



ICCGE-19
2019 OMVPE-19
Keystone, Colorado, USA

**19th International Conference on Crystal Growth and Epitaxy
(ICCGE-19)**

and the

**19th US Biennial Workshop on Organometallic Vapor
Phase Epitaxy (OMVPE-19)**

along with the

**Symposium on 2D and other Low-dimensional Materials
Symposium on Epitaxy of Complex Oxides
Symposium on Ferroelectric Crystals and Textured Ceramics**

PROGRAM BOOK



Table of Contents

[Table of Contents](#)

[Welcome to Keystone, Colorado](#)

[Maps of Conference Area and Resort](#)

[Conference Center Floor Plan](#)

[Conference Corporate Sponsors](#)

[Conference Funding Support](#)

[Scope and Purpose of the Conferences](#)

[Practical Information](#)

[Conference Organizers](#)

[ICCGE-19 International Advisory Committee](#)

[Officers and Executive Committee of the IOCG
\(2016-2019\)](#)

[IOCG Council \(2016-2019\)](#)

[AACG Organization \(2017-2019\)](#)

[OMVPE Workshop Committee \(2019\)](#)

[Sessions and Organizers](#)

[IOCG Prizes](#)

[ICCGE-19/OMVPE-19 .Corporate Exhibition](#)

[Proceedings](#)

[Wednesday Afternoon Group Excursions](#)

[Presentation and Poster Instructions](#)

[ICCGE-19/OMVPE-19 Photo Contest](#)

[Schedule Overview](#)

[Technical Program Schedule](#)

[Monday Schedule](#)
[Tuesday Schedule](#)
[Wednesday Schedule](#)
[Thursday Schedule](#)
[Friday Schedule](#)

** Current as of 6-20-2019. Changes to the schedule will be posted on-site **

Welcome to Keystone, Colorado

Welcome to ICCGE-19 / OMVPE-19! On behalf of the organizing committee, the American Association for Crystal Growth (AACG), the International Organization for Crystal Growth (IOCG) and the OMVPE Workshop Committee, we are honored to host all of you at the 19th International Conference on Crystal Growth and Epitaxy (ICCGE-19) to be held jointly with the 19th US Biennial Workshop on Organometallic Vapor Phase Epitaxy (OMVPE-19) and following the 17th International Summer School on Crystal Growth (ISSCG-17) held the previous week.

ICCGE/OMVPE-19 will provide sessions for presentation and discussion regarding recent research and development activities in all aspects of crystal growth, epitaxy, characterization and applications including both general sessions and special topical symposia. The latter will include the Fourth Symposium on 2D and other Low-Dimensional Materials, the Second Symposium on Epitaxy of Complex Oxides and the Second Symposium on Ferroelectric Crystals and Textured Ceramics.

ICCGE-19 is the latest in a sequence that started with ICCG-1 in Boston, MA, USA in 1966, which marked the formation of the crystal growth community as an independent discipline rather than subsidiary to a number of other fields. The key principle is that the theory and practice of crystal growth is common across a range of materials and applications and that we have much to share with one another.

The OMVPE-19 workshop continues a tradition, started at Cornell in 1983, of bringing together specialists in the OMVPE field from industry, academia and government laboratories in an informal

atmosphere and scenic surroundings. The workshop is an opportunity to present and discuss new results in the OMVPE field and provides a venue for newcomers to familiarize themselves with OMVPE science and technology.

The conferences are composed of cross-cutting and cutting-edge science and technology. Participants are encouraged to move about this technical landscape to maximize interaction with their personal interests. The technical program will include both oral and poster sessions, as well as plenary, invited and award talks. We intend to make this another excellent opportunity to advance the science and technology of crystal growth, epitaxy, characterization, and applications, and to gather old and new friends, colleagues and business associates. The official language of the conference is English. The conference proceedings will be reviewed and published in a thematic issue of Journal of Crystal Growth.

The conference will observe a policy of non-discrimination and affirms the right and freedom of scientists to associate in international scientific activity without regard to such factors as ethnic origin, religion, citizenship, language, political stance, gender, sex or age, in accordance with the Statutes of the International Council for Science. At this meeting no barriers will be made by the conference organizers or the venue that would prevent the participation of bona fide scientists.

This is the fourth crystal growth conference held at the Keystone Resort and Conference Center and we have perfected enjoying this beautiful venue and its surroundings. The Keystone area on the front range of the Rockies has a mountain climate that is temperate in the summer. Keystone has numerous summer activities for all ages and activity levels with hiking, historic tours, shopping,

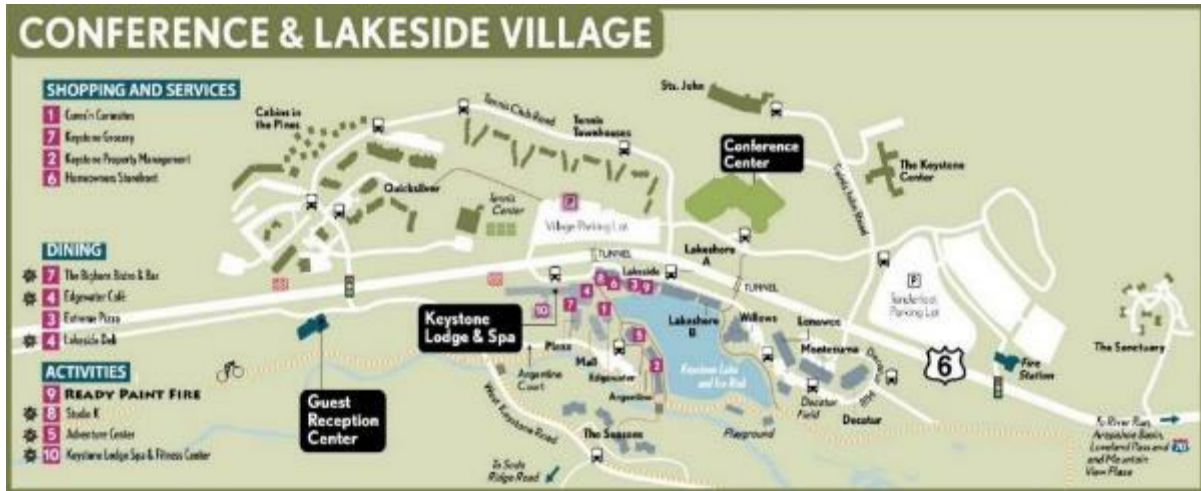
fishing, golf, horseback riding, gondola rides, white water rafting, spa activities and wonderful western cuisine. Welcome to Keystone.

Sincerely yours,

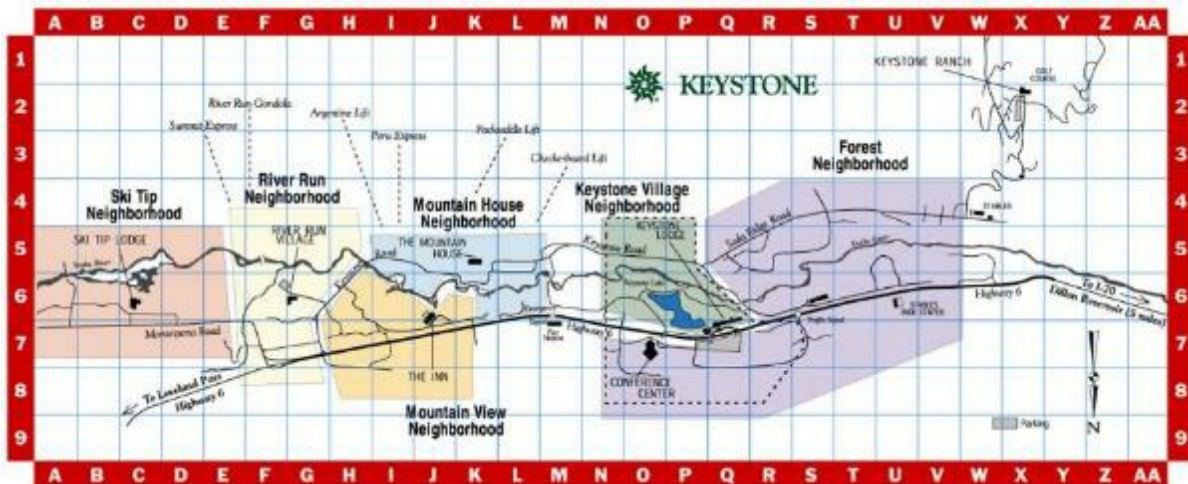
Vince Fratello, Quest Integrated, LLC
Jeff Derby, University of Minnesota
ICCGE Co-chairs

Andy Allerman, Sandia National Labs
OMVPE Workshop Chair

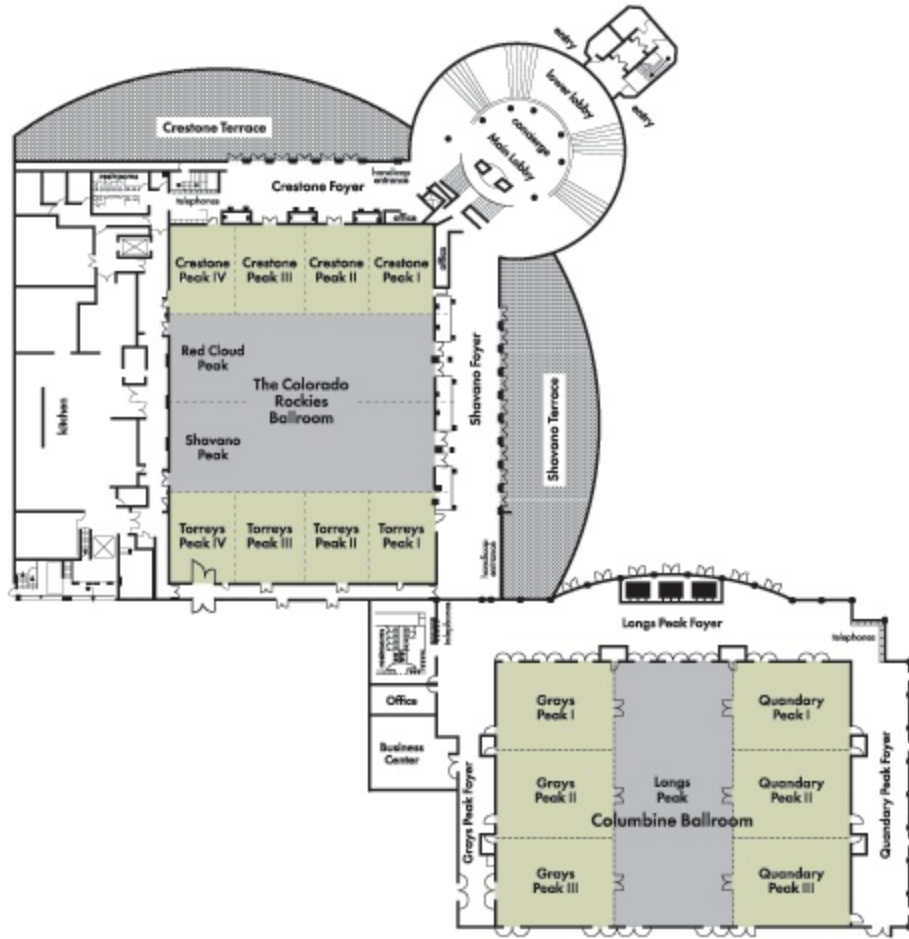
Maps of Conference Area and Resort



Note; the maps above are oriented North up opposite to the South-oriented map below



Conference Center Floor Plan



Conference Corporate Sponsors

At press time, the following companies have generously given their support to this meeting:

- BAE Systems
- Cape Simulations Inc.
- Coherent Advanced Crystal Group
- Elemental Metals
- Elsevier
- Furuya Metal America
- Heraeus
- II-VI Optical Systems
- IPG Photonics
- Johnson Matthey
- Matheson Tri-Gas, Inc.
- Northrop Grumman Synoptics
- ProChem Inc.
- Thermcraft, Inc.
- Wide Bandgap Materials (II-VI Incorporated)
- WEP Control

Conference Funding Support

At press time, the following organizations have graciously offered to support to this meeting:

- International Union of Crystallography (IUCr)
- Lawrence Livermore National Laboratory (LLNL)
- National Science Foundation PARADIM MIP Center (Platform for the Accelerated Realization, Analysis, and Discovery of Interface Materials - Materials Innovation Platform), Cornell
- Penn State 2D Crystal Consortium - Materials Innovation Platform (2DCC-MIP)
- The Olsen Foundation/GHO Ventures

Scope and Purpose of the Conferences

ICCGE-19/OMVPE-19 will provide a forum for the presentation and discussion of recent research and development activities in all aspects of epitaxial thin film and bulk crystal growth; sessions will integrate fundamentals, experimental and industrial growth processes, characterization and applications. Crystal growth is a broad field that attracts people from a wide variety of disciplines. The purpose of the conferences is to bring together scientists and engineers to discuss the entire breadth of activities in crystal growth from bulk to nano, fundamentals to characterization, modeling to equipment design, every type of epitaxy and every type of material from elemental to biological. The conferences feature symposia on important new topics in crystal growth as well as more traditional subjects of enduring interest. Focused and joint sessions have been organized based on the topical distribution of papers and to foster cross-fertilization among fields. Current interest in low dimensional materials, biotechnology and other fields has provided the crystal growth field with many new opportunities and challenges for materials preparation and device research. While the presentations are the core of the

conference schedule, it is the personal interactions with colleagues across the spectrum of crystal growth that give strength to the experience of this meeting and an opportunity to explore fully the issues of importance in the field. The crystal growth community is unique in that the vendor community is intimately integrated with the technical community and the vendor exhibit will give everyone a chance to form and renew commercial and technical relationships. A single registration fee gives attendees access to all the conferences and symposia.

Practical Information

The weather during July and August at Keystone will be temperate, but the sunlight is intense. The air is very dry and the high elevation is also dehydrating. It is a good idea to wear plenty of sunscreen, wear a hat and drink lots of water when enjoying any outdoor activities. Attendees are cautioned that Keystone is at a rather high elevation (9,300 feet or 2,800 m) and some attendees may experience difficulties with the altitude at first. To avoid experiencing altitude sickness, guests are encouraged to limit their physical exertion for the first day or two and drink plenty of water. For some guests, consumption of alcoholic

beverages may aggravate these effects.

It is the responsibility of the conference attendees and their families to have their own medical insurance.

The conference, the organizing committee, the American Association for Crystal Growth, the International Organization for Crystal Growth, the OMVPE Workshop Committee and their officers bear no responsibility for medical care for conferees and their families.

Conference Organizers

ICCGE Conference Chairs

Vincent Fratello, Quest Integrated LLC

Jeffrey Derby, University of Minnesota

OMVPE Conference/Program Chair

Andrew Allerman, Sandia National Labs

ISSCG Chairs

Thomas Kuech, University of Wisconsin

Joan Redwing, Penn State University

ICCGE Program Chairs

Christine Wang, MIT Lincoln Laboratory

Peter Schunemann, BAE Systems

Secretariat

Shoshana Nash, AACG

Treasurer

Luis Zepeda-Ruiz, Lawrence Livermore National
Laboratory

Local Arrangements

John Geisz, National Renewable Energy Laboratory

Kris Bertness, National Institute of Standards and
Technology

Corporate Support

Candace Lynch, Inrad Optics

Luke Mawst, University of Wisconsin

Irina Mnushkina, II-VI, Incorporated

Government Support

Joan Redwing, Penn State University

Industrial Exhibit

Harry Niedecken, WirlNet Inc.

John Geisz, National Renewable Energy Laboratory

Publicity

Merry Koschan, University of Tennessee

ACCGE/ OMVPE Proceedings

Raj Bhat, retired

Catherine Caneau, retired

Bharat Jalan, University of Minnesota

Roger Qiu, Lawrence Livermore National Laboratory

Andrea Zappettini, Italian National Research Council
(CNR)

Thomas Kuech, University of Wisconsin

Chung-Wen Lan, National Taiwan Univ.

Photography Contest

Balaji Raghothamachar, Stony Brook University

IOCG Awards

Elias Vlieg, Radboud University

Web Site & Information Management

Shoshana Nash, AACG

Conference Planner

Dori Nielsen

2D Symposium

Kurt Gaskill, Naval Research Laboratory

Kevin Daniels, University of Maryland

Symposium on Complex Oxides

Ho Nyung Lee, Oak Ridge National Labs

Darrell Schlom, Cornell University

Judith Driscoll, University of Cambridge

Symposium on Ferroelectric Crystals and Textured Ceramics

Zuo-Guang Ye, Simon Fraser University

Shujun Zhang, University of Wollongong

Richard Meyer, Penn State University

Jun Luo, TRS Technologies

Liaison International Advisory Comm.

Antoni Dabkowski, McMaster University

ICCGE-19 International Advisory Committee

Andrey Prokofiev, Vienna University of Technology,
Vienna, Austria

Julian Gale, Curtin University, Perth, Australia

Dominique Maes, Vrije Universiteit, Brussels, Belgium

Bogdan Ranguelov, Bulgarian Academy of Sciences,
Bulgaria

Hanna Dabkowska, McMaster University, Hamilton,
Canada

J. Y. Wang, Shandong University, Jinan, China

Zdenek Kozicek, Institute of Physics of the Czech
Academy of Sciences, Prague, Czech Republic

Thierry Duffar Grenoble Institute of Technology,
Grenoble, France

Wolfram Miller, Leibniz Institute for Crystal Growth
(IKZ), Berlin, Germany

Laszlo Granasy, Hungarian Academy of Sciences,
Budapest, Hungary

Srinivasan Raghavan, Indian Institute of Science,
Bangalore, India

Brian Glennon, University College, Dublin, Ireland

Simon Brandon, Technion – Israel Institute of
Technology, Haifa, Israel

Andrea Zappettini, Italian National Research Council
(CNR), Rome, Italy

Koichi Kakimoto, Kyushu University, Fukuoka, Japan
Janis Virbulis, University of Latvia, Riga, Latvia
Abel Moreno, The National Autonomous University of
Mexico (UNAM), Mexico City, Mexico
Elias Vlieg, Radboud University, Nijmegen, The
Netherlands
Anne-Karin Soiland, Elkem Solar, Oslo/Kristiansand,
Norway
Dobrosława Kasprowicz, Poznan University of
Technology, Poznań, Poland
Horia Alexandru, University of Bucharest, Bucharest,
Romania
Nikolay Leonyuk, Moscow State University, Moscow,
Russia
Evgenii Zharikow, Russian Academy of Sciences,
Moscow, Russia
Kimberly Dick Thelander, Lund University, Lund,
Sweden
Enrico Gianini, University of Geneva, Geneva,
Switzerland
Igor Pritula, Institute for Single Crystals, of National
Academy of Sciences of Ukraine, Kharkiv, Ukraine
Tariq Mahmud, University of Leeds, Leeds, United
Kingdom

Officers and Executive Committee of the IOCG (2016-2019)

Officers

President: K. Kakimoto (Japan)

Co-vice Presidents: T. F. Kuech (USA) and E. Vlieg
(The Netherlands)

Secretary: H. Dabkowska (Canada)

Treasurer: J. Derby (USA)

Immediate Past President: R. Fornari (Italy)

Honorary Principal Founder: Michael Schieber (1928-
2017) (Israel)

Executive Committee

Elected Members

S. L. Baldochi (Brazil)

J. M. García-Ruiz (Spain)

M. Heuken (Germany)

S. Krukowski (Poland)

Y. Mori (Japan)

A. Voloshin (Russia)

J. Y. Wang (China)

J. De Yoreo (USA)

Conference Co-chairs Members of the Executive Committee

Chairs ICCGE-18 Y. Arakawa, K. Kakimoto (Japan)
Chairs ICCGE-19 J. Derby, V. Fratello (USA)

Ex-Officio Executive Committee Members

Representing International Unions

International Union of Crystallography, IUCr: A.
Zappettini (Italy)

International Union on Pure and Applied Physics.
IUPAP: J. Adler (Israel)

International Association of Pure and Applied
Chemistry, IUPAC: J. W. Jost (USA)

Ex-Officio Executive Committee Members Serving as Representatives to International Unions

International Union of Crystallography, IUCr: E. Vlieg
(The Netherlands)

International Union on Pure and Applied Physics.
IUPAP: Vacant

International Association of Pure and Applied
Chemistry, IUPAC: Vacant

IOCG Council (2016-2019)

Councilors Representing National Organizations

Australia: F. Jones

Brazil: S. Baldocchi

China: J. Wang

Czech Republic: Z. Kozisek

France: T. Duffar, F. Puel

Germany: C. Frank-Rotsch, J. Friedrich, W. Miller

Hungary: L. Granasy

India: P. Ramasamy, J. Kumar

Ireland: B. Glennon

Israel: M. Roth

Italy: A. Vecchione

Japan: H. Fuijoka, Y. Takeda, Y. Furukawa

Korea: W. B. Shim, S. M. Kang, J. G. Choi

The Netherlands: A. van der Heijden, H. te Nijenhuis

Poland: D. Pawlak, D. Kasprowicz

Romania H.V. Alexandru

Russia: P. Fedorof, A. E. Voloshin, E. Zharikov

Spain: F. Otalora

Switzerland: E. Giannini

Ukraine: B. Grinyov, V. Semynozhenko, I. Pritula

United Kingdom: J. ter Horst, L. Seton, G. Sadiq

USA: R. Biefeld, J. M. Redwing, M. Zhuravleva

Councilors Representing the General Assembly

Algeria L. Amirouche

Belgium: D. Maes

Bulgaria: V. Tonchev

Canada: A. Dabkowski

Denmark: H. E. Lundager Madsen

Mexico: A. Moreno

Singapore: X. Y. Liu

Sweden: S. Lourdodoss

Taiwan: C. W. Lan

Uruguay: L. Fornaro

AACG Organization (2017-2019)

President: Robert Biefeld (Consultant)

Vice President: Joan Redwing (Pennsylvania State University)

Treasurer: Luis Zepeda-Ruiz (Lawrence Livermore National Labs)

Secretary: Mariya Zhuravleva (University of Tennessee)

Administrator: Shoshana Nash (AACG)

Executive Committee:

Robert Biefeld (Consultant)

Edith Bourret-Courchesne (Lawrence Berkeley National Laboratory)

Antoni Dabkowski (McMaster University)

Parthiv Daggolu (University of Minnesota)

Jeffrey Derby (University of Minnesota)

James De Yoreo (Pacific Northwest National Laboratory)

Govindhan Dhanaraj (Aymont Technology)

Dirk Ehrentraut (Soraa)

Robert Feigelson (Stanford University)

Vincent Fratello (Quest Integrated, LLC)

Kurt Gaskill (Naval Research Laboratory-retired)

John Geisz (National Renewable Energy Laboratory)

Kenneth Jackson (Retired)
David Kisailus (University of California, Riverside)
Seyed Koochpayeh (Johns Hopkins University)
Thomas Kuech (University of Wisconsin)
Candace Lynch (Inrad Optics, Inc.)
Luke Mawst (University of Wisconsin)
Irina Mnushkina (II-VI, Inc.)
Aleksandar Ostrogorsky (Illinois Institute of
Technology)
Joan Redwing (Pennsylvania State University)
Jeffrey Rimer (University of Houston)
J. Carlos Rojo (General Electric)
Peter Schunemann (BAE Systems, Inc.)
David Vanderwater (Consultant)
Peter Vekilov (University of Houston)
Christine A. Wang (MIT Lincoln Laboratory)
Simon P. Watkins (Simon Fraser University)
Matthew Whittaker (Gooch & Housego)
Kevin Zawilski (BAE Systems, Inc.)
Luis Zepeda-Ruiz (Lawrence Livermore National
Laboratory)
Mariya Zhuravleva (University of Tennessee)

Section Presidents:

WEST: Edith Bourret-Courchesne (Lawrence Berkeley
Laboratory)

TENNESSEE: Merry Spurrier-Koschan (University of Tennessee)

OMVPE Workshop Committee (2019)

Andrew Allerman (Sandia National Laboratories)

Robert Biefeld (Consultant)

Russell Dupuis (Georgia Institute of Technology)

John Geisz (National Renewable Energy Laboratory)

Luke Mawst (University of Wisconsin)

Joan Redwing (Pennsylvania State University)

Jae-Hyun Ryou (University of Houston)

Shadi Shahedipour-Sandvik (State University of New York Polytechnic Institute)

Christine Wang (MIT Lincoln Laboratory)

Simon Watkins (Simon Fraser University)

Sessions and Organizers

Special Session: George Gilmer

Chair: Luis Zepeda-Ruiz (Lawrence Livermore
National Laboratory)

Special Session: Michael Schieber

Chair: Jerry Stringfellow (University of Utah)
Edith Bourret-Courchesne (Lawrence Berkeley
National Laboratory)

Fundamentals of Crystal Growth

Co-Chair: Baron Peters (University of Illinois, Urbana-
Champaign)

Co-Chair: Boaz Pokroy (Technion Israel Institute of
Technology)

Jim De Yoreo (Pacific Northwest Laboratory)

Peter Vekilov (University of Houston)

Mu Wang (Nanjing)

Modeling of Crystal Growth Processes

Chair: Simon Brandon (Technion Israel Institute of
Technology)

Wolfram Miller (Leibniz Institute for Crystal Growth)

Moneesh Upmanyu (Northeastern University)

Talid Sinno (University of Pennsylvania)

Thierry Duffar (Grenoble Institute of Technology,
France)

Bulk Crystal Growth

Chair: Merry Koschan (University of Tennessee,
Knoxville)

Seth Bank (University of Texas, Austin)

Michal Bockowski (UNIPRESS, Poland)

Antoni Dabkowski (McMaster University)

Christo Gugushev (Leibniz Institute for Crystal
Growth)

Seyed Koohpayeh (Johns Hopkins University)

Aleks Ostrogorsky (Illinois Institute of Technology)

Nonlinear Optical and Laser Host Materials

Co-Chair: Yasunori Furakawa (OXIDE Corp.)

Co-Chair: Kevin Zawilski (BAE Systems)

Peter Schunemann (BAE Systems)

Biological and Biomimetic Materials

Chair: David Kisailus (University of California,
Riverside)

Detector Materials: Scintillators and Semiconductors

Co-Chair: Edith Bourret-Courchesne (Lawrence
Berkeley National Laboratory)

Co-Chair: Mariya Zhuravleva (University of
Tennessee, Knoxville)

Seth Bank (University of Texas, Austin)

Candace Lynch (Inrad)

Industrial Crystal Growth Technology and Equipment

Chair: Matt Whittaker (Gooch & Housego)

Advanced Equipment and Growth Technology

Chair: Kou Matsumoto (Taiyo Nippon Sanso, Japan)

Michael Heuken (Aixtron)

Xiaohang Li (King Abdullah University of Science and
Technology, Saudi Arabia)

Akinori Ubukata (Taiyo Nippon Sanso, Japan)

Surfaces and Interfaces

Chair: Elias Vlieg (Radboud University)

Martin Albrecht (Leibniz Institute for Crystal Growth)

Kerstin Volz (Philipps-Universität Marburg)

In situ Observation and Characterization

Co-Chair: Matt Highland (Argonne National
Laboratory)

Co-Chair: Katsuo Tsukamoto (Tohoku University)

Characterization Techniques for Bulk and Epitaxial Crystals

Chair: Mark Goorsky (University of California, Los
Angeles)

Mike Dudley (Stony Brook University)

Holger Eisele (Technical University Berlin)

Motoaki Iwaya (Meijo University, Japan)

Thin Film Growth, Epitaxy, and Superlattices

Co-Chair: Ferdinand Scholz (Ulm University)

Co-Chair: Masakazu Sugiyama (University of Tokyo)

Seth Bank (University of Texas, Austin)

Xiuling Li (University of Illinois at Urbana-Champaign)

Kunal Murkherjee (University of California, Santa Barbara)

Kevin Schulte (National Renewable Energy Laboratory)

Nanocrystals, Quantum Dots, and Nanowires

Chair: George Wang (Sandia National Laboratories)

Alok Rudra (EPFL)

Hoe Tan (Australian National University)

2D Materials and Devices

Jim Maslar (NIST)

Suzanne Mohny (Pennsylvania State University)

Joan Redwing (Pennsylvania State University)

Materials for Photovoltaics and Other Energy Technology

Chair: John Geisz (National Renewable Energy Laboratory)

Kamran Forghani (Microlink)

Aaron Ptak (National Renewable Energy Laboratory)

Kevin Schulte (National Renewable Energy Laboratory)

Masakazu Sugiyama (University of Tokyo)

Hoe Tan (Australian National University)

Selective and Patterned Epitaxial Growth

Chair: Yuji Zhao (Arizona State University)

Seth Bank (University of Texas, Austin)

III-V Epitaxial Growth for Devices

Chair: Luke Mawst (University of Wisconsin)

Amy Liu (IQE)

Christopher Pinzone (Thor Labs)

Jae-Hyun Ryou (University of Houston)

Kevin Schulte (National Renewable Energy
Laboratory)

Marcus Weyers (Ferdinand Braun Institute)

III-V's on Silicon

Chair: Kei May Lau (University of Hong Kong)

Seth Bank (University of Texas, Austin)

Bernardette Kunert (IMEC)

Shadi Shahedipour-Sandvik (State University of New
York

Polytechnic Institute)

III-V Wide Bandgap Nitride Semiconductors and Devices

Co-Chair: Tim Wernicke (Technical University Berlin)

Co-Chair: Ramon Collazo (North Carolina State
University)

Co-Chair: Daniel Feezell (University of New Mexico)

Jung Han (Yale University)

Jennifer Hite (NRL)

Isik Kizilyalli (U.S. Department of Energy)

Zetian Mi (University of Michigan)

Hideto Miyake (Mie University)

Yasu Nanishi (Ritsumeikan University)

Christian Wetzel (Rensselaer Polytechnic Institute)

Narrow Bandgap Semiconductors and Devices

Chair: Simon Watkins (Simon Fraser University)

Ganash Balakrishnan (University of New Mexico)

Seth Bank (University of Texas, Austin)

Leon Shterengas (State University of New York,
Stonybrook)

BN Epitaxial Growth and Characterization

Hongxing Jiang (Texas Tech)

Tony Rice (Sandia National Laboratories)

Sergei Novikov (University of Nottingham, UK)

Silicon Carbide Materials and Devices

Chair: Govindhan Dhanaraj (Aymont Technology)

Michael Dudley (State University of New York,
Stonybrook)

Balaji Raghothamachar (Stony Brook University)

Gallium Oxide Materials and Devices

Co-Chair: Shizuo Fujita (Kyoto University, Japan)

Co-Chair: Kevin Stevens (Northrup Grumman
Synoptics)

Fourth Symposium on 2D and Other Low Dimensional Materials:

Co-Chair: Kurt Gaskill (Naval Research Laboratory)

Co-Chair: Kevin Daniels (University of Maryland)

Second Symposium on Complex Oxides

Co-Chair: Ho Nyung Lee (Oak Ridge National Labs)

Co-Chair: Darrell Schlom (Cornell University)

Co-Chair: Judith Driscoll (University of Cambridge)

Second Symposium on Ferroelectric Crystals and Textured Ceramics

Co-Chair: Zuo-Guang Ye (Simon Fraser University)

Co-Chair: Shujun Zhang (University of Wollongong)

Co-Chair: Rich Meyer (Pennsylvania State University)

Co-Chair: Jun Luo (TRS Technologies)

IOCG Prizes

Since 1989 at ICCG-9 (Sendai), the International Organization for Crystal Growth (IOCG) has sponsored two triennial prizes, the Frank Prize and the Laudise Prize. Beginning in 2004 at ICCG-14 (Grenoble), there was a new triennial IOCG prize, the Schieber Prize, sponsored by the Elsevier and the Journal of Crystal Growth. These prizes consist of a commemorative item plus an invitation and financial support to present the work, which is the subject of the award, at the ICCGE meeting at which the award takes place. The winners are expected to deliver invited talks during the conference.

Frank and Laudise Prizes

The IOCG Frank Prize is awarded for significant fundamental (not necessarily theoretical) contributions to the field of crystal growth. The IOCG Laudise prize is presented for significant technological (not necessarily experimental) contributions to the field of crystal growth. Both awards are made for outstanding contributions to the field of crystal growth through technical achievements, publications and presentations and through their impact worldwide on science and technology.

The Frank Prize is jointly awarded to Prof. Darrell Schlom of Cornell University and Dr. Reinhard Uecker of the Leibniz Institute for Crystal Growth (IKZ) for their pioneering contributions to the development of new perovskite substrates enabling strain engineering of functional oxides.

The Laudise prize is awarded to Prof. Kazuo Nakajima, emeritus professor of Tohoku University, for his seminal contributions to the growth of both III-V quaternary layers for optical communication systems and of high-quality Si ingots for high-efficiency solar cells.

Schieber Prize

The IOCG Schieber prize is awarded to a young author to recognize his or her outstanding scientific publications in the field of Crystal Growth. The prize shall be awarded to one person who is an early career worker. The publications for which the award is made should consist of a paper or series of papers, published prior to the opening of that ICCGE. The criteria for selection should be scientific excellence, clarity of presentation and impact on the field of crystal growth. This prize is sponsored Elsevier and the Journal of Crystal Growth in memory of its Founding Editor.

The Schieber Prize is awarded to Dr. Anton Jesche, Center for Electronic Correlations and Magnetism, Institut für Physik, Universität Augsburg, for innovative development of crystal growth processes for complex correlated electron and magnetic materials.

ICCGE/OMVPE Corporate Exhibition

The following exhibitors had registered at press time.

AIXTRON

Ajax TOCCO Magnethermic / PILLAR Induction

Ambrell Induction Heating Solutions

BASF Temperature Sensing

Carlite Gero, part of Verdo Scientific, Inc.

Cyberstar / ECM-USA

DOCKWEILER CHEMICALS GmbH

Elemental Metals

Elsevier

EMD Performance Materials

Eurofins EAG

Freiberg Instruments GmbH

Furuya

Heraeus

II-VI Optical Systems

Johnson Matthey

k-Space Associates, Inc.

Matheson Gas

Mesta Electronics, Inc.

Nouryon

Proto Manufacturing, LTD

SciDre (Scientific Instruments Dresden)

STR Group

Structured Materials Industries, Inc.

WEP Control

Zircar Zirconia, Inc.

Proceedings

Authors who have a paper accepted for oral or poster presentations at the 19th International Conference on Crystal Growth and Epitaxy/19th US Biennial Workshop on Organometallic Vapor Phase Epitaxy are invited to submit manuscripts for consideration for publication in the conference proceedings. Only work actually presented at the conference and that has not been published, nor is in press, or submitted for publication elsewhere will be considered for inclusion in the Proceedings.

The Proceedings will be published as a special thematic issue of the Journal of Crystal Growth. The manuscripts submitted will undergo a peer review process similar to regular publications.

The length of the papers in the Proceedings is limited to 8 printed pages

Manuscript submission deadline: September 29, 2019.

Formatting instructions:

Please follow the formatting recommendations on the Elsevier author instructions website. All manuscripts

will be subject to the review process; submissions will be rejected if they do not describe original, unpublished work or are not of high quality. A single printed column (text only) in the Journal of Crystal Growth is approximately 480 words. Please keep the page length limit in mind when preparing your manuscript.

Instructions to Authors:

<https://www.elsevier.com/journals/journal-of-crystal-growth/0022-0248/guide-for-authors>

Submission Link:

<http://ees.elsevier.com/CRYS/default.asp>

When submitting their papers, authors must select VSI: ICCGE-19/OMVPE-19 as the article type.

ICCGE-19/OMVPE-19 Editors:

Raj Bhat (retired)

Bharat Jalan (University of Minnesota)

Catherine Caneau (retired)

Roger Qiu (Lawrence Livermore National Laboratory)

Andrea Zappettini (Italian National Research Council)

Tom Kuech (University of Wisconsin-Madison)

Chung-Wen Lan (National Taiwan University)

Wednesday Afternoon Group Excursions

Option One: Rafting on the Upper Colorado River

Enjoy beautiful mountain scenery while floating down the Colorado river in a guided raft trip! This trip is suitable for beginners and children at least 4 years old and above. Some paddling is required with basic maneuvers; splashing and jumping off rocks into river pools available for those who choose! Plan on wearing swimsuits and fast-drying clothing. Hats, sunscreen and water bottles recommended. Spare clothing, water, etc., may be left on the bus but no valuables (no phones, watches, wallets), please. More information about the raft trip and outfitters is available at <https://www.madadventures.com/what-to-bring/>.

Depart Keystone in front of Keystone Lodge at 12:30 pm;

Return to Keystone about 5:30 or 6:00 pm.

Please fill out and sign the Participant Agreement prior to arrival at the bus. The document is available here.

Cost: \$110 per person including 10% group discount, transportation, and sack lunch to take on the bus. See registration form for lunch details.

Sign up by July 10, 2019, to ensure space and choice of lunch.

Number of slots and lunch choices will be finalized immediately after this date due to vendor deadlines.

Lunch includes a choice of wrap, fresh fruit salad, red jacket potato salad, cookie duo, and bottled water in a reusable tote. Wrap choices: Buffalo Chicken Salad (chicken breast, pepper jack cheese, buffalo ranch dressing, sliced tomatoes and chopped romaine lettuce), Tuna Salad (white albacore tuna salad, Monterey jack cheese, spinach, sliced pickles and tomatoes on a tomato wrap), or Quinoa Vegetable Salad (shredded kale and black bean hummus on a spinach wrap, dairy free).

Option Two: Scenic Wagon Ride

Relax and enjoy a scenic horse-drawn wagon ride through Soda Creek Valley to Keystone's original homestead. Wranglers will give an historic account of Keystone's original settlement and progression to a ski resort. Learn about the horses pulling the wagons and enjoy refreshments (2 glasses of wine or beer with cheese and crackers) at the barn and deck of the Soda

Ridge Homestead.

Meet at 1:30 p.m. in the Adventure Center located in Lakeside Village for a short bus ride to the horse drawn wagons. The entire event will last 2 - 2 1/2 hours.

Cost: \$50 per person. Sign up by July 10 to ensure availability.

Presentation and Poster Instructions

Oral

- If for any reason you cannot attend the conference or give your presentation, contact the conference organizers at the earliest possible time so as not to disrupt the schedule and to allow another presentation to take its place.
- PC laptop computers will be provided by the conference in each session room. However, you are welcome to bring your own PC or Mac (required if you use Keynote). Each room will also have one LCD projector, a laser pointer, and a microphone.
- Presentations will run on Windows Power Point (versions from 2015-2019) with a resolution of up to 1920x1080 (via HDMI or

UXGA cabling).

- Various adapters will be available upon request.
- Only a single projector is available in the presentation rooms.
- Please arrive and check in with the session chair and audio-visual assistant at least 15 minutes before the session begins either to load your presentation on the conference laptop or to check the connection between your computer and the projector. Note that time lost switching between computers or due to nonfunctioning computer graphics presentations will be deducted from the speaker's allotted presentation time.
- In general, the smaller your presentation (in file size) the easier it is to handle.
- Any movie/image file must be in the same folder as the presentation and must be copied in the folder before being included in the presentation.
- Please direct any presentation questions to the chair for your session.

Time slots

- Plenary talks are 45 minutes total (40 min.

- presentation, 5 min. questions)
- Prize talks are 40 minutes total (35 min. presentation, 5 min. questions)
- Invited ICCGE, OMVPE, and Symposia talks are 30 minutes total (25 min. presentation, 5 min. questions)
- Contributed ICCGE, OMVPE, and Symposia talks are 15 minutes total (12 min. presentation, 3 min. questions)
- Contributed OMVPE evening talks are 20 minutes total (17 min. presentation, 3 min. questions)

Posters

- Poster boards cost money and space is limited. Poster presenters are required to confirm their attendance at the conference by registration or other means. If you have not confirmed your attendance, your poster will be removed from the program. If for any reason you cannot attend the conference or give your poster, contact the conference organizers at the earliest possible time.
- Posters must fit in a 3' wide x 4' tall space. Push pins will be available.
- Poster sessions are scheduled for Monday and

Tuesday afternoons from 5:30 PM - 7:00 PM.

- Please mount your poster from 2:30 – 5:00 PM on the day of the presentation.
- Individual poster boards will be identified with poster numbers. Check the list in the room to determine your poster number and mount your poster in the correct space.
- You or a co-author are expected to be present at your poster during the entire session to answer questions.
- Please remove your poster in a timely manner at the end of the poster session.
- There will be one or more prizes for the best student poster(s).

Make Sure Slides Are Simple and Legible

- Preferred page setup is landscape orientation with high-contrast lettering and readable fonts.
- Use a sans serif non-stylized typeface such as Helvetica or Arial.
- No non-standard fonts as they may not display properly or be illegible.
- The larger the font, the better. Avoid using anything smaller than 24-point font for text and 18-point font for labels. Most of us can't read too small.

- Do not rely solely on color for contrast, but use light text on dark background or vice versa. Some people are colorblind.
- A maximum of 7 lines/slide and 5 words/line will improve the communication value of your slide. Most of us can't read fast enough for excessive content.
- Test slides for legibility and contrast.
- Check spelling and grammar using a spell check program or a proofreader.
- Have an appropriate number of slides for your time. More than one slide per presentation minute is unlikely to be understood by the audience.
- One concept per slide is enough.
- Include your contact information and website URL on the final slide.

Pictures and Graphics

- Do not save pictures as .bmp or .tiff (file size is too big).
- Images with .gif and .jpg extensions are recommended to obtain a light presentation that will load and display readily (other kinds of extensions - recognizable by PowerPoint will be accepted all the same).

- Save the pictures used in your presentation on a USB storage as backup (in case of problems, we can re-insert the original).
- Save the graphics or spreadsheets (Excel) used in your presentation on a separate USB-stick as back up.
- PDFs for presentations that may have been created using a different format are acceptable.

Video

- Movies should not exceed 50 MB each (50 MB is not necessarily the limit; we can handle larger movies without any problems, but the video may not present as smoothly).
- Always bring your movies on a separate USB storage as back up. The best format for videos is .mp4.

ICCGE-19/OMVPE-19 Photo Contest

Sponsored by the Elsevier and the Journal of Crystal Growth

Photographs portraying scientific, technical, or artistic aspects of crystals, crystal growth, or characterization are solicited. The photos will be displayed on the conference website in addition to being displayed in a prominent location at the conference location and as a slide show in the meeting rooms. Submissions will be accepted in two categories:

- 1) Natural untouched micrographs or photographs
- 2) Photographs including digital manipulation (and computational simulations)

Judging and Awards

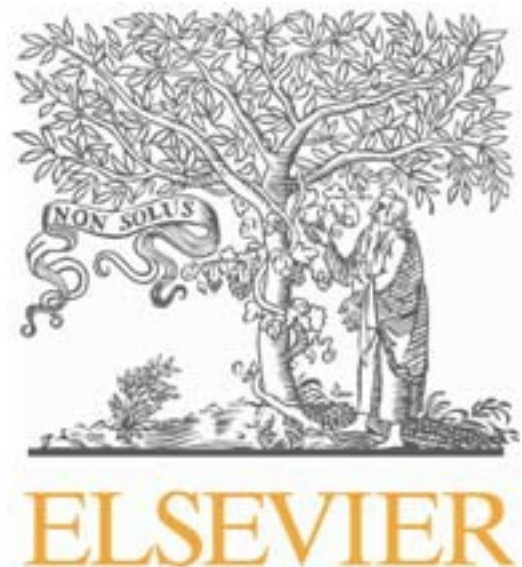
Submissions will be voted on by conference attendees on the conference website. The first-place entries in each category will receive an award certificate and a cash prize of \$300. The best student entry will also receive an award certificate and a cash prize of \$300. Winners will be announced during the Banquet and Awards Ceremony and the Winning photos will be published in the AACG newsletter.

Contest Rules

1. Contest is open only to registered meeting attendees.
2. Each attendee can submit exactly one entry per category.
3. Entries must be submitted by email as a PowerPoint slide (use attached template; limit file size to 10MB).
 - Please do not put text on the photo unless it is part of the image
 - Photo caption should describe the technical significance of the entry and/or the artistry that it represents (50 words or less)
 - Indicate if the entry is a General or Student submission
 - Identify the appropriate category for judging (Natural or Digital/Altered)

Entries should be submitted by email to the photo contest organizer, Balaji Raghothamachar, by **June 30, 2019**. Please direct any questions or comments to the organizer:

Balaji Raghothamachar



Stony Brook University

Phone: 1 (631) 632-4183

Email: balaji.raghothamachar@stonybrook.edu

Overall Schedule

	Sunday 7/28	Monday 7/29	Tuesday 7/30	Wednesday 7/31	Thursday 8/1	Friday 8/2					
7:00-7:30		Breakfast	Breakfast	Breakfast	Breakfast	Breakfast					
7:30-8:00											
8:00-8:30											
8:30-9:00		Intro & Plenary Session	Plenary Session ICCG Press Table	Parallel Sessions W1	Plenary Session	Parallel Sessions F1					
9:00-9:30	Registration Vendor Setup	Registration	Registration	Registration	Registration	Registration					
9:30-10:00							Break	Break	Break	Break	
10:00-10:30							Parallel Sessions M2	Parallel Sessions Tu2	Parallel Sessions W2	Parallel Sessions Th2	Parallel Sessions F2
10:30-11:00							Lunch	Lunch	Exhibition	Lunch, ICCG General Session	End of conference
11:00-11:30							Parallel Sessions M3	Parallel Sessions Tu3		Parallel Sessions Th3	Parallel Sessions F3
11:30-12:00							Break	Break		Break	Break
12:00-12:30							Parallel Sessions M4	Parallel Sessions Tu4		Parallel Sessions Th4	Parallel Sessions F4
12:30-13:00											
13:00-13:30											
13:30-14:00											
14:00-14:30											
14:30-15:00											
15:00-15:30											
15:30-16:00											
16:00-16:30											
16:30-17:00											
17:00-17:30											
17:30-18:00											
18:00-18:30	Posters	Vendor Reception	Posters		Banquet Reception						
18:30-19:00	Welcome Reception	Break	Break								
19:00-19:30											
19:30-20:00		AAOQ ExComm Meeting									
20:00-20:30		OMPE Evening Session	OMPE Evening Session		Banquet						
20:30-21:00											
21:00-21:30											

Monday, July 29, 2019

08:10 - 10:00

Plenary Session

Monday, July 29, 2019

Colorado Rockies Ballroom (Shavano and Red Cloud Peak)

Moderator(s): Christine Wang, USA

08:10 - 08:30

Opening Remarks: Vincent Fratello and Jeffrey Derby

08:30 - 09:15

[\(Plenary\) A RETROSPECTIVE ON THE AMERICAN ASSOCIATION FOR CRYSTAL GROWTH ON ITS 50TH ANNIVERSARY](#)

Robert Feigelson (Stanford University, USA)

09:15 - 10:00

[\(Plenary\) DEFECT ENGINEERING IN BULK CRYSTAL GROWTH](#)

Thierry Duffar (SIMAP EPM, FR)

10:00 - 10:30

BREAK

10:30 - 12:00

Industrial Crystal Growth Technology and Equipment I

Monday, July 29, 2019

Shavano Peak

Moderator(s): Matt Whittaker, USA; Gisele Maxwell, USA

10:30 - 11:00

(Invited) ADVANCES IN SINGLE-CRYSTAL FIBERS AND THIN RODS
GROWN BY LASER HEATED PEDESTAL GROWTH: A REVIEW

Gisele Maxwell (Shasta Crystals, Inc., USA)

11:00 - 11:30

(Invited) ULTRA-FAST AND HIGH-PRECISION CRYSTAL ORIENTATION
AND QUALITY MEASUREMENTS ON CRYSTALLINE SEMICONDUCTORS

Kay Dornich (Freiberg Instruments GmbH, DE)

11:30 - 11:45

CONTROL OF MICROSTRUCTURE AND MECHANICAL PROPERTIES
PLATINUM FIBER FABRICATED BY UNIDIRECTIONAL SOLIDIFICATION

Yuui Yokota (Tohoku University, JP)

11:45 - 12:00

BULK CRYSTAL GROWTH OF TERNARY III-V COMPOUND
SEMICONDUCTORS

Partha Dutta (Rensselaer Polytechnic Institute, NY/USA)

10:30 - 12:00

Wide Bandgap Growth and Characterization

Monday, July 29, 2019

Torreys Peak II-IV

Moderator(s): Daniel Feezell, USA; Tetsuya Takeuchi, JP

10:30 - 11:00

(Invited) GROWTH AND POINT DEFECT CONTROL OF ALGaN FOR U
LASER DIODES

Ramon Collazo (North Carolina State University, USA)

11:00 - 11:15

[POINT DEFECTS IN GAN:MG CRYSTALS GROWN BY AMMONOBASIS METHOD](#)

Robert Kucharski (Institute of High Pressure Physics, Polish Academy of Sciences, PL)

11:15 - 11:30

[CRYSTALLOGRAPHIC POLARITY INVERSION IN NITRIDES ON SI](#)

Alexana Roshko (NIST, CO/USA)

11:30 - 11:45

[GE-DOPING IN ALGAN: DX FORMATION AND COMPENSATION](#)

Ronny Kirste (Adroit Materials Inc, USA)

11:45 - 12:00

[HIGH-TEMPERATURE ANNEALING OF SPUTTERED SCALN FILMS FOR LATTICE-MATCHED ALGAN EPITAXY](#)

Brendan Gunning (Sandia National Laboratories, NM/USA)

10:30 - 12:00

Nonlinear Optical and Laser Host Materials I

Monday, July 29, 2019

Crestone I, II

Moderator(s): Peter Schunemann, USA; Kevin Stevens, USA

10:30 - 11:00

[\(Invited\) FLUORIDE CRYSTALS FOR LASER GAIN AND FARADAY ROTATOR APPLICATIONS](#)

Kevin Stevens (Northrop Grumman SYNOPTICS, NC/USA)

11:00 - 11:15

[OPTICAL SPECTROSCOPY AND MAGNETIC BEHAVIOUR OF \$SM^{3+}\$ - \$A\$ \$EU^{3+}\$ - CATIONS IN \$LI_6EU_{1-X}SM_X\(BO_3\)_3\$ SOLID SOLUTION](#)

Matias Velazquez (SIMaP UMR 5266 CNRS-UGA-G INP, FR)

11:15 - 11:30

[TOP-SEEDED SOLUTION CRYSTAL GROWTH AND CHARACTERIZATION OF NEW ULTRAVIOLET AND DEEP-ULTRAVIOLET NON-LINEAR OPTICAL MATERIALS](#)

P Shiv Halasyamani (Department of Chemistry, University of Houston, TX/U

11:30 - 11:45

[NOVEL \(ER,YB\)YMGB₅O₁₀ PENTABORATE CRYSTALS: FLUX GROWTH AND CHARACTERIZATION](#)

Victor Maltsev (Lomonosov Moscow State University, RU)

11:45 - 12:00

[BRIDGMAN GROWTH OF LARGE SIZE SM:YCOB CRYSTAL FOR QPC APPLICATION](#)

Xiaoniu Tu (Shanghai institute of ceramics, CN)

10:30 - 12:15

Symposium on 2D Materials: Characterization and Devices

Monday, July 29, 2019

Crestone III, IV

Moderator(s): James Maslar, USA; Tanushree Choudhury, USA

10:30 - 11:00

(Invited) NOVEL EXCITONIC EFFECTS IN ATOMICALLY THIN HETEROSTRUCTURES

Cristina Giusca (National Physical Laboratory, GB)

11:00 - 11:15

PHOTOLUMINESCENCE PROPERTIES OF MOS₂/GAN HETERO STRUCTURE

Shinichiro Mouri (Ritumeikan University, JP)

11:15 - 11:30

CHEMICAL VAPOR TRANSPORT SYNTHESIS, CHARACTERIZATION AND COMPOSITIONAL TUNING OF ZRSXSE_{2-X} FOR OPTOELECTRONIC APPLICATIONS

Joshua Fox (Penn State University, USA)

11:30 - 11:45

TUNABLE ELECTRIC AND THERMAL TRANSPORT PROPERTIES IN DEFECT ENGINEERED HF/ZRTE_{5-δ} SINGLE CRYSTAL DURING CVT GROWTH

Shuhua Yao (Nanjing university, CN)

11:45 - 12:00

CHEMICAL SENSING WITH MOS₂/GRAPHENE HETEROSTRUCTURE ON SILICON CARBIDE

Soaram Kim (University of Maryland, MD/USA)

12:00 - 12:15

CRYSTAL GROWTH AND STUDY OF ORBITAL CURRENTS IN THE PSEUDOGAP PHASE OF HIGH-TC CUPRATES

Dalila Bounoua (Laboratoire Léon Brillouin, FR)

10:30 - 12:00

Symposium on Epitaxy of Complex Oxides: Batteries and Epitaxial Nanocomposites

Monday, July 29, 2019

Grays Peak II, III

Moderator(s): Q. X. Jia, USA

10:30 - 11:00

(Invited) RESEARCH DEVELOPMENT OF ALL SOLID-STATE BATTERIES BY USING THIN FILM TECHNOLOGY

Tsuyoshi Ohnishi (National Institute for Materials Science, JP)

11:00 - 11:30

(Invited) NEW PARADIM OF EPITAXY WITH LARGE LATTICE MISMATCH USING NANOCOMPOSITE DESIGNS

Haiyan Wang (Purdue University, USA)

11:30 - 12:00

(Invited) INTERPLAY OF STRAIN, DEFECTS AND INTERFACE ON FUNCTIONAL PROPERTIES OF NANOCOMPOSITES

Aiping Chen (CINT, Los Alamos, NM/USA)

10:30 - 12:00

Symposium on Ferroelectric Crystals and Textured Ceramics: Perovskite Ferroelectric Crystals

Monday, July 29, 2019

Grays Peak I

Moderator(s): YUJI Noguchi, JP; Zuo-guang Ye, CA

10:30 - 11:00

[\(Invited\) ELECTRICAL CONTROL OF FERRIELECTRIC AND FERROELECTRIC PHASES IN BI-BASED POLAR PEROVSKITES.](#)

YUJI Noguchi (Department of Applied Chemistry, The University of Tokyo, JP)

11:00 - 11:30

[\(Invited\) MULTISCALE STRUCTURES AND ORIGINS OF HIGH PIEZO-/FERROELECTRICITY IN COMPLEX PEROVSKITE SINGLE CRYSTALS](#)

Zuo-Guang Ye (Simon Fraser University, BC/CA)

11:30 - 11:45

[GROWTH AND CHARACTERIZATION OF BAPRXND1-XFENB4O15 SINGLE CRYSTALS](#)

Bixia Wang (Argonne National Laboratory, IL/USA)

11:45 - 12:00

[A FERROELECTRIC POLYMER BASED ARTIFICIAL SYNAPSE FOR NEUROMORPHIC APPLICATIONS](#)

Sungjun Kim (School of Electronic and Electrical Engineering, Sungkyunkwan University, KR)

10:30 - 12:00

Special Session - Michael Schieber I

Monday, July 29, 2019

Red Cloud Peak

Moderator(s): Jerry Stringfellow, USA; Edith Bourret-Courchesne, USA

10:30 - 11:00

[\(Invited\) REVIEW OF ROOM TEMPERATURE COMPOUND SEMICONDUCTOR MATERIALS FOR NUCLEAR DETECTION](#)

Kanai Shah (Radiation Monitoring Devices, Inc., MA/USA)

11:00 - 11:30

[\(Invited\) DEVELOPMENTS IN CDZNTE AND OTHER MATERIALS FOR GAMMA-RAY DETECTORS](#)

Mark Goorsky (Dept. of Materials Science and Engineering, University of California Los Angeles, CA/USA)

11:30 - 12:00

[\(Invited\) HEAVY METAL HALIDES FOR ROOM TEMPERATURE NUCLEAR RADIATION DETECTION](#)

Arnold Burger (Fisk University, TN/USA)

12:00 - 13:30

LUNCH

13:30 - 15:00

Special Session - Michael Schieber II

Monday, July 29, 2019

Red Cloud Peak

Moderator(s): Jerry Stringfellow, USA; Edith Bourret-Courchesne, USA

13:30 - 14:00

[\(Invited\) PEROVSKITE CSPBBR3 SINGLE CRYSTAL DETECTOR FOR GAMMA AND ALPHA-PARTICLE SPECTROSCOPY](#)

Duck Young Chung (Argonne National Laboratory, IL/USA)

14:00 - 14:30

[\(Invited\) FURTHER IMPROVEMENT OF CE DOPED CLLB SCINTILLATORS](#)

Mikayel Arzakantsyan (Saint-Gobain Research Paris, FR)

14:30 - 15:00

[\(Invited\) PROGRESSION AND MITIGATION OF FABRICATION CHALLENGES FOR MICROSTRUCTURED SEMICONDUCTOR NEUTRON DETECTORS](#)

D.S. McGregor (Kansas State University, KS/USA)

13:30 - 15:00

Industrial Crystal Growth and Technology II

Monday, July 29, 2019

Shavano Peak

Moderator(s): Matt Whittaker, USA

13:30 - 13:45

[EFFECT OF GROWTH EQUIPMENT STABILITY AND PRECISION ON THE PULLING OF SINGLE CRYSTALS FROM THE MELT](#)

Ahmed Nouri (CYBERSTAR, FR)

13:45 - 14:00

[TOWARDS MODEL PREDICTIVE CONTROL FOR VGF GROWTH USING ARTIFICIAL NEURONAL NETWORKS](#)

Stefan Ecklebe (Technische Universität Dresden, DE)

14:00 - 14:15

[MODELING OF DISLOCATION DYNAMICS IN VGF GAAS CRYSTAL](#)

GROWTH

Vladimir Artemyev (STR Group, Inc. – Soft-Impact, Ltd., RU)

14:15 - 14:30

NUMERICAL SIMULATION OF THE FLOW, HEAT AND MASS TRANSPORTS OF APCVD REACTOR TO OBTAIN THE ULTRA-HIGH FLATTEN SILICON EPITAXY ON 12-INCH DIAMETER SILICON

Chieh Hu (Department of Mechanical Engineering, National Central University, TW)

14:30 - 14:45

COMPUTER MODELING OF HMCZ SI GROWTH

Vladimir Kalaev (STR Group, Inc. – Soft-Impact, Ltd., RU)

14:45 - 15:00

APPLICATION OF MACHINE LEARNING TO MOCVD PROCESS

Gaurab Samanta (Veeco Instruments, NJ/USA)

13:30 - 15:00

Nonlinear Optical and Laser Host Materials II

Monday, July 29, 2019

Crestone I, II

Moderator(s): Shekhar Guha, USA; Yushi Kaneda, JP

13:30 - 14:00

(Invited) EFFICIENT CONTINUOUS-WAVE NONLINEAR FREQUENCY CONVERSION TOWARD DEEP-ULTRAVIOLET

Yushi Kaneda (Oxide Corp., JP)

14:00 - 14:15

[HVPE OF ENGINEERED GRATING STRUCTURES IN OP-GAAS AND OP-GAP](#)

Peter Schunemann (BAE Systems, NH/USA)

14:15 - 14:30

[THICK HVPE GROWTH OF ZNSE ON GAAS SUBSTRATES AND OP-GAAS TEMPLATES FOR MLWIR FREQUENCY CONVERSION](#)

Shivashankar Vangala (Sensors Directorate, Air Force Research Laboratory, OH/USA)

14:30 - 14:45

[LARGE DIAMETER LABGEO₅ SINGLE CRYSTAL GROWTH FOR QPM DEVICE WITH LONG INTERACTION LENGTH](#)

Mitsuyoshi Sakairi (OXIDE Corporation, JP)

14:45 - 15:00

[VAPOR TRANSPORT GROWTH OF ZINC SELENIDE AND ZINC SULPHIDE SINGLE CRYSTALS](#)

Peter Schunemann (BAE Systems, NH/USA)

13:30 - 15:00

Symposium on Epitaxy of Complex Oxides: Freestanding Crystalline Oxide Membranes

Monday, July 29, 2019

Grays Peak II, III

Moderator(s): Steven May, USA

13:30 - 14:00

[\(Invited\) FREESTANDING CRYSTALLINE OXIDE MEMBRANES AND](#)

HETEROSTRUCTURES

Harold Hwang (Stanford University, CA/USA)

14:00 - 14:30

(Invited) FREESTANDING, SELF-FORMED LAALO₃/SRTIO₃ MICRO-MEMBRANES

Fabio Miletto Granozio (CNR-SPIN, IT)

14:30 - 15:00

(Invited) FREESTANDING CRYSTALLINE MONOLAYERS OF OXIDE PEROVSKITES

Yuefeng Nie (Nanjing University, CN)

13:30 - 15:00

**Symposium on Ferroelectric Crystals and Textured Ceramics:
Characterization of Ferroelectric Crystals
Monday, July 29, 2019
Grays Peak I**

Moderator(s): Richard Meyer, USA; Christo Gugushev, DE

13:30 - 14:00

(Invited) GROWTH AND CHARACTERIZATION OF LARGE-LATTICE-PARAMETER PEROVSKITE SUBSTRATE SINGLE CRYSTALS FOR FERROELECTRIC FILMS AND DEVICES

Christo Gugushev (Leibniz Institute for Crystal Growth, DE)

14:00 - 14:30

(Invited) PROCESSING-ELECTROMECHANICAL PROPERTY RELATIONSHIPS IN TEXTURED PMNT

Richard Meyer (Applied Research Lab, Pennsylvania State University, USA)

14:30 – 15:00

[\(Invited\) EXPLORING FERROELECTRIC DOMAIN ENGINEERING THROUGH CERAMICS TEXTURING, FOR UNDERWATER ACOUSTICS APPLICATIONS](#)

Alain Moriana (Institute for Superconducting and Electronic Materials, NSW/AU)

13:30 - 15:00

Symposium on 2D Materials: Beyond Graphene and TMDs

Monday, July 29, 2019

Crestone III, IV

Moderator(s): Kurt Gaskill, USA; Kevin Daniels, USA

13:30 - 13:45

[INTERACTIONS OF TMGA AND NH₃ WITH DEFECTS IN GRAPHENE: TOWARDS A MECHANISTIC UNDERSTANDING OF 2D GAN_x FORMATION](#)

Anushka Bansal (Penn State University, PA/USA)

13:45 - 14:00

[EPITAXIAL GROWTH OF LAYERED \$\beta\$ -IN₂SE₃ THIN FILMS VIA METALORGANIC CHEMICAL VAPOR DEPOSITION](#)

Xiaotian Zhang (The Pennsylvania State University, PA/USA)

14:00 - 14:15

[MOVPE GROWTH OF GAAS ON SINGLE-CRYSTAL 2D LAYERED BI₂SE₃ SUBSTRATES](#)

Andrew Norman (National Renewable Energy Laboratory, CO/USA)

14:15 - 14:30

[HIGH-PRESSURE GROWTH OF THE NEWLY PREDICTED QUANTUM SPIN HALL INSULATOR PT₂HGSE₃](#)

Enrico Giannini (Department of Quantum Matter Physics - University of Geneva, CH)

14:30 - 14:45

[A FAMILY OF RARE EARTH-BASED MAGNETIC TRIANGULAR LATTICE MATERIALS](#)

Shu Guo (Princeton University, NJ/USA)

14:45 - 15:00

[STRUCTURES AND STABILITY OF TWO-DIMENSIONAL MATERIALS COMPOSED OF GROUP III-V AND II-VI ELEMENTS](#)

Toru Akiyama (Mie University, JP)

13:30 - 15:00

Thin Film Growth, Epitaxy, and Superlattices: Nitride and Oxide Thin Films

Monday, July 29, 2019

Torreys Peak II-IV

Moderator(s): Luke Mawst, USA; Roberto Fornari, IT

13:30 - 14:00

[\(Invited\) CHARACTERIZATION OF INTRINSIC COMPOSITIONAL DISORDER IN NITRIDE ALLOYS BY SCANNING TUNNELING ELECTROLUMINESCENCE SPECTROSCOPY](#)

Wiebke Hahn (Laboratoire de Physique de la Matière Condensée, Ecole Polytechnique, CNRS, FR)

14:00 - 14:15

[GROWTH OF LEAD TELLURIDE FILMS BY METAL ORGANIC CHEMICAL VAPOR DEPOSITION](#)

Gary Tompa (Structured Materials Industries, Inc., NJ/USA)

14:15 - 14:30

[IMPROVED CRYSTALLINITY OF ZNO FILM FORMED ON FTO SUBSTRATE WITH INSERTING MULTI-BUFFER FILMS](#)

Xinwei Zhao (Department of Physics, Tokyo University of Science, JP)

14:30 - 14:45

[ZN-IV-N₂ SEMICONDUCTORS FOR GREEN EMISSION: RECENT PROGRESS IN MATERIAL SYNTHESIS](#)

Brooks Tellekamp (National Renewable Energy Laboratory, CO/USA)

14:45 - 15:00

[PROPERTIES OF GALLIUM OXIDE THIN FILMS ON C-PLANE SAPPHIRE GROWN BY REAR-FLOW-CONTROLLED MIST CHEMICAL VAPOR DEPOSITION](#)

SIYOUNG Bae (Korea Ceramic Engineering and Technology, KR)

15:00 -15:30

BREAK

15:30 - 17:45

Symposium on 2D Materials: Graphene and Graphene-Related Processes

Monday, July 29, 2019

Crestone III, IV

Moderator(s): Kevin Daniels, USA; Kurt Gaskill, USA

15:30 - 16:00

[\(Invited\) FUNDAMENTAL EXPERIMENTAL INVESTIGATIONS OF CALCIUM AND MAGNESIUM INTERCALATED GRAPHENE ON SILICON CARBIDE](#)

Jimmy Kotsakidis (Monash University, Department of Physics and Astronomy, AU)

16:00 - 16:30

[\(Invited\) STRONG CORRELATION ENFORCED BY DOPING INTERCALATION IN EPITAXIAL GRAPHENE ON SIC\(0001\)](#)

U Starke (Max-Planck-Institut für Festkörperforschung, DE)

16:30 - 16:45

[MULTI-WAFER BATCH SYNTHESIS OF GRAPHENE ON CU FILMS BY QUASI-STATIC FLOW CHEMICAL VAPOR DEPOSITION](#)

Benjamin Huet (The Pennsylvania State University, PA/USA)

16:45 - 17:00

[LOW-TEMPERATURE DIRECT GROWTH OF GRAPHENE ON R-PLANE SAPPHIRE USING CU VAPOR CATALYST BY CVD](#)

Yuki Ueda (Meijo University, JP)

17:00 - 17:15

[LIQUID-PHASE GROWTH OF FEW-LAYERED GRAPHENE ON SAPPHIRE SUBSTRATES USING GA MELTS](#)

Takahiro Maruyama (Meijo University, JP)

17:15 - 17:30

[EPITAXIAL CU FILMS: AN IDEAL PLATFORM FOR THE GRAPHENE GROWTH, TRANSFER AND DEVICE FABRICATION](#)

Benjamin Huet (The Pennsylvania State University, PA/USA)

17:30 - 17:45

[GROWTH OF INDIUM SELENIDE COMPOUND SEMICONDUCTOR FOR OPTOELECTRONIC APPLICATIONS](#)

Tao Wang (Northwestern Polytechnical University, CN)

15:30 - 17:30

**Bulk Crystal Growth: III-V Wide Bandgap Nitride Semiconductors
Monday, July 29, 2019
Shavano Peak**

Moderator(s): Rafael Dalmau, USA; Michal Bockowski, PL

15:30 - 16:00

[\(Invited\) CRYSTALLIZATION OF GAN BY HVPE METHOD WITH CONTROLLED LATERAL GROWTH](#)

Tomasz Sochacki (Institute of High Pressure Physics PAS, PL)

16:00 - 16:15

[THICK GAN CRYSTALS OF HIGH PURITY GROWN WITH AN INCREASED RATE BY AMMONOBASE METHOD](#)

Mikolaj Amilusik (Institute of High Pressure Physics PAS, PL)

16:15 - 16:30

[SUPPRESSION OF STEP BUNCHING IN GAN CRYSTALS DURING THE NA-FLUX METHOD AT LOW SUPERSATURATION](#)

Kiyoto Endo (Grad. Sch. of Eng., Osaka Univ., JP)

16:30 - 16:45

TEMPERATURE DEPENDENCE OF NITROGEN DISSOLUTION ON SODIUM FLUX GROWTH

Ricksen Tandryo (, JP)

16:45 - 17:00

DETAILED STUDY OF HVPE-GAN DOPED WITH SILICON

Mikolaj Amilusik (Institute of High Pressure Physics PAS, PL)

17:00 - 17:15

HVPE-GAN DOPED WITH CARBON AND/OR MANGANESE

Tomasz Sochacki (Institute of High Pressure Physics PAS, PL)

17:15 - 17:30

GROWTH OF GAN SINGLE CRYSTALS WITH HIGH TRANSPARENCY LI-ADDED NA-FLUX METHOD

Tatsuhiko Nakajima (Osaka University, JP)

15:30 - 17:30

Detector Materials: Numerical Simulation and Semiconductors

Monday, July 29, 2019

Red Cloud Peak

Moderator(s): Jeffrey Derby, USA; Joshua Tower, USA

15:30 - 15:45

MODEL-BASED CONTROL FOR BRIDGMAN GROWTH OF SCINTILLATOR CRYSTALS

Swanand Pawar (University of Minnesota, MN/USA)

15:45 - 16:00

[GROWTH AND PERFORMANCE OF THALLIUM MERCURY IODIDE CRYSTALS FOR GAMMA-RAY DETECTION](#)

Narsingh Singh (University of Maryland, Baltimore County, USA)

16:00 - 16:15

[REQUIREMENTS, GROWTH AND EVALUATION OF GAAS CRYOGEN SCINTILLATOR CRYSTALS](#)

Christiane Frank-Rotsch (Leibniz Institute for Crystal Growth, DE)

16:15 - 16:30

[GROWTH OF HEAVILY-DOPED GERMANIUM SINGLE CRYSTALS FOR MID-INFRARED APPLICATIONS](#)

R Radhakrishnan Sumathi (Leibniz Institute for Crystal Growth, DE)

16:30 - 16:45

[EVALUATION OF AN INVERTED VERTICAL GRADIENT FREEZE METHOD FOR CADMIUM ZINC TELLURIDE](#)

John Roerig (University of Minnesota, MN/USA)

16:45 - 17:00

[NUMERICAL INVESTIGATION OF CDZNTe GROWTH BY THE BORON OXIDE ENCAPSULATED VERTICAL BRIDGMAN METHOD](#)

Carmen Stelian (Université Grenoble Alpes, CNRS, FR)

17:00 - 17:15

[IMPLEMENTATION OF ACCELERATED CRUCIBLE ROTATION TECHNIQUE \(ACRT\) TO ACHIEVE IMPROVED GROWTH RATE AND DETECTOR PERFORMANCE OF CADMIUM ZINC TELLURIDE \(CDZN](#)

Saketh Kakkireni (Washington State University., WA/USA)

17:15 - 17:30

CDZnTe SINGLE-CRYSTAL INGOTS GROWTH BY PRESSURE CONTROLLED BRIDGMAN METHOD

Fan Yang (Northwestern Polytechnical University, CN)

15:30 - 17:30

Epitaxy of III-V Thin Films and Superlattices

Monday, July 29, 2019

Torreys Peak II-IV

Moderator(s): Hitoshi Habuka, JP; Phil Ahrenkiel, USA

15:30 - 16:00

(Invited) QUANTUM CASCADE LASER ACTIVE REGIONS GROWN ON LATTICE-MISMATCHED SUBSTRATES BY OMVPE

Luke Mawst (Department of Electrical and Computer Engineering, University of Wisconsin-Madison, WI/USA)

16:00 - 16:15

AB INITIO STUDY FOR ADSORPTION AND DESORPTION BEHAVIOR OF WETTING LAYER SURFACE OF INAS GROWN ON GAAS(001) SUBSTRATE

Kazuhiro Yonemoto (Mie university, JP)

16:15 - 16:30

LAYER THICKNESS DEPENDENT INTERFACIAL GRADING ANALYSIS FOR STRAINED III-V SUPERLATTICES BY ATOM PROBE TOMOGRAPHY

Ayushi Rajeev (University of Wisconsin Madison, WI/USA)

16:30 - 16:45

[RECENT PROGRESS OF HIGH TEMPERATURE VAPOR PHASE EPITAXY FOR THE GROWTH OF GAN LAYERS](#)

Tom Schneider (TU Bergakademie Freiberg, Institute of Nonferrous-Metallurgy and Purest Materials, DE)

16:45 - 17:00

[IMPROVEMENT OF LUMINESCENCE PROPERTIES OF N-GAN USING TEGA PRECURSOR](#)

Tomáš Hubáček (Institute of Physics, CAS, CZ)

17:00 - 17:15

[MOCVD GROWTH OF ALGAN BACK-ILLUMINATED SEPARATE-ABSORPTION AND MULTIPLICATION ULTRAVIOLET AVALANCHE PHOTODIODES](#)

Russell Dupuis (Georgia Institute of Technology, GA/USA)

17:15 - 17:30

[HETEROEPITAXIAL GROWTH BETWEEN GAN THIN FILM AND A FLEXIBLE SUBSTRATE](#)

Wei Cih Yang (National Chiao Tung University, TW)

15:30 - 17:30

Nonlinear Optical and Laser Host Materials III

Monday, July 29, 2019

Crestone I, II

Moderator(s): Kevin Stevens, USA; Shekhar Guha, USA

15:30 - 16:00

(Invited) LINEAR AND NONLINEAR OPTICAL TECHNIQUES FOR DETERMINATION OF CRYSTAL PROPERTIES

Shekhar Guha (Air Force Research Laboratory, OH/USA)

16:00 - 16:15

TEMPERATURE DIFFERENCE SOLUTION GROWTH OF GASE CRYSTAL BY USING IN FLUX AND SELF-SEEDING METHOD
TEMPERATURE DIFFERENCE SOLUTION GROWTH OF GASE CRYSTAL BY USING IN FLUX AND SELF-SEEDING METHOD

Yohei Sato (Tohoku University, JP)

16:15 - 16:30

IN-SITU SYNTHESIS AND HGF GROWTH OF $BAGa_4S_7$, $BAGa_4SE_7$, AND $BAGa_2GESE_6$

Peter Schunemann (BAE Systems, NH/USA)

16:30 - 16:45

COMPARISON OF $CDSIP_2$ TO $ZNGEP_2$ FOR 2-MICRON PUMPED OPOS

Kevin Zawilski (BAE Systems, NH/USA)

16:45 - 17:00

MEASUREMENT OF D-COEFFICIENTS OF CRYSTALS USING NON-PHASE-MATCHED SECOND HARMONIC GENERATION OF MID-WAVE INFRARED RADIATION

Shekhar Guha (Air Force Research Laboratory, OH/USA)

17:00 - 17:30

(Invited) PROGRESS IN GROWTH OF LARGE LBO CRYSTALS FOR

NON-LINEAR OPTICAL APPLICATIONS

Dan Perlov (IPG Photonics, MA/USA)

15:30 - 17:30

Symposium on Epitaxy of Complex Oxides: Complex Oxides from Metalorganic Precursors

Monday, July 29, 2019

Grays Peak II, III

Moderator(s): Matthew Brahlek,

15:30 - 16:00

(Invited) DEFECT-FREE SYNTHESIS OF QUANTUM HETEROSTRUCTURES VIA METAL-ORGANIC PULSED LASER DEPOSITION

Chang-Beom Eom (University of Wisconsin-Madison, WI/USA)

16:00 - 16:30

(Invited) CONTROLLING THE STOICHIOMETRY IN QUATERNARY COMPLEX OXIDE THIN FILMS BY HYBRID MOLECULAR BEAM EPITAXY

Roman Engel-Herbert (Penn State University, USA)

16:30 - 17:00

(Invited) EPITAXIAL GROWTH OF COMPLEX OXIDE FILMS WITH DESIRED PROPERTIES BY A POLYMER-ASSISTED DEPOSITION

Q X Jia (Univ. at Buffalo, SUNY, Department of Materials Design and Innovation, NY/USA)

17:00 - 17:15

GROWTH OF LINBO₃ FILMS FOR ELECTRO-OPTIC DEVICES BY

CHEMICAL VAPOR DEPOSITION

Gary Tompa (Structured Materials Industries, Inc., NJ/USA)

17:15 - 17:30

ACTIVATING CATION DIFFUSION ACROSS THE INTERFACE FOR MATERIALS DISCOVERY

Yingge Du (Pacific Northwest National Laboratory, WA/USA)

15:30 - 17:30

**Symposium on Ferroelectric Crystals and Textured Ceramics: Doped Relaxor-PT Ferroelectric Crystals
Grays Peak I**

Moderator(s): Qiang Li, ; Ho Nyung Lee, USA

15:30 - 16:00

(Invited) GEN III MN-MODIFIED PMN-PZT SINGLE CRYSTALS FOR HIGH POWER/HIGH FREQUENCY/COMPOSITE APPLICATIONS

Ho-Yong Lee (Ceracomp Co., Ltd., KR)

16:00 - 16:30

(Invited) EFFECT OF MANGANESE DOPING ON MICROSTRUCTURE AND FATIGUE PROPERTY OF PIN-PMN-PT SINGLE CRYSTAL

Qiang Li (Department of Chemistry, Tsinghua University, CN)

16:30 - 17:00

(Invited) THE GROWTH AND PIEZOELECTRIC PERFORMANCE OF RELAXOR-BASED FERROELECTRIC PIN-PMN-PT AND MN DOPED PIN-PMN-PT SINGLE CRYSTALS

Guisheng Xu (Shanghai Institute of Ceramics, Chinese Academy of Sciences,

CN)

17:00 - 17:15
LATE NEWS

17:15 - 17:30
LATE NEWS

MONDAY, JULY 29, 2019

Poster Session

17:30 - 19:00
Poster Session
Monday, July 29, 2019
Columbine Ballroom (Longs and Quandary Peak)

Symposium on 2D Materials / 2D Materials and Devices

MP1.1
[PBI₂ SINGLE CRYSTAL GROWTH AND ITS OPTICAL PROPERTY STUDY](#)

Der Yuh Lin (National Changhua University of Education, TW)

MP1.2
[PRECIPITATION OF MULTILAYER GRAPHENE DIRECTLY ON GALLIUM NITRIDE TEMPLATE USING W CAPPING LAYER](#)

Jumpei Yamada (Meijo University, JP)

MP1.3
[TERAHERTZ GENERATION UTILIZING HOT ELECTRONS INJECTION ACROSS GRAPHENE PLANES](#)

BYOUNG DON Kong (Pohang University of Science and Technology, KR)

Industrial Crystal Growth and Technology

MP2.1

[ATTAINMENT OF DESIRED MORPHOLOGY AND CRYSTAL SIZE DISTRIBUTION OF ALPHA LACTOSE MONOHYDRATE \(\$\alpha\$ -LM\) THROUGH VARIOUS CRYSTALLIZATION METHODOLOGIES](#)

Srinivasan Karuppanagounder (Bharathiar University, IN)

MP2.2

[GROWTH KINETICS OF THE METASTABLE POLYMORPH OF L-HISTIDINE IN AQUEOUS SOLUTION](#)

Lek Wantha (School of Chemical Engineering, Suranaree University of Technology, TH)

MP2.3

[TUNING THE SOLUTION-MEDIATED CONCOMITANT PHASE TRANSFORMATION OUTCOME OF THE PIROXICAM MONOHYDRATE BY TWO HYDROXYL-CONTAINING ADDITIVES: HYDROXYPROPYL CELLULOSE AND H₂O](#)

Lei Wang (Shandong University, CN)

III-V Wide Bandgap Nitride Semiconductors and Devices

MP3.1

[EFFECT OF IN AD LAYER ON MBE GROWTH OF INN BY DERI METHOD](#)

Naoki Goto (Ritsumeikan university, JP)

MP3.2

SINGLE-CRYSTALLINE III-N THIN FILMS FOR FLEXIBLE
PIEZOELECTRIC GENERATORS AND PULSE SENSORS

Jae-Hyun Ryou (University of Houston, USA)

MP3.3

UNINTENTIONALLY INCORPORATED HYDROGEN AS PROBABLE
LUMINESCENCE KILLER IN INGAN/GAN QWS

Alice Hospodková (Institute of Physics, CAS, CZ)

MP3.4

FIRST-PRINCIPLES CALCULATION OF ABSOLUTE SURFACE
ENERGIES OF GAN DURING OXIDE VAPOR PHASE EPITAXY
GROWTH

Takahiro Kawamura (Mie University, JP)

MP3.5

IMPLANTATION OF BERYLLIUM INTO THIN UNINTENTIONALLY
DOPED LAYERS OF GALLIUM NITRIDE CRYSTALLIZED BY
HALIDE VAPOR PHASE EPITAXY

Mikolaj Amilusik (Institute of High Pressure Physics PAS, PL)

MP3.6

LUMINESCENCE RED SHIFT OF INGAN/GAN HETEROSTRUCTURES
BY ENLARGEMENT OF V-PITS

Tomáš Vaněk (Institute of Physics, CAS, CZ)

MP3.7

COMPUTER MODELING OF BULK GAN CRYSTAL GROWTH FROM
NA-GA SOLUTION

Vladimir Kalaev (STR Group, Inc. – Soft-Impact, Ltd., RU)

MP3.8

[STUDIES ON ALGAN PHOTODIODES BASED ON DIFFERENT ALN TEMPLATES](#)

Dunjun Chen (Nanjing University, CN)

MP3.9

[IMPROVING OPTICAL AND ELECTRICAL PROPERTIES OF GAN EPITAXIAL WAFERS AND ENHANCING LUMINESCENT PROPERTIES OF GAN-BASED LIGHT-EMITTING-DIODE WITH EXCIMER LASER IRRADIATION](#)

Yijian Jiang (Beijing Institute of Petrochemical Technology, CN)

MP3.10

[MOCVD PECULIARITIES FOR INGAN/GAN HETEROSTRUCTURES](#)

Oleg Rabinovich (NUST MISIS, RU)

MP3.11

[LED DEGRADATION CONTROL METHOD](#)

Oleg Rabinovich (NUST MISIS, RU)

Nonlinear Optical and Laser Host Materials

MP4.1

[GROWTH AND NONLINEAR OPTICAL PROPERTIES OF LANGASITE CRYSTALS](#)

Haohai Yu (Shandong University, CN)

MP4.2

EFFECT OF L-ARGININE ADDITIVE ON THE GROWTH AND PHYSICAL PROPERTIES OF POTASSIUM DIHYDROGEN PHOSPHATE SINGLE CRYSTALS

Igor Prytula (Institute for Single Crystals of NASU, UA)

MP4.3

METAL ORGANIC POTASSIUM L-ASCORBATE MONOHYDRATE A NEW NONLINEAR OPTICAL MATERIAL

Dhanpal Bairwa (Indian Institute of Science, Bangalore, IN)

MP4.4

POLARIZATION REVERSAL OF HYDROTHERMAL GROWN KTIPOPO₄ AND RB⁺-DOPED KTIPOPO₄ CRYSTALS AT ROOM TEMPERATURE

Li Yang (China Nonferrous Metal (Guilin) Geology and Mining Co., Ltd., CN)

MP4.5

TETRAPHENYLPHOSPHONIUM BROMIDE SINGLE-CRYSTALLINE MICROFIBER FOR MULTIPLE-COLOR STIMULATED RAMAN SCATTERING

YAN Ren (INSTITUTE OF CRYSTAL MATERIALS, CN)

MP4.6

CRYSTAL GROWTH AND OPTICAL PROPERTIES OF Y_{1.5}HO_{1.5}AL₅O₁₂ COMPOUNDS

Brahim Rekik (Laboratory LASICOM Faculty of Science University saad Dahleb Blida 1, DZ)

MP4.7

GROWTH OF MOLYBDENUM AND INDIUM CO-DOPED
LINBO₃ CRYSTALS BY BRIDGMAN METHOD

Tian Tian (Shanghai Institute of Technology, CN)

MP4.8

IMPROVEMENT OF UPCONVERSION PROCESS VIA PLASMONIC
ENHANCED NANOMETER AU FILM ON TM³⁺/YB³⁺/LITHIUM
NIOBITE SINGLE CRYSTAL

Zhihua Liu (Sun Yat-sen University, CN)

MP4.9

EFFECT OF XYLENOL ORANGE ON THE CRYSTALLINE
PERFECTION, OPTICAL AND ELECTRICAL BEHAVIOR OF
UNIDIRECTIONALLY GROWN IMIDAZOLIUM L-TARTRATE SINGLE
CRYSTAL

S Chinnasami (SSN College of Engineering, IN)

MP4.10

STUDIES ON GROWTH ASPECTS AND CHARACTERIZATION OF A
THIRD ORDER NONLINEAR OPTICAL SINGLE CRYSTAL: 1,4 :
OXAZINIUM NITRATE (ON)

H Arul (Kumaraguru College of Technology (Autonomous), IN)

MP4.11

INVESTIGATIONS ON SEMI-ORGANIC SINGLE CRYSTAL BIS(4-
METHOXYBENZYLAMMONIUM) TETRACHLORIDOZINCATE
(4MBZ) FOR NONLINEAR OPTICAL (NLO) APPLICATIONS

Pichan Karuppasamy (SSN College of Engineering, IN)

MP4.12

GROWTH AND CHARACTERIZATION AN ORGANIC QUINOLINE 4-NITROPHENOL (Q4N): A NOVEL SINGLE CRYSTAL FOR NONLINEAR OPTICAL APPLICATIONS

Pichan Karuppasamy (SSN College of Engineering, IN)

MP4.13

EFFECT OF KDP MIXING ON OPTICAL PROPERTIES OF AKDP NLO MIXED CRYSTAL FOR ELECTRO OPTIC MODULATORS

G Iyappan (SSN College of Engineering, IN)

MP4.14

INVESTIGATION ON THE SUPERSATURATION DEPENDENT GROWTH OF METHYL-4-HYDROXY BENZOATE (P-MHB) SINGLE CRYSTALS USING SEEDING TECHNIQUE

Srinivasan Karuppanagounder (Bharathiar University, IN)

MP4.15

STRUCTURAL, THERMAL AND NONLINEAR OPTICAL STUDIES ON ORGANIC IMIDAZOLIUM 4-HYDROXYBENZOATE (IHB) CRYSTAL

H Arul (Kumaraguru College of Technology (Autonomous), IN)

MP4.16

GROWTH AND CHARACTERIZATION OF 4-AMINOPYRIDINIUM 4-NITROPHENOLATE 4-NITROPHENOL (4AP4N) CRYSTAL FOR NONLINEAR OPTICAL APPLICATIONS

Tamilsevan Kamalesh (SSN College of Engineering, IN)

MP4.17

STRUCTURES AND LUMINESCENT PROPERTIES OF Y AT.% EU³⁺-DOPED Y(TA_{1-x}P_x)O₄ PHOSPHOR POWDERS

Degao Zhong (College of Physics, Qingdao University, CN)

MP4.18

[DESIGN, SYNTHESSES AND CRYSTAL GROWTHS OF NEW COMPOUNDS IN KBBF FAMILY](#)

Hongwei Yu (School of Material Science, Tianjin University of Technology, CN)

MP4.19

[PROGRESS IN STUDY OF POTASSIUM TANTALATE NIOBATE SERIES CRYSTALS AS QUADRATIC ELECTRO-OPTIC MATERIAL](#)

Xuping Wang (Qilu University of Technology, SAS, CN)

Nanocrystals, Quantum Dots, and Nanowires

MP5.1

[FORMATION OF GAN NANOWIRES IN MOLECULAR BEAM EPITAXY OBSERVED SIMULTANEOUSLY BY LINE-OF-SIGHT QUADRUPOLE MASS SPECTROMETRY, REFLECTION HIGH ENERGY ELECTRON DIFFRACTION AND OPTICAL REFLECTOMETRY: WHAT CAN WE LEARN USING THESE GROWTH MONITORING TOOLS?](#)

Zbigniew Zytkiewicz (Institute of Physics Polish Academy of Sciences, PL)

MP5.2

[FORMATION PROCESS AND EFFECT OF NANO-OXIDES IN STEEL](#)

Zidong Wang (University of Science & Technology, CN)

MP5.3

[THERMODYNAMIC AND KINETIC CONDITIONS FOR THE](#)

FORMATION OF NANO-OXIDES IN MOLTEN STEEL

Zidong Wang (University of Science & Technology, CN)

MP5.4

USE OF GOLD NANOPARTICLES TO CONTROL SHAPE OF LITHIUM PERCHLORATE CRYSTALS IN CHITOSAN MEMBRANES

Radha Perumal Ramasamy (Anna University, IN)

MP5.5

HOMOGENEITY REGION WIDTH AND CRYSTAL STRUCTURE OF PALLADIUM (II) OXIDE NANOCRYSTALLINE FILMS

Alexander Samoylov (Voronezh State University, RU)

MP5.6

WHISKER PARTICLE GROWTH WITH CR-SIO AND FE-SIO SYSTEMS

Rikuto Tsuda (Tohoku Gakuin University, Miyagi, JP)

MP5.7

ON THE MEDIUM SIZED SILICON NANOPARTICLES: EDIP VS. TERSOFF POTENTIAL

Lynda Amirouche (University of Sciences and Technologie Houari Boumedienne Algeria, DZ)

MP5.8

DETERMINATION OF Zn^{2+} SUPERSATURATION IN THE GROWTH SOLUTION FOR THE SYNTHESIS OF ZNO NANORODS

Nikola Basinova (Institute of Photonics and Electronics of the Czech Academy of Sciences, CZ)

MP5.9

[ON THE EFFECT OF INTERATOMIC POTENTIAL ON THE ENERGETIC AND STRUCTURAL BEHAVIORS OF SOME SILICON CLUSTERS: MOLECULAR DYNAMICS SIMULATIONS](#)

Lynda Amirouche (University of Sciences and Technologie Houari Boumedienne Algeria, DZ)

MP5.10

[INFLUENCE OF THE INTERATOMIC POTENTIAL TYPE ON THE STRUCTURAL PHASE TRANSITIONS AND ENERGETIC PROPERTIES OF LARGE SILICON NANOPARTICLES: MOLECULAR DYNAMICS SIMULATIONS](#)

Lynda Amirouche (University of Sciences and Technologie Houari Boumedienne Algeria, DZ)

MP5.11

[SOLVOTHERMAL SYNTHESIS AND CHARACTERISTICS OF KTA0.63NB0.37O3 AND CU/FE DOPED KTA0.63NB0.37O3 NANOPARTICLES](#)

Yuguo Yang (Qilu University of Technology, SAS, CN)

Modeling of Crystal Growth Processes

MP6.1

[TRANSIENT GLOBAL MODELING FOR THE PULLING PROCESS OF CZOCHRALSKI SILICON CRYSTAL GROWTH. I. PRINCIPLES, FORMULATION AND IMPLEMENTATION OF THE MODEL](#)

Xin Liu (Research Institute for Applied Mechanics, Kyushu University, JP)

MP6.2

[NUMERICAL STUDY OF THE HEAT AND OXYGEN TRANSPORT DURING A CZOCHRALSKI SILICON GROWTH USING DIFFERENT](#)

CRYSTAL-CRUCIBLE ROTATION CONDITIONS AND CUSP-SHAPED
MAGNETIC FIELDS

Thi Hoai Thu Nguyen (National Central University, TW)

MP6.3

COMPUTATIONAL STUDY OF HEAT TRANSFER, FLUID FLOW OF
MELT AND GAS ATMOSPHERE DURING THE SEEDING PROCESS
OF SAPPHIRE KYROPOULOS CRYSTAL GROWTH

SAMIR Zermout (Mouloud Mammeri University of Tizi-Ouzou, DZ)

MP6.4

TOWARDS CONTROLLING GROWTH INTERFACE SHAPE AND
STABLE THERMAL FIELD IN THM GROWTH SYSTEM OF CDZNTE
CRYSTAL

Bangzhao Hong (Tsinghua University, CN)

MP6.5

EFFECTS OF GROWTH RATE ON MELT/CRYSTAL INTERFACE
SHAPE AND TEMPERATURE DISTRIBUTION IN GROWING
CRYSTAL

Shin-ichi Nishizawa (Research Institute for Applied Mechanics, Kyushu
University, JP)

MP6.6

PLATINUM DISSOLUTION MODEL IN PEM FUEL CELL

Shinobu Sekine (Toyota Motor Corporation, JP)

MP6.7

INFLUENCE OF ADDITIONAL INSULATION BLOCK ON MULTI-
CRYSTALLINE SILICON INGOT GROWTH PROCESS IN FURNACE

WITH ADDITIONAL BLOCK DS FURNACE FOR PV APPLICATIONS

Nagarajan S G (SSN College of Engineering, IN)

MP6.8

MODELING OF VARIOUS CRUCIBLE AND SUPPORT SYSTEM
DESIGNS FOR VERTICAL GRADIENT FREEZE GROWTH OF
CDZNTe

Ozden Balbasi (Middle East Technical University, TR)

MP6.9

REDUCTION OF THERMAL STRESS AND DISLOCATION DENSITY
IN MC-SI INGOT USING HEATER MODIFIED DIRECTIONAL
SOLIDIFICATION FURNACE

Sundaramahalingam Sanmugavel (SSN College of Engineering, IN)

MP6.10

INFLUENCE OF ADDITIONAL SIZE INSULATION BLOCK ON MELT-
CRYSTAL INTERFACE SHAPE IN DIRECTIONAL SOLIDIFICATION
SYSTEM: NUMERICAL INVESTIGATION

G Anbu (SSN College of Engineering, IN)

MP6.11

INFLUENCE OF ANNEALING TEMPERATURE DURING THE MC-SI
SOLAR CELL FABRICATION

Gurusamy Aravindan (SSN College of Engineering, IN)

MP6.12

EFFECT OF SCHMIDT NUMBER ON MODELING OF MC- SILICON
GROWTH PROCESS FOR PV APPLICATIONS

Srinivasan Manickam (SSN Research Centre, IN)

MP6.13

GLOBAL MODELING ON MODIFIED CRUCIBLE SHAPE IN DIRECTIONAL SOLIDIFICATION PROCESS TO GROW THE HIGH QUALITY MC-SI CRYSTAL

M Vishnuwaran (SSN College of Engineering, IN)

MP6.14

EFFECT OF HEAT EXCHANGER BLOCK THICKNESS ON GROWN MULTI-CRYSTALLINE SILICON INGOT IN DIRECTIONAL SOLIDIFICATION PROCESS

THIYAGARAJAN M (SSN College on Engineering, IN)

MP6.15

ABSORPTION COEFFICIENT OF SAPPHIRE AT TEMPERATURES UP TO 1420 C.

Aleksandar Ostrogorsky (Illinois Institute of Technology, IL/USA)

Advanced Equipment and Growth Technology

MP7.1

CONTROL OF CRYSTAL SHAPE OF ORGANIC MATERIALS BY FEMTOSECOND LASER ABLATION

Hiroshi Yoshikawa (Saitama University, JP)

Materials for Photovoltaics and Other Energy Technology

MP8.1

STUDY OF DIP CASTING FOR MULTI-CRYSTALLINE SILICON

Chung-Wen Lan (National Taiwan University, TW)

MP8.2

[SYNTHESIS, CRYSTAL CHARACTERIZATION AND PROPERTY ANALYSIS: AN INSENSITIVE HIGH ENERGETIC SALT OF DICARBOHYDRAZIDE BIS\[3-\(5-NITROIMINO-1,2,4-TRIAZOLE\)\]](#)

Dong Chen (China Academy of Engineering Physics, CN)

MP8.3

[INNOVATIVE ELECTRIC CHARGE STORAGE MECHANISM: IDEAL METALLIC SUPERCAPACITORS](#)

Shivam Kansara (Sardar Vallabhbhai National Institute of Technology, IN)

MP8.4

[MAIN DIRECTION OF PHOTOELECTRIC CONVERTERS RESEARCH IN GEORGIA](#)

Lia Trapaidze (Tbilisi State University, GE)

MP8.5

[ONE POT SYNTHESIS OF BI DOPED \$\text{Cu}_2\text{ZnSns}_4\$ NANOPARTICLES](#)

Kusum Rawat (DDU Gorakhpur University, IN)

MP8.6

[A UNIFIED MECHANISM OF ENHANCED MAGNETO-OPTIC AND MAGNETO-CALORIC EFFECTS](#)

Rukang Li (Chinese Academy of Sciences, CN)

MP8.7

[INFLUENCE OF GROWTH INTERRUPTION ON INGAP GROWN BY HYDRIDE VAPOR PHASE EPITAXY](#)

Y. Shoji (National Institute of Advanced Industrial Science and Technology, JP)

MP8.8

[NUMERICAL STUDY OF SURFACE WAVES ENHANCED SILICON REFINEMENT FOR SOLAR GRADE SILICON PRODUCTION](#)

Vadims Geža (University of Latvia, LV)

MP8.9

[EXPERIMENTS ON SURFACE WAVE EXCITATION BY ELECTROMAGNETIC FIELD](#)

Mikus Milgravis (University of Latvia, LV)

Biological and Biomimetic Materials

MP9.1

[PHASE FIELD MODELING OF BIOMINERALIZATION? MICROSTRUCTURE EVOLUTION IN MOLLUSK SHELLS AND CORAL SKELETONS](#)

László Gránásy (Wigner Research Centre for Physics, HU)

MP9.2

[USE OF GOLD CLUSTERS TO CONTROL CONDUCTIVITY OF CHITOSAN MEMBRANES](#)

Radha Perumal Ramasamy (Anna University, IN)

Surfaces and Interfaces

MP10.1

[MODELING BIMETALLIC OXIDE NANOSTRUCTURES.](#)

Olena Chernikova (Kryviy Rih National University, UA)

MP10.2

[SURFACE OXIDATION OF TI PLATES BY USING MICROWAVE PLASMA HEATING SYSTEM](#)

Junji Yamanaka (University of Yamanashi, JP)

MP10.3

[BROMINE-METHANOL ETCHING: AN EXPERIMENTAL STUDY ON THE EFFECTS OF CHEMICAL POLISHING ON SURFACE PROPERTIES OF CDZNTE CRYSTALS](#)

Mustafa Unal (Middle East Technical University, TR)

MP10.4

[IMPURITY SEGREGATION AT MISORIENTED \$\Sigma 3\{111\}\$ TILT BOUNDARIES IN HIGH-PERFORMANCE SI](#)

Y. Ohno (Tohoku University, JP)

Symposium on Ferroelectric Crystals and Textured Ceramics

MP11.1

[GROWTH AND PIEZOELECTRIC PROPERTIES OF LARGE SIZE \$Ca_3Ta\(Al_{0.5}Ga_{0.5}\)_3Si_2O_{14}\$ CRYSTALS WITH LANGASITE STRUCTURE](#)

Kainan Xiong (Shanghai Institute of Ceramics, CN)

MP11.2

[MID-INFRARED EMISSION PROPERTIES OF \$Er^{3+}/Eu^{3+}:PbF_2\$, \$Er^{3+}/Tb^{3+}:PbF_2\$ AND \$Er^{3+}/Nd^{3+}:PbF_2\$ CRYSTALS](#)

Peixiong Zhang (Jinan University, CN)

MP11.3

[GROWTH AND CONSISTENCY OF 5 INCHES CA3TAGA3SI2O14 CRYSTALS](#)

Kainan Xiong (Shanghai Institute of Ceramics, CN)

Monday, July 29, 2019
OMVPE-19 Evening Session

19:30 - 21:30

Advanced MOCVD Technology for the Future

Monday, July 29, 2019

Torreys Peak II-IV

Moderator(s): Masakazu Sugiyama, JP; Akinori Ubukata, JP

19:30 - 20:00

[\(Invited\) HIGH TEMPERATURE OMVPE FOR NEW MATERIALS GROWTH](#)

Gary Tompa (Structured Materials Industries, Inc., NJ/USA)

20:00 - 20:30

[\(Invited\) GROWTH OF HIGH PURITY GAN FOR VERTICAL ELECTRON DEVICES AND CHARACTERIZATION OF ELECTRON AND HOLE TRAPS](#)

Tetsuo Narita (Toyota Central R&D Labs. Inc, JP)

20:30 - 20:50

[FILTERED AND UNFILTERED RESTRICTIVE FLOW ORIFICES IN THE DELIVERY OF ELECTRONIC PROCESS GASES](#)

Rikard Wind (Matheson, CO/USA)

20:50 - 21:10

[CHARACTERIZING LIQUID PRECURSOR DELIVERY FOR DEPOSITION PROCESSES](#)

James Maslar (NIST, USA)

21:10 - 21:30

[THE OPTIMAL PARTITION DESIGN OF THE TRIPLE INJECTOR IN THE HORIZONTAL MOCVD REACTOR FOR THE GAN FILM GROWTH THROUGH THE NUMERICAL SIMULATION](#)

Wei-Jie Lin (National Central University, TW)

Tuesday, July 30, 2019

08:00 - 10:00

Plenary Session: IOCG Prize Talks

Tuesday, July 30, 2019

**Colorado Rockies Ballroom
(Shavano and Red Cloud Peak)**

Moderator(s): Elias Vlieg, NL

08:00 - 08:40

Frank Prize Talk: DEVELOPMENT OF NEW PEROVSKITE SUBSTRATES ENABLING STRAIN ENGINEERING OF OXIDE THIN FILMS

Darrell Schlom (Cornell University, USA) and Reinhard Uecker (Leibniz Institute for Crystal Growth, DE)

08:40 - 09:20

Laudise Prize Talk: DEVELOPMENT OF HIGH-QUALITY CRYSTALS

FOR III-V QUATERNARY OPTICAL SEMICONDUCTORS AND
SOLAR CELL SILICON AND THEIR INDUSTRIAL APPLICATIONS

Kazuo Nakajima (Tohoku University, JP)

09:20 - 10:00

Schieber Prize Talk: THE METAL FLUX AS A POWERFUL TOOL FOR
THE SOLID STATE PHYSICIST

Anton Jesche (Augsburg University, DE)

10:00 - 10:30

BREAK

10:30 - 12:00

Bulk Crystal Growth: Focus on Technology

Tuesday, July 30, 2019

Shavano Peak

Topic: Bulk Crystal Growth

Moderator(s): Christo Gugushev, DE; Jiaqiang Yan, USA

10:30 - 11:00

[\(Invited\) FLUX GROWTH IN A HORIZONTAL CONFIGURATION: AN
ANALOG TO VAPOR TRANSPORT GROWTH](#)

[Jiaqiang Yan](#) (Oak Ridge National Laboratory, TN/USA)

11:00 - 11:15

[FORCED CONVECTION BY HIGH-SPEED ROTATION IN
CZOCHELSKI GROWTH FROM HIGH-TEMPERATURE SOLUTIONS](#)

[Peter Gille](#) (LMU München, GeoDepartment, Crystallography, DE)

11:15 - 11:30

[NEW EXPERIMENTAL APPROACHES FOR RAPIDLY ESTABLISHING CRYSTAL GROWTH CONDITIONS](#)

Peter Khalifah (Stony Brook University, USA)

11:30 - 11:45

[IN-SITU DETECTABILITY OF CRYSTALLIZATION PROCESSES AND SEED SELECTION IN HIGH TEMPERATURE SOLUTIONS](#)

Andreas-Gabriel Schneider (University of Augsburg, DE)

11:45 - 12:00

[IN SITU VISUALIZATION AND DYNAMIC SUPPRESSION OF CRYSTAL GROWTH INTERFACE FLUCTUATIONS BY GROWTH INTERFACE ELECTROMOTIVE FORCE](#)

Yunzhong Zhu (Sun Yat-sen University, CN)

10:30 - 12:00

Industrial Scintillator and Detector Growth

Tuesday, July 30, 2019

Red Cloud Peak

Topic: Industrial Crystal Growth Technology and Equipment

Moderator(s): Matt Whittaker, USA; Mariya Zhuravleva, USA

10:30 - 11:00

[\(Invited\) DEVELOPMENT OF MASS PRODUCTION TECHNOLOGY OF CE:GD₃\(GA,AL\)₅O₁₂ SCINTILLATOR FOR RADIATION IMAGING APPLICATIONS](#)

Kei Kamada (NICHe, Tohoku University, JP)

11:00 - 11:30

[\(Invited\) DEVELOPMENT OF BULK CRYSTAL GROWTH](#)

[TECHNOLOGY FOR NOVEL FUNCTIONAL CRYSTALS AND THEIR SOCIAL IMPLEMENTATION](#)

Akira Yoshikawa (Institute for Materials Research, Tohoku University, JP)

11:30 - 12:00

[\(Invited\) COMMERCIAL-SCALE SOLUTION GROWTH OF THE ORGANIC SCINTILLATOR STILBENE](#)

Candace Lynch (Inrad Optics, Inc., USA)

10:30 - 12:00

Modeling of Crystal Growth Processes I

Tuesday, July 30, 2019

Crestone I, II

Moderator(s): Thierry Duffar, FR; Koichi Kakimoto, JP

10:30 - 11:00

[\(Invited\) ARTIFICIAL INTELLIGENCE IN CRYSTAL GROWTH](#)

Natasha Dropka (Leibniz Institute for Crystal Growth, DE)

11:00 - 11:15

[SIMULATION OF THE CREATION OF A DEFECT STRUCTURE OF DISLOCATION-FREE GERMANIUM SINGLE CRYSTALS](#)

Dmitryi Igorevich Yakymchuk (Department of Computer Science & Software Engineering, Institute of Economics & Information Technology, UA)

11:15 - 11:30

[ONSET OF ISOTROPIC AND ANISOTROPIC SHAPE CHANGES DURING CZOCHRALSKI CRYSTAL GROWTH](#)

Simon Brandon (Technion, IL)

11:30 - 11:45

[UNSTEADY NUMERICAL SIMULATION CONSIDERING EFFECT OF THERMAL STRESS AND HEAVY DOPING ON BEHAVIOR OF INTRINSIC POINT DEFECTS IN LARGE-DIAMETER SI CRYSTAL GROWING BY CZOCHRALSKI METHOD](#)

Yuji Mukaiyama (STR Japan K.K, JP)

11:45 - 12:00

[CONTROLLING NUCLEATION DURING UNSEEDED THM GROWTH OF CDZNTE CRYSTAL](#)

Song Zhang (Tsinghua University, CN)

10:30 - 12:00

**Symposium on 2D Materials: Vapor Phase Synthesis of TMDs
Tuesday, July 30, 2019
Crestone III, IV**

Moderator(s): Joan Redwing, USA; James Maslar, USA

10:30 - 11:00

[\(Invited\) EPITAXIAL GROWTH OF WAFER-SCALE TRANSITION METAL DICHALCOGENIDES BY GAS SOURCE CVD](#)

Tanushree Choudhury (The Pennsylvania State University, PA/USA)

11:00 - 11:15

[MOVPE OF 2D WS₂ AND 2D MOS₂ LAYERS FOR OPTOELECTRONIC APPLICATIONS](#)

Michael Heuken (RWTH Aachen University, DE)

11:15 - 11:30

[WAFER SCALE EPITAXIAL GROWTH OF MONOLAYER WS₂ BY GAS SOURCE CHEMICAL VAPOR DEPOSITION](#)

[Mikhail Chubarov](#) (The Pennsylvania State University, PA/USA)

11:30 - 11:45

[CHEMICAL VAPOR DEPOSITION OF SEMIMETALLIC TO SEMICONDUCTING MoTe₂](#)

[Bhakti Jariwala](#) (The Pennsylvania State University, PA/USA)

11:45 - 12:00

[GAS SOURCE CVD OF HIGHLY CRYSTALLINE GRAPHENE/TUNGSTEN DISULFIDE HETEROSTRUCTURE](#)

[Benjamin Huet](#) (The Pennsylvania State University, PA/USA)

10:30 - 12:00

**Symposium on Epitaxy of Complex Oxides: Defects
Tuesday, July 30, 2019
Grays Peak II, III**

Moderator(s): Julia Mundy, USA

10:30 - 11:00

[\(Invited\) MAKING FUNCTIONAL COMPLEX OXIDE THIN FILMS: EXPLORING THE LIMITATIONS OF CONTROL AND EMBRACING MATERIAL IMPERFECTION](#)

[Lane Martin](#) (University of California, Berkeley, CA/USA)

11:00 - 11:30

[\(Invited\) IDEALIZED OUTCOMES AND SYNTHETIC REALITIES - WORRYING ABOUT WHAT ATOMS ACTUALLY DO IN OXIDE](#)

HETEROEPITAXY

Scott Chambers (Pacific Northwest National Laboratory, WA/USA)

11:30 - 12:00

(Invited) NEW PHENOMENA ENABLED BY THE CONTROL OF OXYGEN VACANCIES IN THE DILUTE LIMIT IN OXIDE THIN FILMS AND SINGLE CRYSTALS

Anand Bhattacharya (Argonne National Laboratory, IL/USA)

10:30 - 12:00

**Symposium on Ferroelectric Crystals and Textured Ceramics: Textured Relaxor-PT Ceramics
Tuesday, July 30, 2019
Grays Peak I**

Moderator(s): Mark Fanton, USA; Gary Messing, USA

10:30 - 11:00

(Invited) FABRICATION OF HIGH QUALITY TEXTURED PIEZOELECTRIC CERAMICS FOR NEXT GENERATION TRANSDUCER APPLICATIONS BY TEMPLATED GRAIN GROWTH (TGG).

Gary Messing (Department of Materials Science & Engineering, Pennsylvania State University, USA)

11:00 - 11:30

(Invited) TEXTURE-ENGINEERED LEAD-FREE PIEZOCERAMICS: PROPERTY ENHANCEMENTS THROUGH CRYSTALLOGRAPHIC TAILORING, DOMAIN ENGINEERING AND COMPOSITE EFFECTS

Yunfei Chang (Harbin Institute of Technology, CN)

11:30 - 12:00

[\(Invited\) MANUFACTURING AND UNIFORMITY OF GRAIN TEXTURED PIEZOELECTRIC CERAMICS](#)

[Mark Fanton](#) (Penn State University, USA)

10:30 - 12:00

Thin Film Growth, Epitaxy, and Superlattices: Novel Materials and Processes

Tuesday, July 30, 2019

Torreys Peak II-IV

Moderator(s): Wiebke Hahn, ; Brooks Tellekamp, USA

10:30 - 10:45

[GROWTH AND CHARACTERIZATION OF GROUP IV SIGESN THIN FILMS USING PLASMA ENHANCED CHEMICAL VAPOR DEPOSITION ON SI \(100\) SUBSTRATES](#)

[Gary Tompa](#) (Structured Materials Industries, Inc., NJ/USA)

10:45 - 11:00

[BORON TRICHLORIDE GAS BEHAVIOUR FOR CHEMICAL VAPOUR DEPOSITION AND ETCHING AT SILICON SURFACE](#)

[Hitoshi Habuka](#) (Yokohama National University, JP)

11:00 - 11:15

[NON-EQUILIBRIUM MOCVD GROWTH WITH PLASMA ENHANCEMENT](#)

[Nathan Smaglik](#) (South Dakota School of Mines and Technology, SD/USA)

11:15 - 11:30

[THREE-DIMENSIONAL ATOMIC SCALE RECONSTRUCTION OF OCTAHEDRAL TILT EPITAXY IN FUNCTIONAL PEROVSKITE THIN FILMS](#)

Yanfu Lu (Pennsylvania State University, PA/USA)

11:30 - 11:45

[TWO-DIMENSIONAL HBN LAYER PROMOTED HETEROEPITAXY IN REACTIVELY SPUTTER-DEPOSITED \$\text{MoS}_2\(0001\)/\text{Al}_2\text{O}_3\(0001\)\$ THIN FILMS](#)

Aditya Deshpande (Dept. of Materials Science and Engineering, University of California Los Angeles, CA/USA)

11:45 - 12:00

[EPITAXIAL MULTIFERROIC SUPERLATTICES COMBINING HEXAGONAL AND CUBIC FERRITES](#)

Rachel Steinhardt (Cornell University, NY/USA)

12:00 - 13:30

LUNCH

13:30 - 15:00

Bulk Crystal Growth: Focus on Silicon

Tuesday, July 30, 2019

Shavano Peak

Moderator(s): Jochen Friedrich, DE; Tomasz Sochacki, PL

13:30 - 13:45

[EXPERIMENTAL AND THEORETICAL ANALYSIS OF THE GROWTH RIDGE GEOMETRY OF CZOCHRALSKI-GROWN SILICON CRYSTALS](#)

Jochen Friedrich (Fraunhofer IISB, DE)

13:45 - 14:00

GROWTH OF SILICON SINGLE CRYSTALS BY THE GRANULATE CRUCIBLE METHOD

Robert Menzel (Leibniz-Institut für Kristallzüchtung, DE)

14:00 - 14:15

GRAIN BOUNDARY EVOLUTIONS AND INTERACTIONS AT THE CRYSTAL/MELT INTERFACE OF SILICON DURING DIRECTIONAL SOLIDIFICATION

Lu-Chung Chuang (Institute for Materials Research, Tohoku University, JP)

14:15 - 14:30

CO CONCENTRATION IN CZ FURNACE

Yoshiji Miyamura (Research Institute for Applied Mechanics, Kyushu University, JP)

14:30 - 14:45

EFFECT OF SEED CRYSTAL ON DISLOCATION DENSITY IN SI SINGLE CRYSTAL

Satoshi Nakano (Research Institute for Applied Mechanics, Kyushu University, JP)

14:45 - 15:00

NON-STATIONARY SIMULATIONS OF HEAT TRANSFER, THERMAL STRESSES AND POINT DEFECT DISTRIBUTION DURING CZ SI SINGLE CRYSTAL GROWTH

Andrejs Sabanskis (University of Latvia, LV)

13:30 - 15:00

Detector Materials: Halide Scintillators

Tuesday, July 30, 2019

Red Cloud Peak

Moderator(s): Mariya Zhuravleva, USA; Akira Yoshikawa, JP

13:30 - 14:00

[\(Invited\) IMPACT OF \$Tl_2LiYCl_6\$ CRYSTAL STRUCTURE EVOLUTION ON CRYSTAL GROWTH](#)

Drew Onken (Lawrence Berkeley National Laboratory, CA, USA)

14:00 - 14:15

[CRYSTAL GROWTH AND SCINTILLATION PROPERTIES OF THALLIUM-BASED HALIDE SCINTILLATORS](#)

Edgar Van Loef (RMD, MA/USA)

14:15 - 14:30

[PRODUCTION OF ELPASOLITE SCINTILLATION CRYSTALS FOR DUAL-MODE RADIATION DETECTION](#)

Joshua Tower (Radiation Monitoring Devices, Inc., MA/USA)

14:30 - 14:45

[GROWTH CHALLENGES OF CESIUM HAFNIUM CHLORIDE SCINTILLATOR](#)

Cordell Delzer (University of Tennessee, TN/USA)

14:45 - 15:00

[EVALUATING MIXED-CATION \$CS_4SRI_6:EU\$ AND \$CS_4CAI_6:EU\$ SCINTILLATORS AND GROWTH OF LARGE DIAMETER \(> 1](#)

INCH) CRYSTALS

Daniel Rutstrom (University of Tennessee Knoxville, TN/USA)

13:30 - 15:00

Modeling of Crystal Growth Processes II

Tuesday, July 30, 2019

Crestone I, II

Moderator(s): Talid Sinno, USA; Toru Ujihara, JP

13:30 - 14:00

(Invited) PHASE-FIELD MODELING OF SPIRAL EUTECTIC DENDRITES

László Rátkai (Wigner Research Centre for Physics, HU)

14:00 - 14:15

MODELING OF ZNO NANOROD GROWTH IN A FLOW REACTOR

Ondrej Cernohorsky (Institute of Photonics and Electronics of the CAS, CZ)

14:15 - 14:30

SELF-ORGANISATION OF SIGE PLANAR NANOWIRES VIA ANISOTROPIC ELASTIC FIELD

Jean-Noël Aqua (Sorbonne Université, FR)

14:30 - 14:45

CRYSTAL GROWTH IN FLUID FLOW REVISITED: HOW TO ESCAPE STEP PINNING?

Dominique Maes (Vrije Universiteit Brussel, BE)

14:45 - 15:00

[EFFECT OF INTENSE CONVECTIVE FLOW ON THE DENDRITE GROWTH](#)

Liubov Toropova (Ural Federal University, RU)

13:30 - 15:00

Semiconductor Quantum Dots and Nanostructures

Tuesday, July 30, 2019

Torreys Peak II-IV

Moderator(s): George Wang, USA; Honghyuk Kim, USA

13:30 - 13:45

[INVESTIGATION OF BI INDUCED THREE-DIMENSIONAL INAS NANOSTRUCTURES ON GAAS \(110\) BY CROSS-SECTIONAL SCANNING TUNNELING MICROSCOPY.](#)

Wjatscheslav Martyanov (TU Berlin, DE)

13:45 - 14:00

[INP QUANTUM DOTS SATURABLE ABSORBERS FOR MODE LOCKING OF SOLID-STATE LASERS](#)

Andrey Krysa (National Centre for III-V Technologies, University of Sheffield, GB)

14:00 - 14:15

[HETEROEPITAXIAL QUANTUM DOTS ON PATTERNED SUBSTRATES](#)

Monika Dhankhar (Indian Institute of Technology Kanpur, IN)

14:15 - 14:45

[IN_{0.8}GA_{0.2}AS QD ACTIVE REGION \(\$\lambda \sim 1.65 \mu\text{M}\$ \) LASER DIODES GROWN BY BLOCK COPOLYMER LITHOGRAPHY AND SELECTIVE](#)

[AREA OMVPE](#)

Honghyuk Kim (University of Wisconsin-Madison, WI/USA)

14:45 – 15:00

LATE NEWS

13:30 - 15:00

Symposium on 2D Materials: Special Topics I: h-BN

Tuesday, July 30, 2019

Crestone III, IV

Moderator(s): Suzanne Mohney, USA; Cristina Giusca, GB

13:30 - 14:00

[\(Invited\) 2D EPITAXY WITH A TWIST: ACHIEVING DIFFERENT COMMENSURATE RELATIONS IN HBN/GRAPHENE HETEROSTRUCTURES BY TUNING HBN GROWTH PARAMETERS AND SUBSTRATE MORPHOLOGY](#)

D J Pennachio (Materials Department, UC Santa Barbara, CO/USA)

14:00 - 14:30

[\(Invited\) EPITAXY OF MONO-TO FEW-LAYER HBN ON TRANSITION METAL SUBSTRATES](#)

Michael Snure (Air Force Research Laboratory, OH/USA)

14:30 - 15:00

[\(Invited\) ELECTRICAL CHARACTERIZATION OF SINGLE CRYSTAL BORON CARBIDE METAL-SEMICONDUCTOR DIODES](#)

MVS Chandrashekhar (University of Southern Carolina, SC/USA)

13:30 - 15:00

Symposium on Epitaxy of Complex Oxides: Binary Oxides
Tuesday, July 30, 2019
Grays Peak II, III

Moderator(s): Scott Chambers, USA

13:30 - 14:00

[\(Invited\) PLASMA-ASSISTED MBE GROWTH OF BETA-GA₂O₃](#)

James Speck (Materials Department, UCSB, CA/USA)

14:00 - 14:30

[\(Invited\) GROWING THIN FILMS OF BERYLLIUM OXIDE AND ALLOYS](#)

Mikk Lippmaa (Institute for Solid State Physics, University of Tokyo, JP)

14:30 - 15:00

[\(Invited\) SUPERCONDUCTING TITANATE FILMS: EPITAXIAL GROWTH AND DISTINCTION OF CRYSTAL PHASES](#)

Kohei Yoshimatsu (Tohoku University, JP)

13:30 - 15:00

Symposium on Ferroelectric Crystals and Textured Ceramics:
Ferroelectric
Relaxor- PT Crystal Growth
Tuesday, July 30, 2019
Grays Peak I

Moderator(s): Jun Luo, USA; Kazuhiko Echizenya, JP

13:30 - 14:00

[\(Invited\) PMN-PT AND PIN-PMN-PT SINGLE CRYSTALS GROWN BY CONTINUOUS FEEDING GROWTH METHOD](#)

Kazuhiko Echizenya (JFE MINEAL COMPANY, LTD., JP)

14:00 - 14:30

(Invited) DEVELOPMENT OF SM-DOPED RELAXOR-PT CRYSTALS WITH ULTRAHIGH PIEZOELECTRIC COEFFICIENT

Jun Luo (TRS Technologies, Inc., USA)

14:30 - 15:00

(Invited) CRYSTAL GROWTH AND APPLICATION OF PMN-PT BASED SINGLE CRYSTALS

Jian Tian (CTS Corporation, IL/USA)

15:00 - 15:30

BREAK

15:30 - 17:30

Bulk Crystal Growth: Semiconductors

Tuesday, July 30, 2019

Shavano Peak

Moderator(s): Aleksandar Ostrogorsky, USA; Merry Koschan, USA

15:30 - 15:45

RECENT DEVELOPMENTS IN GERMANIUM CRYSTAL GROWTH

Johannes Vanpaemel (Umicore EOM, BE)

15:45 - 16:00

SEGREGATION OF BORON IN SILICON GERMANIUM CRYSTALS GROWN BY TRAVELING LIQUIDUS ZONE TECHNIQUE

Toshinori Taishi (Faculty of Engineering, Shinshu University, JP)

16:00 - 16:15

[INFLUENCE OF THE GROWTH INTERFACE SHAPE ON THE DEFECT CHARACTERISTICS IN THE FACET REGION OF 4H-SIC SINGLE CRYSTALS](#)

Matthias Arzig (FAU Erlangen Nürnberg Crystal Growth Lab, DE)

16:15 - 16:30

[HIGH QUALITY AND INCLUSION SUPPRESSION BY SWITCHING FLOW IN 3-INCH SIC SOLUTION GROWTH](#)

Can Zhu (Institute of Materials and Systems for Sustainability, JP)

16:30 - 16:45

[INTERFACE RECONSTRUCTION OF 4H-SIC \(000-1\) IN THE SI-CR BASED SOLVENT](#)

Yuchuan Yao (Institute of Industrial Science, JP)

16:45 - 17:00

[UNDERSTANDING THERMOCHEMICAL AND TRANSPORT LIMITATIONS AND THEIR IMPACT ON CRYSTALLINE QUALITY IN THE CHEMICAL VAPOR TRANSPORT GROWTH OF CUBIC BORON ARSENIDE](#)

David Snyder (Penn State Applied Research Laboratory, PA/USA)

17:00 - 17:15

[TWIN PHENOMENA OF VGF-GROWN INP SINGLE CRYSTALS](#)

Youwen Zhao (Institute of semiconductors, CN)

17:15 - 17:30

[VGF GROWTH OF HIGH QUALITY INAS SINGLE CRYSTALS WITH](#)

LOW DISLOCATION DENSITY

Jun Yang (Institute of Semiconductors, Chinese Academy of Sciences, CN)

15:30 - 17:30

Detector Materials: Oxide Scintillators

Tuesday, July 30, 2019

Red Cloud Peak

Moderator(s): Federico Moretti; V. Ouspenski

15:30 - 15:45

PRECIOUS METAL CRUCIBLE-FREE BULK CRYSTAL GROWTH OF
CE DOPED $\text{GD}_3(\text{GA,AL})_5\text{O}_{12}$ SINGLE CRYSTAL FROM THE MELT

Akira Yoshikawa (Institute for Materials Research, Tohoku University, JP)

15:45 - 16:00

CZOCHEVSKI GROWTH OF 4 INCH DIAMETER
CE:GD₃AL₂GA₃O₁₂ SINGLE CRYSTALS FOR SCINTILLATOR
APPLICATIONS

Vladimir Kochurikhin (General Physics Institute, Russian Academy of Sciences, RU)

16:00 - 16:15

CZOCHEVSKI GROWTH AND SCINTILLATION PROPERTIES OF
LI[±], NA[±], AND K[±], CODOPED LUYAG: PR^{3±} SINGLE CRYSTALS

Camera Foster (University of Tennessee, TN/USA)

16:15 - 16:30

EFFECTS OF LA DOPING ON THE CRYSTAL GROWTH AND
INTRINSIC LUMINESCENCE PROPERTIES OF $\text{LU}_3\text{AL}_5\text{O}_{12}$ SINGLE
CRYSTAL

Karol Bartosiewicz (Institute for Materials Research, Tohoku University, JP)

16:30 - 16:45

[LITHIUM AND SODIUM MOLYBDATE CRYSTALS FOR NEUTRINOLESS DOUBLE BETA DECAY EXPERIMENTS](#)

Joshua Tower (Radiation Monitoring Devices, Inc., MA/USA)

16:45 - 17:00

[BULK \$\text{Li}_2\text{MOO}_4\$ CRYSTALS FOR SCINTILLATING BOLOMETERS USED IN NEUTRINOLESS DOUBLE-BETA DECAY NEXT-GENERATION DETECTION EXPERIMENTS \(ORAL PRESENTATION\)](#)

Matias Velazquez (SIMaP UMR 5266 CNRS-UGA-G INP, FR)

17:00 - 17:15

[CRYSTAL GROWTH AND LUMINESCENCE PROPERTIES OF NOVEL MOLYBDATE SCINTILLATION MATERIALS](#)

Hongbing Chen (Institute of Materials Science & Chemical Engineering, Ningbo University, CN)

17:15 - 17:30

CZOCHEWSKI GROWTH OF LARGE (DIA. > 60 MM) YAP:CE CRYSTALS AND ITS IMPROVED SCINTILLATION PROPERTIES

Jan Kovář (CRYTUR, CZ)

15:30 - 17:30

Bulk and Epitaxial Growth of Gallium Oxide

Tuesday, July 30, 2019

Grays Peak I

Moderator(s): Kevin Stevens, USA; Shizuo Fujita, JP

15:30 - 16:00

[\(Invited\) DEVELOPMENTS IN BULK GROWTH OF \$\beta\$ -GA₂O₃ VIA THE CZOCHRALSKI METHOD AND FABRICATION OF \(010\) EPI-READY SUBSTRATES](#)

[Adam Lindsey](#) (Scintillation Materials Research Center, TN/USA)

16:00 - 16:15

[\$\beta\$ -GA₂O₃ SINGLE CRYSTAL GROWTH OPTIMIZATION BY EFG METHOD AND OPTICAL ANISOTROPY AND IN-PLANE POLARIZATION](#)

[Wenxiang Mu](#) (State Key Laboratory of Crystal Materials, CN)

16:15 - 16:30

[NUMERICAL STRESS MODELING OF \$\beta\$ -GA₂O₃ CRYSTAL GROWTH BY CZOCHRALSKI METHOD](#)

[Masaya Iizuka](#) (YBP 15F, JP)

16:30 - 16:45

[CRYSTAL GROWTH OF A PROMISING SEMICONDUCTOR: \$\beta\$ -GA₂O₃](#)

[Peng Zhao](#) (Beijing Sinoma Synthetic Crystals Co., Ltd., CN)

16:45 - 17:00

[ATOMIC STRUCTURE AND ELECTRONIC PROPERTIES OF THE \$\beta\$ -GA₂O₃\(100\) SURFACE](#)

[Celina Schulze](#) (TU Berlin, DE)

17:00 - 17:15

[SURFACE EVOLUTION OF SINGLE CRYSTALLINE \$\beta\$ -GA₂O₃ WITH](#)

[CHEMICAL MECHANICAL POLISHING AND ANNEALING AT AN ELEVATED TEMPERATURE](#)

Michael Liao (University of California Los Angeles, CA/USA)

17:15 - 17:30

[LOW BACKGROUND CARRIER CONCENTRATION IN AN MOCVD-GROWN \$\beta\$ -GA₂O₃](#)

Nazar Orishchin (Agnitron Technology, Inc., MN/USA)

15:30 - 17:30

III-V Wide Bandgap Devices

Tuesday, July 30, 2019

Crestone III, IV

Moderator(s): Ramon Collazo, USA; Ronny Kirste, USA

15:30 - 16:00

[\(Invited\) EPITAXY OF GAN-BASED VCSELS](#)

Tetsuya Takeuchi (The University of Meijo, JP)

16:00 - 16:30

[\(Invited\) VERTICAL GAN-ON-SILICON POWER DEVICES](#)

Elison Matioli (Ecole Polytechnique Fédérale de Lausanne (EPFL), CH)

16:30 - 16:45

[NONPOLAR GAN-BASED VCSELS WITH NANOPOROUS DISTRIBUTED BRAGG REFLECTOR MIRRORS](#)

Daniel Feezell (University of New Mexico, USA)

16:45 - 17:00

THE INFLUENCE OF SI AND MG CONCENTRATION IN ALGAN-BESED UV-B LASERS

Shunya Tanaka (The University of Meijo, JP)

17:00 - 17:15

EVALUATION AND CONTROL OF MG DIFFUSION EFFECT IN III-NITRIDE UV LIGHT-EMITTING DEVICES

Russell Dupuis (Georgia Institute of Technology, GA/USA)

17:15 - 17:30

TRANSFER-FREE FLEXIBLE SINGLE-CRYSTALLINE III-N FILM DIRECTLY GROWN ON METAL TAPE FOR BENDABLE INORGANIC PHOTONIC AND ELECTRONIC DEVICES

Jae-Hyun Ryou (University of Houston, TX/USA)

15:30 - 17:30

Nanowires

Tuesday, July 30, 2019

Torreys Peak II-IV

Moderator(s): George Wang, USA; Zhaoxia Bi, SE

15:30 - 16:00

(Invited) RESHAPE OF GAN NANOWIRE-MEDIATED NITRIDE PYRAMIDS AND REALIZATION OF FULL VISIBLE COLOR LIGHT EMITTING DIODES

Zhaoxia Bi (Solid State Physics Division, Physics Department, SE)

16:00 - 16:15

AMORPHOUS Al_xO_y AS A NUCLEATION LAYER FOR SELECTIVE AREA FORMATION OF GAN NANOWIRES BY PLASMA-ASSISTED

MOLECULAR BEAM EPITAXY

Marta Sobanska (Institute of Physics, Polish Academy of Sciences, PL)

16:15 - 16:30

HOMOEPITAXIAL GROWTH OF GAN NANORODS VIA IRREGULAR MASKS

Chang-Hsun Huang (National Chiao Tung University, TW)

16:30 - 16:45

BETWEEN GROWTH OF GALLIUM NITRIDE NANOWIRES ON MOS₂ AND ITS PIEZOELECTRIC EFFECT

Wei Ting Lin (National Chiao Tung University, TW)

16:45 - 17:00

ULTRA-THIN-WALLED ZNO MICROTUBE CAVITY FABRICATED BY OPTICAL VAPOR SUPERSATURATED PRECIPITATION FOR NOVEL APPLICATIONS IN NANOPHOTONICS

Yinzhou Yan (Institute of Laser Engineering, Beijing University of Technology, CN)

17:00 - 17:15

TOWARDS SMART COMPOSITE MATERIALS: NANOSCALE FUNCTIONALIZATION OF CARBON FIBERS WITH ZINC OXIDE

Andrea Zappettini (IMEM-CNR, IT)

17:15 - 17:30

PHYSICAL VAPOR TRANSPORT GROWTH OF ZINC PHTHALOCYANINE NANOPILLARS ON GRAPHENE SUBSTRATES

Timothy Mirabito (Penn State University, PA/USA)

15:30 - 17:30

Symposium on Epitaxy of Complex Oxides: Delafossites and Oxides on Semiconductors

Tuesday, July 30, 2019

Grays Peak II, III

Moderator(s): Chang-Beom Eom, USA

15:30 - 16:00

[\(Invited\) THIN-FILM GROWTH OF \$\text{PDCO}_2\$: A LAYERED OXIDE AS CONDUCTIVE AS GOLD](#)

Takayuki Harada (Tohoku University, JP)

16:00 - 16:30

[\(Invited\) GROWTH OF METALLIC DELAFOSSITES BY MOLECULAR BEAM EPITAXY AND PULSED LASER DEPOSITION](#)

Matthew Brahlek (Oak Ridge National Laboratory, USA)

16:30 - 16:45

[GROWTH OF DELAFOSSITE \$\text{PTCO}_2\$ THIN FILMS BY MOLECULAR-BEAM EPITAXY](#)

Jiixin Sun (Cornell University, NY/USA)

16:45 - 17:15

[\(Invited\) ATOMIC CONTROLLED OXIDE HETEROSTRUCTURES ON SI AND III-V SEMICONDUCTORS](#)

Guus Rijnders (University of Twente, MESA+ Institute for Nanotechnology, NI)

17:15 - 17:30

[EPITAXIAL GROWTH OF SRTIO₃ AND FUNCTIONAL OXIDES ON SILICON](#)

Zhe Wang (Cornell University, NY/USA)

15:30 - 17:30

Surfaces and Interfaces

Tuesday, July 30, 2019

Crestone I, II

Moderator(s): Elias Vlieg, NL; Kerstin Volz,

15:30 - 16:00

[\(Invited\) STEP DYNAMICS RESULTING FROM ADSORPTION AT ELECTRON PASSIVATED SEMICONDUCTOR SURFACES](#)

Stanislaw Krukowski (Institute of High Pressure Physics PAS, PL)

16:00 - 16:15

[EFFECTS OF ACIDIC GASES ON ICE SURFACES GROWN FROM WATER VAPOR](#)

Ken Nagashima (Hokkaido University, JP)

16:15 - 16:30

[ADHESIVE PROPERTIES OF BI-MATERIAL INTERFACES FORMED WITH FRESHWATER COLUMNAR ICE](#)

Emily Asenath-Smith (USA Army ERDC CRREL, NH/USA)

16:30 - 16:45

[STEP MORPHOLOGY CONTROL IN HOMOEPITAXIAL GAN GROWTH BY MOCVD](#)

Andrew Klump (North Carolina State University, USA)

16:45 - 17:00

[GROWTH AND MORPHOLOGY OPTIMIZATION OF OMVPE
ALINGAAS/INP SUPERLATTICE STRUCTURES](#)

Oliver Pitts (National Research Council Canada, ON/CA)

17:00 - 17:15

[CREATION OF ATOMICALLY-ORDERED SIDE- AND FACET-
SURFACES ON THE THREE-Dimensionally ARCHITECTED SI
STRUCTURES](#)

Azusa Hattori (The Institute of Scientific and Industrial Research, Osaka
University, JP)

17:15 - 17:30

[THE INTERFACIAL INTERACTIONS BETWEEN FACETED
CRYSTALS: AN IN-SILICO AND ATOMIC FORCE MICROSCOPY
STUDY](#)

Alexandru Moldovan (University of Leeds, GB)

Tuesday, July 30, 2019
Poster Session

17:30 - 19:00

Poster Session

Tuesday, July 30, 2019

Columbine Ballroom (Longs and Quandary Peak)

Symposium on Epitaxy and Complex Oxides

TuP1.1

[SIZE SCALING OF THE IMPROPER FERROELECTRICITY IN LUFeO₃](#)

Megan Holtz (Cornell University, USA)

TuP1.2

[SELF-ASSEMBLY AND PROPERTIES OF DOMAIN WALLS IN BIFEO₃ LAYERS GROWN VIA MOLECULAR-BEAM EPITAXY](#)

Antonio Mei (Cornell University, USA)

TuP1.3

[HIGH MOBILITY LA-DOPED BASNO₃ THIN FILM GROWTH ON LATTICE-MATCHED BA\(SC_{0.5},NB_{0.5}\)O₃ \(001\) SUBSTRATE BY MOLECULAR-BEAM EPITAXY](#)

Hanjong Paik (Cornell University, USA)

Thin Film Growth, Epitaxy, and Superlattices

TuP2.1

[EXOTIC TRANSROTATIONAL CRYSTAL GROWTH IN THIN AMORPHOUS FILMS DISCOVERED BY TEM:"VACUUM EPITAXY", LATTICE-ROTATION NANOENGINEERING, NOVEL AMORPHOUS MODELS](#)

Vladimir Kolosov (Ural Federal University, RU)

TuP2.2

[PREPARATION OF IRIDIUM FILMS BY CHEMICAL VAPOR DEPOSITION ON METAL SUBSTRATES](#)

Hiroki Sato (Tohoku University, JP)

TuP2.3

[SPINODAL DECOMPOSITION WITH THE FORMATION OF A OSCILATIONS OF COMPOSITION AT THE LOW TEMPERATURE](#)

SYNTHESIS OF THE GAINP - GAAS STRUCTURE

Vladimir Kuznetsov (Saint-Petersburg State Electrotechnical University, RU)

TuP2.4

CHANGE OF KINETIC PROCESS IN CRYSTAL GROWTH FROM AMORPHOUS THIN FILM OF α -NPD

HIDEYUKI Kanehara (Nakada-lab, Department of Physical Sciences, College of Science and Engineering, Ritsumeikan University, JP)

TuP2.5

INVESTIGATIONS ON STRUCTURAL, MECHANICAL AND MAGNETIC PROPERTIES OF ELECTROPLATED NIW NANO CRYSTALLINE THIN FILMS FOR MEMS APPLICATIONS

H Arul (Department of Science and Humanities, Kumaraguru College of Technology (Autonomous), IN)

TuP2.6

EPITAXIAL GROWTH OF GAN/GA₂O₃ AND GA₂O₃/III-N HETEROSTRUCTURES

Roberto Fornari (Dept. of Mathematical, Physical and Computer Sciences, University of Parma, IT)

TuP2.7

CHARACTERIZATION OF INTRINSIC COMPOSITIONAL DISORDER IN NITRIDE ALLOYS BY SCANNING TUNNELING ELECTROLUMINESCENCE SPECTROSCOPY

Wiebke Hahn (Laboratoire de Physique de la Matière Condensée, Ecole Polytechnique, CNRS, FR)

Silicon Carbide Materials and Devices

TuP3.1

[NITROGEN DOPED SILICON-CARBON PROTECTIVE MULTILAYER NANOSTRUCTURES ON CARBON OBTAINED BY TVA METHOD](#)

Victor Ciupina (Academy of Romanian Scientists, Ro)

In situ Observation and Characterization

TuP4.1

[CHEX: A NEW BEAMLINER FOR HIGH ENERGY COHERENT X-RAY STUDIES DURING SYNTHESIS](#)

M J Highland (Argonne National Lab, USA)

TuP4.2

[A NEW METHODOLOGY FOR CRYSTAL PHASE IDENTIFICATION OF KIDNEY STONE THIN SECTION BY MICROSCOPIC FT-IR](#)

Koichi Sawada (Osaka University, JP)

TuP4.3

[IN SITU COHERENT X-RAY STUDIES OF SURFACE DYNAMICS DURING OMVPE OF GAN](#)

Carol Thompson, Department of Physics, Northern Illinois University, IL/US)

Bulk Crystal Growth

TuP5.1

[CRYSTAL GROWTH AND LUMINESCENCE STUDIES ON \$\text{Li}_2\text{Mg}_2\(\text{MOO}_4\)_3\$ CRYSTAL GROWN BY CZOCHRALSKI METHOD](#)

Joseph Daniel D. (Kyungpook National University, KR)

TuP5.2

[REVEALING THE ROLE OF CALCIUM CODOPING ON OPTICAL AND SCINTILLATION HOMOGENEITY IN LU₂SIO₅:CE SINGLE CRYSTALS](#)

Yuntao Wu (University of Tennessee, USA)

TuP5.3

[LUMINESCENCE PROPERTIES OF AG DOPED LIF CRYSTAL GROWN BY CZOCHRALSKI METHOD](#)

Joseph Daniel D (Kyungpook National University, KR)

TuP5.4

[DIRECTIONAL GROWTH, PHYSICOCHEMICAL AND QUANTUM CHEMICAL INVESTIGATIONS ON 2-AMINO-5-NITROPYRIDINIUM DIHYDROGEN PHOSPHATE \(2A5NPDP\) SINGLE CRYSTAL FOR NONLINEAR OPTICAL \(NLO\) APPLICATIONS](#)

Sivasubramani V (SSN College of Engineering, IN)

TuP5.5

[SYNTHESIS, GROWTH, OPTICAL TRANSMITTANCE, LASER DAMAGE THRESHOLD, Z-SCAN AND OPTICAL LIMITING STUDIES OF 2-AMINO-4,6-DIMETHOXYPYRIMIDINIUM HYDROGEN \(2R, 3R\)-TARTRATE 2-AMINO-4,6-DIMETHOXYPYRIMIDINE SINGLE CRYSTAL](#)

Ro Mu Jauhar (VIT University, IN)

TuP5.6

[SELECTIVE SAPPHIRE DISSOLUTION TECHNIQUE WITHOUT DISSOLVING GALLIUM NITRIDE IN A SODIUM FLUX ADDED LITHIUM](#)

Takumi Yamada (Osaka university, JP)

TuP5.7

[HIGH-RATE GROWTH OF A THICK FREESTANDING GAN CRYSTAL WITH CH₄ BY OVPE](#)

Masahiro Kamiyama (Osaka University, JP)

TuP5.8

[THE EFFECT OF IMPURITIES ON THE TRANSPARENCY OF GAN CRYSTALS GROWN BY NA FLUX](#)

Mohammed Abo Alreesh (University of California Santa Barbara, USA)

TuP5.9

[EFFECT OF TEMPERATURE GRADIENT ON ALN CRYSTAL GROWTH BY PVT METHOD](#)

Lei Zhang (State Key Lab of Crystal Materials, Shandong University, CN)

TuP5.10

[GROWTH OF GAN CRYSTALS BY SUBLIMATION METHOD](#)

Y. Song (Institute of Physics, Chinese Academy of Sciences, CN)

TuP5.11

[FLUX GROWTH OF 0.64PB\(MG_{1/3}NB_{2/3}\)O₃-0.36PBTIO₃ SINGLE CRYSTALS: TRUE-REMANENT AND RESISTIVE-LEAKAGE INVESTIGATION](#)

Abhilash Joseph (Department of Physics & Astrophysics, University of Delhi, IN)

TuP5.12

[DEVICE GRADE AND THE ULTRA HIGH-QUALITY SB-BASED](#)

[CRYSTAL GROWTH:THE NOVEL CONCEPT OF THE VERTICAL DIRECTIONAL SOLIDIFICATION \(VDS\) BY SLOW FREEZING](#)

Dattatray Gadkari (Consultant, Crystal Growth and Technology, IN)

TuP5.13

[SEARCHING FOR IDEAL TOPOLOGICAL CRYSTALLINE INSULATORS AND TOPOLOGICAL SUPERCONDUCTORS IN PB-SN-IN-TE SYSTEM](#)

Genda Gu (Brookhaven National Laboratory, USA)

TuP5.14

[CRYSTAL GROWTH, MICROSTRUCTURE, AND PHYSICAL PROPERTIES OF SR\(MN1-XZNX\)SB2](#)

Yong Liu (Institute of High Energy Physics, Chinese Academy of Sciences and Dongguan Neutron Science Center, CN)

TuP5.15

[CRYSTAL GROWTH, STRUCTURAL, OPTICAL AND THERMAL PROPERTIES OF TRIPHENYLAMINE \(TPA\) SINGLE CRYSTAL GROWN BY BRIDGMAN](#)

Kasthuri Ramachandran (SSN College of Engineering IN)

TuP5.16

[GROWTH OF Y-TYPE HEXAFERRITE SINGLE CRYSTALS](#)

Dharmalingam Prabhakaran (Clarendon Laboratory, University of Oxford, GB)

TuP5.17

[GROWTH, STRUCTURAL AND OPTICAL PROPERTIES OF](#)

LANGBEINITE-TYPE $\text{RB}_2\text{Ti}_{0.8}\text{YB}_{1.2}(\text{PO}_4)_3$ CRYSTALS

Xiulan Duan (Shandong University, CN)

TuP5.18

INVESTIGATION ON THE STRUCTURAL, CRYSTALLINE PERFECTION, OPTICAL, ELECTRICAL AND MECHANICAL PROPERTIES OF HIPPURIC ACID DOPED FERROELECTRIC TRIGLYCINE SULFATE CRYSTALS

P Rajesh (SSN College of Engineering, IN)

TuP5.19

NUMERICAL SIMULATION ON OXYGEN TRANSFER IN SI MELT UNDER A CUSP-SHAPED MAGNETIC FIELD USING A 3D GLOBAL MODEL

D. Murakami (Institute for Applied Mechanics, Kyushu University, JP)

TuP5.20

DISPERSIONS OF PEROVSKITE STRUCTURE RELAXOR FERROELECTRIC SINGLE CRYSTALS GROWN BY ORIENTED BRIDGMAN METHOD

Xian Wang (Shanghai Institute of Ceramics, Chinese Academy of Sciences, CN)

TuP5.21

SPIN REORIENTATION TRANSITION AND EXCHANGE BIAS IN HALF Y DOPED SMFEO_3 SINGLE CRYSTAL

Bhawana Mali (Indian Institute of Science, IN)

TuP5.22

THE CRYSTAL GROWTH AND CHARACTERIZATION OF SE-SUBSTITUTED BISI BY PHYSICAL VAPOR TRANSPORT METHOD

Bao Xiao (Northwestern Polytechnical University, CN)

TuP5.23

[INFLUENCE OF GROWTH CONDITIONS ON THE OPTICAL SPECTRA OF GAMMA-IRRADIATED \$\text{BAF}_2\$ AND \$\text{CAF}_2\$ CRYSTALS](#)

Irina Nicoara (West University of Timisoara, RO)

TuP5.24

[STUDIES ON SHUBNIKOV-DE HASS OSCILLATIONS IN P- \$\text{SB}_2\text{TE}_2\text{SE}\$ TOPOLOGICAL SINGLE CRYSTALS](#)

Anandha Bab Govindan (Department of Physics, SSN College of Engineering, Rajiv Gandhi Salai, IN)

Detector Materials: Scintillators and Semiconductors

TuP6.1

[REVEALING THE ROLE OF CALCIUM CODOPING ON OPTICAL AND SCINTILLATION HOMOGENEITY IN \$\text{LU}_2\text{SiO}_5:\text{CE}\$ SINGLE CRYSTALS](#)

Yuntao Wu (University of Tennessee, USA)

TuP6.2

[CRUCIBLE-FREE GROWTH OF CE-DOPED \$\(\text{GD,LA}\)_2\text{Si}_2\text{O}_7\$ SINGLE CRYSTALS IN THE AIR ATMOSPHERE FOR SCINTILLATOR APPLICATIONS](#)

Vladimir Kochurikhin (General Physics Institute, Russian Academy of Sciences, RU)

TuP6.3

[CRYSTAL GROWTH AND OPTICAL PROPERTIES OF A](#)

[CE₂Si₂O₇ SINGLE CRYSTAL](#)

Takahiko Horiai (IMR, Tohoku University, JP)

TuP6.4

[METAL HALIDE PEROVSKITE BULK CRYSTALS GROWN FROM SOLUTION FOR ROOM TEMPERATURE NUCLEAR RADIATION DETECTION](#)

Yadong Xu (Northwestern Polytechnical University, CN)

TuP6.5

[SCINTILLATION PROPERTIES OF ZNO:GA SINGLE CRYSTALS GROWN BY TRAVELLING-SOLVENT FLOATING-ZONE METHOD](#)

Y. Ma (Shanghai Institute of Technology, Shanghai, CN)

TuP6.6

[SCINTILLATION IMPROVEMENT OF BABR₂:EU SINGLE CRYSTALS BY AU CO-DOPING](#)

Dongsheng Yuan (Lawrence Berkeley National Lab, USA)

TuP6.7

[THE CRYSTAL GROWTH AND CHARACTERIZATION OF QUASI-ONE-DIMENSIONAL LEAD BASED PEROVSKITE CSPBI₃ CRYSTALS](#)

Bin-bin Zhang (Northwestern Polytechnical University, CN)

TuP6.8

[HPHT SINGLE CRYSTAL DIAMOND SUBSTRATE IIA TYPE CHARACTERIZATION FOR PARTICLE DETECTORS](#)

Oleg Rabinovich (NUST MISIS, RU)

TuP6.9

SYNTHESIS AND PHASE CONTROL OF THE EUROPIUM DOPED
BAF₂-BaCl₂ SYSTEM

Brenden Wiggins (Los Alamos National Laboratory, USA)

TuP6.10

GROWTH DIFFICULTIES AND GROWTH OF CRACK FREE EU²⁺
ACTIVATED KSR2I5 SCINTILLATOR SINGLE CRYSTAL BY
VERTICAL BRIDGMAN-STOCKBARGER TECHNIQUE FOR
RADIATION DETECTION APPLICATIONS

A Raja (SSN College of Engineering, IN)

TuP6.11

SINGLE CRYSTAL GROWTH OF UNDOPED AND TB DOPED LU₂O₃
AND HFO₂ BY INDIRECT HEATING GROWTH METHOD USING ARC
PLASMA

Kei Kamada (NICHe, Tohoku University, JP)

TuP6.12

COMPARISON CO-DOPING EFFECTS BETWEEN MG AND W ON
CE:GD₃GA₃AL₂O₁₂ SCINTILLATOR GROWN BY MICRO PULLING
DOWN METHOD.

Mutsumi Ueno (Institute for Materials Research, Tohoku University, JP)

TuP6.13

BULK CRYSTAL GROWTH OF ALSB FOR ROOM-TEMPERATURE
PHOTODETECTOR

Ziang Yin (Northwestern Polytechnical University, CN)

TuP6.14

UNIDIRECTIONAL GROWTH AND CHARACTERIZATION OF

TRIPHENYLMETHANE SINGLE CRYSTALS FOR SCINTILLATOR APPLICATION

K. Sankaranarayanan (Alagappa University, Karaikudi, IN)

TuP6.15

TAILORING CHEMICAL STRESS TO SUPPRESS CRACKING OF SCINTILLATOR CRYSTALS DURING BRIDGMAN GROWTH

Chang Zhang (University of Minnesota, USA)

TuP6.16

CRYSTAL GROWTH AND CHARACTERIZATION OF $\text{CEBR}_{3-x}\text{I}_x$ SCINTILLATORS

Matthew Lloyd (University of Tennessee, USA)

TuP6.17

GROWTH AND THE INFLUENCE OF CE^{3+} CONCENTRATION ON THE SCINTILLATION PROPERTIES OF $\text{CS}_2\text{LIYCL}_6$ CRYSTALS

Guohao Ren (Shanghai Institute of Ceramics, Chinese Academy of Sciences, CN)

TuP6.18

CRYSTAL GROWTH AND CHARACTERIZATION OF $\text{CH}_3\text{NH}_3\text{PBBR}_3$ SINGLE-CRYSTALS FOR X-RAY PHOTODETECTION

S. Amari (CEA LITEN LCO, Grenoble, FR)

TuP6.19

CS_2HFCL_6 : A NOVEL LARGE DIAMETER SCINTILLATOR CRYSTAL

Rastgo Hawrami (Fisk University, USA)

TuP6.19

LIGHT YIELD IMPROVEMENT OF $\text{BI}_4\text{SI}_3\text{O}_{12}$ SCINTILLATION

CRYSTALS BY DOPING TRANSITION METAL IONS

Jiayue Xu, (Shanghai Institute of Technology, CN)

Gallium Oxide Materials and Devices

TuP7.1

ELECTRICAL AND OPTICAL PROPERTIES OF ZR DOPED β -GA₂O₃ SINGLE CRYSTALS GROWN BY CZOCHRALSKI METHOD

M. Saleh (Washington State University, USA)

TuP7.2

SILICON AND TIN DOPING OF EPSILON-GALLIUM OXIDE EPILAYERS GROWN BY MOVPE

R. Fornari (University of Parma, IT)

TuP7.3

DESIGN, MODELING, AND IMPLANTATION OF AN IMPROVED INDUCTIVELY HEATED SUSCEPTOR FOR GALLIUM OXIDE

G. Tompa(Structured Materials Industries, Inc, USA)

Characterization Techniques for Bulk and Epitaxial Crystals

TuP8.1

YB³⁺ AND YB²⁺ IONS DISTRIBUTION ALONG THE YBF₃ DOPED BAF₂ AND CAF₂ CRYSTALS

Irina Nicoara (West University of Timisoara, RO)

TuP8.2

DIELECTRIC SPECTROSCOPY IN FERRO TRANSITION OF TGS CRYSTAL

Horia Alexandru (University of Bucharest, RO)

TuP8.3

FLOATING-ZONE GROWTH OF FLUORITE STRUCTURE OXIDES

Dharmalingam Prabhakaran (Clarendon Laboratory, University of Oxford, GB)

TuP8.4

GROWTH AND ELECTRIC PROPERTIES OF Ca_2RuO_4 SINGLE CRYSTALS

Antonio Vecchione (CNR - SPIN, IT)

TuP8.5

CORRELATION BETWEEN THE Mg_2Si PRECIPITATES AMOUNT FORMATION AND THE MECHANICAL PROPERTIES OF AL-SI AND AL-SI-MG ALLOYS.

Lynda Amirouche (University of Sciences and Technologie Houari Voumedienne Algeria, DZ)

TuP8.6

INFLUENCE OF Pb^{2+} IONS ON THE OPTICAL PROPERTIES OF GAMMA IRRADIATED BaF_2 AND CaF_2 CRYSTALS

Irina Nicoara (West University of Timisoara, RO)

TuP8.7

OPTICAL CHARACTERIZATIONS OF $Cd_{1-x}Zn_xTe$ BULK SEMICONDUCTORS GROWN BY VERTICAL BRIDGMAN-STOCKBARGER METHOD

Der Yuh Lin (National Changhua University of Education, TW)

Fundamentals of Crystal Growth

TuP9.1

[SOLVATION AND PHASE DISSOCIATION OF CARBONIC DIHYDRAZIDINIUM BIS\[3-\(5-NITROIMINO-1,2,4-TRIAZOLATE\)\] INDUCED BY SOLVENTS](#)

Hongzhen Li (Institute of Chemical Materials, China Academy of Engineering Physics, CN)

TuP9.2

[PHASE EQUILIBRIUMS IN THE BINARY CDAS₂-MN SYSTEM](#)

Oleg Rabinovich (NUST MISIS, RU)

TuP9.3

[MNSB THIN FILMS GROWTH BY PVD METHOD](#)

Oleg Rabinovich (NUST MISIS, RU)

TuP9.4

[TWO-DIMENSIONAL STRUCTURES FORMED BY SPHERICAL PATCHY PARTICLES](#)

Masahide Sato (Information Media Center, Kanazawa University, JP)

TuP9.5

[PRE-NUCLEATION AND PARTICLE ATTACHMENT OF BISMUTH TRI-IODIDE ONTO GRAPHENE SUBSTRATES](#)

Laura Fornaro (CURE, Uy)

TuP9.6

[ROLE OF ELECTRON TUNNELING IN THE THERMALIZATION OF](#)

THE ADSORBATE AT SOLID SURFACES

Stanislaw Krukowski (Institute of High Pressure Physics PAS, PL)

TuP9.7

HABIT MODIFICATION OF L-ARGININE DOPED POTASSIUM DIHYDROGEN PHOSPHATE CRYSTALS GROWN UNDER ELECTRIC FIELD

Ashwini Mahadik (The Maharaja Sayajirao University of Baroda, IN)

TuP9.8

PHOTOCHROMIC COCRYSTAL OF CURCUMIN

Lora Altahrawi (University of Lincoln, GB)

TuP9.9

PHASE FORMATION IN $TbAl_3(BO_3)_4-(K_2MO_3O_{10}-B_2O_3-AL_2O_3)$ FLUX SYSTEM AND CRYSTAL STRUCTURE OF $TbAl_3(BO_3)_4$ MONOCLINIC MODIFICATION

Elena Volkova (Lomonosov Moscow State University, RU)

TuP9.10

UNIFORMLY VALID ASYMPTOTIC SOLUTIONS OF LAMELLAR EUTECTIC GROWTH IN DIRECTIONAL SOLIDIFICATION FOR LIQUID-SOLID INTERFACE SLOPES OF SMALL AND NORMAL ORDER

Xiang-Ming Li (Kunming University of Science and Technology, CN)

TuP9.11

CRYSTALLIZATION IN NON-AQUEOUS MEDIA AND THE ROLE OF WATER

Franca Jones (Curtin University, AU)

TuP9.12

MORPHOLOGY OF A JAPANESE TRADITIONAL SUGAR BALL CAKE, CONPEITOU

Katsuo Tsukamoto (Osaka University, JP)

TuP9.13

SYNTHESIS, CRYSTAL STRUCTURE AND HIRSHFELD SURFACE OF 2-AMINO-3 BENZYLOXY PYRIDINIUM PICRATE (1:1)

Dr Divya Shetty (St Aloysius College (Autonomous), IN)

TuP9.14

ROLE OF A CRYSTAL GROWER IN HIGH TECH INDUSTRIES

Narsingh Singh (University of Maryland, USA)

19:30 - 21:30

Advanced OMVPE Technology for Wide Bandgap III-Nitrides

Tuesday, July 30, 2019

Torreys Peak II-IV

Moderator(s): Russell Dupuis, USA; Jae-Hyun Ryou, USA

19:30 - 19:50

CLOSE COUPLED SHOWERHEAD MOVPE REACTOR FOR UVC LED AND GRAPHENE DEPOSITION

Clifford McAleese (AIXTRON Ltd, GB)

19:50 - 20:10

PHYSICAL VAPOR TRANSPORT GROWN ALN SINGLE CRYSTAL

SUBSTRATES

Rafael Dalmau (HexaTech, Inc., NC/USA)

20:10 - 20:30

DISLOCATION RECOVERY IN AL-RICH ALGAN LAYERS BY HIGH TEMPERATURE ANNEALING

Shun Washiyama (North Carolina State University, NC/USA)

20:30 - 20:50

GROWTH OF ALGAN/INGAN MULTIPLE QUANTUM WELLS AND P-ALGAN LAYERS FOR 369 NM ULTRAVIOLET LIGHT EMITTING DEVICES

Russell Dupuis (Georgia Institute of Technology, GA/USA)

20:50 - 21:10

MOVPE GROWTH OF N-GAN CAP LAYER ON GAINN/GAN MULTI-QUANTUM SHELL LEDS

Nanami Goto (Meijo University, JP)

21:10 - 21:30

STUDY OF THE ORIGINS OF CARBON IMPURITIES ON GAN MOVPE FROM A GAS PHASE REACTION PERSPECTIVE

Yuto Okawachi (Nagoya University, JP)

Wednesday, July 31, 2019

08:00 - 10:00

Bulk Crystal Growth and Detector Materials

Wednesday, July 31, 2019

Shavano Peak

Moderator(s): Luis Stand, Chuck Melcher

08:00 - 08:30

[\(Invited\) CESIUM HAFNIUM CHLORIDE, NOVEL SCINTILLATING MATERIAL](#)

Robert Kral (Institute of Physics of the Czech Academy of Sciences, CZ)

08:30 - 08:45

[GROWTH AND QUALITY IMPROVEMENT OF CE-DOPED \(GD,LA\)₂SI₂O₇ SCINTILLATOR CRYSTALS](#)

Yasuhiro Shoji (Institute for Materials Research, Tohoku University, JP)

08:45 - 09:00

[ELIMINATION OF CRACKS IN LGSO SCINTILLATION SINGLE CRYSTALS DURING CRYSTAL GROWTH](#)

Junya Osada (Oxide Corporation, JP)

09:00 - 09:15

[SINGLE CRYSTAL GROWTH AND SCINTILLATION PROPERTIES OF MO CO-DOPED CE:LYSO CRYSTALS](#)

Kyoung Jin Kim (Institute for Materials Research, Tohoku University, JP)

09:15 - 09:30

[BULK SINGLE CRYSTAL GROWTH OF W, CE:GD₃GA₃AL₂O₁₂ BY](#)

CZOCHELSKI METHOD AND THEIR UNIFORMITY OF
SCINTILLATION PROPERTIES

Mutsumi Ueno (Institute for Materials Research, Tohoku University, JP)

09:30 - 09:45

MULTIPLE SHAPED CRYSTAL GROWTH OF OXIDE
SCINTILLATORS USING MO CRUCIBLE AND DIES BY THE EDGE
DEFINED FILM FED GROWTH METHOD

Kei Kamada (NICHe, Tohoku University, JP)

09:45 - 10:00

PHASE DIAGRAM OF $\text{BaI}_2\text{-LuI}_3$ AND GROWTH OF
 $\text{BaI}_2/\text{LuI}_3$ EUTECTIC SCINTILLATOR

Kazuya Origuchi (Institute for Materials Research, Tohoku University, JP)

08:00 - 10:00

**Fundamentals of Crystal Growth: Impact of Chemical and Structural
Heterogeneities**

Wednesday, July 31, 2019

Crestone I, II

Moderator(s): Mu Wang, Baron Peters,

08:00 - 08:30

(Invited) MESOSCOPIC CLUSTERS AND PREFORMED SOLUTE
DIMERS IN CRYSTAL FORM TRANSITIONS AND GROWTH OF
OLANZAPINE CRYSTALS

Peter Vekilov (USA)

08:30 - 08:45

DYNAMICS OF BUBBLE ENGULFMENT DURING SAPPHIRE

CRYSTAL GROWTH

Linmin Wang (University of Minnesota, MN/USA)

08:45 - 09:00

[AB INITIO STUDY FOR ADSORPTION AND DESORPTION BEHAVIOR AT STEP EDGES OF GAN\(0001\) SURFACE](#)

Toru Akiyama (Mie University, JP)

09:00 - 09:15

[ON THE EFFECT OF BULK DIFFUSION ON THREE-DIMENSIONAL LAMELLAR GROWTH IN THE DISCONTINUOUS PRECIPITATION REACTION: A PHASE-FIELD APPROACH](#)

Aniss Ryad Ladjeroud (USTHB DZ)

09:15 - 09:30

[INVESTIGATING THE ROLE OF \$Mg^{2+}\$ IN \$CaCO_3\$ CRYSTALLIZATION](#)

Matthew Boon (Curtin University, WA/AU)

09:30 - 09:45

[MACROSTEP-HEIGHT DEPENDENCE OF SURFACE VELOCITY FOR A REACTION- \(INTERFACE-\) LIMITED CRYSTAL GROWTH](#)

Noriko Akutsu (Osaka Electro-Communication University, JP)

09:45 - 10:00

[TEMPORAL CHANGE OF CRYSTAL SIZE DISTRIBUTION DURING CHIRALITY CONVERSION BY ULTRASOUND GRINDING](#)

Hiroyasu Katsuno (JP)

08:00 - 10:00
III-V Devices
Wednesday, July 31, 2019
Torreys Peak II-IV

Moderator(s): Luke Mawst, USA; Jae-Hyun Ryou, USA

08:00 - 08:30

[\(Invited\) STATE-OF-THE-ART IN-SITU METROLOGY DURING OMVPE IN ACADEMIC RESEARCH AND INDUSTRY](#)

[Kolja Haberland](#) (Laytec AG, DE)

08:30 - 09:00

[\(Invited\) TRENDS IN MID IR QUANTUM CASCADE AND INTERBAND CASCADE LASERS](#)

[Kevin Lascola](#) (Thorlabs Quantum Electronics, MD/USA)

09:00 - 09:15

[EDGE BREAKDOWN COMPARISON OF OMVPE SINGLE AND DOUBLE DIFFUSION PROCESSES FOR AVALANCHE PHOTODIODES](#)

[Oliver Pitts](#) (National Research Council Canada, ON/Ca)

09:15 - 09:30

[HIGH OPERATING TEMPERATURE INTERBAND CASCADE INFRARED DETECTORS BASED ON TYPE-II SUPERLATTICES GROWN ON GAAS SUBSTRATES](#)

[Łukasz Kubiszyn](#) (Vigo System S.A., PL)

09:30 - 09:45

[GROWTH OF HIGHLY N-TYPE DOPED GAAS AND INGAAS BY METAL ORGANIC VAPOR EPITAXY WITH \$\text{SNCL}_4\$](#)

Reynald Alcotte (IMEC, BE)

09:45 - 10:00
LATE NEWS

08:00 - 10:00
Nanocrystals and Nanostructured Materials
Wednesday, July 31, 2019
Grays Peak I

Moderator(s): George Wang, USA; Erik Bakkers, NL

08:00 - 08:30
[\(Invited\) HEXAGONAL SiGe; GROWTH AND DIRECT BAND GAP EMISSION](#)

Erik Bakkers (Eindhoven University of Technology, NL)

08:30 - 08:45
[AN INSIGHT INTO QUANTUM DOT MOLECULE FORMATION MECHANISM IN HETEROEPITAXY OF \$\text{Si}_{1-x}\text{Ge}_x/\text{Si}\(001\)\$](#)

Monika Dhankhar (Indian Institute of Technology Kanpur, IN)

08:45 - 09:00
[TAILORING WAVELENGTH OF \$\text{CuInS}_2\$ QUANTUM DOTS BY THE CONTROL OF COMPOSITION AND SIZE IN A BOLT-NUT MICROREACTOR](#)

Hyunbin Kim (Korea Advanced Institute of Science and Technology, KR)

09:00 - 09:15
[ON SOFT LANDING DEPOSITION OF SMALL SIZE SILICON CLUSTERS UPON SILICON SUBSTRATE AT 300K: MOLECULAR](#)

DYNAMIC SIMULATIONS

Lynda Amirouche (University of sciences and technologie Houari boumedienne Algeria, DZ)

09:15 - 09:30

[RE³⁺:CAF₂ \(RE=ER, YB\) NANOCRYSTALLITES-CONTAINING OXYFLUOROGERMANOTELLURITE GLASS-CERAMICS \(ORAL PRESENTATION\)](#)

Matias Velazquez (SIMaP UMR 5266 CNRS-UGA-G INP, FR)

09:30 - 09:45

[ALLOY NANO-COMPOSITES FOR HIGH-Q INDUCTORS](#)

Narsingh Singh (University of Maryland, Baltimore County, USA)

09:45 - 10:00

[SKYRMION HOSTING CU₂OSEO₃ NANOCRYSTALS](#)

Arnaud Magrez (Ecole Polytechnique Fédérale de Lausanne, CH)

08:00 - 10:00

Symposium on 2D Materials: Special Topics II: h-BN

Wednesday, July 31, 2019

Crestone III, IV

Moderator(s): Sang-Hoon Bae, USA; Bhakti Jariwala, USA

08:00 - 08:30

[\(Invited\) GROWTH AND APPLICATIONS OF HEXAGONAL BORON NITRIDE](#)

Hyeon Shin (Department of Chemistry and Department of Energy Engineering, Ulsan National Institute of Science and Technology (UNIST),

KR)

08:30 - 08:45

[OPTIMIZATION OF VAPOR PHASE EPITAXY FOR THICK BORON NITRIDE FILMS](#)

Anthony Rice (Sandia National Laboratories, NM/USA)

08:45 - 09:15

[\(Invited\) ATOMIC PRECISION CONTROL OF 2D MATERIALS VIA LAYER RESOLVED SPLITTING](#)

Sang-Hoon Bae (Massachusetts Institute of Technology, MA/USA)

09:15 - 09:45

[\(Invited\) GROWTH, PROPERTIES, AND APPLICATIONS OF HEXAGONAL BORON NITRIDE EPILAYERS](#)

Hongxing Jiang (Texas Tech University, TX/USA)

09:45 - 10:00

[HIGH-THROUGHPUT PRODUCTION OF NOBLE METAL-DECORATED HEXAGONAL BORON NITRIDE \(HBN\) IN A HYDRODYNAMIC REACTOR](#)

Yongju Park (Korea Advanced Institute of Science and Technology (KAIST), KR)

08:00 - 10:00

**Symposium on Epitaxy of Complex Oxides: Beyond the Limits of Traditional Film Growth
Wednesday, July 31, 2019**

Grays Peak II, III

Moderator(s): Susanne Stemmer, USA

08:00 - 08:30

[\(Invited\) MOLECULAR BEAM EPITAXY OF ANTIPEROVSKITES](#)

Hiro Nakamura (Max Planck Institute for Solid State Research, DE)

08:30 - 09:00

[\(Invited\) GAS-SOURCE MBE TO MAKE COMPLEX SULFIDE THIN FILMS](#)

Rafael Jaramillo (MIT, MA/USA)

09:00 - 09:30

[\(Invited\) THIN FILM CRYSTAL GROWTH OF OXIDES AND NITRIDES USING HIGH IMPULSE MAGNETRON SPUTTERING](#)

Jon-Paul Maria (North Carolina State University, USA)

09:30 - 10:00

[\(Invited\) FROM PLD TO MBE AND BEYOND: OXIDE EPITAXY AT HIGH TEMPERATURES](#)

Wolfgang Braun (Max Planck Institute for Solid State Research, DE)

08:00 - 10:00

Special Session - George Gilmer I

Wednesday, July 31, 2019

Red Cloud Peak

Moderator(s): Luis Zepeda-Ruiz, USA

08:00 – 08:30

(Invited) INTRODUCTORY REMARKS AND MY HISTORY WITH GEORGE GILMER

Luis Zepeda-Ruiz, USA

08:30 – 09:00

[\(Invited\) KINETIC MONTE CARLO SIMULATIONS OF RESIDUAL STRESS DEVELOPMENT DURING THIN FILM GROWTH](#)

[Eric Chason](#) (Brown U, RI/USA)

09:00 – 09:30

(Invited) SOLID-LIQUID INTERFACIAL FREE ENERGY CALCULATIONS

[Babak Sadigh](#) (Lawrence Livermore National Laboratory, USA)

09:30 - 10:00

[\(Invited\) GROWTH OF CRYSTALLINE NANORODS](#)

[Hanchen Huang](#) (University of North Texas, TX/USA)

10:00 -10:30

BREAK

10:30 - 12:00

Advanced Equipment and Growth Technology

Wednesday, July 31, 2019

Shavano Peak

Moderator(s): Koh Matsumoto, JP; Michael Heuken, DE

10:30 - 11:00

[\(Invited\) MOCVD IN PRODUCTION-TODAY AND FUTURE CHALLENGES](#)

[J Iwan Davies](#) (IQE plc, GB)

11:00 - 11:15

[IN SITU RECONSTRUCTION OF CRYSTAL SHAPE GROWN IN AN AXISYMMETRIC KYROPOULOS SYSTEM](#)

Thierry Duffar (SIMAP EPM, FR)

11:15 - 11:30

[OPTIMAL GROWTH OF YAG SINGLE CRYSTAL FIBER BY MODIFIED LHPG METHOD](#)

Zhitai Jia (Institute of Crystal Materials & State Key Laboratory of Crystal Materials, Shandong University, CN)

11:30 - 11:45

[LOW COST MODIFIED CZOCHRALSKI TECHNIQUE FOR ORGANIC CRYSTALS: GROWTH, CHARACTERIZATION AND APPLICATION](#)

Binay Kumar (UNIVERSITY OF DELHI, IN)

11:45 - 12:00

[FORMATION OF HIERARCHICAL STRUCTURES OF 3,5-DINITROPYRAZINE-2,6-DIAMINE-1-OXIDE WITH POLYMERIC ADDITIVES AND THEIR ENHANCED MECHANICAL PROPERTIES](#)

Xiaoqing Zhou (Institute of Chemical Materials, China Academy of Engineering Physics, CN)

10:30 - 12:00

Fundamentals of Crystal Growth: Surfaces and Interfaces

Wednesday, July 31, 2019

Crestone I, II

Moderator(s): Boaz Pokroy, IL; F. Spaepen, USA

10:30 - 11:00

(Invited) IN SITU OBSERVATIONS OF STEP DYNAMICS ON GROWING INTERFACES BETWEEN ICE AND SUPERCOOLED WATER

Ken-ichiro Murata (Institute of Low Temperature Science, Hokkaido University, JP)

11:00 - 11:15

FUNDAMENTAL STUDY OF METAL ORGANIC CHEMICAL VAPOR DEPOSITION (MOCVD) OF MGF₂

Gary Tompa (Structured Materials Industries, Inc., NJ/USA)

11:15 - 11:30

ARRANGEMENT OF DISLOCATIONS INTO RING CRYSTAL OF TRANSITION METAL TRICHALCOGENIDES

Masakatsu Tsubota (Gakushuin University, JP)

11:30 - 11:45

QUASI-LIQUID LAYERS CAN EXIST ON POLYCRYSTALLINE ICE THIN FILMS AT A TEMPERATURE SIGNIFICANTLY LOWER THAN ON ICE SINGLE CRYSTALS

Jialu Chen (Institute of Low Temperature Science, Hokkaido University, JP)

11:45 - 12:00

STEP BUNCHING INDUCED BY IMPURITIES IN A SURFACE DIFFUSION FIELD

Masahide Sato (Information Media Center, Kanazawa University, JP)

10:30 - 12:00

**Materials for Photovoltaics and Other Energy Technology: Silicon PV
Wednesday, July 31, 2019**

Torreys Peak II-IV

Moderator(s): Jeffrey Derby, USA; Ted Cizek, USA

10:30 - 10:45

[ASSESSMENT OF THE KYROPOULOS PROCESS TO THE SILICON SINGLE CRYSTAL FOR PV APPLICATIONS](#)

Kader Zaidat (SIMaP-EPM laboratory, INP Grenoble Alpes University, FR)

10:45 - 11:00

[INFLUENCE OF THE VERTICAL TEMPERATURE GRADIENT ON THE GROWTH INTERFACE SHAPE, THERMAL STRESS AND IMPURITIES DISTRIBUTION IN DIRECTIONAL SOLIDIFICATION OF MULTICRYSTALLINE SILICON](#)

Carmen Stelian ((Universit e Grenoble Alpes, CNRS, FR)

11:00 - 11:15

[ANALYSIS OF THE ENGULFMENT OF FOREIGN PARTICLES DURING CRYSTAL GROWTH OF SOLAR SILICON](#)

Chung-Hsuan Huang (University of Minnesota, MN/USA)

11:15 - 11:30

[SILICON INGOT GROWTH FROM NIRTIDE CRUCIBLES MADE FROM KERF-LOSS SILICON DURING DIAMOND WIRE SAWING](#)

Hao-Ting Yu (Dept. of Chem. Eng., National Taiwan University, TW)

11:30 - 11:45

[NUMERICAL INVESTIGATION OF SILICON WALL DEPOSITION IN TRICHLOROSILANE FLUIDIZED BED REACTOR](#)

Shaohua Du (Xi'an Jiaotong University, CN)

11:45 - 12:00
LATE NEWS

10:30 - 12:00
Symposium on 2D Materials: Special Topics III: h-BN
Wednesday, July 31, 2019
Crestone III, IV

Moderator(s): Michael Snure, USA; Benjamin Huet, USA

10:30 - 11:00
[\(Invited\) DEFECT-MEDIATED VAN DER WAALS EPITAXY OF H-BN ON EPITAXIAL GRAPHENE](#)

J Marcelo Lopes (Paul-Drude-Institut für Festkörperelektronik, Leibniz-Institut im Forschungsverbund Berlin, DE)

11:00 - 11:30
[\(Invited\) HIGH-TEMPERATURE MOLECULAR BEAM EPITAXY OF HEXAGONAL BORON NITRIDE](#)

Sergei Novikov (School of Physics & Astronomy, University of Nottingham, GB)

11:30 -12:00

(Invited) STUDYING THE GROWTH OF BN NANOMATERIALS
Nicole Grobert (University of Oxford, GB)

10:30 - 12:00
Symposium on Epitaxy of Complex Oxides: Growth of Stannates by MBE
Wednesday, July 31, 2019
Grays Peak II, III

Moderator(s): Yoshiharu Krockenberger, JP

10:30 - 11:00

[\(Invited\) HIGH-MOBILITY HETEROSTRUCTURES WITH \$\text{BASNO}_3\$](#)

Susanne Stemmer (University of California, Santa Barbara, CA/USA)

11:00 - 11:30

[\(Invited\) SUBOXIDE-RELATED KINETICS, THERMODYNAMICS, AND METAL-EXCHANGE CATALYSIS DURING OXIDE MOLECULAR BEAM EPITAXY](#)

Oliver Bierwagen (Paul-Drude-Institut, DE)

11:30 - 12:00

[\(Invited\) RADICAL-BASED MBE APPROACH FOR COMPLEX OXIDE EPITAXY](#)

Bharat Jalan (University of Minnesota, MN/USA)

10:30 - 12:00

**Symposium on Ferroelectric Crystals and Textured Ceramics and Bulk Crystal Growth: Piezoelectric Single Crystal: Growth and Characterization
Wednesday, July 31, 2019
Grays Peak I**

Moderator(s): Alain Morina: Hiroaki Takeda, JP

10:30 - 11:00

[\(Invited\) DEVELOPMENT OF MELILITE-TYPE SINGLE CRYSTALS FOR HIGH TEMPERATURE PIEZOELECTRIC SENSOR](#)

Hiroaki Takeda (Tokyo Institute of Technology, JP)

11:00 - 11:15

INVESTIGATION ON TERAHERTZ TIME-DOMAIN SPECTROSCOPY
IN MIXED RARE EARTH ORTHOFERRITE

Anhua Wu (Shanghai Institute of Ceramics, CAS, CN)

11:15 - 11:30

THE EFFECT OF GAS ATMOSPHERE AND GROWTH PARAMETERS
ON THE CRYSTALS QUALITY OF LANGATATE ($\text{La}_3\text{Ga}_{5.5}\text{Ta}_{0.5}\text{O}_{14}$)
GROWN BY THE CZOCHRALSKI METHOD

Belkacem Boutahraoui (Laboratoire LASICOM, Université Blida1, DZ)

11:30 - 11:45

LATE NEWS

11:45 - 12:00

LATE NEWS

10:30 - 12:00

Special Session - George Gilmer II

Wednesday, July 31, 2019

Red Cloud Peak

Moderator(s): Luis Zepeda-Ruiz, USA

10:30 - 11:00

(Invited) George Gilmer at Colorado School of Mines: Inspiring folks who run uphill

Cristian Ciobanu (Colorado School of Mines, USA)

11:00 - 11:30

(Invited) Impurity-induced step patterns in vapor and solution growth: From step bunches to Supersteps

Madhav Ranganathan (Indian Institute of Technology Kanpur, Kanpur, India)
and J. Weeks (University of Maryland, College Park)

11:30 - 12:00

(Invited) DEVIL'S STAIRCASES: ARE THEY REAL?

Vasily Bulatov (Lawrence Livermore National Laboratory, USA)

12:00 – 17:00

EXCURSIONS

Thursday August 1, 2019

08:30 - 10:00

Plenary Session

Thursday, August 1, 2019

Colorado Rockies Ballroom (Shavano and Red Cloud Peak)

Moderator(s): Peter Schunemann, USA

08:30 - 09:15

(Plenary) ADVANTAGES AND CHALLENGES OF GROWING III-V
PHOTONIC AND ELECTRON

Kei May Lau (Hong Kong University of Science and Technology, HK)

09:15 - 10:00

(Plenary) THEY CALL IT FREE ENERGY SO, HEY, WHY PAY?

Jim De Yoreo (Pacific Northwest National Laboratory, WA/USA)

10:00 - 10:30

BREAK

10:30 - 12:00

Bulk Crystal Growth & Nonlinear Optical Materials I

Thursday, August 1, 2019

Shavano Peak

Moderator(s): Kevin Zawilski, USA; Shekhar Guha, USA

10:30 - 11:00

[\(Invited\) CRYSTAL GROWTH OF TERBIUM-DOPED AND TERBIUM-CONTAINING MATERIALS FOR OPTICAL ISOLATORS AND FLUORESCENCE STANDARDS](#)

[Daniel Rytz](#) (FEE GmbH, DE)

11:00 - 11:15

[LOW TEMPERATURE LIQUID PHASE GROWTH AND TERAHERTZ OPTICAL PROPERTIES OF VAN DER WAALS CRYSTAL INSE](#)

[Chao Tang](#) (Tohoku University, JP)

11:15 - 11:30

[MULTISCALE CHARACTERIZATION OF THE POINT DEFECT AND ROTATIONAL DISORDERS IN TWO NEW HIGH-TEMPERATURE SOLUTION GROWN RARE-EARTH BORATES \(ORAL PRESENTATION\)](#)

[Matias Velazquez](#) (SIMaP UMR 5266 CNRS-UGA-G INP, FR)

11:30 - 11:45

[GROWTH OF LARGE APERTURE YCOB CRYSTAL FOR OPCPA APPLICATION](#)

[Xiaoniu Tu](#) (Shanghai institute of ceramics, CN)

11:45 - 12:00

[CRYSTAL GROWTH AND OPTIMIZATION OF RE³⁺ DOPED CAGDALO₄ DISORDERED CRYSTALS](#)

Qiangqiang Hu (Institute of Crystal Materials, Shandong University, CN)

10:30 - 12:00

Characterization Techniques for Bulk and Epitaxial Crystals I
Thursday, August 1, 2019
Crestone III, IV

Moderator(s): Michael Dudley, USA ; Balaji Raghothamachar, USA

10:30 - 11:00

[\(Invited\) STRAIN IMAGING WITH NANOSCALE BRAGG DIFFRACTION MICROSCOPY](#)

Martin Holt (Argonne National Laboratory, IL/USA)

11:00 - 11:30

[\(Invited\) GaP LAYERS GROWN ON SI\(001\): HOW CROSS-SECTION SCANNING TUNNELING MICROSCOPY ALLOWS FOR ACCESSING THE ATOMIC STRUCTURES](#)

Andrea Lenz (TU Berlin, DE)

11:30 - 11:45

[CHARACTERIZATION OF DEFECTS IN GAAS SUBSTRATES AND EPITAXIAL WAFERS BY SYNCHROTRON X-RAY TOPOGRAPHY](#)

Hongyu Peng (Department of Materials Science and Chemical Engineering, Stonybrook University, NY/USA)

11:45 - 12:00

LATE NEWS

10:30 - 12:00

Hetero-Epitaxy of III-V on Silicon

Thursday, August 1, 2019

Red Cloud Peak

Moderator(s): Kei May Lau, HK; Shadi Shahedipour-Sandvik, USA

10:30 - 11:00

[\(Invited\) SELECTIVE AREA EPITAXY OF III-V NANOSTRUCTURES AND THIN FILMS FOR INTEGRATED DEVICE PLATFORMS](#)

Qiang Li (Cardiff University, GB)

11:00 - 11:15

[UNDERSTANDING THREADING DISLOCATIONS IN III-ARSENIDE HETEROSTRUCTURES ON SILICON: RECOMBINATION-ENHANCED GLIDE AND PIPE DIFFUSION](#)

Kunal Mukherjee (University of California Santa Barbara, CA/USA)

11:15 - 11:30

[CORRELATION OF MOCVD PROCESS CONDITIONS AND DEFECT EVOLUTION OF GAP/SI HETEROSTRUCTURES VIA ELECTRON CHANNELING CONTRAST IMAGING](#)

Jacob Boyer (Ohio State University, OH/USA)

11:30 - 11:45

[NUCLEATION OF GAP ON V-GROOVED SI SUBSTRATES](#)

Emily Warren (National Renewable Energy Lab, CO/USA)

11:45 - 12:00

[DEFECT ENGINEERING FOR INP EPITAXIALLY GROWN ON \(001\) SI](#)

[BY MOCVD](#)

Bei Shi (University of California, Santa Barbara, CA/USA)

10:30 - 12:00

In Situ Observation and Characterization, I

Thursday, August 1, 2019

Grays Peak I

Moderator(s): M. J. Highland, USA

10:30 - 11:00

[\(Invited\) COHERENT X-RAY MEASUREMENT OF LOCAL STEP-FLOW PROPAGATION DURING GROWTH ON POLYCRYSTALLINE ORGANIC SEMICONDUCTOR THIN FILM SURFACES](#)

Randall Headrick (Department of Physics and Materials Science Program, University of Vermont, VT/USA)

11:00 - 11:30

[\(Invited\) USING HIGH-SPEED, MOLECULARLY-RESOLVED AFM TO INVESTIGATE SOLUTION STRUCTURE AND NUCLEATION AT CRYSTAL SURFACES](#)

Jim De Yoreo (Pacific Northwest National Laboratory, WA/USA)

11:30 - 11:45

[ATOMIC-SCALE VISUALIZATION OF ION BEHAVIOR ON CLAY MINERALS](#)

Yuki Araki (Ritsumeikan University, JP)

11:45 - 12:00

[STEP-SPECIFIC LIGAND INTERACTIONS CONTROL CRYSTALLIZATION OF METAL-ORGANIC FRAMEWORK](#)

HETEROSTRUCTURES

Jinhui Tao (Pacific Northwest National Laboratory, WA/USA)

10:30 - 12:00

Modeling of Crystal Growth Processes III

Thursday, August 1, 2019

Crestone I, II

Moderator(s): Vladimir Kalaev, RU; Lili Zheng, CN

10:30 - 11:00

(Invited) NUMERICAL STUDIES ON OXYGEN TRANSFER IN SI MELT UNDER INHOMOGENEOUS MAGNETIC FIELDS OF TMCZ CONDITION USING A GLOBAL MODEL

Koichi Kakimoto (Research Institute for Applied Mechanics, Kyushu University, JP)

11:00 - 11:15

OPTIMAL ROTATION SPEED AND CONVECTIVE THERMAL INSTABILITIES IN THE SAPPHIRE MELT UNDER THE CZOCHRALSK GROWTH PROCESS

Derradji Bahloul (University of Batna 1, DZ)

11:15 - 11:30

NUMERICAL MODELING OF MELT CONVECTION AND OXYGEN TRANSPORT IN A CZOCHRALSKI PROCESS FOR SOLAR SILICON GROWTH

Daniel Vizman (West University of Timisoara, RO)

11:30 - 11:45

TRANSIENT GLOBAL MODELING FOR THE PULLING PROCESS OF

[CZOCHELSKI SILICON CRYSTAL GROWTH. II. INVESTIGATION ON SEGREGATION OF OXYGEN AND CARBON](#)

Xin Liu (Research Institute for Applied Mechanics, Kyushu University, JP)

11:45 - 12:00

[LIMITATIONS OF THE GROWTH RATE DURING PULLING OF LARGE DIAMETER SILICON CRYSTALS BY THE CZOCHELSKI TECHNIQUE](#)

Jochen Friedrich (Fraunhofer IISB, DE)

10:30 - 12:00

Materials for Novel Energy Technologies
Thursday, August 1, 2019
Torreys Peak II-IV

Moderator(s): Ryan France, USA; Shujun Zhang, AU

10:30 - 10:45

[METAL OXIDE - CARBON COMPOSITE NANOFIBERS FOR ADVANCED LITHIUM STORAGE](#)

Somchate Wasantwisut (Dept. of Chemical and Environmental Engineering, University of California at Riverside, CA/USA)

10:45 - 11:00

[INFLUENCE OF HYDROTHERMALLY SYNTHESIZED TITANIUM DIOXIDE NANORODS/NANOPARTICLES IN DYE-SENSITIZED SOLAR CELL](#)

Rajamanickam Govindaraj (SSN College of Engineering, IN)

11:00 - 11:15

[CRYSTAL GROWTH AND OCTAHEDRA TILTING OF \$\text{BAZRS}_3\$ AND](#)

ITS RUDDLESDEN-POPPER PHASES

Shanyuan Niu (University of Southern California, CA/USA)

11:15 - 11:30

DOPED SINGLE CRYSTAL AND CERAMIC OF KNN BASED COMPOUNDS: AN INVESTIGATION TO FIND NEW GREEN FRIENDLY MATERIAL FOR PIEZOELECTRIC DEVICE APPLICATION

ANA MARIA Santo (Universidade Federal de São Paulo, BR)

11:30 - 11:45

CRYSTAL GROWTH AND CHARACTERIZATION OF $\text{CH}_3\text{NH}_3\text{PBBR}_3$ SINGLE-CRYSTALS FOR X-RAY PHOTODETECTION

Smaïl Amari (CEA, FR)

11:45 - 12:00

EXPERIMENTS ON SURFACE WAVE EXCITATION BY ELECTROMAGNETIC FIELD

Mikus Milgravis (University of Latvia, LV)

10:30 - 12:00

Symposium on Epitaxy of Complex Oxides: Substrates for Complex Oxide Films

Thursday, August 1, 2019

Grays Peak II, III

Moderator(s): Wolfgang Braun, DE

10:30 - 11:00

(Invited) 27 YEARS OF PROGRESS IN PEROVSKITE-TYPE SUBSTRATE CRYSTAL GROWTH AT THE IKZ

Christo Gugushev (Leibniz Institute for Crystal Growth, DE)

11:00 - 11:30

(Invited) CONGRUENTLY MELTING PEROVSKITE SOLID SOLUTIONS

Vincent Fratello (Quest Integrated, LLC, WA/USA)

11:30 - 12:00

(Invited) SPINEL FERRITE THIN FILMS AND HETEROSTRUCTURES FOR SPINTRONICS

Arunava Gupta (The University of Alabama, AL/USA)

12:00 - 13:30

LUNCH, IOCG GENERAL SESSION

13:30 - 15:00

Bulk Crystal Growth & Nonlinear Optical Materials II

Thursday, August 1, 2019

Shavano Peak

Moderator(s): Yushi Kaneda, JP; Adam Lindsey, USA

13:30 - 13:45

IMPLEMENTATION OF ACCELERATED CRUCIBLE ROTATION TECHNIQUE IN CZOCHRALSKI GROWTH OF ND:YAG SINGLE CRYSTALS: MODIFYING ND CONCENTRATION AND SEGREGATION

Muad Saleh (Washington State University, WA/USA)

13:45 - 14:00

GROWTH OF RARE-EARTH DOPED YTTRIUM ALUMINUM GARNET SINGLE CRYSTAL FIBERS

Subhabrata Bera (National Energy Technology Laboratory, PA/USA)

14:00 - 14:15

[PARTITIONING OF MG INTO LI AND NB SITES IN \$\text{LiNbO}_3\$ CRYSTAL DURING GROWTH FROM THE MELT](#)

Satoshi Uda (Tohoku University, JP)

14:15 - 14:30

[CRYSTALLINE GROWTH UNDER ELECTRIC FIELD: TOWARD A NEW ROUTE TO DESIGN DOMAIN MODULATED-STRUCTURES.](#)

Raphael Haumont (Paris-Saclay University - ICMMO SP2M, FR)

14:30 - 14:45

[GROWTH OF THE OPTICAL PERFECT \$\text{LiNbO}_3\$ CRYSTALS](#)

Victoria Sanina (RCTU Mendeleevs, RU)

14:45 - 15:00

[CRYSTAL GROWTH OF QUATERNARY CHALCOGENIDE MID-IR NONLINEAR OPTICAL MATERIALS: AGGS AND AGGSE](#)

Wei Huang (Sichuan University, CN)

13:30 - 15:00

Characterization Techniques for Bulk and Epitaxial Crystals II
Thursday, August 1, 2019
Crestone III, IV

Moderator(s): Mark Goorsky, USA; Holger Eisele, DE

13:30 - 14:00

[\(Invited\) REDUCTION OF THREADING DISLOCATION DENSITY IN](#)

[HIGH-TEMPERATURE ANNEALED ALN ON SAPPHIRE TEMPLATES](#)

Hideto Miyake (Graduate School of Regional Innovation Studies, Mie University, JP)

14:00 - 14:15

[A FUNDAMENTAL STUDY ON SUBSTRATE-INDUCED EPITAXIAL TILT USING HIGH-RESOLUTION X-RAY DIFFRACTION METHODS](#)

Michael Liao (University of California Los Angeles, CA/USA)

14:15 - 14:30

[CHARACTERIZATION OF LINEAGES WITH DISLOCATIONS IN CZOCHRALSKI-GROWN \$\text{LiTaO}_3\$ INGOTS BY DIFFERENTIAL INTERFERENCE CONTRAST MICROSCOPY OF ETCH PITS](#)

Yutaka Ohno (Institute for Materials Research, Tohoku University, JP)

14:30 - 14:45

[DETERMINATION OF AL CONTENT IN AL/SI THERMOMIGRATION FABRICATED STRUCTURES BY X-RAY DIFFRACTION](#)

Boris Seredin (Platov South-Russian State Polytechnic University (NPI), RU)

14:45 - 15:00

[MORE INSIGHTS IN SEMICONDUCTOR MATERIAL QUALITY WITH ADVANCED X-RAY TOPOGRAPHY IMAGING](#)

Jochen Friedrich (Fraunhofer IISB, DE)

13:30 - 15:00

III-V Nano-Devices on Silicon

Thursday, August 1, 2019

Red Cloud Peak

Moderator(s): Bernardette Kunert, BE; Quang Li, Cardiff University, UK

13:30 - 14:00

[\(Invited\) MONOLITHIC INTEGRATION OF GAAS-\(IN,AL\)GAAS BASED NANOWIRE LASERS ON SILICON](#)

Gregor Koblmüller (Walter Schottky Institut, DE)

14:00 - 14:15

[INGAAS NANO-RIDGE ENGINEERING TOWARDS NOVEL III/V DEVICE INTEGRATION ON PATTERNED 300 MM SI SUBSTRATES](#)

Bernardette Kunert (Imec, BE)

14:15 - 14:30

[GROWTH OF GaSb NANO-RIDGES ON PATTERNED 300 MM SI WAFERS](#)

Marina Baryshnikova (Imec, BE)

14:30 - 14:45

[ADVANCED INTEGRATION OF III-V NANOWIRES OPTICAL INTERCONNECTS ON \(100\) SILICON-ON-INSULATOR](#)

Ting-Yuan Chang (University of California, Los Angeles, USA)

14:45 - 15:00

Late News

13:30 - 15:00

In Situ Observation and Characterization II

Thursday, August 1, 2019

Grays Peak I

Moderator(s): Jim DeYoreo, USA

13:30 - 13:45

[STEP DYNAMICS DURING HOMOEPITAXIAL GROWTH OBSERVED WITH IN SITU X-RAY PHOTON CORRELATION SPECTROSCOPY \(XPCS\)](#)

Irene Calvo Almazan (Argonne National Laboratory, IL/USA)

13:45 - 14:00

[IN SITU OBSERVATION OF THE SOLIDIFICATION INTERFACE AND GRAIN BOUNDARY DEVELOPMENT OF TWO SILICON SEEDS WITH SIMULTANEOUS MEASUREMENT OF TEMPERATURE PROFILE AND UNDERCOOLING](#)

Victor Lau Jr (National Taiwan University, TW)

14:00 - 14:15

[STEP-EDGE DIFFUSION BARRIERS STUDIED BY IN SITU SURFACE X-RAY SCATTERING DURING OMVPE OF GAN](#)

Gregory Stephenson (Argonne National Laboratory, IL/USA)

14:15 - 14:45

[\(Invited\) IN-SITU OPTICAL MICROSCOPIC OBSERVATION OF ICE CRYSTAL SURFACES](#)

Gen Sazaki (Institute of Low Temperature Science, Hokkaido University, JP)

14:45 - 15:00

[IN SITU DIAGNOSTICS OF MELTING/SOLIDIFICATION AND SEGREGATION DURING CRYSTAL GROWTH PROVIDED BY ENERGY RESOLVED NEUTRON IMAGING](#)

Anton Tremsin (University of California, CA/USA)

13:30 - 15:00

Modeling of Crystal Growth Processes IV
Thursday, August 1, 2019
Crestone I, II

Moderator(s): Simon Brandon, IL; Moneesh Upmanyu, USA

13:30 - 14:00

[\(Invited\) SURFACE REHYBRIDIAZTION AND STRAIN EFFECTS ON THE COMPOSITION AND THE PROPERTIES OF TERNARY III-NITRIDE ALLOYS.](#)

Liverios Lymperakis (Max-Planck-Institut für Eisenforschung GmbH, DE)

14:00 - 14:15

[AB INITIO ATOMISTIC THERMODYNAMICS OF HOT GAN SURFACES](#)

Pawel Kempisty (Institute of High Pressure Physics PAS, PL)

14:15 - 14:30

[ATOMIC SIMULATION OF CARBON SOLUBILITY IN LIQUID SILICON](#)

Jinping Luo (Xi'an Jiaotong University, CN)

14:30 - 14:45

[THERMODYNAMICS OF VAPOR-SURFACE EQUILIBRIA IN *AB INITIO* MODELLING OF SEMICONDUCTOR GROWTH PROCESSES](#)

Stanislaw Krukowski (Institute of High Pressure Physics PAS, PL)

14:45 - 15:00

[FREE ENERGY OF SILICON CARBIDE PARTICLE NUCLEATION IN CARBON-CONTAINING SILICON MELTS](#)

Abdullah Alateeqi (Department of Chemical and Biomolecular Engineering, University of Pennsylvania, PA/USA)

13:30 - 15:00

III-V Solar Cells

Thursday, August 1, 2019

Torreys Peak II-IV

Moderator(s): Christopher Pinzone, USA; Amy Liu, USA

13:30 - 14:00

[\(Invited\) GRADED BUFFER BRAGG REFLECTORS FOR METAMORPHIC SOLAR CELLS](#)

Ryan France (National Renewable Energy Laboratory, USA)

14:00 - 14:15

[OMPVE GROWTH OF SIX-JUNCTION INVERTED SOLAR CELLS](#)

John Geisz (National Renewable Energy Laboratory, CO/USA)

14:15 - 14:30

[ANALYSIS ON RELATIONS BETWEEN ELECTRICAL CHARACTERISTICS AND MISFIT DISLOCATIONS OF METAMORPHIC SINGLE JUNCTION SOLAR CELLS](#)

Akio Ogura (Japan Aerospace Exploration Agency, JP)

14:30 - 14:45

[HIGH GROWTH RATE \$\text{In}_x\text{Ga}_{1-x}\text{As}\$ METAMORPHIC BUFFER LAYERS BY OMVPE](#)

Kaddour Lekhal (University of Wisconsin-Madison, WI/USA)

14:45 - 15:00

[SINGLE-CRYSTAL-LIKE GaAs THIN-FILM SOLAR CELLS DIRECTLY](#)

ON FLEXIBLE METAL TAPES

Jae-Hyun Ryou (University of Houston, TX/USA)

13:30 - 15:00

Symposium on Epitaxy of Complex Oxides: Ruthenates

Thursday, August 1, 2019

Grays Peak II, III

Moderator(s): Bharat Jalan, USA

13:30 - 14:00

(Invited) EMERGENCE OF ROBUST 2D SKYRMIONS IN SRRUO₃ ULTRATHIN FILM

Bongju Kim (Center for Correlated Electron Systems, Institute for Basic Science, KR)

14:00 - 14:30

(Invited) REALIZATION OF HORIZONTAL AND VERTICAL INTERFACES IN RUTHENATE EPITAXIAL THIN FILMS

Woo Seok Choi (Sungkyunkwan University, KR)

14:30 - 14:45

DEMYSTIFYING THE GROWTH OF SUPERCONDUCTING SR₂RUO₄ THIN FILMS

Hari Nair (Cornell University, NY/USA)

14:45 - 15:00

GROWTH OF HETEROSTRUCTURES OF FERROMAGNETIC SRRUO₃ AND SUPERCONDUCTING SR₂RUO₄ BY MOLECULAR-BEAM EPITAXY

Nathaniel Schreiber (NY/USA)

15:00 - 15:30

BREAK

15:30 - 17:30

Characterization Techniques for Bulk and Epitaxial Crystals III

Thursday, August 1, 2019

Crestone III, IV

Moderator(s): Hideto Miyake, JP; Motoaki Iwaya,JP

15:30 - 16:00

(Invited) [MULTIPHOTON-EXCITATION PHOTOLUMINESCENCE:
NOVEL NONDESTRUCTIVE DEFECT CHARACTERIZATION
TECHNOLOGY](#)

Tomoyuki Tanikawa (Osaka University, JP)

16:00 - 16:15

[SHALLOW DONOR COMPLEXES IN ZNO CONTAINING SN AND LI
STUDIED BY PHOTOLUMINESCENCE SPECTROSCOPY AND
DENSITY FUNCTIONAL THEORY](#)

Manu Hegde (Department of Physics, Simon Fraser University, BC/Ca)

16:15 - 16:30

[EFFECT OF DOPING IN RARE EARTH ORTHOFERRITE SINGLE
CRYSTALS](#)

Suja Saji (Indian Institute of science , IN)

16:30 - 16:45

LATE NEWS

16:45 - 17:00
LATE NEWS

17:00 - 17:15
LATE NEWS

17:15 - 17:30
LATE NEWS

15:30 - 17:30
Bulk Crystal Growth: Focus on Oxides
Thursday, August 1, 2019
Shavano Peak

Moderator(s): Robert Kral, CZ; Jiaqiang Yan, USA

15:30 - 15:45
[ADVANCES IN THE GROWTH OF A- \$\text{GeO}_2\$ CRYSTALS BY TOP SEEDED SOLUTION GROWTH](#)

[Alexandra Pena Revellez](#) (Institut Néel - CNRS/UGA, FR)

15:45 - 16:00
[FABRICATION OF SPRING SINGLE CRYSTALS USING MODIFIED MICRO-PULLING-DOWN METHOD WITH THREE-DIMENSIONAL CONTROL SYSTEM](#)

[Yuui Yokota](#) (Tohoku University, JP)

16:00 - 16:15
[ADDRESSING SURFACE DEFECTS IN EFG-GROWN SAPPHIRE SINGLE CRYSTALS](#)

[Nathan Stoddard](#) (II-VI Optical Systems, PA/USA)

16:15 - 16:30

[IMPACT OF THE CRYSTAL TECHNOLOGY AND SEED ON THE BUBBLES AND STRAIN DISTRIBUTION](#)

[Rekia Bouaita](#) (Institut Lumière Matière, FR)

16:30 - 16:45

[GROWTH OF \$\text{BaSnO}_3\$ SINGLE CRYSTALS FOR WIDE BANDGAP APPLICATIONS](#)

[Joseph Kolis](#) (Clemson University, SC/USA)

16:45 - 17:00

[MECHANICAL PROPERTIES AND DISLOCATIONS NUMERICAL MODELING FOR \$\text{Li}_2\text{MOO}_4\$ CRYSTAL GROWTH](#)

[Abdelmounaim Ahmine](#) (CNRS-SIMAP, FR)

17:00 - 17:15

[GROWTH OF HIGH QUALITY \$\text{Li}_2\text{B}_4\text{O}_7\$ SINGLE CRYSTALS: CORE DEFECT FORMATION REVISITED](#)

[Jose Luis Plaza](#) (Universidad Autonoma de Madrid, ES)

17:15 - 17:30

GROWTH OF LARGE DIAMETER UNDOPED AND RARE EARTH DOPED YTTRIUM ALUMINIUM GARNET (YAG) CRYSTALS BY MODIFIED CZOCHRALSKI METHOD

[Jan Polák](#) (CRYTUR, CZ)

15:30 - 17:30

Fundamentals of Crystal Growth: Crystallization from Melt

Thursday, August 1, 2019

Crestone I, II

Moderator(s): Baron Peters, USA; Jim DeYoreo, USA

15:30 - 16:00

[\(Invited\) CRYSTAL GROWTH OF QUASICRYSTALS](#)

[An-Pang Tsai](#) (Institute of Multidisciplinary Research for Advanced Materials, Tohoku University, JP)

16:00 - 16:15

[CAPILLARY-MEDIATED INTERFACE FIELDS](#)

[Martin Glicksman](#) (Florida Institute of Technology, FL/USA)

16:15 - 16:30

[INVESTIGATION OF SOLUTO-CAPILLARY CONVECTION IN \$Ge_xSi_{1-x}\$ MELTS](#)

[Jan Philipp Wöhrle](#) (Crystallography - Albert-Ludwigs-University Freiburg, DE)

16:30 - 16:45

[ANALYSIS AND IN-SITU OBSERVATION OF SOLID-STATE DIFFUSION IN MELT CRYSTAL GROWTH](#)

[Kerry Wang](#) (University of Minnesota, MN/USA)

16:45 - 17:00

[THE EFFECT OF GRAIN BOUNDARIES ON INSTABILITY AT THE CRYSTALMELT INTERFACE DURING THE UNIDIRECTIONAL GROWTH OF SI](#)

[Kuan-Kan Hu](#) (Institute for Material Research, JP)

17:00 - 17:15

[TWIN BOUNDARY FORMATION DEPENDING ON CRYSTAL/LIQUID INTERFACE MORPHOLOGY IN LITHIUM TETRABORATE](#)

Kensaku Maeda (Institute for materials research, Tohoku University, JP)

17:15 - 17:30

[COHERENT NANOPRECIPITATES WITHIN SINGLE CRYSTALS: FROM CHARACTERIZATION TO UNRAVELING THE MECHANISM OF FORMATION](#)

Boaz Pokroy (Technion Institute of Technology, Il)

15:30 - 17:30

In Situ Observation and Characterization III

Thursday, August 1, 2019

Grays Peak I

Moderator(s): Tsukamoto Katsuo, JP

15:30 - 15:45

[IN SITU OBSERVATION OF CRYSTALLIZATION OF A SALT USING AN ANTISOLVENT BY TRANSMISSION ELECTRON MICROSCOPY](#)

Tomoya Yamazaki (Institute of Low Temperature Science, Hokkaido University, JP)

15:45 - 16:00

[MANIPULATION OF ACETAMINOPHEN CRYSTALLIZATION AND DISCOVERY OF TWO-STEP DISSOLUTION PROCESS BY PLASMONIC OPTICAL TWEEZERS](#)

Hiromasa Niinomi (Institute for Materials Research, Tohoku University, JP)

16:00 - 16:15

[IN-SITU OBSERVATION OF PHASE TRANSITION OF ASPIRIN FORM](#)

II

Yuka Tsuru (Osaka Univ., JP)

16:15 - 16:30

[IN-SITU CURVATURE MONITORING OF ALINN/GAN DBRS](#)

Kei Hiraiwa (Meijo University, JP)

16:30 - 16:45

[VIRTUAL VISUALIZATION SYSTEM FOR INNER STATE IN HIGH-TEMPERATURE SOLUTION GROWTH USING PREDICTION MODEL OF COMPUTATIONAL FLUID DYNAMICS CONSTRUCTED BY MACHINE LEARNING](#)

Toru Ujihara (Graduate School of Engineering and School of Engineering, Nagoya University, JP)

16:45 - 17:00

[IDENTIFICATION OF MICRO CRYSTALS AND VISUALIZATION OF ORGANIC COMPONENTS IN KIDNEY STONES -FOR THE ELUCIDATION OF THE FORMATION MECHANISM OF KIDNEY STONES-](#)

Mihoko Maruyama (Osaka University, JP)

17:00 - 17:15

[HARD X-RAY INSTRUMENTATION FOR *IN SITU* SYNCHROTRON NANOBEAM DIFFRACTION AND COHERENT SCATTERING STUDIES OF COMPLEX OXIDE SOLID PHASE EPITAXY](#)

Samuel Marks (University of Wisconsin, WI/USA)

17:15 - 17:30

[IN SITU NANOCRYSTALLOGRAPHICAL CHARACTERIZATION](#)

STUDIES WITH THE USE OF X-RAY SCATTERING TECHNIQUES

Hans Te Nijenhuis (Malvern Panalytical, NI)

15:30 - 17:30

PV Materials

Thursday, August 1, 2019

Torreys Peak II-IV

Moderator(s): Kevin Schulte, USA; Hoe Tan, AU

15:30 - 16:00

(Invited) FUNDAMENTALS OF COALESCENCE-RELATED DISLOCATIONS

Bill McMahon (National Renewable Energy Laboratory, CO/USA)

16:00 - 16:30

(Invited) STRAIN-BALANCE QUANTUM WELL SOLAR CELLS

NED Ekins-Daukes (University of New South Wales, AU)

16:30 - 16:45

CONTEMPORARY SOLAR CELL BASED ON PEROVSKITE IMPROVEMENTS

Oleg Rabinovich (NUST MISIS, RU)

16:45 - 17:00

III-V SOLAR CELLS ON SPALLED AND POROUS GE FOR SUBSTRATE REUSE

Alessandro Cavalli (NREL, CO/USA)

17:00 - 17:15

POLYCRYSTALLINE CUGASE₂ THIN-FILM GROWTH ON SAPPHIRE
OR ZIRCONIA SUBSTRATES WITH ALKALI-METAL DOPING

Shogo Ishizuka (AIST, JP)

17:15 - 17:30
LATE NEWS

15:30 - 17:30

**Symposium on Epitaxy of Complex Oxides: Superlattices
Thursday, August 1, 2019
Grays Peak II, III**

Moderator(s): Guus Rijnders

15:30 – 16:00
(Invited) PICOSCIENCE OF CHARGE-TRANSFER OXIDE
HETEROSTRUCTURES

Fred Walker (Yale University, CT/USA)

16:00 – 16:30
(Invited) CREATING NEW ANTIFERROELECTRIC MATERIALS
USING INTERFACIAL ELECTROSTATIC ENGINEERING

Julia Mundy (University of California, Berkeley, CA/USA)

16:30 – 17:00
(Invited) COMBINING OXIDE EPITAXY AND TOPOCHEMISTRY:
FROM ELECTRON-DOPED MANGANITES TO LATERAL ANIONIC
HETEROSTRUCTURES

Steven May (Drexel University, PA/USA)

17:00 - 17:15

[EFFECTIVE DIMENSIONALITY-TUNED ELECTRONIC STATES IN METASTABLE NICKEL OXIDE THIN FILMS](#)

Grace Pan (Harvard University, MA/USA)

17:15 – 17:30

[A SUPERLATTICE APPROACH TO ANALYZE THE X-RAY DIFFRACTION OF RUDDLESDEN-POPPER FILMS](#)

Matthew Barone (Cornell University, NY/USA)

15:30 - 17:30

Selective and Patterned Epitaxial Growth

Thursday, August 1, 2019

Red Cloud Peak

Moderator(s): Yuji Zhao, USA; Jung Han, USA

15:30 - 16:00

[\(Invited\) SELECTIVE AREA REGROWTH AND DOPING OF GAN](#)

Jung Han (Yale University, CT/USA)

16:00 - 16:15

[EFFECT OF GROWTH AND PATTERNING CONDITIONS ON AIR-HOLE CHARACTERISTICS IN GAAS-BASED PATTERNED EPITAXIAL GROWTH FOR PHOTONIC CRYSTAL SURFACE EMITTING LASERS \(PCSELS\)](#)

Sadhvikas Addamane (Center for High Tech Materials, NM/USA)

16:15 - 16:30

[ZNO NANORODS GROWN FROM SOLUTIONS ON PATTERNED SUBSTRATES](#)

Jan Grym (Institute of Photonics and Electronics of the CAS, CZ)

16:30 - 17:00

[SELECTIVE AREA GROWTH OF III-V SEMICONDUCTOR NANOSTRUCTURES](#)

Chris Palmstrom (University of California, Santa Barbara, CA/USA)

17:00 - 17:15

[EFFECTIVE SELECTIVE AREA DOPING FOR GAN VERTICAL POWER TRANSISTORS ENABLED BY EPITAXIAL REGROWTH](#)

Houqiang Fu (Arizona State University, AZ/USA)

17:15 - 17:30

LATE NEWS

18:00 - 21:30

BANQUET RECEPTION AND BANQUET

Friday, August 2, 2019

08:00 - 10:00

Biological and Biomimetic Materials I

August 2, 2019

Grays Peak I

Moderator(s): Wei Huang, CN; David Kisailus, USA

08:00 - 08:30

[\(Invited\) ENERGETICS OF AMELOGENIN VARIANTS BINDING TO HYDROXYAPATITE](#)

Jinhui Tao (Pacific Northwest National Laboratory, WA/USA)

08:30 - 08:45

[OCTACALCIUM PHOSPHATE FORMATION AND ENHANCES ITS LAYER STRUCTURE IN THE SYSTEMS OF NA-NH₄](#)

Yuki Sugiura (National Institute of Advanced Industrial Science and Technology, JP)

08:45 - 09:00

[FORMATION OF CALCIUM PHOSPHATES IN SIMULATED BODY FLUID WITH CALCITE CRYSTAL](#)

Hiroki Saito (Department of Physical Sciences, Ritsumeikan University, JP)

09:00 - 09:15

[MULTISCALE TOUGHENING IN ORIENTED ATTACHED BIOLOGICAL NANOCRYSTALLINE HYDROXYAPATITE](#)

Wei Huang (Sichuan University, CN)

09:15 - 09:30

[ORIENTED CRYSTALLIZATION OF BIOGENIC STRONTIUM SULFATE SINGLE CRYSTALS](#)

Vivian Merk (Florida Atlantic University, FL/USA)

09:30 - 09:45

[BIOLOGICAL CRYSTALLIZATION OF ULTRAHARD TEETH AND TRANSLATION TO MULTI-FUNCTIONAL MATERIALS](#)

David Kisailus (Department of Chemical and Environmental Engineering, University of California at Riverside, CA/USA)

09:45 - 10:00

[TOWARDS THE UNDERSTANDING OF MORPHOLOGY CONTROL IN](#)

MAGNETITE BIOMINERALIZATION

Anna Pohl (Max Planck Institute of Colloids and Interfaces, Potsdam, DE)

08:00 - 10:00

Bulk Crystal Growth: Other Materials

August 2, 2019

Shavano Peak

Moderator(s): Christo Gugushev, DE; Luis Stand, USA

08:00 - 08:15

COOLING RATE DEPENDENCE ON MICROSTRUCTURES AND MECHANICAL PROPERTIES OF CO-CR-MO ALLOY FIBERS FABRICATED BY UNIDIRECTIONAL SOLIDIFICATION

Shoki Abe (Institute for Material Research, JP)

08:15 - 08:30

CHIRAL IDENTIFICATION AND CHIRAL CRYSTAL GROWTH OF DIFFICULT ORGANIC MOLECULES

Colin McMillen (Clemson University, USA)

08:30 - 08:45

TERNARY PHASE DIAGRAM STUDIES AND SINGLE CRYSTAL GROWTH OF SOLID SOLUTIONS IN THE GA-PD-SN SYSTEM FOR BASIC RESEARCH IN HETEROGENEOUS CATALYSIS

Kristian Bader (Crystallography Section, Ludwig-Maximilians-Universität München, DE)

08:45 - 09:00

LARGE-SIZED CRYSTAL GROWTH OF $\text{BaCd}(\text{VO})(\text{PO}_4)_2$ AND $\text{Pb}_2(\text{VO})(\text{PO}_4)_2$ BY THE

SELF-FLUX BRIDGMAN METHOD

Zewu Yan (ETH Zurich, CH)

09:00 - 09:15

AQUEOUS SOLUTION GROWTH AT 200°C AND
CHARACTERIZATIONS OF PURE, ¹⁷O- AND D-BASED
HERBERTSMITHITE $ZnCu_3(OH)_6Cl_2$ SINGLE CRYSTALS

Matias Velazquez (SIMaP UMR 5266 CNRS-UGA-G INP, FR)

09:15 - 09:30

ELECTROPHYSICAL PROPERTIES OF GA_{0.03}IN_{0.97}SB SINGLE
CRYSTALS GROWN IN ULTRASONIC FIELD

Gennadiy Kozhemyakin (Shubnikov Institute of Crystallography of Federal Scientific Research Center “Crystallography and Photonics” of Russian Academy of Sciences, RU)

09:30 - 09:45

GROWTH FROM THE MELT, STRUCTURE AND PROPERTIES OF
(ZRO₂)_{1-x}(GD₂O₃)_xSOLID SOLUTION CRYSTALS

Alexey Kulebyakin (Prokhorov General Physics Institute of the Russian Academy of Sciences, RU)

09:45 - 10:00

EFFECT OF GROWTH AMBIENCE AND STUDIES ON HEXAGONAL
DY_(1-x)Y_(x)MNO₃SINGLE CRYSTALS

Anandha Babu Govindan (SSN College of Engineering, IN)

08:00 - 10:00

**Fundamentals of Crystal Growth: Colloids and Crystal Growth in
Solution**

August 2, 2019

Torreys Peak II-IV

Moderator(s): Peter Vekilov, USA; Mu Wang, CN

08:00 - 08:30

[\(Invited\) NUCLEATION, GROWTH AND PERFECTION OF COLLOIDAL CRYSTALS](#)

Frans Spaepen (School of Engineering and Applied Sciences, Harvard University, USA)

08:30 - 08:45

[ANALYSIS OF DIFFUSIONLESS TRANSFORMATIONS IN COLLOIDAL CRYSTALLITES](#)

Talid Sinno (University of Pennsylvania, USA)

08:45 - 09:00

[GROWTH MECHANISM OF BINARY COLLOIDAL CRYSTALS](#)

Jun Nozawa (Institute for Materials Research, Tohoku University, JP)

09:00 - 09:15

[THE ATOMIC SCALE MECHANISM OF GROWTH ADDITIVES FOR NaCl](#)

Elias Vlieg (Radboud University, Institute for Molecules and Materials, NL)

09:15 - 09:30

[MONONUCLEAR AND POLYNUCLEAR GROWTH OF ELECTROLYTE CRYSTALS FROM SOLUTION](#)

Hans Erik Lundager Madsen (Chemistry Department, University of Copenhagen, DK)

09:30 - 09:45

OBSERVATION OF SOLUTION STRUCTURES AND SUPERCOOLING SUPPRESSION IN SEMICLATHRATE HYDRATE RECRYSTALLIZATION

Takeshi Sugahara (Osaka University, JP)

09:45 - 10:00

DETACHED GROWTH PHENOMENON AND THE FUNDAMENTAL SCIENCE BEHIND: NOVEL CRYSTAL GROWTH PROCESS IN VERTICAL DIRECTIONAL SOLIDIFICATION BY SLOW FREEZING

Dattatray Gadkari (, IN)

08:00 - 10:00

**Modeling of Crystal Growth Processes V
August 2, 2019
Crestone I, II**

Moderator(s): Daniel Vizman, RO; Jochen Friedrich, DE

08:00 - 08:30

(Invited) MODELING THE OPTICAL FLOATING ZONE CRYSTAL GROWTH SYSTEM FOR MATERIALS DISCOVERY

Scott Dossa (University of Minnesota, MN/USA)

08:30 - 08:45

NUMERICAL STUDIES ON ASYMMETRIC THREE-PHASE LINE IN THE FLOATING ZONE SILICON

Xuefeng Han (Research Institute for Applied Mechanics, Kyushu University, JP)

08:45 - 09:00

THE FLUCTUATION OF CRYSTAL/MELT INTERFACE INDUCED BY

MELT FLOW INSTABILITY IN LARGE SIZE CZ-SI CRYSTAL GROWTH

Lijun Liu (Xi'an Jiaotong University, CN)

09:00 - 09:15

EFFECT OF NUMERICAL PARAMETERS ON UNSTEADY MELT FLOW FEATURES AND IMPURITY TRANSPORT WITHIN A SIMPLIFIED CZ SI CRYSTAL GROWTH PROCESS GEOMETRY WITH EFFECT OF TRANSVERSE MAGNETIC FIELDS

Vladimir Kalaev (STR Group, Inc. – Soft-Impact, Ltd., RU)

09:15 - 09:30

LATTICE BOLTZMANN SIMULATION OF THREE-DIMENSIONAL INSTABILITIES IN CZOCHRALSKI CRYSTAL GROWTH

Xingchun Xu (Harbin Institute of Technology, CN)

09:30 - 09:45

ADVANCES IN TURBULENCE MODELING OF HEAT AND MASS TRANSPORT DURING CZ SILICON CRYSTAL GROWTH

Vladimir Artemyev (STR Group, Inc. – Soft-Impact, Ltd., RU)

09:45 - 10:00

NEW COLD CRUCIBLE FOR SINGLE CRYSTAL GROWTH

Kader Zaidat (SIMaP-EPM laboratory, INP Grenoble Alpes University, FR)

08:00 - 10:00

Nonlinear Optical and Laser Host Materials IV

August 2, 2019

Red Cloud Peak

Moderator(s): Kevin Zawilski, USA; Peter Schunemann, USA

08:00 - 08:15

[ELABORATION OF LARGE LBO AND RTP CRYSTALS FOR NONLINEAR AND ELECTRO OPTIC APPLICATIONS](#)

Denis Balitsky (Cristal Laser S.A., FR)

08:15 - 08:30

[GROWTH OF HIGH-QUALITY \$\text{SRB}_4\text{O}_7\$ SINGLE CRYSTAL AND ITS OPTICAL PROPERTIES](#)

Yasunori Tanaka (Osaka University, JP)

08:30 - 08:45

[STUDY OF SELF-FLUX COMPOSITION FOR GROWING \$\text{CSLiB}_6\text{O}_{10}\$ CRYSTAL WITH HIGH DUV LASER-INDUCED DEGRADATION TOLERANCE](#)

Masashi Yoshimura (Institute of Laser Engineering, Osaka University, JP)

08:45 - 09:00

[BORATE MATERIALS: FROM BULK SINGLE CRYSTALS TO LOW-DIMENSIONAL STRUCTURES](#)

Nikolay Leonyuk (Lomonosov Moscow State University, Geological faculty, Department of Crystallography and Crystal Chemistry, RU)

09:00 - 09:15

[\(ISO\)CYANURATES WITH NEW TYPES OF \$\pi\$ -CONJUGATED SIX-MEMBERED RING UNITS FOR LINEAR/NONLINEAR OPTICAL APPLICATIONS](#)

Mingjun Xia (Technical Institute of Physics and Chemistry, CAS, CN)

09:15 - 09:30

[NASR3BE3B3O9F4 CRYSTAL GROWTH, DEFECT AND HIGH POWER OF UV LASER GENERATION](#)

Lijuan Liu (Technical Institute of Physics and Chemistry, CN)

09:30 - 09:45

[THEORETICAL INVESTIGATION ON THE MICROSCOPIC MECHANISM OF LATTICE THERMAL CONDUCTIVITY OF ZNXP₂ \(X=SI, GE AND SN\)](#)

Lei Wei (Shandong Academy of Science, CN)

09:45 - 10:00

[THE DESIGN AND SYNTHESSES OF HIGH PERFORMANCE IR NONLIN](#)

Dajiang Mei (Shanghai University of Engineering Science, CN)

08:00 - 10:00

Silicon Carbide Materials and Devices I

August 2, 2019

Crestone III, IV

08:00 - 08:30

[\(Invited\) ADVANCED SILICON CARBIDE SUBSTRATES AND DEFECT CHARACTERIZATION FOR POWER ELECTRONIC INDUSTRY](#)

Santharaghavan Parthasarathy (GT Advanced Technologies, NH/USA)

08:30 - 09:00

[\(Invited\) GROWTH OF LARGE DIAMETER 6H SI AND 4H N+ SIC SINGLE CRYSTALS](#)

Varatharajan Rengarajan (II-VI INCORPORATED WORLD HEADQUARTERS, PA/USA)

09:00 - 09:30

[\(Invited\) MODELING SOLUTIONS FOR SILICON CARBIDE CRYSTAL GROWTH AND EPITAXY](#)

Alex Galyukov (STR USA, Inc., VA/USA)

09:30 - 09:45

[LOW TEMPERATURE GROWTH OF SIC: EVOLUTION OF MORPHOLOGY DURING DISSOLUTION OF AL-SI EUTECTIC](#)

Narsingh Singh (University of Maryland, Baltimore County, USA)

09:45 - 10:00

[IN SITU X-RAY TOPOGRAPHY STUDIES OF 4H-SIC SUBSTRATES AND EPILAYERS](#)

Balaji Raghothamachar (Stony Brook University, NY/USA)

08:00 - 10:00

**Symposium on Epitaxy of Complex Oxides: 5d Transition Metal Oxides
August 2, 2019
Grays Peak II, III**

Moderator(s): Jacobo Santamaria, ES

08:00 - 08:30

[\(Invited\) ENGINEERING THE ELECTRONIC STRUCTURE AND CORRELATIONS IN IRIDATES](#)

Jason Kawasaki (University of Wisconsin Madison, WI/USA)

08:30 - 09:00

[\(Invited\) SYNTHESIS CONTROL OF QUANTUM PHASES IN 3D-5D DOUBLE PEROVSKITE OXIDE HETEROSTRUCTURES](#)

Changhee Sohn (Ulsan National Institute of Science and Technology, KR)

09:00 - 09:30

(Invited) SPIN RECONSTRUCTIONS AT EPITAXIAL OXIDE INTERFACES

Jacobo Santamaria (Universidad Complutense, ES)

09:30 - 09:45

(Invited) GROWTH CONTROL OF INTERFACE STRUCTURE AND SYMMETRY FOR NOVEL FUNCTIONALITIES IN 3D AND 5D OXIDE SUPERLATTICES

Elizabeth Skoropata (Oak Ridge National Laboratory, TN/USA)

09:45 - 10:00

(Invited) SPONTANEOUS HALL EFFECT INDUCED BY LOCAL IR MOMENTS IN THE EPITAXIAL PR₂IR₂O₇ THIN FILMS

Lu Guo (University of Wisconsin, WI/USA)

10:00 - 10:30

BREAK

10:30 - 12:00

Biological and Biomimetic Materials II

August 2, 2019

Grays Peak I

Moderator(s): Anna Pohl, FR; Jinhui Tao, USA

10:30 - 10:45

THE OPTIMUM DESIGN OF DNA-GUIDED NANOPARTICLE

[SUPERLATTICES FOR DIRECT DEHYDRATION](#)

Hayato Sumi (Nagoya Univ, JP)

10:45 - 11:00

[HIERARCHICAL ASSEMBLY AND CHARACTERIZATION OF DNA NANOTUBE NETWORKS](#)

Michael Pacella (Johns Hopkins University, MD/USA)

11:00 - 11:15

[AN ORDERED 2D POLYMER TEMPLATE FOR PROTEIN CRYSTALLIZATION](#)

Elias Vlieg (Radboud University, Institute for Molecules and Materials, NI)

11:15 - 11:30

[PRECIPITANT-FREE CRYSTALLIZATION OF GLUCOSE ISOMERASE SIMPLY BY CONCENTRATION IN A CRYOPROTECTANT SOLUTION](#)

Yoshihisa Suzuki (Tokushima University, JP)

11:30 - 11:45

[BIO-INSPIRED SYNTHESIS AND PHASE TRANSFORMATIONS OF TiO / TiO₂ FOR WATER PURIFYING MEMBRANES](#)

Luz Cruz (Materials Science and Engineering Program, University of California at Riverside, CA/USA)

11:45 - 12:00

[BIOMIMETIC TEMPLATE-FREE SYNTHESIS OF Ta₃N₅ SPHERICAL NANOSHELLS FOR PHOTOCATALYTIC APPLICATIONS](#)

Taifeng Wang (University of California at Riverside, USA)

10:30 - 12:00
HVPE Growth and Devices
August 2, 2019
Torreys Peak II-IV

Moderator(s): Aaron Ptak; Masakazu Sugiyama, JP

10:30 - 11:00
[\(Invited\) HIGH SPEED GROWTH OF III-V MATERIALS USING MOVPE AND HVPE FOR LOW COST PHOTOVOLTAICS](#)

[Takeyoshi Sugaya](#) (National Institute of Advanced Industrial Science and Technology, JP)

11:00 - 11:15
[UNIFORMITY OF GAAS SOLAR CELLS GROWN IN A KINETICALLY-LIMITED REGIME BY DYNAMIC HYDRIDE VAPOR PHASE EPITAXY](#)

[Kevin Schulte](#) (National Renewable Energy Laboratory, CO/USA)

11:15 - 11:30
[HETEROEPITAXY OF GAASP AND GAP ON GAAS BY LOW PRESSURE HYDRIDE VAPOR PHASE EPITAXY](#)

[Yan-Ting Sun](#) (Department of Applied Physics, KTH-Royal Institute of Technology, Se)

11:30 - 11:45
[EVALUATION OF GAAS SOLAR CELLS GROWN WITH DIFFERENT GROWTH REGIMES BY HYDRIDE VAPOR PHASE EPITAXY](#)

[Ryuji Oshima](#) (National Institute of Advanced Industrial Science and Technology, JP)

11:45 - 12:00

[GAAS SOLAR CELLS GROWN AT GROWTH RATES EXCEEDING 300 \$\mu\$ M/H BY DYNAMIC-HYDRIDE VAPOR PHASE EPITAXY](#)

Wondwosen Metaferia (National Renewable Energy Laboratory, CO/USA)

10:30 - 12:00

In Situ Observation and Characterization IV

August 2, 2019

Shavano Peak

Topic: In situ Observation and Characterization - ICCGE/OMVPE

10:30 - 10:45

[HOW MICROGRAVITY EXPERIMENTS LEAD TO A BETTER UNDERSTANDING OF PARTICLE INCORPORATION DURING CRYSTAL GROWTH](#)

Thomas Jauss (University of Freiburg, DE)

10:45 - 11:00

[IN SITU OBSERVATION OF DENDRITE GROWTH IN GALLIUM ANTIMONIDE](#)

Keiji Shiga (Institute for Materials Research, JP)

11:00 - 11:15

[INFLUENCE ON DEFECT TYPES AND DENSITIES OF 4H-SIC WITH VARYING GROWTH CONDITIONS](#)

Melissa Roder (Crystallography, Albert-Ludwigs University Freiburg, DE)

11:15 - 11:30

[IN-SITU SYNCHROTRON X-RAY TOPOGRAPHY STUDIES OF STACKING FAULTS EXPANSION PROCESS IN N-TYPE 4H-SIC](#)

CRYSTALS

Fumihito Fujie (Nagoya University, JP)

11:30 - 11:45

OPTICAL ANOMALY OF GAN AND SIC CRYSTALS AS OBSERVED BY NEW OPTICAL MAIN AXIS MAPPING

Katsuo Tsukamoto (Osaka University, JP)

10:30 - 12:00

Nonlinear Optical and Laser Host Materials V

August 2, 2019

Red Cloud Peak

Moderator(s): Yushi Kaneda, JP

10:30 - 10:45

OPTIMIZATION OF THE GROWTH OF ERBIUM DOPED YAG AND ER-TM CO-DOPED YAG FIBERS BY THE MICRO-PULLING DOWN TECHNIQUE

Abdallah Laidoune (département de physique université Batna 1, DZ)

10:45 - 11:00

CRYSTAL GROWTH, SPECTROSCOPY AND FEMTOSECOND LASER PERFORMANCE OF TM,HO:CNGG DISORDERED GARNET CRYSTAL

Zhongben Pan (Institute of Chemical Materials, China Academy of Engineering Physics, CN)

11:00 - 11:15

RECENT PROGRESS IN $KBe_2(BO_3)_2F_2$ CRYSTAL GROWTH AND APPLICATIONS

Xiaoyang Wang (Technical Institute of Physics and Chemistry, CN)

11:15 - 11:30

[GROWTH, ELECTRICAL, OPTICAL STUDIES AND TERAHERTZ WAVE GENERATION OF ORGANIC NLO CRYSTALS: DSTMS](#)

Bing Teng (College of Physics, Qingdao University, CN)

11:30 - 11:45

[CRYSTAL GROWTH, COMPOSITION, MORPHOLOGY AND THERMAL PROPERTIES OF \$REAL_{2.07}\(B_4O_{10}\)O_{0.60}\$ DIMETABORATES SOLID SOLUTIONS \(\$RE = LA, CE, PR\$ \).](#)

Victor Maltsev (Lomonosov Moscow State University, Geological faculty , RU)

11:45 - 12:00

[PROGRESS ON SELF-FREQUENCY-DOUBLED YB:CA₄YO\(BO₃\)₃ CRYSTAL](#)

Jiyang Wang (Shandong University, CN)

10:30 - 12:00

Silicon Carbide Materials and Devices II

August 2, 2019

Crestone III, IV

Moderator(s): Narsingh Singh, USA; S. Parathasarathy,

10:30 - 11:00

[\(Invited\) EVALUATION OF DEFECTS IN BULK SIC](#)

Michael Dudley (Stony Brook University, NY/USA)

11:00 - 11:30

(Invited) GROWING LARGE DIAMETER 4H SIC BOULES

Govindhan Dhanaraj (Pallidus Inc. , NY/USA)

11:30 - 11:45

EFFECT OF NITROGEN DOPING CONCENTRATION ON LATTICE STRAIN VARIATION IN 4H-SIC SUBSTRATES

Tuerxun Ailihumaer (Department of Materials Science and Chemical Engineering, Stonybrook University, NY/USA)

11:45 - 12:00

DESIGN OF SIC SOLUTION GROWTH CONDITION UTILIZING PREDICTION MODEL CONSTRUCTED BY MACHINE LEARNING AND MATHEMATICAL OPTIMIZATION

Shunta Harada (Nagoya University, JP)

10:30 - 12:00

Symposium on Epitaxy of Complex Oxides: Understanding Film Growth and Solid-Phase Epitaxy

August 2, 2019

Grays Peak II, III

Moderator(s): Lane Martin, USA

10:30 - 11:00

(Invited) A NEXUS IN OXIDES: MOLECULAR BEAM EPITAXY

Yoshiharu Krockenberger (NTT Basic Research Labs, JP)

11:00 - 11:15

INSIGHTS INTO THE DYNAMIC INTERFACE REARRANGEMENT IN LAFeO₃/N-SrTiO₃(001) HETEROJUNCTIONS

Yingge Du (Pacific Northwest National Laboratory, WA/USA)

11:15 - 11:30

[CONTROL OF PHASES AND FUNCTIONALITIES IN EPITAXIAL PEROVSKITE OXIDE THIN FILMS THROUGH FORMATION OF OXYGEN DIODES](#)

Qiyang Lu (Oak Ridge National Laboratory, TN/USA)

11:30 - 11:45

[SOLID PHASE EPITAXY OF \$\text{PrAlO}_3\$ ON \$\text{SrTiO}_3\$: A NEW GROWTH APPROACH FOR COMPLEX OXIDE THIN FILMS AND INTERFACES](#)

Peng Zuo (Department of Materials Science and Engineering, University of Wisconsin-Madison, WI/USA)

11:45 - 12:00

[SOLID-STATE CRYSTALLIZATION OF AMORPHOUS \$\text{Al}_2\text{O}_3\$ ON C-PLANE SAPPHIRE](#)

Omar Elleuch (University of Wisconsin, WI/USA)

10:30 - 12:00

Modeling of Crystal Growth Processes VI

August 2, 2019

Castle Peak III & IV

Moderator(s): Natasha Dropka, DE; Liverios Lymperakis, DE

10:30 - 11:00

[\(Invited\) PREDICTION MODEL OF COMPUTATIONAL FLUID DYNAMICS BASED ON NEURAL NETWORK CONSTRUCTED BY MACHINE LEARNING AND PROCESS OPTIMIZATION OF SIC SOLUTION GROWTH](#)

Toru Ujihara (Graduate School of Engineering and School of Engineering,
Nagoya University, JP)

11:00 - 11:15

[ESTIMATION OF HIGH-TEMPERATURE PHYSICAL PROPERTIES BY
MACHINE LEARNING TOWARD ACCURATE NUMERICAL
MODELING OF CRYSTAL GROWTH](#)

Keisuke Ando (Nagoya University, JP)

11:15 - 11:30

[INVESTIGATION OF PROCESS CONDITIONS ON SURFACE HEIGHT
VARIATION OF KDP CRYSTALS BY RAPID GROWTH TECHNIQUE](#)

Lili Zheng (Tsinghua University, CN)

11:30 - 11:45

[ANALYSIS OF HEAT AND MASS TRANSFER USING ROTATING
BAFFLE IN VERTICAL BRIDGMAN CONFIGURATION](#)

Aleksandar Ostrogorsky (Illinois Institute of Technology, IL/USA)

11:45 - 12:00

[NUMERICAL INVESTIGATION OF THERMAL AND IMPURITIES
DISTRIBUTION IN THE DIRECTIONAL SOLIDIFICATION FURNACE
FOR PHOTOVOLTAIC APPLICATIONS](#)

Kesavan V (SSN College of Engineering, IN)

END OF CONFERENCE

Monday, July 29, 2019

8:10 AM - 10:00 AM

Monday Plenary Session

Location: Shavano Peak

Session Chair(s): Christine Wang

8:10 AM - 8:55 AM

A RETROSPECTIVE ON THE AMERICAN ASSOCIATION FOR CRYSTAL GROWTH ON ITS 50TH ANNIVERSARY

R.S. Feigelson

Stanford University, UNITED STATES OF AMERICA

While a large and successful effort was made to grow large quartz single crystals of during World War II , it wasn't until after the invention of the transistor in 1947 and the slow emergence of the need for growing and characterizing larger and more perfect silicon and germanium single crystals, and later materials for optical applications, that the field of crystal growth started to coalesce. Up until the late 1960's crystal growth research and development papers were presented throughout a variety of society conferences and journals i.e. physics, chemistry, metallurgy, etc. Recognizing that single crystals were becoming very important to the development of advanced electronic and optical devices, as well facilitating materials characterization, a small group of scientists decided to set up a new international effort devoted to bringing together all aspects of crystal growth theory, preparation and characterization into its own "society". This activity was spear headed by the Israeli scientist Michael Schieber in association with some high profile members of the international scientific community, and led in 1966 to the first International Conference on Crystal Growth (ICCG-1) in Boston MA and from that to the formation of the IOCG , the Journal of Crystal Growth, and a series of national organizations, most prominently the American Association for Crystal Growth whose executive committee members had a lot to do with the organization of the ICCG-1. This presentation will take a trip down memory lane to explore the highlights of the AACG's 50 year history. The people involved, the conferences sponsored, the formation of regional chapters and in particular advances in scientific developments and the exploration of new classes of materials during this time period. In addition to

celebrating the AACG, I will also briefly discuss some of the other national organizations such as the BACG which is also celebrating their 50th anniversary this year.

8:55 AM - 9:40 AM

DEFECT ENGINEERING IN BULK CRYSTAL GROWTH

T. Duffar

SIMAP EPM, FRANCE

Most bulk crystal growth processes, such as Czochralski, Bridgman, Verneuil, were invented more than one century ago. Fifty years later, crystals appeared to be key materials for advanced technologies: electronics, optics, sensors and so on. Consequently, these processes have been developed in order to reach industrial standards in terms of productivity, reliability and costs. Anyhow, placed on a very competitive market, companies are continuously facing the need of improving their growth technology in order to get larger, better and cheaper crystals.

Obviously, growth conditions directly control the crystal quality and it is of uppermost importance to understand the physical phenomena involved during the growth and how they affect the defect distribution inside the crystal. This is well known as far as individual, independent, defects are considered so that this basic knowledge can be used for any kind of crystal and growth process. In this respect, I will show how process charts can be drawn in order to quickly define the growth condition for producing a given crystal.

A further step forward concerns the precise design of the process for obtaining given crystals with a given quality. For this, the passed thirty years have seen several groups worldwide developing numerical models in order to investigate the details of the processes. This activity led to the offer of devoted numerical simulation software, which are now commercially available at the industrial level. I will show, on some examples, how numerical simulation can help solving real industrial crystal growth issues.

However, the situation becomes more complex when crystal defects cannot anymore be considered independently. In such situations, it will be shown, through some industrial examples, that an acceptable compromise between contradictory growth parameters is difficult to

obtain. Numerical modelling of such complex coupling remains a challenge.

Monday, July 29, 2019

10:30 AM - 12:00 PM

Industrial Crystal Growth Technology and Equipment I

Location: Shavano Peak

Session Chair(s): Matt Whittaker, Gisele Maxwell

10:30 AM - 11:00 AM

ADVANCES IN SINGLE-CRYSTAL FIBERS AND THIN RODS GROWN BY LASER HEATED PEDESTAL GROWTH: A REVIEW G. Maxwell

Altus Consulting, CA, UNITED STATES OF AMERICA

Single-crystal fibers are an intermediate between laser crystals and doped glass fibers. They have the advantages of both guiding laser light and matching the efficiencies found in bulk crystals, which is making them ideal candidates for high-power laser and fiber laser applications. This work focuses on the growth of a flexible fiber with a core of dopant (Er, Nd, Yb, etc.) and a polycrystalline clad of yttrium aluminum garnet (YAG) that will exhibit good wave guiding properties. Direct growth or a combination of growth and cladding experiments are described. Lasing and amplification results are presented. Industrial applications and the future of the technology are also discussed.

11:00 AM - 11:30 AM

ULTRA-FAST AND HIGH-PRECISION CRYSTAL ORIENTATION AND QUALITY MEASUREMENTS ON CRYSTALLINE SEMICONDUCTORS

N. Schüler, **K. Dornich**, T. Weißbach, H. Bradaczek, H. Berger
Freiberg Instruments GmbH, GERMANY

For a fast and precise crystal orientation of a semiconductor, the so-called omega scan is presented. The crystal orientation of ingots and wafers is of crucial importance e.g. for the quality and properties of deposited epitaxial layers. In most cases the x-ray diffractometry is used, but in a production environment, time is an important factor and

typical x-ray diffractometry measurements of the complete lattice orientation take at least several minutes. In contrast the omega-scan method allows the accurate orientation determination of the complete crystal lattice in only 5 s. Therefore, the omega-scan is especially suited for industrial applications. Because the omega-scan measurement is fast, mapping becomes feasible. Samples with 1 mm diameter up to large ingot with 300 kg are possible. Transfer systems to a saw or other following process steps allow a transfer without loss of orientation accuracy and even an OEM system for a direct implementation into a saw or grinding machine is available. During the omega-scan measurement the crystal rotates with constant speed around an axis, the reference axis of the system. X-ray tube and detector with mask for the reflected beams are in fixed positions. The X-ray beam is twice reflected from lattice planes inclined to the rotation axis and the angular positions of the reflections are measured in the plane perpendicular to the rotation axis (Omega circle). The whole measurement requires only one revolution of the rotary turntable. Not only the crystal orientation but also the minority carrier lifetime is a crucial parameter for the quality of a certain crystal, since it is very sensitive for all electrically active defects as impurities and structural defects. The here presented microwave detected photoconductivity (MDP) is a very sensitive method which allows for fast, destruction free and precise measurements. Here the sample is irradiated with laser light and the generated photoconductivity in the sample is detected via a very sensitive advanced microwave detections system. The minority carrier lifetime is determined from the decrease of the photoconductivity after the light is switched of. Lifetimes of only 20 ns up to several ms can be detected. From temperature dependent measurements even the activation energies of defects such as traps can be investigated, via a technique called MD-PICTS. Both methods are presented on 4H-SiC wafers and epitaxial layers to demonstrate the speed and precision of the omega-scan and MDP method.

11:30 AM - 11:45 AM

**CONTROL OF MICROSTRUCTURE AND MECHANICAL
PROPERTIES OF PLATINUM FIBER FABRICATED BY**

UNIDIRECTIONAL SOLIDIFICATION

Y. Yokota¹, T. Nihei², M. Yoshino¹, A. Yamaji¹, H. Sato¹, Y. Ohashi¹, S. Kurosawa¹, K. Kamada¹, A. Yoshikawa¹

¹Tohoku University, JAPAN, ²C&A Corporation, JAPAN

We have developed an alloy-micro-pulling-down (A- μ -PD) method to fabricate metal and alloy fibers from the melt by a unidirectional solidification. In our previous reports, Iridium (Ir) and Platinum (Pt) fibers could be grown by the A- μ -PD method, and microstructure and mechanical properties of the Ir fiber were investigated. The Ir fiber was composed of elongated large grains and the maximum nominal strain was larger than that of a commercial Ir wire produced by a wire-drawing process. In this study, microstructure and mechanical properties of the Pt fibers fabricated by the unidirectional solidification using the A- μ -PD method were investigated by a Universal Testing Machine and an Electron Backscattered Diffraction (EBSD). The Pt fiber grown by the A- μ -PD method at 10 mm/min growth rate was composed of large grains with $\langle 100 \rangle$ crystal orientation along to the growth direction. The crystal orientation is consistent with the easy axis of the crystal growth on the face-centered-cubic (f.c.c.) structure [Fig.1(c)]. On the other hand, adjacent grains of the Pt fiber grown at 50 mm/min growth rate randomly oriented due to the faster growth rate [Fig.1(e)]. In the tensile tests, the Pt fibers grown by the A- μ -PD method showed extremely different stress-strain curves compared to the commercial Pt wire. The maximum tensile stress of the Pt fiber grown by the A- μ -PD method reached to ~ 100 MPa and the Pt fiber ruptured after 58% nominal strain.

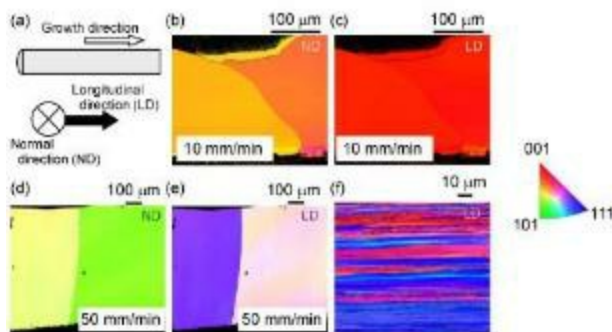


Figure 1 (a) Schematic diagram of the EBSD analysis and (b - e) IPF maps of the Pt fiber grown by A- μ -PD method and (f) the commercial Pt wire.

11:45 AM - 12:00 PM

BULK CRYSTAL GROWTH OF TERNARY III-V COMPOUND SEMICONDUCTORS

P.S. Dutta

Rensselaer Polytechnic Institute, NY, UNITED STATES OF AMERICA

III-V compound semiconductors play a crucial role in modern electronic and photonic technologies. The current applications are met by binary compounds such as GaAs, InP, GaP, InAs, InSb, etc. III-V ternary compound semiconductors offer the freedom to vary band gaps or lattice constants and are necessary for niche applications. However the crystal growth technology and process parameters used for binary compounds cannot yield ternary crystals that are application worthy. This talk will discuss the fundamental challenges that have impeded the progress of ternary crystal growth. Due to the intrinsic separation between liquidus and solidus in the pseudo-binary phase diagrams used for growing ternary crystals, alloy segregation is a major issue. This in turn leads to (a) low yield of wafers with same composition, (b) cracking of crystals due to constitutional supercooling and strain arising from the compositional grading, and (c) non-homogeneous wafers due to curved solid-liquid interface shape. Some of the recent advances made to overcome these challenges for the growth of 50 – 100 mm diameter GaInAs, GaInSb, InAsP and GaInP bulk crystals will be presented. The precise control of heat and mass transport in the melt that is necessary during ternary crystal growth will be discussed. Vertical Bridgman (VB) or vertical gradient freezing (VGF) techniques in conjunction with solute replenishment strategies have been found to be most suitable and successfully employed for growing ternary crystals with a wide range of alloy compositions.

Monday, July 29, 2019

10:30 AM - 12:00 PM

Nonlinear Optical and Laser Host Materials I

Location: Crestone I, II

Session Chair(s): Peter G. Schunemann, Kevin Stevens

10:30 AM - 11:00 AM

FLUORIDE CRYSTALS FOR LASER GAIN AND FARADAY ROTATOR APPLICATIONS

K. Stevens, G. Foundos

Northrop Grumman SYNOPTICS, NC, UNITED STATES OF AMERICA

There are many solid-state laser host crystals available for rare-earth and transition-metal ion doping. In particular, the oxides (YAG, Sapphire, Aluminates) play an important role in commercially available crystals. Their superior mechanical and optical properties have made such hosts preferred materials to designers of solid-state lasers. However, fluoride hosts have become increasingly desired over the past decade due to reduced thermal lensing and a natural birefringence. In addition, there is increased energy storage when compared to other hosts mentioned earlier¹. There are undesirable properties of fluoride crystals (thermomechanical properties), but improvements in the growth and fabrication of these crystals has helped alleviate some of these concerns. Because of the increased demand for the fluoride laser host crystals, there has been much knowledge gained over the years growing and developing large single crystals of LiYbF₄ (YLF). Growth has scaled from boules averaging 25mm in diameter in the 1980s to over a 100mm in diameter with the current technologies. The progress made in crystal growth processes has led to the ability to grow other fluoride crystals. Namely, Faraday rotator crystals such as LiTbF₄ (TLF) and KTb₃F₁₀ (KTF) have been grown on a production scale with good optical quality. We will report recent work on these new Faraday crystals as well as the state of the art in growing large fluoride laser host crystals.

11:00 AM - 11:15 AM

OPTICAL SPECTROSCOPY AND MAGNETIC BEHAVIOUR OF SM³⁺- AND EU³⁺- CATIONS IN LI₆EU_{1-x}SM_x(BO₃)₃ SOLID SOLUTION

M. Velazquez¹, R. Belhoucif², J. Sand³, O. Plantevin⁴, P. Aschehoug⁵, P. Goldner⁵, G. Christian⁴

¹SIMaP UMR 5266 CNRS-UGA-G INP, FRANCE, ²Laboratoire d'Electronique Quantique, USTHB, ALGERIA, ³ICMCB, FRANCE,

⁴CSNSM UMR 8609, FRANCE, ⁵PSL Research University, FRANCE
Rare earth ions dissolved in high bandgap dielectrics are thoroughly investigated because of the many applications as activators and sensitizer that can be envisioned in solid state lasers, infrared (IR) quantum counters, IR to visible converters [1-6]. A new borate solid solution series of powders, $\text{Li}_6\text{Eu}_{1-x}\text{Sm}_x(\text{BO}_3)_3$ ($x=0.35, 0.5, 0.6, 1$), were synthesized by solid-state reaction, characterized and their luminescent properties were investigated. Moreover, a centimeter-sized single crystal was grown by the Czochralski method from an initial $\text{Li}_6\text{Eu}_{0.65}\text{Sm}_{0.35}(\text{BO}_3)_3$ growth load. The absorption spectra indicate that absorption takes place mainly from the $\text{Sm}^{3+}6\text{H}_{5/2}$ ground state, with a strong band at 405 nm. The photoluminescence spectra reveal that the Eu^{3+} red emission intensity strongly depends on the Sm^{3+} content x . Judd-Ofelt analysis was carried out in order to estimate radiative transition rates and emission quantum efficiency. Owing to the energy transfer from Sm^{3+} to Eu^{3+} the intense red light detected at 613 nm at room temperature, under UV or blue light excitation, was improved by ~35% as compared with Sm^{3+} -free samples. This energy transfer was confirmed by faster decay times of Sm^{3+} as energy donors. Magnetic susceptibility measurements of $\text{Li}_6\text{Eu}_{1-x}\text{Sm}_x(\text{BO}_3)_3$ compounds were carried out in the 2-320 K temperature range and were used to compare calculated and experimental energy levels. [1] F. Auzel, P. A. Santa Cruz, G. F. de Sa, *Rev. Phys. Appl.*, **20**, 273-281 (1985). [2] N. Bloembergen, *Phys. Rev. Lett.*, **2**, 84-85 (1959). [3] L. Esterowitz, A. Schnitzler, J. Noonan, J. Bahler, *Appl. Opt.*, **7**, 2053-2070 (1968). [4] L. F. Johnson, H. J. Guggenheim, T. C. Rich, F. W. Ostermayer, *J. Appl. Phys.*, **43**, 1125 (1972). [5] G. F. J. Garlick, *J. Contemp. Phys.*, **17** (1976). [6] D. Serrano, A. Braud, J.-L. Doualan, P. Camy, R. Moncorge, *Proc. SPIE*, **8111**, 811104 (2011).

11:15 AM - 11:30 AM

**TOP-SEEDED SOLUTION CRYSTAL GROWTH AND
CHARACTERIZATION OF NEW ULTRAVIOLET AND DEEP-
ULTRAVIOLET NON-LINEAR OPTICAL MATERIALS**

P..S. Halasyamani, W. Zhang

Department of Chemistry, University of Houston, TX, UNITED STATES OF AMERICA

Nonlinear optical (NLO) materials are critical in generating coherent light through frequency conversion, e.g., second harmonic generation (SHG). From the ultraviolet (UV) to the infrared (IR), NLO materials have expanded the range of the electromagnetic spectrum accessible by solid-state lasers. Wavelengths where NLO materials are still needed include the UV (~200 - 400nm) and deep UV (< 200nm). Coherent deep-ultraviolet (DUV) light has a variety of technologically important uses including photolithography, atto-second pulse generation, and in advanced instrument development. Design strategies will be discussed, as well as synthetic methodologies. In addition, the crystal growth, characterization, and structure-property relationships in new UV and DUV NLO materials discovered in our laboratory will be presented. Finally, our crystal growth capabilities and recent crystal growth of functional materials will be described.



11:30 AM - 11:45 AM

NOVEL (ER,YB)YMGB₅O₁₀ PENTABORATE CRYSTALS: FLUX GROWTH AND CHARACTERIZATION

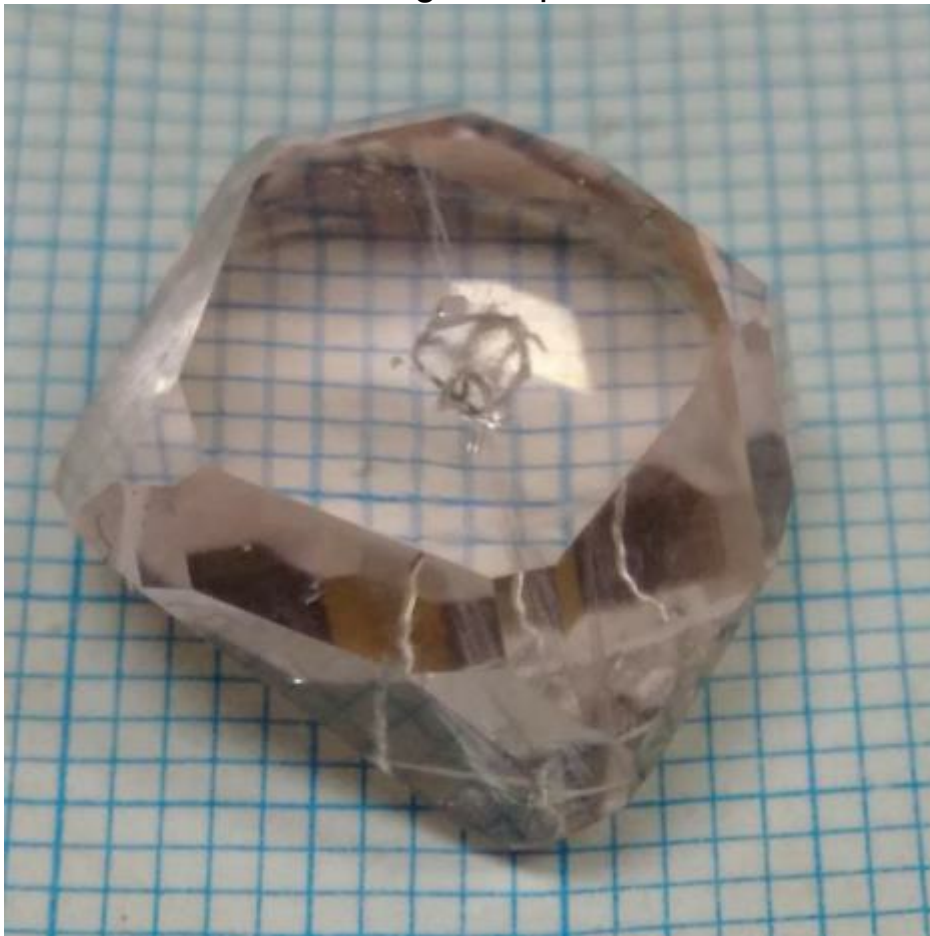
V.V. Maltsev¹, D.D. Mitina¹, N.I. Leonyuk¹, K.N. Gorbachenya², R.V. Deineka², V.E. Kisel², A.S. Yasukevich², N.V. Kuleshov²

¹Lomonosov Moscow State University, Geological faculty, Department of Crystallography and Crystal Chemistry, RUSSIAN FEDERATION,

²Belarusian National Technical University Center for Optical Materials and Technologies, BELARUS

Single crystals co-doped with Er³⁺ and Yb³⁺ have gained much

interest as solid state media for eye-safe lasers emitting around 1.5 μm , which can be used in many important applications [1]. In this connection, after earlier works on borate crystals [2-5], (Er,Yb):LaMgB₅O₁₀ and (Er,Yb):GdMgB₅O₁₀, as representatives of borate family, were recently synthesized [6,7]. Here, an attempt has been made to study crystallization conditions of YMgB₅O₁₀ (YMB) compound and to evaluate its device potential. Visually transparent (Yb,Er):YMB single crystals with size up to 20x10x5 mm were grown from K₂Mo₃O₁₀-containing high-temperature solutions by using the approach named as solution growth on dipped seeds (SGDS) in the temperature range of 865-835°C at a cooling rate of 1-1.5 °C/day. Ytterbium, erbium and yttrium concentrations were measured and their segregation coefficients are close to their concentrations in the nutrient borate of the high-temperature solution.



The thermal conductivity of a YMB crystal was measured to be $6.2 \pm 0.3 \text{ W/m}\cdot\text{K}$. Polarized absorption and emission cross-section

spectra, lifetimes of $^4I_{11/2}$ and $^4I_{13/2}$ energy levels of Er^{3+} and ytterbium-erbium energy transfer efficiencies were investigated. The obtained results make it possible to grow (Er, Yb):YMB single crystals with high optical quality for applications in diode-pumped lasers operating in the eye-safe spectral range of 1.5–1.6 μm . 1. G. Huber et al. J. Opt.Soc.Am.B 2010, 27, B93–B105. 2. P. Wang, et al. Opt.Mater. 2002, 19, 383–387. 3. N.A. Tolstik, et al. Appl.Phys. B 2009, 97, 357–362. 4. Z. Pan, et al. J. Cryst.Growth 2013, 363, 176–184. 5. K.N. Gorbachenya et al. Opt.Lett. 2016, 41, 918–921. 6. Y. Huang et al. J.Alloys and Compounds, 2017, Vol.695, pp.215–220

11:45 AM - 12:00 PM

BRIDGMAN GROWTH OF LARGE SIZE SM:YCOB CRYSTAL FOR QPCPA APPLICATION

X. Tu¹, K. Xiong², S. Wang², E. Shi², Y. Zheng²

¹University of Chinese Academy of Sciences, CHINA, ²Shanghai institute of ceramics, Chinese academy of sciences, CHINA

The good thermal and nonlinear optical property as well as high damage threshold and high transmittance make YCOB ($YCa_4O(BO_3)_3$, Yttrium calcium oxyborate) a key optical element in the SHG and OPCPA process to obtain high repetition rate, multi-petawatt laser pulse. However, typical OPCPA conversion efficiency is less than 25% due to the presence of backward energy transfer among the three interacting waves during the OPCPA process. A new scheme termed “quasi-parametric chirped pulse amplification” (QPCPA) was proposed in 2015. This new technology can effectively improve the conversion efficiency by using the Sm:YCOB crystal to absorb the idler wave (1550 nm). In this work, the growth of Sm:YCOB crystals with the diameter larger than 100 mm by Bridgman method was described for the first time (as shown in Fig. 1). The X-ray powder diffraction, high resolution X-ray diffraction (HRXRD), transmission spectrum, laser induced damage threshold of as grown crystals were measured. The full width at half maximum (FWHM) of the rocking curve of the as grown crystal is lower than 25 seconds. Then, QPCPA and high-repetition rate frequency conversion of YCOB was demonstrated. With

the potential to grow large size Sm:YCOB crystals, we anticipate that QPCPA will be a promising approach for efficiently amplifying optical chirped pulses to unprecedented powers.



Fig. 1. The as grown Sm:YCOB crystal with the diameter of 108 mm

Monday, July 29, 2019

10:30 AM - 12:00 PM

Special Session - Michael Schieber I

Location: Red Cloud Peak

Session Chair(s): Jerry Stringfellow, Edith D. Bourret

10:30 AM - 11:00 AM

**REVIEW OF ROOM TEMPERATURE COMPOUND
SEMICONDUCTOR MATERIALS FOR NUCLEAR DETECTION**

K.S. Shah

Radiation Monitoring Devices, Inc., MA, UNITED STATES OF

AMERICA

Review of Room Temperature Compound Semiconductor

Materials for Nuclear Detection Kanai S. Shah and M.R. Squillante,

Radiation Monitoring Devices, Inc., 44 Hunt Street, Watertown, MA

02472 Abstract This paper, being presented in honor of Prof. Michael

Schieber, a pioneer in room temperature semiconductor research, will

present a broad review of room temperature semiconductor materials

for nuclear detection. Groundbreaking research in CdTe and HgI₂,

performed in 1970s, which is still relevant today, including crystal

growth by travelling heater method (THM) and vapor transport will be

presented. Alloying of CdTe and ZnTe to create CdZnTe (CZT) by

high pressure Bridgman methods in late 1980s to much of 1990s will

also be covered followed by migration to THM for growth of CZT.

Newer wide bandgap materials such as PbI₂, InI and TlBr processed

by zone melting and Bridgman methods will be discussed. In all these

cases, highlights of detection performance will be presented. New and

emerging wide-bandgap semiconductors such as perovskites (e.g.

CsPbBr₃) and chalcogenides (e.g. Tl₆SeI₄) will also be discussed.

Applications of these semiconductor materials in medical imaging,

security and defense, non-destructive testing and physics research

will be covered. Along with crystal results, development of thick films

of some semiconductors (e.g. TlBr, PbI₂ and HgI₂) for X-ray imaging

applications will also be covered.

11:00 AM - 11:30 AM

**DEVELOPMENTS IN CDZNTE AND OTHER MATERIALS FOR
GAMMA-RAY DETECTORS**

M. Goorsky

Dept. of Materials Science and Engineering, University of California

Los Angeles, CA, UNITED STATES OF AMERICA

Professor Michael Schieber was a pioneer in the development of

materials such as Cd_{1-x}Zn_xTe, CdTe, HgI₂, and others with

applications for gamma-ray detectors and spectrometers. My research

group was privileged to be a part of that effort for several years and

the topic here will include our collaborations which focused on relating

defects, interfaces, and surfaces with detector performance. These

developments led to improvements in performance and also helped establish characterization techniques including laboratory-based double crystal x-ray topography, triple axis x-ray scattering measurements for compositional analysis, and mapping techniques based on x-ray diffraction and infra-red imaging that we continue to use to study other electronic materials.

11:30 AM - 12:00 PM

HEAVY METAL HALIDES FOR ROOM TEMPERATURE NUCLEAR RADIATION DETECTION

A. Burger¹, R. Hawrami¹, E. Ariesanti¹, S. Motakef²

¹Fisk University, UNITED STATES OF AMERICA, ²CapeSym, Inc., UNITED STATES OF AMERICA

Abstract— I will review my research journey in the growth of crystals for room temperature nuclear radiation detection that started while working with Michael Schieber in early 1970's on mercuric iodide (HgI_2), a wide bandgap semiconductor and continues today on bright scintillators such as strontium iodide ($\text{SrI}_2:\text{Eu}^{2+}$) and cesium hafnium chloride (Cs_2HfCl_6 or CHC). CHC is a recently discovered non-hygroscopic intrinsic scintillator with a simple cubic crystal structure. In this paper we will present a successful development of a large diameter, crack-free single crystal growth of CHC as well as improvement to its scintillation performance. A single one inch diameter crystals CHC boule is grown using the vertical Bridgman method. Excellent energy resolution of 3.5% (FWHM) at 662 keV and gamma-ray non-proportionality of CHC has been obtained and is compared to those of the commercial NaI:Tl and BGO.

Monday, July 29, 2019

10:30 AM - 12:15 PM

Symposium on 2D Materials: Characterization and Devices

Location: Crestone III, IV

Session Chair(s): James Maslar, Tanushree H. Choudhury

10:30 AM - 11:00 AM

NOVEL EXCITONIC EFFECTS IN ATOMICALLY THIN HETEROSTRUCTURES

C.E. Giusca

National Physical Laboratory, UNITED KINGDOM

Light emission in atomically thin heterostructures is known to depend on the type of materials and the stacking sequence of the constituent layers. Interfacing transition metal dichalcogenides with graphene is a versatile approach for creating a range of electronic and optoelectronic applications, such as field-effect transistors and ultrafast photodetectors. In this talk I will discuss the role of graphene in tuning the electronic and optical properties in atomically thin heterostructures and show that the thickness of the graphene is crucial in modulating the light emission, giving rise to novel excitonic effects. I will describe how the behavior of the photoexcited carriers changes with the graphene thickness and discuss the effect that the interlayer electronic coupling has on the excitonic properties of the heterostructures. This will be supported by direct evidence of spatially-resolved electronic structure changes at the heterogeneous atomic-scale interfaces and associated band offsets that lead to patterned exciton and trion photoluminescence. The findings bring evidence that the electronic and excitonic properties of 2D heterostructures can be effectively tuned by the number of supporting graphene layers, demonstrating ultimate control of the optoelectronic properties at the nanoscale.

11:00 AM - 11:15 AM

PHOTOLUMINESCENCE PROPERTIES OF MOS₂/GAN HETERO STRUCTURE

S. Mouri¹, Y. Komichi¹, K. Shinokita², K. Matsuda², T. Araki¹

¹Ritsumeikan University, JAPAN, ²Kyoto University, IAE, JAPAN

Optical properties of monolayer (1L) transition metal dichalcogenides (TMDs) are interesting because of their direct bandgap response [1], strong light matter interactions [2], large excitonic effects [3] and valley-spin locking optical response [4]. Stacking of TMDs and conventional optical semiconductors such as III-V nitrides is an

effective approach to incorporate these features into practical devices, such as LED or photo-detectors. Here, we have studied the photoluminescence (PL) properties of 1L-MoS₂ exfoliated onto free-standing GaN substrate, especially focusing on the polarity of GaN surface. We prepared the 1L-MoS₂ exfoliated from natural crystal and transferred it onto the +c or -c surface of the free-standing GaN (Chino Nitrides Co.) using a scotch tape and a polymer sheet. The PL intensity of MoS₂ on GaN becomes quarter as compared with that on SiO₂/Si reflecting the electron transfer from MoS₂ to GaN surface at room temperature. More interestingly, the intensities and emission energies of excitons and trions (charged excitons), are different depending on the polarity of surface. Both exciton and trion PL was observed from the 1L-MoS₂ on the Ga polar (+c) surface. On the other hand, trion PL was mainly observed from the 1L-MoS₂ on the N polar (-c) surface. The sign of induced charge by spontaneous polarization of GaN is opposite depending on the surface polarity. Induced holes compensated the initially doped electrons in MoS₂ on the Ga polar (+c) surface while additional electrons were induced in MoS₂ on the N polar (-c) surface. We also carried out the temperature dependent PL measurement for these samples. Trion valley polarization also depends on the surface polarity. The degree of valley polarization of MoS₂ on the Ga polar (+c) surface is finite until 200 K however that on the N polar (-c) surface is finite until 150 K. This might be related to the sign of trions. These results suggest that the polarity of GaN might be important to determine optical properties of TMDs for the application to luminescent devices.

References [1] K. Fai. Mak *et.al.*, Phys. Rev. Lett **105**. 136805 (2010). [2] L. Britnell et al., Science **340**, 1311 (2013). [3] A. Chernikov *et.al.*, Phys. Rev. Lett **113**. 076802 (2014). [4] K. Fai. Mak *et.al.*, Nature. Nanotech. **7**. 494 (2012). This work was supported by JSPS KAKENHI, JP15H03559 JP16H03860, JP16H0615, JP18H04294, Iketani science foundation, and zeroemission energy program of IAE.

11:15 AM - 11:30 AM

CHEMICAL VAPOR TRANSPORT SYNTHESIS,

CHARACTERIZATION AND COMPOSITIONAL TUNING OF ZRSXSE_{2-X} FOR OPTOELECTRONIC APPLICATIONS

J.J. Fox¹, R.L. Cavalero¹, R.M. Lavelle¹, S.M. Oliver², J.D. Joshi², P.M. Vora², D.W. Snyder¹

¹Electronic Materials and Devices Department, Applied Research Laboratory, Pennsylvania State University, PA, UNITED STATES OF AMERICA, ²Department of Physics and Astronomy, George Mason University, VA, UNITED STATES OF AMERICA

Two-dimensional (2D) transition metal dichalcogenides (TMDs) offer a wealth of electronic and optical properties for next-generation optoelectronic devices. Further control of their properties can be achieved through strain and alloy engineering, which provide methods for tuning the bandgap, work functions, lattice constants, and crystal structure of these materials. We seek to explore the properties of ternary alloys comprised of the TMDs ZrS₂ and ZrSe₂, the end components of the ZrS_xSe_{2-x} system, which are highly attractive for optoelectronic technology due to predictions of a strain-tunable indirect bandgap in the visible and near-infrared. Bandgap values are predicted to range from 0 – 2.45 eV for ZrS₂ and 0.45 – 1.2 eV for ZrSe₂. Substitutional alloying of ZrS₂ and ZrSe₂ binary materials has not yet been characterized, though it is postulated that alloying may enable coarse bandgap tuning from 0.45 eV to 1.93 eV in the monolayer^{1,2} while also maintaining or enhancing the strain response of the material. Additionally, theory predicts improvements to light absorption properties of ZrS₂ through incorporation into van der Waals heterostructures, which may be enhanced in the alloying process. We have synthesized the alloy series ZrS_xSe_{2-x} (x = 0, 0.2, 0.5, 0.8, 1.0, 1.2, 1.5, 1.8 and 2) through a chemical vapor transport (CVT) process and iodine carrier gas to produce bulk crystalline flakes in evacuated quartz ampoules with a specific source stoichiometry. The bulk flakes have grown as large as 2 cm side length and consistent cm-scale flakes are achieved for the entire compositional range with macro-scale hexagonal features. Scalability of the flakes was improved through trials with ampoule volume through larger diameter quartz tubing (14 mm OD, 10 mm ID). Characterization via X-ray diffraction is

used to document shifts in reflections of oriented (00 l) for $l = 1, 2, 3, 4$ features as a function of alloy composition, while Raman spectroscopy is used to explore the evolution of the vibrational modes. Raman measurements of bulk ZrS_xSe_{2-x} at 5 K reveal not only significant shifting and broadening of the primary ZrS_2 and $ZrSe_2$ vibrational modes, but also activation of new modes not present in the pure compounds as effects which are known to result from disorder introduced into the crystal due to the alloying process. The alloy stoichiometric ratios, determined through EDS analysis with accuracy $\pm 2-4$ molar %, in the bulk crystals match closely with the targeted ampoule source loaded stoichiometry.

11:30 AM - 11:45 AM

**TUNABLE ELECTRIC AND THERMAL
TRANSPORT PROPERTIES IN DEFECT ENGINEERED Hf/ZrTe_{5- δ}
 δ SINGLE CRYSTAL DURING CVT GROWTH**

S. Yao

Nanjing university, CHINA

Recently, transition-metal pentatelluride have been investigated because of the resistivity abnormality and topological properties. Many experimental and theory works have been carried out to clarify resistivity abnormality and topological character by different methods. Their thermoelectric properties have also been attracted enormous attention because of their potential applications in developing environment-friendly electrical power generators, as well as freon-free refrigerator. Here we tailor the level of Te deficiency by adding different excessive amount of Te into the I_2 vapor transport growth procedure. Series of crystal Hf/ZrTe_{5- δ} have been grown successfully under modified CVT method[1]. We carried out the thermal transport investigation. The analysis of Raman data verifies that mean-free-path of optical phonon at Γ -point is nearly tenfold larger than phonon transport mean-free-path, which strongly suggests that abstract microstructure, rather than conventional an-harmonic phonon-phonon interaction, leads to extremely low thermal conductivity in these two compounds. The electrical and magneto-transport properties of Hf/ZrTe_{5- δ} crystals the extremely large MR effect of sample is

attributed to high carrier mobility and a nearly compensation of the electron and hole carries concentration[2-4]. This work provides a viable route to tune superior MR properties and extra-thermal transport in the similar compounds through defect engineering, which may be promising to develop the novel magnetic memory/sensor devices/thermoelectric devices. Reference: Microstructure, growth mechanism and anisotropic resistivity of quasi-one-dimensional ZrTe₅ crystal ZrTe₅. Y.Y. Lv, S.H.Yao*, Y.B.Chen*, J.Zhou, Y.F.Chen. Journal of Crystal Growth 2017, 457: 250–254. Transition between strong and weak topological insulator in ZrTe₅ and HfTe₅. Z.J.Fan, Q.F.Liang, Y. B. Chen, S.H.Yao & J.Zhou*. Scientific Reports 2017,7:45667. Three-dimensional nature of the band structure of ZrTe₅ measured by high-momentum-resolution photoemission spectroscopy. H. Xiong, J. A. Sobota, S.-L. Yang, H. Soifer, A. Gauthier, M.-H. Lu, Y.-Y. Lv, S.-H. Yao, P. S. Kirchmann, Y.-F. Chen, and Z.-X. Shen. PHYSICAL REVIEW B 95, 195119 (2017). Tunable Resistance or MR Cusp and Extremely Large MR in Defect-Engineered HfTe_{5-δ} Single Crystals.Y.Y. Lv, S.H.Yao*, Y.B.Chen*, J.Zhou, Y.F.Chen. PHYSICAL REVIEW APPLIED. 2018, 9:054049.

11:45 AM - 12:00 PM

CHEMICAL SENSING WITH MOS₂/GRAPHENE HETEROSTRUCTURE ON SILICON CARBIDE

S. Kim¹, J. Park², S. Lee³, S. Krishna³, S. Kang⁴, K.M. Daniels¹

¹Department of Electrical and Computer Engineering, University of Maryland, MD, UNITED STATES OF AMERICA, ²Advanced Instrumentation Institute, Korea Research Institute of Standards and Science, KOREA, REPUBLIC OF, ³Department of Electrical and Computer Engineering, The Ohio State University, UNITED STATES OF AMERICA, ⁴Science of Measurement, University of Science and Technology, KOREA, REPUBLIC OF

In recent years, graphene has attracted much attention with many potential devices such as pressure sensors, batteries, solar cells, field effect transistors, and especially gas sensors. Atomically thin 2D graphene has an exceedingly high surface-to-volume ratio which is

the most important parameter for gas sensor application. In addition, it is suitable for a van der Waals heterostructure devices, stacking 2D architectures atomically with synergistic combinations of nanomaterials. Here, we have prepared vertically grown nanoflower-structures molybdenum disulfide (MoS_2) on graphene (i.e. MoS_2 /graphene heterostructure) for gas sensing application at room temperature. The MoS_2 /graphene heterostructure make the sensor a good candidate for gas sensing due to the high surface-to-volume ratio of both MoS_2 and graphene, resulting in ultimate sensitivity. To synthesize bilayer epitaxial graphene on 6H SiC, the Si thermal sublimation method was used. After that, nanoflower-structures MoS_2 were grown on graphene/SiC directly using metal organic chemical vapor deposition (MOCVD). Molybdenum hexacarbonyl ($\text{Mo}(\text{CO})_6$) and hydrogen sulfide (H_2S) were used as precursor materials, with the partial pressure ratio of 1:1. Carbonaceous impurities were first randomly deposited on graphene/SiC, acting as promoters of nucleation and growth of vertically standing MoS_2 (Stranski-Krastanov growth mode). The growth of MoS_2 was performed at 350 °C with various chamber pressures and growth times. Samples were investigated by scanning electron microscopy (SEM), Raman spectroscopy, and photoluminescence (PL).

12:00 PM - 12:15 PM

CRYSTAL GROWTH AND STUDY OF ORBITAL CURRENTS IN THE PSEUDOGAP PHASE OF HIGH-TC CUPRATES

D. Bounoua¹, J. Jeong¹, L. Mangin-Thro², R. Saint-Martin³, L. Pinsard-Gaudart³, Y. Sidis¹, P. Bourges¹

¹Laboratoire Léon Brillouin, FRANCE, ²Institut Laue-Langevin, FRANCE, ³Paris-Saclay University - ICMMO-SP2M, FRANCE

The onset of an intra-unit cell magnetism (IUC), when entering the pseudogap state ($T=T^*$) of High-Tc cuprates was shown to occur in four different families of layered cuprates, using polarized neutron diffraction (PND) [1]. This IUC magnetism breaks the time reversal symmetry but preserves the translational symmetry of the lattice giving rise to a $q=0$ antiferromagnetic order, consistent with other reports on

time reversal and inversion symmetry breaking at T^* [2]. The T_{mag} corresponding to the IUC magnetism tightly follows the temperature vs hole dependence of the pseudogap state boundary with $T_{\text{mag}}=T^*$. Its magnetic structure factor, as measured by PND, is consistent with the loop current model proposed by C.Varma [3], which predicts the existence of spontaneously circulating orbital currents within the CuO_2 planes, with two-loops per Cu site turning clockwise and anti-clockwise. We probed the signature of such magnetism using PND in a quasi-1D superconducting cuprate family, the so-called “telephone number” series $\text{Sr}_{14-x}\text{Ca}_x\text{Cu}_{24}\text{O}_{41}$, where the existence of such orbital magnetism was predicted by [4]. In this compound, the CuO_2 sheets form arrays of ladders rather than 2D planes. The pure compound is intrinsically hole-doped, with holes localized within the Cu-O chains. The Ca-doping leads to a transfer of holes from the chains subsystem to the ladders subsystem describing a rich phase diagram under pressure. A superconducting transition also occurs for Ca doping, in the range: $10 < x_{\text{Ca}} < 13.6$ [5]. High quality single crystals of composition ($x_{\text{Ca}}=5$ and 8) were grown by the travelling solvent floating zone method in an image furnace. The emergence of a low temperature magnetism, possibly associated with circulating orbital currents, within the ladders subsystem, was evidenced by PND on both compositions. The crystal growth process along with results from PND will be presented and discussed. [1] L. Mangin-Thro *et al.*, Nat. Comm. 6, 7705 (2015) (and references therein) [2] L Zhao *et al.*, Nature Phys. 13, 250 (2017) [3] C.M. Varma, Phys.Rev.B 73,15 (2006) [4] P. Chudzinski *et al.*, Phys. Rev. B 76, 161101(R) (2007) ; Phys. Rev. B 78, 075124 (2008). [5] K. M. Kojima *et al.*, J. Elec Spe Rel Phen 117–118, 237 (2001).

Monday, July 29, 2019

10:30 AM - 12:00 PM

Symposium on Epitaxy of Complex Oxides: Batteries and Epitaxial Nanocomposites

Location: Grays Peak II, III

Session Chair(s): Q. X. Jia

10:30 AM - 11:00 AM

RESEARCH DEVELOPMENT OF ALL SOLID-STATE BATTERIES BY USING THIN FILM TECHNOLOGY

T. Ohnishi

National Institute for Materials Science, JAPAN

Interface properties are essential in solid-state batteries. When battery materials are combined into a solid-state battery, various kinds of interfaces are formed, and these play critical roles in determining the battery performance. Thin film synthesis of battery materials is an effective approach to investigating the interface properties, since it simplifies the interface geometry and provides important information about the interface. Pulsed laser deposition (PLD) is used to form thin films of multication oxides since the deviation in composition between the solid target and the thin film is relatively small compared with other physical vapor deposition methods. However, even the PLD grown films often show somewhat different properties, usually degraded, from those of bulk single crystals by the inclusion of lattice defects in many cases caused by the composition deviating from stoichiometry. We use PLD to grow highly crystalline epitaxial thin films of a cathode material: LiCoO_2 [1-6]. Sputtering is widely used to form wide area films including battery materials. We use RF-sputtering to form amorphous thick films of an oxide solid electrolyte: Li_3PO_4 . Thermal evaporation is used to form metal Li film as an anode material. I will talk about various properties of each film and show some battery performance of the samples consist of these films.

References [1] T. Ohnishi, B.T. Hang, X. Xu, M. Osada, and K. Takada : *J. Mater. Res.*, **25** (2010), 1886-1889. [2] T. Ohnishi and K. Takada : *Appl. Phys. Express*, **5** (2012), 055502. [3] K. Nishio, T. Ohnishi, M. Osada, N. Ohta, K. Watanabe, and K. Takada : *Solid State Ionics*, **285** (2016), 91-95. [4] K. Nishio, T. Ohnishi, K. Akatsuka, and K. Takada : *J. Power Sources*, **247** (2014), 687-691; *ibid.*, **261** (2014), 412-413. [5] K. Okada, T. Ohnishi, K. Mitsuishi, and K. Takada : *AIP Advances*, **7** (2017), 115011. [6] K. Nishio, T. Ohnishi, K. Mitsuishi, N. Ohta, K. Watanabe, and K. Takada : *J. Power Sources*, **325** (2016), 306-310.

11:00 AM - 11:30 AM

NEW PARADIM OF EPITAXY WITH LARGE LATTICE MISMATCH USING NANOCOMPOSITE DESIGNS

H. Wang¹, J. Huang², J.L. Macmanus-Driscoll³, Q..X. Jia⁴

¹Purdue University/Neil Armstrong Engineering Building, UNITED STATES OF AMERICA, ²Purdue University/Neil Armstrong Engineering Building, IN, UNITED STATES OF AMERICA,

³Cambridge University, UNITED KINGDOM, ⁴Univ. at Buffalo - the State University of New York, NY, UNITED STATES OF AMERICA
Self-assembled oxide-based vertically aligned nanocomposite (VAN) thin films offer a unique platform for nanocomposite designs and multifunctionalities. . A large number of oxide VAN systems have been demonstrated and explored for enhancing specific physical properties, such as strain-enhanced ferroelectricity, tunable magnetotransport, and novel electrical/ionic transport properties. The epitaxial growth of the nanocomposite thin films and the coupling at the heterogeneous interfaces are critical considerations for future device applications. In this talk, the advantages of strain coupling along vertical interfaces and film-substrate interfaces in nanocomposite films over conventional single phase films are discussed. Specifically, a unique strain compensation model enabling the epitaxial growth of two-phase nanocomposites having large lattice mismatch with substrates will be discussed. Out-of-plane strain coupling between the two phases is also discussed in terms of designing strain states for desired functionalities.

11:30 AM - 12:00 PM

INTERPLAY OF STRAIN, DEFECTS AND INTERFACE ON FUNCTIONAL PROPERTIES OF NANOCOMPOSITES

A. Chen

CINT, Los Alamos, NM, UNITED STATES OF AMERICA

Strain, Defects and Interface play critical role in controlling functional properties in complex oxide heterostructures. These parameters have been extensively studied in controlled synthesis to control physical properties. How to control these parameters in more complex two

phase vertical heteroepitaxial nanocomposites and how to use these parameters to tailor functionalities in nanocomposites are much less explored. In this talk, I will first talk about the synthesis of a variety of nanocomposite thin films from a perspective of strain, defect and interface. Nanopillar feature size in these two phase nanocomposites has been found to be a critical parameter to control strain, defects and vertical interface density. In the second part of this talk, I will focus on how to use these parameters to tune the functional properties such as magnetism, magnetotransport and magnetoelectric coupling in nanocomposites. Via a combination of controlled synthesis, advanced probing, and theoretical modeling, we are able to reveal the key role of the pillar feature size on determining strain, defects and interface, as well as functionalities in two phase epitaxial nanocomposite films.

Monday, July 29, 2019

10:30 AM - 12:00 PM

Symposium on Ferroelectric Crystals and Textured Ceramics: Perovskite Ferroelectric Crystals

Location: Grays Peak I

Session Chair(s): Yuji Noguchi, Zuo-Guang Ye

10:30 AM - 11:00 AM

ELECTRICAL CONTROL OF FERRIELECTRIC AND FERROELECTRIC PHASES IN BI-BASED POLAR PEROVSKITES.

Y. Noguchi

Department of Applied Chemistry, The University of Tokyo, JAPAN

Because the functions of polar materials are governed primarily by their polarization response to external stimuli, the majority of studies have focused on controlling polar lattice distortions. In some perovskite oxides, polar distortions coexist with nonpolar tilts and rotations of oxygen octahedra. The interplay between nonpolar and polar instabilities appears to play a crucial role, raising the question of how to design materials by exploiting their coupling. Here, we show morphotropic phase boundaries, where 'ferrielectric' appears as a bridging phase between ferroelectrics with rhombohedral and

tetragonal symmetries in $\text{Bi}_{1/2}\text{Na}_{1/2}\text{TiO}_3\text{-BaTiO}_3$ perovskites. Neutron diffraction analysis demonstrates that the intermediate ferrielectric displays a small P_s resulting from up and down polarizations coupled with an in-phase TiO_6 rotation. Our *ab initio* calculations indicate that a staggered Bi-O conformation at an appropriate chemical pressure delivers the ferrielectric-mediated phase boundaries. In addition, we demonstrate that the ferrielectric and ferroelectric phases can be controlled at will by an application of electric fields. The ferrielectric phase exhibits a piezoelectric strain constant d_{33} as high as 1,000 pm/V, which originates from the polarization twist mechanism. Our experimental and first-principles studies provide direct evidence that a ferrielectric perovskite exhibits a large piezoelectric response because of extended polar distortion, accompanied by nonpolar octahedral rotations, as if the twisted polarization relaxes under electric fields.

11:00 AM - 11:30 AM

MULTISCALE STRUCTURES AND ORIGINS OF HIGH PIEZO-/FERROELECTRICITY IN COMPLEX PEROVSKITE SINGLE CRYSTALS

Z. Ye

Simon Fraser University, BC, CANADA

Single crystals of complex perovskite structure, represented by lead magnesium niobate-lead titanate $\text{PbMg}_{1/3}\text{Nb}_{2/3}\text{O}_3\text{-PbTiO}_3$ (PMN-PT) solid solution, exhibit extraordinary piezoelectric performance - with extremely high piezoelectric coefficients, very large electromechanical coupling factors and exceptionally high strain levels, making them the materials of choice for the next generation of high-end electromechanical transducers for a wide range of applications. However, their mesoscopic domain structures, local crystal structures and morphotropic phase boundary (MPB) phase symmetry and components remain poorly understood. In order to unveil the origin of high piezo-/ferroelectricity, it is of particular interest to study the single crystals of the canonical piezo-/ferroelectric lead zirconate-titanate $\text{PbZr}_{1-x}\text{Ti}_x\text{O}_3$ (PZT), which are not only needed for a thorough characterization of the anisotropic properties of this prototype ferroelectric solid solution system, but are also expected to exhibit

superior piezo-/ferroelectric performance over the PZT ceramics, and a higher depoling temperature (T_d) and a higher coercive field (E_c) than the relaxor-based PMN-PT single crystals, suitable for a broader range of advanced applications. Recently, thanks to our capability in growing PZT single crystals with a wide composition range across the MPB and the availability of multiscale characterization and analytical techniques, such as polarized light microscopy, piezoresponse force microscopy (PFM), spherical aberration-corrected transmission electron microscopy, high-resolution neutron total scattering and diffuse scattering, and pair-distribution function analysis, we have gained new insights into the *complex local structure, atomic scale polarization rotation, nano-scale domain structure, intricate phase transition and critical behaviour, and tri-critical points in PZT*. For instance, the atomic structure of PZT crystals is imaged by means of high-resolution TEM. The accurate Pb displacements and their directions are successfully determined relative to the centre of the four B-cations, on the monoclinic mirror plane. The orientation and distribution of local polarizations indicate a mixture of rhombohedral, tetragonal and monoclinic local symmetry, providing the atomistic evidence for the origin of the monoclinic phase in the PZT of MPB compositions. By synchrotron X-ray diffraction, the structural and domain-wall-motion effects in PZT single crystals are measured and the intrinsic and extrinsic contributions to the piezoelectricity are evaluated quantitatively. This series of results provide a better understanding of the relationship between micro-/nano-scopic structure and macroscopic functional properties for the PZT solid solution, but also for the piezo-/ferroelectric materials in general. *This work was supported by the U. S. Office of Naval Research (Grants N00014-12-1-1045 and N00014-16-1-6301) and the Natural Science and Engineering Research Council of Canada (NSERC).*

11:30 AM - 11:45 AM

GROWTH AND CHARACTERIZATION OF BAPRXND1-XFENB4O15 SINGLE CRYSTALS

B. Wang, M. Krogstad, H. Zheng, S. Rosenkranz, R. Osborn, D. Phelan

Argonne National Laboratory, IL, UNITED STATES OF AMERICA

Relaxor ferroelectrics were discovered in the 1950s among the complex oxides with perovskite structure. [1] In recent years, interest in this class of materials has continued to grow owing to their ultra-high electromechanical coupling. The majority of work has been concentrated upon prototypical cubic relaxor systems, such as $\text{Pb}(\text{Mg}_{1/3}\text{Nb}_{2/3})\text{O}_3$ (PMN), $\text{Pb}(\text{Zn}_{1/3}\text{Nb}_{2/3})\text{O}_3$ (PZN) and $(\text{Pb}, \text{La})(\text{Zr}, \text{Ti})\text{O}_3$ (PLZT).[2] In this work, single crystals of $\text{BaPr}_x\text{Nd}_{1-x}\text{FeNb}_4\text{O}_{15}$ ($0 \leq x \leq 1$), which serve as a representative of the three dimensional Ising class of relaxors, have been synthesized by the floating zone technique and characterized by high resolution X-ray scattering and dielectric measurements. Single crystal diffuse X-ray scattering experiments reveal characteristic shapes of diffuse scattering in the relaxor phase of this system. Dielectric properties were studied as a function of temperature, and it was found that the oxygen vacancies have a significant influence on the dielectric behavior. Furthermore, the relations between dielectric properties and local ordering have been investigated. [1] A.A. Bokov and Z.-G. Ye, *J. Mater. Sci.* **41**, 31-52 (2006)
[2] Enwei Sun and Wenwu Cao, *Prog. Mater. Sci.* **65**, 124-210 (2014)

11:45 AM - 12:00 PM

A FERROELECTRIC POLYMER BASED ARTIFICIAL SYNAPSE FOR NEUROMORPHIC APPLICATIONS

S. Kim¹, J. Park²

¹Department of Electrical and Computer Engineering, Sungkyunkwan University, KOREA, REPUBLIC OF, ²Department of Electrical and Computer Engineering, KOREA, REPUBLIC OF

With the coming of 4th Industrial Revolution, represented by Artificial intelligence (AI), Internet of Things (IoT) and Big-data processing, the demand of the new computing scheme for numerous data processing with less energy consumption in a short period time has been rapidly increased. The conventional von Neumann computing architecture which is separating logic and memory blocks faced the challenge of the extensive power consumption and time delay by serial computing to transfer data between each blocks. A neuromorphic computing which mimics human brain functionalities has been considered that it

can overcome the limitation of von Neumann-based computing systems with its characteristics of parallel computing capability with energy efficient data processing. From energy efficiency point of view at neuromorphic system, many candidates for synaptic devices have been suggested such as phase change memory, resistive change memory, conductive bridge memory, and ferroelectric memory. However it is still challengeable to implement low power neuromorphic system with these emerging memories since more switching power reduction should be realized for parallel array application. Among aforementioned applications, ferroelectric device is one of the promising candidates for synaptic devices due to its low power and fast switching characteristics. In this work, we report ferroelectric polymer based artificial synaptic devices for neuromorphic applications. We fabricated ferroelectric polymer devices with the poly (vinylidene fluoride-trifluoroethylene) (P(VDF-TrFE)) as the gate dielectric and 2 dimensional transition metal dichalcogenide (TMD) materials as channel materials. Our devices exhibited a large hysteresis and displayed excellent retention and endurance performance. Additionally, a comprehensive study comparing the ferroelectric properties, e.g. coercive field, remnant polarization and hysteresis is presented with respect to thickness and composition of P(VDF-TrFE). Increasing thickness of PVDF was found to cause enhanced hysteresis window and the possible mechanism of that was qualitatively analyzed using band theory. Additionally, synaptic plasticity such as long-term potentiation and depression (LTP/D) and spike-timing dependent plasticity (STDP) are successfully demonstrated with improved symmetry and linearity between positive and negative update. Our study suggests that ferroelectric organic synaptic devices are considered as one of key technologies for realization of neuromorphic applications in the future.

Monday, July 29, 2019

10:30 AM - 12:00 PM

Wide Bandgap Growth and Characterization

Location: Torrey Peak II-IV

Session Chair(s): Daniel Feezell, Tetsuya Takeuchi

10:30 AM - 11:00 AM

GROWTH AND POINT DEFECT CONTROL OF ALGAN FOR UV LASER DIODES

R. Collazo¹, R. Kirste², P. Reddy³, S. Washiyama⁴, Q. Guo⁵, A. Klump⁴, B. Sarkar⁵, S. Mita³, W. Mecouch³, J. Tweedie³, Z. Sitar³
¹, UNITED STATES OF AMERICA, ², AL, UNITED STATES OF AMERICA, ³Adroit Materials, AL, UNITED STATES OF AMERICA, ⁴North Carolina State University, NC, UNITED STATES OF AMERICA, ⁵North Carolina State University, AL, UNITED STATES OF AMERICA

The AlGaN material system offers unique opportunities to develop next generation UV lasers with emission ranging 210 – 350 nm. However, despite many efforts, no electrically injected laser diode with emission wavelength < 320 nm has been demonstrated yet. Among others, challenges for these devices include low doping and low carrier injection efficiency, absorbing layers and defects, and non-ohmic contacts. Here, we present recent advances in the growth and fabrication of UV laser diodes on single crystal AlN substrates focusing on necessary point defect control schemes during growth by MOCVD. Point defect incorporation in Al/GaN is dependent on the defect formation energy and hence on associated chemical potentials and the Fermi level. For example, the formation energy of C_N or V_{Al} -nSi complexes in Al/GaN varies as chemical potential difference and Fermi level. Here, we demonstrate a systematic point defect control by employing the defect formation energy as tool by (a) chemical potential control and (b) Fermi level control. We derive a relationship between growth parameters, metal supersaturation and chemical potentials demonstrating successful quantitative predictions of C and V_{Al} -nSi complex incorporation as a function of growth conditions in Al/GaN. Hence growth environment necessary for minimal point defect incorporation within any specified constraints may be determined. Fermi level control based point defect reduction is demonstrated by modifying the Fermi level describing the probability of the defect level being occupied/unoccupied i.e. defect quasi Fermi level (DQFL). The DQFL is modified by introducing excess minority carriers (by above

bandgap illumination). A predictable (and significant) reduction in compensating point defects (C_N , H, V_N , V_{Al-nSi}) in (Si, Mg) doped Al/GaN measured by electrical measurements, photoluminescence and secondary ion mass spectroscopy (SIMS) provides experimental corroboration of these control schemes. In terms of UV laser fabrication, all steps needed to achieve electrically injected UV lasing will be described. First, it is shown that the MOCVD growth on AlN substrates results in high quality AlGaN layer with low defect concentration and excellent doping capabilities after implementation of the point defect control schemes. Next, design of the active region (MQW) is discussed and low threshold optically pumped lasing is demonstrated. Considering simulation results, the design and growth of a complete UV laser diode is shown and fabrication challenges are analyzed. Finally, we present electrical data and electroluminescence spectra from fabricated diodes and discuss the challenges that need to be addressed to realize the first electrically injected UV laser diode.

11:00 AM - 11:15 AM

POINT DEFECTS IN GAN:Mg CRYSTALS GROWN BY AMMONOBASED METHOD

M. Zajac¹, R. Piotrkowski¹, E. Litwin-Staszewska¹, K. Sakowski¹, D. Wasik², **R. Kucharski**¹, M. Bockowski¹

¹Institute of High Pressure Physics, Polish Academy of Sciences, POLAND, ²Faculty of Physics, University of Warsaw, POLAND
Ammonothermal method uses supercritical ammonia for the dissolution of feedstock material. The method enables production of GaN substrates with different conductivity, including n-type, p-type and semi-insulating (SI) material with resistivity between 10^6 and 10^{12} Ωcm . A wide range of electrical properties was achieved by controlling concentrations of unintentional oxygen (O) donor and intentional Mg acceptor. However, in case of SI ammonothermal GaN:Mg crystals, there is little knowledge about the participation of intentional and native point defects in the oxygen compensation mechanism. It was suggested that in case of highly resistive GaN:Mg, V_{Ga} -related point defects (mainly $V_{Ga}-H_3$) determine the character of temperature dependence of resistivity [1]. SI GaN:Mg crystals of various Mg and

oxygen concentrations were thoroughly studied by means of resistivity vs temperature measurements in the van der Pauw configuration. It was observed that if the O concentration is $1 \times 10^{18} \text{ cm}^{-3}$, the activation energy (E_A) can be tuned from 1.5 eV, through 1 eV, to 0.5 eV for Mg concentration of $1 \times 10^{18} \text{ cm}^{-3}$, $2 \times 10^{18} \text{ cm}^{-3}$, and $6 \times 10^{18} \text{ cm}^{-3}$, respectively. Additionally, high-temperature Hall effect data (300°C-600°C) reveal n-type conductivity for the first case and p-type conductivity for the two other ones. The results are interpreted in terms of the Fermi level dependent generation of electrons/holes from the deep defect (DD) level located about 1 eV above the valence band maximum (vbm) and attributed to the $V_{\text{Ga}}H_n$ defect. In the n-type crystals ($E_A=1.5 \text{ eV}$) the Fermi level is located in the middle between the DD level and the conduction band minimum (cbm). In the p-type crystals the Fermi level is pinned to the DD level if $E_A=1 \text{ eV}$ and it is in the center between the DD level and the vbm if $E_A=0.5 \text{ eV}$. The results will be quantitatively analyzed by calculations based on neutrality equation and compared with other measurement techniques (FTIR). In addition, the role of Mg-, O-, and Ga vacancy-related defects will be discussed in terms of the temperature dependence of resistivity. The presented results indicate a crucial role of Ga-related defects in optimizing the resistivity of GaN:Mg. [1] M. Zajac et al., Prog. Cryst. Growth Charact. Mat.,64 (2018) 63–74 . This research was supported by the Department of the Navy, Office of Naval Research (ONRG-NICOP-N62909-17-1-2004), by Polish National Science Center through projects No. 2017/25/B/ST5/02897 and 2018/29/B/ST5/00338, by TEAM TECH program of the Foundation for Polish Science co-financed by the European Union under the European Regional Development Fund. (POIR.04.04.00-00-5CEB/17-00).

11:15 AM - 11:30 AM

CRYSTALLOGRAPHIC POLARITY INVERSION IN NITRIDES ON SI

A. Roshko, M. Brubaker, P. Blanchard, T. Harvey, K. Bertness
NIST, CO, UNITED STATES OF AMERICA

III-nitrides grown on Si substrates are attractive for low cost, large scale manufacturing of easily integrable devices. A major challenge to

achieving this objective is control of crystallographic polarity. While AlN polarity can be nominally controlled during growth through the V/III ratio,^[1] it has been found that polarity inversion domains (IDs) are common.^[2,3] In addition, we have recently shown that Al-Si eutectic frequently forms during AlN growth above the eutectic temperature ($T_{\text{eut}} = 577 \text{ }^\circ\text{C}$).^[4] To investigate these issues further, GaN/AlN films were grown on Si(111) substrates and examined with atomic resolution scanning transmission electron microscopy and energy dispersive X-ray spectroscopy. Evidence of eutectic formation, such as hillocks and holes in the Si substrate surface, was found in most of the samples and the concentration of eutectic-phase related defects increased with increasingly Al-rich conditions during the initial stage of growth. The presence of Al-Si eutectic-phase was also correlated with formation of IDs in the nitride layers. Silicon was found at polarity inversion boundaries both within the AlN buffer layers and at the AlN/GaN interface. Spatial nonuniformity in these Si distributions gave rise to narrow regions of vertical IDs. In samples grown with initially very N-rich conditions there was little evidence of eutectic formation and consistent with this IDs were not found in these samples. The results can be described by the following model. An Al-Si eutectic layer is formed under Al-rich conditions and floats on the AlN surface during growth. When the growth is changed to N-rich the eutectic layer is incorporated into the nitride film including the silicon, which can induce polarity inversion. Because the silicon incorporation is nonuniform, the polarity inversion is also nonuniform, leading to vertical inversion domains. AlN growth below the eutectic temperature will also be discussed. [1] Brubaker, et al., *Cryst. Growth Des.* **16**, 596 (2016). [2] Sanchez, et al., *Appl. Phys. Lett.* **78**, 2688 (2001). [3] Auzelle, et al., *J. Appl. Phys.* **117**, 245303 (2015). [4] Roshko, et al., *Crystals* **8**, 366 (2018).

11:30 AM - 11:45 AM

GE-DOPING IN ALGAN: DX FORMATION AND COMPENSATION

R. Kirste¹, P. Bagheri¹, S. Washiyama¹, S. Mita², Q. Guo¹, B. Sarkar¹, J.H. Kim¹, A. Klump¹, Y. Guan¹, R. Collazo¹, Z. Sitar¹

¹North Carolina State University, UNITED STATES OF AMERICA,

²Adroit Materials, UNITED STATES OF AMERICA

Successful n-type doping of GaN and AlGa_xN is crucial for UV lasers and LEDs and next generation high power devices. Si is the most widely used n-dopant. However, high Si-doping typically leads to tensile strain and cracking. Germanium doping of GaN was found to be a good alternative to Si leading to crack free films and high carrier concentrations $n > 10^{20} \text{ cm}^{-3}$. Data on Ge doped AlGa_xN is sparse. For Al-rich AlGa_xN, theoretical calculations predict the crossover point for DX center formation in Al_xGa_{1-x}N to be around $x=0.5$ for Ge. Until now, for Ge-doping no experimental data is available that supports these predictions. In this study, doping of AlGa_xN with Al content of up to 60% is demonstrated and compensations and DX-center formation is investigated. Doped AlGa_xN layers are grown on AlN/sapphire templates by MOVPE. TEG, TMA, and ammonia are used as gallium, aluminum, and nitrogen sources as well as GeH₄ gas for Ge doping. Electronic properties and defect luminescence are characterized by Hall effect measurement, photoluminescence spectroscopy (PL), and XRD. The AlGa_xN layers maintain a good quality upon doping as indicated by a strong and well-defined near band edge luminescence. Almost constant free electron concentration is observed for AlGa_xN:Ge with similar doping levels of $3 \times 10^{19} \text{ cm}^{-3}$ and up to 40% Al content. However, for higher Al content a collapse of the free carrier concentration from $8 \times 10^{18} \text{ cm}^{-3}$ to $1 \times 10^{17} \text{ cm}^{-3}$ is observed. Hall effect measurement in a temperature range from 280 K to 700 K revealed activation energy of below 20 meV in AlGa_xN up to 40% Al content and a sharp increment in activation energy to 90 meV at 50% Al composition, indicating the onset of DX-center formation. This is in excellent agreement with theoretical predictions. In addition to the DX formation, Ge doped Al_{0.4}Ga_{0.6}N layer exhibited reduction in free carrier concentration with increasing Ge concentration above a certain value. Similar to Si doped AlGa_xN, this can be due to metal vacancy-Ge complexes which act as acceptor type point defect. Consequently, self-compensation in Ge-doped AlGa_xN films at 40% Al content can be further shown by emergence of a Ge-vacancy related peak at 2.3 eV in the PL spectra, while a C-related peak at 2.7 eV is dominant in low doping condition acting as a compensator. Finally, it is shown that

self-compensation can be controlled via growth parameters which affect chemical potential and defects formation energy.

11:45 AM - 12:00 PM

HIGH-TEMPERATURE ANNEALING OF SPUTTERED SCALN FILMS FOR LATTICE-MATCHED ALGAN EPITAXY

B. Gunning, A. Allerman, A. Rice

Sandia National Laboratories, NM, UNITED STATES OF AMERICA

AlGaN alloys offer great potential for ultraviolet light emitters and high-power electronics owing to their large band gap and critical electric field. AlGaN films are typically grown on template layers of GaN or AlN on sapphire substrates, or on bulk GaN or AlN substrates. However, the approximately 2.5% in-plane lattice mismatch between AlN and GaN limits the thickness of AlGaN that can be grown before the onset of strain relaxation and subsequent generation of cracks or dislocations. In recent years, research has shown that high-temperature annealing ($>1600^{\circ}\text{C}$) can cause dramatic recrystallization in MOCVD-grown and sputtered AlN films, leading to dislocation densities $\sim 10^8 \text{ cm}^{-2}$, comparable to state-of-the-art high-temperature MOCVD AlN. Unfortunately similar high temperature annealing processes applied to AlGaN alloys does not provide the same reduction in dislocation density due to the lower thermal decomposition temperature of the GaN constituent. As an alternative, we propose the use of sputtered ScAlN which features greater thermal stability and can be lattice-matched to any AlGaN composition using Sc mole fractions from 0-18%. A high-temperature annealed, sputtered ScAlN film could provide a lattice-matched, low-dislocation buffer layer for subsequent AlGaN epi growth. Initially, sputtering and annealing conditions were optimized for AlN sputtered on sapphire. After optimization, as-sputtered AlN films exhibited (0002) and (10-11) XRD rocking curves of ~ 15 and ~ 3000 arcsec, respectively. After high-temperature anneal for 1 hour at $\sim 1800^{\circ}\text{C}$ these films showed dramatically improved (10-11) rocking curve FWHM of ~ 300 arcsec. Switching to an Sc-Al alloy target (5.5 at% Sc) and employing similar process conditions as used for sputtered AlN, we achieved rocking curves of 15 and 4300 arcsec for the (0002) and (10-11) reflections, respectively, for ~ 200 nm thick as-sputtered ScAlN films. XRD and

RBS measurements indicated a Sc composition of ~3.5%. After high temperature anneal at 1750°C (1800°C) for 1 hour, the (10-11) rocking curves were dramatically reduced to 730 (630) arcsec but the (0002) rocking curves broadened to 110 (330) arcsec. The surface after annealing was transformed from of a small-grain texture to one exhibiting highly ordered step bunches. Characterization by TEM and EDX, revealed Sc- and O-rich precipitates and a high density of stacking faults potentially indicative of cubic inclusions. Sandia National Laboratories is a multimission laboratory managed and operated by National Technology & Engineering Solutions of Sandia, LLC, a wholly owned subsidiary of Honeywell International Inc., for the U.S. Department of Energy's National Nuclear Security Administration under contract DE-NA0003525.

Monday, July 29, 2019

1:30 PM - 3:00 PM

Beyond Graphene and TMDs

Location: Crestone III, IV

Session Chair(s): Kurt Gaskill, Kevin M. Daniels

1:30 PM - 1:45 PM

INTERACTIONS OF TMGA AND NH₃ WITH DEFECTS IN GRAPHENE: TOWARDS A MECHANISTIC UNDERSTANDING OF 2D GAN_x FORMATION

A. Bansal, N. Nayir, S. Rajabpour, B. Huet, A. Van Duin, J.M. Redwing

Penn State University, PA, UNITED STATES OF AMERICA

Low dimensional forms of GaN and related group III-nitrides such as nanowires and nanoparticles have attracted significant interest for applications in optoelectronics, displays, gas sensors etc. Recently, ultra-thin, two-dimensional (2D) layers of GaN_x and AlN have been reported, formed by metal intercalation through graphene and subsequent nitridation using metalorganic chemical vapor deposition (MOCVD). Balushi et. al. reported that 2D GaN_x film can be stabilized by the diffusion of Ga and N species to the interfacial gap between

epitaxial graphene (EG) and SiC.¹ Likewise, Wang et. al. reported 2D AlN confined between CVD graphene and Si.² This intercalation-based growth process is believed to rely on many factors including wrinkles, vacancies and other defects in graphene. However, in both cases, the mechanisms of intercalation and nitridation is not well understood. In this study, we apply a combination of experiments, reactive force field (ReaxFF) modeling and density functional theory (DFT) calculations to elucidate the interaction of TMGa and NH₃ precursors with defects in graphene. Transferred monolayer CVD graphene on Si when heated in hydrogen at a pressure of 100 Torr at different temperatures (550°C, 750°C and 950°C) introduced defects into graphene as confirmed by increased I_D/I_G ratio with increasing temperature indicating a higher density of defects. Further, we investigate interaction of Ga and N atoms/clusters with the defects formed and develop a mechanistic understanding of 2D GaN_x formation. Initially, we modeled the decomposition of Ga clusters from TMGa precursor, based on ReaxFF. To examine the influence of the defects in graphene on the intercalation, we considered three representative defect models, namely, single vacancy (SV), divacancy (DV) and 555777 (reconstructed divacancy) and employed the DFT method to compute the binding energy of Ga atom, monomethylgallium (MMG), dimethylgallium (DMG) and trimethylgallium (TMG) to the pristine and defective graphene. SV and DV defects strongly bind the Ga atom with/without methyl group while pristine graphene weakly interacts with Ga. These results show that by introducing the defects into graphene, the binding energies of Ga species can be manipulated, and thus, the Ga intercalation process can be controlled. Similarly, investigating the interaction of NH₃ with the defects will provide us a better understanding and control on the encapsulated growth process. 1. Al Balushi, Z. Y. *et al.* Two-dimensional gallium nitride realized via graphene encapsulation. *Nat. Mater.* **15**, 1166 (2016). 2. Wang, W. *et al.* 2D AlN Layers Sandwiched Between Graphene and Si Substrates. *Adv. Mater.* **31**, 1803448 (2019).

1:45 PM - 2:00 PM

EPITAXIAL GROWTH OF LAYERED β - In_2Se_3 THIN FILMS VIA METALORGANIC CHEMICAL VAPOR DEPOSITION

X. Zhang, S. Lee, A. Bansal, T.N. Jackson, J.M. Redwing
The Pennsylvania State University, PA, UNITED STATES OF AMERICA

2D materials have attracted wide interest because of their potential performance and diversity of function as electronic and optoelectronic materials. Growth of transition metal dichalcogenides (TMDs) such as MoS_2 and WSe_2 typically requires high temperatures ($>700^\circ\text{C}$) for large domain size and epitaxy. This restricts the applications of these materials, especially considering the growing interest in 2D materials integration with silicon in back-end-of-line (BEOL) applications that require processing temperature $< 450^\circ\text{C}$. In contrast, group III metal chalcogenides (indium selenide and gallium selenide) possess lower melting temperatures than TMDs and thus high crystal quality films are anticipated at lower growth temperature. In addition, depending on their stoichiometry and phase, they also have a layered structure that offers interesting physical, electronic, and piezoelectric properties down to the monolayer limit. In the case of indium selenide, there is interest in γ - InSe due to its high carrier mobility ($>1000 \text{ cm}^2/\text{Vs}$) and β - In_2Se_3 and α - In_2Se_3 which are ferroelectric phases. Despite the intriguing properties, there have been few studies thus far aimed at investigating the epitaxial growth and properties of indium selenide films. In this study, we demonstrate the growth of β - In_2Se_3 thin films on various substrates in a vertical cold-wall metalorganic chemical vapor deposition (MOCVD) system at 400°C using trimethylindium (TMIn) and hydrogen selenide (H_2Se) in a H_2 carrier gas. The In_2Se_3 films were grown epitaxially on c-plane sapphire and Si (111) surfaces (Figure 1a,b). The films were identified as β - In_2Se_3 by both Raman (Figure 1c) and XRD (Figure 1d). A low reactor pressure (100 Torr) and high total gas flow rate were required to suppress gas-phase reactions between TMIn and H_2Se based on their Lewis acid and base properties. β - In_2Se_3 films were formed on both c-plane sapphire and Si (111) surfaces in this work, however, γ - In_2Se_3 films were synthesized on amorphous SiO_2/Si substrates indicating the

importance of substrate type determining the crystal structure of the films. Top-gated thin film transistors (TFTs) fabricated on β - In_2Se_3 thin films reasonable mobility and on/off ratio and therefore offer potential applications in electronic devices.

2:00 PM - 2:15 PM

MOVPE GROWTH OF GAAS ON SINGLE-CRYSTAL 2D LAYERED Bi_2Se_3 SUBSTRATES

A.G. Norman¹, C. Melamed¹, T. Saenz², A. Tamboli¹, B. McMahon¹, E. Toberer²

¹National Renewable Energy Laboratory, CO, UNITED STATES OF AMERICA, ²Colorado School of Mines, UNITED STATES OF AMERICA

Motivated by the impact of GaAs substrate cost on GaAs-based solar cells, we have investigated the growth of GaAs on a two dimensional (2D) layered substrate which can be exfoliated for each GaAs deposition, potentially reducing the substrate cost and usage. We have chosen to use Bridgman-grown single-crystal layered-2D $\text{Bi}_2\text{Se}_3(0001)$ substrates for this study because Bi_2Se_3 has a phase diagram that is very suitable for the growth of bulk single crystals from the melt by the Bridgman technique, and has an in-plane lattice-constant favorable for III-V epitaxy. The two challenges addressed by this work are the in-plane lattice-constant mismatch between $\text{GaAs}(111)$ and $\text{Bi}_2\text{Se}_3(0001)$, and the nucleation of GaAs on a 2D layered crystal surface. Both of these challenges were overcome using surface-conversion processes which are quite different from traditional epitaxial processes. To address the lattice-mismatch challenge, we show that exposure to trimethylindium at elevated temperatures converts the surface layers of $\text{Bi}_2\text{Se}_3(0001)$, which is in-plane lattice-matched to $\text{InP}(111)$, to high quality 2D layered $\text{In}_2\text{Se}_3(0001)$, which is in-plane lattice matched to $\text{GaAs}(111)$. GaAs nucleation is also a challenge, partly due to the lack of dangling bonds at the surface of the 2D layered crystals and also because attempts to grow GaAs directly on Bi_2Se_3 produced GaSe compounds. To solve this problem, we surface-convert the Bi_2Se_3 to cubic ZnSe by

exposing $\text{Bi}_2\text{Se}_3(0001)$ to diethylzinc at elevated temperatures. After performing this surface-conversion to $\text{ZnSe}(111)$, which is lattice-matched to $\text{GaAs}(111)$, we were able to epitaxially grow a thin film of highly $\{111\}$ textured GaAs , then exfoliate the resulting film from the underlying 2D layered Bi_2Se_3 substrate.

2:15 PM - 2:30 PM

HIGH-PRESSURE GROWTH OF THE NEWLY PREDICTED QUANTUM SPIN HALL INSULATOR Pt_2HgSe_3

E. Giannini

Department of Quantum Matter Physics - University of Geneva,
SWITZERLAND

In the quest for van der Waals materials suitable for exfoliation and for tuning the physical properties at the atomic limit, a remarkable effort has been made by high-throughput calculations using Density Functional Theory in order to identify a class of 2D materials with expected exciting electronic, magnetic and topological properties [1]. One of the most remarkable outputs of first-principle calculations was the prediction of a large-gap Quantum Spin Hall Insulating state in the compound Pt_2HgSe_3 [2]. Pt_2HgSe_3 is a naturally occurring layered mineral ("*jacutingaite*") only recently discovered and synthesized in powder samples [3]. The phase equilibria in the system Hg-Pt-Se are not known above 400°C and the high-volatility and toxicity of the components render the conventional crystal growth methods unusable. Here I report on the successful growth of Pt_2HgSe_3 crystals at high pressure (1-3GPa), using a cubic anvil isostatic press operating at high temperature in the range $800\text{-}1000^\circ\text{C}$. The growth pressure, temperature and rate were optimized and the largest crystals were grown at 1.5GPa and 900°C , starting from a slightly Hg-rich composition. The most common secondary phase was found to be PtSe_2 , which is stable in the same temperature range and easily grows either as intra-layer defects into Pt_2HgSe_3 or separate crystals with similar morphology and size to those of *jacutingaite*. The control of the Hg-loss was found to be the key point to grow the best Pt_2HgSe_3 crystals with the largest size of $0.6\times 0.4\text{mm}^2$ in the *ab*-plane. The reported crystal structure was confirmed by single-crystal XRD.

As-expected, the crystals exfoliate in the *ab*-plane and experiments of exfoliation to the mono-layer limit are in progress. The bulk crystals are metallic, and preliminary ARPES experiments have shown a very good agreement with the calculated bulk band structure. The similar system Pd-Hg-Se is also studied, thus offering the possibility of tuning the spin-orbit coupling in the lighter Pd-based compound. The successful growth of jacutingaite crystals opens a new perspective towards robust non-trivial 2D topologic materials. [1] Mounet N., et al., *Nat. Nanotech.* 13 (2018) 246–252 [2] Marrazzo A., et al., *Phys. Rev. Lett.* 120 (2018) 117701 [3] Vymazalová A., et al., *Can. Mineral.* 50 (2012) 441-446

2:30 PM - 2:45 PM

A FAMILY OF RARE EARTH-BASED MAGNETIC TRIANGULAR LATTICE MATERIALS

S. Guo¹, A. Ghasemi², T. Kong¹, F..A. Cevallos¹, W. Xie³, C..L. Broholm², R..J. Cava¹

¹Princeton University, NJ, UNITED STATES OF AMERICA, ²Johns Hopkins University, UNITED STATES OF AMERICA, ³Louisiana State University, UNITED STATES OF AMERICA

Geometrically frustrated magnets are typically based on corner- or edge-sharing triangular or tetrahedral units, in which magnetic cations carry the spins. With different arrangements of geometric units, such as triangular lattices, kagomé lattices, and pyrochlores, the frustrating networks display evolving magnetic characteristics. Among them, the 2D triangular lattice is considered to be one of the simplest potentially geometrically frustrated lattice types and thus has received much attention. Considering the rich unpaired electron configurations possible and the various crystal fields that they can be found in, rare earth (*R*) elements are of particular interest as the magnetic atoms in frustrated structures. To date, interesting magnetic ground states have been proposed for several *R*-based materials with frustrating magnetic networks; including spin ice behavior in Ho₂Ti₂O₇ and Dy₂Ti₂O₇, spin liquid behavior in Tb₂Ti₂O₇ and quantum spin liquid behavior in YbMgGaO₄. Here we will report single crystal growth of the KBaR(BO₃)₂ and RbBaR(BO₃)₂ rare earth borates by spontaneous

nucleation from a $\text{KF/RbF-B}_2\text{O}_3$ flux. The crystals are typically hexagonal plates about 1 mm in large dimension with good morphologies. The K variants present off-magnetic-site disorder while Rb variants are fully crystallographically ordered. The crystallographically ordered structures make compounds in the $\text{RbBaR}(\text{BO}_3)_2$ ($R = \text{Gd-Yb}$) system good candidates for further study of magnetic frustration. $\text{RbBaYb}(\text{BO}_3)_2$, as a representative of this family, was grown by spontaneous nucleation for study of its anisotropic magnetic and thermodynamic properties. Our results provide clear evidence of highly anisotropic magnetic properties and a frustrated spin state in $\text{RbBaYb}(\text{BO}_3)_2$.

2:45 PM - 3:00 PM

STRUCTURES AND STABILITY OF TWO-DIMENSIONAL MATERIALS COMPOSED OF GROUP III-V AND II-VI ELEMENTS

T. Akiyama, Y. Hasegawa, K. Nakamura, T. Ito

Mie University, JAPAN

Two-dimensional (2D) materials with honeycomb lattice have been paid much attention due to their potential applications in nanoelectronic devices. As a new class of 2D materials composed of group III-V materials, graphite-like AlN and 2D-GaN have been experimentally reported recently. [1,2] From theoretical viewpoints, we have revealed that in group-III nitrides five-fold coordinated hexagonal (Hex) structure is more stable than wurtzite structure for the films up to 15 bilayers due to interlayer electrostatic interactions. [3] Furthermore, using hybrid density functional (DFT) calculations with spin-orbit coupling and van der Waals (vdW) interaction, Lucking *et al.* have predicted that the double layer honeycomb (DLHC) structure can be realized in various group III-V, II-VI, and I-VII materials, some of which exhibits exotic topological properties. [4] According these results, the Hex structure is expected to be realized for materials containing a first-row element (B, N, and O for instance). However, the relationship between the stable structure and properties in the 2D limit and the constituent elements is still lacking. Here, we systematically investigate the structures and stability of 2D materials composed of group III-V and II-VI elements based on DFT calculations with vdW to

clarify the controlling factor of stable structure in the 2D limit. The calculated cohesive energies for various III-V and II-VI materials with different number of layers demonstrate that the DLHC structure can be stabilized depending on the constituent elements and the number of layers. The number of layers where the DLHC structure has a lower cohesive energy than three-dimensional zinc blende structure is found to be large for AlAs and CdSe. On the other hand, the fivefold coordinated Hex structure is stabilized for group-III nitrides (AlN, GaN, and InN) and CdS with large ionicity. It should be noted that the inversion of electronic bands across the Fermi energy occurs in GaAs and InP with the DLHC structure, indicating the formation of excitonic insulator. [5] These results suggest that various structures and electronic properties can be formed in 2D materials consisting of group III-V and II-VI elements.

References [1] P. Tsipas *et al.*, Appl. Phys. Lett. **103**, 251605 (2013) [2] Z. Y. A. Balushi *et al.*, Nature Materials **15**, 1166 (2016). [3] Y. Tsuboi *et al.*, Phys. Status Solidi **255**, 1700446 (2018). [4] M. C. Lucking *et al.*, Phys. Rev. Lett. **120**, 086101 (2018). [5] D. Jérôme *et al.*, Phys. Rev. **158**, 462 (1967).

Monday, July 29, 2019

1:30 PM - 3:00 PM

Industrial Crystal Growth and Technology II

Location: Shavano Peak

Session Chair(s): Matt Whittaker

1:30 PM - 1:45 PM

EFFECT OF GROWTH EQUIPMENT STABILITY AND PRECISION ON THE PULLING OF SINGLE CRYSTALS FROM THE MELT

A. Nouri, F. Lissalde, G. Quetelart

CYBERSTAR, FRANCE

Crystal growth processes require precise control of the working parameters to obtain the desired crystal size and quality. Such control is in great part related to the precision and stability of the growth equipment including pulling, rotation and weighing devices. This abstract introduces the discussion of several key points in crystal

pullers equipment and their effect on the stability of the growth as well as the quality of the final ingot. While we may suspect the important effect of thermal fluctuation and melt flow instabilities on defect formation, a better understanding of the induced mechanical vibration and movement's precision effect on crystal pulling is also required to properly control the growth environment. Both crystal rotation and translation are discussed in this summary where the achieved ranges of movement precision, stability and steadiness are given and compared.

1:45 PM - 2:00 PM

TOWARDS MODEL PREDICTIVE CONTROL FOR VGF GROWTH USING ARTIFICIAL NEURONAL NETWORKS

S. Ecklebe¹, J. Winkler¹, C. Frank-Rotsch², N. Dropka²

¹Technische Universität Dresden, GERMANY, ²Leibniz Institute for Crystal Growth, GERMANY

The Vertical Gradient Freeze (VGF) crystal growth process is a key technology for the production of compound semiconductors. It is characterized by propagating a temperature field along an ampoule's vertical axis which initially contains the molten material. From a technological point of view the control of this process is a challenging task because growth velocity and interface shape have to be kept within narrow limits without any in-situ measurement information about the process state available. The process is a typical example of the application of optimal control approaches. In this field, input trajectories for the plant are obtained by numerical minimization of a cost functional using a mathematical model of the process. In VGF growth such a cost functional would penalise undercooling of the melt or large deflections of the solid-liquid interface. However, even if sophisticated simulation models of the plant are employed the results may not lead to the expected behaviour due to disturbances acting on the system.

In order to solve this problem measurement information characterizing the process state need to be incorporated into the control system. This can be done by model predictive control (MPC). There, in each time-step only the first part of the optimal process input solution is applied. Between the time-steps, the optimisation problem is solved again

utilizing the current system state as initial value.

It is no secret that the simulation of a realistic plant model requires a fair amount of time. Considering further that this simulation has to be conducted several times by the optimiser to solve the optimal control problem, and that the whole procedure has to be repeated at every time-step during growth raises doubts concerning the applicability of the MPC approach. This is where artificial neuronal networks (ANNs) can be employed.

In contrast to transient simulations, ANNs can be trained to learn the dynamics of the system. Although this process is time-consuming and rather involved, it can be done offline. Thus, the simulation required by the optimiser is transformed to a simple online evaluation whose computation time lies within an acceptable range.

The contribution presents how these methods can be used for feedback control of the VGF process by using experimental data from a production VGF plant.

2:00 PM - 2:15 PM

MODELING OF DISLOCATION DYNAMICS IN VGF GAAS CRYSTAL GROWTH

V. Artemyev¹, A. Smirnov¹, V. Kalaev¹, A. Golubev², L. Beno²

¹STR Group, Inc. – Soft-Impact, Ltd., RUSSIAN FEDERATION,

²CMK, s. r. o., SLOVAK REPUBLIC

Gallium arsenide (GaAs) is a compound semiconductor material widely used in production of opto-electronic components like photodiodes, phototransistors, photoresistors, integrated optical circuits, chips, optical fiber communications and high-efficiency solar panels [1]. During last years GaAs is extensively employed in the development of the new wireless 5G standard of communication. Growing very high-purity GaAs crystals with a low dislocation density is practically difficult problem, which requires knowledge and experience of the growth processes. Experimental approach to improve crystal quality may be long and expensive and takes a lot of time. Computer modeling is an alternative to experiment for the analysis and optimization of GaAs crystal growth processes [2, 3]. For the Vertical Gradient Freeze (VGF) furnace of CMK, we have performed comprehensive analysis of 6-inch GaAs crystal growth

using CGSim software of STR for modeling of cone, body growth, and cooling stage. We have applied unsteady modeling of GaAs crystallization with the account of the melt flow, melt/crystal interface shape evolution, and dislocation density multiplication, analyzing the structure loss phenomenon, as a transition from mono- to multicrystalline material. The Alexander-Haasen model [4] of dislocation density multiplication based on the thermal stress release into dislocations has been used simulating crystal growth and cooling dynamics. Comparison with experimental data has demonstrated reasonable level of predicted dislocation density and its distribution in the crystal. Optimization of hot zone design and temperature recipe using computer modeling focused on reduction of dislocation density helped us to decrease the dislocation density several times compared to the initial values in the crystal before optimization. The possible factors responsible for reduction of the probability of the structure loss phenomenon are discussed. [1] <http://cmk.sk/products/gallium-arsenide/> [2] M. P. Bellman, et al., Journal of Crystal Growth, 312 (2010), p. 2175-2178 [3] Christiane Frank-Rotsch, et al., Woodhead Publishing Series in Electronic and Optical Materials, 2019, p. 181-240 [4] Alexander H., Haasen P. Solid State Phys. 1969. 22 p. 27-158

2:15 PM - 2:30 PM

NUMERICAL SIMULATION OF THE FLOW, HEAT AND MASS TRANSPORTS OF APCVD REACTOR TO OBTAIN THE ULTRA-HIGH FLATTEN SILICON EPITAXY ON 12-INCH DIAMETER SILICON

C. Hu¹, S. Wang¹, W. Lin¹, J. Chen¹, C. Tu², L. Chen²

¹Department of Mechanical Engineering, National Central University, TAIWAN, ²Taisil Electronic Materials Corp., TAIWAN

The 10 nm technology of the semiconductor device requires a very flatness film epitaxy on a 12-inch silicon wafer. At present, the Epi 300 Centura epitaxy equipment is usually used to obtain this ultra-high flatten silicon epitaxy. The obstacle occurred this epitaxy process is that there is peak near the center of the wafer and a valley between the center and the edge. In this study, the three-dimensional numerical simulation is used to investigate the flow motion and the heat and mass transfer inside the chamber. The simulated deposition

rate along the wafer is in good agreement with the experimental one from the real growth system. In this equipment, the preheat ring is installed at the outside of the susceptor to maintain the uniform temperature of susceptor. Since the partitions of the injectors have a better heat transfer from the preheat ring in comparison with the hydrogen gas. It causes the higher temperature at the partitions. The Trichlorosilane concentration declines at the higher temperature state. Therefore, the simulated result shows the non-uniform concentration distribution of Trichlorosilane near the outlet of injectors due to the non-uniform temperature. The non-uniform distribution of Trichlorosilane concentration near the outlet of injectors results in the non-uniformity of deposition rate. The uniformity of the deposition rate on the silicon wafer is achieved by the adjustment of the gas speed of the injectors.

2:30 PM - 2:45 PM

COMPUTER MODELING OF HMCZ SI GROWTH

V. Kalaev

STR Group, Inc. – Soft-Impact, Ltd., RUSSIAN FEDERATION

Nowadays, Cz growth of monocrystalline silicon remains the major crystal growth technology for making wafers for IC applications and PV cells. Industrial Cz growth of Si crystals of 300 mm diameter for electronic applications usually requires DC magnetic fields to avoid hard turbulence producing strong temperature fluctuations in the melt [1,2]. Comparing different MFs, there are several advantages of a transverse (horizontal) MF [2-4], making possible automatic industrial production with a low oxygen concentration and without structure loss. Recently, it was revealed that significant unsteady asymmetric features of Si melt convection during 300 mm HMCz growth may appear at the crystal rotation rate of 10 rpm [3] for the body growth and at increasing the argon flow rate [4] for the seeding stage. In the paper [3], it was concluded that fully 3D unsteady approximation is necessary to simulate the whole Cz system to obtain reasonable agreement with the asymmetric temperature distribution measured experimentally. However, as reported in [2, 4], the flow under the crystal is unsteady and asymmetric even within a combined 2D-3D approach with 2D axisymmetric modeling of global heat transfer and

3D modeling of a limited crystallization zone. We have studied the crystal growth case reported in [3] using the combined 2D-3D numerical approach [2, 4] and have compared our results of 3D modeling to experimental measurements reported in [3]. The study has revealed that, even within 2D-3D approach, the flow structure in Si melt with the horizontal MF is asymmetric but different from that reported in [3]. The reason of the low temperature region ($T < 1687\text{K}$) observed in the experiment [3] far away from the crystallization front is discussed in details and compared to our simulation results. Unsteady features of the melt flow and reasons of changes in asymmetric flow structures are discussed with the analysis of the temperature and velocity fluctuation spectra. A new steady 3D approach is proposed for fast and robust engineering calculations of industrial HMCz cases to growth 300 mm Si crystals, which as well enable the calculation of crystallization front geometry and reproduction of the asymmetric experimental temperature distribution [3] including the low temperature region. [1] O. Graebner et al., Materials Science and Engineering B73 (2000) 130 [2] V.V. Kalaev, Journal of Crystal Growth 303 (2007) 203 [3] R. Yokoyama et al., J. Crystal Growth 468 (2017) 905 [4] M. Iizuka et al., J. Crystal Growth 468 (2017) 510

2:45 PM - 3:00 PM

APPLICATION OF MACHINE LEARNING TO MOCVD PROCESS

G. Samanta

Veeco Instruments, NJ, UNITED STATES OF AMERICA

Micro-LED leads the candidate list for next-generation display technologies. However, challenges remain in its adoption commercially. One of the main challenges is to meet epitaxy specification of wavelength uniformity of 1-2nm within transfer field. Therefore, fast and accurate prediction of wavelength uniformity for a given set of process parameters is of enormous value. To this end, we applied machine learning algorithms on datasets obtained either from computer simulations or experiments to create efficient models with high accuracy. For instance, we developed a neural network (NN) model that can predict growth temperature at any location on wafer surface with >99% accuracy when heater powers are provided as inputs. Since growth temperature uniformity is closely related to

wavelength uniformity, the developed model can be used to predict wavelength uniformity for material grown by MOCVD.

Monday, July 29, 2019

1:30 PM - 3:00 PM

Nitride and Oxide Thin Films

Location: Torrey Peak II-IV

Session Chair(s): Luke J. Mawst, Roberto Fornari

1:30 PM - 2:00 PM

CHARACTERIZATION OF INTRINSIC COMPOSITIONAL DISORDER IN NITRIDE ALLOYS BY SCANNING TUNNELING ELECTROLUMINESCENCE SPECTROSCOPY

W. Hahn¹, J. Lentali¹, S. Nakamura², J.S. Speck³, C. Weisbuch¹, Y. Wu⁴, M. Filoche¹, F. Maroun¹, L. Martinelli¹, Y. Lassailly¹, J. Peretti¹

¹Laboratoire de Physique de la Matière Condensée, Ecole polytechnique, CNRS, FRANCE, ²Materials Department, University of California, CA, UNITED STATES OF AMERICA, ³Materials Department, UCSB, CA, UNITED STATES OF AMERICA, ⁴Graduate Institute of Photonics and Optoelectronics and Department of Electrical Engineering, National Taiwan University, TAIWAN

The emission linewidth of the widely used nitride ternary alloys (such as InGaN and AlGaIn) is affected by two different kinds of compositional fluctuations. Extrinsic fluctuations originate from large scale (100 to 1000nm) structural effects due to growth inhomogeneities. Intrinsic fluctuations are short range (nm scale) disorder due to random positioning of alloy atoms on the crystal lattice [1,2]. This compositional disorder induces potential fluctuations which result in carrier localization [3]. Commonly used photo- or cathodoluminescence microscopy techniques were so far only able to probe the large scale extrinsic fluctuations [4].

We use scanning tunneling electroluminescence (STL) to detect the radiative recombination of electrons locally injected by a scanning tunneling microscope tip in a GaN/InGaIn/GaN single quantum well (QW) located near the surface (Fig.1a). Fluctuations in the emission

spectrum are observed when changing the injecting tip position by a few nm (Fig.1b). Analyzing the linewidth and peak energy of the luminescence spectrum as a function of the tip position we evidence localization effects induced by alloy disorder with 5nm resolution. In addition, narrow peaks characteristic of emission from single localized states are resolved [5] and their variation versus tip position provides information on transport in the disordered potential.

These experimental results are in good agreement with the so-called localization landscape theory [3] which provides an effective potential map for the carriers (holes as well as electrons) exhibiting localization regions on the scale of 5nm Fig.1c.

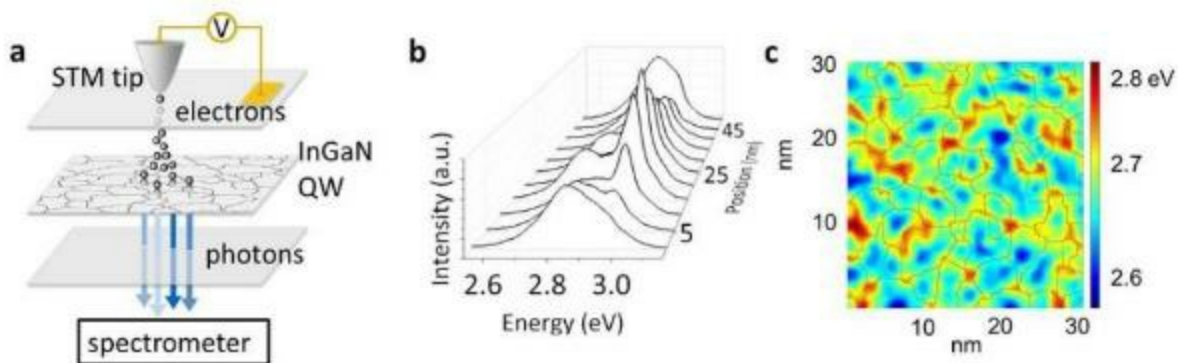


Figure 1: (a) Schematic of the STL experiment. (b) STL spectrum evolution along a 50nm linescan. (c) Effective potential map for electrons calculated by the localization landscape theory in a GaN/In_{0.15}Ga_{0.85}N/GaN QW.

[1] Wu et al., Appl. Phys. Lett. **101**, 083505 (2012).

[2] Watson-Parris et al., Phys. Rev. B **83**, 115321 (2011); Yang et al., J. Appl. Phys. **116**, 113104 (2014); Schulz et al., Phys. Rev. B **91**, 035439 (2015); Auf Der Maur et al., Phys. Rev. Lett. **116**, 027401 (2016).

[3] Arnold et al., Phys. Rev. Lett. **116**, 056602 (2016); Filoche et al., Phys. Rev. B **95**, 144204 (2017); Piccardo et al., Phys. Rev. B **95**, 144205 (2017); Li et al., Phys. Rev. B **95**, 144206 (2017).

[4] Chichibu et al., Appl. Phys. Lett. **71**, 2346 (1997); Sonderegger et al., Appl. Phys. Lett. **89**, 232109 (2006); Pozina et al., Appl. Phys. Lett. **107**, 251106 (2015); Kawakami et al., Phys. Rev. Appl. **6**, 044018 (2016).

[5] Hahn et al., Phys. Rev. B **98**, 045305 (2018).

2:00 PM - 2:15 PM

GROWTH OF LEAD TELLURIDE FILMS BY METAL ORGANIC CHEMICAL VAPOR DEPOSITION

A.C. Arjunan¹, T. Salagaj¹, J. Vanjaria², H. Yu², **G. Tompa**¹

¹Structured Materials Industries, Inc., NJ, UNITED STATES OF AMERICA, ²Arizona State University, AZ, UNITED STATES OF AMERICA

Lead telluride (PbTe), has promising applications such as infrared detectors and optics (in the wavelength region 3-25 μm) due to its narrow band gap, optoelectronics due to its terahertz photoconductivity, and thermoelectric applications due its optimal Seebeck co-efficient and high thermal conductivity. Lead telluride has been grown using vacuum sublimation and chemical vapor deposition methods on silicon and BaF_2 substrates. We herein report on the nucleation and growth of PbTe films silicon and sapphire substrates by metal organic chemical vapor deposition (MOCVD). Tetra ethyl lead and di-isopropyl tellurium were used as precursors for lead and tellurium, respectively. The PbTe films were grown using a vertical flow MOCVD reactor at pressures varied between of 1 to 300 Torr and temperatures varied between 350 to 650°C. Partial pressures of lead and the tellurium were varied from 10 to 50 millitorr. For the growth pressures of above 20 Torr, the films were not continuous and exhibited island growth while no growth occurred above pressures of 36 Torr for a growth temperature of 540°C. The coalesced continuous film growth occurred at a growth pressure of 20 Torr with a temperature of 410 °C. At a growth temperature of 350°C with a pressure of 20 Torr the films exhibited micro grain structures and are not coalesced. We are further studying two step growth process to achieve coalesced high quality PbTe layers. In this two-step process, we will have a step 1 low temperature (400°C) nucleation layer growth followed by a step 2 growth layer at high temperature (550°C) growth layer for coalescing to achieve high quality PbTe layers. We will also further report the structural and morphological characterization of the grown films.

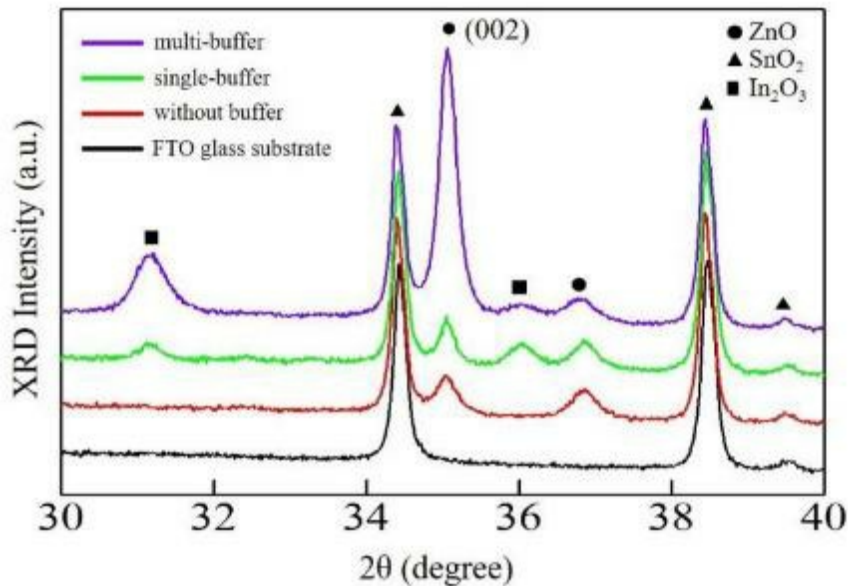
2:15 PM - 2:30 PM

IMPROVED CRYSTALLINITY OF ZNO FILM FORMED ON FTO SUBSTRATE WITH INSERTING MULTI-BUFFER FILMS

X. Zhao¹, A. Mori¹, S. Guan¹, S. Komuro²

¹Department of Physics, Tokyo University of Science, JAPAN,

²Faculty of Science and Engineering, Toyo University, JAPAN



In order to improve the efficiency of transparent solar cells, one reasonable method is to improve the properties of the transparent conductive oxides (TCO). In recent years, indium-doped tin oxide (ITO) has been widely used as a transparent electrode. ITO is with low resistance and high transparency, but it is weak to heat and uses a lot of rare metals. Compared with that, fluorine-doped tin oxide (FTO) is with high conductivity and low cost [1]. However, zinc oxide (ZnO) is difficult to form on FTO substrate, due to the lattice mismatch between them. In order to solve this problem, buffer film was used to improve the incompatibility between them. It has been reported that the crystallinity of ZnO has been improved by inserting multi-buffer films by pulsed laser deposition technique on quartz substrate [2]. In this study, we report that the crystallinity of ZnO film has been successfully improved with inserting multi-buffer films between ZnO@FTO. The buffer and ZnO films were formed on FTO substrate in sequence by radio frequency (RF) magnetron sputtering in argon (Ar) gas. To

improve crystallinity of ZnO film formed on FTO substrate, the multi-buffer films of ZnO/ITO/ZnO/ITO/ZnO were inserted between ZnO and FTO. For comparison, the single buffer (ITO) film had been inserted between ZnO and FTO with same condition. The characterization of the samples was carried out by X-ray diffraction (XRD), DRUV-vis spectra (UV-vis), photoluminescence (PL), X-ray photoelectron spectroscopy (XPS), and room temperature Hall-effect measurements. The XRD result clearly shows that the peak of 002 plane from ZnO has been enhanced with inserting multi-buffer films, and its orientation index increases about 3 times. Moreover, the near-band-edge (NBE) emission results show that the crystallinity of ZnO film has been successfully improved with inserting multi-buffer films. Furthermore, the electrical and optical properties of ZnO film had not been significantly affected, with the inserted multi-buffer films. [1] T. Fukano and T. Motohiro, Sol. Energy Mater. Sol. Cells **82**, 567 (2004). [2] R. Vinodkumar , K.J. Lethy , D. Beena , et al. Reddy Solar Energy Materials & Solar Cells **94**, 68 (2010)

2:30 PM - 2:45 PM

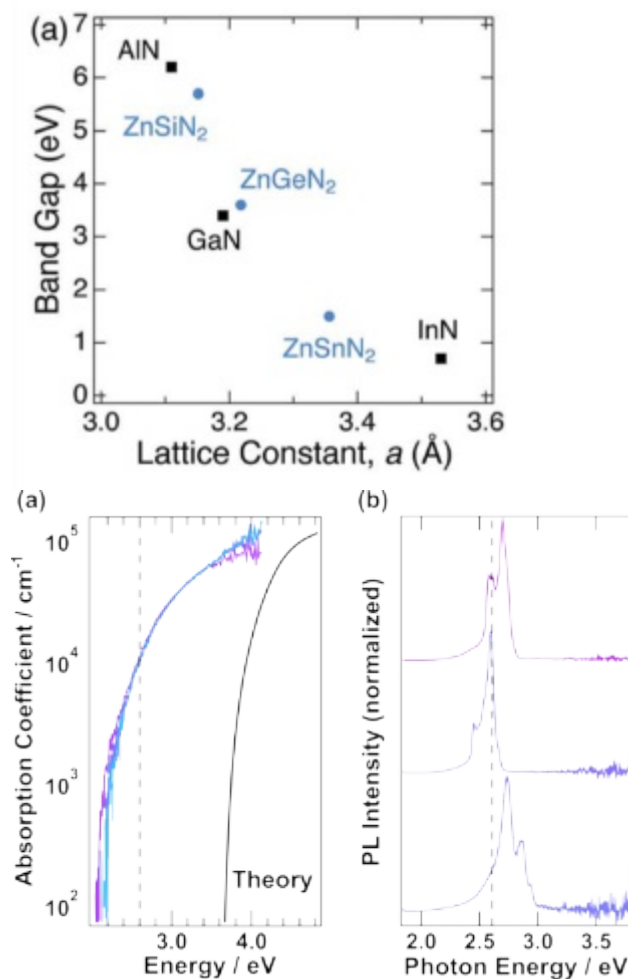
ZN-IV-N₂ SEMICONDUCTORS FOR GREEN EMISSION: RECENT PROGRESS IN MATERIAL SYNTHESIS

B. Tellekamp, C. Melamed, A. Tamboli

National Renewable Energy Laboratory, CO, UNITED STATES OF AMERICA

The 'green gap' refers to the lack of efficient light emitters in the deep green wavelength range 525 nm – 555 nm. Blue to blue-green emitters belong to the GaN/InGaN family, however the increased indium content required to reach the green gap results in increased spontaneous polarization leading to decreased electron-hole wavefunction overlap due to the quantum-confined Stark effect. Increased indium content also results in reduced material quality due to phase separation through the miscibility gap. On the other end of the visible spectrum the AlGaP/AlGaAs system is indirect, resulting in low efficiency emitters above approximately 2 eV. As such, a suitable direct-gap green emitting material is desired to increase efficient green luminescence, a significant factor missing in white light emission which at this point still has to rely on phosphor conversion. The II-IV-

N_2 family of semiconductors represents an optically relevant class of materials with direct gaps across the visible spectrum. The system ZnSnN_2 - ZnGeN_2 spans 1 eV – 3.4 eV, is fully miscible, and possess cation order tunability potentially enabling a decoupled bandgap and lattice parameter. ZnGeN_2 is lattice matched to GaN, providing a mature system for substrates and injection layers. Recent progress in the growth of ZnGeN_2 by molecular beam epitaxy (MBE) will be discussed, also highlighting films deposited by sputtering. Insights into growth regimes and limitations will be given, highlighting practical considerations for the characterization of potentially cation-disordered materials. The optical properties of these films will be presented, with films displaying room temperature photoluminescence in the range 2.4 eV – 2.8 eV (440 nm – 515 nm). Additionally, the role of oxygen anion alloying will be explored, providing an additional method for bandgap tuning.



2:45 PM - 3:00 PM

**PROPERTIES OF GALLIUM OXIDE THIN FILMS ON C-PLANE
SAPPHIRE GROWN BY REAR-FLOW-CONTROLLED MIST
CHEMICAL VAPOR DEPOSITION**

S. Bae, K. Kim, M. Ha, S. Jeong

Korea Ceramic Engineering and Technology, KOREA, REPUBLIC OF

Gallium oxide (Ga_2O_3) has been considered for promising materials semiconductor applications such as high power electronics, ultraviolet (UV) photodetectors, gas sensors, and hybrid light emitters. Ultra-wide band gap (4.9–5.3 eV) can be obtained depending on crystal structure of five polymorphs (α , β , γ , δ , and ε phases). In particular, heteroepitaxy is available on α - Al_2O_3 sapphire substrates. There have been several growth methods to deposit Ga_2O_3 such as molecular beam epitaxy, halide vapor phase epitaxy, pulsed laser deposition, and mist chemical vapor deposition (mist CVD). Among these, mist CVD is attractive for inexpensive process. In this study, the effectiveness of rear-flow-controlled mist CVD has been tried to grow high-quality α - Ga_2O_3 epilayers with two-inch scale. Numerical simulation supports the fluid behaviors to obtain high-uniform thin films. The low velocity of the flow is appropriate to induce upward flow on the growth front without vortex. By minimizing the flow velocity, α - Ga_2O_3 the epilayers have been successfully grown on c-plane sapphire substrates. It featured high quality with 42 arcsec and 1993 arcsec for (0006) and (104) plane reflections, respectively. The thickness was adequately increased as the growth time increases. At the same time, corundum α -phase crystal features were confirmed by XRD 2theta scan and transmittance measurement. Therefore, rear-flow-controlled mist CVD system appropriately provides cost-saving approach to obtain high-quality and uniformity of Ga_2O_3 thin films.

Monday, July 29, 2019

1:30 PM - 3:00 PM

Nonlinear Optical and Laser Host Materials II

Location: Crestone I, II

Session Chair(s): Shekhar Guha, Yushi Kaneda

1:30 PM - 2:00 PM

EFFICIENT CONTINUOUS-WAVE NONLINEAR FREQUENCY CONVERSION TOWARD DEEP-ULTRAVIOLET

Y. Kaneda, Y. Furukawa

Oxide Corp., JAPAN

With the continuing demand for laser sources at wavelength that are not available from the host materials, harmonic conversion has been extensively used in both scientific and industrial applications for both pulsed and continuous-wave (CW) modes. In the past few decades, such demand had extended into CW deep-ultraviolet (DUV) output. For example, at 266nm, the fourth harmonic wavelength of conventional 1064nm laser, CW output powers of up to 2W is commercially available today, and up to 14W was demonstrated in the lab. To arrive that end, single-pass conversion would not be realistic. With only a few pm/V of nonlinearity of the compatible materials, the normalized conversion efficiency for the DUV is of the order of 10^{-4} W^{-1} . With realistic power levels of fundamental (tens of watts or lower), the use of optical resonator is necessary for efficient conversion, bringing the efficiency to tens of percents. In this talk, we review some of the demonstrations of efficient CW DUV generation at 266nm and below, as well as techniques and materials associated with them.

2:00 PM - 2:15 PM

HVPE OF ENGINEERED GRATING STRUCTURES IN OP-GAAS AND OP-GAP

P.G. Schunemann, D.J. Magarrell, L. Mohnkern

BAE Systems, NH, UNITED STATES OF AMERICA

Low-pressure hydride vapor phase epitaxy (HVPE) is offers extremely high growth rates (>100 microns/hour) which enable epitaxial growth of bulk III-V nonlinear optical devices based on orientation-patterned gallium arsenide (OP-GaAs) and gallium phosphide (OP-GaP). These unique materials have enabled exciting advances in frequency-combs for spectroscopy in the molecular fingerprint region beyond the transparency limits of quasi-phase matched (QPM) oxides like periodically-poled lithium niobate (PPLN) and potassium titanyl

phosphate (PPKTP). These QPM compound semiconductors also offer much higher nonlinearities for pump with widely-available laser sources operating at 1- mm (OP-GaP, $d_{14} \sim 70$ pm/V), 1.5 mm (OP-GaP, $d_{14} \sim 35$ pm/V), or 2 mm (OP-GaAs, $d_{14} = 94$ pm/V). A primary advantage of QPM is that the frequency conversion process can be engineered in various ways through the design and layout of the grating structure to achieve discrete and continuous wavelength tuning by translation across multiple adjacent gratings or fan gratings respectively. Tandem grating periods enable sequential processes such as photon recycling for enhanced efficiency, and chirped grating structures allow spectral tailoring of the frequency conversion process. In ferroelectric oxides like PPLN, the periodic QPM structure is created by the use of electric-field poling through a photolithographically defined electrode pattern to periodically reverse the polarity (and hence the sign of the nonlinear coefficient) of alternating domains. Nonlinear optical semiconductors like GaAs and GaP are not ferroelectric, however, so the QPM grating structure must be created instead by polar-on-nonpolar molecular beam epitaxy (MBE) whereby an inverted GaAs (GaP) epi-layer (grown on a thin, lattice-matched non-polar Ge (Si) layer) is photolithographically patterned, etched, and regrown by MBE and then HVPE to produce thick (> 1mm) QPM structures for in-plane laser pumping. Since the domain nucleation and propagation mechanisms are completely different from those in ferroelectric oxides, the challenge of this work was to determine if the same engineered grating structures available in ferroelectric QPM semiconductors could be produced in OP_GaAs and OP-GaP. Here we present our mask designs, growth criteria, domain propagation results, and nonlinear optical device performance.

2:15 PM - 2:30 PM

THICK HVPE GROWTH OF ZNSE ON GAAS SUBSTRATES AND OP-GAAS TEMPLATES FOR MLWIR FREQUENCY CONVERSION

S. Vangala, V. Tassev, M. Snure

Sensors Directorate, Air Force Research Laboratory, OH, UNITED STATES OF AMERICA

ZnSe has excellent optical properties including its high nonlinear

coefficient $d_{ij} \sim 47$ pm/V and better optical transmission from visible to long-wave infrared (LWIR) wavelengths. It has been identified as one of the promising quasi-phase-matched (QPM) materials, beyond GaAs and GaP, for frequency conversion in the mid- and LWIR (MLWIR). However, as a non-linear optical material for orientation-patterned (OP) QPM structures, ZnSe remains relatively unexplored for nonlinear frequency conversion due, in part, to the lack of OP-ZnSe templates and substrates limited by available and high cost of large area single crystal ZnSe. ZnSe has a small lattice mismatch of 0.26% with GaAs, which is a well-developed QPM material with a matured OP template processing technology, and hence GaAs substrates and OP-GaAs templates are expected to be a good alternative for epitaxial growth of ZnSe. Despite this, there are only a few reports on thick growth of ZnSe and OP-ZnSe on GaAs limited to physical vapor transport (PVT), while other more advanced thick epitaxial growth methods such as hydride vapor phase epitaxy (HVPE) have not been explored. In this paper we discuss low pressure HVPE growth of ZnSe on GaAs substrates as a first step towards developing OP-ZnSe QPM material for nonlinear frequency conversion devices. Over 250 μm thick single crystalline quality ZnSe layers have been produced by low-pressure HVPE on GaAs (100) vicinal substrates and on orientation-patterned GaAs (OP-GaAs) templates with good domain fidelity. We show that the crystalline quality of zinc blend ZnSe grown on GaAs is similar to that of a commercially available ZnSe substrate and as mentioned above the smaller lattice mismatch of 0.26% between these two materials is a primary factor for considering the growth of ZnSe on GaAs substrates and OP-GaAs templates. Photoluminescence and Raman measurements confirm the exciton transitions and LO phonon modes consistent with high quality ZnSe, while the direct bandgap is measured at 2.79 eV at 20K. Cross-sectional transmission electron microscopy (XTEM) imaging analysis shows stacking faults at the interface that propagate few microns deep into the growing film. Surface morphology shows the presence of etch pits that have their long axis perpendicular to (1-10) direction. On the OP templates, we have achieved good domain fidelity of total thickness of 115 μm in 2hr growth duration and this presents a unique opportunity to further increase the thickness necessary for frequency

conversion in the MLWIR for infrared countermeasures and other defense/civilian applications.

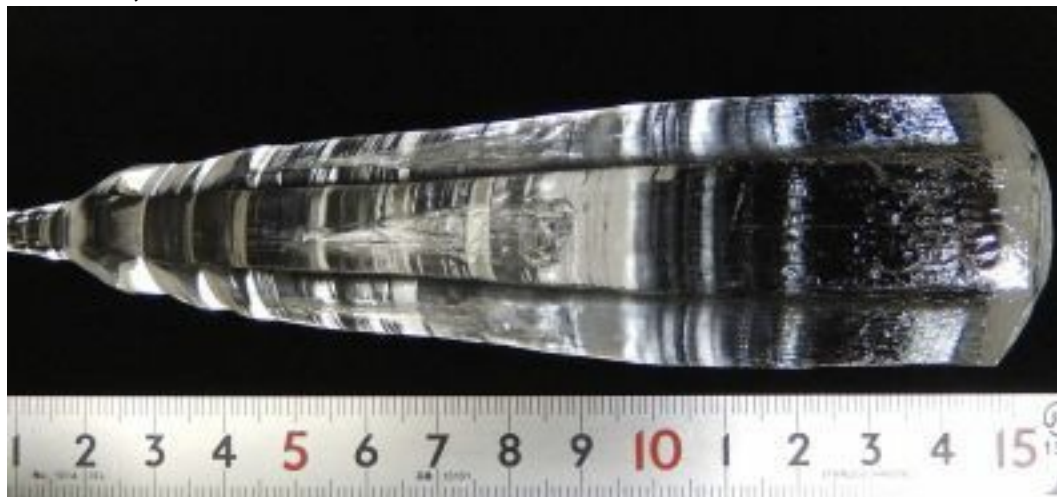
2:30 PM - 2:45 PM

LARGE DIAMETER LaBGeO_5 SINGLE CRYSTAL GROWTH FOR QPM DEVICE WITH LONG INTERACTION LENGTH

M. Sakairi, S. Takekawa, M. Sasaura, J. Hirohashi
OXIDE Corporation, JAPAN

We focused on LaBGeO_5 (LBGO) single crystal as a novel ferroelectric material for quasi-phase-matching (QPM) devices which are suitable for UV generation. LBGO crystal has a wide transmittance wavelength range and the optical absorption edge lies around 195nm. Currently, we reported on the generating UV by periodically poled LBGO (PP-LBGO) devices and the practical use of modules for wavelength conversion and lasers has proceeded. The maximum diameter of LBGO crystal we achieved was limited about 18 mm because the growth of LBGO single crystals is required high supercooling temperature, and the poly-crystallization frequently occurred during the process of increasing crystal diameter. In order to enhance the conversion efficiency of PP-LBGO, it is required to grow large diameter crystal to obtain long PP-LBGO device length. In this paper, we challenged to grow LBGO crystals with more than 30 mm in diameter for pulling up PP-LBGO possibilities. 5N purity raw materials of La_2O_3 , H_3BO_3 and GeO_2 were mixed in the stoichiometric ratio, and the growth was carried out by the Czochralski technique using rf-heating furnace. The growth was conducted with the pulling rates of 0.3 mm/hr, the pulling direction of c-axis and the Pt crucible size of 80 - 100 mm in diameter. In order to investigate the cause of poly-crystallization, a part of polycrystalline LBGO was measured by powder X-ray diffractometer. As a result of the measurement, the polycrystalline parts contained $\text{La}_2\text{Ge}_2\text{O}_7$ phase. By the repetitively growth, $\text{La}_2\text{Ge}_2\text{O}_7$ phase was easily occurred because the melt composition of stoichiometric ratio was changed to B-poor composition by the evaporation of B from the melt. We consider that this might be one of the main causes of poly-crystallization. By optimizing growth conditions, LBGO single crystals with a diameter

greater than 30 mm were successfully obtained and the stable growth conditions for growing large diameter crystal, which is heretofore difficult, was able to be found.



2:45 PM - 3:00 PM

VAPOR TRANSPORT GROWTH OF ZINC SELENIDE AND ZINC SULPHIDE SINGLE CRYSTALS

P.G. Schunemann, K.T. Zawilski

BAE Systems, NH, UNITED STATES OF AMERICA

Polycrystalline Cr:ZnSe and Cr:ZnS have greatly advanced as mid-IR laser host materials in the last 20 years. These materials are also highly attractive as passive q-switches (PSQs) for 1.5- and 2-micron lasers, enabling greatly-simplified laser architectures for compact, multi-watt, pulsed 2-micron lasers and 2-micron-pumped mid-infrared optical parametric oscillators (OPOs). Researchers at the U.S. Army Night Vision Laboratory recently developed a compact, highly-efficient Tm:YAP laser based on commercially available polycrystalline Cr:ZnSe and Cr:ZnS PSQs (IPG Photonics). Unfortunately the lifetime of these devices under intense laser pumping is extremely limited due to grain-boundary (GB) diffusion of the active Cr^{2+} ion away from the pumping region of the PSQ. The PSQ lifetime can be dramatically increased, however, by eliminating rapid GB diffusion of Cr^{2+} through the use of single crystal Cr:ZnSe and Cr:ZnS. However, no commercial (nor domestic) source of single crystal Cr:ZnSe or Cr:ZnS is available. The goal of this work, therefore, was to develop single crystal growth of Cr:ZnSe and Cr:ZnS at BAE Systems. Melt-growth of

twin-free, single crystal ZnS and ZnSe is precluded by the high vapor pressures as well as the low stacking fault energy of these compounds. The highest quality single crystals of ZnSe and ZnS have been produced by physical vapor transport (PVT) as well as chemical vapor transport (CVT), but growth of Cr-doped crystals by these techniques have never been achieved. Here we report the successful growth of high purity single crystal ZnS and ZnSe by CVT and PVT respectively, and Cr-doping was achieved by iodine-assisted vapor transport of CrSe located in a separate temperature-controlled zone. Crystal sizes up to one cubic centimeter have been achieved to date. Spectral properties and device performance will be reported.

Monday, July 29, 2019

1:30 PM - 3:00 PM

Special Session - Michael Schieber II

Location: Red Cloud Peak

Session Chair(s): Jerry Stringfellow, Edith D. Bourret

1:30 PM - 2:00 PM

PEROVSKITE CSPBBR3 SINGLE CRYSTAL DETECTOR FOR GAMMA AND ALPHA-PARTICLE SPECTROSCOPY

D.Y. Chung¹, Y. He², W. Lin², M.G. Kanatizidis²

¹Argonne National Laboratory, IL, UNITED STATES OF AMERICA,

²Northwestern University, IL, UNITED STATES OF AMERICA

Radiation detection at room temperature based on semiconductors is of intense interest because the combined characteristics of direct-conversion detectors can deliver superior spectroscopic performance. Semiconductor detectors allow for facile fabrication and integration with universal front-end electronics systems to achieve high resolution imaging in both energy and spatial sense. Due to the highly proportional response from semiconductor detectors, there is no need for further energy calibration, in contrast to the current heavily-used scintillation detectors, thus leading to superior energy resolution as has been demonstrated in CdTe and Cd_{1-x}Zn_xTe (CZT) semiconductor detectors. We present the all-inorganic perovskite CsPbBr₃ detector

with impressive ambient stability and superior stopping power that exhibits exceptional potential for the next generation radiation detection material. Our CsPbBr₃ detector has shown remarkable energy resolving capability under both X and g rays, particularly in achieving 3.9% (4.8 keV, FWHM) energy resolution for 122 keV ⁵⁷Co g-ray. ¹⁶ Lifetime of hole in CsPbBr₃ detector-grade single crystal was observed to be over 25 μs. The CsPbBr₃ detector was capable of simultaneously resolving both the alpha particle (5.5 MeV) and g ray (59.5 keV) peaks from ²⁴¹Am radiative isotope. This work widens the scope of perovskite detectors to encompass charged radiation as well as high energy X/g rays, and will significantly promote and guide further studies on perovskite materials for radiation detection applications.

2:00 PM - 2:30 PM

FURTHER IMPROVEMENT OF CE DOPED CLLB SCINTILLATORS

M. Arzakantsyan¹, P.R. Menge², V. Ouspenski¹, J. Frank²

¹Saint-Gobain Research Paris, FRANCE, ²Saint-Gobain Crystals, OH, UNITED STATES OF AMERICA

Scintillator crystals are used as detectors for radiation detection devices. We are focused in the search for materials providing better performance and lower cost at industrial scale. Elpasolites with a general formula of A₂BCX₆ first attracted attention as a potential scintillation material in 1989 [1]. Some elpasolites have a cubic crystallographic structure and can provide dual sensitivity for gamma-rays and thermal neutrons when enriched with ⁶Li. The first cubic elpasolite studied was Cs₂LiYCl₆ (CLYC) [1]. Other substitutional compositions like CLYB and CLLB have been discovered by TU Delft [2-4] were later studied by multiple groups. Ce doped CLLB (Cs₂LiLa_(1-x)Ce_xBr₆) [5] has been found to provide the highest light yield and the best energy resolution at 662keV, and has attracted a particular interest for industrial applications. To improve performance we have introduced several dopants at different sites to substitute for Cs, La and Br, for example with Rb. [4]. The crystals are grown by classic Vertical Bridgman technique in vacuum sealed ampoules. The

extracted detectors substituting [0.2at%] Rb for Cs with the size of Ø1"x1" showed an energy resolution of 3.42% compared with standard Ce:CLLB at 3.92%, grown at the same conditions. In parallel, we are studying the impact of alkaline earth and halide substitutions. Non-congruently melting elpasolites are also generally non-stoichiometric and in CLLB will have a deficit of Li in the crystalline matrix at the level of approximately 2-3% causing a host of defects. There are methods to correct this and in particular a LiBr self-flux can be added [5]. By alternating the flux composition from simple LiBr to a more complex one like LiBr+LiI+LaBr₃ we are able to improve stoichiometric proportions for continued improved performance. Using these techniques, non-stoichiometric CLLB crystals grow efficiently at industrially exploitable sizes. Our process currently allows for the manufacture of detectors for gamma+neutron applications with the sizes of at least 60mmx60mmx120mm. We also show a roadmap for continued size increase and performance improvement. [1] C. Reber, H.U. Guedel, G. Meyer, T. Schleid, C.A. Daul, Inorg. Chem., 28, pp. 3249-3258, 1989 [2] C. M. Combes, P. Dorenbos, C. W. E. van Eijk, K. W. Krämer, and H. U. Güdel, J. Lumin., vol. 82, pp. 299–305, 1999 [3] E. V. D. van Loef, P. Dorenbos, C. W. E. van Eijk, K. W. Krämer and H. U. Gödel, J. of Physics: Cond. Matt., Vol 14, 8481-8496, 2002 [4] US Patent 7.525.100 [5] US Patent 9.599.727

2:30 PM - 3:00 PM

PROGRESSION AND MITIGATION OF FABRICATION CHALLENGES FOR MICROSTRUCTURED SEMICONDUCTOR NEUTRON DETECTORS

D.S. McGregor, S.L. Bellinger, R.G. Fronk, L.C. Henson, R.M. Hutchins, W.J. McNeil, T.R. Ochs, B.B. Rice, J.K. Shultis, C.J. Solomon

For over a decade, much research effort has been dedicated to discovering alternatives to conventional ³He thermal-neutron detectors. The thin-film coated neutron detector was a relatively early solution, wherein a thin layer of neutron conversion material, typically ¹⁰B or ⁶LiF, was coated on either a Schottky or *pn*-junction semiconductor diode. Incident neutrons were absorbed in the conversion material layer which subsequently produced charged

particle reaction products. When a reaction product enters the adjacent semiconductor substrate, electron-hole pairs are liberated through Coulombic interactions. These charge carriers are collected which are generally measured as a voltage pulse. Conventional planar devices with either ^{10}B or ^6LiF coated upon a semiconductor diode delivered a maximum intrinsic thermal-neutron detection efficiency of approximately 4%-5%. Unfortunately, these films often detached and peeled from the surface. To improve adhesion of the reactive layer, tiny circular holes were etched periodically across the surface, originally GaAs material, before applying the reactive film. Along with improving adhesion, the miniature features increased the detection efficiency by increasing the neutron absorption probability and reaction product solid angle, and thus, the Microstructured Semiconductor Neutron Detector (MSND) was first realized. During MSND development the substrate has changed from GaAs to Si due to material costs, machinability, and improved background reduction. The reactive layer also changed from ^{10}B to ^6LiF , because the reaction products from the $^6\text{Li}(n,t)^4\text{He}$ reaction have higher energy and longer ranges in materials than $^{10}\text{B}(n,\alpha)^7\text{Li}$ reaction products, allowing for larger feature designs while simultaneously improving the signal to noise ratio. MSNDs underwent multiple design changes and improvements to optimize the diode design and minimize leakage current to enable economical mass production. Presently, MSNDs have straight trenches etched 400- μm deep by 20- μm wide with a 30- μm wide unit cell and an intrinsic thermal-neutron detection efficiency of 30%. Dual-sided MSNDs (DS-MSNDs) were recently developed with improved the detection efficiencies to more closely match those achieved with commercial ^3He detectors. DS-MSNDs have straight trenches on both sides of the diode, with the back-side trenches offset from the front-side trenches to eliminate neutron free streaming paths. First generation DS-MSNDs had poor charge collection efficiency which ultimately limited the thermal-neutron detection efficiency. A redesigned doping profile improved the detection efficiency to approximately 55%. Recent efforts have focused on developing backfill techniques to optimize the ^6LiF packing fraction within the trenches: these efforts coupled with deeper trench etching have

improved the intrinsic thermal-neutron detection efficiency to $69.2\% \pm 0.8\%$.

Monday, July 29, 2019

1:30 PM - 3:00 PM

**Symposium on Epitaxy of Complex Oxides:
Freestanding Crystalline Oxide Membranes**

Location: Grays Peak II, III

Session Chair(s): Steven May

1:30 PM - 2:00 PM

**FREESTANDING CRYSTALLINE OXIDE MEMBRANES AND
HETEROSTRUCTURES**

H. Hwang

Stanford University, CA, UNITED STATES OF AMERICA

The ability to create and manipulate materials in two-dimensional (2D) form has repeatedly had transformative impact on science and technology. In parallel with the exfoliation and stacking of intrinsically layered crystals, the atomic-scale thin film growth of complex materials has enabled the creation of artificial 2D heterostructures with novel functionality and emergent phenomena, as seen in perovskite oxides. We present a general method to create freestanding complex oxide membranes and heterostructures with millimeter-scale lateral dimensions and nanometer-scale thickness. This facilitates many new opportunities we are beginning to explore, and focus here on probing the nanomechanical response and the application of extreme strain states.

2:00 PM - 2:30 PM

**FREESTANDING, SELF-FORMED $\text{LaAlO}_3/\text{SrTiO}_3$ MICRO-
MEMBRANES**

F. Miletto Granozio

CNR-SPIN, ITALY

Two-dimensional electron gases (2DEGs) at oxide interfaces, as $\text{LaAlO}_3/\text{SrTiO}_3$ and its several variants, show multiple functional properties of major physical interest, including a high electron mobility,

superconductivity, a large Rashba spin-orbit coupling, an exceptionally large spin-to-charge conversion efficiency and a yet ill understood, sample-dependent magnetic ground state. Such properties are tunable under external control parameters, as electric field effect. We show that a careful choice of parameters in LaAlO_3 thick film growth allows to select a persistent and fully coherent regime in which a disruptive strain relaxation process eventually place. This results in a surface delamination and in the formation of freestanding, curved, $\text{LaAlO}_3/\text{SrTiO}_3$ micro-sized bilayers. We demonstrate the highly perfect, dislocation-free nature of such micro-heterostructures by studying their curvature from the micro to the atomic scale and by analysing it in terms of standard elasticity theory. We individually contact our flakes after transfer on SiO_2/Si substrates and demonstrate they are metallic down to the lowest measured temperatures. We discuss the peculiar mixed strained state of the SrTiO_3 part of the bilayer, the one hosting the 2DEG, in which orthogonal ferroelectric orders are expected to coexist within few tens of nanometers. Our discoveries demonstrate a method for obtaining bilayer membranes not resorting to any sacrificial layer. The perspectives opened by this work on several aspects of oxide interface science and technology will be discussed.

2:30 PM - 3:00 PM

FREESTANDING CRYSTALLINE MONOLAYERS OF OXIDE PEROVSKITES

Y. Nie

Nanjing University, CHINA

Two-dimensional (2D) materials such as graphene and transition metal dichalcogenides (TMD) have demonstrated how the new electronic phases emerge when a bulk crystal is thinned down to a mono-layer. As transition metal oxide perovskites host a variety of correlated phases, realizing the analogs with transition metal oxide perovskite materials would open the door to a rich spectrum of exotic 2D correlated phases that have not yet been explored. Here we report on the fabrication of freestanding perovskite films with high crystalline quality down to a single unit cell. Using the recently developed method

based on water-soluble $\text{Sr}_3\text{Al}_2\text{O}_6$ as the sacrificial buffer layer^[1,2] we synthesize freestanding SrTiO_3 and BiFeO_3 ultrathin films by reactive molecular beam epitaxy and transfer them to different substrates such as crystalline silicon wafers and holey carbon films. We find that freestanding BiFeO_3 films exhibit an unexpected giant tetragonality and polarization when approaching the ultimate 2D limit. Our results demonstrate the absence of critical thickness for stabilizing the crystalline order in the freestanding ultrathin oxide films. The ability to synthesize and transfer crystalline freestanding perovskite films without thickness limitation onto any desired substrate opens a new field for the 2D correlated electronic phases and interfacial phenomena that technically have not yet been accessible. [1] Hong, S. S., *et al.* **Sci. Adv.** **3**, eaao5173 (2017). [2] Lu, D., Baek, D. J., Hong, S. S., Kourkoutis, L. F., Hikita, Y. & Hwang, Harold Y. **Nat. Mater.** **15**, 1255 (2016).

Monday, July 29, 2019

1:30 PM - 3:00 PM

Symposium on Ferroelectric Crystals and Textured Ceramics: Characterization of Ferroelectric Crystals

Location: Grays Peak I

Session Chair(s): Richard Meyer, Christo Gugushev

1:30 PM - 2:00 PM

GROWTH AND CHARACTERIZATION OF LARGE-LATTICE-PARAMETER PEROVSKITE SUBSTRATE SINGLE CRYSTALS FOR FERROELECTRIC FILMS AND DEVICES

C. Gugushev¹, D. Klimm¹, M. Brützam¹, T.M. Gesing², M. Gogolin², J. Hidde¹, T. Markurt¹, S. Ganschow¹, J. Schwarzkopf¹, M. Bickermann¹, D. Schlom³

¹Leibniz-Institut für Kristallzüchtung, GERMANY, ²University of Bremen, Solid State Chemical Crystallography, Institute of Inorganic Chemistry and Crystallography, GERMANY, ³Department of Materials Science and Engineering, Cornell University, UNITED STATES OF AMERICA

Perovskites have been extensively studied since the foundation of the IKZ in 1992. In the form of epi-ready substrates, the crystals produced at IKZ have served as the literal foundation for the discovery and development of advanced epitaxially grown films with interesting ferroelectric, superconducting, ferromagnetic, piezoelectric, multiferroic, or simply electronic properties. Since rare earth scandates REScO_3 (RE = Dy ... Pr) are proven to be well suited as substrates for films of various ferroelectrics with the perovskite structure, fine adjustments in substrate lattice spacings have allowed the stabilization of novel strained ferroelectric phases and enhanced film properties to be achieved. For such developments we can now demonstrate, that practically any desired pseudo-cubic lattice parameter in the range from about 3.95 and 4.01 Å can be covered by growing solid solutions between neighboring RE scandates. In contrast to this, the availability of perovskite substrate single crystals with lattice parameters above 4 Å is currently very limited and hampers the development of novel devices. For example, until now most of the film work related to ferroelectric field-effect transistors with a semiconducting channel consisting of a chemically and structurally compatible perovskite with high mobility at room temperature, BaSnO_3 , is performed on highly non-lattice matched substrates. The closest is PrScO_3 , which is still mismatched by -2.3% . When BaSnO_3 films are grown on these substrates, the inescapable result for films with device-relevant thicknesses is that the films are riddled with threading dislocations. This high density of dislocations is considered responsible for the significantly lower mobilities seen in thin films of BaSnO_3 compared with BaSnO_3 single crystals. To overcome this bottleneck, we started to explore the solid solution system $(\text{LaLuO}_3)_{1-x}(\text{LaScO}_3)_x$ and expanded the ternary system $\text{La}_2\text{O}_3 - \text{Sc}_2\text{O}_3 - \text{Lu}_2\text{O}_3$ to a quaternary system by the addition of a RE oxide. Using this approach our preliminary results reveal that pseudo-cubic lattice parameters of about 4.086 Å and between 4.12 – 4.15 Å are accessible. These values are promising to improve the quality of heteroepitaxially grown BaSnO_3 thin films. This talk will give insights into our recent bulk crystal growth activities in this regard.

2:00 PM - 2:30 PM

PROCESSING-ELECTROMECHANICAL PROPERTY RELATIONSHIPS IN TEXTURED PMNT

Richard Meyer¹, Mark Fanton², Gary L. Messing²

¹Applied Research Lab, Pennsylvania State University, University Park, UNITED STATES OF AMERICA, ²Penn State University, Freeport, UNITED STATES OF AMERICA

Textured piezoceramics are produced by the templated grain growth (TGG) method, whereby platelet-shaped seed crystals of a perovskite phase are used to control grain growth in the ceramic during thermal processing. These seed crystals are aligned by shear forces during tape casting of a slurry containing the seed crystals and a fine matrix powder. To facilitate further adoption of this technology, PSU has been engaged in a two-prong development effort that is looking at scaling the current processing techniques for manufacturing and also at improving the performance of textured relaxor-based ceramics through composition and processing enhancements. In $\langle 001 \rangle$ textured $(1-x)\text{Pb}(\text{Mg}_{1/3}\text{Nb}_{2/3})\text{O}_3-x\text{PbTiO}_3$ (PMN-PT), strong preferred grain alignment results in more single-crystal-like piezoelectric response. PMN-PT based textured ceramics have been shown to exhibit piezoelectric coefficients of 900-1200 pC/N – about 70-75% of the PMN-PT single crystal value, and a greater than 3-fold improvement over conventional ceramics. These materials also show substantial increases in electromechanical coupling ($k_{33} \geq 0.83$) and dielectric constant ($\epsilon_{T33} \geq 3800$) compared to PZT ceramics. Recent work has focused on harder compositions with low dielectric loss and high mechanical quality factors for higher power transducer applications. This presentation will provide an overview of recent compositional development work and highlight key process-electromechanical property relationships in these newer textured variants.

2:30 PM – 3:00 PM

EXPLORING FERROELECTRIC DOMAIN ENGINEERING THROUGH CERAMICS TEXTURING, FOR UNDERWATER ACOUSTICS APPLICATIONS

A.D. Moriana, Z. Cheng, S. Zhang

Institute for Superconducting and Electronic Materials, NSW,
AUSTRALIA

Many underwater acoustic transducers, are based on piezoelectric materials, taking advantage of the direct (receiver) and converse (transmitter) piezoelectric effects. High-coupling and high-strain relaxor ferroelectric single crystals have been researched actively in recent years due to their significant enhancements to acoustic transducer performance, especially in terms of the sensitivity (high piezoelectric coefficient and electromechanical coupling), frequency bandwidth (high electromechanical coupling) and compactness (large elastic compliance and piezoelectric coefficient). However, single crystals are limited in applications due to the complexity of fabrication, composition inhomogeneity, high cost and time of synthesis as well as the inferior mechanical properties compared to their ceramic counterparts. In parallel to single crystals, textured piezoelectric ceramics are being studied based on the template grain growth process (TGG). This process, uses various types of ceramic systems and has been shown to achieve performances that are close to those of the first generations of relaxor ferroelectric single crystals. Additional advantages include reduced cost of manufacturing, significant performance enhancements compared to polycrystalline piezoelectric ceramics and machinability for easier industrial transition. In this study, several ceramic systems will be explored (PMN-PT and PIN-PMN-PT, etc.) as well as template seed crystals (BT, ST, NN, etc.) in an effort to induce texturing, hence maximising piezoelectric response by focusing on properties favourable for underwater acoustic systems: High electromechanical coupling (k_p), piezoelectric strain constant (d_{33}), mechanical quality factor (Q_m) and coercive field (E_C).

Manufacturability and the impacts of the processing parameters involved in fabricating textured piezoelectric ceramics will also be explored, the relationship of the complex microstructures and engineered ferroelectric domains with macroscopic properties will be established.

Monday, July 29, 2019

3:00 PM - 5:15 PM

Graphene and Graphene-Related Processes

Location: Crestone III, IV

Session Chair(s): Kevin M. Daniels, Kurt Gaskill

3:00 PM - 3:30 PM

FUNDAMENTAL EXPERIMENTAL INVESTIGATIONS OF CALCIUM AND MAGNESIUM INTERCALATED GRAPHENE ON SILICON CARBIDE

J.C. Kotsakidis¹, A. Grubišić-Čabo², A. Tadich³, M. Currie⁴, A.L. Vazquez De Parga⁵, C. Liu¹, R. Myers-Ward⁴, M.T. Dejarld⁴, K.M. Daniels⁶, S.P. Pavunny⁴, M.T. Edmonds², K. Gaskill⁴, M.S. Fuhrer²

¹Monash University, Department of Physics and Astronomy, AUSTRALIA, ²Monash University, Department of Physics and Astronomy, ACT, AUSTRALIA, ³Australian Synchrotron, AUSTRALIA, ⁴U.S Naval Research Laboratory (NRL), DC, UNITED STATES OF AMERICA, ⁵Dep. Física de la Materia Condensada and Condensed Matter Physics Center (IFIMAC), Universidad Autónoma de Madrid, SPAIN, ⁶University of Maryland (UMD), UNITED STATES OF AMERICA

Graphene has not only proven itself an indispensable testing-bed for expanding our understanding of condensed-matter physics, but is a material that may directly enable future technological advancement through use in electrical devices. Recent theoretical and experimental results from literature have suggested that graphene, highly doped with calcium (through intercalation and/or surface decoration), becomes superconducting with relatively high transition temperatures. Furthermore, highly electron-doped graphene may be useful as a low work function and transparent conducting electrode for applications in photovoltaics. Although these systems are physically and technologically interesting, a complete structural understanding of these systems, is thus far, lacking.

In order to fully elucidate the intercalation of graphene, we study both epitaxial monolayer graphene (EMLG) and quasi-free standing (hydrogen intercalated) bilayer graphene (QFSBLG) on 6H-SiC(0001)

substrates. The former consists of monolayer graphene on a carbon interface layer, which is partially covalently back-bonded to the silicon face on the SiC - often termed 'zero layer graphene' or 'the buffer layer'. The latter is formed by hydrogen 'intercalation' of the EMLG, whereby the hydrogen can bond to the silicon on the SiC surface, releasing the interface layer and forming another layer of graphene. This work will present recent experiments on graphene on SiC intercalated with calcium or magnesium, and analysed using X-ray photoemission spectroscopy (XPS), Low Energy Electron Diffraction (LEED), angle resolved photoemission spectroscopy (ARPES) – conducted at the Soft X-ray (SXR) beamline at the Australian Synchrotron and Scanning tunneling microscopy (STM) – conducted in the Fuhrer Laboratory at Monash University on calcium-intercalated graphene.

Our XPS, LEED and STM data suggests that calcium (and magnesium) can intercalate underneath the carbon interface layer and bond with the silicon on the surface of the SiC, freeing the interface layer to form calcium/magnesium-intercalated quasi-free-standing bilayer graphene (Ca-QFSBLG/Mg-QFSBLG). Calcium may also intercalate between the graphene layers, suggested in both XPS and STM data. Furthermore, patterning mesas in the graphene increases the rate of intercalation, shedding light on the intercalation mechanism.

ARPES data indicates a high doping in both calcium and magnesium intercalated samples. Although surprisingly, the Mg-QFSBLG is stable in air exposures of at least 30 minutes, and ARPES results show no shift in the doping level after air exposure. The observed doping in Ca-QFSBLG is also corroborated with quasi-particle interference (QPI) measurements from the STM. Mg-QFSBLG is therefore promising as an air-stable, highly conductive and low work function electrode for implementation into future electronic devices.

3:30 PM - 4:00 PM

**STRONG CORRELATION ENFORCED BY DOPING
INTERCALATION IN EPITAXIAL GRAPHENE ON SiC(0001)**

U. Starke

Max-Planck-Institut für Festkörperforschung, GERMANY

Wafer scale epitaxial graphene grown on Silicon Carbide (SiC) is regarded as a suitable candidate for carbon based electronics. The electronic and structural properties of the graphene layer can be manipulated by functionalizing the graphene/SiC interface on an atomic scale. Intercalation under the first carbon layer can relieve the covalent bonds of its atoms to the SiC(0001) substrate and manipulate the p-band structure in a large range of aspects¹. Au intercalation generates a highly ordered graphene/intercalant/substrate system which leads to significant many-body interactions and a renormalization of the graphene bands. A sharp 2D band structure of its own can be resolved for the gold layer². By controlling the intercalation the dielectric constant of the graphene layer can be tuned. By varying the amount of Au intercalation a semiconductor to metal transition is induced. Extremely high doping regimes can be reached by the intercalation of Gadolinium. As a result, the Van-Hove singularity of the p-bands at the M-point reaches the Fermi level. Thus, the intercalation's influence on the electronic structure of the graphene can be viewed as a topological transition from two hole pockets to one electron pocket. The doping is accompanied by a strong bending of the bands in the vicinity of the Fermi energy, which is attributed to electron-electron interaction. Additionally strong electron-phonon coupling is observed³. We speculate that the high density of states at the Fermi level may potentially allow to access different ordered ground states predicted in highly doped graphene such as unconventional superconductivity or charge and spin density waves⁴.

C. Riedl, C. Coletti, T. Iwasaki, A.A. Zakharov, and U. Starke, Phys. Rev. Lett. 103, 246804 (2009).

S. Forti, S. Link, A. Stöhr, Y. R. Niu, A. A. Zakharov, U. Starke, in preparation.

S. Link, S. Forti, A. Stöhr, K. Müller, M. Roesner, D. Hirschmeier, C. Chen, J. Avila, M.C. Asensio, A.A. Zakharov, T.O. Wehling, A.I. Lichtenstein, M.I. Katsnelson, and U. Starke, in preparation.

A. M. Black-Schaffer and C. Honerkamp, J. Phys.: Condens. Matter 26, 423201 (2014)

4:00 PM - 4:15 PM

MULTI-WAFER BATCH SYNTHESIS OF GRAPHENE ON CU FILMS BY QUASI-STATIC FLOW CHEMICAL VAPOR DEPOSITION

B. Huet¹, X. Zhang², J.M. Redwing², D.W. Snyder¹, J. Raskin³

¹Applied Research Lab-Pennsylvania State University, PA, UNITED STATES OF AMERICA, ²The Pennsylvania State University, PA, UNITED STATES OF AMERICA, ³Université catholique de Louvain, BELGIUM

Large-scale manufacturing of graphene is one of the most challenging tasks for the development of technological applications, particularly when high crystallinity and a strict control over the number of layers are desired. In this work, we report the high-throughput batch production of single-layer highly-crystalline graphene on 3-inch thin Cu film wafers. Thin Cu films pre-deposited on flat and rigid wafers (silicon, quartz or sapphire) emerge as attractive catalytic substrates for the chemical vapor deposition (CVD) of graphene owing to their superior flatness, rigidity, high purity, and compatibility with conventional thin film techniques. In contrast to the widely used Cu foils, Cu films can be placed in a close-packed vertical configuration which enables the production of graphene over a large number of wafers within a relatively small conventional CVD reactor. We first conducted a preliminary set of experiments to study how the graphene growth results are impacted by the substrate configuration (e.g. single horizontal wafer, single vertical wafer with the Cu film facing the CVD reactor outlet or inlet, or multiple vertical wafers). Although the graphene deposition is relatively uniform in the case of one single wafer, for both horizontal or vertical configurations, it is not the case when placing several wafers side-by-side. This poor deposition uniformity is attributed to a modification of the mass transport of the C precursor (i.e. methane) inside the CVD reactor. Computational fluid dynamic (CFD) simulations have been performed to better understand the variation of graphene domain seeding density and growth rate across individual wafers and between wafers within a given lot. Quasi-static gas flow conditions are found to be essential for achieving both optimal size and uniform distribution of graphene domains on a batch of closely-packed vertically-standing wafers. We also demonstrate that graphene can be produced under fully static CVD conditions, that is,

by completely suppressing the convective gas transport of methane. Given the very small amount of carbon required to grow an atomically-thin layer, we show that the growth rate does not significantly vary from one wafer to another, even within a large batch (25 wafers). The batch production of flat high-quality single-layer graphene on Cu films in commercial CVD equipment paves the way to the large-scale industrial production and spur graphene to become a key material in tomorrow's electronic device and sensor technology.

4:15 PM - 4:30 PM

LOW-TEMPERATURE DIRECT GROWTH OF GRAPHENE ON R-PLANE SAPPHIRE USING CU VAPOR CATALYST BY CVD

Y. Ueda, J. Yamada, T. Maruyama, S. Naritsuka

Meijo University, JAPAN

Cu foil is universally used to grow a large-size, high-quality graphene. For the fabrication of devices, however, the transfer process is mandatory. It largely deteriorates the graphene. Therefore, a direct growth of graphene has been strongly required. But an ordinal one needs a high growth temperature above 1000 °C. The substrate is frequently deteriorated by such a high temperature. Teng et al. reported that graphene was satisfactorily grown on SiO₂ even at 950 °C using Cu vapor catalyst in CVD [1]. On the other hand, we found that r-plane sapphire had strong catalytic effect, which was useful to grow a smooth and uniform graphene at low temperature [2]. In this study, direct CVD growth of graphene on r-plane sapphire using Cu vapor catalyst is attempted to lower the growth temperature. R-plane sapphire was used as a substrate, which was covered by a Cu foil. Four holes were punched into the foil for supplying source materials. Mixture-gas of N₂, H₂ and 3-Hexyne (C₆H₁₀) was flown to a reactor for the growth. The growth temperature was systematically changed between 700 °C and 1000 °C. Raman measurements show that graphene was successfully grown on r-plane sapphire above 800°C while no graphene was obtained at 800 °C without using Cu vapor catalyst. The G peak intensity of Raman measurements rather decreased with increasing the growth temperature. It is because the oxygen thermally desorbed from the sapphire will etch the graphene.

AFM observation shows the number of 2-dimensional nuclei also decreased with increasing the growth temperature, which reasonably corresponds to the supersaturation dependence of the growth caused by the etching effect of the oxygen at high temperature. The growth rate of the graphene showed a highest value at 800 °C by the use of the Cu vapor catalyst. On the contrary, no growth was obtained without Cu vapor catalyst, which means that the source materials weren't decomposed at 800 °C. In conclusion, direct growth of graphene was successfully performed by the use of Cu vapor catalyst on r-plane sapphire by CVD even at a low-temperature of 800 °C. Acknowledgement: This work was supported in part by JSPS KAKENHI Grant Numbers 25000011, 26105002, 15H03559. References: [1] P. Y. Teng et al., Nano Lett. 12, 1379 (2012), [2] Y. Ueda et al., MRS Fall Meeting (2018) NM01.11.29.

4:30 PM - 4:45 PM

LIQUID-PHASE GROWTH OF FEW-LAYERED GRAPHENE ON SAPPHIRE SUBSTRATES USING GA MELTS

T. Maruyama, S. Sawada, T. Saida, S. Naritsuka
Meijo University, JAPAN

During recent years, graphene has emerged as a promising candidate for various electronic devices. To realize practical applications, it is significant to synthesize graphene on insulator substrates directly. In this study, using liquid Ga as the melt and amorphous carbon (a-C) as the source material, we performed direct synthesis of graphene films of a few layers (few-layered graphene) on sapphire substrates by liquid-phase growth (LPG) using a slider boat. By optimizing the nucleation time and growth time, we succeeded in several tens micrometer-size monolayer graphene on sapphire substrates by LPG. Thin a-C layers (~0.2 nm in thickness) were deposited on sapphire substrates, which were set in the LPG system. After dissolution of a-C into Ga melts at 1000°C, the substrate temperature was rapidly decreased to 800 °C for nucleation of graphene, followed by gradual temperature decrease to 650°C for graphene growth. After graphene growth, Ga melts were detached from the substrates by sliding the boat. The grown graphene was characterized by optical microscopy, Raman spectroscopy and X-ray photoelectron spectroscopy. The

effects of the nucleation time and growth time on the area, layer and crystallinity of graphene were investigated. When the growth time was 6 h, a number of graphene flakes were formed on the substrates. As the nucleation time decreased from 3 h to 1h, the graphene size was enlarged, indicating the increase of nucleation density. At the same time, G/D ratio of graphene increased, showing the improvement of crystallinity. At the nucleation time of 1 h, several tens of micrometer-sized graphene was formed and most of the grown graphene had 2-3 layers. When the growth time was 8 h, the graphene layers became thinner and 1-2 layers graphene covered most of the substrate surface. In particular, at the nucleation time of 1 h, both area and density of monolayer graphene reached its maximum and the area of some monolayer graphene crystal was about $50 \times 100 \mu\text{m}$. In addition, the G/D ratio was improved by increasing the growth time.

4:45 PM - 5:00 PM

EPITAXIAL CU FILMS: AN IDEAL PLATFORM FOR THE GRAPHENE GROWTH, TRANSFER AND DEVICE FABRICATION

B. Huet¹, J. Raskin², J.M. Redwing³, D.W. Snyder¹

¹Applied Research Lab-Pennsylvania State University, PA, UNITED STATES OF AMERICA, ²Université catholique de Louvain, BELGIUM,

³Penn State University, PA, UNITED STATES OF AMERICA

Owing to its unique combination of physical properties, graphene is envisioned to be a key material in a multitude of energy-efficient technological applications including high-speed electronics, light-emitting diodes, and sensors. Unfortunately, large-scale graphene synthesis and processing techniques are not sufficiently advanced yet to fabricate functional applications realizing graphene's full potential. The chemical vapor deposition (CVD) of graphene on metals is the most advanced synthesis method as it offers a relatively high crystallinity and good control over the number of layers. Although Cu foil has been the most widely used catalytic substrate for the CVD of graphene for about a decade, our experimental results suggest that Cu film pre-deposited on a C-plane sapphire wafer constitutes a superior catalytic platform for the graphene synthesis, transfer and fabrication of devices [1]. Our work demonstrates that the sub-optimal

graphene results obtained on Cu foils mainly arise from its (i) surface morphology, (ii) polycrystalline nature, (iii) thermal expansion, and (iv) flexibility. First, we benchmark the Cu surface roughness of the various type of Cu catalytic substrates that can be used for the graphene growth including Cu foils, polycrystalline Cu films and epitaxial Cu films. We then show how the type of Cu substrate influences the formation of wrinkles and cracks in graphene. Graphene wrinkling and cracking inevitably take place after the graphene growth step when the CVD furnace is cooled down from about 1050°C down to room temperature. In particular, we show that the formation of cracks and wrinkles significantly depends on Cu surface crystallographic orientation, Cu surface surface morphology which disrupt graphene's pinning, and catalyst thermal deformation. Our work also demonstrates that replacing Cu foils by Cu films helps suppressing the growth of undesired additional graphene layers. In addition, our research provides guidelines to grow millimeter-size single-crystalline graphene domains on epitaxial thin Cu films while minimizing the Cu surface roughening that takes place during the high temperature CVD process. Finally, we discuss the challenges and opportunities of the various Cu catalytic platforms in terms of transfer quality/reliability and device fabrication. [1] *B. Huet & J.-P. Raskin, Role of the Cu substrate in the growth of ultra-flat crack-free highly-crystalline single-layer graphene, Nanoscale, 2018, 10, 21898*

5:00 PM - 5:15 PM

GROWTH OF INDIUM SELENIDE COMPOUND SEMICONDUCTOR FOR OPTOELECTRONIC APPLICATIONS

T. Wang, W. Wang, W. Jie

Northwestern Polytechnical University, CHINA

InSe, with the advantages of high electron mobility, high light absorption efficiency and good material stability at room temperature, shows great potential in high-performance electronic and optoelectronic devices. Mechanical exfoliation is a promising way to get large area two-dimensional InSe material where the crystal quality is heritable from the bulk material. However, the growth of high-quality InSe crystals is still a problem, because of the intrinsic structure imperfections, the complex phase transition and the deviation of

stoichiometry caused by the different partial pressures of In and Se. In this work, the vertical Bridgman method and physical vapor transport method were used to grow high quality InSe crystal respectively. The synthesis and growth process parameters were designed according to the phase diagram. The stoichiometry, crystal structure, phase structure and the photoelectric properties of the crystals were characterized. and proved a high quality of the InSe crystals. It was found that the electron Hall mobility from the tip to the tail of the grown crystal by vertical Bridgman method increases from $592 \text{ cm}^2\text{V}^{-1}\text{s}^{-1}$ to $870 \text{ cm}^2\text{V}^{-1}\text{s}^{-1}$, while the mobility of different parts in the crystal grown by the horizontal physical vapor transport method is quite uniform, which is about $750 \text{ cm}^2\text{V}^{-1}\text{s}^{-1}$. Multilayer InSe film samples were obtained by the mechanical exfoliation method. Indium and gold were respectively used as metal contact electrodes. The multilayer InSe device with indium has a field effect mobility of up to $910 \text{ cm}^2\text{V}^{-1}\text{s}^{-1}$, a switching ratio of 10^7 , and optical responsibility up to $9 \times 10^6 \text{ mA/W}$ for light with a wavelength of 465 to 850 nm and external quantum efficiency of 106 %, while the response time is as long as several hundred seconds, probably due to the adsorption of oxygen and water on the surface as a hole trapping center. The gold contact electrode multilayer InSe device has an optical response time as low as $60 \mu\text{s}$, which is lower than all the reported response times of InSe devices. The reason may result from the enhancement of the actual electric field strength by the built-in electric field in the contact barrier, resulting in faster separation and drift of photogenerated carriers. The prepared multilayer InSe device has good room temperature stability, which proves that it has good application potential in optoelectronic devices.

Monday, July 29, 2019

3:30 PM - 5:30 PM

Detector Materials: Numerical Simulation and Semiconductors

Location: Red Cloud Peak

Session Chair(s): Jeffrey J. Derby, Joshua Tower

3:30 PM - 3:45 PM

MODEL-BASED CONTROL FOR BRIDGMAN GROWTH OF SCINTILLATOR CRYSTALS

S. Pawar¹, C. Zhang¹, A.S. Tremsin², D. Perrodin³, E.D. Bourret³, S.C. Vogel⁴, J.J. Derby¹

¹University of Minnesota, MN, UNITED STATES OF AMERICA,

²University of California at Berkeley, CA, UNITED STATES OF AMERICA, ³Lawrence Berkeley National Laboratory, CA, UNITED STATES OF AMERICA, ⁴Los Alamos National Laboratory, NM, UNITED STATES OF AMERICA

The U.S. DOE NNSA Advanced Materials for Detectors project has identified new classes of promising scintillators for gamma ray detection, comprising mixed halides, doped or co-doped with activators. However, the small crystals grown during this exploratory research will require the development of crystal growth processes for their production at larger scale. Toward these goals, we are applying sophisticated computational models for crystal growth to understand the mechanisms of growth of these scintillator crystals. We are developing model-based control schemes that can be used to determine optimal growth conditions in real time, avoiding the extensive, trial and error involved in the development of most growth systems. We present initial results that clarify the dynamics and operating limits of a five-zone Bridgman furnace employed to grow these mixed-halide single crystals. Our objective is then to establish a feedback control strategy for growth using interface measurements made via neutron imaging, followed by the identification of other measurable quantities that may be used to find the position and shape of the interface for control. Ultimately, a model-based state observer and controller will allow for improved growth conditions in commercial applications.

3:45 PM - 4:00 PM

GROWTH AND PERFORMANCE OF THALLIUM MERCURY IODIDE CRYSTALS FOR GAMMA-RAY DETECTION

N.B. Singh

University of Maryland, Baltimore County, UNITED STATES OF AMERICA

During the past decades huge amount of resources have been devoted to develop several materials for radiation detectors. More specifically cadmium zinc telluride (CZT) and mercuric iodide (HgI_2) has been developed for g-ray detection. But due to inherent problems in crystal stoichiometry of CZT and low mt values in HgI_2 , are big road block for wide spread low cost detectors. Also, it is well established that extremely high purity materials are required to increase sensitivity of detectors. Heavy metal based ternary selenides have shown very good multiple properties including wavelength conversion in mid wave infrared and long wave infrared region, acousto-optic and great potential for radiation detection. We have extensively studied thallium based compounds for variety of applications. In this paper we report the results of crystal growth, fabricability and radiation detection characteristics of ternary compounds thallium mercury iodide (Tl_4HgI_6) system by growing single crystals from the melt by Bridgman method. The congruency of material and phase transition was studied by differential thermal analysis. Material melts congruently at 357°C and did not show any other phases between room temperature and melting point. Results of crystal growth, and effect of doping and growth parameters on the quality and properties are reported. Crystals have demonstrated good fabricability. Crystal slabs were fabricated as bulk detector and showed good characteristics for detectivity of X-ray and g-rays. Effect of impurities on performance was evaluated by using source materials of different purity and by purifying synthesized stoichiometric compound. Crystals with high purity source materials and mixed by vibrating method showed resistivity in range of 10^{12}ohm-cm and with a ^{137}Cs g-ray testing showed mt value of 8×10^{-4} .

4:00 PM - 4:15 PM

REQUIREMENTS, GROWTH AND EVALUATION OF GAAS CRYOGENIC SCINTILLATOR CRYSTALS

C. Frank-Rotsch¹, K. Stolze¹, R. Zwierz¹, E.D. Bourret², F. Moretti², S. Derenzo²

¹Leibniz Institute for Crystal Growth, GERMANY, ²Lawrence Berkeley

National Laboratory, CA, UNITED STATES OF AMERICA

Scintillators are promising targets for detecting MeV/c^2 mass dark matter (DM) particles due to scattering of electrons [1]. A recent evaluation of prospective cryogenic scintillation radiation detector materials revealed *n*-type GaAs to be a promising scintillator for DM with scintillation luminosity between 7 and 43 photons/keV [2]. X-ray emission peaks of about 1.46 eV (830 nm) and 1.33 eV (930 nm) have been observed at 10 K. The absence of naturally radioactive Ga and As isotopes is a further advantage and the annihilation of metastable radiative centers by the *n*-type delocalized electrons potentially excludes afterglow. The definition of the requirements for a scintillator, the growth of the corresponding large high-quality crystals, and the analysis and evaluation of the obtained samples are presented. Single crystalline scintillator crystals typically have a diameter of 10 cm. The 10 K scintillation at 1.33 eV is a radiative recombination between a delocalized *n*-type electron and a hole trapped on an acceptor ion. The cryogenic energy gap is 1.52 eV. The electron is correlated to an energy level below the conduction band formed by Si acceptor ions. The hole is correlated to an ionized boron atom acting as an acceptor [2]. Therefore, a well-defined Si and B concentration is required. Furthermore, a low concentration of mid-gap electron traps seem to be necessary. Besides the boron and silicon concentration further dopants, i.e. carbon and zinc were investigated. In order to optimize the dopant household 10 cm GaAs crystals were grown by vertical gradient freeze technique. The crystals were silicon doped in a range of $2\text{--}8 \cdot 10^{17} \text{ cm}^{-3}$ and compensated by carbon as acceptor. The boron concentration varies from $2 \cdot 10^{18}$ to 10^{19} cm^{-3} depending on the growth parameters respectively. Especially the influence of the water content of the used B_2O_3 encapsulant was investigated. Furthermore, experiments with an additional carbon source in the growth container were carried out to increase the acceptor concentration up to the solubility limit of carbon in GaAs. The obtained doping level of Si, B and C were measured by means of secondary-ion mass spectrometry (SIMS). Using single crystalline samples of $10 \times 10 \times 1 \text{ mm}^3$ size luminosity signals between 150 and 3 photons/keV could be observed. The outlook for further work is promising. Reference: [1] S. Derenzo et al., Phys. Rev. D 96, 016026 (2017) [2] S. Derenzo et al., Journal of

Appl. Phys. 123, 114501 (2018)

4:15 PM - 4:30 PM

GROWTH OF HEAVILY-DOPED GERMANIUM SINGLE CRYSTALS FOR MID-INFRARED APPLICATIONS

R..R. Sumathi¹, N. Abrosimov², J. Fischer², M. Czupalla²

¹Leibniz Institute for Crystal Growth, GERMANY, ²Leibniz-Institut für Kristallzüchtung, GERMANY

Heavily-doped germanium (Ge) displays plasma frequencies in the mid-infrared (IR) range, which tends the unique opportunity for optical sensing/detection of molecules (for e.g. gas molecules in the atmosphere or biomolecules in a diagnostic assay). Although very high concentration (10^{19} - 10^{20} cm⁻³) of n-type doping with a tunable plasma frequency has been demonstrated in epitaxial films of Ge grown on silicon, such a doping process during bulk crystal growth of Ge, especially by Czochralski (Cz) method is not simple. Among the shallow-donors of Ge, phosphorus (P) is preferable, but P doping is limited due to lack of stable dopant sources, and P has also a very low segregation coefficient ($k_0 = 0.08$) that creates a positive concentration gradient in the axial direction of the crystal. In contrary to P, the distribution coefficient of acceptor dopant, boron (B) is very high ($k_0 \gg 1$), and so it has the reversal effect (i.e. negative concentration gradient). In this presentation, doping issues in Ge will be addressed and the development of a new doping method from the gas phase will be discussed. The problem with phosphorus doping could be solved using the gaseous source, phosphine (PH₃). The crystals were grown using quartz crucible and doping was carried on by blowing PH₃ to the melt surface using a special nozzle design so that the amount of phosphorus introduced into the melt could be manipulated and controlled. <100> P-doped crystals up to 50 mm in diameter with a carrier concentration in the range from 1×10^{14} cm⁻³ to 5×10^{17} cm⁻³ were grown. The same doping approach was also used for B-doped Ge crystal growth. As a boron source, the gaseous chemical compound diborane (B₂H₆) was chosen. Because of very high segregation of B, continuous replenishment of B in the melt is

necessary. The charge carrier density in the range between $1.5 \times 10^{14} \text{ cm}^{-3}$ and $2.5 \times 10^{16} \text{ cm}^{-3}$ was achieved in B-doped $\langle 100 \rangle$ Ge crystals. We are optimizing further to dope a high concentration (up to 10^{19} cm^{-3}) of P and B into the crystals. High doping often leads to mosaic structures and its evolution will be presented. The crystals were also analysed for their electrical and optical properties and the results will be given in detail. Influence of doping concentration on the bandgap narrowing effect in the grown crystals is being explored.

Acknowledgments: This work was partly supported by the BMBF project InTerFEL, No. BMBF05K2014.

4:30 PM - 4:45 PM

EVALUATION OF AN INVERTED VERTICAL GRADIENT FREEZE METHOD FOR CADMIUM ZINC TELLURIDE

J.J. Roerig, J.J. Derby

University of Minnesota, MN, UNITED STATES OF AMERICA

Cadmium zinc telluride (CZT) is a material of interest for the production of room temperature gamma and infrared sensors. Growth of large, single crystals for use as a substrate in the production of the aforementioned devices has proven difficult with more common methods such as the conventional vertical Bridgman and gradient freeze (VGF) methods. In this presentation, we apply computational models to analyze the potential of an inverted, or destabilizing, VGF method, in which growth starts at the top of the crucible and moves in the downward direction. This method was originally proposed by Taniguchi and Asahi, who filed a U.S. Patent for such a system for CZT growth in 1997. However, there is no evidence that this approach was successful, nor are we aware of any commercial processes that use this configuration. There are several advantages claimed for this method, including greater single-crystal yield and fewer second-phase particles in the grown crystal. To achieve these goals, this process aims to nucleate a single crystal along the free surface of the melt, followed by an enlarging of the crystal via radial expansion. If the crystal-solid interface does not contact the wall until the very last moments of growth, the grown solid is expected to be nearly all single-crystal material. The inverted gradient will also promote mixing in the

melt due to buoyant flows driven by the destabilizing temperature field from the heated bottom of the crucible. This increased mixing will ameliorate morphological instabilities that result in tellurium inclusions at the growth interface. We present computations that assess the possibility of achieving these beneficial outcomes.

4:45 PM - 5:00 PM

NUMERICAL INVESTIGATION OF CDZnTE GROWTH BY THE BORON OXIDE ENCAPSULATED VERTICAL BRIDGMAN METHOD

C. Stelian¹, D. Calestani², M. Velazquez³, A. Zappettini²

¹, FRANCE, ²IMEM-CNR, ITALY, ³SIMaP UMR 5266 CNRS-UGA-G INP, FRANCE

CdZnTe (CZT) crystals with 4.8 cm in diameter were grown by the boron oxide encapsulated vertical Bridgman technique. The quartz ampoule is pulled down at 0.5 mm/h rate in a furnace which has three independent heating zones. The boron oxide layer fully encapsulates the CZT sample and prevents the contact between the crystal and the ampoule. The ingots exhibit good structural quality with large grains and low dislocation density. However, the as-grown crystals contain high densities of Te inclusions. These inclusions originate from Te droplets trapped at the growth interface in the conditions of low vertical temperature gradients at the crystal-melt interface during the crystallization process. In this work, numerical modeling is applied to investigate the temperature gradients, the shape of the growth interface and Zn distribution in CdZnTe crystals grown in a three-zone Bridgman furnace. Global modeling of the furnace is performed by using the finite element code COMSOL Multiphysics. The crucible movement and the shape of the growth interface are computed by applying the deformable mesh technique. Computations performed for the standard furnace configuration show that the crystal-melt interface is concave toward the melt in the conical part of the ampoule, then becomes convex during the growth through the cylindrical part of the ampoule. These results are in agreement with previous experimental characterization of CZT ingots by means of photoluminescence mapping showing slightly convex shape of the interface in the cylindrical part of the ingot [1]. Concave shapes of the interface and

very homogeneous temperature distribution at the ampoule tip promote the growth of a polycrystalline material. The computations show low temperature gradients in the crystal near the growth interface (2-4 K/cm) which allow the trapping of Te inclusions in the growing ingot. The furnace configuration was changed in order to increase the vertical temperature gradient in the crystal to about 7-8 K/cm. A numerical model able to simulate the migration of Te inclusions under temperature gradient field was developed and validated by comparison to experimental results taken from the literature [2]. [1] A. Zappettini, M. Zha, L. Marchini, D. Calestani, CrystEngComm 14 (2012) 5992 [2] Y. He, W. Jie, T. Wang, Y. Xu, Y. Zhou, Y. Zaman, G. Zha, Journal of Crystal Growth 402 (2014) 15

5:00 PM - 5:15 PM

IMPLEMENTATION OF ACCELERATED CRUCIBLE ROTATION TECHNIQUE (ACRT) TO ACHIEVE IMPROVED GROWTH RATE AND DETECTOR PERFORMANCE OF CADMIUM ZINC TELLURIDE (CDZANTE)

S. Kakkireni¹, J.J. McCoy¹, S.K. Swain¹, A. Bolotnikov², K.G. Lynn¹

¹Washington State University., WA, UNITED STATES OF AMERICA,

²Brookhaven National Labs, NY, UNITED STATES OF AMERICA

CdZnTe crystals grown from Te-rich solution, at fast growth speeds comparable to those employed in typical melt growth, is demonstrated by implementing ACRT. The crystals exhibit detector performance comparable to state of the art gamma-ray detectors that are grown at substantially lower rates by commercial techniques such as travelling heater method. Point defects induced by unintentional chemical impurities and extended defects such as inclusions and precipitates of tellurium composition are two of the key factors that limit the transport properties and detector performance in CdZnTe crystals. Growth methods that rely on solvent purification and low growth temperatures to improve purity, are inherently slower to avoid extended defect formation due to constitutional super-saturation (CSS) as a result of high degree of melt off-stoichiometry. Due to melt off-stoichiometry, excess Te is continuously rejected into the melt as the growth progresses. Formation of Te-rich boundary layer adjacent to the solid-liquid interface is responsible for the onset of constitutional

undercooling and capturing of Te droplets in the matrix leading to the formation of second phase extended defects. Here we show that implementation of ACRT with optimized combinations of rotation profile and melt composition can induce flow patterns in the melt, necessary to achieve reduced defect density while growing at fast rates of 2mm/hr. Ingots with sub ppm total impurity concentration, fairly low second phase content with particle sizes of $\sim 2\mu\text{m}$ are reproducibly obtained with corresponding mobility-lifetime products exceeding $5 \times 10^{-2} \text{cm}^2/\text{V}$ which is ideal for high efficiency detector fabrication. Ingots with uniform electrical properties and defect profile are demonstrated with resolutions of $\sim 1.6\%$ @ 662keV achieved in as-grown crystals without any electronic corrections.

5:15 PM - 5:30 PM

CDZnTE SINGLE-CRYSTAL INGOTS GROWTH BY PRESSURE CONTROLLED BRIDGMAN METHOD

F. Yang¹, T. Wang¹, B. Zhou², L. Yin³, M. Wang⁴, N. Jia⁴, S. Xi⁴, G. Zha¹, W. Jie¹

¹Northwestern Polytechnical University, CHINA, ²Tianjin University of Technology, CHINA, ³North China University of Water Resources and Electric Power, CHINA, ⁴Imdetek Corp. Ltd., CHINA

The developments of large dimension CdZnTe (CZT) crystal grows very rapidly due to the increasing requirements on radiation imaging applications. However, the yield of CZT crystal is limited by many problems such as polycrystalline, sub grain boundaries and twins. Furthermore, segregation effect and inhomogeneity of defects cause the material non-uniformity. This will deteriorate detection performance, especially for large dimension CZT detectors. In this work, we report single-crystal ingot growth of CZT with high uniformity by pressure controlled Bridgman method. We utilized Accelerated Crucible Rotation Technique (ACRT) to suppress the constitutional supercooling. By improving the ACRT control parameters the melt convection field during growth was optimized. Thus the solute distribution uniformity and stability of growth interface were improved. The introducing of cadmium pressure dynamic control during growth and annealing suppressed the cadmium evaporation in the melt and

optimized the distribution of point defects. The concentrations of cadmium vacancy and tellurium anti-site were also reduced. Single-crystal ingots with dimensions of 2-inch and 4-inch were reproducibly obtained. Single-crystal wafers, $25 \times 25 \times 5 \text{ mm}^3$ detectors and $40 \times 40 \times 5 \text{ mm}^3$ detectors were cut from the ingots. The diameter of tellurium inclusions was lower than $10 \text{ }\mu\text{m}$ (as-grown without wafer annealing). The wafer uniformity was also determined by resistivity and PL mapping. High $\mu\tau$ values for both electron and hole were observed in the pressure controlled growth ingots, which reached $1 \times 10^{-2} \text{ cm}^2/\text{Vs}$ and $5 \times 10^{-4} \text{ cm}^2/\text{Vs}$, respectively. The $25 \times 25 \times 5 \text{ mm}^3$ pixel detectors showed high uniform charge collection efficiency and energy resolution between the pixels, which further proved the reproducibility of the CZT material.

Monday, July 29, 2019

3:30 PM - 5:30 PM

Epitaxy of III-V Thin Films and Superlattices

Location: Torrey Peak II-IV

Session Chair(s): Hitoshi Habuka, Phil Ahrenkiel

3:30 PM - 4:00 PM

QUANTUM CASCADE LASER ACTIVE REGIONS GROWN ON LATTICE-MISMATCHED SUBSTRATES BY OMVPE

L.J. Mawst¹, A. Rajeev², H. Kim³, J. Kirch¹, K. Oresick¹, B. Knipfer¹, S. Xu³, D. Botez¹, B. Shi⁴, Q. Li⁴, K.M. Lau⁵, T.F. Kuech⁶

¹Department of Electrical and Computer Engineering, University of Wisconsin-Madison, WI, UNITED STATES OF AMERICA, ²University of Wisconsin Madison, WI, UNITED STATES OF AMERICA,

³University of Wisconsin-Madison, WI, UNITED STATES OF AMERICA, ⁴Hong Kong University of Science and Technology, HONG KONG PRC, ⁵HUST, HONG KONG PRC, ⁶Department of Chemical and Biological Engineering, University of Wisconsin-Madison, WI, UNITED STATES OF AMERICA

The heteroepitaxy of III-V alloys onto lattice-mismatched substrates, such as a Si substrate, have drawn much attention for both electronic and optoelectronic applications. Lower substrate cost, epitaxial growth on larger wafer size, as well as monolithic integration onto Si-based photonic platforms are among the motivating factors. The high density of defects, originating from large lattice-mismatch values, however, remain a challenging factor limiting the device performance and reliability. Metamorphic buffer layers (MBLs) have been effective to reduce residual threading-dislocation densities in the device structures grown on mismatched substrates. Employing such MBL techniques has been successful for realizing high performance and reliable diode lasers operating in the important telecom wavelength region on Si. The integration of mid-infrared (IR) sources onto Si photonic platforms would enable new compact sensor systems as well as monolithic Lab-on-Chip setups. Mid-IR-emitting quantum cascade lasers (QCLs) rely on many (500-700) ultra-thin (~1-2 nm) ternary strained-layer

superlattice (SL) materials, which pushes the limits of current crystal-growth technology. To exploit the potential of such devices on Si platforms, a detailed understanding of the interfacial structure and the influence of defects and surface morphology on the SL active region is needed. We will present the characteristics of strain-compensated, as well nominally lattice-matched InAlAs/ InGaAs SL structures and QCL active regions, grown on an InP MBL on either GaAs or Si substrates [1,2]. Since the MBL surface morphology is generally rougher than when using planar substrates, chemical mechanical polishing followed by wet chemical etching or chemical polishing are employed to reduce rms surface roughness prior to the SL growth. The planarity of the constituent layers and interfaces are compared to those grown directly on InP. Full QCL structures on MBLs have been grown by OMVPE and the structural and electroluminescence characteristics were investigated. [1] B. Shi, Q. Li, and K. M. Lau, J. Cryst. Growth, vol. 464, no. September 2016, pp. 28–32, 2017 [2] Ayushi Rajeev, Bei Shi, Qiang Li, Jeremy D. Kirch, Micah Cheng, Aaron Tan, Honghyuk Kim, Kevin Oresick, Chris Sigler, Kei May Lau, Thomas F. Kuech and Luke. J Mawst, Physica Status Solidi, Vol. 216, Jan 2019 The work at University of Wisconsin-Madison was supported by Materials Research Science and Engineering Center (DMR-1121288), NSF ECCS 1806285, and Army Research Office (ARO W911NF-16-1-0298). Work at HKUST was supported by the Research Grants Council of Hong Kong (16245216) and Innovation Technology Fund of Hong Kong (ITS/273/16FP).

4:00 PM - 4:15 PM

AB INITIO STUDY FOR ADSORPTION AND DESORPTION BEHAVIOR OF WETTING LAYER SURFACE OF INAS GROWN ON GAAS(001) SUBSTRATE

K. Yonemoto, T. Akiyama, A.M. Pradipto, K. Nakamura, T. Ito
Mie university, JAPAN

InAs/GaAs(001) heterostructures have been attracted much attention to fabricate three-dimensional island-shaped quantum dots (QDs). To theoretically understand the formation mechanism of InAs QDs, it is necessary to clarify the relationship between surface structure and epitaxial growth processes such as adsorption and desorption

behavior. In our previous studies, we have suggested that the (4×3) surface incorporates In atoms to proceed InAs growth substituting As-As dimers for In-As dimers from 0.63 monolayer (ML) to 0.96 ML. However, InAs growth does not proceed at the (4×3) surface beyond 0.96 ML. [1] The calculated results contradict the STM observations in which the (4×3) and (2×4) domains coexist at InAs coverage $\theta=0.76\pm0.07$ ML. [2] To understand the experimental results, we have predicted that the c(4×4) surface consisting of two In-As and one As-As dimer with $\theta=0.88$ ML appears as an intermediate surface structure between the (4×3) surface consisting of one In-As and two As dimer with $\theta=0.71$ ML and the (2×4) surface with $\theta=1.375$ ML. [3] In this study, the adsorption and desorption behavior for the formation of the (2×4) surface from the c(4×4) in InAs wetting layer on GaAs(001) substrate is systematically investigated using *ab initio*-based approach incorporating growth conditions such as temperature and beam-equivalent pressure. The calculations of surface phase diagrams demonstrate that the adsorption of one In-As dimer and In adatom and desorption of one As-As dimer occurs on the c(4×4) surface, resulting in the formation of the c(4×4) surface with $\theta = 1.13$ ML. For $\theta = 1.13$ ML, it is found that the surface energy of the (2×4) surface with 1.13 ML is lower than that of the c(4×4) surface by 2.52 meV/unit cell. This is because the number of excess electrons on the (2×4) surface is smaller than that on the c(4×4) surface. Furthermore, the adsorption of two In atoms and desorption of one As atom occurs on the (2×4) surface, resulting in formation of the (2×4) α 2 surface. The stabilization of the (2×4) α 2 surface is consistent with the STM observations. [2] These calculated results suggest that the formation of the c(4×4) surface is of importance to understand the formation of InAs QDs on GaAs(001) substrate. [1] T. Ito *et al.*, J. Cryst. Growth **477**, 12 (2017). [2] J. Grabrowski *et al.*, Appl. Phys. Lett. **95**, 233118 (2009). [3] T. Ito *et al.*, Phys. Status Solidi A **216**, 1800476 (2019).

4:15 PM - 4:30 PM

LAYER THICKNESS DEPENDENT INTERFACIAL GRADING ANALYSIS FOR STRAINED III-V SUPERLATTICES BY ATOM PROBE TOMOGRAPHY

A. Rajeev¹, B. Knipfer¹, D. Isheim², J. Kirch¹, S.E. Babcock³, T.F.

Kuech⁴, T. Earles⁵, D. Botez¹, L.J. Mawst¹

¹Department of Electrical and Computer Engineering, University of Wisconsin-Madison, WI, UNITED STATES OF AMERICA,

²Department of Materials Science and Engineering, Northwestern University, IL, UNITED STATES OF AMERICA, ³Department of

Materials Science and Engineering, University of Wisconsin-Madison, WI, UNITED STATES OF AMERICA, ⁴Department of Chemical and

Biological Engineering, University of Wisconsin, WI, UNITED STATES OF AMERICA, ⁵Intraband LLC, WI, UNITED STATES OF AMERICA

Mid-infrared emitting quantum cascade lasers (QCLs) typically contain active regions composed of ~30-40 repetitions of a strained superlattice (SL) motif. This motif contains many quantum wells and barriers of various thicknesses (1-4nm) and compositions in order to achieve emission through conduction band engineering. Precise control over the thickness and composition of each well and barrier is required to attain the designed emission wavelength. Atom probe tomography (APT) has been employed in conjunction with x-ray diffraction to quantify the composition gradients for SL motifs with constant thickness and composition throughout. Analysis of the APT-derived composition profile yielded a self-consistent interdiffusion coefficient across the samples studied and indicated an interdiffusion zone as wide as the half-thickness of the thinnest constituent layers of the QCL [1]. In this study, interfacial intermixing and actual vs. target compositions are characterized, for layers as thin as 1nm, using transmission electron microscopy (TEM) and APT. A strained SL structure was grown on InP by organometallic vapor phase epitaxy (OMVPE) at a temperature of 605°C and reactor pressure of 100 torr, with a 5sec interruption time in between the layers. The SL layers are 2x (1nm:In_{0.44}Al_{0.56}As/ 1nm:In_{0.6}Ga_{0.4}As); 2x (2nm:In_{0.44}Al_{0.56}As/ 2nm:In_{0.6}Ga_{0.4}As); 2x (3nm:In_{0.44}Al_{0.56}As/ 3nm:In_{0.6}Ga_{0.4}As) and 2x (4nm:In_{0.44}Al_{0.56}As/ 4nm:In_{0.6}Ga_{0.4}As) in the growth direction. This entire structure is bound by 50nm of In_{0.53}Ga_{0.47}As towards the substrate and terminated by 50nm of In_{0.52}Al_{0.48}As. Ga⁺ focused ion beam lift out and shaping techniques were used to prepare tips and slices for APT and TEM investigations, respectively. The layer

thicknesses obtained from TEM were used to validate the atom-probe data reconstruction. Preliminary analysis of the 1-D concentration profiles suggests that the 1nm-thick barriers are significantly Al-deficient. The composition gradient at the interfaces determines QCL design modifications, specifically for the thinnest quantum barriers and wells, to minimize the wavelength deviation from design. [1] A. Rajeev et al., *Crystals* **2018**, 8(11), 437 Acknowledgement: This work is supported by Air Force Research Laboratory under Grant FA8650-13-21616 and NSF ECCS 1806285. APT was performed at the Northwestern University Center for Atom-Probe Tomography (NUCAPT) supported with grants from the NSF-MRI (DMR-0420532), ONR-DURIP (N00014-0400798, N00014-0610539, N00014-0910781, N00014-1712870) programs, MRSEC program (NSF DMR-1720139) at the Materials Research Center, the SHyNE Resource (NSF ECCS-1542205), and the Initiative for Sustainability and Energy at Northwestern University. The authors gratefully acknowledge use of facilities and instrumentation at the UW-Madison Wisconsin Centers for Nanoscale Technology partially supported by UW-MRSEC (NSF DMR-1720415).

4:30 PM - 4:45 PM

RECENT PROGRESS OF HIGH TEMPERATURE VAPOR PHASE EPITAXY FOR THE GROWTH OF GAN LAYERS

T. Schneider¹, M. Förste¹, C. Schimpf², C. Röder³, J. Beyer³, E. Niederschlag¹, D. Rafaja², O. Pätzold¹, M. Stelter¹

¹TU Bergakademie Freiberg, Institute of Nonferrous-Metallurgy and Purest Materials, GERMANY, ²TU Bergakademie Freiberg, Institute of Materials Science, GERMANY, ³TU Bergakademie Freiberg, Institute of Applied Physics, GERMANY

The high temperature vapor phase epitaxy (HTVPE) is a physical vapor transport technique, which can be used for the deposition of GaN layers [1]. The precursors are ammonia and thermally evaporated elemental gallium, whereby toxic or aggressive substances or byproducts are widely avoided in the growth process. This contribution presents recent progress in the development of HTVPE for the epitaxial growth of GaN on sapphire substrates with

diameters up to 2 inches. An advanced multi-step HTVPE process that includes the sequential deposition of a nucleation layer (Fig. 1a) and a seed layer (Fig. 1b) is described in detail. The use of seed layers as templates for further overgrowth with an increased growth rate to produce several ten μm thick GaN layers is successfully demonstrated. The properties of the GaN layers are characterized by optical microscopy, scanning electron microscopy (SEM), high-resolution X-ray diffraction, confocal Raman spectroscopy, photoluminescence and GDMS. Impurity concentrations, dislocation densities, and residual stress of seed and overgrown layers are presented and compared with the properties of GaN layers grown by established methods of chemical vapor phase epitaxy. In this context, challenges and prospects of the HTVPE method are discussed. [1] G. Lukin et al., *Physical Status Solidi C* **11**, 491-494 (2014)

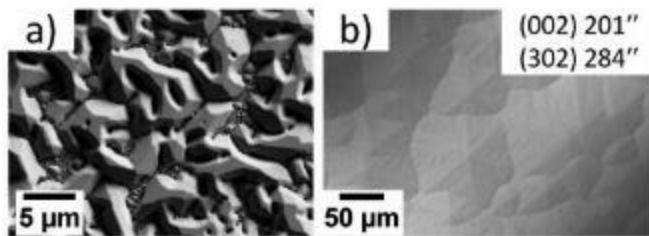


Fig. 1: a) SEM top-view image of a nucleation layer revealing a 3D surface morphology. b) DIC image of a 5 μm thick GaN seed layer and the full width at half maximum of selected X-ray diffraction lines.

4:45 PM - 5:00 PM

IMPROVEMENT OF LUMINESCENCE PROPERTIES OF N-GAN USING TEGA PRECURSOR

T. Hubáček, A. Hospodková, K. Kuldová, M. Slavická-Zíková, F. Hájek, J. Pangrác, J. Oswald, T. Vaněk, A. Vetushka, E. Hulcius
Institute of Physics, CAS, CZECH REPUBLIC

Photoluminescence properties of epitaxially grown GaN buffer layers have been extensively studied and two defect bands at around 2.9 eV (blue band – BB) and 2.2 eV (yellow band – YB) are usually observed. Three different origins of BB have been proposed. The first origin of the BB is related to the Zn_{Ga} acceptor, the second one is related to carbon-hydrogen complexes and the last one was attributed to C_{N} defects that might be also responsible for the YB [1]. Amount of

carbon contamination is very important indicator of the quality of GaN layers. Nowadays, origin of these defect bands and their suppression is still discussed in the GaN community. Suppression of these bands is a quite challenging task and needs specific growth parameters. Trimethylgallium (TMGa) with hydrogen carrier gas is usually used as a precursor during the growth of GaN buffer layers grown by Metal Organic Vapor Phase Epitaxy. The growth temperature is typically over 1000 °C. On the other hand, during the growth of InGaN/GaN heterostructures the growth temperature is much lower (650 – 850 °C) and triethylgallium (TEGa) with nitrogen carrier gas is usually used as a Ga source having an advantage of lower carbon contamination of GaN layers. TEGa is less stable than TMGa, decomposes by β -hydride elimination reaction and suffers from strong parasitic pre-reactions. In our study we will discuss the influence of different growth parameters on the optical and structural properties of the n-type doped GaN buffer layers grown from TEGa precursor. Photoluminescence measurement showed suppression of the YB using nitrogen carrier gas, TEGa precursor and lower growth rate. Influence of other growth parameters on quality of GaN layers, such as growth temperature or V/III ratio will be discussed. Morphology and structural quality measured by AFM and XRD will be discussed as well. Combination of specific growth parameters will be suggested to improve the quality of n-GaN buffer layers. [1] M.A. Reshchikov, et al., Phys. Rev. B **98**, 125207 (2018).

5:00 PM - 5:15 PM

EPITAXIAL GROWTH OF GAN/GA₂O₃ AND GA₂O₃/III-N HETEROSTRUCTURES

R. Fornari¹, S. Leone², M. Bosi³, V. Montedoro¹, L.K. Kirste², V. Polyakov², O. Ambacher²

¹Dept. of Mathematical, Physical and Computer Sciences, University of Parma, ITALY, ²IAF - Fraunhofer Institute for Applied Solid State Physics, GERMANY, ³IMEM-CNR, ITALY

Despite the great progresses made in III-N epitaxy and the commercialization of electronic and optoelectronic devices, there are still technological problems that hinders the full exploitation of nitride

applications, the main being the lack of a suitable substrate with good lattice match and low cost. Sapphire is still the substrate of choice for hexagonal GaN deposition but, despite the use of buffer layers, the high lattice mismatch results in many defects and lowers the nitride crystal quality. Ga₂O₃ is a wide bandgap transparent semiconducting oxide that is receiving a lot of interest for its potential applications in high-power devices and in deep-UV photodetectors. Although b-Ga₂O₃ is the most studied polytype, being the thermodynamically stable one, the other polymorphs such as a and e are getting attention because they can be grown on sapphire and present unique properties such as hexagonal (a) or orthorhombic (pseudo-hexagonal, e), the latter also exhibits spontaneous polarisation and ferroelectric behaviour. We have explored the possibility of inserting an intermediate e-Ga₂O₃ layer, deposited by MOVPE on sapphire substrates, as a template to reduce the lattice mismatch of GaN with the standard sapphire. The GaN layers were deposited at two different temperatures (690°C, 1050 °C), considering that the e-Ga₂O₃ is metastable with a transition temperature around 800 °C. Preliminary electrical and SIMS investigations have evidenced the interdiffusion of oxygen from the e-Ga₂O₃ to the GaN epitaxial layers, which results in a n-type conductivity and a sheet resistance as low as 70 Ohm/sq in a 1 µm thick GaN layer. The rocking curve of the GaN layers indicates a crystal quality worse than for GaN deposited directly on sapphire, however, considering that these are preliminary experiments and that deposition conditions are not yet optimized, is the FWHM of 650 and 850 arcsec for the 00.2 and 10.2 reflections, respectively, looks very promising. In parallel, we utilized GaN layers grown on silicon or sapphire to improve the epitaxial deposition of e-Ga₂O₃ on sapphire. The use of III-N templates for Ga₂O₃ epitaxy evidenced an improvement of the morphology and of the structural quality of the layer. Moreover, the possibility of obtaining n-type e-Ga₂O₃ layers on p-type GaN / silicon opens interesting possibilities for the realization of novel devices.

5:15 PM - 5:30 PM

HETEROEPITAXIAL GROWTH BETWEEN GAN THIN FILM AND A FLEXIBLE SUBSTRATE

W.C. Yang¹, Z.X. Lo¹, W.R. Lo¹, C. Huang¹, Y.H. Chu², Y. Chou¹

¹Department of Electrophysics, National Chiao Tung University, TAIWAN, ²Department of Materials Science and Engineering, National Chiao Tung University, TAIWAN

Nowadays, roll-to-roll fabricated devices are benefit to thin, light and unbreakable products. GaN is known for the applications in the field of high-frequency and power electronic devices such as high electron mobility transistors, RF components, and light-emitting diodes for its high saturated current and wide band gap [1]. Additionally, the fluorophlogopite mica as a flexible substrate is resistant to corrosion, high temperature and collision. Thus, we propose the use of fluorophlogopite mica substrate for GaN growth to form flexible GaN devices. However, the difficulty of epitaxy high-quality crystalline GaN on fluorophlogopite mica is ascribed to and high diversity of thermal expansion coefficient between GaN and fluorophlogopite mica. We will show the synthesis of transparent GaN film on fluorophlogopite mica as heteroepitaxial growth. Due to the large lattice mismatch of mica and GaN, the interface was expected to form Van der Waals bonding[2]. The growth of crystalline GaN film was carried out in hydride vapor phase epitaxy (HVPE) so that rapid growth can be achieved. We fabricated GaN film using two-step growth, including formation of a buffer layer and followed by the growth of dense GaN layer, to improve adhesion and crystal quality compared with conventional growth condition of GaN film. The crystallinity, surface morphology, and photoluminescence of GaN thin film on mica will be discussed. **Reference** 1 Fong, C. Y., Ng, S. S., Yam, F. K., Abu Hassan, H. & Hassan, Z. Effects of Nitridation Temperature on Characteristics of Gallium Nitride Thin Films Prepared Via Two-Step Method. *Acta Metallurgica Sinica (English Letters)* 28, 362-366,(2015) 2 Qin, J.-K. et al. van der Waals epitaxy of large-area continuous ReS₂ films on mica substrate. *RSC Advances* 7, 24188-24194,(2017).

Monday, July 29, 2019

3:30 PM - 5:30 PM

Joint III-V Wide Bandgap Nitride Semiconductors

Location: Shavano Peak

Session Chair(s): Rafael Dalmau, Michal Bockowski

3:30 PM - 4:00 PM

CRYSTALLIZATION OF GAN BY HVPE METHOD WITH CONTROLLED LATERAL GROWTH

T. Sochacki, S. Sakowski, B. Lucznik, M. Amilusik, M. Fijalkowski, M. Iwinska, A. Sidor, I. Grzegory, M. Bockowski

Institute of High Pressure Physics PAS, POLAND

It was shown that ammonothermally grown GaN (Am-GaN) crystals can be successfully used as seeds for Halide Vapor Phase Epitaxy (HVPE). Crack-free and up to 2-mm-thick HVPE-GaN layers can be obtained during growth in the c-direction. Free-standing (F-S) HVPE-GaN crystals sliced from the Am-GaN seeds show high structural as well as optical, electrical, and thermal qualities [1]. However, for 1-inch (lateral size) seed the growth of layer thicker than 2 mm without degradation of its structural quality is difficult. The most important factor limiting the thickness of the deposited layer is anisotropy of the growth [2,3]. The crystal does not only grow in the c-direction but also in lateral direction. Lateral "wings" are formed. This material has different properties (incorporation of unintentional dopants and therefore the lattice parameters) than GaN grown in the c-direction. The wings are the origin of stress during crystallization. The stress increases with the thickness of the deposited layer. Exceeding a certain critical thickness of the deposited layer results in plastic deformation and deterioration of the structural quality of GaN growing in the c-direction. Controlling the growth in lateral directions seems to be a key aspect for obtaining a bulk GaN crystal. This could be realized by formation of a specific thermal field around the growing crystal. A proper thermal field can suppress the lateral growth, lead to the disappearance of the side walls and expansion of the c-plane. In this paper the influence of lateral growth on critical thicknesses and structural quality of crystallized GaN layers by HVPE method will be discussed. Some ways to modify the temperature field and its effect on crystal growth will be investigated and discussed based on numerical simulations and experimental results. A new approach to

HVPE-GaN growth process with modulation of the temperature field at the edge of the crystal will be shown. Reduction of lateral crystallization and growth only in the c-direction will be presented. [1] T. Sochacki et al. Appl. Phys. Expr. 6, 075504 (2013) [2] J.Z. Domagala et al. J. Cryst. Growth 456 (2016) 80. [3] B. Lucznik et al. J. Cryst. Growth 456 (2016) 86.

4:00 PM - 4:15 PM

THICK GAN CRYSTALS OF HIGH PURITY GROWN WITH AN INCREASED RATE BY AMMONOBASIC METHOD

R. Kucharski¹, K. Grabianska¹, M. Zajac¹, D. Wlodarczyk², **M. Amilusik**¹, A. Suchocki², L. Konczewicz¹, E. Litwin-Staszewska¹, R. Piotrkowski¹, M. Bockowski¹

¹Institute of High Pressure Physics, Polish Academy of Sciences, POLAND, ²Institute of Physics, Polish Academy of Sciences, POLAND

Ammonothermal method is regarded as one of key technologies for bulk GaN crystallization. It uses supercritical ammonia to dissolve feedstock material and crystallize GaN on native seeds at due to supersaturation at temperatures 450-550 °C. In this method C-plane growth is conducted on N-face of a GaN seed with a rate of 40-50 μm/day [1]. Recently, a twofold increase of the growth rate was achieved [2] by controlling the supersaturation conditions and the fluid convection velocity. In addition, elimination of the lateral growth in *a*- and *m*-directions was performed by an appropriate seed masking. This lead to diminishing the stress generated at the crystal's edges by growth anisotropy. Such one-directional growth in a higher-growth-rate (HGR) regime enabled an increase in the crystal's thickness to about 6 mm [2] during one process. The crystals are highly conductive with free electron concentration at about $1 \times 10^{19} \text{ cm}^{-3}$, since unintentional doping of oxygen is a common problem in ammonothermal method. In this communication we show a successful reduction of oxygen concentration to $1-2 \times 10^{18} \text{ cm}^{-3}$ by the use of a getter at HGR conditions, leading to thick (4-5 mm) crystals. Concentrations of residual metals (Mg, Mn, Fe, Zn) did not exceed $5 \times 10^{16} \text{ cm}^{-3}$. The crystals were characterized by SIMS, temperature-dependent Hall

effect, and Raman scattering spectroscopy. Hall effect data at room temperature revealed electron concentration of $5-8 \times 10^{17} \text{ cm}^{-3}$, resistivity of $2-3 \times 10^{-2} \text{ } \Omega\text{cm}$, and mobility of $400-450 \text{ cm}^2/\text{Vs}$. The electron concentration is uniform, within the accuracy of 30%, along the c-axis of a crystal. This was confirmed by Raman scattering (plasma coupled phonon modes) mapping performed on an *m*-plane cross-section of the obtained crystal. To conclude, a successful reduction of oxygen in together with an increase of the ammonothermal crystal's thickness (4-5 mm) was achieved. This improvement enables an efficient multiplication of high-purity crystals and highly efficient wafer-to-wafer technology. The obtained substrates can be used for epitaxy by HVPE method of drift layers with outstanding structural quality for vertical transistors. [1] M. Zajac et al., Prog. Cryst. Growth Charact. Mat.64 (2018) 63–74. [2] R. Kucharski et al, presented at International Workshop on Nitride Semiconductors, November 11-16, 2018, Kanazawa (Japan). This research was supported by the Department of the Navy, Office of Naval Research (ONRG-NICOP-N62909-17-1-2004), by Polish National Science Center through projects No. 2017/25/B/ST5/02897 and 2018/29/B/ST5/00338, as well as by TEAM TECH program of the Foundation for Polish Science co-financed by the European Union under the European Regional Development Fund. (POIR.04.04.00-00-5CEB/17-00).

4:15 PM - 4:30 PM

SUPPRESSION OF STEP BUNCHING IN GAN CRYSTALS DURING THE NA-FLUX METHOD AT LOW SUPERSATURATION

K. Endo¹, T. Yamada¹, K. Murakami¹, M. Imanishi¹, M. Yoshimura², Y. Mori¹

¹Grad. Sch. of Eng., Osaka Univ., JAPAN, ²Institute of Laser Engineering, Osaka University, JAPAN

GaN-based transistors and diodes are excellent candidates for high-voltage and high-power electronics, due to its superior material properties. In order to realize such GaN-based devices, the fundamental causes for the leakage current in GaN crystals needs to be further solved. Recent reports suggested that the leakage current

in Na-flux-grown GaN crystals was mainly caused by the micro-facet-growth sector in which GaN crystals grew with step bunching on the side of terrace in *c*-growth sector [1]. Therefore, in order to suppress that sector, it is significant to reduce the step bunching, in short, increase of step height in *c*-growth sector. In this work, we focused on growth temperature, and investigated the step-bunching height in GaN crystals grown at 870°C (Conventional) and 900°C (Low supersaturation). GaN substrate, Ga, Na, and carbon were placed in a crucible. The starting Ga:Na:C composition was 27:73:0.5. The growth proceeded with nitrogen dissolution into a Ga-Na melt at 870°C and 900°C under N₂ pressure of 4.0 MPa, and the film thickness of both GaN crystals was made uniform. The step-bunching height was observed in several places of the GaN crystal with a confocal laser scanning microscope. Figure 1 shows the measurement results of the step-bunching height in GaN crystals grown at 870°C (named 870°C-GaN) and 900°C (named 900°C-GaN). As shown in Fig.1, the step-bunching height of 900°C-GaN was much lower than that of 870°C-GaN. These results showed that GaN crystals having less step bunching can be realized with Na-flux growth at low supersaturation. Figure 2 shows the scanning electron microscope (SEM) images of (a-1)870°C-GaN, (b-1)900°C-GaN and the nomarski differential interference-contrast (DIC) images of (a-2)870°C-GaN, (b-2)900°C-GaN. Figure 3 shows DIC and schematic images of the cross section in hillocks, respectively. As shown in Fig. 2 and 3, Some hillocks are observed in both the GaN crystals. The slope angle of hillocks observed in 870°C-GaN was 0.3 degrees, whereas that in 900°C-GaN was 0.07 degrees. From the results, it is expected that the growth rate of spiral steps in 900°C-GaN was lower than 870°C-GaN, and attractive interactions between steps are suppressed because of low supersaturation condition [2,3]. In summary, GaN crystals with step bunching free can be obtained at low supersaturation condition.

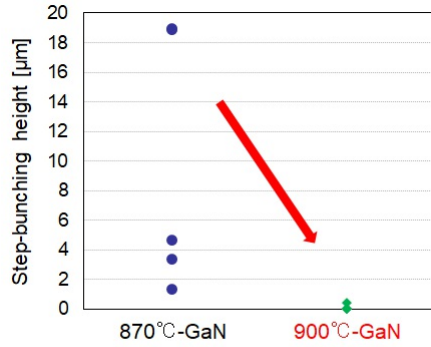


Fig. 1 The step-bunching height of the 870°C-GaN and the 900°C-GaN

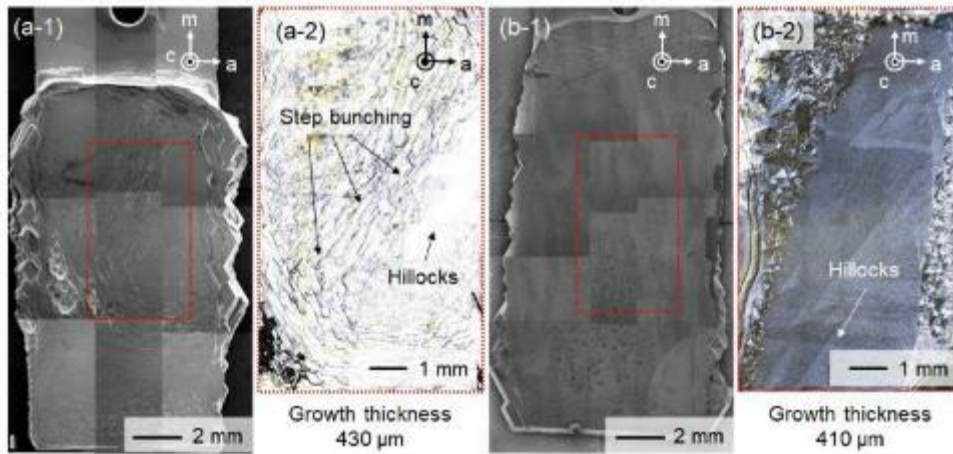


Fig. 2 SEM images of the (a-1)870°C-GaN, (b-1)900°C-GaN and DIC images of the (a-2)870°C-GaN, (b-2)900°C-GaN

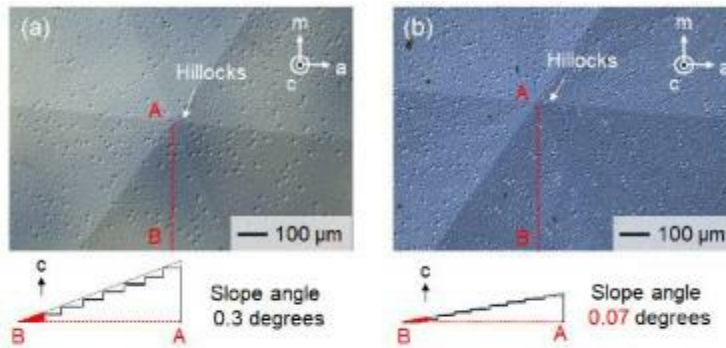


Fig. 3 DIC images of hillocks in the (a)870°C-GaN, (b)900°C-GaN and schematic images of the cross section in hillocks.

[1] T. Hamachi *et al.*, The 65th JSAP Spring Meeting, 18p-E202-5 (2018). [2] A. A. Chernov, *Sov. Phys. Usp.*, **4** R06 (1961). [3] A.C. Redfield *et al.*, *Phys. Rev. B* **46** 4289 (1992).

4:30 PM - 4:45 PM

TEMPERATURE DEPENDENCE OF NITROGEN DISSOLUTION ON

SODIUM FLUX GROWTH

R. Tandryo, K. Murakami, K. Okumura, T. Yamada, T. Kitamura, M. Imanishi, M. Yoshimura, Y. Mori

Graduate School of Engineering, Osaka University, JAPAN

High-quality and Large Diameter bulk Gallium Nitrides (GaN) are desired to popularize GaN-based devices and lower its cost. Sodium Flux is a promising method to grow large diameter GaN crystals with low dislocation density. Even though it is important to understand the growth process, there are only a few studies reporting the mechanism of sodium flux growth. In particular, temperature dependence of nitrogen dissolution has not been elucidated yet. In this work, we used electrical resistance measurement^[1] to investigate the temperature dependence of nitrogen dissolution. The electrical resistance of Ga-Na melt was investigated with 4-point probe method. Gallium and Sodium with starting Ga:Na composition of 27:73 were heated and melted at 870°C and 900°C. Nitrogen gas pressure of 4 MPa was applied to Ga-Na melt on each experiment. Crystals growth were also performed under the same condition with Multi-point seed substrates. Dipping method was employed to kept substrates at the vapor phase for various keeping duration, then dipped it into the Ga-Na melt for growth for 3 hours. Initial c-axis growth rate of different temperature was investigated as the parameter. Electrical resistance change of Ga-Na melt is shown in figure 1. Linear slope which indicates the nitrogen dissolution rate in case of 870°C was much lower than that of 900°C which showed significant increase rate of the electrical resistance value. Evaluation of c-axis growth rate (thickness) on growth temperature of 870°C showed the saturation for longer keeping duration while thickness increase in case of 900°C remained unchanged. Initial growth rate was driven by nitrogen concentration (supersaturation) which were different for each keeping duration. In the case of 870°C with long keeping duration, growth rate was high but slow nitrogen dissolution process cannot maintain the growth rate, which resulted in the saturation of thickness. High nitrogen dissolution rate helped to maintain the increase of c-direction growth at constant. These results showed that temperature dependence of nitrogen dissolution was successfully revealed with electrical resistance measurement and the results matched with crystal growth.

References: [1] R. Tandryo et al., LEDIA'19, LEDIA-6-02, 2019

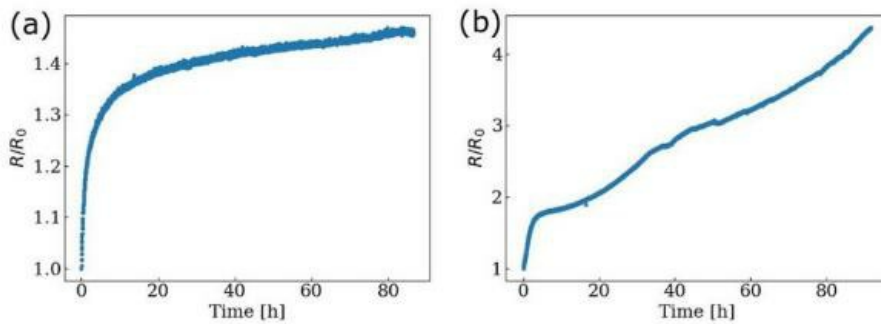


Fig 1. Electrical resistance change of Ga-Na melt when pressurized by 4 MPa of nitrogen gas at (a) 870°C, (b) 900 °C

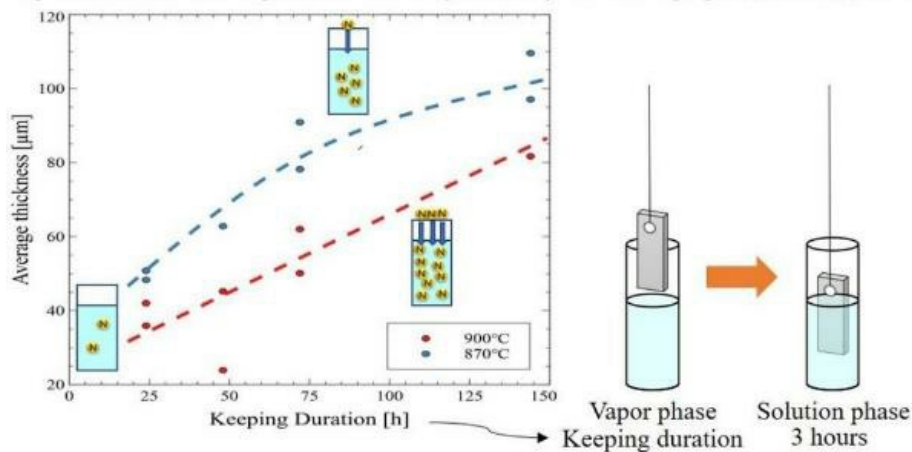


Fig 2. Schematic illustration of crystal growth with dipping method and the average thickness of grown crystal as the function of keeping duration at 870°C and 900°C

4:45 PM - 5:00 PM

DETAILED STUDY OF HVPE-GaN DOPED WITH SILICON

M. Amilusik, T. Sochacki, M. Iwinska, M. Fijalkowski, B. Lucznik, A. Sidor, M. Zajac, I. Grzegory, M. Bockowski

Institute of High Pressure Physics PAS, POLAND

Hydride Vapor Phase Epitaxy (HVPE) method enables growth of GaN crystals with low levels of background impurities. Generally, the impurity concentration on the c-plane of HVPE-GaN grown without intentional doping in the c-direction lies between 10^{16} cm^{-3} and 10^{17} cm^{-3} . In turn, the free carrier concentration is usually not higher than $2\text{-}4 \times 10^{16} \text{ cm}^{-3}$. It is well known that the main impurity in undoped HVPE-GaN is silicon. Silicon concentration was investigated in free-standing (F-S) HVPE-GaN and differences in its values on N-polar and Ga-polar faces were demonstrated. According to SIMS measurements the Ga-polar face had $[\text{Si}] = 2 \times 10^{17} \text{ cm}^{-3}$, while the N-

polar face had $[Si] = 2 \times 10^{16} \text{ cm}^{-3}$. The Si concentration gradient was also observed in F-S HVPE-GaN grown with intentionally incorporated silicon. For a constant dichlorosilane (precursor of silicon) flow during a crystallization process the concentration of silicon varied by more than one order of magnitude and was higher close to the (0001) surface. For example, Si concentration level could change from $2 \times 10^{18} \text{ cm}^{-3}$ to $2 \times 10^{19} \text{ cm}^{-3}$. A gradient was also observed in the free carrier concentration, investigated by Raman spectroscopy, and the value was always higher close to the Ga-polar surface. Additionally, SIMS and Hall measurements performed on the (0001) HVPE-GaN:Si surfaces showed that with an increase of silicon concentration in GaN the free carrier concentration decreased. In order to understand and investigate the described above phenomena a many HVPE-GaN:Si crystallization processes (on native seeds) were performed with varying growth parameters (i.e. growth temperature, reactants and dichlorosilane flows, total pressure, time). Morphology, structural quality and growth rate of the obtained crystals were investigated and determined. The Ga-polar, N-polar surfaces as well as cross sections (the m-planes) of the samples were examined. The crystals were studied by optical and electron microscopies, X-Ray diffraction, SIMS, photoetching (PEC, a technique which reveals areas with different electrical properties), Hall measurements, and Raman spectroscopy. The determined free carrier concentration was compared to the silicon concentration. It was shown that the cause of silicon gradient in HVPE-GaN:Si was associated with the silicon deposition inside the reactor, in the dichlorosilane line. In turn, the drop of the efficiency of Si doping was caused by gallium vacancies and complexes of gallium vacancies with silicon atoms.

5:00 PM - 5:15 PM

HVPE-GAN DOPED WITH CARBON AND/OR MANGANESE

T. Sochacki, M. Amilusik, M. Fijalkowski, M. Iwinska, A. Sidor, B. Lucznik, E. Litwin-Staszewska, R. Piotrkowski, I. Grzegory, M. Bockowski, M. Zajac

Institute of High Pressure Physics PAS, POLAND

Gallium nitride of the highest purity can be grown by halide vapor phase epitaxy (HVPE) method. In general, HVPE-GaN without

intentional doping is n-type with free carrier concentration at the level of $2\text{-}5 \times 10^{16} \text{ cm}^{-3}$. The main unintentionally incorporated donors are silicon and oxygen. Intentional incorporation of acceptors is required when the goal is to compensate the residual donors. This should lead to semi-insulating properties of the crystallized material. Manganese seems to be an ideal acceptor due to its energy level close to the middle of the bandgap (activation energy of 1.7-1.8 eV). Resistivity of GaN with Mn concentration of 10^{19} cm^{-3} exceeds $10^8 \Omega \cdot \text{cm}$ at 560 K. At room temperature it is difficult to measure the resistivity value. Hall measurements, however, reveals n-type conductivity at high temperature. The second candidate for an acceptor in GaN is carbon. The energy level connected to carbon is situated at about 1 eV above the valence band maximum. Carbon-doped GaN is highly resistive at room temperature (exceeding $1 \times 10^8 \Omega \cdot \text{cm}$) and becomes p-type at high temperature. In this paper advantages and challenges connected to the two dopants in GaN (Mn and C) crystallized by HVPE will be described. GaN crystals and their structural, electrical and optical properties will be presented. Results of doping of HVPE-GaN with carbon, manganese, as well as co-doping with and carbon and manganese will be investigated. The motivation for this work is to increase the resistivity of crystallized material as well as obtain p-type bulk GaN.

5:15 PM - 5:30 PM

GROWTH OF GAN SINGLE CRYSTALS WITH HIGH TRANSPARENCY BY LI-ADDED NA-FLUX METHOD

T. Nakajima, T. Yamada, K. Murakami, M. Imanishi, M. Yoshimura, Y. Mori

Osaka University, JAPAN

For the widespread use of the GaN devices, it is necessary to fabricate low-dislocation GaN wafers. We have developed Na-flux point-seed-technique by thin-flux-method for fabrication of the GaN crystal with large dislocation-free area [1]. As shown Figure 1, GaN crystals grown by this method are mainly composed of {10-11}-growth-sector which easily incorporates oxygen impurities resulting in blackening [2]. Therefore, it is necessary to suppress oxygen incorporation to improve transparency of {10-11}-growth-sector. We

reported that in Na-flux-method, GaN crystal generally grows in nitrogen poor condition [3]. In the condition, oxygen impurities are easily incorporated into crystals [4]. High nitrogen concentration is effective for obtaining transparent {10-11}-growth-sector. Thus, in this study we attempted to increase the nitrogen concentration by adding Li [5]. GaN substrate and Ga, Na, C, and Li were placed in a crucible. We used Y_2O_3 which is hard to be corroded by Li and alumina as crucible. The starting Ga:Na:C:Li composition was 27:73:0.5:0.3. The growth temperature, nitrogen pressure, and growth period were 870 °C, 4.0 MPa and 72 h, respectively. Figure 2 shows optical and bird's-eye SEM images of crystals grown in Y_2O_3 crucible (sample1) and alumina crucible (sample2). From Figure 1 and Figure 2, it was found that transparency in {10-11}-growth-sector of sample1 was improved and that of sample2 was the same as a conventional crystal. In sample1, Li additive enabled high nitrogen concentration in flux, resulting in having high transparency. In sample2, the reason for blackening of {10-11}-growth-sector is estimated due to the high oxygen concentration by crucible melting. It is reported that an alumina easily reacts with Li [6]. In fact, alumina crucible decreased in weight more than Y_2O_3 crucible after growth. This result means that oxygen impurities from a corroded alumina crucible had more effective than increase of nitrogen concentration by Li additive, on oxygen concentration in GaN crystals. We concluded that GaN grown with Li additive in Y_2O_3 crucible enables high nitrogen concentration, with low oxygen concentration, and high transparent GaN wafers were successfully obtained. [1] T. Nakajima *et al.*, The 37th EMS. Th2-14 (2018) [2] M. Imanishi *et al.*, Cryst. Growth. Des. **17** (2017) 3806 [3] F. Kawamura *et al.*, J. Mater. Sci. Mater. Electron, **16** (2005) 29 [4] F. Wright *et al.*, J. Appl. Phys. **98** (2005) 103531 [5] M. Morishita *et al.*, J. Cryst. Growth **284** (2005) 91 [6] J. Konys *et al.*, J. Nucl. Mater. **131** (1985) 158



Figure 1. Photo images of GaN crystal on PS grown by thin-flux method

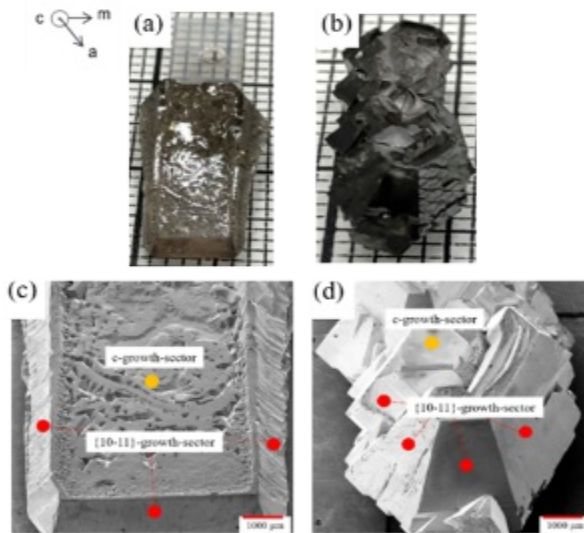


Figure 2. Photo images of grown GaN crystal using (a) yttrium oxide crucible (sample1), (b) alumina crucible (sample2) and bird's-eye Scanning Electron Microscope (SEM) images of (c) sample1 (d) sample2 with the scheme describing the growth-sector

Monday, July 29, 2019

3:30 PM - 5:30 PM

Nonlinear Optical and Laser Host Materials III

Location: Crestone I, II

Session Chair(s): Kevin Stevens, Shekhar Guha

3:30 PM - 4:00 PM

LINEAR AND NONLINEAR OPTICAL TECHNIQUES FOR DETERMINATION OF CRYSTAL PROPERTIES

S. Guha, J. Murray, J. Wei

Air Force Research Laboratory, UNITED STATES OF AMERICA

Nonlinear optical crystals are used for conversion of lasers from wavelengths easily available commercially to other wavelengths of interest. To maximize the conversion efficiency, refractive indices of the crystals need to be known with high degree of accuracy, preferably over a wide temperature and wavelength range. The method outlined by Moss [1] and used more recently for accurate measurement of refractive indices of GaAs [2] have been used in our laboratory for the determination of refractive indices of various anisotropic nonlinear optical crystals such as CdSiP₂ and ZnGeP₂ as well as isotropic crystals with potential for quasi-phase matching such as GaSb and InAs, for which accurate temperature dependent Sellmeier equations are not easily available.

Along with the linear refractive index values, it is also important to know the values of the second order nonlinear optical coefficient d of the crystals, and especially the values of the different components of the d tensor. The Maker fringe technique, involving the interference between the free and bound second harmonic waves in a parallel plate of nonlinear optical medium, is a method that allows determination of various d components. However, a general theoretical treatment of Maker fringes obtained from plane parallel plates of anisotropic (or isotropic) media is not easily available. Using our recent derivation of the detailed expressions for SHG transmission (SHG-T) and SHG reflection (SHG-R) using the plane-wave theory outlined by Pavlides and Pugh [3] for crystals of arbitrary symmetry and orientation and through fitting of experimentally observed Maker fringes at various wavelengths from a thin parallel plates of oriented wafer, values of all the non-zero d coefficients of several nonlinear optical crystals were measured.

A review of these techniques and their relative benefits and drawbacks with respect to other 'standard' methods will be provided.

1. T. S. Moss, S. D. Smith, and T. D. F. Hawkins. "Absorption and dispersion of indium antimonide," in *Proc. Phys. Soc. B* **70**, 776 (1957).

2. T. Skauli, P. S. Kuo, K. L. Vodopyanov, et al. "Improved dispersion relations for GaAs and applications to nonlinear optics." J. Appl. Phys. **94**, 6447-6455 (2003).
3. P. Pavlides and D. Pugh, "General theory of Maker fringes in crystals of low symmetry, Journal of Physics: Condensed Matter", **3**, (8) (1991)

4:00 PM - 4:15 PM

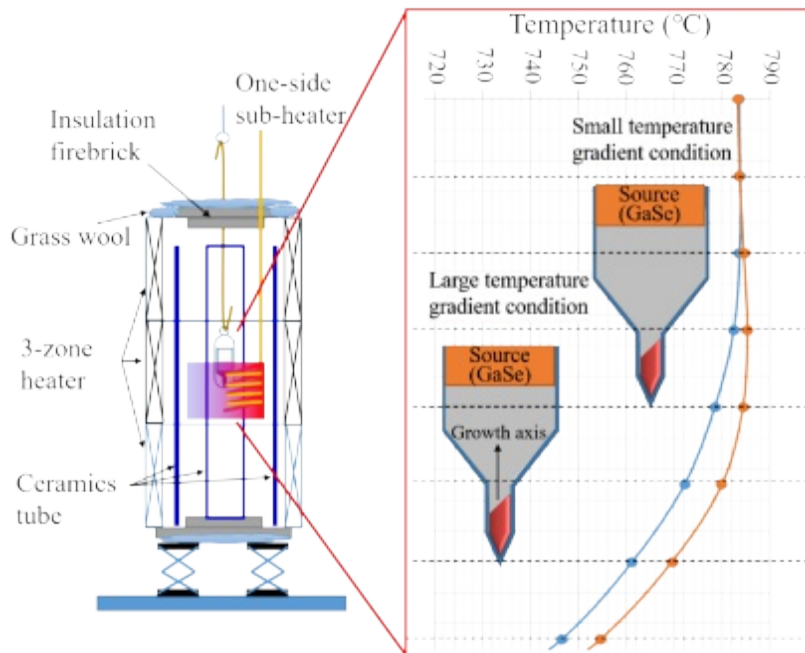
**TEMPERATURE DIFFERENCE SOLUTION GROWTH OF GASE CRYSTAL BY USING IN FLUX AND SELF-SEEDING METHOD
TEMPERATURE DIFFERENCE SOLUTION GROWTH OF GASE CRYSTAL BY USING IN FLUX AND SELF-SEEDING METHOD**

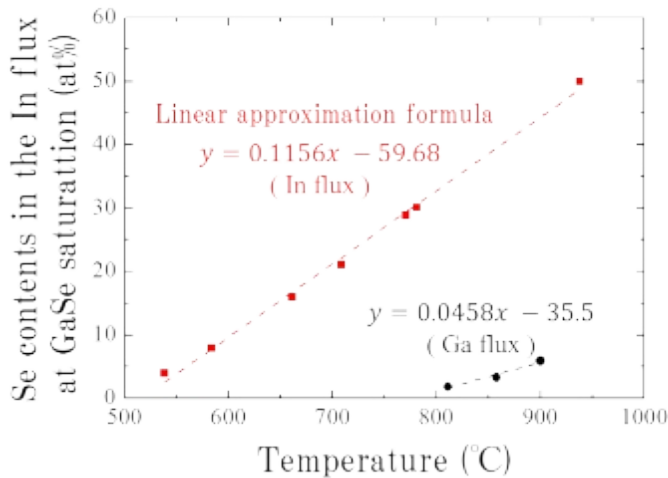
Y. Sato¹, C. Tang¹, W. Katsuya¹, J. Osaki¹, T. Yamamoto², T. Tanabe¹, Y. Oyama¹

¹Department of Materials Science and Engineering, Tohoku University, JAPAN, ²Graduate School of Environmental Studies, Tohoku University, JAPAN

Gallium selenide (GaSe) is one of the most essential key materials for the highly efficient, widely frequency-tunable THz light source via difference frequency generation by collinear phase matching. In our laboratory, we grow GaSe crystal by Temperature Difference Method under Controlled Vapor Pressure (TDM-CVP). TDM-CVP enables growth of GaSe crystal at lower temperature than melting point by precipitation of GaSe crystal from Ga solution saturated Se. In addition, TDM-CVP also enables to suppress dissociation of Se from solution and control the stoichiometry of grown crystal by applying Se vapor pressure during crystal growth. Compared with GaSe crystal grown by Bridgman method, transparency of GaSe crystal grown by TDM-CVP is improved at near IR and THz frequency range by low temperature growth and controlling of stoichiometric composition. Furthermore, conversion efficiency of THz wave generation at 9.41 THz per unit length of GaSe crystal grown by TDM-CVP was 4 times higher than that from Bridgman-grown crystal. However, the conversion efficiency of THz wave per unit length of the crystal increased, but output power of THz wave did not go up because thickness perpendicular to (001) of GaSe crystal grown from Ga-Se

solution is thin (thickness : about 300 μ m). This slow growth rate along $\langle 001 \rangle$ is because of a low solubility and small concentration difference to temperature difference of Se in the Ga solvent. In the collinear phase matching, the thicker thickness of GaSe crystal is, the longer interaction length of excited light is. Therefore, it is expected to improve the output power of generated THz wave by using GaSe crystal which has optimal thickness considered with optical absorption. In this work, Gallium selenide (GaSe) ingrot crystals were grown from In flux by temperature difference solution growth without seed crystal. The schematic view of the equipment for crystal growth is shown in Fig. 1. As shown in Fig.2, compared with the case of dissolving Se in Ga flux, Se solubility and concentration difference increased in In flux at GaSe saturation. Thickness of GaSe crystal grown from In flux for 7 days (5.4 mm) is 18 times thicker than that of GaSe crystal grown from Ga flux for 14 days (300 μ m). Finally, from visual examination of the grown crystal and the results of computational fluid dynamics and mass transfer simulation for large and small temperature gradient conditions, we consider which large or small temperature gradients is suitable for single crystal growth.





4:15 PM - 4:30 PM

***IN-SITU* SYNTHESIS AND HGF GROWTH OF $BaGa_4S_7$, $BaGa_4Se_7$, AND $BaGa_2GeSe_6$**

P.G. Schunemann, K.T. Zawilski

BAE Systems, NH, UNITED STATES OF AMERICA

Two new mid-IR NLO materials - barium thiogallate ($BaGa_4S_7$) and barium selenogallate ($BaGa_4Se_7$) – have recently been reported to exhibit notably wide band gaps (3.54 eV and 2.64 eV respectively), deep infrared transparency (cut-off at 13.7 mm and 18 mm respectively), moderately high nonlinear coefficients (5 pm/V and 20 pm/V), and favorable growth of high-optical-quality crystals from stoichiometric melts. To evaluate this final claim, and to establish a viable commercial source for these materials, we investigated the growth of these compounds in transparent furnaces using the Horizontal Gradient Freeze (HGF) technique. The compounds were synthesized *in-situ* from high-purity elemental starting materials by two-temperature vapor transport, followed by self-seeding and directional solidification (~ 1 mm/hr) by slow cooling in a shallow axial temperature gradient. direct synthesis in carbon-coated boats in fused-silica ampoules. Crack-free single crystals (up to 27-mm diameter x 150-mm length) were grown with good optical quality. FTIR and VIS/NIR spectral measurements confirmed the low losses and wide transparency range of these materials. Furthermore, we also investigated synthesis and growth of a the promising new quaternary

analog BaGa₂GeSe₆, or BGGSe, which is characterized by a significantly higher nonlinear coefficient ($d_{11} \sim 66$ pm/V), transparency out to 17 mm, a slightly smaller band gap band gap (2.38 eV), and a high laser damage threshold of 11J/cm² for a 10.6 mm pump. Its birefringence is quite large (~0.08-0.11), allowing phase-matched frequency conversion throughout most of its transparency range. *In-situ* synthesis from high purity elementary starting materials by two-temperature vapor transport in sealed quartz ampoules, followed by self-seeded horizontal gradient freeze growth on a transparent furnace was used to produce single crystals several centimeters in length with 16 x 25 mm² apertures. As-grown crystals exhibited low scattering losses, and were oriented, cut, and polished for device testing.

4:30 PM - 4:45 PM

COMPARISON OF CDSIP₂ TO ZNGEP₂ FOR 2-MICRON PUMPED OPOS

K.T. Zawilski¹, P.G. Schunemann¹, F..K. Hopkins², C. Liebig², S. Guha², K. Averett², L. Pomeranz¹, J.C. Mccarthy¹, L. Goldberg³, B. Cole³

¹BAE Systems, NH, UNITED STATES OF AMERICA, ²Air Force Research Laboratory, UNITED STATES OF AMERICA, ³US ARMY RDECOM CERDEC, UNITED STATES OF AMERICA

CdSiP₂ (CSP) is a nonlinear optical chalcopyrite semiconductor developed as a wider-band-gap analog of ZnGeP₂ (ZGP) to enable mid-infrared generation with widely-available 1- and 1.55-micron pump laser sources. Due to defect related absorption, ZGP cannot be pumped at either 1- or 1.55 microns. CSP has a higher nonlinear coefficient ($d_{36}=84.5$ pm/V) than ZGP ($d_{36}=79$ pm/V), and its lower thermal conductivity (13.6 W/mK vs 35 W/mK for ZGP) is more than offset by nearly 10-fold lower absorption losses in the 1.06- to 2.1-micron wavelength range, making CSP an attractive alternative to ZGP even for power-scaling 2-micron-pumped OPOs. CSP growth presents significant crystal growth challenges compared to ZGP including: a higher melting point and vapor pressure that push the limits of fused silica based growth technology, a higher reactivity with

boat materials and fused silica ampoules, an increased incidence of twin formation, and a negative c-axis thermal expansion coefficient (which makes it prone to cracking). Despite these difficulties, recent advances in crystal growth from stoichiometric melts using the horizontal gradient freeze (HGF) technique have resulted in scaling boule diameters from 19 to 28 millimeters. Thermal conductivity measurements as a function of temperature along the major crystallographic axes are reported. For the first time, CSP has outperformed ZGP in an OPO operating near 2 microns. To reach this conclusion, parts cut from each material with identical dimensions were compared in the same 1.94-micron Tm:YAP laser setup. Thermal lensing measurements on both ZGP and CSP in the presence of a 2 micron pump source are also reported, along with recent laser frequency results using 1.5 micron sources.

4:45 PM - 5:00 PM

MEASUREMENT OF D-COEFFICIENTS OF CRYSTALS USING NON-PHASE-MATCHED SECOND HARMONIC GENERATION OF MID-WAVE INFRARED RADIATION

S. Guha¹, J. Murray¹, J. Wei¹, K.T. Zawilski², P.G. Schunemann²

¹Air Force Research Laboratory, UNITED STATES OF AMERICA,

²BAE Systems, UNITED STATES OF AMERICA

Non-phase matched second harmonic generation and the interference of bound and free second harmonic waves giving rise to Maker fringes can be used to determine the values of the nonlinear optical coefficients of thin crystals. An advantage of this technique is that crystals having several millimeter thickness are not needed. For currently important nonlinear optical crystal such as CdSiP₂, the value of d has been measured using phase-matched second harmonic generation (SHG) of 4.6 μm radiation [1,2]. However, reliable values at shorter wavelengths, more relevant to short wavelength pumping, are not easily available. We present here a measurement of the values of the two distinct non-zero d coefficients (d_{14} and d_{36}) of CdSiP₂ and several other nonlinear optical crystals through fitting of Maker fringes observed by SHG of a 10 ps duration, wavelength-tunable optical pulse in thin plane parallel single crystal plates having known surface

orientation with respect to the principal dielectric axes. From the measurement of the generated SHG energy as a function of the incident fundamental beam irradiance, the absolute values of the d coefficients are obtained. The measurements are made over a range of wavelengths spanning 2700 nm to 4700 nm. The theoretical treatment of Maker fringes obtained from plane parallel plates of arbitrary symmetry class and surface orientation, and for arbitrary incidence angle and beam polarization direction is derived from the treatment presented by Pavlides and Pugh [3]. The refractive indices values needed for the calculation are obtained from recent measurements.

References [1] L.P. Gonzalez, D. Upchurch, J.O. Barnes, P.G. Schunemann, K.T. Zawilski and S. Guha, Second harmonic generation in CdSiP₂, Proceedings Volume 7197, Nonlinear Frequency Generation and Conversion: Materials, Devices, and Applications VIII; 71970N (2009). [2] V. Petrov, F. Noack, I. Tunchev, P. Schunemann, and K. Zawilski, The nonlinear coefficient d_{36} of CdSiP₂, Proceedings Volume 7197, Nonlinear Frequency Generation and Conversion: Materials, Devices, and Applications VIII; 71970M (2009). [3] P. Pavlides and D. Pugh, General theory of Maker fringes in crystals of low symmetry, Journal of Physics: Condensed Matter, Volume 3, Number 8, (1991). [4] J. Wei, J.M. Murray, F.K. Hopkins, D.M. Krein, K.T. Zawilski, P.G. Schunemann, and S. Guha, Measurement of refractive indices of CdSiP₂ at temperatures from 90 to 450 K, Optical Materials Express, Vol. 8, Issue 2, 235-244 (20).

5:00 PM - 5:30 PM

PROGRESS IN GROWTH OF LARGE LBO CRYSTALS FOR NON-LINEAR OPTICAL APPLICATIONS

D. Perlov¹, A. Novoselov¹, P. Czechowicz¹, A. Sadovsky², I. Zhurkova², S. Zhurkov², M. Artyushenko², V. Sukharev²

¹IPG Photonics, MA, UNITED STATES OF AMERICA, ²IPG IRE-Polus, RUSSIAN FEDERATION

Over recent years Lithium Borate (LBO) crystal became a backbone of

frequency conversion in the laser industry. It has the largest by far commercial market among all non-linear crystals. Significant progress has been achieved by several independent companies in a stride towards elevated LBO boule size. A few kilogram boules have been reported grown from Lithium Molybdate flux by a modified Top-Seeded Solution Growth (TSSG) method. Unfortunately it requires several months to grow such a boule using a common approach. Additionally, as-grown boules frequently suffer from flux inclusions, striations and elevated optical absorption. We have developed a unique rapid growth process for large LBO boules in mass production. It is based on common TSSG with pulling. However, due to a precise control of the system supersaturation we have achieved growth rates exceeding those reported in literature by 10-20 times. Thus, we have been able to demonstrate unparalleled growth rates up to 10 mm/day. The full growth cycle for a typical 2 kg LBO boule has been reduced from a several months to a couple of weeks. Most importantly these extreme conditions did not impact crystal quality. On the contrary, as-grown boules demonstrate superior morphology and higher optical quality compared to conventional ones. They are completely striation/inclusion free which is quite uncommon for LBO. Absolute optical absorption of this material has been reduced to the record level of ~0.5 ppm/cm at 1064 nm.

Monday, July 29, 2019

3:30 PM - 5:30 PM

Symposium on Epitaxy of Complex Oxides: Complex Oxides from Metalorganic Precursors

Location: Grays Peak II, III

Session Chair(s): Matthew Brahlek

3:30 PM - 4:00 PM

DEFECT-FREE SYNTHESIS OF QUANTUM HETEROSTRUCTURES VIA METAL-ORGANIC PULSED LASER DEPOSITION

C. Eom

University of Wisconsin-Madison, WI, UNITED STATES OF AMERICA

The ability to reduce point defects in material systems opens new functionalities. For example, even though the concept of the transistor was first proposed in 1926, the practical solid state transistor was realized about a quarter-century later only when the fabrication of high purity germanium was accomplished. In complex oxide thin films reducing point defects remains challenging, due largely to their overwhelming numbers, arising mostly from non-stoichiometry. Here, we report a defect-free synthesis of $\text{LaAlO}_3/\text{SrTiO}_3$ (LAO/STO) quantum heterostructures *via* newly-developed metal-organic pulsed laser deposition (MOPLD) growth technique, which uses titanium tetraisopropoxide (TTIP) as a Ti source during laser ablation of a SrO target. X-ray diffraction and Raman spectroscopy show that there is a wide window of TTIP flux resulting in stoichiometric STO growth. Depth-resolved cathodoluminescence spectroscopy reveals that STO films grown by MOPLD possess fewer oxygen vacancies than even bulk single crystal STO. We find that the low temperature mobility of electrons in the LAO/STO interfacial two-dimensional electron gas is six times higher with MOPLD-grown STO than using bulk STO, resulting in clear Shubnikov–de Haas oscillations. This state-of-the-art deposition technique provides a new opportunity not only for fabrication of high performance complex oxide thin films and their heterostructures but also for exploring new underlying physics in oxide heterostructures. This work has been done in collaboration with J. W. Lee, A. L. Edgeton, N. Campbell, B. A. Noesges, J. L. Schad, K. Wada, J. Moreno-Ramirez, N. Parker, T. R. Paudel, H. Lee, Y. Chen, K. Eom, J. H. Kang, N. Pryds, E. Y. Tsybal, D. A. Tenne, L. J. Brillson, and M. S. Rzchowski

4:00 PM - 4:30 PM

CONTROLLING THE STOICHIOMETRY IN QUATERNARY COMPLEX OXIDE THIN FILMS BY HYBRID MOLECULAR BEAM EPITAXY

R. Engel-Herbert

Penn State University, UNITED STATES OF AMERICA

Complex oxides with perovskite structure that contain a transition metal element is a particularly interesting material class for electronic application. Owed to the rich functionality arising from the coupling of

spin, orbital, charge and lattice degree of freedom competing ground states with dramatically different electronic, optical and magnetic properties exist. The d orbitals of the transition metal elements form a narrow conduction band and free carriers exhibit sizeable electron correlation effects, giving rise to intriguing phenomena, such as electronic phase transitions in the vicinity of quantum critical points. Harnessing these properties in applications and studying these fascinating phenomena requires the growth of high quality thin films, which has been proved very challenging. In this talk I will discuss how the quantum critical point of the quaternary oxide $\text{La}_{1-x}\text{Sr}_x\text{VO}_3$ can be accessed avoiding the creation of unintentional defects in the film by employing hybrid molecular beam epitaxy. This method combines the advantages of chemical vapor deposition and conventional solid source molecular beam epitaxy for the growth of oxides in an ideal way. I will show that for both end members of the complete solid solution $\text{La}_{1-x}\text{Sr}_x\text{VO}_3$ an adsorption controlled growth window can be accessed in which cation stoichiometry of the film is achieved in a self-regulated fashion. Record high residual resistivity ratios in excess of 200 for the end member SrVO_3 , a correlated metal, and the lowest optical absorption for below band gap excitation of the Mott insulator LaVO_3 are testimony of the excellent quality achieved by this growth method and evidencing that complex oxide thin films can be grown that way with a low defect concentration that has been unprecedented thus far. Transport measurements of the quaternary compound along with the detailed analysis of the end members will be discussed revealing a much more detailed electronic phase diagram as a function of temperature and composition.

4:30 PM - 5:00 PM

EPITAXIAL GROWTH OF COMPLEX OXIDE FILMS WITH DESIRED PROPERTIES BY A POLYMER-ASSISTED DEPOSITION

Q..X. Jia¹, Y. Lin², A.K. Burrell³, T.M. Mccleskey⁴

¹University at Buffalo - the State University of New York, UNITED STATES OF AMERICA, ²University of Electronic Science and Technology of China, CHINA, ³The National Renewable Energy Laboratory, UNITED STATES OF AMERICA, ⁴Los Alamos National

Laboratory, UNITED STATES OF AMERICA

Tremendous advances have been made in growing epitaxial complex oxide films with controlled microstructures and desired physical properties using either physical- or chemical-vapor deposition techniques. However, one of the challenges in chemical solution-based processes for complex oxide films has been the growth of high quality epitaxial films with desired physical properties. In this talk, I will discuss a polymer-assisted deposition (PAD) technique to grow epitaxial complex oxide films with desired physical properties. Different from other conventional chemical solution-based deposition techniques, PAD uses water-soluble polymers to prevent metal ions from unwanted chemical reactions, to deliver stable and homogeneous solutions, and to keep the precursor solution stable. Using epitaxial VO_2 and BaTiO_3 as model systems, I will explain the process, microstructures, and physical properties of such epitaxial films grown by PAD. The ability to grow a range of epitaxial complex oxide films with desired physical properties by PAD suggests that such a technique is an effective approach to the growth of high-quality epitaxial complex oxide films.

5:00 PM - 5:15 PM

GROWTH OF LiNbO_3 FILMS FOR ELECTRO-OPTIC DEVICES BY CHEMICAL VAPOR DEPOSITION

A.C. Arjunan¹, T. Salagaj¹, M. Maurer², C.T. Middlebrook², **G. Tompa**¹

¹Structured Materials Industries, Inc., NJ, UNITED STATES OF AMERICA, ²Michigan Technological University, MI, UNITED STATES OF AMERICA

LiNbO_3 is a near ideal material for electro-optic devices due to its high electro-optic coefficient and excellent transparency in the visible and near infrared. Lithium niobate single crystals can be grown from the melt using the Czochralski process and are readily available commercially. To produce devices, such as electro optic modulators, efficient ridge wave guide structures need to be fabricated on LiNbO_3 substrates. The Ridge waveguide should have higher refractive index than LiNbO_3 in order to efficiently produce optical confinement, reduce

propagation loss and better concentrate the electric fields. This is presently achieved by ion implanting Ti into Li:NbO₃ and then annealing - this results in a diffused ridge boundary and hence large than optimal waveguide circuits. A more ideal approach would be either blanket ion implantation and pattern and etch- or even better - growing a doped an epitaxial film on LiNbO₃ and then patterning and etching. However patterning and etching single crystal LiNbO₃ is difficult. Whereas patterning and etching amorphous LiNbO₃ films are easy to pattern to form a waveguide and subsequent annealing will convert these films to epitaxial films. The desire to pattern and etch the films for marking devices is that the resultant structures will be smaller – saving space and requiring less voltage and will provide tighter more repeatable tolerances. We used CVD to grow films of titanium doped LiNbO₃ using precursors of Lithium butoxide, Niobium ethoxide and titanium propoxide – mixed in a toluene solvent – where the precursor solution is flash evaporated for delivery as a vapor to the ROR reactor. The precursors by flash evaporated between 180 to 250 °C and deposited on Lithium niobite substrates at temperatures between 350 to 600 °C. We have demonstrated growth rates as high 1.1 micron/hr for growth temperatures above 500 °C. We routinely deposited film with thicknesses of 3-4 microns. The grown films were studied for composition using XRF, XPS, and for structural quality using X-ray diffraction. Further, the grown films were annealed at temperatures 900-1000 °C to crystallize the titanium doped LiNbO₃ films. Further, optical properties of the films were determined using ellipsometry. The impact of growth parameters such as growth temperature, precursor concentration, pressure of growth on the film characteristics will be reported on.

LiNbO₃ is a near ideal material for electro-optic devices due to its high electro-optic coefficient and excellent transparency in the visible and near infrared. Lithium niobate single crystals can be grown from the melt using the Czochralski process and are readily available commercially. To produce devices, such as electro optic modulators, efficient ridge wave guide structures need to be fabricated on LiNbO₃ substrates. The Ridge waveguide should have higher refractive index than LiNbO₃ in order to efficiently produce optical confinement, reduce

propagation loss and better concentrate the electric fields. This is presently achieved by ion implanting Ti into Li:NbO₃ and then annealing - this results in a diffused ridge boundary and hence large than optimal waveguide circuits. A more ideal approach would be either blanket ion implantation and pattern and etch- or even better - growing a doped epitaxial film on LiNbO₃ and then patterning and etching. However patterning and etching single crystal LiNbO₃ is difficult. Whereas patterning and etching amorphous LiNbO₃ films are easy to pattern to form a waveguide and subsequent annealing will convert these films to epitaxial films. The desire to pattern and etch the films for marking devices is that the resultant structures will be smaller – saving space and requiring less voltage and will provide tighter more repeatable tolerances. We used CVD to grow films of titanium doped LiNbO₃ using precursors of Lithium butoxide, Niobium ethoxide and titanium propoxide – mixed in a toluene solvent – where the precursor solution is flash evaporated for delivery as a vapor to the ROR reactor. The precursors by flash evaporated between 180 to 250 °C and deposited on Lithium niobite substrates at temperatures between 350 to 600 °C. We have demonstrated growth rates as high 1.1 micron/hr for growth temperatures above 500 °C. We routinely deposited film with thicknesses of 3-4 microns. The grown films were studied for composition using XRF, XPS, and for structural quality using X-ray diffraction. Further, the grown films were annealed at temperatures 900-1000 °C to crystallize the titanium doped LiNbO₃ films. Further, optical properties of the films were determined using ellipsometry. The impact of growth parameters such as growth temperature, precursor concentration, pressure of growth on the film characteristics will be reported on.

5:15 PM - 5:30 PM

ACTIVATING CATION DIFFUSION ACROSS THE INTERFACE FOR MATERIALS DISCOVERY

Y. Du¹, L. Wang², Z. Yang², M. Bowden²

¹Pacific Northwest National Laboratory, WA, UNITED STATES OF AMERICA, ²Pacific Northwest National Laboratory, UNITED STATES OF AMERICA

Epitaxial growth is a powerful way to realize emergent properties and functionalities. In most materials design, we expect the degree of interface diffusion and intermixing to be small. In this work, we show cation diffusion during epitaxial growth can be exploited for the synthesis of novel energy materials and architectures with tunable properties. LiCoO₂, one of the most widely used cathode materials for lithium ion batteries, can be epitaxially grown on SrTiO₃(111) and (001) with lithium conducting planes either parallel or 55 degree to the interface, respectively. The subsequent growth of Li-free transition metal oxides (e.g., WO₃, MoO₃, and TiO₂) on LiCoO₂ can directly incorporate lithium from the underneath layers due to the low Li diffusion barrier. Depending on the orientation and growth temperature, nanostructures and thin films with different lithium stoichiometry and atomic structure can be synthesized with an epitaxial relationship to LiCoO₂. The resulting architectures can be ideal model systems for fundamental studies aiming to understand the ion transport processes across solid-solid interfaces.

Monday, July 29, 2019

3:30 PM - 5:30 PM

Symposium on Ferroelectric Crystals and Textured Ceramics: Doped Relaxor-PT Ferroelectric Crystals

Location: Grays Peak I

Session Chair(s): Qiang Li, Ho Nyung Lee

3:30 PM - 4:00 PM

GEN III MN-MODIFIED PMN-PZT SINGLE CRYSTALS FOR HIGH POWER/HIGH FREQUENCY/COMPOSITE APPLICATIONS

H. Lee

Ceracomp Co., Ltd., KOREA, REPUBLIC OF

Analogous to acceptor doping in hard PZT polycrystalline ceramics, Mn-modified PMN-PT/PMN-PZT single crystals exhibited enhanced mechanical quality factor [$Q_m \sim 1,000$] with low dielectric loss [$\tan \delta \sim 0.2\%$], while maintaining ultrahigh electromechanical coupling factor [$k_{33} \sim 0.9$], inherent in domain engineered relaxor-PT single crystals.

The effect of acceptor doping was evident in the build-up of an internal

bias [$E_1 > 1.0$ kV/cm], shown by a horizontal offset in the polarization-field behavior. The FOM Qd for Mn- modified PMN-PT/PMN-PZT crystals was also found to be one order of magnitude higher than both unmodified single crystals and hard PZT ceramics. These results show that Mn-doped PMN-PT/PMN-PZT single crystals, because they are piezoelectrically hard and simultaneously have high piezoelectric and electromechanical properties, have great potential in many piezoelectric application fields such as ultrasound transducers (medical, HIFU and NDA), SONAR transducer, piezoelectric actuators, piezoelectric sensors, ultrasonic motors, piezoelectric composites and piezoelectric energy harvesting, etc. Contrary to unmodified single crystals, Mn-doped single crystals do not show the scaling effect (property degradation with decreasing thickness), so they are expected to be good for high frequency (very thin plates less than 100 μ m) as well as single crystal-epoxy composite (fine pitch dicing than 200 μ m) applications. For production of Gen III “Mn-modified” PMN-PT/PMN-PZT single crystals, we did the scale-up test of solid-state single crystal growth (SSCG) method and evaluated its production cost, productivity, and reproducibility. The solid-state single crystal growth (SSCG) method was selected owing to its inherent benefit of cost-effectiveness as well as maintaining dopant uniformity in a solid solution, unlike the melt Bridgman process. After the scale-up test, the dielectric and piezoelectric properties of Mn-modified PMN-PT/PMN-PZT single crystals were characterized. Especially, crystal uniformity test (within a plate, between plates from the same boule, and between boules), modifier concentration gradient inside a single crystal, polarization fatigue test, and phase transition under electric field and stress were made. These results demonstrate that Gen III “Mn-modified” PMN-PT/PMN-PZT single crystals can be successfully mass produced and thus the SSCG method can be their primary crystal growth method.

4:00 PM - 4:30 PM

EFFECT OF MANGANESE DOPING ON MICROSTRUCTURE AND FATIGUE PROPERTY OF PIN-PMN-PT SINGLE CRYSTAL

Q. Li, Y. Zhou, Q. Yan, C. Xu

Department of Chemistry, Tsinghua University, CHINA

PIN-PMN-PT ferroelectric single crystals with high dielectric, piezoelectric, and T_c are widely used in advanced actuators, sensors, and transducers. In the past decades, rare studies devoted to domain switching and polarization fatigue in novel PIN-PMN-PT and Mn-doped PIN-PMN-PT single crystals though it was essential to explore the underlying mechanisms of fatigue behaviors for the better applications of new general ferroelectrics. In order to understanding the domain switching process under bipolar electric field, in-situ polarized light microscopy was introduced. By the domain configuration analysis, the domain switching paths in pure and Mn-doped PIN-PMN-PT crystals underwent only one-step 71° switching, accompanied by the observed domain walls whose traces on the (001) plane are along 45° or 135° direction, were confirmed. Polarization and strain loops during cyclic electric field were studied in depth as a function of switching cycles. Polarization fatigue appeared obviously above 1000 bipolar cycles in PIN-PMN-PT samples, while Mn-doped PIN-PMN-PT samples exhibited almost fatigue-free characteristics. This result indicated that the Mn-modification would not affect the domain switching paths, but it could increase the energy barrier of domain switching, leading to the improved fatigue behaviors.

4:30 PM - 5:00 PM

THE GROWTH AND PIEZOELECTRIC PERFORMANCE OF RELAXOR-BASED FERROELECTRIC PIN-PMN-PT AND MN DOPED PIN-PMN-PT SINGLE CRYSTALS

G. Xu, J. Liu, X. Zhu

Shanghai Institute of Ceramics, Chinese Academy of Sciences, CHINA

The relaxor-based ferroelectric single crystals have been paid great attention due to their ultrahigh piezoelectric properties, which will lead to a great breakthrough of imaging quality of medical ultrasonic probes and projective and/or receiving properties of acoustic transducers. In order to optimize the piezoelectric performance of relaxor-based ferroelectric single crystals, our group first reported the growth of large size ternary system PIN-PMN-PT single crystals by a modified Bridgman method in 2006 and 2007. Since then, PIN-PMN-PT single crystals have attracted a great interest and have been called

“generation two” relaxor-based crystals. Compared with “generation one” relaxor-based crystals PMN-PT, PIN-PMN-PT crystals present higher Curie temperature T_c , higher phase transition temperature T_{rt} and higher coercive field E_c , which are beneficial to the increase of temperature stability and work power of transducers. However, ternary system PIN-PMN-PT crystals face greater challenges, such as compositional segregation and property consistence in the process of growth due to more complicated chemical compositions than binary system PMN-PT. On the other hand, the mechanical quality factors are not enough high for some high-power applications. In this talk, we will introduce the new progress in the growth of relaxor-based ferroelectric single crystals in our research group. Both of “generation two” PIN-PMN-PT and “generation three” Mn:PIN-PMN-PT crystals were grown by a modified Bridgman method, and their composition and property variation along growth direction and wafer diameter were measured by composition and structure analysis and dielectric, piezoelectric and ferroelectric characterization methods. Moreover, the temperature, stress and field dependence of the piezoelectric properties of the samples with different composition were also presented. Up to present, the PIN-PMN-PT and Mn:PIN-PMN-PT crystals grown along [001] and [110] have been enlarged to about 4 inches and exhibit excellent and uniform piezoelectric performance, which can meet the needs of large size wafers in medical ultrasonic imaging probes. Mn:PIN-PMN-PT crystals have higher mechanic quality factors Q_m as well as higher coercive field E_c than pure PIN-PMN-PT crystals, which are in favor of the increase of projective power of transducers.

Monday, July 29, 2019

5:30 PM - 7:00 PM

Poster Session - Monday

Location: Quandary Peak

Session Chair(s):

5:30 PM - 5:30 PM

PBI₂ SINGLE CRYSTAL GROWTH AND ITS OPTICAL PROPERTY

STUDY

D.Y. Lin¹, B. Guo¹, Z. Dai¹, H. Hsu²

¹National Changhua University of Education, TAIWAN, ²Ming Chi University of Technology, TAIWAN

In this study, we reported the growth and optical characterizations of Pbl₂ single crystals, which were grown by chemical vapor transport (CVT) method using iodine as a transporting agent. The layered property and surface morphology were investigated by scanning electron microscope (SEM). A good composition ratio and uniformity were demonstrated by energy dispersive X-ray diffraction spectroscopy (EDS) and electron probe microanalysis (EPMA). We also carried out X-ray diffraction (XRD) measurement to confirm its diffraction patterns and structure. Following these measurements for checking its crystal structure, composition and quality, A prototype photodetector with a lateral metal–semiconductor–metal (MSM) configuration was fabricated to evaluate its photoelectric properties by using photoconductivity spectrum (PC), persistent photoconductivity experiment (PPC), reflectance spectroscopy, and PL spectroscopy. The band gap energy is determined to be 2.3 and 2.41 eV at 300 and 20 K, respectively. We also measure the response time and photogain of the Pbl₂ crystal by persistent photoconductivity experiment (PPC). Finally, through the absorption spectroscopies the temperature dependence of band gap energy has been studied.

5:30 PM - 5:30 PM

PRECIPITATION OF MULTILAYER GRAPHENE DIRECTLY ON GALLIUM NITRIDE TEMPLATE USING W CAPPING LAYER

J. Yamada, Y. Ueda, T. Maruyama, S. Naritsuka

Meijo University, JAPAN

Because of its outstanding characteristics, graphene is highly expected to apply to a wide range of application fields. One of them is a transparent electrode on LEDs, which replaces ITO. For example, graphene is used as the transparent electrode of ultraviolet LEDs. However, in most cases, graphene is grown on a metal foil by a conventional CVD and transferred onto the top of the LEDs. The transfer process not only requires skilled operators but also deteriorates the properties of graphene by producing structural defects

and contaminating it with impurities. In addition, large-area graphene is particularly difficult to transfer. Therefore, it is desirable to grow graphene directly on a required substrate without the use of a transfer process. We have succeeded in direct growth of graphene on a sapphire substrate [1]. In this study, graphene is directly precipitated on a GaN template with systematically changing the precipitation temperature to check the effect. Ni (300 nm), amorphous carbon (a-C) (1 nm) and a capping layer of W (20 nm) were deposited sequentially on a GaN template substrate using electron beam deposition. The samples were annealed at 500, 700 and 900 °C for 15 min in a vacuum. After annealing, the catalyst layers were removed using a dilute aqua regia solution to directly obtain the graphene on the template. The G and G' peaks were clearly observed on the Raman spectra at each temperature. The quality of the graphene was improved with increasing the precipitation temperature because the peaks became narrow and the intensity of the D peak decreased with increasing the process temperature. In addition, XPS measurements of a precipitated graphene at 700 °C indicate the existence of a honeycomb structure of carbons, which is consisted of carbon sp² bonds. This is confirmed by a shake-up satellite peak at around 290 eV on C1s peak. Graphene was also precipitated directly on a double-sided polished sapphire substrate under the same condition, which showed a high transmittance of 91% at a wavelength of 550 nm. From these results, we conclude that multilayer graphene was successfully precipitated directly on GaN layer using a W capping layer. [1] J. Yamada et al. Jpn. J. Appl. Phys. 55, 100302 (2016).

Acknowledgment: This work was supported in part by JSPS KAKENHI Grant Numbers 2660089, 15H03558, 26105002, and 25000011.

5:30 PM - 5:30 PM

TERAHERTZ GENERATION UTILIZING HOT ELECTRONS INJECTION ACROSS GRAPHENE PLANES

B.D. Kong

Pohang University of Science and Technology, KOREA, REPUBLIC
OF

Terahertz generation has been a subject of interest due to the expected impacts on biomedical and scientific applications initially.

However, a compact tunable emission source in this frequency regime still remains as a challenging topic. In this report, it is explored the possibility of utilizing hot electrons injection across the graphene plane as a frequency tunable terahertz generation mechanism. Light generation from solid requires electron transition between conduction and valence band (inter-band transition). It has been known that, due to the unique electron energy dispersion of graphene, which is often described as massless Dirac fermion, the hot electrons injected along the graphene plane (parallel to graphene plane) can generate only intra-band transition, and inter-band transitions are strictly prohibited by selection rules. However, a recent theoretical development reveals that in the case of high energy electrons traveling across the graphene planes can generate inter-band transitions. Moreover, this transition energy can be precisely tuned by controlling the Fermi energy level of graphene. Our study shows that the scattering rate, which decides the efficiency of energy transfer from the hot electrons to the electrons in graphene, is a strong function of energy level and the incident angle of the injected hot electrons. We investigate the potential of this novel light generation mechanism and estimate their limits, theoretically. The efficiency among the different emitter materials will be compared to find the best emitter-graphene hybrid structures. Additionally, the tactics to improve emission efficiency will also be discussed.

5:30 PM - 5:30 PM

ATTAINMENT OF DESIRED MORPHOLOGY AND CRYSTAL SIZE DISTRIBUTION OF ALPHA LACTOSE MONOHYDRATE (α -LM) THROUGH VARIOUS CRYSTALLIZATION METHODOLOGIES

V. Kandasamy, **S. Karuppannagounder**

Bharathiar University, INDIA

Lactose (β -D- galactopyranosyl (1-4) -D-glucopyranose), the main sugar of milk, is an important raw material widely used in food and pharmaceutical industries. Lactose exists in two isomeric forms, alpha (α -L) and beta (β -L) lactose, which differs only in one special position of hydroxyl group on the first carbon of glucose moiety. In aqueous solution, both α -L and β -L will mutually transform from one to the other, to maintain an equilibrium ratio between them by changing the position of the hydroxyl group through mutarotation. α -L crystallizes

below 93.5 °C as a monohydrate whereas β -L crystallizes above 93.5 °C as anhydrous form. From aqueous solution only α -L crystallizes as a monohydrate form i.e. α -Lactose monohydrate (α -LM) and is the only thermodynamically stable form at ambient environmental conditions hence it is widely used as a more suitable candidate for the dry powder inhaler (DPI) applications. Moreover, the food (i.e., dairy) products require larger (i.e., > 100 μ m) α -LM crystals with narrow crystal size distribution (CSD). Even in pharmaceutical products, the size and shape of α -LM crystals are important because they influence powder flow, blending, mixing, compaction, caking and drug delivery efficiency. In the present work, three different crystallization methodologies such as (i) antisolvent crystallization, (ii) gas phase diffusion crystallization and (iii) swift cooling crystallization procedures were adopted to attain the desired morphology and CSD of the α -LM crystals. Crystallization experiments with DMSO as the primary solvent and ethanol and water as antisolvents enabled to attain the required supersaturation to obtain the nucleation of α -LM crystals with desired morphology. Gas-phase diffusion crystallization process yielded α -LM crystals of high purity within shorter induction periods. Swift cooling crystallization method facilitated to attain different levels of supersaturation and the desired needle like morphology with CSD usable for various applications. Detailed procedure adopted and the confirmation of the form of crystallization through XRD and DSC analyses are to be discussed.

5:30 PM - 5:30 PM

GROWTH KINETICS OF THE METASTABLE POLYMORPH OF L-HISTIDINE IN AQUEOUS SOLUTION

L. Wantha

School of Chemical Engineering, Suranaree University of Technology, THAILAND

For the polymorphic crystallization, nucleation, growth, and dissolution rates, and the transformation of crystallizing polymorphs should be controlled individually. This leads to the determination of the crystallization (nucleation and growth) and dissolution kinetics, and thermodynamics are important for characterization of the crystallization behavior and transformation of the polymorphs. In this

study L-histidine (L-his) is the model substance; it is one of the essential amino acids and is significant in the food, pharmaceutical, and feed industries. There are two known polymorphic forms, the metastable form B and stable form A. In this study, the growth kinetics of the metastable polymorph of L-his in aqueous solution were measured at different temperatures using desupersaturation technique. The experiments were performed isothermally in an agitated batch crystallizer at 10, 25, and 40 °C. The effect of the initial supersaturation and seed mass on crystal growth were also studied. The particle sizes were measured by microscope. The solute concentration were measured by refractometer. The seed crystals of the metastable polymorph were prepared by antisolvent crystallization. The growth kinetics were determined using the desupersaturation curve and during the curve before the transformation of the metastable polymorph into the stable polymorph. These polymorphic forms were identified by microscope and Raman spectroscopy. The results showed that the growth rates increase with increasing temperature and the amount of seeds. Growth kinetics of the metastable polymorph of L-his will be used to begin characterization of the polymorphic transformations and the overall crystallization rate of L-histidine.

5:30 PM - 5:30 PM

TUNING THE SOLUTION-MEDIATED CONCOMITANT PHASE TRANSFORMATION OUTCOME OF THE PIROXICAM MONOHYDRATE BY TWO HYDROXYL-CONTAINING ADDITIVES: HYDROXYPROPYL CELLULOSE AND H₂O

L. Wang, C. Yao, S. Song, Z. Wang

State Key Lab of Crystal Materials, Shandong University, CHINA

Solution-mediated concomitant phase transformation (SMCPT) of the Piroxicam (PCM) monohydrate was found. The PCM monohydrate could simultaneously transform to block Form I and needle Form II in acetone at 31 °C. But the Form I and the Form II can be selectively grown in the presence of 0.04 mg/ml HPC and 1 % H₂O, respectively. In addition, the morphology of Form I is changed from block to rod-like or even needle with the increase of the concentration of HPC. Based on these phenomena, the role of Hydroxypropyl cellulose (HPC) and

H₂O in the solution-mediated concomitant phase transformation were studied. The mechanisms of HPC and H₂O to affect the process of SMCPT of the PCM monohydrate are different. In the presence of 0.04 mg/ml HPC, the interactions between the HPC molecules and the PCM molecules was the main factor that governed the process of SMCPT of the PCM monohydrate. But in the presence of 1 % H₂O, the driving force of SMCPT played the main role. In our work, the outcome of SMCPT could be tuned directly by additives for the first time, which provide a good guide to obtain the pure polymorph in the SMCPT for pharmaceutical industry.

5:30 PM - 5:30 PM

EFFECT OF IN ADLAYER ON MBE GROWTH OF INN BY DERI METHOD

K. Watanabe, **N. Goto**, S. Mouri, T. Araki, Y. Nanishi
Ritsumeikan university, JAPAN

We have proposed DERI (droplet elimination by radical-beam irradiation) process to obtain high quality InN film by RF-MBE [1]. This method essentially consists of the two growth processes, namely, metal-rich growth process (MRGP) and droplet elimination process (DEP). Following InN growth under In-rich condition, extra nitrogen radical beam is irradiated to remove In droplets, which yields droplet-free flat InN film. Nevertheless, detailed growth mechanism and role of In adlayer have not been fully understood. In order to further understand these mechanisms, we have investigated effect of In adlayer on quality of InN grown by DERI method. Three kinds of InN films with a thickness of approximately 370 nm were grown on GaN/sapphire templates. N₂ gas flow, RF power, In flux and growth temperature were kept constant at 2.0 sccm, 100 W, 7.2×10^{-7} Torr and 425 °C, respectively. The growth time of each MRGP was fixed at 1 min and time for DEP was varied. MRGP and DEP were alternately repeated by 50 times. For sample A, DEP was stopped at the point where In adlayer became no more than two monolayers on the surface. This point corresponds to the time when RHEED intensity just started to increase. Under our growth condition, we found that 15 seconds were needed to completely eliminate two monolayers of In on

the surface during DEP. For sample B, DEP was stopped at 6 seconds after A point, where almost half of In adlayer is expected to remain on the surface. For sample C, DEP carried out until In adlayer was completely eliminated. These three samples were characterized by using AFM and Hall effect measurement. Among three AFM images of these InN films, sample B showed the best surface morphology. Three-dimensional islands started to form on the surface of sample A. Higher mobility and lower carrier concentration were obtained in sample A and sample B. We have found that InN films with higher crystal quality in terms of surface morphology and electrical property were obtained when MRGP was re-started at the condition where In adlayer still remains on the surface at each DERI cycle. These results suggested that such an In adlayer either enhances atom migration on the surface acting as surfactant or decreases ion induced damage acting as protecting barrier. This work was supported by JSPS KAKENHI 15H 03559, JP16H06415, JP16H03860. [1] T. Yamaguchi and Y. Nanishi, Appl. Phys. Express 2, 051001 (2009)

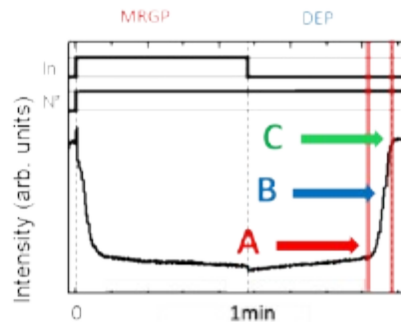


Fig. 1 Schematic view of RHEED intensity variation during DERI process. MRGP time is fixed at 1 min. DEP stopped at A, B, C points which correspond to the time where 2 ML, almost 1 ML and no In adlayer remains on the surface, respectively.

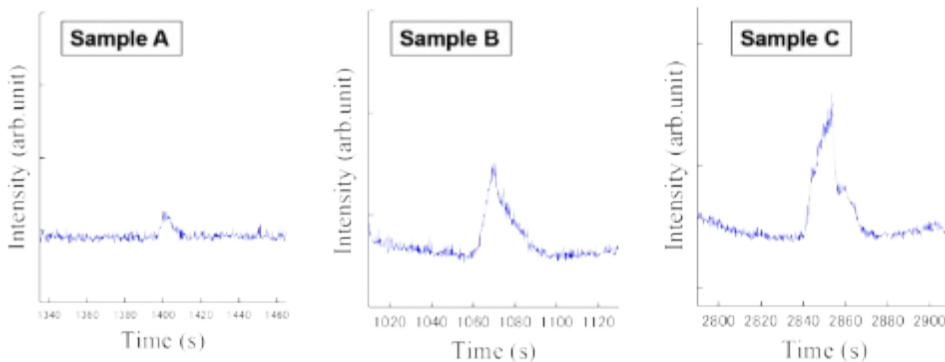


Fig. 2 In situ monitored RHEED intensity variations for each type(A, B, C) of the growth cycle.

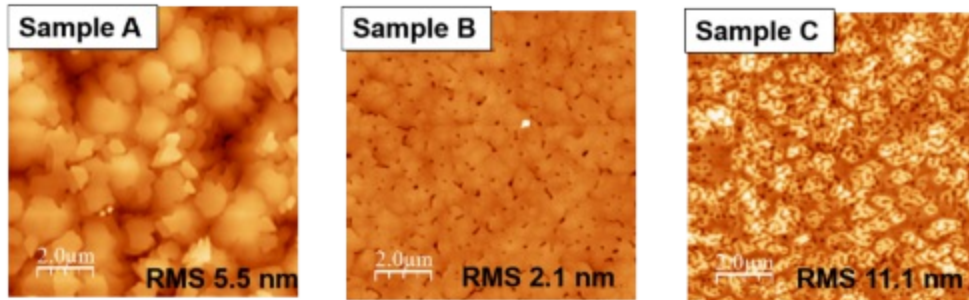


Fig. 3 Morphology of the surface of each film measured by AFM.

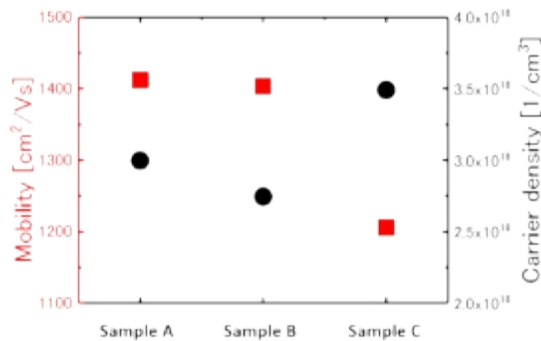


Fig. 4 Carrier concentration and mobility of each film determined by Hall effect measurements.

5:30 PM - 5:30 PM

MOCVD GROWTH OF ALGaN BACK-ILLUMINATED SEPARATE-ABSORPTION AND MULTIPLICATION ULTRAVIOLET AVALANCHE PHOTODIODES

M. Bakhtiary-Noodeh, M. Ji, C. Tsou, H. Jeong, E. Gazda, A..N. Otte, S. Shen, T. Detchprohm, **R. Dupuis**

Georgia Institute of Technology, GA, UNITED STATES OF AMERICA

AlGaN optical detectors can have a high sensitivity in the solar-blind region. Their adjustable direct bandgap energies provide controllable wavelength detection and high optical gain, low dark current, high detection sensitivity, high breakdown field, etc., make them promising candidates for deep-UV photodiodes. Back-illuminated separate absorption and multiplication (SAM) avalanche photodiodes (APDs) are capable of multiplication noise reduction, gain intensification, elimination of light blocking issues and higher hole ionization coefficient (compared to front illumination). The main challenge for wide-bandgap AlGaN materials is the limited free-carrier concentration of *p*-doped layers, which is essential for solar-blind APD detectors. In addition, some properties of available compatible substrates impede

the development of back-side-illuminated AlGaN APDs. Currently, bulk AlN substrates exhibit large absorption below $\sim 265\text{nm}$. While AlN/sapphire templates provide better optical transparency down to 210 nm , however, other issues such as lattice mismatch, different thermal expansion coefficients, and strain-induced defects act as a source of leakage current and result in the degradation of the device performance. In this study, $\text{Al}_x\text{Ga}_{1-x}\text{N}$ *p-i-n-i-n* SAM-APD epitaxial layers were grown by a metalorganic chemical vapor deposition (MOCVD) with a target cut-off wavelength of 250 nm at $x=0.65$. X-ray diffraction (XRD) was used for the characterization of the quality of the structure and the alloy composition of $\text{Al}_x\text{Ga}_{1-x}\text{N}$ layers. In this study, AlN/c-plane sapphire templates were used to calibrate the APD growth conditions prior to growth on AlN substrates. Rocking curves results for AlN templates show full-width at half maximum (FWHM) values of 274 and 537 for (002) and (102) respectively. Hall-effect characterization was used in order to measure the electrical properties of the doped layers. The grown epitaxial layers on AlN/sapphire templates include AlN/AlGaN short-period superlattice layers (SPSLs), $0.4\text{ }\mu\text{m}$ thick *n*- $\text{Al}_{0.71}\text{Ga}_{0.29}\text{N}$ layer ($n\sim 8\times 10^{18}\text{cm}^{-3}$), $0.24\text{ }\mu\text{m}$ thick *u*- $\text{Al}_{0.65}\text{Ga}_{0.35}\text{N}$ layer (absorption layer), $0.03\text{ }\mu\text{m}$ thick *n*- $\text{Al}_{0.595}\text{Ga}_{0.405}\text{N}$ layer (launcher layer, $n\sim 8\times 10^{18}\text{cm}^{-3}$), $0.17\text{ }\mu\text{m}$ thick *u*- $\text{Al}_{0.595}\text{Ga}_{0.405}\text{N}$ layer (multiplication layer), $0.1\text{ }\mu\text{m}$ thick *p*- $\text{Al}_{0.37}\text{Ga}_{0.63}\text{N}$ layer, $0.04\text{ }\mu\text{m}$ thick graded *p*- $\text{Al}_x\text{Ga}_{1-x}\text{N}$ layer, and $0.02\text{ }\mu\text{m}$ thick p^{++} -GaN layer. To confirm the doping profile of the layers, secondary ion mass spectrometry (SIMS) measurements were performed confirming the Hall data. The surface morphology and the corresponding root-mean-square (RMS) were studied by atomic force microscopy. The RMS value of $1\times 1\text{ }\mu\text{m}^2$ and $5\times 5\text{ }\mu\text{m}^2$ scan sizes are 0.25 nm and 4.98 nm respectively. The details of growth, characterization, and fabrication processes, as well as preliminary device data, will be discussed in the talk.

5:30 PM - 5:30 PM

**SINGLE-CRYSTALLINE III-N THIN FILMS FOR FLEXIBLE
PIEZOELECTRIC GENERATORS AND PULSE SENSORS**

J. Chen¹, N. Nabulsi¹, W. Wang¹, H. Johnson², S.K. Oh¹, S. Shervin¹, S. Pouladi¹, **J. Ryou**¹

¹University of Houston, TX, UNITED STATES OF AMERICA,

²Brigham Young University, UNITED STATES OF AMERICA

Single-crystalline group III-nitride (III-N) thin films obtained by epitaxy have been widely used in electronic and optoelectronic devices, such as transistors, light emitting diodes (LEDs) and photodiodes, as great progress has been made to achieve high crystal quality. Besides, III-N thin films are good candidates to make piezoelectric devices, since high piezoelectric coefficient is readily available without electrical poling as the atoms are already well aligned in the as-grown single-crystalline thin film. Compared with conventional piezoelectric materials such as lead zirconate titanate (PZT), zinc oxide (ZnO) and polyvinylidene fluoride (PVDF), III-N thin films have the advantages of good biocompatibility without containing toxic elements, high durability being chemically stable, and simple process without extra electrical poling. Unfortunately, applications in piezoelectric devices such as generators and sensors which usually require flexibility are still underdeveloped, due to the brittleness of III-N thin film and difficulty to be flexible since they are usually grown on rigid substrates. In this research, flexible piezoelectric generator (F-PEG) and flexible piezoelectric pulse sensor (F-PPS) were developed with single-crystalline III-N thin film, which is composed of an AlN buffer layer, Al_xGa_{1-x}N interlayers and a top GaN layer, by transferring the as-grown thin film from the Si (111) substrate to a foreign flexible substrate. Large-area and defect-free flexible single-crystalline III-N thin film was obtained by this layer-transfer method. The III-N thin-film F-PEG can generate an open-circuit voltage of 50 V, a short-circuit current of 15 μA, and a maximum power of 167 μW with a corresponding optimum load resistance of 5 MΩ. The III-N thin-film F-PEG is able to directly power electronics such as light-emitting diodes and electric watches, and charge commercial capacitors and batteries. The III-N thin-film F-PPS is sensitive enough to convert the subtle deflection caused by the arterial pulse into electrical signal and detect the pulse waveform with detailed characteristic peaks from most arterial pulse sites. Both the F-PEG and the F-PPS showed high

durability and stable outputs after being subjected to long-term tests. The piezoelectric devices made from single-crystalline III-N thin films have great potential applications in future flexible wearable electronics, such as the energy harvester and active pulse sensor.

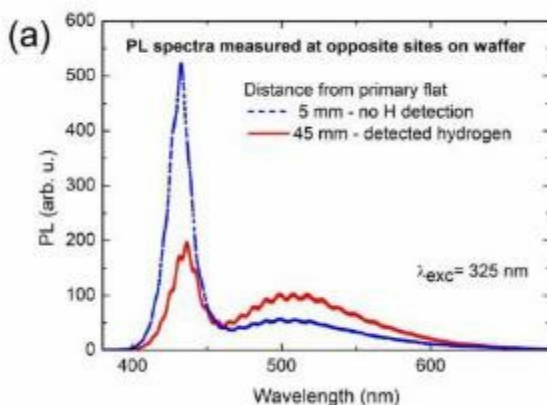
5:30 PM - 5:30 PM

UNINTENTIONALLY INCORPORATED HYDROGEN AS PROBABLE LUMINESCENCE KILLER IN INGAN/GAN QWS

A. Hospodková, T. Hubáček, M. Slavická-Zíková, T. Vaněk, F. Hájek, K. Kuldová

Institute of Physics, CAS, CZECH REPUBLIC

Although InGaN/GaN multiple quantum well (MQW) structures are widely used for light LEDs and laser diodes for more than two decades, there are still some not answered questions. An example of such a problem, which is still waiting to be fully explained, is why a single InGaN QW or the deepest QWs in the MQW structure suffer with a high non-radiative recombination rate. Improvement of luminescence efficiency of InGaN/GaN MQW active region can be achieved by introduction of In containing prelayers such as InGaN layers, InGaN/GaN superlattice or InAlN layers. Formation of bigger V-pit size is widely used hypothesis explaining luminescence improvement by prelayers. However, some results on structures without V-pits suggest that the V-pit formation may not be the dominant mechanism which helps to suppress the Shockley-Read-Hall (SRH) non radiative recombination.



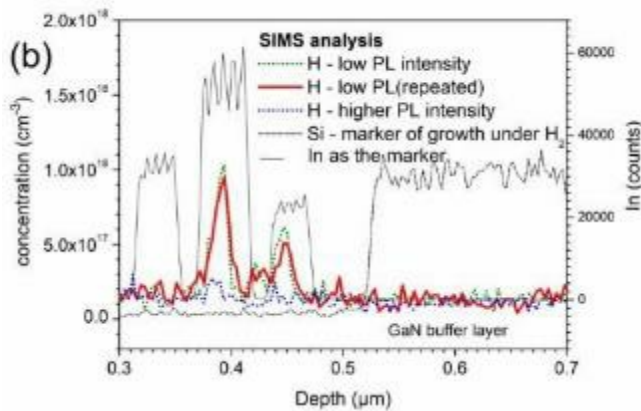


Fig. 1. (a) PL spectra measured at different places across the wafer and (b) results of SIMS analysis for hydrogen concentration measured at places with the highest and the lowest PL intensity. Our work suggests new explanation why the deepest QWs in the multiple quantum well (MQW) structure suffer with a high non-radiative recombination rate. According to SIMS results and photoluminescence measurements we have recognized that hydrogen atoms most probably play a dominant role in non-radiative SRH recombination of the deepest QWs in InGaN/GaN MQW structures, see Fig.1. The probable non-radiative center is $V_{\text{Ga}}-3\text{H}$ [1]. Hydrogen atoms originating in the buffer layers, grown at higher temperatures and under H_2 atmosphere are transported to the InGaN/GaN MQW region by diffusion, where they are very effectively trapped in InGaN layers. Trapping hydrogen atoms by InGaN layers is also the most important mechanism why the widely used In containing prelayers help to increase the luminescence efficiency of the InGaN/GaN MQW active region grown above them. Several experimental results supporting this conclusion will be presented. Low hydrogen detectivity by SIMS combined with efficient SRH non-radiative recombination at low H concentration is the reason why the hydrogen was not identified as the luminescence killer till now. Understanding the mechanism of non-radiative recombination in the deepest QWs may be very important for LED community and can help to develop new improved technologies for the growth of InGaN/GaN MQW active region. [1] C. E. Dreyer, A. Alkauskas, J. L. Lyons, J. S. Speck, and Ch. G. Van de Walle, Appl. Phys. Lett. **108**, 141101 (2016).

5:30 PM - 5:30 PM

FIRST-PRINCIPLES CALCULATION OF ABSOLUTE SURFACE ENERGIES OF GAN DURING OXIDE VAPOR PHASE EPITAXY GROWTH

T. Kawamura¹, A. Kitamoto², M. Imanishi², M. Yoshimura², Y. Mori², Y. Morikawa², Y. Kangawa³, K. Kakimoto³

¹Mie University, JAPAN, ²Osaka University, JAPAN, ³RIAM, Kyushu Univ, JAPAN

High-quality and large bulk GaN crystals are required for fabrication of high-quality and low-cost GaN devices. Oxide vapor phase epitaxy (OVPE) method has attracted interest as a bulk GaN growth method because solid by-products that disturb continuous growth are not formed [1]. However, further improvement of growth rate and crystal quality are demanded for practical use. In particular, high oxygen impurity concentration ($1 \times 10^{18} \text{ cm}^{-3}$ [2]) is a major problem. We have worked on investigation of surface structures and oxygen adsorption and desorption processes during the GaN growth using first-principles calculations [3]. In this study, we compared absolute surface energies of polar (0001) and (000-1), nonpolar (11-20) and (1-100), and semipolar (1-101) and (1-10-1) GaN surface under the OVPE growth conditions and we comprehensively discussed stable surface structures. We used the first-principles molecular dynamics simulation program "STATE-Senri" [4]. Surface energy ΔE is given by $\Delta E = E_{tot} - E_{ref} - \sum_i n_i \mu_i$ [5], where E_{tot} and E_{ref} are the total energy of the surface model and the reference (ideal) model, respectively. n_i is the number of atoms of the i th species added to the reference surface. μ_i is the chemical potential of gas-phase atom or molecule [6]. In addition, we calculated absolute surface energies of the polar, nonpolar, semipolar ideal surfaces of GaN [7]. These values were added to ΔE and it allows us to compare the surface energies of different surface orientation. Under the typical OVPE growth conditions (the temperature $\sim 1500 \text{ K}$, the Ga pressure $\sim 1 \times 10^{-3} - 1 \times 10^{-2} \text{ atm}$, the H_2 pressure $\sim 0.1 \text{ atm}$), (0001) surface with an O atom on the surface was the most stable. When Ga pressure was lower than 10^{-4} atm , (000-1) surface with an O atom incorporated into a N vacancy site

became stable. Nonpolar surfaces with an O atom incorporated into a N vacancy site appeared to be next stable under the typical growth conditions. This work was supported by JSPS KAKENHI Grant Numbers JP18K04957 and JP16H06418.

References [1] M. Imade et al., J. Cryst. Growth **312**, 676 (2010). [2] Y. Bu et al., J. Cryst. Growth **392**, 1 (2014). [3] T. Kawamura et al., Jpn. J. Appl. Phys. **57**, 115504 (2018). [4] Y. Morikawa, Phys. Rev. B **51**, 14802 (1995). [5] C. G. Van de Walle et al., Phys. Rev. Lett. **88**, 066103 (2002). [6] Y. Kangawa et al., Surf. Sci. **493**, 178 (2001). [7] T. Akiyama et al., Phys. Rev. Materials **3**, 023401 (2019).

5:30 PM - 5:30 PM

IMPLANTATION OF BERYLLIUM INTO THIN UNINTENTIONALLY DOPED LAYERS OF GALLIUM NITRIDE CRYSTALLIZED BY HALIDE VAPOR PHASE EPITAXY

M. Amilusik¹, T. Sochacki¹, M. Iwinska¹, M. Fijalkowski¹, B. Lucznik¹, A. Sidor¹, M. Zajac¹, I. Grzegory¹, R. Jakiela², A. Barcz², M. Bockowski¹

¹Institute of High Pressure Physics PAS, POLAND, ²Institute of Physics PAS, POLAND

HVPE can be used for growing thin, up to 200 μm , GaN layers of high purity and low free carrier concentration. Deposition of such material on conductive n-type GaN seeds results in a structure which is the basis of some vertically operating electronic devices. It should be stressed that thickness of this GaN with low free carrier concentration influences the breakdown voltage of the devices. Therefore, HVPE becomes the main epitaxial technology for crystallizing such layers. The method allows to crystalize GaN with a relatively high growth rate of about 100 $\mu\text{m}/\text{h}$. It makes HVPE crucial for preparing transistor structures with breakdown voltage higher than a few or several kV. The main goal of this paper is to investigate implantation of beryllium (Be) acceptors into thin (10-100 μm) unintentionally doped layers of GaN crystallized by HVPE on native seeds. A nitride structure comprising of an n-type layer of low free carrier concentration with implanted regions with p-type conductivity or semi-insulating and a highly conductive n-type substrate will be obtained. Basic parameters

of HVPE-GaN growth processes (reagent flows, growth temperature) as well as parameters of ion implantation will be determined. Post-implantation damage, which occurs in the implanted layers, will be removed by high-temperature (1000-1480°C) annealing at high nitrogen pressure, up to 1 GPa. Influence of the annealing temperature, pressure and time on structural quality of implanted layers as well as on diffusion mechanisms of Be in the material will be investigated in detail. Structural, optical, and electrical parameters of implanted and annealed GaN will be presented. The samples will be characterized prior to and after ion implantation. The effective diffusion coefficients and the activation energy for Be diffusion in GaN will be determined.

5:30 PM - 5:30 PM

LUMINESCENCE RED SHIFT OF INGAN/GAN HETEROSTRUCTURES BY ENLARGEMENT OF V-PITS

T. Vaněk¹, T. Hubáček¹, F. Hájek², K. Kuldová², J. Oswald², J. Pangrác², M. Slavická-Zíková², A. Hospodková²

¹Technical University of Liberec, CZECH REPUBLIC, ²Institute of Physics, CAS, CZECH REPUBLIC

V-pits in InGaN/GaN heterostructures are known for their positive properties for the light yield in the LED because they increase the light extraction efficiency and isolate threading dislocations from active quantum wells (QWs). However, for very thick active layer needed in photovoltaics or scintillator applications the V-pits are oversized since their size is growing with the active layer thickness and their density is increasing due to the generation of new misfit dislocations caused by the strain relaxation of thick strained structure [1], see the smaller V-pits in the SEM image of sample C (Fig.1).

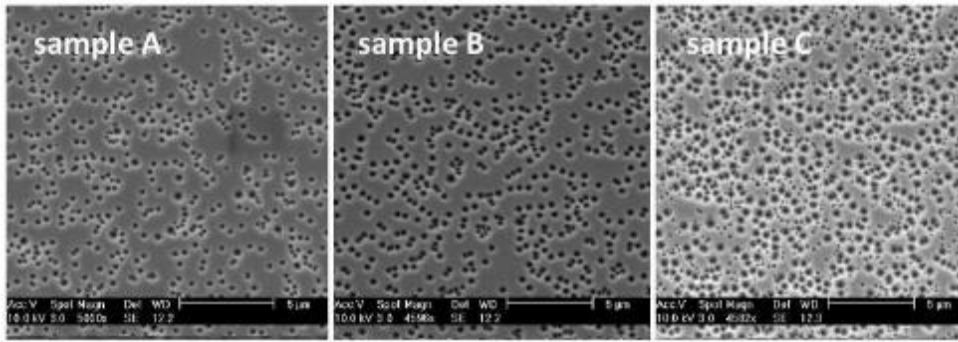


Fig.1. SEM

pictures of structures with increasing size and density of V-pits. (A) only one size, (B) bigger V-pits of one size, (C) two generations of V-pits. However, new dislocation formation and deteriorated surface almost completely covered by V-pits surprisingly does not decrease the integral photoluminescence (PL) intensity, which remains very high. Additionally, structures with high V-pit density evince strong unexpected red shift of QW luminescence, compare SEM images of samples A – C and their PL spectra in Fig. 2. QWs in all three samples were prepared with the same technological procedure the only difference is the V-pit size and density.

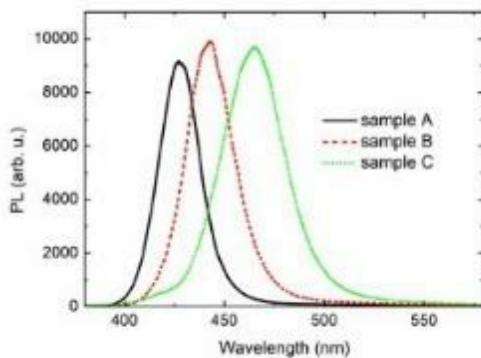


Fig.2. PL results of structures with different V-pit size and density for excitation at 325 nm, laser power density 5 W/cm². The aim of this work is to explain the origin of this QW luminescence red shift, which correlates with surface coverage by V-pits. We suppose that increased size and V-pit density has a consequence in a smaller flat area with <0001> orientation where the indium incorporation to QWs is preferred and thus thicker QWs with higher concentration of indium are grown. Similar behavior was also observed for trench defects [2]. Luminescence results of InGaN/GaN multiple quantum well (QW) structures (from 10 to 50 QW) grown by MOVPE with the MQW active

region thickness up to 1.17 mm will be shown in this work. The PL red shift with increasing V-pit size will also be demonstrated by cathodoluminescence measured for different penetration depth of electrons. The strong red shift of PL spectrum accompanied by increasing the integral PL intensity might be important for luminescence as well as solar cell applications. [1] F. C. P. Massabuau, et. al, Appl. Phys. Lett.101, 212107 (2012). [2] P. M. F. J. Costa, et. al, Phys. Stat. Sol. (a) 203, No. 7, 1729–1732 (2006).

5:30 PM - 5:30 PM

COMPUTER MODELING OF BULK GAN CRYSTAL GROWTH FROM NA-GA SOLUTION

A. Vorobiev, A. Kondratyev, A. Smirnov, **V. Kalaev**

STR Group, Inc. – Soft-Impact, Ltd., RUSSIAN FEDERATION

High quality GaN is required for production of blue light emitting diodes (LED), semiconductor lasers, high frequency and high power electronic devices. For fabrication of high quality bulk GaN substrates one needs a reliable and low-cost bulk growth technology. The Na flux method, first introduced in 1997 [1], relies upon a much higher solubility of nitrogen in a sodium-gallium melt in comparison with a pure gallium one. This method requires a quite simple equipment with moderate pressures (30-50 atm) and temperatures (750-900°C). The major limitations are related to a low diffusion coefficient of nitrogen atoms through the Na-Ga melt and parasitic deposition of GaN polycrystals near the melt free surface. Currently the liquid phase epitaxy (LPE) based on the Na flux method allows production of GaN substrates of up to 6 inch diameter at growth rate of up to 50-100 mm/hr and threading dislocation density of approximately $\times 10^3 \text{ cm}^{-2}$. The present work focuses on development of a 2D-3D simulation tool coupled with an advanced chemical model extended to cover wide range variation of such process parameters as composition of the gallium-sodium melt, the growth temperature, and nitrogen pressure. Our approach uses the available experimental data on the temperature dependence of nitrogen solubility in a pure gallium melt and accounts for nitrogen pressurization. As a solution, one obtains the solubility values, which allows accurate specification the boundary conditions for the nitrogen transport. The calculated solubility and

estimation of the GaN growth rate as a function of temperature, composition and pressure agrees well with the experiments available in literature. A number of 2D computations have been performed on a set of experimental data obtained with LPE Na flux furnaces of Osaka University [2-4]. The dependence on the nitrogen pressure exhibited a slightly sublinear ascending trend. Heating up the crucible bottom over the melt free surface initiates natural thermal convection, which intensifies nitrogen atoms delivery towards the substrate and increases the growth rate. Our model reproduces the growth rate increase with the temperature drop. The model is built into the commercial computational software CGSim™ [5] and should serve as a convenient tool for optimization of growth technology. [1] H. Yamane et al., Chem. Mater. 9 (1997) 413. [2] R. Gejo et al., Jpn. J. Appl. Phys. 46 (2007) 7689. [3] D. Kashiwagi et al., J. Cryst. Growth 310 (2008) 1790–1793 [4] Y. Mori, et al., Phys. Status Solidi C 8 (2011) 1445. [5] <http://www.str-soft.com/products/CGSim>

5:30 PM - 5:30 PM

STUDIES ON ALGAN PHOTODIODES BASED ON DIFFERENT ALN TEMPLATES

D. Chen, Z. Xie, P. Chen
Nanjing University, CHINA

Solid-state AlGa_N photodiodes are attracting more and more attention because they have the irreplaceable advantage of detecting very weak light signals in the deep ultraviolet (UV) spectral region thanks to their wide band-gap and high chemical and physical stabilities. However, the demonstration of AlGa_N photodiodes with high gain and low noise still remains great challenge due to high density of dislocations, low p-type doping efficiency, and low impact ionization coefficient of carriers in high-Al-content AlGa_N alloys. Recently, we have fabricated a series of AlGa_N photodiodes structures based on various AlN templates by metal-organic chemical vapor deposition. We found that using the nano-pattern AlN template can significantly reduce extended dislocation density in heteroepitaxy AlGa_N film. On basis of the epitaxial AlGa_N structure, we have demonstrated high-gain AlGa_N photodiodes by exploiting polarization and heterostructure energy-band engineering. We found that the performances of AlGa_N

photodiodes can be significantly improved by designing a beneficial polarization electric field in the multiplication region. Furtherly, employing a low-Al-content multiplication layer together with a photonic-crystal structure as solar-blind optical window instead of intrinsic solar-blind AlGa_N layer is also an effective way to realize high-gain solar-blind AlGa_N photodiodes. These improved AlGa_N photodiodes exhibit one order of magnitude higher gain and a much lower dark current density compared with their conventional counterparts. In addition, some particular device processes, such as photo-electrochemical treatment, field-plate structure, and mesa terminal process, for AlGa_N photodiodes will also be introduced. Finally, we investigated the leakage current mechanisms and found that electron tunneling along 4 core or 5/7 core edge threading dislocations from the valence band of p-AlGa_N to the conduction band of i-AlGa_N is responsible for the leakage and the premature breakdown behavior of AlGa_N photodiodes by a combined theoretical and experimental analysis.

5:30 PM - 5:30 PM

IMPROVING OPTICAL AND ELECTRICAL PROPERTIES OF GAN EPITAXIAL WAFERS AND ENHANCING LUMINESCENT PROPERTIES OF GAN-BASED LIGHT-EMITTING-DIODE WITH EXCIMER LASER IRRADIATION

Y. Jiang¹, H. Tan², L. Hao²

¹Beijing Institute of Petrochemical Technology, CHINA, ²Institute of Laser Engineering, Beijing University of Technology, CHINA

The effect of 248 nm KrF excimer laser irradiation on the properties of epitaxial wafers with a p-GaN surface were investigated. The GaN epitaxial wafers with a p-GaN surface were irradiated with an excimer laser at different energy densities and pulse numbers. The irradiated samples were annealed in oxygen. The laser irradiation-induced changes in optical and electrical properties of GaN epitaxial wafers were examined using PL, I-V, XPS, SIMS and Hall test system measurements. Experimental results show that under an appropriate laser irradiated condition, optical and electrical properties of the samples were improved to different degrees. The samples which were annealed after irradiation have better electrical properties such as the

hole concentration and sheet resistance than those without annealing. We hypothesize that the pulsed KrF excimer laser irradiation dissociates the Mg–H complexes and annealing treatment allows the hydrogen to diffuse out more completely under the oxygen atmosphere at a proper temperature. Under appropriate laser conditions and O₂-activated annealing, the light output of the laser-irradiated GaN-Based LED sample is about 1.44 times that of a conventional LED at 20 mA. It is found that the wall plug efficiency is 10% higher at 20 mA and the reverse leakage current is 80% lower at 5V.

5:30 PM - 5:30 PM

MOCVD PECULIARITIES FOR INGAN/GAN HETEROSTRUCTURES

O. Rabinovich, A. Savchuk

NUST MISIS, RUSSIAN FEDERATION

Low-temperature amorphous buffer (nucleus) InGaN/GaN layer, the oxygen influence on the epitaxial growth, the island growth process special additional doping profile were investigated. Based on this the density of penetrating, structural line dislocations upto 10^8cm^{-2} was reduced, charge carriers mobility risen and improve the uniformity of surface morphology. The influence of defects occurs from III/V flows ratio and doping barriers by Indium atoms was detected. Decrease in the V/III ratio upto 1320 at the stage of the precipitated growing low-temperature nuclei leads to the formation of growth islands, and also increases the growth rate in the lateral direction. This leads to a decrease in the dislocations density. a-GaN films on the r-Al₂O₃ substrate by the MOCVD with good surface morphology were grown. The acceptor and donor impurities concentrations were $8 \cdot 10^{17} \text{cm}^{-3}$ and $4 \cdot 10^{18} \text{cm}^{-3}$, correspondently.

5:30 PM - 5:30 PM

LED DEGRADATION CONTROL METHOD

O. Rabinovich¹, S. Nikiforov², A. Savchuk¹, M. Orlova¹, S. Podgornaya¹

¹NUST MISIS, RUSSIAN FEDERATION, ²Arhilight, RUSSIAN

FEDERATION

The investigations of the degradation mechanisms of crystals and LEDs production based on them are very important. Establishing the dependence between the degradation rate of the most important LEDs parameters determination makes it possible to forecast the LEDs lifetime at the production stage. The main parameter taken for the LEDs investigation is the luminous flux F . Based on the model for the emitting area structure in the form of parallel connected nanoLEDs (p - n junctions) with different characteristics, it is possible to establish a link between changes in the total characteristics of the entire structure and its individual components. The nonuniform distribution of the $\text{In}_x\text{Ga}_{1-x}\text{N}$ composition in the active region shows interesting results. This statement well explains the fact of the emission energy parameters redistribution but not their quantitative change. According to this model, the LED is a set of parallel-connected microdiodes having the same parameters of wide-gap n - GaN and p - GaN emitters, but differing from each other in indium content in quantum wells. Huge degradation will be in the structure areas with small Indium atoms concentration $X = 0.15\text{--}0.17$, through which currents with high density flows. As a result, the emission spectra is shifted to the long-wavelength area during the working time, since the shorter-wave part of the spectral distribution degrades faster. The decrease in luminous flux with a slight increase in U_f and long-wavelength area shift may be due to the redistribution and migration of structural defects in the form of non-radiative recombination centers with low resistance (which are leakage channels) that are parallel to the included in the whole structure. In this redistribution, the total direct voltage of the structure varies slightly, and the shunting effect of these sites increases significantly, reducing the total luminous flux. The existing LEDs sorting is carried out at one current value - 20 mA. It has been detected that the criteria for sorting LEDs should be made at high current densities through the crystal, and also that the proposed method of such sorting makes it possible to make a reliable the LEDs quality produced (to detect more than 95 % of potentially unsuitable devices) and to adjust the necessary technological operations possible damage at the exit.

5:30 PM - 5:30 PM

GROWTH AND NONLINEAR OPTICAL PROPERTIES OF LANGASITE CRYSTALS

H. Yu, H. Zhang, J. Wang
Shandong University, CHINA

Mid-infrared lasers using nonlinear optical (NLO) crystals have essential applications in science as well as daily life, such as infrared remote sensing, biological tissue imaging, environmental monitoring, and minimally invasive medical surgery. For generating mid-infrared lasers in the spectral range of 3–20

5:30 PM - 5:30 PM

EFFECT OF L-ARGININE ADDITIVE ON THE GROWTH AND PHYSICAL PROPERTIES OF POTASSIUM DIHYDROGEN PHOSPHATE SINGLE CRYSTALS

I.M. Prytula¹, E.I. Kostenyukova¹, O.N. Bezkrovnaya¹, V.Y. Gayvoronsky², A.N. Levchenko³

¹Institute for Single Crystals of NASU, UKRAINE, ²Institute of Physics NAS of Ukraine, UKRAINE, ³V.N. Karazin Kharkiv National University, UKRAINE

Potassium dihydrogen phosphate (KDP) single crystals doped with L-arginine (L-arg) amino acid were grown from aqueous solutions onto a point seed using the temperature reduction method. The incorporation of L-arg molecules into the crystal was verified by means of ninhydrin reaction. Undoped and L-arginine doped KDP crystals were characterized by XRD method and structure perfection of the doped crystals was shown to correspond to the one of pure KDP. It was established that incorporation of L-arg molecules into KDP crystal had an effect on the formation of additional bonds in the crystal structure, that manifested itself in the thermal properties of the doped crystals. Investigation of $\epsilon_{\perp}/\epsilon_{\parallel}$ value which characterizes the dielectric permittivity anisotropy showed that it was minimal at 0.5-1.0 wt% L-arg concentrations. In this case, the introduced L-arg seems to lead to creation of additional hydrogen bonds and disappearance of proton vacancies bound up with aliovalent impurities. Since the crystals contain different impurity defects, L-arg molecules are oriented in the

lattice in a different way, depending on the type of the defects, and diminish the anisotropy. The present study testifies that the attenuation of the values of DC conductivity, dielectric permittivity and loss tangent at L-arg concentrations of ~1 wt% is probably related to the content decrease of the proton vacancies and the impurity-proton vacancy complexes dipoles, formed due to incorporation of the impurity ions into the crystal. The incorporation of L-arg molecules into the crystalline matrix results in an order of magnitude enhancement of the refractive nonlinear optical (NLO) response efficiency and its sign turn to self-focusing effect versus the self-defocusing obtained in the nominally pure KDP crystal. Similar kind of the NLO response efficiency rise in the KDP single crystals doped with TiO₂ nanoparticles. The phenomenon can produce the enhancement of the optical harmonics generation efficiency due to the laser radiation localization and improvement of phase matching conditions realization.

5:30 PM - 5:30 PM

METAL ORGANIC POTASSIUM L-ASCORBATE MONOHYDRATE A NEW NONLINEAR OPTICAL MATERIAL

D. Bairwa¹, K.R. Rao², D. Swain³, T.n.G. Row³, H.I. Bhat⁴, S. Elizabeth¹

¹Department of Physics, Indian Institute of Science, INDIA, ²PES University, INDIA, ³Solid State and Structural Chemistry Unit, Indian Institute of Science, INDIA, ⁴Center for Soft Matter Research, INDIA
Crystal play important role in LASER technology and Nonlinear optics. In Nonlinear optics, crystals with large size with properties such as non centrosymmetry, higher conversion efficiency, higher laser damage threshold, low cut off wavelength, low coast and non toxicity are the favoured prerequisites.

Saccharides are chiral molecules which always crystallize with noncentrosymmetric structure and generally fulfil the basic requirements for application in Nonlinear optics. However crystal growth of saccharides involves careful calculations of temperature, PH and chemical inertness as their solution is subject to oxidation during growth.

Nontoxic, environment friendly, low cost, large size (35mm× 35mm × 20mm) single crystals of potassium l-ascorbate monohydrate (KLAM), ($\text{KC}_6\text{H}_7\text{O}_7 \cdot \text{H}_2\text{O}$) are grown using solution growth technique employing modified Holden's Rotary Crystallizer. Crystals were grown by cooling the solution at the rate of 0.01°C/h , as the material has positive temperature coefficient of solubility in water. The structure of KLAM was solved by single crystal XRD. It crystallizes in non-centrosymmetric, monoclinic, $P2_1$ space group with lattice parameters $a=7.030(5) \text{ \AA}$, $b=8.811(5) \text{ \AA}$, $c=7.638(5) \text{ \AA}$ and $\beta = 114.891(5)^\circ$. The monoclinic structure (biaxial dielectric frame), presents a challenge and the identification of the phase matching curves is quite involved. Due to multi-directional hydrogen bonding, crystal has bulky morphology in all three directions with (100), (-100), (-110), (0-1-1), (0-11), (001) and (00-1) prominent faces, identified by solving the morphology using WinXMorph software. TGA and DSC measurements show that KLAM is stable up to 90°C . KLAM shows good transparency down to 260 nm. Second harmonic conversion efficiency measured on powder sample is 3.5 times of that of potassium dihydrogen phosphate (KDP). Collinear phase matching reveals that KLAM crystal is phase matchable. The crystal was oriented using Laue XRD and the phase matching directions were measured experimentally on oriented crystal plates. Analysis of SHG conical sections originating from noncollinear phase matching, helps to locate the collinear phase matching directions. Presence of third order noncollinear SHG rings suggests large magnitude of birefringence and large nonlinear optical coefficients. Laser damage threshold value of the crystal for single pulse is found to be $3.07 \text{ GW}=\text{cm}^2$, for 1064 nm wavelength in b direction.

5:30 PM - 5:30 PM

POLARIZATION REVERSAL OF HYDROTHERMAL GROWN KTiOPO_4 AND RB^+ DOPED KTiOPO_4 CRYSTALS AT ROOM TEMPERATURE

L. Yang¹, X. He², C. Zhang², W. Wu¹, H. Zhou², Y. Zuo², F. Lu², M. Ren²

¹Photoelectric technology of Guilin Bairay Co., Ltd., CHINA, ²China Nonferrous Metal (Guilin) Geology and Mining Co., Ltd., CHINA

A research of polarization reversal of hydrothermal grown KTiOPO_4 and Rb^+ doped KTiOPO_4 crystals with polished Z-cut planes under an external electric field at room temperature has been implemented. The coercive electric field obtained from ferroelectric hysteresis loop of KTiOPO_4 and Rb^+ doped KTiOPO_4 crystals are about 5.88KV/cm and 8.65KV/cm, respectively, which are somewhat higher than that of ones estimated by the method of high voltage DC power supply. It is revealed that the electrical resistivity, which the polarization reversal of high electrical resistivity KTiOPO_4 crystals are more difficult than that of low electrical resistivity ones, of KTiOPO_4 crystal plays the major role in coercive electric field, and the approximately linear relationship between electrical resistivity and coercive electric field has been concluded roughly. Polarization switching of hydrothermal grown KTiOPO_4 and Rb^+ doped KTiOPO_4 crystals under a pulsed voltage have also been achieved, and the results show that a higher peak voltage is required for a pulsed voltage with lower duty cycle to realize polarization reversal of KTiOPO_4 and Rb^+ doped KTiOPO_4 crystals. The coercive electric field of hydrothermal grown KTiOPO_4 and Rb^+ doped KTiOPO_4 crystals are lower than that of flux grown ones obviously, which the coercive of flux grown KTiOPO_4 and Rb^+ doped KTiOPO_4 crystal at room temperature are about 20KV/cm and 60KV/cm respectively¹, suggesting that the hydrothermal grown KTiOPO_4 and Rb^+ doped KTiOPO_4 crystals are better candidates for polarization reversal. The observations presented above may also be a good guidance for the fabrication of periodically poled KTiOPO_4 and Rb^+ doped KTiOPO_4 crystals.

5:30 PM - 5:30 PM

TETRAPHENYLPHOSPHONIUM BROMIDE SINGLE-CRYSTALLINE MICROFIBER FOR MULTIPLE-COLOR STIMULATED RAMAN SCATTERING

Y. Ren

INSTITUTE OF CRYSTAL MATERIALS, CHINA

We report an organic single-crystal microfiber of tetraphenylphosphonium bromide (TPPB). Using fast solution method [1,2], we successfully grow high quality one-dimensional organic single-crystal microfiber of tetraphenylphosphonium bromide (TPPB). Experimentally, the TPPB single-crystal microfiber growing process exhibits a unique ambient-condition-dependent behavior. Fast evaporation and cooling in high supersaturation solution benefits to the formation of TPPB crystal in one-dimension. The length-to-diameter ratios of TPPB single-crystalline microfibers are typically over $10^4:1$ with the diameters ranging from less one micron to tens of micron. In optical experiments, we find that TPPB single-crystal microfibers exhibit excellent optical wave-guiding properties and efficient multiple-color SRS generation under a continuous-wave pump at 532 nm. Three main SRS peak at 562.35 nm, 581.45 nm and 636.15 nm are detected, all of which originate from the first-order Stokes shifts of TPPB at 1000 cm^{-1} , 1586 cm^{-1} , and 3067 cm^{-1} respectively. The SRS generation threshold of TPPB single-crystal microfiber is showed to be less than 0.7 mW determined by a CCD image of the signal at the exit of the microfiber. To the best of our knowledge, the single-pass SRS generation threshold of TPPB single-crystal microfiber is far less than that of bulk crystal in a cavity under continuous laser excitation. The low threshold also indicates that the power of a common laser pointer may be enough to pump TPPB single-crystalline microfiber to give efficient SRS. The TPPB single-crystal microfiber developed here may find practical use in miniature optical frequency devices such as compact Raman lasers to provide varied laser wavelengths for applications in imaging, spectroscopy or medicine.

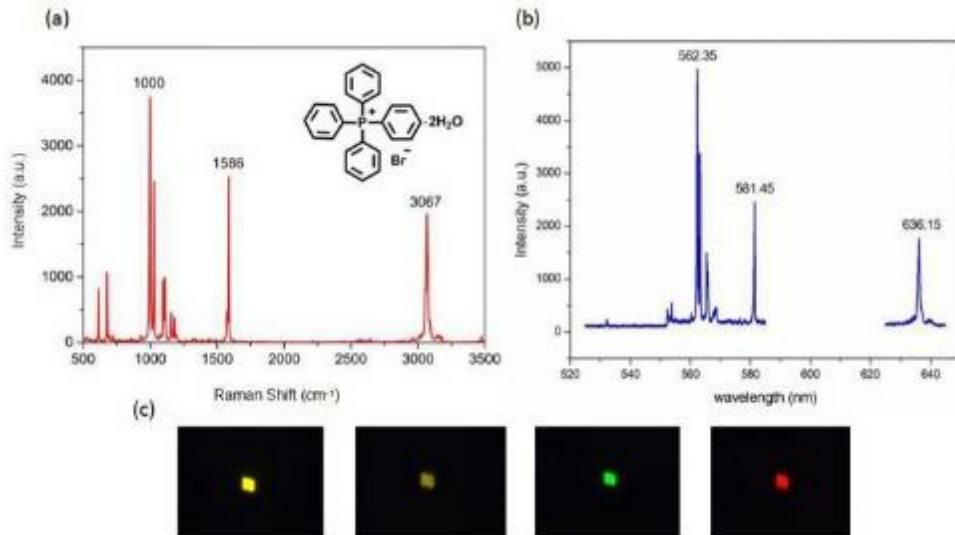


Fig. 1. (a) Spontaneous Raman spectrum; (b) stimulated Raman scattering spectrum of TPPB pumped by a CW 532 nm laser; (c) SRS images recorded by a CCD camera at the exit of TPPB single-crystal microfiber. Yellow: SRS images involving multiple wavelength, Gold: SRS at 562.35 nm, Yellow green: SRS at 581.45 nm, Red: SRS at 636.15 nm. **Acknowledgement** We thank Dr. L. Deng (NIST) and Dr. E.W. Hagley (NIST) for critical helps in this research project.

References [1] Y. Ren, X. Zhao, L. Deng and E. W. Hagley, "Ambient-condition growth of high-pressure phase centrosymmetric crystalline KDP microstructures for optical second harmonic generation," *Sci. Adv.* **2**, e1600404 (2016). [2] Y. Ren and S. J. Zhang, "Optical quality tetragonal phase single-crystal microfiber of potassium di-hydrogen phosphate with efficient second-harmonic generation," *CrystEngComm* **19**, 767-771 (2017).

5:30 PM - 5:30 PM

CRYSTAL GROWTH AND OPTICAL PROPERTIES OF $Y_{1.5}HO_{1.5}AL_5O_{12}$ COMPOUNDS

B. Rekik, I. Lanez

Laboratory LASICOM Faculty Of Science University saad Dahleb
Blida 1, ALGERIA

In order to investigate the optical properties of rare earth activator; Holmium ion, Ho^{3+} in Yttrium Aluminium Garnet crystal Fibers $Y_{1.5}Ho_{1.5}Al_5O_{12}$, and to study the pulling rate effects on morphologie of this compound, we have it grown by laser heated pedestal Growth

(LHPG) technical, in rang of 0.1mm/mn until 1mm/mn using a CO₂ laser , these fibers were transparent and free of defect, and inclusions, or cracks, with High-quality, in the shape of 7-10 cm in length and rang 450-1000 μm diameters , The X-ray diffraction pattern well indexed with the cubic structure of YHoAG (space group: Ia3d, JCPDS: 00-033-040). the samples of Y_{1.5}Ho_{1.5}Al₅O₁₂ fibers crystals were adopted and its MEB morphologies were studied, Optical properties of the Y_{1.5}Ho_{1.5}Al₅O₁₂ were studied with UV-Vis absorption spectroscopy, The spectra show the absorption bands in the UV-VIS-regions which are ³H₅+³H₆(~361 nm), ⁵G₄+³K₇(~385 nm), ⁵G₅(~417 nm), ⁵G₆(~452 nm), ⁵F₂+³K₆(~472 nm), ⁵F₃ (~485 nm), ⁵F₄+⁵S₂(~537nm), ⁵F₅(~642nm) and ⁵I₆(~1147 nm) Spectrum photoluminescence were measured through excitation wavelength at the 540, 645, 900 and 1200 nm, to yield the emissions in Infra red rang, give the emission wavelength ⁵I₆ → ⁵I₈ (1160 nm) , ⁵I₇ → ⁵I₈ (1200 nm), The X ray luminescence spectra of the Y_{1.5}Ho_{1.5}Al₅O₁₂ fibers crystals were measured when exciting by X ray tube (Cu anticathode, U = 30 kV, I = 30 mA,). Which show the intensity of the UV visible luminescence in the range 200–800 nm provided by transitions corresponding to the ⁵G₄ → ⁵I₈ (360nm), ⁵G₄ → ⁵I₈ (360nm) , ⁵G₅ → ⁵I₈ (411nm), ⁵F₄ → ⁵I₈(490nm), ⁵S₂ → ⁵I₈ (550nm), ⁵F₅ → ⁵I₈ (658nm) and ⁵I₄ → ⁵I₈ (757nm). FTIR and Raman spectra of The Fibers crystals (Y_{1.5} Ho_{1.5})Al₅ O₁₂ were established in the wave number range from 400-4000 cm⁻¹, its show the vibrations of the isolated [AlO₄] at 790 and [AlO₆] at 695 , 564 cm⁻¹ in Tetrahedral and Octahedral sites respectively. The vibration modes peaks of Y(Ho)-O stretching and bending were located at the dodecahedral Sit corresponding to the peaks 508 and 723 cm⁻¹ respectively.

5:30 PM - 5:30 PM

GROWTH OF MOLYBDENUM AND INDIUM CO-DOPED LINBO₃ CRYSTALS BY BRIDGMAN METHOD

T. Tian, Y. Xiaodong, Y. Wen, J. Xu
Shanghai Institute of Technology, CHINA

Lithium niobate (LiNbO_3 , LN) crystal is one of the most prominent materials for applications in many practical fields such as holographic storage, waveguides, integrated optics devices and 3D dynamic holographic display. However, LN crystal has disadvantages such as the low photorefractive response speed, which still limits it realize real time 3D dynamic holographic display. It has been reported that the photorefractive response speed of LN can be greatly improved by co-doping resistant photorefractive elements and molybdenum, and the response speed can be dramatically enhanced. Recently, the photorefractive properties of molybdenum and indium co-doped LiNbO_3 crystals (LN:In, Mo) grow by Czochralski method were reported, but the real threshold of indium still unknown in LN:In, Mo crystals. Besides, Czochralski method is not suit for screening out the best doping method because the low produce efficiency. But Bridgman method can grow multiple crystals in a furnace each time. So we grew a series of LN:In, Mo crystals with various indium doping concentrations and 0.5mol molybdenum by Bridgman method. The polycrystalline powders were analyzed by X-ray diffraction and DTA to make sure the pure phase and small difference in melting points. The crystals were grown along [001] with micro-convex growth interface, the growth speed is 0.5-1mm/h and the temperature gradient is 15-25 °C/cm. The absorption spectrum of the crystals were determined and showed a strong absorption band in the visible range. Meanwhile, the photorefractive response speed faster with more indium doped, more details are still need further measure.

5:30 PM - 5:30 PM

IMPROVEMENT OF UPCONVERSION PROCESS VIA PLASMONIC ENHANCED NANOMETER AU FILM ON $\text{TM}^{3+}/\text{YB}^{3+}$ /LITHIUM NIOBITE SINGLE CRYSTAL

Z. Liu, B. Wang

Sun Yat-sen University, CHINA

Upconversion (UC) luminescence on single crystal has long time been suffocated by the low quantum efficiency. However, the strategy of concentration optimizing yields little due to the frangibility of heavy-doped single crystal. Moreover, methods are mainly appropriate for

the nanoparticles but bulk materials. Thus, the restricted method urges the putting forward of external treatment to enhance the UC intensity. We firstly coat Au film with different thickness on $\text{Tm}^{3+}/\text{Yb}^{3+}$ /lithium niobite (LN) wafer to enhance upconversion luminescence, as shown in Fig. 1 (a, b). The upconversion spectra are recorded in Fig. 1(c) and the intensity of blue and red emission have achieved 6.8 and 14 folds enhancement under 980 nm excitation, respectively, which is the firstly reported on bulk material. Additionally, the UC intensity shows irregular variation with the thickness of Au film. Due to the different thickness of Au film, the resonance frequency varies correspondingly, which has been proved by UV-Vis absorption spectra. Meanwhile, the results of time-resolved measurement consistent with conclusion as well. This study revealed that surface plasmons supported upconversion enhancement can be achieved on bulk materials, which shed light on promotion of upconversion properties on bulk materials via aftertreatment.

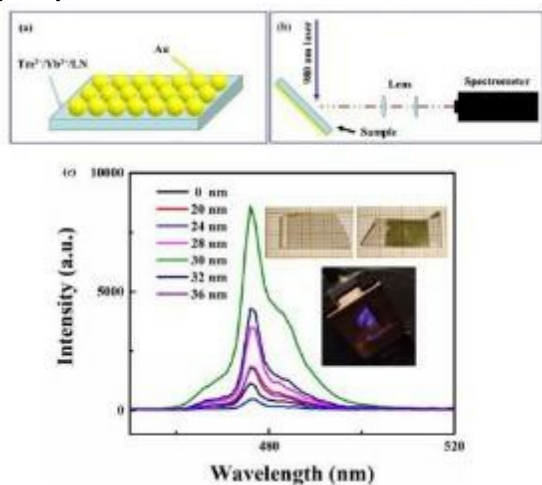


Fig. 1 (a) The schematic of the Au coated $\text{Tm}^{3+}/\text{Yb}^{3+}/\text{LN}$ single crystal, (b) The emission collected by reflection, (c) The upconversion emission of Au coated $\text{Tm}^{3+}/\text{Yb}^{3+}/\text{LN}$ single crystal under 980 nm, the inserts are the picture of LN single crystal wafer before and after Au coating.

5:30 PM - 5:30 PM

EFFECT OF XYLENOL ORANGE ON THE CRYSTALLINE PERFECTION, OPTICAL AND ELECTRICAL BEHAVIOR OF UNIDIRECTIONALLY GROWN IMIDAZOLIUM L-TARTRATE

SINGLE CRYSTAL

S. Chinnasami, P. Rajesh, P. Ramasamy
SSN College of Engineering, INDIA

Abstract: Pure and 0.1 mol % xylenol orange (XO) doped imidazolium L-tartrate (IMLT), an organic nonlinear optical (NLO) single crystal, has been grown to a dimension of 100 mm and 25 length and 15 and 10 mm diameter respectively by Sankaranarayanan–Ramasamy (SR) method of uniaxial solution crystallization. The grown crystals were subjected to powder XRD, HRXRD, FT-IR, UV–vis, photoluminescence, dielectric, Vickers microhardness, and piezoelectric studies. The powder XRD results confirm that the addition of XO has not changed the basic structure of the IMLT crystal. The crystalline perfection of the grown crystal has been studied by HRXRD rocking curve measurements. The functional groups of pure and doped IMLT crystals were affirmed by FTIR spectral analysis. UV-vis NIR spectra show that both crystals are good transparency in the entire visible region which is an important requirement for an NLO crystal. Dielectric studies were evaluated for the grown crystals for different various frequencies and temperatures. Vickers microhardness studies have been measured by the mechanical strength of the grown crystals. Good piezoelectric behavior was observed for pure and doped IMLT crystals.

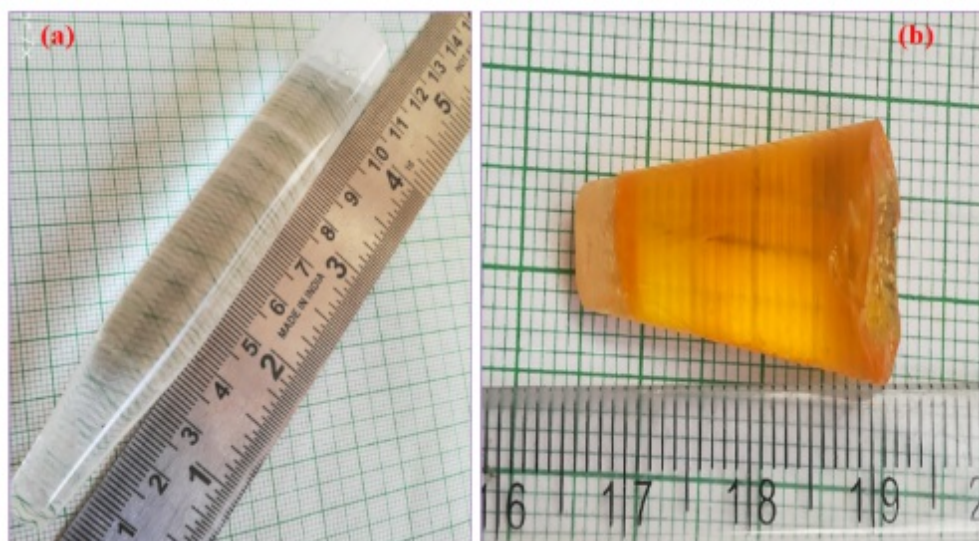


Figure 1. As grown crystals (a) Pure IMLT (b) XO doped IMLT

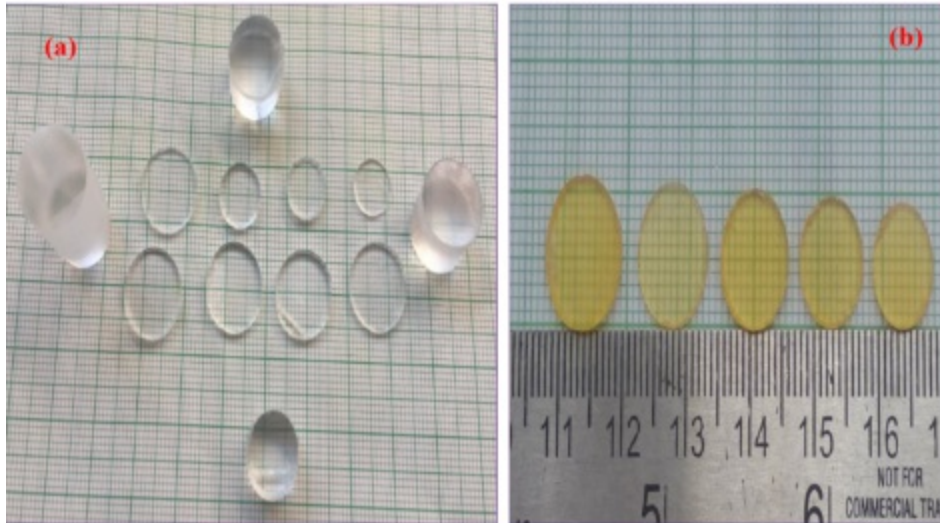


Figure 2. Cut and polished SR method grown crystal (a) Pure IMLT (b) XO doped IMLT

5:30 PM - 5:30 PM

STUDIES ON GROWTH ASPECTS AND CHARACTERIZATION OF A THIRD ORDER NONLINEAR OPTICAL SINGLE CRYSTAL: 1,4 : OXAZINIUM NITRATE (ON)

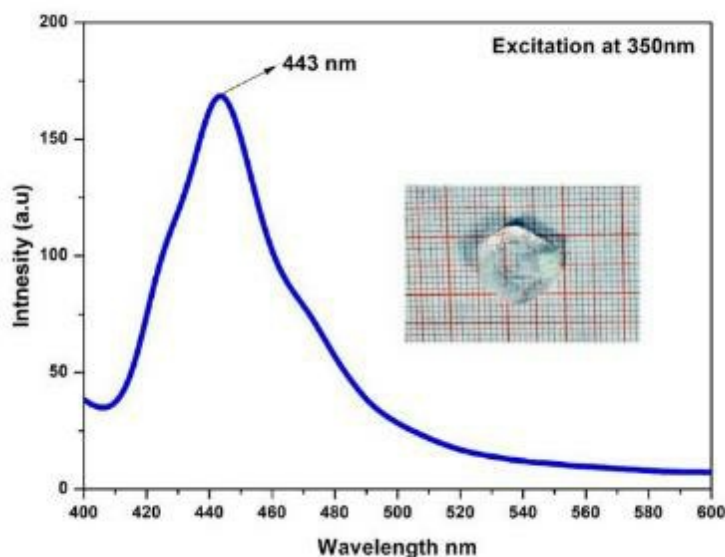
H. Arul, S. Edward, R. Kannan

Department of Science and Humanities, Kumaraguru College of Technology (Autonomous), INDIA

There has been a great interest for academic researchers to discover new materials exhibiting nonlinear optical properties in combination with other desirable properties such as optical transparency, thermal and mechanical stability. The use of third order optical nonlinearity for all optical signal processing devices has been a goal for many years. Therefore it is still challenging task to make high quality optical switching devices responding on picoseconds time scale.

Incorporation of an inorganic additive with an organic molecule provides high optical nonlinearity, chemical flexibility, thermal stability and excellent transmittance in the visible region. 1,4 : Oxazine is a kind of secondary aliphatic amine. The incorporation of nitrogen into the six member ring exposes the lone electron pair on nitrogen and makes the molecule as a good nucleophile. Semi-organic nonlinear optical single crystal ON was grown by controlled evaporation method at room temperature. Unit cell parameter was confirmed by single

crystal XRD. FT-IR spectra revealed the presence of corresponding functional groups. UV-Vis-NIR analysis was taken for the grown crystal and it shows that the crystal is transparent in the visible region. Optical band gap was calculated as 3.4 eV using Tauc's plot. Photoluminescence spectrum was recorded in the wavelength length range of (300-800 nm). The refractive index of ON crystal was measured as 1.4274. Thermal analysis of the sample revealed that the crystal retains the texture up to 192°C. The grown crystal was subjected to Vickers microhardness test to estimate the hardness properties. This shows that the material is exhibiting Reverse Indentation Size effect. Third order nonlinear optical behaviour was confirmed by Z-Scan technique and the parameters such as nonlinear refractive index (n_2), nonlinear absorption (β) and third order nonlinear susceptibility ($\chi^{(3)}$) was also calculated



C. Bosshard, Adv Mater. 8(1996) 385-392 Z. Dega-Szafran, I. Gszczyk, D. Maciejewska, M. Szafran, E. Tykarska, I. Wawer, J. Mol. Struct. 560(2001) 261-273.

5:30 PM - 5:30 PM

INVESTIGATIONS ON SEMI-ORGANIC SINGLE CRYSTAL BIS(4-METHOXYBENZYLAMMONIUM) TETRACHLORIDOZINCATE (4MBZ) FOR NONLINEAR OPTICAL (NLO) APPLICATIONS

P. Karuppasamy¹, D. Joseph Daniel², H.j. Kim², M. Senthil Pandian¹, P. Ramasamy¹

¹SSN College of Engineering, INDIA, ²Kyungpook National University, KOREA, REPUBLIC OF

A semi-organic nonlinear optical single crystal of bis(4-methoxybenzylammonium) tetrachloridozincate (4MBZ) has been grown by slow evaporation solution growth technique. The single crystal XRD analysis confirms that the grown crystal belongs to the Monoclinic system with non-centrosymmetric space group $P2_1$.

Powder X-ray diffraction analysis was carried out for the grown sample in the 2θ range of $20 - 70^\circ$. The crystalline perfection was analyzed by high-resolution X-ray diffraction (HRXRD) and found that the quality of the grown single crystal is quite good. Thermal behaviour of the grown crystal was analyzed by Thermogravimetric analysis (TGA) and differential Scanning calorimetry analysis (DSC). The mechanical behaviour of the grown crystal was studied using Vickers microhardness tester. Nonlinear optical characteristics of 4MBZ have been studied using Q-switched Nd:YAG laser ($\lambda=1064$ nm). The second harmonic generation conversion efficiency of 4MBZ was analyzed.

5:30 PM - 5:30 PM

GROWTH AND CHARACTERIZATION AN ORGANIC QUINOLINE 4-NITROPHENOL (Q4N): A NOVEL SINGLE CRYSTAL FOR NONLINEAR OPTICAL APPLICATIONS

P. Karuppasamy¹, T. Kamalesh¹, D. Joseph Daniel², M. Senthil Pandian¹, P. Ramasamy¹, S. Verma³, H.j. Kim²

¹SSN College of Engineering, INDIA, ²Kyungpook National University, KOREA, REPUBLIC OF, ³Raja Ramanna Centre for Advanced Technology (RRCAT), INDIA

Good quality organic single crystals of quinoline 4-nitrophenol (Q4N) were successfully grown by slow evaporation solution technique (SEST) at room temperature using methanol as solvent. Primarily, the (hkl) reflections of the grown crystal were collected by single crystal X-ray diffraction (SXRD) analysis and its structure was solved by the direct method using SHELXS program and refined using SHELXL

program. The crystalline planes, phase purity were analyzed by powder XRD (PXRD) measurement. Different functional groups of Q4N crystal were confirmed by Fourier transform infrared (FTIR) spectral analysis. The optical quality and its band tail perfection were analyzed by UV-Vis NIR spectral analysis. The grown crystal has good optical transparency in the range 410 – 1100 nm. The thermal stability of the Q4N single crystal has been investigated by thermogravimetric and differential thermal analysis (TG-DTA). The laser damage threshold (LDT) was measured using an Nd: YAG laser. The third-order nonlinear optical properties such as refractive index (n_2), absorption coefficient (β) and susceptibility ($\chi^{(3)}$) were studied using the Z-scan technique.

5:30 PM - 5:30 PM

EFFECT OF KDP MIXING ON OPTICAL PROPERTIES OF AKDP NLO MIXED CRYSTAL FOR ELECTRO OPTIC MODULATORS

G. Iyappan¹, P. Rajesh¹, R. P¹, K.k. Maurya², S. Venugopal Rao³

¹SSN College of Engineering, INDIA, ²CSIR –National Physical Laboratory, INDIA, ³University of Hyderabad, INDIA

Mixed crystal of Ammonium Dihydrogen Phosphate (ADP) - Potassium Dihydrogen Phosphate (KDP) in the ratio of 85:15 was grown using slow cooling technique. The grown crystal's crystalline perfection is evaluated using High-Resolution X-Ray Diffractometry (HR-XRD). The full width at half maximum (FWHM) shows good crystalline perfection of the grown mixed crystal. The homogeneity of KDP along the length of mixed crystal was analysed by studying the UV-Vis NIR spectra for different as-grown regions. In the entire visible region, a good optical transmission was obtained. Technological vital optical constants like optical conductivity (EMBED Equation.3), extinction coefficient (K), refractive index (n) and reflectance (R) were evaluated. The Urbach Energy (EU) value of 0.91eV of the crystal grown indicates a good crystallinity. Etch pit density of the grown mixed crystal was found using chemical etching studies. To determine the mechanical strength of the crystal, the vickers micro hardness (Hv) along the plane (100), reverse indentation size effect (RISE), work

hardening coefficient(n), dislocation density(p), yield strength(EMBED Equation.3 of the crystal were calculated. The positive photoconductive nature of the crystal was confirmed from photoconductivity studies. Compared to pure ADP and KDP crystals, a higher piezoelectric coefficient is seen in the grown mixed crystal. The laser damage threshold of mixed crystal was found at 532 nm using Nd:YAG laser.

5:30 PM - 5:30 PM

INVESTIGATION ON THE SUPERSATURATION DEPENDENT GROWTH OF METHYL-4-HYDROXY BENZOATE (P-MHB) SINGLE CRYSTALS USING SEEDING TECHNIQUE

S. Karuppanagounder, M. Vajaravel

Bharathiar University, INDIA

Methyl-4-Hydroxy benzoate (p-MHB) has been identified as one of the efficient organic nonlinear optical single crystals belongs to alkyl esters group with the chemical formula ($C_8H_8O_3$). p-MHB crystallizes in monoclinic system with non-centrosymmetric space group exhibits high nonlinear hyperpolarizability compared to other materials of current interest. Growth of smaller size single crystals from solutions with selected organic solvents by self-nucleation is always possible at normal supersaturation conditions. But problem begins when the growth experiment was continued with a seed crystal in the solution medium in order to grow large dimensional single crystals and also at elevated supersaturation conditions. After a period of growth and also above a certain level of supersaturation, the crystal develops along one of the polar directions largely when compared to the other and also with the fan-out of various internal defects towards the fast growing direction of the crystal. This deteriorates the quality of the grown single crystal. To understand the asymmetric growth behavior of p-MHB single crystal, in this present work, we have carried out a series of slow cooling crystal growth experiments of p-MHB from the solution with ethyl acetate as a solvent and at different saturation levels with seed. Results indicate that growth rate and morphology of the p-MHB single crystal very much supersaturation dependent. Though solvent has an effect on the growth morphology of p-MHB crystal over and above our observation shows that the crystal grows

unidirectionally along one of its polar directions.

5:30 PM - 5:30 PM

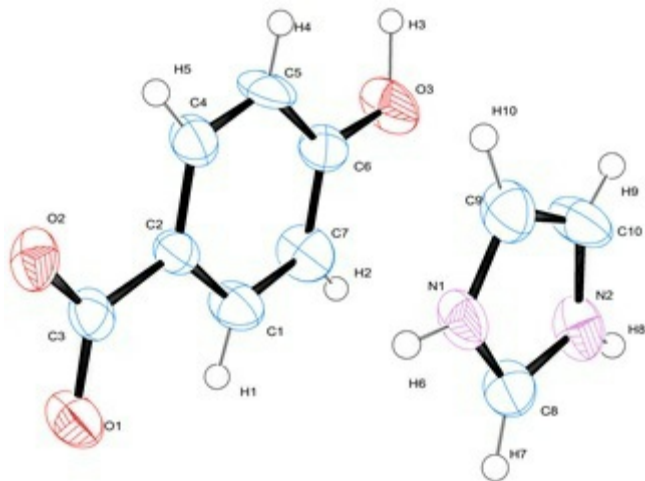
STRUCTURAL, THERMAL AND NONLINEAR OPTICAL STUDIES ON ORGANIC IMIDAZOLIUM 4-HYDROXYBENZOATE (IHB) CRYSTAL

S. Edward¹, R. Kesavasamy², **H. Arul**¹, R. Thirumurugan³, S. Babu⁴

¹Department of Science and Humanities, Kumaraguru College of Technology (Autonomous), INDIA, ²Department of Physics, Sri Ramakrishna Engineering College, INDIA, ³Department of Physics, Madurai Kamarajar University, INDIA, ⁴National Chung Hsing University, TAIWAN

A novel organic proton transfer compound Imidazolium 4-hydroxybenzoate (IHB) was synthesized experimentally and optically good quality single crystals were grown for X-ray diffraction by slow evaporation method. Single crystal X-ray diffraction analysis elucidated its 3-dimensional molecular structure in monoclinic crystal system with a centrosymmetric spacegroup of $P2_1/n$. The molecular packing arrangement is largely contributed by N—H \cdots O and O—H \cdots O intermolecular contacts. The energy minimized molecular geometry of IHB has been computed by Density functional theory (DFT) studies and compared with with crystal structure. The vibrational spectra of both FTIR and FT-Raman were recorded well for IHB compound to probe its vibrational modes. The chemical constructions of initial synthesized compound of IHB has been affirmed in great mode by (¹H and ¹³C) NMR spectral analysis. The electronic transition of title molecule is probed by UV-Vis absorption spectrum (both experimental and theoretical). Thermal perspectives such as melting point (212 °C) and decomposition stages of IHB compound were examined using TG-DTA analysis. Third order nonlinear optical properties were studied by Z-scan measurement. Hirshfeld surface analysis disclosed that more than 75 % of inter contacts are associated with H \cdots H (44.9 %), O \cdots H (19.6 %) and H \cdots O (16.4 %) interactions. The chemical reactivity of IHB has been established by calculating HOMO, LUMO, electronegativity, hardness, softness and electrophilicity index. The formation and locations of intermolecular interactions in IHB is

recognized by Mulliken atomic charge distribution and molecular electrostatic potential (MEP) map analysis by DFT method using 6-311++G(d,p) basis set level of theory.



5:30 PM - 5:30 PM

GROWTH AND CHARACTERIZATION OF 4-AMINOPYRIDINIUM 4-NITROPHENOLATE 4-NITROPHENOL (4AP4N) CRYSTAL FOR NONLINEAR OPTICAL APPLICATIONS

T. Kamalesh¹, P. Karuppasamy¹, M. Senthil Pandian¹, P. Ramasamy¹, S. Verma²

¹SSN College of Engineering, INDIA, ²Raja Ramanna Centre for Advanced Technology (RRCAT), INDIA

Organic nonlinear optical (NLO) 4-aminopyridinium 4-nitrophenolate 4-nitrophenol (4AP4N) single crystals were grown by the slow evaporation solution growth technique at room temperature using methanol as a solvent. The cell parameters of 4AP4N single crystals were confirmed by single crystal XRD (SXRD) measurement. The crystallinity and phase purity were analyzed by the powder XRD (PXRD). Optical quality and optical band gap energy were analyzed by the UV-Vis-NIR spectral analysis. Photoluminescence studies reveals that the crystal has high intense emission. The electro-optical behaviour of the 4AP4N crystal was analyzed by the photoconductive measurement. Thermal and mechanical stability of the grown crystal were analyzed using TG/DTA and Vickers microhardness measurement respectively. The dislocation density of 4AP4N crystal was analyzed and it observed in less dislocations. Dielectric measurement was carried out at room temperature. The laser damage

threshold was investigated. The second harmonic generation (SHG) and third order optical susceptibility were analyzed using Kurtz-Perry powder and Z-scan technique respectively.

5:30 PM - 5:30 PM

STRUCTURES AND LUMINESCENT PROPERTIES OF Y AT.% EU³⁺-DOPED Y(TA_{1-x}P_x)O₄ PHOSPHOR POWDERS

D. Zhong

College of Physics, Qingdao University, CHINA

UV-activated phosphors for solid state lighting europium ion doped yttrium tantalate-phosphate phosphors were synthesized by high temperature solid-state method. The crystalline structures and luminescent characteristics of Eu³⁺ activated Y(Ta_{1-x}P_x)O₄ powders were investigated in detail for the first time by X-ray diffraction (XRD), Fourier transform infrared spectroscopy (FT-IR), scanning electron microscopy (SEM) and photoluminescence (PL) measurements. It is found in our experiment that the maximum doping concentration of phosphate in tantalate is 1%, which is also the concentration with the most efficient luminous performances. The excitation bands of Eu³⁺ 615 nm emission are mainly composed of charge transfer bands of TaO₄³⁻ (peak center is located in 230 nm) and Eu³⁺ (peak center is located in 250 nm) which indicates that TaO₄³⁻ has a certain energy transfer effect on Eu³⁺ 615 nm emission. The characteristic emissions of Eu³⁺ excited by 250 nm ultraviolet light occurred at 595 nm and 615 nm assigned to ⁵D₀→⁷F₁ and ⁵D₀→⁷F₂ charge transition, respectively, and the full width at half maxima is 3 nm of 615 nm emission. Fluorescence lifetime is 1.2720±0.0738 ms. Increasing sintering temperature and holding time can effectively enhance luminous intensities, so Y(Ta_{0.99}P_{0.01})O₄:5 at.% Eu³⁺ is synthesized under the optimal condition of holding temperature at 1300 °C for 10 h. In addition, changing the doping concentrations of Eu³⁺ can change the color coordinates in the yellow-red region and the doping concentration of Eu³⁺ with the strongest luminous intensity and the highest purity is 7 at.% .

5:30 PM - 5:30 PM

DESIGN, SYNTHESSES AND CRYSTAL GROWTHS OF NEW COMPOUNDS IN KBBF FAMILY

H. Yu, Z. Hu

School of Material Science, Tianjin University of Technology, CHINA
Nonlinear optical (NLO) crystals are essential materials for generation of coherent UV light in solid state lasers. KBBF is the only material that can achieve coherent light below 200 nm by direct second harmonic generation (SHG). However, its strong layer habits and the high toxicity of the beryllium oxide powders required for synthesis limit its application. Based on the molecular structure engineering design, a series of new UV nonlinear optical materials with KBBF-like structures, including $\text{Cs}_3\text{Zn}_6\text{B}_9\text{O}_{21}$, $\text{Rb}_3\text{Ba}_3\text{Li}_2\text{Al}_4\text{B}_6\text{O}_{20}\text{F}$ and $\text{Pb}_2\text{BO}_3\text{I}$ have been successfully synthesized. They cannot only overcome the processing limitations of KBBF, but also enhance the SHG responses of the KBBF family. For the high performance $\text{Rb}_3\text{Ba}_3\text{Li}_2\text{Al}_4\text{B}_6\text{O}_{20}\text{F}$ and $\text{Cs}_3\text{Zn}_6\text{B}_9\text{O}_{21}$, the crystals with sizes $12 \times 8 \times 7.6 \text{ mm}^3$ and $5 \times 5 \times 3 \text{ mm}^3$ have been grown by the top seeded solution growth method, respectively.

Reference

- 1. Yu, H.;** Koocher, N. Z.; Rondinelli, J. M.; Halasyamani, P. S., $\text{Pb}_2\text{BO}_3\text{I}$: A Borate Iodide with the Largest Second-Harmonic Generation (SHG) Response in the $\text{KBe}_2\text{BO}_3\text{F}_2$ (KBBF) Family of Nonlinear Optical (NLO) Materials. *Angew. Chem. Int. Ed.* **2018**, *57*, 6100-6103.
- 2. Yu, H.;** Young, J.; Wu, H.; Zhang, W; Rondinelli, J. M.; Halasyamani, S., The Next-Generation of Nonlinear Optical Materials: $\text{Rb}_3\text{Ba}_3\text{Li}_2\text{Al}_4\text{B}_6\text{O}_{20}\text{F}$ -Synthesis, Characterization, and Crystal Growth. *Adv. Opt. Mater.* **2017**, *5*, 1700840.
- 3. Yu, H.;** Wu, H.; Pan, S.; Yang, Z.; Hou, X.; Su, X.; Jing, Q.; Poeppelmeier, K. R.; Rondinelli, J. M., $\text{Cs}_3\text{Zn}_6\text{B}_9\text{O}_{21}$: a chemically benign member of the KBBF family exhibiting the largest second harmonic generation response. *J. Am. Chem. Soc.* **2014**, *136*, 1264-1267.

5:30 PM - 5:30 PM

FORMATION OF GAN NANOWIRES IN MOLECULAR BEAM EPITAXY OBSERVED SIMULTANEOUSLY BY LINE-OF-SIGHT QUADRUPOLE MASS SPECTROMETRY, REFLECTION HIGH ENERGY ELECTRON DIFFRACTION AND OPTICAL REFLECTOMETRY: WHAT CAN WE LEARN USING THESE GROWTH MONITORING TOOLS?

Z. Zytewicz¹, M. Sobanska¹, K.P. Korona², A. Daniluk³, K. Klosek¹

¹Institute of Physics Polish Academy of Sciences, POLAND, ²Faculty of Physics, Institute of Experimental Physics, University of Warsaw, POLAND, ³Department of Applied Computer Science, Institute of Computer Science, Maria Curie-Skłodowska University, POLAND

Controlled formation of GaN nanowires (NWs) by MBE requires *in-situ* monitoring of the growth process. The most advanced studies of GaN NW growth kinetics involve the line-of-sight quadrupole mass spectrometry (QMS) [1-3]. The technique has allowed to distinguish three stages of nanowires' evolution: (i) an incubation preceding the formation of GaN islands, (ii) nucleation and transformation of GaN islands into the NW shape and (iii) further anisotropic growth. Characteristic physical processes for each stage have been determined and analyzed. However, application of QMS requires that one MBE source port is occupied by the spectrometer, thus limiting the number of cells available for growth. Therefore, QMS is usually used in dedicated research MBE set-ups. On the other hand each MBE system is equipped with RHEED tool while laser reflectometry (LR) can be easily installed using standard optical viewports of the system. Both RHEED and LR have been used already for *in-situ* monitoring of GaN NW formation by MBE [4,5]. However, the results were not directly combined with the QMS analysis on the same sample making interpretation of the data difficult. In this work for the first time we use simultaneously QMS, RHEED and LR for monitoring self-assembled formation of GaN NWs on Si(111) by plasma-assisted MBE. Intensity of RHEED and LR signals were recorded as a the growth proceeded together with the QMS signal that was a measure of amount of GaN deposited on the substrate. Kinematical diffraction theory and an effective medium approach were used to simulate RHEED and LR data, respectively. This allowed unambiguous

correlation of characteristic features of the three profiles. The experimental results were combined with studied *ex-situ* morphology of the samples with different growth durations to show a relationship of QMS, RHEED and LR signals with the onset of GaN nucleation and temporal changes of the fill factor, density of NWs, their length and length fluctuations. Finally, we discuss effectiveness of all three techniques for real time monitoring of GaN NW formation by MBE indicating strong and weak points of each technique. [1] S. Fernandez-Garrido et al., *Nano Lett.* 13 3274 (2013). [2] M. Sobanska et al., *Nanotechnology* 27 325601 (2016). [3] M. Sobanska et al., *Nanotechnology* 30 154002 (2019). [4] M. Sobanska et al., *Cryst. Growth Des.* 16 7205 (2016). [5] P. Corfdir et al., *Cryst. Eng. Comm.* 20 3202 (2018). This work was supported by the Polish NCN grants 2016/21/N/ST3/03381 and 2016/23/B/ST7/03745.

5:30 PM - 5:30 PM

FORMATION PROCESS AND EFFECT OF NANO-OXIDES IN STEEL

Z. Wang

School of Materials Science and Engineering, University of Science & Technology Beijing, CHINA

It has been found that when alumina is used for deoxidation in molten steel, the size of the added aluminum is an important factor influencing the size of the oxide formed. This paper gives the size of oxides formed during the steel making process by adding aluminum rods or aluminum wires of different diameters. The data show that when the diameter of the aluminum wire is less than 2mm, the size of the oxide is less than 10 micron, and most of the oxide particles are less than 20 nm. These particles can be used as the crystal core of the crystal grains to refine the solidification structure of the steel; they can also be used as the core of sulfides and silicates to refine inclusions such as sulfides and silicates, the outstanding effect is improved the mechanical properties of the material.

5:30 PM - 5:30 PM

THERMODYNAMIC AND KINETIC CONDITIONS FOR THE FORMATION OF NANO-OXIDES IN MOLTEN STEEL

Y. Zheng¹, **Z. Wang**²

¹Wuxi Open University, CHINA, ²School of Materials Science and Engineering, University of Science & Technology Beijing, CHINA

When melting steel, the conventional method of removing oxide is to make the inclusions grow as much as possible, and then let them float up and removed in a certain period of time, but this method can only partially remove the inclusions in the molten steel because it is difficult to form large-sized inclusions when the oxygen content is low. In order to improve the mechanical properties of the material, our method is to control the reaction of oxygen with aluminum to form nano-oxides such as alumina when the oxygen content is low. The thermodynamic and kinetic conditions for the formation of nano-oxides are given in this paper, providing a theoretical basis for the formation of nano-oxides in steel. When melting steel, the conventional method of removing oxide is to make the inclusions grow as much as possible, and then let them float up and removed in a certain period of time, but this method can only partially remove the inclusions in the molten steel because it is difficult to form large-sized inclusions when the oxygen content is low. In order to improve the mechanical properties of the material, our method is to control the reaction of oxygen with aluminum to form nano-oxides such as alumina when the oxygen content is low. The thermodynamic and kinetic conditions for the formation of nano-oxides are given in this paper, providing a theoretical basis for the formation of nano-oxides in steel.

5:30 PM - 5:30 PM

USE OF GOLD NANOPARTICLES TO CONTROL SHAPE OF LITHIUM PERCHLORATE CRYSTALS IN CHITOSAN MEMBRANES

R.P. Ramasamy

Department of Applied Science and Technology, Anna University,,
INDIA

Lithium ion batteries are an important area of research. In this research the effect of gold nanoparticles upon LiClO_4 included in chitosan solution is studied. Chitosan solution was prepared by adding 1 gm of chitosan in 100 ml of water containing 1.5 gm of acetic acid. When allowed to dry, the solution forms chitosan films. When LiClO_4

was incorporated in chitosan solution, the dried films had several rectangular parallelepiped shaped crystals of sizes in the range 1-3 microns. XRD analysis showed the presence of crystallites. When maghemite nanoparticles (20 nm) were added to 100 ml of chitosan solution containing LiClO_4 (50% wt of chitosan) and dried to form films rod shaped crystals formed. The length of the rod shaped crystals increased with increase in LiClO_4 concentration. When chloroauric acid (1mM) was included in 100 ml chitosan solution and heated, gold nanoparticles formed. The size of the gold nanoparticles was 20-50 nm. When LiClO_4 (50% wt of chitosan) was added to it and cast as films, dough nut shaped structures were observed using SEM. The diameter of the outer ring was approximately 1.3 microns. These had networks in it. Interestingly chitosan-1mM HAuCl_4 – 50% LiClO_4 – 10% maghemite composite films had uniformly sized globules cover the entire sample surface. These globules had network like structures with nanoparticles embedded in it. Dielectric spectroscopy is a useful tool to understand the relaxation behavior and conductivity in membranes. Dielectric spectroscopy analysis showed that the relaxation behavior of chitosan was modified due to LiClO_4 , Gold nanoparticles and maghemite nanoparticles. This research shows that incorporation of small amounts of gold nanoparticles can be used to control the morphology and dielectric characteristics of Lithium containing chitosan films. Various characterization techniques such as vibrating sample magnetometer, SEM, XRD, Dielectric relaxation spectroscopy, FTIR were used for this research. This research could benefit the use of nanoparticles such as gold nanoparticles and maghemite in lithium ion battery technology.

5:30 PM - 5:30 PM

HOMOGENEITY REGION WIDTH AND CRYSTAL STRUCTURE OF PALLADIUM (II) OXIDE NANOCRYSTALLINE FILMS

A.M. Samoylov, A. Dontsov, S. Ivkov, D. Pelipenko, M. Sharov, V. Tsyganova

Voronezh State University, RUSSIAN FEDERATION

The prototypes of gas sensors based on palladium (II) oxide nanostructures showed good sensitivity, signal stability, operation

speed, short recovery period, and reproducibility of the sensor response at detection of carbon monoxide, ozone, and nitrogen dioxide [1–2]. In this work the influence of oxidation temperature and oxygen partial pressure on crystal structure of nanocrystalline palladium (II) oxide thin films (thickness is about 35 - 40 nm) has been studied by X-ray diffraction (XRD). PdO films on SiO₂/Si (100) substrates were prepared by oxidation in ambient air and dry oxygen atmosphere of previously vacuum deposited pure palladium nanolayers. It has been found that at oxidation temperature interval $T = 570 - 1020$ K regardless of oxidation atmosphere the lattice constants and unit cell volume of tetragonal crystal structure of homogeneous nanocrystalline PdO film increased monotonically with the rise of oxidation temperature. However, the absolute values of an increment of lattice constants and unit cell volume of PdO films prepared by oxidation in ambient air atmosphere were essentially less in comparison with the PdO samples oxidized in dry oxygen atmosphere at identical temperature. For both cases (oxidation in dry oxygen and in ambient air) the dependence of calculated X-ray density values upon the oxidation temperature has U-form with minimum at $T_{ox} = 920 - 1020$ K. On the basis of experimental data the calculation of homogeneity region width of PdO films has been performed using the known values of palladium (+2) and oxygen (-2) ionic radii for tetrahedral and square coordination. According to the calculation results the maximal homogeneity region within interval $-0.27 < \delta < +0.11$ mole fraction has been found for nanocrystalline PdO films prepared by oxidation in dry oxygen atmosphere. The obtained experimental data specify that the deviation from stoichiometry, excess oxygen concentration, and *p*-type conductivity of PdO films can be caused by interstitial oxygen atoms in palladium (II) oxide crystal structure.

References [1] V.M. Ievlev, S.V. Ryabtsev, A.M. Samoylov, A.V. Shaposhnik, S.B. Kushev, A.A. Sinelnikov (2018) *Sensors and Actuators B* 255 (2): 1335–1342. [2] A.M. Samoylov, S.V. Ryabtsev, V.N. Popov, P. Badica. Palladium (II) Oxide Nanostructures as Promising Materials for Gas Sensors. In book: *Novel Nanomaterials Synthesis and Applications* // Edited by George Kyzas. UK, London : IntechOpen Publishing House, 2018: 211–229.

5:30 PM - 5:30 PM

WHISKER PARTICLE GROWTH WITH CR-SiO AND FE-SiO SYSTEMS

R. Tsuda¹, M. Sato¹, K. Sasaki¹, T. Awano¹, H. Suzuki²

¹Faculty of Engineering, Tohoku Gakuin University, JAPAN, ²1-13-1, JAPAN

Nanoparticles are easily produced by a gas evaporation method. When some metals are evaporated in an inert gas atmosphere, the vapor is condensed immediately and particles are produced. The particles rise on a convection flow like a smoke. Cr nanoparticles with a few nanometers embedded in an amorphous SiO particle were found by evaporating a Cr and SiO mixture powder in an Ar gas collected 10 mm from the evaporation source. Comet-like whisker particles which had CrSi₂ nuclei and Si tail covered with amorphous SiO₂ layer were found by the same method collected above 100 mm. By using Fe-SiO mixture powder, the whisker particles which had a FeSi₂ or and Si crystal tail were produced. The whisker particle grows by a vapor-liquid-solid (VLS) growth like mechanism model ¹). If the Si tail of the whisker particle grows by the eutectic reaction with the metal (Cr, Fe) and Si in SiO, the whisker particle can be produce by using a mixture powder with SiO rich ratio. But the ratio of the mixed powders was not indicated in detail in the report¹). To elucidate the whisker particle production condition of the metal-SiO mixture powder, we tried to evaporate the mixture powder of Cr-SiO and Fe-SiO systems with several ratios in Ar gas. Mixture powders of Cr-SiO and Fe-SiO were evaporated by heating a W boat as a evaporation source in the Ar gas pressure at 10 kPa. Produced particles were collected on the glass plate set above 100 mm from the evaporation source. The collected particles were observed by TEM (JEOL JEM-2000FX II). The ratio of mixture powder are Cr or Fe : SiO = 2:8, 3:7, 4:6, 5:5, 6:4, 7:3, 8:2. The whisker particles were produced with CrSi₂ nucleus and Si tail in the mixture ratio of Cr:SiO = 2:8, 3:7, 4:6, 5:5 in the Cr-SiO system. In the Fe-SiO system, the whisker the whisker particles with FeSi₂ nucleus and Si tail were produced in the mixture ratio of Fe:SiO = 2:8, 3:7, 4:6. In the both systems, the whisker particles were produced on

the excess-SiO condition. These results supposed the VLS-like growth mechanism model of the whisker particles. The eutectic reaction took place between Cr and Si or Fe and Si respectively in SiO on the coalescence growth of the particles in the smoke. 1) C. Kaito et al., J. Crystal Growth 200 (1990) 271.

5:30 PM - 5:30 PM

ON THE MEDIUM SIZED SILICON NANOPARTICLES: EDIP VS. TERSOFF POTENTIAL

L. Amirouche¹, N. Boulkaboul¹, S. Erkoç²

¹Theoretical Physics Laboratory, Faculty of Physical Sciences, USTHB, P.O. Box 32, El-Alia, Bab Ezzouar, Alger, Algeria, ALGERIA,

²Department of Physics, Middle East Technical University, 06800 Ankara, Turkey, TURKEY

In the present work, attention is paid, by means of molecular dynamics simulation, to the study of structural, energetic and thermal behaviors of silicon nanoparticles of medium sizes ranging from **20** to **70** atoms.

In this context, we have used the well-known Tersoff¹ and **EDIP**² (Environment Dependent Interaction Potential) empirical interatomic potentials to model the interactions between silicon atoms. Lowest energy structures were obtained at **1 K**, starting from an atomic closed spherical shells (**ACSS**) geometry chosen as an initial configuration for our simulation set. Phase transitions were also investigated by plotting caloric curves of the corresponding system. We find out that Tersoff potential gives rise to structures that are lower in energies than those obtained by **EDIP**. The higher coordination number does not seem to play a significant role if any on the stability of the clusters. That is to say, lowest energy structures obtained using **EDIP** have higher coordination numbers compared to those obtained using Tersoff potential. However, the latter gives rise to more stable structures according to the binding energies. Furthermore, lowest energy geometries found out using **EDIP** appear to be more compact and exhibit highly coordinated endohedral atoms. Tersoff potential's lowest energy clusters, on the other side, are characterized by slightly elongated geometries. On the other hand, caloric curves don't reveal phase transitions, but rather present isomerization processes that are

observed for both **EDIP** and Tersoff potential. That is, the change in the caloric curve slope arises from a structural transition of the clusters. An isomerization followed by a fragmentation is observed only for some clusters such as **Si₂₃** and **Si₂₇** obtained using Tersoff potential. No fragmentation can be observed in the case of **EDIP**. To check whether the observed fragmentation depends on the initial configuration, we have carried out the same investigation starting from a different initial configuration: Fragment of diamond structure (**FDS**). It is observed that, for Tersoff potential, **Si₂₃** cluster fragments around the same temperature **1800 K** but according to a different fragmentation pathway. We notice that, in this case, the cluster **Si₂₇** doesn't undergo a fragmentation process. It turns out that the observed fragmentation is not only sensitive to the initial configuration but it is also size dependent. ¹ J. Tersoff, Phys. Rev. Lett. **56**, 632 (1986); Phys. Rev. B **37**, 6 991 (1988). ² M.Z. Bazant, E. Kaxiras, and J.F. Justo. Phys. Rev. B, **56**:8542–8552 (1997).

5:30 PM - 5:30 PM

DETERMINATION OF ZN²⁺ SUPERSATURATION IN THE GROWTH SOLUTION FOR THE SYNTHESIS OF ZNO NANORODS

N. Basinova, O. Cernohorsky, J. Grym

Institute of Photonics and Electronics of the Czech Academy of Sciences, CZECH REPUBLIC

Zinc oxide nanostructures are recently extensively studied for their potential applications in electronics and photonics. A variety of physical and chemical deposition techniques are available for their synthesis. Chemical bath deposition on a seeded substrate is one of the frequently used methods to prepare arrays of ZnO nanorods. This method is easily accessible, non-expensive and has many adjustable parameters to produce desired nanostructures. To be able to control the growth process, it is necessary to control the growth conditions in an appropriate way to obtain well-ordered nanorods. The growth process significantly depends on the properties of precursor solutions; it is essential to understand how the supersaturation of zinc ions in the solution develops, because the supersaturation is a key parameter affecting the mechanism by which the nanorods grow. In our studies,

we use chemical system consisting of zinc nitrate and hexamethylenetetramine (HMTA) equimolar solution. Zinc nitrate supplies zinc ions and HMTA supplies hydroxyl ions, both needed to produce ZnO. The OH⁻ ions are in excess to Zn²⁺ ions; therefore, it is important to evaluate the zinc ion concentration decrease with time, which is related to the incorporation into the ZnO crystal. An effective tool for this purpose is a quantitative chemical analysis - titration. Titration is an accessible and reliable analytical method that provides information about unknown concentration of identified substance in an analyte solution. To determine concentration of zinc in the growth solution and its time and temperature dependence, a chelatometric titration was used. From the analytically obtained data together with the SEM image analysis of the grown nanorods, the zinc ion supersaturation was calculated. As the growth process takes place in a common batch reactor where the solution is being continuously depleted, the kinetics of the reaction that is obtained from the measured data, offers the way to determine the growth mechanisms of ZnO nanorods.

5:30 PM - 5:30 PM

ON THE EFFECT OF INTERATOMIC POTENTIAL ON THE ENERGETIC AND STRUCTURAL BEHAVIORS OF SOME SILICON CLUSTERS: MOLECULAR DYNAMICS SIMULATIONS

A. Ouatzerga, L. Amirouche

Laboratoire de Physique Théorique, Faculté de Physique, U. S. T. H. B., BP 32, El-Alia, BabEzzouar 16311, ALGERIA

A Molecular Dynamics (MD) simulation has been carried out, on small and medium sized silicon clusters, by using the LAMMPS (Large-scale Atomic/Molecular Massively Parallel Simulator) software package. Two interatomic potentials, namely Tersoff and EDIP (Environment Dependant Interatomic Potential) have been used for comparison purposes. The size range investigated, spreading from 3 to 100 atoms, comprises 3 groups of clusters exhibiting, each one, a typical lowest energy structure, according to experimental observations and theoretical predictions [1-3]: (i) for the first one, corresponding to sizes from 3 to 10 atoms, the geometry is rather molecular; (ii) for the second one, prolate or elongated structures are observed up to 26

atoms and (iii) the third one, which includes clusters presenting sizes varying from 27 to 100 atoms, corresponds to compact geometries. All the clusters investigated, through our simulations, are subject to simulated annealing and then quenching in order to optimize their structures and approach the global minimum. The lowest energy structures obtained are observed to depend on the initial configuration. It is shown that clusters commonly accepted in the literature are reproduced for sizes ranging from 3 to 20 atoms. With respect to the size range, situated between 20 to 30 atoms, the geometries obtained suggest a shape transition from elongated to compact structures at about $N=27$. It should be noted that this size range is still subject to controversy, in the sense that a clear divergence is observed in the literature with regard to the exact size beyond which the nanoparticle geometry passes from an elongated shape to a spherical one [4]. For the third group of clusters, the preferred shape is observed to be compact whatever the initial configuration used (diamond fragment or spherical clusters). [1] K-M. Ho et al, Nature, **392**, 582, (1998). [2] S.E. Schönborn, S. Goedecker, S. Roy, A. R. Oganov, J. of Chem. Phys. 130, (14):144108 (2009). [3] Ding, Li Ping et al, Nature, 5, 582, (2015). [4] M. Horoi et K. A. Jackson, Chem. Phys. Lett., **427**, 147, (2006).

5:30 PM - 5:30 PM

INFLUENCE OF THE INTERATOMIC POTENTIAL TYPE ON THE STRUCTURAL PHASE TRANSITIONS AND ENERGETIC PROPERTIES OF LARGE SILICON NANOPARTICLES: MOLECULAR DYNAMICS SIMULATIONS

D. Bendris, **L. Amirouche**

Laboratoire de Physique Théorique, Faculté de Physique, U. S. T. H. B., BP 32, El-Alia, BabEzzouar 16311, ALGERIA

Silicon nanoparticles have attracted great attention in the past decades because of their intriguing physical properties, active surface state, distinctive photoluminescence and biocompatibility [1]. In the present contribution, we investigate, by molecular dynamics simulations, the energetics and the structural phase transitions of Si nanoparticles for sizes ranging between 100 and 900 atoms. The software package LAMMPS (Large-scale Atomic/Molecular Massively Parallel Simulator) was used to evaluate the system's energies at

different temperatures for the nanoparticles and the corresponding bulk Si system. The nanoparticles' behavior and some other thermodynamics properties have been examined for two different force-fields: (i) Stillinger-Weber (SW) potential and (ii) EDIP (Environment Dependent Interatomic Potential). The structural phase transitions have been studied through the different caloric curves that were obtained by plotting nanoparticles' total energy against temperature. The nanoparticles' behavior was analysed in terms of size effects dependence, in particular for Si_N clusters with $N= 123, 211, 317, 413, 501, 603, 705, 801$ and 903 atoms, which correspond to magic numbers. The melting temperatures ranges were, as expected, below the corresponding bulk system's melting temperature, except for $N= 801$ and 903 atoms. It turns out that the (SW) potential is more adequate to describe nanoparticles' phase transitions than EDIP, which is in good agreement with the literature [2]. [1] Chang Huan and Sun Shu-Qing, Chinese Physics B, (2014), **23**, 8 . [2] Luca Sementa et al, Phys. Chem. Chem. Phys., (2018), **20**, 1707.

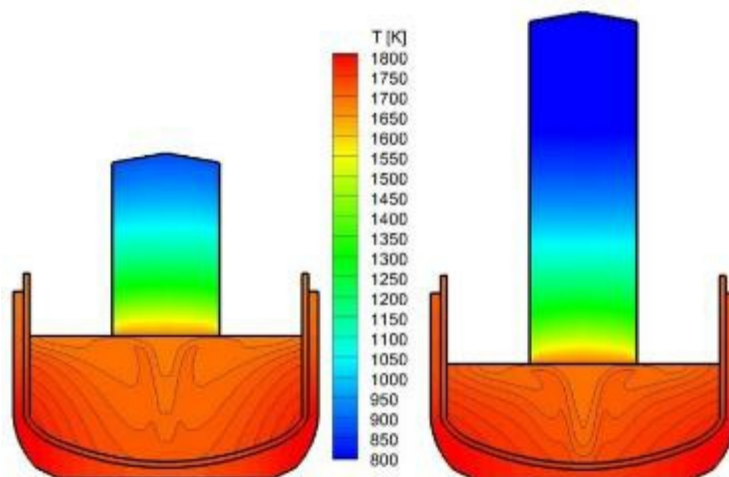
5:30 PM - 5:30 PM

TRANSIENT GLOBAL MODELING FOR THE PULLING PROCESS OF CZOCHRALSKI SILICON CRYSTAL GROWTH. I. PRINCIPLES, FORMULATION AND IMPLEMENTATION OF THE MODEL

X. Liu, H. Harada, Y. Miyamura, X. Han, S. Nakano, S. Nishizawa, K. Kakimoto

Research Institute for Applied Mechanics, Kyushu University, JAPAN
Transient global modeling of the Czochralski silicon (CZ-Si) crystal growth process has long been proposed for understanding the dynamic behaviors of the heat and mass transport in the crystallization set-up. Furthermore, segregation of impurities and dopants could also be predicted dynamically by the transient global simulation. However, most of the transient global simulations for CZ-Si crystal growth neglected the melt flow and mass transport due to the complexity of convection modeling. It is impossible to reproduce the segregation curves of the impurities and dopants without the predication coupled melt convection and mass transport. In the present study, the transient global model for the crystal pulling process was developed for CZ-Si

growth with the cusp-shaped magnetic field (CMF). Heat transfer by solid conduction, melt convection, and diffuse grey radiation is taken into account for the crystal, melt and other components in the furnace. The mesh adaption and view factor updating for the dynamic pulling process were realized by the structured grid deformations for different domains. The necking and tailing stages were neglected due to the difficulty of the varying crystal diameter. By imposing the thermal boundary conditions in the vicinity of the triple point, a virtual proportional integral derivative (PID) controller for the temperature was introduced to realize power control of the heater, which heated the lifting crucible. The applied CMF suppressed the turbulent melt flow and stabilized the heat and mass transport. The interface shape, the v/G ratio at the growth interface were dynamically predicted for the different pulling stages. This developed transient global model will be applied for the segregation predictions of impurities (oxygen and carbon) and dopants in CZ-Si growing process.



Local thermal fields of different solidified fractions: 20% solidified and 40% solidified.

5:30 PM - 5:30 PM

NUMERICAL STUDY OF THE HEAT AND OXYGEN TRANSPORT DURING A CZOCHRALSKI SILICON GROWTH USING DIFFERENT CRYSTAL-CRUCIBLE ROTATION CONDITIONS AND CUSP-SHAPED MAGNETIC FIELDS

T.H.T. Nguyen¹, J. Chen¹, C. Hu¹, C. Chen²

¹Department of Mechanical Engineering, National Central University,

TAIWAN, ²Research and Development Division, GlobalWafers Co., Ltd., TAIWAN

The industrial Czochralski furnace with cusp type magnet for growing 8-inch diameter single silicon crystals was used in this numerical study. The effects of a balanced/unbalanced cusp magnetic field (CMF) with crystal-crucible iso/counter-rotation on the heat, flow, and oxygen transport were investigated. Balanced or unbalanced CMF is indicated by the magnetic ratio (MR) defined as a ratio of the lower coil and upper coil current. In this work, MR1 and MR1.5 indicating a balanced and an unbalanced CMF, respectively, are considered. The simulation results show that the oxygen concentration along the crystal-melt interface gets more uniform in the case with a balanced CMF than the case with an unbalanced one under an iso-rotation condition with the crystal rotated faster than the crucible. Using an unbalanced cusp-shaped magnetic field and iso-rotation reduces significantly the formation of point defect. This is implied by decreasing significantly the Voronkov parameters. Moreover, a convex crystal-melt interface induced in iso-rotation cases is good for growing the defect-free crystals due to the outward diffusion of point defects from the central region to the edge of the ingot. The axial temperature gradient is enhanced in iso-rotation cases. This may allow the faster pulling of crystal from the silicon melt and prevent the super-cooling during the growth.

5:30 PM - 5:30 PM

COMPUTATIONAL STUDY OF HEAT TRANSFER, FLUID FLOW OF MELT AND GAS ATMOSPHERE DURING THE SEEDING PROCESS OF SAPPHIRE KYROPOULOS CRYSTAL GROWTH

S. Zermout¹, F. Mokhtari², A. Nehari³, I. Lasloudji²

¹Department of Mechanical Engineering, Mouloud Mammeri University of Tizi-Ouzou, B.P.17 RP, 15000, Algeria., ALGERIA, ²LTSE

Laboratory, University of Science and Technology Houari Boumediene, BP 32 Elalia, Bab Ezzouar, Algiers, Algeria., ALGERIA,

³Université de Lyon, Université Claude Bernard Lyon 1, CNRS, Institut Lumière Matière, F-69622 Villeurbanne, France., FRANCE

Oxide single crystals such as sapphire has widespread applications in

several fields such as lasers, nonlinear optics, substrates, and so on. The Kyropoulos (KY) method is one of the most important techniques for producing such single crystals. A successful growth of perfect single crystals requires the control of heat and mass transport in all media because the quality of the grown crystal is closely related to its thermal history and the transport phenomena in the furnace. For the seeding process of the Ky crystal growth of sapphire, the flow and temperature field as well as the seed-melt interface shape have been studied numerically using the finite element method. The configuration used in our Ky crystal growth process consists of a crucible, graphite susceptor, induction coil, insulation, melt and gas. At first, the electromagnetic field produced by the radio frequency (RF) coil in the whole system and the volumetric distribution of heat inside the graphite by Ohm's effect were calculated. Using this heat distribution as a source, the fluid flow and temperature field were determined in the whole system. We have considered two cases: (1) configuration without gas convection and (2) with gas convection. It was shown that gas convection influences markedly the temperature and flow field of the gas in the chamber and partly also in the melt. Doing these calculations, we try to find an optimal temperature distribution for the seeding process.

5:30 PM - 5:30 PM

TOWARDS CONTROLLING GROWTH INTERFACE SHAPE AND STABLE THERMAL FIELD IN THM GROWTH SYSTEM OF CDZnTE CRYSTAL

B. Hong¹, S. Zhang¹, L. Zheng¹, H. Zhang¹, C. Wang², B. Zhao²

¹Tsinghua University, CHINA, ²Ruiyan Technology Co. Ltd., CHINA

Thermal field is an important control factor in CdZnTe crystal growth since the low thermal conductivity of CdZnTe crystal makes it difficult for heat extraction from the growth interface while maintaining a stable interface. In this study, we focus on optimizing the thermal field to achieve stable crystal growth process by introducing a support with cold finger at the bottom of crucible. Both experiment and numerical simulation studies were carried out for CdZnTe crystal growth from Te-solution by the traveling heater method (THM). Several ingots with diameter of 27mm were grown by THM with/without crucible support.

The growth temperature is 750°C and the growth rate is 5mm/day. It is found that the surface temperature of crucible increases gradually with the pulling process of growth, caused by low thermal conductivity of CdZnTe crystal accumulated on the bottom of the crucible. Simulation results show that the changed temperature profile may lead migration of the growth interface and also increase the curvature of the growth interface, which is not favorable for stable growth of large grains. Subsequent simulation results indicate that a particular crucible support can stabilize the surface temperature profile of crucible, meanwhile the growth interface can be maintained at a relatively flat level with slight concave. A crucible support that consist of a hollow support and a cold finger with high thermal conductivity was designed to modify the thermal field. An ingot grown under the changed thermal field shows the formation of new grains after a period of crystal growth. A stable temperature profile and columnar crystal were observed in the improved experiment.

5:30 PM - 5:30 PM

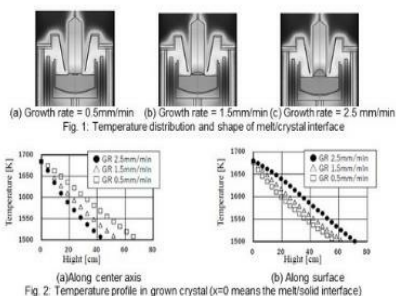
EFFECTS OF GROWTH RATE ON MELT/CRYSTAL INTERFACE SHAPE AND TEMPERATURE DISTRIBUTION IN GROWING CRYSTAL

S. Nishizawa, H. Harada, Y. Miyamura

Research Institute for Applied Mechanics, Kyushu University, JAPAN

Temperature distribution in the growing crystal is the most important parameter that determines the grown-in-defects, growth rate, etc. Abe et al discussed that temperature gradient in growing crystal at the melt/crystal interface decreases as increasing the growth rate, based on the experiment [1&2]. But in general understanding, higher growth rate leads to the larger thermal gradient. In this study, in order to make clear the reason of this discrepancy, the effects of growth rate on the shape of melt/crystal interface, and temperature distribution in growing crystal were investigated by numerical modeling. As show in Fig.1, as increasing the growth rate, the shape of melt/crystal interface becomes more convex toward the crystal. And Fig.2 shows that temperature gradient along center axis increases as increasing the growth rate. On the other hand, temperature gradient along surface decreases as increasing the growth rate. To obtain higher growth rate,

heat transfer should be enhanced. Along the center axis, heat transfer in vertical direction (conduction along the center axis) is dominant. Then convex interface shape and larger thermal gradient along center axis were obtained. Inside the grown crystal near the triple points, because of convex interface shape, heat transfer in radial direction, and radiative heat transfer from growing crystal become important. Then smaller thermal gradient along surface was obtained. This surface temperature profile agrees well with Abe's measurement results. It is cleared that (1) higher growth rate leads to the higher heat transfer, and (2) melt/crystal interface shape, and temperature distribution in growing crystal are determined by the balance of growth rate and heat transfer (conduction in vertical direction, and radiation in radial direction). [1] T.Abe, H.Harada and J.Chikawa, *Physica B*, **116**, 139 (1983). [2] K.Shirai and T.Abe, *J.Crystal Growth*, **351**, 141 (2012).



5:30 PM - 5:30 PM

PLATINUM DISSOLUTION MODEL IN PEM FUEL CELL

S. Sekine¹, K. Higashi², H. Kumei¹

¹Toyota motor corporation, Higashifuji technical center, JAPAN, ², JAPAN

In order to solve environmental issues, we have developed power sources including proton-exchange membrane fuel cells (PEMFCs). To improve the durability of PEMFC, maintaining the activity of catalysis and the electrochemical surface area (ECSA) are an

important matter. For this purpose, we develop a catalysts model of oxidation and dissolution of nanoscale platinum particles supported on carbon[1,2,3]. In this talk, we discuss the process of the change in particle distributions within the catalyst layer of PEMFC based on Ostwald ripening. During high potentials, Pt is dissolved as Pt ion; subsequently diffuses to larger particles in the ionomer phase. When the potential descends to a sufficiently low level, Pt ions are precipitated onto large Pt particles. In this process, the surface tension of the Pt particle is a very important parameter, but we cannot measure this value directly. In our model, this physical property is treated as a kind of fitting parameter. We would like to discuss how to measure these parameters. [1] R. M. Daring and J. P. Meyers, *J. Electrochem. Soc.*, 150,A1523 (2003). [2] R. M. Daring and J. P. Meyers, *J. Electrochem. Soc.*, 152,A242 (2005). [3] R. K. Ahluwalia, D. D. Papadias, N. N. Nariuki, J.K.Peng, X. P. Wang, Y. Tsai, D. G. Graczyk, and D. J. Myers, *J Electrochem Soc*, **165**, F3024 (2018).

5:30 PM - 5:30 PM

INFLUENCE OF ADDITIONAL INSULATION BLOCK ON MULTI-CRYSTALLINE SILICON INGOT GROWTH PROCESS DS FURNACE WITH ADDITIONAL BLOCK DS FURNACE FOR PV APPLICATIONS

N. S G, M. Srinivasan, P. Ramasamy
SSN College of Engineering, INDIA

Directional solidification process is the main process for producing the multi-crystalline silicon ingots. It is economically beneficial to grow the good quality mc-Si ingots with lower power consumption. We have carried out numerical simulation for analysing the impact of addition of an insulation block on the DS furnace. The addition of the insulation block has been implemented experimentally and the quality of the grown ingot was evaluated by the minority carrier lifetime measurement. Though the temperature gradient and hence the growth rate are higher in the insulation block added DS furnace, the generated dislocation density has not increased beyond the acceptable limit 10^8 1/m². The power used by the DS furnace has been reduced considerably by the addition of the insulation block. The good quality mc-Si ingot with higher minority carrier lifetime has been

obtained along with minimum power consumption by the addition of small insulation block in the DS system which could be put to beneficial use by lowering the manufacturing cost.

5:30 PM - 5:30 PM

MODELING OF VARIOUS CRUCIBLE AND SUPPORT SYSTEM DESIGNS FOR VERTICAL GRADIENT FREEZE GROWTH OF CDZNTe

O. Balbasi, M. Unal, D. Bender, M. Unalan, M. Parlak, R. Turan
Middle East Technical University, TURKEY

Cadmium Zinc Telluride ($\text{Cd}_{1-x}\text{Zn}_x\text{Te}$) has become a crucial material for X-ray and gamma ray detection due to its wide band-gap, high atomic number and high density, which offer high efficiency and sharp spectroscopic resolution at room temperature. In addition, due to being lattice matched, it can also be used as substrate for the epitaxial growth of HgCdTe, a critical semiconductor for high resolution infrared detection. Hence, increasing the single crystal yield of CdZnTe gained importance for further advancements in detector technology. In this study, an axisymmetrical global temperature model was created based on multi-zone Vertical Gradient Freeze (VGF) furnace at Middle East Technical University - Crystal Growth Laboratories (METU-CGL) and modeling approach has been applied to various growth crucible and support system designs along with different materials in order to achieve *the Cold Finger* effect. Conventional V-shaped, rounded V-shaped, flat-bottomed and hemispherical from geometrical point of view, quartz, graphite and pyrolytic boron-nitride from material point of view were compared. Combination of mentioned crucibles with multiple support system designs and materials such as graphite, platinum, silicon carbide and stainless steel were investigated for both temperature distribution and axial heat flux behavior. In addition, solid-liquid interface shapes were also investigated for quasi-stationary models to predict single crystal yields.

5:30 PM - 5:30 PM

REDUCTION OF THERMAL STRESS AND DISLOCATION DENSITY IN MC-SI INGOT USING HEATER MODIFIED DIRECTIONAL SOLIDIFICATION FURNACE

S. Sanmugavel¹, P. Ramasamy²

¹Research Centre, SSN College of Engineering, INDIA, ²SSN College of Engineering, INDIA

95% of the total PV production is based on wafer based silicon PV technology in which multi-crystalline silicon contributes 62%. The efficiency has been increased from 12% to 17% in the last decade for the wafer based modules. The efficiency of wafer based technology of 26.7% has been achieved using crystalline silicon whereas the multi-silicon holds 22.3%. Even though the efficiency of crystalline silicon based solar cell is higher, it is very difficult to grow crystalline silicon in industrial scale. Also it is high in cost. The growth of mc-Si is easier than the growth of mono-crystalline silicon. The directional solidification process is a widely accepted method for the growth of multi-crystalline silicon in industries. But because of the presence of grain boundaries, dislocations and impurities, the efficiency of the multi-crystalline silicon solar cells is lower than that of mono crystalline silicon solar cells. By reducing the defect and dislocation we can achieve high conversion efficiency. The present work focuses on the time dependent numerical simulation on the industrial directional solidification furnace for the growth of multi-crystalline silicon ingot using CGSim software. The thermal field will be controlled by the side heaters in order to get a high quality mc-Si ingot in the DS process. The temperature distribution of both conventional and modified DS process has been studied and the melt-crystal interface was analysed. The volumetric flow of the melt has been discussed. The influence of temperature distribution on the thermal stress has been investigated. The dislocation densities of both conventional and modified DS furnaces have been discussed.

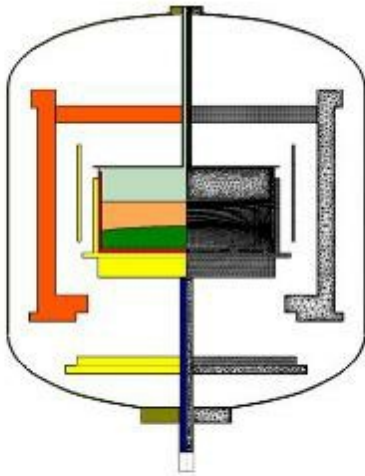


Fig. 1. Directional Solidification Furnace

5:30 PM - 5:30 PM

INFLUENCE OF ADDITIONAL SIZE INSULATION BLOCK ON MELT-CRYSTAL INTERFACE SHAPE IN DIRECTIONAL SOLIDIFICATION SYSTEM: NUMERICAL INVESTIGATION

G. Anbu, N. S G, M. Srinivasan, P. Ramasamy

SSN College of Engineering, INDIA

Heat transfer properties of Directional Solidification (DS) system are highly non-linear. Numerical simulation is the better way to solve such type of problems. Here we have carried out the numeration simulation for DS system for growing multi-crystalline silicon (mc-Si) ingot. Controlled dissipation of heat flux can determine the quality of mc-Si ingot. Thermal Stress, melt-crystal interface shape and dislocation density are the main factors that can determine the efficiency of solar cells. Thermal stress and dislocation density can be controlled by controlling of heat dissipation rate which can be employed by controlling of heater power and insulation opening rate during the solidification process. But controlling the same melt-crystal interface shape throughtout the solidification process is very challenging. The shape of melt-crystal interface plays main role which can determine the optimal grain growth and segregate the impurity atoms in beneficial way. The simulation resulsts revealed that the effective controll of melt-crystal interface shape has been obtained by establishing the additional insulation block in DS system. At particular

size of insulation block the optimal melt-crystal interface shape has been established during the solidification process which can enhance the mc-Si ingot quality.

5:30 PM - 5:30 PM

INFLUENCE OF ANNEALING TEMPERATURE DURING THE MC-SI SOLAR CELL FABRICATION

G. Aravindan¹, S. Sanmugavel¹, N. S G¹, V. Kesavan¹, M. Srinivasan¹, K.L. Narasimhan², B.M. Arora², R. P¹

¹SSN College of Engineering, INDIA, ²National Centre for Photovoltaic Research and Education, INDIA

The boron doped multi-crystalline silicon (mc-Si) ingot was grown using the directional solidification process. Grown ingots were converted into bricks and then to wafers. We have fabricated silicon solar cells from the multi-crystalline silicon wafers. The minority carrier lifetime of the wafers is around 15-25 ms. The investigation on the annealing temperature has been carried out. Annealing the device at 583⁰C for 5 sec gives better results. Typical open circuit voltage (V_{oc}) of the devices is around ~540-550mV. The best cell had a power conversion efficiency of ~9 % with a typical acceptor doping density ~ 2.35 E+15 per cm³ (The devices reported here do not have AR coating layer and the surfaces are also not textured).

5:30 PM - 5:30 PM

EFFECT OF SCHMIDT NUMBER ON MODELING OF MC- SILICON GROWTH PROCESS FOR PV APPLICATIONS

S. Manickam, P. Ramasamy
SSN Research Centre, INDIA

Multi-crystalline silicon is an important material with advantages of low production cost and high conversion efficiency of PV solar cells.

Numerical simulations have been performed on molten silicon during directional solidification for various Schmidt numbers at critical Prandtl number $Pr=0.01$. The simulation is performed in the framework of the incompressible Navier-Stokes equation with convection-conduction equations. The diffusion model is mainly used in this simulation. The computations are carried out in two-dimensional(2D) axisymmetric

model by the finite-volume method. Schmidt number is mainly used to study the mass transport phenomena. There is still no study on the Schmidt number during the mc-silicon growth process. In this paper, we have simulated and analysed the diffusion flux of impurities (Oxygen, Carbon and Nitrogen) and dopants (phosphorus, boron) for various Schmidt numbers $Sc= 0.5$, $Sc= 5$ and $Sc= 10$ during directional solidification of silicon process. It is used to control the formation of impurities and dopants in grown mc-silicon ingot. We have found that the Schmidt number $Sc=0.5$ is suitable for growing better quality mc-Si crystals. A global modelling of heat transfer was performed to study the melt/crystal interface, generation of creep stress and formation of dislocations in multi-crystalline silicon at the various growth stages for the various modified DS system. The aim is to reduce the impurities distribution and dislocation density. We have found suitable dimensionless numbers, bottom groove DS block and suitable insulation speed. The obtained simulation results may be used to grow the better quality mc-silicon ingot in the PV industry.

5:30 PM - 5:30 PM

GLOBAL MODELING ON MODIFIED CRUCIBLE SHAPE IN DIRECTIONAL SOLIDIFICATION PROCESS TO GROW THE HIGH QUALITY MC-SI CRYSTAL

M. Vishnuwaran, M. Srinivasan, V. Kesavan, P. Ramasamy
SSN College of Engineering, INDIA

Unlike silicon crystals used in the electronics industry, purity, crystal perfection and homogeneity need not necessarily be highest on the list of desirable attributes for crystalline silicon incorporated into commercial PV modules. The majority of PV solar cells are fabricated from bulk silicon crystals, which may be either single-crystalline or multi-crystalline. Multi-crystalline silicon (mc-Si) is an important material with advantages of low-production cost and high conversion efficiency. It has a market share of more than 60% in all photovoltaic materials. Directional solidification (DS) method has become the leading technique for producing mc-Si because of its better feedstock tolerance, higher throughput and easier operation. Solar cell efficiency is decreased by impurities, precipitates, and structural defects in the mc-Si ingots. The generation and distribution of these are investigated

using numerical analyses in this paper. A global modelling of heat transfer was performed to study the generation of various type of stresses, impurities and formation of dislocations in multi-crystalline silicon at the various growth stages for the modified crucible shape in DS system.

5:30 PM - 5:30 PM

EFFECT OF HEAT EXCHANGER BLOCK THICKNESS ON GROWN MULTI-CRYSTALLINE SILICON INGOT IN DIRECTIONAL SOLIDIFICATION PROCESS

T. M¹, N. S G¹, S. M¹, P. Ramasamy²

¹SSN COLLEGE OF ENGINEERING, INDIA, ²SSN College of Engineering, INDIA

Numerical investigation was carried out for analyzing the von-Mises stress of growing multi-crystalline silicon ingot during the Directional Solidification Process. DS furnace with Various thickness of heat exchanger block 10 mm, 20 mm, 30 mm, 40 mm, 50 mm, 100 mm, 150 mm, 180 mm, 200 mm, 220 mm, and 250 mm has been simulated and their response to solidification process has been analyzed. The axial and radial temperature, maximum principal stress, maximum shear stress study has been carried out for analyzing the von Mises stress distribution. By varying the thickness of the heat exchanger block the axial temperature distribution has been altered. From simulation results, we concluded that there should be a match with the axial and radial temperature gradient for getting the lower von-Mises stress. Here we have optimized the axial temperature distribution which is optimal to the radial temperature distribution for obtaining minimum von-Mises stress by changing the thickness of the heat exchanger block.

5:30 PM - 5:30 PM

ABSORPTION COEFFICIENT OF SAPPHIRE AT TEMPERATURES UP TO 1420 C.

A.G. Ostrogorsky

Illinois Institute of Technology, IL, UNITED STATES OF AMERICA
Infrared absorbance spectra of Al_2O_3 at temperatures up to 1420 °C were measured in an external tantalum furnace, under high vacuum (-10^{-6} Torr enclosure with ZnSe windows) using modulated radiation from the Fourier Transform Infrared (FTIR) spectrometer (Nicolet MAGNA 560). The IR transmission spectra were collected using 2 mm and 4 mm thick sapphire disks. The absorption coefficient of sapphire was determined by subtracting the spectra, thus eliminating the losses due to reflection. The range of wavelengths considered was $1.33 \mu\text{m} < \lambda < 16 \mu\text{m}$. In the 3.5 μm to 5.5 μm region, the transmittance of sapphire decreases with increasing temperature. The data are extrapolated to the melting point of Al_2O_3 and compared to the data available in the literature.

5:30 PM - 5:30 PM

CONTROL OF CRYSTAL SHAPE OF ORGANIC MATERIALS BY FEMTOSECOND LASER ABLATION

H.Y. Yoshikawa¹, D. Suzuki¹, C. Wu², J. Ikeyama¹, M. Yamaji¹, T. Sugiyama³, S. Nakabayashi¹

¹Department of Chemistry, Saitama University, JAPAN, ²Department of Applied Chemistry, National Chiao Tung University, TAIWAN,

³Graduate School of Materials Science, Nara Institute of Science and Technology, JAPAN

Control of crystal shape is crucial for various scientific and industrial fields such as X-ray/Neutron crystallographic studies, pharmaceuticals, optoelectronic devices, and food industries because these factors significantly influence quality, functionality, handling, and storage of end-products. However, due to relatively weak interaction natures of organic materials, it is still very challenging to obtain crystals with desired shape, even with the systematic optimization of environmental parameters such as temperature and concentration. In contrast, one

of the authors, Yoshikawa, have recently developed an innovative method for the promotion of crystal growth of proteins by locally destroying the crystal structures via laser ablation [Nat Photon 2016]. The paper reported that local etching (several micrometers in diameter) of protein crystal surfaces by femtosecond laser ablation enhances crystal growth rates without deterioration of crystal quality. The underlying mechanism can be explained by the generation of energetically favorable crystal growth mode (spiral growth mode), which is a fundamental growth mode for various organic crystals. Based on the previous demonstration with protein crystals, we now consider that femtosecond laser ablation may provide a new approach for control of shape of various organic crystals without complicated optimization of environmental parameters. In this presentation, we will introduce our recent development for the control of organic crystal shape by femtosecond laser ablation [Cryst Growth Des 2018 etc]. We here used small organic compounds, amino acids, which are basic components of proteins and used for various scientific and industrial fields such as pharmaceuticals and foods. Our systematic investigation clearly revealed that femtosecond laser ablation with energy close to ablation threshold can enhance growth rate of the irradiated crystal face with the minimum damage to crystal structure, which allows the shape control of single crystals of organic materials. In addition, in-situ monitoring of nanometer-scale crystal growth dynamics by advanced interference microscopy clearly revealed that crystal growth of not only proteins but also smaller organic compounds can spatiotemporally be controlled by the generation of spiral growth via femtosecond laser ablation. The fine-tuned, spatiotemporal cue given by femtosecond laser ablation will provide a facile means to obtain crystals of organic materials with desired shape.

5:30 PM - 5:30 PM

STUDY OF DIP CASTING FOR MULTI-CRYSTALLINE SILICON

C. Lan, H. Yang

Dept. of Chem. Eng., National Taiwan University, TAIWAN

The silicon wafer-based solar cells continue to dominate the photovoltaic market. However, the wafer cost remains high due to slicing and the kerf loss that wastes too much valuable polysilicon.

The dip casting, or the so-called crystallization on dipped substrate (CDS), is a potential technology that could further reduce the wafer cost. However, the progress of this technology is slow and the understanding of its fundamentals is rather limited. The dip casting uses a cold substrate to dip into the melt. Crystal growth is thus carried out on the substrate forming the multi-crystalline wafer. If the substrate does not stick with the wafer, the wafer could be easily detached and the substrate could be reused for the next dipping. The substrate and the melt temperatures, as well as the contact time, need to be carefully controlled, and the substrate materials needs to be carefully chosen for dip casting. In this report, some preliminary results will be presented for silicon dip casting, and the factors that control the thickness and smoothness, as well as the grain size, of the cast wafer will be discussed.

5:30 PM - 5:30 PM

SYNTHESIS, CRYSTAL CHARACTERIZATION AND PROPERTY ANALYSIS: AN INSENSITIVE HIGH ENERGETIC SALT OF DICARBOHYDRAZIDE BIS[3-(5-NITROIMINO-1,2,4-TRIAZOLE)]
D. Chen

Institute of Chemical Materials, China Academy of Engineering Physics, CHINA

The energetic salts based on nitrogen-rich heterocycles, especially the triazole or tetrazole ring, exhibits intrinsically lower vapor pressure, higher positive heat of formation, better thermal stability, and higher densities than their atomically similar nonionic compounds, so they have unique advantages in many aspects. CBNT is a typical triazole energetic ion salt, which consists of one carbonyl hydrazide cation and one BNT²⁻ anion, both are with two charges. The measured density of CBNT is 1.95 g cm⁻³ and the calculated detonation velocity is 9316.89 m s⁻¹, so it was considered as an alternative substitution of RDX. However, the single crystal of CBNT is very difficult to obtain and its crystal structure have not been revealed. Since carbonyl hydrazine contains two hydrazine groups, it can receive one or two protons to form monovalent or two valent cations. So, in order to verify whether BNT and carbonyl hydrazine can be combined in different ratios into new energetic salts, and to obtain more assistant information of

CBNT, we conducted experiments. The new compound may have similar characteristics and properties compared with CBNT. In the text, Dicarbohydrazide bis[3-(5-nitroimino-1,2,4-triazole)] (DCBNT) was firstly synthesized by ions exchange and salt formation reaction. A combination of single-crystal X-ray diffraction (SXRD), FTIR, ¹H NMR, ¹³C NMR, and elemental analysis was utilized to analyze the structural character and composition of DCBNT. DCBNT exhibits high detonation velocity of 9234.87 m s⁻¹ and detonation pressure of 31.73 GPa calculated by EXPLO5 v6.02 program. In addition, DCBNT was investigated in the aspect of sensitivities (impact sensitivity >40 J, H50 value of 90 cm and friction sensitivity is 216 N) and thermal stability (>230 °C). Moreover, we measured solubility of DCBNT in 12 common solvents by a polythermal method system which demonstrates its poor solubility in common organic solvents and water. These excellent physicochemical properties make DCBNT an environmental-friendly low sensitives high explosives.

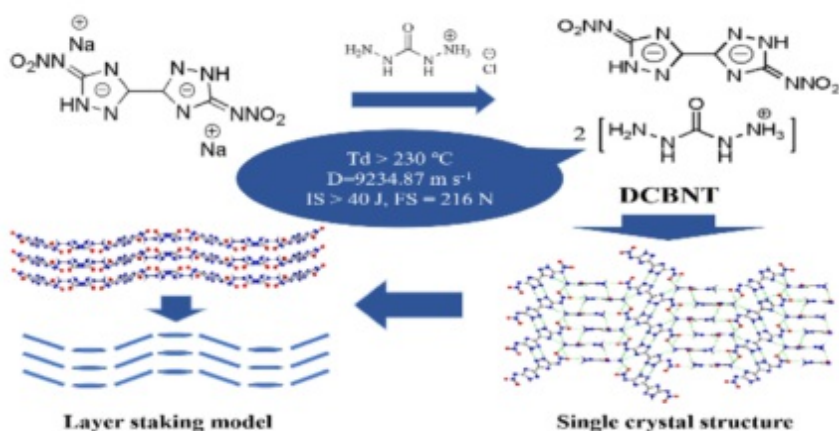


Fig.1 DCBNT, a new compound, exhibits low friction and impact sensitivities, good thermal stability, promising detonation pressure and detonation velocity.

5:30 PM - 5:30 PM

INNOVATIVE ELECTRIC CHARGE STORAGE MECHANISM: IDEAL METALLIC SUPERCAPACITORS

S. Kansara¹, S.K. Gupta², Y.A. Sonvane¹

¹Sardar Vallabhbhai National Institute of Technology, INDIA, ²St Xavier, INDIA

We report the first time that metallic homo-structure of aluminene (Al)

and antimonene (Sb) materials are the promising materials for the electric charge storage as a supercapacitor. In this work, we proposed two phases of capacitor namely hexagonal (H) - and trigonal (T) - phase. Here, we have investigated the electronic properties, visualization of molecular orbitals, van der Waals (vdW) energy between layers and supercapacitance properties such as dipole moment (P), charge stored (Qs), energy stored (Es) and capacitance (C). It is found that the Sb- bilayer has higher capacitance values than Al- bilayer. Our investigated energy storage, charge and capacitance values are in better agreement with the previously reported works. The capacitance values increased accordingly to the external electric field and behave as an ideal nanocapacitor. The results suggest that Al- and Sb- homo-bilayer could be flexible method for building nanoscale capacitor and nanocircuits.

5:30 PM - 5:30 PM

MAIN DIRECTION OF PHOTOELECTRIC CONVERTERS RESEARCH IN GEORGIA

L. Trapaidze¹, R. Chikovani², I. Trapaidze³, G. Goderdzishvili³, T. Minashvili²

¹Dep. of Physics, Tbilisi State University, GEORGIA, ²Dep. of Physics, Georgian Technical University, GEORGIA, ³Dep. of Physics, Georgian Technical University, GEORGIA

Georgia together with use of traditional energy resources attaches a very large importance of using renewable energy sources. Due to the geographical location of Georgia, the emanation of the Sun is rather high. Note, that the East part of Georgia it is sunnier than the West. Solar energy perspective for Georgia, because of its geographical allocation on the territory and application of solar energy is an important term for providing the population with the objects which are so important for life (supply with the energy the mountainous regions of small numbers of population). In most regions of the country there are 250-280 sunny days in a year, which is approximately 1900-2000 hours per year. The total annual solar energy potential in Georgia is estimated to be 108 MW. The prospects of development of photovoltaics in Georgia are analyzed. It is noted that the photoelectric

method of conversion of the solar energy based on semiconductor materials is especially promising. Main directions of research photoelectric convertors in Georgia are: Creation and use low power photoelectric convertors on the basis of Silicon. Processing of convertors on the basis of GaAlAs and other semiconductive compounds. At present it is very important to obtain high efficiency photoelectric convertors on the basis of these compounds with quantum dots and quantum wells creating in nanostructure. Research of possibility of creation high efficiency photoelectric convertors by using silicon-germanium. We've studied photoelectric convertors on the basis of silicon, also GaAlAs. After investigation we observed that convertor obtained on the basis of semiconductive compound of GaAlAs is more effective (2-2.5 times), than converter with silicon.

5:30 PM - 5:30 PM

ONE POT SYNTHESIS OF BI DOPED $\text{Cu}_2\text{ZnSnS}_4$ NANOPARTICLES

K. Rawat¹, K. Jha²

¹Department of Electronics, DDU Gorakhpur University, INDIA,

²Department of Physics, Bhagalpur college of engineering, INDIA

Among the various solar cell absorber materials, chalcopyrite semiconductor $\text{Cu}_2\text{ZnSnS}_4$ (CZTS) is a fascinating absorber because of the suitable narrow direct bandgap of ~ 1.50 eV with high absorption coefficient $> 10^4 \text{ cm}^{-1}$. In the previous works, bismuth (Bi) dopant has been introduced in absorber layers like CIGS, CdTe and SnS absorber material which resulted in the enhancement of electrical and optical properties of the absorber materials.

In this present work, Bismuth (Bi) doped $\text{Cu}_2\text{ZnSnS}_4$ (CZTS) nanoparticles were synthesized by a simple one pot chemical method with different doping concentrations. The x-ray diffraction patterns revealed the formation of nanoparticles with tetragonal kesterite single CZTS phase structure. It was observed that the incorporation of Bi has improved the crystalline quality of CZTS nanoparticles without altering their current phase. The average particle size was found to increase with doping concentration as measured by x-ray diffraction and Scanning electron micrograph (SEM) images. The diffraction peak of

(112) plane of CZTS was found to shift towards smaller diffraction angles with increasing dopant concentration. The Raman results also confirm the formation of CZTS phase and peak intensity found to increase with doping concentration. SEM images show the increase in uniform particle size of CZTS nanoparticles with Bi doping. These results indicate that the Bi dopant makes synergetic effects on CZTS absorber material properties for the applications in photovoltaics

5:30 PM - 5:30 PM

A UNIFIED MECHANISM OF ENHANCED MAGNETO-OPTIC AND MAGNETO-CALORIC EFFECTS

R. Li

Technical Institute of Physics and Chemistry, Chinese Academy of Sciences, CHINA

Both magneto-optic (MO) and magneto-caloric (MC) effects rely on the magnetic ions occupying the special sites of a given crystal lattice. As the main MO crystal for visible or near IR spectrum range, Tb^{3+} containing compounds like $Tb_3Ga_5O_{12}$ (TGG) are usually employed. Whereas, $Gd_3Ga_5O_{12}$ (GGG) is the preferable MC material for temperature range between 10-1K. We found in preferential cases, single ion anisotropy of Tb^{3+} ion can both enhance the MO and MC effects by 50% or more and more importantly can extend the working temperature of the MC material to above liquid hydrogen temperature. The theoretical analysis and experimental results of the model crystals will be presented and new direction to search for materials with improved properties will be discussed.

5:30 PM - 5:30 PM

PHASE FIELD MODELING OF BIOMINERALIZATION? MICROSTRUCTURE EVOLUTION IN MOLLUSK SHELLS AND CORAL SKELETONS

L. Gránásy, L. Rátkai, T. Pusztai

Wigner Research Centre for Physics, HUNGARY

We explore the question whether phase-field models developed for describing complex polycrystalline structures can be adapted to model crystallization in biological systems. We investigate two cases, where

detailed microstructural information is available from synchrotron experiments: the microstructure of mollusk shells [1] and coral skeletons [2]. In attempting to model these microstructures, we rely on phase-field techniques [3, 4] that were successfully applied to describe complex polycrystalline structures, such as spherulites, crystal sheaves, disordered dendrites, and fractallike polycrystalline aggregates and spiraling eutectic dendrites. We show that with appropriate choice of the model parameters microstructures resembling closely to the experimental ones can be obtained [5] (Fig. 1).

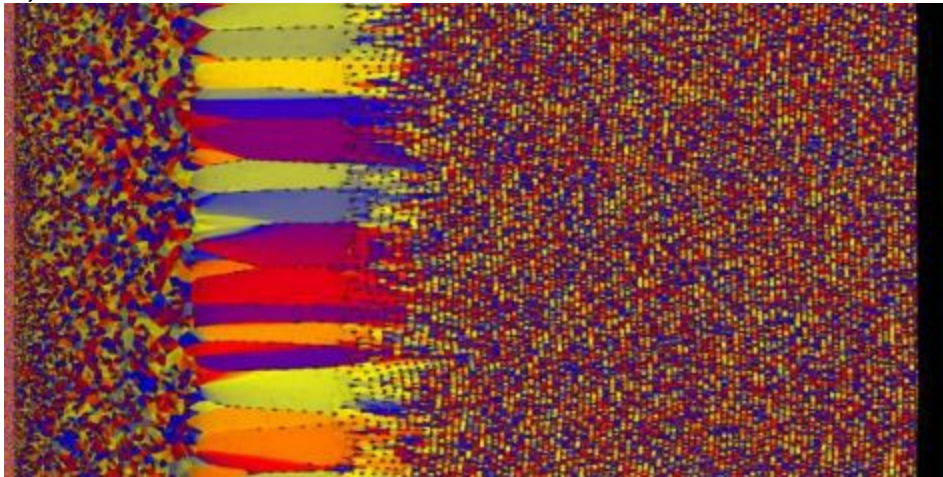


Fig.1: Predicted microstructure for mollusk shell. Different colors stand for different crystallographic orientation. [1] I. Zlotnikov, V. Schoeppler, *Adv. Funct. Mater.* **27**, 1700506 (2017). [2] C.-Y. Sun et al., *ACSNano* **11**, 6612 (2017). [3] L. Gránásy et al., *Nature Mater.* **4**, 650 (2004). [4] L. Rátkai et al., *J. Chem. Phys.* **142**, 154501 (2015). [5] V. Schoeppler et al., *Adv. Mater.* **30**, 1803855 (2018).

5:30 PM - 5:30 PM

GROWTH AND CONSISTENCY OF 5 INCHES $\text{Ca}_3\text{TaGa}_3\text{Si}_2\text{O}_{14}$ CRYSTALS

K. Xiong¹, Y. Zheng¹, X. Tu¹, S. Wang¹, T. Karaki², E. Shi¹

¹Shanghai institute of ceramics, CHINA, ²Toyama Prefectural University, JAPAN

As new sensor technology develops, searching for new kinds of high temperature piezoelectric crystals becomes increasingly urgent. Because of their high piezoelectric and excellent high temperature

properties. Langasite-type crystals are promising new piezoelectric materials for fabrication of sensors. Since the 1980s, crystals with langasite structure, such as disordered $\text{La}_3\text{Ga}_5\text{SiO}_{14}$ (LGS), and $\text{La}_3\text{Ga}_{5.5}\text{Ta}_{0.5}\text{SiO}_{14}$ (LGT), ordered $\text{Ca}_3\text{TaGa}_3\text{Si}_2\text{O}_{14}$ (CTGS), $\text{Ca}_3\text{NbGa}_3\text{Si}_2\text{O}_{14}$ (CNGS), $\text{Sr}_3\text{TaGa}_3\text{Si}_2\text{O}_{14}$ (STGS), $\text{Sr}_3\text{NbGa}_3\text{Si}_2\text{O}_{14}$ (SNGS), $\text{Ca}_3\text{TaAl}_3\text{Si}_2\text{O}_{14}$ (CTAS) and $\text{Ca}_3\text{NbAl}_3\text{Si}_2\text{O}_{14}$ (CNAS), have been grown and gained much attention. The ordered crystals possess lower dielectric permittivity and piezoelectric coefficients when compared to the disordered crystal. As the SAW devices develop toward large size and low cost, the crystal growth technology makes progress in larger size and lower cost. In this work, 5 inches CTGS crystals were grown by Czochralski technique along $\langle 110 \rangle$ and $\langle 100 \rangle$ direction. Polycrystalline materials were prepared by mixing of 4N pure CaCO_3 , Ta_2O_5 , Ga_2O_3 and SiO_2 powers at the stoichiometric ratio. The (110), (100) and (001) crystal faces are strongly exposed, and the growth rates of (001) is obviously faster than that of (110) and (100). The consistency of crystal quality, chemical composition and piezoelectric properties of the grown crystals will be studied.





Figure 1. The picture of as-grown CTGS crystals pulled along directions of (L) $\langle 100 \rangle$ and (R) $\langle 110 \rangle$.

5:30 PM - 5:30 PM

USE OF GOLD CLUSTERS TO CONTROL CONDUCTIVITY OF CHITOSAN MEMBRANES

R.P. Ramasamy

Department of Applied Science and Technology, Anna University,,
INDIA

Quantum clusters are an important area of research. In this research the effect of inclusion of protein encapsulated gold quantum clusters upon conductivity of chitosan membranes is studied. Chitosan solution (1 wt%) was prepared by adding 1 gm of chitosan to 100 ml of water containing 1.5 gm of acetic acid. The solution was stirred for 30 min for the chitosan powder to dissolve completely. Upon drying, the chitosan solution formed films. Protein templated gold nanoparticles were prepared by the following method. Bovine serum albumin (BSA) was dissolved in water to have a concentration of 25 mg/ml. To this solution 100 mM chloro-auric acid was added in drops while stirring to have a final concentration of 5 mM. To this solution appropriate amount of NaOH was added to have NaOH concentration of 50 mM. The solution was stirred for 12 hours. It was then dialyzed using dialysis membrane in water to have a pH of 7 and the solution was freeze dried to obtain a red powder. The powder glowed red under UV

light indicating the formation of fluorescent gold quantum clusters. The as obtained quantum clusters were added in different amounts to chitosan solution and then cast as films. It was observed that the relaxation behavior, conductivity and morphology of the chitosan films were influenced by the presence of gold quantum clusters. A detailed temperature dependent analysis (30 -100 deg C) for dielectric analysis were also carried out. Various characterization techniques such as SEM, XRD, Dielectric relaxation spectroscopy, FTIR were used for this research. This research could benefit the use of gold clusters in energy storage technology.

5:30 PM - 5:30 PM

MODELING BIMETALLIC OXIDE NANOSTRUCTURES.

O.M. Chernikova

Kyryviy Rih National University, UKRAINE

Of particular interest are fuel cells (PEs), which are an integral part of energy devices. As a catalytic component in PE, as a rule, use platinum. Its main disadvantages include degradation during long-term work in the PE, as well as high cost. The solution of these problems is associated with the development of multi-component catalytic systems based on platinum with the inclusion of other metals. The strategies of their development really depend on a detailed understanding of the mechanisms of oxidation of fuel and the recovery of oxygen [1]. The direct relationship between activity on Pt-based RVC catalysts and Pt-M catalysts from the distances between the immediate Pt-Pt layers has been described in many papers. The smaller the distance, the stronger is the catalytic activity relative to the RVC [2]. We study the physical mechanisms of heterogeneous catalytic oxidizing reactions methanol oxidation with using bimetallic film layered mechanically strained PtNi and PtCu-based catalysts. The main research methods are theoretical calculations based on the density functional theory and the "ab initio" pseudopotential method. According to the results of calculations using the author's software code [3], the mechanical stress and the presence of dissociated oxygen have the greatest impact on increasing electron bimetallic catalyst activity during the oxidation of methanol with using bimetallic layered mechanically strained PtNi and PtCu-based catalysts. The compression of the

platinum film pushes the electron density outside the film and it gives the density an elongated form and increases the chemical and absorption activity of the film. The methods of the functional of electron density and pseudopotential from the first principles obtained distributions of the density of valence electrons and electronic energy spectra of bimetallic catalysts on the basis of Pt to determine the mechanisms of their increased catalytic activity. It was found that mechanical stresses and the presence of dissociated oxygen play the greatest influence on the increase of the electronic activity of the catalyst.

References 1. Yoshiyuki Show, Yutavo Ueno Formation of platinum catalyst on carbon black using on in-liquid plasma method for fuel cells// J. Nanomaterials, 2017, V.7, pp. 31-40. 2. Kuln S., Strasser P. Oxygen electrocatalysis on dealloed Pt nanocatalysts // Springer Catalysis J., 2016, V. 59, pp. 1628-1637. 3. Balabay RM, Grishchenko N.V. A complex of programs for calculations of ab-initio solid-state structures // Photoelectronics. 1998. №8, pp. 25-29.

5:30 PM - 5:30 PM

SURFACE OXIDATION OF TI PLATES BY USING MICROWAVE PLASMA HEATING SYSTEM

J. Yamanaka¹, M. Shirakura¹, Y. Miyazawa¹, S. Shinozuka¹, M. Katsumata¹, T. Takamatsu², T. Arai¹, K. Nakagawa¹

¹University of Yamanashi, JAPAN, ²SST Inc., JAPAN

We developed our original microwave-plasma heating system which distinctive characteristic is that no matching system was installed. We realized to heat transition metals up to 1000C in a few seconds by using this system. We have been applying this new equipment mainly for local heating of metal-semiconductor specimens in previous. We utilized this machine for surface oxidation of Ti plates in this study, as a new application of this system. Commercially available Ti foils and plates were used for this study. First, the Ti foils/plates were cut into 10 mm squared. Second, the Ti foils/plates were deoxidized in hydrogen plasma atmosphere to remove their natural oxide on the surface. After this treatment, the specimens were oxidized in oxygen-plasma atmosphere under various pressure/gas-flow-rate conditions.

The duration time of the oxidation was 10 to 150 seconds. We checked the uniformity of each specimen using an optical microscope. Optical micrographs showed that most of the specimens were uniform. Then selected specimens, they all showed uniform color, were characterized using X-ray photoelectron Spectroscopy (XPS) and it was revealed that the surface oxide layer was TiO_2 . We also carried out cross-sectional transmission electron microscopic (TEM) observations. We used a 200 kV type FE-TEM (FEI, Tecnai Osiris) equipped with a super high-sensitivity energy dispersive X-ray spectroscopy (EDX). TEM images exhibited that the surface oxide layers were about 50 nm or less and they were very uniform in each specimen. As a cross-check of the XPS, we carried out EDX analysis and it was also indicated that the oxide was TiO_2 . In conclusion, we were succeeded in producing very uniform thin TiO_2 on the Ti surface by using our original microwave-plasma heating system. It is considered that our plasma system are very useful for surface treatment of metals and alloys.

5:30 PM - 5:30 PM

BROMINE-METHANOL ETCHING: AN EXPERIMENTAL STUDY ON THE EFFECTS OF CHEMICAL POLISHING ON SURFACE PROPERTIES OF CDZnTE CRYSTALS

M. Unal¹, D. Bender¹, M. Unalan¹, O. Balbasi², M. Parlak¹, R. Turan¹
¹Crystal Growth Laboratory, TURKEY, ²Physics Department, TURKEY

Cadmium Zinc Telluride ($\text{Cd}_{1-x}\text{Zn}_x\text{Te}$) semiconductor crystals have gained attention in the field of X-ray and gamma-ray detection applications over the past years owing to developments in crystal growth and preparation processes. Unlike Si and Ge semiconductors, CdZnTe detectors can operate at room temperature due to its wide band-gap, high atomic number and high density. In addition, by changing the fraction of Zn content in the crystal matrix, both mechanical and electrical properties of the crystal can be altered. For an optimal CdZnTe detector to be used in X-ray and gamma-ray detection systems, Zn concentration is usually kept around 10%. In the detector crystal preparation process, surface condition is crucial to

be able to obtain successful metallic contacts and low leakage currents. Mechanical lapping and polishing remove damage due to wire saw and flattens the surface. However, all mechanical processes on CdZnTe creates a damaged and contaminated layer over crystalline CdZnTe in addition to surface oxide. In this study, we present an attempt to remove damaged overlayer by bromine-methanol solution with 1% concentration. The effect of chemical polishing on surface properties were also investigated. Surface properties of the crystals were characterized by scanning electron microscopy, atomic force microscopy and X-ray photoelectron spectroscopy. In addition, CdZnTe crystals were investigated by photoluminescence spectroscopy to be able to observe the effect of chemical process on defect centers on the crystal. Moreover, I-V characteristics comparison study has been conducted between a crystal that was chemically etched by bromine-methanol solution and a crystal that was only mechanically polished.

5:30 PM - 5:30 PM

GROWTH AND PIEZOELECTRIC PROPERTIES OF LARGE SIZE $\text{Ca}_3\text{Ta}(\text{Al}_{0.5}\text{Ga}_{0.5})_3\text{Si}_2\text{O}_{14}$ CRYSTALS WITH LANGASITE STRUCTURE

K. Xiong¹, Y. Zheng¹, X. Tu¹, S. Wang¹, T. Karaki², E. Shi¹

¹Shanghai institute of ceramics, CHINA, ²Toyama Prefectural University, JAPAN

Piezoelectric materials have been widely used in sensors, resonators, filters and so on. Recently, because of the advantage of excellent high-temperature piezoelectric properties, high resistivity and high-temperature stability, langasite-type crystals have been gained huge attention and become promising materials for ultrahigh-temperature applications. However, the high content of gallium made these crystals much more expensive compared than quartz, so their application are limited strongly. Fortunately, ordered single crystals $\text{Ca}_3\text{TaAl}_3\text{Si}_2\text{O}_{14}$ (CTAS) and $\text{Ca}_3\text{NbAl}_3\text{Si}_2\text{O}_{14}$ (CNAS) were grown by Czochralski method successfully, and the cost of raw materials is similar to that of quartz while its piezoelectric property are much better than that of quartz. But the growth of CTAS single crystals is much more difficult

than that of $\text{Ca}_3\text{TaGa}_3\text{Si}_2\text{O}_{14}$ (CTGS). In order to overcome the difficulty, 50% Al^{3+} ions were substituted with Ga^{3+} ions in CTAS crystals, and $\text{Ca}_3\text{Ta}(\text{Al}_{0.5}\text{Ga}_{0.5})_3\text{Si}_2\text{O}_{14}$ (CTAGS) single crystals still have the advantage of low cost of raw materials. The CTAGS single crystal was grown by Czochralski technique. The single crystal was grown along $\langle 110 \rangle$ direction using a CTGS crystal as seed, with pulling and crystal rotation rates being in the range of 0.3-1 mm/h and 15-20 rpm respectively. At the end of growth, the crystals were cooled down to room temperature at a rate of 35 °C/h. The obtained CTAGS crystal with the dimensions of 65 mm in thickness, 78 mm in width and 136 mm in length is shown in Figure 1. The single crystal was transparent and slightly green. In this work, the structure, crystal quality, chemical composition, piezoelectric properties, electric resistivity and optical properties of the grown crystals were studied.



Figure 1. The picture of as-grown CTAGS single crystal.

5:30 PM - 5:30 PM

IMPURITY SEGREGATION AT MISORIENTED $\Sigma\{111\}$ TILT BOUNDARIES IN HIGH-PERFORMANCE SI

Y. Ohno¹, T. Tamaoka², S. Takeda², Y. Shimizu¹, N. Ebisawa¹, K. Inoue¹, Y. Nagai¹, K. Kutsukake³, N. Usami⁴

¹IMR, Tohoku University, JAPAN, ²ISIR, Osaka University, JAPAN,

³RIKEN, JAPAN, ⁴GSE, Nagoya University, JAPAN

Grain boundaries (GBs) are inevitably introduced in polycrystalline silicon (Si) ingots for solar cells, and they have substantial influences on electronic properties, such as carrier recombination activity, via the segregation of impurity atoms. Especially, asymmetric GBs with higher GB energy are frequently introduced in Si ingots, and they severely degrade the photovoltaic properties since they have a large segregation ability for impurity atoms with respect to low-energy symmetric GBs [1]. Therefore, a comprehensive knowledge of their segregation ability, depending on their atomistic structure, is indispensable to produce cost-effective high-efficiency solar cells by controlling the formation of detrimental GBs.. We examined asymmetric $\Sigma\{111\}$ GBs in which the tilt angle and the GB plane orientation were off from their ideal values, in a high-performance Si ingot for commercial solar cells. Those asymmetric $\Sigma\{111\}$ GBs had a high carrier recombination activity, even when the degree of misorientation was small. The activity evaluated by photoluminescence imaging was as high as ~ 0.6 for an asymmetric $\Sigma\{111\}$ GB whose tilt angle was slightly off from the ideal angle of 70.5° . Most parts of the asymmetric GBs were composed of arrays of GB dislocations lying on the symmetric $\Sigma\{111\}$ GB segments. Oxygen atoms would segregate at the atomic sites under tensile stresses above about 2 GPa, which were introduced along the GB dislocations [1]. Small amount of carbon atoms also segregated, while they would locate only nearby the dislocation cores. Considering that the effect of oxygen atoms segregating at GBs on the recombination activity is rather small [2], carbon atoms segregating at GB dislocations would severely influence the recombination activity. We also found an asymmetric $\Sigma 3$ GB whose GB plane was off from $\{111\}$; it was composed of nanofacets lying on $\{111\}$ and $\{112\}$. Even though the faceted GB would have a high segregation ability due to strains around the edges of the nanofacets [3], its recombination activity of ~ 0.3 was smaller in comparison with dislocated GBs. This result suggests that the misorientation in the tilt angle, rather than that in the GB plane orientation, would impact on the recombination activity, as well as on the segregation ability of GBs. [1] Y. Ohno, *et al.*, J. Microsc. **268** (2017) 230. [2] Y. Ohno, *et al.*, Appl. Phys. Lett. **109**

(2016) 142105. [3] C. L. Liebscher, *et al.*, Phys. Rev. Lett. 121 (2018) 015702.

5:30 PM - 5:30 PM

INFLUENCE OF GROWTH INTERRUPTION ON INGAP GROWN BY HYDRIDE VAPOR PHASE EPITAXY

Y. Shoji¹, R. Oshima¹, K. Makita¹, A. Ubukata², T. Sugaya¹

¹National Institute of Advanced Industrial Science and Technology, JAPAN, ²Taiyo Nippon Sanso Corporation, JAPAN

III–V multi-junction solar cells have achieved the high conversion efficiency exceed to 40%. Currently, metal organic vapor phase epitaxy (MOVPE) is a mainstream to fabricate these devices. However, their applications are still limited to space and concentrator devices due to expensive manufacturing cost and low throughput performance. Hydride vapor phase epitaxy (HVPE) can reduce the deposition cost because the group III materials are supplied through the reaction of less-expensive pure metals with the hydrogen chloride (HCl) gas with high material utilization efficiency. Furthermore, it can attain a high growth rate of ~100 mm/h. Up to date, we demonstrated InGaP single-junction solar cells with 12.4% efficiency using our HVPE. In order to improve the cell performance, control of InGaP/InGaP interfaces would be a key factor. This study focuses on the influence of growth interruption on InGaP/InGaP interfaces. In our HVPE system (H260, Taiyo Nippon Sanso), the reactor consists of two growth chambers and a preparation chamber; each growth chamber is used for GaAs or InGaP deposition. The preparation chamber is placed between two growth chambers and is used for the growth interruption under AsH₃ and PH₃ supplies until the gas flow is stabilized in each growth chamber. Undoped 1.6 mm thick-InGaP layer on the GaAs (100) substrates miscut 4° toward (111)B at 660°C were fabricated. We compare two kinds of InGaP layers; one is a continuously grown InGaP film and the other is a film grown with four times of growth interruptions for 18 s in the preparation chamber under PH₃ supply at each 0.32 mm thickness. Finally, both samples were capped by thin GaAs layers. GaCl and AsH₃ gases were continuously supplied at the GaAs growth chamber during the InGaP

deposition to grow the cap layer without any interruption. A time resolved photoluminescence of the sample with growth interruption showed a shorter decay of 0.10 ns compared than that of 0.72 ns for the continuously grown sample. From the scanning transmission electron microscope-energy dispersive X-ray analysis, we observed that 3~4% of P atoms were replaced with As atoms at the InGaP/InGaP interfaces. It is likely that thin InGaAsP layers were unintentionally formed at the interfaces caused by the contamination from either the neighbor GaAs growth chamber or the preparation chamber.

5:30 PM - 5:30 PM

MID-INFRARED EMISSION PROPERTIES OF ER³⁺/EU³⁺: PBF₂, ER³⁺/TB³⁺: PBF₂ AND ER³⁺/ND³⁺: PBF₂ CRYSTALS

P. Zhang, Z. Chen, Z. Li
Jinan University, CHINA

Mid-infrared laser, especially ~3μm laser, is widely used in the fields of optical communication, sensing technology, medical surgery owing to the strong absorption peak of water at this wavelength. Meanwhile, Er³⁺ is a well-known candidate for ~3μm lasers, which corresponds to the transition from ⁴I_{11/2} to ⁴I_{13/2} level. However, a detrimental self-termination bottleneck effect is possible for this transition, owing to the much longer lifetime of the ⁴I_{13/2} level than that of the ⁴I_{11/2} level.

Therefore, a series of methods were used to enhance the intensity of photoluminescence around 2.7μm, including co-doping with other rare-earth ions, such as Tm³⁺, Ho³⁺, Pr³⁺. In the current work, we find Eu³⁺, Tb³⁺, Nd³⁺ ion as deactivator to quench the lower level of Er³⁺:

⁴I_{13/2}. As far as we know, the use of Eu³⁺, Tb³⁺, Nd³⁺ co-doped for the enhancement of the transition of Er³⁺: ⁴I_{11/2} → ⁴I_{13/2} ~3μm emissions

was observed in the PbF₂ laser crystal for the first time. The Er³⁺:

PbF₂, Er³⁺/Eu³⁺: PbF₂, Er³⁺/Tb³⁺: PbF₂, Er³⁺/Nd³⁺: PbF₂ single crystals were successfully grown by using the Bridgman method, and the crystals' fluorescence emission properties and energy transfer mechanisms of series crystals were investigated. In the Er³⁺/Eu³⁺:

PbF₂ single crystal, the Eu³⁺ ion depopulates the lower laser level of Er³⁺: ⁴I_{13/2}, and has little effect on the upper laser level of Er³⁺: ⁴I_{11/2} at the same time. Moreover, the energy transfer efficiency from the Er³⁺: ⁴I_{13/2} level to the Eu³⁺: ⁷F₆ level is as high as 88.07%. In addition, Tb³⁺ greatly increased Er³⁺ 2.7μm emission by depopulating the Er³⁺: ⁴I_{13/2} level while having little influence on the Er³⁺: ⁴I_{11/2} level, and the energy transfer efficiency from Er³⁺: ⁴I_{13/2} to Tb³⁺: ⁷F₀ is as high as 90.27%, indicating that Tb³⁺ ion is an excellent deactivator with which self-termination bottleneck effect was effectively suppressed. In the Er³⁺/Nd³⁺: PbF₂ single crystal, the lower energy level of Er³⁺: ⁴I_{13/2} has been depopulated through the Nd³⁺ ion, and the upper energy level of Er³⁺: ⁴I_{11/2} has been populated at the same time. Simultaneously, the energy transfer efficiency from the Er³⁺: ⁴I_{13/2} level to the Nd³⁺: ⁴I_{15/2} level is 84.06%, and from the Nd³⁺: ⁴F_{3/2} level to the Er³⁺: ⁴I_{11/2} level is 55.81%, respectively. These advantageous spectroscopic characteristics suggest that these crystals are likely to be promising materials for 2.7μm laser applications.

5:30 PM - 5:30 PM

SOLVOTHERMAL SYNTHESIS AND CHARACTERISTICS OF KTA0.63NB0.37O3 AND CU/FE DOPED KTA0.63NB0.37O3 NANOPARTICLES

Y. Yang, H. Yu, X. Wang, L. Wei, B. Liu

Advanced Materials Institute, Qilu University of Technology
(Shandong Academy of Sciences), CHINA

KTa_{0.63}Nb_{0.37}O₃ (KTN), Cu doped KTN and Fe doped KTN particles were synthesized by a mixed solvothermal method at 200°C for 24 h. The phase and microstructure of the synthesized particles were investigated by XRD and TEM measurements. The effects of Cu and Fe doping on the phase and microstructure of the synthesized particles were also investigated. The TEM images show that the synthesized pure KTN, Cu doped KTN and Fe doped KTN particles have the cubic morphology and the particles sizes are in the range of

nanometer. The doped Cu and Fe lead to the changes of lattice parameters and grain sizes of KTN particles. Moreover, the doped Cu and Fe help to the homogeneous distribution of the synthesized KTN particles. When the doping concentrations of Cu and Fe are respectively higher than 1.5mol% and 1.8mol%, impure phase is formed in KTN particles.

5:30 PM - 5:30 PM

NUMERICAL STUDY OF SURFACE WAVES ENHANCED SILICON REFINEMENT FOR SOLAR GRADE SILICON PRODUCTION

V. Geža, Ģ. Zāģeris, V. Dzelme

University of Latvia, LATVIA

One of the most perspective methods to produce solar grade silicon is refinement via the metallurgical route. The most critical part of this route is refinement from boron and phosphorus due to high segregation coefficients. One possible approach to remove boron is the use of reactive gas on the surface of the silicon melt. An approach of creating surface waves on silicon melt's surface is proposed in order to enlarge its area and accelerate the removal of boron via chemical reactions. This paper focuses on the numerical analysis of surface wave creation by means of the low-frequency electromagnetic field. A coupled numerical model is presented which accounts for time-harmonic electromagnetic field and force and calculates the shape of the free surface. Results show that the frequency of the magnetic field and its amplitude significantly change the character of surface waves with most changes occurring when waves become nonlinear. Another question of interest is the dependence of boron removal rate on the surface wave character, amplitude, and total surface area. Boron removal rate is strongly dependent on surface wave amplitude, and if the amplitude is smaller than a certain threshold, which is determined by diffusion length, there is no enhancement of removal rate.

5:30 PM - 5:30 PM

PROGRESS IN STUDY OF POTASSIUM TANTALATE NIOBATE SERIES CRYSTALS AS QUADRATIC ELECTRO-OPTIC MATERIAL

X. Wang¹, Y. Yang¹, L. Wei¹, J. Wang²

¹Advanced Materials Institute, Qilu University of Technology (Shandong Academy of Sciences), CHINA, ²Shandong University, CHINA

Electro-optic crystal is one of the basic materials of all-solid-state laser, which can be used to modulate the laser propagation characteristic. Electro-optic modulation has a lot of advantages such as high efficiency, good stability, quick response and inertialessness etc. Development of novel highly efficient electro-optic crystal is of great significant for the all-solid-state laser technique. Potassium Tantalate Niobate crystal is a famous multifunctional crystal, which remarkable for its electro-optic effect and photorefractive effect. In this work, a Kerr-Effect-Enhanced Cu:KTN crystal with gradient refractivity effect was prepared by the ion doped method. The physical mechanism of Kerr-effect-enhance and refractivity-amplify effect in Cu:KTN crystal have been investigated. An abnormal laser deflection phenomenon in the crystal is demonstrated. A near-50 mrad beam deflection angle is observed when a voltage of 1.2 kV was applied to a Cu:KTN block with size of 2.8 mm×1.2 mm×7.5 mm at room temperature. The special features of this deflection phenomenon are that the laser beam deflection direction is perpendicular to the electric field direction, and the beam deflection angle remains unchanged when the electric field direction is reversed. The operating principle of the phenomenon is investigated and the origin of the deflection phenomenon is attributed to an interaction between the graded refractivity effect and the quadratic electro-optic effect of the crystal. Ion doping method to format the great and uniform refractive index gradient is a promising discovery in E-O materials and laser scanner investigation field.

Monday, July 29, 2019

7:30 PM - 9:30 PM

Advanced MOCVD Technology for the Future

Location: Torrey Peak II-IV

Session Chair(s): Masakazu Sugiyama, Akinori Ubukata

7:30 PM - 8:00 PM

HIGH TEMPERATURE OMVPE FOR NEW MATERIALS GROWTH

G. Tompa¹, M.E. Tawfik¹, A. Feldman¹, T. Salagaj¹, L..G. Provost¹,
A.C. Arjunan¹, K. Li², X. Li², S. Watkins³, M. Hegde³

¹Structured Materials Industries, Inc., NJ, UNITED STATES OF AMERICA, ²King Abdullah University of Science and Technology (KAUST), Advanced Semiconductor Laboratory, SAUDI ARABIA,

³Department of Physics, Simon Fraser University, BC, CANADA

The successful development and advancement of thin film materials often hinges not only on the tools to produce them; but also on the reasonableness of subsequently scaling the processes developed in such tools. OMVPE is one of the primary tools used in the production of semiconductor (II-VIs, III-Vs, III-nitride, III-oxides, and IV-IVs) and optical materials, superconductors, TCOs, TMDCs/chalcogenides, and metal fluorides, among many other materials. While the OMVPE principles are largely the same – these diverse material systems span a wide range of atmospheres that may be reactive/corrosive and temperatures that may range from a few hundred degrees to >2000 °C and thus require unique process environment materials of construction. Researchers also need economically flexible tools that can easily adapt from one material system to another in response to evolving materials of interest. The two main scalable heating methodologies are filament and induction heating with each having benefits (notably higher temperatures are achievable with induction heating) and detriments (notably temperature uniformity is more difficult to achieve with induction heating), which we will review in this work. We will also review our recent design developments for elegantly achieving film uniformity for a broad uniform heating temperature range with a common showerhead for each of the aforementioned environments/material systems. The resultant tool has provided a simple, common platform, means for researching multiple materials. We also compare the trade-offs between using interchangeable induction heated susceptors versus interchangeable filament heated assemblies.

8:00 PM - 8:30 PM

GROWTH OF HIGH PURITY GAN FOR VERTICAL ELECTRON

DEVICES AND CHARACTERIZATION OF ELECTRON AND HOLE TRAPS

T. Narita¹, K. Tomita¹, K. Kanegae², M. Horita³, Y. Tokuda⁴, T. Kogiso⁴, H. Yoshida⁴, T. Kachi³, J. Suda²

¹Toyota Central R&D Labs. Inc, JAPAN, ²Kyoto University, JAPAN,

³Nagoya University, JAPAN, ⁴Aichi Institute of Technology, JAPAN

Reduction of energy consumption is crucial for sustainable human development and has been investigated. A GaN-based vertical power device is one of the key components to achieve highly-efficient energy conversion in high-power systems such as hybrid/electric vehicles. To obtain the ideal on-state resistance and the blocking voltage based on the simulation, we have investigated the growth technology of highly-pure GaN crystal involving the well-controlled donor/acceptor impurities and the sufficiently-reduced sources of carrier compensation. Recent growth technology allows a fine doping control of donor/acceptor impurities, while the effective donor/acceptor concentrations can be modified by traps compensating carriers. Moreover, their traps are generally varied from position-to-position in a wafer. Therefore, the accurate estimation of trap concentration at each position is required. In the case of n-type GaN, the electron and hole traps around $E_C - 0.6$ eV and $E_V + 0.88$ eV act as compensation sources, where the latter hole trap is assigned as an acceptor-like state of a carbon on nitrogen site (C_N). The concentration of electron trap at $E_C - 0.6$ eV can be mapped by the isothermal capacitance transient spectroscopy (ICTS) using a conventional capacitance meter, indicating a small concentric variation below 10^{14} cm⁻³ in a wafer. The well-controlled growth condition allows suppressing carbon concentration ($[C]$) of a few times 10^{15} cm⁻³. However, it is difficult to evaluate the hole trap concentration due to C_N because holes are absent in an n-type epilayer. Thus, p-n junction structure to inject holes or hole excitation using light source is required to estimate the trap concentrations. We have suggested the optical ICTS using hole captures generated by illuminating a sub-bandgap light source, allowing uniform excitation under the measured electrode. However, the illumination simultaneously leads to hole emissions, resulting in the hole filling factor below unity. By comparing the trap

concentrations obtained from the optical ICTS and the ICTS using a current pulse for a p-n diode, we successfully determined the accurate hole trap concentration corresponding to [C]. We also revealed that a C_N has a donor-like charged state compensating a hole at $E_V + 0.29$ eV. Accordingly, two different charged states originating from the identical C_N can compensate an electron and a hole in n-type and p-type layers, respectively. The trap concentration due to the C_N in a p-type GaN exhibited concentric distribution plausibly resulting from the wafer rotation during MOVPE-growth. This work was supported by MEXT GaN R&D Project and by CSTI-SIP funded by NEDO.

8:30 PM - 8:50 PM

FILTERED AND UNFILTERED RESTRICTIVE FLOW ORIFICES IN THE DELIVERY OF ELECTRONIC PROCESS GASES

R. Wind¹, M. Raynor¹, D. Scott²

¹Matheson Gas Products, CO, UNITED STATES OF AMERICA,

²Matheson Gas Products, PA, UNITED STATES OF AMERICA

Restrictive flow orifices (RFOs) installed in cylinder valve outlets of pyrophoric and toxic gases provide a significant safety benefit. RFOs greatly reduce gas flow during an accidental release by use of a simple and inexpensive safety device. RFOs have no moving parts; they limit gas flow by the use of an orifice with a typical diameter of 150–1500 μ m. While greatly improving safety, the small diameter of some orifices makes them susceptible to partial blockage by particles that may be generated by actuating the valve. These blockages can produce unexpectedly lower flow rates delivered from the cylinder. This is normally not an issue as a larger RFO can be employed. However, if the flow rate delivered by the RFO is set close to the tool process flow rate, for safety or compliance reasons, partial blockage of the RFO may result in tool shut-down, because the process flow cannot be maintained. In order to overcome the problem with blockages, Matheson has evaluated the use of RFOs that come with an integral 2 μ m steel filter to protect the orifice from foreign material. This is an effective method to prevent particles entering/blocking the orifice. However, it introduces a porous, high surface-area material which can entrain elevated levels of moisture into the gas-stream. For

III-V semiconductor applications, moisture in the gas stream must be tightly controlled. Semiconductor grade gases are specified with moisture levels below 100ppbv to minimize oxygen incorporation in deposited layers. Atmospheric moisture that enters the gas connections during cylinder change-out can lead to significantly elevated levels of moisture. In order to remove the moisture in the connections, a sequence of “cycle purges” is performed by alternating between a high pressure of inert gas and vacuum. This has been shown to be a very effective moisture removal method for process lines. In this study, Matheson shows the efficacy of cycle purging to remove moisture trapped behind an RFO with and without the presence of a porous steel filter. We examine the moisture levels in a gas using a cavity ring-down spectrometer, showing the purging time required to achieve baseline moisture levels. The results show that filtered RFOs can be effectively purged of moisture and will not affect process gas purity. We conclude that filtered RFOs may be preferable for certain gases to achieve consistent, equivalent flow rates to those delivered by unfiltered RFOs, without running the risk of blockage or moisture entrainment.

8:50 PM - 9:10 PM

CHARACTERIZING LIQUID PRECURSOR DELIVERY FOR DEPOSITION PROCESSES

J. Maslar¹, B. Sperling¹, W. Kimes¹, W. Kimmerle², K. Kimmerle², E. Woelk³

¹NIST, UNITED STATES OF AMERICA, ²NSI, UNITED STATES OF AMERICA, ³CeeVeeTech, UNITED STATES OF AMERICA

Liquid precursors are utilized in deposition processes for a wide variety of compounds. These precursors are commonly delivered in an inert carrier gas from a bubbler (an ampoule with a dip tube) or a vapor draw ampoule (an ampoule with no dip tube: the gas in and gas out ports open directly into the ampoule headspace). While it is relatively simple to implement a delivery system based on such ampoules, it can be difficult to reproducibly deliver liquids from such ampoules, a situation that can lead to undesired film properties. The goal of this work is to obtain a better understanding of the factors

influencing liquid delivery from bubblers and vapor draw ampoules. Of particular interest is the degree to which evaporative cooling limits the amount of liquid delivered (evaporative cooling reduces the compound vapor pressure and hence the amount of material entrained in the carrier gas). To achieve the goals of this investigation, both the amount of liquid delivered from an ampoule and the temperature distribution of the liquid in the ampoule were measured under a range of process conditions, in bubblers and vapor draw ampoules. The amount of liquid delivered and the liquid temperature vertical distribution in the ampoule were measured using in situ optical diagnostics and a five-element temperature sensor array, respectively. These data were used to determine the degree to which the amount of liquid delivered was correlated to evaporative cooling in the ampoule. For bubblers, this determination was relatively straight-forward as bubbling tended to homogenize the liquid temperature. For vapor draw ampoules, however, this determination was complicated by a temperature gradient that existed during flow. The focus of this investigation was on hexane, which was selected as a simulant for trimethylgallium. In addition, water was examined in order to compare the behavior of two liquids with significantly different vapor pressures at the delivery temperature. The results from this work could facilitate development of deposition recipes, delivery control methods, and improved ampoule designs.

9:10 PM - 9:30 PM

THE OPTIMAL PARTITION DESIGN OF THE TRIPLE INJECTOR IN THE HORIZONTAL MOCVD REACTOR FOR THE GAN FILM GROWTH THROUGH THE NUMERICAL SIMULATION

W. Lin, J. Chen, C. Hu, J. Lin

Department of Mechanical Engineering, National Central University, TAIWAN

Horizontal MOCVD reactor with triple injector is used to growing the GaN epitaxy film. The structure of the triple injector includes two partitions to separate the inlet into upper, middle and bottom injectors. The mixture of TMG and H₂ is ejected from the middle injector, while the mixture of NH₃ and H₂ is supplied from the others. In this study, an axisymmetric numerical model is employed to study the relation

between the relative position and diameter of the partitions, the gas phase reaction and the deposition curve. The Nelder-Mead optimization method is adopted to figure out the optimal position and diameter of the triple injector. The weighted sum method is applied and the average deposition rate and uniformity on the wafer is considered in the test function for optimization. The result shows that the pyrolysis reaction of the TMG is affected by the distance between the lower partition and the susceptor when the upper partition is fixed. As the distance between the lower position and the susceptor is smaller than thickness of thermal boundary layer, the TMG ejected by middle injector reaches the high temperature area before it is mixed with NH₃. In this condition, pyrolysis reaction dominates in the gas phase reaction. The higher molar concentration of the MMG makes the higher slope of the deposition rate on the wafer. However, the average deposition rate on the wafer decreases if the distance between the lower partition and the susceptor is much larger than the thickness of the thermal boundary layer. When the injector diameter increases, the reaction sources are mixed at a higher temperature region that causes stronger pyrolysis reaction. On the other hand, the area of cross section of the injector increase with the diameter. This makes the velocity of the flow at the injector decrease and the mixing area is pushed to downstream. With stronger pyrolysis reaction and lower flow velocity, the deposition rate of the film increases and the peak of the depletion curve moving toward to the downstream. An optimal diameter of the partitions and a best position of the lower partition are found by the Nelder-Mead method.

Tuesday, July 30, 2019

10:30 AM - 12:00 PM

Bulk Crystal Growth: Focus on Technology

Location: Shavano Peak

Session Chair(s): Christo Gugushev, Jiaqiang Yan

10:30 AM - 11:00 AM

FLUX GROWTH IN A HORIZONTAL CONFIGURATION: AN ANALOG TO VAPOR TRANSPORT GROWTH

J. Yan

Oak Ridge National Laboratory, TN, UNITED STATES OF AMERICA
Materials synthesis and crystal growth in molten fluxes have proven to be excellent routes to new materials with intriguing properties. The components of the target compound are dissolved in a flux, which is usually molten salt or metal inside of an oxide or metal crucible; crystal growth takes place under supersaturation controlled by cooling or evaporating the flux. This kind of crystal growth is normally performed in a vertical configuration. And the reaction between flux and crucible materials should be avoided as it can change the flux composition and usually leads to crystal contamination or even growth failure. In my talk, I will talk about the flux growth of novel materials in a horizontal configuration: the principles, some growth examples, and how it complements to the growth in the conventional vertical configuration.[1] I will also briefly talk about our exploratory synthesis of new superconductors by using the reaction between flux and crucible materials.[2] This work was supported by the US Department of Energy, Office of Science, Basic Energy Sciences, Division of Materials Sciences and Engineering. [1] J.-Q. Yan, B. C. Sales, M. A. Susner, and M. A. McGuire. Phys. Rev. Materials 1, 023402 (2017), arXiv:1706.02339 [2] J.-Q. Yan, J. crystal growth, 416, 62 (2015)

11:00 AM - 11:15 AM

FORCED CONVECTION BY HIGH-SPEED ROTATION IN CZOCHRALSKI GROWTH FROM HIGH-TEMPERATURE SOLUTIONS

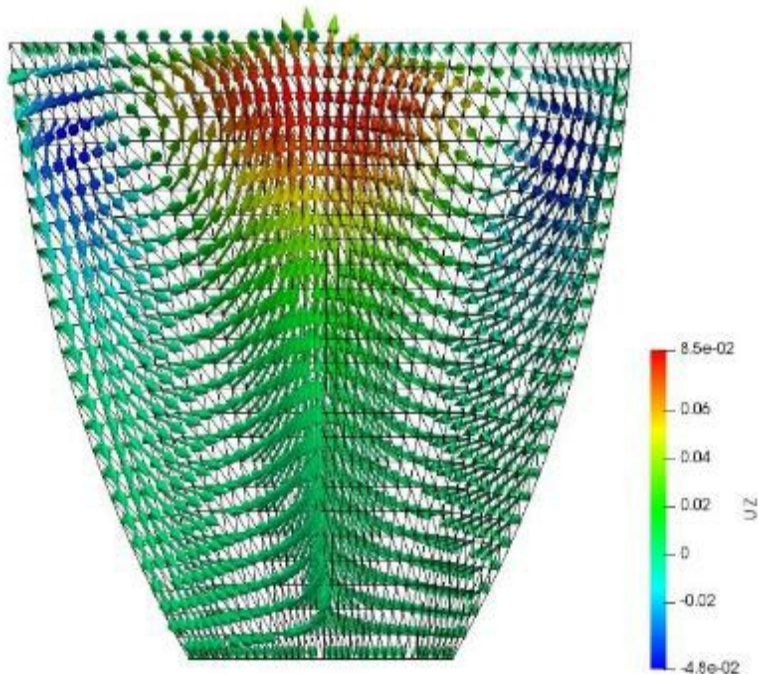
O. Harder¹, P. Eschenbacher¹, E. Hanfstaengl¹, K. Dadzis², **P. Gille**¹

¹LMU München, GeoDepartment, Crystallography, GERMANY,

²Leibniz-Institut für Kristallzüchtung, GERMANY

In crystal growth of intermetallics, the Czochralski method has proved to be a powerful technique for bulk single crystals¹. Many intermetallic compounds show peritectic melting behavior and can, therefore, only be crystallized from incongruent melts below their decomposition temperature which is sometimes relatively low. Combined with a restricted solubility, material transport in the solution next to the growth interface is the limiting factor for growth rates. Even with very

low pulling rates of 25–50 $\mu\text{m/h}$, fluid inclusion formation due to constitutional supercooling often indicates unsatisfactory mixing of the liquid adjacent to the growing crystal. Various techniques of forced convection, i.e., ACRT² or IRB³ are known from literature to effectively increase convective mixing and, thus, may avoid inclusion formation.



Since in the Czochralski method crystal and crucible counter-rotation is anyway part of the technique, we studied the impact of high-speed

crystal rotation on forced convection of the metallic melt. The crystal can be described as a rotating disc attached to the melt surface which is an old model analytically solved long time ago and treated for Czochralski growth purposes by Hurle⁴ The most important result is a reduced diffusion boundary layer thickness δ (here called Ekman layer) according to $\delta \sim (\nu/\omega)^{1/2}$ (ν : kinematic viscosity; ω : disc rotation rate). A combined experimental and numerical modelling study is presented investigating the influence of high crystal rotation rates on fluid flow in Czochralski growth of intermetallic compounds from metallic solutions. Numerical simulation with the computational fluid dynamics package OpenFOAM was applied to investigate forced convection flow patterns. Experimental proof in growth of Ga₃Ni₂ and Ga₇Pd₃, both from Ga-rich solutions could be achieved. Suppressed inclusion formation was taken as decisive criterion for fast enough forced convection. What has been considered most important is the very high flow velocities next to the growth interface, i.e., where it is needed to reduce the diffusion boundary layer thickness. Inclusion-free single crystal growth of Ga₃Ni₂ and Ga₇Pd₃ could be demonstrated with crystal rotation rates exceeding 400 rpm.

References [1] P. Gille, in: *Crystal Growth of Intermetallics*, P. Gille, Yu. Grin (Eds.), de Gruyter, Berlin/Boston, 2019, pp. 61-90. [2] H.J. Scheel, *J. Crystal Growth*, **13/14**, 560-565, 1972. [3] M. Pillaca et al., *J. Crystal Growth*, **475**, 346-353, 2017. [4] D.T.J. Hurle, in: *Advanced Crystal Growth*, P.M. Dryburgh et al. (Eds.), Prentice Hall, New York, 1987, pp. 97-123. **Acknowledgments:** Experimental contributions by Christina Glassl are gratefully acknowledged.

11:15 AM - 11:30 AM

NEW EXPERIMENTAL APPROACHES FOR RAPIDLY ESTABLISHING CRYSTAL GROWTH CONDITIONS

P. Khalifah

Stony Brook University, NY, UNITED STATES OF AMERICA

Improved methods for the flux growth of single crystals of the important battery material LiFePO₄ have been developed, allowing the facile preparation of single crystals up to 1 cm across with well-developed facets at relatively low temperatures suitable for both

structural and properties characterization. Growths were carried out for compositions within the $\text{Li}_3\text{PO}_4 - \text{FePO}_4 - \text{FeCl}_2 - \text{LiCl}$ reciprocal salt phase diagram. Rapid identification of primarily solidification regime boundaries for the major components of this phase diagram was carried out by using the net mass of grown crystals to calculate vectors relating the starting composition and the composition at which crystallization occurred, an efficient method for which no literature precedent could be found. Novel and general *in situ* approaches to quickly obtain complementary information about the solidification temperature for different compositions are in progress.

11:30 AM - 11:45 AM

IN-SITU DETECTABILITY OF CRYSTALLIZATION PROCESSES AND SEED SELECTION IN HIGH TEMPERATURE SOLUTIONS

A.F. Schneider, A. Jesche

University of Augsburg, GERMANY

Solution growth is a powerful tool for single crystal growth of various materials [1] and particularly useful for basic research in solid state physics and chemistry. A decrease of the formation temperatures of the desired compounds by several hundred degrees as well as high diffusion rates can be achieved. Accessing the exact nucleation temperature on the other hand and thereby the instant of nucleation remains almost impossible. A prediction of this instant gets also hampered by the uncertainties of the published liquidus temperatures (if available at all). This gets aggravated by supercooling, which stays undetected at all during the growth procedure. The difference between the displayed furnace temperature and the actual sample temperature makes this even more difficult. Here we present a way to accurately measure the complete time-temperature profile including small temperature changes caused by dissolution or nucleation. Without the necessity of a reference crucible, the signal-to-noise ratio approaches the level of conventional DTA-signals. The detection of nucleation enables crystal selection using oscillations within a well-defined temperature range. The setup can be applied to all common growth systems including aqueous solutions and has been proven up to 1300°C . The reaction chamber can be flooded with inert gas, while a direct contact between solution and sensor is avoided. Single crystals

of the component PdBi successfully enlarged by seed selection are shown in comparison to conventionally grown crystals. [1] M. M. Kanatzidis, R. Pöttgen, and W. Jeitschko. *Metal flux review: A preparative tool for the exploration of intermetallic compounds*. Angew. Chem. Int. Ed., 44, 6996 - 7023, 2005.

11:45 AM - 12:00 PM

IN SITU VISUALIZATION AND DYNAMIC SUPPRESSION OF CRYSTAL GROWTH INTERFACE FLUCTUATIONS BY GROWTH INTERFACE ELECTROMOTIVE FORCE

Y. Zhu, B. Wang

Sun Yat-sen University, CHINA

Defects have deleterious effects on the performance, reliability and degradation behavior of bulk crystals, as well as is a major problem for sophisticated electronic and optical solid-state crystalline materials. Especially in Czochralski system, the changeful flow pattern and elusory temperature field around growth interface are tough issues that fluctuate crystallization, enrich defects and damage the uniformity of a crystal boule. Since the *in situ* detection in real growth system is considered unattainable, although methods have been tried to generalize interface fluctuation, apparent contradictions still exist among recent theoretical and experimental simulations of the complex melt flow. In addition, without the direct feedback of growth interface, growth optimization and fluctuation suppression approaches can hardly perform as expected. Our study solves these issues via the sensitive response of growth interface electromotive force (GEMF) to crystallization and supercooling phenomena [1,2], which, for the first time, (as shown in Fig. 1a-c) visualizes and quantifies the real-time state of subtle growth rate and temperature fluctuations, depicts the regularity of coupled melt convection and spoke flow pattern, draws the micron-scale movement of growth interface, and even predicts a gradient surface morphology to demonstrate the outstanding sensitivity and accuracy of GEMF method [3]. Above achievements offer significant evidence to reveal convection instability and visual guidance to optimize a melt growth system *in situ*. More importantly, based on the GEMF feedback and PID controller, a closed-loop convection control system could be built to serve the dynamic

suppression of interface fluctuation. Specifically, as shown in Fig. 1d and e, benefiting from the GEMF-controlled unsteady crystal rotation configuration, an impressive suppression ratio of convection fluctuation over 60% is achieved, which reduces the dislocation density of the as-grown crystal drastically. In sum, GEMF method is a novel view to solve the pressing issues of crystal growth, and possesses good potential for scientific research and industrial application. [1] Y. Zhu, *et al. CrystEngComm*, **2019**, 21, 1107. [2] Y. Zhu, *et al. J. Cryst. Growth*, **2018**, 487, 120. [3] Y. Zhu, *et al. J. Cryst. Growth*, **2017**, 475, 70.

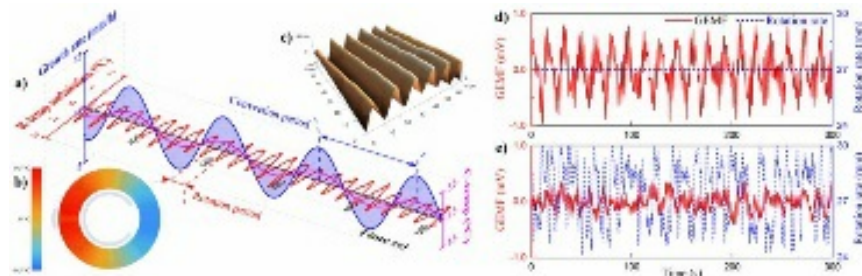


Fig. 1 (a) The *in situ* visualization of crystal growth rate, azimuthal and axial temperature (R-temp and C-temp) fluctuations. (b) The pie graph visualizes the spoke flow pattern and azimuthal temperature fluctuation of growth interface (c) The gradient morphology of crystal surface scanned by AFM. (d, e) GEMF variations at constant and PID-controlled unsteady rotation rates, respectively.

Tuesday, July 30, 2019

10:30 AM - 12:00 PM

Industrial Scintillator and Detector Growth

Location: Red Cloud Peak

Session Chair(s): Matt Whittaker, Mariya Zhuravleva

10:30 AM - 11:00 AM

**DEVELOPMENT OF MASS PRODUCTION TECHNOLOGY OF
CE:GD₃(GA,AL)₅O₁₂ SCINTILLATOR FOR RADIATION IMAGING
APPLICATIONS**

K. Kamada¹, Y. Shoji², V. Kochurikhin³, G. Luidmila⁴, M. Yoshino⁵,
K.J. Kim⁵, A. Yamaji⁵, Y. Yokota⁶, Y. Ohashi⁷, A. Yoshikawa⁵

¹C&A, JAPAN, ²C&A Corporation, JAPAN, ³General Physics Institute,

Russian Academy of Sciences, RUSSIAN FEDERATION, ⁴C&A corporation, JAPAN, ⁵Institute for Materials Research, Tohoku University, JAPAN, ⁶NICHe, Tohoku University, JAPAN, ⁷Tohoku University, JAPAN

Scintillators find their applications in many fields such as high-energy physics, medical imaging and diagnostics (Positron Emission Tomography: PET, X-ray CT), security check (baggage CT in an airport, goods containers) oil logging and agriculture. Especially, demand for radiation monitoring devices was immediately increased in the accident of Fukushima Daiichi nuclear power plants in 2011. Our research group have made our effort to combinatorial search of an optimal chemical composition for $(\text{Gd,RE})_3(\text{Al,Ga})_5\text{O}_{12}$ (Re= Lu, Y) using crystal growth method called micro-pull-down (μ -PD) [1] method from 2009. Among this research, our group reported about Ce:Gd₃(Ga,Al)₃O₁₂ (GGAG) single crystal and scintillation response of about ~90 ns at emission around 520 nm, excellent light yield of about 56000 photon/MeV, and density of 6.7 g/cm³[2]. Ce:GGAG is now mass-produced in 3 inch diameter size by Cz method and widely used for radiation imaging application as survey meter, gamma camera, Compton camera etc. including the decontamination application for Fukushima area. In 2015, we reported that Mg co-doping in Ce:GAGG improved its timing resolution to 160ps from 400ps of Ce:GAGG standard[3]. Mg co-doped in Ce:GAGG was also mass-produced for PET application due to its fast timing property. In my talk, the combinatorial search, development of large size crystal growth, improvement of scintillation properties of Ce:GAGG will be presented. Furthermore, application example such gamma camera mounted on a helicopter for radiation dose mapping from the sky, Compton camera and PET compatible medical imaging scanner will be introduced.

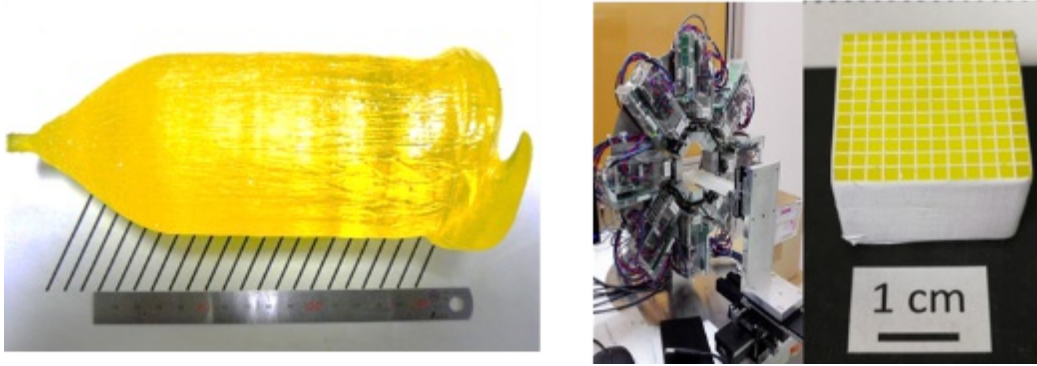


Fig. 3 inch diameter Ce:GAGG single crystal grown by Cz method(left), a example of medical imaging scanner and scintillator array (right).
 References [1] K. Kamada, et al., Crystal Growth & Design, 11(2011)4484 [2] K. Kamada, et al., Opt. Mater. 36(2014)1942 [3] K. Kamada, et al., IEEE Trans. Nucl. Sci.63 (2016)443 – 447

11:00 AM - 11:30 AM

DEVELOPMENT OF BULK CRYSTAL GROWTH TECHNOLOGY FOR NOVEL FUNCTIONAL CRYSTALS AND THEIR SOCIAL IMPLEMENTATION

A. Yoshikawa¹, Y. Yokota², K. Kamada², V. Kochurikhin³, M. Nikl⁴, Y. Ohashi², S. Kurosawa², A. Yamaji¹, M. Yoshino¹, H. Sato², K. Inoue⁵

¹Institute for Materials Research, Tohoku University, JAPAN, ²NICHe, Tohoku University, JAPAN, ³C&A corporation, JAPAN, ⁴Institute of Physics, CZECH REPUBLIC, ⁵Piezo Studio Inc., JAPAN

Solid-state functional materials play a significant role in number of important technical applications. One of the important application is scintillator. The application includes medical imaging, natural resource survey, radon detection in geology, border security and industrial inspection systems, non-destructive analysis of complex objects, and many others. In most cases, single-phase and single-crystalline substances are used as a material detecting nature, intensity, and spatial distribution of the irradiation. In order to develop novel scintillating material, the fusion of the knowledge in different fields are important such as solid state chemistry, band gap engineering (BGE), understanding of co-doping effects and so on. Recent our R&D studies on Ce: {Gd,RE}₃(Ga,Al)₅O₁₂ (RE=Y, Lu) (Ce:GAGG), (La,Gd)₂Si₂O₇ (Ce:La-GPS), Eu:SrI₂ single crystals and eutectic

materials will be introduced taking their social implementation into account. Though the lattice constant, volume and emission wavelength changes linearly, LY has maxima at the specific ratio. This is explained as the result of suitable BGE. From the crystal chemistry point of view, partial substitution of Ga in Al site or partial substitution of RE in Gd site is effective to make the garnet phase congruent. The study on investigate the role of Ce^{4+} become popular as a co-doping effect on Ce:GAGG. Crystal growth technology is also the key to obtain high performance scintillators in your hand. Eu:SrI₂ is the typical example. we have developed a novel VB method using the μ -PD furnace with the removable chamber to grow bulk single crystals of hygroscopic halide materials. 2 inch bulk crystal growth of Eu:SrI₂ was established. Other application is piezoelectric material. Piezoelectricity is exploited in a number of useful applications, such as the production and detection of sound, piezoelectric inkjet printing, generation of high voltages, electronic frequency generation for timing devices and so on. Recent our R&D studies on $Ca_3TaGa_{3-x}Al_xSi_2O_{14}$ with langasite type structure will be introduced together with the feature of the devices.

11:30 AM - 12:00 PM

COMMERCIAL-SCALE SOLUTION GROWTH OF THE ORGANIC SCINTILLATOR STILBENE

C. Lynch¹, J. Freese¹, T. Caughey¹, S. Selin²

¹Inrad Optics, Inc., UNITED STATES OF AMERICA, ²Inrad Optics, Inc., AL, UNITED STATES OF AMERICA

The organic scintillation crystal stilbene (C₁₄H₁₂) has long been recognized as an excellent material for detection of fast neutrons in a gamma ray background, but its widespread use has historically been limited by the low availability of melt-grown material. Recently, solution crystal growth was proposed by Zaitseva as a cost-effective route for production of organic scintillators. We have leveraged the existing commercial solution growth capability at Inrad Optics and scaled up production of stilbene. Stilbene crystals grown at Inrad Optics have dimensions suitable for parts up to 5" in diameter and have been machined into geometries such as cylinders, bars, cones, and thin

plates. Characterization and results from selected customers will be presented along with an overview of promising applications.

Tuesday, July 30, 2019

10:30 AM - 12:00 PM

Modeling of Crystal Growth Processes I

Location: Crestone I, II

Session Chair(s): Thierry Duffar, Koichi Kakimoto

10:30 AM - 11:00 AM

ARTIFICIAL INTELLIGENCE IN CRYSTAL GROWTH

N. Dropka¹, M. Holena², S. Ecklebe³, C. Frank-Rotsch¹, J. Winkler³

¹Leibniz Institute for Crystal Growth, GERMANY, ²Leibniz Institute for Catalysis, GERMANY, ³Technische Universität Dresden, GERMANY

A next generation of smart crystal growth factories will use artificial intelligence (AI) and automation to keep costs low and profits high. The AI based on artificial neural networks (ANNs) is trying to mimic biological processes in the human brain by detecting the patterns and relationships in data and by experiential learning. ANNs represent a powerful modeling technique, especially for non-linear data sets which are common in crystal growth processes. ANN has an ability to correlate very high number of variables and an ability to work in the stand-alone mode with high accuracy in predictions. ANNs can describe both static and dynamic data, where the latter means that ANN can have a memory. In that case, ANN response at any given time depends not only on the current input, but on the history of the input sequence.

Based on these facts, there are two feasible applications of ANN in crystal growth:

pattern recognition by static ANN crystal growth process automation by dynamic ANN.

The pattern recognition means to find complex correlation between static process parameters from one side and crystal size/deflection of crystallization front/crystal quality from another. Once derived, ANN can be used for the fast optimization of the former for the growth of

perfect crystals. Application in process automation means to use ANN for fast real time predictions of the transient growth process parameters e.g. temperatures in various points in the growth furnace, shape and position of crystallization front after usage of certain growth recipe etc. These real time predictions are necessary for the process control, since their direct measurement, particularly in the melt and crystal may cause contamination and therefore is not feasible. A large database that is needed for generation and training of ANNs is a bottleneck of ANN applications. Fortunately, crystal growth data can be obtained experimentally or by numerical CFD simulations. Our recent results on the application of various ANNs to the optimization of electro-magnetic parameters of magnetic driven vertical gradient freeze growth (VGF) and to fast forecasting of common VGF crystal growth process will be presented and critical issues such as the amount of data and the choice of ANN type and architecture will be discussed.

11:00 AM - 11:15 AM

SIMULATION OF THE CREATION OF A DEFECT STRUCTURE OF DISLOCATION-FREE GERMANIUM SINGLE CRYSTALS

V.I. Talanin, I.E. Talanin, V.V. Zhdanova, V.V. Kondratiev, **D.I. Yakymchuk**

Department of Computer Science & Software Engineering, Institute of Economics & Information Technology, UKRAINE

Over the past ten years, we have created a diffusion model for the formation and transformation of structural imperfections during the growth of dislocation-free silicon single crystals. The diffusion model is based on the elastic interaction of intrinsic point defects and impurities with each other near the crystallization front of a crystal. The diffusion model allows at any stage of growing a crystal or creating an instrument using software tools to control or set the defect structure of silicon crystals. The main results of our research are presented in the monograph [1]. We believe that the diffusion model can also be used to describe the creation and development of the defect structure of other perfect crystals (without dislocations). In order to verify this assumption, we modeled using the diffusion model the creation and development of a defect structure of dislocation-free germanium single

crystals. We first estimated the recombination parameters for regions of high and low temperatures in germanium. Thermodynamic calculations show that the aggregation of point defects in germanium prevails over the recombination process between its own point defects. The contribution of the recombination process at high temperatures to the aggregation process is negligible. Consequently, vacancies and interstitial atoms of implantation coexist in thermal equilibrium. Thus, both types of internal point defects are involved in the aggregation process simultaneously. The decomposition of a supersaturated solid solution of point defects is caused by the cooling of two mechanisms: vacancy and interstitial, which leads to the formation of impurity-vacancy and impurity-interstitial agglomerates. This means that the processes of formation of defects in silicon and germanium proceed in the same way and can be described using the model of high-temperature precipitation [2]. It is shown that the complexation process occurs near the crystallization front. Compared with silicon in germanium, this value is an order of magnitude less [1]. The critical radii of oxygen and carbon precipitates near the crystallization front are determined. The further development of the defective structure of germanium during the cooling of the crystal during its growth is shown. [1]. V.I. Talanin and I.E. Talanin. The Formation of Structural Imperfections in Semiconductor Silicon. Cambridge Scholars Publishing, UK, 2018. [2]. V.I. Talanin, I.E. Talanin, V.V. Zhdanova, D.I. Yakymchuk and A.V. Rybalko The Basic Principle of Calculation and Analysis of the Defective Structure of Solids. In: Mechanical Design, Materials and Manufacturing (Ed. Sandip A. Kale). Nova Science Publishers, New York, 2019.

11:15 AM - 11:30 AM

ONSET OF ISOTROPIC AND ANISOTROPIC SHAPE CHANGES DURING CZOCHRALSKI CRYSTAL GROWTH

S. Brandon, O. Weinstein
Technion, ISRAEL

In a recent paper [1] a model was presented and applied for the analysis of anisotropy in a Czochralski crystal growth system. The model and associated numerical formulation is based on a three dimensional and transient analysis of heat transport and melt flow

using Lattice Boltzmann models (LBMs), and accounts for two physical phenomena involving anisotropy. These are interface attachment kinetics, implemented using the approach described in [2], and an orientation-dependent growth angle applied using an ad-hoc formulation loosely based on specific experimental measurements. Calculations demonstrated how combined anisotropy of interface attachment kinetics and growth angle (capillarity) can influence crystal shape evolution. Specifically, it was shown how growth angle anisotropy can either increase or decrease the impact of interface attachment kinetics on shape anisotropy, depending on the manner in which growth angle values vary with the melt/crystal interface orientation at the crystal/melt/gas triple phase line. In this contribution we extend the analysis to examine more carefully the onset of shape changes during the growth process. When doing this we test, in certain cases, a more rigorous formulation for growth angle anisotropy. Phenomena to be discussed include those related to changes in growth mechanism (e.g. due to the appearance of a screw dislocation on a previously dislocation free faceted melt/crystal interface) as well those related to changes in the structure of the crystal/melt interface during shouldering (e.g. due to the appearance of facets on the crystal/melt interface at the crystal/melt/gas triple phase line). [1] O. Weinstein, W. Miller and S. Brandon, J. Crystal Growth, **509** 71-86 (2019) [2] O. Weinstein and S. Brandon, J. Crystal Growth **284**, 235 (2005).

11:30 AM - 11:45 AM

UNSTEADY NUMERICAL SIMULATION CONSIDERING EFFECT OF THERMAL STRESS AND HEAVY DOPING ON BEHAVIOR OF INTRINSIC POINT DEFECTS IN LARGE-DIAMETER SI CRYSTAL GROWING BY CZOCHRALSKI METHOD

Y. Mukaiyama¹, M. Iizuka¹, V.M. Mamedov², S. Maeda³, K. Sueoka⁴

¹STR Japan K.K, JAPAN, ²STR Group - Soft Impact, Ltd., RUSSIAN FEDERATION, ³GlobalWafers Japan Co., Ltd., JAPAN, ⁴Okayama Prefectural University, JAPAN

We developed and studied a novel numerical simulation model for the prediction of the transient behavior of intrinsic point defects in growing silicon (Si) crystal by the Czochralski (Cz) method. Especially, the

effects of the thermal stress and heavy doping of typical impurities are applied to the calculation of the thermal equilibrium concentration of the intrinsic point defects. In this paper, we present the transient behavior of the point defects in growing large-diameter Si crystal under the high thermal stress and heavy doping, using dynamical unsteady numerical modeling. Over many years, researchers have suggested several theoretical and numerical models on the behavior of point defects in growing Si crystal by Cz method. However, the effects of thermal stress and doping have not been considered in these models. Recently, Sueoka *et al.* and Kobayashi *et al.* have claimed the importance of the effect to explain and engineer the intrinsic point defect in large-diameter single Si crystals grown by the Cz method [1-2]. Nowadays, we have elaborated a theoretical model of the thermal equilibrium concentration of intrinsic point defects (vacancy V and self-interstitial Si I) as functions of the thermal stresses, type and concentration of dopant, and concentration of interstitial oxygen in growing Cz -Si crystal, and implemented into *CGSim* package of STR. [3]. By the extended *CGSim* version, it is possible to predict the transient behavior of point defects, accounting for the thermal stress and dopant incorporated from the melt by segregation within the unsteady dynamical crystal growth model, starting from the crystal shoulder and finishing at the tail formation. We have numerically predicted and analyzed, the distributions of V and I concentrations inside a growing Si ingot with varying doping type, concentration, and growth condition (Figure 1).

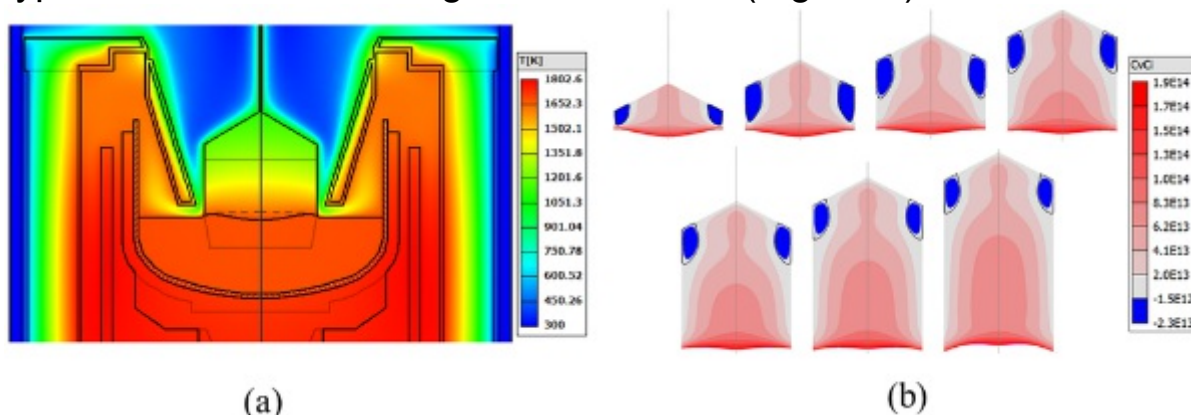


Figure 1: Simulation results of Cz 400mm silicon growth. (a) Temperature distribution in hot zone of puller furnace. (b) Cv-Ci distributions in the growing silicon crystal. [1] K. Sueoka, K. Nakamura

and J. Vanhellefont, J. Cryst. Growth 474 (2017) 89–95 [2] K. Kobayashi, S. Yamaoka, K. Sueoka and J. Vanhellefont, J. Cryst. Growth 474 (2017) 110–120 [3] <http://www.str-soft.com/products/CGSim/>

11:45 AM - 12:00 PM

CONTROLLING NUCLEATION DURING UNSEEDED THM GROWTH OF CDZnTE CRYSTAL

S. Zhang¹, B. Hong¹, L. Zheng¹, H. Zhang¹, C. Wang², B. Zhao²

¹Tsinghua University, CHINA, ²Ruiyan Technology Co. Ltd., CHINA

Unseeded THM growth of CdZnTe have attracted much attention as it is a much more economic and convenient method to prepare high-quality CdZnTe crystal. However, there are always undesired grains formed at the beginning of unseeded growth which deteriorate the crystal quality greatly. In this paper, several ingots with diameter of 27mm were grown by unseeded THM method with built-in-house furnace to study the method to control the nucleation process. The Influence of crucible bottom geometry, nucleation temperature, temperature gradient including vertical and lateral temperature gradient, and accelerated crucible rotation technique (ACRT) were studied under the growth temperature of 750°C and the growth rate of 5mm/day. Also numerical simulation of thermal and fluid field was also conducted for the THM process to study the nucleation process. The simulation results show that great temperature change during the nucleation and enlarge process is the main reason for crystal quality deterioration. Dummy crystal was introduced in order to control the stability of temperature field during the early stage of crystal growth. With dummy crystal introduced stable temperature field was obtained during the nucleation and also large column grains were formed from the beginning to the end of the ingot. And also cold fingers were designed for further optimization.

Tuesday, July 30, 2019

10:30 AM - 12:00 PM

Novel Materials and Processes

Location: Torrey Peak II-IV

Session Chair(s): Wiebke Hahn, Brooks Tellekamp

10:30 AM - 10:45 AM

GROWTH AND CHARACTERIZATION OF GROUP IV SIGESN THIN FILMS USING PLASMA ENHANCED CHEMICAL VAPOR DEPOSITION ON SI (100) SUBSTRATES

J. Vanjaria¹, A.C. Arjunan², Y. Wu¹, H. Yu¹, T. Salagaj², **G. Tompa²**

¹Arizona State University, AZ, UNITED STATES OF AMERICA,

²Structured Materials Industries, Inc., NJ, UNITED STATES OF AMERICA

The development of group IV materials towards achieving integrated Si photonics has attracted significant scientific interest in recent years. The goal is to integrate group IV based Si photonics with established CMOS technology on a single chip for high speed infra-red on chip communication. Silicon germanium tin (SiGeSn) is a promising group IV material because it has a direct band gap at high Sn concentration (Sn >10%), high carrier mobility, ability to be grown on Si and form emitter and detector structures on Si. However, growing the material is challenging due to available precursor chemistry (specifically limitations with Sn chemistry) and due to the tendency of Sn to segregate (phase separate) out of the material owing to its low solubility in Ge and Si. The large lattice mismatch with the Si substrate is also a challenge. Non-equilibrium growth techniques are thus appealing to deposit homogenous SiGeSn thin films with Sn concentrations which are scientifically and technologically relevant. In this work, plasma enhanced chemical vapor deposition (PECVD) was used to deposit SiGeSn films using an in-house developed PECVD reactor. The reactor supports film growth on wafers up to 100mm in diameter. Germane (GeH₄), disilane (Si₂H₆) and tin tetrachloride (SnCl₄) were used as precursors. The use of plasma enabled growth at low deposition temperatures. Low temperatures were found to be beneficial to incorporate higher concentrations of Sn in the films by limiting Sn diffusion and segregation. High quality SiGeSn films were grown using Ge and SiGe buffer layers. The deposited films were analyzed using optical interference for thickness, X-ray fluorescence for composition, X-ray diffraction and Raman for structural quality, and

Rutherford Back Scattering (RBS) for atomic composition. The films were annealed by Rapid Thermal Annealing (RTA) to improve their crystalline quality and relieve stresses in the films. Growth rates of 16 nm/min and 25nm/min were achieved for Ge and SiGe films respectively at susceptor temperature of 700°C. SiGeSn films with a Sn concentration of up to 2% were deposited at growth conditions of 450°C and 15-30 Torr. A growth rate of 2nm/min was observed for the SiGeSn films at these conditions.

10:45 AM - 11:00 AM

BORON TRICHLORIDE GAS BEHAVIOUR FOR CHEMICAL VAPOUR DEPOSITION AND ETCHING AT SILICON SURFACE

H. Habuka, M. Muroi, A. Saito

Yokohama National University, JAPAN

A chemical behaviour of boron trichloride gas was studied over wide ranges of temperature and concentration for developing a safe and effective boron doping process for silicon epitaxial growth, instead of that using a toxic and burnable gas of diborane. A (100) silicon wafer was placed in a horizontal cold wall reactor, into which the boron trichloride gas and the dichlorosilane gas were introduced with the hydrogen gas at atmospheric pressure. The real time *in situ* monitoring was performed for analyzing the gas phase chemical compounds and for evaluating the byproduct deposition at the exhaust, utilizing the quadrupole mass spectra (QMS) analyzer and the quartz crystal microbalance (QCM), respectively. The chemical condition of the silicon surface was *ex situ* evaluated using the X-ray photoelectron spectroscopy (XPS). (i) The chemical reaction of the boron trichloride gas at the silicon surface was first evaluated. The boron trichloride gas at 20 % in ambient hydrogen produced the boron film at the temperatures between 1073 K and 1323 K, by the thermal decomposition. At the temperatures higher than 1373 K, the silicon surface was etched with producing chlorosilane gases. Because the chlorosilane gas production stopped immediately after terminating the boron trichloride gas supply, both the deposition and etching behaviour were due to the boron trichloride gas. These two opposite processes were considered to occur by the balance between the boron deposition rate by the boron trichloride gas and the etching rate

by the in-situ-produced hydrogen chloride gas. At high temperatures, the amount of hydrogen chloride gas produced by the boron film deposition became significant to increase the etching rate exceeding the boron deposition rate, particularly, in the downstream region. (ii) Taking into account the behaviour depending on the temperature, the gas mixture of boron trichloride and dichlorosilane at the concentration of 10 % and 2 %, respectively, was used at 1073 K for producing a boron-doped silicon film at the silicon surface. Because the obtained film contained both silicon and boron, the boron doped silicon film formation was possible using the boron trichloride gas. In conclusions, the boron trichloride gas can work as a dopant and an etchant at the silicon surface depending on the temperatures low and high, respectively.

11:00 AM - 11:15 AM

NON-EQUILIBRIUM MOCVD GROWTH WITH PLASMA ENHANCEMENT

N. Smaglik, N. Pokharel, X. Pasala, P. Ahrenkiel

South Dakota School of Mines and Technology, SD, UNITED STATES OF AMERICA

The use of plasma enhancement for non-equilibrium growth of III-V compound semiconductor materials by metal-organic chemical vapor deposition (MOCVD) is being examined, to aid in establishing greater control and understanding of the underlying growth mechanisms for their uses in photovoltaic and solid-state lighting devices. While plasma is commonly used with group-IV materials, such as silicon, few studies have examined the impact of plasma enhancement on III-V material growth. A plasma-enhanced MOCVD (PE-MOCVD) method using radio-frequency coupling was developed for the deposition of elemental Al from trimethylaluminum, which is not generally possible by conventional methods. PE-MOCVD provides improved decomposition of metalorganic precursors driven by hydrogen plasma excitation, rather than either hydride reactions or thermal pyrolysis. The PE-MOCVD approach can also enable lower temperature growth, the uses of alternative precursors, improvements in interface abruptness, and lower production costs. Textured, elemental Al films grown by PE-MOCVD show distinct crystallographic texturing, offering

a step towards epitaxial Al layers, which have potential roles as buffer layers for III-Vs and in ultraviolet plasmonics. We have demonstrated PE-MOCVD of GaAs at temperatures as low as 300 °C, and the use of plasma as a handle to control spontaneous atomic ordering in GaInP. The latter is the basis for our investigations into forming order/disorder AlInP unicompositional heterostructures, which are appealing candidates for red/amber light-emitting diodes. Growth for this work is performed with a home-built PE-MOCVD system, with supporting characterization by transmission electron microscopy, transmission electron diffraction, energy-dispersive X-ray spectrometry, and X-ray diffraction. In its current implementation, films grown by PE-MOCVD are subject to plasma damage during growth, resulting in microstructural degradation. Improvements in the system design and growth sequences are at the focus of on-going efforts.

11:15 AM - 11:30 AM

THREE-DIMENSIONAL ATOMIC SCALE RECONSTRUCTION OF OCTAHEDRAL TILT EPITAXY IN FUNCTIONAL PEROVSKITE THIN FILMS

Y. Lu, Y. Yuan, S.B. Sinnott, V. Gopalan

Pennsylvania State University, PA, UNITED STATES OF AMERICA

It is recognized that tuning octahedral tilts, which are the most ubiquitous distortions in perovskite-related structures, can dramatically influence functional properties such as polarization, magnetism, and electronic orders; yet the paradigm of “tilt epitaxy” in thin films is barely explored. Commensurately imprinting a substrate tilt pattern into the film requires ultrathin films, and it is a formidable challenge to experimentally non-destructively characterize such epitaxy in three-dimensions for low symmetry complex tilt systems composed of low atomic number anions. Here we demonstrate that a non-polar earth-abundant mineral, calcium titanate, when grown as ultrathin films on different substrates, can transform into high temperature polar oxides with polar distortions that can last above 900 K. This directly arises from interfacial tilt epitaxy, which is exclusively revealed by reconstructing the 3-dimensional electron density maps across film-substrate interfaces with atomic resolution using Coherent Bragg Rod Analysis (COBRA). These maps reveal unit-cell-by-unit-cell, all the

atomic positions, the three components of the polarization as well as three independent oxygen octahedral tilts (a-b+c-) in ultrathin films on substrates. Density functional theory calculations reveal that strain gives rise to a large out-of-plane displacement of Ti-cations inside the TiO_6 octahedral cages responsible for the strain induced polarization. The study could serve as a broader template for non-destructive, 3-dimensional atomic resolution probing of complex low symmetry functional interfaces. Yuan, Y.; Lu, Y.; Stone, G.; Wang, K.; Brooks, C. M.; Schlom, D. G.; Sinnott, S. B.; Zhou, H.; Gopalan, V. *Nat. Commun.* **2018**.

11:30 AM - 11:45 AM

TWO-DIMENSIONAL HBN LAYER PROMOTED HETEROEPITAXY IN REACTIVELY SPUTTER-DEPOSITED $\text{MoS}_2(0001)/\text{Al}_2\text{O}_3(0001)$ THIN FILMS

A. Deshpande¹, K. Hojo², K. Tanaka¹, P. Arias¹, H. Zaid¹, M. Liao¹, M. Goorsky¹, S. Kodambaka¹

¹Dept. of Materials Science and Engineering, University of California Los Angeles, CA, UNITED STATES OF AMERICA, ²Graduate Department of Micro-Nano Mechanical Science and Engineering, Nagoya University, JAPAN

Two-dimensional (2D) layered materials have gained a lot of attention over the past decade for a variety of applications including their use as templates for the epitaxial growth of crystalline solids. Here, we report on the use of one such layered material, hexagonal boron nitride (hBN) ($a = 0.250$ nm and $c = 0.667$ nm), as the buffer layer for the heteroepitaxial growth of MoS_2 thin films on $\text{Al}_2\text{O}_3(0001)$. MoS_2 layers are deposited via ultra-high vacuum direct current magnetron sputtering of Mo target in 20 mTorr Ar with 1% H_2S gas mixtures at 1073 K on bare and hBN-covered $\text{Al}_2\text{O}_3(0001)$ substrates. hBN layers are grown via pyrolytic cracking of borazine ($\sim 6 \times 10^4$ L) onto $\text{Al}_2\text{O}_3(0001)$ at 1373 K. Cross-sectional TEM observation reveals that the film thickness is approximately 20.5 nm. The as-deposited MoS_2 layer composition and crystallinity are determined using a combination of X-ray diffraction (XRD), Raman spectroscopy, and X-ray

photoelectron spectroscopy (XPS). ω -2 θ and ω rocking curve XRD scans obtained from all the MoS₂/Al₂O₃(0001) samples reveal only 000/ reflections, indicative of highly-oriented crystal growth. Compared to the XRD spectra of the films deposited on bare Al₂O₃(0001), XRD data from MoS₂/hBN/Al₂O₃(0001) layers show Laue oscillations around the reflection at 2 θ = 14.40 degrees with a full width of half maximum of 781 arc second and 173 arc seconds in ω -2 θ scan and ω rocking curve, respectively. Raman spectra of the MoS₂ thin films show characteristic peaks with higher intensities in layers deposited on hBN-covered Al₂O₃(0001) compared to those on bare substrates. Our results indicate that hBN layers enhance the crystallinity of sputter-deposited layers.

11:45 AM - 12:00 PM

EPITAXIAL MULTIFERROIC SUPERLATTICES COMBINING HEXAGONAL AND CUBIC FERRITES

R. Steinhardt¹, M.E. Holtz¹, P. Barrozo Da Silva², B. Prasad², J.A. Mundy³, R. Ramesh², D. Schlom⁴

¹Cornell University, UNITED STATES OF AMERICA, ²University of California Berkeley, UNITED STATES OF AMERICA, ³Harvard University, UNITED STATES OF AMERICA, ⁴Department of Materials Science and Engineering, Cornell University, UNITED STATES OF AMERICA

Hexagonal rare earth ferrites offer a promising and relatively unexplored area for multiferroic materials design. An exciting new method for creating multiferroic materials by combining rare earth ferrites into epitaxial superlattices has previously been developed using LuFeO₃ for its ferroelectric properties and LuFe₂O₄ for its ferrimagnetism [1]. While these lutetium ferrite superlattices demonstrated magnetoelectric coupling near room temperature, for device applications we seek materials that have stronger magnetism at higher temperatures. We use molecular beam epitaxy to combine ferroelectric hexagonal LuFeO₃ and ferrimagnetic cubic spinel ferrite into a superlattice. Depending on growth conditions, the spinel can form as surface polycrystalline precipitates [2], ordered 3D epitaxial

structures, or well-ordered superlattices (figure 1.). The resulting superlattices show both strong magnetism and ferroelectricity above room temperature, which is promising for device applications. Multiferroic properties such as magnetoelectric coupling are currently being investigated. 1. Mundy, Julia A., et al. "Atomically engineered ferroic layers yield a room-temperature magnetoelectric multiferroic." *Nature* 537.7621 (2016): 523-527. 2. Moyer, J. A., et al. "Intrinsic magnetic properties of hexagonal LuFeO₃ and the effects of nonstoichiometry." *APL Materials*, 2.1 (2014): 012106

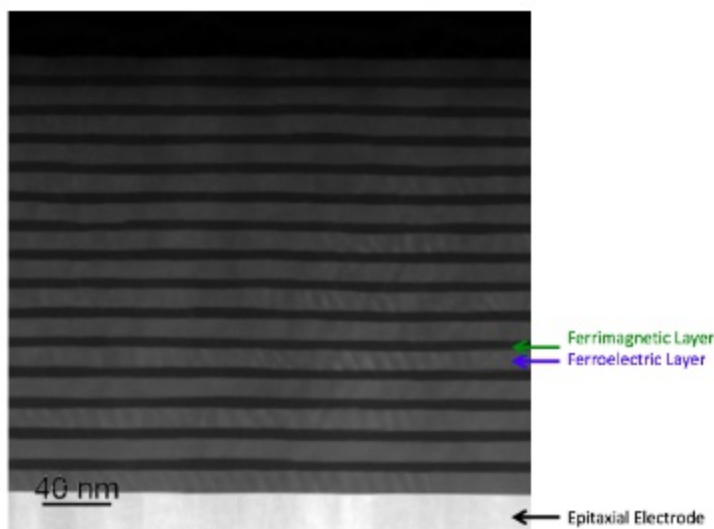


Figure 1.) STEM image of superlattice

Tuesday, July 30, 2019

10:30 AM - 12:00 PM

Symposium on 2D Materials: Vapor Phase Synthesis of TMDs

Location: Crestone III, IV

Session Chair(s): Joan Redwing, James Maslar

10:30 AM - 11:00 AM

EPITAXIAL GROWTH OF WAFER-SCALE TRANSITION METAL DICHALCOGENIDES BY GAS SOURCE CVD

T.H. Choudhury, M. Chubarov, X. Zhang, J.M. Redwing

The Pennsylvania State University, PA, UNITED STATES OF

AMERICA

Monolayer transition metal dichalcogenides (TMDs) possess a range of intriguing optical and electronic properties including direct bandgap, valley polarization, etc. A major hurdle to utilizing these properties is the availability of large area uniform epitaxial films. Our research is aimed at the development of an epitaxial growth technology for layered dichalcogenides based on gas source chemical vapor deposition (CVD). This approach provides a high overpressure of chalcogen species needed to maintain stable growth at elevated temperature and excellent control of the precursor partial pressures to achieve monolayer growth over large area wafers. Our initial studies have focused on the epitaxial growth of binary TMD monolayers including MoS_2 , WS_2 , WSe_2 and MoSe_2 using metal hexacarbonyl and hydride chalcogen precursors to deposit on 2" sapphire substrates in a cold-wall CVD reactor. Growth of sulfur-containing TMDs require a significantly higher chalcogen/metal inlet gas ratio compared to selenium-containing TMDs due to the reduced sticking coefficient of sulfur on the sapphire surface at typical growth temperatures (600-950°C). A multi-step precursor modulation growth method was developed to independently control nucleation density and the lateral growth rate of monolayer domains on the substrate [1]. This approach also enables measurement of metal-species surface diffusivity and domain growth rate as a function of growth conditions providing insight into the fundamental mechanisms of monolayer growth. Using this approach, uniform, coalesced monolayer and few-layer TMD films were obtained on 2" sapphire substrates at growth rates on the order of ~ 1 monolayer/hour. In-plane X-ray diffraction demonstrates that the films are epitaxially oriented with respect to the sapphire with narrow X-ray full-width-at-half-maximum indicating minimal rotational misorientation of domains within the basal plane [2]. Post-growth transmission electron microscopy carried out on monolayers removed from the sapphire by a wet transfer method demonstrate that the films are single crystal and include anti-phase grain boundaries that result from a merging of 0° and 60° oriented domains that form on sapphire. Growth of $(\text{Mo,W})\text{S}_2$ alloy monolayers was also achieved over the entire composition range by controlling the

inlet gas phase ratio of Mo and W hexacarbonyl precursors. Applications and challenges of this technique for the growth of vertical 2D heterostructures will also be discussed. [1] X. Zhang, T.H. Choudhury, M. Chubarov, Y. Xiang, B. Jariwala, F. Zhang, N. Alem, G.C. Wang, J.A. Robinson and J.M. Redwing, Nano Lett. 18, 1049 (2018). [2] M. Chubarov, T.H. Choudhury, X. Zhang and J.M. Redwing, Nanotechnology 29 055706 (2017).

11:00 AM - 11:15 AM

MOVPE OF 2D WS₂ AND 2D MOS₂ LAYERS FOR OPTOELECTRONIC APPLICATIONS

A. Grundmann¹, D. Andrezejewski², T. Kümmell², G. Bacher², **M. Heuken**¹, H. Kalisch¹, A. Vescan¹

¹RWTH Aachen University, GERMANY, ²University Duisburg-Essen, GERMANY

Due to their unique properties, 2D transition metal dichalcogenides (TMDC) such as tungsten disulfide (WS₂) and molybdenum disulfide (MoS₂) are primed for a variety of future (opto)electronic applications. Unlike chemical vapor deposition (CVD), metal-organic vapor phase epitaxy (MOVPE) provides a reproducible and easily scalable technology with excellent homogeneity. However, optimum growth conditions for MOVPE processes of TMDC to enable industrial production of atomically thin high-performance devices have not yet been established. Here, we report on the systematic investigation of key MOVPE parameters for homogeneous 2D WS₂ and 2D-MoS₂ monolayers. The samples are grown on sapphire (0001) substrates using a hydrogen sulfide (H₂S)-free MOVPE process in a commercial AIXTRON planetary hot-wall reactor in 10 × 2" configuration. Tungsten hexacarbonyl (WCO, 99.9 %), molybdenum hexacarbonyl (MCO, 99.9 %) and di-tert-butyl sulfide (DTBS, 99.9999 %) were used as MO sources. All samples were characterized using Raman spectroscopy, photoluminescence (PL) spectroscopy and scanning electron microscopy. Prior to all deposition processes, a substrate prebake step in a pure H₂ atmosphere is performed. Following the prebake step, growth processes were carried out at 30 hPa in pure N₂

atmosphere. During all processes, the DTBS flow was kept constant. Previous investigation determined the optimum growth temperature for WS₂ and MoS₂ to be at around 820 °C. According to literature, nucleation and growth are mainly controlled by the metal species. Therefore, in our first WS₂ series, the impact of the WCO flow on lateral growth in 10 h growth processes was investigated with the aim of maximizing the edge length of the triangular crystals as well as their total surface coverage. In the second WS₂ series, the growth time was extended gradually up to 20 h at optimized WCO flow conditions. This yields fully coalesced 2D-WS₂ samples without parasitic carbon-related Raman peaks and with only sparse bilayer nucleation. PL mapping reveals homogeneous PL emission, evidencing uniform growth of the 2D-WS₂ layer. After removal from the sapphire substrate, a fully coalesced 2D-WS₂ film was implemented into a vertical p-i-n light emitting device showing homogeneous red electroluminescence (EL) from a 6 mm² area at a bias voltage of 6.5 eV. The growth of coalesced MoS₂ monolayers has proven to be more challenging because bilayer nucleation of MoS₂ is more pronounced than for WS₂. Therefore, lateral growth rates compete with the process of secondary nucleation on top of the coalescing monolayer.

11:15 AM - 11:30 AM

WAFER SCALE EPITAXIAL GROWTH OF MONOLAYER WS₂ BY GAS SOURCE CHEMICAL VAPOR DEPOSITION

M. Chubarov¹, T.H. Choudhury¹, D. Reifsnyder Hickey², S. Bachu², T. Zhang², M. Terrones², N. Alem², J.M. Redwing¹

¹The Pennsylvania State University, Materials Research Institute, PA, UNITED STATES OF AMERICA, ²The Pennsylvania State University, Department of Materials Science and Engineering, PA, UNITED STATES OF AMERICA

Tungsten disulfide (WS₂) has been widely investigated due to its outstanding properties, such as its bandgap of 2 eV, relatively high theoretical electron mobility, and valley spin polarization. Commonly, the films are grown on amorphous substrates and contain high-angle

grain boundaries after coalescence due to the random orientation of domains. These can act as scattering and recombination centers for charge carriers, limiting device performance. To avoid this, a crystalline substrate and epitaxial growth is typically employed for general thin-film deposition, although this approach has not been extensively investigated for 2D TMD monolayers. Large-area growth is also crucial to show technological feasibility of the material for wafer-scale device fabrication. In this work, we employ gas source chemical vapor deposition for the growth of WS_2 films on 2" (0001) $\alpha-Al_2O_3$. To achieve coalesced monolayer growth over the entire substrate, we implemented a multi-step growth process, modulating the metal precursor concentration during each of the steps. $W(CO)_6$ and H_2S were used as precursors in H_2 carrier gas. The deposition experiments were conducted over the temperature range from 750 °C to 1000 °C at a pressure of 50 Torr. Characterization of the resulting samples was conducted using atomic force microscopy (AFM), in-plane X-ray diffraction (XRD), Raman and photoluminescence (PL) spectroscopies, and transmission electron microscopy (TEM). Initial studies showed that the WS_2 films exhibit multiple crystal orientations that evolve with growth temperature. Among others, the orientation with an epitaxial relation of $(10-10) WS_2 // (10-10) \alpha-Al_2O_3$ was present at all temperatures. It was established that the additional orientations can be suppressed by increasing the H_2S concentration. Further adjustment of the growth parameters and use of the multi-step growth process led to the formation of a coalesced epitaxial monolayer of WS_2 on $\alpha-Al_2O_3$ with XRD FWHM of the 10-10 peak in ω being 0.09°. This value suggests well in-plane oriented domains with low edge dislocation density. A high-intensity, narrow (FWHM=40 meV) PL peak positioned around 2 eV was observed for the WS_2 films. Low-temperature PL also indicated the formation of good-quality crystalline material as nearly no defect-bound exciton emission was observed. Monolayer formation was confirmed from the AFM height profile ($D=0.9$ nm) and ultra-low frequency (0-100 cm^{-1}) Raman measurements. Dark-field TEM was used to visualize antiphase domains. It was found that the formation of antiphase domains can be

suppressed and that the formation of a 95% antiphase free (single-crystal) WS₂ monolayer film can be achieved.

11:30 AM - 11:45 AM

CHEMICAL VAPOR DEPOSITION OF SEMIMETALLIC TO SEMICONDUCTING MoTe₂

B. Jariwala, R. Zhao, J. Robinson
PA, UNITED STATES OF AMERICA

Semiconducting 2H-MoTe₂ is of interest due to its direct band gap of 1.1 eV in the monolayer limit, which enables its application in the silicon photonics devices as closely match to Si band gap (~1.1 eV)[1][2]. Furthermore, it is known that this material system undergoes a semiconducting (2H) to metallic (1T') phase transition with an electric field [3], thus making large area MoTe₂ is of interest. Here, we report the synthesis of MoTe₂ by hybrid chemical-physical vapor deposition (HPCVD). The synthesis of semi-metallic (1T' phase) to semiconductor (2H phase) films indicates strong dependence on carrier gas, precise control of the temperature profile and local Te-vapor pressure during the growth. A growth optimization was performed for different growth temperatures (500C – 700C), carrier gases and Te-vapor pressure by vary Te-powder location in growth set-up. Scattered and random nucleation is observed mainly when only Ar is used as a carrier gas, while growths using forming gas (Ar/H₂) results in a continuous deposition of MoTe₂ film over the entire substrate (~1×1 cm of SiO₂). Films grown under Te-rich environment exhibit more 2H- phase vibrational modes (

11:45 AM - 12:00 PM

GAS SOURCE CVD OF HIGHLY CRYSTALLINE GRAPHENE/TUNGSTEN DISELENIDE HETEROSTRUCTURE

B. Huet¹, T.H. Choudhury², M. Chubarov², X. Zhang², D. Snyder¹, J.M. Redwing²

¹Applied Research Lab-Pennsylvania State University, PA, UNITED STATES OF AMERICA, ²2D Crystal Consortium, Materials Research Institute, PA, UNITED STATES OF AMERICA

The co-integration of graphene with other 2D-materials constitutes an

important technological step toward the development of 2D electronic and optoelectronic devices. In order to fully exploit the semi-metal behavior of graphene and the semiconducting nature of transition metal dichalcogenides (TMDs) in functional applications, it is of central importance to control the number of layers, their crystallinity, the presence of defects, the cleanliness of the interface, and the formation of wrinkles. In this work, we demonstrate the growth of WSe₂ by gas source chemical vapor deposition (CVD) on top of CVD grown graphene. Isolated millimeter-size graphene single-crystalline domains are first produced by CVD on Cu substrates and transferred on a gas-source CVD process-compatible substrate. This graphene template is then used as synthesis substrate for the high temperature growth of WSe₂ using tungsten hexacarbonyl (W(CO)₆) and hydrogen selenide (H₂Se) as precursors. We observed that WSe₂ grown on graphene exhibits a lower seeding density compared with the direct deposition on C-plane sapphire, thus leading to the formation of WSe₂ with a lateral size exceeding 1 micron. Our work also focuses on studying the epitaxial relationship of WSe₂ with both graphene and the underlying substrate, like sapphire. Graphene can act as a transparent buffer layer which allows WSe₂ to grow epitaxially with the underlying substrate. Successively transferring a few layers of graphene increases the distance between WSe₂ nuclei and sapphire, and screens their interaction. Given that the graphene transfer process inherently leads to impurity intercalation, we investigate the impact of annealing under various atmospheres (low/ambient pressure, oxidative or reducing) on the cleanliness of graphene/graphene and WSe₂/graphene interfaces. Finally, we show that the type of substrate employed as support for graphene plays a role in the formation of wrinkles in the graphene/WSe₂ heterostructure. The formation of wrinkles has been attributed to the high temperature required for the TMD growth process, the difference in thermal coefficient between 2D materials and the underlying substrate, and the weak van der Waals interaction. This work presents a scalable route for the fabrication of van der Waals 2D hetero-structures and helps better understanding the role of the substrate on the fundamental growth mechanisms of WSe₂.

Tuesday, July 30, 2019

10:30 AM - 12:00 PM

Symposium on Epitaxy of Complex Oxides: Defects

Location: Grays Peak II, III

Session Chair(s): Julia A. Mundy

10:30 AM - 11:00 AM

MAKING FUNCTIONAL COMPLEX OXIDE THIN FILMS: EXPLORING THE LIMITATIONS OF CONTROL AND EMBRACING MATERIAL IMPERFECTION

L.W. Martin

University of California, Berkeley, CA, UNITED STATES OF AMERICA

Despite our best intentions and efforts, our ability to manipulate and control complex materials remains rudimentary as compared to the precise control of materials demonstrated in other fields (*e.g.*, the ppb-level control of defects in traditional semiconductor materials). In complex oxide thin films, although modern approaches to epitaxial thin-film growth have enabled unprecedented control of single/multi-layer systems, emergent physical phenomena, and marked advances in our fundamental understanding of these materials, controlling material chemistry, and in turn, defects at even the 0.1-1% level is challenging. In turn, defects, be they intrinsic or extrinsic in nature, play a critical role in the evolution of material properties and phenomena. In this talk, we will investigate a multi-year perspective of our limitations in producing complex-oxide materials with the level of control we desire to have, what those limitations mean for the study, understanding, and utilization of these materials for devices, and, in turn, the opportunities for the community to embrace these defects and utilize their presence as a new design parameter. We will call upon examples of processing-defect-property relationships in a range of epitaxial thin-film materials including SrTiO₃, LaAlO₃, NdNiO₃, BaTiO₃, PbTiO₃, BiFeO₃, and others. We will highlight the role of the synthesis process in determining defect structures, how epitaxy can influence defect formation and ordering, what the presence of these defects does to properties, how to probe and study such defects, and

also how to deterministically produce defects in a way that enhances or improves material performance. We will end with an exploration of what further growth of defect-engineering approaches might enable in the way of novel function and applications in these materials.

11:00 AM - 11:30 AM

IDEALIZED OUTCOMES AND SYNTHETIC REALITIES - WORRYING ABOUT WHAT ATOMS ACTUALLY DO IN OXIDE HETEROEPITAXY

S.A. Chambers

Pacific Northwest National Laboratory, WA, UNITED STATES OF AMERICA

Oxide heteroepitaxy has tremendous potential for generating novel, artificially structured material systems to facilitate the discovery of emerging properties. However, these systems have many degrees of freedom, and the number increases with the number of elements. Moreover, the use of transition metals with their range of stable valences generates even more possible outcomes. In striving to discover exotic new physics, the intricacies and complexities of materials synthesis are often overlooked. It is frequently assumed that depositing multi-layer structures is like making something out of Legos – all one has to do is deposit the right atoms, and they will automatically snap into place and stay put. In reality, this never happens. If we provide enough thermal energy to effect crystallization, we also provide enough energy to drive a range of processes. Film deposition involves both heterogeneous (gas/solid) and solid-state chemistry. As practitioners, we need to be aware of, and have a strategy for monitoring, the plethora of phenomena that can occur as we deposit atoms at elevated temperature. These include surface and bulk diffusion, local chemistry that may differ from our intended outcome, point defect generation including vacancies, anti-sites and interstitials, non-uniform distributions of elements, and deviations from the intended stoichiometry. If these go undetected, the outcome can be “imperfection-driven” functional properties which, if interpreted based on an idealized model of the material, can lead to incorrect understanding. In this talk, I will present some examples of these phenomena from our recent investigations. These include band

alignment and interface structure at $\text{LaFeO}_3/\text{SrTiO}_3(001)$ heterojunctions, band bending and charge transfer at $\text{SrNb}_x\text{Ti}_{1-x}\text{O}_3/\text{Si}(001)$ interfaces, and the structural, compositional and optical properties of epitaxial Fe_2CrO_4 on $\text{MgAl}_2\text{O}_4(001)$ among others, as time allows.

11:30 AM - 12:00 PM

NEW PHENOMENA ENABLED BY THE CONTROL OF OXYGEN VACANCIES IN THE DILUTE LIMIT IN OXIDE THIN FILMS AND SINGLE CRYSTALS

A. Bhattacharya

Argonne National Laboratory, IL, UNITED STATES OF AMERICA

In thin films of complex oxides, properties can often be tuned by varying stoichiometry, thickness, strain and heterostructuring.

However, determining stoichiometry in films, particularly for oxygen, remains a challenge. In some situations, properties may be sensitive to small variations in oxygen stoichiometry, which may not be possible to determine independently with accuracy - and thus difficult to correlate with measured properties. In high mobility samples, electronic transport measurements can be sensitive to low levels of oxygen vacancies - though they are not a quantitative measure of vacancy concentration. I will present two examples of materials where we have controlled oxygen stoichiometry by introducing or removing vacancies at relatively low concentrations to realize new properties. In particular, I will discuss electronic states realized in high mobility films of LaNiO_3 , and in very dilutely doped (reduced) high mobility single crystals of SrTiO_3 , mostly in the context of transport properties. These materials, while having been studied for decades, may still have some surprises in store for us. I hope these findings will again highlight the need to characterize and understand oxygen vacancies in the dilute limit.

Tuesday, July 30, 2019

10:30 AM - 12:00 PM

Symposium on Ferroelectric Crystals and Textured

Ceramics: Textured Relaxor- PT Ceramics

Location: Grays Peak I

Session Chair(s): Mark Fanton, Gary L. Messing

10:30 AM - 11:00 AM

FABRICATION OF HIGH QUALITY TEXTURED PIEZOELECTRIC CERAMICS FOR NEXT GENERATION TRANSDUCER APPLICATIONS BY TEMPLATED GRAIN GROWTH (TGG).

G. Messing¹, M. Brova¹, B. Watson¹, R. Walton¹, E. Kupp¹, M. Fanton², R. Meyer³

¹Department of Materials Science and Engineering, Pennsylvania State University, UNITED STATES OF AMERICA, ²Applied Research Laboratory, Pennsylvania State University, UNITED STATES OF AMERICA, ³Applied Research Lab, Pennsylvania State University, UNITED STATES OF AMERICA

The templated grain growth process consists of crystallographically orienting a minority of single crystal particles in a finer grain size matrix. Densification and subsequent grain growth results in a textured ceramic having the same orientation as the aligned single particles.

The TGG process, first reported in 1997¹, has been shown to yield textured piezoelectric ceramics with properties comparable to the single crystal analog^{2,3}. In this presentation we present key process steps for achieving high quality texture fraction and orientation, and how template size and concentration impact the quality of the textured microstructure. Finally, we correlate the electromechanical properties with the process parameters required to achieve dense, fully textured PIN-PMN-PT and PZN-PMN-PT via reactive RTGG and TGG. ¹M. M. Seabaugh, I. H. Kerscht and G. L. Messing, *J. Am Ceram. Soc.* 80 [5] 1181-88 (1997). ²G. L. Messing, S. Trolier-McKinstry, E. M. Sabolsky, C. Duran, S. Kwon, B. Brahmaroutu, P. Park, H. Yilmaz, P. W. Rehrig, K. B. Eitel, E. Suvaci, M. Seabaugh & K. S. Oh (2004) Templated Grain Growth of Textured Piezoelectric Ceramics, *Critical Reviews in Solid State and Materials Sciences*, 29:2, 45-96. ³G.L. Messing, S.F. Potala, Y. F. Chang, T. Frueh, E.R. Kupp, B.H. Watson III, R.L. Walton, M. J. Brova, A. Hofer, R. Bermejo and R. J. Meyer, "Texture-

Engineered Ceramics – Property Enhancements Through Crystallographic Tailoring” (Review), *Journal of Materials Research*, 32 (17) 3219-3241 (2017)

11:00 AM - 11:30 AM

TEXTURE-ENGINEERED LEAD-FREE PIEZOCERAMICS: PROPERTY ENHANCEMENTS THROUGH CRYSTALLOGRAPHIC TAILORING, DOMAIN ENGINEERING AND COMPOSITE EFFECTS

Y. Chang¹, Y. Liu¹, Y. Sun¹, J. Wu¹, F. Li², S. Zhang³, B. Yang¹, W. Cao⁴

¹Harbin Institute of Technology, CHINA, ²Xi'an Jiaotong University, CHINA, ³Nanjing University, CHINA, ⁴The Pennsylvania State University, UNITED STATES OF AMERICA

Piezoelectric energy harvesting has recently received extensive attention due to the strong demand of sustainable power sources for wireless sensor networks and portable/wearable electronics.

Unfortunately, relatively low energy density and poor long-term stability seriously hinder the implementation of BaTiO₃ (BT)-based piezoelectrics as high-efficiency energy harvesters. In this work, we proposed to integrate crystallographic texture and composite design strategies into BT-based ceramics to resolve the above challenges. Novel 0-3 type (Ba, Ca)(Zr, Ti)O₃/BaTiO₃ (BCZT/BT) composites with highly [001]_c oriented and “core-shell” structured grains were developed by templated grain growth. Benefited from the piezoelectric anisotropy, the favorable domain configuration, and the formation of smaller sized domains, high piezoelectric coefficient (d_{33}) of 755 pC/N and large piezoelectric strain coefficient (d_{33}^*) of 2027 pm/V were simultaneously achieved at a textured degree F_{001} of 98.6%.

Meanwhile, the inclusion of low- ϵ_r BT microcrystals inside the oriented BCZT grains effectively suppressed the dielectric permittivity of the composite, thus remarkably improving piezoelectric voltage coefficient g_{33} to be about 34.3×10^{-3} Vm/N. Significantly enhanced fatigue resistance was observed in the highly textured composites up to 10^6 bipolar cycles, which can be attributed to the enhanced domain mobility, less defect accumulation, and thus suppressed crack

generation/propagation. Encouragingly, the cantilever energy harvesters based on such textured composites possessed ~9.8 times enhancement in output power density at 1 g acceleration relative to the non-textured counterpart, with stable output features maintained up to 10^6 vibration cycles. This work represents a remarkable advancement in the field of lead-free piezoelectrics, and can largely expand their applications into high-efficiency energy harvesting field.

11:30 AM - 12:00 PM

MANUFACTURING AND UNIFORMITY OF GRAIN TEXTURED PIEZOELECTRIC CERAMICS

M. Fanton¹, R. Meyer², G. Messing³, E. Kupp³, B. Watson³, M. Brova³, R. Walton³, J.J. Fox¹

¹Penn State University, UNITED STATES OF AMERICA, ²Applied Research Lab, Pennsylvania State University, UNITED STATES OF AMERICA, ³Department of Materials Science and Engineering, Pennsylvania State University, UNITED STATES OF AMERICA

Directional tailoring of performance for oxide materials has been largely limited to taking advantage of anisotropies in single crystal materials. This presentation outlines the process technology and scale up considerations for tailoring directionally oriented ceramic microstructures, with a focus on achieving near single crystal performance from highly oriented ceramic piezoelectric materials in the PIN-PMN-PT, and PMN-PZT families of materials. The engineering challenges associated with scaling each step of the manufacturing process to yield 150mm square by 10mm thick tiles will be outlined as will observations regarding process variability within a given tile and between tiles. In addition, we will discuss modifications to these textured compositions and processes to control performance characteristics such as loss factor and coercive field. The electro-mechanical performance and performance trade-offs of materials for acoustic applications where power loss and self-heating are a significant issue will be the primary focus.

Tuesday, July 30, 2019

1:30 PM - 3:00 PM

Bulk Crystal Growth: Focus on Silicon

Location: Shavano Peak

Session Chair(s): Jochen Friedrich, Tomasz Sochacki

1:30 PM - 1:30 PM

EXPERIMENTAL AND THEORETICAL ANALYSIS OF THE GROWTH RIDGE GEOMETRY OF CZOCHRALSKI-GROWN SILICON CRYSTALS

J. Friedrich¹, L. Stockmeier², C. Kranert³, P. Fischer³, B. Epelbaum¹, C. Reimann¹, G. Raming², A. Miller²

¹Fraunhofer IISB, GERMANY, ²Siltronic AG, GERMANY, ³Fraunhofer THM, GERMANY

We present a contactless, non-destructive approach based on surface topography to measure the geometrical parameters of the growth ridge and apply it to silicon crystals grown by the Czochralski method. This method gives an easy access to the temperature gradient at the crystal edge during growth. From theoretical considerations¹, it is well known that the temperature gradient, edge facet growth and the growth ridge are tightly connected. Also the geometry of the growth ridge and its quantitative dependence on the temperature gradient was theoretically predicted¹, but experimental results have not been published yet. Using the results from our experiments for a large variety of industrially grown Czochralski silicon crystals, we confirm the universal validity of that theory². This confirmation in turn allows directly correlating the geometrical parameters of the growth ridge to the temperature gradient. Therefore, fluctuations as well as absolute values of the temperature gradient can be extracted from the measurements, making this a powerful tool for the assessment of crystal growth processes.

References [1] V.V. Voronkov, *Izvestiy Akademii Nauk SSSR Seriya Fizicheskaya* **49**, 2467–2472, 1985. [2] L. Stockmeier, C. Kranert, P. Fischer, B. Epelbaum, C. Reimann, J. Friedrich, G. Raming, A. Miller, *J. Cryst. Growth* (submitted), 2019.

1:30 PM - 1:30 PM

GROWTH OF SILICON SINGLE CRYSTALS BY THE GRANULATE

CRUCIBLE METHOD

R. Menzel, K. Dadzis, A. Nikiforova, N. Lorenz-Meyer, B. Faraji-Tajrishi, N. Abrosimov, H. Riemann

Leibniz-Institut für Kristallzüchtung, GERMANY

The Silicon Granulate Crucible (SiGC) method is a novel growth concept we have proposed for the production of high-quality silicon single crystals needed for application in photovoltaics and electronic devices [1,2]. The SiGC growth concept has the potential to combine the advantages and avoid the disadvantages of the industrial established methods, i.e. the Czochralski (Cz) and the Floating Zone (FZ) process. We have developed a set-up for growth of SiGC crystals of a industrially relevant diameter of 4 inch. During SiGC growth the crystal is pulled from an inductively heated melt pool that is not in contact to a contaminant. High-purity is achievable due to the use of electronic grade fluidized bed silicon granules as containment for the melt and as raw material. FTIR measurements on grown material showed a low oxygen content $<10^{16}$ atoms/cm³, at the level of FZ Si. Because of the continuous replenishment of raw material to the melt pool a homogeneous axial resistivity distribution as in FZ is achievable. Gas phase doping using phosphane allowed the growth of crystals with n-type resistivity of 10 Ωcm. For the first time, the growth of single crystals was demonstrated (see Fig.1). To obtain monocrystalline material, suitable values for pull rate and heater power during seeding were identified. A special technique using a moveable susceptor was applied to generate the thermal conditions and stable phase boundaries for seeding, growth of a Dash neck and crystal shoulder. The filling level of the melt pool must be held constant, within a small tolerance of only several mm. Any contact of granules with the triple-phase-line must be avoided. The process stability was improved with the help of a developed finite element model for the time-dependent calculation of the high-frequency electromagnetic- and temperature field, including shape of the solid-liquid interfaces for all process phases. For crystal diameter control a low order model of the SiGC process was derived.



[1] Menzel, R.; et al., Proc.: Electrotechnol. for Material Processing, Hannover, June 6-9, 2017. [2] Riemann, H., et al.: Method and apparatus for producing single crystals composed of semiconductor material, International Patent, WO2011063795 A1, 2011.

1:30 PM - 1:30 PM

GRAIN BOUNDARY EVOLUTIONS AND INTERACTIONS AT THE CRYSTAL/MELT INTERFACE OF SILICON DURING DIRECTIONAL SOLIDIFICATION

L. Chuang¹, K. Maeda¹, K. Shiga¹, H. Morito¹, W. Miller², K. Fujiwara¹
¹Institute for Materials Research, Tohoku University, JAPAN, ²Leibniz-Institut für Kristallzüchtung, GERMANY

The origin of small-angle grain boundaries (SAGBs) and the interactions between $\Sigma 3$ GBs, SAGBs, and general GBs at a silicon crystal/melt interface are studied by in situ observation during directional solidification. SAGBs are confirmed by preferential etching due to the aggregation of dislocations at the solid/melt interface. Dislocations self-arrange by polygonization into an energetically favorable SAGB configuration. The misorientation of the SAGBs increases during crystal growth, possibly through the continual incorporation of dislocations. The interactions between various GBs

exhibit a dependence on the misorientation angle of participating GBs. SAGBs, which possess a low misorientation and are composed of dislocation arrays, can propagate through $\Sigma 3$ GBs, but this behavior transitions into coalescence with $\Sigma 3$ s when the misorientation approaches the limit of a SAGB, which is typically 15° . GBs with a misorientation around 15° are capable of absorbing $\Sigma 3$ GBs, but the resulting GBs are unstable and prone to form new $\Sigma 3$ GBs at the crystal/melt interface. General GBs, in which dislocation structure is indistinguishable owing to high misorientation, show the ability to terminate $\Sigma 3$ GBs steadily and continuously. The present findings suggest that the presence of intrinsic dislocations in GBs plays a role in GB interactions. The intrinsic GBDs in SAGB would decompose into partial dislocations at the $\{111\}$ plane of the $\Sigma 3$ GB. When the liquid atoms in the melt solidify at the junction of the deformed boundary plane and the crystal/melt interface, a new dislocation network grows on the other side of the boundary as if a SAGB penetrates a $\Sigma 3$ GB. In contrast, there is no distinguishable intrinsic dislocation structure in high-misorientation general GBs, and this fact means that the decomposition of boundary structure at the $\Sigma 3$ boundary plane is not probable during growth. Consequently, $\Sigma 3$ GBs terminate in the encounter with the general GBs owing to the strong disorder of the general GB structure.

1:30 PM - 1:30 PM

CO CONCENTRATION IN CZ FURNACE

Y. Miyamura, H. Harada, S. Nakano, S. Nishizawa, K. Kakimoto
Research Institute for Applied Mechanics, Kyushu University, JAPAN
Since carbon impurities in silicon become nuclei of oxygen precipitates in the thermal process[1], reduction of carbon is required for high performance devices. In crystal growth process of CZ silicon, carbon contamination is caused by CO gas generated in the CZ furnace [2]. CO gas is generated mainly by (i) degassing during heating-up, (ii) reaction between quartz crucible and graphite, (iii) reaction between SiO gas evaporated from silicon melt and carbon materials. In order to clarify the contribution of each reaction, we measured the concentration of CO gas in the CZ furnace during the heating process by gas chromatography. 4-inch crucibles were

installed in 18-inch hot zone CZ furnace and heated at 60 kW in 5 torr. The argon gas flow rate was 20 slm. CO concentration was measured by sampling the gas from the furnace exhaust every 24 minutes. Four batches of heating were performed. Bat#1: placing two 4-inch graphite crucibles. Bat#2: setting a quartz crucible in each of two graphite crucibles. Bat#3: charging and melting 100 g of poly Si in each of two quartz crucibles. Bat#4: charging and melting 100 g of poly Si in each of four quartz crucibles. Figure 1 shows CO concentration during heating. The CO concentration of Bat#1 increases for one and a half hours up to 2×10^{-11} mol/cm³, and then decreases. CO in Bat#1 is caused by (i) degassing. Therefore it decreases after peak of degassing. The CO concentration in Bat#2 does not continue to decrease after degassing peak and becomes 9×10^{-12} mol/cm³. It is generated by (ii) reaction between quartz and graphite. In Bat#3, all of poly-Si melted in 3 hours. The CO concentration after melting increases up to 2×10^{-11} mol/cm³. It is generated by both (ii) reaction between quartz and graphite and (iii) reaction between SiO gas and carbon materials. In Bat#4, the CO concentration after melting is 4×10^{-11} mol/cm³, twice of that in Bat#3. From those results, it is possible to estimate the contribution to CO generation of each reactions. [1] S. Kishino, Y. Matsushita, M. Kanamori, T. Iizuka, Jpn. J. Appl. Phys. 21 (1982) 1. [2] X. Liu, S. Nakano, K. Kakimoto, Cryst. Res. Technol. 52 (2017) 1600221. This work was partly supported by the New Energy and Industrial Technology Development Organization (NEDO) under the Ministry of Economy, Trade and Industry (METI).

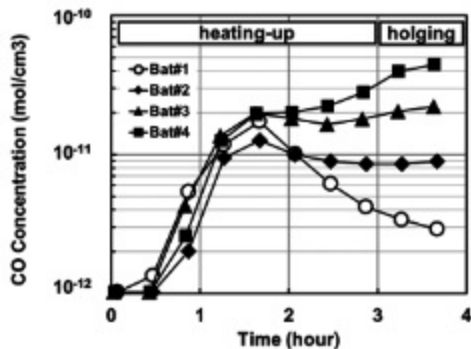


Figure 1. CO gas concentration in CZ furnace
 Bat#1: two graphite crucibles
 Bat#2: two set of quartz and graphite crucible
 Bat#3: two set of poly-Si (100g) in quartz and graphite crucible
 Bat#4: four set of poly-Si (100g) in quartz and graphite crucible

1:30 PM - 1:30 PM

EFFECT OF SEED CRYSTAL ON DISLOCATION DENSITY IN SI SINGLE CRYSTAL

S. Nakano, X. Liu, X. Han, K. Kakimoto

Research Institute for Applied Mechanics, Kyushu University, JAPAN

Monocrystalline silicon is mainly produced by the Czochralski method. This method can produce high-quality silicon ingot, but production cost is high. Multicrystalline silicon is one of the major materials because of its low production costs and high throughput. However, dislocation density is one of the main problems that affects the quality of silicon ingots for solar cells [1]. Seeded directional solidification, which uses a monocrystalline seed crystal in the bottom of the crucible to grow the Si in one crystallographic orientation. This technique could be produced high-efficient and low-cost mono-like Si ingots. It has been reported that oxygen atoms in the Si single crystal adhere to dislocation and immobilize it by anchoring effect [2]. Therefore, dislocation multiplication in the Si single crystal is inhibited by anchoring effect of oxygen atoms. In this study, we focused on the effect of different seed crystals, which is grown by Czochralski method and Floating zone method on the dislocation density. These seed crystals have different levels for oxygen concentration, which could be effect on dislocation generation. We investigated the relationship between the dislocation density and different seed crystals by using numerical analysis [3-5]. Acknowledgement This work was partly supported by the New Energy and Industrial Technology Development Organization (NEDO) under the Ministry of Economy, Trade and Industry (METI). Reference [1] M. M'Hamdi, E. A. Meese, E. J. Øvrelid, and H. Laux, Proceedings 20th EUPVSEC (2005) 1236. [2] M. Imai, K. Sumino Phil. Mag. A 47 (1983) 599. [3] H. Alexander, P. Haasen, Solid State Phys. 22 (1968) 27. [4] M. Suezawa, K. Sumino, I. Yonenaga, Phys. Stat. Sol. A 51 (1979) 217. [5] B. Gao, S. Nakano, H. Harada, Y. Miyamura, K. Kakimoto, Cryst. Growth Des 13 (2013) 2661.

1:30 PM - 1:30 PM

NON-STATIONARY SIMULATIONS OF HEAT TRANSFER,

THERMAL STRESSES AND POINT DEFECT DISTRIBUTION DURING CZ SI SINGLE CRYSTAL GROWTH

A. Sabanskis, J. Virbulis

University of Latvia, LATVIA

During the growth of silicon (Si) single crystals using the Czochralski (CZ) technique, the crystal pull rate and the heater power are adjusted to maintain a predefined crystal shape. The CZ process is strongly non-stationary, i.e., the temperature and point defect concentration fields depend on their past values. In the present work the CZ process is studied numerically using non-stationary mathematical models which allow to predict the evolution of the CZ system in time, including Dash neck, cone and cylindrical growth stages. The model system implemented in the computer program CZ-Trans [1,2] considers heat transfer, point defects dynamics, thermal stresses and their influence on the point defects [3]. In the present study the influence of the model parameters on the thermal stresses and point defects are investigated. The impact of the process parameters (crystal pull rate, heater power) is also studied. The results are compared with the experimental data such as [4].

References [1] A. Sabanskis, K. Bergfelds, A. Muiznieks, T. Schröck, and A. Krauze, *J. Cryst. Growth* **377**, 9–16, 2013. [2] A. Sabanskis, J. Virbulis, *IOP Conf. Ser.: Mater. Sci. Eng.* **355**, 012003, 2018. [3] K. Sueoka, E. Kamiyama, J. Vanhellefont, and K. Nakamura, *Phys. Stat. Sol. B* **251**, 2159-2168, 2014. [4] T. Abe, K. Hagimoto, *Solid State Phen.* **47-48**, 107–114, 1996. **Acknowledgments** The present research has been supported by the PostDoc Latvia Project No. 1.1.1.2/VIAA/2/18/280.

Tuesday, July 30, 2019

1:30 PM - 3:00 PM

Detector Materials: Halide Scintillators

Location: Red Cloud Peak

Session Chair(s): Mariya Zhuravleva, Akira Yoshikawa

1:30 PM - 2:00 PM

IMPACT OF TL₂LIYCL₆ CRYSTAL STRUCTURE EVOLUTION ON

CRYSTAL GROWTH

D.R. Onken¹, D. Perrodin¹, D. Yuan¹, A. Canning¹, A.S. Tremsin², S.C. Vogel³, E.D. Bourret¹

¹Lawrence Berkeley National Laboratory, CA, UNITED STATES OF AMERICA, ²University of California at Berkeley, CA, UNITED STATES OF AMERICA, ³Los Alamos National Laboratory, NM, UNITED STATES OF AMERICA

Investigations of elpasolite scintillators containing ⁶Li (A_2LiLnX_6 , Ln-lanthanide and X-halogen) have been a focal point in the development of inorganic radiation detector materials with gamma-neutron discrimination. A benchmark in this area has been Ce-doped Cs_2LiYCl_6 , which is grown commercially using the vertical Bridgman technique. Despite the propensity of this compound to phase separate during growth, the growth is aided by the cubic crystal structure, minimizing the anisotropic thermal stress which can lead to cracking during post-growth cooling. Recently, a number of studies have looked at replacing Cs with Tl in these dual-mode elpasolite scintillators to improve density and gamma stopping power. However, introducing Tl^+ in place of Cs^+ also introduces lower-symmetry p-orbitals, and the crystal structure of many of these Tl-containing elpasolites show a slight distortion from the cubic structure, resulting in a tetragonal space group at room temperature which complicates crystal growth. In this study, we use high-temperature neutron diffraction on Tl_2LiYCl_6 to study how the crystal structure may change during post-growth cooling. We have identified a phase transition around 165°C, and we examine the anisotropic thermal expansion which arises as the cubic symmetry is broken in this crystal during cooling. First-principles electronic structure and formation energy calculations also predict the breaking of cubic symmetry at low temperature. Our experimental and theoretical work examining the crystal structure evolution of Tl_2LiYCl_6 assists in refining the crystal growth. The impact of these temperature-dependent stresses may be assessed through acoustic monitoring for crack detection during the growth process. Growth optimization of Tl_2LiYCl_6 , informed by careful study of the crystal structure evolution, may serve as a basis for future development of Tl-based elpasolites

for dual-mode radiation detection. This work is supported in part by the US Department of Energy/NNA/DNN R&D and carried out at Lawrence Berkeley National Laboratory under contract #AC02-05CH11231 and in part by the U.S. Department of Energy, Office of Science under competitive award number DE-SC0015793.

2:00 PM - 2:15 PM

CRYSTAL GROWTH AND SCINTILLATION PROPERTIES OF THALLIUM-BASED HALIDE SCINTILLATORS

E. Van Loef, G. Ciampi, U. Shirwadkar, L.S. Pandian, K.S. Shah
RMD, MA, UNITED STATES OF AMERICA

In this paper we report on the crystal growth and characterization of thallium-based halide scintillators of composition Tl_2MX_n ($M = La, Hf$; $X = Cl, Br$; $n = 5, 6$). Single zone Vertical Bridgman furnaces were used to grow crystals of Tl_2LaCl_5 and Tl_2LaBr_5 doped with different Ce concentrations. In the case of Tl_2HfCl_6 and Tl_2HfBr_6 , crystals were grown using a low melting point halide flux to control the high vapor pressure of the hafnium tetrahalide starting materials. In two separate cases however, crystals of Tl_2HfCl_6 and Tl_2HfBr_6 were grown by first sintering $TlCl$ ($TlBr$) with $HfCl_4$ ($HfBr_4$) under reduced pressure before the crystal growth commenced. Crystals thus obtained were typically 1 cm^3 or smaller. Radioluminescence spectra of $Tl_2LaCl_5:Ce$ and $Tl_2LaBr_5:Ce$ crystals exhibit a broad emission band peaking at about 385 nm and 416 nm, respectively. Light yields of small crystals of $Tl_2LaCl_5:Ce$ and $Tl_2LaBr_5:Ce$ typically are $\geq 60,000\text{ ph/MeV}$, while energy resolutions as high as $\sim 3\%$ (FWHM) at 662 keV have been measured. The scintillation decay curve of $Tl_2LaCl_5:Ce$ and $Tl_2LaBr_5:Ce$ is best fitted with a two decay component model. In the case of $Tl_2LaCl_5:10\%$ Ce, the short decay component has a lifetime of about 43 ns (98%) while the longer decay component has a lifetime of about 550 ns (2%). For $Tl_2LaBr_5:3\%$ Ce the numbers are 28 ns (98%) and 150 ns (2%). Note that in the case of $Tl_2LaCl_5:Ce$, the lifetimes and contributions of the short and long decay component to the overall scintillation decay are very much dependent on the Ce concentration. Typically however, the higher the Ce concentration the faster the

decay. Radioluminescence spectra of Tl_2HfCl_6 and Tl_2HfBr_6 crystals exhibit a broad emission band peaking at about 425 and 550 nm, respectively. Light yields of small crystals of Tl_2HfCl_6 and Tl_2HfBr_6 typically are $\geq 20,000$ ph/MeV. Energy resolution measurements are underway and will be reported in the full paper. The scintillation decay curve of Tl_2HfCl_6 and Tl_2HfBr_6 is best fitted with a two decay component model. In the case of Tl_2HfCl_6 , the short decay component has a lifetime of about 240 ns while the longer decay component has a lifetime of about 1.2 μ s. Finally, pulse shape discrimination (PSD) between alpha particles and gamma rays was attempted with Tl_2HfCl_6 using a CAEN system. A PSD Figure of Merit of 1.5 was obtained at a cut off energy of about 300 keVee.

2:15 PM - 2:30 PM

PRODUCTION OF ELPASOLITE SCINTILLATION CRYSTALS FOR DUAL-MODE RADIATION DETECTION

J. Tower¹, C. Hines¹, P. O'Dougherty¹, M. Spens¹, C. Ji¹, J. Glodo², K.S. Shah³

¹Radiation Monitoring Devices, Inc., MA, UNITED STATES OF AMERICA, ²Radiation Monitoring Devices, MA, UNITED STATES OF AMERICA, ³RMD, MA, UNITED STATES OF AMERICA

The elpasolite family of scintillation crystals has been developed for “dual-mode” detection of neutrons and gamma rays simultaneously. This family of crystals exhibits excellent gamma ray energy resolution as a result of its extraordinarily proportional response and strong light output. Neutron response is generated primarily by the reaction of lithium-6 with thermal neutrons, which produces a Q-value of 4.78 MeV. Discrimination between gamma ray and neutron signals can be effectively achieved through pulse height or pulse shape techniques. We report on the crystal development and scale-up efforts at Radiation Monitoring Devices (RMD), which has established production processes for growth of elpasolite crystals that are used for radiation security instruments. The first of these crystals to be offered commercially was $Cs_2LiYCl_6:Ce$ (CLYC) in 2012, which was followed by $Cs_2LiLa(BrCl)_6:Ce$ (CLLBC) in 2018. Crucial elements of the

processes include pre-purification of the raw materials, control of stoichiometry and doping, and vertical Bridgman growth conditions. The challenge has been to reduce defects, such as cracks, grain boundaries, and inclusions, while increasing the crystal size. We will review the development of CLYC and CLLBC with emphasis on the current status and commercialization progress. Finally, we will describe a promising composition that is still in the early stages of development, $Tl_2LiYCl_6:Ce$ (TLYC), which has extraordinary gamma detection efficiency resulting from its high effective-Z value. This work has been supported by the US Defense Threat Reduction Agency, under competitively awarded contracts HDTRA1-14-C-0005 and HDTRA1-17-C-0053. It has also been supported by the US Department of Energy, under competitively awarded contract DE-SC0015793. This support does not constitute an express or implied endorsement on the part of the Government.

2:30 PM - 2:45 PM

GROWTH CHALLENGES OF CESIUM HAFNIUM CHLORIDE SCINTILLATOR

C. Delzer, M. Zhuravleva, J. Hayward, L. Stand, C.L. Melcher
University of Tennessee, TN, UNITED STATES OF AMERICA
Our ability to detect radiation in homeland security application could be significantly improved if a better scintillator were able to replace NaI. One candidate for this is cesium hafnium chloride. It has been shown to have a high energy resolution of 3.3% with a light yield of 36,000 photons per MeV. Also, due to its cubic structure, it has also shown an ability to be grown quickly by the Bridgman method with growth rates at 0.5 mm/hr for high quality crystals. Since the potential for this scintillator has been shown, the next step is to scale up to crystals larger than 12 cubic centimeters, to be comparable in efficiency to available hand held detectors. As scale up of this crystal has been pursued several challenges mostly resulting formation of a secondary phase in the form of inclusion due to the volatility of $HfCl_4$. These inclusion are composed of CsCl, as confirmed by EDS, after $HfCl_4$ sublimes. In the study we investigate the causes of this segregation in to the crystal and several way to improve the growth of

this scintillator, while continuing to scale up the size of crystals produced. This includes growth parameters such as thermal gradient, precursor synthesis methods, and stoichiometry. Using a solution synthesis method, developed at Lawrence Livermore National Laboratory, we are able to produce precursor powder with increased purity while reducing the amount of HfCl_4 lost during growth. Using this precursor, we can grow crystals up to 1 inch in diameter and have achieved a resolution below 4% at 662 keV.

2:45 PM - 3:00 PM

EVALUATING MIXED-CATION $\text{Cs}_4\text{SrI}_6:\text{Eu}$ AND $\text{Cs}_4\text{CaI}_6:\text{Eu}$ SCINTILLATORS AND GROWTH OF LARGE DIAMETER (> 1 INCH) CRYSTALS

D. Rutstrom¹, L. Stand¹, M. Koschan², C.L. Melcher², M. Zhuravleva³

¹Scintillation Materials Research Center, TN, UNITED STATES OF AMERICA, ²University of Tennessee, TN, UNITED STATES OF AMERICA, ³Department of Materials Science and Engineering,

University of Tennessee, TN, UNITED STATES OF AMERICA

$\text{Cs}_4\text{SrI}_6:\text{Eu}$ and $\text{Cs}_4\text{CaI}_6:\text{Eu}$ single crystal scintillators have shown promising properties for use in gamma spectroscopy applications, with energy resolution as low as 3.2% at 662 keV and approximately 70,000 ph/MeV light yields. A study was recently conducted to determine the effects of divalent cation substitution on scintillation performance in terms of energy resolution and light yield for mixed compositions $\text{Cs}_4\text{Sr}_{1-x}\text{Ca}_x\text{I}_6:\text{Eu}$ 7%. Single crystals were grown at a size of $\text{Ø}7$ mm using the vertical Bridgman method with nominal values of $x = 0.10, 0.20, 0.40, 0.60, 0.80,$ and 0.90 . Thermal, structural, and scintillation properties were evaluated. Differential scanning calorimetry (DSC) results showed a near linear relationship between melting point and Ca concentration for compositions between $\text{Cs}_4\text{SrI}_6:\text{Eu}$ and $\text{Cs}_4\text{CaI}_6:\text{Eu}$ ($T_m = 533^\circ\text{C}$ and $T_m = 555^\circ\text{C}$, respectively). Powder X-ray diffraction (XRD) revealed that the trigonal crystal structure and space group $R\bar{3}c$ were maintained for all compositions. Rietveld refinement of the structural models was performed to determine the change in lattice parameter caused by the cation substitution. The refined 'a' lattice parameters decreased

linearly with composition from 14.6665(7) Å for Cs₄SrI₆:Eu 7% to 14.5228(7) Å for Cs₄CaI₆:Eu 7%. The same trend was observed for the 'c' lattice parameter. Vegard's Law was applied to determine the approximate compositions and compared against the nominal values. The measured compositions were all within 5% of the nominal values, with the exception of x = 0.60 which deviated by about 10%. Energy resolution was maintained at 3.2% for 0.10 < x < 0.60 with a maximum light yield of 76,000 ph/MeV being obtained with x = 0.60. These results are promising in that a wide variety of Cs₄Sr_{1-x}Ca_xI₆:Eu compositions can be evaluated without degrading the scintillation performance and could potentially be beneficial for optimizing the crystal growth parameters. Future work will address the effects on crystal growth and homogeneity at large sizes. Additionally, Ø1 inch crystals of Cs₄SrI₆:Eu 3% and Cs₄CaI₆:Eu 3% were successfully grown using the vertical Bridgman method. A thermal gradient of 33 °C/cm was used and crystals were translated at a rate of 0.5 mm/hr and cooled at 5 °C/hr. The crystals were transparent and mostly crack-free, however, macroscopic defects were present. While these defects are not fully understood yet, we currently attribute them to impurity-related growth striations. Ongoing work will investigate the exact causes of these defects and potential solutions for preventing them.

Tuesday, July 30, 2019

1:30 PM - 3:00 PM

Modeling of Crystal Growth Processes II

Location: Crestone I, II

Session Chair(s): Talid Sinno, Toru Ujihara

1:30 PM - 2:00 PM

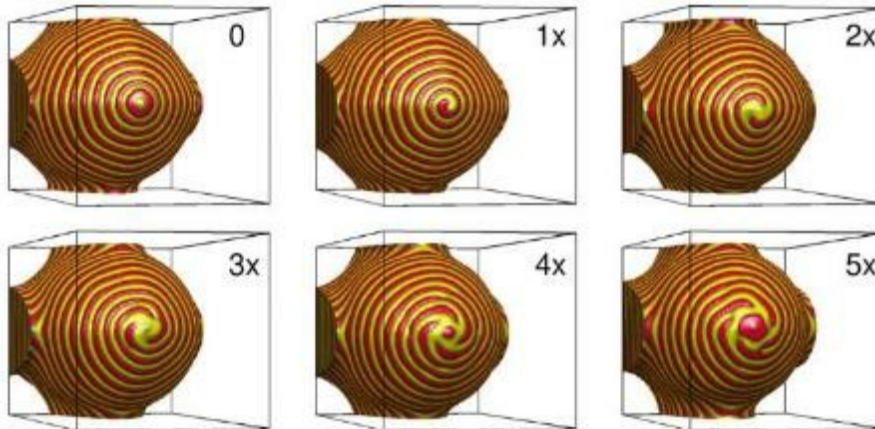
PHASE-FIELD MODELING OF SPIRAL EUTECTIC DENDRITES

T. Pusztai, L. Rátkai, L. Gránásy

Wigner Research Centre for Physics, HUNGARY

Eutectic systems are capable of forming regular microstructures in a self-organizing manner. Well known examples are the lamellar and rod-like eutectic structures. In special cases, however, more exotic

microstructures may also form, such as two-phase eutectic dendrites with a helical inner structure [1]. We have used a simple phase-field model of a ternary alloy to model these spectacular growth forms. We show that different stable structures may develop (spirals with one, two, or even more arms) under the same physical conditions, selected by the thermal fluctuations present in the system. We demonstrate that anisotropy plays an essential role in stabilizing the eutectic dendrite [2,3].



[1] Akamatsu, S., Perrut, M., Bottin-Rousseau, S., & Faivre, G. (2010). Spiral Two-Phase Dendrites. *Physical Review Letters*, 104(5), 056101. [2] Pusztai, T., Rátkai, L., Szállás, A., & Gránásy, L. (2013). Spiraling eutectic dendrites. *Physical Review E*, 87(3), 032401. [3] Rátkai, L., Szállás, A., Pusztai, T., Mohri, T., & Gránásy, L. (2015). Ternary eutectic dendrites: Pattern formation and scaling properties. *The Journal of Chemical Physics*, 142(15), 154501.

2:00 PM - 2:15 PM

MODELING OF ZNO NANOROD GROWTH IN A FLOW REACTOR

O. Cernohorsky, H. Faitova, N. Basinova, S. Kucerova, J. Grym
Institute of Photonics and Electronics of the Czech Academy of
Sciences, CZECH REPUBLIC

Preparation of metal-oxide nanostructures from aqueous solutions by chemical bath deposition has been widely used for its low temperature conditions, low cost, and simple experimental setup. Using this technique, nanostructures of various shapes, dimensions, and crystal structures can be obtained; however, the detailed understanding of this process is still far from complete. To control the nanostructure

growth, it is important to understand how the growth conditions/parameters affect the supersaturation at the interface between the growth solution and the nanostructures. The supersaturation is directly affected by the reaction kinetics of chemical precursors. Moreover, the supersaturation at the solution/nanostructure interface is generally different from that in the bulk solution. Particularly when the rate of the incorporation of the growth units is high in comparison with the diffusion, the reactants are consumed so quickly, that they cannot be supplied from the bulk solution. In this diffusion limited regime, the inhomogeneity of the reactant supersaturation is formed and the supersaturation is lower than in the bulk solution. On the other hand, when the rate of incorporation is small and the diffusion is fast, the system is in the reaction limited regime and the interface supersaturation is virtually the same as in the growth solution. To study the correlation between the interface concentration and the growth habit of nanostructures, we have used ZnO nanorods grown in batch reactors and flow reactors as a model material. Two structures were grown: (a) nanorod arrays on ZnO seed layers with a different seed density, and (b) periodic nanorod arrays on GaN substrates patterned by focused ion beam (FIB) lithography. In the batch reactors, the supersaturation can be considered to be constant over the sample surface at a given time; however, it decreases with time as the growth units are consumed by both homogeneous nucleation within the growth solution and heterogeneous nucleation on the substrate. Flow reactors, on the other hand, ensure time independent reactant concentration, which, however, decreases with the distance from the reactor inlet. The interface concentration of the growth units was estimated using diffusion/reaction model, where experimentally measured growth velocities were used as input data into the model. The modeling of the concentration profile over the patterned substrates was performed using the COMSOL Multiphysics finite element method package and the computed results were used for the estimation of the growth velocities.

2:15 PM - 2:30 PM

SELF-ORGANISATION OF SIGE PLANAR NANOWIRES VIA

ANISOTROPIC ELASTIC FIELD

J. Aqua¹, K. Liu², I. Berbezier², L. Favre², A. Ronda², T. David², M. Abbarchi², P. Gaillard³, T. Frisch³

¹Sorbonne Université, FRANCE, ²IM2NP, FRANCE, ³Université Côte d'Azur, FRANCE

Strained epitaxial SiGe on vicinal Si(001) substrates develop a morphological instability perpendicular to the steps unlike the usual growth instabilities on vicinal substrates, eventually leading to planar nanowires. We assess both theoretically and experimentally the effect of strain anisotropy on the 1D elongation of the Asaro-Tiller-Grinfeld (ATG) instability. The anisotropy of strain relaxation due to the presence of step edges is considered in a continuum model with two different effective strains in the surface plane. We show that the measured in-plane strain anisotropy and the theoretical model are consistent with the experimental morphologies. Nice network of ultrasmall aligned elongations are predicted resulting from a complex interplay of kinetic and energetic phenomena associated with strain anisotropy.

2:30 PM - 2:45 PM

CRYSTAL GROWTH IN FLUID FLOW REVISITED: HOW TO ESCAPE STEP PINNING?

D. Maes¹, J.F. Lutsko²

¹Vrije Universiteit Brussel, BELGIUM, ²Universite Libre de Bruxelles, BELGIUM

A key factor determining the dynamics of crystallization is the effect of impurities on step growth. For over 50 years, all discussions of impurity–step interaction have been framed in the context of the Cabrera–Vermilyea (CV) model for step blocking, which has nevertheless proven difficult to validate experimentally. We performed extensive kinetic Monte Carlo simulations which clearly falsify the CV model, suggesting a more complex picture. In our early studies we found that the CV model only applies in the case of effectively large impurity clusters with long surface residency times¹⁻³. Smaller clusters and point impurities require much higher impurity densities to induce step blocking because thermal fluctuations are likely to drive

the system past the limit implied by the Gibbs-Thomson effect. Here we report on our recent studies of crystal growth and crystal growth cessation in the presence of fluid flows. Flows parallel to the crystal face and perpendicular to the step affect step growth in predictable ways depending on their direction: flows in the opposite direction of the growth raise the local supersaturation and enhance step velocity while those parallel the direction of step growth lower the local supersaturation and can even lead to dissolution of the crystal. Surprisingly, the combination of the two effects on an island causes spontaneous transport of the island in the opposite direction of the flow. Furthermore, we find strong, unexpected effects of flow *parallel* to the step face: effects strong enough to overcome step pinning by impurities. We show that these are due to the same physics as in the case of perpendicular flows but acting on the capillary fluctuations of the step front. This analogy extends to behaviour corresponding to the spontaneous movement of isolated islands. 1. J.F. Lutsko, N. González-Segredo, M.A. Durán-Olivencia, D. Maes, A.E.S. Van Driessche and M. Sleutel, Crystal Growth Cessation Revisited: The Physical Basis of Step Pinning, Cryst Growth and Design, 14, 6129–6134, 2014. 2. M. Sleutel, J.F. Lutsko, D. Maes, and A.E.S. Van Driessche, Mesoscopic Impurities Expose a Nucleation-Limited Regime of Crystal Growth, Phys. Rev. Lett. 114, 245501, 2015. 3. J.F. Lutsko, A.E.S. Van Driessche, M.A. Durán-Olivencia, D. Maes, and M. Sleutel, Step Crowding Effects Dampen the Stochasticity of Crystal Growth Kinetics, Phys. Rev. Lett., 116, 015501, 2016.

2:45 PM - 3:00 PM

EFFECT OF INTENSE CONVECTIVE FLOW ON THE DENDRITE GROWTH.

L. Toropova¹, D. Alexandrov¹, P. Galenko²

¹Ural Federal University, RUSSIAN FEDERATION, ²Friedrich-Schiller-Universität-Jena, GERMANY

A model for the n -fold symmetric dendrites growing under convective flow has been formulated with allowance for the new convective-type heat and mass balance conditions imposed at the dendritic interface. In addition, the Gibbs-Thomson condition connecting the phase transition temperature, solute concentration and interface curvature

has been taken into account with allowance for the kinetic contribution arising from the effect of attachment kinetics at the phase transition boundary. Using the linear stability analysis and solvability theory, a new selection criterion for thermally and solute controlled growth of the dendrite has been found. The obtained selection criterion determines the stable mode of dendritic growth, i.e. it gives an additional relation connecting the dendrite tip velocity and dendrite tip diameter in the case of intensive convective heat and mass transfer near the growing dendritic tips.

Tuesday, July 30, 2019

1:30 PM - 3:00 PM

Semiconductor Quantum Dots and Nanostructures

Location: Torrey Peak II-IV

Session Chair(s): George T. Wang, Honghyuk Kim

1:30 PM - 1:45 PM

INVESTIGATION OF BI INDUCED THREE-DIMENSIONAL INAS NANOSTRUCTURES ON GAAS (110) BY CROSS-SECTIONAL SCANNING TUNNELING MICROSCOPY.

W. Martyanov¹, R.B. Lewis², H. Janssen¹, C.S. Schulze¹, P. Farin¹, R. Zielinski¹, A. Lenz¹, L. Geelhaar², H. Eisele¹

¹TU Berlin, GERMANY, ²Paul-Drude-Institut für Festkörperelektronik, GERMANY

While on GaAs(001) three-dimensional (3D) growth of InAs quantum-dots (QD) is observed on GaAs surfaces, such as (110), the InAs deposition typically results in a two-dimensional (2D) growth and the misfit relaxes plastically. But {110} facets often form the sidewalls in self-assembled GaAs nanowires. And the growth of 3D nanostructures like quantum dots on these sidewalls is of interest for light emitting devices [1]. Recent investigations show that the presence of surface Bismuth (Bi) induces 3D growth on GaAs(110) by reducing the surface energy [2]. Furthermore, Bi exposure on already grown 2D InAs layers causes a morphological phase transition, resulting in a rapid re-organization of the 2D layer into 3D nanostructures. These so-called 3D islands have optical properties of quantum dots and open the

possibility to generate linearly polarized single photons [2]. We investigate these 3D InAs islands grown on GaAs(110) substrate using cross-sectional scanning tunnelling microscopy (XSTM). For this purpose, we cleaved the sample containing capped InAs/GaAs(110) layers with four different growth conditions and Bi contents in ultra-high vacuum perpendicularly to the growth [110] direction. Atomically resolved XSTM images allow for the characterization of the geometric structures in terms of size, density, and atomic composition depending on the presence of Bi. Furthermore, we carry out stoichiometric analysis of the chemical composition by analyzing the variation of local lattice parameter [3]. Thus, we are able to contribute to better understanding of the growth mechanisms of InAs/GaAs(110) with Bi in order to improve the properties for device applications.

References:

- [1] P. Corfdir et al. Phys. Rev. B 96, 045435 (2017)
- [2] R. B. Lewis et al. Nano Lett, 17, 4255-4260 (2017)
- [3] A. Lenz et al. J. Vac. Sci. Technol. B 29, 04D104 (2011).

1:45 PM - 2:00 PM

INP QUANTUM DOTS SATURABLE ABSORBERS FOR MODE LOCKING OF SOLID-STATE LASERS

A.B. Krysa¹, T. Walther¹, S. Ghanbari², K.a. Fedorova³, E.u. Rafailov³, A. Major²

¹University of Sheffield, UNITED KINGDOM, ²University of Manitoba, CANADA, ³Aston University, UNITED KINGDOM

InP quantum dots (QDs) embedded in (Al)GaInP on GaAs have received great attention as an active medium in the edge- and surface emitting lasers. Also, InP QDs showed some promise in single photon emitters and spintronics applications. QDs can offer low saturation fluence within their optical absorption spectrum and short recovery time. In this work, we exploited the above properties of InP QDs, and explored the possibility of using them in semiconductor saturable absorber mirrors (SESAMs) to achieve a high repetition rate operation in passively mode-locked solid-state lasers based on Alexandrite crystals. The spectral tuning of the optical activity of InP QDs can be

achieved by controlling the QD size, composition and surrounding matrix. The growth variable parameters studied were the growth temperature, QD deposition rate, QD deposition time and substrate miscut angle from (100). Thus, a wide spectral range of ~700-800 nm (at room temperature) was covered. A further long wavelength shift of the QD emission up to at least ~900 nm was achieved by adding arsenic during QD growth and forming nominally ternary InPAs QDs. In general, a higher QD deposition rate, a higher growth temperature, a shorter deposition time and a higher miscut angle promoted a shorter wavelength InP QD emission. For device fabrication, substrates with a relatively low miscut (3° off) and extremely high miscut (i.e. (211) plane) angles were not used due to the CuPt type ordering, which deteriorated the crystalline quality of the matrix, and an added complexity with cleaving samples, respectively. Thus, a miscut angle of 10° off towards $\langle 111 \rangle_A$ was used as a compromise. The full SESAM structures consisted of an AlAs/AlGaAs distributed Bragg mirror completed with an InP/GaInP QD layer. This structure was used as one of the plane end mirrors of the laser cavity. A passively mode-locked Alexandrite laser was demonstrated. Pulses with duration as short as 380 fs and 420 fs with an average output power of 295 mW and 325 mW, respectively, were generated. The laser was pumped with up to 7.3 W at 532 nm and operated around 775 nm as defined by the QD optical absorption and the spectral position of the reflectivity stopband of the DBR. The fluence on the saturable absorber was $\sim 590 \mu\text{J}/\text{cm}^2$ and no damage to the SESAM structure was observed.

2:00 PM - 2:15 PM

HETEROEPITAXIAL QUANTUM DOTS ON PATTERNED SUBSTRATES

M. Dhankhar, M. Ranganathan

Indian Institute of Technology Kanpur, INDIA

Quantum dots are very small crystals with typical size ranging from 1 nm to 100 nm. In heteroepitaxial growth, the elastic strain due to the lattice mismatch leads to spontaneous quantum dot formation.

However, these dots, such as the silicon-germanium quantum dots on a flat Si(001) substrate, exhibit a large size distribution and spatial

disorder. One approach to direct the size and organization of the quantum dot arrays in these systems is to use pre-patterned substrates as a template for growth. We construct a theoretical framework based on continuum mechanics to study the growth of quantum dots on patterned substrates. The corresponding numerical resolution is performed using a small slope approximation and a pseudospectral method to resolve the elastic problem[1-3]. The competition between the length scale of the pattern and the intrinsic quantum dot size leads to a rich behaviour where localization of dots can be modified with respect to the features of the patterns. In cubic elastic materials such as silicon and germanium, the alignment tendency due to the elastic anisotropy also changes the location of the quantum dots. In our work, we show that, indeed, this elastic anisotropy is crucial in order to reproduce the key experimental results on quantum dot formation on substrates that has Gaussian pit-like patterns[4].

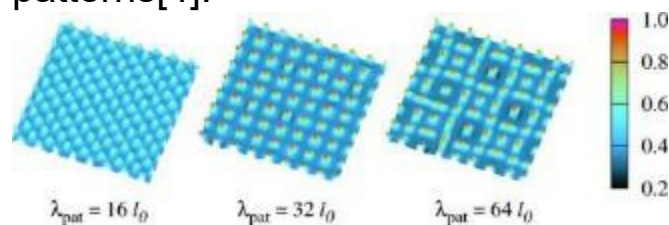


Fig 1: Snapshot showing quantum dot growth starting with different pattern wavelengths (λ_{pat}) indicated. The colour bar refers to the height of the film in units of l_0 ($1 l_0 = 8.8 \text{ nm}$). The system size is 128×128 in units of l_0 and the initial thickness of the film above the patterned substrate is $\sim 8 \text{ ML}$ or 2.19 nm .

References

- [1] J.-N. Aqua, X. Xu, Surf. Sci. 639 (2015) 20.
- [2] G.K. Dixit, M. Ranganathan, J. Phys. Condens. Matter 29 (2017) 375001.
- [3] G.K. Dixit, M. Ranganathan, Nanotechnology 29 (2018) 365305.
- [4] J. M. Amatya, J. A. Floro, Appl. Phys. Kett. 109 (2016) 193112.

2:15 PM - 2:45 PM

IN_{0.8}GA_{0.2}AS QD ACTIVE REGION ($\lambda \sim 1.65 \mu\text{M}$) LASER DIODES GROWN BY BLOCK COPOLYMER LITHOGRAPHY AND SELECTIVE AREA OMVPE

H. Kim¹, W. Wei², T.F. Kuech³, P. Gopalan², L.J. Mawst¹

¹Department of Electrical and Computer Engineering, University of Wisconsin-Madison, WI, UNITED STATES OF AMERICA,

²Department of Material Science and Engineering, University of Wisconsin-Madison, WI, UNITED STATES OF AMERICA,

³Department of Chemical and Biological Engineering, University of Wisconsin-Madison, WI, UNITED STATES OF AMERICA

The formation of InAs QDs by Stranski-Krastonov (SK) growth mode for the emission wavelength near the telecom C-band (1.55 μ m) on InP substrate remains challenging, in comparison to that on GaAs substrate, due to the smaller driving force for the nucleation of InAs QDs stemming from the smaller lattice mismatch [1]. On the other hand, nanopatterning and selective organometallic vapor phase epitaxy (SA-OMVPE) offer a more controllable pathway for QD formation, allowing the QD size to be decoupled from the strain state of the material. However, the processing related damages involved in the sample preparation for the SA-OMVPE has also remained a problematic issue. In this study, an *in situ* etching by CBr₄ was employed prior to the SAE of QD growth, in order to reduce processing related damages introduced during pattern transfer process, which was established by using the real time reflectance measurements beforehand. *in situ* etching performed on either In_{0.53}Ga_{0.47}As or InP at a fixed PH₃ overpressure resulted in a mirror-like smooth surface morphology with relatively controllable etching rates (0.042 and 0.1 nm/sec, respectively). On the other hand, *in situ* etching on In_{0.53}Ga_{0.47}As at the same amount of AsH₃ overpressure exhibited degraded surface morphology accompanied with rapid reduction in the real time reflectance. *in situ* etching on InP under AsH₃ overpressure didn't show an apparent degradation in the real-time reflectance. Based on this established *in situ* etching condition together with InP sacrificial layer, laser diodes, where its In_{0.8}Ga_{0.2}As QD active region was formed by nanopatterning, defined by diblock copolymer lithography, and subsequent selective epitaxy (SAE) on InP substrate, were grown, fabricated for edge emitters, and tested near room temperature (RT) under pulsed operation. The fabricated devices exhibit a low RT threshold current density (\sim 1.6kA/cm²) and

ground-state emission from the QDs for long cavity length devices (4mm-long). The relatively low optical gain from the single layer QD active region leads to a transition from the ground state to excited state as the heat sink temperature increases. In addition, the 2-mm long and 4mm-long QD devices show an insensitivity in the lasing wavelength from 10°C to 25°C and 15°C to 50°C respectively [2]. This work is supported by University of Wisconsin Materials Research Science and Engineering Center (DMR-1121288) and Army Research Office (ARO W911NF-16-1-0298). [1] C. Gilfert *et al*, *Appl. Phys. Lett.* .98, (2011) :201102 [2] H. Kim, et al. *IEEE International Semiconductor Laser Conference (ISLC)* (2018)

Tuesday, July 30, 2019

1:30 PM - 3:00 PM

Symposium on 2D Materials: Special Topics I: h-BN

Location: Crestone III, IV

Session Chair(s): Suzanne Mohny, Cristina E. Giusca

1:30 PM - 2:00 PM

2D EPITAXY WITH A TWIST: ACHIEVING DIFFERENT COMMENSURATE RELATIONS IN HBN/GRAPHENE HETEROSTRUCTURES BY TUNING HBN GROWTH PARAMETERS AND SUBSTRATE MORPHOLOGY

D.j. Pennachio¹, C.c. Ornelas-Skarin², N.s. Wilson¹, E.c. Young¹, S.g. Rosenberg³, K.M. Daniels⁴, R.I. Myers-Ward⁴, K. Gaskill⁵, C.r. Eddy, Jr.⁵, C.j. Palmstrøm¹

¹Materials Department, UC Santa Barbara, CO, UNITED STATES OF AMERICA, ²Electrical Engineering and Computer Science, UC Irvine, CA, UNITED STATES OF AMERICA, ³American Society for

Engineering Education, AL, UNITED STATES OF AMERICA, ⁴National Research Council, DC, UNITED STATES OF AMERICA, ⁵U.S. Naval Research Laboratory, DC, UNITED STATES OF AMERICA

⁴National Research Council, DC, UNITED STATES OF AMERICA,

⁵U.S. Naval Research Laboratory, DC, UNITED STATES OF AMERICA

Many of the intriguing properties of single-crystal 2D devices rely on the relative rotational alignment between layers. For instance,

graphene's band structure highly depends on the interlayer rotational alignment in the graphene/hBN heterostructure [1]. A misalignment in this system may be beneficial if graphene's innate properties, such as high room-temperature electrical mobility, are desired [2]. To allow for scalable graphene/hBN heterostructure formation, this work investigates hBN growth on single-crystal epitaxial graphene (EG) on macrostepped SiC(0001) substrates. The presented results suggest that the EG/SiC(0001) macrosteps influence hBN epitaxy such that a metastable, 30° in-plane hBN/EG rotational alignment is more favorable in certain growth regimes than the fully commensurate hBN/EG alignment, despite their similar crystal structures. Plasma-enhanced chemical beam epitaxy (PE-CBE), an ultra-high vacuum (UHV) compatible process, was utilized to provide a clean environment for examination of the hBN structural, electrical, and chemical properties via *in-situ* and *in-vacuo* characterization methods. To determine the effect of substrate macrostep morphology, SiC (0001) substrates with a 4°-offcut toward <11-20> and nominally on-axis substrates were tested. The alignment of the hBN/EG/SiC(0001) heterostructure was studied by relating *in-situ* electron diffraction to nuclei edge directions found using *ex-situ* atomic force microscopy (AFM). Preferential alignment of the hBN nuclei edges to the SiC macrosteps was found in growths with a lower precursor flux (3 nm/hr. growth rate), while far lower preference was found for higher-flux depositions (7 nm/hr. growth rate). In addition, cross-sectional TEM confirmed the registry and rotational alignment of the hBN to the EG/SiC substrate for both growth conditions, while plan-view TEM showed a single crystal alignment. Energy dispersive X-ray spectroscopy (EDS) during scanning TEM showed the graphene layers remained after the growth process and an atomically sharp hBN/EG interface was present. No hBN/EG intermixing between the layers was detected in either EDS or X-ray photoelectron spectroscopy (XPS). High-resolution topographic and electrical measurements of the hBN layer were performed using *in-vacuo* surface probe microscopy. The macrostep-directed epitaxy of hBN on EG highlighted in this work shows how different levels of commensurability can be achieved solely by tuning growth parameters during van der Waals epitaxy, thus reducing the reliance on manual

rotation during film transfer and increasing the viability of scalable, single-crystal heterostructure growth.

[1] M. Yankowitz, *et al.*, *Nat. Phys.* **8**, 382 (2012).

[2] J. R. Wallbank, *et al.*, *Nat. Phys.* **15**, (2019).

2:00 PM - 2:30 PM

EPITAXY OF MONO-TO FEW-LAYER HBN ON TRANSITION METAL SUBSTRATES

M. Snure, G. Siegel, S.C. Badescu

Air Force Research Laboratory, OH, UNITED STATES OF AMERICA

Hexagonal boron nitride (hBN) has shown to play a critical role in the field of two dimensional (2D) materials and devices serving both complementary roles as a weakly interacting substrate or passivation layer for other 2D materials and primary roles in emitters and tunneling devices. Yet, even with the expanding number of 2D materials it remains one of the only insulators. As a dielectric passivation or buffer layer, hBN has shown to effectively preserve properties of 2D materials by screening effects of surface impurities, phonons, roughness, *ect.* from 3D substrates as well as greatly improving chemical stability of sensitive 2D materials. This is owed to hBN's atomically smooth defect free surface, high phonon energy, and excellent thermal and chemical stability. As such, the demand for hBN has increased significantly driving research on growth of large area, high quality materials with controlled thickness. To meet these needs a variety of methods are being explored including molecular beam epitaxy and chemical vapor deposition (CVD). Under the umbrella of CVD, hBN is largely grown from single precursors (borazine or ammonia borane) on metallic substrates. The morphology and alignment of these layers depends on lattice mismatch and interactions between BN and the metal's d shell electrons. Here we present on metal organic vapor phase epitaxy (MOVPE) of hBN on (111) transition metal films. Metals with partially filled (Ni) and filled (Cu) d shells are explored. As will be discussed the (111) surface of these cubic metals provides both an excellent template for growth of well aligned hBN layers and as a catalyst for growth at relatively low temperatures (<1000C). Separate B (triethylborane (TEB)) and N (NH₃) precursors are used, as opposed single precursors, providing a

great deal of control over the process and chemistry. Using this approach we have demonstrated growth of mono- to many-layer hBN with excellent alignment between this van der Waals material and the metallic substrate. We will also present models to describe growth of mono-to many-layer hBN as the catalytic substrate is covered becoming nearly inert.

2:30 PM - 3:00 PM

ELECTRICAL CHARACTERIZATION OF SINGLE CRYSTAL BORON CARBIDE METAL-SEMICONDUCTOR DIODES

M. Chandrashekar¹, M. Straker², A. Ajilore³, W.A. Phelan⁴, M. Spencer³

¹University of Southern Carolina, SC, UNITED STATES OF AMERICA, ²Morgan State University, UNITED STATES OF AMERICA, ³Morgan State University, AL, UNITED STATES OF AMERICA, ⁴Johns Hopkins University, UNITED STATES OF AMERICA

We report on the current-voltage (I-V) and capacitance-voltage (C-V) characteristics of Ti/Au/B₄C metal/semiconductor diodes grown using a laser-diode float zone technique. Such ultra-hard, highly conductive, refractory borides melt congruently, and are lattice matched to the wide and ultra-wide bandgap (UWBG) III-Nitrides, of interest for power electronics, and other extreme applications. In addition, B₄C (lattice matched with GaN) is used in military armor, where single crystals will aid in characterizing the mechanical properties of such armor, and clarify the failure mechanisms in this anisotropic icosahedral material. The B₄C single crystals were grown using a 1kW 985nm laser diode in a float-zone configuration from commercially purchased high-purity B₄C hot-pressed ceramic rods, at an estimated temperature of ~2400°C. After growth, 2mm thick crystals were oriented into the <101>h plane using Laue white-beam x-ray technique, cut, and polished with diamond grit down to 0.1µm to an RMS roughness <5nm. Powder x-ray diffraction, and electron dispersive spectroscopy (EDS) both showed B/C~4, as expected. Glow discharge mass spectroscopy showed purity in the ppm range. Ti/Au contacts were evaporated on the as-polished surface using a shadow mask to

eliminate the need for lithography.

The I-V curves were linear below 0.05V. Analysis of the nonlinear symmetric I-V's above this voltage suggested trap-related tunneling into the B4C from the metal, manifesting as a 104x increase in current over 0.5V. This was supported by weak temperature dependence down to 80K. Our presentation of the first ever C-V measurements of B4C showed the clear presence of holes as the charge carriers, at a concentration $\sim 10^{20}\text{cm}^{-3}$ at a depletion depth $\sim 3\text{nm}$, again supporting tunneling transport across the metal/semiconductor junction. Given that the impurity concentration is in the ppm range, we attribute the origin of these carriers to intrinsic point defects. We reconcile these measurements with previously reported defect levels within the bandgap of B4C, and discuss the implications of these results on the engineering of B4C for electronic applications. Given that these metal-semiconductor devices are strongly rectifying, they may be used for high temperature thermoelectrics, as well as neutron detection.

Tuesday, July 30, 2019

1:30 PM - 3:00 PM

Symposium on Epitaxy of Complex Oxides: Binary Oxides

Location: Grays Peak II, III
Session Chair(s): Scott A. Chambers

1:30 PM - 2:00 PM

PLASMA-ASSISTED MBE GROWTH OF BETA-GA₂O₃

J.S. Speck

Materials Department, UCSB, CA, UNITED STATES OF AMERICA
Beta-Ga₂O₃ (GO) is a promising wide bandgap semiconductor for power electronics due to its ~4.8 eV bandgap, realization of shallow donors via group IV dopants (Si, Ge, or Sn) on the Ga site, reasonable electron mobility, the availability of large area melt grown substrates by a variety of techniques, and the ability to form heterostructures by alloying on the group III site. In this presentation, we provide an overview of UCSB work on the development of plasma-assisted MBE growth of β -Ga₂O₃, systematic doping studies with Sn and Ge, etching and contact studies, and the development of the heterostructure system β -(Al_xGa_{1-x})₂O₃/β-Ga₂O₃. Recently we realized modulation doping of β -(Al_xGa_{1-x})₂O₃/β-Ga₂O₃ and demonstrated basic MODFET transistors with sheet charge densities as high as $1.2 \times 10^{13} \text{ cm}^{-2}$. Under normal growth conditions, the GO growth temperature is limited by decomposition via suboxide formation. We highlight recent work on the marked impact of growth with a catalytic indium adlayer on the surface (the technique of metal oxide catalyzed oxide epitaxy (MOCATAXY) where the catalytic indium adlayer reacts with molecular oxygen to increase the effective oxygen flux for growth and exchanges the oxygen with gallium at the growth surface. We show an increase of growth temperature of ~250 C over conventional PAMBE growth. We summarize the many open issues in growth science and opportunities for device technology.

2:00 PM - 2:30 PM

GROWING THIN FILMS OF BERYLLIUM OXIDE AND ALLOYS

M. Lippmaa

University of Tokyo, JAPAN

Beryllium oxide is one of the lightest stable oxides, with a band gap of 10.6 eV and a very high Debye temperature of 1270 K, which means

that the thermal conductivity of the highly insulating oxide is comparable to copper at room temperature. BeO is therefore used as a low-loss heat sink material in microwave power devices and as an oxygen diffusion barrier in semiconductor devices. Our aim was to study the behavior of Be in the pulsed laser deposition process and explore the possibility of developing a high-energy particle detector material with the smallest cross-section for radiation damage. Epitaxial BeO films were obtained on sapphire (001) and Nb:SrTiO₃ (111) substrates. A peculiar feature of BeO growth is that epitaxial films can be obtained even at room temperature, while the film growth rate drops sharply above 500 C, possibly due to sublimation of unoxidized Be metal from the film surface. Since BeO is isostructural with ZnO, (Be,Zn)O alloy phase growth was explored. Crystalline films were obtained only within 20% alloying range near the BeO and ZnO end compositions and only moderate band gap tuning was obtained for Zn-rich compositions due to strong band gap bowing. (Be,Zn)O alloy phases could be grown when using mixed oxide targets prepared by conventional powder ceramic methods. Attempts to grow (Be,Zn)O films by alternate depositions from BeO and ZnO targets resulted in a complete loss of Be from the film, apparently due to resputtering by Zn. In situ time-of-flight plume current measurements were used to analyze the plume composition and the kinetic energy of the species in the BeO_x plume.

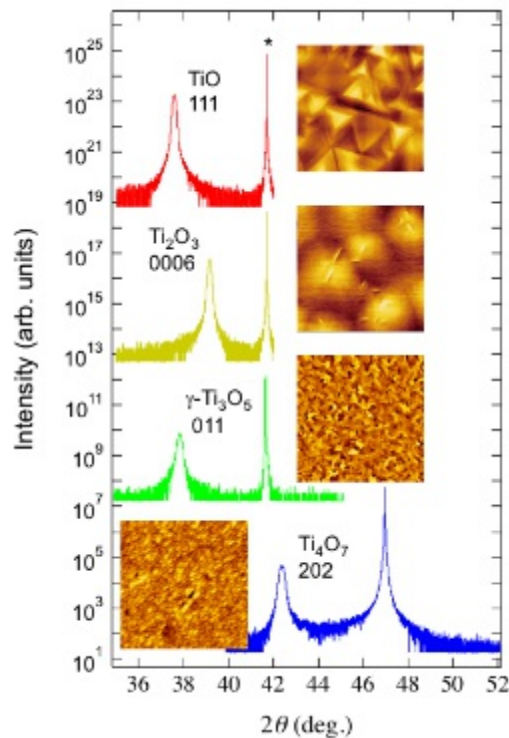
2:30 PM - 3:00 PM

SUPERCONDUCTING TITANATE FILMS: EPITAXIAL GROWTH AND DISTINCTION OF CRYSTAL PHASES

K. Yoshimatsu¹, H. Kurokawa², A. Ohtomo²

¹Tohoku University, JAPAN, ²Tokyo Institute of Technology, JAPAN
Recently, we [1] and other groups [2, 3] reported on superconductivity of titanates in thin-film form. Interestingly, the proposed chemical formula was different among the groups: Ti₃O₅ and Ti₄O₇ [1], TiO [2], and Rh₂O₃-type Ti₂O₃ [3]. The difference was caused by rich crystal phases in titanates. In order to develop research of superconducting titanate films, we should establish characterization methods to distinguish the crystal phase of titanate films we grew. In this study,

we fabricated titanate films using pulsed-laser deposition (PLD) under wide temperature and pressure conditions. The x-ray diffraction patterns indicated clear film reflections at each detection angle (Fig. 1). In addition, the surface morphology was unique with each film (insets of Fig. 1). These results suggest that various titanates (TiO , Ti_2O_3 , $\gamma\text{-Ti}_3\text{O}_5$, and Ti_4O_7) can be obtained in thin-film form by using PLD. In this talk, we will also introduce resistivity and electronic structures which are also keys to distinguish the crystal phase of titanate films.



Reference [1] K. Yoshimatsu *et al.*, Scientific Reports 7, 12544 (2017)., H. Kurokawa, K. Yoshimatsu *et al.*, J. Appl. Phys. 122, 055302 (2017). [2] C. Zhang *et al.*, npj Quantum Mater. 2, 2 (2017). [3] Y. Li *et al.*, NPG Asia Materials 10, 521 (2018).

Tuesday, July 30, 2019

1:30 PM - 3:00 PM

Symposium on Ferroelectric Crystals and Textured Ceramics: Ferroelectric Relaxor- PT Crystal Growth

Location: Grays Peak I

Session Chair(s): Jun Luo, Kazuhiko Echizenya

1:30 PM - 2:00 PM

PMN-PT AND PIN-PMN-PT SINGLE CRYSTALS GROWN BY CONTINUOUS FEEDING GROWTH METHOD

K. Echizenya, K. Nakamura, K. Mizuno

JFE MINEAL COMPANY, LTD., JAPAN

$\text{Pb}(\text{Mg}_{1/3}\text{Nb}_{2/3})\text{-PbTiO}_3$ (PMN-PT) and $\text{Pb}(\text{In}_{1/2}\text{Nb}_{1/2})\text{O}_3\text{-}$

$\text{Pb}(\text{Mg}_{1/3}\text{Nb}_{2/3})\text{O}_3\text{-PbTiO}_3$ (PIN-PMN-PT) single crystals have

excellent piezoelectric properties. These single crystals have been widely utilized for medical ultrasound transducers to provide better image quality. The single crystal boules grown by the conventional Bridgman method show large fluctuations of the piezoelectric properties. The cause is the compositional variation along the growth direction due to the segregation phenomena. We have therefore developed a continuous feeding growth method to eliminate the compositional segregation. The main feature of this new technique is to continuously feed material into the melt during crystal growth. The melt composition is controlled in a tight range by optimizing the feed conditions such as the material composition and the feed rate. As a result, the property uniformity in the single crystal boules was dramatically improved compared to the conventional Bridgman method. Another advantage of the continuous feeding growth method is that crystal boules are grown from a smaller melt volume than the conventional method. This effectively reduces damage to the crucible which holds the melt. Therefore large size single crystal boules of 80 mm in diameter and 320 mm in length have been successfully grown by the continuous feeding growth method.

2:00 PM - 2:30 PM

DEVELOPMENT OF SM-DOPED RELAXOR-PT CRYSTALS WITH ULTRAHIGH PIEZOELECTRIC COEFFICIENT

J. Luo¹, S. Taylor¹, F. Li², S. Zhang³, T. Shrout⁴, W. Hackenberger¹

¹TRS Technologies, Inc., UNITED STATES OF AMERICA, ²Xi'an

Jiaotong University, CHINA, ³University of Wollongong, AUSTRALIA,

⁴Pennsylvania State University, UNITED STATES OF AMERICA

The development of relaxor-ferroelectric single crystals (relaxor-PT),

such as $\text{Pb}(\text{Mg}_{1/3}\text{Nb}_{2/3})\text{O}_3\text{-PbTiO}_3$ (PMN-PT) and $\text{Pb}(\text{Zn}_{1/3}\text{Nb}_{2/3})\text{O}_3\text{-PbTiO}_3$ (PZN-PT), over twenty years ago was a milestone achievement in ferroelectric research as they achieved highest piezoelectric coefficients (d_{33}) and brought breakthroughs to the advanced transducers and sensors applications. Sponsored by the Office of Naval Research (ONR), TRS has developed a modified Bridgman process for relaxor-PT crystal growth and commercialized $\text{Pb}(\text{Mg}_{1/3}\text{Nb}_{2/3})\text{O}_3\text{-PbTiO}_3$ (PMN-PT) and $\text{Pb}(\text{In}_{1/2}\text{Nb}_{1/2})\text{O}_3\text{-Pb}(\text{Mg}_{1/3}\text{Nb}_{2/3})\text{O}_3\text{-PbTiO}_3$ (PIN-PMN-PT) crystals. The diameter of these crystals has been scaled up to 100mm in the current production. Recently, in collaboration with Material Research Institute at Pennsylvania State University (PSU MRI), TRS have successfully grown Sm-doped PMN-PT single crystals with ultrahigh piezoelectric coefficients (d_{33}) and dielectric permittivity (K) ranging from 3400 to 4100 pC/N and from 11700 to 12430 respectively. TRS also grew Sm-doped PIN-PMN-PT crystals with d_{33} values in the range of 2000-2500pC/N and K values in the range of 5950-8200, which are much higher than the values of the undoped counterparts. Furthermore, it was verified that the property variation along the PMN-PT and PIN-PMN-PT crystals can be significantly suppressed by doping Sm during the Bridgman crystal growth process. For the Bridgman-grown undoped PMN-PT and PIN-PMN-PT crystals, the d_{33} and K vary dramatically along the length in the rhombohedral section owing to the inevitable composition segregation. It is seen that Sm doped PMN-PT and PIN-PMN-PT crystals exhibit at least 25% less variations of piezoelectric coefficient. In this talk, the efforts that TRS has taken on commercialization of PMN-PT and PIN-PMN-PT crystals and on development of the Sm doped relaxor-PT crystals will be reviewed.

2:30 PM - 3:00 PM

CRYSTAL GROWTH AND APPLICATION OF PMN-PT BASED SINGLE CRYSTALS

J. Tian

CTS Corporation, IL, UNITED STATES OF AMERICA

Lead magnesium niobate-lead titanate (PMN-PT) based single crystals were grown with modified Bridgman technique. Binary PMN-

PT single crystals with boule diameter up to 4" are grown routinely along $\langle 001 \rangle$ and $\langle 011 \rangle$ crystallographic directions. In the past decade, ternary single crystals, lead indium niobate-lead magnesium niobate-lead titanate (PIN-PMN-PT), have demonstrated improved electrical and thermal properties while maintaining excellent dielectric and piezoelectric properties. Such improvements are important for transducers requiring a high driving field and/or better temperature stability. The typical usable length of a crystal boule with modified Bridgman growth is about 50 mm. In recent years efforts focus on improved crystal growth techniques to reduce the cost of single crystals as well as improve crystal property uniformity. PMN-PT single crystals with usable length of 100 mm were obtained with double melt crystal growth. Crystals demonstrate uniform in-wafer property before and after the second melt, comparable to production crystals with modified Bridgman technique. Double melt crystal growth is promising in reducing cost of single crystals. One of the issues of Bridgman growth with PMN-PT based single crystals is compositional segregation during crystal growth. Because of the segregation, crystals from the beginning of the growth and end of the growth have different compositions and properties. This limits the usable length of a boule and poses challenges for some underwater applications where property uniformity across parts is critical. Continuous feed crystal growth provides an effective means of controlling property variation along crystal growth direction. Results from continuous feed crystal growth will be presented. The binary PMN-PT crystals have been commercialized in medical ultrasound imaging since 2004. Application of piezoelectric crystals in medical ultrasound has become increasingly popular. Ternary PIN-PMN-PT crystals have been adopted in many higher frequency ultrasound imaging applications in recent years. In addition, excellent crystal performance has been demonstrated in other applications including lower frequency sonar transducers. For high-frequency application, crystal composite was fabricated to fully exploit the excellent properties of single crystals. Crystal composite has greatly improved electromechanical coupling factor enabling transducers to work more efficiently. High frequency crystal composite has been successfully adopted in the state-of-the-art IVUS catheters with broader bandwidth, higher sensitivity and

improved image quality.

Tuesday, July 30, 2019

3:30 PM - 5:30 PM

Bulk and Epitaxial Growth of Gallium Oxide

Location: Grays Peak I

Session Chair(s): Kevin Stevens, Shizuo Fujita

3:30 PM - 4:00 PM

DEVELOPMENTS IN BULK GROWTH OF β -GA₂O₃ VIA THE CZOCHRALSKI METHOD AND FABRICATION OF (010) EPI-READY SUBSTRATES

G. Foundos¹, **A. Lindsey**¹, L. Sande¹, K. Stevens¹, J. Blevins²
¹Northrop Grumman - SYNOPTICS, NC, UNITED STATES OF AMERICA, ²Air Force Research Laboratory, UNITED STATES OF AMERICA

Beta-gallium oxide (the most stable polymorph of Ga₂O₃) has garnered recent interest as the widest bandgap transparent semiconducting oxide which can be produced in bulk using melt-growth techniques. Its bandgap of $\approx 4.8\text{eV}$ enables a high critical breakdown electric field of 8 MV/cm (theoretical) potentially allowing power devices to be fabricated with higher performance at a smaller scale. With support from the Air Force Research Laboratory (AFRL), we are developing a manufacturing process to (1) grow large single crystal boules pulled along [010] using Czochralski puller technology developed at our facility and (2) fabricate and polish 500 μm thick (010) oriented substrates targeting 1-2 Å surface roughness with rocking curves below 100 arcsecs (FWHM). We present our recent progress on growth and fabrication of epi-ready substrates with characterization provided by our project collaborators at AFRL and various universities across the country.

4:00 PM - 4:15 PM

β -GA₂O₃ SINGLE CRYSTAL GROWTH OPTIMIZATION BY EFG METHOD AND OPTICAL ANISOTROPY AND IN-PLANE

POLARIZATION

W. Mu¹, Z. Jia², Y. Yin², X. Tao²

¹State Key Laboratory of Crystal Materials, CHINA, ²Institute of Crystal Materials & State Key Laboratory of Crystal Materials, Shandong University, CHINA

As a wide-bandgap semiconductor with the bandgap of 4.8 eV, β -Ga₂O₃ is attracting more and more attention in recent years, because it has a lot of new applications include: deep ultraviolet photodetectors, light-emitting diodes (LEDs), Schottky diodes, high voltage transistors and high temperature gas sensors. In this work, our objective is to grow high quality and large size β -Ga₂O₃ single crystals and develop its potential applications. We have chosen the EFG method to grow the β -Ga₂O₃ single crystal, since it is convenient for the growth of high quality β -Ga₂O₃ single crystals. In this method the Ir-particles, floating on the surface of the melt, do not disturb the growth process and the solid-liquid interface is stable. Moreover, the crystal growth process has been optimized from the views of temperature gradient on the top of the Ir die, crystal crack, Ga₂O₃ raw material decomposition and volatilization, and the Ir crucible erosion. High quality crystals have been grown with the full width at half maximum (FWHM) of the rocking curve was as narrow as 35.6 arcsec, as shown in Fig 1. A simple method for quick and non-destructive determination of carrier concentration was established based on mid-IR transmission. The anisotropy of optical properties and valence band structure as well as the in-plane angle-resolved transmittance spectra of the three main crystal planes were investigated in detail. The optical bandgap of unintentionally doped β -Ga₂O₃ of (100), (010) and (001) planes were found to be 4.70, 4.55 and 4.70 eV, respectively. The valence band maximum of (100), (010) and (001) planes were 3.37, 3.26 and 3.37 eV obtained by VB-XPS. A 0.04 eV larger surface band bending was found in (100) and (001) than that of (010) plane. The transmitted intensity as a function of in-plane polarization angles was established, as shown in Fig 2. The results indicating that β -Ga₂O₃ could be used in polarizing filters and spectrally selective photodetectors in the UVC band which was

demonstrated by two vertically stacked (100) single crystal wafers

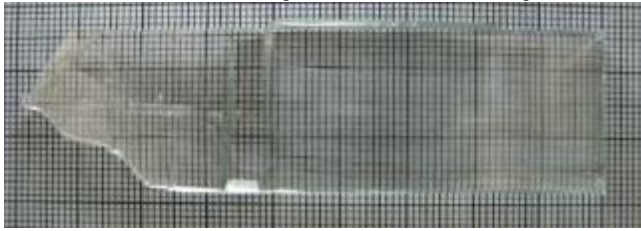


Fig 1. Single crystal grown by EFG method

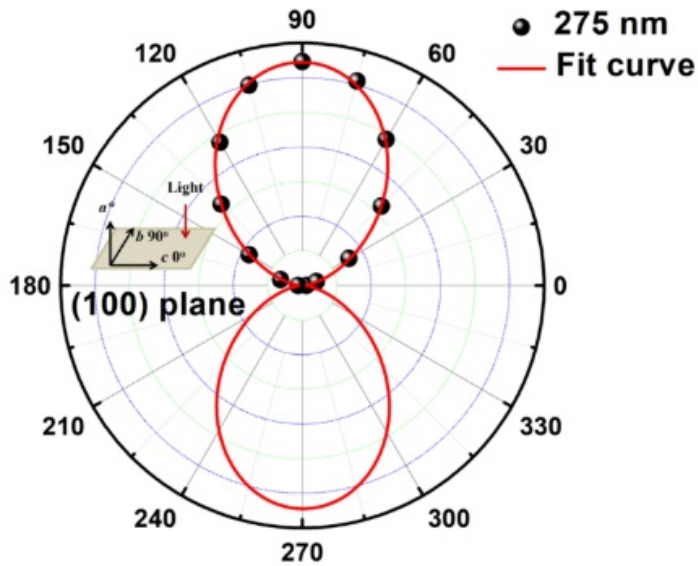


Fig 2. In-plane angle-resolved UV transmittance of β -Ga₂O₃

4:15 PM - 4:30 PM

NUMERICAL STRESS MODELING OF β -GA₂O₃ CRYSTAL GROWTH BY CZOCHRALSKI METHOD

M. Iizuka¹, Y. Mukaiyama¹, V. Artemyev², V. Mamedov², A. Smirnov², V. Kalaev²

¹STR Japan K.K., JAPAN, ²STR Group, Inc. – Soft-Impact, Ltd., RUSSIAN FEDERATION

In the present study, we have performed numerical modeling of β -Ga₂O₃ crystal growth by the Czochralski (Cz) method to investigate controlling of the thermal stress in the crystal. An important issue from the point of view of β -Ga₂O₃ crystal growth is heat transfer around the melt/crystal interface especially through the semitransparent crystal by internal radiation. We have paid special attention to accurate treatment of radiative heat transfer in the semitransparent crystal

using varying absorption coefficient as a function of a doping level to study the effect of transparency on the thermal stress. Growing the β - Ga_2O_3 crystal by Cz method, the control of the thermal stress in the crystal is one of the important factors from the viewpoint of the crystal quality. Especially, it is known that defects are assumed to be generated by a high thermal stress, in particular, near melt-crystal-gas tri-junction point during crystal body growth. Suppressing defects generation, refined adjustment of growth conditions is usually required. Generally, the stress is related to the temperature and composition gradients in the crystal and can be changed by optimization of growth condition, such as crystal shape and doping level. It is known that the absorption coefficient increases as a function of the free electron concentration by doping, which affects internal radiative heat transfer in the semitransparent crystal [1]. The internal radiative heat flux through the crystal can be reduced as increasing absorption coefficient, which leads to higher temperature gradient in the crystal, especially, near the tri-junction point, producing high levels of the thermal stress. To understand comprehensively the phenomena in the β - Ga_2O_3 crystal growth, we used CGSimTM software and add-on module Cz dynamics [2], to carry out 2D unsteady axisymmetric modeling and detailed analysis of global heat transfer in the whole Cz furnace (see Figure 1(a)) with different crystal shapes, shoulder angles, and doping levels, which affect significantly the distribution of the thermal stress in the crystal (see Figure 1(b)).

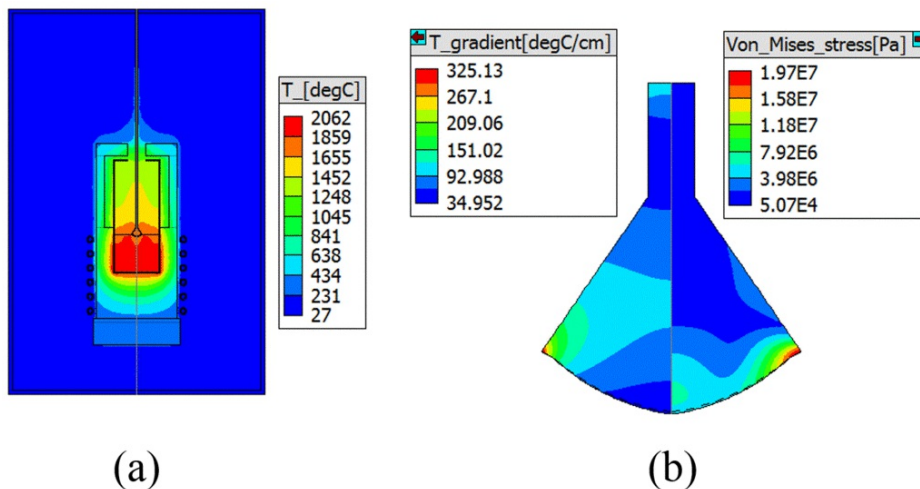


Figure 1: Simulation results of Cz single β - Ga_2O_3 growth. (a) Temperature distribution in the whole Cz furnace. (b) Temperature

gradient distribution (left) and Von Mises stress distribution (right) in the crystal. [1] Zbigniew Galazka *et al.*, J. Cryst. Growth 404 (2017) 184–191 [2] <http://www.str-soft.com/products/CGSim/>

4:30 PM - 4:45 PM

CRYSTAL GROWTH OF A PROMISING SEMICONDUCTOR: β -GA₂O₃

P. Zhao

Beijing Sinoma Synthetic Crystals Co., Ltd., CHINA

Wide band gap semiconductors have become one of the hottest topics of the day to their unique properties and application potentials in various fields. Among them, β -Ga₂O₃ crystal as a third-generation wide band gap semiconductor has shown excellent performances in many fields, including high-temperature gas sensors, deep ultraviolet optoelectronic devices and ultra-high voltage power devices. N-type semiconductors have been successfully prepared and the carrier concentration can be controlled to a certain extent. However, the preparation of p-type semiconductors is still a major problem, which also restricts its applications as devices. Recently, the our group has devoted huge efforts to the research of β -Ga₂O₃ crystals.

4:45 PM - 5:00 PM

ATOMIC STRUCTURE AND ELECTRONIC PROPERTIES OF THE β -GA₂O₃(100) SURFACE

C.S. Schulze¹, J.K. Hofmann¹, C. Bruckmann¹, M. Franz¹, Z. Galazka², W. Martyanov¹, H. Eisele¹

¹TU Berlin, GERMANY, ²Leibniz Institute for Crystal Growth, GERMANY

β -Ga₂O₃ belongs to the transparent conducting oxides (TCOs), being promising candidates for a wide field of devices like solar cells and high-power devices. The physical properties of device operation is highly dependent on the actual parameters of doping and defects, which are highly influenced by the growth and post-growth sample preparation. Scanning tunneling microscopy and spectroscopy (STM/STS) are powerful experimental methods in order to gather

information on the structural and electronic properties at the atomic scale. We present results of clean, freshly-cleaved β -Ga₂O₃ surfaces. The semiconducting bulk β -Ga₂O₃ crystals were grown from the melt [1] and cleaved *in situ* under a base pressure below 1×10^{-8} Pa. Atomically resolved STM images of the β -Ga₂O₃(100) surface show a flat cleavage surface with identified surface unit cells. On the flat (100) β -Ga₂O₃ cleavage surface dark contrast with an estimated volume density of 10^{18} cm⁻³ were observed. This darker contrasts can be assigned to oxygen vacancies below the surface. By low energy electron diffraction measurements on the freshly-cleaved β -Ga₂O₃(100) surface an unreconstructed surface with a (1×1) diffraction pattern was observed. Scanning tunneling spectra show intrinsic electronic states within the band gaps, partially induced by the transition level of oxygen vacancies. This project was supported by the Leibniz Association, Leibniz Science Campus GraFOx, project C2-3. [1] Z. Galazka et al. ECS J. Solid State Sci. Technol. 6, Q3007 (2017).

5:00 PM - 5:15 PM

SURFACE EVOLUTION OF SINGLE CRYSTALLINE β -GA₂O₃ WITH CHEMICAL MECHANICAL POLISHING AND ANNEALING AT AN ELEVATED TEMPERATURE

M.E. Liao, C. Li, M. Goorsky

University of California Los Angeles, CA, UNITED STATES OF AMERICA

The surface evolution of β -Ga₂O₃ with chemical mechanical polishing (CMP) and annealing was investigated in this study. In the current literature, there is a deficiency of β -Ga₂O₃ CMP studies. One recent CMP study investigated the effect of diamond slurry in NaOH during CMP of β -Ga₂O₃.¹ However, slurry particles can induce subsurface damage in substrates and removal rates are too aggressive for thin-layer applications.² In this work, abrasive-free solutions of HCl or NaOH were used to polish (010) substrates at 4 kPa of applied pressure. The solutions were prepared such that the H⁺ and OH⁻

concentrations from HCl and NaOH used were equal. The HCl solution resulted in a removal rate of 90 nm/hr while the NaOH solution resulted in a removal rate of 20 nm/hr. This is interesting considering a study that reported the free etch rate of β -Ga₂O₃ in NaOH was ~8 times faster than in HCl for the same OH⁻ and H⁺ concentrations. We also employed x-ray diffraction triple axis ω scans of the (020) reflection to monitor the effect of the CMP. The tails of the (020) peak were narrower after polishing, indicating the removal of subsurface damage. Smooth surfaces without any surface pits were achieved with a roughness below 1 nm. Epi-ready ($\bar{2}01$) and (010) substrates were annealed at 900 °C to study the surface evolution at elevated temperatures. Atomic force microscopy (AFM) images of the annealed substrates showed parallel striations formed on the surface. We propose that the mechanism of these striations is due to the surfaces reconfiguring itself towards the most energetically favorable planes, which are the (100) and (001) for β -Ga₂O₃.^{1,3} AFM shows that the striations for the ($\bar{2}01$) sample were observed along the (201) planes and the angle at which these striations made with the substrate surface ranged from 1° to 15°. These corresponded to many planes such as ($\bar{9}04$), ($\bar{5}03$), and ($\bar{3}01$). All of these planes associated with each striation are planes that suggest the substrate surface is reconfiguring its surface towards either the (100) or (001) planes. Striations also formed on the annealed (010) substrates. In these samples, the striations made angles ranging from 0.5° to 2° from the surface – towards the (001) plane.

References 1. C. Huang, et al., RSC Adv., 8, 6544 (2018) 2. S.J. Brightup, et al., ECS Trans., 33(4), 383 (2010) 3. E.G. Villora, et al., Proc. Of SPIE, 8987, 89871U (2014)

5:15 PM - 5:30 PM

LOW BACKGROUND CARRIER CONCENTRATION IN AN MOCVD-GROWN β -GA₂O₃

N. Orishchin¹, A. Osinsky¹, F.L. Alema¹, Y. Zhang², A. Mauze², J.S. Speck²

¹Agnitron Technology, Inc., MN, UNITED STATES OF AMERICA,

²Materials Department, UCSB, CA, UNITED STATES OF AMERICA
The prospect of using β -Ga₂O₃ for high voltage vertical power devices is dependent on the capability of epitaxial growth methods to realize low background carrier concentration and high electron mobility. In this work, we report on the use of MOCVD for the growth of high quality β -Ga₂O₃ epitaxial films with low carrier concentration and high electron mobility. Homoepitaxial β -Ga₂O₃ thin films have been grown using TEGa and TMGa as a source for Ga precursor, and N₂O was used as an oxidizer. Unlike the growth of β -Ga₂O₃ using pure O₂, the use of N₂O as an oxygen precursor leads to incorporation of nitrogen and hydrogen impurities into the films. However, the incorporation of these two impurities is strongly dependent on the MOCVD process. Under optimal growth conditions, incorporation of N and H impurities below SIMS detection limit is possible, effectively leading to a UID β -Ga₂O₃ epitaxial layers with very low electron concentration. The MOCVD grown films were analyzed using SIMS, Hall measurement, HRXRD, and AFM. No N and H incorporation was observed in the films as the concentration of both impurities were below the detection limit of the SIMS instrument. The HRXRD and AFM measurements have shown that the films have an XRD FWHM of ~ 43.0 arcsec and RMS ~ 0.8 nm with distinct atomic steps. The Hall measurement showed an electron mobility 150 cm²/Vs with a free carrier concentration 2.4×10^{14} cm⁻³. Such a low background concentration with high electron mobility is the first to be demonstrated and is attributed to the use of N₂O as an oxygen source along with the optimal growth conditions. In this paper, we will also discuss the effect of water vapor, which was added to the other oxidizers for the growth of β -Ga₂O₃ with a reduced background concentration.

Tuesday, July 30, 2019

3:30 PM - 5:30 PM

Bulk Crystal Growth: Semiconductors

Location: Shavano Peak

Session Chair(s): Aleksandar G. Ostrogorsky, Merry Koschan

3:30 PM - 3:45 PM

RECENT DEVELOPMENTS IN GERMANIUM CRYSTAL GROWTH

J. Vanpaemel, K. Dessein, R. Kurstjens

Umicore EOM, BELGIUM

After its initial prominent role in the development of transistor technology, germanium crystals have since been in the shadow of its fellow group IV element, silicon. Although germanium crystals are not being used for CMOS technology, it has found its use in different applications, where it plays a crucial role in the functioning of the device. Umicore has a long tradition in dealing with bulk germanium crystal growth, offering solutions to markets ranging from infrared optics to gamma ray detectors. Today, most of the germanium crystals are processed into epi-ready wafers. These wafers are used as a growth substrate for space triple-junction solar cells. A key selling point of these Umicore crystals is their dislocation-free nature and the fact that they possess only a minimal number of voids caused by vacancy clustering. Until recently, 4 inch germanium crystals/wafers were the standard product in the solar cell market. One wafer would typically fit 2 solar cells. In order to reduce the labor cost associated with the manual lay-down of the cells, larger cell types needing 6 inch wafers are becoming increasingly popular. Our 6 inch wafer volume is today outweighing that of 4 inch, also thanks to recent improvements to the crystal growth. In parallel, the development of industrial length 8 inch crystals has been initiated, as there is a strong market pull for this product. In this presentation, we will show how we tackled the issues of void formation while maintaining dislocation-free growth for 6" crystals and share the status of large diameter Ge crystal growth developments.

3:45 PM - 4:00 PM

SEGREGATION OF BORON IN SILICON GERMANIUM CRYSTALS GROWN BY TRAVELING LIQUIDUS ZONE TECHNIQUE

T. Taishi¹, K. Kawakami¹, K. Ogawa¹, Y. Arai²

¹Faculty of Engineering, Shinshu University, JAPAN, ²Japan Aerospace Exploration Agency, JAPAN

Silicon germanium ($\text{Si}_x\text{Ge}_{1-x}$) is a complete solid solution, which can change electric properties such as bandgap and carrier mobility by changing compositions of Si and Ge. In order to precisely control carrier concentration in $\text{Si}_x\text{Ge}_{1-x}$ crystals, segregation phenomena of impurities such as boron (B) and phosphorus are very important. But, few reports about segregation of impurities in $\text{Si}_x\text{Ge}_{1-x}$ at the intermediate composition of $x=0.5$ are available. In the present study, segregation of B in $\text{Si}_x\text{Ge}_{1-x}$ crystals grown in traveling liquidus zone (TLZ) technique is investigated. Several crystals doped with B were grown by TLZ technique in carbon crucible. B doping were carried out by two kinds methods. One is that all B atoms were doped in Ge liquidus zone by arranging a B-doped Si thin wafers above a Ge block. Another is that B atoms were continuously doped in Ge liquidus zone by arranging a B-doped Si block on the Ge block. The composition of Si and Ge in crystals was controlled to be $x=0.5$, and the B concentration in the Ge liquidus zone was controlled to be approximately 10^{18} cm^{-3} . After the crystal growth, crystals were cut vertically along the growth direction, and B concentration was evaluated by TOF-SIMS analysis and Hall-effect measurement. It was found that B concentration decreased gradually with increasing solidified fraction in $\text{Si}_{0.5}\text{Ge}_{0.5}$ crystals, indicating that the segregation coefficient of B in $\text{Si}_{0.5}\text{Ge}_{0.5}$ crystal growth is larger than 1. In addition, the decrease tendencies were different in two kinds B doping methods. From these experimental results, segregation of B in $\text{Si}_{0.5}\text{Ge}_{0.5}$ crystals were discussed.

4:00 PM - 4:15 PM

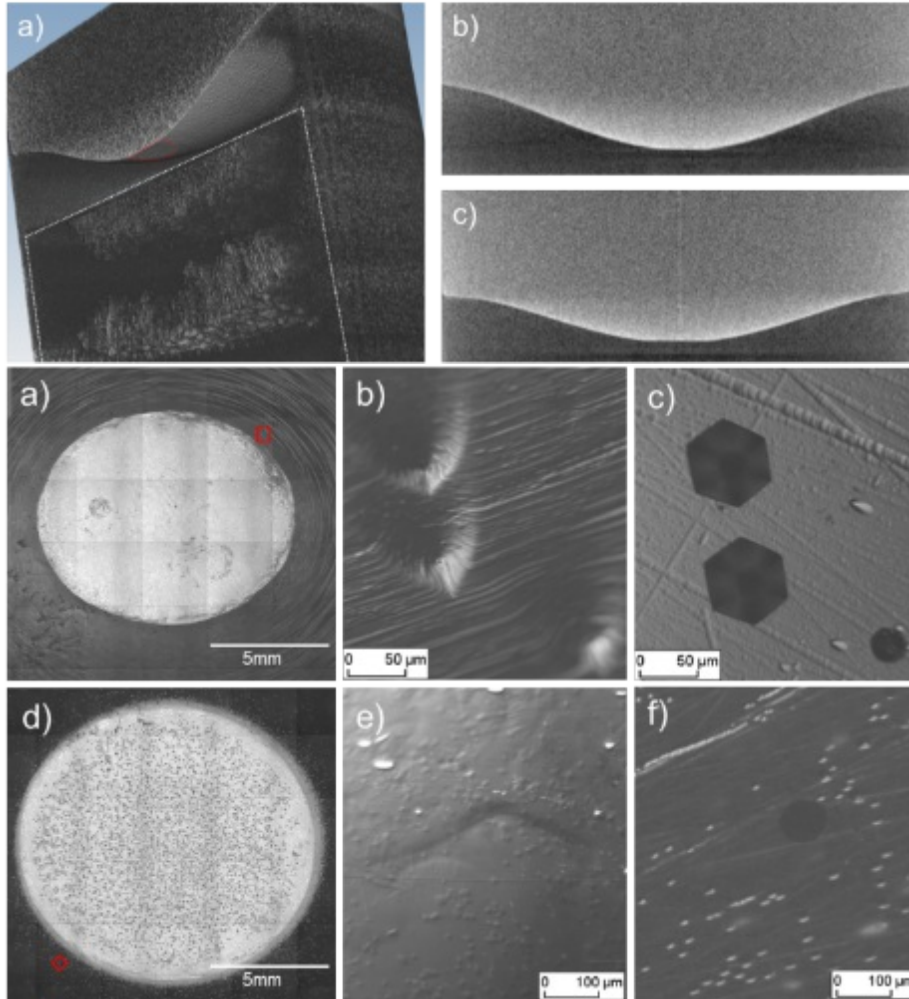
INFLUENCE OF THE GROWTH INTERFACE SHAPE ON THE DEFECT CHARACTERISTICS IN THE FACET REGION OF 4H-SiC SINGLE CRYSTALS

M. Arzig¹, M. Salamon², T.C. Hsiao³, N. Uhlmann², P.J. Wellmann¹

¹Crystal Growth Lab, Materials Department 6 (i-meet), University of Erlangen-Nürnberg (FAU), GERMANY, ²Fraunhofer Institute for Integrated Circuits, Development Center for X-Ray Technology (EZRT), GERMANY, ³Industrial Technology Research Institute of

Taiwan (ITRI), TAIWAN

With this study we want to evaluate how the shape of the growth interface influences the characteristic defects found near the facet during 4H-SiC PVT-growth. Utilizing our in-situ X-ray Computer Tomography we can observe in-situ how a larger radial thermal gradient leads to the formation of a smaller facet and steeper crystal flanks than it's the case for a smaller thermal gradient. Two 3inch 4H-SiC crystals were grown in our standard PVT setup with an argon background pressure set to 20mbar and Nitrogen is added to stabilize the 4H polytype. The growth temperature at the seed is estimated to be around 2150°C from numerical simulation. Wafers are cut close to the facet, polished and etched in molten KOH at 560°C for defect characterization. CT measurements are conducted several times during the experiment enabling to record how the mass distribution inside the crucible changes and how the crystal evolves during growth, as depicted in Figure 1a). From the 2D cuts through the CT data depicted in Figure 1b) and c), the difference in the curvature of the growth interface for the two grown crystals gets obvious. For crystal #1 the inclination between facet and crystal flanks is more pronounced than for crystal #2, which grows rather flat. It can also be seen that the stronger inclination leads to a smaller size of the facet for crystal #1. With a pronounced curvature of the interface, the step flow morphology at the crystal flanks changes as denoted by Figure 2. A larger angle between the basal plane of the facet and the growth interface in the step flow area leads to the formation of bigger surface steps (Figure 2 b). For crystal #2 the smaller surface steps are only visible in the higher magnified image depicted in Figure 2e. With KOH defect etching, micropipes are revealed as big hexagonal pits visible in Figure 2c) and f). Figure 2b) and e) show the influence of these specific defects to the morphology at the point where the surface is penetrated, respectively. In the case for steeper crystal flanks, the micropipes perturb the step flow morphology stronger than in the case for the more flat growth interface. In the conference paper a detailed examination of the interaction of different step heights with defects intersecting the surface will be investigated regarding lateral overgrowth mechanisms. Process conditions that cause overall defect reduction will be discussed.



4:15 PM - 4:30 PM

HIGH QUALITY AND INCLUSION SUPPRESSION BY SWITCHING FLOW IN 3-INCH SiC SOLUTION GROWTH

C. Zhu¹, T. Endo², H. Lin², H. Koizumi¹, S. Harada², M. Tagawa², T. Ujihara¹

¹Institute of Materials and Systems for Sustainability (IMaSS), JAPAN,

²Department of Materials Process Engineering, Nagoya University, JAPAN

In the solution growth of SiC, threading dislocations conversion by the macrosteps were observed, and ultra-high-quality crystal were achieved. On the other hand, the development of macrosteps leads to the formation of macroscopic defects such as solvent inclusion, which degrade the crystal quality. Therefore, it is necessary to control the development of macrosteps. In our pervious study, to stabilize step

flow over the entire crystal, the switching flow method was proposed. In this study, we investigated the effect of switching flow on the TSD conversion and the inclusion suppression in 3-inch SiC growth. The crystal growth experiments were conducted by TSSG method. The simulation was calculated by CGSim (STR Japan). By changing the rotation speed of seed and crucible rod, 2 favorable solution flow patterns were achieved, as shown in Fig. 1. Condition 1 is that the solution flow near the seed crystal is from the center to the outer periphery, and condition 2 is that the solution flow is from the outer periphery to the center. Next, we conducted the solution growth with only condition 1 (ACRT), and periodically switching solution flow with conditions 1 and 2 (Switching flow). 1 ϕ off-axis 3-inch 4H-SiC with the (0001) Si face was used as a seed crystal. The growth temperature was 1900 °C and the growth time is 6 h. Fig. 2 shows the surface morphology and X-ray topography images of 3-inch crystal after the ACRT and switching flow growth. Inhomogeneous surface morphology was obtained after ACRT growth. TSD conversion was observed in the upstream area. However, in the downstream area, the destroyed X-ray topography image was observed, which means the inclusions were generated in the downstream area. After crystal growth with switching flow, relatively uniform surface morphology was formed. In the upstream area, a partial BPD-free region was obtained, and in the downstream area, clear X-ray topography image with TSD conversion contrasts was observed, which indicates that the formation of the inclusions was successfully suppressed by the switching flow growth. The average TSD density in this crystal is about 29 cm⁻². The results show that inclusion-free 3-inch SiC crystal with low TSD density can be grown by the switching flow technique.

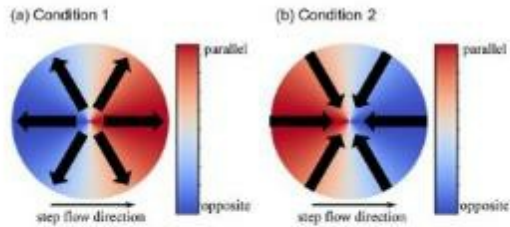


Fig. 1. The two favorable solution flow near the seed crystal distributions: (a) Condition 1, that tendency is from the center to the outer periphery, (b) Condition 2, that tendency is from the outer periphery to the center.

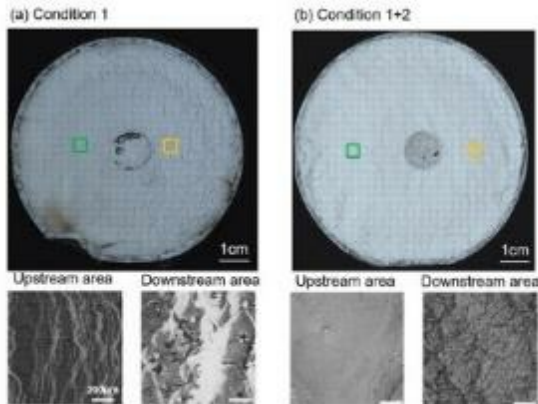


Fig. 2 The surface morphology and X-ray topography images of 3-inch crystal after growth with (a) condition 1 only and (b) condition 1+2

4:30 PM - 4:45 PM

INTERFACE RECONSTRUCTION OF 4H-SiC (000-1) IN THE Si-Cr BASED SOLVENT

Y. Yao¹, T. Yoshikawa¹, D. Chaussende²

¹Institute of Industrial Science, The University of Tokyo, JAPAN,

²SIMAP, Univ. Grenoble Alpes, CNRS, FRANCE

Solution growth is a promising method to grow high-quality SiC bulk crystals because the growth interface is close to the thermal equilibrium. A maximum growth rate of 2 mm/h has been reported by using Si-Cr based solvent. However, solvent inclusions in grown crystals and polytype control are still important issues in solution growth, both of which are presumably related to the step-bunching at the growth interface. Previous works showed that surface roughness and step-bunching greatly differed when using different solvents such as Fe-Si, Si-Cr, and Si-Ti based alloys, and small addition of Al (~1mol%) in solvent effectively suppressed the step-bunching, while reasons for above phenomena are still under discussion. Thus, the new methodology on step-bunching analysis is strongly required for understanding the step-bunching and investigate the solvent effects in

solution growth. In this work, we performed interface reconstruction experiment, where step-bunching is isolated from the crystal growth process, for the off-axis 4H-SiC (000-1) substrate in Si-Cr solvents with and without additives. Then we conducted the kinetic analysis on step-bunching to determine the rate-limiting step of reconstruction process and to analyze the effects of additives on the elementary reaction steps in the step-bunching.

4:45 PM - 5:00 PM

UNDERSTANDING THERMOCHEMICAL AND TRANSPORT LIMITATIONS AND THEIR IMPACT ON CRYSTALLINE QUALITY IN THE CHEMICAL VAPOR TRANSPORT GROWTH OF CUBIC BORON ARSENIDE

D. Snyder, R. Cavalero, R. Lavelle, J.J. Fox

Penn State Applied Research Laboratory, PA, UNITED STATES OF AMERICA

Cubic Boron Arsenide (BAs) has been theoretically predicted to have an ultra-high thermal conductivity material ($k_{\text{BAs}}=1400 \text{ W/mK}$), second to diamond ($k_{\text{diamond}}=2200 \text{ W/mK}$), and superior to all other bulk solid materials, due to the distinctive phonon band structure [1]. Recent reports have experimentally demonstrated the ultra-high thermal conductivity [2,3,4]. Furthermore, theoretical calculation suggests that BAs has excellent carrier transport properties, with electron and hole mobilities predicted to be $1400 \text{ cm}^2/\text{V-sec}$ and $2110 \text{ cm}^2/\text{V-sec}$, respectively [5]. The superior thermal conductivity has attracted interest in BAs for device integration for thermal management of electronics. In addition, the excellent electronic transport properties raise even greater potential for BAs as a semiconductor for homoepitaxial devices for next-generation electronics for a very wide range of applications. The extremely slow growth of BAs using conventional Chemical Vapor Transport (CVT) approach has been well documented. We describe results from our thermochemical analysis using HSC Chemistry in which we explored a range of transport agents, temperatures, and temperature gradients to understand the fundamental limitations. Experimentally we have demonstrated the unseeded CVT growth of BAs and have characterized BAs crystals as large as several mm. We have explored

the impact of transport limitations by varying the ampoule diameter, ampoule length, orientation (horizontal vs. vertical) temperature, temperature gradient and iodine concentration. We have also explored the effect of arsenic overpressure and total system pressure on growth. Fundamental limitations in transport rate are discussed in terms of an 'axial gradient transport' approach and we describe the potential benefits of a halide chemical vapor deposition process to overcome thermochemical limitations associated with conventional CVT growth.

5:00 PM - 5:15 PM

TWIN PHENOMENA OF VGF-GROWN INP SINGLE CRYSTALS

Y. Zhao, M. Duan, W. Lu

Institute of semiconductors, CHINA

It is well-known that InP has a high probability to twin in the single crystal growth process due to its low stacking fault energy. Usually, the probability of twinning increases with the decrease of temperature gradient in the single crystal growth process. Thus, the yield of InP single crystal grown by temperature gradient freezing (VGF) method is rather low since the temperature gradient of VGF is much lower than that of liquid encapsulated Czochralski (LEC) method. It is significant to study the twin phenomena of VGF-InP and increase the yield of single crystal via suppressing twin formation. In this work, we report the statistical results about twin of 3 inch and 4 inch diameter (100)InP single crystals grown by VGF. Undoped, S-doped and Fe-doped twin-free (100)InP have been obtained frequently, but most of the InP ingots grown by VGF have one or more twins. Fortunately, generation probability of lamella twin with two or more bands, which don't change the ingot orientation, is quite high. The ingots are still useful to slice 2 inch, 3 inch or 4 inch wafers with a good yield in these cases, as shown in figure 1 and figure 2. In addition, short lamella twins with length of 1-3 cms in the interior of some ingots are also observed after the ingots are sliced into (100) wafers. This kind of lamella twin is observed more frequently in Fe-doped and undoped InP ingots. Twin generation phenomena in VGF-InP are different from LEC-InP in which single twin appears frequently and growth orientation of the ingot change completely. The twin behavior of VGF-InP is discussed

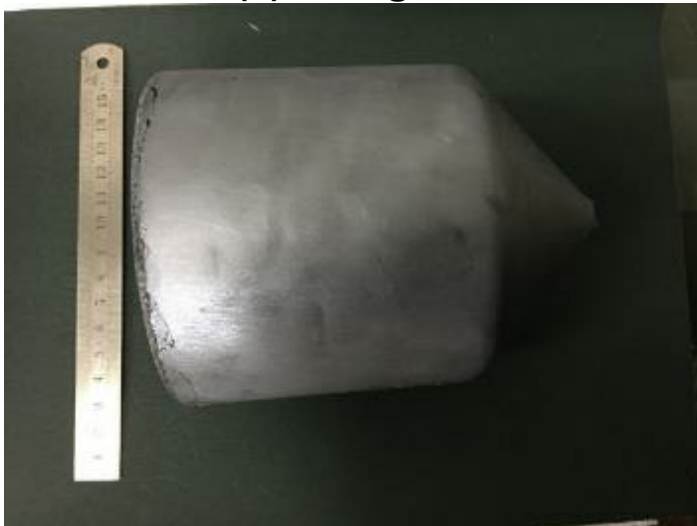
and compared based on the unique thermal condition and growth condition, such as low temperature gradient, small temperature fluctuation, good stoichiometry and temperature gradient variation with doping related thermal conductivity, ingot length, etc.







(a) (b) (c) Figure 1 S-InP(100) ingots grown by VGF: (a) a twin-free ingot ;(b) an ingot with lamella twin band and (100) orientation; (c) a single twin on the lower part of an (100) ingot





(a) (b) (c) **Figure 2 Fe-InP(100) ingots grown by VGF: (a) a twin-free ingot ; (b) patch twins on the shoulder of an (100) ingot (c) an ingot with a lamella twin band and (100) orientation**

5:15 PM - 5:30 PM

VGF GROWTH OF HIGH QUALITY INAS SINGLE CRYSTALS WITH LOW DISLOCATION DENSITY

J. Yang

Institute of Semiconductors, Chinese Academy of Sciences, CHINA

InAs single crystal is becoming an important substrate for the

development of infrared lasers and detectors operated at mid to long IR wavelength. Commercial InAs single crystal is currently grown by liquid encapsulated Czochralski (LEC) method. However, LEC-InAs single crystal usually has etch pit dislocation density (EPD) as high as 10^4cm^{-2} due to the existence of large temperature gradient and thermal stress in the growth process. It is necessary to grow InAs single crystal with low EPD for the development of infrared devices with high performance. In this work, we report the results of InAs single crystals grown by vertical temperature gradient freezing method (VGF) which has low temperature gradient during the growth process. InAs single crystals with (100) and (111) orientation, diameter up to 4 inch have been grown by VGF. Twin-free single crystal ingots with length around 150-200mm have been obtained reproducibly. Etch pit dislocation density (EPD) of the VGF-InAs single crystals is 1000-3000 cm^{-2} . As-expected, X-ray rocking curve of the VGF-InAs single crystal exhibits a narrower FWHM than LEC-InAs single crystal, indicating a better lattice perfection. In contrast, undoped n type VGF-InAs single crystal has a better electrical property, such as higher electron mobility, lower free electron concentration.



Tuesday, July 30, 2019

3:30 PM - 5:30 PM

Detector Materials: Oxide Scintillators

Location: Red Cloud Peak

Session Chair(s): Federico Moretti, V. Ouspenski

3:30 PM - 3:45 PM

PRECIOUS METAL CRUCIBLE-FREE BULK CRYSTAL GROWTH OF CE DOPED $Gd_3(Ga,Al)_5O_{12}$ SINGLE CRYSTAL FROM THE MELT

A. Yoshikawa¹, V. Kochurikhin², H. Sato³, M. Yoshino³, A. Yamaji³, Y. Ohashi¹, K. Kamada¹, Y. Yokota¹, S. Kurosawa¹, M. Nikl⁴

¹NICHE, Tohoku University, JAPAN, ²C&A corporation, JAPAN, ³IMR, Tohoku University, JAPAN, ⁴Institute of Physics, CZECH REPUBLIC

The $Gd_3(Ga,Al)_5O_{12}:Ce$ (GAGG:Ce) scintillator, was developed in 2011. It becomes well known to be attractive material for application in many fields such as nuclear science, industry, environmental monitoring, gamma ray astronomy, and medical imaging. The melting temperature of GAGG is around 1800 degree C, therefore, we have to use Ir crucible for the growth. We use inert atmosphere to protect Ir crucible, then, beta-Ga₂O₃ is decomposed under this atmosphere. It generates not only the oxygen vacancy but also cation vacancy. So far, the majority of the functional single crystalline materials including scintillators are fabricated as bulk crystals using the Czochralski (Cz) or Bridgman (BS) methods. Therefore, we need extensive machining process such as cutting, slicing, polishing and so on. Moreover, the atmosphere is limited as we use Ir crucible, which is easily oxidized by oxygen (above 2 % of partial pressure) in high temperature. This low oxygen partial pressure induces the oxygen vacancy, which can be the origin of slow component or non-radiative transition. We investigated the opportunity to use skull melting technique for the formation and keeping GAGG melt without a crucible. The growth process itself was performed with the use of rotated seed by slow pulling up like at ordinary Czochralski technique. Such combined technique allows to solve both mentioned problems of conventional Cz process for GAGG. Due to the absence of Ir crucible there is no

growth limitation caused by Ir crucible deformation. Also, the absence of Ir crucible gives the opportunity to apply any growth atmosphere (including air or even pure Oxygen). As a result, melt overheating needed for gas bubbles removing can be realized easily without beta-Ga₂O₃ evaporation. GAGG crystals were grown in air without use of Ir crucible using pulling up from the cold container. Such technique gives the opportunity to avoid growth problems typical for traditional Czochralski method.

3:45 PM - 4:00 PM

CZOCHELSKI GROWTH OF 4 INCH DIAMETER CE:GD₃AL₂GA₃O₁₂ SINGLE CRYSTALS FOR SCINTILLATOR APPLICATIONS

V. Kochurikhin¹, K. Kamada², Y. Shoji², M. Yoshino², A. Yoshikawa²
¹C&A corporation, JAPAN, ²IMR, Tohoku University, JAPAN

Oxide materials with the garnet structure are promising candidates for scintillator applications. Ce-doped Gd₃Al₂Ga₃O₁₂ garnet (Ce:GAGG) is one of the most prospective materials due to high light yield (up to 56000 photon/Mev) which is exceeding by 30-40 % the well known Ce:LYSO crystal. Earlier, our group reported the successful Czochralski growth of Ce:GAGG crystals with 2 inch [1] and 3 inch [2] in diameter. However, the further increasing of the crystal diameter for the cost reduction is needed. In this report the production of 4 inch diameter Ce:GAGG crystals by the Czochralski technique will be reported for the first time. All 4 inch Ce:GAGG crystals were grown using Ir crucible of 150 mm in diameter and 150 mm in length. At our previous experiments with 2-3 inch GAGG growth we always applied Ar+1-2% O₂ gas mixture as a growth atmosphere. However, in the case of large Ir crucible used for 4 inch growth such atmosphere was an origin of too many Ir oxide particles on the melt surface. These particles were intensively absorbed by the grown crystal. They produced internal stresses and as a result cracks formation. For this reason N₂ + 20-25 % CO₂ mixture was used. Under such growth atmosphere the formation of Ir particles and tendency for cracking were decreased dramatically. 4 inch Ce:GAGG crystals were grown with the body part length up to 50 mm. In principle, the increasing of

crystal length was possible, however due to the notable difference in crystal composition at the top and the bottom of crystal, increasing of the crystal length over 50 mm led to the formation of cracks. Exactly the same optimal solidification fraction (0.23) was found earlier for 3 inch Ce:GAGG crystal [2]. The transmission spectra and the scintillation properties (light yield and decay time) of the grown 4 inch Ce:GAGG crystals were measured and compared with the samples cut from the smaller crystals grown at Ar+O₂ atmosphere. Their close identity has been confirmed. [1] K. Kamada, T. Yanagida, T. Endo, K. Tsutumi, Y. Usuki, M. Nikl, Y. Fujimoto, A. Fukabori, A. Yoshikawa, J. Cryst. Growth, 352 (2012) 88 [2] K. Kamada, Y. Shoji, V. Kochurikhin, S. Okumura, S. Yamamoto, A. Nagura, J.Y. Yeom, S. Kurosawa, Y. Yokota, Y. Ohashi, M. Nikl, A. Yoshikawa, J. Cryst. Growth, 452 (2016) 81

4:00 PM - 4:15 PM

CZOCHELSKI GROWTH AND SCINTILLATION PROPERTIES OF LI⁺, NA⁺, AND K⁺, CODOPED LUYAG: PR³⁺ SINGLE CRYSTALS

C. Foster, Y. Wu, M. Koschan, C.L. Melcher

Scintillation Materials Research Center, TN, UNITED STATES OF AMERICA

Many rare-earth aluminum garnet scintillators fail to reach their full potential due to intrinsic defects that reside within the host matrix, namely anti-site defects and oxygen vacancies. Current efforts to improve the scintillation properties of these multicomponent garnets include both admixing rare earth elements, i.e. Lu, Y, and Gd, and codoping. Most recently, the benefits of codoping garnet scintillators (GGAG: Ce³⁺, LuAG: Ce³⁺, and LuYAG: Pr³⁺) with monovalent ions such as Li⁺, Na⁺, or K⁺ have been reported as increased light yield, improved energy resolution and faster scintillation decay time. In this paper, we combine the strategies of admixing rare-earth elements in the host matrix and monovalent codoping to alter the scintillation properties of praseodymium-doped (Lu_{0.75}Y_{0.25})₃Al₅O₁₂ (LuYAG: Pr³⁺) single crystals with respect to Li⁺, Na⁺, and K⁺ codopants. Scintillation light yield, energy resolution, and scintillation decay time were measured for each of these samples and their results are presented

and compared to a non-codoped LuYAG: Pr³⁺ single crystal. Thermal annealing experiments in different atmospheres were carried out on these samples as an investigative method to further enhance the scintillation performance. In addition to the scintillation properties of these materials, substantial effort was given into optimizing the growth process to mitigate cracking. Because of the heavy stoichiometric mixing and doping in the garnet matrix, cracking has occurred in many of the codoped LuYAG: Pr³⁺ crystals beginning around the shoulder region and continuing throughout the boule. To combat this challenge, parameters such as the geometry, growth rate, cool down rate, and thermal field within the furnace were altered.

4:15 PM - 4:30 PM

EFFECTS OF LA DOPING ON THE CRYSTAL GROWTH AND INTRINSIC LUMINESCENCE PROPERTIES OF LU₃AL₅O₁₂ SINGLE CRYSTAL

K.A. Bartosiewicz¹, S. Kurosawa², A. Yamaji¹, M. Nikl³, A. Yoshikawa¹, Y. Zorenko⁴

¹Institute for Materials Research, Tohoku University, JAPAN, ²NICHE, Tohoku University, JAPAN, ³Institute of Physics, Academy of Science, CZECH REPUBLIC, ⁴Institute of Physics, Kazimierz Wielki University, POLAND

Lu₃Al₅O₁₂ (LuAG) single crystal host lattice attracts much interest in the scintillator applications due to favorable characteristics such as high density, mechanical hardness, good chemical and radiation stability and easy doping with RE ions [1]. LuAG belongs to the system with the most stable garnet phase and can be easily obtained as a single phase from the melt [2]. However, in this system antisite defects (AD) (Lu³⁺ ion at Al³⁺ site, Lu_{Al}) occurs due to high preparation temperature during the growth of the single crystal from the melt [3]. The AD can localize low energy electronic excitation (excitons or electrons and holes) causing intrinsic UV emission. The intrinsic UV luminescence in LuAG can be enhanced by La doping. Large La³⁺ (1.165 Å) ions are localized in LuAG exclusively in the dodecahedral sites of Lu³⁺ cations (0.977 Å) forming La_{Lu} centers. This process

stimulates displacement Lu^{3+} ions in the octahedral Al^{3+} sites forming Lu_{Al} AD. Both La_{Lu} and Lu_{Al} centers are responsible for UV emission in LuAG crystals. However, large La atom prefers to form aluminum perovskite phase. Moreover, a large difference between ionic radii between La^{3+} and Lu^{3+} (0.188 Å) hampers to incorporate the La in dodecahedral site in LuAG single crystal. The aim of this research is to reveal the maximum available La doping concentration in LuAG garnet single crystal and to study the effect of La on the AD luminescence. The single crystals were grown using the micro-pulling-down method [4] with radiofrequency inductive heating using an iridium crucible with a die of 3 mm in diameter. The growth was performed from a slightly overheated melt to decrease the melt viscosity and increase wettability allowing the melt to spread over the whole diameter of the die. The hot-zone and afterheater were modified to keep a very steep vertical temperature gradient and mild radial gradient to improve the crystal quality. Single crystals were characterized by optical absorption, photoluminescence excitation, and emission and radioluminescence spectra and photoluminescence decay kinetic measurements. Scintillation properties of the crystals were studied by means of light yield value and scintillation decay time analysis. The garnet phase is confirmed by powder X-ray diffraction. [1] M. Nikl, et al., Prog. Cryst. Growth Charact. 59 (2013) 47-72. [2] X. Xu, et al, Acta Mater. 67 (2014) 232-238. [3] M. Ashurov et al., Phys. Stat. Sol. (a) 42 (1977) 101. [4] A. Yoshikawa, et al., Opt. Mater. 30 (2007) 6-10

4:30 PM - 4:45 PM

LITHIUM AND SODIUM MOLYBDATE CRYSTALS FOR NEUTRINOLESS DOUBLE BETA DECAY EXPERIMENTS

J. Tower¹, L. Winslow², H. Hong¹, Y. Ogorodnik¹, J. Glodo³, E. Van Loef⁴, A. Giuliani⁵, D. Poda⁵, L. Berge⁵, L. Dumoulin⁵, H. Khalife⁵, P. De Marcillac⁵, S. Marnieros⁵, C. Nones⁶, V. Novati⁵, E. Olivieri⁵, T. Redon⁵, A. Zolotarova⁵, M.R. Squillante¹, K.S. Shah⁴

¹Radiation Monitoring Devices, Inc., MA, UNITED STATES OF AMERICA, ²Massachusetts Institute of Technology, UNITED STATES OF AMERICA, ³Radiation Monitoring Devices, MA, UNITED STATES

OF AMERICA, ⁴RMD, MA, UNITED STATES OF AMERICA,
⁵CSNSM, Univ. Paris-Sud, CNRS/IN2P3, Université Paris-Saclay,
FRANCE, ⁶IRFU, CEA, Université Paris-Saclay, FRANCE

The Majorana nature of neutrinos and the lepton number violation are among the most important questions being pursued in physics today. This has given the search for neutrinoless double beta decay ($0\nu\beta\beta$) a high priority among proposed nuclear physics experiments. Recent advances in cryogenic bolometer technology have significantly improved detector sensitivity and background rejection. In this work, the objective was to evaluate several molybdenum-containing crystal compositions for possible use as scintillating bolometers in $0\nu\beta\beta$ research. The research reported here investigates the synthesis, purification, and crystal growth of sodium and lithium molybdate, and the testing of these materials as scintillating bolometers at cryogenic temperatures. Single-crystals of sodium molybdate ($\text{Na}_2\text{Mo}_2\text{O}_7$ or NMO) and lithium molybdate (Li_2MoO_4 or LMO) were grown by Czochralski in sizes up to two inches diameter. The crystal compounds were synthesized in a separate step prior to crystal growth. Transparent colorless crystals were produced when materials of suitable purity were used. We will report on the production and physical characteristics of the crystals. Scintillating bolometer data were measured from both LMO and NMO crystals at around 20 mK using a pulse-tube cryostat of an aboveground cryogenic laboratory of CSNSM (France). A scintillation light output, found at low-temperature, enables an efficient separation between alpha and beta/gamma emissions in light-vs-heat analysis. Pulse shape analysis was also shown as a viable method of particle identification as well. This capability is crucial for background reduction in $0\nu\beta\beta$ research. This work has been supported by the US Department of Energy SBIR grant No. DE-SC0015200.

4:45 PM - 5:00 PM

**BULK Li_2MOO_4 CRYSTALS FOR SCINTILLATING BOLOMETERS
USED IN NEUTRINOLESS DOUBLE-BETA DECAY NEXT-
GENERATION DETECTION EXPERIMENTS (ORAL
PRESENTATION)**

M. Velazquez¹, P. Veber², C. Stelian¹, P. De Marcillac³, A. Giuliani³, D. Poda³, A. Ahmine¹, T. Duffar¹, S. Marnieros³, C. Nones⁴, V. Novati³, E. Olivieri³, A. Zolotarova³, H. Cabane⁵, T. Redon³

¹SIMaP UMR 5266 CNRS-UGA-G INP, FRANCE, ²Institut Lumière Matière UMR 5306, FRANCE, ³CSNSM, Univ. Paris-Sud, CNRS/IN2P3, Université Paris-Saclay, FRANCE, ⁴IRFU, CEA, Université Paris-Saclay, FRANCE, ⁵Cristal Innov, FRANCE

A unique probe of the new physics beyond the Standard Model will be realized in the upcoming decade by several next-generation experiments, in particular CUPID, aiming at the detection of neutrinoless double-beta decay [1]. The basic option for CUPID is to exploit the infrastructure of the recently started CUORE experiment with a tonne-scale bolometer array. The key points addressed for a bolometric technique to be applied in CUPID are reproducible crystal growth and detector technologies satisfying the project requirements on the production, purity and performance. A technology of mass production of high quality, radiopure, natural and ⁶Li-enriched Li₂MoO₄ (LMO) scintillators is being developed in the CLYMENE R&D program. Crystals with varied diameters were grown in two different Czochralski configurations. The first configuration based on inductive heating (RF coil coupled with Pt crucible) was used to grow crystals of 3 to 4 cm in diameter. We investigated the detector performances and radiopurity of a cracked 158 g crystal and an uncracked 13.5 g crystal. In the latter, a good energy resolution (2–7 keV FWHM @ 0.2–5 MeV), one of the highest light yield (0.97 keV/MeV) amongst LMO scintillating bolometers, an efficient alpha particles discrimination (10

5:00 PM - 5:15 PM

CRYSTAL GROWTH AND LUMINESCENCE PROPERTIES OF NOVEL MOLYBDATE SCINTILLATION MATERIALS

H. Chen, P. Chen, Z. Wang, R. Wei, L. Jiang

Institute Materials Science & Chemical Engineering, Ningbo University, CHINA

The neutrinoless double beta ($0\nu\beta\beta$) decay as a rare nuclear event, which could provide the unique information about the neutrino mass hierarchy, has aroused a great interest for the nuclear physics

researchers. As an important technical route for the experimental observatory of $0\nu\beta\beta$ decay, the nuclear physics researchers have been trying to develop a cryogenic bolometer operating at underground laboratory. In recent years, a series of molybdate scintillation crystals, such as ZnMoO_4 , CaMoO_4 , CdMoO_4 and Li_2MoO_4 , were investigated as the key materials used in the cryogenic bolometer. All these molybdate crystals reported in literatures contain the isotope ^{100}Mo , which has a high energy release ($Q = 3034.40 \text{ keV}$) and a large natural isotopic abundance ($d = 9.82\%$). In order to provide the scintillation materials applied in cryogenic bolometer, a series of molybdate crystals, such as ZnMoO_4 , CaMoO_4 , CdMoO_4 and Li_2MoO_4 , were grown by Crochralski method or Bridgman process in our laboratory. The crystallization behaviors and the crystal defects of these molybdate crystals were investigated systematically under Bridgman or Crochralski process. Using the polycrystalline material synthesized via solid-state reaction, a series of molybdate crystals with a size of 1~2 inch in diameter were grown by Crochralski method or Bridgman process. The spectral properties and scintillation properties of as-grown molybdate crystals were investigated systematically by measuring the transmittance spectra, laser or cosmic rays stimulated luminescence spectra as well as luminescence decay time. The crystal samples with a size of $\text{Ø}44\times 45 \text{ mm}$ were applied for assembling the prototype cryogenic bolometers. By evaluating the research results acquired from the radiation observatory, Li_2MoO_4 single crystal with riched ^{100}Mo isotope has been considered to be a most promising material for the cryogenic bolometer applied in $0\nu\beta\beta$ decay research. A mass amount of molybdate crystals maybe required in the nuclear physics project organized by CUPID-China Cooperative group in the next years.

Tuesday, July 30, 2019

3:30 PM - 5:30 PM

III-V Wide Bandgap Devices

Location: Crestone III, IV

Session Chair(s): Ramon Collazo, Ronny Kirste

3:30 PM - 4:00 PM

EPITAXY OF GAN-BASED VCSELS

T. Takeuchi, S. Kamiyama, M. Iwaya, I. Akasaki

Meijo University, JAPAN

Recently GaN-based VCSELS have been rapidly developed towards novel light sources for illuminations, displays, and communication systems. There seem two approaches to achieve GaN-based VCSELS. One is to form conventional VCSEL cavity structures by following the infrared GaAs-based VCSELS already showing the great successes. In this case, semiconductor-based DBRs and semiconductor-based current/optical confinement structures are desired, requiring epitaxial growth developments. The other approach is to form unique cavity structures by considering GaN-based material properties. In this case, putting aside such semiconductor-based structures, other materials, mostly oxide materials, are utilized as double dielectric DBRs and ITO apertures with device process developments. Our group has been developing GaN-based VCSELS along with the former approach by using MOVPE. In this talk, we present our MOVPE developments of high-reflectivity AlInN/GaN DBRs and low-resistivity nitride tunnel junctions for optical confinement towards GaN-based VCSELS. It is not straightforward to grown high-quality AlInN because the optimum growth conditions of AlN and InN are very different. In addition, typically low growth rate is preferred to obtain high-quality In-contained nitride materials, which is not appropriate for a thick DBR growth. We found that even using relatively high growth rate, 0.5 $\mu\text{m}/\text{h}$, reasonably high-quality 90 nm AlInN layers were obtained by using low growth pressure and relatively high growth temperature. Our 40-pair AlInN/GaN DBRs for 410 nm and 520 nm target wavelengths showed 99.9% and 99.4% reflectivity values, respectively. We then demonstrated a RT-CW operation of the VCSEL with the bottom AlInN/GaN DBR emitting 410 nm with 4.2 mW. We also developed Si-doped conductive DBRs, and the VCSEL with the conductive DBR showed 1.8 mW with a low series resistance of 90 Ω . Note that these VCSELS still had the lossy ITO apertures. Regarding the tunnel junction, we first developed lateral Mg activation, in which hydrogen atoms can laterally move in the p-layers

towards device mesa sidewalls. This method circumvents the difficulty of acceptor activation in p-layers capped with n-layers. We then found that GaInN layers and overlapped Mg and Si doped regions were effective to obtain low resistivity values, $2-3 \times 10^{-4} \Omega\text{cm}^2$, comparable to a decent conventional p-contact resistivity. Finally, we obtained a RT-CW operation of the VCSEL with a buried tunnel junction, a bottom undoped AlInN/GaN DBR, and a top dielectric DBR. Now the GaN-based VCSEL structure is getting close to the infrared GaAs-based VCSEL structure. Acknowledgements: This work was supported by MEXT GaN R&D Project.

4:00 PM - 4:30 PM

VERTICAL GAN-ON-SILICON POWER DEVICES

E. Matioli

Ecole Polytechnique Fédérale de Lausanne (EPFL), SWITZERLAND

The outstanding properties of Gallium Nitride semiconductors grown on cost-effective Silicon substrates have led to the demonstration and commercialization of high-performance lateral GaN power devices with large breakdown voltage and low on-resistance. The breakdown voltage (BV) in lateral device scales proportionally with the gate-to-drain spacing, thus requiring large device area for high voltage operation. However, beyond a specific gate-to-drain separation, the BV is dictated by the thickness and quality of the buffer layers grown on Silicon. Lateral devices are also severely affected by trap states and high electric fields present at the surface, which lead to current collapse and other reliability issues.

These drawbacks are not present in vertical devices, as the electric field peaks far away from the surface, and the breakdown voltage depends mainly on the thickness of the drift layer, independently of the device area. Vertical p-i-n diodes and transistors on bulk GaN substrates have already been reported with nearly ideal ON- and OFF-state performances, which was possible due to the low defect density and the ability to homo-epitaxially grow thick layers on these substrates. Yet, bulk GaN substrates are still prohibitively expensive. The recent progress on hetero-epitaxial growth of thick GaN layers on large area Silicon substrates offers a cost-effective platform to develop vertical GaN-on-Si power devices, taking advantage of large scale and

mature fabrication technology of Si substrates.

This talk will discuss the state of the art of high-voltage GaN-on-Si vertical devices, starting by the initial demonstrations of quasi-vertical devices, including GaN-on-Si p-i-n diodes, and MOSFETs. The challenge of quasi-vertical devices is the severe performance limitation due to current crowding in the bottom n-GaN layer, which significantly increases the $R_{on,sp}$. To address these challenges, here we present the recent first demonstration of fully-vertical GaN-on-Si power MOSFET based on a robust fabrication process to selectively remove the Si substrate and resistive buffer layers under the devices. Fully-vertical GaN-on-Si power MOSFETs fabricated on a 6.6 μm -thick n-p-i-n GaN epitaxial structure grown on 6-inch Si substrate presented large forward current density, small $R_{on,sp}$, along with high BV of 520 V. This talk will discuss technologies to mitigate self-heating issues, including localized CVD diamond heat spreaders. These technologies open a promising pathway for the development of cost-effective GaN-on-Silicon vertical devices for future power applications.

4:30 PM - 4:45 PM

NONPOLAR GAN-BASED VCSELS WITH NANOPOROUS DISTRIBUTED BRAGG REFLECTOR MIRRORS

S.M. Mishkat-UI-Masabih¹, A.A. Aragon¹, M. Monavarian¹, T.S. Luk²,
D.F. Feezell¹

¹University of New Mexico, UNITED STATES OF AMERICA, ²Sandia National Laboratory, UNITED STATES OF AMERICA

GaN-based vertical-cavity surface-emitting lasers (VCSELs) have drawn increasing interest in recent years for their potential applications in data storage, laser printing, solid-state lighting, optical communications, sensing, and display technologies. The small active volume in VCSELs is favorable for single-mode emission, low threshold current, high modulation bandwidth, and high-density 2D array formation. Furthermore, VCSELs have circular low-divergence beam profiles simplifying fiber coupling and on-chip testing. Despite the impressive properties of VCSELs, they are one of the more difficult optoelectronic devices to fabricate. Precisely controlling the length of the cavity is one such challenge. The cavity length essentially

determines the how much of the electric field is coupled into the active region to maximize the enhancement factor. Cavity length is also important for correctly aligning the gain peak with the cavity mode and controlling the number of longitudinal modes in the cavity. In this work, we used photoelectrochemically (PEC) etched marker layers to accurately calibrate and grow our VCSEL epilayers. PEC etching works by the wavelength selective etching of lower bandgap materials such as $\text{In}_{0.1}\text{Ga}_{0.9}\text{N}$ when illuminated under a lower wavelength light in an etchant. From cross-sectional SEM imaging, we determined the thickness of the n-cladding, active, and p-cladding regions. Another issue we addressed in this work is the formation of high-reflectance nanoporous epitaxial DBRs. Group III-nitrides lack lattice-matched materials with the high refractive index contrast necessary for obtaining a high reflectance mirror. Although several research groups have demonstrated electrically injected GaN-based VCSELs using $\text{Al}_{0.82}\text{In}_{0.18}\text{N}/\text{GaN}$ epitaxial DBRs, maintaining the correct composition is often very difficult to form defect free mirrors. Also, the low index contrast results in a narrow DBR stopband and requires many pairs to obtain high-reflectance. Here, we introduce nanoporous layers with alternating doped/undoped regions that undergo anodic electrochemical (EC) etching. The selective formation of the nanopores in the doped layers effectively lowers the refractive index compared to the adjacent undoped GaN layers. As a result, we obtain lattice-matched mirrors with very high reflectance. Using this approach, we demonstrated the first electrically injected nonpolar *m*-plane GaN-based VCSELs with nanoporous bottom DBRs. Stimulated emission was observed under pulsed operation with record high output powers (~ 1.5 mW) in the *m*-plane orientation at 409 nm. All tested devices were linearly polarization-pinned along the *a*-direction with high polarization ratios (>0.9). The demonstration shows that the nanoporous DBR approach is a viable candidate for mitigating some issues affecting GaN-based VCSELs.

4:45 PM - 5:00 PM

THE INFLUENCE OF SI AND MG CONCENTRATION IN ALGAN-BESED UV-B LASERS

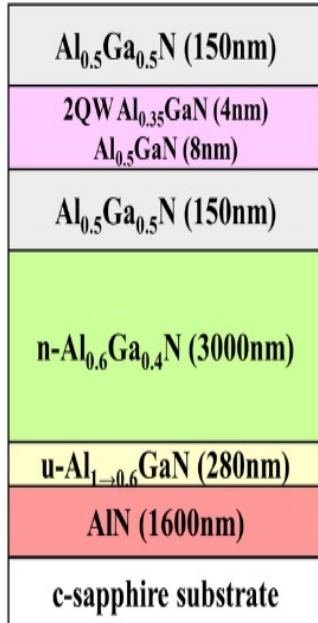
S. Tanaka, K. Sato, S. Yasue, Y. Ogino, M. Iwaya, T. Takeuchi, S.

Kamiyama, I. Akasaki

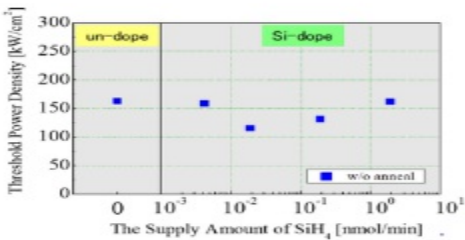
The University of Meijo, JAPAN

Abstract Realization of UV-B and UV-C AlGaN-based semiconductor lasers is very important academically and industrially. To realize it, it is one of the most important issues to find a device structure that improves carrier injection efficiency and internal loss reduction. Generally, the electron blocking layer of the active layer is often used in visible lasers of nitride semiconductors. Therefore, impurities are often added to the guide layer as well. However, since doping into the guide layer leads to an increase in internal loss, the optimum doping concentration is designed. Martens *et al.* have reported the influence of Mg-doping on the optical absorption of photoexcited lasers with the Mg-doped ($\sim 1 \times 10^{20} \text{cm}^{-3}$) region in the waveguide layer [1]. However, the dependency of Mg and Si concentration in the guide layer is not much investigated. Furthermore, the optical loss of Mg concentration and Si concentration in the cladding layer is unknown. In this study, the Mg and Si doping concentration of the guide layer and the cladding layer in the UV-B laser was changed and the results of the photoexcited laser characteristics were investigated. Samples were prepared on AlN template grown on sapphire substrate by MOVPE method. After forming a 1- μm -thick AlN template of at 1350 °C, 3- μm -thick n-AlGaN ($8.7 \times 10^{18} \text{cm}^{-3}$), a 150-nm-thick 1st Al_{0.5}Ga_{0.5}N guide layer, a 2-pairs Al_{0.35}Ga_{0.65}N (4 nm)/Al_{0.5}Ga_{0.5}N (8 nm) quantum well active layer, a 150-nm-thick 2nd Al_{0.5}Ga_{0.5}N guide layer were sequentially stacked. The emission wavelength from 2QW active layer was approximately from 290 nm to 300 nm. In this study, the Si and Mg concentrations of the 1st Al_{0.5}Ga_{0.5}N guide layer and the 2nd Al_{0.5}Ga_{0.5}N guide layer were changed by changing the supply amounts of SiH₄ and Cp₂Mg, and the threshold power density dependence of the photoexcited lasers was investigated. Si concentration and Mg concentration changed from unintentionally doped to about 10^{19}cm^{-3} greatly. As a result, the threshold power density of the photoexcited laser increased sharply as Mg and Si doping concentrations were increased. An increase in the threshold power density is explained by an increase in the optical loss.

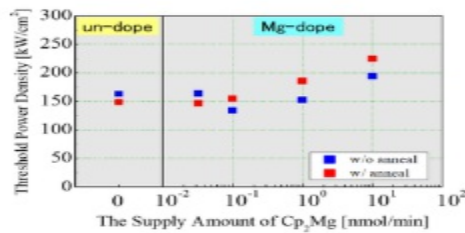
Therefore, investigation of optimum doping concentration and carrier injection is necessary. **Reference** [1] M. Martens et al, Appl. Phys. Lett., **110**, 081103 (2017).



Sample Structure



Si-doped in down waveguide layer



Mg-doped in down waveguide layer

5:00 PM - 5:15 PM

EVALUATION AND CONTROL OF MG DIFFUSION EFFECT IN III-NITRIDE UV LIGHT-EMITTING DEVICES

T. Detchprohm, C. Tsou, H. Jeong, Y.J. Park, K. Mehta, P. Chen, P.D. Yoder, S. Shen, **R. Dupuis**

Georgia Institute of Technology, GA, UNITED STATES OF AMERICA
We are developing InGaN/AlGaN-based vertical-cavity surface-emitting lasers (VCSELs) with an emission wavelength of 369.5 nm for portable Yb⁺ atomic clocks. We have previously demonstrated optically pumped VCSELs lasing at 375 nm with a 1λ optical cavity. In this work we have introduced and optimized Si- and Mg-doped AlGaN layers for current injection by forming resonant-cavity light emitting diodes (RCLEDs) targeting 370nm emission. In these RCLED structures, the bottom DBR mirror was a 5-pair 3/4- n⁺-Al_{0.014}Ga_{0.986}N (n~2E19 cm⁻³)/Al_{0.045}Ga_{0.955}N stack on top of strain management AlGaN layers, followed by a 6l-cavity LED consisting of n-Al_{0.08}Ga_{0.92}N (n~8E18cm⁻³) spacer/InGaN-AlGaN MQW/p-AlGaN electron blocking layer (EBL)/p-Al_{0.08}Ga_{0.92}N (p~3E17cm⁻³) spacer/graded p⁺-AlGaN ([Mg] >1E20 cm⁻³). However, we observed PL intensity degradation in the active region at an early period of the device growth cycle. The degradation appeared in both intensity level, and intensity ratio before and after Mg thermal activation process. This degradation behavior was found to be sensitive to the Cp₂Mg supply in the EBL. The decrease of MQW PL intensity was approximately 25% for as-grown samples and additional reduction of 35-40% after the thermal activation within small number of runs followed the initial optimum Cp₂Mg supply. We observed [Mg] as high as 1E19 cm⁻³ in the last two InGaN quantum wells (QWs). The degradation got worse when there was poor surface morphology developed at the beginning of DBR growth. The [Mg] of 5E18 cm⁻³ or more distributed across the whole MQW active region although the morphology was recovered in the first few pairs of DBR growth. Therefore, we implemented two approaches of (1) alleviating such poor surface development via modifying growth transition step, and (2) introducing delay and re-optimizing Cp₂Mg in EBL to mitigate this issue. For the latter approach, we tested the Cp₂Mg doping modification with the LED structure without the bottom DBR layers in order to shorten the cycle time. The PL intensity of an optimized as-grown LED showed no sign of degradation and it only dropped about 13-26% after thermal activation. The fabricated LED with ITO as p-type contact electrode,

showed improved L/I characteristics at high injection current, e.g., with an increase of 50% or more of light output power at 330 A/cm^2 as well as small leakage current in the reverse I - V characteristics by 2-3 order of magnitudes lower than the LED with large diffused [Mg] in the active region. We will discuss these results and present data on our optimized RCLEDs.

5:15 PM - 5:30 PM

TRANSFER-FREE FLEXIBLE SINGLE-CRYSTALLINE III-N FILM DIRECTLY GROWN ON METAL TAPE FOR BENDABLE INORGANIC PHOTONIC AND ELECTRONIC DEVICES

S. Shervin¹, K. Alam¹, M. Ji², K. Shervin¹, S.K. Oh¹, T. Detchprohm³, J. Bao¹, R. Dupuis³, **J. Ryou**¹

¹University of Houston, TX, UNITED STATES OF AMERICA,

²Georgia Institute of Technology, UNITED STATES OF AMERICA,

³Georgia Institute of Technology, GA, UNITED STATES OF AMERICA

This work presents a flexible metal tape substrate with directly grown single-crystalline gallium nitride (GaN) on top for flexible photonic and electronic III-N based devices. We have developed transfer-free and epitaxially grown single-crystalline III-N films on the polycrystalline flexible Cu foil using graphene as an intermediate layer (IL). Although the flexible electronics and mechanically bendable devices are emerging, there are several fundamental limitations need to be overcome. Challenges such as instability in harsh environment and elevated temperatures, limited bendability, low materials quality, high production cost, and low device performance make flexible device vulnerable. In this work, an inorganic (metal) foil is developed to serve as a flexible substrate for III-N materials and devices, which can stand high-growth temperatures to reach device-quality III-N materials. The easily implementable and direct-growth features make this method a scalable platform for roll-to-roll (R2R) growth and continues production of high quality III-N materials on bendable substrates for fabrication of flexible/stretchable electronic and photonic devices. Graphene is grown on the Cu foil by well-established chemical vapor deposition (CVD) method. AlN seed layer was deposited on graphene

intermediate layer via DC magnetron reactive ion sputtering method using pure Al as the target. Standard blue-LED structure is grown by metalorganic chemical vapor deposition (MOCVD) method on flexible AlN/graphene/Cu foil. The crystal structure and surface morphology of AlN and GaN layers are characterized. X-ray diffraction analyses (XRD) show that the *c*-plane of AlN film (from (0002) peak in 2θ - ω scan) is preferably grown on graphene, and GaN is grown epitaxially on the AlN/Cu. XRD phi scan on GaN (102) plane show six-fold symmetry features which confirms the single-crystal-like wurtzite structure is formed during growth. Also, electron back-scattering diffraction (EBSD) pole figure analyses on GaN (102) plane confirms high crystalline quality of GaN film. Using XRD and photoluminescence (PL) characterization methods, it is confirmed that MQW layers were grown successfully. The PL map also confirms the uniformity of the LED structure on Cu foil. The directly grown epitaxial III-N films on Cu tape using graphene IL are easily bendable. Our current focus is to fabricate inorganic flexible LED on Cu foil using the developed structure. This work offers a solution for low-cost and large-scale production of III-N based electronic and photonic devices by enabling R2R and continuous fabrication on the developed flexible GaN template serving as a flexible substrate for various bendable III-N based devices.

Tuesday, July 30, 2019

3:30 PM - 5:30 PM

Nanowires

Location: Torrey Peak II-IV

Session Chair(s): George T. Wang, Zhaoxia Bi

3:30 PM - 4:00 PM

RESHAPE OF GAN NANOWIRE-MEDIATED NITRIDE PYRAMIDS AND REALIZATION OF FULL VISIBLE COLOR LIGHT EMITTING DIODES

Z. Bi¹, F. Lenrick², J. Colvin², A. Gustafsson¹, O. Hultin³, A. Nowzari¹, T. Lu¹, R. Wallenberg⁴, R. Timm², A. Mikkelsen², B..J. Ohlsson¹, K. Storm³, B. Monemar¹, L. Samuelson¹

¹Solid State Physics Division and NanoLund, Physics Department, Lund University, SWEDEN, ²Division of Synchrotron Radiation Research and NanoLund, Physics Department, Lund University, SWEDEN, ³RISE Acreo AB, SWEDEN, ⁴Center for Analysis and Synthesis/nCHREM, Lund University, SWEDEN

In this work, we demonstrate a new InGaN template platform enabling III-nitride light emitting diodes (LEDs) with blue, green and red light emissions. The green and red LEDs have similar strain and quantum confined Stark effect in InGaN quantum wells (QWs) as the well-developed traditional GaN blue LEDs by growing InGaN QWs on this InGaN template. The platform of dislocation-free and relaxed InGaN platelets in sub-micron dimensions is defined by a top (0001) and six inclined (10 $\bar{1}$ 1) planes. Smooth top (0001) surface and indium contents up to 18% make such platelets a perfect template for nitride LEDs covering full visible color spectrum. Our approach to form InGaN platelets starts from hexagonal InGaN pyramids defined by six equivalent (10 $\bar{1}$ 1) planes. InGaN pyramids are selectively grown on small GaN nanowire seeds nucleated from 100 nm-sized openings in a SiN mask on (0001)-oriented GaN/Si or GaN/sapphire substrate. With in-situ high temperature annealing under a NH₃ flow, InGaN pyramids decompose downwards from the apex, resulting in platelet formation with a top (0001)-plane while the inclined (10 $\bar{1}$ 1) planes are intact. Such a shape transformation can also be achieved with ex-situ chemical mechanical polishing (CMP) on InGaN pyramids. With an InGaN regrowth on the as-formed (0001) plane of the platelets, high quality surface showing single bilayer steps can be obtained (refer to figure 1). In this work, we also fabricate GaN platelets through annealing a GaN pyramids sitting on a thick GaN pillar (obtained with GaN radial shell growth on a GaN nanowire) via a mass transportation mechanism (also refer to figure 1).

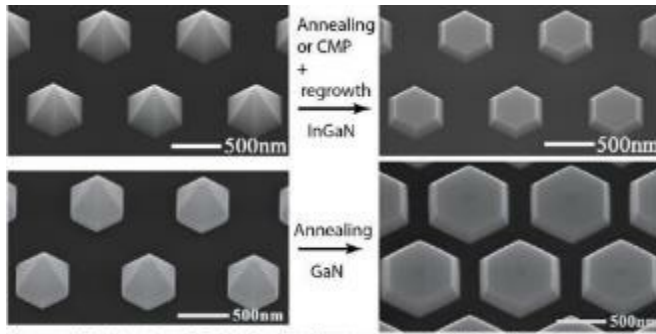
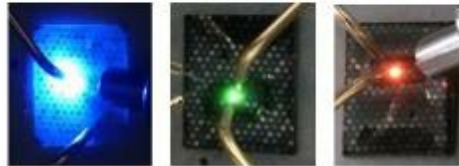
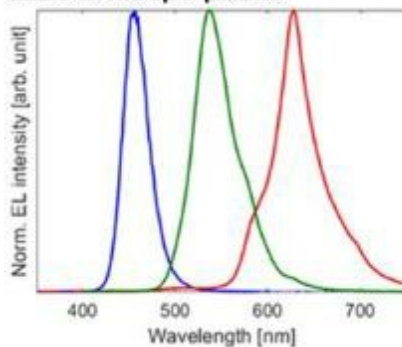


Figure 1 Fabrication of GaN platelets (bottom row) and InGaN platelets (top row) with high temperature annealing.

InGaN QWs can be grown on the top (0001) plane of such dislocation-free and relaxed platelets with blue, green and red light emissions on GaN, $\text{In}_{0.09}\text{Ga}_{0.91}\text{N}$ and $\text{In}_{0.18}\text{Ga}_{0.82}\text{N}$ platelets, respectively. No visible QW growth on inclined (10 $\bar{1}$ 1) planes was observed under transmission electron microscopy, thanks to the extremely low growth rate on such planes. After QW and p-(In)GaN growth, each platelet possesses a complete LED structure. In this work, we will present two processes, either in an ensemble way to fulfill different application purposes (such as microLEDs) or on a single platelet as ultra-small light sources (emitter size about 200 nm) for optogenetic applications (refer to figure 2).

LEDs on multiple platelets



Blue LED on single platelets

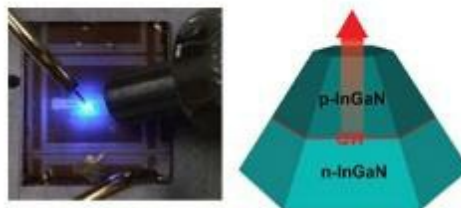
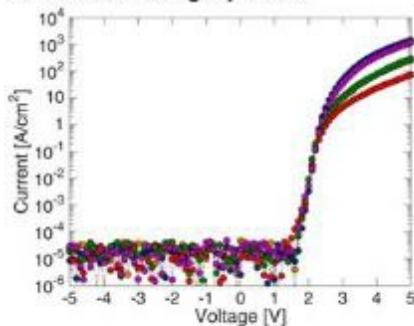


Figure 2 EL characteristics of LEDs processed on multiple platelets (top row) or a single platelet (bottom row).

4:00 PM - 4:15 PM

AMORPHOUS Al_xO_y AS A NUCLEATION LAYER FOR SELECTIVE AREA FORMATION OF GaN NANOWIRES BY PLASMA-ASSISTED MOLECULAR BEAM EPITAXY

M. Sobanska¹, Z. Zytkeiwicz¹, K. Klosek¹, R. Kruszka², K. Golaszewska², S. Gieraltowska¹

¹Institute of Physics Polish Academy of Sciences, POLAND, ²Institute of Electron Technology, POLAND

We recently reported that self-assembled formation of GaN nanowires (NWs) can be achieved by plasma-assisted MBE on crystalline sapphire if the substrate is covered by an amorphous Al_xO_y (a- Al_xO_y) layer grown by atomic layer deposition [1]. Moreover, much faster nucleation of GaN NWs was observed on such a- Al_xO_y films than on commonly used nitridated Si substrates (Si_xN/Si) under the same growth conditions [2, 3]. Despite these promising advantages, high density of NWs and controlling of their spatial distribution on a substrate still remain an issue. In this work GaN growth was performed on GaN/sapphire and Si_xN/Si substrates with 12 μm wide stripes of 15 nm thick a- Al_xO_y . Formation of GaN NWs well-aligned perpendicularly to the substrate surface was found on a- Al_xO_y stripes, while a rough compact GaN layer was obtained on bare, crystalline parts of GaN/sapphire template. Since the compact layer forms under N-rich conditions while the growth of GaN NWs takes place under local excess of Ga [4, 5], the ratio of NW length h to the thickness of the compact layer d can be tailored by adjusting the Φ_N/Φ_{Ga} flux ratio and the growth temperature. The respective modelling was performed taking into account the NW incubation time as a function of growth parameters [6]. In agreement with calculations we found that the value of h/d ratio can be increased by increasing the Φ_N/Φ_{Ga} flux ratio. On the other hand pure selective area growth (SAG) of GaN NWs was observed on Si_xN/Si substrates with a- Al_xO_y stripes. This was achieved by adjusting the growth parameters that nucleation of GaN on Si_xN was prevented (incubation time longer than the growth

duration), so GaN NW growth took place on a-Al_xO_y stripes only. Importantly, the same effect of pure SAG was found for PECVD-deposited Si_xN on GaN/sapphire templates. In that way, our results pave the way for SAG of GaN NWs on a wide variety of dissimilar materials by using a-Al_xO_y as a nucleation layer. [1] M. Sobanska et al., *J. Appl. Phys.* **115** 043517 (2014). [2] M. Sobanska et al., *J. Appl. Phys.* **118** 184303 (2015). [3] M. Sobanska et al., *Cryst. Growth Des.* **16** 7205 (2016). [4] S. Fernandez-Garrido et al., *Nano Lett.* **13** 3274 (2013). [5] M. Sobanska et al., *Nanotechnology* **27** 325601 (2016). [6] M. Sobanska et al., *Nanotechnology* **30** 154002 (2019). This work was partly supported by the Polish Nacional Science Centre grants 2016/21/N/ST3/03381, 2016/23/B/ST7/03745 and 2016/21/B/ST5/03378.

4:15 PM - 4:30 PM

HOMOEPITAXIAL GROWTH OF GAN NANORODS VIA IRREGULAR MASKS

C. Huang¹, W. Lee², Y. Chou¹

¹Department of Electrophysics, National Chiao Tung University, TAIWAN, ²Department of Electrophysics, TAIWAN

It is well known that GaN nanorods (NRs) of high crystal quality are served as promising building materials of current optoelectronics and high-power electronic devices [1]. Compared with films of GaN, the rods of it permit more strain relaxation and possess large surface-to-volume ratio, which can be used for quantum-wells with core-shell structures to control light extraction with tunable bandgap [2].

Furthermore, GaN NRs with c-orientation provide non-polar and semi-polar facets for reducing the quantum-confined Stark effect (QCSE) and thus increase the emission efficiency and intensity of optical devices [3]. In this research, we propose a less complex and low cost approach using irregular masks for GaN NR fabrication on GaN substrate through hydride vapor phase epitaxy with a rapid growth rate. The grown GaN NRs are isolated by SiO₂ islands, served as irregular masks, and GaN NRs can be confined in the pits, created by annealing and nitridation at high temperature on GaN substrate. The selection of mask amount is investigated to achieve reasonable NR

density (high coverage) and lattice quality (single crystalline; better quality than as-grown layer under same growth ambient). Using this growth method with appropriate parameter, GaN NRs grew along c-orientation with high aspect ratio of ~ 25.6 and high growth rate of $\sim 0.93 \mu\text{m}/\text{min}$. The growth mechanism of GaN NRs is also demonstrated with several scanning electron microscopy images, illusions, and statistic plots. The conditions of growth temperature are found to critically influence the NR aspect ratio and height. The unique morphology of GaN NRs are investigated by transmission electron microscopy (TEM). Cathodoluminescence measurements show a GaN-related near bandgap emission peak and improved luminescence intensity. The residual strain released in the grown GaN NRs is discovered by the Raman spectrum and TEM.

References [1] P. Deb et al. "GaN Nanorod Schottky and p-n Junction Diodes." *Nano Lett.* 2006, 6, 2893-2898. [2] X. Wang et al. "Continuous-flow MOVPE of Ga-polar GaN column arrays and core-shell LED structures." *Cryst. Growth Des.* 2013, 13, 3475-3480. [3] H. P. T. Nguyen et al. "Controlling electron overflow in phosphor-free InGaN/GaN nanowire white light-emitting diodes." *Nano Lett.* 2012, 12, 1317-1323.

4:30 PM - 4:45 PM

BETWEEN GROWTH OF GALLIUM NITRIDE NANOWIRES ON MoS_2 AND ITS PIEZOELECTRIC EFFECT

W.T. Lin, C. Huang, Y. Chou

Department of Electrophysics, National Chiao Tung University,
TAIWAN

Gallium Nitride (GaN), with wide direct bandgap of 3.4eV as semiconductor, affords it special properties for application in optoelectronic, high-power, etc. In recent years, GaN nanowires (NWs) have been synthesized with vapor-liquid-solid (VLS) mechanism, which is a catalyst assisted-process. Metal particle formed by annealing a metal film on the substrate will grow by precursor [1]. Due to its non-centrosymmetric wurtzite structure, GaN NWs has a great potential in development of piezoelectric device [2]. Molybdenum disulfide (MoS_2) is one of the most typical transition metal dichalcogenides (TMDCs) which is an indirect bandgap

semiconductor with negligible photoluminescence. When the MoS₂ crystal is thinned to monolayer, however, a strong photoluminescence emerges, indicating a direct bandgap transition, thus making it scientific and industrial importance. MoS₂, which could realize band engineering with the modulation of its number of layers, creates a great potential to fabrication of transistors, solar cells, etc. Here, we report GaN NWs grown on few-layers MoS₂, synthesized by (NH₄)₂MoS₄ solution [3], via hydride vapour phase epitaxy (HVPE) using Au/Ni as catalyst. We found that nucleation density on pristine and defect-free MoS₂ is low due to lack of dangling bonds and small area. Additionally, piezoelectric effect between GaN NWs and MoS₂ will be discussed by applying strain along piezoelectric polarization direction (c-axis) which modifies the heterogeneous energy bandgap height.

4:45 PM - 5:00 PM

ULTRA-THIN-WALLED ZNO MICROTUBE CAVITY FABRICATED BY OPTICAL VAPOR SUPERSATURATED PRECIPITATION FOR NOVEL APPLICATIONS IN NANOPHOTONICS

Y. Yan, Y. Jiang

Institute of Laser Engineering, Beijing University of Technology,
CHINA

ZnO optical microcavities have shown great promise as a potential core component material/structure for ultraviolet lasers, light-emitting diodes and photonic sensors due to their outstanding optoelectronic properties. Here the ultra-thin-walled ZnO (UTW-ZnO) microtubes with hexagonal cross-section are fabricated by optical vapor supersaturated precipitation (OVSP) in an optical image furnace. The growth mechanism is revealed and the process parameters are optimized for time-saving fabrication. The dimensions of the UTW-ZnO microtube are >5 mm in length and ~50-200 μm in diameter with the wall thickness down to 500 nm. The UTW-ZnO microtube cavity supports multiple types of optical modes, e.g. in-tube Fabry–Perot modes, in-wall Fabry–Perot modes and wave-guided whispering gallery modes (WG-WGMs). The free-exciton recombination rate and exciton–exciton collisions are promoted in the cavity. The intensities of

near-band edge (UV light) and X-band (blue light) emission are therefore increased at least one order of magnitude in the temperature range of 0–500°C. Meanwhile, the temperature-sensitive multicolor luminescence of the UTW-ZnO microtubes in the visible band from near-white to bluish-violet is demonstrated. Low-threshold UV lasing is also achieved in the UTW-ZnO microtube by WG-WGMs, in which the excitation threshold is down to 5.50 μ W. The self-absorption effect in UTW-ZnO microtube cavity on excitonic luminescence is studied as well. The trapping structure regulates the X-band and NBE emission via various excitation-detection geometries. The self-absorption in the microcavity results in a high concentration of exciton and boosts the amplified spontaneous emission. The enhancement ratio for the UV band emissions can be up to 40 folds. Furthermore, light harvesting in the microtube cavity is beneficial to boosting the ZnO catalytic performance for photodegradation of organic dyes. The UTW-ZnO microtube demonstrates compatibility to microfluidic channels for recyclable on-chip degradation. The present work provides new opportunities to design novel tubular wide-bandgap semiconductor devices for a variety of optoelectronic applications in micro/nanophotonics.

5:00 PM - 5:15 PM

TOWARDS SMART COMPOSITE MATERIALS: NANOSCALE FUNCTIONALIZATION OF CARBON FIBERS WITH ZINC OXIDE

A. Zappettini, D.M. Nikolaidou, D. Delmonte, D. Calestani, N.

Coppedé, M. Villani

IMEM-CNR, ITALY

Nowadays providing real-time feedback on the integrity of mechanical structures is a challenging goal in different technological fields: many real-world examples include aerospace (aircrafts, satellites), civil and mechanical engineering (buildings, bridges), robotics (exoskeletons), therefore the availability of a net of transducers embedded in these structures would own a paramount importance. Carbon fiber (CF) as the backbone of lightweight and high performance composites (CFRP), is the material of choice with enormous potential in the aforementioned industries, however CFRP laminates are extremely susceptible to generate micro-damages when extrinsic sensors are

applied within the polymer matrix. Recently the possibility to achieve a fully integrated piezoelectric sensor, by nanoscale functionalization with ZnO, has been demonstrated [1]. The nano-engineered transducer, consisting of zinc oxide nanorods grown *in situ* on carbon fibers, has been characterized by means of dynamic hysteresis and capacitance measurements. The device has been stimulated using both static and dynamic stress: the occurrence of characteristic current vs. voltage polarization lobes of a ferroelectric material (stressed piezoelectric), have been recorded under static stress application. Under dynamic stress, a 400% capacitance increase has been measured with respect to the unstressed device. It is noteworthy that these results have been achieved using the carbon fiber itself as conductive element, without the need for external wiring, providing a true integration of the piezoelectric transducer into carbon fiber based materials. The functionalization process has been extended to tows made of one thousand fibers, like those commonly used in industrial processing, resulting in the creation of “smart” sensing carbon fiber composites. A stress-sensing device made of two functionalized tows, fixed with epoxy resin and crossing like in a typical carbon fiber texture, was successfully tested [2]. Piezoelectric properties of single nanorods, as well as those of CFRP, are measured and discussed. Noteworthy the proposed device, integrated into CFRP composite material, affects CFRP mechanical properties to a very low extent (about 5%). Overall, one of the most impressive features is the possibility to have stress/vibration sensors network distributed and embedded into the structural material itself (e.g. CFRP), which is the backbone of the high-performance structural materials of today. References [1] M. Villani et al, *J. Mater. Chem. A.*, 2016, **4**, 10486–10492 [2] D. Calestani et al., *Nanotechnology*, 2018, **29**, 335501

5:15 PM - 5:30 PM

PHYSICAL VAPOR TRANSPORT GROWTH OF ZINC PHTHALOCYANINE NANOPILLARS ON GRAPHENE SUBSTRATES

T. Mirabito¹, B. Huet¹, D.W. Snyder¹, A. Briseno²

¹Applied Research Lab-Pennsylvania State University, PA, UNITED STATES OF AMERICA, ²Pennsylvania State University, PA, UNITED

STATES OF AMERICA

Zinc phthalocyanine (ZnPc) is important for organic electronic devices because of its good thermal and chemical stability. It is also well characterized and inexpensive which makes it an ideal system to investigate the morphology, and interfacial properties by systematically varying its interaction with graphene-based substrates. Since the ZnPc microstructure is strongly dependent on the underlying substrate, we study the growth of graphene on a wide range of substrates including Si, SiO₂, SiC, and sapphire. Building upon the work of Briseno et al. [1], we investigate the growth mode of ZnPc on graphene-based substrates. Graphene, a one-atom-thick carbon layer, serves as a buffer layer, with the advantage of helping decouple the ZnPc from the substrate for transferring onto other materials. To investigate the potential effects of the graphene growth process, thickness and substrate material, graphene grown from chemical vapor deposition (CVD) as well as epitaxial graphene grown on silicon carbide from thermal decomposition were investigated. We also investigated the effect of graphene thickness using single layer graphene (SLG) grown from CVD and multilayer graphene produced by multiple transfers as well as single layer and few layer graphene (FLG) grown by thermal decomposition. The oriented crystallization of ZnPc nanowires onto the graphene templates has been performed utilizing a pressure-controlled physical vapor transport (PVT). The effects of process parameters (substrate temperature, source temperature, pressure) have been investigated. Characterization of these samples through Scanning Electron Microscopy, Raman Spectroscopy, and 3D Optical Profilometry show grass like morphologies of vertically oriented nanowires when grown on SLG. Additionally, deposition on FLG silicon carbide has revealed two segregated regions of bulkier ZnPc morphology on the thicker graphene areas and the thinner nanowires along the basal plane step edges. Our experimental results explore the influence of substrate material, or graphene character on the nucleation and growth mode of the organic material. Ultimately, these experiments help us establish a better understanding of the correlation between ZnPc growth behavior and the substrate physical properties. [1] Zhang, Y., Diao, Y., Lee, H., Mirabito, T., Johnson, R., Puodziukynaite, E., John, J., Carter, K.,

Emrick, T., Mannsfeld, S. and Briseno, A. (2014). Intrinsic and Extrinsic Parameters for Controlling the Growth of Organic Single-Crystalline Nanopillars in Photovoltaics. Nano Letters

Tuesday, July 30, 2019

3:30 PM - 5:30 PM

Surfaces and Interfaces

Location: Crestone I, II

Session Chair(s): Elias Vlieg, Kerstin Volz

3:30 PM - 4:00 PM

STEP DYNAMICS RESULTING FROM ADSORPTION AT ELECTRON PASSIVATED SEMICONDUCTOR SURFACES

S. Krukowski, P. Strak, P.T. Kempisty, K. Sakowski

Institute of High Pressure Physics PAS, POLAND

Results of *ab initio* extensive simulations of adsorption of the species at semiconductor surfaces show that the important contribution to adsorption energy stems from the electron transfer from or to the newly created quantum surface states. The effect called Intrasurface Electron Transition Contribution to Adsorption Energy may amount to several eVs, drastically changing the adsorption energy. The magnitude of this contribution is fixed for the Fermi energy pinned at the surface state. At some coverage, the surface states are fully occupied and empty, and at this surface state the Fermi level is shifted from one pinning state to another. This is accompanied by the adsorption energy change of order of the electronvolts. This is singular point in the vapor-surface equilibrium as the equilibrium vapor pressure changes by several orders of magnitude while the surface coverage remains almost constant. The examples of such behavior include N at AlN(0001) [1], Ga, H₂ and NH₃ at GaN(0001) and GaN(000 $\bar{1}$)[2-4], Si at SiC(0001) [5] surfaces. Thus this behavior is universal, typical for all semiconductor surfaces. The drastic variation of the adsorption energy affects the diffusion at the surface terraces, strongly deviating from standard BCF behavior [7]. The underlying step dynamic is resolved for adatom diffusion, typical for Si at SiC(0001) and N at AlN(0001) surfaces and also complex dynamics of

Ga adatoms moving over the surface under mixed $\text{NH}_2\text{-NH}_3\text{-NH-H}$ coverage. [1] P. Strak, K. Sakowski, P. Kempisty, S. Krukowski, J. Appl. Phys. 119 (2015) 095705 [2] P. Kempisty, P. Strak, K. Sakowski, S. Krukowski, Surf. Sci. 662 (2017) 12 [3] P. Kempisty, S. Krukowski, AIP Adv. 4 (2014) 117109 [4] P. Kempisty, P. Strak, K. Sakowski, Y. Kangawa, S. Krukowski, Phys. Chem. Chem. Phys. 19 (2017) 29676 [5] J. Soltys, J. Piechota, P. Strak, S. Krukowski, Appl Surf. Sci. 393 (2017) 168 [6] P. Kempisty, P. Strak, K. Sakowski, S. Krukowski, J. Cryst. Growth 390 (2014) 71

4:00 PM - 4:15 PM

EFFECTS OF ACIDIC GASES ON ICE SURFACES GROWN FROM WATER VAPOR

K. Nagashima, G. Sazaki, T. Hama, K. Murata, Y. Furukawa
Institute of Low Temperature Science, Hokkaido University, JAPAN
Ice has a great influence on the global environment, due to its abundance on the earth. Surfaces of ice have attracted considerable attention as “reaction sites” where atmospheric gases cause various heterogeneous chemical reactions in nature. In addition, the ice crystal surfaces near melting point are covered with quasi-liquid layers (QLLs), which may lead great influence on the chemical reactions. Hence, so far there have been many spectroscopy studies on such chemical reactions on ice surfaces, yet revealing effects of atmospheric gases on ice surfaces remains an experimental challenge. In this study, we directly visualized effects of acidic gases (HNO_3 and HCl) on ice surfaces by laser confocal microscopy combined with differential interference contrast microscopy (LCM-DIM), which can visualize the individual 0.37-nm-thick elementary steps on ice crystals [1]. In the absence of acidic gas, QLLs on ice basal faces disappear at temperature $T < -2^\circ\text{C}$ [2]. In the presence of acidic gas, the QLLs stably existed even at $T < -15^\circ\text{C}$ [3], showing that QLLs were not pure bulk water but acidic solution. Therefore, the acidic droplets can stably exist on ice surfaces at $T < -15^\circ\text{C}$. In addition, under supersaturated water vapor conditions, HNO_3 and HCl gases show different effects. The HNO_3 droplets on ice surfaces can stably remain on ice surfaces, whereas the HCl droplets are

embedded in ice crystals. In the case of the HNO_3 droplets, the ice-droplet interface grows evenly by the vapor-liquid-solid growth mechanism utilizing macrosteps formed on the ice-droplet interface. In contrast, in the case of HCl droplets, the growth of ice starts from the ice-droplet-vapor interfaces (contact lines), and the subsequent growth proceeds on the surfaces of the droplets, resulting in the embedding of the droplets in the ice crystals. After the sublimation of the ice, the embedded HCl droplets reappear on ice crystal surfaces [4]. This difference should be due to the differences between the physical and chemical properties between HNO_3 and HCl. However revealing the details is a future challenge. The insights obtained in this study may open a new avenue for the study of the uptake of atmospheric gases on natural ice. [1] Sazaki et al., PNAS 107, 19702 (2010). [2] Chen, et al., Cryst. Growth Des. 19, 116 (2019). [3] Nagashima et al., Cryst. Growth Des. 16, 2225 (2016). [4] Nagashima, et al., Cryst. Growth Des. 18, 4117 (2018).

4:15 PM - 4:30 PM

ADHESIVE PROPERTIES OF BI-MATERIAL INTERFACES FORMED WITH FRESHWATER COLUMNAR ICE

E. Asenath-Smith, G.R. Hoch, V.R. Gisladdottir, D.T. O'Connor, R.B. Haehnel

US Army ERDC CRREL, NH, UNITED STATES OF AMERICA

Ice adhesion threatens the safety and success of systems around the globe: transportation is halted; power is lost; communications are severed; aerial vehicles are grounded. All these scenarios have severe consequences for both military and civilian operations. Coating technologies present a highly appealing 'promise' to passively reduce ice accretion or adhesion without increasing mass or energy requirements of related equipment. Yet, after decades of research and the development of numerous low ice adhesion coatings, few are commercialized, and there are even fewer examples of their successful implementation. Underlying this disparity is the reality that there are no standard methods for measuring ice adhesion. The adhesion of ice is determined by measuring the force required to delaminate ice from the surface of interest. Essentially a bi-material interfacial fracture event, ice adhesion data has been historically

analyzed as a cohesive materials strength problem; by calculating the maximum force divided by the contact area. While this is a reasonable approach to qualitatively compare samples tested under identical conditions, it does not have the quantitative rigor needed to thoroughly evaluate the effectiveness of a surface treatment to modulate the adhesive properties of ice. In addition, the materials properties of the coatings influence the force required to delaminate ice from a surface, and these quantities are not accounted for in the 'strength' analysis. Moreover the properties of ice affect the measurement; ice type, microstructure, and temperature are all important. Leveraging our historical role in ice adhesion testing and evaluation, the US Army Corps of Engineer's Cold Regions Research and Engineering Laboratory (CRREL) is performing research on ice adhesion to develop a rigorous quantitative analysis of ice adhesion measurements. This presentation will address our progress on this effort, by first discussing methods we have developed to crystallize freshwater columnar ice on substrates. Subsequently we will report on techniques to measure the adhesion of freshwater ice along with data analysis approaches, which are consistent with the physics of ice adhesion experiments. Through this presentation, we will address the role of surface and ice material properties in ice adhesion studies so that coating technologies can be utilized to control ice adhesion across a wide range of settings.

4:30 PM - 4:45 PM

STEP MORPHOLOGY CONTROL IN HOMOEPITAXIAL GAN GROWTH BY MOCVD

A. Klump¹, P. Reddy², Y. Guan¹, S. Washiyama¹, S. Mita², R. Collazo³, Z. Sitar²

¹North Carolina State University, NC, UNITED STATES OF AMERICA, ²Adroit Materials, UNITED STATES OF AMERICA, ³North Carolina State University, UNITED STATES OF AMERICA
Commercially available native GaN substrates offer exciting new potential for the next generation of gallium nitride (GaN) based vertical power devices. Previously, GaN epitaxial layers suffered from a high density of dislocations due to growth on foreign substrates. These

dislocations resulted in a rough surface morphology, limiting sharp layer transitions and introducing doping non-uniformities. Growth on native substrates eliminates the lattice mismatch between film and substrate, and ultimately the presence of these dislocations. In this work, homoepitaxial GaN growth is explored. Particularly, the relationship between substrate offcut and growth supersaturation on the surface morphology was examined to establish a kinetic/process map to identify the conditions for obtaining smooth step-flow morphology. This analysis will be based on surface kinetic approaches within the context of BCF theory. All films were grown via MOCVD on vicinal (0001) HVPE or ammonothermal GaN substrates. For all growths, temperature was 950°C, diluent gas was H₂, total pressure was 20 Torr, and total flow was kept at 7 slm. Substrate offcut and V/III ratio (by ammonia flow) were the parameters varied in the experiments. Atomic force microscopy (AFM) was utilized to measure offcuts, step heights, and surface morphologies. From the substrate perspective, decreasing the offcut from 0.3° to 0.2° at a fixed growth supersaturation (2000 V/III ratio) shifted the morphology from bi-layer steps to sinusoidal undulations. These undulations were considered to lower the energy at low offcuts by decreasing the stress domains of long-range straight steps. In this work, the step height perpendicular to the undulation direction was the same as the bilayer step growth. However, there was a height change observed between peak-valley-peak along a step in the undulation direction - undesirable for optimal performance. From the growth supersaturation perspective, reducing the V/III ratio from 2000 to 100 at a fixed offcut of 0.3° led to a step-bunched morphology. This transition from bi-layer steps to step-bunching is understood as the decrease in supersaturation with decreasing V/III ratio (i.e. NH₃ partial pressure). Preventing this undesired morphology thus is accomplished by decreasing the offcut or controlling the supersaturation. In general, these results indicate the impact of the vicinal offcut and growth conditions on the surface morphology of GaN homoepitaxy and provide the kinetic/process boundaries for achieving smooth surfaces required by power devices.

4:45 PM - 5:00 PM

GROWTH AND MORPHOLOGY OPTIMIZATION OF OMVPE

ALINGAAS/INP SUPERLATTICE STRUCTURES

O.J. Pitts, O. Salehzadeh, X. Wu, A.J. Springthorpe
National Research Council Canada, ON, CANADA

Alln(Ga)As layers grown on InP are an important and attractive material system for a number of device applications, including directly-modulated lasers, avalanche photodiodes and high electron mobility transistors. The growth of a high quality interface between InP and Alln(Ga)As by OMVPE presents significant challenges, with strained interface layers and surface morphology degradation having been reported. However, most previous reports have focused on the growth of device structures containing at most only a small number of repeats of this interface [1-2]. In this work, we report a detailed study of the OMVPE growth of a superlattice structure specifically designed to characterize interface quality. The superlattice structure contains 20 repeats of InP/AllnGaAs/InP, grown under a variety of growth conditions. The interface quality is characterized by *in situ* reflectivity monitoring, photoluminescence (PL) spectroscopy, optical microscopy, laser scattering mapping, high resolution x-ray diffraction (HRXRD) and transmission electron microscopy (TEM) with energy-dispersive x-ray spectroscopy analysis (EDX). Under non-optimized conditions we observe the formation of a strained layer at the AllnGaAs-on-InP interface due to intermixing on the group V sublattice. This is accompanied by the formation of localized three-dimensional growth features starting after the fourth repeat of the superlattice structure. We report optimized growth conditions that allow the growth of the 20 period superlattice structure with minimized interfacial strain and no observable interface morphology degradation. [1] Misao Takakusaki, Hajime Momoi, Kouji Kakuta and Hirofumi Nakata, "Comparison of InAlAs/InP Hetero-interface Properties -MBE vs. MOCVD-," *Proc. of International Conference on Compound Semiconductor Mfg.*, 2003. [2] K. Borgi, M. Hjiri, F. Hassen, H. Maaref, V. Souliere, Y. Monteil, "Optical study of inverted interface in InP/InAlAs/InP structures grown by MOCVD," *Microelectronic Engineering* 51–52 (2000) 299–308.

5:00 PM - 5:15 PM

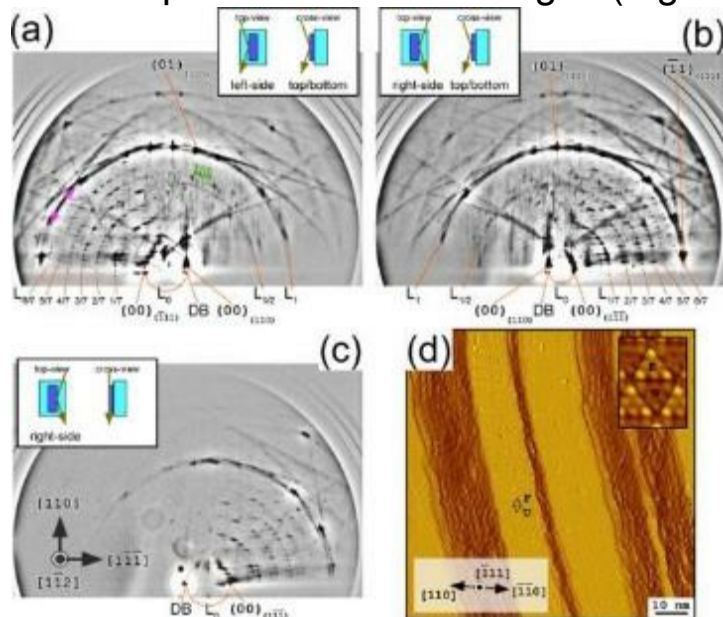
CREATION OF ATOMICALLY-ORDERED SIDE- AND FACET-

SURFACES ON THE THREE-DIMENSIONALLY ARCHITECTED SI STRUCTURES

A.N. Hattori

The Institute of Scientific and Industrial Research, Osaka University, JAPAN

The creation of atomically-ordered Si{100}2×1, {110}2×16, and {111}7×7 ordered side- and facet- surfaces on the three-dimensionally (3D) architected Si substrate is realized for the first time. We have established the original methodology that enable to observe atomic orderings and arrangements of "surfaces with arbitrary directions" on 3D figured structures, by developing reflection high-energy electron diffraction (RHEED) and scanning tunneling microscope (STM). RHEED pattern and STM images (Figure)



prove the realization atomically-reconstructed Si{111}7×7 side-surfaces, which are perpendicular to planar substrate surfaces on 3D patterned Si substrates. We have also developed the atomically-ordered 3D nanofabrication technique, where the material stacking direction is switched from the general out-of-plane to in-plane direction, and realized the formation ultra-thin epitaxial films in 3D space. The resistance investigation for the Au wires crossing over 3D facet edges with an angular shape revealed the enlargement of the resistance originated from conduction electron scattering along the angular path. Our results would contribute to the progress in surface science for 3D nanostructure and the fundamental understanding of

electron transport in 3D angular metal-interconnects.

5:15 PM - 5:30 PM

THE INTERFACIAL INTERACTIONS BETWEEN FACETED CRYSTALS: AN IN-SILICO AND ATOMIC FORCE MICROSCOPY STUDY

A. Moldovan, A. Bayly, R. Hammond, S. Connell

University of Leeds, UNITED KINGDOM

In this work, we have probed the interactions between specific organic crystal surfaces using Molecular Mechanics and Atomic Force Microscopy. This allows us to identify the impact of surface chemistry onto inter-particulate interactions. The formulation of pharmaceutical products has historically been a time and resource extensive endeavour. Excipients are used in formulations to enhance product performance and improve manufacturability. The compatibility between the active pharmaceutical ingredient (API) and the excipients used plays a critical role in the final product performance. The cohesive (API-API) and adhesive (API-Excipient) balance (CAB) between an API-excipient can be used to describe the likelihood of two powders sticking together. The ability to pre-screen API-Excipient compatibility in-silico would allow formulators to make a more informed decision on the experimental studies to be carried out, thus reducing the development time and resources required to get a molecule from discovery to product. However, as with any computational model, this must be validated with experimental data. For the in-silico approach, a molecular mechanics (MM) framework has been developed to calculate the interfacial interactions between faceted organic crystals. The Surface-Surface Interaction Model (SSIM) is designed to calculate the interaction energy between two slabs at an atomistic scale. By focusing on facet-specific interactions both computationally and experimentally, energetics associated with the surface chemistry can be identified. A surface compatibility ranking system has been developed allowing relative comparisons to be made between adhesive and cohesive forces. Atomic force microscopy (AFM) is being used to measure the adhesive force between defined crystal planes of paracetamol. These faceted surfaces will also be measured against a range of excipients (α -L-Glutamic Acid and β -D-

Mannitol). AFM studies have been previously carried out using colloidal probes and coated cantilevers, however, there is a lack of fully faceted organic crystal adhesion data. This work has significant applications within pharmaceutical research by offering a piece of the puzzle that has always been difficult to probe. The impact of surface chemistry based on facet-specific termination has been tested both computationally and experimentally

Tuesday, July 30, 2019

3:30 PM - 5:30 PM

Symposium on Epitaxy of Complex Oxides: Delafossites and Oxides on Semiconductors

Location: Grays Peak II, III

Session Chair(s): Chang-Beom Eom

3:30 PM - 4:00 PM

THIN-FILM GROWTH OF PdCoO_2 : A LAYERED OXIDE AS CONDUCTIVE AS GOLD

T. Harada, A. Tsukazaki

Tohoku University, JAPAN

Insulating and semiconducting substrates used in industry often belong to hexagonal systems as exemplified by sapphires, gallium nitrides, and silicon carbides. Hexagonal metals with matched lattice constants will offer a possibility to develop devices with epitaxial interfaces. As a promising hexagonal electrode material, we focus on a delafossite metal PdCoO_2 , which has a unique layered crystal structure with two-dimensional Pd sheets and triangular lattices of CoO_2 octahedra. Despite being an ionic oxide, a PdCoO_2 bulk single crystal has very high room-temperature conductivity comparable to elemental Au, with a bulk mean-free path reaching $20 \mu\text{m}$ (ref^{1,2}). In spite of its prominent electrical properties, research on PdCoO_2 has been limited in bulk crystals. Stabilizing PdCoO_2 in a thin-film form will offer new heterostructures and devices utilizing its superior electrical properties on hexagonal substrates. In this talk, we will discuss the thin-film growth of PdCoO_2 by pulsed laser deposition and its physical

properties. Stoichiometric *c*-axis oriented PdCoO₂ thin films are successfully grown on *c*-Al₂O₃, by alternately ablating polycrystalline PdCoO₂ and mixed-phase PdO_x targets. The surface morphology and the crystal structure of the PdCoO₂ thin films are characterized by atomic force microscopy, X-ray diffraction and transmission electron microscopy. The PdCoO₂ thin films have triangular domains with one of the base parallel to the [1-100]_{Al₂O₃} direction. The room-temperature sheet resistance $R_s < 100 \Omega/\text{sq}$ is achieved for highly transparent ultrathin films of 4 nm: the optical transmittance $T_{\text{film}} > 70\%$ for visible light and $T_{\text{film}} > 90\%$ for near infrared light, demonstrating the superior properties as hexagonal electrodes³. We will discuss the current status and possible challenges in the thin-film growth of PdCoO₂, aiming at the bulk level of conductivity. We also show our recent attempt to fabricate functional devices exploiting the unique crystal structure of PdCoO₂.

References ¹ A.P. Mackenzie, Rep. Prog. Phys. 80, 032501 (2017). ² R. Daou *et al.*, Sci. Technol. Adv. Mater. 18, 919 (2017). ³ T. Harada *et al.*, APL Mater. 6, 046107 (2018).

4:00 PM - 4:30 PM

GROWTH OF METALLIC DELAFOSSITES BY MOLECULAR BEAM EPITAXY AND PULSED LASER DEPOSITION

M. Brahlek

Oak ridge national laboratory, TN, UNITED STATES OF AMERICA

The ABO₂ delafossite oxides are a unique class of oxides with layered A-BO₂-A-BO₂ structure with inplane trigonal coordination. For A=Pd and Pt this structural motif gives rise to natural 2D electronic behavior with inplane conductivity rivaling that of the noble metals. In this talk I will discuss the successes and failures in the pursuit of growing thin films of the metallic delafossite oxides PdCoO₂ and PdCrO₂ by both molecular beam epitaxy and pulsed laser deposition. The key challenges are threefold: (1) optimizing conditions to form oxides of Pd, (2) maintaining the correct A:B stoichiometry, and (3) navigating the complex space of nucleation and kinetics on various surfaces. Structural and transport data will be presented that highlight these

challenges and how to overcome them. Understanding the synthesis science of ABO₂ delafossites is the first step towards creation of a new generation of layered quantum oxides.

This work was supported by the U.S. Department of Energy, Office of Science, Basic Energy Sciences, Materials Sciences and Engineering Division.

4:30 PM - 4:45 PM

GROWTH OF DELAFOSSITE PtCoO₂ THIN FILMS BY MOLECULAR-BEAM EPITAXY

J. Sun¹, H. Paik², D. Schlom¹

¹Department of Materials Science and Engineering, Cornell University, NY, UNITED STATES OF AMERICA, ²Platform for the Accelerated Realization, Analysis, & Discovery of Interface Materials (PARADIM), Department of Materials Science and Engineering, Cornell University, NY, UNITED STATES OF AMERICA

PtCoO₂ and PdCoO₂ are layered complex oxides with the highest conductivities per carrier among all known materials. This in combination with their large spin-orbit coupling makes them of interest for fundamental studies and possible applications. These oxides belong to the delafossites family. Due perhaps to the difficulty to oxidize platinum, the growth of PtCoO₂ thin films by molecular-beam epitaxy (MBE) has been unexplored. Here we report the first successful synthesis of PtCoO₂ (0001) thin films with platinum inclusions on *c*-plane sapphire. These films were grown in an adsorption-controlled growth regime in which an excess of platinum was supplied in an ambient of distilled ozone and thermodynamics led to the vaporization of the excess platinum. Although the residual resistivity ratio (ρ_{300K}/ρ_{4K}) of 2 achieved for the MBE-grown PtCoO₂ films rivals that of the best of PdCoO₂ films reported in the literature, the in-plane resistivity of the resulting PtCoO₂ films at 300 K (34.6 $\mu\Omega$ -cm) is an order of magnitude larger than bulk PtCoO₂ single crystals (2.1 $\mu\Omega$ -cm). Possible routes to improve the transport properties of the epitaxial delafossites films will be discussed further.

4:45 PM - 5:15 PM

ATOMIC CONTROLLED OXIDE HETEROSTRUCTURES ON SI AND III-V SEMICONDUCTORS

G. Rijnders

University of Twente, MESA+ Institute for Nanotechnology,
NETHERLANDS

In recent years, it has been shown that novel functionalities can be achieved in oxide heterostructures in which the interfaces are atomically controlled, in terms of atomic stacking as well as in terms of the local symmetry. Correlated transition metal oxide perovskites receive a lot of attention due to their unique physical properties, which are largely driven by distortion of the BO_6 octahedral network. In bulk, the control of the octahedral network is normally obtained by cation substitutions in a random alloy. Similar to the charge donors in semiconductors, cation substitutions will introduce scattering and disorder. The development of artificial heterostructures offers unprecedented opportunities to lattice engineering to achieve desired properties. We, for instance, demonstrated a structural analogue of modulation doping in nickelate heterostructures through the interfacial transfer of tilt patterns. Modulation tilt control was used to remotely control the Ni–O bonds in the compound SmNiO_3 and thereby its critical temperature for optimal optical switching application.

In this contribution, I will highlight the recent developments in atomic controlled growth of epitaxial oxides by pulsed laser deposition, with a focus on heterostructures showing manipulated magnetic and electronic properties.

Furthermore, integration of epitaxial complex oxides in Si and III-V technologies has recently attracted a lot of attention in science and industry. Such complex oxides include, amongst others, ferro- and piezo-electrics and materials for resistive switching devices. In this presentation I will focus on the integration of complex oxides such as SrRuO_3 and $\text{Pb}(\text{Zr},\text{Ti})\text{O}_3$ as well oxide heterostructures with Si and III-V semiconductor devices.

5:15 PM - 5:30 PM

EPITAXIAL GROWTH OF SrTiO_3 AND FUNCTIONAL OXIDES ON

SILICON

Z. Wang¹, B.H. Goodge¹, D.J. Baek¹, M.J. Zachman¹, X. Huang¹, X. Bai¹, C. Brooks¹, H. Paik¹, A.B. Mei¹, J. Brock¹, J. Maria², L. Kourkoutis¹, D. Schlom¹

¹Cornell University, NY, UNITED STATES OF AMERICA, ²North Carolina State University, UNITED STATES OF AMERICA

Growing epitaxial SrTiO₃ films on silicon, the backbone of semiconductor industry, has been a challenging task for decades. Here we detail the growth procedure for integrating epitaxial (001) SrTiO₃ films on (001) Si using molecular-beam epitaxy. The structural perfection and defect microstructure of epitaxial (001) SrTiO₃ films grown on (001) Si was assessed by a combination of x-ray diffraction and scanning transmission electron microscopy (STEM). Conditions were identified that yield 002 SrTiO₃ rocking curves with full width at half maximum (FWHM) below 0.03° for films ranging from 2-300 nm thick. These rocking curves are comparable or even narrower than the 002 rocking curve of typical SrTiO₃ single crystals. Examination of a SrTiO₃/Si film with a 002 rocking curve FWHM of the 0.008° by STEM showed it to contain ~ threading dislocations per cm², about 6 orders of magnitude higher than SrTiO₃ single crystals. How it is possible for a SrTiO₃ film that contains a threading dislocation density more than six orders of magnitude higher than a SrTiO₃ single crystal to exhibit an 002 SrTiO₃ rocking curve narrower than that of the single crystal? The answer is that the threading dislocations in the SrTiO₃/Si film have pure edge character, making the 002 peak insensitive to them. Our results show that one narrow rocking curve peak is insufficient to characterize the structural perfection of epitaxial films. Despite the high density of threading dislocations and extended defects containing dislocations and out-of-phase boundaries in these SrTiO₃/Si films, they do represent a significant improvement in the quality of SrTiO₃/Si films as demonstrated by the properties of functional oxides that have been achieved on top of them. For example, an epitaxial SrRuO₃ film with a residual resistivity ratio (rou_{300K} / rou_{4K}) of 11 has been achieved on a 14 nm thick SrTiO₃ film on silicon. This value rivals

those of epitaxial SrRuO₃ films produced directly on SrTiO₃ single crystals by most thin film growth techniques other than MBE. Similarly, epitaxial La-doped BaSnO₃ films of room temperature mobility of 128 cm² V⁻¹ s⁻¹ has been achieved on a 18 nm thick SrTiO₃ film on silicon, which compares favorably to those of La-doped BaSnO₃ films grown by all techniques other than MBE on single-crystal oxide substrates.

Tuesday, July 30, 2019

5:30 PM - 7:00 PM

Poster Session - Tuesday

Location: Quandary Peak

Session Chair(s):

5:30 PM - 5:31 PM

**SIZE SCALING OF THE IMPROPER FERROELECTRICITY IN
LUFeO₃**

M.E. Holtz¹, R. Steinhardt¹, P. Barrozo Da Silva², B. Prasad², J.A. Mundy³, R. Ramesh², D. Schlom¹

¹Cornell University, NY, UNITED STATES OF AMERICA, ²University of California Berkeley, UNITED STATES OF AMERICA, ³Harvard University, UNITED STATES OF AMERICA

Ferroelectric materials are of key importance in functional memory devices. Of particular interest are improper ferroelectrics, which have a structural transition that drives ferroelectricity. Because the order parameter for the transition is structural, and not the polarization, this opens pathways towards exciting phenomena such as the coupling of ferroelectricity with magnetism, and ferroelectricity in ultra-thin films. Hexagonal oxides, such as $R(\text{Mn,Fe})\text{O}_3$ where $R = \text{Y, Ho - Lu}$, have a trimerization distortion that drives ferroelectricity, and have recently been incorporated into room-temperature multiferroic superlattices. Here we investigate the thickness dependence of ferroelectric properties in epitaxially stabilized hexagonal LuFeO₃ on (111) oriented cubic metal electrodes such as platinum. The film and electrodes are grown by molecular beam epitaxy (MBE) without breaking vacuum, resulting in epitaxial and atomically smooth interfaces with

indiscernible interdiffusion. We vary the LuFeO_3 thickness from 150 nm down to 0.5 unit cells (a single formula unit). We investigate ferroelectric switching with frequency-dependent capacitor measurements, observing a decrease in the coercive field as the films become thinner, to below 200 mV in 10 nm thick films. Atomic-resolution scanning transmission electron microscopy shows an onset of ferroelectricity in the first monolayer of the LuFeO_3 film, and thickness dependent measurements are underway. This low-coercivity in thin improper ferroelectrics opens the door to making thin film low power logic and memory devices.

5:31 PM - 5:32 PM

SELF-ASSEMBLY AND PROPERTIES OF DOMAIN WALLS IN BIFEO3 LAYERS GROWN VIA MOLECULAR-BEAM EPITAXY

A.B. Mei¹, D. Schlom²

¹Cornell University, UNITED STATES OF AMERICA, ²Department of Materials Science and Engineering, Cornell University, UNITED STATES OF AMERICA

Bismuth ferrite BiFeO_3 layers, ~200-nm-thick, are deposited on SrRuO_3 -coated $\text{DyScO}_3(110)_o$ substrates in a step-flow growth regime via adsorption-controlled molecular-beam epitaxy. Structural characterizations establish phase-pure films of high structural perfection with substrate-limited mosaicity (0.012 deg x-ray diffraction ω -rocking curve widths). Film surfaces are atomically smooth (0.2 nm root-mean-square height fluctuations) and consist of 260-nm-wide $[1-11]_o$ -oriented terraces and unit-cell-tall (0.3 nm) step edges. The combination of electrostatic and symmetry boundary conditions promotes two monoclinically-distorted BiFeO_3 ferroelectric variants, which self-assemble into a pattern of unprecedented long-range order, consisting of 145-nm-wide striped domains separated by $[001]_o$ -oriented 71 deg. domain walls. The walls exhibit electrical rectification and enhanced conductivity.

5:32 PM - 5:33 PM

EXOTIC TRANSROTATIONAL CRYSTAL GROWTH IN THIN AMORPHOUS FILMS DISCOVERED BY TEM: "VACUUM

EPITAXY", LATTICE-ROTATION NANOENGINEERING, NOVEL AMORPHOUS MODELS

V.Y. Kolosov

Ural Federal University, RUSSIAN FEDERATION

Exotic thin crystals with unexpected **transrotational nanostructures** [1] have been discovered by transmission electron microscopy (TEM) for crystal growth in thin (10-100 nm) amorphous films of different chemical nature (oxides, chalcogenides, metals and alloys) prepared by various methods (thermal/laser/e-beam evaporation, melt spinning, pyrolysis, diffusion in solid state). We use primarily our TEM bend-contour technique [2] incorporating usual selected area electron diffraction, bright and dark field imaging. HREM, AFM and optical microinterferometry were used in due cases (preferentially for correlative microscopy). The unusual crystal growth we study is in general dislocation independent. It can be often traced *in situ* in TEM column during local e-beam heating or annealing: regular internal bending of crystal lattice planes in a growing crystal, Fig.1a-b. Such **transrotation** (translation of the unit cell is complicated by small **rotation** realized round an axis lying in the film plane) can carry strong regular lattice orientation gradients (up to $300^\circ/\mu\text{m}$) of different geometry/topology: cylindrical, ellipsoidal (2 types), toroidal, saddle-like, etc., Fig.1b. The most distinctive features of the structure appear at the meso-scale (100-1000 nm) where strong regular rotation of the lattice is attained. The possible mechanisms of the phenomenon are discussed, Fig.1d. Initial amorphous state and surface nucleation of the crystal growth are most essential factors. The last fact accompanied by anisotropy of crystal growth rate and obvious tendency for regular change of interatomic distances of the crystal propagating from the surface layers inside the bulk material resembles specific epitaxy, "vacuum epitaxy". The **transrotation** phenomenon is the basis for novel lattice-rotation nanoengineering of functional, smart thin-film materials suitable also for strain nanoengineering.

Transrotational micro crystals have been eventually recognized by different authors in some thin film materials vital for applications, e.g. phase change materials (PCM) for memory [3-5]. New nanocrystalline models of amorphous state are proposed: fine-grained structures with internal lattice curvature, Fig.1e. Thus different transrotational lattice

geometry inside fine crystal grains in the static model corresponds to different amorphous structures. Going to 3D clusters of positive/negative curvature and dynamics we propose the hypothesis of “dilaton” and “contracton” pulsating or/and circulating in amorphous film. [1] V.Yu. Kolosov, A.R. Tholen, *Acta Mater.* **48** (2000) 1829-1840. [2] I.E. Bolotov, V.Yu. Kolosov, *Phys. Stat. Sol.* **69a** (1982) 85-96. [3] B.J. Kooi, J.T.M. De Hosson, *J. App. Phys.* **95** (2004), 4714-4721. [4] J. Kalb et al., *J. Appl. Phys.* **98** (2005), 054902. [5] E. Rimini et al, *J. App. Phys.* **105** (2009), 123502.

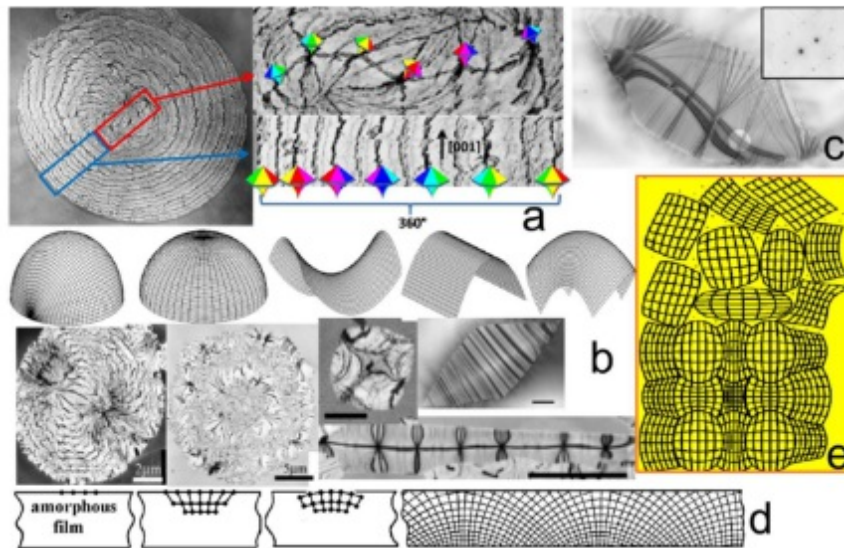


Fig. 1. TEM of thin crystals grown in different amorphous films (a, b) with crystal lattice planes curvature shown (b, upper row: ellipsoidal of 2 types, saddle-like, cylindrical, toroidal - corresponding to TEM micrographs placed in a row below). See “transrotational” single crystal with regular bend-contour patterns demonstrating additional evidence for “transrotation” from series of SAED (c); model for “vacuum epitaxy” in film cross-section (d); new model of the amorphous state based on fine transrotational crystal grains (e).

5:33 PM - 5:34 PM

PREPARATION OF IRIIDIUM FILMS BY CHEMICAL VAPOR DEPOSITION ON METAL SUBSTRATES

H. Sato¹, T. Goto¹, Y. Yokota¹, M. Yoshino², A. Yamaji², Y. Ohashi¹, S. Kurosawa¹, K. Kamada¹, A. Okuno³, A. Yoshikawa¹

¹New Industry Creation Hatchery Center, Tohoku University, JAPAN,

²Institute for Materials Research, Tohoku University, JAPAN, ³SANKO Co., Ltd., JAPAN

Chemical vapor deposition (CVD) of noble metals has a significance for practical applications in electronics, protective coating and catalyst

industries. The potentiality of applications is due to the valuable combination of the intrinsic properties of these metals, including high thermal and chemical stability, high electrical conductivity and catalytic activity. CVD of iridium (Ir) is of interest to prepare oxidation protective coatings on high-melting-temperature metals such as molybdenum (Mo), tantalum and tungsten. Thick enough coatings are essential to offer an effective corrosion and oxidation protection. Laser chemical vapor deposition (LCVD) of Ir was carried out in a cold-wall chamber made of stainless steel. Mo plates with the size of $10 \times 10 \times 0.15 \text{ mm}^3$ and $12 \times 12 \times 1.0 \text{ mm}^3$ were used as metal substrates. An Ir acetylacetonate, $\text{Ir}(\text{acac})_3$ precursor used as the source material was heated to maintain a high vapor pressure. After the Mo substrate was pre-heated to 873 K, the evaporated $\text{Ir}(\text{acac})_3$ precursor was transported into the chamber with Argon gas and the chamber was evacuated to 200-1000 Pa. The Nd:YAG laser was then introduced into the chamber through a quartz window, with an optical lens expanding the beam to about 10 mm in diameter so that the entire substrate is irradiated. The crystal phase of prepared films was identified by X-ray diffraction. It was found that the initial phase of the films was Ir-Mo alloy such as Mo_3Ir and $\text{Ir}_{1.02}\text{Mo}_{0.98}$. It is expected that Ir single phase can be obtained by optimizing the deposition time and thickness. Microstructure was observed with a scanning electron microscope. The Ir films prepared by LCVD and the thermal CVD using a carbon resistive heater as a heating element were compared.

5:34 PM - 5:35 PM

SPINODAL DECOMPOSITION WITH THE FORMATION OF A OSCILLATIONS OF COMPOSITION AT THE LOW TEMPERATURE SYNTHESIS OF THE GAINP - GAAS STRUCTURE

V. Kuznetsov¹, P. Moskvina², S. Skuratovskiy²

¹Saint-Petersburg State Electrotechnical University, RUSSIAN FEDERATION, ²Zhitomir state technological University, UKRAINE
An important consequence of the supersaturated state of the solid phase, which was synthesized under conditions close to the boundaries of thermodynamic instability, is the modulation effect of the solid solution composition, which is theoretically predicted and

experimentally observed [1,2]. The essence of this effect lies in the formation of micro-oscillations of the solid solution composition with the superstructure creation. Accounting of the energy of the components mixture and the energy of the elastically strained inclusions of the new phase leads to the following adapted form of the stationary equation for analyzing the concentration fields:

$$\beta \frac{d^2 c}{dz^2} = \alpha^S c \cdot (1-c) + RT [c \ln c + (1-c) \ln(1-c)] + \lambda_{ijk} \cdot N_o a (a - a_s)^2 / 4 - \mu,$$

where "z" is the coordinate in the direction of the layer growth; β, c - coefficient at the concentration gradient in the decomposition of the free energy of mixing of the solid phase [1] and the concentration of the GaP component in the solid solution $Ga_c In_{1-c} P$; N_o, λ_{ijk} - Avogadro number and combination of elastic moduli according to [3], a, a_s - the current period and the period of the crystal lattice of the stabilizing substrate; α^S - the parameter of interaction between the components of the solid phase; μ - chemical potential. A typical distribution of the composition of the layers in the $Ga_c In_{1-c} P$ - GaAs (111)

heterostructure depending on coordinate "z" are shown in Fig.1. In these figures, the periodic structure of the distribution of solid solution composition in the direction of the layer growth is visible. At the same time, the concentration profiles of the components differ significantly from the form corresponding to harmonic oscillations. The calculated result of Fig. 1 clearly illustrates the process of structure appearance with the periodic distribution of the solid phase composition which grown under thermodynamic conditions close to the boundaries of the spinodal decomposition.

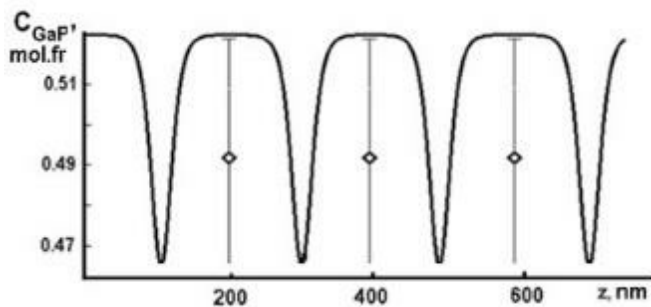


Fig. 1. The distribution of the composition over a layer of $Ga_c In_{1-c} P$ solid solution synthesized on a GaAs (111) substrate at $T=993K$ with an average composition 0.5 mol.fr. The presence of modulation of the

composition of a solid solution with a period at the level of tens of nanometers must be taken into account especially when forming nanostructures based on A^3B^5 solid solutions, when the thicknesses of the deposited layers become commensurate with the modulation period.

References 1. Cahn J.W. On spinodal decomposition. *Acta Metallurgica*, 1961, V.9, p.81. 2. Khachaturyan A.G., *Theory of Structural Transformations in Solid*, Wiley, New York, 1983. 3. Kuznetsov V.V., Moskvin P.P, Sorokin V.S. *J. Crystal Growth*, 1988, v.88.p. 241.

5:35 PM - 5:36 PM

CHANGE OF KINETIC PROCESS IN CRYSTAL GROWTH FROM AMORPHOUS THIN FILM OF α -NPD

H. Kanehara¹, H. Katsuno², T. Nakada²

¹Department of Physical Sciences, Ritsumeikan University, JAPAN,

²Department of Physical Sciences, Ritsumeikan University, JAPAN

Crystallization of amorphous organic thin films often causes degradation of practical devices. To avoid degradation, crystallization processes of amorphous NPD (N'-di-1-naphthyl -N,N'-diphenylbenzidine) thin films, which have been used as standard hole transport material for organic light emitting diode, have been investigated for years. However, the crystallization mechanism of NPD films has not been fully understood so far. In this study, we studied the kinetic process of the crystallization of NPD amorphous thin films by observing the crystallization processes in detail. Amorphous NPD thin films were prepared on glass substrates at room temperature using vacuum deposition at a pressure of 3×10^{-3} Pa. The deposition rate was 0.1-0.2 nm/s. Immediately after the deposition, the thin films were transferred into an environmental chamber, in which temperature were controlled at 50 °C in atmosphere. After taking out the specimens from environmental chamber temporarily, we observed the NPD films and measured the growth rate using optical and atomic force microscopy (AFM). After the annealing, crystalline regions appeared in the NPD films within a few hours. Figure 1 shows a typical optical microscope image of the crystalline region of NPD thin film annealed for 702

hours. AFM observation revealed that the circular crystalline is composed of aggregation of fibril crystals. Figure 2 shows the radius of crystalline regions versus annealing time in log-log plot. As shown in this figure, the slope clearly changes at a few tens of hours, suggesting that the kinetics of the crystallized process changes.

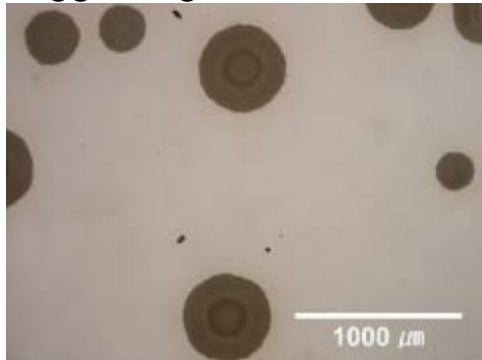


Figure 1. Optical microscope image of crystalline region in 110 nm-thick NPD film under 50 °C after 702 hours.

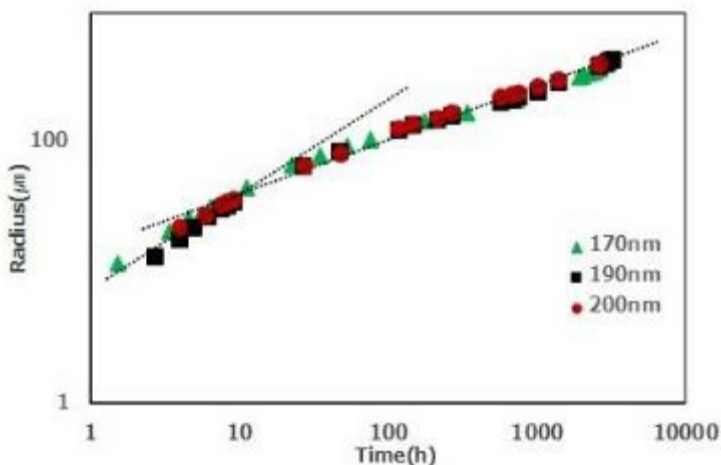


Figure 2. Radius of crystalline regions versus annealing time at 50 °C in log-log plot.

5:36 PM - 5:37 PM

INVESTIGATIONS ON STRUCTURAL, MECHANICAL AND MAGNETIC PROPERTIES OF ELECTROPLATED NIW NANO CRYSTALLINE THIN FILMS FOR MEMS APPLICATIONS

R. Kannan, M. Selvambikai, H. Arul, S. Jyothi

Department of Science and Humanities, Kumaraguru College of Technology (Autonomous), INDIA

The nano crystalline Nickel – Tungsten (NiW) thin films were

electroplated on the copper surface at constant current density of 1 A/dm² with two different bath temperatures like 35°C and 70°C. The micro structural and chemical elemental analysis of NiW thin films have been analysed by SEM and EDAX. The crystalline nature of coated thin films were investigated by XRD pattern. The surface roughness of coated NiW thin films was determined by using stylus profilometer. The electrochemical behaviour of NiW thin films have been analysed by using polarization and impedance results. The magnetic property of electroplated NiW thin films were also studied by VSM. The SEM micrograph reveals that the coated NiW thin films are bright, uniform and crack free. The XRD pattern shows the existence of FCC crystalline structure in NiW thin films with crystalline size are in the range of few tens of nanometre. NiW thin films synthesised at 35°C and 70°C have average roughness value of 0.38 and 0.34 µm respectively. The NiW thin films coated at lower bath temperature exhibit the better Inhibition efficiency of 78.58 % with polarization resistance of 2130.1 KΩ compared with higher bath temperature. The NiW thin film coated at 70°C exhibit the excellent soft magnetic property with lower coercivity of 62.174 G and higher saturation magnetization of 22.25×10^{-3} emu (retentivity of 999.31×10^{-6} emu). The NiW thin films plays an important role for the fabrication of MEMS devices due to its excellent soft magnetic property with better corrosion resistance.

5:37 PM - 5:38 PM

NITROGEN DOPED SILICON-CARBON PROTECTIVE MULTILAYER NANOSTRUCTURES ON CARBON OBTAINED BY TVA METHOD

V. Ciupina¹, C. Lungu², R. Vladoiu³, G. Prodan³, C. Porosnicu², E. Vasile⁴, M. Prodan³, V. Nicolescu⁵, A. Mandes³, V. Dinca³

¹Academy of Romanian Scientists, ROMANIA, ²National Institute for Lasers, Plasma and Radiation Physics, ROMANIA, ³Ovidius University of Constanta, ROMANIA, ⁴University Politehnica of Bucharest, ROMANIA, ⁵CERONAV Constanta, ROMANIA

To improve the oxidation resistance properties of Carbon, Nitrogen doped Silicon-Carbon multilayer coatings on Carbon are deposited

using Thermionic Vacuum Arc (TVA) method. The initial carbon layer has been deposited on a silicon substrate in the absence of nitrogen, and then a 3nm Si thin film to cover carbon layer was deposited. Further, seven Si and C layers were alternatively deposited in the presence of nitrogen ions at substrate temperature between 200°C and 1000°C. In order to form silicon carbide at the interface between silicon and carbon layers, all carbon, silicon and nitrogen ions energy has increased up to 150eV using a negative bias voltage up to -1000V. The characterization of microstructure and electrical properties of as-prepared N-Si-C multilayer structures were done using Transmission Electron Microscopy (TEM, STEM) techniques, Thermal Desorption Spectroscopy (TDS) and electrical measurements. The retention of oxygen in the protective layer of N-Si-C is due to the following phenomena: The reaction between oxygen and silicon carbide resulting in silicon oxide and carbon dioxide; The reaction involving oxygen, nitrogen and silicon resulting silicon oxynitride with a variable composition; Nitrogen acts as a trapping barrier for oxygen. To perform electrical measurements, ohmic contacts were attached on the samples. Electrical conductivity was measured in constant current mode. To explain the temperature behavior of electrical conductivity we assumed a thermally activated electric transport mechanism.

5:38 PM - 5:39 PM

CHEX: A NEW BEAMLINE FOR HIGH ENERGY COHERENT X-RAY STUDIES DURING SYNTHESIS

M..J. Highland¹, R.p. Winarski², G.B. Stephenson¹

¹Materials Science Division, Argonne National Lab, IL, UNITED STATES OF AMERICA, ²Advanced Photon Source, Argonne National Laboratory, IL, UNITED STATES OF AMERICA

The upgrade of the Advanced Photon Source (APS-U) is a large-scale project to improve the properties of the APS such that it is ideally suited for high energy coherent x-ray studies. As part of the APS-U a number of new feature beamlines will be constructed, including the Coherent High Energy X-ray beamlines for in-situ science (CHEX). One of the principle scientific focuses of CHEX will be to perform coherent x-ray studies during synthesis. To that end CHEX will feature

a number of synthesis systems designed for OMVPE, rf-sputtering, molecular beam epitaxy, and bulk crystal growth. The beamline will also be equipped with general purpose x-ray scattering instruments and infrastructure capable of accommodating custom built synthesis and processing systems. This new beamline will enable a variety of real-time in-situ studies including observation of nucleation and growth, defect formation, and thin film relaxation in complex environments. I will describe the planned capabilities of the CHEX beamline, anticipated initial experiments, and the insight that in-situ coherent x-ray studies will be able to provide into various synthesis processes.

5:39 PM - 5:40 PM

A NEW METHODOLOGY FOR CRYSTAL PHASE IDENTIFICATION OF KIDNEY STONE THIN SECTION BY MICROSCOPIC FT-IR

K.P. Sawada¹, M. Maruyama¹, Y. Tanaka², R. Tajiri³, K. Momma⁴, Y. Furukawa⁵, R. Fujimoto¹, Y. Tsuru¹, R. Mori⁶, Y. Kamihira⁷, Y. Sugiura⁸, K. Taguchi², S. Hamamoto², R. Ando², T. Kato², R. Unno², T. Sugino², M. Isogai², K. Hasebe², J. Yamanaka⁹, T. Okuzono⁹, A. Toyotama⁹, H. Miura¹⁰, Y. Ohtomo¹¹, M. Nakamura¹², H.Y. Yoshikawa¹³, K. Tsukamoto⁵, A. Okada², M. Yoshimura⁷, T. Yasui², Y. Mori¹

¹Graduate School of Engineering, Osaka University, JAPAN, ²Nagoya City University Graduate School of Medical Sciences, JAPAN, ³Tajiri Thin-section Lab., JAPAN, ⁴National Museum of Nature and Science, JAPAN, ⁵Graduate School of Science, Tohoku University, JAPAN, ⁶Graduate School of Science, Osaka University, JAPAN, ⁷Institute of Laser Engineering, Osaka University, JAPAN, ⁸National Institute of Advanced Industrial Science and Technology, JAPAN, ⁹Graduate School of Pharmaceutical Sciences, Nagoya City University, JAPAN, ¹⁰Graduate School of Natural Sciences, Nagoya City University, JAPAN, ¹¹Graduate School of Engineering, Hokkaido University, JAPAN, ¹²Graduate School of Engineering, Nagoya Institute of Technology, JAPAN, ¹³Department of Chemistry, Saitama University, JAPAN

Recently, the prevalence of urolithiasis has been increasing up to 10 %. Endourology and shock wave lithotripsy are main remedies for it. They are invasive ways and further the recurrence rate in 5 years is more serious than 50 %. The elucidation of a kidney stone forming mechanism is essential to improve conventional remedy and prevention for urolithiasis. Main component of most kidney stones is calcium oxalate, and the crystalline phase are calcium oxalate monohydrate (COM) and calcium oxalate dihydrate (COD). Although COD is less stable than COM in physiological condition, nucleation of COD is easier at high supersaturation because COD is metastable. The past several studies^{1),2)} showed the importance of phase transformation from COD to COM; however, the phase identification and distribution of COM and COD in micrometer order is difficult because their overall spectra of IR and/or Raman are too similar to identify. Therefore, we established the identification method by focusing on the peak at 780 cm^{-1} where the influence of other crystalline components is relatively small. We synthesized pure COM and COD inorganically by the method of past study³⁾, then mixed them at various ratios. We obtained IR spectra of each mixed sample, then calculated the expected COM/COD ratio depending on patent JP3524968B⁴⁾. We compared the actual COM/COD ratios with the calculated ratios, then refined the method by least-squares method. After that, we obtained several kidney stone sections by the resin embedding method and succeeded in making samples capable of observing the structure without impairing the intrinsic information of the stones as much as possible. The samples enabled us to obtain fine IR spectra at a resolution of approximately $20\text{ }\mu\text{m}$ by reflection method of microscopic FT-IR. We identified COM/COD ratio by the refined method of patent JP3524968B⁴⁾ using the obtained IR spectra. By the combination with various optical microscopy observations, we could identify crystal phases in micrometer order with maintaining the spatial information. In our presentation, we discuss the formation mechanism of calcium oxalate stone by phase identification, tissue observation, and analysis using the above method. 1) V. Castiglione et al., PLOS ONE, **13**(2018) e0201460. 2) Bazin et al., C. R. Chimie, **19**(2016) 1492e1503. 3) L. Lepage et al., Journal of Pharmaceutical

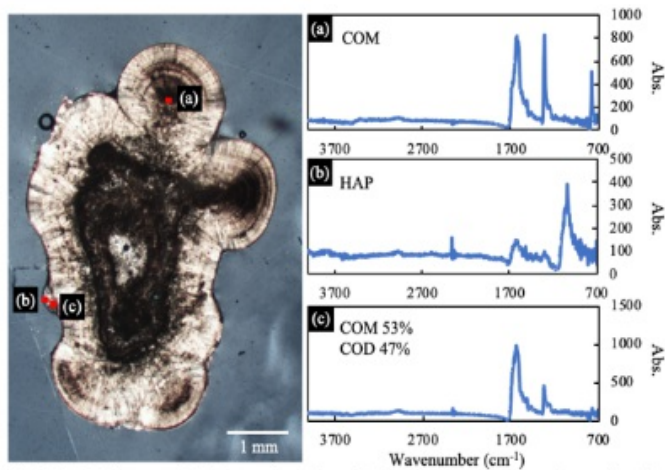


Fig.1 Optical image of a thin section (Sample No.3900) and IR spectrum of each measurement point indicated in the image (point (a) ~ (c)). We obtained spectra like (a) in most places, but locally obtained spectra like (b) and (c).

5:40 PM - 5:41 PM

IN SITU COHERENT X-RAY STUDIES OF SURFACE DYNAMICS DURING OMVPE OF GAN

C. Thompson¹, G. Ju², D. Xu³, M..J. Highland⁴, J.A. Eastman⁴, P. Zapol⁴, G.B. Stephenson⁵

¹Department of Physics, Northern Illinois University, IL, UNITED STATES OF AMERICA, ²Arizona State University, AZ, UNITED STATES OF AMERICA, ³Huazhong University of Science and Technology, CHINA, ⁴Argonne National Laboratory, IL, UNITED STATES OF AMERICA, ⁵Argonne National Lab, IL, UNITED STATES OF AMERICA

We have been exploring the use of X-ray photon correlation spectroscopy to observe the atomic-scale dynamics of surface morphology in situ during OMVPE growth of GaN. These studies were carried out at a relatively high X-ray energy (~26 keV) to penetrate the OMVPE environment and chamber and minimize X-ray disturbance of the OMVPE process. Because the surface features scatter weakly and the coherent X-ray flux decreases strongly at higher energy, we developed methods to use the full 'pink beam' bandwidth of the undulator harmonic to study surface features. In this presentation we

will summarize the results of several studies. Using two-time correlations, we observed persistent island arrangements during layer-by-layer growth on the m-plane surface [1]. We also used XPCS to reveal the dynamics during steady-state step-flow growth on the c-plane surface, and observed growth producing 'crenulate' steps on m-plane hillock facets tilted towards $[1 -2 1 0]$. These results will be compared with Kinetic Monte Carlo simulations of growth on c- and m-plane GaN [2]. [1] G. Ju, D. Xu, M. J. Highland, Carol Thompson, H. Zhou, J. A. Eastman, P. H. Fuoss, P. Zapol, H. Kim, and G. B. Stephenson, to appear in Nature Physics (2019). [2] D. Xu, P. Zapol, G. B. Stephenson, and Carol Thompson, Journal of Chemical Physics 146, 144702 (2017).

5:41 PM - 5:42 PM

CRYSTAL GROWTH AND LUMINESCENCE STUDIES ON $\text{Li}_2\text{Mg}_2(\text{MOO}_4)_3$ CRYSTAL GROWN BY CZOCHRALSKI METHOD

J.D. D¹, H..J. Kim¹, I.R. Pandey¹, M. Tyagi²

¹Kyungpook National University, KOREA, REPUBLIC OF, ²Technical Physics Division, Bhabha Atomic Research Centre, Trombay, Mumbai 400085, India, INDIA

There is a long history of using molybdates family materials for different practical applications, such as; solid state lighting, acoustic-optical elements, and laser host materials [1-3]. For the past few decades, number of new facilities have been built worldwide to develop large inorganic scintillating crystals of molybdates in search for $0\nu\beta\beta$ decay [4]. There are different Molybdate content compounds with a general formula XMoO_4 ($\text{X} = \text{Li}, \text{Ca}, \text{Cd}, \text{Zn}, \text{Pb}, \text{Sr}, \text{Mg}$) and double molybdate of $\text{Li}_2\text{Zn}_2(\text{MoO}_4)_3$ have been developed for the $0\nu\beta\beta$ decay search experiments. In this present study, $\text{Li}_2\text{Mg}_2(\text{MoO}_4)_3$ crystal has been grown by Czochralski method. The polycrystalline compound have been synthesised using standard solid-state reaction method. The phase purity of the synthesised compound have been analysed through powder X-ray diffraction method. Single crystal growth was carried out using Czochralski chamber with air atmosphere and the pulling rate was maintained nearly 6 mm/h with a rotation rate of 4–6 rpm. The grown crystal sample exhibits an intrinsic

emission band in the wavelength range from 320 to 600 nm with a peak center at 400 nm. As shown in Fig.1, with decreasing temperature, a significant increase in emission intensity is observed as well as the blue shift in the peak position. The temperature dependent luminescence spectra were studied in the temperature range of 10 – 300 K. Low temperature thermoluminescence glow curve recorded to study the trap centers in the temperature range of 10 -300 K. The foregoing results suggest that $\text{Li}_2\text{Mg}_2(\text{MoO}_4)_3$ crystal can be used for luminescence applications.

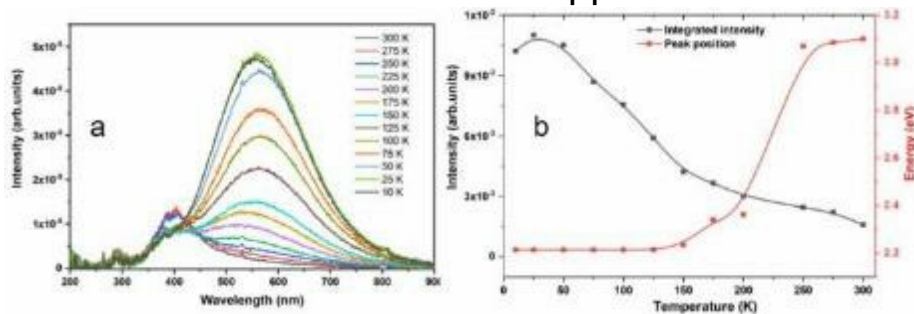


Fig.1 a) Temperature dependent emission spectra b) Temperature dependent Integrated intensity and peak position Reference: A. Khanna and P. S. Dutta, "Narrow spectral emission CaMoO_4 : Eu^{3+} , Dy^{3+} , Tb^{3+} phosphor crystals for white light emitting diodes," *J. Solid State Chem.* **198**, 93 (2013). A. S. Shcherbakov, A. O. Arellanes, and S. A. Nemov, "Transmission function of collinear acousto-optical interaction occurred by acoustic waves of finite amplitude," *Opt. Eng.* **52**, 064001 (2013). H. Yu *et al.*, "A continuous wave SrMoO_4 Raman laser.," *Opt. Lett.* **36**, 579 (2011). F. A. Danevich, "Development of Crystal Scintillators From Enriched Isotopes for Double β Decay Experiments," *IEEE Trans. Nucl. Sci.* **59**, 2207 (2012).

5:42 PM - 5:43 PM

REVEALING THE ROLE OF CALCIUM CODOPING ON OPTICAL AND SCINTILLATION HOMOGENEITY IN Lu_2SiO_5 :Ce SINGLE CRYSTALS

Y. Wu¹, M. Koschan¹, Q. Li², I. Greeley¹, C.L. Melcher¹

¹University of Tennessee, TN, UNITED STATES OF AMERICA, ²IBM Thomas J Watson Research Center, UNITED STATES OF AMERICA
The presence of impurities and dopants (or codopants) can influence

solute transport at the solid-liquid interface and its stability during bulk crystal growth, which ultimately affect the crystal uniformity. Codoping with Ca^{2+} can significantly improve the performance of $\text{Lu}_2\text{SiO}_5:\text{Ce}$ single crystals, well-known scintillators for nuclear medical imaging, albeit at the expense of growth stability due to surface tension reduction. However, an understanding of the correlation between crystal growth properties and radial performance uniformity in Czochralski-grown $\text{LSO}:\text{Ce},\text{Ca}$ single crystals is still lacking. In this work, we reveal this essential correlation by studying the roles of Ca^{2+} concentration on the radial distribution of stable Ce^{3+} ions and oxygen vacancy (V_{O}) related defects as well as solute transport at the solid-liquid interface. Through mapping of optical and scintillation properties across cross-sections of 0.1 at% and 0.4 at% Ca codoped boules and the defect formation energies derived from density functional theory (DFT) calculations, a direct link between Ca^{2+} ions, stable Ce^{3+} or Ce^{4+} ions, and $\{\text{Ca}_{\text{Lu}}+V_{\text{O}}\}$ complex defects is established. The light yield enhancement in Ca^{2+} codoped $\text{LSO}:\text{Ce}$ single crystals is attributed to the dissociation of spatially correlated Ce ions and oxygen vacancies. Based on the quantitative comparison of photoluminescence (PL) and radioluminescence (RL) emissions from Ce1 (seven-coordinated) and Ce2 (six-coordinated) sites, the preferential occupation of stable Ce^{4+} is believed to depend on the concentration of stable Ce^{4+} . The underlying causes of symmetry and variation in the radial distribution of optical and scintillation properties, as consequences of Ca^{2+} distribution, are discussed from the perspective of crystal growth.

5:43 PM - 5:44 PM

LUMINESCENCE PROPERTIES OF AG DOPED LIF CRYSTAL GROWN BY CZOCHRALSKI METHOD

I.R. Pandey¹, J.D. D¹, M. Tyagi², H.j. Kim¹

¹Kyungpook National University, KOREA, REPUBLIC OF, ²Technical Physics Division, Bhabha Atomic Research Centre, Trombay, Mumbai 400085, India, INDIA

Lithium fluoride is a good radiation sensitive material and has been

widely used in radiation dosimetry, optoelectronics and integrated optics [1,2] application. Since the development of thermoluminescence technique (TL), phosphor of LiF has attracted much attention and lithium fluoride doped with Mg and Ti (TLD-100) is used as dosimetry application [3]. Many reports can be found on phosphorus of this material as a storage material [4] but luminescence properties of bulk single crystal for this material has been poorly studied. If the crystal has a high light yield at low temperature, this could be also used for dark matter search experiment. LiF crystal is also an alternate material for neutron detection and used along with other material like LiF(ZnS) [5]. Bulk crystal of LiF can also be directly used for neutron imaging by optically stimulating luminescence centers of crystal [6]. In this study, luminescence properties of a single crystal of LiF (0.2 mol% of Ag) grown using the Czochralski technique has been studied at various temperature (10 to 550 K). Fig.1 shows the photograph of as grown and cut and polished crystals of LiF crystal. X-ray induced emission spectra reveals the peak at 414 nm. Absorption spectra of pure and Ag doped LiF crystal was carried out and studied the band gap of the crystal which is found to be 4.5 eV. Temperature dependent emission spectra have been measured under 280 nm LED excitation source at 10 -300 K. Decay time of the crystal varies from $\sim 26 \mu\text{s}$ (300 K) to $\sim 31 \mu\text{s}$ (75 K). Low temperature trap centers were analysed through thermoluminescence glow curves. From the high temperature TL glow curve measurement three-glow peaks were observed at 383, 416, and 461 K respectively. The activation energy of the main TL peak was calculated around 1.13 eV.

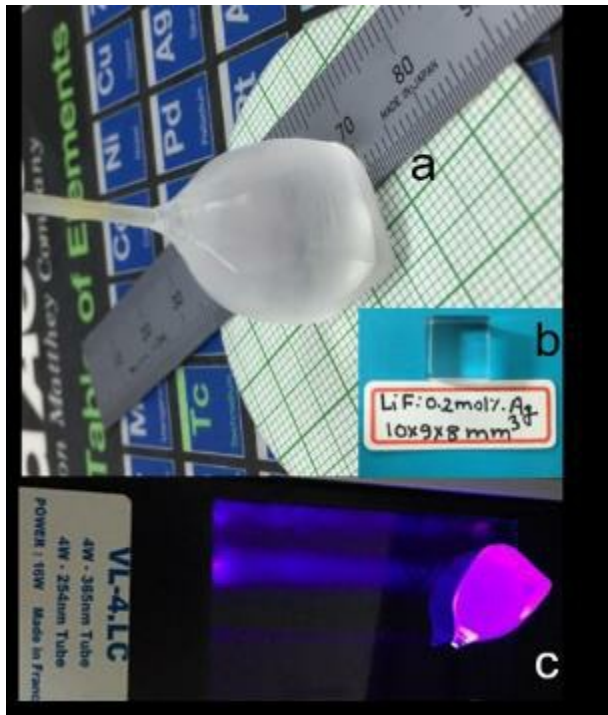


Fig.1 a) Photograph of as grown crystal b) cut and polished crystal c) under UV excitation Reference: A. T. Davison et al., *J Appl. Phys.* **86**, 1410 (1999). R. M. Montoreali et al., *Appl. Phys. Lett.* **78**, 4082 (2001). Harshaw Chemical Co. USA., (n.d.). K. Meijvogel et al., *Radiat. Meas.* **24**, 411 (1995) C.W.E. Van Eijk, A. Bessiere, P. Dorenbos, *Nucl. Inst. Methods Phys. Res. A* **529**, 260 (2004). M. Matsubayashi et al., *Nucl. Inst. Methods Phys. Res. A* **622**, 637 (2010).

5:44 PM - 5:45 PM

DIRECTIONAL GROWTH, PHYSICO-CHEMICAL AND QUANTUM CHEMICAL INVESTIGATIONS ON 2-AMINO-5-NITROPYRIDINIUM DIHYDROGEN PHOSPHATE (2A5NPDP) SINGLE CRYSTAL FOR NONLINEAR OPTICAL (NLO) APPLICATIONS

S. V, M. V, M. Senthil Pandian, P. Ramasamy

SSN College of Engineering, INDIA

Semi-organic nonlinear optical 2-amino-5-nitropyridinium dihydrogen phosphate (2A5NPDP) single crystal has been grown by the modified Sankaranarayanan-Ramasamy (SR) method. The major difficulties for the growth of 2A5NPDP single crystal have been resolved with the aid of temperature lowering method. After optimizing the growth conditions, transparent 2A5NPDP single crystal was harvested with

the size of 80 mm length and 15 mm diameter over a period of 60 days. The growth rate of the modified SR method grown crystal was found to be 10 times higher than the conventional slow evaporation solution technique (SEST) grown crystal. The unit cell parameters of the grown crystal were ascertained by the single crystal X-ray diffraction (SXRD) analysis. The degree of crystallinity of the grown crystal was analyzed by the powder X-ray diffraction (PXRD) analysis. The presence of multifarious functional groups of the 2A5NPDP crystal were confirmed by Fourier transform infrared (FT-IR) and Fourier transform Raman (FT-Raman) spectral analyses. The thermal property was assessed by the thermogravimetric and differential thermal analysis (TG-DTA). It shows that the grown crystal withstands upto 175°C. The crystalline perfection of the 2A5NPDP crystal was carried out using high-resolution X-ray diffraction (HRXRD) analysis. It confirms that the modified SR method grown crystal possesses higher crystalline perfection which can be used for practical device applications. Comparative analysis between the conventional and the modified SR method grown crystals was made using UV-Vis NIR, third-order nonlinearity (Z-Scan) and optical limiting (OL) studies. It reveals a significant enhancement in the properties of the crystal grown by the modified SR method. The optical limiting threshold of conventional method grown crystal is 5.7 mW/cm², whereas the modified SR method grown crystal is 4.7 mW/cm². Low value of limiting threshold indicates that the grown crystal has minimum defects. The theoretical calculations were performed by B3LYP/6-311++G (d,p) basis set. The charge transfer characteristic of 2A5NPDP compound was studied by frontier molecular orbital (FMOs) analysis. The first-order hyperpolarizability of the present molecule was calculated and it was found to be 3.788×10^{-29} e.s.u, which is 108 times higher than the standard urea molecule (3.50×10^{-31} e.s.u). The hydrogen bonding of the title molecule was confirmed by Natural Bond Orbital (NBO) analysis. The obtained experimental and theoretical results lead to conclude that the grown 2A5NPDP crystal is a promising candidate for nonlinear optical (NLO) and optoelectronic device applications.



Figure 1. 2A5NPDP single crystal grown by the modified SR method

5:45 PM - 5:46 PM

SYNTHESIS, GROWTH, OPTICAL TRANSMITTANCE, LASER DAMAGE THRESHOLD, Z-SCAN AND OPTICAL LIMITING STUDIES OF 2 -AMINO- 4,6- DIMETHOXPYRIMIDINIUM HYDROGEN (2R, 3R)-TARTRATE 2-AMINO-4,6- DIMETHOXPYRIMIDINE SINGLE CRYSTAL

R.M. Jauhar¹, P. Era², G. Vinitha¹, P. Murugakoothan²

¹VIT University, INDIA, ²Pachaiyappas College, INDIA

An organic nonlinear optical (NLO) crystal, 2 -amino- 4,6- dimethoxypyrimidinium hydrogen (2R, 3R)-tartrate 2-amino-4,6- dimethoxypyrimidine was synthesized and grown by slow evaporation technique. The crystals obtained from the slow evaporation technique were further grown adopting temperature lowering technique. The formation of the crystalline compound was confirmed by single crystal X-ray diffraction study. The title compound crystallizes in the monoclinic crystal system with space group, $P2_1$. Optical transmittance study showed that the grown crystal is transparent in the entire visible region with the lower cut-off wavelength of 228 nm. The laser induced surface damage threshold of the grown crystal was measured to be 1.9 GW/cm^2 for 1064 nm Nd:YAG laser radiation. The Z-scan method was carried out to determine the nonlinear refractive index and nonlinear absorption coefficient. Optical limiting study of the title crystal was found to saturate with the threshold of 35 mW/cm^2 and amplitude of 1.8 mW/cm^2 .

5:46 PM - 5:47 PM

SELECTIVE SAPPHIRE DISSOLUTION TECHNIQUE WITHOUT DISSOLVING GALLIUM NITRIDE IN A SODIUM FLUX ADDED LITHIUM

T. Yamada¹, M. Imanishi¹, K. Murakami¹, K. Nakamura¹, M. Yoshimura², Y. Mori¹

¹Osaka university, JAPAN, ²Institute of Laser Engineering, Osaka University, JAPAN

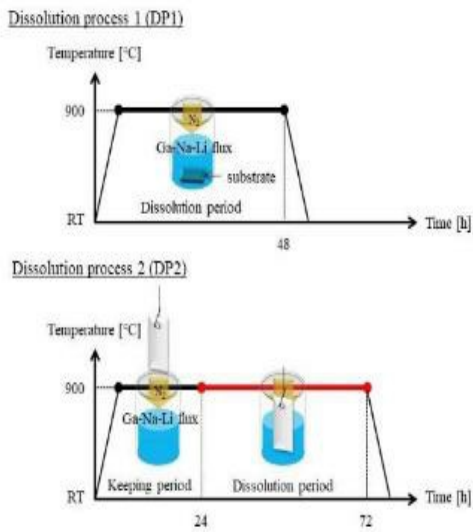


Fig.1 Schematic drawing of experimental process

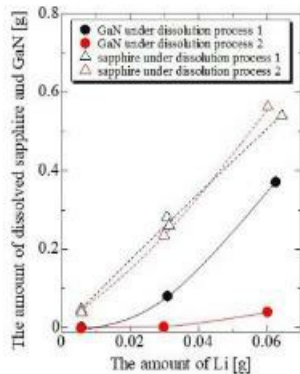


Fig.2 The amount of dissolved sapphire and GaN substrates as a function of the amount of Li in the flux in dissolution processes 1 and 2.

Large-diameter GaN substrates are indispensable for the realization of

low-cost GaN-based electronic devices. In a previous study, we succeeded in fabricating 1-in. GaN substrate using sapphire dissolution technique after GaN crystals were grown on c-GaN templates (GaN on sapphire) by the Na-flux method [1]. This technique is useful for avoiding stress due to the differences of thermal expansion coefficient between GaN and sapphire. In this method, Li reacts with Al_2O_3 and dissolves sapphire substrate in a Ga-Na-C-Li flux. However, Li is also liable to dissolve GaN, because Li changes GaN solubility in the flux [2]. [MI1] Therefore, in this study, we investigated sapphire and GaN solubility in the flux and found out the way to dissolve sapphire selectively without dissolving GaN. Two dissolution processes were performed as shown in Fig. 1. In the dissolution process 1 (DP1), sapphire and GaN substrates were set at the bottom of a crucible with a Ga-Na-Li-C flux, and these substrates were dissolved in the flux at 900°C under a pressure of 4 MPa of N_2 for 48h. In the dissolution process 2 (DP2), these substrates were kept above the flux and nitrogen was dissolved into the flux for 24h. After that, these substrates were dipped into the flux and were dissolved under the same condition as DP1. The ratio of the Li content to the total Ga+Na+C content was 0, 2.5 and 5.0 mol%. Figure 2 shows the amount of dissolved sapphire and GaN substrates as a function of the amount of Li in the flux in each dissolution process. In DP1, the amount of dissolved these substrates increased with the amount of Li. On the other hand, in DP2, the amount of dissolved sapphire increased with the amount of Li as well as in DP1. In contrast, the amount of dissolved GaN didn't drastically increase with the amount of Li in comparison with DP1. This means that a reaction between sapphire and Li doesn't depend on the amount of nitrogen dissolved in a solution, but a reaction between GaN and Li depends on that. In DP2, little GaN was dissolved because enough nitrogen not to dissolve GaN was dissolved in the solution. To increase the amount of nitrogen in the flux enable to suppress dissolution of GaN and to dissolve sapphire substrate selectively. [1] T. Yamada *et al.*, IWN2018 GR4-6. [2] M. Morishita *et al.*, J. Cryst. Growth **284** (2005).

5:47 PM - 5:48 PM

HIGH-RATE GROWTH OF A THICK FREESTANDING GAN

CRYSTAL WITH CH₄ BY OVPE

M. Kamiyama¹, Y. Gunji², H. Kobayashi¹, T. Oshiba¹, A. Kitamoto¹, M. Imanishi³, M. Yoshimura⁴, M. Isemura⁵, T. Sumi⁶, J. Takino⁶, Y. Okayama⁶, Y. Mori³

¹Osaka university, JAPAN, ²Osaka University, JAPAN, ³Graduate School of Engineering, Osaka University, JAPAN, ⁴Institute of Laser Engineering, Osaka University, JAPAN, ⁵Itochu Plastics Inc, JAPAN, ⁶Panasonic corporation, JAPAN

We have been developing a method using Ga₂O vapor for the growth of GaN crystals (Oxide Vapor Phase Epitaxy: OVPE). The advantages of this method are that it is HCl-free and produces no solid by-product, allowing for long-term growth of large-sized GaN crystals [1].

However, thick OVPE-GaN layers over 50- μm at high-rate growth over 100 $\mu\text{m}/\text{h}$ have not been obtained due to the formation of polycrystalline GaN crystals. In our previous study, it was confirmed that H₂O vapor which originated from by-product of Ga₂O and GaN formation reactions led to the increasing of polycrystal density [2].

Thus, to decrease H₂O partial pressure, CH₄ gas was introduced into the reactor by the reaction of CH₄ with H₂O to produce CO and H₂. As a result, a 400- μm thick GaN layer was obtained at a growth rate of 40 $\mu\text{m}/\text{h}$ with CH₄ by decreasing polycrystal density [3]. In this study, we attempted to fabricate a thick freestanding GaN crystal with CH₄ at high-rate growth. However, the H₂O partial pressure at high-rate growth is higher than that at low-rate growth because the H₂O partial pressure increases with the Ga₂O partial pressure. For this reason, we investigated dependence of polycrystal density on flow rate of CH₄ gas at high-rate growth. Next, at CH₄ flow rate optimized, we investigated dependence of polycrystal density on growth rate. We used a +c-plane freestanding GaN fabricated by HVPE as seed substrates. During the growth periods, CH₄ gas was introduced into the reactor at flow rate of 0 to 600 sccm. In growth period of 1 h at a growth rate of 70 $\mu\text{m}/\text{h}$, polycrystal densities decreased with the increase in CH₄ flow rate. Further, polycrystal densities in growth period of 1 h at a growth rate of 70 to 100 $\mu\text{m}/\text{h}$ decreased at a CH₄

flow rate of 400 sccm compared to those without CH₄ gas. We fabricated a 421- μm thick GaN layer at a growth rate of 70 $\mu\text{m}/\text{h}$ and a CH₄ flow rate of 400 sccm. Full width at half maximum of GaN (0002) and (10-12) X-ray rocking curve of this as-grown layer were almost the same as those of the seed substrate. Finally, the front and back surface was polished to fabricate a freestanding OVPE-GaN crystal with 297- μm -thickness. In this presentation, we will report the details on structural properties and discuss effects of CH₄ additive at high-rate growth in OVPE method.

[Reference]

- [1] M. Imade *et al.*, *J. Cryst. Growth* **312**, 676 (2010).
- [2] Y. Yamaguchi *et al.*, *Jpn. J. Appl. Phys.* **55**, 05FB04 (2016).
- [3] A. Kitamoto *et al.*, *Jpn. J. Appl. Phys.*, *in press*.

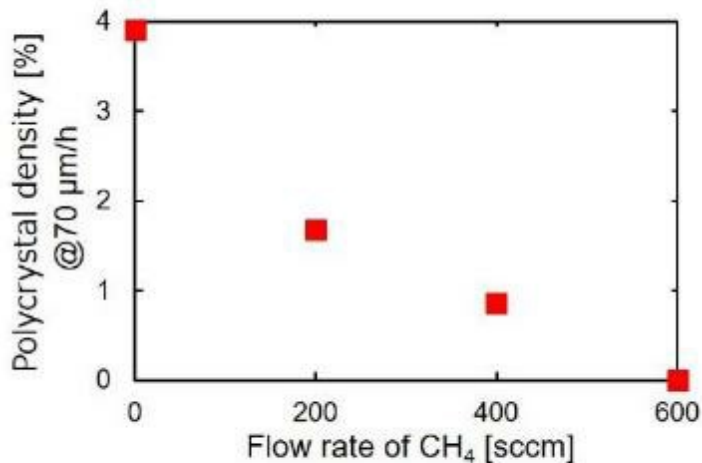


Fig. 1. Dependency of Polycrystal density on Flow rate of CH₄

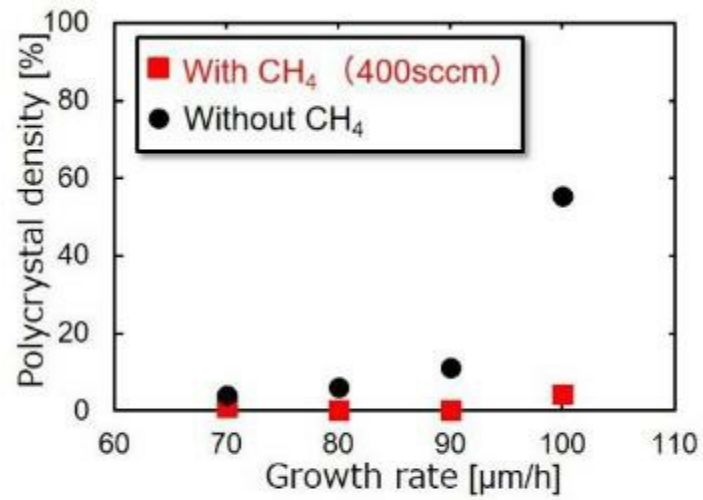


Fig. 2. Dependency of Polycrystal density on Growth rate

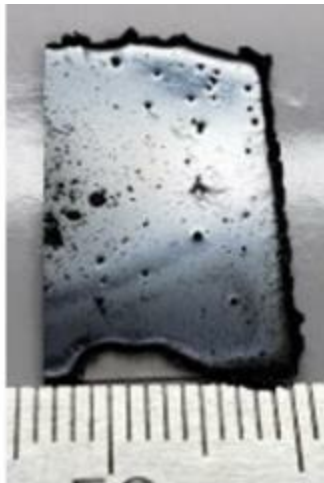


Fig. 3. 421- μm thick GaN layer grown by OVPE



Fig. 4. Freestanding 297- μm thick GaN crystal fabricated by OVPE

5:48 PM - 5:49 PM

THE EFFECT OF IMPURITIES ON THE TRANSPARENCY OF GAN CRYSTALS GROWN BY NA FLUX

M. Abo Alreesh¹, P. Von Dollen¹, T. Malkowski¹, T. Mates¹, H. Albrithen², S. Denbaars¹, S. Nakamura¹, J. Speck¹

¹, UNITED STATES OF AMERICA, ², SAUDI ARABIA

We investigated several impurities in bulk GaN crystals grown by the sodium flux technique. In our system, black GaN is in general associated with oxygen, sodium, and molybdenum concentrations in excess of 10^{19} atoms/cm³. We report on the correlation of high levels of oxygen with opaque crystals. Samples that contain oxygen concentrations above 10^{19} atoms/cm³ are highly absorbing regardless of the presence of other impurities. Experiments with partially submerged seeds indicated material grown mainly above the nominal liquid surface was more transparent and had a generally lower impurity concentration, especially oxygen. In optically transparent regions, concentrations of oxygen, sodium, and carbon were as low as 7×10^{16} , 2×10^{16} , and 5×10^{16} atoms/cm³, respectively, while the concentration of molybdenum was below the detection limit.

5:49 PM - 5:50 PM

EFFECT OF TEMPERATURE GRADIENT ON ALN CRYSTAL

GROWTH BY PVT METHOD

L. Zhang¹, G. Wang¹, Y. Shao¹, C. Chen², Y. Wu¹, X. Hao¹

¹State Key Lab of Crystal Materials, Shandong University, CHINA,

²Energy Research Institute, Qilu University of Technology (Shandong Academy of Sciences), CHINA

Aluminum nitride (AlN) has excellent properties such as ultra-wide direct bandgap (6.2 eV), high breakdown electric field, high thermal conductivity, good UV transmittance and strong radiation resistance. It has great application prospects in fields such as high-efficiency optoelectronic devices and high-power high-frequency electronic devices. In this study, physical vapor transport (PVT) method was used to grow AlN crystal. The effects of different temperature field distributions on the growth of spontaneous nucleation AlN crystal was investigated through simulation and experiment. It was found that the axial temperature gradient was the main factor affecting the growth rate of AlN crystal, and the radial temperature gradient was the driving force for expanding the diameter of AlN crystal. High-quality 5×5 mm AlN single crystal was successfully grown by optimizing the temperature field distribution.

5:50 PM - 5:51 PM

GROWTH OF GAN CRYSTALS BY SUBLIMATION METHOD

Y. Song, K. Zhu

Institute of Physics, Chinese Academy of Sciences, CHINA

GaN crystals on graphite and SiC substrates, respectively, with GaN powder as evaporation source were prepared by sublimation method.

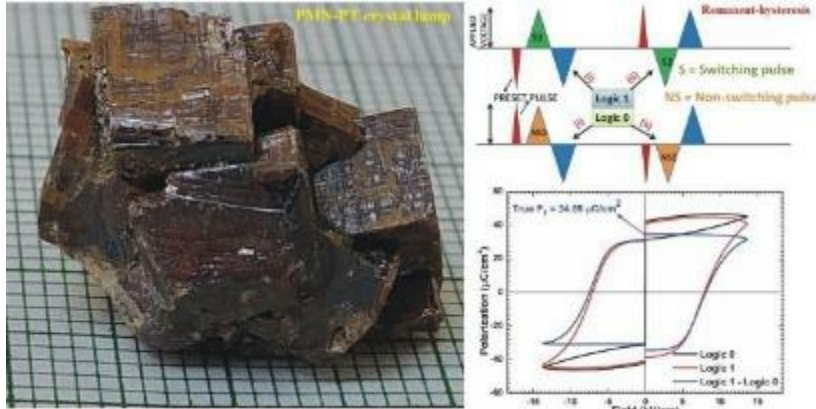
The influence of growth conditions involving the pressures, the temperatures of substrates, the temperature gradient between evaporation source and substrates on the growth of GaN was investigated, appropriate growth conditions were found. GaN single crystals with the morphology of platelet were obtained on graphite substrates, and the maximum sizes of the crystals reached 6×1×0.2mm³ and 2×2×0.2 mm³; on SiC substrate, GaN epitaxy layer with a thickness of 600μm was grown. The quality of these crystals was checked by the rocking curve, PL spectra, Raman spectra etc.

5:51 PM - 5:52 PM

FLUX GROWTH OF $0.64\text{Pb}(\text{Mg}_{1/3}\text{Nb}_{2/3})\text{O}_3\text{-}0.36\text{PbTiO}_3$ SINGLE CRYSTALS: TRUE-REMANENT AND RESISTIVE-LEAKAGE INVESTIGATION

A.J. Joseph, B. Kumar

Department of Physics & Astrophysics, University of Delhi, INDIA



Ferroelectric single crystals of $0.64\text{Pb}(\text{Mg}_{1/3}\text{Nb}_{2/3})\text{O}_3\text{-}0.36\text{PbTiO}_3$ (PMN-PT) has been successfully grown in the vicinity of morphotropic phase boundary, using high temperature solution method with $\text{PbO/B}_2\text{O}_3$ as flux. The crystals were characterized for its dielectric, ferroelectric, piezoelectric and pyroelectric properties along with the investigation of its domain structure. The FESEM analysis revealed the step-like growth pattern visible on the surface of the as grown crystal. A high Curie temperature ($T_c = 190^\circ\text{C}$) was observed in the dielectric study. Well-saturated ferroelectric hysteresis loops with high remanent polarization, good switching and fatigue resistant nature indicated the high ferroelectric quality of the crystals. A high value of piezoelectric coefficient ($d_{33}^* = 1398 \text{ pm/V}$) was obtained from the butterfly loops. True-remnant hysteresis study was used to isolate the practically usable/switchable polarization value, which actually serves as memory component in devices. Time-dependent compensated hysteresis analysis was done to examine the frequency dependent components of polarization present in the PMN-PT crystal which provides information about the resistive-leakage nature of the grown crystals. Weibull statistics was used to analyze the distribution of hardness number and to find the values of critical load for the flux grown PMN-PT crystals which helps to critically analyze materials

suitability for device fabrication.

5:52 PM - 5:53 PM

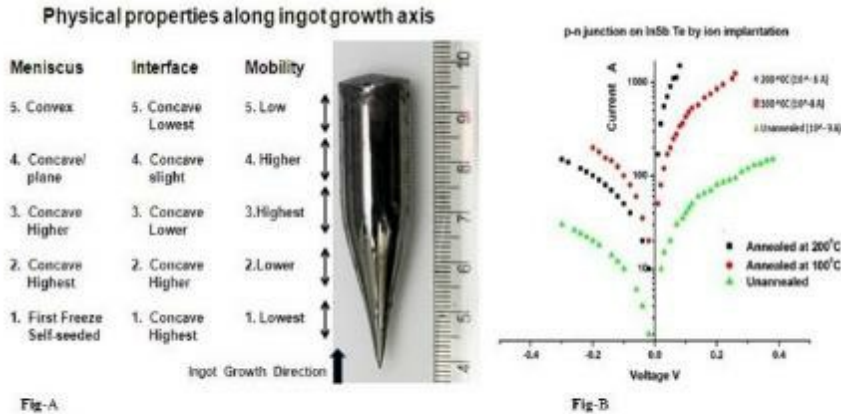
DEVICE GRADE AND THE ULTRA HIGH-QUALITY SB-BASED CRYSTAL GROWTH: THE NOVEL CONCEPT OF THE VERTICAL DIRECTIONAL SOLIDIFICATION (VDS) BY SLOW FREEZING

D. Gadkari

Freelance Research and Consultant, Crystal Growth and Technology,,
INDIA

In this paper, experimental results on detached growth of Sb-based single crystals in VDS with industrially relevant diameter and geometry are presented [1]. Sb-based high grade crystals have necessity in tiny solid-state lasers, flat-panel displays. Also, it is hard-to-predict the spin-offs will produce new categories of the electronic products, and the image courtesy hardware-Multilayer Switch Feature Card (MSFC). The crystals with unprecedented elevation of structural perfection is achieved by the reduced buoyant thermo-gravitational convection in a melt [2]. The entire detached solidification of Sb-based crystals were experimentally grown on Earth by VDS [3, 4], its properties showed highest than the crystal grown ever [5,6]. The Hall mobility along crystal axis and its statistical analysis is used to predict a model for mobility relation with the meniscus and interface along the crystal growth axis in Fig-A [9]. The *p-n* junction, Schottky diode and MOS structures fabrication on Sb-based VDS-substrates showed lower leakage (dark) current $<0.1\text{nA}$ at 300K [7,8]. The I-V characteristics of *p-n* diode by Ion implantation at 300K, Fig-B [7]. *Forward bias*: Semi-log I-V curves for the ion implanted Te for the p-type InSb:Te, (current- μA , voltage-V) is shown in Fig-B. I-V curves reveal ideality factors (η) for i) as deposited, ii) annealed at 373K, and iii) at 473K for 10 minutes are 1.11, 1.21, 1.27 respectively. A *p-n* diode shows corresponding increase in the rectification with decrease in a barrier height (BH). The ideality factor η increases with temperature. *Reverse bias*: The leakage current or dark currents is measured for *p-n* diode at 0.3V; the samples annealed at 473K have a maximum increase in leakage current. On annealing both bias showed the thermal defects generated into high-quality VDS-substrates. For reverse bias, as deposited samples showed very low reverse current (dark or leakage)

for smooth, constant breakdown reverse voltage greater than $V_r = -4V$. While, the depletion layer formation shows the presence of high series and low shunt resistance with no defects. Reversed dark current $I_r = 25nA$ at $-0.4V$ is lowest in comparison to InSb traditional diode at the ambient temperature (300K). Defect components have entered into junctions on annealing by increasing g-r, and SRH process. A $p-n$ diode process will be discussed.



Figures- A- The Hall mobility along the axis of detached crystal [9], B- the p-n Junction diode fabricated on the p-type VDS- substrate [7].
References: [1] J Cry Growth 173 (1997) 585, [2] Mater Chem-Phys 139 (2013) 375, [3] Int J Energy Res Sci Engg Tech 5(2) (2016) 2092, [4] Journal of Materials Science and Engineering A 3 (5) (2013) 338, [5] J. Chem. Chem. Eng. 6 (2012) 65, [6] J. Chem. Chem. Eng. 6 (2012) 250, [7] J Electr Commun Eng IOSR-JECE 12 (2017) 51, [8] J Electr Commun Eng IOSR-JECE 13 (2018) 51, [9] Intern J Sci Res Public. 4(5)(2014) 2250

5:53 PM - 5:54 PM

SEARCHING FOR IDEAL TOPOLOGICAL CRYSTALLINE INSULATORS AND TOPOLOGICAL SUPERCONDUCTORS IN Pb-Sn-IN-TE SYSTEM

G. Gu

Brookhaven National Laboratory, NY, UNITED STATES OF AMERICA

The discovery of 3D topological insulator materials and topological superconductor open up a new research field in the condensed matter physics. In order to search for the topological superconductor, we have grown a large number of the single crystals of Pb-system (Pb-Sn-In-Te) topological crystalline insulator and their topological superconductor. We have measured the physical properties on these single crystals by various techniques. We have studied the effect of crystal growth condition, impurity and composition on the bulk electrical conductivity of these single crystals. We try to find out which composition and crystal growth condition is the best for the ideal

topological insulator, topological crystalline insulator and topological superconductor. We have got the bulk topological superconductor with $T_c=5K$.

5:54 PM - 5:55 PM

CRYSTAL GROWTH, MICROSTRUCTURE, AND PHYSICAL PROPERTIES OF SR(MN_{1-X}ZN_X)SB₂

Y. Liu¹, T. Ma², L. Zhou², D. Vaknin², R. McQueeney²

¹Dongguan Neutron Science Center, CHINA, ²Ames Laboratory, UNITED STATES OF AMERICA

Single crystals of Sr(Mn_{1-x}Zn_x)Sb₂ (0≤x≤1) were grown by the self-flux method. Magnetic susceptibility measurements reveal an antiferromagnetic (AFM) transition at $T_N = 295$ K for SrMnSb₂. With increasing Zn doping level, the AFM transition temperature is suppressed and vanishes at x=0.6. However, de Haas–van Alphen (dHvA) effect is observed from the sample x=0 to the highest doping x=1. By extracting the oscillatory component, the effect of Zn doping on the quantum oscillations is investigated. Interestingly, transmission electron microscopy (TEM) reveals the existence of stacking faults in the crystals, which result from a horizontal shift of Sb atomic layers suggesting possible ordering of Sb vacancies in the crystals. The role of Sb vacancies will be discussed.

5:55 PM - 5:56 PM

CRYSTAL GROWTH, STRUCTURAL, OPTICAL AND THERMAL PROPERTIES OF TRIPHENYLAMINE (TPA) SINGLE CRYSTAL GROWN BY BRIDGMAN

K. Ramachandran, A. Raja, M. Senthil Pandian, R. P

SSN College of Engineering, INDIA

Optically transparent Triphenylamine (TPA) single crystal has been grown by Bridgman-Stockbarger method with optimized temperature gradient. The grown organic TPA single crystal belongs to monoclinic crystal system with non-centrosymmetric space group of Cc, which is obtained from the single crystal X-ray diffraction (SXRd) study. The powder X-ray diffraction (PXRD) pattern of title crystal revealed good crystalline nature and the diffraction peaks (2θ) values exactly

matched with the standard CIF File. The chemical bonding structure of TPA crystal has been obtained from the Fourier transform infrared (FTIR) spectral study. The optical transmittance spectrum of the grown organic single crystal was obtained from the UV-Visible NIR spectrum analysis and the high optical transmittance observed in the UV-visible to near infrared (IR) region. Thermal stability and melting point of the TPA single crystal were identified by using thermogravimetric / differential thermal (TG-DTA) analysis. The intermolecular interactions of title crystal were investigated by Hirshfeld surface (HS) and two dimensional (2D) fingerprint analyses.

5:56 PM - 5:57 PM

GROWTH OF Y-TYPE HEXAFERRITE SINGLE CRYSTALS

D. Prabhakaran, F. Chmiel, J. Chen, P. Radaelli

Clarendon Laboratory, University of Oxford, UNITED KINGDOM

Recent advancement in both experimental and theoretical work leads to understand the coupling between ferroelectricity and magnetism which helps to develop new multiferroic materials. In particular interaction between ferroelectric and ferromagnetic domain walls are very important to switch the polarization using applied magnetic or electric field. Among the known multiferroic materials, hexaferrite found to be promising candidate for the practical applications at room temperature. In particular Y-type exhibit ferroelectricity associated with non- collinear magnetic orders in relatively low magnetic field and at high-temperature. Y-type hexaferrite melts incongruently and hence flux technique is the viable method to grow high quality single crystal. We will report the growth optimisation and different transition metal substitutions in order to increase the crystal quality and transition temperature. Maintaining the chemical stoichiometry is very challenging, in particular controlling the oxygen stoichiometry is very important to keep the resistivity very high for pyroelectric measurement. To address this problem, we have annealed the crystals under oxygen pressure at different temperatures.

5:57 PM - 5:58 PM

GROWTH, STRUCTURAL AND OPTICAL PROPERTIES OF LANGBEINITE-TYPE $\text{Rb}_2\text{Ti}_{0.8}\text{Yb}_{1.2}(\text{PO}_4)_3$ CRYSTALS

X. Duan, Z. Li

State key laboratory of crystal materials, Institute of crystal materials, Shandong University, CHINA

$\text{Rb}_2\text{Ti}_{0.8}\text{Yb}_{1.2}(\text{PO}_4)_3$ crystals with langbeinite-type structure have been obtained by high-temperature solution method. The chemical composition was determined using electron probe microanalysis. Detailed structural investigation was performed through single crystal X-ray diffraction technique. The as-grown crystals crystallized in cubic system with space group $P2_13$, and the lattice parameters were determined to be $a = b = c = 10.2114(9) \text{ \AA}$, $\alpha = \beta = \gamma = 90^\circ$, $V = 1064.8(3) \text{ \AA}^3$. The thermal stability was studied and the specific heat was measured to be $0.485\text{-}0.575 \text{ J}/(\text{mol}\cdot\text{K})$ in the temperature range of $25\text{-}300 \text{ }^\circ\text{C}$. The UV-visible diffuse reflectance spectrum showed the obvious Yb^{3+} absorption lines due to the transition from $^2F_{7/2}$ ground state to $^2F_{5/2}$ excited state. Blue cooperative up-conversion emission was observed at 486 nm under 980 nm excitation. The results indicate that $\text{Rb}_2\text{Ti}_{0.8}\text{Yb}_{1.2}(\text{PO}_4)_3$ crystal is a potential up-conversion phosphor material.

References [1] Y. Shen, Y. Yang, S. Zhao, X. Li, Q. Ding, Y. Li, S. Liu, Z. Lin, J. Luo, A Langbeinite-Type Yttrium Phosphate $\text{LiCs}_2\text{Y}_2(\text{PO}_4)_3$, *Inorganic chemistry*, 57 (2018) 13087-13091. [2] S. Sadhasivam, P. Manivel, K. Jeganathan, C. Jayasankar, N. Rajesh, Bright blue cooperative upconversion emission of Yb^{3+} from langbeinite $\text{K}_2\text{Ti}_{1.887}\text{Yb}_{0.113}(\text{PO}_4)_3$ single crystal, *Materials Letters*, 188 (2017) 399-402.

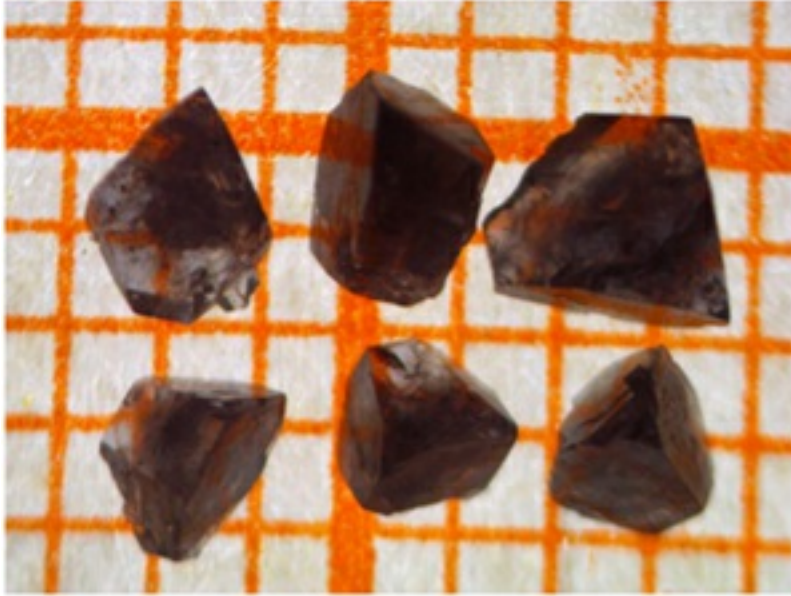


Fig. 1. Photograph of as-grown $\text{Rb}_2\text{Ti}_{0.8}\text{Yb}_{1.2}(\text{PO}_4)_3$ crystals.

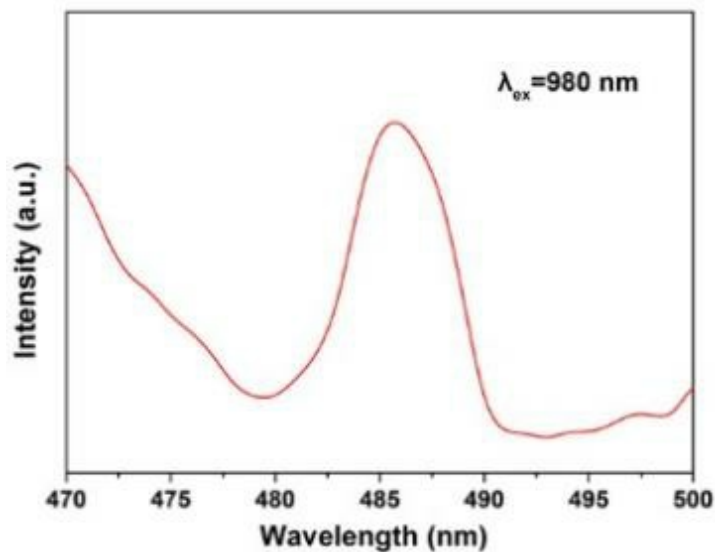


Fig.2. Cooperative up-conversion emission spectrum excited at 980 nm for langbeinite-type $\text{Rb}_2\text{Ti}_{0.8}\text{Yb}_{1.2}(\text{PO}_4)_3$ crystal.

5:58 PM - 5:59 PM

INVESTIGATION ON THE STRUCTURAL, CRYSTALLINE PERFECTION, OPTICAL, ELECTRICAL AND MECHANICAL PROPERTIES OF HIPURIC ACID DOPED FERROELECTRIC TRIGLYCINE SULFATE CRYSTALS

A. Steephen Raj, S. Chinnasami, P. Rajesh, G. Babu Rao
SSN College of Engineering, INDIA

Abstract: Pure and 1 mol % hippuric acid (HA) doped triglycine sulfate (TGS), an inorganic single crystal, has been grown to a dimension of 110 and 100 mm lengths and 30 and 30 mm diameter respectively by Sankaranarayanan–Ramasamy (SR) method. The effects of dopants on the growth, structural, electrical, optical, and mechanical properties have been investigated. The powder XRD studies confirm that the addition of 1 mol % HA has not changed the basic structure of the TGS crystal. The crystalline perfection of the grown crystal has been studied by HRXRD rocking curve measurements. UV-Visible transmittance shows that the HA doped TGS possesses higher transparency compared to pure. The emission and excitation peaks of both pure and doped TGS crystal can be observed by photoluminescence studies. Dielectric studies were evaluated for the grown crystals for different various frequencies and temperatures. Low dislocation density for HA doped TGS crystal is observed from chemical etching studies. The Vicker's hardness studies carried out at room temperature, it shows that increased hardness of the doped crystals.

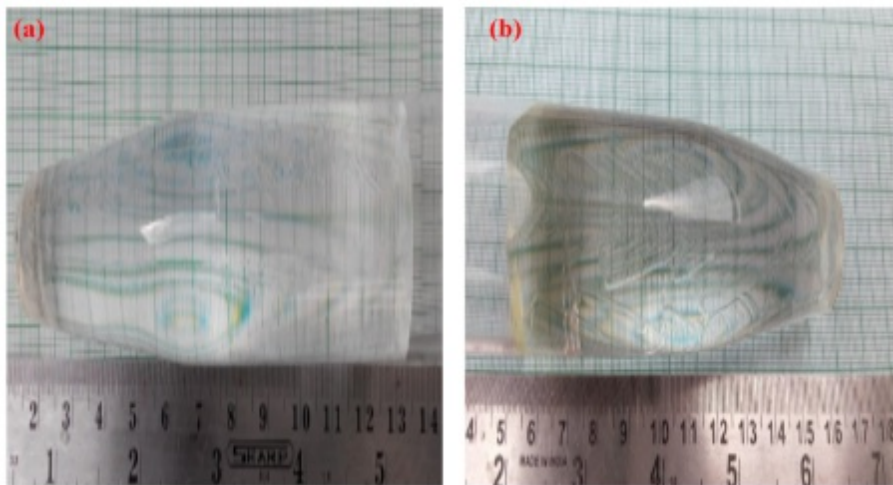


Figure 1. As grown crystals (a) Pure TGS (b) HA doped TGS

5:59 PM - 6:00 PM

NUMERICAL SIMULATION ON OXYGEN TRANSFER IN SI MELT UNDER A CUSP-SHAPED MAGNETIC FIELD USING A 3D GLOBAL MODEL

D. Murakami¹, **K. Kakimoto**², **X. Liu**², **S. Nakano**², **H. Harada**², **Y. Miyamura**²

¹Research institute for applied mechanics, Kyushu university, JAPAN,
²Research Institute for Applied Mechanics, Kyushu University, JAPAN
 In order to investigate the effect of cusp-shaped magnetic field (CMF) configuration on oxygen transfer in Si melt, numerical simulations were conducted for growth of a Czochralski (CZ) crystal in the CMF using a 3D global model. Based on the partly 3D global model proposed by Liu and Kakimoto [1], the 3D global model which can generate CMF by calculating integration of Biot-Savart equation was developed. The CMF with its symmetry plane 4mm above the half-depth of the melt plane (upper), along the half-depth plane (middle) and 4mm below the half-depth plane (lower) were investigated. The results showed that the melt temperature is almost axisymmetric in the middle case and the lower case. However, the non-uniformity of melt temperature in the azimuthal direction was observed in the upper case. As the position of the symmetry plane of the CMF become lower, the shape of the growth interface become flat. Furthermore, the oxygen concentration at the growth interface decreased when the symmetry plane of the CMF shifted from the top toward the bottom of the crucible. The results indicated that the growth interface shape and the oxygen concentration at the growth interface can be controlled effectively by optimizing the distribution of CMF.

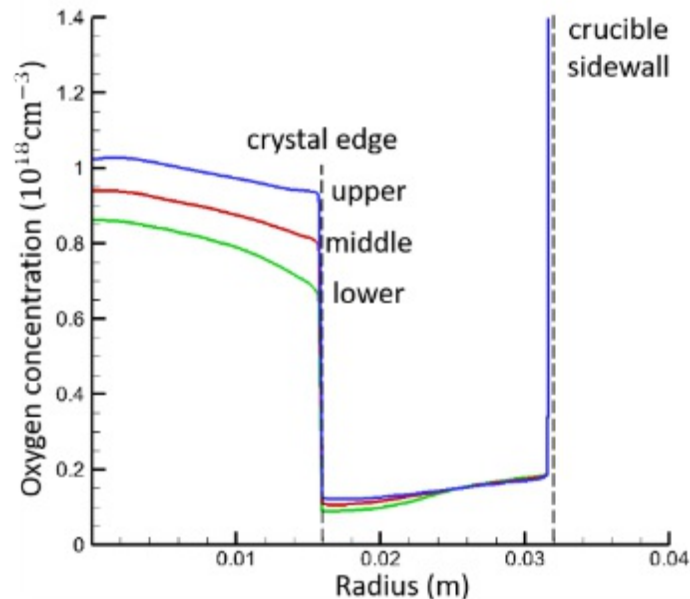


Fig.1 Radial distribution of oxygen concentration at the top of the melt.

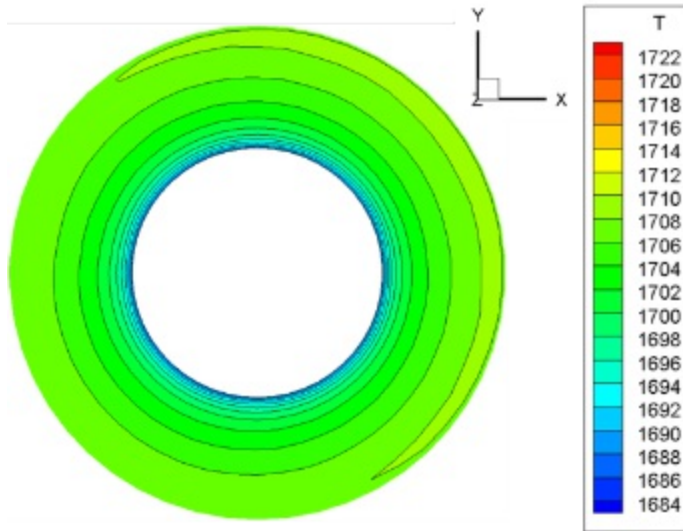


Fig.2 Thermal field at the top of the melt in the upper case. Reference [1] Lijun Liu, Koichi Kakimoto, Int. J. Heat Mass Transfer 48 (2005)4481-4491.

6:00 PM - 6:01 PM

DISPERSIONS OF PEROVSKITE STRUCTURE RELAXOR FERROELECTRIC SINGLE CRYSTALS GROWN BY ORIENTED BRIDGMAN METHOD

X. Wang, D. Lin, H. Xu, H. Luo

Shanghai Institute of Ceramics, Chinese Academy of Sciences, CHINA

The relaxor ferroelectric single crystals, such as PMN-PT and PIN-PMN-PT with perovskite structure, have attracted more and more attentions, because of ultrahigh piezoelectric performances. The large-size single crystals, aiming at the practical applications, have been grown successfully by Bridgman method. The dispersions of these single crystals have existed and only been ignored after the successful growth. After the crystal wafer will be annealed in different atmospheres, such the experiments as X-ray diffractions and X-ray Photoelectron Spectroscopy are performed to clarify the reasons of the grown boule with dispersion. The di-/piezo-/ferroelectric properties are characterized to elucidate the influences of the annealings.

6:01 PM - 6:02 PM

SPIN REORIENTATION TRANSITION AND EXCHANGE BIAS IN HALF Y DOPED SMFeO₃ SINGLE CRYSTAL

B. Mali, S.E. Saji

Indian Institute of Science, INDIA

The prospect of controlling magnetization of a material is relevant from the fundamental physics point of view as well as in emerging spintronics applications. The family of rare-earth orthoferrite compounds RFeO₃ (R = rare-earth element) exhibits striking physical properties of spin switching and magnetization reversal induced by temperature and/or external magnetic field. Further, a range of novel properties - magnetic, magneto-optic, and multiferroic – reported in this class of materials has been attracting more and more researchers in recent years. Spin reorientation is a magnetic phase transition in which the easy axis of magnetization vector rotates from one crystallographic axis to another consequent to changes in temperature or magnetic field. For example, in SmFeO₃, this occurs from the c-axis above 480 K to a-axis below 450 K, and is known as $\Gamma_4-\Gamma_2$ transition. This work involves the synthesis of a new single-crystal perovskite, namely Sm_{0.5}Y_{0.5}FeO₃ and reports its characteristics as a function of temperature and magnetic field. In addition to the spin reorientation, this compound reveals exchange bias properties as evidenced from MH isotherms at various temperatures. Exchange bias phenomenon generally manifests as a unidirectional magnetic shift along the field axes. The behaviour was confirmed by employing the training protocol with measurement of field-cooled MH loops. Being single phase in nature, this compound has potential application in spintronics devices.

6:02 PM - 6:03 PM

THE CRYSTAL GROWTH AND CHARACTERIZATION OF SE-SUBSTITUTED BISI BY PHYSICAL VAPOR TRANSPORT METHOD

B. Xiao, M. Zhu, B. Zhang, Y. Xu, W. Jie

Northwestern Polytechnical University, CHINA

Quasi-one-dimensional Bismuth Chalcogenide BiSI and BiSeI have immense potential for diverse applications, such as thermoelectric, photoelectric and ferroelectric, *etc.* However, up to now, their crystal

size and quality were still limited for the further applications. In this work, we have developed an effective synthesis and growth method to obtain pure phase $\text{BiS}_{1-x}\text{Se}_x\text{I}$ crystal with large size and high quality. The results show that synthesis at 550 °C and homogenization at 400 °C are the optimal routes to obtain pure polycrystalline $\text{BiS}_{1-x}\text{Se}_x\text{I}$, and strip-shaped single crystal with the largest size of $\sim 80 \times 4 \times 0.5 \text{ mm}^3$ was successfully grown below 500 °C by the physical vapor transport method. To investigate the substitution effect of Se atom for S, XRD and Raman measurements were performed to investigate the evolution of crystal structure by the Se substitution. The compositions and morphologies of $\text{BiS}_{1-x}\text{Se}_x\text{I}$ were determined by SEM. The band-gap of as-grown $\text{BiS}_{1-x}\text{Se}_x\text{I}$ crystal showed a nonlinear dependence on the Se content, which decreased from 1.53 eV to 1.29 eV with the increasing of Se content according to the UV-Vis diffuse reflectance spectra. Our results may stimulate further investigation into V-VI-VII compounds for their applications.

6:03 PM - 6:04 PM

INFLUENCE OF GROWTH CONDITIONS ON THE OPTICAL SPECTRA OF GAMMA IRRADIATED BaF_2 AND CaF_2 CRYSTALS

I. Nicoara, M. Stef, D. Vizman

West University of Timisoara, ROMANIA

BaF_2 and CaF_2 crystals are widely used in science and technology, like as optical windows and lenses, as scintillators and detectors for different radiations. The radiation damage of the crystals is caused by the formation of color centers after irradiation. The damage depends on the various impurities in crystals [1] and on the structural defects formed during the growth process [2]. The goal of this paper is to investigate the influence of growth conditions (temperature gradient (TG) during the crystallization process, trace of Pb^{2+} , Yb^{2+} , O^{2-} ions) on the optical spectra of γ -irradiated BaF_2 (B) and CaF_2 (C) crystals. The crystals were obtained by Bridgman method using a shaped graphite furnace [3]. The samples were irradiated at room temperature from a ^{60}Co source. The optical absorption (OA) spectra were recorded before and after irradiation. Depending on the growth

conditions, the dislocation density of the samples varies along the boule and the crystal type. The OA spectra of the two types of crystals reveal different kind of behavior after γ -irradiation. No g-rays induced absorption bands were observed for the B1 crystal (TG=16⁰C/cm, without impurities, low dislocation density). The B2 crystal has trace of Pb²⁺ and O²⁻ ions, TG=24⁰C/cm. For the samples from the middle of B2 crystal very weak induced absorption bands appear. The dislocation density of these samples is lower than of the top of the crystal B2, but higher than of B1 crystal. The samples remain colourless and transparent. In the case of the samples from the top (end) of B2 boule, with high dislocation density, two broad absorption bands were observed. The samples are brown. In the case of CaF₂ crystals, the dislocation density of the C1 samples (TG=17⁰C/cm, trace of Yb²⁺ ions) is lower than of the C2 samples (TG=32⁰C/cm, trace of Pb²⁺). After γ irradiation no new absorption bands appear in C1 samples, they are colourless. Two broad absorption bands are present in C2 samples; the samples are light green. The samples of crystal C3 (high dislocation density, no impurities) the characteristic F centers are observed. The samples are blue. The peaks intensities depend on the γ -dose and on the dislocation density. The type of induced colour centres is indicated for every sample. [1] L.I. Bryukvina, E.E. Penzina, J. Appl. Spectroscopy, 77(2010) 104. [2] Z. W. Yin, Mat. Res. Soc. Symposia Proceedings, 348(1994) 65. [3] D. Nicoara, I. Nicoara, Mater. Sci. Eng. A, 102(1988) L1.

6:04 PM - 6:05 PM

UNRAVELLING THE CRITICAL ROLE OF SITE OCCUPANCY OF LITHIUM CODOPANTS IN LU₂SIO₅:CE³⁺ SINGLE-CRYSTALLINE SCINTILLATORS

Y. Wu¹, J. Peng², D. Rutstrom¹, M. Koschan¹, C. Foster¹, C.L. Melcher¹

¹University of Tennessee, TN, UNITED STATES OF AMERICA,

²Beihang University, CHINA

Lithium codoping has emerged as an effective strategy to enhance the light yield of oxide scintillators for radiation detection applications, but

the understanding of the actual role played by Li^+ remains unclear. In this work, we comprehensively study the effects of Li codoping on optical and scintillation properties of $\text{Lu}_2\text{SiO}_5:\text{Ce}$ (LSO:Ce) single crystals, and reveal the critical role of site occupancy of Li. High quality LSO:Ce single crystals codoped with 0.05, 0.1 and 0.3 at% Li ions were grown by the Czochralski method. The optical absorption spectra confirm non-conversion of stable Ce^{3+} to Ce^{4+} in Li-codoped LSO:Ce regardless of Li codoping concentration. The photoluminescence decay kinetics suggest an enhanced ionization of the excited $5d_1$ state of Ce^{3+} centers in highly codoped samples. A simultaneous improvement of scintillation light yield, decay time, and afterglow is achieved in LSO:Ce codoped with low concentrations of Li. The preferential occupation of Li at interstitial spaces and lutetium sites is proven to rely on its codoping concentration by using ^7Li nuclear magnetic resonance technique. The concentration-dependent site occupancy of Li alters the defect structures of LSO:Ce, in particular resulting in a distinct change in the number of cerium-spatially-correlated oxygen vacancies confirmed by thermoluminescence and afterglow measurements.

6:05 PM - 6:06 PM

CRUCIBLE-FREE GROWTH OF CE-DOPED $(\text{Gd},\text{La})_2\text{Si}_2\text{O}_7$ SINGLE CRYSTALS IN THE AIR ATMOSPHERE FOR SCINTILLATOR APPLICATIONS

V. Kochurikhin¹, K. Kamada², Y. Shoji², M. Yoshino², A. Yoshikawa¹

¹C&A corporation, JAPAN, ²IMR, Tohoku University, JAPAN

Ce-doped $(\text{La},\text{Gd})_2\text{Si}_2\text{O}_7$ scintillators have fast decay time and high light yield (41000 ph/MeV) at the temperature range up to 150 C. Such properties make it a prospective scintillator for oil well logging [1].

However, the wide application of Ce- $(\text{La},\text{Gd})_2\text{Si}_2\text{O}_7$ single crystal is still limited due to the serious difficulties in production of high quality bulk crystals. The Czochralski (Cz) is the main technique applying for the growth of Ce- $(\text{La},\text{Gd})_2\text{Si}_2\text{O}_7$ crystals of 1-2 inch in diameter [2]. A considerable disadvantage of the Cz growth of Ce- $(\text{La},\text{Gd})_2\text{Si}_2\text{O}_7$ crystals is associated with the short lifetime of Ir crucible used as a

melt container during the growth process and presence of Oxygen vacancies in the grown crystals. During many years there is the well-known crystal growth technique called “Scull melting” or “Cold container” [3]. This technique uses the fact that many oxide melts at high temperature have enough high electric conductivity and can be heated directly by the high frequency electric field without use of metal crucible. In this work we investigated the opportunity to use scull melting technique for the formation and keeping Ce-(La,Gd)₂Si₂O₇ melt without a crucible. The growth process itself was performed with the use of rotated seed by slow pulling up like at ordinary Czochralski technique. Such combined technique allows to solve many problems of conventional Cz process for Ce-(La,Gd)₂Si₂O₇. The absence of Ir crucible gives the opportunity to apply any growth atmosphere (including air or even pure Oxygen). Such conditions look appropriate for the suppression of Oxygen vacancies in the grown crystal. Grown crystals were up to 10 mm in diameter and up to 20 mm in length. Optical and scintillation properties of the grown crystals were measured and compared with the properties of crystals grown by the traditional Czochralski technique in inert atmosphere. [1] S. Kurosawa, T. Shishido, T. Sugawara, A. Nomura, K. Yubuta, A. Suzuki, J. Pejchal, Y. Yokota, K. Kamada, A. Yoshikawa, Nucl. Inst. Methods Phys. Res., 772 (2015) 72 [2] A. Yoshikawa, Y. Shoji, S. Kurosawa, V. Chani, R. Murakami, T. Horiai, K. Kamada, Y. Yokota, Y. Ohashi, V. Kochurikhin, J. Cryst. Growth, 452 (2016) 57 [3] V. V. Osiko, M. A. Borik, E. E. Lomonova, Ann. Rev. Mater. Sci., 17 (1987) 101

6:06 PM - 6:07 PM

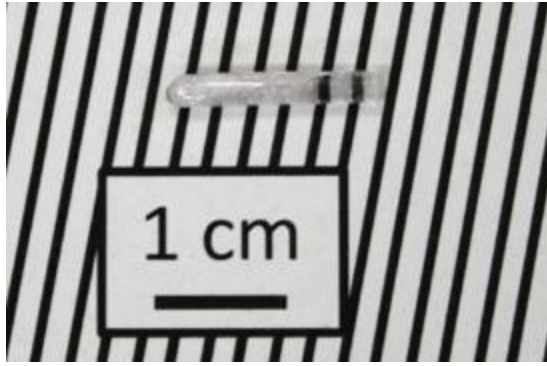
CRYSTAL GROWTH AND OPTICAL PROPERTIES OF A CE₂SI₂O₇ SINGLE CRYSTAL

T. Horiai¹, S. Kurosawa², R. Murakami³, Y. Shoji³, J. Pejchal⁴, M. Yoshino¹, A. Yamaji¹, H. Sato², Y. Ohashi², K. Kamada³, Y. Yokota², A. Yoshikawa³

¹IMR, Tohoku University, JAPAN, ²NICHe, Tohoku University, JAPAN, ³C&A corporation, JAPAN, ⁴Institute of Physics CAS, CZECH REPUBLIC

Scintillation crystals convert ionizing radiation to ultraviolet or visible

light, and are used in many fields as radiation detectors. The Ce-doped $(\text{Gd},\text{La})_2\text{Si}_2\text{O}_7$ (Ce:La-GPS) has been reported to have a high light yield ($\sim 41,000$ photons/MeV), short decay time (~ 46 ns) and good energy resolution ($\sim 5.0\%$, 662 keV, FWHM) [1,2]. One of the main reasons for a high light yield of Ce-doped crystals is that Ce^{3+} 5d-4f transition is a parity-allowed one. Since the involved Ce^{3+} 5d orbital are not shielded by outer electrons, the emission and excitation spectra strongly depend on the host crystal structure. In previous study, the crystal structures of Ce:La-GPS and $\text{Ce}_2\text{Si}_2\text{O}_7$ (CePS) have been investigated, and rare-earth sites in Ce:La-GPS and CePS were found [3,4]. From the ref. 4, it was found that the CePS structure is composed of CeO_8 polyhedra and SiO_4 tetrahedra with two inequivalent Ce^{3+} sites in the structure. Since the optical and scintillation properties of CePS single crystal have not been reported except fabrication of nanocrystals and films [5,6], we tried to grow a relatively large mm-scale CePS single crystal to clarify the relationship between the number of Ce^{3+} sites and scintillation properties. The $\text{Ce}_2\text{Si}_2\text{O}_7$ single crystal was grown from the melt using the micro-pulling-down (μ -PD) method. As starting materials, we used CeO_2 and SiO_2 powders the purities of which were at least 99.99%. After growth, we evaluated the phase by the powder X-ray diffraction (XRD) analysis, and performed the Rietveld analysis to estimate the atomic coordinates in $\text{Ce}_2\text{Si}_2\text{O}_7$ single crystal. In addition, we measured optical and scintillation properties. We succeeded in growing a transparent crystal as shown in the figure 1. From the result of the powder XRD analysis, the crystal system was determined to be monoclinic (space group: $P2_1/n$), $a=13.0770$ Å, $b=8.7230$ Å, $c=5.4045$ Å and $\beta=90.1278^\circ$. In this work, we report the crystal growth and discuss the optical and scintillation properties. [1] A. Suzuki, A. Yoshikawa, et al., Appl. Phys. Express **5** (2012) 102601. [2] S. Kurosawa, A. Yoshikawa, et al., Nucl. Instrum. Methods Phys. Res. A **772** (2015) 72. [3] R. Murakami, A. Yoshikawa, et al., J. Alloy. Compd. **748** (2018) 404. [4] A.C. Tas, et al., J. Amer. Ceram. Soc. **77** (1994) 2968. [5] W.C. Choi, et al., Appl. Phys. Lett. **75** (1999) 2389. [6] L. Kępiński, et al., J. Alloy. Compd. **341** (2002) 203.



6:07 PM - 6:08 PM

METAL HALIDE PEROVSKITE BULK CRYSTALS GROWN FROM SOLUTION FOR ROOM TEMPERATURE NUCLEAR RADIATION DETECTION

Y. Xu, X. Liu, F. Wang, Q. Sun

Northwestern Polytechnical University, CHINA

Rapid development on X-ray and γ -ray spectrometers and imaging arrays result in tremendous opportunities in the field of astronomy, high energy physics, nuclear medicine, non-destructive inspection, and national security. To achieve a higher spatial and energy resolution, semiconductor detectors have exhibited significant advantages, due to the direct photoelectric conversion. Recently, there has been considerable interest in identifying new low-cost, heavy element, chemically robust compound materials for room-temperature radiation detection. Among the various semiconductors, the metal halide perovskites are receiving attention as potential radiation detection materials [1, 2]. Here, we report centimeter-sized detector-grade APbBr₃ (A=Methylammonium, Cs) perovskite crystals grown using solution method [3, 4]. The morphology and phase evolution of APbBr₃ crystals have been discussed according to the molar ratios of precursors and the growth anisotropy. The resulting detector grade crystals exhibited high resistivity in the range of $10^8 \sim 10^9 \Omega \cdot \text{cm}$. The mobility-lifetime (mt) products are measured under ²⁴¹Am @ 5.48 MeV alpha particles, with the values in the range of $10^{-4} \sim 10^{-3} \text{ cm}^2/\text{V}$ for both electrons and holes. Simultaneously, the electrons and holes mobility are estimated using the alpha particles induced transient waveforms. Finally, the enhanced X-ray sensitivity

was achieved under continuous X-ray beam by both surface engineering and electrode modification.

References: [1] H. Wei, Y. Fang, P. Mulligan, W. Chuirazzi, H.-H. Fang, C. Wang, B. R. Ecker, Y. Gao, M. A. Loi, L. Cao, and J. Huang, **Nat. Photonics**, 2016, 10, 333-339. [2] C. C. Stoumpos, C. D. Malliakas, J. A. Peters, Z. Liu, M. Sebastian, J. Im, T. C. Chasapis, A. C. Wibowo, D. Y. Chung and A. J. Freeman, **Cryst. Growth Des.**, 2013, 13, 2722-2727. [3] H. Zhang, X. Liu, J. Dong, H. Yu, C. Zhou, B. Zhang, Y. Xu, **Cryst. Growth Des.** 2017, 17, 6426-6431. [4] X. Liu, H. Zhang, B. Zhang, J. Dong, W. Jie, and Y. Xu, **J. Phys. Chem. C**, 2018, 122 (26), 14355-14361.

6:08 PM - 6:09 PM

SCINTILLATION PROPERTIES OF ZNO:GA SINGLE CRYSTALS GROWN BY TRAVELLING-SOLVENT FLOATING-ZONE METHOD

Y. Ma¹, Y. Jiang², J. Xu¹

¹Shanghai Institute of Technology, CHINA, ²Institute of Laser Engineering, Beijing University of Technology, CHINA

ZnO: Ga crystal was a multifunctional semiconductor with direct- and wide-band gap, combining with the characteristics of transparent conduction, ultra-fast scintillation and ultraviolet emission, etc.. The growth of cm-sized ZnO: Ga crystals with high dopant amount and multicomponent covering large dopant range, and the optical properties as a function of Ga₂O₃ dopant amount were researched systematically. The GZO (ZnO: x wt% Ga₂O₃; x=0, 0.05, 0.1, 0.2, 0.3, 0.4, 0.5, 0.6, 0.7, 0.8, 0.9, 1.0) single crystals were grown out by the travelling solvent floating zone technique. Room photoluminescence (PL) and X-ray luminescence (XRL) of ZnO: Ga crystals showed that the strong near-band edge emissions blue-shift and broad with increasing Ga doping amount. Temperature dependence of photoluminescence showed that the strong near-band edge emissions blue-shift and narrow down with increasing Ga doping amount. Room temperature pulsed X-ray decay curves showed GZO-0.5 wt% crystal was of shortest decay time 0.79 ns, which represents 94% of the total light yield. However, 325nm laser emission decay curve of the GZO sample was well fitted with two exponential decay components with

two decay times of 0.04ns (95 %), 1.2ns (5%). The TEM、 Raman spectrum and XPS spectra of GZO crystals were also tested for studying on composition-structure-property relationship and obtaining the optimum Ga doping amount.

6:09 PM - 6:10 PM

SCINTILLATION IMPROVEMENT OF BABR2:EU SINGLE CRYSTALS BY AU CO-DOPING

D. Yuan, F. Moretti, D. Perrodin, E.D. Bourret

Lawrence Berkeley National Laboratory, CA, UNITED STATES OF AMERICA

Abstract: Co-doping strategy has been used to improve the performance of scintillator materials, including the widely used $\text{LaBr}_3:\text{Ce}$ and $\text{NaI}:\text{Tl}$. Few studies have attempted co-doping halides activated by Eu^{2+} until it was shown that $\text{BaBrCl}:\text{Eu}$ co-doped with Au has a significantly improved light output [1]. Herein, we report the effect of Au co-doping on optical and scintillation properties of $\text{BaBr}_2:\text{Eu}$. BaBr_2 single crystals doped with Eu and with or without the Au co-dopant were grown by the vertical Bridgman method using identical growth parameters. Both photo- and radio-luminescence show the same Eu^{2+} emission spectrum for Eu doped and Au co-doped BaBr_2 samples suggesting that Au introduction has no influence on the Eu^{2+} luminescence center characteristics. Co-doping, on the other hand, improves remarkably the light output (at least 50% higher for the co-doped samples). It also reduces the weight of slow components in the scintillation decay kinetics of $\text{BaBr}_2:\text{Eu}$. Moreover, a clear reduction in the thermally stimulated luminescence intensities was observed after the co-doping. These results suggest that Au co-doping is the cause of a substantial reduction in charge carriers trapped at defects sites, likely due to lower concentration of intrinsic defects, notably Br vacancies. It is not clear now what is the role of Au during the crystal growth that results in the defect concentration reduction. Previous results obtained on BaBrCl indicate that practically no Au remains inside the grown crystals, implying that Au might act as a sort of catalyst at the growth interface. We cannot exclude other possibilities, including that AuBr_3 behaves as a bromine source during

growth. The effectiveness of such a co-doping in other bromide scintillator single crystals is also currently investigated. *This work is supported by the Department of Energy/NNSA/DNN R&D and carried out at Lawrence Berkeley National Laboratory under contract #AC02-05CH1123. Reference:* [1] T. Shalapska, F. Moretti, E. Bourret, G. Bizarri, Effect of Au codoping on the scintillation properties of BaBrCl:Eu single crystals, *Journal of Luminescence*, 202 (2018), 497.

6:10 PM - 6:11 PM

THE CRYSTAL GROWTH AND CHARACTERIZATION OF QUASI-ONE-DIMENSIONAL LEAD BASED PEROVSKITE CSPBI₃ CRYSTALS

B. Zhang, B. Xiao, X. Liu, Y. Xu, W. Jie

Northwestern Polytechnical University, CHINA

Quasi-one-dimensional lead based perovskite CsPbI₃ exhibits increasing interests in quantum dots, solar cells, *etc.* However, high quality large CsPbI₃ bulk crystals are still unexplored. Here we report CsPbI₃ crystal growth from solution by tailoring the solubility. The morphology and crystal structure of CsPbI₃ are characterized by SEM and XRD, which reveal the stick-like structure with the space group *Pnma* and lattice parameters $a=10.46 \text{ \AA}$, $b=4.80 \text{ \AA}$, and $c=17.78 \text{ \AA}$. Ultra violet-visible transmission spectra substantiate CsPbI₃ being a direct-gap semiconductor with a band-gap $\sim 2.69 \text{ eV}$. In addition, a broad emission at 550~580 nm with a large Stokes shift of 0.60~0.75 eV and the corresponding dissociation energy 7.58 meV was found using temperature and power dependent PL spectra. This emission was attributed to a strong electron-phonon coupling induced "self-trap excitons" in CsPbI₃. Interestingly, high resistivity of $7.4 \times 10^9 \text{ W}\cdot\text{cm}$ and large carrier mobility-life time product of $3.63 \times 10^{-3} \text{ cm}^2\cdot\text{V}^{-1}$ along *b* axis bring out the CsPbI₃ detector with a low X-ray detection limit of $0.219 \text{ mGy}\cdot\text{s}^{-1}$ and high sensitivity of $2.37 \text{ mC}\cdot\text{Gy}^{-1}\cdot\text{cm}^{-2}$ under $4.17 \text{ V}\cdot\text{mm}^{-1}$ (50 kVp), which is at least an order of magnitude larger than the previous reported halide perovskite single crystals, such as MAPbBr₃, Cs₂AgBiBr₆, Cs₃Bi₂I₉. The enhanced sensitivity may be attributed to the shallower-defects assistant gain or charge collection

efficiency up to 1045% (50kVp) under $4.17 \text{ V}\cdot\text{mm}^{-1}$. Our finding shields more light on the crystal growth, structure, optical properties and potential applications of the low dimensional perovskite materials.

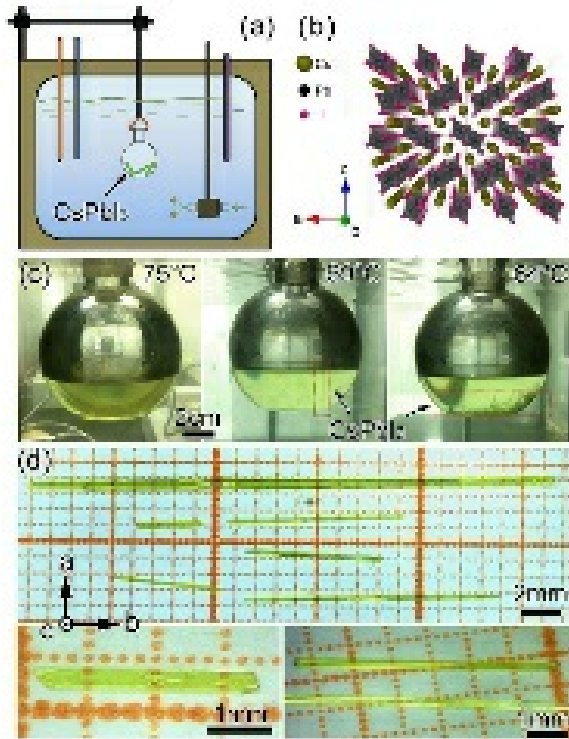


Fig. 1. (a) Schematic of experimental apparatus for CsPbI₃ crystals grown from solution. (b) Structure schematic of quasi-one-dimensional CsPbI₃. (c) The pictures of the processes for the crystal growth at 75 °C, 69 °C and 64 °C. (d) As-grown stick-like CsPbI₃ crystals.

6:11 PM - 6:12 PM

HPHT SINGLE CRYSTAL DIAMOND SUBSTRATE IIA TYPE CHARACTERIZATION FOR PARTICLE DETECTORS

O. Rabinovich, S. Chernykh, A. Chernykh, E. Trifonov, K. Shcherbachev, D. Kiselev, N. Polushin, M. Kondakov, S. Didenko, S. Didenko

NUST MISIS, RUSSIAN FEDERATION

In recent years, diamond detectors have been widely developed. Wide band gap (5.5 eV) and high resistivity (up to $10^{14} \Omega\cdot\text{cm}$) together with high transport parameters of non-equilibrium current carrier give possibility for such detectors to be used up to a temperature – 300 °C with no serious change in their characteristics. Moreover, due to the

high displacement energy of the atoms in the crystal lattice (43 eV), diamond has a significant radiation tolerance. The combination of the above mentioned diamond characteristics makes detectors based on it ideal candidates for working in extreme conditions. The paper presents the results of HPHT single-crystal diamond substrates Ila type characterization for particle detectors. The used diamond substrates [(100), with size 4×4 mm and with thickness 0.5 mm] were produced by company “New Diamond Technology”. The diamond substrates were investigated by X-ray diffraction, Fourier transform infrared spectroscopy and by atomic force microscopy. It has been shown that substrates have significant crystalline perfection. No crystallites inclusions with a different orientation were detected. At rocking curves measuring, no physical broadening was detected. The dislocation density in the current substrates is at a level below of the method sensitivity $< 10^3 \text{ cm}^{-2}$. The nitrogen and boron concentrations in the substrates were estimated at 10 and 50 ppb, correspondently. To create a test detector, contacts ($3.5 \times 3.5 \text{ mm}^2$) based on Pt (thickness – 150 Å) were applied to both substrate sides. Deposition was made through a metal mask using ion-plasma sputtering. At a next step, the charge transport properties were investigated by alpha spectrometry method. For this, the dependence of the charge collection efficiency versus bias voltage under irradiation with α -particles (5.499 MeV) from ^{238}Pu and different polarities of the bias voltage on the detector was measured. The obtained results were correlated with the deep centers parameters investigation by the DLTS method. The correlation of the measured diamond substrates electro-physical parameters with their crystalline perfection was discussed. This work was supported by the Ministry of Science and Higher Education of the Russian Federation within the framework of the State Job No. 075-02-2018-210 dated 2018.11.26, RFMEFI57818X0266.

6:12 PM - 6:13 PM

SYNTHESIS AND PHASE CONTROL OF THE EUROPIUM DOPED BAF_2 - BACL_2 SYSTEM

B. Wiggins, C. Richards, D. Williams, M. Hehlen

Los Alamos National Laboratory, NM, UNITED STATES OF AMERICA

Mixed halide systems have attractive optical properties that make these materials applicable to radiation detection, imaging, optical data storage and fundamental science. This study investigates the synthesis of BaFCl:Eu^{2+} through flux growth techniques and its corresponding optical properties. Crystals up to $0.5 \times 0.5 \times 0.5 \text{ mm}^3$ and lower in size were grown through flux growth techniques. The crystals were characterized by fluorescence, x-ray diffraction and SEM-EDX. The successful control of the mixed halide compositional space enables the development of pixelated composite imaging screens applicable to medical imaging. The composites can support respectable scintillation light transport and high detection efficiency.

6:13 PM - 6:14 PM

GROWTH DIFFICULTIES AND GROWTH OF CRACK FREE EU²⁺ ACTIVATED KSR₂I₅ SCINTILLATOR SINGLE CRYSTAL BY VERTICAL BRIDGMAN-STOCKBARGER TECHNIQUE FOR RADIATION DETECTION APPLICATIONS

A. Raja, R. P

SSN College of Engineering, INDIA

The parent compound of Strontium Iodide (SrI_2), Potassium Iodide (KI) and Europium Iodide (EuI_2) was purified by homemade Zone-refinement experimental set-up. Insoluble impurities were filtered by specially designed dual chamber quartz ampoule with frit filter method. The Europium activated potassium strontium iodide ($\text{KSr}_2\text{I}_5:\text{Eu}^{2+}$) compound melt was filtered by frit filtering method. Steep temperature profile of this growth furnace is also measured to growth a quality single crystal of $\text{KSr}_2\text{I}_5:\text{Eu}^{2+}$. The $\text{KSr}_2\text{I}_5:\text{Eu}^{2+}$ single crystal was grown by homemade vertical transparent Bridgman-Stockbarger technique. The photoluminescence excitation and emission spectra indicated the typical $4f \rightarrow 5d - 4f$ transition. The broad emission peak was at 443 nm. The X-ray excited radioluminescence broad emission was observed at 452 nm. The scintillation properties of the grown crystal were tested by gamma ray spectrometer. The energy resolution of the $\text{KSr}_2\text{I}_5:\text{Eu}^{2+}$

crystal was found to be 4.1% at 662 KeV under ^{137}Cs sealed gamma source and scintillation decay time was also determined and calculated value is 1.25 μs .

6:14 PM - 6:15 PM

SINGLE CRYSTAL GROWTH OF UNDOPED AND TB DOPED LU₂O₃ AND HFO₂ BY INDIRECT HEATING GROWTH METHOD USING ARC PLASMA

R. Murakami¹, **K. Kamada**², V. Kochurikhin³, K.J. Kim⁴, Y. Shoji⁵, M. Yoshino⁶, A. Yamaji⁴, S. Kurosawa⁷, Y. Ohashi⁷, Y. Yokota⁸, A. Yoshikawa⁴

¹Tohoku University, JAPAN, ²C&A, JAPAN, ³General Physics Institute, Russian Academy of Sciences, RUSSIAN FEDERATION,

⁴Institute for Materials Research, Tohoku University, JAPAN, ⁵C&A Corporation, JAPAN, ⁶IMR, JAPAN, ⁷NICHe, Tohoku University, JAPAN, ⁸New Industry Creation Hatchery Center, Tohoku University, JAPAN

Inorganic scintillators have been playing a major role in many fields of radiation detection, including medical imaging, security, astrophysics, and well logging. In these applications, heavy scintillator composed of high effective atomic number ions are strongly needed, For example, Lu₂O₃ have 9.42 g/cm³ of density and containing high effective atomic ion of (Lu:71). HfO₂ has also attracted attention due to its high density of 9.7 g/cm³, a high effective atomic number (Hf:72) and negligible intrinsic background. These materials itself and their compounds can be promising host materials as acintillators. However Lu₂O₃ and HfO₂ have generally high melting temperatures of more than 2490 and 2700 °C, respectively. Conventional growth technique using Ir crucible such Chochralski, Bridgman-Stockbarger and micro-pulling down method. Especially, quick materials survey using single crystals is important to discover novel scintillators. Crucible free growth technique such skull melting and floating zone (FZ) method can be adapted to high melting temperature materials, but these technique are unsuitable for quick materials survey due to their difficulty coming from massive raw material and power supply capacity, frequent replacement of power

supply equipment, time-consuming sintering and preparing of raw materials, difficulty of crystal growth and heating difficulty for high transmittance crystal against to FZ beams. In this study, we propose a novel indirect heating growth method using arc plasma and Ir metal melt for materials survey. Figure 1 (left) shows the schematic drawing of this growth method. Arc plasma preferentially heats metal due to the difference of electrical conductivity. Oxide material melts on the molten Ir metal and is melted by the heated molten metal. After the gradual cooling by decreasing arc plasma power, single crystal of synthesized oxide can be obtained. The presence of metal enables control of heating and cooling, and promotes directional solidification. Figure 1 (right) shows the grown undoped and Tb doped Lu_2O_3 crystal. These crystals show enough transparency and size for radiation response measurements. The Tb doped sample shows green Tb^{3+} emission under UV light. Details of growth procedure, growth results of HfO_2 , crystal phase, XRC, optical and scintillation properties will be presented.

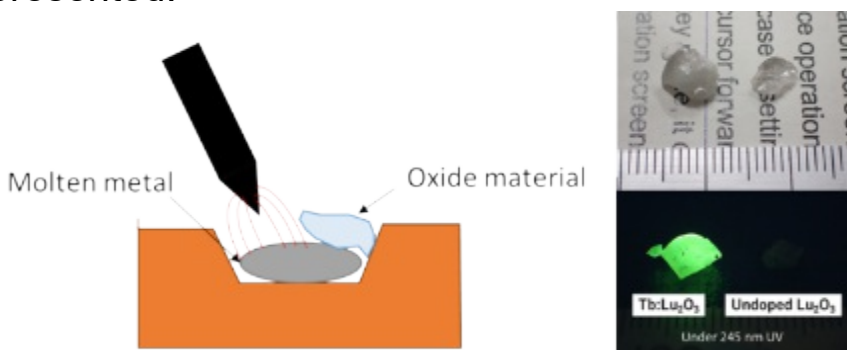


Figure 1. Schematic drawing of the growth method and grown undoped and Tb:Lu₂O₃ crystals

6:15 PM - 6:16 PM

COMPARISON CO-DOPING EFFECTS BETWEEN MG AND W ON CE:GD₃GA₃AL₂O₁₂ SCINTILLATOR GROWN BY MICRO PULLING DOWN METHOD.

M. Ueno¹, K.J. Kim¹, K. Kamada², T. Nihei³, M. Yoshino¹, A. Yamaji¹, S. Kurosawa⁴, Y. Yokota⁵, Y. Ohashi⁴, A. Yoshikawa¹, H. Sato⁴

¹Institute for Materials Research, Tohoku University, JAPAN, ²C&A corporation, JAPAN, ³C&A Corporation, JAPAN, ⁴NICHE, Tohoku

University, JAPAN, ⁵New Industry Creation Hatchery Center, Tohoku University, JAPAN

Inorganic scintillators with high density and high light yield are of major interest for applications in high energy physics and medical imaging detectors, etc. Especially positron emission tomography (PET) is very effective tool to analyze the distribution of target molecules and playing an important role in small animal molecular imaging. To improve the PET performance, higher light yield and shorter decay time are effective. From previous research, alkali earth ions co-doping effects were investigated for garnet scintillators such as $Gd_3Ga_3Al_2O_{12}$ (Ce:GGAG), $Lu_3Al_5O_{12}$, $Y_3Al_5O_{12}$. In the case of Ce:GGAG the light yield of Mg0.2% co-doped Ce:GGAG showed 59% of light yielded comparing with Ce GGAG standard with 56000 photons/MeV, the decay time was accelerated by Mg 0.2% co-doping compared with the standard crystal and decay value decreased down to 26 ns from 75 ns. In this study, to optimize the co-dopants concentration, we made the Ce:GGAG single crystal by micro-pulling down method with various W concentration as 200, 500, 1000, 3000 ppm. As a result, W 200 ppm co-doped Ce:GGAG showed the largest increase of 121% light yield comparing to non co-doped Ce:GGAG standard. There was no effect on decay time by W co-doping even in high W concentration. These tendency is opposite to Mg co-doping. The detail of the relationship between co-dopant concentration and scintillation characteristic will be shown. Furthermore, difference between W and Mg of the improvement mechanism is discussed.

Scintillator properties of W co-doped Ce:GGAG single crystals grown by μ -PD method.		
codopants concentration (ppm)	light yield (Photons/MeV)	first decay time
0	41400	53.6 ns 46.0%
200	50000	55.2 ns

		42.2%
500	44800	53.6 ns 46.0%
1000	45800	55.9 ns 40.6%
3000	44000	57.5 ns 43.0%

6:16 PM - 6:17 PM

BULK CRYSTAL GROWTH OF ALSB FOR ROOM-TEMPERATURE PHOTODETECTOR

Z. Yin, T. Wang, X. Zhang, W. Wang, W. Jie
Northwestern Polytechnical University, CHINA

The Aluminum Antimonide (AlSb) crystals show great potential for room-temperature radiation detection applications, which has been considered as the only dual-carrier compound semiconductor detector to supplant high purity Germanium. However, the development of AlSb was greatly limited in the realization of theoretical prediction performance due to the difficulties in synthesis and crystal growth. The main problems with AlSb crystal growth consists of the high reactivity of Al with crucible and the evaporation of Sb. Here we introduced high purity pBN crucible in the crystal growth of AlSb by vertical Bridgman method (VB method). The pBN crucible was placed in a quartz ampoule with a graphite cover to suppress the high reactivity of Al and depress the evaporation loss of Sb. A two-setup growth process was implemented, which consists of a temperature oscillation period for synthesis and the growth in a VB mode. The AlSb crystal ingots with a diameter of 22mm were successful obtained and monocrystal wafers of 5×5×2 mm³ were able to cut from the ingots. The crystal structure of as-grown AlSb was a single phase of zinc blende structure determined by powder XRD. The composition of as-grown AlSb crystal was analyzed by EDS, with Al and Sb ratio of 49.52 : 50.48. The optical and electrical properties of undoped and Te-doped AlSb samples were characterized. The optical energy bandgap of as-grown AlSb at room-temperature was about 1.6 eV, identified by the UV-vis

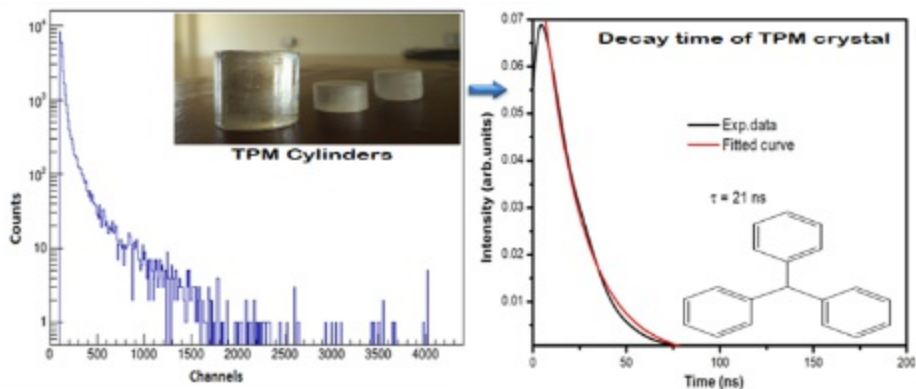
transmittance spectrum. The low temperature photoluminescence (PL) spectra revealed a new DAP peak, which was related to Te dopants. With Te compensation, the conductivity type was converted from P-type to N-type with decrease in the density of carriers, which was determined by Hall test. A significantly increase from 10^2 to $10^6 \Omega \cdot \text{cm}$ in the resistivity of as-grown AISb was observed by I-V test. The wafers were illuminated by pulsed LED light with several different wavelength of 375~600nm with a power of ~1mW under 0.1V bias. The photo-response of AISb revealed that the ratio of photocurrent to dark current was about 100. It can be inferred that AISb has high external quantum efficiency content in the visible light, indicates a promising future for the development of the AISb-based optoelectrical devices.

6:17 PM - 6:18 PM

UNIDIRECTIONAL GROWTH AND CHARACTERIZATION OF TRIPHENYLMETHANE SINGLE CRYSTALS FOR SCINTILLATOR APPLICATION

K. Sankaranarayanan¹, D. Joseph Daniel², G. V¹, K. H.J²

¹Alagappa University, INDIA, ²Kyungpook National University, KOREA, REPUBLIC OF



Organic scintillators have great impact in recent years due to detection of high energy particles in defective environment. In this aspect, the triphenylmethane has been crystallized unidirectionally by temperature gradient SR method with cylindrical dimension. Highly transparent large size (80 mm length and 15 mm diameter) single crystal was grown during the crystallization period of 25 days. The grown crystal cylinder was subjected to various physico-chemical investigations to

establish its structural details both by X-ray diffraction and by infrared analysis, to study its thermal behaviour under gravimetric and calorimetric analyses, to record its photo response in the vicinity of UV-Visible wavelength and with the excitation wavelength of 385 nm and to explore the mechanical modulus by Vicker's microhardness test. The scintillation of the crystal cylinder under gamma radiation shows intense emission in the wavelength of interest and a decay time of 21 ns was noticed. These important results suggested the feasibility of this material for high energy radiation detection. **Reference: V. Govindan**, D. Joseph Daniel, H. J. Kim, K. Sankaranarayanan, "Unidirectional crystal growth, luminescence and Scintillation Characteristics of t-stilbene Single Crystals" *Dyes and Pigments*. 160 (2019) 848-852. **V. Govindan**, D. Joseph Daniel, H. J. Kim, K. Sankaranarayanan, "Crystal Growth and Characterization of 1,3,5-triphenylbenzene organic scintillator crystal" *Journal of Materials Chemistry and Physics*. 223 (2019) 183-189. **V. Govindan**, K. Sankaranarayanan, B. Venkatraman, M.T. Jose, A system for growing a unidirectional organic single crystal compound and method thereof, Patent No: 201641011210.

6:18 PM - 6:19 PM

TAILORING CHEMICAL STRESS TO SUPPRESS CRACKING OF SCINTILLATOR CRYSTALS DURING BRIDGMAN GROWTH

C. Zhang¹, B. Gao², A.S. Tremsin³, D. Perrodin⁴, G.A. Bizarri⁴, E.D. Bourret⁴, D.R. Onken⁴, S.C. Vogel⁵, J.J. Derby¹

¹University of Minnesota, MN, UNITED STATES OF AMERICA,

²Wuhan University, CHINA, ³University of California at Berkeley, CA,

UNITED STATES OF AMERICA, ⁴Lawrence Berkeley National

Laboratory, CA, UNITED STATES OF AMERICA, ⁵Los Alamos

National Laboratory, NM, UNITED STATES OF AMERICA

The U.S. DOE NNSA Advanced Materials for Detectors project has identified new classes of promising scintillators for gamma ray detection, comprising mixed halides, doped or co-doped with activators. However, the small crystals grown during this exploratory research will require the development of crystal growth processes for their production at larger scale. This has traditionally been a long and

arduous endeavor, since the operation of a large-scale melt crystal growth process is typically limited by minimal real-time diagnostics. Thus, process development relies on slow, iterative improvements usually based on indirect, post-growth destructive observations. In this presentation, we discuss how these approaches are synergistically addressing the many challenges to grow large, single crystals of scintillator materials. We specifically consider europium-doped barium bromium chloride, BaBrCl:Eu, which is representative of these promising, new materials. Like many scintillator crystals, BaBrCl:Eu is plagued by cracking during crystal growth, which adversely impacts yield and increases production costs. We present an overview of models for crystal growth and stress arising from thermal and compositional effects. Via the application of these models, we find that BaBrCl:Eu, grown under different conditions, exhibit Eu profiles that may promote or inhibit crack propagation due to chemical stresses. Using model simulations, we explain the underlying mechanisms of flow and segregation that give rise to such stress distributions. Growth experiments are demonstrated to be consistent with model predictions. Significantly, we find that growth can be tailored to produce a compressive stress field at the surface of the crystal, thereby suppressing crack propagation. Similar outcomes can be obtained by varying heat flows through the melt and crystal using different furnace thermal profiles. Ultimately, the understanding obtained by model and experiment will truly allow the closing of the loop between materials quality, growth conditions, and process development.

6:19 PM - 6:20 PM

CRYSTAL GROWTH AND CHARACTERIZATION OF $\text{CEBR}_{3-x}\text{I}_x$ SCINTILLATORS

M. Loyd¹, L. Stand¹, D. Rutstrom¹, J. Glodo², K.S. Shah³, M. Koschan¹, C.L. Melcher¹, M. Zhuravleva¹

¹University of Tennessee, TN, UNITED STATES OF AMERICA,

²Radiation Monitoring Devices, MA, UNITED STATES OF AMERICA,

³RMD, MA, UNITED STATES OF AMERICA

The search for a scintillator that has optimal properties for national

security applications is ongoing. CeBr_3 is an intrinsic scintillator that has promising performance capabilities such as 60,000 ph/MeV and ~4% energy resolution at 662 keV. It has been shown that halide mixing can improve the properties of single halide scintillators. In this work we attempted to improve on CeBr_3 by creating a mixed halide composition $\text{CeBr}_{3-x}\text{I}_x$. 13 mm diameter crystals were grown using the vertical Bridgman technique, with x values between 0.03 and 1. The $\text{CeBr}_{2.5}\text{I}_{0.5}$ crystal segregated into two sections, colorless and green, while the CeBr_2I crystal was entirely green. The green and colorless phases were examined using powder X-ray diffraction and dynamic vapor sorption. All crystals were characterized using photoluminescence, radioluminescence, decay time, and gamma spectroscopy. Decay time increased as iodine concentration increased. All clear phase crystals reached < 4.5% energy resolution at 662 keV and > 65,000 ph/MeV, with the $\text{CeBr}_{2.94}\text{I}_{0.06}$ crystal achieving 3.9% energy resolution at 662 keV. The green phase crystals both reached light yields of 78,000 ph/MeV, the highest ever recorded for a CeI_3 phase crystal.

6:20 PM - 6:21 PM

GROWTH AND THE INFLUENCE OF Ce^{3+} CONCENTRATION ON THE SCINTILLATION PROPERTIES OF $\text{Cs}_2\text{LiYCl}_6$ CRYSTALS

G. Ren¹, Q. Wang¹, H. Li¹, J. Shi¹, S. Wang¹, J. Chen¹, S. Pan²

¹Shanghai Institute of Ceramics, Chinese Academy of Sciences, CHINA, ²School of Material Sciences and Chemical Engineering, Ningbo University, CHINA

The $\text{Cs}_2\text{LiYCl}_6:\text{Ce}$ (CLYC) crystal is regarded as a kind of promising scintillator to identify gamma-rays and neutrons. Several $\text{Cs}_2\text{LiY}_{1-x}\text{Cl}_3:\text{Ce}_x$ crystals doped with different Ce ($x=0, 0.001, 0.01, 0.02$) were grown by Vertical Bridgman method. The crystals boule could be separated into translucent, transparent and opaque parts from bottom to the top. The translucent part contains some unwanted secondary phases except CLYC and the transparent part is only composed of CLYC single crystals with elpasolite structure. It is suggested that CLYC is an incongruent compound. For the transparent part, two

optical absorption bands, 220nm and 350nm can be observed. In the X-ray excited luminescence, a strong emission band between 350-450nm can be fitted into two peaks, 374nm and 397nm, which are corresponding to the transitions of electron from $5d_1-^2F_{5/2}$ and $5d_1-^2F_{7/2}$ of Ce^{3+} respectively. In addition, a very weak luminescence band around 300nm was also observed and is suggested to result from the core-valence luminescence (CVL). It was found that that the luminescence intensity of CVL and the emission wavelength of Ce^{3+} are affected by the concentrations of Ce ions in the crystals. The overlap between PLE and PL spectra demonstrated that self-absorption effect exists in $Cs_2LiYCl_6:Ce^{3+}$ single crystal. Of all samples doped with different Ce concentration, the best energy resolution, 5.9%@622keV was achieved at a concentration of 0.1mol% Ce^{3+} . Three different luminescence decay component: CVL, direct electron-hole capture by Ce^{3+} , binary V_k and electron diffusion could be identified. The scintillation decay time of direct electron-hole capture by Ce^{3+} decreasing with increasing Ce^{3+} concentration proved Ce^{3+} concentration quenching effect in Cs_2LiYCl_6 crystals. The calculated light yield is 18000 ± 1000 Ph./MeV, which is closed to that reported in literature.

6:21 PM - 6:22 PM

CS2HFCL6: A NOVEL LARGE DIAMETER SCINTILLATOR CRYSTAL

R. Hawrami¹, E. Ariesanti¹, A. Burger¹, S. Motakef²

¹Fisk University, TN, UNITED STATES OF AMERICA, ²CapeSym, Inc., MA, UNITED STATES OF AMERICA

Abstract— Cs_2HfCl_6 (CHC) is a recently discovered non-hygroscopic intrinsic scintillator with a simple cubic crystal structure. In this paper we will present a successful development of a large diameter, single crystal, and crack free growth of Cs_2HfCl_6 (CHC) as well as improvement to its radiometric and scintillation performance. A single one-inch diameter crystals CHC boule is grown using the vertical Bridgman method. Samples retrieved from the boule are characterized for their scintillation properties. Excellent energy resolution of 3.5%

(FWHM) at 662 keV has been obtained. Excellent gamma-ray non-proportionality of CHC compared to those of NaI:TI and BGO is also reported.

6:22 PM - 6:23 PM

DIELECTRIC SPECTROSCOPY IN FERRO TRANSITION OF TGS CRYSTAL

H.V. Alexandru

University of Bucharest, ROMANIA

Triglycine sulphate crystal (TGS) has a typical second order phase transition around 49°C. Alpha-A Novocontrol spectrometer was used for dielectric measurements (1-10⁶ Hz), between 65°C and -120°C at a pace of 0.6°C/minute. Four distinct temperature stages (T_c-45-40-35-30/25°C) of the dielectric parameters were found, walking the temperature down-up-down, crossing the Curie point. The conduction component of the imaginary component of permittivity and other associate parameters, show an instability in all three runs performed and a non-Arrhenius temperature dependence on the interval 45°C-T_c, not mentioned in the literature. In the Cole-Cole representation, there are two main relaxations. The **higher frequency** one $\tau_H \sim 5 \cdot 10^{-7}$ **sec**, associated with the group Glycine **GI** from the structure, is related with the “critical slowing down” mechanism involved in the long distance order in the lattice and with the second order transition in TGS. The **lower frequency** relaxation $\tau_L \sim 10^{-3}-10^{-1}$ **sec**, related with the ferroelectric domain evolution has an Arrhenius temperature dependence with the activation energy of **0.65-0.70 eV**. An unusual, smaller **middle frequency relaxation** $\tau_M \sim 10^{-4}$ **sec**, not mentioned in the literature so far, was found present only on the temperature range T_c-35°C. This relaxation seems to be associated with the dynamic of the glycine group **GII-GIII**, joined by a Hydrogen bridge in the structure of TGS. From the temperature dependences of conductivity and of the frequency coefficient N (also temperature dependent) we have concluded the influence of 49°C ferroelectric transition of TGS, was really finished at 30/25°C.

6:23 PM - 6:24 PM

FLOATING-ZONE GROWTH OF FLUORITE STRUCTURE OXIDES

D. Prabhakaran¹, J. Harrison¹, M. Schulze², R. Schondube², A. Boothroyd¹

¹Clarendon Laboratory, University of Oxford, UNITED KINGDOM,

²SciDre- Scientific Instruments Dresden GmbH, GERMANY

Compounds with the general formula $A_2B_2O_6O'$ have been extensively studied to explore their magnetic and structural properties. Among these, cubic pyrochlore compounds are well studied due to interesting properties such as magnetic monopoles, spin-liquid phases and metal-insulator transitions. In contrast, rare earth hafnate and zirconate compounds with fluorite structure are less studied. Due to the absence of an O' oxygen site, the magnetic properties of these compounds vary as a result of rare earth interaction. Both hafnate and zirconate have a very high melting point ($>2300^\circ\text{C}$) and also have high temperature structural transition ($> 1500^\circ\text{C}$) which limits the crystal size. Volatility of the hafnium oxide is another challenging problem. We have grown the crystals using Xenon lamp floating-zone furnace, Scientific Instruments, Dresden. The purity of the material was confirmed both before and after the crystal growth process. We will discuss the growth conditions, magnetic properties and crystal quality.

6:24 PM - 6:25 PM

GROWTH AND ELECTRIC PROPERTIES OF Ca_2RuO_4 SINGLE CRYSTALS

A. Vecchione¹, C. Cirillo¹, G. Avallone², V. Granata², R. Fittipaldi¹, A. Ubaldini¹, A. Avella², C. Attanasio²

¹CNR - SPIN, ITALY, ²Università di Salerno, ITALY

We report on the growth by floating zone technique of single crystals of Ca_2RuO_4 showing a unique insulator-metal transition even at room temperature induced by applying a relatively low level voltage or d.c. current. This transition is accompanied by a bulk structural change of the system. By combining two different experimental probes, namely electrical transport measurements and X-Ray Diffraction, a study of

the conduction response of the Mott insulators Ca_2RuO_4 from macroscopic to microscopic scales is presented. In particular, the $\rho(J,T)$ phase diagram for both the ab-plane and c-axis configurations is traced, which provides useful information concerning the intermediate region between the insulating and the metallic states. The results are supported by a microscopic analysis of the crystallographic changes occurring during the change in the conduction regimes.

6:25 PM - 6:26 PM

CORRELATION BETWEEN THE Mg_2Si PRECIPITATES AMOUNT FORMATION AND THE MECHANICAL PROPERTIES OF AL-SI AND AL-SI-MG ALLOYS.

Z. Sersour¹, L. Amirouche²

¹Université M'Hamed Bougara de Boumerdès, ALGERIA, ²University of sciences and technologie Houari boumedienne Algeria, ALGERIA
In this study, the effect of Mg_2Si precipitates amount, formed in the as-cast state and after heat-treatments of some Al-Si based alloys, is investigated. Destined to automotive industry, Al-Si alloys are used at eutectic and near-eutectic compositions, due to their remarkable mechanical properties, already at the as-cast state [1]. Moreover, the addition of ternary and even quaternary elements, such Mg and Cu, makes these alloys heat treatable, giving rise to an enhancement in their hardness and their tensile properties, mainly due to hardening precipitates formation such as Mg_2Si and Al_2Cu . Three different alloys AS13, AS10G and AS7G06, having various Mg amounts (0% , 0.22%, 0.44%) respectively, were prepared through casting process in the form of test bars. In the present experimental investigation, the test bars were divided into three groups of samples. Whereas the first group was kept in the as-cast state for comparison, the other groups were subject to T6 and T5 treatments in the aim to detect a peak hardness. Thus, the second group underwent a T6 process, consisting of homogenizing at 540°C for 10 h, followed by quenching in cold water and then aging for 4h at 160°C . The last group was subject to a T5 process consisting of isothermal annealing, at different temperatures, for times ranging from 0.5 h to 8 h. It should be noted

that T6 treatment is mostly used in industry due to its particular efficiency [1-2]. All the samples (as-cast and heat treated) were characterized with scanning electron microscopy, X-Ray Diffraction and Vickers microhardness measurements. The latter were analysed along with tensile tests to estimate the mechanical properties enhancement. The quantities of Mg_2Si precipitates formed in the microstructures, of the three alloys corresponding to different Mg amounts, were examined using a semi-quantification of the XRD patterns. It was observed that in the as-cast condition, the highest value of microhardness is obtained, as expected, for AS7G06 alloys. As well, after heat treating, the peak hardness was surprisingly observed, for the same alloy in the T5 condition: after annealing at $500^\circ C$ for 5h. It turns out, that T5 treatment has proven to be more efficient, in terms of Mg_2Si precipitates amount formation and peak hardness location, than T6 process. However, the latter was observed to be more adequate for tensile properties improvement. [1]Musa Yıldırım, Dursun Ozyurek, Materials and Design **51** (2013) 767–774 [2]Mohamed F.Ibrahim et al, International Journal of Metalcasting, **11** (2017) 274-286

6:26 PM - 6:27 PM

INFLUENCE OF Pb^{2+} IONS ON THE OPTICAL PROPERTIES OF GAMMA IRRADIATED BaF_2 AND CaF_2 CRYSTALS

I. Nicoara, M. Stef, D. Vizman

West University of Timisoara, ROMANIA

Pure BaF_2 and CaF_2 are transparent from ultra-violet to far-infrared region. Exposed to radiations, various absorption bands appear due to the formation of color centers. This effect is usually related to impurities and/or structural defects in the crystals [1, 2, 3]. The purpose of this study is to investigate the influence of small amount of Pb ions on the optical properties of the γ -irradiated BaF_2 and CaF_2 crystals. In spite of the fact that the addition of PbF_2 (~ 4%) in the BaF_2 and CaF_2 melt is used as scavenger in the crystal growth process, sometimes a trace of Pb^{2+} are found in the obtained crystals. Pure and PbF_2 doped BaF_2 and CaF_2 crystals have been obtained

using the conventional Bridgman technique [4]. The samples were irradiated at room temperature with γ rays from a ^{60}Co source. Optical absorption (OA) spectra were recorded before and after irradiation. The additional absorption spectra ($\Delta A = \alpha - \alpha_0$, where α and α_0 are the absorption coefficient after and before γ -irradiation) were calculated and decomposed by Gaussian multi-peak fit in order to identify the main absorption bands and to analyze the effect of irradiation. In the case of BaF_2 , a very broad band (300-840 nm) is present in the OA spectra with maximum at 460 nm. The following color centers were identified: new lead centers [5] $\text{Pb}^+(1)$, $\text{Pb}^+(1) - \text{Pb}^{2+}$ dimer and V_k , F centers. Two broad peaks, centered on 400 nm and 730 nm, characterizes the OA spectra of γ irradiated $\text{PbF}_2:\text{CaF}_2$ samples. The following types of centers were observed: $\text{Pb}^0(2)$, $\text{Pb}^+(1) - \text{Pb}^{2+}$, V_k , F and F_i^0 . The optical properties of the γ -irradiated crystals are significantly affected by the presence of trace quantities (at the 40 ppm level) of lead ions, so they are not good material for applications in which the new optical absorption bands are undesirable.

References: [1] C. Pandurangappa, B.N. Lakshminarasappa, J. of Luminescence 138 (2013) 61. [2] D. W. Cooke, B. L. Bennett, J. Nuclear Materials 321 (2003) 158. [3] L. Su, et al., S.S. Communications 132 (2004) 757-760. [4] D. Nicoara and I. Nicoara, Mater. Sci. Eng. A 102 (1988) L1. [5] M. Fockele, F. Lohse, J-M. Spaeth, R.H. Bartram, J. Phys.: Condens. Matter 1 (1989)13.

6:27 PM - 6:28 PM

SOLVATION AND PHASE DISSOCIATION OF DARBONIC DIHYDRAZIDINIUM BIS[3-(5-NITROIMINO-1,2,4-TRIAZOLATE)] INDUCED BY SOLVENTS

H. Li, J. Ren, D. Chen

Institute of Chemical Materials, China Academy of Engineering Physics, CHINA

Solid-state stability is one of the most important properties of explosives because it is strongly related with energy, safety, reliability and lifespan of weapon. However, explosive crystals exist different solid forms, i.e., polymorphs, solvates, salts, cocrystals, which have

variable detonation performance, mechanical and safety properties as well as physicochemical properties such as density, stability, solubility, and hygroscopicity. A search for new solid forms of an energetic compound is an integral part of the explosive product development process. The studied compound, carbonic dihydrazidinium bis[3-(5-nitroimino-1,2,4-triazolate)] (CBNT), is a recently synthesized high energy low sensitivity explosive with potential applications in weapon systems. The main aim of this study was to investigate the crystal structure evolution and search for new solid forms of CBNT under different conditions via solvent screening method. The solid forms screening experiments were carried out in a systematic way. In details, five different crystallization methods were used in this work such as quick cooling, slow cooling, quick evaporation, slow evaporation and slurry methods. Ten different solvents, i.e., DMSO, DMF, DEF, NMP, BL, H₂O, MT, EA, DMF/H₂O and BL/H₂O, were used in the solid forms screening experiments. Ten powder samples and four single crystal samples were obtained under those crystalline conditions. The dihydrate of CBNT·2H₂O can be obtained in water solvent. In the solvent of DMSO and BL/H₂O, CBNT was dissociated into H₂BNT and (NH₃NH)₂CO, and then H₂BNT was combined with DMSO and H₂O to form the single crystals of H₂BNT·2DMSO and H₂BNT·2H₂O, respectively. In the solvent of DMF/H₂O, CBNT was also dissociated into H₂BNT and (NH₃NH)₂CO, and then the crystals of [NH₂(CH₃)₂⁺]₂[BNT²⁻]·2H₂O were formed. The crystal structures of four new crystals were confirmed by single-crystal X-ray diffraction and reported for the first time. The results indicated that the crystal structure of CBNT is dissociated easily in polar solvents, i.e., DMSO, DMF, DEF, etc, which must be avoided to process CBNT. The molecular interactions of four new crystals were analyzed by theoretical simulations of Hirshfeld surface and molecular electrostatic potentials and explain the plausible mechanism for the crystal structure evolutions of CBNT.

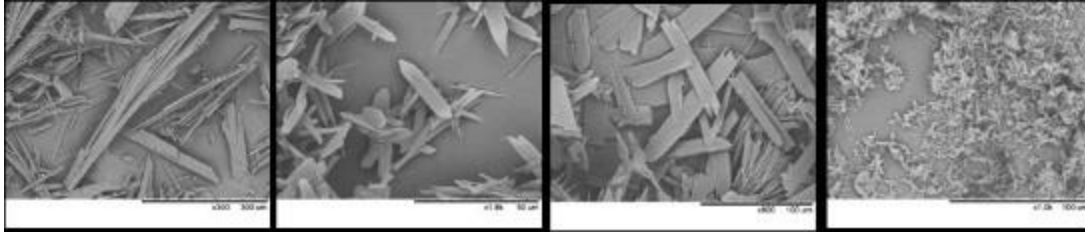


Figure 1. SEM images of $\text{CBNT} \cdot 2\text{H}_2\text{O}$, $\text{H}_2\text{BNT} \cdot 2\text{DMSO}$, $\text{H}_2\text{BNT} \cdot 2\text{H}_2\text{O}$, and $[\text{NH}_2(\text{CH}_3)_2^+]_2[\text{BNT}^{2-}] \cdot 2\text{H}_2\text{O}$

6:28 PM - 6:29 PM

PHASE EQUILIBRIUMS IN THE BINARY CdAs_2 -MnAs SYSTEM

O. Rabinovich¹, S. Marenkin¹, A. Ril², I. Fedorchenko², S. Sizov¹

¹NUST MISIS, RUSSIAN FEDERATION, ²Kurnakov Institute of General and Inorganic Chemistry, Russian Academy of Science, RUSSIAN FEDERATION

The giant magnetoresistance and tunnel magnetoresistance effects magnitude in magnetically granular structures is less than in superlattices, but these structures have some advantages.

Components that form an eutectic composition and have low inter solubility are more preferred for a magneto-granular structure in semiconductor-ferromagnet systems. In that case simultaneous components crystallization of an eutectic melt during the cooling takes place. This leads to the specific fine-dispersed structure creation. The ultra-high alloy supersaturation leads to a significant supercooling of all phases, and causes metastable crystallization. These factors leads to a synergistic effect, contributing to nanostructuring for granular structure creation. In this work the interaction in the CdAs_2 – MnAs system is investigated. CdAs_2 is a semiconductor with a band gap 0.9 eV (1.14 eV at 0 K), and has considerable anisotropic of optical and electric properties. It is crystallized in the tetragonal structure (space group $I4_122$) with the unit cell parameters: $a=7.954 \text{ \AA}$, $c=4.678 \text{ \AA}$. The chemical bonding peculiarities in the CdAs_2 crystal (there are As-As bond, along with Cd-As bonds) contribute to the semiconductor crystallization with significant supercooling. In order to choose optimal compositions and synthesis parameters for grained structures, we have studied phase equilibrium in the CdAs_2 – MnAs system using a

set of physicochemical methods. CdAs₂—MnAs system was investigated by X-ray powder diffraction (XRD), differential thermal analysis (DTA), optical and scanning electron microscopy (SEM). Differential scanning calorimetry (DSC) of the samples was carried out in a Q20 system (TA Instruments) at heating and cooling rates from 6 to 18 °/min in temperature interval 0-100 °C. Heating and cooling cycles DTA of the alloy 94 mol % CdAs₂ and 6 mol% MnAs are presented in Fig. 1. The DSC curves showed the structural transformation effect from hexagonal to orthorhombic modification of the $\alpha \rightarrow \beta$ MnAs. The curve clearly shows the reversible thermal effect. CdAs₂—MnAs system phase diagram was investigated by DTA, X-ray and SEM data and presented in Fig. 2. The eutectic coordinates are 94 mol.% CdAs₂ and 6 mol.% MnAs, with $T_{\text{melt}}=614$ °C.

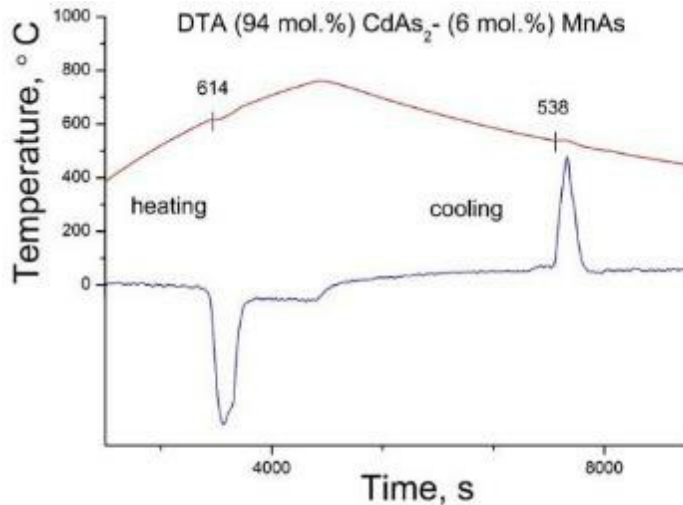


Figure 1

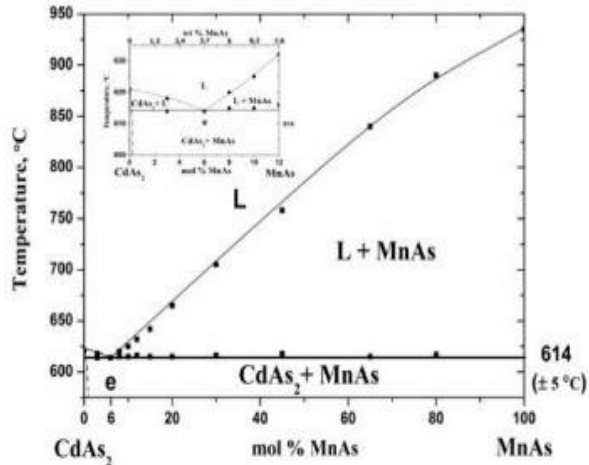


Figure 2

6:29 PM - 6:30 PM

MNSB THIN FILMS GROWTH BY PVD METHOD

O. Rabinovich¹, S. Marenkin¹, A. Ril², I. Fedorchenko², S. Sizov¹, M. Orlova¹

¹NUST MISIS, RUSSIAN FEDERATION, ²Kurnakov Institute of General and Inorganic Chemistry, Russian Academy of Science, RUSSIAN FEDERATION

Manganese antimonide is a ferromagnetic semimetal with a high Curie temperature up to 600 K. This compound attracts attentions due to unique properties, such as ferromagnetism, magneto-optical effect and high magnetic anisotropy. Nowadays hybrid structures of ferromagnetic semimetal-semiconductor are widely investigated. Such structures synthesis is possible both as films and as system with ferromagnetic micro- and nanoclusters embedded in semiconductor matrix. It was predicted that the superconducting state in MnSb compound will be at low temperatures under the external pressure influence. The crystalline and electrical MnSb properties compatibility with semiconductor compounds is valuable for the hybrid structures at the effective spin diodes or transistors production. Manganese antimonide films are generally synthesized by molecular-beam epitaxy. This method is complicated and does not allow obtaining films with a thickness more than 10-15 nm. Due to the low manganese antimonide content, the films have a low sensitivity to the magnetic

field. The films with bigger thickness could be synthesized by vacuum thermal evaporation. The method limitation is the incongruent character of the manganese antimonide evaporation $\text{MnSb}_{\text{con}} = \text{Mn}_{1+x}\text{Sb}_{\text{con}} + \text{Sb}_{\text{gas}}$. Manganese and antimony evaporation temperatures for achieving the MnSb stoichiometric composition were selected based on the metal vapor flux density calculations. The investigation of temperature influence on adhesion and structural perfection showed that the optimum temperature range for films annealing was from 380 to 420 °C. The composition, structure, and nanocrystallites size in the films were determined by X-ray diffraction and microstructural analysis. The structure of the films, their composition and elements distribution were investigated by X-ray phase analysis (XRD), optical and scanning electron microscopy (SEM).

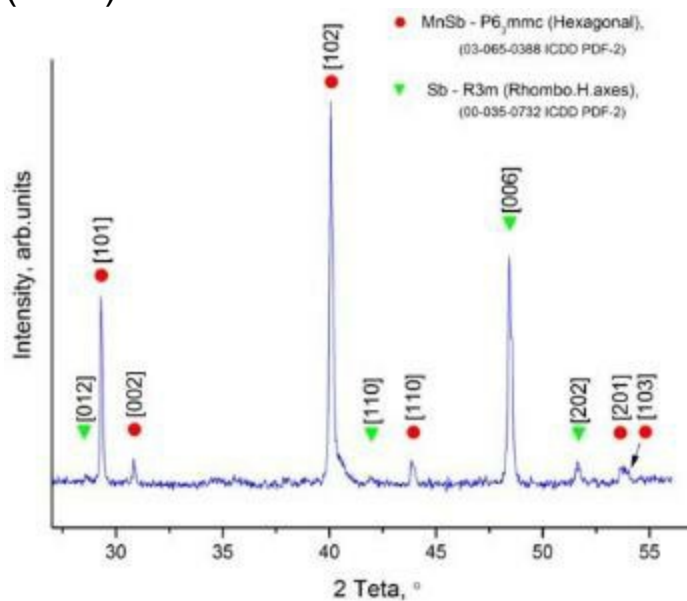


Figure 1. Mn + Sb films diffraction patterns after annealing at 400 °C.

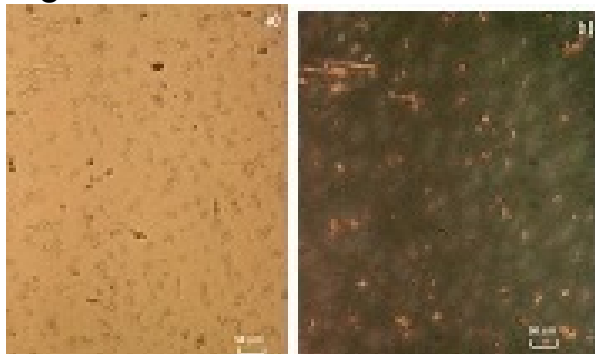


Figure 2. a) film microstructure with Mn and Sb layers, $d \sim 400$ nm; b)

the same film after annealing at 400°C.

6:30 PM - 6:31 PM

TWO-DIMENSIONAL STRUCTURES FORMED BY SPHERICAL PATCHY PARTICLES

M. Sato

Information Media Center, Kanazawa University, JAPAN

Colloidal particles with site-specific directional interactions, which we call patchy particles, are promising candidates as building blocks for materials forming complex structures. By carrying out theoretical studies and simulations, many groups have studied the equilibrium structures that the patchy particles form, but the process of reaching the equilibrium structures have not studied sufficiently. We carry out Monte Carlo simulation and Brownian dynamics simulation for spherical patchy particles having one attractive patch, and study two-dimensional structures and the process of formation the structures. In our simulation, we use the Kern-Frenkel potential as an attractive potential between patchy particles and show how two-dimensional structures depend on the ratio of patch area and the attraction length. When the attraction length is long and the ratio of patchy region is small, particles form square clusters, which are not formed with a short length interaction. The square clusters arrange regularly when the particle density is large. When the ratio of patch region to the entire surface area increases but is smaller than 50%, two rows of particles form string-like structure. With a high pressure, a structure in which the rows of triangular lattice and that of square lattice appears alternatively is formed. In the both cases we mentioned above, the patch direction is mainly in the plane where the particles are set. When the ratio of patchy region exceeds 50%, the patch direction is perpendicular to the plane and the particles form a square lattice.

6:31 PM - 6:32 PM

PRE-NUCLEATION AND PARTICLE ATTACHMENT OF BISMUTH TRI-IODIDE ONTO GRAPHENE SUBSTRATES

L. Fornaro, D. Ferreira, H. Bentos Pereira, A. Olivera

CURE, URUGUAY

Nucleation of BiI_3 was performed by physical vapor deposition (PVD)

onto graphene TEM grids as substrates. Depositions were characterized by High Resolution Transmission Electron Microscopy (HR-TEM), Selected Area Electron Diffraction (SAED), Energy Dispersive Spectrometry (EDS), and Scanning Electron Microscopy with Field Emission Gun (SEM-FEG). Crystalline entities about 5-10 nm in size were observed. Plates up to about 50-100 nm in size were also obtained, similar when imaged by TEM and by SEM. TEM images show clear Moiré diagrams of these plates, which were evaluated and compared with similar ones obtained for other van der Waals superstructures. In addition to these structures, amorphous entities about 2-3 nm in size can be clearly observed. They remain even under the TEM beam, suffer rapid transformations between ordered and disordered structures, as video captures show. FFTs of such structures reveal they are amorphous. Given their size and amorphous character, these last entities result to be very similar to the ones reported as pre-nucleation clusters in solution and chemical vapor deposition (CVD) systems in the framework of non-classical nucleation research. Furthermore, results were similar to previous ones obtained for bismuth tri-iodide onto amorphous substrates, although with differences dictated by the crystalline substrate. Although we cannot say if we are observing pre-nucleation clusters or amorphous nanoparticles, formed by the aggregation of pre-nucleation clusters, these entities are an intermediate metastable phase, are not crystals -as should be according to Classical Nucleation Theory (CNT)-, and such phase is not the one of the bulk crystal, as CNT dictates as well. Then, we conclude that they are not nucleus but pre-nucleation entities. On the other hand, the oriented attachment of entities about 2-3 nm in size giving larger ones of about 10-20 nm can be observed. Nanoparticles neither grow by adding new ions, atoms or molecules, nor form a larger circular one by coalescence as CNT predicts, but interact among them by oriented attachment, giving a stable and oriented structure, crystalline and oriented. This is in agreement with the crystallization by particle attachment (CPA) mechanism, in the framework of non-classical nucleation investigations. Results are in accordance with similar ones obtained for several compounds in solution-solid and vapor-solid systems, and may be valuable contributions to develop a general theory to non-

classical nucleation mechanisms in all kind of systems. Furthermore, they contribute to the development of 2D van der Waals materials and may be valuable for several technological applications.

6:32 PM - 6:33 PM

ROLE OF ELECTRON TUNNELING IN THE THERMALIZATION OF THE ADSORBATE AT SOLID SURFACES

S. Krukowski, P. Strak, P.T. Kempisty, K. Sakowski

Institute of High Pressure Physics PAS, POLAND

A new type of the thermalization of the adsorbates at solid surfaces is presented. The scenario is based on an existence of the electric dipole layer at solid surfaces in which the electron wavefunctions extend beyond the positive ions line creating strong local electric field which drags the electrons into the solid interior and repels the positive ions. During adsorption of any molecular or atomic species, the field enforces the electrons tunnelling into the solid interior. In the process they are drastically accelerated acquiring high kinetic energy which is transported into the depth of the crystals. The electron stripping of the adsorbates creates positive charged ions (atoms or molecules) which are retarded by the field, losing most of the excess kinetic energy. In the results they are located smoothly into the adsorption sites.

According to the scheme, the excess kinetic energy is not dissipated locally thus avoiding local melting of the lattice or creation of defects at the impact site. That explains the absence of kinetic surface damage which is in accordance with the experiments. The scenario is supported by the *ab initio* calculation results including density function theory of the slabs representing AlN surface and the Schrodinger equation for time evolution of hydrogen-like atom at the solid surface [1,2]. [1] P. Strak, P. Kempisty, K. Sakowski, S. Krukowski, *Phys. Chem. Chem. Phys.* **19** (2017) 9149 [2] P. Strak, P. Kempisty, K. Sakowski, S. Krukowski, *J. Phys. Astron.* **5** (2017) 4

6:33 PM - 6:34 PM

HABIT MODIFICATION OF L-ARGININE DOPED POTASSIUM DIHYDROGEN PHOSPHATE CRYSTALS GROWN UNDER ELECTRIC FIELD

A.S. Mahadik¹, P.H. Soni², A.R. Mithani³

¹The Maharaja Sayajirao University of Baroda, INDIA, ²The Maharaja Sayajirao University of Baroda, INDIA, ³PARUL UNIVERSITY, INDIA

Abstract: Potassium Dihydrogen Phosphate (KDP) crystal is a versatile dielectric material having good NLO properties. KDP crystals have prototype habits when grown from solution. We have grown the crystals under applied electric field and have observed habit change of L-Arginine (1 mol%) doped KDP crystals grown in presence of constant applied electric field. Both pure and L-Arginine (1 mol%) doped KDP crystals were grown using slow evaporation method at room temperature in presence as well as in absence of electric field. We found that the crystals grown in presence of electric field differ in size compared to the crystals grown in absence of electric field. The dopant inclusion in the crystals was confirmed using Fourier transform infrared (FT-IR) spectroscopy and Powder X-Ray Diffraction (XRD). The XRD results also confirm the tetragonal structure with lattice parameters $a=b=7.45 \text{ \AA}$ and $c=6.98 \text{ \AA}$. Using the FTIR spectra the presence of functional groups of crystals was analyzed. Both the pure and doped KDP crystals were characterized using Raman Spectroscopy, UV-Visible spectroscopy and Dielectric analysis. For band gap evaluation, UV-Vis spectra were used. The crystals grown in electric field exhibit good transparency as compared to the crystals grown without applied electric field. The results are discussed.

6:34 PM - 6:35 PM

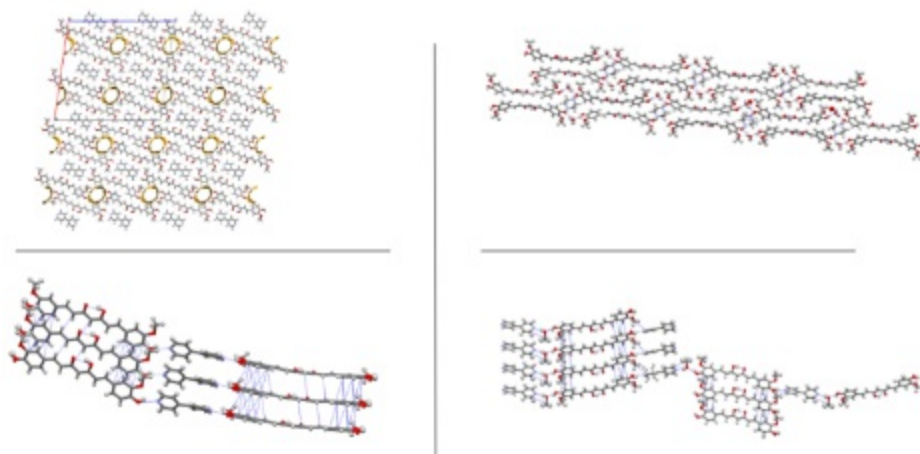
PHOTOCHROMIC COCRYSTAL OF CURCUMIN (POSTER PRESENTATION)

L.K. Altahrawi

university of Lincoln, UNITED KINGDOM

Curcumin, (1E,6E)-1,7-bis (4-hydroxy- 3-methoxyphenyl) -1,6-heptadiene-3,5-dione, is extracted from the spice turmeric and within the context of cuisine is utilized for its distinctive orange to yellow colour¹ Curcumin has been known for its poor propensity for both direct crystallization and co-crystallization to alter physiochemical properties such as solubility. The attrition rate for curcumin co-crystallization is about 1%. Therefore, the careful choice of the cofomers' functional groups and the cocrystallization solvents are crucial for successful hydrogen bond interaction. As a dye, curcumin is

a potential component of crystal with chromic behavior. In this regard, the aim was to target the hydroxyl group of curcumin with amine and pyridine nitrogen and study the packing and motif features. Therefore, this contribution is to highlight the outcomes to date on the co-crystallization of curcumin with piperazine, 4,4' bipyridine. Crystallization was undertaken using a solvent evaporation approach and will be presented. To date even with curcumin's poor propensity for crystal growth, three different binary cocrystals with piperazine and, 4,4' bipyridine, figure 2, have been obtained. The phenolic hydroxyl group of curcumin was found to participate in the hydrogen bond formation in all the resultant cocrystals. Moreover, the solvent choice was shown to be affecting the polymorphism of the 4,4' bipyridine cocrystals. The cocrystals were characterized using SC-XRD, PXRD, DSC, and IR.



References: 1. A. Marchiani, C. Rozzo, A. Fadda, G. Delogu and P. Ruzza, *Curr. Med. Chem.*, 2014, 21, 204–22.

6:35 PM - 6:36 PM

PHASE FORMATION IN $TBaAl_3(BO_3)_4-(K_2MO_3O_{10}-B_2O_3-AL_2O_3)$ FLUX SYSTEM AND CRYSTAL STRUCTURE OF $TBaAl_3(BO_3)_4$ MONOCLINIC MODIFICATION

E. Volkova, E. Latanova, O. Reutova, N. Leonyuk
Lomonosov Moscow State University, RUSSIAN FEDERATION
Rare-earth aluminum borates with the general formula $RAI_3(BO_3)_4$ ($R=Y$ or lanthanide) have come into the focus of interest as a multifunctional solids with favorable physical and chemical properties,

such as perfect chemical and mechanical stability, high transparency, high thermal coefficient, and, in particular, a very high nonlinear optical coefficient. Among them, $\text{TbAl}_3(\text{BO}_3)_4$ (TbAB), can be explored as magneto-optic borate matrix [1,2]. However, there is a lack of data on crystal growth, thermal and optical properties of $\text{TbAl}_3(\text{BO}_3)_4$ so far. In this connection, this presentation mainly concerns with the basic results on the investigation of growth conditions of TbAl-borate crystals with subsequent comprehensive characterization of their functional properties. Taking into account peculiarities of phase formation in previously studied borate-based complex flux systems, in particular $\text{YAl}_3(\text{BO}_3)_4\text{-K}_2\text{Mo}_3\text{O}_{10}\text{-B}_2\text{O}_3\text{-Y}_2\text{O}_3$, $\text{GdAl}_3(\text{BO}_3)_4\text{-K}_2\text{Mo}_3\text{O}_{10}\text{-B}_2\text{O}_3\text{-Gd}_2\text{O}_3$, and $\text{YbAl}_3(\text{BO}_3)_4\text{-K}_2\text{Mo}_3\text{O}_{10}\text{-B}_2\text{O}_3\text{-Yb}_2\text{O}_3$ [3,4], phase relationships in the $\text{TbAl}_3(\text{BO}_3)_4\text{-K}_2\text{Mo}_3\text{O}_{10}\text{-B}_2\text{O}_3\text{-Tb}_2\text{O}_3$ system have been studied in the temperature range 1150 -800°C. Spontaneous crystallization of TbAl-borate has been investigated for 15, 17, 20 and 25 wt.% of borate concentration in the fluxed melt. As a result, phase formation features, as well as effect of the flux composition on the crystal size and morphology, are discussed. Structural investigation of TbAB crystals established the formation of monoclinic modification besides of common for all $\text{RAl}_3(\text{BO}_3)_4$ solids huntite-type form. This structure has been assigned to the $C2$ space group on the basis of XRD measurements. This research was supported in part by the RFBR grant # 18-29-12091 mk. [1] J. Lu, C. Fu, and J. Chen, *Applied optics*, 2011, 50, 116. [2] M. I. Pashchenko *et al.*, *Low temperature physics*, 2017, 43, 631. [3] N.I. Leonyuk and L.I. Leonyuk, *Prog. crystal growth and charact.*, 1995, 31, 179. [4] L.V. Nekrasova and N.I. Leonyuk, *J. Crystal Growth*, 2008, 311(1), 7.

6:36 PM - 6:37 PM

ELECTRICAL AND OPTICAL PROPERTIES OF ZR DOPED $\beta\text{-G}_2\text{O}_3$ SINGLE CRYSTALS GROWN BY CZOCHRALSKI METHOD

M. Saleh¹, J.B. Varley², S. Swain¹, A. Bhattacharyya³, J. Jesenovec¹, S. Krishnamoorthy³, K. Lynn¹

¹Washington State University, WA, UNITED STATES OF AMERICA,

²Lawrence Livermore National Laboratory, CA, UNITED STATES OF

AMERICA, ³The University of Utah, UT, UNITED STATES OF AMERICA

β -Ga₂O₃ possesses uniquely advantageous physical properties over traditional semiconductors such as Si, GaN and SiC. To fully realize its disruptive potential in microelectronics and opto-electronics, understanding of defects, doping and their relation to crystal growth conditions is critical. Tunable n-type conductivity of β -Ga₂O₃ single crystals grown from the melt over a wide range of free carrier concentration up to 10¹⁹cm⁻³ has been demonstrated in the literature with controllable doping in the range of 10¹⁵-10¹⁹ cm⁻³ using Sn, Si, and Ge doping. Zirconium (Zr) doping is used in this study to investigate approaches to increase and control n-type conductivity in β -Ga₂O₃ grown using the Czochralski method employing atomistic hybrid functional calculations in conjunction with a range of electro-optical characterization techniques including UV-VIS-NIR, Hall Effect, I-V, and C-V, deep level transient spectroscopy (DLTS), thermoelectric effect spectroscopy (TEES), and positron annihilation spectroscopy (PAS). Single crystals with initial Zr doping between 0.05-0.25 at% were grown from the melt using Czochralski and vertical gradient freeze methods in Ar+O₂ environment using Iridium crucible. Relatively lower vapor pressure of Zr as compared to Sn, which has been the dopant of choice for n-type conductivity in β -Ga₂O₃, offers the advantage of incorporating higher doping concentrations. In this study, atomistic hybrid functional calculations show that Zr can be more readily incorporated in β -Ga₂O₃ than Sn. Dopant incorporation was confirmed by secondary-ion mass spectrometry (SIMS) measurements. Donor level with activation energy at ~10meV is detected; which is predicted to be due to Zr substituting for Ga_{II} octahedral site. Hybrid functional calculations predict shallow donor behavior of Zr with energy <100meV. Zr doped β -Ga₂O₃ studied here has electron mobility ~112cm²/Vs, resistivity ~0.07 ohm-cm, and room temperature carrier density of 10¹⁷-10¹⁸ cm³. Additionally, local chemical environment induced by Zr doping in as grown and post growth annealed crystals is also examined by PAS. PAS data in conjunction with DLTS and TEES are used to infer

possible defect formed in Zr:Ga₂O₃, upon comparison with Mg:Ga₂O₃ and undoped crystals grown using the same method.

6:37 PM - 6:38 PM

SILICON AND TIN DOPING OF EPSILON-GALLIUM OXIDE EPILAYERS GROWN BY MOVPE

R. Fornari¹, A. Bosio¹, M. Bosi², A. Parisini¹, Z. Zolnai³, A. Lamperti⁴,
V. Montedoro¹, C. Borelli¹, M. Pavese¹

¹Dept. of Mathematical, Physical and Computer Sciences, University of Parma, ITALY, ²IMEM-CNR, ITALY, ³Institute for Technical Physics, HAS, HUNGARY, ⁴IMM-CNR, ITALY

The different crystallographic phases (α , β , δ , ϵ , γ) of gallium oxide (Ga₂O₃) have been widely studied in the last years. Among the phases, the thermodynamically stable monoclinic β is the most investigated due to promising applications in deep-UV detection and power electronics. However, the orthorhombic ϵ -phase is also attracting attention thanks to its wide bandgap (about 4.6 eV), higher crystallographic symmetry and lower deposition temperature than the β -phase. It has been successfully deposited by MOVPE on various substrates [1] but so far there were no reports about efficient n-type doping. In this presentation we will report on two different experimental approaches for doping of ϵ -Ga₂O₃ epilayers deposited on c-oriented sapphire: i) addition of diluted silane to gaseous precursors during the MOVPE process and ii) post-growth diffusion of Sn in nominally undoped films. The latter process is carried out in two steps: first, a thin layer of SnO_x, few nm thick, is deposited by DC reactive sputtering on undoped films, followed by annealing at 600°C for at least 4 hours. After this procedure, the room-temperature (RT) resistivity of ϵ -Ga₂O₃ drops down to (1-5) Ω cm. A repeated SnO_x deposition (on the film surface accurately cleaned by chemical etching from the residuals of the first partially in-diffused SnO_x) and annealing provides further Sn incorporation, and finally brings the RT resistivity below 1 Ω cm.

Donor concentrations of up to 2×10^{18} cm⁻³ were obtained with both Si and Sn incorporation. The electrical characterization however showed

that Hall mobilities are low and suggested that the conduction takes place via hopping between localized states (impurity band conduction). Nevertheless, the resistivity of the doped layers is several orders of magnitude lower than in nominally-undoped ϵ -Ga₂O₃. The lowest RT resistivity was about 0.5 Ω cm, which opens the way to applications, although a better understanding of the donor behavior is still necessary in order to make the epilayers fully suitable for device fabrication.

We shall discuss the relative advantages and disadvantages of the two doping procedures, also considering the results of ToF-SIMS and Rutherford backscattering (RBS). The first technique was applied for semi-quantitative investigation of doping uniformity, while RBS allowed for analysis and modelling of the diffusion mechanisms that occur during thermal anneal of the SnO_x-coated epilayers.

[1] F. Boschi et al.: Hetero-epitaxy of ϵ -Ga₂O₃ layers by MOCVD and ALD; J. Crystal Growth 443 (2016) 25–30

6:38 PM - 6:39 PM

DESIGN, MODELING, AND IMPLANTATION OF AN IMPROVED INDUCTIVELY HEATED SUSCEPTOR FOR GALLIUM OXIDE

G. Tompa, M.E. Tawfik, T. Salagaj, A.C. Arjunan

Structured Materials Industries, Inc., NJ, UNITED STATES OF AMERICA

Ga₂O₃ is a wide bandgap semiconductor material, with properties appealing to produce power control devices and UV sensors. Ga₂O₃ is currently grown epitaxially on sapphire and Ga₂O₃ substrates using variety of techniques; such as, Mist -Chemical Vapor Deposition (Mist-CVD), Pulsed Laser Deposition (PLD), Molecular Beam Epitaxy (MBE), Hydride Vapor Phase Epitaxy (HVPE), and Metal Organic Chemical Vapor Deposition (MOCVD). Amongst these techniques, MOCVD is the most versatile for research and for industrial applications due its scalability, high growth rates, and proven electronic material manufacturability. The use of inductive heating is appealing in research reactors because it is easy to configure and provides access to wide temperature range (to $\sim 1200^\circ\text{C}$). Further, the heat is concentrated in the susceptor and thus minimizes the pre-reaction or

decomposition of precursors. Standard induction heating involves a disc which is immersed in the induction coil that provides a coupling with field, predominantly to the side of the susceptor which heats the center of the susceptor through conduction. Such a conduction-based heating can lead to a large thermal gradient resulting in a wafer property non-uniformity (thickness composition and quality). In order to achieve high yield epitaxial layers even in a small research scale reactor it is necessary to control the coupling geometry – this can be done with the coils and or susceptor geometry. We have designed, modeled, fabricated and tested a range of coils and susceptors. We report on our patent pending heater assembly that has shown a significant improvement in susceptor temperature uniformity. The technology reported here is applicable to many other materials systems; such as: III-Nitrides, Carbides, Silicides, 2-D materials, and other oxides among others.

6:39 PM - 6:40 PM

Yb³⁺ AND Yb²⁺ IONS DISTRIBUTION ALONG THE YbF₃ DOPED BAF₂ AND CAF₂ CRYSTALS

I. Nicoara, M. Stef, D. Vizman

West University of Timisoara, ROMANIA

Pure and doped fluoride type crystals are widely used as optical materials for various purposes. The use of doped crystals needs a homogeneous dopant distribution along the ingot, therefore the investigation of ions distribution provides better understanding of structural properties of these materials. The purpose of this paper is to study the distribution of Yb²⁺ and Yb³⁺ ions along the YbF₃ doped BaF₂ and CaF₂ crystals. The influence of YbF₃ concentration on the Yb ions distribution along the crystals and on the segregation coefficient has been investigated. BaF₂ and CaF₂ crystals doped with 0.1 and 0.2 mol % YbF₃ were grown in our crystal research laboratory using vertical Bridgman method [1]. The optical absorption spectra of the crystals reveal the characteristic absorption bands of the Yb³⁺ and Yb²⁺ ions in the as-grown crystals. The strongest characteristic absorption peaks of the Yb³⁺ ions are 968 nm for BaF₂ and 979 nm for

CaF₂. The Yb²⁺ ions have a well-defined peak at 353 nm (BaF₂), respectively at 365 nm (CaF₂). These peaks were used to study the Yb ions distribution along the crystals. The crystals were cut into 10-16 slices. The corresponding optical absorption coefficient, α (for every slice) was estimated from the optical absorption spectrum. The absorption coefficient is proportional to the impurity concentration (the Beer-Lambert law), so the dopant distribution along the crystal can be estimated from the optical absorption spectra. Non-uniform distribution of the Yb³⁺ and Yb²⁺ ions along the crystals were observed. The unevenness is stronger in BaF₂ crystals than in CaF₂ crystals. As the YbF₃ concentration increases in the crystals, the non-uniform distribution of the ions is more obvious. The segregation coefficient (k) was calculated by using the optical absorption method [2]. The value of k depends on the YbF₃ concentrations and on the crystal type. For Yb³⁺ ions, the value of k varies between 0.91 and 1 for CaF₂, respectively 0.7 and 0.84 for BaF₂. The value of k for Yb²⁺ ions varies between 0.91 and 0.92 for CaF₂, respectively, 0.66 and 0.82 for BaF₂. References: [1] D. Nicoara and I. Nicoara, Mater. Sci. Eng. A 102 (1988) L1-L4. [2] Y. Kuwano, J. Crystal Growth 57 (1982) 353.

6:40 PM - 6:41 PM

SYNTHESIS, CRYSTAL STRUCTURE AND HIRSHFELD SURFACE OF 2-AMINO-3 BENZYLOXY PYRIDINIUM PICRATE (1:1)

D.D.N. Shetty¹, M.S. Kumar², A.A. L³, S. Abraham¹

¹St Aloysius College (Autonomous), INDIA, ²Mangalore University, INDIA, ³CFTRI, INDIA

The crystal and molecular structure of 2-amino-3-benzyloxy pyridinium picrate (**ABPP**) have been elucidated using spectroscopic (MS, NMR and FTIR) and single crystal X-ray diffraction. In **ABPP**, the piperidine and phenyl ring are perpendicular to each other and intramolecular hydrogen bonds (N2---H2B...O1 and C12---H12...O1) are observed. The intermolecular hydrogen bonds of the type C6---H6B...O2, C3---H3...O5 and N2---H2C...O7 connects the molecules within the crystal structure. Intermolecular interactions are visualized and quantified using Hirshfeld surfaces computational method. The intercontact, O...

H contributes more to the Hirshfeld surfaces in both molecules. The electrostatic potential surfaces plotted over the co-crystal signify the electropositive and electronegative regions over the co-crystals. The thermo gravimetric analysis (TGA) measurement provided the thermal degradation of the **ABPP** to be from 230-320 °C. In addition, the emission spectrum was measured using fluorescence spectrometer and the **ABPP** was excited at 321 nm.

6:41 PM - 6:42 PM

ROLE OF A CRYSTAL GROWER IN HIGH TECH INDUSTRIES

N.B. Singh

University of Maryland, Baltimore County, UNITED STATES OF AMERICA

With changing funding situations role of a crystal growers have totally emerged as a multidisciplinary responsible scientist and engineer well aware with design and performance of crystal-based devices and systems. Although materials control not only performance but the market of the systems, funding for crystals growth is shrinking. In this situation one crystal growers are trying to squeeze the time for design, development and transfer the technology for insertion into systems. From the beginning of design, crystal growers have to be aware of the systems requirements and fundamental limit of materials to solve the problems. We will present examples of bulk, thin film and nanocrystal-based crystal based developments and technologies which have evolved to become produces. Specific examples of development and technology transfer of solution grown crystals for missile warning systems, Bridgman grown heavy metal chalcogenides, halides and chalcogenides as multifunctional materials for radiation detection, mid-wave infrared (MWIR) and long wave infrared (LWIR) lasers, all electronic beam deflectors, PVT grown crystals for hyperspectral imagers, nanocrystalline materials for high operating temperature (HOT) infrared detectors and radiation detectors will be presented. Bulk, nano and micro crystalline materials have been grown and characterized for identifying the key parameters and their effect on the performance of detectors. In order to understand effect of morphology on performance, we have shown variety of morphologies including cubic, hexagonal, octagonal and pyramidal structures with different

properties. The level of the oxidation processes and filling of selenium vacancies with oxygen may be the reason for resistivity to increase several orders of magnitude. Another very important area involves crystals for the high-power RF and microelectronics materials for substrates and heat spreader with large thermal conductivity and large mobility. Unavailability of high thermal conductivity semiconductor is still a road block for wide applications of high mobility high power large bandgap active layers. Because of very high temperature growth temperature impurity incorporations, and polytypes based defects, crystal growers have started design and development of low temperature reactive flux process for production of this class of materials. We will present examples of temperature flux growth for 2H-SiC and modified b-Ga₂O₃ crystals can be used and favorable properties for epitaxial growth of gallium nitride (GaN).

6:42 PM - 6:43 PM

CRYSTALLIZATION IN NON-AQUEOUS MEDIA AND THE ROLE OF WATER

F. Jones, S. Javaid

Curtin University, WA, AUSTRALIA

The role of water in crystallisation is being hotly debated currently, with the realisation that many systems do not crystallise via incorporation of growth units or nucleate according to the 'classical' mechanism. It has been determined that ions cluster in solution to form 'inorganic polymers' (called DOLLOPs) in the case of calcium carbonate and can 'nucleate' as amorphous solids before transforming to crystalline products (1). In addition, how these structures then grow (either by classical mechanisms or by aggregative mechanisms leading to meso-crystals) can be referred to as non-classical.

Inorganic solids are normally crystallised and investigated in aqueous media but some recent work has looked at the formation of gypsum in non-aqueous solvents and other minerals (dolomite, barium sulfate) (2, 3). However, the lack of water in a system that normally crystallises in an aqueous environment can also be used to gain information about how water is involved in the process. To this end, we investigated barium sulfate solids crystallisation in dimethyl sulfoxide (DMSO). This is a solvent miscible with water and DMSO has a reasonably high

dielectric constant. The results show that the particles do not grow substantially over time. In addition, the system has an unusually low nucleation rate. The particles remain in the nanometer range (see image below) and are relatively crystalline from the early stages according to infrared spectra. We have begun to investigate the causes of these phenomena and determine whether the nucleation inhibition is by impurity effects. If impurities are not responsible, these results suggest that removal of water may be more rate limiting than the amorphous to crystalline transition.

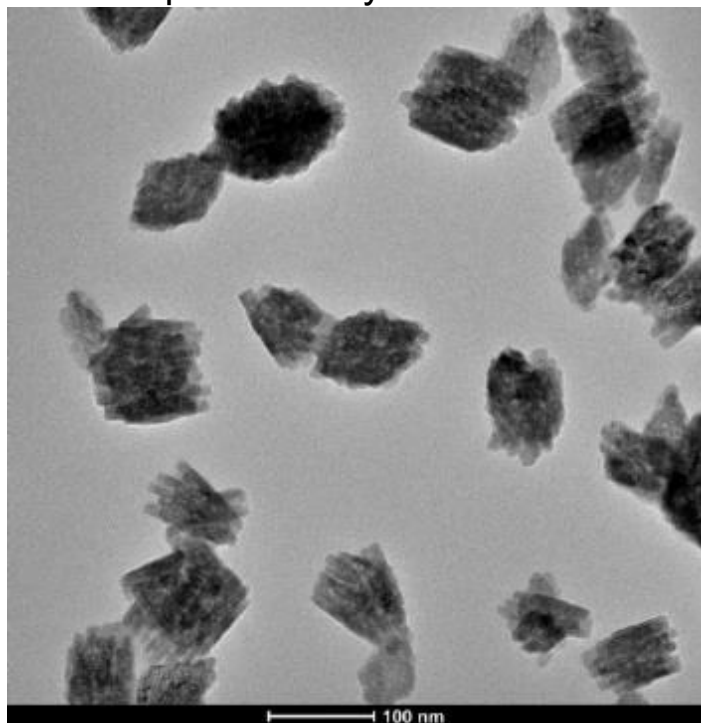


Figure 1. TEM image of barite particles formed in DMSO

References: 1. D. Gebauer, M. Kellermeier, J. D. Gale, L. Bergström, H. Cölfen, 2014, *Chem Soc Rev.*, 43, 2348-2371. 2. U. Tritschler, M. Kellermeier, C. Debus, A. Kempter, H. Cölfen (2015) *CrystEngComm*, 17, 3772-3776. 3. J. Xu, et al., *PNAS*, 110, 17750-17755 (2013); Y. Chen et al., *J. Chem. Sci.*, 119, 319–324 (2007).

6:43 PM - 6:44 PM

MORPHOLOGY OF A JAPANESE TRADITIONAL SUGAR BALL CAKE, CONPEITOU

K. Tsukamoto¹, H. Miura², Y. Kimura³, H. Satoh⁴

¹Graduate School of Science, Tohoku University, JAPAN, ²Nagoya

City University, JAPAN, ³Institute of Low Temperature Science, Hokkaido University, JAPAN, ⁴Mitsubishi Materials Corporation, JAPAN

Konpeitou (confetti) is a traditional Japanese sugar ball cake with horn-like prongs on the surface which was originally imported from Portugal to Japan in the middle of 16th century. The shape was very simple and irregular when imported but Japanese craftsmanship improved the ball sugar cakes to elegant and pretty ones as shown in fig. Because of the interesting shapes, Konpeitou was used as a gift to the Shogun of the Tokugawa era (Edo period 1603-1867). Interesting enough, Konpeitou with the prongs number of 36 was reported to be used. There have been discussions in history on the origin and the number of the horn-like prongs. However, the discussions were more or less philosophical based on a kind of morphological instability, judged from the outer shapes and there was no report from the internal texture, which is important for mineralogical approach to study the origin. This is the aim of this study. We will discuss on the following points: 1) origin of horn-like prongs, 2) the number of the prongs, how they are determined during the processing. In Kyoto there is a famous factory shop of Konpeitou which opened more than 100 years ago. Two weeks are needed to make the Konpeitou, in the first few days the craftsmen try to develop prongs from the seeds. In the rest of the days, they grow Konpeitou larger keeping prongs alive. We have employed X-ray CT scan and SEM for the bulk cakes and birefringence microscopy for the thin sections. The seeds are made of a small irregular porous rice balls, about 1mm large, and thus no definite shape can be seen at the beginning. But the shape of the seeds becomes nearly polyhedral in a day. The corners of the developing seeds with a nearly polyhedral form were found to develop as the prongs. If the seeds become aggregates of sugar crystals, uniform numbers of prongs would not develop. This is real craftsmanship and related to crystallization. It follows from the observation that the number of the horn-like prongs are mainly determined by the shape, namely the number of corners, of the crystalline seeds that craftsmen try to grow larger.



6:44 PM - 6:45 PM

**UNIFORMLY VALID ASYMPTOTIC SOLUTIONS OF
LAMELLAR EUTECTIC GROWTH IN DIRECTIONAL
SOLIDIFICATION FOR LIQUID-SOLID INTERFACE SLOPES OF
SMALL AND NORMAL ORDER**

X. Li

Kunming University of Science and Technology, CHINA

This paper considers system of steady lamellar eutectic growth under directional solidification. Uniformly valid steady solutions were obtained by using asymptotic expansion method and matching method as tangent of the contact angle is small and normal order, respectively. The necessary conditions for existing uniformly valid solution were obtained. Results show that liquid-solid interface shape is determined by coupling of the curvature undercooling and the solute undercooling. The amplitude of liquid-solid interface is a function of the product of the square root of the pulling speed and the temperature gradient. The relationship of the overall average interfacial undercooling with the eutectic spacing is also presented. The dimensional average undercooling in front of both phases are not equal and exhibits a minimum at the critical eutectic spacing. The relationship of critical eutectic spacing with pulling velocity is in agreement with the experimental results.

6:45 PM - 6:45 PM

STUDIES ON SHUBNIKOV-DE HASS OSCILLATIONS IN P-SB₂TE₂SE TOPOLOGICAL SINGLE CRYSTALS

A.B. Govindan¹, G. Govindhan¹, E.P. Amaladass², S. Ganesamoorthy², A. Mani²

¹Department of Physics, SSN College of Engineering, Rajiv Gandhi Salai,, INDIA, ²Condensed Matter Physics Division, Materials Science Group, IGCAR, Kalpakkam, INDIA

Transverse and longitudinal magneto-resistance measurements on Sb₂Te₂Se (STS) topological insulator single crystals are reported.

Electrical resistivity (ρ_{xx}) on STS measured in the temperature range 300-3 K showed a metallic behavior. Hall measurements indicate that the carriers are p-type. The magneto-transport behavior exhibits distinct Shubnikov-de Hass (SdH) oscillations only when the magnetic field is perpendicular to the sample surface. The SdH oscillations have been analyzed using Lifshitz-Kosevich (LK) equation, and the material parameters have been derived from the fit. The value of the Berry phase (β) determined from a Landau level fan diagram is 0.7 suggesting the parallel contribution of surface and bulk states.

6:45 PM - 6:45 PM

LIGHT YIELD IMPROVEMENT OF BI₄SI₃O₁₂ SCINTILLATION CRYSTALS BY DOPING TRANSITION METAL IONS

J. Xu¹, T. Tian¹, H. Feng¹, Z. Li¹, X. Xiao²

¹Shanghai Institute of Technology, CHINA, ²Key Laboratory of Physics and Photoelectric Information Functional Materials Sciences and Technology, North Minzu University, CHINA

Bismuth silicate Bi₄Si₃O₁₂ (BSO) crystal is a fast scintillator which has potential applications in high energy physics, nuclear physics, computed tomography and dosimetry. Compared with famous Bi₄Ge₃O₁₂ (BGO) crystal, BSO has some better scintillation properties such as a faster decay time, greater radiation hardness and a lower raw material cost, so it is considered to be the substitute for an alternative to BGO crystals. Recently, the large size BSO crystals up

to 35mm in diameter and 230mm in length have been grown by the modified vertical Bridgman method in our lab. The scintillation properties of rare earth doped BSO crystals have been investigated and BSO crystal doped with small amount Dy₂O₃ increases its light yield remarkably. In the present work, we reported the successful growth of transparent BSO crystals doped with different transition metal ions. The light yields of as-grown crystals were measured. It was found that Ta⁴⁺ doping can improve the light yield of BSO crystal to 1.5 times and the luminescence mechanism was suggested.

6:45 PM - 6:45 PM

HIGH MOBILITY LA-DOPED BASNO₃ THIN FILM GROWTH ON LATTICE-MATCHED BA(SC_{0.5},NB_{0.5})O₃ (001) SUBSTRATE BY MOLECULAR-BEAM EPITAXY

H. Paik¹, C. Guguschev², Z. Chen³, K. Peters⁴, D. Jena⁵, D.A. Muller⁵, D. Schlom⁶

¹Cornell University, UNITED STATES MINOR OUTLYING ISLANDS, ²Leibniz Institute for Crystal Growth, GERMANY, ³ UNITED STATES OF AMERICA, ⁴CrysTec GmbH, GERMANY, ⁵Cornell University, UNITED STATES OF AMERICA, ⁶Department of Materials Science and Engineering, Cornell University, UNITED STATES OF AMERICA
We report high mobility of La-doped BaSnO₃ thin films grown on lattice-matched single-crystal Ba(Sc_{0.5},Nb_{0.5})O₃ (001) substrate by adsorption-controlled molecular-beam epitaxy technique. Perfectly lattice-matched Ba(Sc_{0.5},Nb_{0.5})O₃ single crystal with regards to BaSnO₃ (0.017% mismatch) is grown by Czochralski technique, prepared as 10×10 mm² Ba(Sc_{0.5},Nb_{0.5})O₃ (001) substrates. Our best mobility of La-doped BaSnO₃ thin film grown on the 10×10 mm² Ba(Sc_{0.5},Nb_{0.5})O₃ (001) substrate is as high as 192 cm²·V⁻¹·s⁻¹ at room-temperature and 402 cm²·V⁻¹·s⁻¹ at 10 K at carrier concentration of 3×10¹⁹ cm⁻³. An atomically abrupt interface between La-doped BaSnO₃ film and Ba(Sc_{0.5},Nb_{0.5})O₃ substrate without any threading dislocations across the entire film thickness is verified by scanning transmission electron microscopy. The highest crystalline

quality of La-doped BaSnO₃ thin film by x-ray diffraction is identified as 0.0064° (23 arcsec) of full-width at half maximum value of 002 ω-rocking curve, which is substrate limited value. Our work demonstrates the highest quality of La-doped BaSnO₃ thin film on the lattice-matched Ba(Sc_{0.5},Nb_{0.5})O₃ (001) substrates. This lattice-matched growth approach can be extended to the potential two dimensional modulation doping or interfacial strain engineering among perovskite stannate (Ba, Sr, Ca)SnO₃ heterostructure with minimum interfacial defects density.

6:45 PM - 6:45 PM

OPTICAL CHARACTERIZATIONS OF CD_{1-x}ZN_xTE BULK SEMICONDUCTORS GROWN BY VERTICAL BRIDGMAN-STOCKBARGER METHOD

D.Y. Lin¹, C.W. Chen¹, H.P. Hsu², Y.F. Wu², K. Strzalkowski³, P. Sitarek⁴

¹National Changhua University of Education, TAIWAN, ²Ming Chi University of Technology, TAIWAN, ³Nicolaus Copernicus University, POLAND, ⁴Wrocław University of Science and Technology, POLAND

Cadmium zinc telluride (CZT) is a tunable band gap II–VI compound semiconductor, which has driven considerable attention due to its wide applications such as solar cells and radiation detectors. We have studied the optical properties of the ternary compound semiconductors Cd_{1-x}Zn_xTe composed from the end-members of ZnTe and CdTe grown by vertical Bridgman-Stockbarger method in the whole range of zinc composition 0<x<1. We measured the band gap energy and optical responsivity for each of the samples by transmission spectroscopy and photoconductivity (PC) spectroscopy, respectively. From the experimental results we found that the band gap energy of CdTe located at around 1.44 eV, and increased to 1.65 eV as increasing the Zn composition to 0.5; which constant increasing toward 2.07 eV for x close to 1. We also performed temperature-dependent transmission measurements to study the temperature dependence of band gap energy. Based on the above analysis, the relationship between the energy gap offset and the doping ratio are

verified and discussed. Furthermore, we will study the optical defects and recombination mechanism by using temperature-dependent PL experiments and modulation spectroscopy.

Tuesday, July 30, 2019

7:30 PM - 9:30 PM

Advanced MOVPE Technology for Wide Bandgap III-Nitrides

Location: Torrey Peak II-IV

Session Chair(s): Russell Dupuis, Jae-Hyun Ryou

7:30 PM - 7:50 PM

CLOSE COUPLED SHOWERHEAD MOVPE REACTOR FOR UVC LED AND GRAPHENE DEPOSITION

C. Mcaleese¹, D. Meyer², O. Feron², O. Rockenfeller², A. Debal², B. Conran¹, J. O'Dowd¹, K. Allen¹, M. Mason¹, A. Boyd², A. Pakes¹, K. Teo¹, M. Heuken²

¹AIXTRON Ltd, UNITED KINGDOM, ²AIXTRON SE, GERMANY
AlGaIn-based UVC LEDs, emitting at a wavelength of 220-280 nm, have a broad range of applications including water, air and surface disinfection. UVC LEDs offer considerable advantages over alternative technologies due to their small size, efficiency and lack of toxic materials. However, MOVPE growth is particularly challenging as high growth temperatures are required for good quality AlN layers, while gas phase pre-reactions result in poor precursor efficiency and impact growth uniformity and reactor stability. In this contribution, we report on new aspects of Close Coupled Showerhead[®] (CCS) technology that bring improvements to both uniformity and reproducibility for systems capable of 1400°C susceptor surface temperatures. These will be discussed for a range of reactor size configurations from 3x2" for R&D to the larger 19x2"/5x4" for mass production. The developments centre around removable insert segments between wafers on the carrier, and a removable cover-plate attached to the showerhead. These parts improve the temperature homogeneity during process and can be easily exchanged and cleaned outside of

the reactor, reducing maintenance time. Uniformity improvements will be presented for AlN buffer layers, n-AlGaIn layers and AlGaIn/AlGaIn MQW structures. Highlights include <1% on-wafer thickness uniformity std. dev. for AlN layers on 2" sapphire substrates and 1 μm thick n-Al_{0.65}Ga_{0.35}N layers with sheet resistance of 90 ± 3 Ω/sq. Additionally 3 period AlGaIn based MQW structures have been grown on an n-AlGaIn/ AlN buffer on 2" sapphire with 1.8 nm on-wafer PL wavelength uniformity std. dev. at a wavelength of 280 nm. The reproducibility was evaluated using this MQW structure over a 5 run series, during which the mean peak wavelength remained within a 2 nm range. Furthermore, a high temperature MOVPE reactor can potentially be used for deposition of other materials such as graphene and h-BN, and we demonstrate direct growth of high quality monolayer graphene on sapphire substrates without the use of a metal catalyst.

7:50 PM - 8:10 PM

PHYSICAL VAPOR TRANSPORT GROWN ALN SINGLE CRYSTAL SUBSTRATES

R. Dalmau, J. Britt, R. Schlessner

HexaTech, Inc., NC, UNITED STATES OF AMERICA

Ultrawide bandgap (UWBG) nitride semiconductors are attracting increasing attention for use in power electronics, UV optoelectronics, and extreme-environment applications. As many device performance metrics scale with the bandgap, AlGaIn alloys, with bandgaps ranging from ~3.4 eV of GaN to ~6.0 eV of AlN, possess the potential for improved performance over a wide range of devices. Research into the materials and device physics of these alloys is accumulating evidence for device benefits, but remains at an early stage. Substrate technology is a critical component to mature this field. High-quality native substrates that possess low lattice and thermal expansion mismatches to the overgrown device layers result in lower densities of extended defects, which are known to compromise device performance and lifetime. Aluminum nitride (AlN) possesses a close lattice match to high Al mole fraction nitride alloys and a high thermal conductivity, which make it an excellent substrate for UWBG nitride devices. Physical vapor transport (PVT) growth of AlN bulk crystals has emerged as the most promising technique for the production of

large, high-quality single crystal substrates. HexaTech has developed seeded growth technology enabling iterative expansion of single crystal size, while maintaining low dislocation densities. X-ray diffraction analysis was used to determine the primary dislocation types in AlN bulk crystals and their likely formation mechanisms, and to establish that low angle grain boundary (LAGB) formation during boule growth was eliminated by proper design of the thermal gradients inside the growth crucible. X-ray topography images demonstrated that the expanded diameter of freestanding AlN boules, grown without contacting the growth assembly or polycrystalline material around the boule periphery, contained low densities of threading dislocations ($<10^4 \text{ cm}^{-3}$) and no basal plane dislocations or LAGBs. Demonstration of AlN diameter expansion without additional defect formation represents a crucial development for substrate production at 2-inch diameter and above. Substrates fabricated from these boules possessed surfaces suitable for AlGaIn epitaxy and absorption coefficients below 100 cm^{-1} at 265 nm, enabling UVC emitters that require light transmission through the substrate. This talk will review diameter expansion and defect mitigation in PVT growth of AlN single crystals.

8:10 PM - 8:30 PM

DISLOCATION RECOVERY IN AL-RICH ALGAN LAYERS BY HIGH TEMPERATURE ANNEALING

S. Washiyama¹, Y. Guan¹, K. Wang¹, P. Bagheri¹, A. Klump¹, Q. Guo¹, J. Tweedie², S. Mita², R. Collazo¹, Z. Sitar¹

¹North Carolina State University, NC, UNITED STATES OF

AMERICA, ²Adroit Materials, UNITED STATES OF AMERICA

High temperature annealing, as proposed by Fukuyama and Miyake [1], is a promising technique to achieve low dislocation density below 10^9 cm^{-2} in AlN on sapphire. Recently, we proposed that this recovery is controlled by dislocation climb via vacancy diffusion at an elevated temperature. In this study, the dislocation recovery is applied to Al-rich AlGaIn layers that would facilitate strain management in AlGaIn based devices. A 200 nm-thick $\text{Al}_x\text{Ga}_{1-x}\text{N}$ layer was grown on 2-inch c-plane sapphire substrate by metalorganic chemical vapor deposition. Al

mole fraction in the AlGa_xN layer was varied from 0.3 to 0.8 by metalorganic flow rates. The AlGa_xN sample was annealed for 1 hour in a nitrogen ambient (1 atm). The annealing temperature was varied from 1550°C to 1700°C. X-ray diffraction (XRD) 2θ-ω scan and ω rocking curve were carried out to estimate the Al mole fraction, strain state and dislocation density in AlGa_xN layer before and after annealing. Atomic force microscopy (AFM) was carried out to investigate the influence of annealing of surface morphology. Prior to dislocation reduction by annealing, AlGa_xN alloy stability was investigated since the recovery is expected to occur at a temperature above 1600°C. Al_{0.3}Ga_{0.7}N surface AFM image exhibited a high density of pits after annealing at 1630°C. This could be caused by decomposition of the Al_{0.3}Ga_{0.7}N layers. As a consequence, effective dislocation density reduction was not realized for low Al content samples. The AFM observation on Al-rich AlGa_xN layers (x=0.70 and 0.8) showed a smooth surface with bilayer steps after annealing at 1630°C. Therefore, Al mole fraction needs to be high enough to achieve dislocation recovery. Edge dislocation density in as-grown Al_xGa_{1-x}N layers estimated from AlGa_xN (302) XRD rocking curve was mid 10¹⁰ cm⁻² on average. Dislocation density was reduced to 4×10⁹ cm⁻² in Al_{0.8}Ga_{0.2}N by annealing at 1650°C. Therefore, high temperature annealing could be employed to obtain low dislocation Al-rich AlGa_xN templates for AlGa_xN-based devices. The role of point defects that could generate vacancies will be discussed in the context of the dislocation climb mechanism. [1] Fukuyama et al., Jpn. J. Appl. Phys. 55 (05FL02) 2016

8:30 PM - 8:50 PM

GROWTH OF ALGAN/INGAN MULTIPLE QUANTUM WELLS AND P-ALGAN LAYERS FOR 369NM ULTRAVIOLET LIGHT EMITTING DEVICES

P. Chen, C. Tsou, Y.J. Park, T. Detchprohm, P.D. Yoder, S. Shen, **R. Dupuis**

Georgia Institute of Technology, GA, UNITED STATES OF AMERICA

In this study, AlGa_xN/InGa_xN multiple quantum wells (MQWs) and p-AlGa_xN contact layers for 369 nm light emitting devices have been

epitaxially grown by metal-organic chemical vapor deposition (MOCVD) and a series of growth procedures have been experimentally investigated. During the MOCVD epitaxial growth of AlGaIn/InGaIn MQWs, the ramping rate from a lower temperature for InGaIn quantum wells (QWs) to a higher one for AlGaIn quantum barriers (QBs) is intentionally changed from 1.0 °C/s to 4.0 °C/s. Atomic force microscopy (AFM) images shows that AlGaIn QBs have a smooth surface with clear step flow patterns. The surface morphology of InGaIn QWs, which is improved by a thermal annealing effect when the growth temperature rises to the set value of the AlGaIn QBs, varies with different temperature ramping rates. The results of optically pumped stimulated emission studies indicate that the laser threshold pumping power density of MQWs is decreased with increasing temperature ramping rate from 1.0 °C/s to 3.0 °C/s, and then slightly increased when the ramping rate is 4.0 °C/s. This phenomenon is believed to result from the thermal degradation effect during the temperature ramp step. A long-time high-temperature annealing will reduce the density of indium-rich microstructures as well as the corresponding localized state density, which is assumed to contribute to the radiative recombination in the InGaIn QWs. Given the great difference between optimal growth temperatures for AlGaIn and InGaIn layers, a higher ramping rate would be more appropriate for the growth of ultraviolet AlGaIn/InGaIn MQWs. A series of p-AlGaIn with various p⁺⁺-(Al)GaIn layers were also grown, and the contact characteristics were studied by using circle transmission line model (CTLM) method. These AlGaIn/InGaIn MQWs and p-type layers have been applied to the fabrication of our 369 nm ultraviolet light emitting devices. These results will be described and the performance of the corresponding UV LEDs will be presented.

8:50 PM - 9:10 PM

MOVPE GROWTH OF N-GAN CAP LAYER ON GAINN/GAN MULTI-QUANTUM SHELL LEDS

N. Goto

Meijo University, JAPAN

Three-dimensional GaInN/GaN multi-quantum shell (MQS) nanowires are promising for high-performance light-emitting devices, because of

their advantages such as non-polar surface orientation, dislocation-free and tolerance of misfit strain due to small size crystal. Particularly, the core-shell geometry of GaInN/GaN grown in lateral m-plane can suppress the quantum confined Stark effect, which usually causes the significantly efficiency-droop in conventional thin film light-emitting diodes (LEDs). Furthermore, it is possible to enhance the optical confinement factor to achieve low threshold lasing and high output for MQS-nanowire based laser diodes (LDs). As it is known, indium tin oxide (ITO) is one the most widely used transparent conducting material in planar LEDs as well as in MQS-nanowire LEDs. In fact, to a certain extent, ITO can induce a high light absorption loss as well as poor conformal deposition on the nanowire structures. By applying tunnel junction (TJ) structures, it is possible to increase the current diffusion efficiency with low resistance and low light absorption rate. In order to realize these features, suppression of the Mg diffusion and voids formation in MQS-nanowire LEDs with TJ are indispensable during the growth of n-GaN cap layer. In this study, we report the investigation of n-GaN cap layer growth on MQS-nanowires covered with TJ. Crystal growth was performed by using metalorganic vapor phase epitaxy (MOVPE). First, an array of hole patterns was prepared on a commercial n-GaN/sapphire template by nanoimprint lithography and plasma etching. Afterwards, n-GaN NW was grown on the template, followed by MQS, p-GaN shell and TJ structures. Finally, the n-GaN cap layer growth was carried to bury the MQS-LEDs. The morphology and the optical characteristics of the samples were investigated by scanning electron microscopy (SEM) and cathodoluminescence (CL). Different growth conditions for n-cap layer has been systemically studied to suppress the Mg diffusion and voids formation. At high temperature (> 960 °C), the growth rate on semipolar decreased, forming large voids in the bottom area of the nanowires. As temperature decrease to 800 °C, the growth rate on both m-plane and semi-polar was increased, hence the size of voids was decreased. It has been demonstrated that the growth with extremely low V/III ratio of 20 at low temperature, can further promote the lateral growth rate. In addition, the CL mappings exhibited a significantly enhancement of band-edge emission of GaN on the sidewall region, which was attributed to the suppressed Mg diffusion

from TJ.

9:10 PM - 9:30 PM

STUDY OF THE ORIGINS OF CARBON IMPURITIES ON GAN MOVPE FROM A GAS PHASE REACTION PERSPECTIVE

Y. Okawachi¹, K. Chokawa¹, M. Araidai², A. Kusaba³, Y. Kangawa³, K. Kakimoto³, S. Yo¹, Y. Honda¹, S. Nitta¹, H. Amano¹, K. Shiraishi¹

¹Graduate School of Engineering, Nagoya Univ, JAPAN, ²IMaSS, Nagoya Univ, JAPAN, ³RIAM, Kyushu Univ, JAPAN

GaN is a promising semiconductor material for next generation power device, and the crystal growth of high-quality GaN by MOVPE has been intensively studied for the mass production. One of the main issues in GaN-MOVPE for vertical power devices is carbon contamination during the growth procedure. The carbon concentration greatly affects the electronic states, resulting in the degradation of the inherent performance of GaN. In this study, we theoretically investigate the origin of carbon contamination, from the viewpoint of gas phase reaction. We define the gas phase reactions as in Table 1. The direction of each reaction is determined by the difference of Gibbs free energy between reactants and products (formation energy), which can be calculated by the statistical-mechanical approach together with the first-principles calculations [1]. Each formation energy is related to the equilibrium constant of each reaction which can be written by the partial pressure of reactants and products. Setting the partial pressures of source gasses: $\text{Ga}(\text{CH}_3)_3$ and NH_3 , and carrier gasses: N_2 and H_2 , to the experimental condition, we can obtain the partial pressures of gas molecules. The details of thermodynamic approach are given in Ref. 2. The equilibrium partial pressures of gas molecules at 1300K, which is the typical growth temperature in GaN-MOVPE, are listed in Table 2. We immediately find from Table 2 that Ga and GaH are the main sources of Ga in GaN-MOVPE at 1300K [3]. On the other hand, the relatively large amount of $\text{Ga}(\text{CH}_3)$ remains undissolved, which means that the main source of carbon contamination is $\text{Ga}(\text{CH}_3)$. The ratio of the partial pressure of GaH to that of $\text{Ga}(\text{CH}_3)$ is 10^3 . If $\text{Ga}(\text{CH}_3)$ molecules are adsorbed onto the surface of GaN

substrate with the same ratio, the amount of carbon impurity is 10^{19} /cm³. Actually, the methyl of Ga(CH₃) blocks the adsorption.

Therefore, the value is expected to approach the experimental value: $\sim 10^{17}$ /cm³ [4]. In the presentation, we also discuss one of the other candidates for carbon impurities, HCN. [1] Y. Kangawa, et al., Surf. Sci. **493**, 178 (2001). [2] Inatomi, et al., Jpn. J. Appl. Phys. **56**, 38002 (2017). [3] K. Sekiguchi, et al., Jpn. J. Appl. Phys. **57**, 04FJ03 (2018). [4] S. Nitta and H. Amano (private communication).

1	Ga(CH ₃) ₃	+	2NH ₃	→	HGa(CH ₃) ₂	+	2NH ₂	+	CH ₄
2	HGa(CH ₃) ₂	+	2NH ₃	→	H ₂ Ga(CH ₃)	+	2NH ₂	+	CH ₄
3	H ₂ Ga(CH ₃)			→	Ga(CH ₃)	+	H ₂		
4	H ₂ Ga(CH ₃)	+	2NH ₃	→	GaH ₃	+	2NH ₂	+	CH ₄
5	Ga(CH ₃)	+	2NH ₃	→	GaH	+	2NH ₂	+	CH ₄
6	GaH ₃			→	GaH	+	H ₂		
7	GaH			→	Ga	+	$\frac{1}{2}$ H ₂		
8	2CH ₄			→	C ₂ H ₆	+	H ₂		
9	C ₂ H ₆			→	C ₂ H ₄	+	H ₂		
10	C ₂ H ₄			→	C ₂ H ₂	+	H ₂		

Table.1 List of the gas phase reactions. No.1-7 are the main decomposition processes of TMG. No.8-10 are reactions of hydrocarbons molecules.

TMG	DMGH	MMGH ₂	MMG	GaH ₃	GaH
2.64×10^{-14}	5.87×10^{-11}	2.13×10^{-10}	3.16×10^{-7}	2.25×10^{-8}	1.46×10^{-4}
Ga	CH ₄	NH ₃	NH ₂	H ₂	N ₂
1.71×10^{-5}	4.90×10^{-4}	0.165	1.67×10^{-7}	0.500	0.334
C ₂ H ₆	C ₂ H ₄	C ₂ H ₂			
6.34×10^{-8}	4.44×10^{-8}	3.13×10^{-4}			

Table.2 Equilibrium partial pressure(atm) at 1300K

Wednesday, July 31, 2019

8:00 AM - 10:00 AM

Bulk Crystal Growth and Detector Materials

Location: Shavano Peak

Session Chair(s): Luis Stand, Chuck Melcher

8:00 AM - 8:30 AM

CESIUM HAFNIUM CHLORIDE, NOVEL SCINTILLATING MATERIAL

R. Kral¹, V. Vanecek¹, J. Paterek¹, V. Babin¹, V. Jary¹, M. Buryi¹, P. Zemenova¹, M. Kohoutkova², S. Kodama³, S. Kurosawa⁴, Y. Yokota³, A. Yoshikawa⁴, M. Nikl¹

¹Institute of Physics, Czech Academy of Sciences, CZECH REPUBLIC, ²University of Chemistry and Technology Prague, CZECH REPUBLIC, ³Institute for Materials Reserach, Tohoku University, JAPAN, ⁴NICHe, Tohoku University, JAPAN

Recently, the cesium hafnium chloride (Cs_2HfCl_6) was discovered as a prospective material for cost effective radiation detection. Its high effective atomic number $Z = 58$, high light yield up to 54 000 ph/MeV, energy resolution of 3.3 % at 662 keV, scintillation response of 4.4 us (95 % of energy) at 662 keV, and moderate density of 3.86 g/cm³ [1] together with its low hygroscopicity [2] makes it a suitable candidate for scintillator applications. The scintillating mechanism in the undoped Cs_2HfCl_6 was ascribed to intrinsic luminescence originating in a self-trapped excitons [3], however, details of the mechanism still requires further analysis. The Cs_2HfCl_6 is formed by cesium chloride and hafnium chloride mixed together in stoichiometric ratio 2:1 congruently melting at 826 °C [4]. The Cs_2HfCl_6 crystallizes in cubic structure with lattice parameters $a = 10.42 \pm 0.01 \text{ \AA}$ (space group Fm-3m), which is isostructural to K_2PtCl_6 and analogous to anti-fluorite CaF_2 structure [5]. This work is focused on the preparation and crystal growth of Cs_2HfCl_6 by the vertical Bridgman method. The X-ray fluorescence and X-ray diffraction analyses of the as-grown crystals together with the thermogravimetry and differential scanning calorimetry contributed to the optimization of the technological process. Grown crystals were cut and polished for further characterizations by means of absorbance, radioluminescence, and photoluminescence emission, excitation, and decay kinetics and their temperature dependence. Influence of various excitation sources on the photoluminescence emission spectra will be discussed. Furthermore, the electron paramagnetic resonance was applied as a useful tool to reveal the origin of the luminescence mechanism. **Acknowledgment:** The

support of Czech Science Foundation by project no. 18-17555Y is gratefully acknowledged. The authors thank to Mr. A. Cihlář and A. Bystřický for preparation and purification of starting materials.

References: [1] A. Burger et al., Appl. Phys. Lett., 107 (2015) 143505. [2] S. Lam et al., J. Cryst. Growth, 483 (2018) 121-124. [3] R. Král et al., J. Phys. Chem. C, 121 (2017) 12375-12382. [4] D.A. Asvestas et al., Can J Chem., 55 (1977) 1154–66. [5] S. Maniv, J Appl Crystallogr., 9 (1976) 245.

8:30 AM - 8:45 AM

GROWTH AND QUALITY IMPROVEMENT OF CE-DOPED (GD,LA)₂S₂O₇ SCINTILLATOR CRYSTALS

Y. Shoji¹, V. Kochurikhin¹, K. Kamada¹, S. Hayasaka¹, S. Kurosawa², M. Yoshino², A. Yamaji², Y. Yokota², Y. Ohashi², A. Yoshikawa¹

¹C&A corporation, JAPAN, ²Tohoku University, JAPAN

Ce-doped (Gd,La)₂Si₂O₇ (Ce:La-GPS) crystals have been studied as the prospective material for oil well logging due to the fact that La-GPS crystals had been demonstrated light output of 41,000 photons/MeV, an energy resolution of 4.4% (662 keV, FWHM) at room temperature. These crystals are known for keeping such high performance up to 150 °C¹⁻². In recent years, the large diameter Ce:La-GPS crystals were designed with above mentioned properties. Based on our previous researches, we encountered some problems related to the large diameter Ce:La-GPS crystals growth by Czochralski method: (1) crucible deformation due to the abnormal behavior of thermal expansion coefficients; (2) bubbles was captured by the Ce:La-GPS crystals from the melt. In this study, we aimed the yield improvement of grown Ce:La-GPS crystals by the creation of optimal growth conditions for bubble free bulk crystal production. We have found that during melting of the mixed raw materials a large amount of gas was entrapped inside the crystals due to the high viscosity of Ce:La-GPS melt. Therefore, we have grown 2 inch diameter Ce:La-GPS crystals using several techniques to eliminate bubbles from the melt; the detailed consideration of these techniques for the bubbles elimination will be discussed and the scintillator properties of the grown crystals in this condition will be compared. 1.

S. Kurosawa et al. Performance of Ce-doped $(\text{La,Gd})_2\text{Si}_2\text{O}_7$ scintillator with an avalanche photodiode, Nucl. Instrum. Methods Phys. Res. A 744 (2014) 30–34. 2. A. Yoshikawa, Y. Shoji, et al. Czochralski growth of 2 in. Ce-doped $(\text{La,Gd})_2\text{Si}_2\text{O}_7$ for scintillator application, Journal of Crystal Growth, 452 (2016) 57–64

8:45 AM - 9:00 AM

ELIMINATION OF CRACKS IN LGSO SCINTILLATION SINGLE CRYSTALS DURING CRYSTAL GROWTH

J. Osada, S. Asai, S. Takekawa, A. Miyamoto, H. Ishibashi
Oxide Corporation, JAPAN

LGSO ($\text{Lu}_{2-x}\text{Gd}_x\text{SiO}_5:\text{Ce}$, $x\sim 0.2$) has a high stopping power and a short decay time, which already makes it very suitable for PET. LGSO has a monoclinic structure with space group C2/c. A single crystal LGSO can be grown by CZ method. Lu_2O_3 , Gd_2O_3 , SiO_2 and CeO_2 with purity of 99.99% or more are mixed as starting materials and are charged in iridium (Ir) crucible. Ir crucible is induction-heated to melt the starting materials up to temperature of the melting point of about 2100 °C in a nitrogen or oxygen-containing atmosphere. The crystal is pulled slowly upwards at a rate of 0.3 to 1.5 mm/h with a seed rotation rate of 1 to 5 per minute. After the growth, the crystal boule is cut off from the melt and is gradually cooled. It was, however, difficult to grow a crack-free single crystal LGSO due to its anisotropic thermal expansion. In this work, we have investigated the optimization of crystal growth conditions to eliminate cracks. As a result, we could mass-produce crack-free LGSO boules by changing a temperature gradient in the growth furnace. Impact of growth orientation on cracks was also considered. Performance of crack-free LGSOs will be presented.

9:00 AM - 9:15 AM

SINGLE CRYSTAL GROWTH AND SCINTILLATION PROPERTIES OF MO CO-DOPED CE:LYSO CRYSTALS

K.J. Kim¹, K. Kamada², M. Yoshino¹, Y. Shoji¹, V. Kochurikhin³, A. Yamaji¹, S. Kurosawa², Y. Yokota², Y. Ohashi², A. Yoshikawa¹

¹Institute for Materials Research, Tohoku University, JAPAN, ²NICHE,

Tohoku University, JAPAN, ³General Physics Institute, Russian Academy of Sciences, RUSSIAN FEDERATION

Scintillator materials combined with photodetectors are used to detect high energy photons and particles e.g., in X-ray computed tomography (CT), positron emission tomography (PET) and other medical imaging techniques, high energy, and nuclear physics detectors, etc. In the last decades, great R&D effort brought several new material systems, namely the Ce-doped orthosilicates as Gd_2SiO_5 (GSO), Lu_2SiO_5 (LSO), $Lu_{2(1-x)}Y_{2x}SiO_5$ (LYSO), pyrosilicates based on $RE_2Si_2O_7$ (RE=Lu, Y, Gd) and most recently LaX_3 (X=Cl, Br) single crystal hosts. Ce:LSO and Ce:LYSO single crystals co-doped with Ca^{2+} have been recently investigated and improvement in their scintillation characteristics were claimed which is based on the suppression of slow delayed recombination processes. The positive role of stable Ce^{4+} centers has been proposed to explain the improved scintillation performance. Also, Mo co-doping with Pr^{3+} and Ce^{3+} in the several host materials such as $YAlO_3$ (YAP), $LuAlO_3$ (LuAP), $Lu_xY_{1-x}AlO_3$ (LuYAP), and $Lu_3Al_5O_{12}$ (LuAG) were investigated. Those studies showed that the co-doping of Mo is capable of improving the scintillation properties. However, there was no report about the Mo co-doping with Ce for LYSO host. In this study, we investigated Mo co-doping effect on optical, luminescence and scintillation properties of Ce:LYSO single crystal scintillators. The Mo co-doped Ce:LYSO single crystals were prepared by the micro-pulling down (μ -PD) and Czochralski (Cz) method with a wide concentration range of the co-dopants. Variations of the chemical composition along the growth axis of the Ce:LYSO crystals were examined. And absorption, radioluminescence, PLE and PL spectra were measured together with scintillation characteristics to reveal the effect of Mo co-doping. The three absorption bands of Ce^{3+} within 250nm–380nm have been observed in the non co-doped and Mo co-doped LYSO crystals. There was no evidence of the characteristic CT absorption transition of Ce^{4+} in the UV spectral range. The difference in the emission peak around 540 nm was observed in the radioluminescence spectra. The light output was increased with a small amount of Mo concentration.

Maximum light output of about 110% compared to the non co-doped Ce:LYSO was observed in a sample with Mo 500ppm co-doping. However, the scintillation decay time with the Mo co-doping concentration was not changed significantly from the value of the non co-doped Ce:LYSO.

9:15 AM - 9:30 AM

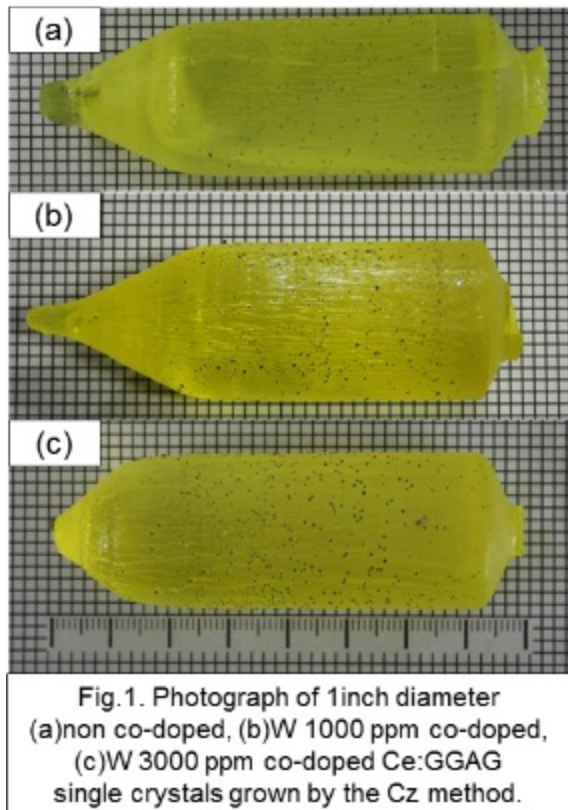
BULK SINGLE CRYSTAL GROWTH OF W, CE:GD₃GA₃AL₂O₁₂ BY CZOCHRALSKI METHOD AND THEIR UNIFORMITY OF SCINTILLATION PROPERTIES

M. Ueno¹, K.J. Kim¹, K. Kamada², T. Nihei³, M. Yoshino¹, A. Yamaji¹, H. Sato⁴, S. Kurosawa⁴, Y. Yokota⁵, Y. Ohashi⁴, A. Yoshikawa¹

¹Institute for Materials Research, Tohoku University, JAPAN, ²C&A corporation, JAPAN, ³C&A Corporation, JAPAN, ⁴NICHe, Tohoku University, JAPAN, ⁵New Industry Creation Hatchery Center, Tohoku University, JAPAN

Large size scintillator single crystals grown by Czochralski (Cz) method were widely used in industrial fields of radiation detection such as high-energy physics, medical imaging, geological exploration and homeland security. Recently 3 inch diameter Ce:Gd₃(Ga,Al)₃O₁₂ (GGAG) single crystal is in mass production. Scintillation response of about ~90 ns at emission around 520 nm, excellent light yield of about 56000 photons/MeV, and density of 6.7 g/cm³ were reported. Most recently, improvements of light yield by W ion co-doping on Ce activated GGAG grown by the micro pulling down method were reported using small samples with 0.5 mm thickness. However, it is necessary to evaluate scintillation properties such timing resolution, self absorption, energy resolution using thick samples to determine their potential for gamma-ray detection applications. In addition, ununiformity of co-dopants and activator coming from their segregation and evaporation often cause ununiformity of the scintillation performance and a decrease in production yield. In this research, W co-doped ,Ce:GGAG were grown by Cz method to evaluate relationship between ununiformity of co-dopants and scintillation properties. W 0, 1000, 3000 ppm co-doped Ce:GGAG single crystals were grown by Cz method as showed in the figure.

Quantitative chemical analyses of the crystals for the W, Ce, Gd, Ga and Al content along the radius and growth direction were performed by EPMA and ICP-MS analysis. The relationship between the chemical composition and scintillation performance such light yield, decay time, timing resolution, absorption length, liminality of radiation response in whole bulk crystals was investigated looking ahead the mass production of large size crystals.



9:30 AM - 9:45 AM

MULTIPLE SHAPED CRYSTAL GROWTH OF OXIDE SCINTILLATORS USING MO CRUCIBLE AND DIES BY THE EDGE DEFINED FILM FED GROWTH METHOD

K. Kamada¹, T. Kotaki², H. Saito², F. Horikoshi², M. Miyazaki², M. Yoshino³, A. Yamaji⁴, K.J. Kim⁵, S. Kurosawa⁴, Y. Yokota⁴, Y. Shoji⁶, A. Yoshikawa⁵

¹C&A corporation, JAPAN, ²Adamant Namiki Precision Jewel Co., Ltd, JAPAN, ³IMR, JAPAN, ⁴Tohoku University, JAPAN, ⁵Institute for Materials Research, Tohoku University, JAPAN, ⁶C&A Corporation,

JAPAN

Scintillator materials are used for radiation detection applications such as medical imaging techniques, high energy, homeland security, well logging, nuclear physics detectors, etc. In the last two decades, great R&D effort brought several novel scintillator material systems, namely the Ce-doped orthosilicates as Lu_2SiO_5 (LSO), Y_2SiO_5 (YSO), pyrosilicates based on $(\text{La},\text{Gd})_2\text{Si}_2\text{O}_7$ (La-GPS), aluminum perovskites as LuAlO_3 (LuAP), LuAlO_3 (YAP) and garnets as $\text{Lu}_3\text{Al}_5\text{O}_{12}$ (Ce:LuAG), $\text{Y}_3\text{Al}_5\text{O}_{12}$ (Ce:YAG), $\text{Ce}:\text{Gd}_3(\text{Al},\text{Ga})_5\text{O}_{12}$ (GAGG). These scintillator single crystals are commercially produced by the Czochralski method using Ir crucibles because of their high melting point around 1900-2130 °C. At the production higher material cost of Ir crucible and their repairing cost occupy most of the crystals cost. Scintillator crystals are used mainly as rectangular shaped pixels which are processed from 3-4 inch diameter bulk single crystals. These processing costs are substantially an economic burden, too. Up to now, shaped crystal growth of sapphire single crystal with shapes of tube, plate, fiber, etc was commercially developed by Edge defined Film Fed Growth (EFG) method [2]. Recently a few companies are producing shaped sapphire single crystal by EFG method using Mo crucible and die. Mo is several hundreds times lower cost material than Ir. Shaped growth by the EFG method using the low cost Mo crucible and die is a today's factor of cost reduction of sapphire. In this study, possibility of mass production of above mentioned oxide scintillators by the EFG method using Mo crucible and die is investigated. At the beginning of this study, reactivity and contact angles of these oxides melts and Mo were investigated. For example, Ce doped LuAG and YAG were grown using 8 multiple 1 x 10 mm Mo dies and 200 mm diameter Mo crucible at a growth rate of 0.1mm/min under Ar atmosphere using $\langle 100 \rangle$ LuAG seeds. 8 plates with 1 x 10 x 300mm size of Ce doped LuAG and YAG was successfully grown by the multiple EFG method. In our presentation, details on reactivity, Crucible and die designs, growth conditions, Mo contamination, chemical composition analysis, optical and scintillation properties of the grown crystals will be discussed.

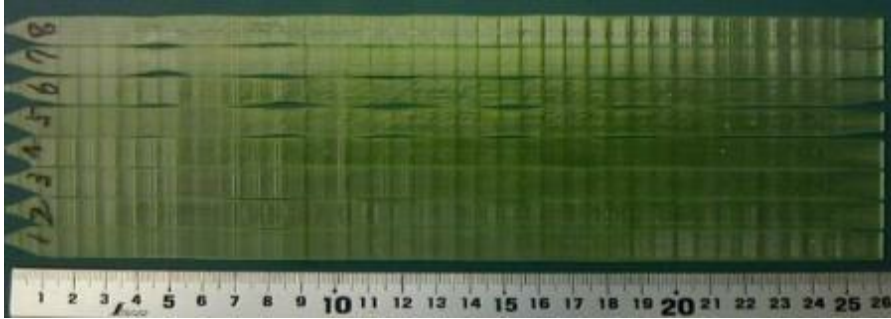


Fig.1 Ce:YAG single crystal plates grown by 8 multiple EFG method

9:45 AM - 10:00 AM

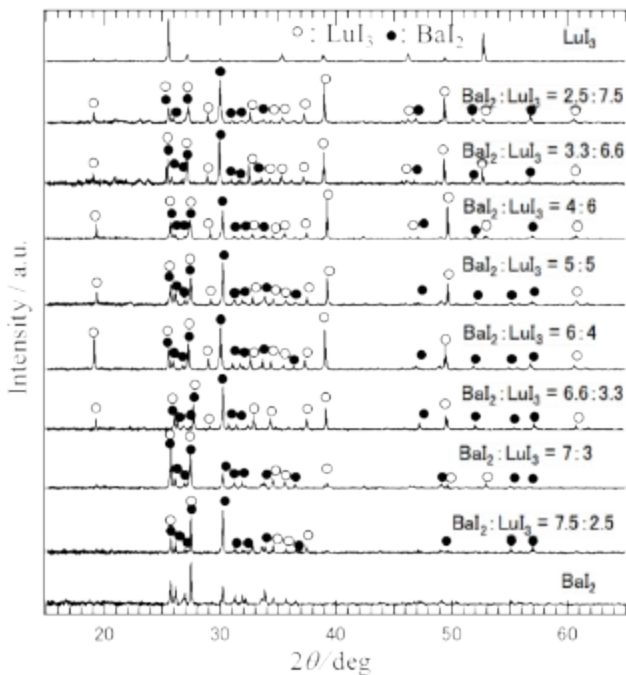
PHASE DIAGRAM OF BaI_2 - LuI_3 AND GROWTH OF BaI_2/LuI_3 EUTECTIC SCINTILLATOR

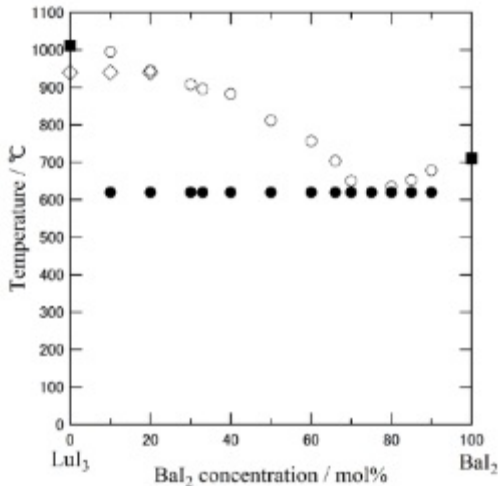
K. Origuchi¹, Y. Yokota², R. Kral³, M. Yoshino¹, A. Yamaji¹, H. Sato², Y. Ohashi², S. Kurosawa⁴, K. Kamada², A. Yoshikawa²

¹Institute for Materials Research, Tohoku University, JAPAN, ²NICHE, Tohoku University, JAPAN, ³Institute of Physics, Czech Academy of Sciences, CZECH REPUBLIC, ⁴Facility of Science, Yamagata University, JAPAN

Scintillator single crystals are required to improve the light yield and the energy resolution under irradiation for the high performance of radiation detectors using the scintillator single crystals. In addition, large effective atomic number and density are necessary to increase a detection efficiency of gamma-rays. Therefore, halide scintillator single crystals have been energetically studied because of their high light yield, small energy resolution, large effective atomic number and large density. However, many halide materials have high hygroscopicity and there are many unknown diagrams of the pseudo-binary system such as rare-earth ions and alkaline-earth metal ions. It is necessary to investigate the phase diagrams to develop new halide scintillator single crystals. If the phase diagram has an eutectic point, we can grow a eutectic scintillator. On the other hand, if it has a new compound with congruent composition, we can grow a single crystal from the melt. In this study, we focused on BaI_2 - LuI_3 system with large atomic number and tried to create the phase diagram of BaI_2 - LuI_3 system. In addition, we tried to grow a new scintillator in the phase diagram. BaI_2 and LuI_3 powders (> 3N) were mixed as various molar

ratios in a dry room or glove box. The mixed powder was set in a carbon crucible and it was melted in Ar using the Halide- μ -PD furnace after vacuuming to 10^{-4} Pa. Phases of the samples were identified by the X-ray diffraction (XRD) measurement. In addition, the mixed powders were set in a sealed quartz ampule after evacuating the inside of the ampule and thermal analyses were performed by the differential scanning calorimetry (DSC). In the powder XRD patterns of the melted samples, there were only diffraction peaks from the BaI_2 and LuI_3 and there was no new compound (Fig.1). In the results of thermal analyses, there were two or three endothermic peaks in elevated temperature process except for the 75 mol% BaI_2 75%/25 mol% LuI_3 . The 75 mol% BaI_2 75%/25 mol% LuI_3 showed just one endothermic peak at 620 °C and it was observed for all composition ratios. The results of the thermal analysis are summarized in Fig.2. The results of XRD and DSC measurements suggest that the BaI_2 - LuI_3 system has a eutectic point around 75 mol% BaI_2 75%/25 mol% LuI_3 in the phase diagram and an eutectic scintillator with the composition can be grown from the melt. Details of the phase diagram, crystal growth of the eutectic scintillator and the scintillation properties will be reported.





Wednesday, July 31, 2019

8:00 AM - 10:00 AM

Fundamentals of Crystal Growth: Impact of Chemical and Structural Heterogeneities

Location: Crestone I, II

Session Chair(s): Mu Wang, Baron Peters

8:00 AM - 8:30 AM

MESOSCOPIC CLUSTERS AND PREFORMED SOLUTE DIMERS IN CRYSTAL FORM TRANSITIONS AND GROWTH OF OLANZAPINE CRYSTALS

P.G. Vekilov¹, M. Warzecha², A. Florence², M. Safari¹

¹University of Houston, UNITED STATES OF AMERICA, ²Strathclyde University, UNITED KINGDOM

The classical mechanisms of crystallization assume that crystals nucleate and grow by sequential association of single solute molecule. Recent results have highlighted deviations from the accepted models whereby preformed nanostructures facilitate crystal nucleation and integrate into growing crystals. Here we explore non-classical pathways for crystallization and crystal form transitions of the antipsychotic drug olanzapine; olanzapine is known to assemble into 60 distinct polymorphs and crystal solvates. We demonstrate the presence of mesoscopic solute-rich clusters in olanzapine solutions. The clusters constitute a unique phase comprised of domains whose

size is insensitive to the solution thermodynamics, yet the amount of olanzapine captured in the clusters increases exponentially with the solute chemical potential. We show that the clusters host the nucleation of crystal forms of increased stability. In contrast to their role in nucleation, the clusters do not integrate into growing crystals, but instead incorporate as unstructured occlusions. The majority of the known olanzapine solid forms are comprised of centrosymmetric dimers. NMR and Raman spectroscopies demonstrate the presence of olanzapine dimers as a minority component in solutions in water-ethanol mixtures. Analyses of the crystal growth kinetics from a monomer/dimer mixture predict a parabolic correlation between the step velocity v and the total olanzapine concentration C for the case where the crystal grows by dimer association. The kinetics of layer spreading reveal a congruent $v(C)$ in a broad C range, suggesting that the olanzapine dimer is the preferred growth unit. Models of olanzapine association in the tested solvent suggest that precursory dimerization eliminates ethanol and water molecules strongly bound to monomers. As solvent dissociation from kinks and incoming solutes constitutes the rate determining step in crystal assembly, strongly bound solvent would significantly retard monomer association. The residual weakly bound solvent, associated to the dimers, contributes to a lower kinetic barrier and faster rate of crystallization via the dimer pathway. To our knowledge, these results represent the first definitive evidence of crystal growth by oligomer association.

8:30 AM - 8:45 AM

DYNAMICS OF BUBBLE ENGULFMENT DURING SAPPHIRE CRYSTAL GROWTH

L. Wang¹, C. Huang¹, D.B. Joyce², J.J. Derby¹

¹University of Minnesota, MN, UNITED STATES OF AMERICA,

²Crystal Systems Innovations, MA, UNITED STATES OF AMERICA
Bubbles of 10-100 microns in size are typically observed in sapphire crystals grown from the melt. Bubbles act as defects, ruining the precise uniformity of large-surface-area wafers, reducing the yield of high-quality material, and increasing costs. A better understanding of the fundamentals of bubble engulfment will provide a basis for improved material quality, increased process yields, and reduced

costs. We present our initial efforts to develop, validate, and apply computational models to elucidate the mechanisms of bubble engulfment during sapphire crystal growth. This research builds upon prior steady-state and dynamic models at the continuum level that have been developed to study the pushing or engulfment of a solid particle at a moving, solid-liquid interface. Prior results have revealed new mechanisms that impact the engulfment of silicon carbide particles engulfed during the growth of multi-crystalline silicon. The engulfment of bubbles during solidification is determined by a balance of repulsive van der Waals forces between the bubble and the solidification interface and drag forces arising from the flow around the bubble and into a thin liquid gap between particle and interface, typically on the order of 10 nanometers in thickness. When drag forces overcome repulsive forces, the bubble is engulfed, otherwise it is steadily pushed ahead of the advancing interface. Since drag increases with bubble size and velocity, there exists a critical velocity at which a bubble of a certain size is engulfed. However, drag forces are strongly dependent upon the shape of the solid-liquid interface as the bubble approaches. Thus, the critical velocity is affected by significant and nonlinear interactions involving heat transfer, premelting, and Gibbs-Thomson phenomena.

8:45 AM - 9:00 AM

AB INITIO STUDY FOR ADSORPTION AND DESORPTION BEHAVIOR AT STEP EDGES OF GAN(0001) SURFACE

T. Akiyama, T. Ohka, K. Nakamura, T. Ito
Mie University, JAPAN

The surface morphology during epitaxial growth is of importance on the efficiency of epitaxially grown quantum devices. It has been experimentally known that smooth GaN layers in the step-flow mode are obtained by both metal-organic vapor phase epitaxy and Ga-rich plasma-assisted molecular beam epitaxy (PAMBE). [1,2] Furthermore, hexagonal hillock morphology appears for GaN under N-rich condition in PAMBE. [1,2] These behaviors are attributed to the kinetic effects. It is believed that there is an energy barrier located at step-edges called Ehrlich-Schwoebel barrier (ESB), in which adatoms need to overcome to diffuse down the step and attach to the lower step-edge. [3] Since

the presence of ESB makes the asymmetry of adsorption-desorption behavior of adatoms, it induces specific self-assembled surface features such as step bunching and meandering. In our previous study, we have theoretically investigated adsorption-desorption behavior on GaN surface during the epitaxial growth and revealed characteristic features of adatoms depending on the growth condition. [4] To clarify the effects of ESB on the growth processes, we here systematically investigate the adsorption and desorption behavior of adatoms at step edges of GaN(0001) surface on the basis of *ab initio* calculations. Our calculations of step edges to the [1-100] direction clarify that the structure depends on the growth condition. The step edge for the surface with Ga adatoms is stabilized over the wide range of Ga chemical potential, whereas the step edge with adlayer is favorable under Ga-rich condition. The adsorption behavior of Ga and N adatoms close to the step edges is found to be dependent on these structures. Under moderately Ga-rich condition, Ga adatoms are preferentially incorporated at the step edge with low adsorption energy (-3.7 eV) and the ESB with 1.6 eV is recognized. In contrast, Ga adatoms can adsorb on both step edges and terrace region and the ESB is negligibly small within 0.1 eV. These results suggest that the nucleation preferentially occurs in the center of terrace under Ga-rich condition, reasonably consistent with experimental results in the MBE. [5]

References [1] C. Adelman *et al.*, J. Appl. Phys. **91**, 9638 (2002). [2] G. Koblmüller *et al.*, Jpn. J. Appl. Phys. **44**, L906 (2005). [3] R. L. Schwoebel and E. J. Shipsey, J. Appl. Phys. **37**, 3682 (1966). [4] T. Akiyama, *Epitaxial Growth of III-Nitride Compounds*, ed. T. Matsuoka and Y. Kangawa (Springer, Berlin, 2018). [5] H. Zheng *et al.*, Phys. Rev. B **77**, 045303 (2008).

9:00 AM - 9:15 AM

ON THE EFFECT OF BULK DIFFUSION ON THREE-DIMENSIONAL LAMELLAR GROWTH IN THE DISCONTINUOUS PRECIPITATION REACTION: A PHASE-FIELD APPROACH

A.R. Ladjeroud¹, L. Amirouche², M. Plapp²

¹Laboratoire de Physique Théorique, Faculté de Physique, U. S. T. H. B., BP 32, El-Alia, BabEzzouar 16311, ALGERIA, ²Laboratoire PMC,

Ecole Polytechnique, CNRS, 91128 Palaiseau, FRANCE

We have previously developed a phase-field model for the discontinuous precipitation, which is a solid-state transformation during which a supersaturated mother phase α_0 decomposes into a two-phase lamellar structure of β precipitates and depleted α phase. The two daughter phases grow via an advancing reaction front that consists of: an interphase boundary α_0/β and a grain boundary α_0/α , which meet with a third α/β interface, at a trijunction line. Since grain-boundary diffusion is faster than bulk diffusion in solid state, theoretical investigations predict that the rate-controlling step for the reaction is interface diffusion [1]. However, a previous two-dimensional (2D) phase-field investigation of the discontinuous precipitation has shown that volume diffusion played also a crucial role, at least in the initiation of the reaction [2]. Moreover, our simulations, that could reproduce many observed features of the discontinuous precipitation, such as the presence of a whole range of lamellar spacings for a given supersaturation and the bounding of the growing front, have revealed that when volume diffusion was dominating, the precipitate's behaviour was analogous to that of a crystal finger growing in a channel [3]. Motivated by our previous findings, we investigate in the present contribution the role of volume diffusion on the behavior of a three-dimensional (3D) precipitate as a function of the usual key parameters such as supersaturation (the main driving force) and lamellar spacing. Our simulations have revealed that, for a given spacing, low supersaturations give rise to a flat reaction front, whereas high supersaturations result in a curved α_0/β interface with a flat grain boundary. Thus, while the curvature of the grain boundary is required for its migration, the latter is prevented by an unexpected curvature of the α/β interface just beneath the trijunction. In both cases of low and high supersaturations, a fold singularity is obtained. The role played by the width of the growing lamellae is examined. It turns out that surface tensions, at the trijunction line, play a crucial role in the sense that though the gap of the transformation of a seed into a lamella is overcome, a steady-state growth of the latter cannot be observed. [1] P.Zieba Archives of Metallurgy and Materials 62(2), 955-968 2017. [2] L. Amirouche and

M. Plapp, Solid State Phenomena 172-174 2011. [3] L. Amirouche and M. Plapp. Acta Materialia, 57(1):237– 247, 2009.

9:15 AM - 9:30 AM

INVESTIGATING THE ROLE OF Mg^{2+} IN $CaCO_3$ CRYSTALLIZATION

M. Boon

Curtin University, WA, AUSTRALIA

Bulk precipitation of $CaCO_3$ has been widely studied over the years, examining the impact of one or two ions. However, in realistic systems the bulk solution is never as pure as the laboratory growth conditions. One realistic system is the growth of $CaCO_3$ in synthetic seawater, a solution containing 11 different inorganic ion species such as high magnesium and sulfate levels. The formation of aragonite from solution based precipitation has been well documented within the literature. It has been known that Mg^{2+} ions within the growth solution influences the formation of aragonite over calcite, despite aragonite being less thermodynamically stable. Multiple theories have been suggested in the literature to explain why this is. The second main theory is the adsorption of the Mg^{2+} ions onto the surface of calcite, increasing the surface free energy of Mg-Calcite making it energetically less favourable than aragonite. Due to the dense unit cell of aragonite, incorporation of Mg^{2+} into aragonite has been thought to be energetically unfavourable. This body of work suggests that due to a synergistic effect between Mg^{2+} and SO_4^{2-} , Mg^{2+} can incorporate into aragonite albeit at low levels. This has been observed using high resolution TEM and EBSD. The reasons for this are explored using molecular modelling.

9:30 AM - 9:45 AM

MACROSTEP-HEIGHT DEPENDENCE OF SURFACE VELOCITY FOR A REACTION- (INTERFACE-) LIMITED CRYSTAL GROWTH

N. Akutsu

Osaka Electro-Communication University, JAPAN

Controlling the self-assembly and disassembly of faceted macrosteps is an important aspect of fabricating semiconductor crystals [1]. For

the step-bunching during the diffusion-limited crystal growth, Chernov and co-workers [2] show the macrostep-height dependence of the step advancement rate theoretically. However, for the reaction-limited crystal growth, theoretical studies are not sufficient. In this work, the effect of macrostep height on the growth velocity is studied during reaction- (interface-) limited crystal growth. We adopted the Monte Carlo method for the non-conserved molecules based on the restricted solid-on-solid model with point-contact-type step-step attraction (p-RSOS model) [3]. Since the surface tension of the model is discontinuous at low temperatures, a faceted macrostep is the most stable configuration on the vicinal surface at equilibrium [4]. The results that were found are that the surface velocity decreases as the height of the faceted macrostep increases [5]. When the height of the faceted macrostep is large, the number of elementary steps on the terrace is small. Hence, the total number of kinks decreases to reduce surface velocity. We show the significant variation in surface velocity similar to recently reported by Onuma et al. [6] in a study based on 4H-SiC. The macrostep-height dependence of terrace slope, elementary-step velocity, and elementary-step kinetic coefficient are also shown. Acknowledgments

This work was supported by the Japan Society for the Promotion of Science (JSPS) KAKENHI Grant numbers JP25400413 and JP17K05503. [1] T. Mitani et al. *J. Cryst. Growth*, **423**, 45–49 (2015); A. Usui et al. *Jpn. J. Appl. Phys.* **36**, L899–L902 (1997); A. F. Khokhryakov et al. *Cryst. Growth Des.* **18**, 152–158 (2018); A.A. Shklyayev and A.V. Latyshev, *App. Surf. Sci.* **465** 10–14 (2019). [2] A. A. Chernov, *Sov. Phys. USP*, **4**, 116–148 (1961); T. Nishinaga, C. Sasaoka, and A. A. Chernov, Ed. I. Sunagawa, *Morphology and Growth Unit of Crystals* (Terra Scientific Publishing Company, Tokyo, 1989) 139–151. [3] N. Akutsu, *Appl. Surf. Sci.* **256**, 1205–1209 (2009); *J. Cryst. Growth* **318**, 10–13 (2011); *J. Phys.: Condens. Matter* **23**, 485004 (2011); *J. Cryst. Growth*, **401**, 72–77 (2014). [4] N. Akutsu, *AIP Adv.*, **6**, 035301 (2016); *Adv. Condens. Matter Phys.* **2017**, 2021510 (2017). [5] N. Akutsu, *Crystals*, **7**, cryst7020042, (2017); *Phys. Rev. Materials* **2**, 023603 (2018).

[6] A. Onuma, et al., Cryst. Growth Des. **17**, 2844–2851 (2017).

9:45 AM - 10:00 AM

TEMPORAL CHANGE OF CRYSTAL SIZE DISTRIBUTION DURING CHIRALITY CONVERSION BY ULTRASOUND GRINDING

H. Katsuno¹, M. Uwaha²

¹Ritsumeikan University, JAPAN, ²Aichi Institute of Technology, JAPAN

Viedma discovered amplification of the crystal enantiomeric excess (CEE) of NaClO₃ in a saturated solution by grinding with glass beads (Viedma ripening). Noorduin et al. reported that Viedma ripening is also observed for organic materials. The chiral cluster reaction model is one of theoretical models that can reproduce the CEE amplification. In the model, the crystal size distribution (CSD) is assumed to be steady. However, Hein et al. found spread of the CSD during the CEE amplification and the CSD returns to the initial form after the CEE amplification. In the experiment, ultrasound is also applied in the glass bead grinding. With the use of the generalized Becker-Döring model, we study time change of the CSD in Viedma ripening under grinding. The model includes crystallization of chiral clusters, in addition to monomers, for each chiral crystal. Two types of grinding are considered: crystals of various sizes are emitted uniformly in glass bead grinding and small fragments are produced from large crystals in ultrasound grinding. Our numerical calculation shows that the CEE is amplified under both grinding models. The steady CSD is realized during the CEE amplification under the glass bead grinding. In contrast, the CSD spreads at the end of the CEE amplification, and the final steady CSD is similar to the initial one under the ultrasound grinding. Since many chiral clusters are produced under the ultrasound grinding, crystals grow fast during the CEE amplification, which leads to the change of the CSD. The temporal spread of the CSD, however, is not the necessary condition for chirality conversion.

Wednesday, July 31, 2019

8:00 AM - 10:00 AM

III-V Devices

Location: Torrey Peak II-IV

Session Chair(s): Luke J. Mawst, Jae-Hyun Ryou

8:00 AM - 8:30 AM

STATE-OF-THE-ART IN-SITU METROLOGY DURING OMVPE IN ACADEMIC RESEARCH AND INDUSTRY

K. Haberland

Laytec AG, GERMANY

MOCVD - or OMVPE - is one of the first and most complex manufacturing step in the production of many semiconductor devices. Among these widely used devices are light-emitting-diodes in various spectral ranges from IR to UV, edge emitting lasers, vertical cavity surface emitting lasers, power transistors, solar cells and much more. Tightening industry requirements in terms of cost reduction and yield improvement have led to an increased usage of in-situ metrology for advanced process control. Consequently, optical in-situ metrology has become an integral part of process control in the production of optical and electronical semiconductor devices in recent years. Various measurement techniques are used in different control scenarios, ranging from real-time control loops to run-to-run control or tool-to-tool matching. New devices with new challenges, such as micro-LEDs or UV-LEDs, continuously add new requirements to control of important growth parameters such as wafer temperature, on-wafer uniformity or ternary composition. Apart from semiconductor industry, academic research is also widely employing in-situ metrology, but with a different approach. For research applications, not yield improvement and automated control is the goal, but the possibility to study new materials, understand physical processes and provide an insight into the "black box" of the growth system. Other measurement techniques and a different way of data analysis is employed. In this talk we will present recent improvements of the optical in-situ metrology equipment for both academia and semiconductor industry. This will include full spectroscopic reflectance measurements, that are perfectly suited for studying complex heterostructures. Examples will be shown from monitoring of LEDs, laser structures, transistors and other devices. We will also show examples for close-loop control concepts that provide direct benefit to manufacturing. It will also be shown, that

the in-situ analysis can be complemented by ex-situ measurements, such as two-dimensional wafer mapping. While in-situ metrology provides real-time information about all growing layers, including those optically not accessible after growth, the post growth ex-situ mapping provides spatial information about the uniformity of the layers, that is not available in-situ. We will show powerful combinations of in-situ and ex-situ measurements.

8:30 AM - 9:00 AM

TRENDS IN MID IR QUANTUM CASCADE AND INTERBAND CASCADE LASERS

K. Lascola, F. Xie, Y. Dikmelik, Y. Okuno, Y. Li, J. Abell, F. Towner, C. Pinzone

Thorlabs Quantum Electronics, MD, UNITED STATES OF AMERICA
Quantum Cascade and Interband Cascade Lasers (QCLs and ICLs) have become among the most important sources in the infrared. As the emission characteristics of these devices is determined primarily through layer thicknesses, rather than composition, a broad range of emission wavelengths, spanning 3 μ m into the THz, is achievable using only three material systems (InP, GaAs, GaSb). In addition, the ability to cascade active stages allows for custom tailored gain profiles for use in tunable lasers and applications requiring broad gain. This talk will begin with a short overview of the operating principles of both QCLs and ICLs and the key requirements for crystal growth of these devices. This will be followed by a discussion of state of the art performance for high power, high efficiency Fabry-Perot and Distributed Feedback lasers. A review of broad gain devices, monolithic tunables will be presented, including recent research in the areas of ICL VCSELs and QCL frequency combs and the suitability of these devices for various applications in chemical analysis and sensing. We will conclude with a performance comparison of devices grown by MBE and OMVPE as well as our view of potential future research in crystal growth for these devices.

9:00 AM - 9:15 AM

EDGE BREAKDOWN COMPARISON OF OMVPE SINGLE AND DOUBLE DIFFUSION PROCESSES FOR AVALANCHE

PHOTODIODES

O.J. Pitts, O. Salehzadeh, M. Hisko, A.J. Springthorpe
National Research Council Canada, ON, CANADA

Processing of avalanche photodiodes (APDs) using Zn diffusion in an OMVPE reactor, with dimethylzinc (DMZn) as the source, has been shown to be advantageous for uniformity and reproducibility, and has been optimized to achieve low dark current devices [1]. Control of the edge breakdown effect remains a challenging issue, however.

Methods of edge breakdown suppression, including the double diffusion method, have relied on the assumption that edge breakdown is due to the junction curvature around the edge of the diode active area. In this work, we present evidence that an additional contribution arises from enhanced Zn diffusion near the edge of diffusion apertures, leading to the observation of edge breakdown in APDs processed with a double diffusion in the OMVPE reactor. Imaging by scanning electron microscopy (SEM), as well as a novel dopant selective etching method using an electrochemical capacitance-voltage (ECV) profiler, are used to estimate the Zn distribution of diffused samples in cross-section and plan view, and are correlated with two-dimensional mapping of the electric field distribution of finished devices by the photocurrent scanning method. Finally, we present results using an alternative technique, combining selective area growth and a single diffusion in the same aperture [2]. The Zn distributions and photocurrent maps of devices processed using this single-diffusion technique show that it is effective in counteracting enhanced Zn diffusion at the mask edges, and results in effective edge breakdown suppression. O. J. Pitts, M. Hisko, W. Benyon, S. Raymond, A. J. SpringThorpe, "Optimization of MOCVD-diffused p-InP for planar avalanche photodiodes," *J. Cryst. Growth*, vol. 393, pp. 85-88, May 2014. O. J. Pitts, M. Hisko, W. Benyon, G. Bonneville, C. Storey, A. J. SpringThorpe, "Planar avalanche photodiodes with edge breakdown suppression using a novel selective area growth based process," *J. Cryst. Growth*, vol. 470, pp. 149-153, July 2017.

9:15 AM - 9:30 AM

**HIGH OPERATING TEMPERATURE INTERBAND CASCADE
INFRARED DETECTORS BASED ON TYPE-II SUPERLATTICES**

GROWN ON GAAS SUBSTRATES

Ł. Kubiszyn¹, K. Michalczewski², K. Lipski¹, J. Boguski¹, K. Murawski¹, P. Martyniuk¹, J. Rutkowski¹, J. Piotrowski²

¹Institute of Applied Physics, Military University of Technology, POLAND, ²VIGO System S.A., POLAND

Interband cascade is a design of infrared (IR) detector aiming for improved performance at high and above-room temperatures. Interband cascade IR detectors (IB CIDs) are built from several stages containing absorber region and specially designed transport region. In this work, we report on the growth and characterization of IB CIDs on IR-transparent, low-cost GaAs substrates buffered with GaSb. The absorbers of the devices are based on type-II InAs/GaSb or InAs/InAsSb superlattice. High resolution X-ray diffraction and photoluminescence are used for the layers characterization. The performance of the devices with different number of stages and absorber material is discussed. The devices exhibit spectral response up to 370 K in mid-wave part of IR spectrum.

9:30 AM - 9:45 AM

GROWTH OF HIGHLY N-TYPE DOPED GAAS AND INGAAS BY METAL ORGANIC VAPOR EPITAXY WITH SnCl_4

R. Alcotte¹, M. Baryshnikova¹, Y. Mols¹, R. Langer¹, B. Kunert²

¹Imec, BELGIUM, ²KU Leuven, BELGIUM

A high doping level is a key parameter to produce efficient and powerful devices. Increased doping concentration leads to reduced parasitic resistance and hence lower heat dissipation. In most III-V systems (GaAs/AlGaAs, InGaAs/InP), the commonly used n-type dopants are sulfur (S), selenium (Se), tellurium (Te), silicon (Si) and tin (Sn). Moreover, in the case of III-V integration on a Si platform, it is beneficial to grow doped layers at low temperature to be more CMOS compatible. Among, all these dopants, Sn has several properties that makes it attractive to explore its application. Here, we will report on the growth of GaAs and InGaAs doped with Sn in a 300 mm metal organic vapor phase epitaxy (MOVPE) reactor. Both materials are considered as contact layers in selective area growth of III/V nano-ridge devices on 300 mm patterned Si wafers. Tintetrachloride (SnCl_4)

is investigated as a new doping source due to its lower decomposition temperature in comparison to more commonly employed precursors such as tetramethyltin (TMSn) and tetraethyltin (TESn). Firstly, we explored the Sn-incorporation into GaAs and InGaAs grown at temperatures from 350°C to 580°C with varying Sn/III ratios from 0 to 0.028. Then, the V/III ratio dependence, the impact of annealing and the gas switching sequence were investigated. Inspection of the layers was done by atomic force microscopy (AFM), high-resolution X-ray diffraction (HRXRD), Hall effect measurement, secondary ion mass spectrometry (SIMS) and Rutherford backscattering spectrometry (RBS). Sn droplet formation at the surface was observed at high growth temperature and Sn/III ratio. Reducing the growth temperature below 450°C leads to a very smooth surface morphology (roughness < 1 nm) even for high Sn concentration up to 10%. Hall measurements indicate that only a fraction of Sn-atoms is active as donors at low growth temperatures. Under optimized growth conditions a maximal carrier concentration of $3 \times 10^{19} \text{ cm}^{-3}$ was achieved, which is comparable to what has been reported before. But a clear advantage of applying SnCl_4 is the low carbon concentration in heavily doped layers. For high doping concentrations ($> 1 \times 10^{19} \text{ cm}^{-3}$) a significant lower C-incorporation was observed by SIMS compared to layers grown with TMSn or TESn as it will be presented in detail. In InGaAs, a doping concentration of up to $1 \times 10^{20} \text{ cm}^{-3}$ was achieved for a Sn/III of 0.026. Growth and composition control is more difficult in comparison to GaAs as SnCl_4 induces indium etching, which easily leads to surface degradation.

Wednesday, July 31, 2019

8:00 AM - 10:00 AM

Nanocrystals and Nanostructured Materials

Location: Grays Peak I

Session Chair(s): George T. Wang, Erik Bakkers

8:00 AM - 8:30 AM

HEXAGONAL SIGE; GROWTH AND DIRECT BAND GAP

EMISSION

E. Bakkers

Eindhoven University of Technology, NETHERLANDS

It has been predicted that SiGe in the hexagonal crystal structure is a semiconductor exhibiting a direct bandgap for germanium contents exceeding ~70%. In this work we discuss the growth of high quality hexagonal SiGe structures using an epitaxial template. The composition can be tuned in the full range from pure Si to pure Ge. Under certain growth conditions a new type of defect can be formed, which has been analyzed in detail. We demonstrate direct band gap emission from this novel material, which is tunable in the range from 1.9 μm to 3.5 μm . We show emission of pure hexagonal germanium up to room temperature.

8:30 AM - 8:45 AM

AN INSIGHT INTO QUANTUM DOT MOLECULE FORMATION MECHANISM IN HETEROEPITAXY OF $\text{Si}_{1-x}\text{Ge}_x/\text{Si}(001)$

M. Dhankhar, M. Ranganathan

Indian Institute of Technology Kanpur, INDIA

Heteroepitaxy of SiGe/Si(001) has been of interest over the past several decades because of its importance in the microelectronics industry and as a model system to illustrate the concepts of heteroepitaxial epitaxial growth. In kinetically controlled conditions, a $\text{Si}_{0.7}\text{Ge}_{0.3}$ system shows morphologies evolving into ridges and structures called quantum dots molecules (QDM), which consist of a symmetric assembly of four quantum dots around a central pit. This represents a particularly interesting morphology and a possible alternate route towards strain relief from the usual quantum dots. To understand the process of QDM formation, we construct a theoretical framework based on continuum mechanics to study the behavior of a film of SiGe on Si. We incorporate both surface energy anisotropy and elastic anisotropy. The resulting elastic problem is solved numerically using a small slope approximation. A pseudospectral method with an Euler time integration is used to generate the resulting evolution. Our results show the spontaneous formation of QDMs under appropriate conditions as a means for strain and surface energy relaxation. Their transient nature justifies their appearance in the kinetically limited

regime of growth. Finally, we shed some light on the mechanism underlying the growth of QDMs.

References [1] J.L. Gray, R. Hull and J. A. Floro, App. Phys. Lett. 81, 2445 (2002). [2] T. E. Vandervelde et al Appl. Phys. Lett. 83, 5205 (2003). [3] J. L. Gray et al, Phys. Rev. B 72, 155323 (2005). [4] G.K. Dixit, M. Ranganathan, J. Phys. Condens. Matter 29, 375001 (2017).

8:45 AM - 9:00 AM

TAILORING WAVELENGTH OF CuInS_2 QUANTUM DOTS BY THE CONTROL OF COMPOSITION AND SIZE IN A BOLT-NUT MICROREACTOR

H. Kim, D.H. Kim

Korea Advanced Institute of Science and Technology, KOREA,
REPUBLIC OF

Quantum dot has received a great deal of attentions due to its outstanding optoelectronic properties which can be applied to various fields such as photovoltaic, lighting, and display devices. Among them, CuInS_2 quantum dot conforms to the global environmental issues as a cadmium-free quantum dots. By controlling the composition and size, we could tailor the wavelength of quantum dots from 500 nm to 750 nm. CuInS_2 , CuS, and InS quantum dot with zinc sulfide shell were synthesized in a bolt-nut microreactor at 230 °C with different core size and Cu/In ratio. Core size was controlled by adjusting core reaction time, and Cu/In ratio was regulated with precursor concentration of copper and indium. For quantum dot synthesis, conventional batch reactors suffer from the insufficient heat and mass transfer, slow mixing, and difficulty in the control of reaction condition which hinder the effective synthesis of quantum dots. We developed a novel bolt-nut microreactor which can be applied to various reactions with wide temperature range. The reactor is composed of stainless steel threaded bolt and nut. The crest of thread of bolt was flattened to make the space for fluid flow forming the spiral microfluidic channels. Reactor volume can be controlled by connecting the several sets of bolt and nut, and the cleaning of reactor is easy as reactor can be freely separated.

9:00 AM - 9:15 AM

ON SOFT LANDING DEPOSITION OF SMALL SIZE SILICON CLUSTERS UPON SILICON SUBSTRATE AT 300K : MOLECULAR DYNAMIC SIMULATIONS

E.F. Kherbouche¹, L. Amirouche²

¹USTHB, ALGERIA, ²University of sciences and technologie Houari boumedienne Algeria, ALGERIA

A Molecular Dynamics (MD) simulation has been carried out, on small silicon clusters, by using LAMMPS software (Large-scale Atomic/Molecular Massively Parallel Simulator), which is a MD program performed from Sandia National Laboratories [1]. The clusters' sizes that have been investigated, namely 4, 6 and 10, are chosen for their magic numbers character and hence their enhanced energetic stability. In order to simulate a soft landing, the clusters deposition is carried out, with no initial speed, on a substrate consisting of a set of many atomic shells, the top of which supposed to present dangling bonds. The behavior of the clusters is examined for two different force-fields, namely: (i) Tersoff potential [2] and (ii) EDIP (Environment Dependent Interatomic Potential) [3]. Moreover, the clusters' interactions with the substrate are analyzed by acting on the initial position (height) of their deposition, provided that its location is comprised in the cutoff. It turns out that for EDIP potential, all the clusters can be deposited without being affected by their initial position. However, for Tersoff potential, the achievement of the deposition is observed to depend on the clusters' initial position. Thus, once deposited, a cluster can get closer or further from the substrate's surface, which is reminiscent to the physics behind the pair interaction between Si atoms. As a result, Tersoff potential, though being very adequate to describe Si clusters behavior mainly at equilibrium, is restricted to a two-body interaction between particles. The two-body interaction strongly depends on the distance between the clusters and the substrate, which means that the clusters deposition may be achieved if the latter are in the attractive region of the potential and may fail if they are in the repelling zone. In such a case, the clusters are observed to leave far away from the substrate. Furthermore, the binding energy to the substrate is observed to be more important for EDIP clusters' than for Tersoff ones, which could be attributed to the

three-body contribution that is absent in Tersoff potential. [1]S. Plimpton, J. Comput. Phys. 117 (1995) 1 [2] Tersoff, Phys Rev B, 37, 6991 (1988) [3] Justo, Bazant, Kaxiras, Bulatov and Yip, Phys Rev B, 58, 2539 (1998)

9:15 AM - 9:30 AM

RE³⁺:CAF₂ (RE=ER,YB) NANOCRYSTALLITES-CONTAINING OXYFLUOROGERMANOTELLURITE GLASS-CERAMICS (ORAL PRESENTATION)

M. Velazquez¹, H. Zanane², D. Denux³, P. Goldner⁴, A. Ferrier⁴, A. Kermaoui², H. Kellou², M. Lahaye⁵, S. Buffière³, F. Weill³, J. Duclère⁶, J. Cornette⁶

¹SIMaP UMR 5266 CNRS-UGA-G INP, FRANCE, ²Faculté de Physique, Laboratoire d'Électronique Quantique, USTHB, ALGERIA, ³CNRS, Université de Bordeaux, ICMCB, UMR 5026, FRANCE, ⁴PSL Research University, Chimie ParisTech - CNRS, Institut de Recherche de Chimie Paris, FRANCE, ⁵PLACAMAT, UMS 3626, CNRS-Université Bordeaux, FRANCE, ⁶IRCER Centre Européen de la Céramique, FRANCE

New Yb³⁺- or Er³⁺-doped oxyfluorogermanotellurate glasses (30 GeO₂-30 TeO₂-15 ZnO-10 Na₂CO₃-10 CaF₂-3 La₂O₃-2 YbF₃/ErF₃) have been synthesized and submitted to varied heat treatments to provoke crystallization in its matrix. In the Yb³⁺-doped materials, the nanocrystallites formed have been found to measure typically 80-100 Å and be composed of ~1.2 mol. % Yb³⁺-doped CaF₂, by X-ray Diffraction, High-Resolution Transmission Electron Microscopy, Energy Dispersive Spectrometry in scanning TEM mode, emission spectroscopy, emission lifetime and magnetic susceptibility measurements techniques. In particular, it was established that in the most crystallized samples the experimental emission cross-section at 977.5 nm increases up to 7.7·10⁻²¹ cm², the experimental lifetime reaches 1.07 ms and the average effective Yb³⁺ cations magnetic moments are the highest. Absorption spectra in cross-section units were also obtained and preliminary Yb³⁺ 4f electrons energy levels positioning was performed. The glass and glass ceramics contain

significant amounts of Tm^{3+} and Er^{3+} impurities, as demonstrated by anti-Stokes emissions and their non resonant transients. Similar nanocrystallites were obtained in Er^{3+} -doped and thermally treated oxyfluorogermanate glasses, but cycling around the glass transition and crystallization temperatures by means of a Vibrating Sample Magnetometer did not reveal the same Van Vleck-to-Curie-Weiss “crossover” behavior. This is likely to be due to the different crystal field splitting of the ground state multiplet as found by optical spectroscopy investigations in these samples (absorption, emission, lifetime measurements and related Judd-Ofelt and crystal field analysis).

9:30 AM - 9:45 AM

ALLOY NANO-COMPOSITES FOR HIGH-Q INDUCTORS

N.B. Singh¹, T. Knight², F. Choa³, B. Arnold³, L. Kelly³

¹University of Maryland, Baltimore County, UNITED STATES OF AMERICA, ²Northrop Grumman Corporation, MD, UNITED STATES OF AMERICA, ³University of Maryland Baltimore County, MD, UNITED STATES OF AMERICA

Nanoparticles of several ferrites were embedded in polymer matrix to prepare composites which have the potential that will improve the performance of RF on-chip inductors. Different composites of nanomaterial were synthesized and used. We used spin spray method also to demonstrate the feasibility of deposition on silicon wafer also by spin spray method. Detailed studies were performed with three alloys of $Fe_{70}Al_5Cu_5Si_{20}O_d$, $Co_{70}Fe_9Cu_6Si_{15}O_d$, and $Co_{70}Al_5Fe_{20}Si_5O_d$ compositions. These composites of ferrite magnetic nanomaterials were fabricated into the ring structures and to measure properties such as permeability, resistivity, and loss to correlated with morphology and concentration of the alloy in the matrix. Fabricated single coil coplanar inductors were characterized for the electrical and magnetic properties of these materials at 100 to 100,000 Hz range. The measurement showed performances improvement in the measured frequency range up to 1000KHz. Results showed that the Co/Fe nanocomposite sample has a permeability and a flat response as function of voltage and frequency making it a very good embedded

inductor material. These composites provided inductance in the range up to 10 mH a value significantly high compared to literature values.

9:45 AM - 10:00 AM

SKYRMION HOSTING CU₂OSeO₃ NANOCRYSTALS

A. Magrez, P.R. Baral, B. Truc, W. Bi, V. Ukleev, J.W. Seo, I. Zivkovic, H. Ronnow, J.S. White, O. Yazyev

Ecole Polytechnique Fédérale de Lausanne, SWITZERLAND

In magnets lacking inversion symmetry, the magnetic structure can form spirals or more complicated magnetic chiral textures such as so-called skyrmions [1]. Chiral magnets were first of substantial interest for fundamental condensed matter physics due to topological effects. The robustness and small size of skyrmions and their high mobility make them promising candidates for applications such as in memory devices. Cu₂OSeO₃ is the first discovered insulator material exhibiting skyrmions under magnetic field at 60K [2]. All of the studies on skyrmions in Cu₂OSeO₃ have been performed using large crystals produced by Chemical Vapour Transport (CVT) at high temperature. [3] The fundamental research, based on macroscopic crystals grown by CVT, has led to the understanding of the mechanisms underlying the creation, [4] annihilation, [5] and motion of skyrmions [6] in Cu₂OSeO₃. However, the crystal size effect on the properties of skyrmions remains unexplored. In this contribution, we will report on the synthesis of Cu₂OSeO₃ nanocrystals achieved by a solid to solid transformation which driving force is an acid-base neutralization with low activation energy. The size, crystal structure, crystallinity of the solid precursor as well as the strength of the basic medium in addition to temperature and pressure of the hydrothermal process are exciting playgrounds to fine-tune the crystal size and morphology of Cu₂OSeO₃ nanocrystals. These parameters are also influencing the kinetics and mechanism of the transformation which was studied by *in-situ* measurements including X-Ray diffraction. This original chemical process produces high crystallinity 30nm to 450nm crystals with narrow size distribution. By combining AC and DC susceptibility measurements with neutron diffraction and Small Angle Neutron Scattering, we could reveal a remarkable effect of the crystal size on

the magnetic phase diagram of Cu_2OSeO_3 nanocrystals which is different from the one of bulk Cu_2OSeO_3 crystals. [7] We acknowledge the Swiss National Science Foundation for supporting the NanoSkyrmionics project (SNSF Sinergia grant number 171003), the Swiss Norwegian Beamline of the ESRF for *in-situ* X-Ray Diffraction, the Rutherford Appleton Laboratory for small angle neutron scattering and neutron diffraction experiments.

REFERENCES: [1] ROESSLER, et al 2006. *Nature*, 442, 797-801. [2] SEKI, S., et al 2012. *Science*, 336, 198-201. [3] DYAKIN, V., et al 2014. *Phys. Rev. B*, 89, 140409. [4] LEVATIC. I., et al 2016, *Scientific Reports*, 6, 21347. [5] HUANG, P., et al 2018. *Nano Letters*, 18, 5167-5171. [6] RAJESWARI, et al 2015. *PNAS*, 7, 10552-10562. [7] BARAL, P.R., et al *to be published*

Wednesday, July 31, 2019

8:00 AM - 10:00 AM

Special Session - George Gilmer I

Location: Red Cloud Peak

Session Chair(s): Luis Zepeda-Ruiz, Christine Wang

8:00 AM - 8:30 AM

KINETIC MONTE CARLO SIMULATIONS OF RESIDUAL STRESS DEVELOPMENT DURING THIN FILM GROWTH

E. Chason

Brown U, RI, UNITED STATES OF AMERICA

Polycrystalline thin films often develop stress during deposition. We would like to understand how the stress depends on the growth conditions (growth rate, temperature, particle energy) and microstructure (grain size) so that we can predict and control it. In past work, we have developed rate equations for this dependence that focus on different stress-generating mechanisms at the grain boundaries. This work makes approximations for the complex stress field so that analytical formulae can be derived. In the current work, we use a KMC approach to obtain a greater understanding of how these mechanisms operate on the atomic level. We are able to incorporate stress into the KMC by using the same approximations

used in the rate equation models. This enables us to simulate the evolution of the film surface and corresponding stress for different growth rates and temperatures. In particular, the KMC shows how the surface supersaturation induced by the flux of deposited atoms leads to compressive stress in the film.

8:30 AM - 9:00 AM

GROWTH OF CRYSTALLINE NANORODS

H. Huang

University of North Texas, TX, UNITED STATES OF AMERICA

As engineers, we conduct scientific researches with the aim of technological and societal impacts. Taking metallic glue as an example, this presentation covers the three aspects of such engineering researches: scientific discoveries, technological developments, and commercialization. Accompanying the interplay of these three aspects is that of sponsoring agencies such as NSF and DOE Office of Basic Energy Sciences, NSF Innovation Corps and tech industries, and customers and investors. The scientific discoveries of metallic glue include the new diffusion kinetics responsible for nanorod growth, new theories of nanorod growth in two modes and for their transitions, experimental realization of small and well-separated nanorods. The developed technologies include a high-quality and pricy metallic glue that is based on the small and well-separated metallic nanorods, and a lower-quality and more economic metallic glue that is based on nano particles/fibers and eutectic alloys. The commercialization of a startup company (MesoGlue, LLC) at this stage builds on the tool kit for the lower-quality and more economic metallic glue (<http://mesoglue.com/index.php/products-2/mesoglue-samplekit/>).

Wednesday, July 31, 2019

8:00 AM - 10:00 AM

Symposium on 2D Materials: Special Topics II: h-BN

Location: Crestone III, IV

Session Chair(s): Sang-Hoon Bae, Bhakti Jariwala

8:00 AM - 8:30 AM

GROWTH AND APPLICATIONS OF HEXAGONAL BORON NITRIDE

H.S. Shin

Department of Chemistry and Department of Energy Engineering,
Ulsan National Institute of Science and Technology (UNIST), KOREA,
REPUBLIC OF

Large-scale growth of high-quality hexagonal boron nitride (h-BN) has been a challenge in two-dimensional (2D)-material-based electronic and energy devices. In this talk, I will demonstrate wafer-scale and wrinkle-free epitaxial growth of multi-layer h-BN on a sapphire

substrate by using high-temperature and low-pressure chemical vapor deposition. Microscopic and spectroscopic investigations and theoretical calculations reveal that synthesized h-BN has a single rotational orientation with Bernal stacking order. A facile method for transferring h-BN onto other target substrates were developed, which provides the opportunity for using h-BN as a substrate in practical electronic circuits. A graphene field effect transistor fabricated on our h-BN sheets shows highly improved carrier mobility, because the ultra-flatness of the h-BN surface can reduce the substrate-induced degradation of the carrier mobility of 2D materials. And, I will show some potential applications of h-BN for a shell layer capping Au nanoparticles in surface-enhance Raman scattering, an encapsulation (or passivation) layer to protect unstable transition metal dichalcogenides (TMDs), and a proton exchange membrane to replace the Nafion film in a polymer electrolyte membrane (PEM) fuel cell. Lastly, I will demonstrate spatially controlled conversion of h-BN to graphene on an array of Pt nanoparticles to realize an array of uniform graphene quantum dots (GQDs) embedded in an h-BN sheet.

8:30 AM - 8:45 AM

OPTIMIZATION OF VAPOR PHASE EPITAXY FOR THICK BORON NITRIDE FILMS

A. Rice, A. Allerman, M. Crawford, M. Smith, G. Pickrell, P. Sharps
Sandia National Laboratories, NM, UNITED STATES OF AMERICA
Thick layers of hexagonal boron nitride (hBN) are an attractive option for direct radiation detection due to the large neutron capture cross section of ^{10}B combined with low gamma ray sensitivity. However, thicknesses on the order of 100 μm are necessary for $\sim 90\%$ absorption of even low energy thermal neutrons. In this study, hBN was deposited on SiC wafers in a cold-walled, RF-heated reactor using triethylboron (TEB) and NH_3 as precursors with N_2 and H_2 diluent gases. The deposition temperature was varied from 1200 $^\circ\text{C}$ to 1900 $^\circ\text{C}$, as measured by optical pyrometry of the susceptor, and the total chamber pressure was varied from 5 to 500 torr. It was found that the deposition rate was nearly temperature independent at 5 or 50 Torr total pressure, while the deposition rate increased with increasing temperature at 500 Torr. The deposition rate at 1800 $^\circ\text{C}$ increased as

the square root of total chamber pressure for fixed input flows. The deposition rate as a function of TEB flow was slightly sub-linear at a constant V/III ratio of 50, with a fourfold increase of TEB flow from 42 $\mu\text{mol}/\text{min}$ to 168 $\mu\text{mol}/\text{min}$ yielding a 3.4-fold increase in deposition rate. The deposition rate varied by less than 10% for V/III ratios between 25 and 200. Films exhibited a yellow hue when deposited with V/III ratios less than 25 and were clear but rapidly roughened when deposited with V/III ratios greater than 200. For hBN films deposited at 1800°C, room temperature photoluminescence showed near band edge emission with a peak at 216 nm and a broad peak centered at ~ 220 nm, thought to be emission of the optical phonon replica of free exciton and defect bound exciton, respectively. The addition of silane (SiH_4) during deposition at a SiH_4/TEB ratio of 0.01 reduced the 220 nm defect bound exciton emission as well as deep level photoluminescence centered at ~ 320 nm. Optimization of conditions allowed for a maximum deposition rate of approximately 4 $\mu\text{m}/\text{hr}$ and optically-clear films up to 40 μm thick to be deposited on SiC without delamination. Supported by the Laboratory Directed Research and Development program at Sandia National Laboratories, a multimission laboratory managed and operated by National Technology and Engineering Solutions of Sandia, LLC., a wholly owned subsidiary of Honeywell International, Inc., for the U.S. Department of Energy's National Nuclear Security Administration under contract DE-NA-0003525.

8:45 AM - 9:15 AM

ATOMIC PRECISION CONTROL OF 2D MATERIALS VIA LAYER RESOLVED SPLITTING

S. Bae¹, J. Kim²

¹Massachusetts Institute of Technology, UNITED STATES OF AMERICA, ²Massachusetts Institute of Technology, MA, UNITED STATES OF AMERICA

2D material based heterostructures formed by weak van der Waals interactions have introduced an interesting physics and new device functionalities. However, fabrication of 2D material based heterostructure is quite challenging in terms of scalability and layer-

controllability. Currently, most of research relies on a tape mechanical exfoliation method which can produce perfect crystalline 2D materials. However, the size of 2D materials is limited to hundreds of microns only and it relies on trial-and-error based operation. Accordingly, people have put intensive effort in growing 2D materials and their heterostructure. However, it has been noted that controlling the kinetic of 2D materials is even more challenging because of easy-additional nuclei formation on top of the initial nuclei. In this regard, an alternative way has been required to demonstrate large scale, monolayer 2D materials. Here, we report a layer-resolved splitting (LRS) for 2D materials that allows precise control of the number of layer of 2D materials at wafer scale. We studied underlying mechanics for LRS to precisely control the 2D materials at atomic resolution. Based on the mechanics, we successfully produced multiple monolayer of 2D materials, including WS_2 , hBN , WSe_2 , MoS_2 and $MoSe_2$, from one multilayer 2D material. Through this LRS, large scale 2D materials based heterostructures were demonstrated and multiple functionalities were also observed. We believe that LRS will open up a new venue for 2D material research community.

9:15 AM - 9:45 AM

GROWTH, PROPERTIES, AND APPLICATIONS OF HEXAGONAL BORON NITRIDE EPILAYERS

H. Jiang¹, J. Lin²

¹Texas Tech University, UNITED STATES MINOR OUTLYING ISLANDS, ², UNITED STATES OF AMERICA

Due to its wide bandgap (> 6 eV) and layered structure, hexagonal BN (h -BN) is an ideal platform for probing fundamental 2D properties of wide bandgap semiconductors. In this talk, a brief overview of synthesis and electrical and optical properties of wafer-scale h -BN epilayers will be presented [1-7]. The unique 2D structure of h -BN induces exceptionally high density of states, large exciton binding energy and high optical absorption and emission intensity. By growing h -BN under high V/III ratios, epilayers exhibiting pure free exciton emission have been obtained [4]. Photocurrent excitation spectroscopy results directly provided a room temperature bandgap

value for *h*-BN in between 6.4 and 6.5 eV and a free exciton binding energy (E_x) of 0.73 eV [5]. The growth of layer-structured B-rich BGaN alloys, heterostructures, and quantum wells and their optical properties have also been explored and will be discussed. Thermal neutron detectors fabricated from 100% B-10 enriched *h*-BN epilayers of thicknesses exceeding 50 nm have attained the highest detection efficiency to date among all solid-state detectors at about 58% [6, 7]. These solid-state neutron detectors have become increasingly desirable for a wide range of applications from fissile materials sensing to well logging, because ^3He gas detectors are inherently bulky, require high pressurization and high voltage application, slow response time, and expensive. We will also discuss many technologically important applications of *h*-BN ranging from deep UV optoelectronics, radiation detectors, to novel layered-structured photonic and electronic devices.

- [1] R. Dahal, J. Li, S. Majety, B.N. Pantha, X. K. Cao, J. Y. Lin, and H.X. Jiang, *Appl. Phys. Lett.* **98**, 211110 (2011).
- [2] S. Majety, J. Li, X. K. Cao, R. Dahal, B. N. Pantha, J. Y. Lin, and H. X. Jiang, *Appl. Phys. Lett.* **100**, 061121 (2012).
- [3] H. X. Jiang, and J. Y. Lin, *Semicon. Sci. Technol.* **29**, 084003 (2014).
- [4] X. Z. Du, J. Li, J. Y. Lin, and H. X. Jiang, *Appl. Phys. Lett.* **106**, 021110 (2015); **108**, 052106 (2016).
- [5] T. C. Doan, J. Li, J. Y. Lin, and H. X. Jiang, *Appl. Phys. Lett.* **109**, 122101 (2016).
- [6] A. Maity, T. C. Doan, J. Li, J. Y. Lin, and H. X. Jiang, *Appl. Phys. Lett.* **109**, 072101 (2016).
- [7] A. Maity, S. J. Grenadier, J. Li, J. Y. Lin, and H. X. Jiang, *Appl. Phys. Lett.* **111**, 033507 (2017) and *J. Appl. Phys.* **123**, 044501 (2018).

9:45 AM - 10:00 AM

HIGH-THROUGHPUT PRODUCTION OF NOBLE METAL-DECORATED HEXAGONAL BORON NITRIDE (HBN) IN A HYDRODYNAMIC REACTOR

J. Jeong¹, **Y. Park**¹, Y. Cha², D. Seo³, D.H. Kim¹

¹Korea Advanced Institute of Science and Technology (KAIST),
KOREA, REPUBLIC OF, ²KAIST, KOREA, REPUBLIC OF, ³, KOREA,
REPUBLIC OF

We report the high-throughput production of noble metal-decorated hexagonal boron nitride (hBN) using a hydrodynamic process for the selective alcohol oxidation catalyst. Fluid mechanics of a hydrodynamic process based on a Taylor–Couette flow provides a high shear stress field and fast mixing process. Unique fluidic behavior efficiently exfoliates bulk hBN into hBN nanosheets dispersed in water solution, in which ionic liquid (IL) is used as the stabilizing agent to prevent the restacking of the hBN nanosheets. The deposition of noble metal on a hBN surface is also performed using a hydrodynamic process, resulting in the uniform decoration of noble metal nanoparticles. Synthesized noble metal/hBN catalyst has been applied for the oxidation of a wide variety of alcohol, including biomass-derived 5-hydroxymethylfurfural (HMF) under environmentally benign condition. The catalyst exhibited a high mechanical stability, and no leaching of the metal was observed during the reaction. These features ensured the reusability of the catalyst for several times for the selective oxidation of biomass-derived HMF to 2,5-diformylfuran (DFF) and furfuryl alcohol to furfural.

Wednesday, July 31, 2019

8:00 AM - 10:00 AM

Symposium on Epitaxy of Complex Oxides: Beyond the Limits of Traditional Film Growth

Location: Grays Peak II, III

Session Chair(s): Susanne Stemmer

8:00 AM - 8:30 AM

MOLECULAR BEAM EPITAXY OF ANTIPEROVSKITES

H. Nakamura

Max Planck Institute for Solid State Research, GERMANY

Antiperovskite with A_3BO ($A=Ca, Sr, \text{ or } Ba; B=Sn \text{ or } Pb$) structure are theoretically predicted to host a variety of topological phases, including bulk three-dimensional (3D) Dirac electrons and surface

states protected by crystalline symmetry. Epitaxial thin film of such materials could offer a new avenue to engineered topological states, because the lattice constants of these materials are close enough to allow epitaxial heterostructures, in close analogy to what has been achieved in conventional oxides. However, little is known thus far regarding the thin film growth of A₃BO-type antiperovskites. In this presentation, we show our results on molecular beam epitaxy (MBE) of Sr₃PbO and Sr₃SnO [1,2]. The key factor to realize phase-pure antiperovskites has been to appreciate that these compounds are not oxides but better viewed as alkaline-earth (Sr) compounds. Thus, a first important step to hit the growth window was to control Sr flux carefully [1], just like O₂ is tuned for a conventional oxide growth. We also show recent results on shuttered MBE approach, which improved the film quality dramatically. We aim to provide initial insights on the chemistry and physics of antiperovskites films, based on extensive characterization using RHEED, LEED, XRD, XPS, and transport.

1. D. Samal, H. Nakamura, H. Takagi, APL Mat. 4, 076101 (2016).
2. H. Nakamura, J. Merz, E. Khalaf, P. Ostrovsky, A. Yaresko, D. Samal, H. Takagi, arXiv:1806.08712.

8:30 AM - 9:00 AM

GAS-SOURCE MBE TO MAKE COMPLEX SULFIDE THIN FILMS

R. Jaramillo

MIT, MA, UNITED STATES OF AMERICA

Sulfides and selenides in the distorted-perovskite and related structures (“complex chalcogenides”) are predicted by theory to be semiconductors with band gap in the visible-to-infrared and may be useful for optical, electronic, and energy conversion technologies. We will present progress towards making films of complex sulfides by gas-source MBE, including thermodynamic modeling and gas-source optimization. We use computational thermodynamics to predict the pressure-temperature phase diagrams for select chalcogenide perovskites. We highlight the windows of thermodynamic equilibrium between solid chalcogenide perovskites and the vapor phase. For $ABCh_3$ ($Ch = S, Se$) materials with B = transition metal, the growth windows lie at very high temperature and low pressure that are

challenging for most MBE chambers. The growth window becomes much more accessible for materials for which the quasi-binary phase diagram includes a compound (e.g. SnS) with high vapor pressure. We also report on the effect of hydride gas source placement in our growth chamber on the growth of chalcogenide films using hydrogen sulfide (H₂S) and hydrogen selenide (H₂Se) gas sources. Taking a cue from the history of complex oxides, we hypothesize that the location of the gas injectors is quite important for optimizing film growth. We test this hypothesis by measuring gas cracking by a heated substrate and the growth of binary sulfides (including SnSe) for several gas injector configurations, supported by Monte Carlo simulations. We will then report on physical property measurements of targeted materials BaZrS₃ (perovskite) and Ba₃Zr₂S₇ (n=2 Ruddlesden Popper). Optical measurements including time-resolved photoluminescence suggest that Ba₃Zr₂S₇ has promising opto-electronic properties, including long minority-carrier lifetime and benign surfaces. Impedance spectroscopy shows that these materials are highly-polarizable, which may be expected for complex-structured materials but is unusual for semiconductors with band-gap in the visible and near-IR.

9:00 AM - 9:30 AM

THIN FILM CRYSTAL GROWTH OF OXIDES AND NITRIDES USING HIGH IMPULSE MAGNETRON SPUTTERING

J. Maria¹, K.P. Kelley², K. Ferri², J. Hayden², A. Cleri², J. Nordlander², E. Runnerstrom², A. Klump³, R. Collazo⁴, Z. Sitar³

¹North Carolina State University, AL, UNITED STATES OF AMERICA,

²The Pennsylvania State University, Department of Materials Science and Engineering, PA, UNITED STATES OF AMERICA, ³North

Carolina State University, NC, UNITED STATES OF AMERICA, ⁴, UNITED STATES OF AMERICA

This presentation will discuss thin film crystal growth using reactive pulsed magnetron sputtering specifically in the region referred to as high power impulse magnetron sputtering, or HIPIMS. HIPIMS is characterized by duty cycles less than approximately 10%, and

magnetron power densities in excess of 1 kW/cm^2 . These intense impulses produce high ionization fractions of both the gas and sputtered species, they can be sustained in atmospheres containing substantial fractions of O_2 or N_2 with only modest re-sputtering, and they can be tuned so as to minimize target poisoning. Pulsed dc plasmas have been applied routinely to promote thin film adhesion, to achieve high deposition rates, and to produce extremely hard and wear resistant coatings. Their introduction to electronic materials has been much less rapid. The intent of this presentation is to demonstrate the utility of pulsed dc plasmas, and specifically the HIPIMS regime, for electronic materials, including oxides and nitrides which require reactive environments that can in many cases can be challenging to realize. Two case studies will be presented: 1) epitaxial growth of CdO thin films for IR optoelectronic applications, and 2) epitaxial growth of GaN thin films for wide bandgap applications. The basic instrumentation of this interesting plasma method will be discussed, and how it offers advantages for controlling defect chemistry, and this transport properties, in CdO, and for enabling epitaxy at surprisingly low temperatures in GaN, with excellent control of surface morphology. In both cases the specific connections between plasma parameters, temperature, pressure, growth mode, and ultimately physical properties will be stressed. The intent is to demonstrate how this less-well explored region of plasma processing space offers possible advantages to crystal growth of electronic materials of contemporary interest.

9:30 AM - 10:00 AM

FROM PLD TO MBE AND BEYOND: OXIDE EPITAXY AT HIGH TEMPERATURES

W. Braun, J. Mannhart

Max Planck Institute for Solid State Research, GERMANY

The success of traditional III-V molecular beam epitaxy (MBE) is largely based on its prevalent adsorption-controlled growth mode, in which the growth rate of the epitaxial layer is defined by the arrival rate of the non-volatile species (e.g. Ga), while the volatile component (e.g. As) is supplied in excess, but only incorporated in the exact stoichiometric ratio when the crystal unit cell forms. Under these

conditions, highly perfect epitaxial layers can be grown at low pressures in a large range of process conditions. On oxide surfaces, high surface mobilities suitable for the epitaxy of structurally high quality layers can be obtained at much lower substrate temperatures relative to the melting point. At these temperatures, desorption is usually negligible, which has led to the development and success of pulsed laser deposition (PLD) for the epitaxy of complex oxide heterostructures. Using a CO₂ laser based substrate heating system in PLD, we find that oxide substrate surfaces can be prepared with remarkable quality, largely independent of the material, when heated to temperatures where desorption sets in. To study layer growth under these conditions similar to classical III-V epitaxy, PLD, however, no longer is the method of choice, since a constant flux of one or more components is required to stabilize the surface and to explore adsorption-controlled growth modes with their promise of ultra-low defect densities. We have therefore begun to study the thermal laser evaporation of various elements that pose problems in oxide MBE in a setup conceptually very similar to PLD. We find that this method dramatically expands the accessible parameter range for oxide epitaxy and low-pressure epitaxy in general, leading to the vision of a fully laser-powered epitaxial setup which aims to combine the advantages of both PLD and MBE, while avoiding their respective shortcomings.

Wednesday, July 31, 2019

10:30 AM - 12:00 PM

Advanced Equipment and Growth Technology

Location: Shavano Peak

Session Chair(s): Koh Matsumoto, Michael Heuken

10:30 AM - 11:00 AM

MOCVD IN PRODUCTION-TODAY AND FUTURE CHALLENGES

J..I. Davies

IQE plc, UNITED KINGDOM

Key Enabling Technologies (KETs) e.g. Microelectronics and Photonics, are integral to all advanced products, being embraced

globally as the core solution to Societal Challenges and economic success. Compound Semiconductors (CS) such as Gallium Arsenide (GaAs), have fundamentally enabled several major technology revolutions over the last 30 years, particularly in KETs. The global photonics market is a \$7 billion industry covering an extremely diverse range of applications with lasers and sensors made from CS being a major portion of this marketplace. For example, market predictions show e.g. from Yole research of market growth for IR solid state light sources for illumination growing from \$450M in 2016 to \$1550M in 2022, with the Vertical Cavity Surface Emitting Laser (VCSEL) share increasing from 21% to 48%. Datacom and industrial markets would add considerably to this market growth. Evidence of such expansion is provided in the manufacturing of VCSEL-based devices, which have in recent years, entered a rapid growth phase, with companies benefitting from an extensive market pull. In order to prepare for a GaAs/AlGaAs-based VCSEL MOCVD epitaxial wafer process, focussing on improvements required prior to mass manufacturing, many areas have to be addressed. This includes collaboration with supply chain partners that supports a cost-reduction for VCSEL epi-wafers - required to meet new ambitious targets. These include scalability, such as a move to 6" production, automated loading/unloading, integrated test routines and in-situ process control. Given that the technology is now growing rapidly and increasingly addressing mass market applications, e.g. in Sensing and predicted soon to involve LIDAR, the target will be to acquire manufacturing capabilities through e.g. yield and throughput improvements, close to a level achieved in existing mass-manufacturing industries.

11:00 AM - 11:15 AM

IN SITU RECONSTRUCTION OF CRYSTAL SHAPE GROWN IN AN AXISYMMETRIC KYROPOULOS SYSTEM

T. Duffar¹, G. Sen¹, L. Braescu²

¹SIMAP EPM, FRANCE, ²Institut National de la Recherche Scientifique -, QC, CANADA

The Kyropoulos growth system is used to grow large high quality sapphire crystals. But since they grow inside a sealed furnace, there is no established monitoring system to allow observing the growth. This

makes it difficult to control the growth parameters ensuring a desired geometrical shape. In the present work a melt-height monitoring system is imagined in the growth system, which would allow the acquisition of the evolving melt level along with the pulling distance of seed and the measured weight of the growing crystal submerged in the melt. Based on all these parameters, it is demonstrated that it would be possible to trace in-situ and in real time the shape of the growing crystal. The needed accuracy for the measurement tools is studied.

11:15 AM - 11:30 AM

OPTIMAL GROWTH OF YAG SINGLE CRYSTAL FIBER BY MODIFIED LHPG METHOD

Z. Jia, J. Zhang, X. Tao

Institute of Crystal Materials & State Key Laboratory of Crystal Materials, Shandong University, CHINA

Compared to traditional silica fiber, YAG crystal has lower Brillouin gain coefficient, higher pump power and thermal conductivity, almost 10 times that of silica. Furthermore, there is no evaporation during crystal growth process, it is considered that YAG crystals are easy to grow making it a very suitable choice of material for single crystal fiber (SCF). In this work, we have successfully fabricated Yb:YAG SCFs with the diameter fluctuation under $\pm 2\%$ and the length of more than 200 mm using LHPG method. In order to improve the quality of the crystal, SCFs were grown under different parameters (atmosphere, pulling rate and pulling ratio). We found that Yb³⁺ is evenly distributed in the YAG SCF and SCFs still maintain a good thermal conductivity at high Yb³⁺ concentrations compared to YAG bulk crystal. The quality of the SCFs were measured by Laue diffraction and High-resolution X-ray diffraction for the first time.

11:30 AM - 11:45 AM

LOW COST MODIFIED CZOCHRALSKI TECHNIQUE FOR ORGANIC CRYSTALS: GROWTH, CHARACTERIZATION AND APPLICATION

B. Kumar

UNIVERSITY OF DELHI, INDIA

Czochralski technique is a well established method to grow many technologically important crystals. However, this technique has been seldomly used for the growth of organic crystals. Due to high cost and complex infrastructure of CZ setup, crystal growth activities at smaller universities are mostly confined to solution growth for organic crystals. In the present work a low cost CZ setup was devised which can be used to grow quality single crystals of organic/ semi organic materials of low melting point. It has been shown that even an 'oil bath' can be used in place of furnaces. The problem of attaining required temperature profile, high vapor pressure, toxic evaporation, etc. are resolved. We have recently grown many organic/semiorganic single crystals of Benzophenone, 8-Hydroxyquinoline, biphenyl, etc. by a simple modified Czochralski set-up [1-4]. It was found that it is difficult to maintain required temperature profile for a low melting point material (less than 100 °C) in a cylindrical resistive furnace. Therefore, a specially designed oil bath was used in place of high temperature furnace. Further, problem of excessive toxic evaporation was solved by placing whole growth chamber within a closed glass enclosure in which inert gas was flown at high pressure. The structural (XRD & SCXRD), optical (UV-Vis, PL, Raman), electric (dielectric, piezoelectric, ferroelectric), etc. properties of CZ grown crystals are compared with their solution grown counterpart. It has been found that apart from better size and directionality, CZ grown crystals are more suited for device fabrication owing to their superior crystallographic, optical and electrical properties. These crystals are used to fabricate communication devices (like GHz patch antenna) and energy harvesting devices. This work has opened the door for the crystal growth of organic crystals by CZ method.

References: Enhancement of Optical Piezoelectric, and Mechanical Properties in Crystal Violet Dye-Doped Benzophenone Crystals Grown by Czochralski Technique. Binay et al., Crystal Growth and Design 15 (2015) 4908–4917 Modified low temperature Czochralski growth of xylenol orange doped benzophenone single crystal for fabricating dual band patch antenna. Binay et al., Journal of Crystal Growth, 450 (2016) 74–80 Growth of 8-Hydroxyquinoline Single Crystal by Modified Czochralski Growth Technique and its Characterization, Binay et al. , CrystEngComm, 20 (2018) 624-630

Anisotropic electrical and optical studies of organic biphenyl single crystal grown by modified Czochralski technique, Binay et al., Journal of Materials Science: Materials in Electronics (2019) DOI: 10.1007/s10854-019-00676-8

11:45 AM - 12:00 PM

FORMATION OF HIERARCHICAL STRUCTURES OF 3,5-DINITROPYRAZINE-2,6-DIAMINE-1-OXIDE WITH POLYMERIC ADDITIVES AND THEIR ENHANCED MECHANICAL PROPERTIES

X. Zhou, J. Shan, H. Li

Institute of Chemical Materials, China Academy of Engineering Physics, CHINA

Morphology of molecules and materials has a significant impact on their properties and functions. The strategies of morphology control have attracted much interest of chemists and materials scientists. A good model for morphology control is found in biominerals, which form inorganicorganic composites with hierarchically organized morphologies under mild conditions. Inspired by biological approaches, many hierarchical structures of inorganic crystals have been prepared through controlling growth in the presence of polymeric additives. In recent years, hierarchical structures of organic crystals have also been studied, which have great potential for many applications in various areas including pharmaceuticals, food, pigments, and explosives. For explosives, formation of hierarchical structures is especially important since the crystal morphology of explosives can not only determine their mechanical and safety properties, but also influence their formulation and manufacturing processes such as extrusion or melt casting. Hence, it is significant to explore an effective crystallization methodology to obtain hierarchical structures of explosive crystals to improve their properties and expand their applications. In this paper, 3,5-dinitropyrazine-2,6-diamine-1-oxide (LLM-105) was selected as a model organic explosive molecular, which has potential applications in insensitive boosters, detonators, and main charges in specialty munitions because of its excellent thermal stability and safety. However, LLM-105 crystals are manufactured by the conventional crystallization method as long needle-like shapes, which will produce the problems such as poor flow

properties, low bulk density, and poor mechanical properties. Herein, we developed a facile polymer-induced antisolvent crystallization method to crystallized hierarchical structures of LLM-105. The results show that the formation of the hierarchical structures and their size, morphology and porosity depend strongly on the polyvinyl pyrrolidone (PVP) concentration. Furthermore, LLM-105 hierarchical structures exhibit enhanced mechanical properties. Based on our results, we propose a possible mechanism for the formation of hierarchical structures of LLM-105 based on the self-assembly principle. Overall, in this work we used the crystallization of LLM-105 hierarchical crystals in the presence of PVP as additive as a model system to better understand the effects of polymeric additives on the crystallization of organic hierarchical crystals.

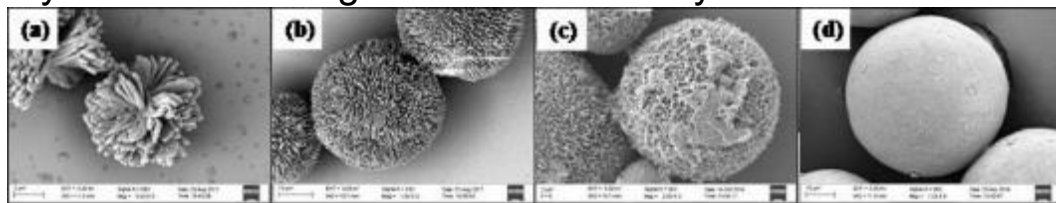


Figure 1. SEM images of obtained LLM-105 hierarchical structures with different PVP concentration.

Wednesday, July 31, 2019

10:30 AM - 12:00 PM

Fundamentals of Crystal Growth: Surfaces and Interfaces

Location: Crestone I, II

Session Chair(s): Boaz Pokroy, F. Spaepen

10:30 AM - 11:00 AM

IN SITU OBSERVATIONS OF STEP DYNAMICS ON GROWING INTERFACES BETWEEN ICE AND SUPERCOOLED WATER

K. Murata, G. Sazaki

Institute of Low Temperature Science, Hokkaido University, JAPAN

Ice crystallization from supercooled water, more generally, crystallization from its own supercooled melt (the so-called melt growth), is one of the fundamental phase transitions seen everywhere in nature. Despite its ubiquity, the microscopic picture of the melt

growth is still far from completely understood, contrary to the crystal growth from vapor and solutions. This mainly comes from the experimental difficulties of direct and precise observations of crystal-melt interfaces during the melt growth in an in-situ manner. For instance, compared with the vapor and solution growth, a crystal growth rate in melt is known to be significantly higher even for a low degree of supercooling. Moreover, the small mismatch in the refractive indices between crystal and melt, namely the extremely low reflectivity, also hampers optical microscopic observations with high sensitivities. The microscopic understanding of the melt growth, including the difference from the vapor and solution growth, still remains a persistent challenge. In this study, to overcome these difficulties, we prepare a specific growing/melting interface between ice and supercooled water, fixed normal to the optical axis, by applying a temperature gradient crossing the melting point along this axis. This experimental system allows us to follow the dynamics of ice interfaces with a moderate growth rate by accurately controlling the temperature gradient. We then make in-situ observations of this interface with our advanced optical microscopy, laser confocal microscopy combined with differential interference microscopy (LCM-DIM), whose resolution in the height direction reaches the order of an angstrom. As a result, we find that bunching-like steps flow on the growing interface while keeping an equal step spacing, which are mediated by screw dislocations (the spiral growth). Interestingly, these bunching-like steps behave as the so-called step density waves. Unlike the usual steps on facets, the interference pattern, reminiscent of ripples, appears on the interface when step arrays, having different spiral centers and advancing in different directions, coalesce with each other. We will discuss an intimate link between this step behavior and the step bunching instability of vicinal surfaces, first proposed by Chernov [1]. Reference [1] A. A. Chernov, *J. Cryst. Growth* **118**, 333-347 (1992)

11:00 AM - 11:15 AM

FUNDAMENTAL STUDY OF METAL ORGANIC CHEMICAL VAPOR DEPOSITION (MOCVD) OF MGF₂

A.C. Arjunan, T. Salagaj, M.E. Tawfik, **G. Tompa**

Structured Materials Industries, Inc., NJ, UNITED STATES OF AMERICA

MgF₂ is a deep UV transparent dielectric material which makes it useful for mirrors, antireflection coatings, interference coatings, and other applications. An important astronomical application is protective coatings on Al surfaces. MgF₂ films are typically deposited by evaporation, sputtering, ion beam assisted deposition (IBAD), and more recently were demonstrated by alternating layer deposition (ALD) [1]. Deposition of MgF₂ films by MOCVD has not been well studied. We report here on initial growth studies using Cp₂Mg as a magnesium source and Fluorobenzene and sulfur hexafluoride (SF₆) as Fluorine (F) sources in a rotating disk reactor. Growth was examined in the temperature range from 350 to 450°C on substrates of Si and sapphire at a pressure of 150 Torr in a background gas mixture of Argon and Hydrogen. We will present film property results including growth rates (100 to 400 nm/hr), n and k values, and crystallinity among other measurements as a function of F:Mg ratio, precursor concentration, deposition temperature, and other parameters. We found that while optically smooth films could be grown, carbon is an ongoing concern with C-F based precursor growth; whereas the SF₆ provides an abundance of F without C. Also, we found that SF₆ did not incorporate sulfur in to our films from X-ray fluorescence studies. Further, films grown using SF₆ precursor are transparent compared to films grown using fluorobenzene which are darker due fluorine deficiency. As next steps, we plan to investigate additional process chemistries, annealing in a F based environment, and extending the range of process parameters evaluated in general. [1] John Hennessy, April D. Jewell, Frank Greer, Michael C. Lee, and Shouleh Nikzad, , J. Vac. Sci. Technol. A 33(1), 01A125-1-6.

11:15 AM - 11:30 AM

ARRANGEMENT OF DISLOCATIONS INTO RING CRYSTAL OF TRANSITION METAL TRICHALCOGENIDES

M. Tsubota, M. Watanabe

Gakushuin University, JAPAN

Although defects are contained in the crystal, its density and

arrangement vary depending on the synthesis condition. MX_3 (M=Nb or Ta, X=S or Se) is a needle-shaped crystal with triangular prism in which six chalcogenes surround a metal parallel to an axis. Topological crystals of MX_3 , known as ring and Möbius shaped, is already known since 2002¹⁾. In order to bend the single crystal, invasion of defects is indispensable, but it is not obvious how to arrange them. In this study, we have synthesized micrometer-scale ring crystals and polyhedral ring crystals of MX_3 by the chemical vapor transportation method, and have observed morphological change due to annealing. The polyhedral ring crystals are closed-loop crystals with several vertices²⁾. In the case of closed-loop, dislocations does not go away from the edge. We investigated the crystallinity and flatness of the facets by the electron backscatter diffraction technique and found that the orientation of the crystal axis changed abruptly at several points. We classified ring-polyhedral crystals as a phase diagram of in terms of radius and thickness. We also proposed a mechanism of polygonization in which the vertices of the polyhedral crystals were formed from concentrated dislocations as a result of distance-dependent interactions between them. As a result of annealing the needle-crystal at 753 K, the crystal spontaneously bended in one direction. Recrystallization occurred with a curvature ¹⁾ S. Tanda et al , "A Mobius strip of single crystals," *Nature*, 417, 397-398 (2002). ²⁾ M. Tsubota *et al*, "Polyhedral Topological Crystals," *Crystal Growth & Design*, 11, 4789-4793 (2011).

11:30 AM - 11:45 AM

QUASI-LIQUID LAYERS CAN EXIST ON POLYCRYSTALLINE ICE THIN FILMS AT A TEMPERATURE SIGNIFICANTLY LOWER THAN ON ICE SINGLE CRYSTALS

J. Chen, K. Nagashima, K.I. Murata, G. Sazaki

Institute of Low Temperature Science, Hokkaido University, JAPAN

Surface melting of ice crystals proceeds below the melting point (0 °C), and forms thin liquid water layers, called quasi-liquid layers (QLLs), which govern a wide variety of phenomena in nature. Hence, many studies have been performed so far, however the lowest temperature above which QLLs exist on ice crystal surfaces varied

from -90 to -1 °C. To reveal the cause of such significant variations, here we show, by laser confocal microscopy combined with Michelson interferometry, the behavior of QLLs on polycrystalline ice thin films that include a large amount of grain boundaries and defects. [1] Polycrystalline ice thin films were prepared by ultrapure water dropped on cover glasses cooled using liquid nitrogen (-196 °C). The ice thin film was cut into a small piece (0.6×0.6 mm²) to reduce the amount of water vapor necessary to grow the ice thin film. In our optical microscopy system, one can distinguish optically isotropic QLL surfaces from optically anisotropic surfaces of the polycrystalline ice thin films, in which ice grains are randomly oriented. We observed QLLs formed on the polycrystalline ice thin films under various temperatures. Then we found that the droplet-type QLLs can exist stably on the polycrystalline ice thin films even at -16.2 °C (the lowest temperature adopted in this study), although the QLLs on ice single crystals disappear at temperature lower than -2.4 ± 0.5 °C. This result clearly emphasizes the importance of grain boundaries and defects for the presence of QLLs. In addition, from the moving directions of the interference fringes by the Michelson interferometer, we could judge whether the QLL was growing or shrinking under various water vapor pressures. Then we also found that critical water vapor pressure above which the QLLs can stably exist is always higher than the solid-vapor equilibrium curve, indicating that the QLLs are formed in a metastable state by the deposition of supersaturated water vapor, as in the case of ice single crystals. **Reference:** [1] J. Chen et al., *Cryst. Growth Des.* **2019**, 19, 116-124.

11:45 AM - 12:00 PM

STEP BUNCHING INDUCED BY IMPURITIES IN A SURFACE DIFFUSION FIELD

M. Sato

Information Media Center, Kanazawa University, JAPAN

Impurities attaching to a vicinal surface cause step bunching, which is well known and studied by many groups. However, effects of a surface diffusion field on the step bunching has not been studied sufficiently. Thus, we carry out Monte Carlo simulations using a simple lattice model and study how the surface diffusion field affects the step

bunching induced by impurities. We study three cases, (1) neither impurities nor adatoms evaporate and impurities are immobile on a surface, (2) at least impurities evaporate and impurities are immobile on a surface, and (3) both impurities and adatoms are evaporate and impurities migrate on a surface. In our simulation, we keep the impingement rates of both impurities and adatoms constant. The step bunching occurs when the impingement rate of adatoms are small smaller than a critical value. In the first and second cases, where the migration of impurities is neglected, step bunches is tight. The evaporation of impurities decreases the bunch size in steady state. In the third case, where the impurities migrate on the surface, the migration weakens clean-up of surface by step passing and the difference between the impurity density at the rear side of step and that in front of step decreases. The decrease in impurities has step bunches loose, and the separation of single steps from bunches repeatedly occurs. The bunch size grows by both collisions of small bunches and collisions between small bunches and single steps. In our talk, we will show how the impurity density on surface and that incorporated in solid depends on parameters.

Wednesday, July 31, 2019

10:30 AM - 12:00 PM

Silicon PV

Location: Torrey Peak II-IV

Session Chair(s): Jeffrey J. Derby, Ted Cizek

10:30 AM - 10:45 AM

ASSESSMENT OF THE KYROPOULOS PROCESS TO THE SILICON SINGLE CRYSTAL FOR PV APPLICATIONS

K. Zaidat, A. Nouri, G. Chichignoud, Y. Delannoy

SIMaP-EPM laboratory, INP Grenoble Alpes University, FRANCE

The efficiency of photovoltaic silicon cells depends dramatically on the crystalline structure, which is related to the manufacturing process. Single crystalline silicon cells, due to a lower defect density, have a better efficiency than polycrystalline cells. The final ingot, obtained from the Czochralski method, is a cylindrical silicon single crystal. Yet

photovoltaic cells have a square geometry. In order to get both the best photoelectric efficiency and material yield, a square single crystal ingot is required. The present work deals with the adaptation of the Kyropoulos process for silicon. Kyropoulos process is generally used for sapphire but it should be relevant for silicon. This process would reduce the dislocation density and improve therefore the efficiency of photovoltaic cells. Indeed, the growth takes place in a low-temperature region within a low temperature gradient, minimizing stress. Moreover, as the shape of the final ingot is square, the material yield is expected to be largely improved. For that purpose, facets growth and engineering will be implemented. A Cyberstar Bridgman furnace has been adapted for the Kyropoulos crystallization of silicon. Experimental studies were carried out to investigate favorable thermal conditions for growth from the seed. Crystals were grown from the seed. To improve the size of this crystal, the control of the heat fluxes, near the corners and faces of the crucible and in the seed area, is necessary. Modifications of the heat zones inside the furnace were assessed to allow a larger lateral growth. As coupled phenomena play an important role, a modeling approach is also carried out, complementary to experiments. 3D modeling is developed and implemented using ANSYS Fluent. Thermal and fluid mechanics maps are calculated for a range of conditions. Process condition and geometry are more particularly investigated. The main objective is to provide a set-up suitable for both lateral and longitudinal crystal growths. Influence of process parameters upon the quality of the growth from the seed is assessed using XRD and EDSD characterizations. In this presentation, we will propose an assessment of this technique on the PV applications.

10:45 AM - 11:00 AM

INFLUENCE OF THE VERTICAL TEMPERATURE GRADIENT ON THE GROWTH INTERFACE SHAPE, THERMAL STRESS AND IMPURITIES DISTRIBUTION IN DIRECTIONAL SOLIDIFICATION OF MULTICRYSTALLINE SILICON

C. Stelian, M. Velazquez

SIMaP UMR 5266 CNRS-UGA-G INP, FRANCE

Three dimensional modeling is applied to investigate the shape of the

growth interface, thermal stress and impurities distribution during directional solidification of the silicon. The transient computations are performed for a domain containing a square-shaped quartz crucible and the silicon charge with a volume of $40 \times 40 \times 10 \text{ cm}^3$. The solidification process is investigated by applying different temperature profiles as boundary conditions at the outer surface of the crucible. The shape of the moving crystal-melt interface is computed by using the deformable mesh technique. The k - ϵ model is applied for modeling the turbulent flow in the melt. Computations performed with a vertical temperature profile characterized by a high gradient ($G_C=10 \text{ K/cm}$ in the crystal) show a concave shape of the crystal-melt interface (seen from the melt) with a small curvature. The interface deflection increases from 0.1 cm at the beginning of the solidification to 0.2 cm at the middle stage of the growth process. Thermal stress computations are performed by applying boundary conditions with and without crucible constraint. The case computed without crucible constraint shows higher thermal stress in the central region of the ingot (20 MPa in the center) as compared to the crystal periphery. The computations performed by considering the crucible as a rigid boundary show that the von Mises stress increases by more than one order of magnitude at the crystal periphery. The modeling of the case with low temperature gradient ($G_C=3 \text{ K/cm}$ in the crystal) shows that the interface deflection increases by a factor of two. In this case, the von Mises stress decreases at the ingot center, but increases at the crystal periphery due to larger interface curvature in this growth system. These results are in agreement with the experiments of Ma et al. [1] showing that the average conversion efficiency of solar cells increases in the case of silicon ingots grown in the conditions of high vertical temperature gradient. Transient computations of carbon and boron distribution are performed for the case with high temperature gradient. Numerical results show nearly homogeneous solute distribution in the transversal section of the ingot, which can be explained by low interface curvatures in this system. [1] W. Ma, G. Zhong, L. Sun, Q. Yu, X. Huang, L. Liu, *Solar Energy Materials and Solar Cells* 100 (2012) 231.

11:00 AM - 11:15 AM

ANALYSIS OF THE ENGULFMENT OF FOREIGN PARTICLES DURING CRYSTAL GROWTH OF SOLAR SILICON

C. Huang¹, B. Druecke¹, C. Reimann², J. Friedrich², T. Jaus³, T. Sorgenfrei³, J.J. Derby¹

¹University of Minnesota, MN, UNITED STATES OF AMERICA,

²Fraunhofer IISB, GERMANY, ³University of Freiburg, GERMANY

A major challenge for the growth of multi-crystalline silicon via directional solidification is the nucleation and growth of carbide and nitride (SiC and Si_3N_4) particles in the melt that are engulfed by the solidification front to form inclusions. These inclusions lower solar cell efficiency and can lead to wafer breakage and sawing defects. Minimizing the number of these engulfed particles will promote lower cost and higher quality silicon and will advance progress in commercial solar cell production. To better understand the physical mechanisms responsible for such inclusions during crystal growth, we have developed finite-element, moving-boundary analyses to assess particle dynamics during engulfment via solidification fronts. This numerical approach allows for an accurate representation of forces and dynamics previously inaccessible by approaches using analytical approximations. We present initial computations for the case of silicon nitride particle engulfment in this system. Since both the thermal conductivity and the morphology of silicon nitride particles differ significantly from those of silicon carbide, we expect substantial differences in engulfment behavior. These computations will be compared with recent experiments on silicon nitride engulfment from terrestrial and microgravity experiments.

11:15 AM - 11:30 AM

SILICON INGOT GROWTH FROM NITRIDE CRUCIBLES MADE FROM KERF-LOSS SILICON DURING DIAMOND WIRE SAWING

C. Lan, C. Liu, H. Yu, H. Yang

Dept. of Chem. Eng., National Taiwan University, TAIWAN

The broken used quartz crucibles and kerf-loss silicon during wafer slicing have been the two major wastes from photovoltaic (PV) industry. In this work, we demonstrated a process of recycling kerf-

loss silicon to produce reaction bonded silicon nitride (RBSN) crucibles for multi-crystalline silicon (mc-Si) ingot growth through acid leaching refining, slip casting, and nitridation. First, the kerf-loss silicon was treated with acid leaching with mixed acids and then nitric acid; the recycled silicon could reach 5N purity, which was purer than quartz crucibles and comparable with the silicon nitride powder used for the releasing agent during mc-Si ingot casting. The cleaned silicon was then mixed with deionized water at a proper pH value and solid content for slip casting. The green body was dried for a few days and calcined in air at 500 °C for 3 h for removing organics. To make RBSN, the crucible was heated to 900°C in vacuum to remove oxides and then nitridated slowly under nitrogen with 5% hydrogen at higher temperature; the final temperature was over the melting temperature of silicon. Before ingot casting, the RBSN crucible was oxidized in air at 1050 °C for 5 h. This step was crucial to prevent the crucible from infiltration of silicon melt during casting. The RBSN crucibles could be reused for a few times. With increasing number of runs, we found that the ingot resistivity increased, indicating that boron was slowly leached out by the silicon melt. And the grown ingot quality was found better than those grown from the quartz crucibles, which could only be used once.

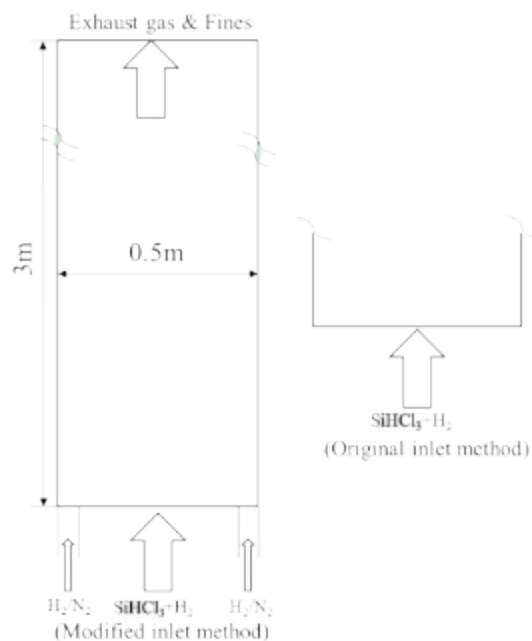
11:30 AM - 11:45 AM

NUMERICAL INVESTIGATION OF SILICON WALL DEPOSITION IN TRICHLOROSILANE FLUIDIZED BED REACTOR

S. Du¹, L. Liu²

¹Xi'an Jiaotong University, CHINA, ²Xi'an Jiaotong University, CHINA
The fluidized bed method, using trichlorosilane as the reactant gas to pyrolyse and deposit on the surface of granular silicon, has become a significant alternative technology to manufacture high purity polysilicon. However, some unsolved problems such as uneven heating and silicon wall deposition restrict the usage of this technology. Therefore, it is necessary to investigate and reduce the silicon wall deposition during the granular silicon growth process in fluidized bed. In this paper, a 2D unsteady simulation is carried out to describe the granular silicon growth process inside the fluidized bed. The gas-solid two-phase flow model, trichlorosilane homogeneous

pyrolysis and heterogeneous deposition reaction models are incorporated. In addition, simulation of the silicon epitaxial growth on a silicon substrate in a single-wafer reactor is carried out to validate the effectiveness of the silicon wall deposition reaction model [1]. Then the silicon wall deposition process is investigated, and an optimized gas inlet configuration is proposed to reduce the silicon wall deposition. As shown in Fig. 1, the original inlet configuration is the uniform mixed gas inlet, thus the trichlorosilane is able to contact with wall immediately when the mixed gas flow into the reactor. Thus to prevent the contact between trichlorosilane and wall, a modified inlet configuration is proposed. As shown in Fig. 1 (left), Pure hydrogen or nitrogen is fed into the reactor from the side inlet near the wall. The wall deposition rates under original (uniform inlet) and modified (H_2 or N_2 at different inlet velocities) inlet conditions are shown in Fig. 1 (right). It is clear that the wall deposition mainly occurs near the inlet under the original inlet condition. In addition, the modified inlet configuration can significantly reduce the silicon wall deposition rate especially near the inlet. [1] H. Habuka, J.P. Suzuki, Y. Takai, H. Hirata, S.I. Mitani. Silicon epitaxial growth process using trichlorosilane gas in a single-wafer high-speed substrate rotation reactor. *J. Cryst. Growth* 327 (2011) 1-5.



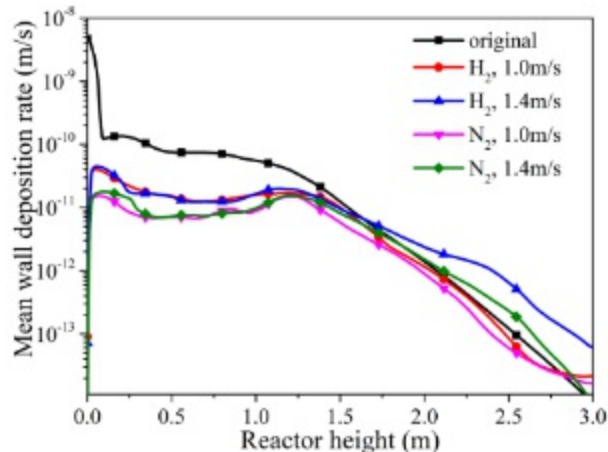


Fig. 1. Configuration of original and modified inlet design (left) and comparison of wall deposition rates under different inlet condition (right).

Wednesday, July 31, 2019

10:30 AM - 12:00 PM

Symposium on 2D Materials: Special Topics III: h-BN

Location: Crestone III, IV

Session Chair(s): Michael Snure, Benjamin Huet

10:30 AM - 11:00 AM

DEFECT-MEDIATED VAN DER WAALS EPITAXY OF H-BN ON EPITAXIAL GRAPHENE

J..M. Lopes

Paul-Drude-Institut für Festkörperelektronik, Leibniz-Institut im Forschungsverbund Berlin, GERMANY

In recent years two-dimensional (2D) hexagonal boron nitride (h-BN) has attracted great attention due to its possible integration as a dielectric layer in 2D heterostructures with graphene, which could be useful for several applications in electronics. Here van der Waals (vdW) epitaxy of atomically thin h-BN films on epitaxial graphene/SiC appears as a promising approach for the scalable fabrication of h-BN/graphene heterosystems [1]. However, the weak out-of-plane interaction between the 2D materials may impede homogeneous nucleation and thus subsequent formation of high-quality h-BN layers on epitaxial graphene.

In this contribution I will report on the recent research at the Paul-Drude-Institute, which aimed at the direct synthesis of h-BN on epitaxial graphene on SiC(0001) via plasma-assisted molecular beam epitaxy (PAMBE) [2]. Results on defect-mediated nucleation and vdW epitaxy of few-layer thick h-BN films on epitaxial graphene over a growth temperature range from 600 to 1000°C will be presented. A comparison with results achieved for PAMBE of h-BN on Ni templates utilizing very similar conditions will be made [3]. Finally, I will also show how surface modification of epitaxial graphene can be used to tailor nucleation and growth of h-BN. Strikingly, such an approach also promote the formation of unconventional BN nanostructures whose phase has only been predicted so far to be stable at high pressures/high temperatures.

Robinson, ACS Nano 10, 42 (2016).

Heilmann et al., 2D Materials 5, 025004 (2018). [3] Nakhaie et al., J. Appl. Phys. 125, 115301 (2019).

11:00 AM - 11:30 AM

HIGH-TEMPERATURE MOLECULAR BEAM EPITAXY OF HEXAGONAL BORON NITRIDE

T.S. Cheng¹, A. Summerfield¹, C.J. Mellor¹, C. Elias², P. Valvin², T. Pelini², B. Gil², G. Cassabois², L. Eaves¹, C.T. Foxon¹, P.H. Beton¹, **S.V. Novikov¹**

¹School of Physics & Astronomy, University of Nottingham, UNITED KINGDOM, ²Laboratoire Charles Coulomb, UMR5221 CNRS-Université de Montpellier, Montpellier, FRANCE

Research studies on the growth and properties of hexagonal boron nitride (hBN) have recently attracted a lot of attention. First, the lattice parameter of hBN is very close to that of the recently discovered graphene. The surface of hBN is atomically flat and will provide an ideal chemically inert dielectric substrate for 2D-structures. Secondly, the band gap of hBN is about 6 eV and that has triggered the interest in hBN as a wide gap material for deep-ultraviolet device (DUV) applications. There are now world-wide attempts to develop a reproducible technology for the growth of large area hBN layers by chemical vapour deposition (CVD), metal-organic chemical vapour

deposition (MOCVD) and molecular beam epitaxy (MBE). In this work we present our recent results on the high-temperature plasma-assisted molecular beam epitaxy (PA-MBE) of hBN monolayers with atomically controlled thicknesses for 2D applications and on the growth of significantly thicker hBN layers for potential DUV applications. We also report our recent results on the high-temperature PA-MBE growth of hBN layers using a high-efficiency RF plasma source with high active nitrogen fluxes. Despite more than a three-fold increase in nitrogen flux with this new source, we saw no significant increase in the growth rates of the hBN layers, indicating that the growth rate of hBN layers is controlled by the boron arrival rate. To characterise the hBN surface structure, we performed atomic force microscopy (AFM) measurements of the hBN monolayers. We used variable angle spectroscopic ellipsometry (VASE) to study the thickness of the hBN layers. We combine DUV photoluminescence and reflectance spectroscopy to study the optical properties of hBN. Our results demonstrate that PA-MBE growth on highly oriented pyrolytic graphite (HOPG) substrates at temperatures $\sim 1400^\circ\text{C}$ can achieve mono- and few-layer thick hBN with a control of the hBN coverage and atomically flat hBN surfaces, which is essential for 2D applications of hBN layers. The hBN monolayer coverage can be reproducibly controlled by the PA-MBE growth temperature, time and B:N flux ratios. Significantly thicker hBN layers have been achieved at higher B:N flux ratios. We observed a gradual increase of the hBN thickness by decreasing the growth temperature from $\sim 1400^\circ\text{C}$ to $\sim 1100^\circ\text{C}$. However, by decreasing the MBE growth temperature below 1250°C , we observe a rapid degradation of the optical properties of hBN layers. Therefore, high-temperature PA-MBE, above 1250°C , is a viable approach for the growth of high-quality hBN layers for 2D and DUV applications.

Wednesday, July 31, 2019

10:30 AM - 12:00 PM

Symposium on Epitaxy of Complex Oxides: Growth of Stannates by MBE

Location: Grays Peak II, III

Session Chair(s): Yoshiharu Krockenberger

10:30 AM - 11:00 AM

HIGH-MOBILITY HETEROSTRUCTURES WITH BaSnO_3

S. Stemmer

University of California, Santa Barbara, CA, UNITED STATES OF AMERICA

Recent reports of room temperature mobilities of $\sim 300 \text{ cm}^2 \text{ V}^{-1} \text{ s}^{-1}$ in single crystals of La-doped BaSnO_3 have generated significant excitement. BaSnO_3 has a wide band gap ($\sim 3 \text{ eV}$), which makes it of interest as a new transparent conducting oxide and as a wide band gap semiconductor for power electronics. Furthermore, it would allow for integration of functional perovskite oxides on a lattice- and symmetry-matched, high-mobility, semiconducting channel. Electronic devices require the growth of high-quality films with low defect densities. Here we discuss the growth studies of high-mobility BaSnO_3 using a modified molecular beam epitaxy (MBE) method, which supplies pre-oxidized SnO_x . We will discuss approaches to improve carrier mobilities and to reduce carrier densities. We will also discuss recent progress in developing functional heterostructures and field effect devices that combine high dielectric constant materials, such as $(\text{Ba,Sr})\text{TiO}_3$, with high-mobility BaSnO_3 . We discuss how such heterostructures enable scaled heterostructure field effect transistors for high-frequency amplification.

11:00 AM - 11:30 AM

SUBOXIDE-RELATED KINETICS, THERMODYNAMICS, AND METAL-EXCHANGE CATALYSIS DURING OXIDE MOLECULAR BEAM EPITAXY

O. Bierwagen

Paul-Drude-Institut für Festkörperelektronik, GERMANY

In_2O_3 , SnO_2 and Ga_2O_3 are prototypical oxide semiconductors with application potential for power electronics, UV sensing, and heterostructure devices. This talk will address fundamental aspects of oxide molecular beam epitaxy with the examples of these oxides.

In_2O_3 , SnO_2 , and Ga_2O_3 possess the suboxides In_2O , SnO , and Ga_2O whose formation and desorption causes decreased growth rates under metal-rich growth conditions as well as oxide layer etching by a metal flux only.[1] Increased growth temperatures further decrease the growth rate,[2] an effect that is stronger for Ga_2O_3 than In_2O_3 and SnO_2 due to the higher Ga_2O vapor pressure than that of In_2O and SnO .[3,4] A given flux of plasma-activated oxygen can oxidize significantly more In and Sn than Ga.[1] This higher oxidation efficiency and lower suboxide vapor pressure correspond to kinetic advantages enabling significantly higher growth rates for In_2O_3 and SnO_2 than for Ga_2O_3 . The dependence of the growth rate on all growth parameters found above can be well described and quantitatively modeled by a two-step growth: In a first step the suboxide is rapidly formed. The competition between its desorption and its oxidation to the full oxide determines the growth rate.[4] Despite the kinetic advantages for the formation of In_2O_3 a preferred incorporation of Ga into $(\text{In}_x\text{Ga}_{1-x})_2\text{O}_3$ was observed and explained by the thermodynamic preference of the stronger Ga-O bonds than In-O bonds.[5] A strong enhancement of the Ga_2O_3 growth rate in the presence of an additional In flux at high growth temperatures has been demonstrated: In this metal-exchange catalysis process, In_2O_3 is rapidly formed (due to its kinetic advantage) followed by an exchange of the In by Ga (due to the stronger Ga-O bonds) producing free In. [6,7] We will demonstrate efficient suboxide sources based on the reaction of the metal with its oxide requiring significantly lower effusion cell temperatures than for the decomposition of the pure oxide into its suboxide. Such a SnO source will be used to grow BaSnO_3 . [1] P. Vogt and O. Bierwagen, Appl. Phys. Lett. **106**, 081910 (2015). [2] P. Vogt and O. Bierwagen, Appl. Phys. Lett. **108**, 072101 (2016). [3] P. Vogt and O. Bierwagen, Appl. Phys. Lett. **109**, 062103 (2016). [4] P. Vogt and O. Bierwagen, Phys. Rev. Materials **2**, 120401(R) (2018). [5] P. Vogt and O. Bierwagen, APL Materials **4**, 086112 (2016). [6] P. Vogt, et al., Phys. Rev. Lett. **119**, 196001 (2017). [7] P. Mazzolini et al., APL Materials **7**, 022511 (2018).

11:30 AM - 12:00 PM

RADICAL-BASED MBE APPROACH FOR COMPLEX OXIDE EPITAXY

B. Jalan

University of Minnesota, MN, UNITED STATES OF AMERICA

Synthesis of metal oxides using ultra high vacuum (UHV) approach can be non-trivial. This is particularly true for metals having low oxidation potential, i.e. hard to oxidize. Controlling and tuning of point and line defects can further be challenging. Using stannate as a model material system, I will present a novel radical-based molecular beam epitaxy (MBE) approach for the growth of metal oxides of stubborn metals. Through detailed thin film growth, synchrotron x-ray scattering, electronic transport, and first-principles calculations, we show detailed MBE growth, and epitaxial stabilization of different polymorphs of SrSnO_3 (SSO) at room temperature (RT) in thin film form. Compressive strain stabilized the high-symmetry tetragonal phase of SSO at RT, which, in bulk, exists only at temperatures above 1062 K. A mobility enhancement of over 300% in doped tetragonal phase of SSO films compared with the low temperature orthorhombic polymorph was achieved. We will discuss these results in the context of the role of strain, doping and disorder on structure and electronic transport of doped SSO films. Work supported by AFOSR YIP and NSF DMR.

Synthesis of metal oxides using ultra high vacuum (UHV) approach can be non-trivial. This is particularly true for metals having low oxidation potential, i.e. hard to oxidize. Controlling and tuning of point and line defects can further be challenging. Using stannate as a model material system, I will present a novel radical-based molecular beam epitaxy (MBE) approach for the growth of metal oxides of stubborn metals. Through detailed thin film growth, synchrotron x-ray scattering, electronic transport, and first-principles calculations, we show detailed MBE growth, and epitaxial stabilization of different polymorphs of SrSnO_3 (SSO) at room temperature (RT) in thin film form. Compressive strain stabilized the high-symmetry tetragonal phase of SSO at RT, which, in bulk, exists only at temperatures above 1062 K. A mobility enhancement of over 300% in doped tetragonal phase of SSO films compared with the low temperature orthorhombic polymorph was achieved. We will discuss these results in the context of the role of

strain, doping and disorder on structure and electronic transport of doped SSO films. Work supported by AFOSR YIP and NSF DMR.

Wednesday, July 31, 2019

10:30 AM - 12:00 PM

Symposium on Ferroelectric Crystals and Textured Ceramics: and Bulk Crystal Growth: Piezoelectric Single Crystal: Growth and Characterization

Location: Grays Peak I

Session Chair(s): Alain Morina, Hiroaki Takeda

10:30 AM - 11:00 AM

DEVELOPMENT OF MELILITE-TYPE SINGLE CRYSTALS FOR HIGH TEMPERATURE PIEZOELECTRIC SENSOR

H. Takeda, H. Kusakabe, H. Usui, T. Hoshina, T. Tsurumi

Tokyo Institute of Technology, JAPAN

Aim of this study is to investigate a potential of melilite-type single crystals as high temperature piezoelectric sensor, especially, combustion pressure sensor. Among a plenty of melilite-type crystals, we firstly focused on calcium aluminate silicate $\text{Ca}_2\text{Al}_2\text{SiO}_7$ (CAS) single crystal because its contained only elements having abundant amounts of resources. However, the CAS single crystals with a clear cleavage plane may have low mechanical strength. This is why we synthesized modified CAS single crystals with higher mechanical strength by substitution for pressure sensor use. Strontium substituted CAS (Sr-CAS) single crystals were grown by Czochralski technique. The Sr-CAS crystal substrate with $(XYt)25^\circ$ rotation cut showed the rupture strength of 220 MPa, which is 1.4 times of that of CAS. Moreover, we also attempted to synthesize new melilite-type crystals by clarifying the relationship between crystal structure, piezoelectric properties and mechanical properties. We successfully synthesize the crystals substrate without phase transition but with the rupture strength over 800 MPa and the piezoelectric constant comparable with that of quartz.

Aim of this study is to investigate a potential of melilite-type single crystals as high temperature piezoelectric sensor. Among a plenty of

melilite-type crystals, we have focused on calcium aluminate silicate $\text{Ca}_2\text{Al}_2\text{SiO}_7$ (CAS) single crystal. For pressure sensor use, we attempted to synthesize modified CAS single crystals with higher mechanical strength by substitution. This is because the CAS single crystals with a clear cleavage plane may have low mechanical strength. Strontium substituted CAS (Sr-CAS) single crystals were successfully grown by Czochralski technique. The Sr-CAS crystal substrate with (XYt)25o rotation cut showed the rupture strength of 220 MPa, which is comparable to that of quartz.

11:00 AM - 11:15 AM

INVESTIGATION ON TERAHERTZ TIME-DOMAIN SPECTROSCOPY IN MIXED RARE EARTH ORTHOFERRITE

A. Wu

Shanghai Institute of Ceramics, CAS, CHINA

In this research, Mixed Rare earth orthoferrites single crystals were selected as the media for studying. The crystals were grown by optical floating zone method, using the high purity oxide as the starting materials. Terahertz time-domain spectroscopy (THz-TDS) was used to study the ferromagnetic mode and antiferromagnetic mode of Mixed Rare earth orthoferrites single crystals which excited by THz pulse. The resonant amplitude and frequency of antiferromagnetic mode were significantly changed in the spin reorientation transition temperature range, which demonstrates that the antiferromagnetic mode can be directly and non-thermally excited. The room temperature terahertz time-domain spectroscopies of $\text{Sm}_{0.4}\text{Er}_{0.6}\text{FeO}_3$ demonstrate that the antiferromagnetic mode and ferromagnetic mode can be excited when the magnetic field of THz pulse were parallel and vertical to magnetic vector of rare earth orthoferrites, respectively. Our measurement demonstrates that the terahertz time-domain spectroscopy is a sensitive mean to explore the spin reorientation transition in rare earth orthoferrites.

11:15 AM - 11:30 AM

THE EFFECT OF GAS ATMOSPHERE AND GROWTH PARAMETERS ON THE CRYSTALS QUALITY OF LANGATATE

($\text{La}_3\text{Ga}_{5.5}\text{Ta}_{0.5}\text{O}_{14}$) GROWN BY THE CZOCHRALSKI METHOD

B. Boutahraoui¹, M. Derbal¹, K. Lebbou²

¹Laboratoire LASICOM, Université Blida1, ALGERIA, ²Institut Lumière Matière, FRANCE

Because of its thermal stability, performed piezoelectric properties and no phase transformation up to melting point, $\text{La}_3\text{Ta}_{0.5}\text{Ga}_{5.5}\text{O}_{14}$ (LTG) langatate single crystal has been widely used as a sensor material in high temperature applications. The chemical composition of this crystal belongs to La_2O_3 - Ta_2O_5 - Ga_2O_3 ternary complex equilibrium diagram, the field of congruent composition, if exists, is very narrow and strongly depend on the solid solution of LGT. Melt composition control is the most critical parameter to adjust the LGT crystal growth from the melt. Moreover, the melt has a small selective Ga_2O_3 evaporation and the composition does change with time, it induces inclusions, cracks and limits the crystal yield. Langatate crystals were successfully grown along X, Y and Z axes by Czochralski technique in argon and mixed argon- O_2 atmospheres. The coloration and the performance of langatate crystals were strongly connected to the starting chemical composition, the gas atmosphere and the growth parameters. Any deviation from the LGT composition generates macroscopic defects such as cracks and grains boundary causing a deterioration of the crystals performance. Based on the growth of more than 40 crystals, through DTA/TG on the crystals and ceramic single phase, it was concluded that LGT is no-congruent material and has a peritectic transition relation to LaGaO_3 compound. The Ga_2O_3 loses minimization will be a key to improve the crystal growth under stationary stable regime.

Thursday, August 1, 2019

8:30 AM - 10:00 AM

Thursday Plenary Session

Location: Red Cloud Peak

Session Chair(s): Peter G. Schunemann

8:30 AM - 9:15 AM

ADVANTAGES AND CHALLENGES OF GROWING III-V PHOTONIC AND ELECTRON

K.M. Lau

HUST, HONG KONG PRC

RF and optoelectronic devices made with III-V semiconductors have been widely used since the 1970s, primarily in discrete form or low level integration. The conventional wisdom has been that lattice-matched crystal structures must be grown on native substrates with minimal crystalline defects to ensure good performance and reliable devices. With limited availability of last-area and low-cost substrates, large scale integration of III-V devices, circuits, and system is still in its infancy compared with Si CMOS that has been scaled following the Moore's law for more than five decades. Despite of the sustainability of the Moore's law, the exponential growth of big data traffic compared with the barely linear improvements in system energy-efficiency leading to a widening of the "energy gap" posts serious challenges. To fulfil the needs of energy-efficient high-performance computing and data-communication, increasing adoption and integration of optics and electronics using silicon photonics is necessary. Application of silicon photonic technologies to integrated systems will significantly impact future generations of high-performance and energy-efficient mobile and stationary data center systems, with much reduced form factor and power consumption. Design and implementation of compound semiconductor components on a silicon material platform for photonic and electronic integration is the most logical path forward. This III-V on silicon platform strongly leverages the enormous capabilities and infrastructure of Si CMOS, extending them to photonic and electronic integrated devices/circuits for high speed, wide bandwidth, and energy-efficient applications. Most communication wavelength lasers with excellent device performance have been grown on III-V substrates and bonded to silicon. For monolithic integration, growth and fabrication of such lasers on III-V/ Si compliant substrates is another option. However, this approach is challenging and was deemed intractable for decades. There is no perfect solution. Various III-V /Si compliant substrates have been explored and led to impressive device performance and reliability results. The compliant substrates will never be identical to the native substrates. We seek a

total solution combining novel epitaxial material systems, growth techniques, and device designs to demonstrate components with respectable performance metrics. I will discuss recent success of III-V active medium with quantum dots grown on compliant III-V/Si substrates exhibiting excellent lasing characteristics in whispering-gallery-mode (WGM) micro-lasers and conventional Fabry Perot lasers. Another approach involves nano-ridge lasers with embedded quantum wells grown on stripes patterned on thin SOI. InP/InGaAs nano-ridge lasers emitting from 1.3 to 1.5 microns at room temperature are excellent candidates for on-chip integration with silicon photonics.

9:15 AM - 10:00 AM

THEY CALL IT FREE ENERGY SO, HEY, WHY PAY?

J. De Yoreo

University of Washington, WA, UNITED STATES OF AMERICA

Nucleation is the seminal process in the formation of ordered structures ranging from simple inorganic crystals to macromolecular membranes. Recent observations have revealed a rich set of hierarchical pathways involving higher-order species ranging from multi-ion clusters to dense liquid droplets to transient amorphous or crystalline phases. Despite their complexity, a holistic framework for understanding such pathways based on classical concepts emerges when the effects of complexities in free energy landscapes and kinetic factors are considered. I illustrate that framework using in situ TEM and AFM studies of inorganic, organic, and macromolecular systems. The results show that introduction of size-dependent phase stability or high driving force coupled with the existence of metastable polymorphs leads to true two-step pathways characterized by the initial appearance of a bulk precursor. Creation of micro-states representing local free energy minima stabilized by chemical or structural factors also drives hierarchical pathways, but the intermediates can only exist as transient microscopic entities that may, nonetheless, provide the easiest path to the final ordered state. Reduction in molecular mobility can freeze in non-equilibrium structural states for kinetic reasons, while formation of highly mobile clusters at high supersaturations can lead to hierarchical growth due

to the dynamics of collision and assembly. The findings provide a common basis for understanding nucleation of ordered states in diverse materials systems.

Thursday, August 1, 2019

10:30 AM - 12:00 PM

Bulk Crystal Growth & Nonlinear Optica Materials I

Location: Shavano Peak

Session Chair(s): Kevin T. Zawilski, Shekhar Guha

10:30 AM - 11:00 AM

CRYSTAL GROWTH OF TERBIUM-DOPED AND TERBIUM-CONTAINING MATERIALS FOR OPTICAL ISOLATORS AND FLUORESCENCE STANDARDS

D. Rytz

FEE GmbH, GERMANY

Various types of crystals based on Tb-doped or Tb-containing compounds are currently grown and characterized at FEE. An overview will be provided on the technical challenges in growing single crystals with adequately low defect densities suited for optical isolators and fluorescence standards. The achieved performances will be compared to the state-of-the-art in the field. As examples the following crystals and their growth processes will be described: KTbW = $\text{KTb}(\text{WO}_4)_2$, TbAB = $\text{TbAl}_3(\text{BO}_3)_4$, Tb_2O_3 , TGG = $\text{Tb}_3\text{Ga}_5\text{O}_{12}$, and CALTO = CaTbAlO_4 , using TSSG for KTbW, TbAB, Tb_2O_3 , and the Czochralski technique for TGG and CALTO.

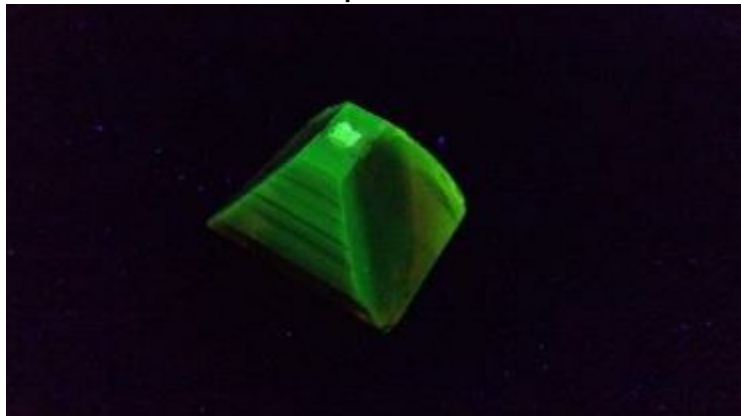




Figure caption: $KTb(WO_4)_2$ (KTbW, left, length of edge is 23 mm, crystal is illuminated by 365 nm source) grown by TSSG (“Top-Seeded Solution Growth”) and $CaTbAlO_4$ (CALTO, diameter is 25 mm) grown by the Czochralski technique.

11:00 AM - 11:15 AM

LOW TEMPERATURE LIQUID PHASE GROWTH AND TERAHERTZ OPTICAL PROPERTIES OF VAN DER WAALS CRYSTAL INSE

C. Tang, Y. Sato, W. Katsuya, J. Osaki, T. Tanabe, O. Yutaka
Tohoku University, JAPAN

The transition-metal monochalcogenides (TMMs) including InSe and GaSe, have been attracted more and more attention because of their novel thermal, magnetic, mechanical, optical and electrical properties. InSe is typical van der Waals crystal with bandgap energy of about 1.3 eV, which makes InSe one of the promising materials for high sensitive infrared detector and 2D spintronics device. Until now, most bulk InSe crystals have been prepared using the Bridgman-Stockbarger technique, in which temperatures at the melting point and a moving crucible (or a moving temperature distribution) are required. To simplify the crystal growth procedure and avoid the formation of defects generated by the drop in temperature and the mechanical disturbance suffered during the growth process, we used a low temperature liquid phase growth method called the temperature difference method under controlled vapor pressure (TDM-CVP), with which InSe can be grown motionlessly at a lower temperature than

that used in the Bridgman method (Fig. 1). The as-grown crystals were confirmed as the γ -InSe with favorable crystallinity by characterizations such as XRD (Fig. 2) and Raman spectroscopy. Moreover, the optical properties in terahertz frequency range were investigated using both the terahertz time domain spectroscopy (THz-TDS) and monochromatic terahertz spectroscopy via different frequency generation (DFG) process. It was shown that the absorption in terahertz range of InSe was far smaller than that of GaSe, a typical THz-generating nonlinear optical crystal (Fig. 3). The conducted Hall effect measurements were compared with the THz-TDS results in view of the carrier mobility and it was indicated that the estimation of carrier dynamics from THz spectroscopy was valid under some measurement conditions. The present study has clarified the practicability of TDM-CVP to prepare high quality InSe crystal and potential of InSe to be applied as nonlinear optical crystal for THz generation.

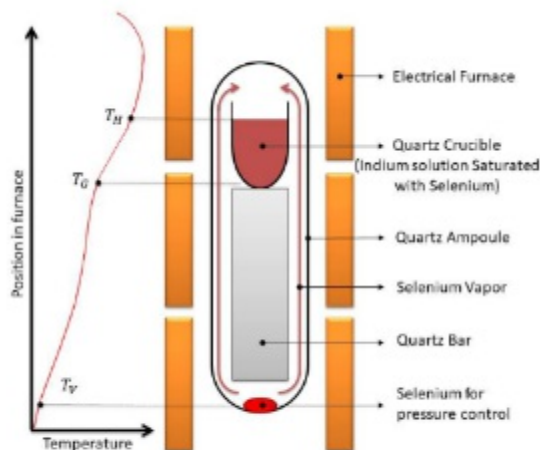


Fig.1. Schematic diagram of the temperature difference method under controlled vapor pressure

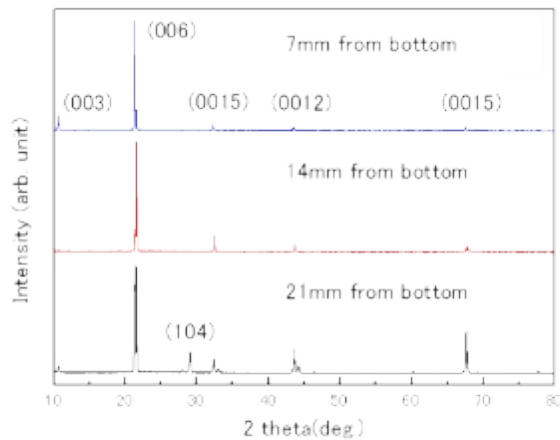


Fig. 2. XRD spectra of InSe perpendicular to the (001) direction. Samples were taken from 7, 14, and 21mm from the bottom of the ingot

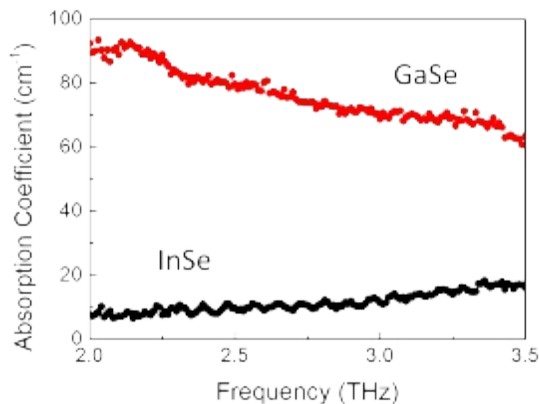


Fig. 3. THz range absorption spectra of InSe (red) and GaSe (black) tested by using coherent THz waves generated via DFG process.

11:15 AM - 11:30 AM

MULTISCALE CHARACTERIZATION OF THE POINT DEFECT AND ROTATIONAL DISORDERS IN TWO NEW HIGH-TEMPERATURE SOLUTION GROWN RARE-EARTH BORATES (ORAL PRESENTATION)

M. Velazquez¹, **S. Péchev**², **O. Pérez**³, **M. Duttine**², **A. Wattiaux**², **C. Labrugère**⁴, **P. Veber**⁵, **S. Buffière**²

¹SIMaP UMR 5266 CNRS-UGA-G INP, FRANCE, ²ICMCB, UMR 5026 CNRS-Université de Bordeaux-Bordeaux INP, FRANCE,

³CRISMAT UMR 6508 CNRS-ENSICaen-UCBN, FRANCE,

⁴PLACAMAT, UMS3626, CNRS-Université Bordeaux, FRANCE,

⁵Institut Lumière Matière UMR 5306, FRANCE

Rare-earth-doped or highly substituted (oxy)borates are extensively investigated for their remarkable physical properties. For example, in recent years, tremendous efforts have been dedicated to the search for and development of a significant number of Tb-based new crystals, essentially because of their potentially remarkable optical, magnetic and magneto-optic properties for the prospects of Faraday rotator, solid state lasers, phosphors and biological cell imaging [1-8]. New $\text{Sr}_6\text{Tb}_{0.94}\text{Fe}_{1.06}(\text{BO}_3)_6$ single crystals have been grown by high-temperature solution growth in controlled atmosphere and their crystal structure has been characterized by XRD. The type of point defects found in the crystals is different from the one found in similar powder phase materials. Moreover, the point defects disorder was investigated at small (~ 1 unit cell) and middle (~ 10 -1000 unit cells) distances by diffuse reflectance and Mössbauer spectroscopies, which evidenced an Fe/Tb disorder not seen in the average over large distances XRD-based crystal structure. The low temperature Mössbauer spectra also complemented the specific heat and magnetic susceptibility data, and the absence of Tb^{4+} cations was established by XPS measurements. In this communication, we will also present single crystals and selected physical properties of a recently discovered oxyborate phase of approximate composition $\sim \text{Li}_3\text{K}_2\text{Pr}_{11}(\text{BO}_3)_7\text{O}_9$, the crystal structure of which exhibits both point defect and BO_3^{3-} -groups rotational disorders. [1] P. Veber, M.

Velázquez, G. Gadret, D. Rytz, M. Peltz, R. Decourt, *CrystEngComm*, **17**, 492 (2015). [2] P. Chen, R. K. Li, *J. Alloys Comp.*, **622**, 859 (2015). [3] K. Shimamura *et al.*, *Cryst. Growth Des.*, **10**, 3466 (2010). [4] F. Guo, X. Chen, Z. Gong, X. Chen, Z. Xiang, B. Zhao, J. Chen, *Opt. Mater.*, **47**, 543-547 (2015). [5] P. W. Metz, D.-T. Marzahl, A. Majid, C. Krankel, G. Huber, *Laser Phot. Rev.*, **10**, 335–344 (2016). [6] W. Di, X. Wang, B. Chen, X. Zhao, *Chemistry Letters*, **34**, 566-567 (2005). [7] T. Oya, D. Nakauchi, G. Okada, N. Kawaguchi, T. Yanagida, *Nucl. Instr. & Meth. Phys. Res. A*, **866**, 134-139 (2017). [8] G. Sotiriou, D. Franco, D. Poulikakos, A. Ferrari, *ACS Nano*, **6**, 3888 (2012).

11:30 AM - 11:45 AM

GROWTH OF LARGE APERTURE YCOB CRYSTAL FOR OPCPA APPLICATION

X. Tu, S. Wang, K. Xiong, E. Shi, Y. Zheng

Shanghai Institute of Ceramics, Chinese academy of sciences, CHINA

The good thermal and nonlinear optical property as well as high damage threshold and high transmittance make YCOB ($\text{YCa}_4\text{O}(\text{BO}_3)_3$, Yttrium calcium oxyborate) a key optical element in the SHG and OPCPA process to obtain high repetition rate, multi-petawatt laser pulse. Growth of YCOB crystal with large size (diameter larger than 100 mm) is essential for high-power SHG and OPCPA applications. YCOB single crystals has been obtained by Czochralski method and congruent melting behavior has been observed. However, successful growth of large size YCOB crystal was seldom reported. In this work, the growth of YCOB crystals with the diameter larger than 100 mm by both Czochralski and Bridgman method was described. The largest crystal element cut from the as-grown crystal is up 102mm×100mm×18mm for the first time (as shown in Fig. 1). The rocking curve and the transmission spectrum were tested. Then, the influence of defects on laser induced damage threshold of YCOB crystal was studied. High-repetition rate frequency conversion of YCOB was demonstrated, and ~70% conversion at 1 Hz has been achieved.



Fig. 1. YCOB element with the aperture of 102mm×100mm×18mm

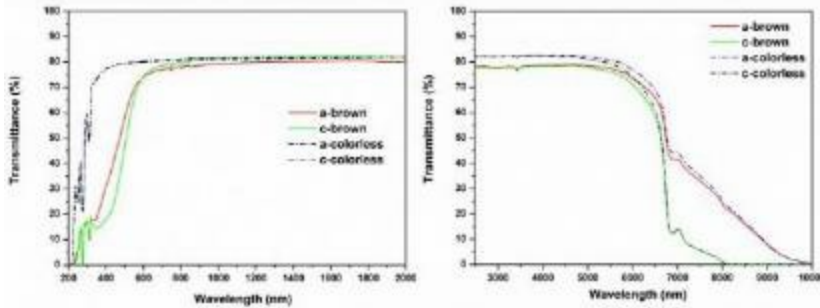
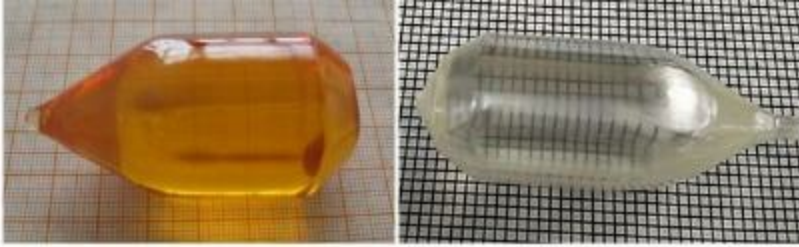
11:45 AM - 12:00 PM

CRYSTAL GROWTH AND OPTIMIZATION OF RE³⁺ DOPED CaGdAlO₄ DISORDERED CRYSTALS

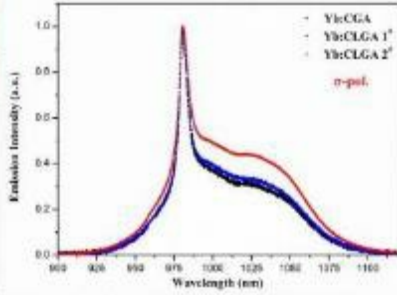
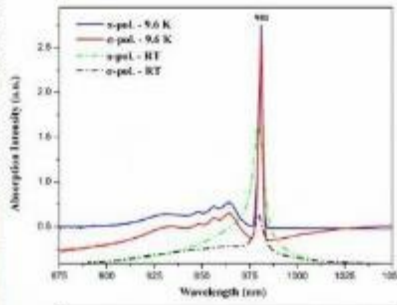
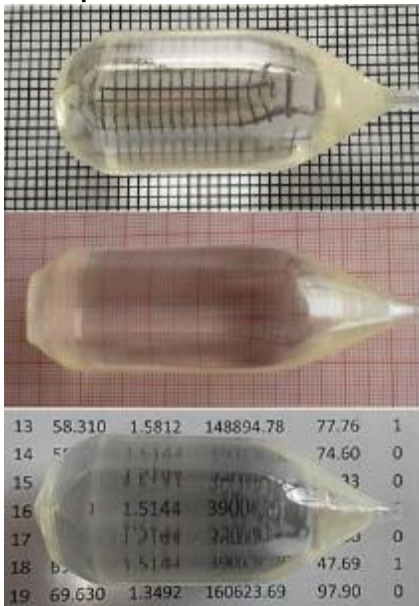
Q. Hu, Z. Jia, X. Tao

Institute of Crystal Materials & State Key Laboratory of Crystal Materials, Shandong University, CHINA

Crystals with disorder structure have drawn extensive attentions due to the wide application of the directly diode-pumped femtosecond lasers in the field of physics, chemistry, biology, and laser spectroscopy. Structural disorder can lead to differing crystal-field potentials at spatially differing active ion sites. As a result, the absorption and emission spectra can be inhomogeneously broadened, which provides great convenience for laser diode pumping and mode locking in the generation of ultrafast laser. Among the disorder crystals, CaGdAlO₄ (CGA) crystal is one of the most promising host candidates for high power and ultrashort pulse laser thanks to its broad and flat emission band and high thermal conductivity. How to design and optimize its disorder structure, and further to get better laser capacity is a critical research issue. In the past years, a series of high quality Re³⁺ doped CaGdAlO₄ crystals were successfully grown by the Czochralski (CZ) method in our group. Brown and colorless undoped CaGdAlO₄ crystals have been successfully grown in atmospheres with different oxygen partial pressures, and the fundamental properties were systematically investigated with respect to the influence of the different colors and corresponding color centers on the crystal density, hardness as well as thermal and optical properties.



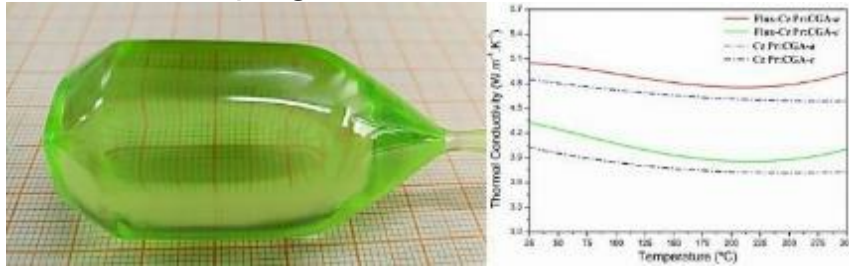
An even more disordered structure has been successfully designed by introducing Lu^{3+} ions into the $\text{Yb}:\text{CaGdAlO}_4$ crystal. The absorption spectra at 9.6 K provided clear evidence for the disordered structure of this crystal. Moreover, further spectral broadening was achieved compared to that of the $\text{Yb}:\text{CGA}$ crystal.



13	58.310	1.5812	148894.78	77.76	1
14	58.310	1.5812	148894.78	74.60	0
15	58.310	1.5812	148894.78	73	0
16	58.310	1.5144	390000.00	73	0
17	58.310	1.5144	390000.00	73	0
18	58.310	1.5144	390000.00	47.69	1
19	69.630	1.3492	160623.69	97.90	0

Due to the low phonon energy, CGA host crystals may also be suitable for visible lasers based on Pr^{3+} as the active ion. $\text{Pr}:\text{CaGdAlO}_4$ ($\text{Pr}:\text{CGA}$) crystals have been grown and investigated for the first time. A Na^+ -flux was creatively utilized to overcome the growth striations problem in the Czochralski method growth. The $\text{Pr}:\text{CGA}$ crystals grown by the Flux-Czochralski method show greatly improved

properties in terms of crystallinity, optical homogeneity and thermal conductivity and this technique may be applied to CGA crystals doped with other doping ions as well in future.



Thursday, August 1, 2019

10:30 AM - 12:00 PM

Characterization Techniques for Bulk and Epitaxial Crystals I

Location: Crestone III, IV

Session Chair(s): Michael Dudley, Balaji Raghothamachar

10:30 AM - 11:00 AM

STRAIN IMAGING WITH NANOSCALE BRAGG DIFFRACTION MICROSCOPY

M.V. Holt

Argonne National Laboratory, IL, UNITED STATES OF AMERICA
Scanning hard X-ray Bragg diffraction microscopy using nanoscale focusing optics is a synchrotron imaging technique capable of mapping structural perturbations such as crystallographic strain and phase within crystalline materials at a real space spatial resolution of ~20nm. Using the high penetrating power of hard x-rays and a fundamental sensitivity to lattice strain of 10^{-5} dc/c, this technique enables an extremely powerful visualization of local structure/function relationships within volumes of complex materials without sample sectioning. Recently developed coherent methods such as Bragg Projection Ptychography enable phase sensitive 3D imaging of crystalline thin films at a resolution beyond the focused beam size with a flexible field of view that can correlate lattice response to interfacial mechanics or chemical heterogeneity. The worldwide development of Diffraction Limited Storage Rings (DLSRs) in the hard x-ray regime

stands to significantly advance the use of high numerical aperture focussing optics for nanoscale synchrotron x-ray microscopy by making direct use of increased source brilliance and phase coherence. Current progress and future directions will be discussed in the context of recent results.

11:00 AM - 11:30 AM

GAP LAYERS GROWN ON SI(001): HOW CROSS-SECTION SCANNING TUNNELING MICROSCOPY ALLOWS FOR ACCESSING THE ATOMIC STRUCTURES

A. Lenz

TU Berlin, GERMANY

Epitaxial growth of III-V layers on Si(001) substrates is highly desirable for tandem solar cells, silicon photonics, or chip-to-chip interconnects. Due to the small lattice mismatch between Si and GaP, this particular III-V semiconductor is used preferentially. Nevertheless, as it occurs on all polar to nonpolar interfaces, the growth of GaP on Si(001) substrates also leads to the formation of undesired antiphase domains.

Within this presentation, samples grown by metal-organic vapor phase epitaxy are investigated on the atomic scale, by using cross-sectional scanning tunneling microscopy (XSTM). After cleaving the samples within an ultra-high vacuum chamber the atomic arrangement of the GaP-to-Si interface, the size and shape of the remaining antiphase domains within the first tens of nm's, and the detailed progression of antiphase boundaries can be determined. Studying antiphase boundaries by XSTM is just performed recently [1] and could be used to build up a structural model for an entire antiphase domain cross-section, including the determination of its antiphase boundary fact-types [2]. Furthermore, using the data of over 50 antiphase domains analyzed on perpendicular cleavage planes, has made it possible to develop a true-to-scale three-dimensional model of antiphase domains in GaP layers [3].

This work is supported by projects LE 3317/1-1 and 1-2 of the DFG.

[1] C. Prohl *et al.*, J. Vac. Sci. Technol. A **34**, 031102 (2016). [2] A.

Lenz *et al.*, J. Appl. Phys. **125**, 045304 (2019).

[3] P. Farin *et al.*, J. Phys.: Condens. Matter **31**, 144001 (2019).

11:30 AM - 11:45 AM

CHARACTERIZATION OF DEFECTS IN GAAS SUBSTRATES AND EPITAXIAL WAFERS BY SYNCHROTRON X-RAY TOPOGRAPHY

H. Peng, M. Dudley, B. Raghothamachar, T. Ailihumaer

Department of Materials Science and Chemical Engineering,
Stonybrook University, NY, UNITED STATES OF AMERICA

Synchrotron white beam X-ray topography in transmission has been widely utilized to characterize defects such as dislocations in bulk crystals while grazing incidence X-ray topography provides us with more detailed information of these features formed during epitaxial growth. In this study, we have applied these techniques to study $(\text{Al}_x\text{Ga}_{1-x})_{0.5}\text{In}_{0.5}\text{P}$ epitaxial layers grown on GaAs substrates with 15 degree offcut. Defects such as inclusions, threading dislocations and misfit dislocations were directly observed in grazing incidence X-ray topographs. To relax the lattice mismatch between epi layer and substrate, misfit dislocations can be formed, most of which are generated by the glide of threading dislocations with specific burgers vector when the critical thickness of epi layer is reached[2]. In addition, some interfacial dislocations generated by the expansion of dislocation half loop nucleated from the surface were also observed. To have a better understanding of these misfit dislocations and the lattice relaxation, we carried out ray tracing simulation to determine the burgers vector of threading dislocations, which plays a significant role in the formation of misfit dislocations[1] [3]. Meanwhile, grazing incidence X-ray topographs also reveal precipitate images consisting of a series of dark circles corresponding to the series of angular steps used to image the entire wafer, an observation reported for the first time. To study the relationship between the strain field and the size and depth of the precipitates, we carried out ray tracing simulation to relate the strain field model to the contrast on grazing-incidence X-ray topographs. The simulated images and the experimental images will be discussed in this paper, and detailed information on the precipitates and dislocations in GaAs epitaxial wafers will be provided. Ref. [1] S J Barnett et al 1995 J. Phys. D: Appl. Phys. 28 A17 [2] J. W. Matthews, S. Mader, T. B. Light 1970 Journal of Applied Physics 41(9) :3800-3804 [3] C.R. Whitehouse et al. /Journal of Crystal Growth 150

(1995) 85-91

Thursday, August 1, 2019

10:30 AM - 12:00 PM

Hetero-Epitaxy of III-V on Silicon

Location: Red Cloud Peak

Session Chair(s): Kei May Lau, Shadi Shahedipour-Sandvik

10:30 AM - 11:00 AM

SELECTIVE AREA EPITAXY OF III-V NANOSTRUCTURES AND THIN FILMS FOR INTEGRATED DEVICE PLATFORMS

Q. Li

Cardiff University, UNITED KINGDOM

Monolithic integration of III-V on silicon is attracting growing interest due to its potential to bring optical capabilities to silicon integrated circuits. To overcome the fundamental challenges associated with lattice mismatched heteroepitaxy, here I present two integration platforms, V-groove epitaxy and catalyst-free nanowire epitaxy, both enabled by selective area growth with metal organic chemical vapour deposition. The V-groove epitaxy platform was developed in conjunction with the aspect ratio trapping technique on standard (001) silicon wafers. By initiating selective epitaxy in oxide confined trenches on etched (111) silicon surfaces, it prevents antiphase domains and provides a geometric approach for defect trapping and filtering. Such a platform has supported various nanostructures and coalesced thin films covering GaAs, InP and GaSb material systems. Successful demonstrations of high-performance quantum dot devices and nanoridge lasers were also achieved. In contrast to the V-groove epitaxy, vertical nanowire growth on (111) substrates relies on an elastic relaxation process taking place in lateral directions to accommodate the lattice mismatch strain. Here I will review our recent work on growing nanowire structures for avalanche photodiode and nanowire laser applications.

11:00 AM - 11:15 AM

UNDERSTANDING THREADING DISLOCATIONS IN III-ARSENIDE

HETEROSTRUCTURES ON SILICON: RECOMBINATION-ENHANCED GLIDE AND PIPE DIFFUSION

K. Mukherjee¹, E. Hughes¹, B. Bonafant¹, R.D. Shah², B.B. Haidet¹, P.G. Callahan¹

¹University of California Santa Barbara, CA, UNITED STATES OF AMERICA, ²Massachusetts Institute of Technology, CA, UNITED STATES OF AMERICA

Understanding the electronic and mechanical properties of threading dislocations is key to improving device efficiency and reliability in lattice-mismatched III-V on silicon. It is known that a difference in the thermal expansion coefficients of GaAs and Si leads to large residual stresses when the films are cooled down to room temperature. Using both MOCVD and MBE grown films, we directly observe how non-radiative recombination at threading dislocations couples to this residual stress and leads to enhanced dislocation glide even at room temperature.¹ We will show that in-situ cathodoluminescence (CL) and electron channeling contrast imaging (ECCI) capture this motion of threading dislocations with high spatial and temporal resolution, down to single dislocations. This enables a study of the dynamics of such processes via the dependence of dislocation glide velocities on temperature and carrier injection. Our results provide insight into device degradation behavior and the character of the different populations of threading dislocations in typical GaAs and AlGaAs films on Si. As dislocation motion due to carrier injection is implicated in degrading III-V on silicon optoelectronic devices,² we will show how alloying small quantities of indium suppresses recombination-enhanced glide. We speculate that alloy hardening leads to this, as opposed to a reduction in non-radiative recombination or the formation of Cottrell impurity atmospheres at dislocations. To understand better the role of such materials modification, we will present results from a newly developed combination of ECCI and atom probe tomography to probe directly the composition at individual dislocations in III-V on Ge/Si films for the first time.³ We see fast pipe diffusion of atomic species along threading dislocations through the heterostructure. However, we do not find evidence for lateral segregation of indium to the dislocation core, supporting our hypothesis of alloy hardening.

More generally, this technique clearly shows that the composition around dislocations in conventional III-V on silicon films can indeed be very different from the matrix. This has important implications for the electronic properties of extended crystal defects and indeed for any effort in modeling non-radiative recombination from first principles. ¹ P.G. Callahan, B.B. Haidet, D. Jung, G.G.E. Seward, and K. Mukherjee, Phys. Rev. Materials **2**, 081601 (2018). ² D. Jung, J. Norman, Y. Wan, S. Liu, R. Herrick, J. Selvidge, K. Mukherjee, A.C. Gossard, and J.E. Bowers, Physica Status Solidi (A) **216**, 1800602 (2019). ³ B. Bonef, R.D. Shah, and K. Mukherjee, Nano Lett. (2019).

11:15 AM - 11:30 AM

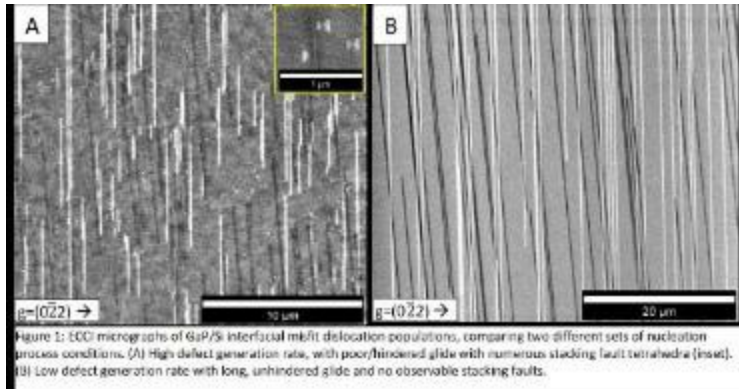
CORRELATION OF MOCVD PROCESS CONDITIONS AND DEFECT EVOLUTION OF GaP/Si HETEROSTRUCTURES VIA ELECTRON CHANNELING CONTRAST IMAGING

J. Boyer, D. Lepkowski, A. Blumer, Z. Blumer, F. Rodriguez, T. Grassman

Ohio State University, OH, UNITED STATES OF AMERICA

III-V/Si photovoltaics and optoelectronics offer an attractive combination of tunable, high-performance III-V alloys with inexpensive and processible Si platforms. Epitaxially-integrated GaP/Si is a straightforward bridge between both material systems and has thus received considerable development, especially in recent years. The slight lattice mismatch between GaP and Si, interface heterovalency, and the high potential for the formation of nucleation related defects (e.g. antiphase disorder, stacking faults, etc.) all complicate the production of low defect density GaP/Si virtual substrates which are required for producing high-performing devices. A variety of growth processes have been demonstrated, in MBE and MOCVD, as capable of nucleating and growing GaP/Si without nucleation related defects and to result in low threading dislocation density (TDD). However, across the many available reports, there is insufficient insight regarding the connection between the differing epitaxial processes and both the extent and evolution of the resulting crystal defects. To this end, we have undertaken an extensive study of MOCVD-based GaP/Si growth, considering a range of important epitaxial parameters, including Si surface pretreatment (e.g. annealing in various ambients,

homoepitaxial growth), layer-by-layer GaP nucleation (e.g. precursor pulse sequence, timing), and bulk GaP overgrowth conditions (e.g. temperature, V:III ratio). Electron channeling contrast imaging (ECCI) was used to image and quantify misfit dislocation arrays at the GaP/Si heterointerface resulting from the different MOCVD process conditions.



Using ECCI micrographs, examples of which are presented in Figure 1, relevant attributes of the misfit dislocation networks can be extracted. Aspects such as average misfit length and endpoint (i.e. threading dislocation) density are found to vary by $>20\times$ for the most critical GaP nucleation conditions, while changes in other growth conditions have little impact on the resultant misfit arrays. In addition, dependences have been identified between the GaP nucleation process conditions and the sensitivity of GaP bulk growth conditions toward TDD and surface morphology, suggesting that certain nucleation procedures result in a more stable overall heteroepitaxial configuration, thus far enabling low- 10^6 cm^{-2} TDD GaP/Si templates. Quantitative analytical models describing and predicting dislocation nucleation and glide are being developed from the vast array of misfit network statistics extracted from ECCI datasets. Nominally, this analysis will elucidate quantitative correlations between process parameters and the limiting defect generation and evolution mechanisms occurring during GaP/Si growth. With these studies, we hope to understand the complex interactions and mechanisms that dictate the heteroepitaxial process in this relatively simple heterovalent materials system and beyond.

11:30 AM - 11:45 AM

NUCLEATION OF GaP ON V-GROOVED Si SUBSTRATES

E.L. Warren¹, T. Saenz², E. Makoutz¹, B. McMahon¹, J. Zimmerman²

¹National Renewable Energy Lab, CO, UNITED STATES OF AMERICA, ²Colorado School of Mines, UNITED STATES OF AMERICA

The direct heteroepitaxy of III-V materials such as GaP on Si for high efficiency optoelectronic and photovoltaic applications has progressed greatly in recent years, but most studies have focused on offcut wafers polished using an expensive chemical-mechanical planarization process. An alternative is to pattern nominally (100) Si surfaces with linear gratings, and then use selective etching to fabricate (111)-faceted v-groove structures. This v-grooved geometry suppresses antiphase boundaries (APBs), thereby enabling defect-free nucleation of polar III-V materials on nonpolar Si. However, for applications where cost is important, it also brings with it the challenge of creating the v-grooved pattern in a cost-effective way, without an expensive wafer-polishing step. Here we demonstrate the use of cost-effective patterning approaches to fabricate the required submicron v-grooves in unpolished Si substrates. Additionally, we present the nucleation and growth of GaP on Si by OMVPE substrates patterned with v-grooves, using both polished (100) wafers and unpolished PV-grade wafers, and demonstrate the absence of APBs.

11:45 AM - 12:00 PM

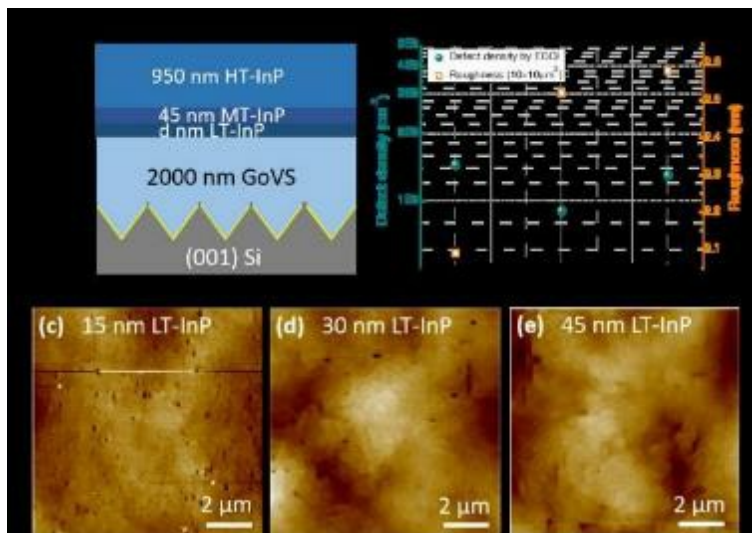
DEFECT ENGINEERING FOR INP EPITAXIALLY GROWN ON (001) Si BY MOCVD

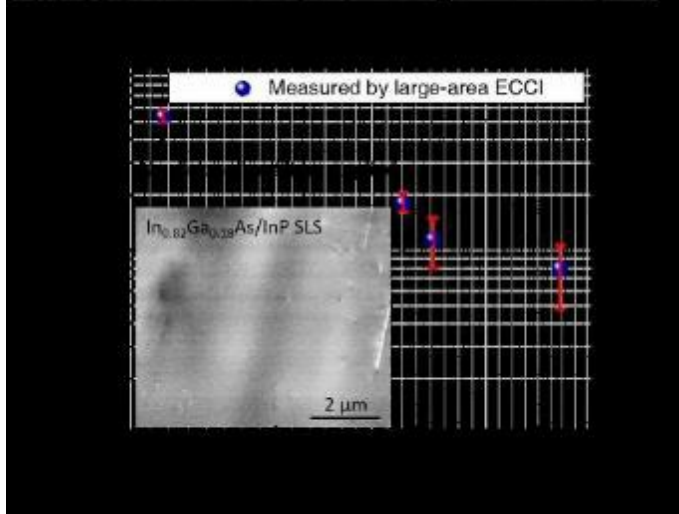
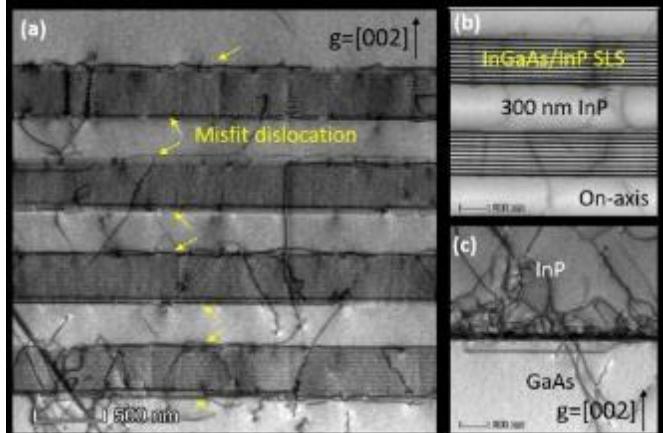
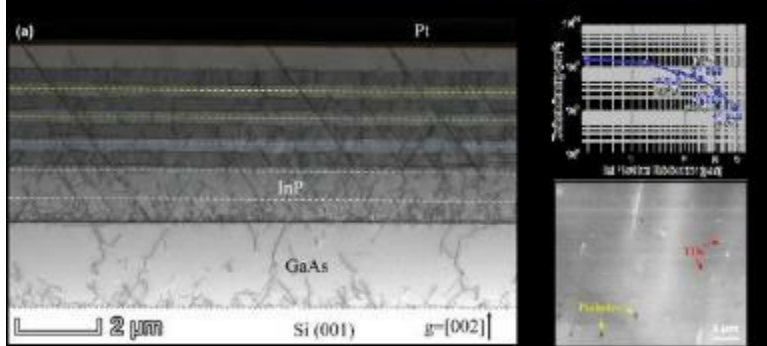
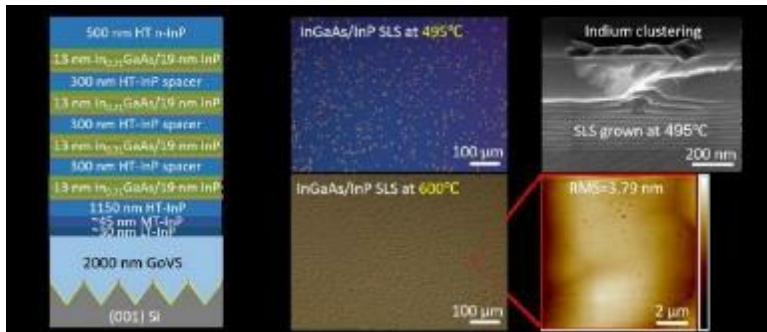
B. Shi, S. Suran Brunelli, A. Taylor, L. Wang, J. Klamkin

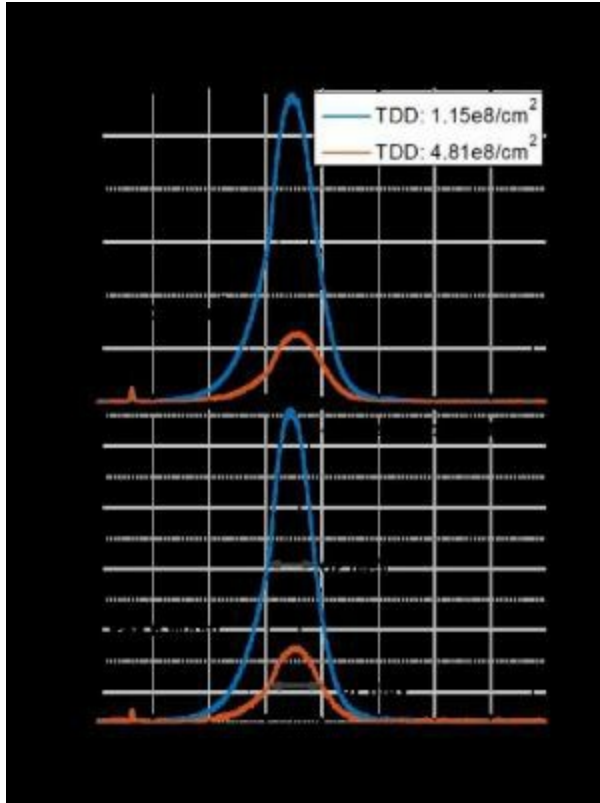
University of California, Santa Barbara, CA, UNITED STATES OF AMERICA

Monolithic integration of indium phosphide (InP) and its related lattice matched alloys on Si substrates have been extensively investigated in the past decades. The challenges in this heteroepitaxy mainly exist in a high threading dislocation density (TDD) due to a larger lattice mismatch (8%) than the GaAs/Si, as well as anti-phase boundaries (APBs) during the polar/non-polar growth. To address the APB issue, one robust methodology applied in this work is to grow III-V materials on the V-groove patterned Si substrates. On the other hand, except

the graded buffer approach, here we grew a GaAs intermediate buffer to well accommodate the lattice mismatch between InP and Si. The high density of TDs generated at the InP/GaAs heterointerface can be partially filtered by the $\text{In}_x\text{Ga}_{1-x}\text{As}/\text{InP}$ SLS during TD propagation. In this work, we demonstrated a defect reduction from 5.6×10^8 to $7.9 \times 10^7 \text{ cm}^{-2}$ for InP monolithically grown on a V-groove patterned (001) Si substrates, by optimizing the $\text{In}_x\text{Ga}_{1-x}\text{As}/\text{InP}$ strained layer superlattices (SLSs). It is uncovered that high density of hillocks emerge for SLSs grown at low temperatures due to Indium clustering. By increasing the SLS growth temperature, a cluster-free InP surface can be obtained, with a smooth morphology. Furthermore, a 7-fold reduction in defect density was achieved by introducing $\text{In}_{0.82}\text{Ga}_{0.18}\text{As}/\text{InP}$ SLSs, as characterized by large-area ECCI. The interaction of dislocations with SLSs were analyzed based on the cross-sectional STEM images. To further lower down the defect density, our next step is to replace the InGaAs/InP SLS with the strain-compensated $\text{In}_x\text{Ga}_{1-x}\text{As}/\text{In}_y\text{Ga}_{1-y}\text{As}$ superlattices to intensify the lateral movement of the TDs.







Thursday, August 1, 2019

10:30 AM - 12:00 PM

In Situ Observation and Characterization I

Location: Grays Peak I

Session Chair(s): M. J. Highland

10:30 AM - 11:00 AM

COHERENT X-RAY MEASUREMENT OF LOCAL STEP-FLOW PROPAGATION DURING GROWTH ON POLYCRYSTALLINE ORGANIC SEMICONDUCTOR THIN FILM SURFACES

R. Headrick¹, J.G. Ulbrandt¹, P. Myint², J. Wan¹, Y. Li¹, A. Fluerasu³, Y. Zhang³, L. Wiegart³, K.F. Ludwig, Jr.²

¹Department of Physics and Materials Science Program, University of Vermont, VT, UNITED STATES OF AMERICA, ²Division of Materials Science and Engineering, Boston University, MA, UNITED STATES OF AMERICA, ³National Synchrotron Light Source II, NY, UNITED STATES OF AMERICA

Vacuum physical vapor deposition of C60 on a graphene-coated surface is investigated in real-time by utilizing 9.65 keV X-rays from the CHX coherent hard X-ray synchrotron beamline at NSLS-II. X-ray Photon Correlation Spectroscopy is performed in the Grazing Incidence Small Angle X-ray Scattering (GISAXS) mode to achieve surface-sensitive conditions. Local step-flow is monitored through the observation of oscillatory correlations in the later stages of growth after crystalline mounds have formed. An important aspect of the work is that coherent X-rays do not average over complex structures, and this allows us to monitor the growth on polycrystalline surfaces without loss of information. This is important since in conditions where mounds form, the surface is too rough to observe layer-by-layer oscillations; this greatly limits the type of information that can be obtained from experimental techniques that employ low-coherence X-rays or electrons. The experimental results show that the step-flow velocity is nonuniform, and we model the velocity of each step-edge as being a simple function of the lengths of the terraces above and below it. This model predicts that the steps become almost stationary near the edges of the mounds where the local terrace length is very small, and the average slope of the surface is large. It was not previously known that such nonuniform and disordered step arrays as we have observed would follow such a simple growth law. We also find that the sensitivity to local step-flow is increased due to coherent mixing of X-rays scattered from the average mound structure with those scattered from the step array. This effect is a version of heterodyne scattering, where the scattering from the average step array can be considered to be a quasi-static reference signal. This work shows that the use of coherent X-ray scattering provides an approach to better understand surface dynamics and fluctuations during crystal growth. We have also extended these measurements to additional materials systems, including the growth of organic semiconductor small molecules with a lower symmetry than C60, such as diindenoperylene.

11:00 AM - 11:30 AM

USING HIGH-SPEED, MOLECULARLY-RESOLVED AFM TO INVESTIGATE SOLUTION STRUCTURE AND NUCLEATION AT

CRYSTAL SURFACES

J. De Yoreo¹, B.A. Legg¹, E. Nakouzi², S. Zhang², M. Baer², C.J. Mundy², G.K. Schenter²

¹University of Washington, WA, UNITED STATES OF AMERICA,

²Pacific Northwest National Laboratory, WA, UNITED STATES OF AMERICA

Investigating nucleation from solutions is challenging, because it is a consequence of unstable density fluctuations, making the structures and events that must be probed both transient and small in spatial extent. Moreover, processes like nucleation are inherently linked to the structure and dynamics of the interfacial region between solution and crystal interface, particularly when nucleation is heterogeneous. Here we use the high-speed and molecular-scale resolution of modern AFM to investigate nucleation of Gibbsite ($\text{Al}(\text{OH})_3$) on muscovite mica in order to quantify the cluster distributions and their dynamics and to observe the evolution from individual adsorbates to stable nuclei. We further take advantage of the AFM's exquisite force sensitivity to map the solution structure at the mica surface as a function of electrolyte type and concentration, as well as the distribution of ions on the surface. Results on Gibbsite nucleation indicate that hydrolyzed aluminum $\text{Al}(\text{OH})_2^+$ precursor species are concentrated near the interface and that aluminum hydroxide clusters form within this precursor-rich region. The cluster populations drop off exponentially with size and subcritical clusters show dynamic fluctuations that are consistent with classical predictions from Monte Carlo simulations. Density functional Theory suggests the mica surface acts as a proton sink and creates a region with an effective pH higher than that of the bulk, driving formation and adsorption of the hydrolyzed species. When the driving force for nucleation is increased, film growth occurs from multiple sites through a process of coalescence and coarsening. The results show that a direct atomistic-to-molecular view of nucleation reveals both consistencies and the deviations from the simple classical picture. Results from AFM mapping of the interfacial region above the mica surface for a variety of electrolytes show that the solution exhibits similar structuring in that the distance between hydration layers and the lateral variations in density are similar for all

electrolytes investigated. Comparison to X-ray reflectivity (XRR) data reveal reasonable agreement in vertical layering. However, the strength of the hydration layering grows dramatically with electrolyte concentration indicating that interfacial chemical gradients and hydration forces also exhibit a strong dependence on concentration. In contrast, analysis of the position and coverage of the cations on the mica surface show clear discrepancies with XRR data and call into question current assumptions about the nature of the AFM tip-substrate interaction which must be accounted for in order to correctly interpret the data.

11:30 AM - 11:45 AM

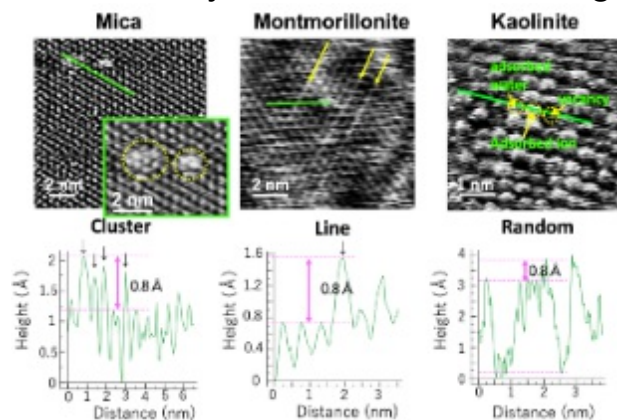
ATOMIC-SCALE VISUALIZATION OF ION BEHAVIOR ON CLAY MINERALS

Y. Araki¹, M. Okumura², Y. Ando³, H. Satoh⁴, K. Kobayashi¹, H. Yamada¹

¹Kyoto University, JAPAN, ²Japan Atomic Energy Agency (JAEA), JAPAN, ³National Institute of Advanced Industrial Science and Technology (AIST), JAPAN, ⁴Mitsubishi Materials Corporation, JAPAN

Recently, ion adsorption on clay mineral surfaces has been investigated in atomic-level by simulations, X-ray reflectivity and atomic force microscopy (AFM). Previous studies found that varieties of adsorption sites [Kobayashi *et al.* (2017) *Langmuir* 33, 3892-3899], effect of interfacial water [Bourg *et al.* (2017) *J. Phys. Chem. C* 121, 9402-9412], and dynamics of adsorbed ions [Ricci *et al.* (2017) *Nano Lett.* 17, 4083-4089] at the muscovite mica surface. However, it has not been explained clearly how the surface charge density of clay minerals and the hydration water contribute the ion adsorption. In this study, we performed in situ atomic-scale observation of cesium adsorption on several clay minerals with different layer charges by the frequency modulation AFM (FM-AFM). The basal plane of phyllosilicate minerals with 2:1 layer type (muscovite mica and montmorillonite) and 1:1 layer type (kaolinite) was observed in 100 mM CsCl solution under room temperature. The surfaces of mica and montmorillonite are negatively charged due to Al³⁺ incorporated in Si-O tetrahedral layer and divalent cations (Mg²⁺, Ca²⁺) in Al-O

octahedral layer, respectively. On the other hand, kaolinite is electrically neutral. We observed different adsorption behavior on these minerals. On the mica substrate, the hexagonal cluster of cesium ions was observed and they desorbed in 20 seconds. Analyzing the height of adsorbed cesium by compared with the position of adsorbed water at the mica surfaces, it is suggested that the cesium cluster was adsorbed above the Si-O tetrahedra (IS2 site) of the (001) face of mica. This result show that the adsorbed ions at IS2 site is mobile. Next, adsorbed cesium which were distributed one-dimensional row was observed on the montmorillonite surface [Araki *et al.* (2017) *Surf. Sci.* 665, 32-26]. The line cesium was stable over 10 minutes at the same place, and we found that these cesium ions were strongly adsorbed in the center of silicate rings (IS1 site). On the other hand, on the kaolinite surface, we observed vacancies, adsorbed water and highest (brightest) protrusions suggesting cesium adsorption nevertheless of their neutral charge. The distribution of highest protrusions was random, and their occupancy was almost 50 % in the scanning area ($5 \times 5 \text{ nm}^2$). In our presentation, we will discuss the adsorption site at kaolinite surfaces by the detail comparison of FM-AFM images and simulations. Also, how the dynamics of adsorbed ions is determined will be discussed with the results of hydration structure imaging at clay surfaces.



11:45 AM - 12:00 PM

STEP-SPECIFIC LIGAND INTERACTIONS CONTROL CRYSTALLIZATION OF METAL-ORGANIC FRAMEWORK HETEROSTRUCTURES

J. Tao¹, M. Lee¹, Z. Zhang², S. Akkineni³, D. Banerjee¹, M. Bowden¹, P. Thallapally¹, Y. Shin¹, M. Sushko¹, J. De Yoreo¹, J. Liu¹

¹Pacific Northwest National Laboratory, UNITED STATES OF AMERICA, ²Xiamen University, CHINA, ³University of Washington, UNITED STATES OF AMERICA

Designing metal-organic framework (MOF)/metal oxide heterostructures highlights the importance of controlling the ligand-substrate interface for MOF formation. Beyond simple principles of lattice matching, our combined in-situ atomic force microscopy (AFM) and ab initio molecular dynamics (AIMD) study reveal that a model MOF, ZIF-8 formation is dictated by interaction between the component ligand, 2-methyl-imidazole (2-MIM) and the ZnO surface dissolution step, on (-120)/(100) step the 2-MIM monodentate structure lengthens Zn-O bond weakening Zn binding to the lattice O and thus enhances the ZnO dissolution rate, while on (001)/(100) step the bidentate 2-MIM configuration shortens Zn-O bond and inhibits the dissolution. The competition between 2-MIM N atom and lattice O atom in binding with step Zn atoms shifts lattice Zn-O bond strength, which controls the ZnO dissolution and the nucleation and growth rate of ZIF-8 particles. This complex synergy between substrate dissolution step and ligand provides a new avenue for controlling heterostructure orientation, composition and formation kinetics in solution.

Thursday, August 1, 2019

10:30 AM - 12:00 PM

Materials for Novel Energy Technologies

Location: Torrey Peak II-IV

Session Chair(s): Ryan M. France, Shujun Zhang

10:30 AM - 10:45 AM

METAL OXIDE - CARBON COMPOSITE NANOFIBERS FOR ADVANCED LITHIUM STORAGE

S. Wasantwisut¹, L. Cruz², H. Tang¹, D. Kisailus¹

¹Department of Chemical and Environmental Engineering, University of California at Riverside, CA, UNITED STATES OF AMERICA,

²Materials Science and Engineering Program, University of California at Riverside, CA, UNITED STATES OF AMERICA

Diminishing fossil fuel reserves worldwide have led to an increased demand for renewable energy generation and efficient energy storage systems. Li-ion batteries (LIBs) are widely used in portable electronic devices due to their high charge capacity per weight ratio. However, LIBs still suffer from limited specific capacity and poor electrical conductivity. Hence, there has been a growing interest in developing porous carbon-based metal oxide composites as viable candidates for LIBs anodes. Here, we investigate the synthesis conditions and subsequent electrochemical performance of cobalt oxide nanoparticles embedded in graphitic carbon fibers (Co_3O_4 -GCFs) as anodes in LIBs. We discuss the formation mechanism of these Co_3O_4 -GCFs, synthesized from an electrospun solution containing metal oxide based precursors within a polymer matrix. We investigate the nucleation and growth of these nanoparticles and their catalysis of graphitic structures. Subsequently, we study the effect of nanoparticle loading on the resulting ultrastructural features of the fibers and their electrochemical performance. When tested as an anode material for LIBs, the Co_3O_4 -GCFs exhibited high specific capacity and excellent cycling stability, which can be attributed to the outstanding structural and electrical properties of the porous carbon-metal oxide nanostructure, which enhance the charge transfer ability, Li storage capacity, and lifespan of LIBs anodes.

10:45 AM - 11:00 AM

INFLUENCE OF HYDROTHERMALLY SYNTHESIZED TITANIUM DIOXIDE NANORODS/NANOPARTICLES IN DYE-SENSITIZED SOLAR CELL

R. Govindaraj, N. Santhosh, M. Senthil Pandian, P. Ramasamy
SSN College of Engineering, INDIA

In recent years, the nanocrystalline based dye-sensitized solar cells (DSSCs) have received much attention owing to their low-cost and high power conversion efficiency (PCE). In the traditional fabrication process, nanocrystalline- TiO_2 nanoparticles have been widely used as the scaffold layer to support the dye molecules. One-dimensional (1D)

nanomaterials have shown a significant advantage for the energy conversion applications. Aligned 1D nanostructures have been studied to improve electron transport properties in DSSC. However, such aligned 1D structure suffers from inefficient dye loading due to the lower surface area than traditional 20 nm size nanoparticles. Therefore, a careful synthesis strategy is needed to synthesize TiO₂ materials, which is still a challenging task. In this approach, a novel TiO₂ nanorods/nanoparticles (NRs/NPs) were prepared via different hydrothermal conditions. The crystallographic information of the prepared materials was confirmed by powder X-ray diffraction, which shows larger fraction of crystalline anatase phase of TiO₂. From the electron microscopy analysis, the formation of NRs/NPs is clearly found. Several solar cells have been fabricated and their performances were evaluated under illumination of 100 mW/cm². The high power conversion efficiency of 9 % has been achieved with NRs/NPs employed device.

11:00 AM - 11:15 AM

CRYSTAL GROWTH AND OCTAHEDRA TILTING OF BAZRS₃ AND ITS RUDDLESDEN-POPPER PHASES

S. Niu¹, W. Li², T. Salters³, B. Zhao¹, E. Bianco⁴, M.E. Mcconney⁵, R. Haiges¹, P. Khalifah³, A. Janotti², J. Ravichandran¹

¹University of Southern California, UNITED STATES OF AMERICA,

²University of Delaware, UNITED STATES OF AMERICA, ³Stony

Brook University, UNITED STATES OF AMERICA, ⁴Cornell

Univerisity, UNITED STATES OF AMERICA, ⁵Air Force Research

Laboratory^[SEP], UNITED STATES OF AMERICA

Transition metal perovskite chalcogenides have gained increased attention as a new class of semiconductors for optoelectronic applications such as solar energy conversion, light emission and detection. Growth of high quality crystals is of vital importance to study the intrinsic properties for these emerging materials. We report the crystal growth and physical property study of BaZrS₃ and its Ruddlesden-Popper phases, Ba₃Zr₂S₇ and Ba₂ZrS₄. Single crystals were grown with salt flux methods. Laboratory and synchrotron based

X-ray diffraction were performed to study the crystal structure and octahedra tilting in these materials. Photoluminescence (PL) measurements were performed to study the optical properties. Optical band gap of 1.82 eV, 1.28 eV and 1.33 eV for BaZrS_3 , $\text{Ba}_3\text{Zr}_2\text{S}_7$, and Ba_2ZrS_4 , respectively, were extracted from steady state PL at room temperature. Such band gap evolution trend is different from that observed in oxide and halide counterparts. The effect of octahedra tilting in determining the electronic structure were explored with theoretical calculations.

11:15 AM - 11:30 AM

DOPED SINGLE CRYSTAL AND CERAMIC OF KNN BASED COMPOUNDS: AN INVESTIGATION TO FIND NEW GREEN FRIENDLY MATERIAL FOR PIEZOELECTRIC DEVICE APPLICATION

A.M.E. Santo¹, M.V.S. Silva¹, S.L. Baldochi², M. Cochez³, M. Ferriol³, J.A. Eiras⁴, M.H. Lente¹

¹Universidade Federal de São Paulo - UNIFESP, BRAZIL, ²Instituto de Pesquisas Energeticas e Nucleares-IPEN/CNEN, BRAZIL,

³Universite de Lorraine, IUT de Moselle-Est, Département Chimie, FRANCE, ⁴Universidade Federal de São carlos, BRAZIL

Lead-based ceramics are the most efficient piezoelectric in electronic devices. An important issue which concerns manufacturing is the toxicity of Pb element for the environment and human health. Lead zirconate titanate (PZT) is one of the most successful compounds for this purpose. Therefore, worldwide researchers do efforts to develop new green-friendly materials with high-performance as piezoelectric transducer. Usually, single-crystals present enhanced properties than their respective ceramics. Among the most promising lead-free materials, sodium potassium niobate (KNN) is considered a potential candidate to replace the PZT compounds because of its good piezoelectric and ferroelectric properties. . We have grown KNN based crystals doped with metallic ions by Micro-pulling-down and also as sintered ceramic by Spark Plasma Sintering techniques with compositions near the morphotropic phase boundary. Therefore, we compared the physical properties of polycrystalline ceramics and

single crystals. We have found that the dopant nature plays an important role in the melting behavior. Our results also have shown that single crystals present enhanced properties than ceramics of same composition in this material.

11:30 AM - 11:45 AM

CRYSTAL GROWTH AND CHARACTERIZATION OF $\text{CH}_3\text{NH}_3\text{PbBr}_3$ SINGLE-CRYSTALS FOR X-RAY PHOTODETECTION

S. Amari¹, J. Verilhac¹, O. Baussens², E. Gros D'Aillon², A. Martinent¹, A. Ibanez³, J. Zaccaro³

¹CEA LITEN LCO, FRANCE, ²CEA LETI LDET, FRANCE, ³Institut Néel, CNRS et Université Grenoble Alpes, BP 166, FRANCE

Organic-Inorganic Halide Perovskites (OIHPs) exhibit promising properties for optoelectronic applications. Devices such as solar cells, LEDs, or photodetectors can easily be made by solution-processing methods. In particular, it is quite easy to obtain $\text{CH}_3\text{NH}_3\text{PbBr}_3$ bulk crystals by different methods such as Inverse Temperature Crystallization (ITC) or AntiSolvent Vapor assisted (ASV) [1]. The record properties to date have been obtained with single-crystals [2]. However, to obtain bulk crystals of high quality is much more delicate and require to perfectly control the growth conditions. The main objective of the work presented here is to explore the impact of the growth conditions on the crystalline quality to later correlate it with optoelectronic properties and determine the intrinsic properties (charge carrier transport, resistivity) of this hybrid material.

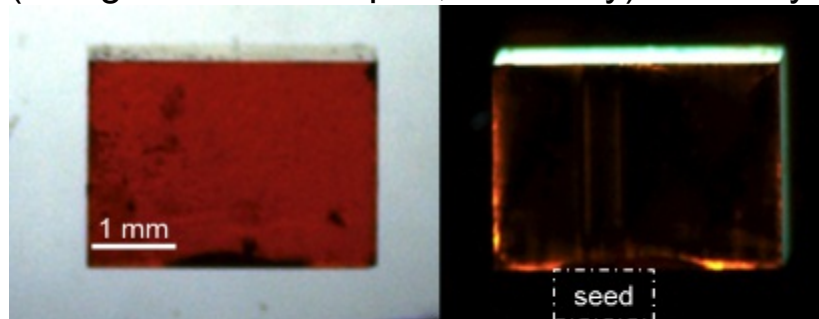


Figure 1 : Bulk crystal (left) between crossed polarizers (right) free of strain

We will present our latest results on the crystal growth of

CH₃NH₃PbBr₃ single-crystals through the ITC method using dimethylformamide (DMF) as solvent. The effect of key parameters on reproducibility and crystal quality of this material will be discussed, in particular, the effect of temperature, supersaturation, and fluid dynamics. Crystalline quality has been characterized using different methods such as visible spectroscopy, polarized light to detect strain (photoelasticity), chemical etching to visualize dislocations, and ICP-MS to quantify impurities. A non-optimized protocol for crystal growth - derived from literature [3]- gives single-crystals free from visible defects, but heavily strained and with high dislocation density. Optimizing the growth conditions lead to the growth of high quality crystals, without any significant strain (Figure 1) and dislocation densities 10 times smaller (Figure 1). Optoelectronic characterizations are in progress, the first results tend to indicate an improvement of the properties as a function of the crystalline quality.

References 1. Babu, R. et al, *Cryst. Growth Des.* **18**, 2645–2664 (2018). 2. Liu, Y. et al. *Mater. Today* **22**, 67–75 (2019). 3. Saidaminov, M. I. et al. *Nat. Commun.* **6**, 7586 (2015).

11:45 AM - 12:00 PM

EXPERIMENTS ON SURFACE WAVE EXCITATION BY ELECTROMAGNETIC FIELD

M. Milgravis, A. Bojarevičs, V. Geža, A. Gaile
University of Latvia, LATVIA

In various purifying processes generation of surface waves can enhance the effectiveness of impurity removal by increasing free surface through which the impurities can escape. A contactless, electromagnetic approach is proposed for the excitation of the surface waves for electrically conductive materials. One of such potential applications is Silicon refinement. Experimental study is done by table-top model using GaInSn alloy. Surface waves are generated by alternating magnetic field, additionally scaling possibility is investigated by an externally applied static magnetic field. Similar wave patterns can be achieved by an alternating magnetic field or adding a static magnetic field to a much lower intensity alternating field. External static magnetic field leads to power saving for AC field generation at least 10 times. Results demonstrate the potential to

scale the technology to industrial size with aim to increase free surface. Figure 1 demonstrates free surface of GalnSn alloy under alternating and static magnetic field. Experimental setup for Silicon refinement process is designed and during the conference the first result will be demonstrated.

Figure 1. GalnSn alloy under alternating (left) and alternating and static (right) magnetic field. Process scaling potential is demonstrated by increasing melt reservoir diameter and adding static magnetic field.

Acknowledgment

This work was funded by European Regional Development Fund under contract “Refinement of metallurgical grade silicon using smart refinement technologies” (No. 1.1.1.1/16/A/097).

Thursday, August 1, 2019

10:30 AM - 12:00 PM

Modeling of Crystal Growth Processes III

Location: Crestone I, II

Session Chair(s): Vladimir Kalaev, Lili Zheng

10:30 AM - 11:00 AM

NUMERICAL STUDIES ON OXYGEN TRANSFER IN SI MELT UNDER INHOMOGENEOUS MAGNETIC FIELDS OF TMCZ CONDITION USING A GLOBAL MODEL

K. Kakimoto

Research Institute for Applied Mechanics, Kyushu University, JAPAN

A numerical investigation has been carried out to clarify the mechanism of oxygen transfer in silicon melt in 3D configuration using a global model. The melt was set under inhomogeneous magnetic fields of transverse magnetic fields of Czochralski (CZ) crystal growth condition. In the TMCZ method with inhomogeneous magnetic fields, distribution of magnetic fields affects the flow structure of the melt.

Then, oxygen transfer in the melt is modified by the inhomogeneous magnetic fields based on the modification of the flow structure. The mechanism was discussed using a local model which impose the temperature boundary condition around a crucible wall. To investigate the effect of distribution of inhomogeneous magnetic fields on the

transfer of oxygen as well as interface shape, 3D global model considering electromagnetic and heat transfer has been developed. The results show that the radial distribution of oxygen concentration at the top of the melt. The notations of Lower, Middle, Upper mean the relative position between the inhomogeneous magnetic fields and the melt surface. The relative position of Higher provides lower oxygen concentration in the crystal. The results show iso-contour of electric potential in the melt. Convection transferred oxygen along the potential in the melt. Oxygen concentration in the melt is determined by the modification of convection by the inhomogeneous magnetic fields.

11:00 AM - 11:15 AM

OPTIMAL ROTATION SPEED AND CONVECTIVE THERMAL INSTABILITIES IN THE SAPPHIRE MELT UNDER THE CZOCHRALSKI GROWTH PROCESS

D. Bahloul¹, H. Azoui¹, A. Laidoune², N. Soltani³

¹Université de Batna 1, Faculté des Sciences de la Matière.

PRIMALAB, ALGERIA, ²département de physique université Batna 1,

ALGERIA, ³Université de Batna 2, Faculté des Sciences de l'ingénieur, ALGERIA

We have accomplished a three-dimensional numerical investigation in order to find the optimal conditions for efficient growth of high quality sapphire crystals with good mechanical, thermal and optical properties. We have studied convective heat transfer near the melt-crystal interface and the thermal instabilities during the Czochralski growth (Cz) process. Our simulations were performed in cylindrical coordinates using the FFT in order to analyze temperature fluctuations. A detailed investigation on the effects of the crystal rotation speed and the temperature distribution on thermal instabilities of sapphire melt under forced convection are presented. The forced convection in the melt, the radiative heat transfer and the Marangoni convection, are studied for Al₂O₃ melt in the crucible. We have been able to determine the optimal rotation speed enabling a planar crystal-melt interface while the flow symmetry is conserved. We have also studied the temperature fluctuations just below the crystal-melt

interface. These fluctuations give important information about the melt-crystal interface, which plays an important role on the quality of the sapphire crystal.

11:15 AM - 11:30 AM

NUMERICAL MODELING OF MELT CONVECTION AND OXYGEN TRANSPORT IN A CZOCHRALSKI PROCESS FOR SOLAR SILICON GROWTH

D. Vizman¹, A. Popescu¹, M. Bellmann²

¹West University of Timisoara, ROMANIA, ²SINTEF Materials and Chemistry, NORWAY

Even the Czochralski silicon (Cz-Si) market is actually below the multicrystalline silicon one, it is expected to increase in the next years as fabrication techniques are optimized and the cost is reduced . Although, Si produced with Cz method is considered of high purity and homogeneity, there are always defects introduced during the process. The Cz-Si process for solar cells is still facing important challenges with the incorporation of impurities (with two main sources: crucible and feedstock) and their interaction with defects. One of those defects are striations caused by inhomogeneous doping concentration across the ingot's length. The aim of this paper is to investigate by numerical modelling the effect of crucible rotation on the temperature and oxygen distribution and fluctuation in order to design the best scenario for the crystal quality improvement. An accelerated crucible rotation technique (ACRT), first proposed by Scheel and Schulz-Dubois [J. Cryst. Growth 8 (1971) 304] will be considered. The focus will be put on the dependence of temperature and oxygen fluctuations under the solid -liquid interface on the different scenario for crucible rotation (counter-rotation, iso-rotation or ACRT). Numerical simulations, using STHAMAS 3D software, were carried out in order to predict the temperature and impurities concentration fluctuation in the melt, induced by natural convection and forced convection due to crucible and crystal rotation in a 200mm Cz-Si process. Temperature boundary conditions for the local 3D – simulation were imported from a 2D global simulation of the Cz-process. The numerical modelling show a significant amplitude of temperature and oxygen concentration fluctuations near S-L interface for most of the cases. It can be

observed that on one side the iso rotation damp the temperature fluctuations, but on the other side increase the oxygen level. The characteristics of temperature and oxygen fluctuations will be compared with the striation fluctuations along the crystal obtained by Lateral Photovoltaic Scanning (LPS). The frequency range (obtained by FFT) are in good agreement with the numerical simulations, which show a good correlation between patterns in doping gradients with temperature fluctuations in the melt. Different ACRT parameters will we analyzed in order to propose the best scenario to reduce the temperature and oxygen fluctuations.

11:30 AM - 11:45 AM

TRANSIENT GLOBAL MODELING FOR THE PULLING PROCESS OF CZOCHRALSKI SILICON CRYSTAL GROWTH. II. INVESTIGATION ON SEGREGATION OF OXYGEN AND CARBON

X. Liu¹, H. Harada¹, Y. Miyamura¹, X. Han¹, S. Nakano¹, S. Nishizawa², K. Kakimoto¹

¹Research Institute for Applied Mechanics, Kyushu University, JAPAN,

²Research Infittute for Applied Mechanics, Kyushu University, JAPAN

Transient global modeling of the Czochralski silicon (CZ-Si) crystal growth process is essential for understanding the dynamic behaviors of the heat and mass transport in the crystallization set-up. Oxygen (O) and carbon (C) are the major impurities in CZ-Si growth. Excessive O and C can both degrade the crystal and wafer by forming the precipitates and micro-defects. Therefore, transport and segregation of O and C must be investigated for the pulling process. Numerical simulation could be applied to obtain much more details on impurity transport and distribution than discrete measurements on the sliced crystal. Furthermore, segregations of impurities and dopants could also be predicted dynamically by the transient global simulation. In the present study, the transient global simulation for the crystal pulling process was conducted for CZ-Si growth with the cusp-shaped magnetic field (CMF). Generation, transport, and segregation of O were considered for the crystal growing process. Incorporation, accumulation, and segregation of C were also predicted at the basis of our previous studies for CZ-Si growth. The distributions of O at the

growth interface were dynamically predicted for different pulling stages, as shown in Fig. 1. The segregation curves of O and C were plotted as the function of crystal length, as shown in Fig. 2. The radial and axial homogeneities of O and C were investigated for the growing crystal. The applied CMF suppressed the turbulent melt flow and stabilized the heat and impurity transport. The O concentration along the axis decreased with the increase of the length of the crystal. Due to the continuous contamination and the lower segregation coefficient, the C concentration increased with the increase of the crystal length. The developed transient global model is also applicable for the segregation prediction of other dopants and impurities in CZ-Si growing process.

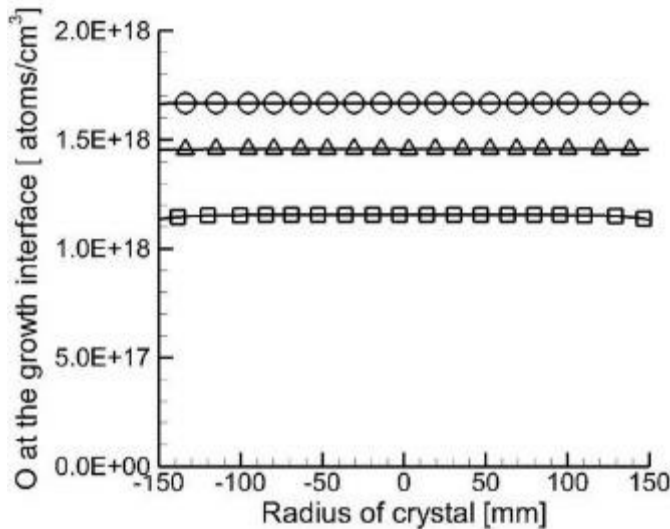


Fig. 1 O at the growth interface during pulling.

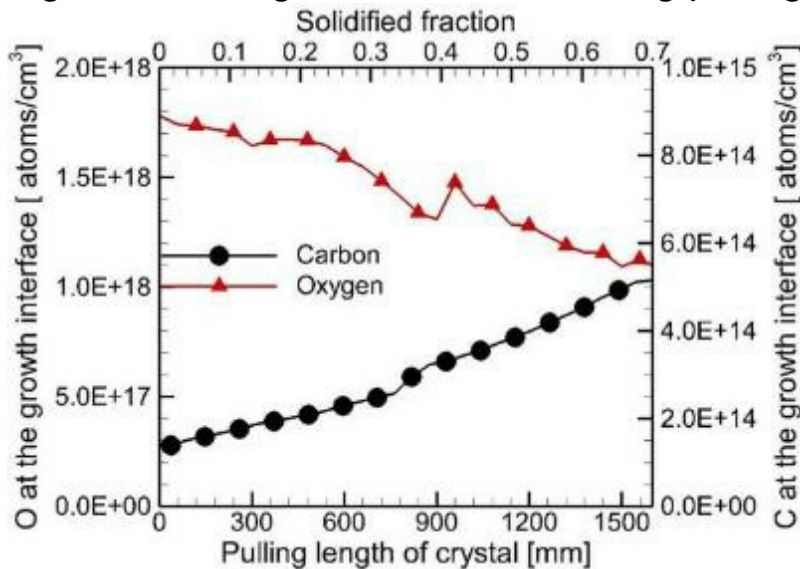


Fig. 2 Segregations of O and C at the growth interface.

11:45 AM - 12:00 PM

LIMITATIONS OF THE GROWTH RATE DURING PULLING OF LARGE DIAMETER SILICON CRYSTALS BY THE CZOCHRALSKI TECHNIQUE

J. Friedrich¹, T. Jung¹, M. Trempa¹, C. Reimann¹, A. Denisov², A. Muehe²

¹Fraunhofer IISB, GERMANY, ²PVA Tepla Crystal Growing Systems GmbH, GERMANY

The major production process of dislocation free, single-crystalline silicon for electronic and solar application is the Czochralski method. Especially in PV industry cost reduction is the main technology driver. Therefore, there is a continuous development towards larger charge weights which requires larger hot zones, and towards an increase of the pulling speed which necessitates sophisticated heat shield designs. Numerical “multi physics” modeling of the heat and oxygen transport phenomena have proven to strongly support the engineers in finding such technical solutions and in improving the understanding of the various processes and phenomena. We developed an advanced numerical model for the description of the Cz process that takes into account a 3D description of the melt flow which is coupled to a 2D model of the surrounding furnace. The numerical model contains all important physical effects. This model has been shown to be very accurate in the prediction of the phase boundary shape and oxygen concentrations. In this contribution, we used this model to investigate in detail the limitations of the growth rate during pulling of silicon crystals with weight of up to 300kg in crucibles with up to 28” diameter. It will be shown that the so-called crystal twisting, where the crystal loses its cylindrical shape, is mainly limiting the pull rate. The thermal stress in the crystal is usually far below the stress values where cracks are experimentally and is not considered to limit the pull rate. The same is valid for the ratio V/G with pull rate V and axial temperature gradient G in the crystal at the solid-liquid interface. The V/G values along the radial position in the crystal are typically exceeding the critical V/G ratio by far, i.e. the crystals grow vacancy rich and not interstitial rich. The later growth conditions are known to

be unfavorable because interstitials will reduce the minority carrier lifetime, which is an important material parameter for solar cells. From the analysis of results above we make conclusions how the hot zone of the Czochralski puller can be optimized to increase the pull speed further.

Thursday, August 1, 2019

10:30 AM - 12:00 PM

Symposium on Epitaxy of Complex Oxides: Substrates for Complex Oxide Films

Location: Grays Peak II, III

Session Chair(s): Wolfgang Braun

10:30 AM - 11:00 AM

27 YEARS OF PROGRESS IN PEROVSKITE-TYPE SUBSTRATE CRYSTAL GROWTH AT THE IKZ

C. Guguschev, S. Ganschow, D. Klimm, M. Brützam, I.M. Schulze-Jonack, M. Bickermann

Leibniz-Institut für Kristallzüchtung, GERMANY

The growth of perovskite substrate single crystals in Berlin, Germany was intensified with the foundation of the IKZ in 1992. During the ensuing 27 years, a myriad of bulk perovskite oxide crystals with pseudocubic lattice parameters in the 3.7 to 4.2 Å range have been mainly grown by using the Czochralski technique (Fig. 1). This work required increased scientific understanding of phase diagrams and melt behavior as well as surmounting technological hurdles to yield high quality single crystal substrates with size sufficient to yield 1 cm x 1 cm substrates. The epi-ready substrates produced from these crystals served as the fundamental basis for the discovery and development of advanced mixed oxide layers with interesting ferroelectric, ferromagnetic, multiferroic, or simply electronic properties. By growing these layers epitaxially on substrates with lattice mismatches up to a few percent, so that the resulting thin films are commensurately strained to the underlying substrates, the Gibbs free energy of the layers is influenced by a contribution from elastic distortion at the interface. Quite often, the structure of these epitaxially

grown layers is orthorhombically distorted. Rare earth scandates REScO_3 ($\text{RE} = \text{Pr} \dots \text{Dy}$) proved to be especially well suited as substrates, because they are orthorhombic from their high melting points near or beyond 2000°C down to room temperature and exhibit almost square (101) lattice meshes with spacings around 4 \AA , which is close to the lattice parameters of many advanced perovskite oxides. The fruitful cooperation between the IKZ group and Prof. Schlom's group resulted in work that served as the cornerstone of modern strain engineering of oxides. Specifically, Haeni et al. (2004) [1] could shift the Curie temperature of the ferroelectric-to-paraelectric transition of SrTiO_3 from non-existent to room temperature by imparting 1% biaxial strain through strain engineering to DyScO_3 substrates. Depending on the epitaxial layer, the choice of appropriate substrates allows the adjustment of elastic strains stepwise, by the choice of proper RE ions. This talk will give an overview of important achievements in bulk single crystal growth, how solid solutions can extend the range of accessible substrate lattice parameters [2] and it will also give insights into our recent crystal growth activities in the fascinating field of perovskites and how they relate to emerging technologies.

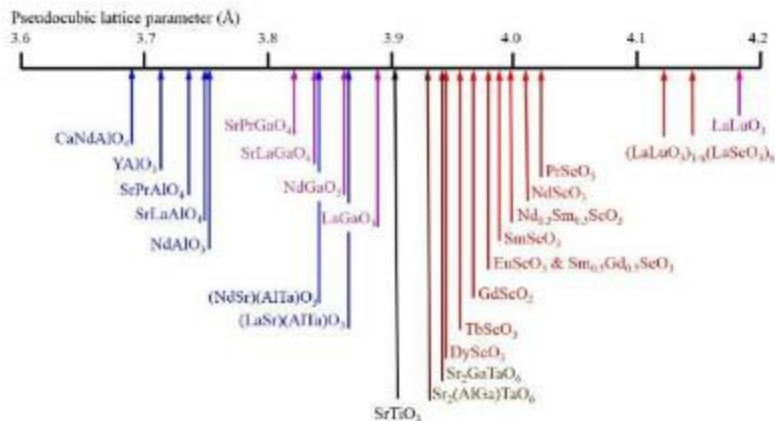


Fig. 1: Selection of perovskite-type substrate single crystals. [1] J.H. Haeni et al., Nature, 430 (2004) 758-761. [2] R. Uecker et al., Journal of Crystal Growth, 457 (2017) 137-142.

11:00 AM - 11:30 AM

CONGRUENTLY MELTING PEROVSKITE SOLID SOLUTIONS

V.J. Fratello¹, L.A. Boatner², H. Dabkowska³, A. Dabkowski³, T. Siegrist⁴, K. Wei⁴

¹Quest Integrated, LLC, WA, UNITED STATES OF AMERICA, ²Oak Ridge National Laboratory (retired), TN, UNITED STATES OF AMERICA, ³McMaster University, CANADA, ⁴Florida State University, UNITED STATES OF AMERICA

If a crystal is non-congruent, has a high liquidus temperature, contains volatile ingredients and is desired in a thin film, multilayer or superlattice, then epitaxy is the required growth method. Good epitaxial growth typically requires a high-quality substrate that is a structural and lattice-parameter match to the film. Perovskites include the most common minerals in the earth's crust, but also comprise technologically important materials that are ferroelectric, electrooptic, ferromagnetic, ferrimagnetic, antiferromagnetic, multiferroic, piezoelectric, pyroelectric, paraelectric, magnetoresistive, colossal magnetoresistive (CMR), magneto optic, photovoltaic, photoluminescent, insulating, conducting, semiconducting, superconducting, ferroelastic, magnetostrictive, catalytic, etc.

Researchers have developed complex perovskite multilayer thin films for potential device applications ranging from spintronics to ferroelectric transistors. There are currently limits on the available substrates for film growth with substrates such as strontium titanate, potassium tantalate and the rare earth scandates being small in size, high in cost and limited in availability. Above 0.3865 nm in the primitive perovskite unit cell lattice parameter, there are no commercial perovskite substrates and there are not even any experimental substrates available in the important range of 0.403-0.416 nm. A class of low-cost perovskite solid solutions has been identified that are congruently melting at a temperature minimum indifferent point and that have a cubic structure with no structural phase transition – i.e., qualities that make them more useful as substrates. In fact, there are a few relevant compounds already reported in the literature - including the technologically important perovskite substrate material lanthanum strontium aluminum tantalate. While having two phases in equilibrium at a point seems to violate the usual expression of Gibbs' phase rule, a more detailed look shows that this is thermodynamically possible if the coefficient matrix has a zero determinant. It requires an uncommon balancing of various terms of the free energy for the required condition. The factors that have

been found to produce such a congruently melting minimum cubic perovskite solid solution include a common ion(s) among the end members, similar sized ions, similar melting temperatures (within 300°C) and, most profoundly, a Goldschmidt tolerance factor T close to unity, preferably 0.98-1.02. This contributes to a thermodynamic energy minimum, and it was found to shift the position of the minimum melting composition to optimize T . Nine new compositions have now been identified with cubic lattice parameters from 0.387 to 0.410 nm. A preliminary unseeded Bridgman growth run of one of the compounds produced a predictably polycrystalline sample with good structure and uniformity.

11:30 AM - 12:00 PM

SPINEL FERRITE THIN FILMS AND HETEROSTRUCTURES FOR SPINTRONICS

A. Gupta

The University of Alabama, AL, UNITED STATES OF AMERICA
Spinel ferrite thin films have numerous technological applications in areas such as telecommunications (microwave and millimeter wave devices), magneto-electric coupling devices and are also promising candidates for future spintronic devices. Unlike perovskites, the investigation of high quality spinel ferrite films is quite limited, in part because of the complex crystal structure with a large unit cell consisting of many interstitial sites and that the transition metal cations can adopt various oxidation states. Usually films of spinel ferrite such as NiFe_2O_4 (NFO), grown both by both physical and chemical deposition techniques, suffer from a number of structural and magnetic drawbacks, e.g. formation of antiphase boundaries and high magnetic saturation fields. We show that by using substrates having similar crystal structure and low lattice mismatch, one can avoid formation of antiphase boundaries and thereby obtain magnetic properties comparable to bulk single crystal. We used spinel MgGa_2O_4 , CoGa_2O_4 and ZnGa_2O_4 substrates, which have 0.6%, 0.1% and 0.05% lattice mismatch, respectively, with NFO to grow epitaxial films that are essentially free of antiphase boundaries and exhibit sharp magnetic hysteresis characteristics. Moreover, ferromagnetic resonance linewidths similar to those in single crystals are obtained.

We have compared these results with NFO film grown on another spinel substrate MgAl_2O_4 , which has 3.1% lattice mismatch, that has antiphase boundaries and clearly exhibits degraded properties. We have also investigated spin transport properties of the films grown on the three substrates via the longitudinal spin Seebeck effect (LSSE). An increase in the spin voltage signal with reduction in lattice mismatch is observed, which is in correspondence with similar improvements in structural and magnetic properties. Improvements in the magnetic and spin Seebeck properties are also observed using the lattice-matched substrates for other spinel ferrites, including CoFe_2O_4 and Fe_3O_4 .

Thursday, August 1, 2019

1:30 PM - 3:00 PM

Bulk Crystal Growth & Nonlinear Optica Materials II

Location: Shavano Peak

Session Chair(s): Yushi Kaneda, Adam Lindsey

1:30 PM - 1:45 PM

IMPLEMENTATION OF ACCELERATED CRUCIBLE ROTATION TECHNIQUE IN CZOCHRALSKI GROWTH OF ND:YAG SINGLE CRYSTALS: MODIFYING ND CONCENTRATION AND SEGREGATION

M. Saleh, S. Kakkireni, J. Mccloy, K. Lynn

Washington State University, WA, UNITED STATES OF AMERICA

Nd:YAG is a well-known and widely used laser material with diverse applications. Nd:YAG is typically grown from the melt using the Czochralski (CZ) technique, and like many other materials grown from the melt, Nd:YAG suffers from Nd segregation along the growth axis due to Nd's large ionic size compared to Y. This segregation results in an average Nd concentration far less than that in the melt (~5 times less) and Nd concentration variation along the growth axis; this leads to limitations on the usable crystal length, and in turn the laser power obtainable. There have not been any published improvement in the open literature to counter the issue of Nd segregation in CZ grown Nd:YAG. The methods used currently to reduce the effect of

segregation, such as growth in larger diameters from large melt volumes or hot-loading, lead to increased crucible sizes, growth costs, and wasted materials. In this paper, the Nd segregation is addressed by the successful implementation of the Accelerated Crucible Rotation Technique (ACRT). Using ACRT, promising Nd uniformity is achieved with much higher Nd incorporation in the matrix than that attained by conventional techniques (over 3% Nd). In addition to the Nd uniformity, the ACRT-CZ grown crystals showed no signs of core breakdown. The concentration of Nd and the distribution along the crystal show dependency on the ACRT profile used and the initial Nd concentration in the melt. It is observed that some crystals had higher Nd concentration than initial Nd in the overall charge. The Nd concentration did not show dependence on the thermal gradients in the growth system or on the crystal diameter. The crystals were grown with diameters ranging from 20-35 mm and lengths up to 120 mm. The rotation profile also affected the solid/liquid interface shape and thus the radial segregation. ACRT thus appears very promising for close control of dopant concentration and gradient in CZ grown YAG.

1:45 PM - 2:00 PM

GROWTH OF RARE-EARTH DOPED YTTRIUM ALUMINUM GARNET SINGLE CRYSTAL FIBERS

S. Bera¹, P. Ohodnicki¹, K. Collins², M. Fortner³

¹National Energy Technology Laboratory, PA, UNITED STATES OF AMERICA, ²National Energy Technology, OR, UNITED STATES OF AMERICA, ³US&S - E2, OR, UNITED STATES OF AMERICA

Single crystal (SC) fibers have shown great potential in optical fiber applications where conventional glass fibers are not suitable due to limitations inherent to the material properties of glasses. However, SC fibers have seen very limited commercial applications because unlike conventional glass fibers, SC fibers cannot be grown with a core-clad structure. Since SC fibers are grown from low viscosity liquid melts, a preform geometry cannot be transferred to the final fiber. In this study, we report an attempt at creating a graded index fiber leveraging the auto-segregation of different dopants in a crystal fiber matrix.

Neodymium and holmium doped yttrium aluminum garnet (YAG) SC

fibers were grown using the laser heated pedestal growth technique and the cross-sectional dopant concentration was measured using electron-probe micro-analysis. It was observed that the degree of auto-segregation of the rare-earth dopant depended on the difference in ionic size of the dopant ion and the Y^{3+} ion in the YAG matrix. While holmium, which is similar in size to yttrium, showed very little tendency to self-segregate, the concentration of Nd ions varied as much as 25% across the cross-section of the fiber. A strong correlation between the dopant concentration profile and fiber draw speed was also demonstrated. Since the local refractive index of the crystal depends on the concentration of dopants, a refractive index profile can be achieved through a dopant profile across the fiber cross-section. This, in turn, can be realized by varying the growth conditions, the dopant, the crystal matrix, etc. Such an approach shows a great promise in developing monolithic SC fibers with graded-index profile.

2:00 PM - 2:15 PM

PARTITIONING OF MG INTO LI AND NB SITES IN $LiNbO_3$ CRYSTAL DURING GROWTH FROM THE MELT

S. Uda, Y. Horie

Tohoku University, JAPAN

Impurities in a melt are partitioned into different sites in a crystal during crystal growth from the melt, and the equilibrium partition coefficient, k_0 , is not the same for each site. In the present study, partitioning of Mg into Li and Nb sites in a $LiNbO_3$ (LN) crystal grown from a congruent melt doped with MgO was investigated. Considering the degrees of freedom for each of the crystal sites [1], Mg goes to either Li or Nb sites, but not into both sites as long as anti-site Nb exists at Li sites. When congruent LN (c-LN) doped with MgO is synthesized by sintering, Mg first goes to Li sites. As the amount of MgO is increased, anti-site Nb at Li sites decreases in quantity and eventually disappears. Further increasing the amount of MgO causes Mg to become located at both Li and Nb sites [2]. MgO partitioning into LN crystal sites from the melt is different to that for solid-state reactions. In the present study, LN crystals were grown at a rate of 5 mm/h along the *c*-axis via the micro-pulling-down (μ -PD) method from

c-LN melts doped with various amounts of MgO ranging from 0 to 7.0 mol%. Steady-state growth was quenched by shutting off the heater power. The MgO distribution along the axial direction across the interface gives the equilibrium partition coefficient for Mg, k_{E0} , which is influenced by the intrinsic electric field at the interface. The dependence of k_{E0} on the MgO content in the melt is shown in Fig. 1. A discontinuity is observed around 3.7 mol% MgO, and is attributed to a change in Mg occupation from Li sites to both Li and Nb sites, where the partitioning mode changes discontinuously. Application of a regular solution model to the chemical potentials of Mg in Li and Nb sites gives k_{E0} for each of these sites and indicates that the mixing enthalpy, ΔH_{mix} , associated with Mg incorporation is several times larger for Nb sites than for Li sites, which suggests that the preferential sites for Mg are Li sites. References S. Uda, in *Handbook of Crystal Growth*, Eds. Nishinaga, Rudolph, and Kuech, Elsevier (2014) pp. 188-189. C. Koyama, J. Nozawa, K. Maeda, K. Fujiwara, and S. Uda, *J. Appl. Phys.* **117**, 014102 (2015).

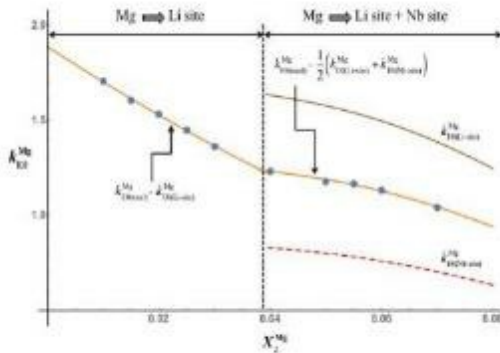


Fig. 1. Variation of the equilibrium partition coefficient for Mg, k_{E0}^{Mg} , for Li sites and Nb sites as a function of the MgO content in the c-LN melt.

2:15 PM - 2:30 PM

CRYSTALLINE GROWTH UNDER ELECTRIC FIELD: TOWARD A NEW ROUTE TO DESIGN DOMAIN MODULATED-STRUCTURES.

R. Haumont, M. Pellen, G. Paris, R. Saint-Martin, C. Decorse
Paris-Saclay University - ICMMO SP2M, FRANCE

Single crystals of CaTiO_3 , BaTiO_3 , and LiNbO_3 were prepared by the

floating method (FZ) method in which a high external electric field (≥ 3 kV.cm⁻¹) is applied. Such an electric field is a new powerful tool, in crystalline growth, able to create new chemical structures and original new materials with new physical properties. By varying crystal growth velocity and electric field strength, we show that we can control the macroscopic shape of single crystals, and we can alter the crystalline orientation of domains; Applying an in-situ high electric field during crystalline growth is a new tool to design domain modulated-structures. Recent works reported the role of the electric field on kinetic and thermodynamic processes during crystalline growth. In the selection, orientation and distribution of piezoelectric domains, we have shown that an electric field acts like an external force [1,2]. The electric field can act on thermodynamic equilibrium and on a solid/liquid interface [3]. Its application during growth modifies the partition coefficient of species [4] and the possible modification phases diagrams of a material [5]. Indeed ions within a difference of electric potentials see their energy changing, which implies a new thermodynamic equilibrium [5]. Thus, applying an intense electric field during compound growth is a new parameter to affect the direction of polarization and possibly to amplify the value of polarization by exacerbating ionic displacements. [1] P. Hicher, R. Haumont, R. Saint-Martin, X. Mininger, P. Berthet, A. Revcolevschi. *J. Cryst. Growth*, 409(1) pp. 23-26 (2014) [2] M. Pellen, R. Haumont, R. Saint-Martin, journal of crystal growth, in press [3] R. Simura, K. Nakamura, S. Uda. *J. Cryst. Growth*, 310(16), pp. 3873-3877 (2008) [4] S. Uda, W. A. Tiller. *J. Cryst. Growth*, 121(1-2), pp. 93-110 (1992) [5] S. Uda, X. Huang, S-Q. Wang. *J. Cryst. Growth*, 275(1-2), pp. 1513-1519. (2005)

2:30 PM - 2:45 PM

GROWTH OF THE OPTICAL PERFECT LiNa₅Mo₉O₃₀ CRYSTALS

V. Sukharev, E. Sukhanova, I. Avetissov, **V. Sanina**, A. Sadovsky
RCTU Mendeleevs, RUSSIAN FEDERATION

Single crystals of LiNa₅Mo₉O₃₀ 130x60x30 mm in size and more than 200 g in weight were successfully grown by the Czochralski method (fig. 1). Mathematical modeling of the crystal growth setup has been carried out. The optimal conditions for crystal growth have been determined. The duration of the crystal growth process were less than

100 hours. The grown crystals had no visible defects, cracks, striations, bubbles. Grown crystals were optically perfect: optical absorption at a wavelength of 1064nm was less than 500 ppm. The crystal destruction threshold was determined as 16 GW/cm² with a pulse time of 5 s. The values of the dielectric constant of the crystal are determined along the axes a, b, c which were respectively 5.8, 10, 9.5

2:45 PM - 3:00 PM

CRYSTAL GROWTH OF QUATERNARY CHALCOGENIDE MID-IR NONLINEAR OPTICAL MATERIALS: AGGS AND AGGSE

W. Huang, S. Zhu, B. Zhao, Z. He, B. Chen, S. Fu, Y. Zhao
Sichuan University, CHINA

$\text{AgGaGe}_n\text{S}_{2(n+1)}$ and $\text{AgGaGe}_n\text{Se}_{2(n+1)}$ are promising quaternary chalcogenide nonlinear crystals for mid-IR laser applications which could satisfy the lack of materials which are able to convert a 1.064 μm pump signal (Nd:YAG laser) to wavelengths higher than 2 μm , up to 12 μm . In this work, $\text{AgGaGe}_n\text{S}_{2(n+1)}$ ($n=1, 2, 3, 4$ and 5) and $\text{AgGaGe}_n\text{Se}_{2(n+1)}$ ($n=3$ and 5) polycrystal are synthesized by vapor transport and mechanical oscillation method with unique cooling processes in a two-zone rocking furnace with specially designed temperature profile. The problem of explosions and composition segregation were solved by careful control of the heating and cooling cycle. Besides, $\text{AgGaGe}_n\text{S}_{2(n+1)}$ and $\text{AgGaGe}_n\text{Se}_{2(n+1)}$ single crystals with 15~30 mm diameter and 20~50 length have been grown by the modified Bridgman method. The crystals have good homogeneity and high transparency in the 0.5–11.5 μm spectral range, making them suitable for laser experiments. At last, different thermal annealing treatment have been conducted to eliminate the absorptions in the mid-IR range of $\text{AgGaGe}_n\text{S}_{2(n+1)}$ and $\text{AgGaGe}_n\text{Se}_{2(n+1)}$ single crystals, and band gap all widen.

Thursday, August 1, 2019

1:30 PM - 3:00 PM

Characterization Techniques for Bulk and Epitaxial Crystals II

Location: Crestone III, IV

Session Chair(s): Mark Goorsky, Holger Eisele

1:30 PM - 2:00 PM

REDUCTION OF THREADING DISLOCATION DENSITY IN HIGH-TEMPERATURE ANNEALED ALN ON SAPPHIRE TEMPLATES

H. Miyake¹, K. Shojiki¹, K. Uesugi², S. Xiao¹

¹Graduate School of Regional Innovation Studies, Mie University, JAPAN, ²Organization for Promotion of Regional Innovation, Mie University, JAPAN

For the realization of highly efficient deep-ultraviolet light-emitting diodes (DUV-LEDs) based on III-nitride semiconductors, it is essential to improve the crystalline quality of the AlN templates for crystal growth of AlGaN. Our group has suggested sputtering deposition and post-deposition high-temperature face-to-face annealing (FFA) as a fabrication method of AlN films with low threading dislocation density (TDD) on sapphire substrates. Although the FFA enables reduction of TDDs, it possibly causes a cracking for AlN films due to a large thermal expansion coefficient mismatch between AlN and sapphire. In this work, we controlled the residual stress in AlN films by modifying the sputtering conditions. Consequently, we achieved crack-free AlN films with low TDDs compared with the previous studies. A series of AlN films with 160 - 850 nm thicknesses were deposited on vicinal sapphire (0001) substrates by RF sputtering. For the AlN deposition, the sputtering pressure was varied among 0.05 - 0.40 Pa, while the substrate temperature, amount of supplied N₂ gas, and RF power were fixed. After the deposition, FFA was performed at 1650 – 1725 °C under N₂ ambient for 3 h. Finally, AlN films were grown by metalorganic vapor phase epitaxy (MOVPE) on the AlN templates. From high resolution X-ray diffraction (HR-XRD) measurements, it is observed that a larger compressive stress is accumulated in the AlN films deposited at lower sputtering pressure. As the sputtering pressure decreases, the cracking occurred during FFA is suppressed even in the sample with a thicker AlN film. It is considered that the compressive stress introduced to the AlN films during the sputtering deposition enhanced the tolerance of the AlN films against the tensile stress applied to the AlN films during FFA. In addition, the X-ray rocking curve full width at half maximum (XRC-FWHM) values from the asymmetric planes of annealed AlN films decrease as the AlN thickness increase, which indicates the crystalline quality improvement of the AlN films. Figures 1(a) and 1(b) show plan-view scanning transmission electron microscopy (STEM) images observed from the annealed AlN template with various thickness and annealing

temperatures. Figure 1(c) shows the relationship between thickness of the annealed AlN templates and TDDs evaluated from the STEM images. It was revealed that a TDD of $2.07 \times 10^8 \text{ cm}^{-2}$ was achieved for AlN templates with submicron thicknesses.

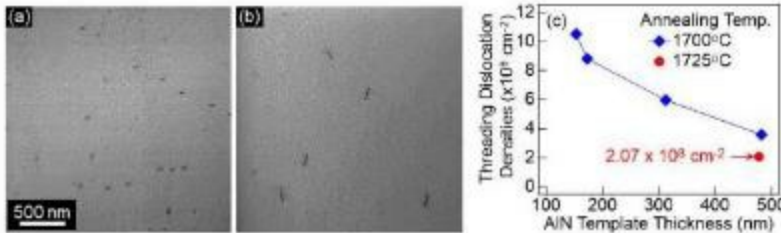


Fig. 1. Plan-view STEM images of (a) a 177-nm-thick AlN template annealed at 1700 °C and (b) a 477-nm-thick AlN template annealed at 1725 °C. (c) Relationship between the AlN template thickness and the TDDs estimated from the STEM images.

2:00 PM - 2:15 PM

A FUNDAMENTAL STUDY ON SUBSTRATE-INDUCED EPITAXIAL TILT USING HIGH-RESOLUTION X-RAY DIFFRACTION METHODS

M.E. Liao, M. Goorsky

University of California Los Angeles, CA, UNITED STATES OF AMERICA

In this study, a refined theory of the origin of epitaxial tilt is presented. In the current literature, there are many reports that cite the so-called Negai tilt as the mechanism for epitaxial tilt.¹⁻³ The basis of Negai tilt is that lattice mismatch and atomic terraces on the substrate surface are the factors that induce epitaxial tilt. This theory neglects the mechanical deformation induced by the entire substrate and thus, we argue, the origin of the observed tilt in epitaxial layers is due to shear stresses. It has been shown for the cubic crystal system that (001), (110), and (111) oriented substrates do not have any component of shear, and thus would not induce any epitaxial tilt.⁴ However, all other orientations including miscut wafers have some component of shear and would correspondingly induce tilt in epitaxial layers: (211), (311), and (221) orientated substrates are some examples of orientations with the largest component of shear. In fact, the first report of Negai tilt examined epilayers on miscut (001) and (111) GaAs substrates.¹ While miscut wafers do have atomic terraces on their surfaces, this is not believed to be the origin of epitaxial tilt. It is the fact that a miscut

wafer's surface orientation can be represented by a different plane. Since the surface is no longer parallel to one of the zero-shear orientations, there is some component of shear present in all epilayers grown on miscut substrates. Reciprocal space analysis is employed in this study to systematically explain how miscut substrates can lead to epitaxial tilt and the degree of tilt can be used to quantify the amount of shear stress present. X-ray diffraction reciprocal space maps of GaAs epitaxially grown on a (211) Si substrate are analyzed to determine the amount of shear stress present as well as the direction of the tilt.

References 1. H. Negai, J. of Appl. Phys., 45, 3789 (1974) 2. F. Riesz, J. of Crys. Growth, 140, 213 (1994) 3. X.R. Huang, et al., Appl. Phys. Lett. 86, 211916 (2005) 4. L. De Caro, et al., Phys. Rev. B, 48(4), 2298 (1993)

2:15 PM - 2:30 PM

CHARACTERIZATION OF LINEAGES WITH DISLOCATIONS IN CZOCHRALSKI-GROWN LITAO₃ INGOTS BY DIFFERENTIAL INTERFERENCE CONTRAST MICROSCOPY OF ETCH PITS

Y. Ohno¹, Y. Kubouchi², T. Kajigaya²

¹Institute for Materials Research, Tohoku University, JAPAN,

²Materials Laboratories, Sumitomo Metal Mining, JAPAN

Lithium tantalite (LiTaO₃) with a R_{3c} pseudo-ilmenite structure is an indispensable material in optical applications due to their excellent piezoelectric and nonlinear optic properties depending on their crystallographic direction. Especially, LiTaO₃ wafers for surface acoustic wave applications, cut from high-quality single-crystalline ingots grown by the Czochralski (CZ) method, have a great demand in the telecommunications mobile phone handset market. One important issue of CZ-LiTaO₃ ingots is polycrystallization during the CZ growth, that would result in the shattering of the growing ingots. It is considered that the polycrystallization is correlated with lineages, i.e., arrays of dislocations introduced due to thermal stresses during the CZ growth. Therefore, in order to control the generation and development of lineages, we need to understand the distribution and nature of dislocations in CZ-LiTaO₃ ingots. For this purpose, we have

developed an analytical method to determine the characteristic of each individual dislocation in CZ-LiTaO₃ (0001) wafers by differential interference contrast microscopy of the etch pit of the dislocation. (0001) wafers of 0.5 mm thick, both sides of which were polished to a mirror finish, were cut from a high-quality CZ-LiTaO₃ single crystal with the growth direction rotated by 42° from [0-110] towards [0001] (42° RY, Sumitomo Metal Mining). Poling processes were executed after the growth so that distributions of composition and point defects were uniform. Two-dimensional distribution of lineages in each wafer was determined by x-ray topography. Each wafer was then etched chemically for 15 min in a mixture of HF and HNO₃ (1:2) at temperature of 353 K to form etch pits of dislocations [1], and the etch pits of dislocations forming lineages were observed by differential interference contrast microscopy. The characteristic on the typical etch pit images was correlated with the Burgers vector **b** of the corresponding dislocations, determined by transmission electron microscopy (TEM). X-ray topography revealed that lineages were introduced along {11-20} and {10-10} planes. The former lineage was composed of an array of edge dislocations with **b** = <11-20>. Meanwhile, the latter lineage was composed of a set of a dislocation array with **b** = <2-1-10> and that with **b** = <11-20>, arranged near each other. Polycrystallization took place beneath the ingot surfaces at which a high density of {10-10} lineages existed. The polycrystallization mechanism will be discussed in terms of the generation and expansion of {10-10} lineages. [1] Y. Ohno and Y. Kubouchi, Japanese Patent Application No. 2018-013246.

2:30 PM - 2:45 PM

DETERMINATION OF AL CONTENT IN AL/SI THERMOMIGRATION FABRICATED STRUCTURES BY X-RAY DIFFRACTION

B.M. Seredin¹, A. Lomov², A. Belov³

¹Platov South-Russian State Polytechnic University (NPI), RUSSIAN FEDERATION, ²Valiev Institute of Physics and Technology of RAS, RUSSIAN FEDERATION, ³FSRC "Crystallography and Photonics" of RAS, RUSSIAN FEDERATION

One of the initial steps in forming both planar and channel silicon p-n

junctions consists in injection of dopant impurity. Boron and phosphorus diffusion is widely used to fabricate power high-voltage devices. But blurring of the p-n interfaces leads to device degradation. As an alternative, zone-gradient melting (thermo-migration technique) can be used. An advantage Al/Si thermomigration process [1] is its high rate which exceeds by two or three orders the rate of conventional diffusion based techniques. It is one of the promising approaches to overcome the disadvantage and increase the efficiency of devices. In addition, by means of Al/Si thermomigration one can fabricate a micro silicon matrix composed of connected photocells with p-n junction channels on faces normal to the working surface of conventional Si wafers [2]. For metrological control of the dopant concentration and structural defects (Al_xO_y precipitates and so on) generated by thermomigration process X-ray diffraction techniques can be applied. Here, using a combination of the X-ray diffraction data and first-principles density functional calculations with ABINIT code [3], we determined the Al content in different structures produced by Al/Si thermomigration, in particular, in planar layers and channels. In DFT calculations Al was assumed to occupy substitutional positions. Additional calculations of lattice distortion due to Al in a number of interstitial positions were carried out on the basis on a many-body interatomic potential [4]. Results of spectroscopic (SIMS) and microscopic (EDX) investigations were used for comparison. It was found that the aluminum content in the Al/Si thermomigration channel and film is $(0.95 \div 1.05) \cdot 10^{19} \text{ cm}^{-3}$. [1]. V.N. Lozovskii, L.S. Lunin, and V.P. Popov. *Temperature- Gradient Zone Recrystallization of Semiconductor Materials*. Metallurgiya, Moscow, 1987 [in Russian]. [2]. V.N. Lozovskii, A.A. Lomov, L.S. Lunin, B.M. Seredin, and Yu.M. Chesnokov. "Crystal Defects in Solar Cells Produced by the Method of Thermomigration". *Semiconductors*, **51**, n.3, pp. 285–289, 2017. [3] X. Gonze, J.-M. Beuken, R. Caracas et al. "First-principles computation of material properties: the ABINIT software project". *Comp. Mater. Science*, **25**, pp. 478-492 (2002). [4]. B. Jelinek, S. Groh, M.F. Horstemeyer, J. Houze, S.G. Kim, G.J. Wagner, A. Moitra, M.I. Baskes. "Modified embedded atom method potential for Al, Si, Mg, Cu and Fe alloys". *Phys. Rev. B*, **85**, pp. 2451021(18), 2012.

2:45 PM - 3:00 PM

MORE INSIGHTS IN SEMICONDUCTOR MATERIAL QUALITY WITH ADVANCED X-RAY TOPOGRAPHY IMAGING

J. Friedrich¹, R. Weingaertner¹, C. Reimann¹, E. Meissner¹, P. Berwian¹, U. Preckwinkel²

¹Fraunhofer IISB, GERMANY, ²Rigaku Europe SE, GERMANY

Characterization of structural defects in semiconductor materials is an important task to understand the influence of the production conditions on the material quality of substrates and epilayers and to correlate the impact of structural defects on the performance and reliability of devices manufactured out of the substrates and epilayers. State of the art characterization of structural defects in single crystalline material like dislocations, dislocation networks, and slip lines is done by defect selective etching (DSE), Cathodoluminescence (CL), Photoluminescence (PL) or by X-ray topography (XRT). Unfortunately DSE is a destructive method and leads to a significant yield loss, especially important for expensive substrate materials. CL could be used only on small samples and needs a high sample preparation effort. CL and PL are applicable only for electrically active defects. PL is not easily available for semiconductors with high band gaps like AlN. XRT measurements were done in the past mostly at synchrotron radiation sources, are highly complex and the accessibility is not satisfying. Meanwhile advanced X-ray topography tools for use in a laboratory are on the market like the XRTmicron which allows high quality 2D and 3D topograms due to the usage of a novel highly focusing anode. The availability of such advanced tools gives the possibility to investigate crystallographic defects such as the amount and different types of dislocations, slip lines, dislocation networks, (small angle) grain boundaries, inclusions, precipitates, pits, scratches, etc. with high speed and high resolution on full wafer scale on bare wafers, wafers with epilayers, partially processed wafers as well as bonded wafers. In this contribution we give an overview of the principle of the XRTmicron tool and present examples how it can be used to analyze e. g. the slip line formation in 300 mm silicon wafers, the different kinds of dislocation types (threading screw, threading etch and basal plane dislocations) in 4H-SiC substrates and epilayers, the quality of differentially grown AlGaN layers on sapphire, and the

defect propagation in AlN-bulk growth.

Thursday, August 1, 2019

1:30 PM - 3:00 PM

III-V Nano-Devices on Silicon

Location: Red Cloud Peak

Session Chair(s): Bernardette Kunert, Seth Bank

1:30 PM - 2:00 PM

MONOLITHIC INTEGRATION OF GAAS-(IN,AL)GAAS BASED NANOWIRE LASERS ON SILICON

T. Stettner, P. Schmiedeke, A. Thurn, J. Bissinger, D. Ruhstorfer, J.J. Finley, **G. Koblmüller**

Walter Schottky Institut and Physics Department, Technical University of Munich, GERMANY

Semiconductor nanowire (NW) lasers are unique Fabry-Perot type nanoscale coherent light sources, which exhibit single-mode low-threshold lasing characteristics, and properties suitable for monolithic integration onto silicon (Si) photonic circuits [1]. In this work, we first show monolithically integrated GaAs-based vertical-cavity NW lasers on silicon-on-insulator (SOI) platform with direct coupling of lasing emission to proximal Si waveguides (WG) [2]. Individual NW-lasers grown directly on prepatterned Si WG using molecular beam epitaxy (MBE), exhibit clear “s-shape”-characteristics, linewidth narrowing and threshold values down to $20 \mu\text{J}/\text{cm}^2$ under optical pumping. The lasing mode of individual NW lasers couples efficiently into propagating modes of the underlying Si WG, and preserves the lasing characteristics during propagation in the WG in good agreement with finite-difference time-domain (FDTD) simulations [3]. Although propagation of the lasing mode within the Si WG extends beyond $> 60 \mu\text{m}$, strong absorption losses prevail at the lasing wavelength of $\sim 820 \text{ nm}$ given by the bulk GaAs gain material. By replacing the bulk GaAs as the active gain medium by $\text{In}_x\text{Ga}_{1-x}\text{As}$ multiple quantum wells (MQW) in a radial core-shell NW heterostructure, the gain spectrum can be tuned and the emission wavelength shifted towards longer wavelengths [4]. Specifically, we illustrate how the NW-MQW lasing

performance is impacted by InGaAs-QW/AlGaAs-barrier design principles and deviations from ideality as influenced by In-incorporation kinetics, alloy intermixing, and structural integrity. Using correlated scanning transmission electron microscopy (TEM), atom probe tomography (APT) and confocal photoluminescence (PL) spectroscopy, the growth mediated effects on the quality of the InGaAs QW are illustrated in two growth series with variable III/V ratio and temperature. Low-temperature shell growth conditions and GaAs interlayers surrounding the InGaAs QWs give rise to enhanced In-incorporation and reduced alloy intermixing in the MQW structure. Clear evidence of lasing (s-shaped LL-curve, SE clamping and linewidth-narrowing) was found from the InGaAs MQW active region with lasing emission tunable over a wide spectral range. Particularly, the lasing emission was red-shifted by ~400 meV to ~1.2 eV (~1.1 μm) in GaAs-InGaAs MQW NW lasers, compared to pure GaAs-AlGaAs MQW NW lasing structures [4]. These results pave the way for future all-optical on-chip communication platform at a favorable low-loss range in the telecommunication wavelength regime. [1] G. Koblmüller, et al., *Semicond. Sci. Technol.* 32, 053001 (2017) [2] T. Stettner, et al., *ACS Photon.* 4, 2537 (2017) [3] J. Bissinger, et al., under review (2019) [4] T. Stettner, et al., *Nano Lett.* 18, 6292 (2018)

2:00 PM - 2:15 PM

INGAAS NANO-RIDGE ENGINEERING TOWARDS NOVEL III/V DEVICE INTEGRATION ON PATTERNED 300 MM SI SUBSTRATES

B. Kunert¹, M. Baryshnikova¹, Y. Mols¹, H. Han¹, T. Hantschel¹, Y. Shi², D. Van Thourhout², Y. De Koninck¹, C.I. Ozdemir¹, M. Pantouvaki¹, J. Van Campenhout¹, O. Syshchyk¹, R. Puybaret¹, B. Vereecke¹, V. Motsnyi¹, R. Langer¹

¹Imec, BELGIUM, ²INTEC Ghent University, BELGIUM

Key requirements for the co-integration of III/V devices with Si based integrated circuits are a low defect density in the active III/V device region and a CMOS compatible integration approach. Selective area growth (SAG) on an oxide pattern with high aspect ratio benefits from efficient defect trapping of mismatch induced crystal defects and

allows III/V deposition only in defined regions. Hence, this is a very promising integration concept to meet both requirements. Especially the growth in narrow trenches leads to an efficient defect reduction [1] and at the same time offers the possibility of nano-ridge engineering to increase the total III/V volume and to define an optimal nano-ridge shape for device integration on top of the pattern. The potential of this novel III/V integration approach was already demonstrated by a GaAs based nano-ridge laser [2]. In this study we present the growth of InGaAs nano-ridges with different In-composition by metal vapor phase epitaxy (MOVPE) on 300 mm patterned Si substrates. The fully relaxed nano-ridge defines the buffer lattice constant for the deposition of further hetero-structures. Realizing various In-concentrations in the InGaAs nano-ridge and hence different buffer lattice constants provides an additional freedom in device design as there is no restriction to the lattice constant of binary compound materials anymore. The crystal properties of InGaAs nano-ridges investigated by scanning electron microscopy (SEM), high-resolution X-ray diffraction (HRXRD), transmission electron microscopy (TEM) and electron channeling contrast imaging (ECCI) techniques will be discussed as a function of the growth conditions and In-concentration. A low defect density in the out-grown InGaAs nano-ridge is only achieved with optimized growth conditions which enhance misfit nucleation at the III/V-Si interface and ensure sufficient gliding of threading dislocations towards the trench oxide in order to be trapped. Investigating the In-distribution in nano-ridges with different shapes emphasises that the growth control of ternary alloys is clearly more complex in comparison to binary materials because the In-incorporation varies on the different nano-ridge crystal facets. The deposition of different hetero-structure lattice matched or pseudomorphically strained as well as the growth of first doped layers will be presented and discussed in view of III/V device integration on Si substrates. [1] Kunert et al., *Semicond. Sci. Technol.* 33 (2018) 093002 [2] Shi et al., *Optica*, 4, No 12 (2017) 1468

2:15 PM - 2:30 PM

GROWTH OF GASB NANO-RIDGES ON PATTERNED 300 MM SI WAFERS

M. Baryshnikova¹, Y. Mols¹, R. Alcotte¹, H. Han¹, T. Hantschel¹, Y. Ishii², N. Bosman¹, O. Richard¹, M. Pantouvaki¹, J. Van Campenhout¹, R. Langer¹, B. Kunert¹

¹Imec, BELGIUM, ²Sony Semiconductor Solutions Corporation, JAPAN

The integration of III/V materials on Si substrate holds great potential for the fabrication of new multifunctional devices but is also challenging. To combine optoelectronic applications in the near- and mid-IR spectral regions with Si electronics, it is of great interest to develop a growth process of GaSb based narrow band gap compounds on Si substrate. The essential requirement for an efficient device performance is a low threading dislocation density in the active layer. One of the techniques to achieve a high crystal quality in mismatched III/V-Si hetero-epitaxy is based on the selective area growth (SAG) in high-aspect-ratio structures patterned on a Si substrate. The strain induced plastic relaxation occurs in a restricted region close to the hetero-interface, e.g. inside a narrow trench. This leads to a confinement of threading dislocations inside the trench and allows the grown-out nano-ridge material to be free of defects. This so-called aspect ratio trapping (ART) approach reduces the defect density and was already successfully demonstrated for different material systems [1]. It is important to note here that the III/V integration applying SAG together with ART has the potential to be fully compatible with CMOS technology and mass production. In our study we deposit GaSb layers in narrow trenches formed in a several hundred nanometer thick SiO₂ layer. The inspection of material properties of the samples is carried out by means of scanning electron microscopy (SEM), atomic force microscopy (AFM), high-resolution X-ray diffraction (HRXRD), transmission electron microscopy (TEM) and electron channeling contrast imaging (ECCI) techniques. In this study we investigate the defect reduction by ART in GaSb layers using different seed layers and grown out from the trenches of varying sizes. The first results indicate that the threading dislocation density is improved in GaSb nano-ridges grown on GaAs seed layers. Values below $5 \cdot 10^6 \text{ cm}^{-2}$ can be reached which are comparable with results for GaAs fins. Another significant aspect of the GaSb nano-ridge

growth is the control of its shape. By applying specific deposition conditions, it is possible to deposit GaSb fins with “funnel”, “diamond” and “box” profiles. The growth parameters leading to a flat (001) surface on top of the nano-ridges and the lowest defect density have been used to grow very first heterostructures based on $\text{In}_x\text{Ga}_{1-x}\text{Sb}$ and InAs. [1] Kunert et al., 2018 *Semicond. Sci. Technol.* 33 093002

2:30 PM - 2:45 PM

ADVANCED INTEGRATION OF III-V NANOWIRES OPTICAL INTERCONNECTS ON (100) SILICON-ON-INSULATOR

T. Chang¹, H. Kim¹, W. Lee², D.L. Huffaker²

¹University of California, Los Angeles, UNITED STATES OF AMERICA, ²Cardiff University, UNITED KINGDOM

The demand in massive data transfer has been growing exponentially as the advent of internet of things (IoT), exascale computing and big data applications. Optical interconnects with high communication bandwidth and promise in scalability have become an emerging technology in building the next-generation communication system. The silicon photonic platform, owing to the inherent nature of indirect band gap, requires the heterogeneous integrations of III-V optoelectronic devices. Selective area epitaxy has shown great potential to integrate III-V nanowires on silicon substrate regardless of lattice-mismatch and the induced strain. However, the growth of vertical nanowires is generally limited to (111) crystal surfaces, which constrains the applications in industry. In this study, we demonstrate the monolithic integration of III-V nanowire 1D array on (100) silicon-on-insulator (SOI) substrate by selective area epitaxy using MOCVD. Inclined GaAs NW array was grown on Si(111) planes that were exposed by using TMAH wet etching while the array maintained 100% yield and decent uniformity by careful controlling of growth condition. The nanobeam array was integrated with a silicon waveguide and grating as output coupler. The presentation will include the design of 3D grating, inclined NW growth and optical characterization of the NW optical interconnects. It is worth noting that, by altering the NW axial heterostructure and photonic design, the prototype shows great potentials to achieve wavelength-tunable III-V NW photonic crystal

lasers that can be integrated in on-chip optical links in silicon photonic industry.

Thursday, August 1, 2019

1:30 PM - 3:00 PM

III-V Solar Cells

Location: Torrey Peak II-IV

Session Chair(s): Christopher Pinzone, Amy W.K. Liu

1:30 PM - 2:00 PM

GRADED BUFFER BRAGG REFLECTORS FOR METAMORPHIC SOLAR CELLS

R.M. France¹, P. Espinet-Gonzalez², N. Ekins-Daukes³, H. Guthrey¹, M. Steiner¹, J.F. Geisz¹

¹National Renewable Energy Laboratory, UNITED STATES OF AMERICA, ²California Institute of Technology, CA, UNITED STATES OF AMERICA, ³University of New South Wales, AUSTRALIA

Distributed Bragg reflectors and compositionally graded buffers are both thick, somewhat complex III-V device components that serve different purposes. Compositionally graded buffers transition the lattice constant away from the substrate to access lattice-mismatched materials with useful properties, and distributed Bragg reflectors provide a wavelength-specific reflection within the semiconductor. While these two components require careful design of alloys and thicknesses, here we show that it is possible to combine their functions into one, dual-function material that serves both purposes. We design and integrate an AlGaInAs “graded buffer Bragg reflector” within metamorphic multijunction solar cells and compare the reflectivity and threading dislocation density to devices with independently-grown reflectors and buffers. The reflectance is close to that of a similar AlGaAs Bragg reflector external to a buffer as well as the reflectance predicted by the transfer matrix model, indicating that the roughness of the buffer does not drastically reduce the reflection. 72%, 91%, and 98% reflectance are shown in 2 μm , 4 μm , and 8 μm buffers using AlGaInAs layers that alternate between 30% and 70%

aluminum content. Using a 2 μm graded buffer Bragg reflector, $\text{Ga}_{0.7}\text{In}_{0.3}\text{As}$ with 2% lattice-mismatched has a minor increase in threading dislocation density compared to a standard graded buffer and a small, 20 mV, loss in voltage. As the buffer is thickened, the voltage loss is recuperated and excellent subcell voltages are achieved, indicating that the Bragg reflector is not severely hindering dislocation glide. We demonstrate the benefits of the reflection from a graded buffer Bragg reflector for multijunction solar cells with optically thin subcells and subcells containing partially-absorbing quantum wells. We conclude that Bragg reflectors can effectively be implemented within graded buffers and are useful for metamorphic optoelectronic devices.

2:00 PM - 2:15 PM

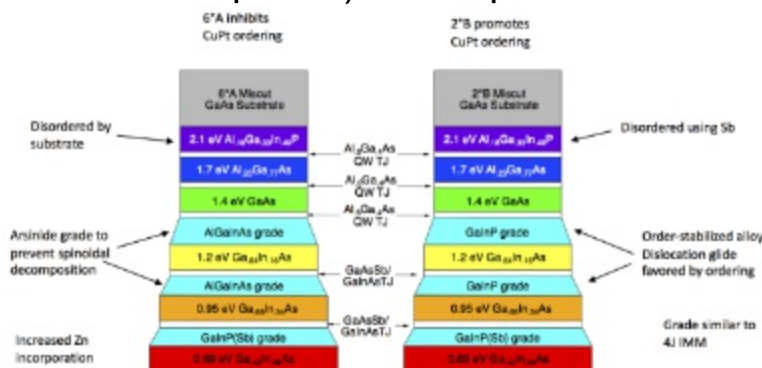
OMPVE GROWTH OF SIX-JUNCTION INVERTED SOLAR CELLS

J.F. Geisz, R.M. France, K. Schulte, M. Steiner

National Renewable Energy Laboratory, CO, UNITED STATES OF AMERICA

A well-designed six-junction (6J) solar cell has the potential to achieve over 50% solar conversion efficiency when operated at high concentration. Inverted metamorphic (IMM) solar cells designs enables the monolithic growth of multijunction solar cells with a broad range of bandgaps, but a 6J IMM design presents several crystal growth challenges. The OMPVE growth of a 6J IMM solar cells is accomplished by growing the first three junctions (2.1 eV AlGaInP , 1.7 eV AlGaAs , and 1.4 eV GaAs) lattice-matched to GaAs , then step-grading the lattice constant progressively to 1.2 eV, 0.95 eV, and 0.69 eV compositions of $\text{Ga}_x\text{In}_{1-x}\text{As}$. We have demonstrated high efficiency operation of 6J IMM solar cells grown on both 6°A and 2°B misorientations from (001) GaAs by modifying the growth to compensate for the different type and magnitude of CuPt atomic ordering that these substrates induce. Initially, 6°A substrates were used to promote the disordering required for the high bandgap of the first AlGaInP junction, but AlGaInAs grades were required to prevent spinodal decomposition in the metamorphic buffer. The ordering promoted on 2°B substrates stabilizes metastable GaInP alloys within the metamorphic buffers and reduces the energies required for facile

dislocation glide resulting in lower dislocation densities and thus higher performance of the metamorphic junctions grown on 2°B. Eventually, disordering of the high bandgap AlGaInP was also achieved using a Sb surfactant on 2°B substrates making this the preferred substrate. We have demonstrated record 39% efficiency at one-sun AM1.5G irradiance with these 6J IMM solar cells grown on 2°B. The main challenge for high concentration operation is the diffusion of Zn during subsequent growth from phosphide back-surface fields (BSF) into the tunnel junctions and junction bases which results in an effective resistance that degrades the fill factor at high currents. We have investigated various alternatives to Zn-doped phosphide BSF, such as C-doped and Zn-doped AlGa(In)As BSFs as well as spacer layers to reduce the effects of Zn diffusion. Significant progress here has lowered this effective internal resistance so that the peak efficiency of 6J IMM solar cells is achieved at several hundred suns with efficiencies approaching the 46% record of the 4J devices. Accurate efficiency measurements at high concentration (currently under development) will be presented at the conference.



2:15 PM - 2:30 PM

ANALYSIS ON RELATIONS BETWEEN ELECTRICAL CHARACTERISTICS AND MISFIT DISLOCATIONS OF METAMORPHIC SINGLE JUNCTION SOLAR CELLS

A. Ogura¹, H. Suzuki², M. Imaizumi¹

¹Japan Aerospace Exploration Agency, JAPAN, ²University of Miyazaki, JAPAN

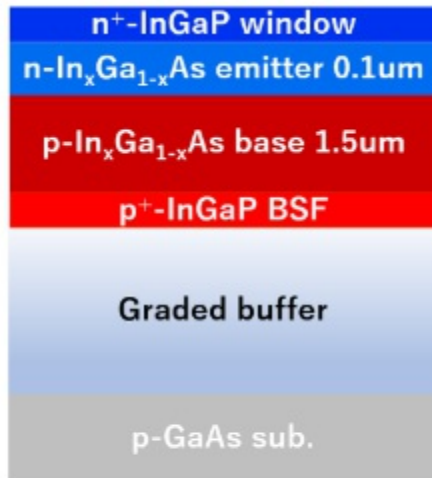


Figure 1. Sample structure of upright metamorphic InGaAs solar cell.

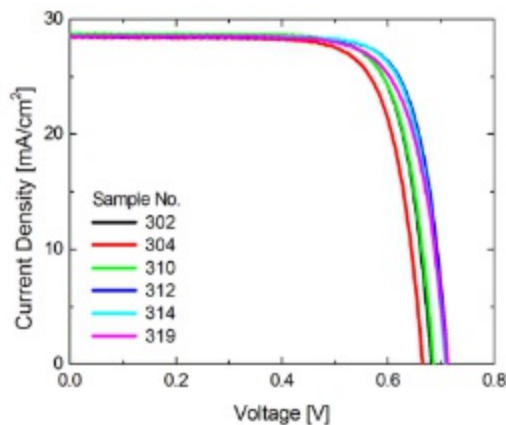


Figure 2. Light IV curves under AM0, V_{oc} and J_{sc} of each sample, metamorphic InGaAs solar cell.

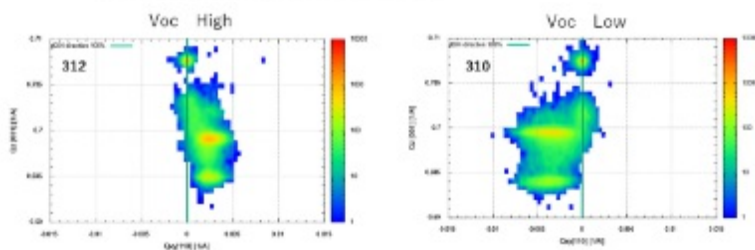


Figure 3. (004) reciprocal space mapping obtained from x-ray [1-10].

Multijunction solar cells combine various bandgap materials to attain higher conversion efficiency, decreasing thermalization and transmission loss. Recently, inverted metamorphic (IMM) technology has been so active. This technology enables us to adapt solar cells with lattice-mismatched materials. Therefore, more appropriate combinations can be selected from numbers of materials. However,

graded buffer layers have to be inserted to connect different lattice constant materials. In order to relax strain due to the lattice mismatch, misfit and threading dislocations are generated in buffer layers. Threading dislocations directly affects the electrical properties of solar cells. Thus, it is very important to optimize buffer layer structures and understand the generation mechanisms of dislocations. This study reports relations between electrical characteristics and misfit dislocations of metamorphic InGaAs single junction solar cells. InGaAs upright metamorphic single junction solar cells were grown on a p-type GaAs (001) substrate by metal organic chemical vapor deposition (MOCVD). The substrate is miscut by 2° towards [100]. Figure 1 shows the sample structure. The size of the cells was 1.0×1.0 cm and six samples were selected from a same wafer. The current voltage characteristics measurement under simulated solar light (LIV) was performed at JAXA Tsukuba Space Center. The LIV measurements were performed under the standard condition (AM0, $1\text{sun}=136.7\text{mW}/\text{cm}^2$, 25°C). Open circuit voltage (V_{oc}) of three samples, Group A, was below 0.7V and others, Group B, were over. Figure 2 indicates the LIV curves. Table 1 summarizes V_{oc} and short circuit current density (J_{sc}) of each sample. The indium composition and strain of InGaAs solar cells were determined from reciprocal space maps (RSMs) of symmetric (004) and asymmetric (115) Bragg reflections in high resolution x-ray diffraction (XRD) using Panalytical X-Pert Pro. The x-ray incident azimuths, [110] and [1-10], were selected so that dislocation anisotropies can be observed. RSMs obtained from the x-ray incident [110] and [1-10] were used to analyze α and β dislocations, respectively. The relaxation process of Group B was quite different from one of Group A. In particular, slip plane anisotropies due to β dislocations is clearly seen. Figure 3 depicts the RSMs of Groups A and B to analyze the relaxation process of β dislocation in their buffer layers. The different relaxation process due to α dislocations could be also found at each group.

Table 1. Voc and Jsc of each sample.

Group	Sample No	Voc [V]	Jsc [mA/cm ²]
A	302	0.6819	28.6695
	304	0.66606	28.444
	310	0.68539	28.7169
B	312	0.71186	28.4793
	314	0.70759	28.5519
	319	0.71074	28.5347

2:30 PM - 2:45 PM

HIGH GROWTH RATE $\text{In}_x\text{Ga}_{1-x}\text{As}$ METAMORPHIC BUFFER LAYERS BY OMVPE

K. Lekhal¹, A. Rajeev², S. Xu³, H. Kim², O. Elleuch¹, T. Kuech¹, L.J. Mawst²

¹Department of Chemical and Biological Engineering, University of Wisconsin-Madison, WI, UNITED STATES OF AMERICA,

²Department of Electrical and Computer Engineering, University of Wisconsin-Madison, WI, UNITED STATES OF AMERICA,

³Department of Materials Science and Engineering, University of Wisconsin-Madison, WI, UNITED STATES OF AMERICA

Metamorphic buffer layers (MBLs) have received great interest for developing new semiconductor devices employing alloy compositions that we cannot typically be grown on readily available substrates like GaAs or InP. However, the growth of a fully-relaxed MBL with low threading dislocation is challenging. The growth of thick MBLs is required in order to achieve a fully-relaxed structure, at least until the onset of the "work hardening" regime. The typically lower growth rates by molecular beam epitaxy (MBE) and organometallic vapor phase epitaxy (OMVPE) has hampered the development of thick MBLs (> 10 μm). The common method used in the growth of thick MBL structures is hydride vapor phase epitaxy (HVPE), but it shows the formation of a high density of hillocks [1,2]. There are few studies on the application of high growth rate OMVPE to ternary materials, such as InGaAs. In this work, we studied the growth of step-graded $\text{In}_x\text{Ga}_{1-x}\text{As}$ MBLs grown at high growth rate of $\sim 9 \mu\text{m/h}$ on GaAs (001)

substrate with 4° miscut→[111]B and zero miscut using OMVPE method. Ten step compositionally-graded structures were grown at different temperatures, 700°C and 750°C. The final cap thickness was ~5 μm with $x_{InAs} \sim 22\%$ equivalent to the lattice parameter required for short wavelength (<3.5 μm) quantum cascade laser (QCLs) and corresponding calibration superlattice (SL) growth [1]. Composition and relaxation were determined from reciprocal space maps of the (004) and (-2-24) reflections of the MBLs. It was found that the top cap layer of the step-graded $In_xGa_{1-x}As$ MBL structure with $x_{InAs} \sim 22\%$ grown at 750°C has improved surface morphology, lower etch pit density ($\sim 1 \times 10^6/cm^2$) and increased strain relaxation (> 90%) compared with the $In_xGa_{1-x}As$ MBL structure grown at 700°C. This is consistent with the result obtained recently with the HVPE method [2]. Higher growth temperature can promote dislocation glide and may reduce the work hardening effect. Then, strained-layer InGaAs/AlInAs SLs representative of those needed for QCLs were grown on the top of MBLs. The FWHM of the SL XRD fringes were found to improve when the higher temperature MBL (grown at 750°C) is utilized. Such data paves the way to the development of efficient QCLs in mid-IR on MBL structures grown by high growth rate OMVPE.

Acknowledgement: NSF ECCS 1806285, NSF MRSEC [1] A. Rajeev et al. , *Journal of Crystal Growth*, 452, 268-271 (2016) [2] K. Schulte et al. *Journal of Crystal Growth*, 370, 293-298 (2013)

2:45 PM - 3:00 PM

SINGLE-CRYSTAL-LIKE GAAS THIN-FILM SOLAR CELLS DIRECTLY ON FLEXIBLE METAL TAPES

S. Pouladi, M. Rathi, D. Khatiwada, P. Dutta, S. Shervin, J. Chen, W. Wang, V. Selvamanickam, **J. Ryou**

University of Houston, TX, UNITED STATES OF AMERICA

We develop a technology that can provide high-quality epitaxial semiconductor thin films on low-cost metal foils bypassing expensive wafer substrates while also offering scalability and flexibility. The epitaxial (Al)GaAs semiconductor thin films are grown on the biaxially textured Ge thin film which is grown on the polycrystalline metal tape through crystallinity-transitional buffer layers from poly- to single-

crystalline-like material, consisting of biaxially textured oxide layers. The single-crystal-like thin-film (Al)GaAs device structure layers are developed to the flexible SJ GaAs SC with front illumination geometry due to the presence of insulating buffer layers. The photovoltaic characteristics of the proof-of-concept flexible SJ GaAs SC under AM 1.5G 1-Sun illumination are promising. This study demonstrates the first flexible single-junction III-V photovoltaic solar cells (PVSCs) based on single-crystal-like GaAs thin films on a low-cost metal substrate by direct and continuous deposition, which can bypass expensive single crystal wafer fabrication. The 2-dimensional modeling of the GaAs SC is developed and used to study feasibility of single-crystal-like GaAs thin films for high performance SC devices. A promising SC device performance characteristic with an open-circuit voltage of 560 mV and short circuit current of 19.4 mA/cm², resulting in a conversion efficiency of ~7.6%, is demonstrated. This approach offers a new technology platform which has the potential for next-generation low-cost high efficiency flexible SCs.

Thursday, August 1, 2019

1:30 PM - 3:00 PM

In Situ Observation and Characterization II

Location: Grays Peak I

Session Chair(s): Jim Deyoreo

1:30 PM - 1:45 PM

STEP DYNAMICS DURING HOMOEPITAXIAL GROWTH OBSERVED WITH IN SITU X-RAY PHOTON CORRELATION SPECTROSCOPY (XPCS)

I. Calvo Almazan¹, M..J. Highland¹, J.A. Eastman¹, C. Thompson²,
H.C. Kang³, D. Fong¹, M.I. Richard⁴, G.B. Stephenson¹

¹Argonne National Laboratory, IL, UNITED STATES OF AMERICA,

²Northern Illinois University, UNITED STATES OF AMERICA,

³Chosun University, KOREA, REPUBLIC OF, ⁴Institut Matériaux
Microélectronique et Nanoscience de Provence, FRANCE

In this presentation we describe preliminary observations of step

dynamics during the homoepitaxial growth of an oxide material, TiO₂, using x-ray photon correlation spectroscopy (XPCS). This coherent x-ray method allows the observation of dynamics under steady state conditions, such as step-flow growth, that cannot be probed using traditional, incoherent x-ray methods. To test the power of XPCS to reveal the microscopic dynamics underlying growth, we have measured a set of time-evolving speckle patterns on the crystal truncation rod of the (110) surface of rutile-structured TiO₂ during magnetron sputter deposition. We investigated a temperature range of 700 to 850 °C, at growth rates of 0.2 to 1.5 x 10⁻² monolayers per second in a 30 mTorr, 3.3 % O₂-in-Ar environment. We extract the wavenumber dependence of the correlation time of speckle intensity, which encodes the information about the step dynamics. The experimental results are compared with different models and kinetic Monte-Carlo simulations that predict the signature of step flow dynamics in XPCS. These results highlight the potential of this new method to reveal the dynamics underlying step-flow growth processes most relevant to the synthesis of technologically promising materials. In the future, we expect XPCS will become even more powerful for in situ studies of crystal growth dynamics because of the new generation synchrotrons coming online with orders-of-magnitude higher coherent x-ray flux.

1:45 PM - 2:00 PM

IN SITU OBSERVATION OF THE SOLIDIFICATION INTERFACE AND GRAIN BOUNDARY DEVELOPMENT OF TWO SILICON SEEDS WITH SIMULTANEOUS MEASUREMENT OF TEMPERATURE PROFILE AND UNDERCOOLING

C. Lan¹, V. Lau Jr²

¹Dept. of Chem. Eng., National Taiwan University, TAIWAN, ²National Taiwan University, TAIWAN

Multi-crystalline silicon naturally possesses a large amount of grain boundaries which act as natural breeding grounds for lattice defects, and these directly affect the minority carrier lifetimes and efficiencies of directionally grown crystals. Therefore, the study of the factors that affect the formation and development of grain boundaries is of great

importance in improving and optimizing the growth process. In this regard, the undercooling at the solidification interface groove of two different orientation grains acts as the main driving force for solidification and development of the grain boundary. This paper aims to study this development by in situ observation of the solidification process with simultaneous measurement of the temperature profile and undercooling. Adjacent silicon seeds of (100) and (100)+20° growth orientations were partially melted in an argon-rich environment before being directionally solidified. In situ visualization and temperature measurements were performed using an infrared microscope, whereas the crystallographic orientations were confirmed using electron backscatter diffraction analysis. Results from the in situ visualization of the solidification process prominently show the development of the groove along the bisector of the two silicon grains and its subsequent transformation. Electron backscatter diffraction analysis confirm the orientation of the seed crystals and the development direction of the grain boundary. Temperature profile measurements along the axis of growth demonstrate the expected consistency of the undercooling driving force to the interface development by showing its relationship with the measured interface growth speed. More interesting is the measurement of the negative temperature gradient inside the groove formed by the (111) facets of the (100) and (100)+20° silicon grains. The actual measurement of the theoretically conjectured cause of the increasing instability of the interface during directional growth provides information and insights on the exact effect of the undercooling to the ensuing grain competition between two different orientation seeds and the resulting grain boundary.

2:00 PM - 2:15 PM

**STEP-EDGE DIFFUSION BARRIERS STUDIED BY IN SITU
SURFACE X-RAY SCATTERING DURING OMVPE OF GAN**

G.B. Stephenson¹, G. Ju², D. Xu³, M..J. Highland¹, J.A. Eastman¹, P. Zapol¹, C. Thompson⁴

¹Argonne National Laboratory, IL, UNITED STATES OF AMERICA,

²Arizona State University, AZ, UNITED STATES OF AMERICA,

³Huazhong University of Science and Technology, CHINA, ⁴Northern Illinois University, IL, UNITED STATES OF AMERICA

On vicinal c-plane (001) surfaces of GaN, the ABAB stacking sequence results in steps that have alternating structures and properties, for a given step direction. This can explain the alternating terrace widths often observed on c-plane GaN surfaces. In particular, for low-energy steps lying in the (100) planes, the Ehrlich-Schwoebel (ES) step-edge barrier for diffusion is predicted to have alternately high and low values [1]. We have tested this prediction by performing in situ surface X-ray scattering during OMVPE growth of GaN. The observed (10L) and (01L) crystal truncation rods have different shapes, indicating that the alternating terrace widths are not equal. Furthermore, these shapes differ for various steady-state growth rates and conditions. By extracting the terrace width ratio during growth, we can infer the relative magnitudes of the ES barriers for the two types of steps. We will discuss the recent improvements to the experimental setup that has made these measurements possible, such as the use of micron-scale beams. [1] D. Xu, P. Zapol, G.B. Stephenson, and C. Thompson, J. Chem. Phys. 146, 144702 (2017).

2:15 PM - 2:45 PM

IN-SITU OPTICAL MICROSCOPIC OBSERVATION OF ICE CRYSTAL SURFACES

G. Sasaki, M. Inomata, K. Murata, K. Nagashima, J. Chen, Y. Furukawa

Institute of Low Temperature Science, Hokkaido University, JAPAN
Ice is one of the most abundant materials on the earth, and its phase transition governs a wide variety of phenomena, such as weather, environment-related issues, life in a cryosphere. Hence the molecular-level understanding of ice crystal surfaces is crucially important. However, an ice crystal is one of the materials on which the molecular-level in-situ observation is very difficult, since popular techniques, such as atomic force microscopy and electron microscopy, cannot be applied near the melting point. Hence, we developed advanced optical microscopy: laser confocal microscopy combined with differential interference contrast microscopy (LCM-DIM), which enables us to observe individual elementary steps on ice

crystal surfaces [1]. We first show the recent measurement of the growth kinetics of elementary steps on ice basal faces [2]. We measured the lateral growth rate of isolated elementary spiral steps under various supersaturation in a temperature range $-26.0 \leq T \leq -2.7^\circ\text{C}$. Then we determined the temperature dependence of the step kinetic coefficient β , for the first time. When $-6.2 \leq T \leq -2.7^\circ\text{C}$, the value of β decreased significantly with decreasing T . In contrast, when $-15.0 \leq T \leq -6.2^\circ\text{C}$, the value of β increased with decreasing T , and had the maximum at $T \sim -15^\circ\text{C}$. When $-26.0 \leq T \leq -15.0^\circ\text{C}$, the value of β decreased monotonically with decreasing T . Such complicated temperature dependence of β strongly implies the existence of unknown phenomena in the temperature range examined. We discuss the relation between the temperature dependence of β and disordered topmost layers recently found on ice basal faces by sum-frequency generation spectroscopy [3]. In addition, we also briefly show the following phenomena recently observed: macrosteps on water-ice interfaces, the interaction of atmospheric gasses with vapor-ice interfaces [4], and QLLs on vapor-polycrystalline ice thin film interfaces [5].

References [1] G. Sazaki, et al., *Proc. Nat. Acad. Sci. USA.*, **107**, 19702-19707 (2010). [2] M. Inomata, et al., *Crystal Growth & Design*, **18**, 786-793 (2018). [3] M.A. Sánchez, et al., *Proc. Natl. Acad. Sci.*, **114**, 227-232 (2017). [4] K. Nagashima, et al., *Crystal Growth & Design*, **18**, 4117-4122 (2018). [5] J. Chen, et al., *Crystal Growth & Design*, **19**, 116-124 (2019).

2:45 PM - 3:00 PM

IN SITU DIAGNOSTICS OF MELTING/SOLIDIFICATION AND SEGREGATION DURING CRYSTAL GROWTH PROVIDED BY ENERGY RESOLVED NEUTRON IMAGING

A.S. Tremsin¹, D. Perrodin², A.S. Losko³, S.C. Vogel³, A.M. Long³, T. Shinohara⁴, K. Oikawa⁴, T. Kai⁴, J.H. Peterson⁵, J.J. Derby⁵, W. Kockelamnn⁶, D.R. Onken², G.A. Bizarri², E.D. Bourret²

¹University of California at Berkeley, CA, UNITED STATES OF AMERICA, ²Lawrence Berkeley National Laboratory, CA, UNITED STATES OF AMERICA, ³Los Alamos National Laboratory, NM,

UNITED STATES OF AMERICA, ⁴Japan Atomic Energy Agency, JAPAN, ⁵University of Minnesota, MN, UNITED STATES OF AMERICA, ⁶Rutherford Appleton Laboratory, UNITED KINGDOM

Detection of gamma and neutron radiation in most devices relies on the conversion of incoming particles into either visible photons (e.g. by scintillators) or electrons (semiconductor devices). The efficiency of this conversion is determined by the characteristics of the converting material. Discovery of new materials for these applications, typically performed on powder or small crystal samples, needs to be followed by the growth of large single crystals. Uniformity of the crystals is critical as light scattering and charge trapping occurring at defects substantially degrade the performance of detection devices. It is the development of crystal growth recipes, which in many cases, becomes the most difficult, long and expensive part of novel material transition from the discovery phase into large scale production for detection devices. The trial and error approach frequently used in the past is very costly and time consuming as growth can take days to weeks. Inherently many crystal growth techniques do not allow direct measurements during the growth, such as in case of hygroscopic or highly reactive materials, which are usually grown in a vacuum-sealed container by the Bridgman-Stockbarger technique. Energy-resolved neutron imaging provides the means for in-situ diagnostics during crystal growth due to high penetration capability of neutrons. In this paper we present the results of our latest experiments where the location and the shape of the interface between the solid and liquid phases is optimized in a multi-zone Bridgman furnace. We also demonstrate how the speed of crystal growth can be optimized through neutron imaging, which also provides information on the elemental distribution in both liquid and solid phases and can even quantify the diffusion of some elements within and between these two phases.

Thursday, August 1, 2019

1:30 PM - 3:00 PM

Modeling of Crystal Growth Processes IV

Location: Crestone I, II

Session Chair(s): Simon Brandon, Moneesh Upmanyu

1:30 PM - 2:00 PM

SURFACE REHYBRIDIZATION AND STRAIN EFFECTS ON THE COMPOSITION AND THE PROPERTIES OF TERNARY III-NITRIDE ALLOYS.

L. Lymparakis, C. Freysoldt, J. Neugebauer

Max-Planck-Institut für Eisenforschung GmbH, GERMANY

The family of III-Nitride alloys - AlN, GaN, and InN - as well as their ternary solid solutions have revolutionized lighting as well as power electronics applications. However, the growth of high quality ternary alloys such as InGaN with high In content to achieve green emission, is challenging: The large lattice mismatch and strong differences in the formation enthalpies of the end constituents constitute the major challenge in the growth of these alloys as well as in exploiting their full potential. These have been proposed to considerably affect the thermodynamics of these alloys and result in limited In incorporation, spinodal decomposition and phase separation. Furthermore, surfaces play a dominant role on the properties of epitaxially grown materials. Efficient strain relaxation as well as different than bulk coordination at surfaces may shift the chemical potential of the species at the surfaces and result in composition pulling or surface segregation phenomena. Although these mechanisms and their effects have been investigated in details, the effect of surface rehybridization and reconstructions on the composition and the properties of semiconductor alloys have been scarcely investigated in the past. In the present work we investigate in details the atomistic mechanisms of rehybridization and surface reconstruction of ternary III-Nitride alloys. More specifically, the surfaces of InGaN as well as of B_{0.5}Ga_{0.5}N and B_{0.25}Al_{0.25}N are studied by employing DFT calculations. Our calculations reveal a novel mechanism, *elastically frustrated rehybridization*, that (i) results to surface geometries which contradicts our understanding of surface relaxations and reconstructions of compound semiconductors and (ii) plays a dominant role on the compositional limits of these alloys [1,2]. More specifically, the interplay between the two symmetry and rehybridization inequivalent cation sites at the 2×2 N adatom reconstruction, i.e. $\times 4$ coordinated and sp^3 hybridized vs $\times 3$

coordinated and sp^2 hybridized sites, results in strict upper limits of 25% for both In and B surface content as well as in thermally stable ordering induced at the surfaces during growth. Furthermore, the physics governing the above mentioned mechanisms as well as the interplay between surface and bulk thermodynamics and the effect of substrate strain on the compositional limits of these alloys will be discussed in details. [1] L. Lympirakis *et al.*, Phys. Rev. Materials **2**, 011601(R) (2018) [2] L. Lympirakis, AIP Advances **8**, 065301 (2018)

2:00 PM - 2:15 PM

AB INITIO ATOMISTIC THERMODYNAMICS OF HOT GAN SURFACES

P.T. Kempisty

Institute of High Pressure Physics PAS, POLAND

Surface thermodynamics is extremely important for epitaxially grown materials, but unfortunately some information are not straightforwardly accessible in typical growth experiments. Molecular structure of the surfaces can change in function of temperature, what makes it difficult to control the growth processes and the introduction of specific dopants or avoiding impurities. Therefore, theoretical studies are still needed to improve our knowledge and quantitative models. Methods for analyzing surface phenomena at the atomic level are desirable. In particular, density functional theory (DFT) calculations are very popular, but unfortunately this method describes the system at the temperature of absolute zero. Typical questions that fall when presenting the results of such calculations include interpretations and references to real growth processes occurring at high temperatures. I will show the methodology of thermodynamic analysis for a system representing the GaN surface in contact with the gas phase based on data derived from DFT calculations. In the standard approach, the effect of temperature is taken into account only in the chemical potential of the gas phase. An innovative element in the form of first principles phonon calculations will be introduced, which allow to determine several temperature-dependent surface properties. The results confirm that there are significant discrepancies in temperature dependencies of free energy between individual surfaces, especially when undissociated molecules or radicals are present on the surface.

Acknowledgements: This work was supported by the National Science Centre of Poland under grant no. 2017/27/B/ST3/01899

2:15 PM - 2:30 PM

ATOMIC SIMULATION OF CARBON SOLUBILITY IN LIQUID SILICON

J. Luo¹, A. Alateeqi², T. Sinno², L. Liu¹

¹School of Energy and Power Engineering, Xi'an Jiaotong University, CHINA, ²Department of Chemical and Biomolecular Engineering, University of Pennsylvania, PA, UNITED STATES OF AMERICA

The nucleation and growth of SiC precipitates in liquid silicon are technologically important processes in the solidification of multicrystalline silicon, and depend strongly on the supersaturation of carbon relative to the precipitate phase. Here, we investigate the question of whether existing empirical interatomic potentials for the Si-C binary system are useful for describing this process by computing the carbon solubility in liquid silicon relative to the bulk β -SiC phase. An important characteristic of the β -SiC/liquid Si system is that Si is both the solvent and a component of the solute. We employ a modification of a multi-step approach previously used for computing the solubility of halide salts in water ^[1]. In particular, we calculate the free energy of liquid Si-C mixtures as a function of composition, the carbon concentration in liquid Si-C as a function of Si and C chemical potential difference, and the free energy of bulk β -SiC. The calculations are repeated using several available empirical potentials, including multiple variants of the Tersoff potential ^[2-5] and the modified embedded atom method (MEAM) ^[6]. We also investigate carbon solubility associated with finite-sized β -SiC particles using large-scale molecular dynamics simulations and interpret the results in the context of the Ostwald-Freundlich model coupled with a Tolman correction to the inferred surface tension. We find that several potential models predict good to excellent agreement with published experimental measurements of carbon solubility ^[7]. However, this agreement is confined to temperatures at or near the Si melting point predicted by each of the potential models. Unfortunately, the majority of the potentials over-predict the Si melting temperature by up to 50%. By

analyzing the chemical potentials of crystalline and liquid Si predicted by each potential, we identify that the source of this problem likely arises from errors in the description of the liquid phase. [1] J. L. Aragones, E. Sanz and C. Vega, J. Chem. Phys. 136, 244508 (2012). [2] J. Tersoff, Phys. Rev. B 39, 5566 (1989). [3] J. Tersoff, Phys. Rev. B 49, 16349 (1994). [4] P. Erhart and K. Albe, Phys. Rev. B 71, 035211 (2005). [5] L. Pastewka, A. Klemenz, P. Gumbsch and M. Moseler, Phys. Rev. B 87, 205410 (2013). [6] M. Baskes, Phys. Rev. B 46, 2727 (1992). [7] F. Durand and J. Duby, J Phase. Equilib. 20, 61 (1999).

2:30 PM - 2:45 PM

THERMODYNAMICS OF VAPOR-SURFACE EQUILIBRIA IN *AB INITIO* MODELLING OF SEMICONDUCTOR GROWTH PROCESSES

S. Krukowski¹, P. Strak¹, P.T. Kempisty¹, Y. Kangawa², K. Sakowski¹

¹Institute of High Pressure Physics PAS, POLAND, ²RIAM, Kyushu Univ, JAPAN

Thermodynamic foundations of ab initio modeling of vapor-solid and vapor-surface equilibrium are presented. It is shown that the chemical potential change during vaporization process may be divided into enthalpy and entropy change during the process. Due to singular technical problem with the assessment of these two contributions: entropy which is singular at $T = 0\text{K}$ and the enthalpy which has to be calculated at this temperature, these two contribution have to be calculated using different paths. The entropy path avoids singular point at zero temperature overcoming solid-vapor transition at normal conditions, where standard evaporation entropy is calculated. The enthalpy path includes ab initio term at $T = 0\text{K}$. In addition, the thermal changes are calculated. The chemical potential difference contribution of the following terms: vaporization enthalpy, vaporization entropy, the temperature-entropy related change, the thermal enthalpy change and mechanical pressure is obtained. The latter term is negligibly small for the pressure typical for epitaxy. The thermal enthalpy change is two order smaller than the three first terms which have to be taken into account explicitly. The configurational vaporization entropy change is derived for adsorption processes. The same formulation is derived for

vapor-surface equilibrium using various vapors at GaN(0001) and AlN(0001) surfaces as examples. The critical factor is dependence of enthalpy of evaporation (desorption energy) on the pinning of Fermi level bringing drastic change of the adsorption energy value. In summary, a complete and exact formulation of vapor-solid and vapor-surface equilibria is presented [1]. [1] P. Kempisty, P. Strak, K. Sakowski, Y. Kangawa, S. Krukowski, *Phys. Chem. Chem. Phys.* **19** (2017) 29676

2:45 PM - 3:00 PM

FREE ENERGY OF SILICON CARBIDE PARTICLE NUCLEATION IN CARBON-CONTAINING SILICON MELTS

A. Alateeqi¹, J. Luo², L. Liu², T. Sinno¹

¹Department of Chemical and Biomolecular Engineering, University of Pennsylvania, PA, UNITED STATES OF AMERICA, ²Xi'an Jiaotong University, CHINA

Micron-scale silicon carbide (SiC) precipitates are known to detrimentally impact multi-crystalline silicon (mc-Si) ingots grown from the melt. Large precipitates can act as electron-hole recombination sites, lowering the efficiency of PV-cells [1]. They may also cause wire-sawing defects during ingot sawing, reducing yields [2]. Although the size and structure of SiC precipitates suggest that they form in molten silicon during the solidification process [3,4], the mechanism and conditions under which they form are still not well understood. Here we employ atomistic simulations based on several empirical interaction potentials to calculate the free energy of nucleation of crystalline precipitates in liquid silicon. The free energy calculations are based on a recently-developed biased sampling technique [5] that allows for efficient evaluation of nucleation free energy curves as a function of precipitate size. The nucleation of both β -SiC and pure Si crystallites in a liquid silicon system are studied as a function of undercooling and carbon impurity supersaturation in the liquid. The results are compared across different interaction potential models in order to generate a coherent view of the precipitation process. We also discuss the impact of the order parameter that is used to estimate precipitate size for a given set of atomic coordinates. Finally, we

describe preliminary investigations of heterogeneous nucleation of β -SiC precipitates on Si surfaces.

References: [1] Breitenstein, O., et al. (2007). "Material-induced shunts in multicrystalline silicon solar cells." *Semiconductors* **41**(4): 440-443. [2] G. Du, and N. Chen, P. Rossetto, On-wafer investigation of SiC and Si₃N₄ inclusions in multicrystalline Si grown by directional solidification, *Solar Energy Materials and Solar Cells* **92**(9), 1059 (2008). [3] Möller, H. J., et al. (2009), *Applied Physics A* **96**(1): 207-220 [4] A. Lotnyk, J. Bauer, O. Breitenstein, and H. Blumtritt, A TEM study of SiC particles and filaments precipitated in multicrystalline Si for solar cells. *Solar Energy Materials and Solar Cells* **92**(10), 1236 (2008). [5] E. Xi, S. Marks, S. Fialoke, and A. J. Patel, Sparse sampling of water density fluctuations near liquid-vapor coexistence, *Molecular Simulation* **44**:13-14, 1124 (2018).

Thursday, August 1, 2019

1:30 PM - 3:00 PM

Symposium on Epitaxy of Complex Oxides: Ruthenates

Location: Grays Peak II, III

Session Chair(s): Bharat Jalan

1:30 PM - 2:00 PM

EMERGENCE OF ROBUST 2D SKYRMIONS IN SRRUO₃

ULTRATHIN FILM

B. Kim¹, **B. Sohn**¹, **S.Y. Park**¹, **T.W. Noh**¹, **C. Kim**¹, **H.Y. Choi**², **J.Y. Moon**², **T. Choi**³, **Y.J. Choi**², **H. Zhou**⁴, **J.W. Choi**⁵, **S.H. Chang**³, **J.H. Han**⁶

¹Center for Correlated Electron Systems, Institute for Basic Science, KOREA, REPUBLIC OF, ²Department of Physics, Yonsei University, KOREA, REPUBLIC OF, ³Department of Physics, Chung-Ang University, KOREA, REPUBLIC OF, ⁴Advanced Photon Source, Argonne National Laboratory, UNITED STATES OF AMERICA, ⁵Center for Spintronics, Korea Institute of Science and Technology, KOREA, REPUBLIC OF, ⁶Department of Physics, Sungkyunkwan University, KOREA, REPUBLIC OF

Magnetic skyrmions have fast evolved from a novelty, as a realization of topologically protected structure with particle-like character, into a promising platform for new types of magnetic storage device. Recently, significant engineering progress was achieved in the synthesis of compounds hosting room-temperature skyrmions in metal based magnetic heterostructures, with the interfacial Dzyaloshinskii-Moriya interactions (DMI) conducive to the skyrmion formation. Here we report new findings of ultrathin skyrmion formation in a few layers of SrRuO₃ grown on top of SrTiO₃ substrate without the heavy-metal capping layer. Measurement of the topological Hall effect (THE) reveals a robust stability of skyrmions in this platform to the external magnetic field. Atomically precise structural analysis of the ultrathin film by the Coherent Bragg Rod Analysis (COBRA) method reveals the nontrivial atomic rumpling of the Ru-O lattice plane near to surface to be the source of inversion symmetry breaking and DMI. First-principles calculations based on the structure obtained from COBRA find significant magnetic anisotropy in the SrRuO₃ film to be the main source of skyrmion robustness. These features promise a few-layer SrRuO₃ to be an important platform for skyrmionics, without the necessity of introducing the capping layer to boost the spin-orbit coupling strength artificially

2:00 PM - 2:30 PM

REALIZATION OF HORIZONTAL AND VERTICAL INTERFACES IN RUTHENATE EPITAXIAL THIN FILMS

W.S. Choi

Oak Ridge National Laboratory, UNITED STATES OF AMERICA

An interface formed in transition metal oxide heterostructures often reveal extraordinary physical properties. A horizontal interface between dissimilar oxides promotes physics of quantum confinement, charge transfer, and dimensional crossover. A vertical interface between the same material, on the other hand, i.e., a grain boundary, also lets us examine intriguing physical behaviors related to the grain boundary scattering, local strain effect, and crystallographic orientation. In this presentation, we show the realization of horizontal and vertical interfaces in Ruthenates, using pulsed laser epitaxy. In the first part, we will discuss the dimensional crossover in oxide

superlattices with horizontal interfaces. A strongly coupled electronic and magnetic phases have been observed as reducing the dimension of SrRuO₃ (SRO) in SRO/SrTiO₃ (STO) superlattices (SLs). The alignment of O-2p bands across the SRO/STO interface lead to the absence of the charge transfer in this system, which prevails in most oxide heterostructures. The absence of the charge transfer across the interface enable us to explore an intrinsic dimensional crossover effect of SRO. The study suggests the realization of spin ordered quasi-2D hole liquid, demonstrating a close correlation among the electronic structure, transport properties, and magnetic ordering via atomically and electronically sharp oxide interface in SRO/STO SLs system. In the second part, we present epitaxial polycrystalline SRO thin films with vertical interfaces using atomically flat polycrystalline substrates. The existence of grain boundaries and mixed crystallographic orientation in epitaxial thin films influence the electronic and thermal transport behaviors, as well as the optical and magnetic properties. Based on the results, the advantage of using epitaxial polycrystalline thin film for combinatorial study will be highlighted.

2:30 PM - 2:45 PM

DEMYSTIFYING THE GROWTH OF SUPERCONDUCTING SR₂RUO₄ THIN FILMS

H.P. Nair¹, N.J. Schreiber¹, J. Ruf¹, L. Miao¹, M. Grandon¹, D. Baek¹, B.H. Goodge¹, L. Kourkoutis¹, K. Shen¹, D. Schlom²

¹Cornell University, NY, UNITED STATES OF AMERICA,

²Department of Materials Science and Engineering, Cornell University, UNITED STATES OF AMERICA

Sr₂RuO₄ is an unconventional superconductor with potentially a spin-triplet, odd-parity topologically nontrivial $p_x \pm ip_y$ superconducting ground state. There are many reports of high purity single crystals of Sr₂RuO₄ with a T_c of up to 1.5 K. To date, however, there are only four published reports of superconducting Sr₂RuO₄ thin films. The three others than ours have T_c s significantly below 1.5 K. This relative paucity of superconducting thin films is likely due to the extreme sensitivity of the odd-parity superconducting ground state in Sr₂RuO₄

to disorder. Thin films provide a pathway for scalability, which is critical for potential practical applications of spin-triplet superconductors such as qubits for ground-state quantum computing. Here, we outline and demonstrate a thermodynamic growth window to achieve repeatable growth of superconducting Sr_2RuO_4 with higher T_c , up to 1.8 K. This T_c is higher than all prior thin films and even higher than unstrained Sr_2RuO_4 single crystals.

2:45 PM - 3:00 PM

GROWTH OF HETEROSTRUCTURES OF FERROMAGNETIC SrRuO_3 AND SUPERCONDUCTING Sr_2RuO_4 BY MOLECULAR-BEAM EPITAXY

N.J. Schreiber¹, H.P. Nair¹, J. Ruf², L. Miao², M. Grandon¹, D.J. Baek³, B.H. Goodge⁴, L. Kourkoutis⁴, K. Shen², D. Schlom⁵

¹Department of Materials Science and Engineering, Cornell University, NY, UNITED STATES OF AMERICA, ²Department of Physics, Cornell University, NY, UNITED STATES OF AMERICA, ³School of Electrical and Computer Engineering, Cornell University, NY, UNITED STATES OF AMERICA, ⁴School of Applied and Engineering Physics, Cornell University, NY, UNITED STATES OF AMERICA, ⁵Department of Materials Science and Engineering, Cornell University, UNITED STATES OF AMERICA

Sr_2RuO_4 is an unconventional superconductor with a T_c of 1.5 K for unstrained single crystals, and has been proposed as a candidate material for quantum computation. Our group recently reported a thermodynamic growth window for reproducible growth of Sr_2RuO_4 thin films [1,2]. The capability to reproducibly grow these films opens up new avenues to elucidate the unconventional superconducting order parameter in Sr_2RuO_4 using heterostructures of Sr_2RuO_4 and ferromagnetic SrRuO_3 . Here, we will describe the growth of $\text{SrRuO}_3/\text{Sr}_2\text{RuO}_4$ heterostructures using molecular-beam epitaxy with a focus on achieving abrupt interfaces between the SrRuO_3 and superconducting Sr_2RuO_4 layers. In addition, we will present the results of the structural and electrical characterization of these

heterostructures. 1) H.P. Nair, Y. Liu, J.P. Ruf, N.J. Schreiber, S.-L. Shang, D.J. Baek, B.H. Goodge, L.F. Kourkoutis, Z.-K. Liu, K.M. Shen, and D.G. Schlom, *APL Mater.* **6**, 046101 (2018). 2) H.P. Nair, J.P. Ruf, N.J. Schreiber, L. Miao, M.L. Grandon, D.J. Baek, B.H. Goodge, J.P.C. Ruff, L.F. Kourkoutis, K.M. Shen, and D.G. Schlom, “Demystifying the Growth of Superconducting Sr_2RuO_4 Thin Films,” *APL Mater.* **6**, 101108 (2018).

Thursday, August 1, 2019

3:00 PM - 5:00 PM

Characterization Techniques for Bulk and Epitaxial Crystals III

Location: Crestone III, IV

Session Chair(s): Hideto Miyake, Motoaki Iwaya

3:00 PM - 3:30 PM

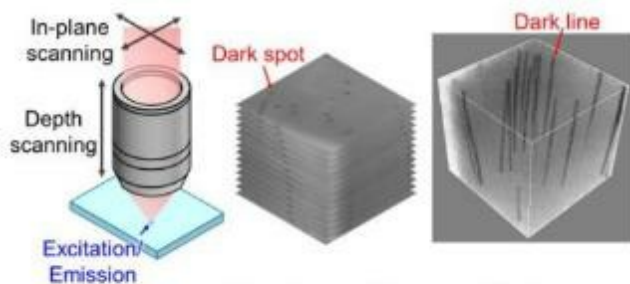
MULTIPHOTON-EXCITATION PHOTOLUMINESCENCE: NOVEL NONDESTRUCTIVE DEFECT CHARACTERIZATION TECHNOLOGY

T. Tanikawa¹, T. Matsuoka²

¹Osaka University, JAPAN, ²Institute for Materials Research, Tohoku University, JAPAN

Widegap semiconductors, GaN, SiC, Ga_2O_3 , and diamond, have attracted attention for high power devices with high power conversion efficiency. These materials often suffer from crystal defects, which often degrade the device performances. In order to avoid such “killer” defects, it is important to precisely characterize the properties of crystal defects. Recently we have proposed multiphoton-excitation photoluminescence (MPPL) as a novel technique for characterizing crystal defects without any destructive preparation. In this study, we demonstrate the nondestructive observation of threading dislocations in GaN crystals using the MPPL method. Relationship between three-dimensional surface feature during the selective area growth and propagation properties of threading dislocations is also characterized. Three-dimensional photoluminescence properties of GaN crystals

were measured using the MPPL method. Figure 1 shows schematic illustration of the MPPL system. An infrared femtosecond laser was focused into the inside of the crystal. MPPL occurs at the focal point. Near-band-edge emission and deep luminescence are corrected individually by dividing optical paths using optical filters. The focal point was scanned in in-plane direction and in-depth direction using a galvo scanner and stepping motor, respectively. Since dislocations act as nonradiative centers in GaN, they are visualized as dark spots and dark lines in 2D and 3D images as shown in Figs. 1(b) and 1(c), respectively. By comparing the intensity between near-band-edge emission and deep luminescence, relative distribution of point defects and/or impurities can be investigated. Concentrations of point defects are often influenced by the growth facets. Therefore three-dimensional feature during the selective area growth can also be characterized using the MPPL method. This technology can utilize as a nondestructive defect characterization method and it will enhance the epitaxial technology of novel materials with decreased defect density.



(a) MPPL mapping (b) Stacking of 2D frames (c) 3D MPPL image
 Fig. 1. Construction of three-dimensional imaging of threading dislocations.

3:30 PM - 3:45 PM

SHALLOW DONOR COMPLEXES IN ZNO CONTAINING SN AND LI STUDIED BY PHOTOLUMINESCENCE SPECTROSCOPY AND DENSITY FUNCTIONAL THEORY

A. Nakhband¹, M. Hegde¹, L.A. Boatner², S. Watkins¹

¹Department of Physics, Simon Fraser University, BC, CANADA, ²Oak Ridge National Laboratory (retired), TN, UNITED STATES OF AMERICA

Lithium has been investigated in detail as a possible acceptor impurity in zinc oxide for many years. Li interstitials are highly mobile in ZnO under Zn rich conditions and diffuse easily at temperatures as low as

300C. In contrast Li substituting for Zn sites is a known deep acceptor and is formed at much lower concentrations under O-rich conditions. [1]. The high mobility of Li ions means that the formation of defect pairs between Li and various oppositely charged impurities should be easily formed. Defect pairs have been proposed as possible candidates for p-doping in ZnO as well as for quantum qubits, and therefore the subject is of general technological interest. In this work we study the low temperature photoluminescence (PL) of high quality ZnO single crystals grown by chemical vapor transport, and co-doped with Sn and Li. A well known donor bound exciton PL feature labeled I_{10} has recently been shown to include Sn substituting for Zn sites.[2] In this study we show that an additional constituent, likely substitutional Li is also involved. Annealing Sn-doped samples under oxygen poor conditions results in a complete suppression of I_{10} , while diffusion of Li in air at $\sim 700\text{C}$ results in a clear enhancement of I_{10} . Density functional theory within the GGA+U approximation has been used to investigate the formation energy and defect transition energies of $\text{Sn}_{\text{Zn}}\text{-Li}_{\text{Zn}}$ nearest neighbour complexes in ZnO. These calculations indicate that the Sn-Li complex is indeed a shallow donor as expected on simple charge considerations. [1] K.E. Knutsen et al., J. Appl. Phys. 113, 023702 (2013) [2] J. Cullen et al., Appl. Phys. Lett. 102, 192110 (2013)

3:45 PM - 4:00 PM

EFFECT OF DOPING IN RARE EARTH ORTHOFERRITE SINGLE CRYSTALS

S.E. Saji¹, T. Chakraborty²

¹Indian Institute of science, INDIA, ²Indian Institute of Science, INDIA
Rare earth orthoferrites constituting the family of RFeO_3 have attracted great interest since they offer scope for fundamental research as well due to their potential for technological applications. These distorted perovskites generally crystallize in orthorhombic structure with $Pbnm$ space group and possess two inequivalent magnetic sub-lattices of partially filled 4f shell of R^{3+} and 3d shell of Fe^{3+} . This results in R–R, Fe–Fe, and R–Fe interactions among which the last one yields very interesting magnetic properties, such as spin

reorientation, spin switching or spin-flop, and magnetization reversal. Magnetization measurements on solid solutions of HoFeO_3 and DyFeO_3 reveal two spin reorientation transitions, $\Gamma_4 \rightarrow \Gamma_1$ and $\Gamma_1 \rightarrow \Gamma_2$ in the cooling cycle. Characteristics of twofold spin reorientation and evolution of magnetic states in $\text{Ho}_x\text{Dy}_{1-x}\text{FeO}_3$ are investigated in this work. Crystal growth was initiated in a four-mirror optical floating zone furnace using polycrystalline samples of $\text{Ho}_x\text{Dy}_{1-x}\text{FeO}_3$ prepared by solid state synthesis. Single crystals were grown in air and oxygen ambient and studied after orienting them using Orient Express program in the Laue back-reflection patterns. Magnetic measurements on oriented crystals revealed two spin reorientations of Fe^{3+} magnetic sublattice at temperatures, T_{sr1} and T_{sr2} . It is perceived that a large field is likely to disrupt the spin reorientation process. Measurements of isothermal magnetization along c-axis confirmed the occurrence of field-induced transitions of the type $\Gamma_1 \rightarrow \Gamma_4$ within the temperature window $T_{\text{sr1}} - T_{\text{sr2}}$.

Thursday, August 1, 2019

3:30 PM - 5:30 PM

Bulk Crystal Growth: Focus on Oxides

Location: Shavano Peak

Session Chair(s): Robert Kral, Jiaqiang Yan

3:30 PM - 3:45 PM

ADVANCES IN THE GROWTH OF $\alpha\text{-GeO}_2$ CRYSTALS BY TOP SEEDED SOLUTION GROWTH

A. Pena Revellez¹, J. Debray¹, D. Balitsky², P. Villeval², P. Armand³, P. Papet³, P. Segonds¹, B. Boulanger¹, B. Ménaert¹

¹Institut Néel - CNRS/UGA, FRANCE, ²Cristal Laser S.A., FRANCE, ³ICGM, FRANCE

Piezoelectric crystals showing a very high temperature sustaining capability are sought for applications in automotive, aerospace and energy industries. $\alpha\text{-GeO}_2$, which are isostructural to $\alpha\text{-SiO}_2$, crystallizes in the space group $P3_121$ or $P3_221$ and is one of the

promising piezoelectric materials, without Pb, to be used for high temperatures applications. Whereas the thermal stability of α -GeO₂ crystals grown by the hydrothermal method is limited to temperatures close to 100 °C, crystals grown by high temperature solutions are thermally stable up to 600 °C.^{1,2} Recently, bulk crystals of α -GeO₂ have been grown by the Top Seeded Solution Growth technique from the chemical system GeO₂-K₂Mo₄O₁₃.³ Even though, the quality of the obtained crystals was good, the system lacks of reproducibility, due to a bad solubilization of the solute (GeO₂) in the solvent (K₂Mo₄O₁₃), so its implementation is difficult. We have study the system GeO₂-K₂Mo₄O₁₃-K₆P₄O₁₃, which benefits from the high solubility of GeO₂ in phosphate solvents, achieving a perfect reproducibility of the process and the growth of bulk crystals with volumes up to 3.5 cm³.⁴ The volume of the obtained crystals and the improved quality, almost complete disappearance of Brazil twins, allowed us to cut and polish oriented slabs that have been used by two research groups to determine the piezoelectric properties at high temperature and the fabrication of a α -GeO₂ MEMS resonator. Nowadays the growth of bulk crystals with volumes > 3.5 cm³ is being done in Cristal Laser S.A.. The nonlinear optical properties of α -GeO₂, that is a positive uniaxial ($n_o < n_e$) crystal, are under study. Preliminary results on an oriented ($\theta = 70^\circ$) slab allow us to determine that phase matching condition of type I second harmonic generation is at $\lambda_\omega = 1.3 \mu\text{m}$. In order to determine the phase matching curves and the Sellmeier equations in the α -GeO₂ transparency range (0.2-6 μm) a cylinder shaped sample obtained from one of the grown α -GeO₂ crystals will be used. [1] D. V. Balitsky, V. S. Balitsky, Yu. V. Pisarevsky, O. Yu. Silvestrova, D. Yu. Pushcharovsky, *Ann. Chim. Sci. Mat*, **2001**, 26, 183. [2] A. Lignie, W. Zhou, P. Armand, B. Rufflé, R. Mayet, J. Debray, P. Hermet, B. Ménaert, P. Thomas, P. Papet, *ChemPhysChem*, **2014**, 15, 118. [3] A. Lignie, B. Ménaert, P. Armand, A. Peña, J. Debray, P. Papet, *Cryst. Growth. Des.*, **2013**, 13, 4220. [4] G. Baret, R. Madar, C. Bernard, *J. electrochem. Soc.*, **1991**, 138, 2830.

3:45 PM - 4:00 PM

FABRICATION OF SPRING SINGLE CRYSTALS USING MODIFIED MICRO-PULLING-DOWN METHOD WITH THREE-DIMENSIONAL CONTROL SYSTEM

Y. Yokota¹, T. Takasugi¹, Y. Ohashi¹, K. Inoue², M. Yoshino¹, A. Yamaji¹, H. Sato¹, S. Kurosawa¹, K. Kamada¹, A. Yoshikawa¹

¹Tohoku University, JAPAN, ²Piezo Studio Inc., JAPAN

A conventional micro-pulling-down (μ -PD) method can grow a single crystal from the melt using a crucible with a hole at the bottom. In addition, shape-controlled single crystals can be grown by the μ -PD method using a specialized crucible. However, only two-dimensional control of the grown single crystal can be achieved by the conventional μ -PD method because cross-sectional shape of the grown single crystal is controlled by shape of the bottom of the crucible. In this study, we developed a modified μ -PD method with a three-dimensional (3D) control system and this process was named as a three-dimensional-micro-pulling-down (3D- μ -PD) method [Fig.1(a)]. Spring-shaped sapphire single crystals could be grown by the 3D- μ -PD method using specialized molybdenum (Mo) crucibles. Then, spring-shaped sapphire single crystals were grown using various Mo crucibles with different shapes of the bottom and effects of the shape of the bottom on the growth stability and the shape-control of the spring-shaped single crystals were investigated. Spring-shaped sapphire single crystals with smaller helical pitch and larger helical radius could be obtained using a crucible with a sharp conical bottom compared to a crucible with a blunt conical bottom. Cross-sectional planes of spring-shaped sapphire single crystals grown using the crucible with the sharp conical bottom became an elliptical shape. On the other hand, a crucible with an inversed conical bottom could grow spring-shaped sapphire single crystals with smaller helical pitch compared to the crucibles with the conical bottom [Fig.1(b)]. Pole figure measurements using X-ray revealed that the crystal orientation of the spring-shaped sapphire single crystal was maintained during the crystal growth.

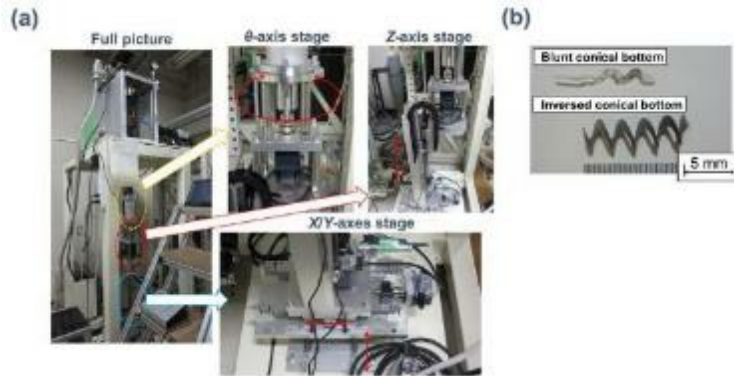


Fig.1 (a) Developed 3D- μ -PD furnace. (b) Spring-shaped sapphire single crystals grown using the crucibles with the blunt and incersed conical bottoms.

4:00 PM - 4:15 PM

ADDRESSING SURFACE DEFECTS IN EFG-GROWN SAPPHIRE SINGLE CRYSTALS

N. Stoddard¹, M. Seitz², M. Seitz²

¹II-VI Optical Systems, PA, UNITED STATES OF AMERICA, ²II-VI Optical Systems, CA, UNITED STATES OF AMERICA

Single crystal growth by the edge-defined film-fed growth method (EFG) has been commercially practiced for over 40 years. State of the art crystals can be over 300mm wide, 10mm thick and 1m long. In addition to well-known defects such as bubble inclusions and bulk structure loss, we describe a crystalline defect occurring uniquely at the outer surfaces of the sapphire panel. Termed 'surface crystals', they penetrate less than 1mm into the depth of the A-plane panel and can originate and terminate multiple times in a single panel. We demonstrate clear correlations with both temperature and ambient conditions and present micro-scale characterization to elucidate the nature of these defects.

4:15 PM - 4:30 PM

IMPACT OF THE CRYSTAL TECHNOLOGY AND SEED ON THE BUBBLES AND STRAIN DISTRIBUTION

R. Bouaita¹, G. Alombert-Goget¹, O. Benamara¹, A. Nehari², V. Motto-Ros¹, K. Lebbou¹

¹Univ Lyon, Université Claude Bernard Lyon 1, CNRS, Institut Lumière Matière, FRANCE, ²Commissariat à l'énergie atomique et aux énergies alternatives, Département des Technologies Solaires, Laboratoire des Matériaux et Procédés pour le Solaire, FRANCE

Sapphire is a material with exceptional mechanical, thermal and optical properties such a high tensile strength (400 MPa) and surface hardness (9 in the Mohs scale), a high thermal conductivity (few tens of $\text{W}\cdot\text{m}^{-1}\cdot\text{K}^{-1}$ at room temperature) and a wide range of transparency (0.24 – 4 μm) [1]. It is also extremely biocompatible [2]. With these properties, sapphire is used for various significant applications involving controlled shapes (medical, military, and laser). The production of sapphire single crystals in the particular geometries can be obtained by different growth shaping techniques [2-4]. In this work undoped single crystal sapphire rods ($\varphi=3\text{mm}$) were successfully grown by micro-pulling-down technique. Shaped sapphire single crystals almost always contain the microscopic and macroscopic defects such: bubbles of average diameter higher than 100 μm , micro-bubbles of diameter smaller than 10 μm , color centers, dislocations and mosaic [5,6]. These defects strongly affect the crystal fibers properties and decrease the optical and mechanical performances. The composition of this “micro-voids” was investigated by Laser-Induced Breakdown Spectroscopy measurements. In parallel, we studied the effect on the density and distribution of bubbles, as well as the internal strain generated in the sapphire crystal, of the seed (crystallographic orientation), the growth rate and the thermal gradient changes around the capillary die. The strain measured on rods and in bulk sapphire grown by Verneuil, Czochralski and μPD techniques are compared to confirms the effect of the crystal growth technique on the sapphire quality.

References: [1] V. Pishchik, L.A. Lytvynov, E.R. Dobrovinskaya, Sapphire, Springer US, Boston, MA, 2009. doi:10.1007/978-0-387-85695-7. [2] V.N. Kurlov, Sapphire: Properties, Growth, and Applications, *Encycl. Mater. Sci. Technol.* (2001) 8259–8264. doi:10.1016/B0-08-043152-6/01478-9 [3] F.A. Ponce, D.P. Bour, Nitride-based semiconductors for blue and green light-emitting devices, *Nature*. 386 (1997) 351–359. doi:10.1038/386351a0. [4] P.F. Moulton, Spectroscopic and laser characteristics of Ti : Al₂O₃, *J. Opt.*

Soc. Am. B. 3 (1986) 125–133. [5] E. a Ghezal, H. Li, A. Nehari, G. Alombert-Goget, A. Brenier, K. Lebbou, M.F. Joubert, M.T. Soltani, Effect of Pulling Rate on Bubbles Distribution in Sapphire Crystals Grown by the Micropulling Down (μ -PD) Technique, Cryst. Growth Des. 12 (2012) 4098–4103. doi:10.1021/cg300589h. [6] H. Li, E. a Ghezal, A. Nehari, G. Alombert-Goget, A. Brenier, K. Lebbou, Bubbles defects distribution in sapphire bulk crystals grown by Czochralski technique, Opt. Mater. (Amst). 35 (2013) 1071–1076. doi:10.1016/j.optmat.2012.12.022.

4:30 PM - 4:45 PM

GROWTH OF BaSnO_3 SINGLE CRYSTALS FOR WIDE BANDGAP APPLICATIONS

J. Kolis, R. Terry, C. Mcmillen

Clemson University, SC, UNITED STATES OF AMERICA

Barium stannate represents a unique opportunity among wide bandgap semiconductors and transparent conducting oxides. It is an ideal cubic perovskite with a relatively large lattice parameter (4.12\AA), is thermally stable and inert to air and water. It is a slightly indirect bandgap material with a band edge near 3.1eV . One significant advantage of the material is that the lowest valence bands are primarily constructed from s orbitals of tin atoms and are thus highly dispersed, making it potentially an excellent electrical conductor. It can be readily n-doped with La^{3+} ions so its conductivity can be increased to very high values ($>200\text{cm}^2/\text{v-sec}$) with very low electron effective mass ($<0.4m_e$) Thus the material can act like a high conductivity wide bandgap oxide with the enormous chemical flexibility of a typical perovskite. It is desirable to grow large single crystals of BaSnO_3 both for determination of bulk properties and as a substrate for devices by epitaxial growth of doped layers. As with most tetravalent tin oxides, a significant challenge to high quality single crystal growth lies in the fact that they are quite refractory, and usually melt only at very high temperatures (ca. $\geq 2000^\circ\text{C}$). At these temperatures the Sn^{4+} ion is unstable and tends to extrude oxygen, creating oxide lattice defects and lower valent tin defects. Flux growth has also demonstrated some promise but also has considerable limitations due to flux incorporation

and lattice defects. This lack of availability of barium stannate single crystal substrates also means that most epitaxial work employs heteroepitaxial substrates with either significant lattice mismatch like SrTiO₃, or exotic, poorly available materials like PrScO₃. We found that a high temperature hydrothermal approach is suitable for the growth of high quality BaSnO₃ single crystals. In aqueous phases at 680°C and 200MPa, large single crystals of BaSnO₃ can be grown using simple feedstocks and CsOH mineralizer. The sealed conditions and relatively low temperatures lead to very high quality single crystals with few lattice defects. Details of the crystal growth will be discussed. A number of bulk properties have been measured for these crystals and will be reported here. The crystals have been polished for use in preliminary epitaxial device work. In addition a series of doped single crystals have been grown of formula La_xBa_(1-x)SnO₃ (x = 0.03), and properties of these materials will also be presented.

4:45 PM - 5:00 PM

MECHANICAL PROPERTIES AND DISLOCATIONS NUMERICAL MODELING FOR Li₂MOO₄ CRYSTAL GROWTH

A. Ahmine¹, M. Velazquez¹, H. Cabane², C. Josserond¹, G. Kapelski¹, H. Roussel³, P. Veber⁴, M. Dumortier², P. De Marcillac⁵, A. Giuliani⁵, T. Duffar¹

¹SIMaP UMR 5266 CNRS-UGA-G INP, FRANCE, ²Cristal Innov, FRANCE, ³Univ. Grenoble Alpes, CNRS, Grenoble INP, LMGP, FRANCE, ⁴Institut Lumière Matière UMR 5306, FRANCE, ⁵CSNSM, Univ. Paris-Sud, CNRS/IN2P3, Université Paris-Saclay, FRANCE

Heat scintillation cryogenic bolometers (HSCBs), the core of which is made of bulk single crystals, turn out to be very sensitive tools for the search and detection of rare events in astro-particle physics. Large Li₂MoO₄ single crystals of good radio purity levels are excellent candidates to build such detectors. We have successfully grown Li₂MoO₄ single crystals up to 820 g by the Czochralski method. Some of these crystals have been machined to build HSCB for detection of neutrinoless double-beta decay events. During cutting of one crystal crack occurred, likely to be due to residual stresses in the crystal. This

fracture proved to affect dramatically the performances of the HSCB built from the crystal, especially in terms of energy resolution. Our goal is to understand and control the generation of dislocations and then residual stresses within Li_2MoO_4 crystals during their growth and subsequent cooling. Temperature and thermal stress fields at different growth stages were obtained by pseudo-stationary calculations. These results allowed calculating the dislocation density distribution using a self-developed simulation based on Alexander and Haasen model. All numerical computations are performed with Comsol Multiphysics®. Direct measurements have been performed, at several temperatures, of the compressive critical shear stress of Li_2MoO_4 single crystals, under appropriate crystallographic orientations for single slip. This allowed determining the different parameters of the model.

5:00 PM - 5:15 PM

GROWTH OF HIGH QUALITY $\text{Li}_2\text{B}_4\text{O}_7$ SINGLE CRYSTALS: CORE DEFECT FORMATION REVISITED

J.L. Plaza

Universidad Autonoma de Madrid, SPAIN

Lithium tetraborate is a well known piezoelectric crystal with a wide variety of applications in the field of Surface Acoustic Wave (SAW) devices and also as a strong candidate for the fabrication of high performance personal dosimetry systems [1]. However, it is well known the tendency of this crystal to form a central core which greatly affects to its physical properties. Although this issue has been studied four decades ago [2], it seems that some issues regarding to the core formation in lithium tetraborate crystals still remain to be understood. In this work we analyse the effect of the thermal gradient and some other parameters like rotation speed and growth rate on the core formation in order to ascertain the best growth conditions to obtain high quality single $\text{Li}_2\text{B}_4\text{O}_7$ crystals. Several lithium tetraborate crystals have been grown by standard Czochralski technique and the formation of the core region has been analysed by using techniques like Scanning Electron Microscopy (SEM), Electric Force Microscopy (EFM), X Ray Diffraction (XRD) and optical absorption. Resistivity mappings from core-free and core-containing wafers from Electroless

resistivity measurements (COREMA) give also an interesting overall record of the defective regions inside the crystals. [1] G. D. Patra, S.G.Singh, A.K.Singh, M.Tyagi, D.G.Desai,B.Tiwari, S.Sen, S.C. Gadkari, Journal of Luminescence 157 (2015) 333–337. [2] D.S. Robertson, I. M. Young, J. Mat Sci 17 (1982) 1729-1738.

Thursday, August 1, 2019

3:30 PM - 5:30 PM

Fundamentals of Crystal Growth: Crystallization from Melt

Location: Crestone I, II

Session Chair(s): Baron Peters, Jim Deyoreo

3:30 PM - 4:00 PM

CRYSTAL GROWTH OF QUASICRYSTALS

A. Tsai

Institute of Multidisciplinary Research for Advanced Materials, Tohoku University, JAPAN

Crystal Growth of Quasicrystals

Quasicrystals reveal diffraction patterns with symmetries forbidden in crystallography, and quasi-periodicity, have been found to be stable phases in several alloy systems. Thanks to their stability, one can grow single grained quasicrystals with large scale by means of traditional crystal-growth techniques. Consequently, single grains of quasicrystals with highly-ordered structure and grain sizes efficient for studying their surfaces, neutron scattering and structures. Single grains of quasicrystals have been successfully grown by various techniques recently. In the talk, we will firstly brief introduction of the structure for quasicrystal and then describe growth mechanisms of quasicrystals in terms of their atomic structures.

4:00 PM - 4:15 PM

CAPILLARY-MEDIATED INTERFACE FIELDS

M.E. Glicksman¹, K. Ankit²

¹Florida Institute of Technology, FL, UNITED STATES OF AMERICA,

²Arizona State University, UNITED STATES OF AMERICA

We determined that solid-melt microstructures formed during crystal growth support capillary-mediated fields that redistribute small rates of thermal energy along curved interfaces. These scalar energy fields locally modulate an interface's mean motion, and auto-stimulate pattern evolution at spatial scales from 10 nm up to several millimeters. The presence of these capillary-mediated energy fields was originally predicted by application of the Leibniz-Reynolds transport theorem, which imposes *omnimetric* energy conservation, i.e., accounts for higher-order energy balances at *all* continuum length scales on crystal-melt interfaces. Surprisingly, the standard conservation paradigm used in crystal growth- viz. the Stefan balance- for satisfying interfacial energy/solute conservation, excludes capillarity, and thereby fails to provide the desired energy/mass balance at shorter length scales. Stefan balances provide net growth speeds and overall transformation rates, and, consequently, do not identify the cause of pattern formation during unstable crystal growth. As a result, selective amplification of noise, proposed over 40 years ago, is accepted as the microscopic physics accounting for interfacial pattern formation in both natural crystal growth and technical crystallization processes.

Capillary energy fields on curved crystal-melt interfaces were recently measured using phase-field simulation of grain boundary grooves constrained by a thermal gradient. The presence of capillary energy fields introduces a small non-linear component in the interface thermo-potential that are related to small thermal fluxes on the interface from gradients in the Gibbs-Thomson interface temperature. By subtracting the applied gradient's linear potential distribution from the measured interfacial thermo-potential produced a "residual" that is proportional to the capillary-mediated energy rate. The distribution of interface residuals was measured for a variety of stationary grain boundary grooves to an accuracy of ± 5 ppm using multiphase-field simulation. Capillary fields so revealed confirm quantitatively prior analytic predictions of persistent capillary "bias fields" on grain boundary grooves derived from sharp-interface thermodynamics. Phase-field simulations and post-processing measurements provide the first independent quantitative support for the presence of predicted

capillary-mediated fields along solid-liquid interfaces. These results, initially prompted by crystal shape changes observed experimentally in microgravity, help answer a long-standing question in crystal growth science: *What is the fundamental mechanism that stimulates interface pattern formation, and provides a possible pathway to improve microstructure-/level interface control?*

4:15 PM - 4:30 PM

INVESTIGATION OF SOLUTO-CAPILLARY CONVECTION IN $\text{Ge}_x\text{Si}_{1-x}$ MELTS

J.P. Wöhrle¹, T. Jauss², A. Cröll³, T. Sorgenfrei²

¹Crystallography - Albert-Ludwigs-University Freiburg, GERMANY,

²University of Freiburg, GERMANY, ³University of Alabama in Huntsville, AL, UNITED STATES OF AMERICA

The requirements for industrial semiconductor materials used for device applications are constantly rising – one example is the upcoming development of the 5G mobile network technology and the following advancement of autonomous driving. To solve the technical obstacles, a profound comprehension of the respective material systems is required. Especially in mixed systems, additional challenges concerning the homogeneity of the grown material are rising due to varying properties of the different chemical composition of the components, such as germanium and silicon.

$\text{Ge}_x\text{Si}_{1-x}$ is an elemental semiconductor material which is extremely attractive for various applications like thermoelectrics, microelectronics, photovoltaic, or various functional applications due to its lattice constant and band gap tuning based on the composition. A major challenge in growing high quality $\text{Ge}_x\text{Si}_{1-x}$ bulk crystals from melt, is the fact that the surface tension of Si is 30% higher than Ge, but on the other hand the density is only half as large. Due to the large segregation coefficient of Si in Ge of $k_0 \leq 5$, germanium is enriched in front of the solid/liquid interface, which leads to a strong soluto-capillary convection and solutal buoyancy convection. It is shown that this specific type of convection is significantly influencing the shape of the solid-liquid interface and consequently the complete growth process, if a growth technique with free melt surfaces is used (e.g.

Float-Zone, detached Bridgman, etc.). Therefore, a deeper understanding of the influence of convection flux and capillary phenomena on the resulting crystal quality is needed. Under normal gravity conditions on earth (1g), it is not possible to investigate the effect of the buoyancy force and different surface-tension-driven convections separately on the crystal growth process – in microgravity (μg) the influence of density-driven convection is suppressed. Experiments under μg conditions provide the possibility to investigate the flow behavior directly on and in the liquid phase without the disturbing impact of the buoyancy convection. Therefore, we use parabolic flight experiments which provide several μg phases up to 22 seconds, where we can quantitatively and qualitatively determine the effect of soluto-capillary convection in the Ge-Si system by analyzing the movement of small tracer particles on the melt surface during solidification of several Ge_xSi_{1-x} mixtures (3-35 at% Si) inside a double ellipsoid mirror furnace. A current view on the results of the parabolic flight campaigns of the last years will be presented.

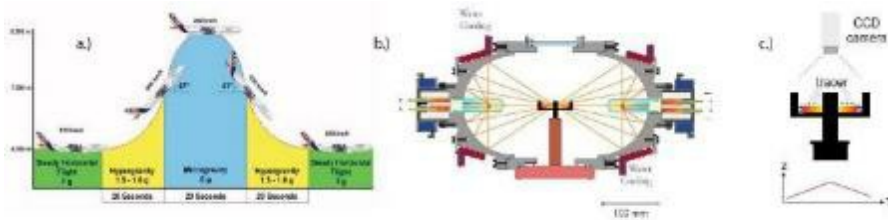


Figure 1: Schematic draw of a.) the gravity phases during a parabolic flight (image by Novespace), b.) used double ellipsoid furnace, c.) crucible, melt, tracer, and high-speed CCD camera and the supposed temperature gradient.

4:30 PM - 4:45 PM

ANALYSIS AND IN-SITU OBSERVATION OF SOLID-STATE DIFFUSION IN MELT CRYSTAL GROWTH

K. Wang¹, J.H. Peterson², A.S. Tremsin³, D. Perrodin⁴, A.S. Losko², S.C. Vogel², T. Shinohara⁵, K. Oikawa⁵, G.A. Bizarri⁴, E.D. Bourret⁴, J.J. Derby¹

¹University of Minnesota, MN, UNITED STATES OF AMERICA, ²Los Alamos National Laboratory, NM, UNITED STATES OF AMERICA,

³University of California, CA, UNITED STATES OF AMERICA,

⁴Lawrence Berkeley National Laboratory, CA, UNITED STATES OF

AMERICA, ⁵Japan Atomic Energy Agency, JAPAN

Understanding diffusion in the solid state is very important for many high-temperature crystal growth systems. For example, the final distribution of dopants and impurities in melt-grown crystals is often significantly affected by solid-state diffusion acting on inhomogeneous fields arising from segregation during growth. However, analyses of these effects are typically quite challenging, since values for solid-state diffusion coefficients are rarely known with a high degree of confidence and their direct measurement is arduous, typically requiring extensive and destructive measurements of concentration profiles in samples from diffusion couple experiments. We discuss a novel and exciting approach to directly measure solid-state diffusion in real time using neutron imaging of a vertical gradient freeze crystal growth system. Energy-resolved neutron imaging is employed for in-situ observation of europium (Eu) diffusion in a mixed halide scintillator crystal, barium bromo-chloride or BaBrCl. The unique capability of neutron imaging to quantitatively map elemental concentration with 0.1-0.2 mm spatial resolution is used to study the dynamics of Eu migration across the solid-liquid interface and its diffusion within the solid material. We mathematically model the transient evolution of the initial dopant profile in this system using a coupled system of one-dimensional diffusion equations and discuss their analytical solution via finite Fourier transform techniques. This analytical solution to the transient concentration profile is then used to estimate both solid-state and liquid diffusion coefficients. Results for high-temperature Eu diffusion in the BaBrCl system will be presented, and the application of this approach to other systems will be discussed.

4:45 PM - 5:00 PM

THE EFFECT OF GRAIN BOUNDARIES ON INSTABILITY AT THE CRYSTALMELT INTERFACE DURING THE UNIDIRECTIONAL GROWTH OF SI

K. Hu¹, K. Maeda², K. Shiga³, H. Morito⁴, K. Fujiwara⁴

¹Institute for Material Research, JAPAN, ²Institute for materials research, Tohoku university, JAPAN, ³Institute for Materials Research,

JAPAN, ⁴Institute for Materials Research, Tohoku University, JAPAN

The morphology of the crystal/melt interface has been found to be an important part of both monocrystalline and multicrystalline Si ingots during unidirectional growth because of its strong effects on impurity segregation and defect formation [1, 2]. Recently, our own group study the instability at a planar crystal/melt interface during the solidification of single crystal Si using an in situ observation system [3]. It was found that wavy perturbations at interface were amplified in conjunction with the formation of a negative temperature gradient leading to a morphological transformation from a planar interface to a zig-zag faceted interface. However, the role of grain boundaries during the morphological transformation is still not fully understood, even though a significant number of grain boundaries can be formed during the solidification of multicrystalline Si. An in situ observation system consisting of a furnace and microscope was used to investigate the instability of crystal/melt interfaces including frequent $\Sigma 3$, small-angle and large-angle grain boundaries during the unidirectional growth of Si. After solidification, the resulting video recording was analyzed using image processing software and grain-boundary characterization was performed using Electron backscattering diffraction (EBSD) measurement. Planar crystal/melt interfaces including $\Sigma 3$ or small-angle grain boundaries were found to undergo local morphological transformation at the grain-boundary positions during high-velocity progression of interface. The observations also confirmed that the critical growth velocity for the appearance of instability at a crystal/melt interface including grain boundaries is significantly lower than that for a single crystal Si/melt interface. In contrast, crystal/melt interfaces including large-angle grain boundaries formed faceted-faceted grooves at a low growth velocity, and no significant morphological changes were found at a high growth velocity. These results are due to the formation of two $\{111\}$ facets in an atomically planar interface at the LAGB position. We calculate the ambient thermal field at the crystal/melt interfaces including grain boundaries and discuss the mechanisms associated with the observed morphological transformation at grain-boundary positions. We propose that the local negative temperature gradients at grain-boundary positions as a result of the reduced thermal

conductivity are the primary reason for the observed morphological transitions at crystal/melt interfaces incorporating grain boundaries. [1] T. Duffar, A. Nadri, *Scr. Mater.* 62 (2010) 955–960. [2] R. Gotoh et al, *Appl. Phys. Lett.* 100 (2012) 021903. [3] K. Fujiwara et al, *Acta Mater.* 59 (2011) 4700–4708.

5:00 PM - 5:15 PM

TWIN BOUNDARY FORMATION DEPENDING ON CRYSTAL/LIQUID INTERFACE MORPHOLOGY IN LITHIUM TETRABORATE

K. Maeda, K. Fujiwara, S. Uda

Institute for Materials Research, JAPAN

We succeed in observation the crystal/liquid interface behavior during unidirectional melt growth of twinned lithium tetraborate ($\text{Li}_2\text{B}_4\text{O}_7$; LB4) crystal. LB4 is a vacuum-UV transparent nonlinear optical crystal and non-ferroelectric. A poling method for ferroelectrics cannot apply to this, however twinning in this crystal accompanies the reverse of the c-axis and the sign of the nonlinear optical coefficient. Periodically twinned LB4 can function as a quasi-phase-matching device like in ferroelectrics, and we developed a method for the formation of periodically twinned crystal. The twin boundary (TB) orientations were dependent on the crystal growth direction. (100) TB forms when the growth direction is around $\langle 010 \rangle$. In contract, (010) TB forms when the growth direction is around $\langle 100 \rangle$. The TB direction can be controlled by temperature distribution around crystal/liquid interface. In the case of melt growth, the morphology of crystal/liquid planer interface changes to zigzag faceted planes and/or cellular structure by latent heat and segregated impurities. In this study, we clarified the TB formation depending on crystal/liquid interface morphology on LB4 melt growth. When the growth rate was zero or small, a straight crystal/liquid interface formed parallel to the isothermal line, and TB orientation in the grown crystal was $\{100\}$. On the other hand, crystal/liquid interface changed to zigzag shape, that formed by (100) and (010) faceted planes, when the growth rate increased as shown in Fig.1. Formed twin boundaries were perpendicular to the facet growth plane. Therefore, twin boundaries must reach to the re-entrant corner of zigzag interface. Then $\{110\}$ twin boundaries formed

between the (100) and (010) facet grown areas.

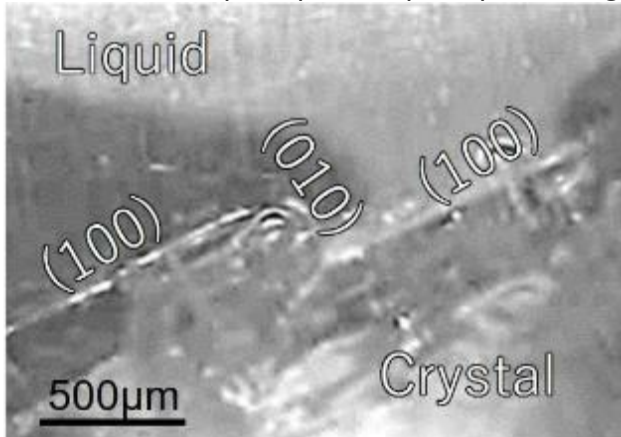


Fig. 1 Facetted crystal/liquid interface of $\text{Li}_2\text{B}_4\text{O}_7$ melt growth.

5:15 PM - 5:30 PM

COHERENT NANOPRECIPITATES WITHIN SINGLE CRYSTALS: FROM CHARACTERIZATION TO UNRAVELING THE MECHANISM OF FORMATION

B. Pokroy

Technion Institute of Technology, ISRAEL

We recently discovered a unique biostrategy for strengthening and toughening brittle crystals of calcite [1]. Our studies on the atomic- and nano-structure of the mineralized lenses of the brittle star *Ophiocoma wendtii* revealed the presence of metastable coherent nanoprecipitates that induce compressive stress on the crystal. Although the final nanostructure is akin to the Guinier–Preston (GP) zones well known in classical metallurgy the brittle star achieves this nanostructure via a completely novel mechanism, in which crystals are formed at ambient conditions from a supersaturated amorphous precursor having coherently aligned nanoprecipitates and coherently alternating stress and elastic modulus layers. This induces compressive stress, which strengthens and toughens the mineralized tissue. In this talk I will present our study on the characterization of such crystals utilizing state-of-the-art techniques and will discuss possible mechanisms of their formation both in biological and synthetic systems. [1] I. Polishchuk I et al. *Science*. 358 1294 (2017)

Thursday, August 1, 2019

3:30 PM - 6:30 PM

In Situ Observation and Characterization III

Location: Grays Peak I

Session Chair(s): Tsukamoto Katsuo

3:30 PM - 3:45 PM

IN SITU OBSERVATION OF CRYSTALLIZATION OF A SALT USING AN ANTISOLVENT BY TRANSMISSION ELECTRON MICROSCOPY

T. Yamazaki, Y. Kimura

Institute of Low Temperature Science, Hokkaido University, JAPAN

In situ observation of crystallization is one of the important methods for understanding the process. Recent advancements of in situ observation using transmission electron microscopy (TEM) combined with a liquid cell is gradually unveiling the primary step of crystallization which is called nucleation. The observations revealed that the classical and non-classical nucleation pathways are co-existing in the calcium carbonate system and the amorphous phases appeared on the route of nucleation of crystalline phases. Thus, this method is promising to develop our further understanding of nucleation and accompanying crystallization phenomena. The difficulty of in situ TEM studies of nucleation is the small observable area; therefore, capturing a moment of nucleation requires a lot of attempts with great patience. In order to overcome this problem, supersaturation should be controlled and increased actively while the process is monitored. Here, we try to use an anti-solvent for a sample solute for increasing a supersaturation during in situ observation and enhance nucleation rates in the liquid cell TEM. We used the TEM holder which can enclose the liquid cell and has the injection ports for solutions. We enclosed sodium chlorate and acetone solutions in the liquid cell and the injection port, respectively. The two solutions were mixed while the solution in the liquid cell was observed by TEM with a field-emission gun at an acceleration voltage of 200 keV. Immediately after mixing the solutions, we could not observe any crystallization event. However, after a short time, the crystallization events were observed when the sample was irradiated by the electron beam. The observed crystal was dendritic-shaped, indicating that the

supersaturation was high. In this presentation, the detailed results of observation which include analysis of the nucleated crystal and mechanisms of the crystallization will be discussed.

3:45 PM - 4:00 PM

MANIPULATION OF ACETAMINOPHEN CRYSTALLIZATION AND DISCOVERY OF TWO-STEP DISSOLUTION PROCESS BY PLASMONIC OPTICAL TWEEZERS

H. Niinomi¹, T. Sugiyama², M. Tagawa³, T. Ujihara³, K. Miyamoto⁴, T. Omatsu⁴, J. Nozawa¹, J. Okada¹, S. Uda¹

¹Institute for Materials Research, Tohoku University, JAPAN,

²Department of Applied Chemistry, National Chiao Tung University,

TAIWAN, ³Institute of Materials and Systems for Sustainability

(IMaSS), JAPAN, ⁴Graduate School of Engineering, Chiba University, JAPAN

Complete spatiotemporal control of crystallization from a solution impacts on detailed exploration on dynamics of early stage of crystallization because the stochastic nature of nucleation hinders us to chase its early stage. Tremendous efforts have been recently devoted to control crystallization by trapping molecular clusters in a solution with optical tweezers using laser focused by an optical lens. This strategy has actually achieved to induce forced crystallization of organic molecules from the focal spot even from an unsaturated solution. Although recent progress in nanoscience including research on nucleation dynamics demands to tightly manipulate nanoscopic objects, required enhancement of trapping force is intrinsically limited by the diffraction limit because the force strength is proportional to the gradient of the square of electrical field generated by light focusing. To overcome this limitation, here we applied near-field generated by the excitation of surface plasmon resonance (SPR) on metal nanostructures because its nanoscopically confined field is equivalent to focused light beyond the diffraction limit. Au gammadion nanolattice was fabricated on a cover glass by electron beam lithography (Figure 1). An aqueous solution of acetaminophen, as a model compound, saturated at room temperature (24°C) was dropped on the nanolattice, and then solution thin layer was formed on the nanolattice by

capillarity. Continuous-wave left-handed circularly polarized laser ($\lambda = 1064 \text{ nm}$, $6.4 \times 10^9 \text{ W/m}^2$) was focused to the nanolattice supporting the solution thin layer by passing through an objective lens equipped on an inverted polarized-light microscope. In-situ microscopic observation was performed simultaneously with the laser irradiation. After the laser irradiation, crystals with the size of around 1000 nm were precipitated $19 \mu\text{m}$ away from the focal spot in annular pattern (Figure 2). The position of the annular pattern moved while following the change of in-plane position of the focal spot via dissolution/precipitation process, indicating that position of the crystallization is manipulatable. When the plasmon excitation was stopped, the crystals were disappeared via two-step dissolution process; the crystals first transformed to liquid droplets, and then the droplet disappeared through molecular diffusion. Generally, large temperature gradient generates when SPR was excited because of heat generation through electron-phonon scattering, resulting that thermophoretic force outward from the focal spot is exerted on the molecules whereas the electrical field gradient force attracts them. The annular-patterned precipitation can be interpreted as the consequence of the balance between the two forces. Therefore, our observation strongly suggested that plasmonic optical tweezers can precisely “manipulate” crystallization.

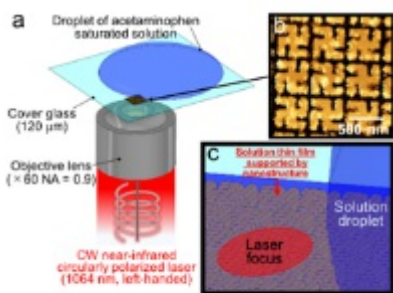


Figure 1 a schematic illustration of the experimental setup b atomic force microscopic image of the plasmonic Au nanolattice c the position of the laser focus.

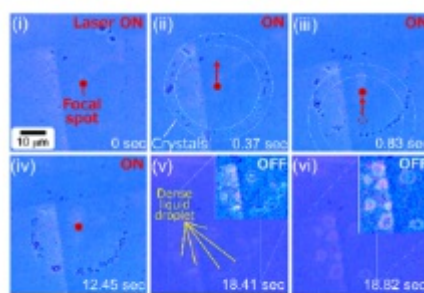


Figure 2 time-lapse micrographs showing the dynamics of the plasmonic trapping-induced crystallization and the two-step dissolution process.

4:00 PM - 4:15 PM

IN-SITU OBSERVATION OF PHASE TRANSITION OF ASPIRIN FORM II

Y. Tsuru¹, M. Maruyama¹, H.Y. Yoshikawa², S. Okada³, H. Adachi³, K. Takano⁴, K. Tsukamoto⁵, M. Imanishi¹, M. Yoshimura⁶, Y. Mori¹

¹Graduate School of Engineering, Osaka University, JAPAN,
²Department of Chemistry, Saitama University, JAPAN, ³SOSHO Inc., JAPAN, ⁴Graduate School of Life and Environmental Science, Kyoto Prefectural University, JAPAN, ⁵Graduate School of Science, Tohoku University, JAPAN, ⁶Institute of Laser Engineering, Osaka University, JAPAN

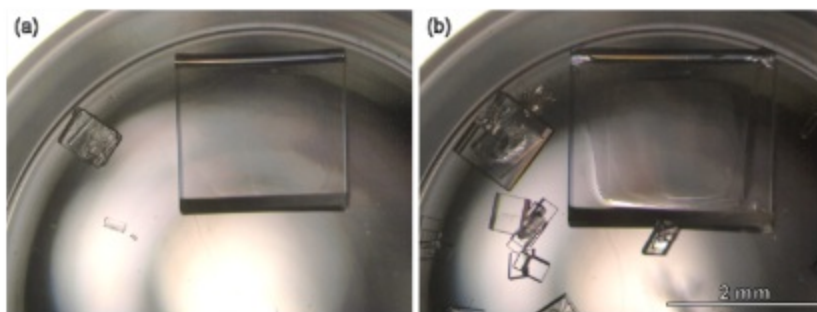


Fig. 1 Optical microscope images showing the phase transformation. (a) was taken immediately after adding form I and (b) was taken after 18 minutes.

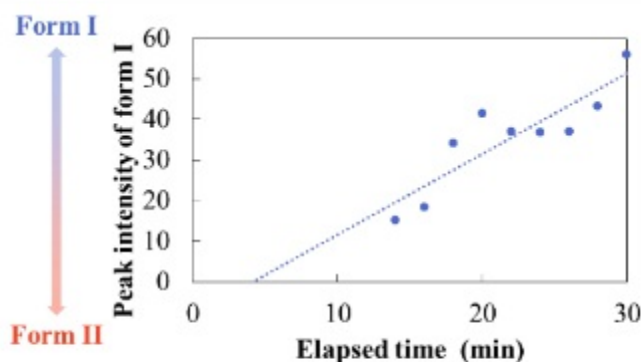


Fig. 2 Change of the peak intensity of form I.

In pharmaceutical industry, polymorph screening and control are very important issues. In a previous study, we have developed laser-induced crystallization technique.¹⁾ In order to apply this technique to crystallization of polymorphs of various compound, we used aspirin as a challenging material. Aspirin has form II (metastable phase), in which the molecular arrangement resemble form I (stable phase). Therefore, intergrown crystals are often obtained, and crystallization of a pure form II is difficult.²⁾ In this study, we selectively crystallized form II by laser irradiation and observed phase transformation of the

obtained pure form II. Furthermore, we investigated phase transformation of the initial stage of the crystal growth by in-situ observation. Solution of aspirin (form I) in acetonitrile were prepared (91.8-95.6 mg/mL) and dispensed into glass vials. They were cooled to 25°C (degree of supersaturation $\sigma=0.18-0.23$). After confirming the absence of spontaneous crystallization, laser pulses ($\tau=250$ fs, $\lambda=800$ nm, 1 kHz) were irradiated into the solutions. With 30 s irradiation with energy of 30 $\mu\text{J}/\text{pulse}$, many crystals, mixture of form I and form II, were obtained. With irradiation of 1.5 $\mu\text{J}/\text{pulse}$ for 0.5 s, a pure form II crystal was obtained. The crystal was stable more than 1 day. After that, we induced phase transformation under a micro-scope by adding form I into the saturated solution including the pure form II. The form II crystal surface became rough, and then form I grew on the form II (Fig. 1). This result indicates that even if form II nucleates, form I easily covers the form II, and finally form II transforms into form I. Therefore, we investigated a crystal form of the initial stage of the growth by Raman spectroscopy. Crystals were grown with adding microcrystals into supersaturated solution prepared as above. We chose one of the crystals and measured the Raman spectrum of the crystal every 2 min, the intensity of the characteristic peak of form I, which appears 290 cm^{-1} , rose (Fig. 2). This result suggests that we succeeded the in-situ observation of phase transformation from form II into form I with a crystal growth. 1) K. Ikeda *et al.*, Appl. Phys. Express, **8**, 045501 (2015). 2) A.D. Bond *et al.*, Angew. Chem. Int. Ed., **46**, 618 (2007).

4:15 PM - 4:30 PM

IN-SITU CURVATURE MONITORING OF ALINN/GAN DBRS

K. Hiraiwa¹, M. Muranaga¹, S. Iwayama¹, T. Takeuchi¹, S. Kamiyama², M. Iwaya², I. Akasaki³

¹Meijo University, JAPAN, ²The University of Meijo, JAPAN, ³Akasaki Research Center, JAPAN

GaN-based VCSELs have been studied because of a low threshold current density and unique emission wavelengths from ultraviolet to green. It is important to control an InN molar fraction of AlInN to be lattice-matched with GaN for high-quality AlInN/GaN DBRs. In-situ

wafer curvature monitoring is one of the methods of the control, and the study of AlInN/GaN DBRs have been published, reporting estimations of InN molar fractions. At the same time, a difference of the curvature changes from AlInN growth temperature to GaN growth temperature between at the first pair and at the last pair was not well explained. Furthermore, a thermal expansion coefficient difference was neglected in the estimation. In this study, we developed and investigated a model considering a total epi layer thickness progression and thermal expansion coefficients for the in-situ curvature. We fabricated three AlInN/GaN DBRs on 2 μm GaN templates on sapphire substrates by MOVPE. Growth temperatures of the AlInN layers in the three DBRs were 830, 835 and 840 $^{\circ}\text{C}$. The designed wavelength was 520 nm. With the lower growth temperature at AlInN, a slope of the in-situ curvature profile at the DBR went to a negative direction (convex direction), suggesting that more In was incorporated in AlInN. We then simulated the experimental in-situ curvature profile results with three different models based on Stoney's equation. The first one is without considering a total epi layer thickness progression and thermal expansion coefficients, which should be the same as that in previous report. Note that the curvature change (measured to be 50 km^{-1} from another experiment) due to the temperature gradient from the top surface to the bottom of the sapphire substrate was incorporated. The second one contained the thickness progression, and the third one contained both the thickness progression and the thermal expansion coefficients. Note that an only InN molar fraction value is a fitting parameter to fit the experimental and the simulated profiles. We found that the second and third simulations showed excellent fitting to all the three experimental in-situ curvature profiles. In addition, the InN molar fraction values from third one were much better agreement with those from ex-situ XRD measurements. As a result, our model is the most suitable one for evaluating curvatures and it enable to control InN molar fractions of AlInN to be lattice-matched with GaN for high-quality AlInN/GaN DBRs much better.

4:30 PM - 4:45 PM

VIRTUAL VISUALIZATION SYSTEM FOR INNER STATE IN HIGH-

TEMPERATURE SOLUTION GROWTH USING PREDICTION MODEL OF COMPUTATIONAL FLUID DYNAMICS CONSTRUCTED BY MACHINE LEARNING

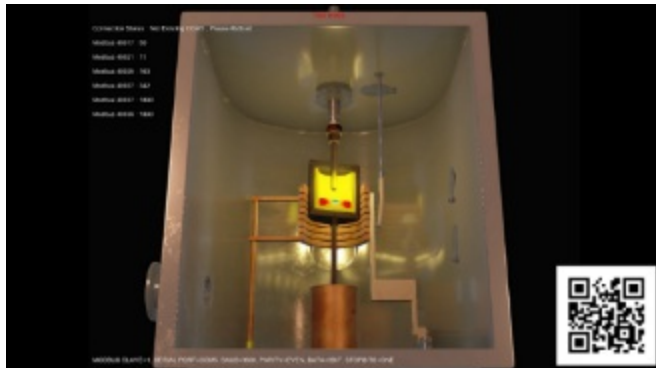
T. Ujihara¹, G. Hatasa², K. Murayama¹, Y. Tsunooka², S. Harada¹, M. Tagawa²

¹Institute of Materials and Systems for Sustainability (IMaSS), JAPAN,

²Department of Materials Process Engineering, Nagoya University, JAPAN

Our final objective is to realize a mode-based development in the field of crystal growth. In this system, crystal growth is completely duplicated in a computer, growth conditions are automatically decided on a computer, and then a crystal growth is experimentally performed under the optimized conditions. In this method, it is essential to construct crystal growth model in a computer. We already made a high-speed and exact regression model to predict temperature-, concentration- and fluid velocity-distributions calculated by computational fluid dynamics (CFD) simulation based on neural network by using machine learning. Moreover, we actually tried to optimize the growth condition and perform SiC solution growth using this system. Another application of the high-speed regression model is the prediction of inner solution situation from log data and a few measurements. Thus, we can know the inner solution situation only from the limited data. In this study, we developed the virtual visualization system of inner solution situation in SiC solution growth using the high-speed prediction model. The CFD simulation of about 100-300 cases are performed and the regression model is constructed on neural network by machine learning. The growth conditions and a few temperature data are given as input data and then the temperature-, concentration- and flow velocity-distributions as outputs are predicted immediately. The prediction time (typically less than 0.1 s) is much 5-7 order shorter than the CFD simulation time. Figure 1 shows the computer graphics of our equipment for SiC solution growth. The temperature distribution predicted by this system is superimposed on this graphics. The conversion time from data to graphics is less than 1 s. Thus, this system is a virtual in-situ observation system. We can visualize the concentration- and fluid velocity- distribution. In our lab, the computer graphics is directly

projected on the surface of the crystal growth equipment. We can virtually observe the inside of the equipment and we can feel more immersed.



4:45 PM - 5:00 PM

IDENTIFICATION OF MICRO CRYSTALS AND VISUALIZATION OF ORGANIC COMPONENTS IN KIDNEY STONES -FOR THE ELUCIDATION OF THE FORMATION MECHANISM OF KIDNEY STONES-

M. Maruyama¹, Y. Tanaka², K.P. Sawada¹, K. Momma³, R. Tajiri⁴, Y. Furukawa⁵, R. Fujimoto¹, Y. Tsuru¹, R. Mori¹, Y. Kamihira¹, Y. Sugiura⁶, R. Ando², S. Hamamoto², K. Taguchi², T. Kato², K. Hasebe², R. Unno², T. Sugino², M. Isogai², J. Yamanaka⁷, T. Okuzono⁷, A. Toyotama⁷, H. Miura⁸, Y. Ohtomo⁹, H.Y. Yoshikawa¹⁰, M. Nakamura¹¹, K. Tsukamoto⁵, A. Okada², M. Yoshimura¹², T. Yasui², Y. Mori¹

¹Graduate School of Engineering, Osaka University, JAPAN, ²Nagoya City University Graduate School of Medical Sciences, JAPAN,

³National Museum of Nature and Science, JAPAN, ⁴Tajiri Thin-section Lab., JAPAN, ⁵Graduate School of Science, Tohoku University,

JAPAN, ⁶National Institute of Advanced Industrial Science and Technology, JAPAN, ⁷Graduate School of Pharmaceutical Sciences, Nagoya City University, JAPAN, ⁸Nagoya City University, JAPAN,

⁹Graduate School of Engineering, Hokkaido University, JAPAN,

¹⁰Department of Chemistry, Saitama University, JAPAN, ¹¹Graduate School of Engineering, Nagoya Institute of Technology, JAPAN,

¹²Institute of Laser Engineering, Osaka University, JAPAN

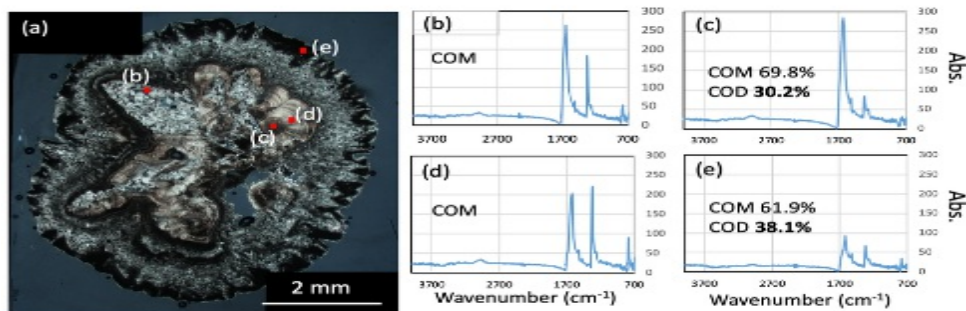


Fig.1 (a) Optical image of a thin section of No.1003-9. (b)-(d) IR spectrum of each point indicated in (a).

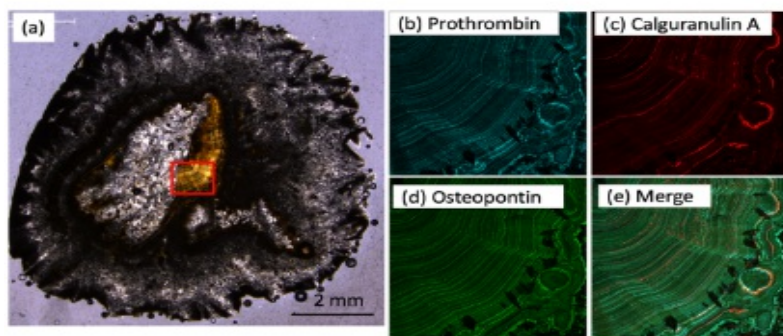


Fig.2 (a) Optical image of another thin section of No.1003-9. Distribution mapping of proteins by fluorescent immunostaining; Prothrombin(b), calgranulinA (c), osteopontin (d) and the merged image (e).

Kidney stones contain more than 90% crystal components and ~10% organic materials. Information such as crystal form, structure and size distribution provide us history of kidney stone formation inside of patients.¹⁾Prevention and treatment based on stone formation mechanism will improve the lifetime incidence and relapse rate of urolithiasis. We aimed to analyze two-dimensional information of crystal components and organic materials. Calcium oxalate stone was targeted in this study. We obtained several stone sections from one stone without demineralization. We observed the thin sections by several optical microscopy for the purpose of observing their constructions. IR spectroscopy (FT/IR6100 JASCO) was used for determination of crystal form. For the precise determination of calcium oxalate monohydrate (COM) and calcium oxalate dihydrate (COD), we

introduced an analyze method of patent JP3524968B with original refinement. Using another thin section, 2D maps of matrix protein; osteopontin, Prothrombin and Calcgranulin-A was analysed by fluorescent immunostaining. We show the data of sample No.1003-9 as an example. The stone size was about 7 mm in long diameter. The stone had variety of structure such as layered (Fig.1 (a)) and micro crystal texture (Fig.1 (b)). Characteristic external edges of the stone were narrow blade like shape, and the area is also filled with micro crystals. IR spectrums showed that these structures were almost COM. A few COD crystals existed in the external edge of the stone or the center of the layered structure. From these structure features, we have hypothesis that the stone consisted with large blade like COD crystals, then transformed into COM crystals. The immunochemical study using the osteopontin, prothrombin and calcgranulin-A antibodies showed positive staining of the stone section. Osteopontin and prothrombin distributed in stripes in a layered structure composed of COM, and intense fluorescence was observed at intervals of several micrometers. Calcgranulin-A also showed relatively thick bands, but there was no apparent periodicity. We would like to discuss the behavior of organic molecules in the stone formation process by associating the crystal phase and structure with the features of organic molecular distribution. 1) Frochot & Daudon, *International Journal of Surgery***36**, 624-632, (2016).

5:00 PM - 5:15 PM

**HARD X-RAY INSTRUMENTATION FOR *IN SITU* SYNCHROTRON
NANOBEAM DIFFRACTION AND COHERENT SCATTERING
STUDIES OF COMPLEX OXIDE SOLID PHASE EPITAXY**

S. Marks¹, P. Quan¹, Y. Chen¹, G.B. Stephenson², T. Kuech³, P.G. Evans⁴

¹University of Wisconsin, WI, UNITED STATES OF AMERICA,

²Argonne National Laboratory, IL, UNITED STATES OF AMERICA,

³Department of Chemical and Biological Engineering, University of Wisconsin-Madison, WI, UNITED STATES OF AMERICA,

⁴Department of Materials Science and Engineering, University of Wisconsin-Madison, WI, UNITED STATES OF AMERICA

Solid phase epitaxy (SPE) is a promising route toward the synthesis of complex oxide thin-films that circumvents the kinetic and thermodynamic challenges of epitaxial growth from the vapor phase by separating the deposition and crystallization steps of thin-film synthesis. Using SPE, an amorphous thin-film can be deposited at room temperature before being annealed in a controlled gas or vacuum atmosphere to drive the crystallization. Nucleation of the crystalline phase can either occur at the interface with the substrate or from nanocrystals in seeded SPE. In both cases, the final orientation of the crystalline thin-film is templated by the orientation of the substrate or seed. Important challenges remain in the structural characterization of the thin-films at all stages of synthesis that, once met, will shape our understanding of the underlying mechanisms driving the amorphous-to-crystalline structural transformation. To address the characterization challenges of thin-film synthesis by SPE, we are developing new instrumentation for the analysis of the deposition and crystallization of oxide thin-films. This instrument incorporates a novel vacuum chamber design that accommodates x-ray focusing optics needed to enable *in situ* x-ray nanodiffraction studies of thin-film synthesis by SPE. The scattering arrangement will permit studies employing nanobeam diffraction, coherent scattering, reflectivity and near-edge x-ray absorption spectroscopy. Structural phenomena of interest include changes of local atomic structure near amorphous-crystalline interfaces during crystallization, the development of texture and mosaicity in the crystalline phase, and the temperature dependence of crystallization. This approach will make it possible to conduct such measurements for a diverse set of thin-film compositions and geometries afforded by the wide compositional scope of amorphous deposition and the potential to use seeding to develop intricate 3-D geometries.

5:15 PM - 5:30 PM

***IN SITU* NANOCRYSTALLOGRAPHICAL CHARACTERIZATION STUDIES WITH THE USE OF X-RAY SCATTERING TECHNIQUES**

H. Te Nijenhuis, M. Gateshki

Malvern Panalytical, NETHERLANDS

In crystal growth studies, both the morphology or microstructure and

the crystallographic structure contain valuable information needed to understand the growth processes. X-ray diffraction has been long recognized as a useful, accurate and effective analytical method for the structural characterization of chemical compounds. It is widely applied for routine types of analysis such as phase identification, semi-quantitative and quantitative analysis of compounds and mixtures. It is therefore not surprising that it has found its way as a standard technique into analytical laboratories in university as well as in industry. Recent interest in the understanding of physical and chemical properties of nanomaterials has increased the need to analyze structures on a local scale. However, the atomic structures of nanostructured and amorphous materials are not accessible by conventional methods used to study crystalline materials, because of the short ordering range in these materials. Nanostructures can be studied using total scattering pair distribution function (PDF) analysis with total X-ray scattering. The pair distribution function provides information about the probability of finding atoms separated at a certain distance. We have applied total X-ray scattering techniques on a standard laboratory X-ray diffraction system employing characteristic Ag *K α* radiation with an energy of 22 keV, corresponding to a wavelength of 0.05564 nm. Samples of different nature –crystalline, nanocrystalline, amorphous solid and even liquid -have been used to test the applicability of the PDF calculations on the lab measurements. Time-resolved measurements with repeated scans make it possible to monitor crystallization of compounds in real time over a long time range. With the addition of non-ambient chambers, the experiments could also be executed at non-ambient temperatures. Phase transitions within the nanocrystals are revealed.

Thursday, August 1, 2019

3:30 PM - 5:30 PM

PV Materials

Location: Torrey Peak II-IV

Session Chair(s): Kevin L. Schulte, Hoe Tan

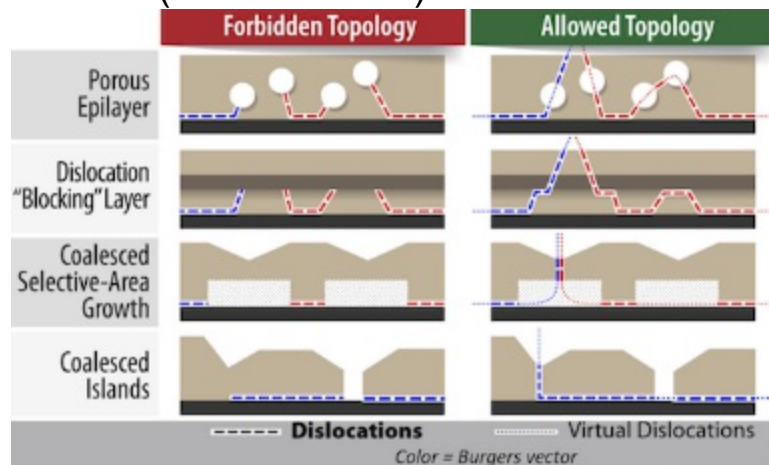
3:30 PM - 4:00 PM

FUNDAMENTALS OF COALESCENCE-RELATED DISLOCATIONS

B. McMahon

National Renewable Energy Laboratory, CO, UNITED STATES OF AMERICA

In materials synthesis, the goal is often to create a material with a very specific structure over a large area or volume. However, this is often done on a foundation—substrate—that doesn't exactly match the structure of the desired material. Adding to the difficulty, synthesis often begins with many small structures that later coalesce into a single, large structure (i.e. a crystalline or layered material), and this coalescence can introduce defects (in the form of dislocations) into the final material. The topology of coalescence-related structural defects is universal over a wide range of materials and applications, and lessons learned from one application can aid in the development of another. This presentation will describe some universal fundamentals of coalescence-related dislocations, illustrated with a range of examples relevant to crystal growth and epitaxy applications. The examples to be discussed include layered-2D, porous and lattice-mismatched crystalline materials. Layered-2D systems provide an excellent starting point for visualization, and enable a discussion of possible layer-interconnection topologies. Porous systems illustrate how subtle changes to the interconnection topology can have a drastic impact on the final defect content. And finally, a solid understanding of coalescence-related dislocations in lattice-mismatched materials greatly facilitates the evaluation of the myriad low-cost "virtual-substrate" strategies being investigated for large-area optoelectronic devices (i.e. solar cells).



4:00 PM - 4:30 PM

STRAIN-BALANCE QUANTUM WELL SOLAR CELLS

N. Ekins-Daukes

University of New South Wales, AUSTRALIA

Abstract: The concept of placing quantum wells into photovoltaic devices can be traced back to the early 1980s when researchers attempted to make absorbing junctions with tailored absorption edges. These early attempts produced disappointing results since the quantum well stack did not permit diffusive transport and resulted in poor carrier collection. In the early 1990s a p-i-n design for the quantum well solar cell was demonstrated that demonstrated unity carrier collection. This approach added the requirement that the QW stack remains depleted, which limits the optical thickness of the device and places stringent demands on the purity of the epitaxial growth. The background doping should be low, ($<1E15\text{cm}^{-3}$) to ensure that the QW stack remains depleted at the solar cell operating voltage. Also the wide depletion region makes the device particularly susceptible to Shockley-Read-Hall recombination. Early devices using AlGaAs/GaAs MQW stacks proved the principle, but InGaAs/GaAs held a particular technological benefit for tailoring the absorption of sub-cells in InGaP based multi-junction solar cells. However, the advent of strain-balanced GaAsP/InGaAs structures barriers provided the key to high photovoltaic device efficiency, eliminating strain related structural defects and with remarkably low background impurity growth. The technique has resulted in some highly efficient devices: a 26% one sun device and a 36.5% triple junction cell. Under solar concentration a 28.3% single junction solar cell was achieved and 42.5% in triple junction configuration. The strain-balance quantum well technique has also been applied to thermophotovoltaic devices, with a InGaAs/InGaAs on InP device achieving an absorption edge of 1.98 μm .

4:30 PM - 4:45 PM

CONTEMPORARY SOLAR CELL BASED ON PEROVSKITE IMPROVEMENTS

O. Rabinovich, D. Saranin, S. Yurchuk, M. Orlova, S. Didenko, S.

Sizov

NUST MISIS, RUSSIAN FEDERATION

Pero-photovoltaics that recently have created a fastest growing solar cell efficiency in the history, needs efficiency improving. In-series tandem generates the minimal current of the subcell with lowest I_{SC} . A parallel connection allows to obtain I_{SC} which is sum of two currents, and two organic photovoltaic (OPV) have created tandems with semitransparent carbon nanotubes (CNT) interlayers. The pero-photovoltaics with laminated AgNW/CNT have been simulated and after it compared with experimental results. Tandem device front view is presented in the figure 1, where perovskite sub-cell is installed directly on the top of GaAs sub-cell (shading area).

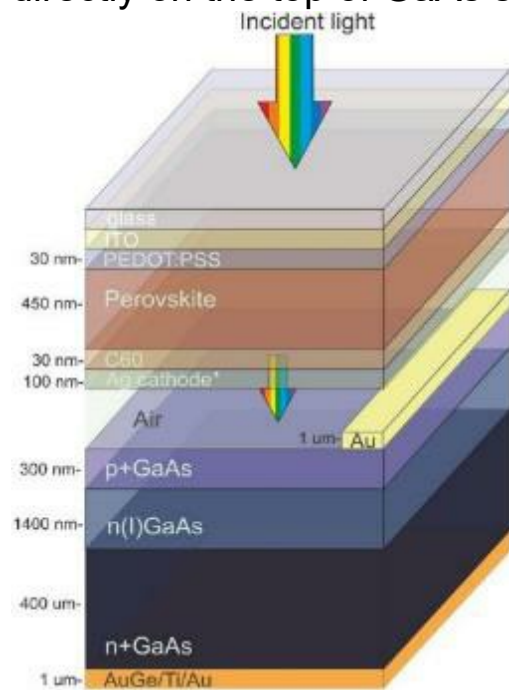


Figure 1 Tandem device schematics (GaAs- perovskite tandem at short circuit regime) The cells connection can be either in-parallel or in-series. It is important to understand how the parameters and characteristics of individual structures affect the characteristics and efficiency of the tandem. The aim of this work is to find trends for different tandem configurations using high – current sub-cells, based on GaAs p-i-n detector structure and $\text{CH}_3\text{NH}_3\text{PbI}_3$ perovskite. So for output parameters extraction we simplified the calculation route to single diode model.

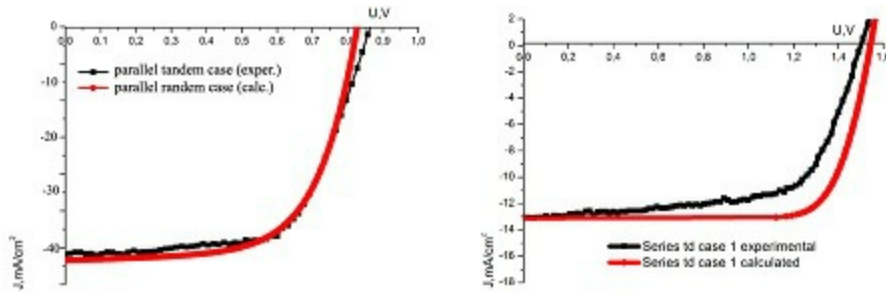


Figure 2 Simulated and experimental dependences with connecting in-parallel and in-series Analyzing the results of this work, it should be noted that GaAs and perovskite technologies are the most effective and promising at the moment for applications in their areas –substrate and solid-state technology, thin-film technology of organometallic semiconductors. The main advantage of this device is the high photocurrent production, which allows to obtain high power. Therefore, in this paper we have developed a tandem in-parallel, nonmonolithic connection showing a high short-circuit current 41 mA from a square centimeter and obtained an efficiency of about 22 %. The approach presented in this paper clearly shows the advantages of parallel tandems over in-series ones with appropriate balancing the output characteristics: the filling factor and the idling voltage. Calculation of a simplified single diode model let us to assume that a parallel connection allows to have not only advantage in the sum of the sub-cell currents, but also eliminates shunt leakage and possible tandem imbalance in the filling factor.

4:45 PM - 5:00 PM

III-V SOLAR CELLS ON SPALLED AND POROUS GE FOR SUBSTRATE REUSE

A. Cavalli¹, B. Ley², N. Alkurd², S. Johnston¹, D. Sulas¹, J. Simon¹, K. Schulte¹, C. Packard², D. Young¹, A. Ptak¹

¹NREL, CO, UNITED STATES OF AMERICA, ²Colorado School of Mines, UNITED STATES OF AMERICA

III-V solar cells are the highest efficiency photovoltaic devices available, but high costs limit their applications. Despite recent interest in substrate reuse, the single-crystalline substrate remains a major cost component of III-V devices. Here we present two paths for device lift off and potential substrate cost mitigation: controlled spalling from

Ge wafers and regrowth on a reformed porous Ge layer. In this work, we demonstrate proof-of-concept solar cells grown on these substrates, evaluate efficiency-limiting defects, and identify paths forward. Both of these technologies rely on epitaxial growth on imperfect Ge surfaces – without additional surface re-preparation – to be economically successful. In the case of controlled spalling, which uses a stressor layer deposited on a substrate to form a crack parallel to the surface and enable device exfoliation, regrowth is hindered by the presence of large arrest lines that develop during the spalling process. Shallow arrest lines do not have a significant effect on performance, but deep arrest lines result in non-radiative recombination centers, as well as introduce disconnected regions that prevent carrier collection. For porous Ge, which uses annealing to reform a continuous layer over an electrochemically etched porous structure, the regrowth challenge is the quality and smoothness of the reformed layer. After annealing porous Ge films, we observe coral-like structures at the surface and sub-surface pore coalescence with embedded porosity, which results in shunted devices upon epitaxial growth. We then develop a procedure that uses a HBr pre-anneal treatment and an ultrasonicated water post-anneal treatment to decrease the roughness in the final microstructure, but further improvement of the roughness and uniformity of the annealed porous Ge surface is needed. We characterize the imperfections in these Ge templates using a variety of characterization techniques, including PL, EL and DLIT, and demonstrate GaAs heterojunction solar cells with an efficiency of 12.8% grown directly on the remaining spalled Ge substrate surface without additional surface re-preparation, and an efficiency of 7.5% on a reformed porous Ge surface, both without an anti-reflection coating. These results show that with better control of the surface features that appear in Ge after spalling and during the annealing reformation process, we would achieve acceptable performance. These two technologies represent possible paths to effective substrate reuse and III-V device cost reduction.

5:00 PM - 5:15 PM

**POLYCRYSTALLINE CUGASE₂ THIN-FILM GROWTH ON
SAPPHIRE OR ZIRCONIA SUBSTRATES WITH ALKALI-METAL**

DOPING

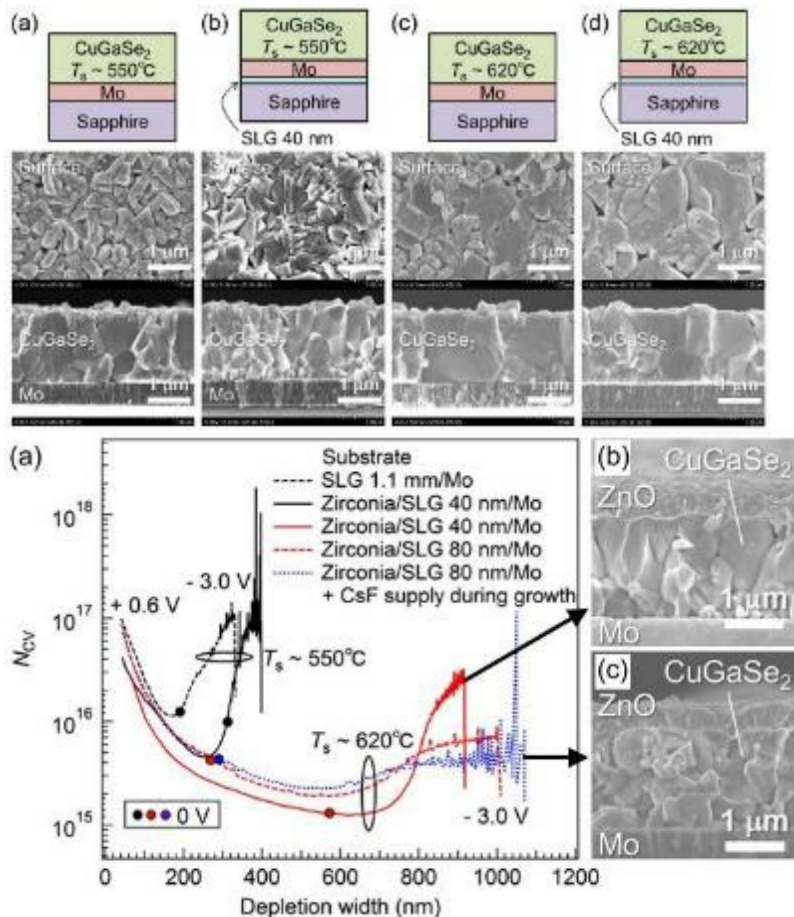
S. Ishizuka¹, P.J. Fons²

¹Research Center for Photovoltaics, AIST, JAPAN, ²Nanoelectronics Research Institute, AIST, JAPAN

CuGaSe₂, with a band-gap energy of 1.7 eV, is one of promising candidates for wide-gap top cells in tandem structure type solar cells as well as photo-electrochemical water splitting devices.

Polycrystalline Cu(In,Ga)Se₂ solar cells, including ternary CuGaSe₂ cells, are generally grown on soda-lime glass (SLG) substrates to obtain high photovoltaic efficiencies due to the so-called alkali-beneficial effects which occur with alkali-metal diffusion from substrates to Cu(In,Ga)Se₂ films during growth, though detailed mechanisms behind the alkali-effects are still open for discussion. In this work, polycrystalline CuGaSe₂ thin-film growth by the three-stage co-evaporation process is studied under alkali-free and -containing conditions using sapphire or zirconia substrates with a focus upon film growth kinetics and alkali-metal effect analyses. Alkali-doping levels in films are controlled using SLG thin layers (40-80 nm in thickness) deposited on substrates by sputtering and/or alkali-halide (such as NaF or CsF) evaporation during film growth. The use of sapphire or zirconia substrates enables CuGaSe₂ film growth at higher temperatures than that conventionally used for the growth on SLG substrates (~550°C) and thus the effects of high growth temperatures (> 600°C) are also examined. Figure 1 shows surface and cross sectional scanning electron microscopy (SEM) images for CuGaSe₂ films grown on sapphire/Mo substrates at 550 or 620°C using SLG thin films as an alkali-metal source. It is found that the use of high growth temperature reasonably leads to large CuGaSe₂ grain sizes, whereas alkali-addition leads to small grain sizes regardless of growth temperature. Figure 2 shows nominal acceptor concentration as a function of depletion width calculated from capacitance-voltage measurements and shows cross sectional SEM images for CuGaSe₂ devices (structure: Mo/p-CuGaSe₂/n-CdS/ZnO-TCO) grown at 620°C with different alkali-metal contents. Note that the use of thicker SLG thin layers leads to higher alkali-metal concentration in films. First, the

longer depletion widths observed with the higher growth temperature are expected to be due to the large grain sizes. In fact, however, it is found in the present work that the reason for lower acceptor concentrations with longer depletion widths are due to the reduction of Cu-vacancy defects (the origin of hole carriers) in CuGaSe_2 grown at 620°C and are independent of the grain size. It is also found that alkali-metals have an effect of improving adhesion of CuGaSe_2 films onto Mo back contacts. Such effects are also expected to be important roles of alkali-metals in CuGaSe_2 devices.



Thursday, August 1, 2019

3:30 PM - 5:30 PM

Selective and Patterned Epitaxial Growth

Location: Red Cloud Peak

Session Chair(s): Yuji Zhao, Jung Han

3:30 PM - 4:00 PM

SELECTIVE AREA REGROWTH AND DOPING OF GAN

B. Li, M. Nami, **J. Han**

Yale University, CT, UNITED STATES OF AMERICA

GaN electronic devices have drawn a lot of attention lately due to their promises in high frequency and high power performances. Based on the history of development in field-effect transistors and diodes from silicon (Si) and silicon carbide (SiC) material systems, it is imperative to have the capability of selective area doping (SAD) for optimal device performance and flexibility. In Si and SiC devices, SAD is readily achieved by implant and/or diffusion of dopant. However, particular material properties, namely the high-temperature instability, have made SAD through implant or diffusion very challenging. In this talk we will review the progress of SAD of GaN and focus on the approach of SAD through epitaxial regrowth and selective growth. The tasks of selective area doping, in our laboratory, are divided into several directions: (1) understanding preexisting defects and impurities before regrowth, (2) in-situ treatment and cleaning of regrowth surfaces, and (3) control and characterizations of planar and non-planar growth. This is an on-going study and our investigation with preliminary electrical characterization will be presented. This work is supported by ARPA-E under the PNDIODES program managed by Dr Isik Kizilyalli.

4:00 PM - 4:15 PM

EFFECT OF GROWTH AND PATTERNING CONDITIONS ON AIR-HOLE CHARACTERISTICS IN GAAS-BASED PATTERNED EPITAXIAL GROWTH FOR PHOTONIC CRYSTAL SURFACE EMITTING LASERS (PCSELS)

S.J. Addamane¹, A. Sharma¹, K. Reilly¹, E. Renteria¹, A.R.K. Kalapala², C. Dix¹, W. Zhou², G. Balakrishnan¹

¹CHTM, University of New Mexico, UNITED STATES OF AMERICA,

²University of Texas at Arlington, UNITED STATES OF AMERICA

Air-hole retained epitaxial growth on patterned substrates is an efficient method to integrate a low-index material with a high-quality III-V semiconductor. Among other applications, this method has more

recently been used in realizing photonic crystal surface emitting lasers (PCSELS).

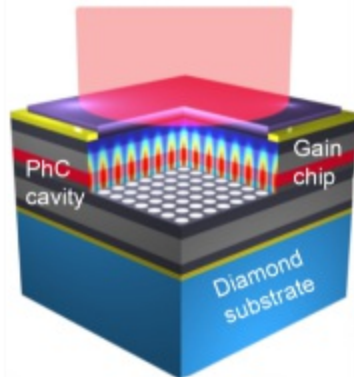


Fig.1: Typical PCSEL configuration

PCSELS utilize a 2-dimensional (2-D) photonic crystal resonant cavity in the vicinity of an active layer to isolate a single mode and direct light in the vertical direction (Figure 1). The photonic crystal cavity is a 2-D array of air-holes formed by regrowth on a patterned substrate that consists the active region (usually quantum wells). Consequently, control over the formation and dimensions of the air-holes is vital to realizing desirable device characteristics. In this talk, we study the effect of varying growth (growth temperature, III-V ratio, and growth rate) and patterning conditions (dose, pre-growth hole dimensions, pitch) on the characteristics of the air-hole. PCSEL fabrication usually involves an initial epitaxy step (for lower cladding and active layer), followed by patterning, which is followed by a regrowth (for upper cladding). With a goal of fabricating PCSELS around the $1\mu\text{m}$ wavelength range based on InGaAs quantum wells (QWs) grown on GaAs, most of the regrowth experiments described here to form air-holes are carried out on GaAs substrates. The samples discussed in this study are grown using molecular beam epitaxy (MBE) in a VG Semicon V80H reactor. The patterning is carried out using electron-beam lithography (EBL) and dry-etched using an inductively coupled plasma (ICP) reactor with BCl_3 gas (Figure 2). These patterned samples are then cleaned and loaded back into the MBE reactor for the regrowth step. Plan-view and cross-section scanning electron microscopy (SEM) were used to characterize the quality of the regrowth and the characteristics of the air-hole. The optical quality of the air-holes and its effects on device parameters are studied using

photoluminescence (PL) from the InGaAs QWs beneath the air-holes. It is found that the growth temperature and the growth rate have a substantial effect on the profile (tear-drop shape) and dimensions of the air-holes. On the other hand, we found that increasing dosage during EBL results in longer air-holes with an increased taper in the profile (Figure 3). The aspect ratio of the holes (before regrowth) is also shown to have an effect on the hole dimensions. A preliminary study exploring different cleaning techniques post-patterning and before re-growth and their effect on air-hole formation will also be discussed.

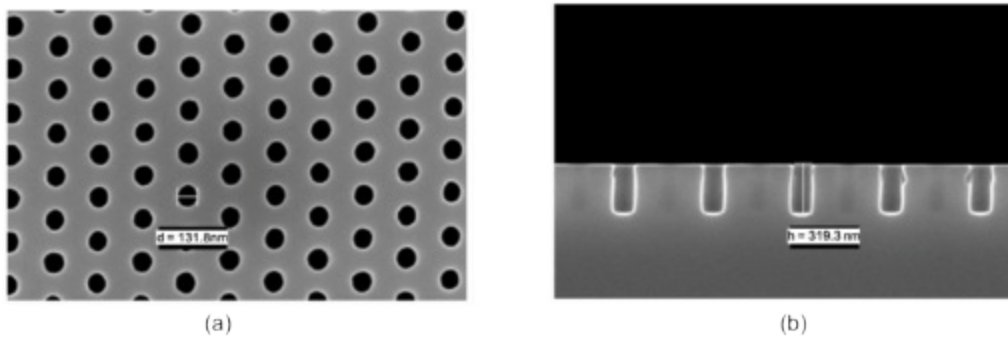


Fig. 2: Plan-view (a) and cross-section (b) SEM images of patterned GaAs substrates

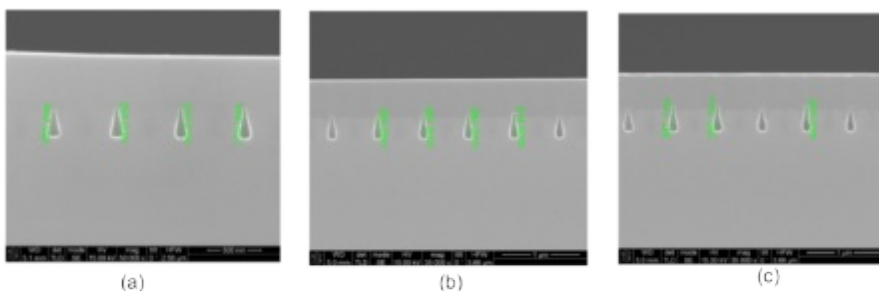


Fig. 3: Cross-section SEM images of variation in air-hole size for different EBL dosages:

(a) $130 \mu\text{C}/\text{cm}^2$ (b) $165 \mu\text{C}/\text{cm}^2$ (c) $190 \mu\text{C}/\text{cm}^2$

4:15 PM - 4:30 PM

ZNO NANORODS GROWN FROM SOLUTIONS ON PATTERNED SUBSTRATES

J. Grym, H. Faitova, S. Kucerova, O. Cernohorsky, N. Bašínová, R. Yatskiv, S. Tiagulskyi, J. Vaniš

Institute of Photonics and Electronics of the CAS, CZECH REPUBLIC

ZnO is a direct wide bandgap semiconductor with a series of unique properties: a large exciton binding energy; good optical transmittance in the visible region; high optical gain; piezoelectricity; room

temperature ferromagnetism; mechanical stability given by the high melting point and large cohesive energy; radiation hardness; or biological compatibility [1]. These properties allow for applications of ZnO in UV light-emitting devices and detectors, field-effect transistors, solar cells, piezoelectric nanogenerators, or chemical sensors [2]. For the majority of these applications, upright standing arrays with controlled positioning, sizes, and physical properties are desirable. Despite a large number of applications, the growth of ZnO from solutions is not well understood and the growth technology mostly relies on empirical results. We investigate the growth of ZnO vertical nanorod arrays on patterned substrates and seed layers in both conventional batch reactors and non-conventional continuous-flow reactors and point out the differences. Unlike the batch reactors, in continuous-flow reactors the solution supersaturation can be accurately controlled [3], which enables to control the growth rates, the aspect ratio, the incorporation of dopants and impurities, and the density of defects. We further report on fundamental mechanisms of nucleation and growth of the nanorods on the substrates modified by focused ion beam (FIB). Thanks to FIB processing we are able to control the nucleation and positioning of the nanorods. This method enables the nucleation to be uniform even on substrates whose morphology is originally non-uniform. Representative examples of substrates with non-uniform morphology are GaN epitaxial templates, which are commercially widely used as an alternative of expensive GaN monocrystals. We study the impact of several parameters of FIB (e.g. the ion energy, the dose, the beam profile) on the geometry and physical properties of the nanostructures. Moreover, we present measurements of electronic transport in a single vertically oriented n-type ZnO nanorod on p-type GaN substrate using a nanoprobe in a scanning electron microscope. [1] Ahmad M., Zhu J., ZnO based advanced functional nanostructures: synthesis, properties and applications, *Journal of Materials Chemistry* 21/3, 599-614 (2011). [2] D. Panda and T.Y. Tseng, One-dimensional ZnO nanostructures: fabrication, optoelectronic properties, and device applications. *Journal of Materials Science*, 48/20, 6849-6877 (2013). [3] S.A. Morin, M.J. Bierman, J. Tong and S. Jin, Mechanism and Kinetics of Spontaneous Nanotube Growth Driven by Screw Dislocations. *Science*, 328/5977,

476-480 (2010).

4:30 PM - 5:00 PM

SELECTIVE AREA GROWTH OF III-V SEMICONDUCTOR NANOSTRUCTURES

C. Palmstrom

University of California, Santa Barbara, CA, UNITED STATES OF AMERICA

Some proposed scalable designs for Majorana based qubit devices involve semiconductor nanowire networks with induced topological superconductivity and semiconductor quantum dots. These can potentially be realized by post growth top down lithography and etching of two-dimensional epitaxial layers or by patterning dielectric covered III-V surfaces followed by selective area growth. We have used chemical beam epitaxy selective area growth of InAs on SiO₂ covered InP substrates with various crystal orientations to obtain an understanding of the influence of substrate as well as the in-plane crystal orientations on the shape and defect formation of selective area grown InAs nanowires. Going beyond selective area growth, by adding an additional dielectric layer, confined epitaxial lateral epitaxy can also be investigated. In this presentation I will discuss our progress in the use of selective area growth of InAs and InSb based nanostructures with potential applications for Majorana devices and topological quantum computer applications. I will also compare this approach with the vapor-liquid-solid growth of InAsSb and InSb nanowire structures and networks. In addition, I will also present results on confined epitaxial lateral overgrowth of InP nanostructures on InP substrates.

5:00 PM - 5:15 PM

EFFECTIVE SELECTIVE AREA DOPING FOR GAN VERTICAL POWER TRANSISTORS ENABLED BY EPITAXIAL REGROWTH

H. Fu, K. Fu, H. Liu, S. Reddy, F. Ponce, Y. Zhao

Arizona State University, AZ, UNITED STATES OF AMERICA

Vertical GaN power transistors have recently garnered considerable interests due to their large current and voltage handling capabilities and small chip area. However, one of critical components that is still

missing is lateral or patterned p-n junctions. They can be realized by two methods: ion-implantation and epitaxial regrowth. Ion-implantation is far from mature in GaN devices due to GaN decomposition at high post-implantation annealing temperatures and poor implanted p-GaN. Epitaxial regrowth is regarded as an alternative route to realizing patterned p-n junctions. In this work, we explored several important topics in the regrowth of p-n junction. Large reverse current leakage is the major limiting factor in realizing high performance usable regrown p-n junctions. This is mainly due to the dry etching damages before the regrowth. Inductively coupled plasma (ICP) etching is usually used to form trenches for regrowth; however, it also induces plasma damages on the regrowth surfaces. Influences of different dry etching processes on GaN regrown p-n diodes have been comprehensively investigated. The reverse leakage current in the regrown samples was significantly suppressed and close to that in as-grown samples, by reducing the etching power combined with appropriate wet etching treatments such as HF and a suitable insertion layer. This improvement is attributed to the decrease of charge concentrations at the regrowth interface. Furthermore, this method could also improve the ideality factor for regrown p-n diodes. In addition, a non-uniform Mg distribution in p-GaN regrown on patterned trench structures was observed by spot mode cathodoluminescence (CL) spectroscopy and CL mapping. The sidewall (i.e., non-basal planes) has a much lower Mg concentration compared with p-GaN along the (0001) direction. This is attributed to crystal orientation effects on the Mg incorporation efficiency. A growth method that provides a dominant (0001) plane growth can be used to solve this issue. Furthermore, a large amount of impurities including Si and O was found to accumulate at the regrowth interface by SIMS. O may come from the atmosphere and/or metalorganic precursors; however the origin of Si is still unclear. These impurities serve as donors and can adversely affect the device current leakage and breakdown voltages. Possible methods to mitigate this effect include HF treatment, insertion layer, p-type compensation layer, etc. In conclusion, this work investigated critical challenges and solutions for demonstrating high for regrown p-n junctions, and can be serve as important references for future developments of advanced high voltage GaN power electronics.

Thursday, August 1, 2019

3:30 PM - 5:30 PM

**Symposium on Epitaxy of Complex Oxides:
Superlattices**

Location: Grays Peak II, III

Session Chair(s): Guus Rijnders

3:30 PM - 3:30 PM

**PICOSCIENCE OF CHARGE-TRANSFER OXIDE
HETEROSTRUCTURES**

F.J. Walker

Yale University, CT, UNITED STATES OF AMERICA

A diverse toolkit has been developed by the thin film oxide community for the control of physical and electronic structure to realize new material properties. This includes the use of epitaxial strain, charge transfer, and polarization at interfaces in superlattices or heterostructures. One example of this approach involves the growth of oxide heterostructures that have atomically abrupt changes in transition metal chemistry designed to promote charge transfer between layers. In this talk, I will describe examples of *in situ* and *in operando* synchrotron x-ray spectroscopic and diffraction methods that can be used to verify that the physical and electronic structure at interfaces is as designed. Crystal truncation rod measurements reveal the lattice polarization that accompanies charge transfer, and soft x-ray absorption spectroscopy measurements demonstrate changes in the transition metal oxidation state. Finally, more advanced synchrotron methods, such as resonant inelastic x-ray scattering and coherent soft x-ray scattering, provide a detailed picture of electronic spin and electronic configurations at charge transfer interfaces. The combination of atomic layer synthesis and picoscale characterization is a powerful approach that guides the development of new materials.

3:30 PM - 3:30 PM

**CREATING NEW ANTIFERROELECTRIC MATERIALS USING
INTERFACIAL ELECTROSTATIC ENGINEERING**

J.A. Mundy

Harvard University, UNITED STATES OF AMERICA

Dielectric capacitors hold a tremendous advantage for energy storage due to their fast charge/discharge times and stability in comparison to batteries and supercapacitors. A key limitation to today's dielectric capacitors, however, is the low storage capacity of conventional dielectric materials. To mitigate this issue, antiferroelectric materials have been proposed, but relatively few families of antiferroelectric materials have been identified to date. Here, we propose a new design strategy for the construction of lead-free antiferroelectric materials using interfacial electrostatic engineering. We begin with a ferroelectric material with one of the highest known bulk polarizations, BiFeO_3 . We use atomically-precise reactive oxide molecular-beam epitaxy to construct high-quality superlattices of BiFeO_3 and a confining dielectric. We show that this electrostatic confinement of BiFeO_3 induces a new metastable antiferroelectric structure.

Application of an electric field reversibly switches between this new phase and a ferroelectric state; in addition, tuning of the dielectric layer causes coexistence of the ferroelectric and antiferroelectric states. Precise engineering of the structure generates an antiferroelectric phase with energy storage comparable to that of the best lead-based materials. The use of electrostatic confinement provides a new pathway for the design of engineered antiferroelectric materials with large and potentially coupled responses that could be applicable to other oxide systems.

3:30 PM - 3:30 PM

COMBINING OXIDE EPITAXY AND TOPOCHEMISTRY: FROM ELECTRON-DOPED MANGANITES TO LATERAL ANIONIC HETEROSTRUCTURES

S. May

Drexel University, PA, UNITED STATES OF AMERICA

The ability to carry out topochemical reactions on epitaxial complex oxide films is an enabling strategy for expanding the accessible chemistries in oxide heterostructures and realizing lateral superstructures with precise geometries. Using recent work on

SrMnO_{2.5-δ}F_γ as an example, I will discuss the fluorination reaction used to incorporate fluorine into as-grown SrMnO_{2.5} films. In this compound, the fluorine substitutes for oxygen, resulting in electron-doped (mixed Mn^{3+/2+} valence) manganite films. The resultant physical properties of the manganite oxyfluoride will be discussed, highlighting the contrast in electronic, magnetic, and optical behavior obtained through anion substitution as compared to A-site substituted La_{1-x}Ce_xMnO₃. In the second half of the talk, I'll present how topochemical reactions can be spatially controlled through lithographically-defined hard masks, allowing for the realization of in-plane SrFeO_{2.5}/SrFeO₃ and SrFeO_{2.5}/SrFeO₂F superlattices. These lateral heterostructures exhibit many features distinct from traditional patterned materials such as tunable anisotropy, non-binary properties, and reconfigurability, offering the potential for dynamic control over lateral patterns.

3:30 PM - 3:30 PM

EFFECTIVE DIMENSIONALITY-TUNED ELECTRONIC STATES IN METASTABLE NICKEL OXIDE THIN FILMS

G.A. Pan¹, Q. Song¹, C.M. Brooks¹, D. Renaud¹, H. Paik², J.A. Mundy¹

¹Harvard University, UNITED STATES OF AMERICA, ²Platform for the Accelerated Realization, Analysis, & Discovery of Interface Materials (PARADIM), Department of Materials Science and Engineering, Cornell University, NY, UNITED STATES OF AMERICA
The rare-earth nickelates (RNiO₃) have been heralded as strongly correlated electron materials with a rich phase diagram, including metal-to-insulator transitions with concomitant magnetic ordering. The layered Ruddlesden-Popper phases of the nickelates have the potential to display distinct electronic and magnetic ground states from the RNiO₃ counterpart due to the changes in nickel valence, dimensionality, and structure. Here, we use reactive oxide molecular-beam epitaxy to synthesize the first Ruddlesden-Popper phases of parent compound NdNiO₃, Nd_{n+1}Ni_nO_{3n+1} with $n = 1 - 5$. We will present the unique synthetic challenges of preparing this series of

samples as well as the change in electronic properties with varying n .

3:30 PM - 3:30 PM

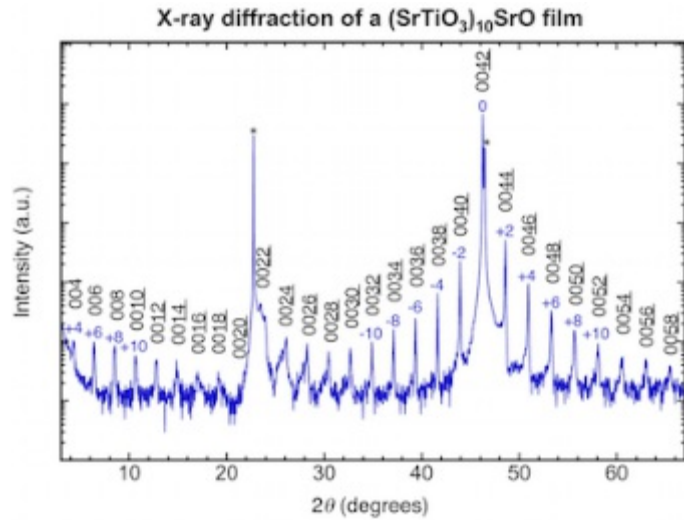
A SUPERLATTICE APPROACH TO ANALYZE THE X-RAY DIFFRACTION OF RUDDLESDEN-POPPER FILMS

M. Barone¹, N. Dawley¹, H. Nair¹, T. Heeg², Y. Nie³, D. Schlom¹

¹Department of Materials Science and Engineering, Cornell University, UNITED STATES OF AMERICA, ²Heeg Vacuum Engineering, GERMANY, ³Nanjing University, CHINA

Ruddlesden-Popper phases are an important class of superlattices composed of perovskite (ABO_3) and rock salt (AO) with general formula $(ABO_3)_nAO$. Diverse properties including high-temperature superconductivity and record-breaking tunable dielectrics have been observed in Ruddlesden-Popper films grown by molecular-beam epitaxy, but the quality of these films is limited by the precision of the calibration method. To improve the layering perfection of Ruddlesden-Popper superlattices, we apply an x-ray diffraction (XRD) based approach developed for superlattices of III-V semiconductors to quantitatively compute flux corrections to Ruddlesden-Popper films grown by molecular-beam epitaxy. We demonstrate the precision of this approach by synthesizing an $n=10$ Ruddlesden-Popper phase, $(SrTiO_3)_{10}SrO$, with unparalleled layering perfection and by iteratively improving $(SrSnO_3)_2SrO$ films as seen in Figure 1. We also modify Nelson-Riley analysis to make it applicable to superlattices and demonstrate the generality of our approach by analyzing another homologous series, the Aurivillius phases.

a)



b)

X-ray diffraction of sequential $(\text{SrSnO}_3)_2\text{SrO}$ films

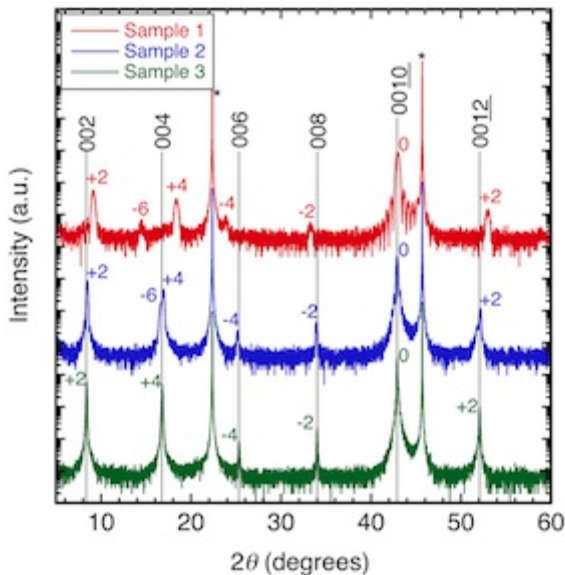


Figure 1 X-ray diffraction of **a)** an impeccable $n=10$ $(\text{SrTiO}_3)_{10}\text{SrO}$ film and **b)** three $(\text{SrSnO}_3)_2\text{SrO}$ films grow sequentially, showing dramatic improvement from the first to the second sample and an essentially perfect third sample.

Friday, August 2, 2019

8:00 AM - 10:00 AM

Biological and Biomimetic Materials I

Location: Grays Peak I

Session Chair(s): Wei Huang, David Kisailus

8:00 AM - 8:30 AM

ENERGETICS OF AMELOGENIN VARIANTS BINDING TO HYDROXYAPATITE

J. Tao¹, Y. Shin², R. Jayashinha Arachchige², S.D. Burton¹, G.W. Buchko³, W.J. Shaw¹, B.J. Tarasevich²

¹Pacific Northwest National Laboratory, WA, UNITED STATES OF AMERICA, ²Pacific Northwest National Laboratory, AL, UNITED STATES OF AMERICA, ³School of Molecule Biosciences, Washington State University, WA, UNITED STATES OF AMERICA

The exceptional functional properties of enamel, one of hardest biomaterials in nature, arise from its intricate hierarchical structure and cannot be reproduced *in vitro* inorganically. *In vivo* the formation of enamel depends on the ~180-residue protein amelogenin, the predominant protein in the enamel matrix. A testament to amelogenin's importance is that a single amino acid substitution to the primary amino acid sequence of amelogenin can lead to drastic changes in enamel phenotype, resulting in *amelogenesis imperfecta* (AI), enamel that is defective and easily damaged. Our aim was to develop an energetic understanding to explain how a single amino acid variation can affect steps in the biomineralization process and lead to malformed enamel. High resolution, *in situ* atomic force microscopy (AFM), solid state NMR (ssNMR) and *in vitro* mineralization were employed to study the energetics, structure and mineralization kinetics of murine amelogenin (wild-type, two naturally occurring single amino acid variants associated with AI (T21I and P41T), and a model variant (P71T)) interacting with single crystal hydroxyapatite (100). *In situ* AFM showed that altering one amino acid resulted in an increase in the quantity of protein adsorbed onto hydroxyapatite and the formation of multiple protein layers. Quantitative analysis of the equilibrium adsorbate amounts revealed that the protein variants had higher protein-protein binding energies. ssNMR suggested that the stronger HAP binding results in less interfacial protein mobility. Mineralization and MMP20 enzyme degradation studies showed that the amino acid variants inhibited the growth and phase transformation of hydroxyapatite and slowed the

degradation of amelogenin by MMP20. The amelogenin variants cause malformed enamel because they bind excessively to hydroxyapatite and disrupt the normal hydroxyapatite growth and enzymatic degradation processes. These *in situ* methods we applied to determine the molecular level energetics and structures of amelogenin binding to hydroxyapatite are powerful tools to be further exploited towards understanding the mechanisms of biomineralization. The ultimate result of such understanding is the predictive synthesis of functional materials tailored by macromolecular design.

8:30 AM - 8:45 AM

OCTACALCIUM PHOSPHATE FORMATION AND ENHANCES ITS LAYER STRUCTURE IN THE SYSTEMS OF NA-NH₄

Y. Sugiura, Y. Makita

AIST, JAPAN

Octacalcium phosphate (OCP) is a layered type of calcium phosphate that shows promise for pharmaceutical and biomedical applications because it offers both excellent biocompatibility and a unique, robust crystal structure that readily accepts substitution by various molecules. Although several cations can be incorporated into the OCP crystal lattice by ionic substitution, little is known about the relative probability of different ions to substitute into the OCP crystal lattice. In this study, we focus on Na and NH₄, which are known to enter the OCP crystal lattice by ionic substitution. We investigate which of these two is most likely to substitute into OCP in a system containing both ions. In this work, OCP is fabricated from monocalcium phosphate monohydrate via hydrolysis in a solution containing 1 mol L⁻¹ (NH₄)₂HPO₄ with NaCl concentrations ranging from 0 to 100 mmol L⁻¹. X-ray diffraction and thermal analyses indicate that the structure characteristic of NH₄ ionic substitution in OCP is attenuated as the Na concentration increases. Furthermore, when the Na concentration exceeds 50 mmol L⁻¹ (Na/NH₄ ≥ 1/20), the structure characteristic of NH₄ ionic substitution into OCP almost completely disappears. These results indicate that Na is more likely to be ionically substituted into the OCP crystal structure than NH₄ and thereby inhibits the structural change of OCP caused by ionic substitution of NH₄.

8:45 AM - 9:00 AM

FORMATION OF CALCIUM PHOSPHATES IN SIMULATED BODY FLUID WITH CALCITE CRYSTAL

H. Saito¹, T. Hirai², H. Katsuno³, T. Nakada³

¹, JAPAN, ²Department of Physical sciences, Ritsumeikan University, JAPAN, ³Department of Physical Sciences, Ritsumeikan University, JAPAN

Recently, Ohtsuki et al. showed that hydroxyapatite (HAp: $\text{Ca}_{10}(\text{PO}_4)_6(\text{OH})_{10}$) layers formed on the surfaces of CaO-SiO₂-based glasses in simulated body fluid (SBF). Authors pointed out that the dissolution of calcium ion from the CaO-SiO₂-based glasses induced the nucleation of calcium phosphate and silanol (Si-OH) groups emerged on the surface. Based on their results, we attempted to form HAp and discussed the process of the formation on the surface of SiO₂ glasses by using calcite (CaCO₃) as a source of calcium ion. Fig. 1 shows an image of scanning electron microscope (SEM) of the surface of the SiO₂ glass substrate with a calcite crystal after soaking in SBF for 5 days. Numerous spherical precipitates with the size of 1-15 micrometers were observed around the calcite crystal. The size distribution of the precipitates was larger in nearby calcite, indicating the dissolution fields of calcium ion from the calcite crystal. X-ray Diffraction analysis suggested that amorphous calcium phosphates (ACP) transformed into CaHPO₄ · 2H₂O (DCPD: dicalcium phosphate dihydrate) crystals around 10 days. It is expected that ACP tends to transform HAp in relatively higher pH (>7.0) in general. DCPD crystals observed in the solution although local pH would be higher value around dissolving calcite. We will also report the results of *in-situ* observations of calcium phosphate formation.

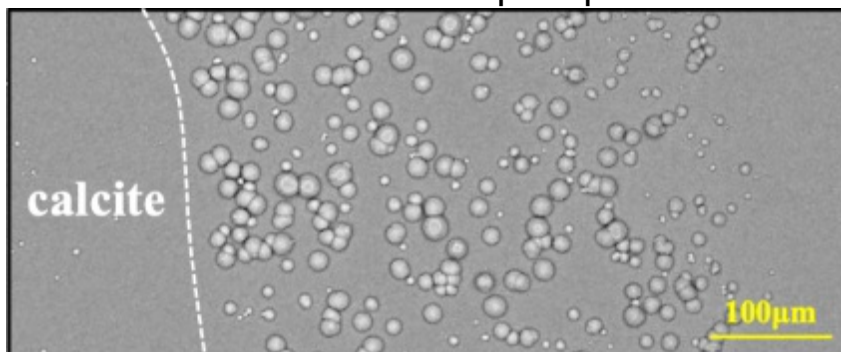


Fig. 1 SEM image of a SiO₂glass substrate with a calcite crystal in SBF for 5 days. The calcite crystal was on the left side of the substrate, which was removed.

9:00 AM - 9:15 AM

MULTISCALE TOUGHENING IN ORIENTED ATTACHED BIOLOGICAL NANOCRYSTALLINE HYDROXYAPATITE

W. Huang¹, D. Kisailus²

¹Department of Chemical and Environmental Engineering, University of California, CA, UNITED STATES OF AMERICA, ²Department of Chemical and Environmental Engineering, University of California at Riverside, CA, UNITED STATES OF AMERICA

Biomaterial composites found in natural organisms such as nacre, antler and the dactyl club of mantis shrimp show remarkable toughness and impact resistance. The impact speed of the dactyl clubs can reach ~20 m/s at an acceleration of ~10,000g during the daily feeding activities of mantis shrimp. The nanocrystalline hydroxyapatite (HAP) found in these dactyl clubs plays an important role in terms of impact energy dissipation and damping. The surface consists of densely packed (~ 88 vol%) ~60 nm hydroxyapatite nanoparticles, which were found to consist of oriented attached ~10-20 nm HAP single crystals. Under high strain rate (~10⁴ s⁻¹) impact, these particles rotate, translate and fracture at low angle grain boundaries, providing significant energy dissipation. Imperfections in the nanocrystals such as dislocations and amorphization are generated during the impact events, which are additional toughening mechanisms at the atomic scale. As a result, the impact damage is localized and limited to a specific region on the surface, thus protecting the whole dactyl club from crack propagation and catastrophic failure under high speed impacts.

9:15 AM - 9:30 AM

ORIENTED CRYSTALLIZATION OF BIOGENIC STRONTIUM SULFATE SINGLE CRYSTALS

V. Merk, J. Walker, P. Smeets, D. Joester

Northwestern University, UNITED STATES OF AMERICA

The marine protozoa *Acantharia* builds endoskeletons from intricate, smoothly curved strontium sulfate (SrSO_4) spicules, whose long axes coincide with the crystallographic *a*-axis. To address the question how crystal texture is biologically controlled in the vesicular compartment, we employed a combination of electron-optical imaging and synchrotron-based techniques. Strikingly, biogenic strontium sulfate displays a highly ordered orthorhombic single crystal structure. However, based on high resolution synchrotron XRD we discovered a small anisotropic effect in coherence length and a roughly 14-fold higher strain in the biomineral in comparison with their geological counterpart. To explore the origin of local lattice perturbations, we investigated the distribution of intercalated biomolecules on various length scales. As markers for intracrystalline organic matter, sulfur-bearing amino acids and di-sulfides were detected across the protist's skeleton by microbeam X-ray absorption spectroscopy (XANES) at the sulfur *K*-edge. Highly anisotropic small-angle X-ray scattering signals correspond to nanoscale electron density variations parallel to the crystallographic *a*-axis, which are consistent with buried interphases in the SrSO_4 biomineral. Similarly, scanning TEM Z-contrast imaging showed nanodomains with a lower atomic number around the spicule center, which may guide the crystallographic orientation of a primary seed crystal. In the diffraction contrast image from the spicule cross-section, we observed concentric layers reflective of fluctuating growth. Taken together, we present experimental evidence for the occlusion of intracrystalline biomolecules in biologically produced strontium sulfate crystals. Our findings suggest that biomolecules interact specifically with (*h00*) planes and subsequently become introduced into the growing crystal, which may be related to the fixed crystallographic orientation of *Acantharian* spicules.

9:30 AM - 9:45 AM

BIOLOGICAL CRYSTALLIZATION OF ULTRAHARD TEETH AND TRANSLATION TO MULTI-FUNCTIONAL MATERIALS

D. Kisailus

Department of Chemical and Environmental Engineering, University of California at Riverside, CA, UNITED STATES OF AMERICA

There is an increasing need for the development of multifunctional

lightweight materials with high strength and toughness. Natural systems have evolved efficient strategies, exemplified in the biological tissues of numerous animal and plant species, to synthesize and construct composites from a limited selection of available starting materials that often exhibit exceptional mechanical properties that are similar, and frequently superior to, mechanical properties exhibited by many engineering materials. These biological systems have accomplished this feat by establishing controlled synthesis and hierarchical assembly of nano- to micro-scaled building blocks. This controlled synthesis and assembly require organic that is used to transport mineral precursors to organic scaffolds, which not only precisely guide the formation and phase development of minerals, but also significantly improve the mechanical performance of otherwise brittle materials.

In this work, we investigate an organism that have taken advantage of hundreds of millions of years of evolutionary changes to derive structures, which are not only strong and tough, but also demonstrate abrasion resistance. All of this is controlled by the underlying organic-inorganic components. Specifically, we discuss the formation of heavily crystallized radular teeth the chitons^[1-4], a group of elongated mollusks that graze on hard substrates for algae.

From the investigation of synthesis-structure-property relationships in these unique organisms, we are now developing and fabricating multifunctional engineering materials for energy conversion and storage. We discuss the crystallization of these materials and their subsequent impact on performance.



Figure 1. Ultrahard abrasion resistant radular teeth of the giant chiton.

- [1]. "Competing mechanism in the wear resistance behavior of biomineralized rod-like microstructures," E. Escobar de Obaldia et al., *Journal of the Mechanics and Physics of Solids*, 96 (2016) 511-534.
- [2]. "Stress and Damage Mitigation from Oriented Nanostructures within the Radular Teeth of *Cryptochiton stelleri*," L.K. Grunenfelder et al., *Adv. Funct. Mater.*, 24 (2014) 6093-6104.
- [3]. Phase transformations and structural developments in the radular teeth of *Cryptochiton stelleri*," Q. Wang, M. Nemoto, et al., *Adv. Funct. Mater.*, **23** (2013) 2908–2917.
- [4]. "Analysis of an ultra hard magnetic biomineral in chiton radular teeth," J. Weaver, QQ. Wang, et al., *Materials Today*, **13** (2010) 42-52.

9:45 AM - 10:00 AM

TOWARDS THE UNDERSTANDING OF MORPHOLOGY CONTROL IN MAGNETITE BIOMINERALIZATION

A. Pohl¹, C.T. Lefèvre², N. Menguy³, K.G. Blank⁴, D. Faivre²

¹Max Planck Institute of Colloids and Interfaces, GERMANY,

²CEA/CNRS/ Aix-Marseille Université, FRANCE, ³Sorbonne Université, Muséum National d'Histoire Naturelle, FRANCE, ⁴Max

Planck Institute of Colloids and Interfaces, FRANCE

Magnetotactic bacteria are a diverse group of motile aquatic prokaryotes that biomineralize magnetite crystals within their cells. These bacterial magnetite nanoparticles have outstanding properties, such as their single crystalline structure in the size range of magnetic single domains, and their strain-specific morphologies. Magnetotactic bacteria of the *Deltaproteobacteria* class, for example, mineralize anisotropic crystals that defy crystallographic rules. Such morphologies are extremely difficult to obtain synthetically. Magnetite biomineralization is genetically controlled and the interaction of biomacromolecules with magnetite is hypothesized to be essential for morphology control. However, many of these molecular players are still unknown.

We are investigating several protein candidates that are putatively responsible for growth control of anisotropic magnetite crystals with the goal of understanding the molecular processes determining nanoparticle morphologies. In the study presented here, we introduce one highly conserved protein that is unique to bacteria, which mineralize anisotropic magnetite crystals. Quartz crystal microbalance measurements of the recombinantly expressed protein prove that this protein binds to magnetite sensor surfaces almost irreversibly. This result is confirmed when the magnetite interaction of the most conserved region is probed with atomic force microscope-based single-molecule force spectroscopy. These experiments reveal that the strong binding is the result of a slow off-rate combined with a fast on-rate, originating from the high concentration of binding sites on the magnetite surface. This new magnetite-binding protein is used for the production of functionalized magnetite nanoparticles in a bioinspired synthesis approach.

The outcome of this study provides new insights into the molecular mechanisms that determine biomineralization processes. Magnetite nanoparticles synthesized *via* the before mentioned green synthesis route can find various applications in bio- and nanotechnologies.

Friday, August 2, 2019

8:00 AM - 10:00 AM

Bulk Crystal Growth: Other Materials

Location: Shavano Peak

Session Chair(s): Christo Gugushev, Luis Stand

8:00 AM - 8:15 AM

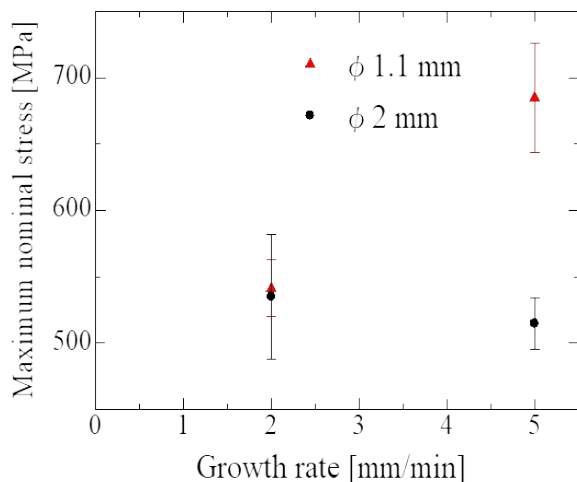
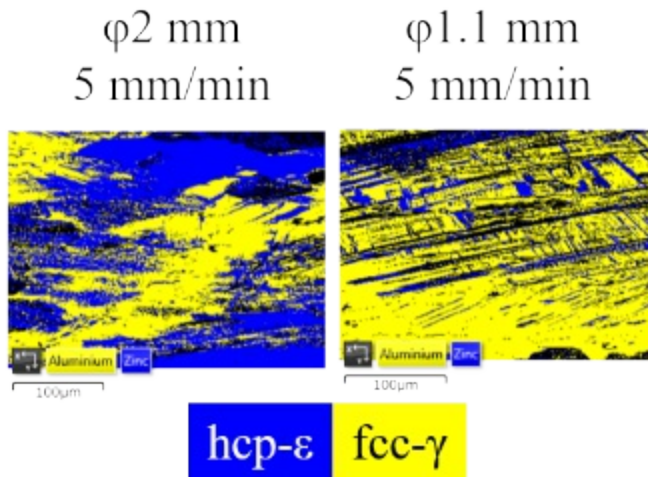
COOLING RATE DEPENDENCE ON MICROSTRUCTURES AND MECHANICAL PROPERTIES OF CO-CR-MO ALLOY FIBERS FABRICATED BY UNIDIRECTIONAL SOLIDIFICATION

S. Abe¹, Y. Yokota², M. Yoshino¹, A. Yamaji¹, H. Sato², Y. Ohashi², S. Kurosawa², K. Kamada², A. Yoshikawa³

¹Institute for Material Research, JAPAN, ²NICHE, Tohoku University, JAPAN, ³C&A corporation, JAPAN

Poor workability of some alloys with high functionalities increases the manufacturing cost in the processing. Therefore, we developed an alloy-micro-pulling-down (A- μ -PD) method which could fabricate alloy fibers from the melt directly. In our previous studies, we could fabricate Ir and Pt fibers from the melts by the A- μ -PD method. [1-2] Moreover, we could grow Co-Cr-Mo (CCM) alloys fibers with poor workability which had been applied as a stent and dental implant. [3] In the study, the ratio of a fcc-g phase in the CCM fiber grown by the A-m-PD method increased with increasing growth rate due to the increase of cooling rate. The fcc-g phase improves tensile ductility and cold workability. Therefore, in this study, we tried to increase the cooling rate during the fabrication of the CCM fiber to reveal the effects of cooling rate on microstructures and mechanical properties of the CCM alloy and achieve the further improvements of mechanical properties. Starting materials, Co, Cr and Mo powders (<3N), were mixed according to the chemical composition of Co-28Cr-6Mo. The mixed powder was pelletized by arc melting furnace under Ar atmosphere. The pellets were set in an alumina crucible with a hole of ϕ 2 mm or ϕ 1.1 mm at the center of the bottom. After melting of the pellets by a high-frequency induction heating under Ar+3%H₂ atmosphere, a CCM fiber was fabricated using an Ir seed. After the mechanical polishing of the fabricated fiber, surface was treated by a cross section polisher and the microstructure was observed using an electron back scattered diffraction pattern (EBSD). In addition,

mechanical properties were investigated by tensile tests. Figure 1 shows phase maps of a $\phi 2$ mm and a $\phi 1.1$ mm CCM fibers grown at 5 mm/min. The CCM fibers were composed of the fcc- γ and hcp- ϵ phases. By the thinning of fiber diameter, ratio of the fcc- γ phase increased due to the increase of cooling rate. Figure 2 shows the maximum tensile stress of the CCM fibers fabricated with different growth rates and diameter. The $\phi 1.1$ mm CCM fibers grown at 5 mm/min indicated the highest maximum tensile stress. Detail results of microstructures and mechanical properties on CCM fibers grown at various growth rates, diameters and temperature gradients will be reported.



[1] Y. Yokota, *et al.*, *Adv. Eng. Mater.* **20** (2018) 1700506 [2] T. Nihei, *et al.*, *J. Cryst. Growth* **468** (2017) 403 [3] S. Abe, *et al.*, *MS&T* (2018) P3-81

8:15 AM - 8:30 AM

CHIRAL IDENTIFICATION AND CHIRAL CRYSTAL GROWTH OF DIFFICULT ORGANIC MOLECULES

C. Mcmillen, B. Brummel, K. Lee, D. Whitehead, J. Kolis
Clemson University, SC, UNITED STATES OF AMERICA

Since the time of Pasteur's groundbreaking work on sodium ammonium tartrate crystals, the study of molecular chirality has become a centerpiece in fields of chemistry, crystallography, medicine, and materials science. Incredible effort is devoted to identifying the absolute stereochemistry of molecules, and ultimately, resolving enantiomers and diastereomers. This often requires elegant, specialized techniques that do not necessarily translate across a wide range of candidate systems. Here, we present a new, robust approach to chiral identification and resolution using a fusion of crystal growth, crystallography, and synthetic organic chemistry. Ubiquitous substrates such as alcohols and amines, which themselves resist crystallization, are converted to sulfates, and then crystallized as salts using simple counterions such as guanidinium. Crystals of the sulfate salts are ideal for straightforward absolute structure determination using X-ray crystallography. The approach can be extended to diastereomers by using a counterion that itself has stereocenters, such as chiral guanidine derivatives. The resulting hydrogen bonding networks enable the growth of very large crystals. Extended crystal growth can then be used as an approach to chiral or diastereomeric resolutions, and the resolved salts returned to their original substrate via hydrolysis. Several case studies of systems that otherwise resist crystallization are described, as well as the complete, routine identification of all stereocenters in complex molecules.

8:30 AM - 8:45 AM

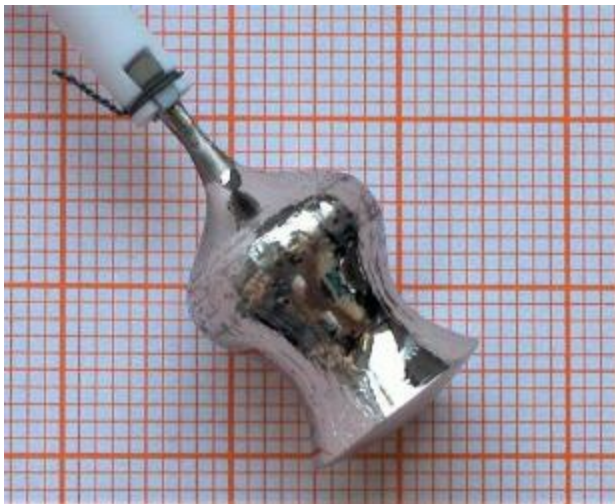
TERNARY PHASE DIAGRAM STUDIES AND SINGLE CRYSTAL GROWTH OF SOLID SOLUTIONS IN THE GA-PD-SN SYSTEM FOR BASIC RESEARCH IN HETEROGENEOUS CATALYSIS

K. Bader, A. Dorner, P. Gille

LMU München, GeoDepartment, Crystallography, GERMANY

According to recent studies, intermetallic compounds may have better

catalytic properties than presently used industrial catalysts that are based on elements or substitutional alloys [1]. Those suffer diffusion and segregation under operation conditions, while intermetallics have structures with well-defined atomic sites. Therefore, they may have better long-term stability and considerably higher catalytic selectivity, according to the *active-site isolation concept* [2]. The intermetallic compounds GaPd and GaPd₂ have been found to be promising candidates for heterogeneous catalysis in hydrogenation processes, with catalytically active Pd sites, being well isolated. Both compounds have already been grown with the Czochralski technique from Ga-rich solutions in cm³-sized single crystals [3] which are being used for fundamental studies in surface physics and crystallography. GaPd₂ and the isostructural SnPd₂ crystallize in the Co₂Si structure type (*Pnma*) and form a complete solid solution series. Therefore, Ga substitution by Sn in GaPd₂ is a powerful approach to discriminate and understand catalytic properties, arising from either structural or electronic influences, by uncoupling these effects. Pure SnPd₂ cannot be grown from a liquid phase, but decomposes in a peritectoid reaction at 820°C [4]. Thus, ternary Ga_{1-x}Sn_xPd₂ crystal growth by the Czochralski method is expected to result in an upper limit for Sn substitution.



Due to first successful experiments on Ga_{1-x}Sn_xPd₂ the substitution of Ga by Sn in GaPd also came into focus. The end members GaPd (*P2₁3*) and SnPd (*Pnma*) can be grown from solution, but no complete miscibility is present. This study presents the results of a high number

of simple cooling pre-experiments in order to investigate parts of the unknown liquidus surface and the relevant tie-lines for crystal growth in the ternary Ga-Pd-Sn system and the resulting growth of well oriented, cm³-sized single crystals of Ga_{1-x}Sn_xPd₂ and Ga_{1-x}Sn_xPd by the Czochralski technique from (Ga,Sn)-rich solutions.

References [1] M. Armbrüster, R. Schlögl, Yu. Grin, *Sci. Technol. Adv. Mater.*, **15**, 1-17, 2014. [2] W.M.H. Sachtler, *Catal. Rev. Sci. Engin.*, **14**, 193-210, 1976. [3] J. Schwerin, D. Müller, S. Kiese, P. Gille, *J. Crystal Growth*, **401**, 613-616, 2014. [4] T.B. Massalski et al., *Binary Alloy Phase Diagrams*, ASM International, Ohio, 1990.

Acknowledgments: The authors are grateful to the Deutsche Forschungsgemeinschaft for financial support under grant no. Gl 211/15-1.

8:45 AM - 9:00 AM

LARGE-SIZED CRYSTAL GROWTH OF BACD(VO)(PO₄)₂ AND PB₂(VO)(PO₄)₂ BY THE SELF-FLUX BRIDGMAN METHOD

Z. Yan, S. Gvasaliya, A. Zheludev
ETH Zurich, SWITZERLAND

The family of layered vanadophosphates are one of the most intensively studied of the J₁-J₂ frustrated square lattice models, manifesting an novel quantum phases theoretically predicted as spin nematic state. In order to study the extrem geometric frustrations correlated with the spin lattice and chemical structure of the compounds and to better understand the exotic magnetic order underlying physics, achievement of single crystals large enough for being used in physical measurements is one of the biggest challenges. In principle, different members of the AB(VO)(PO₄)₂ (A,B=Pb, Sr, Zn, Cd, Ba and Ca) family need a different crystal growth condition to obtain large-sized and high-quality stoichiometric single crystals. In this paper we report on single crystal growth techniques of one of the most promising candidates of BaCd(VO)(PO₄)₂ with total mass up to 160 mg and one of the most studied members of Pb₂(VO)(PO₄)₂ with total mass up to 1500 mg using the self-flux Bridgman

technique. We present X-ray power diffraction, Laue diffraction and neutron diffraction rocking curves, showing the quality of both of our as-grown single crystals, as well as magnetic susceptibilities, magnetocaloric effect, low temperature specific heat and isothermal magnetization for $\text{BaCd}(\text{VO})(\text{PO}_4)_2$, revealing a low temperature phase; and inelastice neutron scattering for $\text{Pb}_2(\text{VO})(\text{PO}_4)_2$, revising this compound is less geometrically frustrated than previous report.

[1] K. Y. Povarov, V. K. Bhartiya, Z. Yan, A. Zheludev, Thermodynamics of a frustrated quantum magnet on a square lattice, Phys. Rev. B 99 (2019) 024413. [2] S. Bettler, F. Landolt, . M. Aksoy, Z. Yan, S. Gvasaliya, Y. R. Qiu, K. E. Beauvois, S. Raymond, A. Pono-maryov, S. Zvyagin, A. Zheludev, Magnetic structure and spin waves in the frustrated ferro-antifeero magnet $\text{Pb}_2\text{VO}(\text{PO}_4)_2$, <https://arxiv.org/abs/1902.11172>.

9:00 AM - 9:15 AM

AQUEOUS SOLUTION GROWTH AT 200°C AND CHARACTERIZATIONS OF PURE, ^{17}O - AND D-BASED HERBERTSMITHITE $\text{ZnCu}_3(\text{OH})_6\text{Cl}_2$ SINGLE CRYSTALS

M. Velazquez¹, F. Bert², P. Mendels², D. Denux³, P. Veber⁴, M. Lahaye⁵, C. Labrugère⁵

¹SIMaP UMR 5266 CNRS-UGA-G INP, FRANCE, ²Laboratoire de Physique des Solides, CNRS, Univ. Paris-Sud, Université Paris-Saclay, FRANCE, ³ICMCB, UMR 5026 CNRS-Université de Bordeaux-Bordeaux INP, FRANCE, ⁴Institut Lumière Matière UMR 5306, FRANCE, ⁵PLACAMAT, UMS3626, CNRS-Université Bordeaux, FRANCE

Spin liquids represent an exotic class of quantum matter where, despite strong exchange interactions, spins do not order or freeze down to zero temperature [1]. While well established in 1D for e.g. the Heisenberg spin $S = \frac{1}{2}$ antiferromagnetic chain, it has been recognized that in higher dimension, frustration is the major ingredient to stabilize such a class of exotic states, which generates a true playground for novel concepts. In two dimensions, this physics is best represented by the now famous example of the **Kagome Heisenberg**

AntiFerromagnetic (KHAF) Hamiltonian. On the kagome lattice, frustrated triangles share corners and there is a consensus that the threefold combination of such a reduced connectivity, of $S=1/2$ quantum spins and of frustration leads to a **Quantum Spin Liquid (QSL)** state with fractional excitations. After 15 years of exploration, herbertsmithite $ZnCu_3(OH)_6Cl_2$ was the first true and now emblematic QSL [2]. Here, $S=1/2$ spins are organized in perfect, well decoupled, 2D kagome layers with large nearest neighbor interactions $J \sim 190$ K dominating any other one by more than a factor of 20. In this work, we have investigated the influence of temperature and temperature cycling on the growth rate, volume and Cu_{Zn}^x antisite disorder of the single crystals, characterized by powder XRD, XPS, EPMA/WDS, ICP/AES, coupled TGA-MS and magnetic susceptibility. The morphology of the crystals was characterized by the Laue method, and a correlation between the Cu_{Zn}^x antisite disorder and the c-lattice parameter was established. [1] L. Balents, *Nature*, **464**, 199 (2010). [2] M. Shores, E. Nytko, B. Barlett and D. Nocera, *J. Am. Chem. Soc.*, **127**, 13462 (2005).

9:15 AM - 9:30 AM

ELECTROPHYSICAL PROPERTIES OF $Ga_{0.03}In_{0.97}Sb$ SINGLE CRYSTALS GROWN IN ULTRASONIC FIELD

G.N. Kozhemyakin

Shubnikov Institute of Crystallography of Federal Scientific Research Center "Crystallography and Photonics" of Russian Academy of Sciences, RUSSIAN FEDERATION

$Ga_xIn_{1-x}Sb$ solid solutions with a band gap from 0.73 to 0.17 eV are of great interest for optoelectronic devices, because their wavelength can be varied in the range of 1.7–7 μm [1,2]. However, a polycrystalline growth, axial and radial compositional inhomogeneities etc., impede the achievement of high electrophysical properties of $Ga_xIn_{1-x}Sb$ crystals. To reduce of the components inhomogeneity in the single crystals, Czochralski method with ultrasound can be employ [3]. $Ga_xIn_{1-x}Sb$ single crystals were grown by a modified Czochralski method using InSb seed single crystals in the $\langle 111 \rangle_B$ direction. The melt mass did not exceed 80 g. The pulling and rotation rates of the

crystals were 3 mm/h and from 1 to 10 rpm, respectively. A fused silica crucible was not rotated. Ga, In and Sb of 6N were used as source materials. The crystals were pulled in high purity Ar. Ultrasound at frequencies of 0.72 and 1.44 MHz was introduced into the melt from a piezotransducer through a fused silica waveguide. The direction of ultrasonic waves was parallel to the pulling axis. These crystals were cut from regions grown without and with ultrasound, parallel to the pulling axis using electrical discharge machine. The measurements of carrier concentration in $\text{Ga}_x\text{In}_{1-x}\text{Sb}$ single crystals were carried out using Hall effect. Magnetic field induction was equal to 0.18 T. 4-point probe was used to perform the resistivity measurements. The occurring voltage in the crystal samples was measured using two cope probes. The resistivity has a tendency of reducing in the samples grown in the presence of ultrasound. Simultaneously the carrier mobilities in samples of crystal pulled with ultrasonic field increase on 23÷46 %. The reduction of the resistivity and increase in the carrier mobility in the crystal samples grown under ultrasound can be explained by the decrease in carrier diffusion due to compositional homogeneity. Additionally, the measured thermo emf in these crystal samples was larger on 22÷32 % than that in the crystal samples obtained without ultrasound. [1] R. Pino, Y. Ko and P.S. Dutta, *J. Appl. Phys.*, **2004**, V. 96, 5349-5352. [2] S. Collins, A.G. Birdwell, R. Glosser, *J. Appl. Phys.*, **2002**, V. 91, 1175-1178. [3] G.N. Kozhemyakin, *J. Cryst. Growth*, **1995**, V. 149, 266-268.

9:30 AM - 9:45 AM

GROWTH FROM THE MELT, STRUCTURE AND PROPERTIES OF $(\text{ZrO}_2)_{1-x}(\text{Gd}_2\text{O}_3)_x$ SOLID SOLUTION CRYSTALS

A.V. Kulebyakin¹, M.A. Borik¹, V.T. Bublik², E.E. Lomonova¹, F.O. Milovich², V.A. Myzina¹, V.V. Osiko¹, P.A. Ryabochkina³, N.Y. Tabachkova²

¹Prokhorov General Physics Institute of the Russian Academy of Sciences, RUSSIAN FEDERATION, ²National University of Science and Technology «MISIS», RUSSIAN FEDERATION, ³Ogarev Mordovia State University, RUSSIAN FEDERATION

Zirconia based materials have a variety of unique physicochemical,

electrical and mechanical properties including high strength, hardness, impact toughness, wear resistance, low coefficient of friction, high melting point, chemical inertness, low heat conductivity and biocompatibility. These properties account for the wide range of applications, from wear resistant bearings to medical and surgical instruments. The aim of this work is to study the effect of the stabilizing impurity concentration on the phase composition, structure and properties of partially stabilized zirconia (PSZ) crystals. Gadolinium oxide stabilized (concentration range 2.0–4.0 mol.%) PSZ crystals were grown by directional melt crystallization in a cold crucible at a 10 mm/h crystallization rate. The chemical composition of the crystals was determined by X-ray spectral analysis under a JEOL 5910 LV electron scanning microscope. Analysis of the gadolinium oxide distribution on the length of the crystal showed that the composition of all the samples is homogeneous and impurity concentration practically corresponds to its content in the starting material. The phase composition and crystal structure of the material was studied using X-ray diffraction, Raman spectroscopy and transmission electron microscopy. The studies showed that the PSZ crystals have two tetragonal phases (t and t') with different tetragonal distortion degrees. TEM studies showed that the crystals of all compositions are a complex twinned domain structure, which is formed during the transformation from the cubic to the tetragonal phase during the cooling of the crystal. Mechanical characteristics were measured by vickers indentation technique. The microhardness and fracture toughness for different crystallographic planes have been tested by indentation with different indenter diagonal orientations. The maximum fracture toughness has been obtained on the specimen of $ZrO_2 - 2.8 \text{ mol.}\% \text{ Gd}_2O_3$ crystal for the $\{100\}$ plane and the $\langle 100 \rangle$ indenter diagonal orientation. In addition, the effect of high-temperature annealing in air (1600 °C) and in vacuum (2100 °C) on the characteristics of the crystals was investigated. The work was supported by research grants № 18-13-00397 of the Russian Science Foundation.

9:45 AM - 10:00 AM

EFFECT OF GROWTH AMBIENCE AND STUDIES ON

HEXAGONAL $Dy_{(1-x)}Y_{(x)}MnO_3$ SINGLE CRYSTALS

P..A. Kumar¹, **A.B. Govindan**¹, S. Ganesamoorthy²

¹SSN College of Engineering, INDIA, ²Indira Gandhi Centre for Atomic Research, INDIA

Rare earth manganites $RMnO_3$ ($R = La^{3+} - Lu^{3+}, Y^{3+}$) represent a fascinating family of multiferroic compounds due to an interplay between their charge, lattice and spin. The possible application of these materials is in random access memory devices based on the magnetoelectric coupling driven by the prospect of controlling polarization by the magnetic field and magnetization by an electric field. Among these compounds, $DyMnO_3$ can be crystallized in both orthorhombic ($Pnma$) and hexagonal ($P6_3cm$) structures by carefully choosing a growth ambience. We report here, a systematic study on the crystal growth of the hexagonal $Dy_{(1-x)}Y_{(x)}MnO_3$ ($x = 0.0, 0.25, 0.50, 0.75,$ and 1.00) by optical floating zone technique. High-quality single crystals (Fig. 1(a)) were successfully obtained and the growth conditions were optimized very carefully. The atmosphere pressure, growth rate, feed/seed rotation, and growth atmosphere are found to be the most important parameters. Powder X-ray Diffractions data clearly demonstrated the grown $Dy_{(1-x)}Y_{(x)}MnO_3$ ($x = 0.25, 0.50, 0.75,$ and 1.00) single crystals are single phase. All the diffraction peaks were indexed to hexagonal structure (Fig. 1(b)) with space group $P6_3cm$ (#185). The Rietveld refinement was performed using the FULLPROF program. Quality of the all grown single crystals was ascertained by Laue pattern. The magnetic properties of these crystals were characterized by magnetic susceptibility, magnetization vs magnetic field (M-H) loop and specific heat measurements.



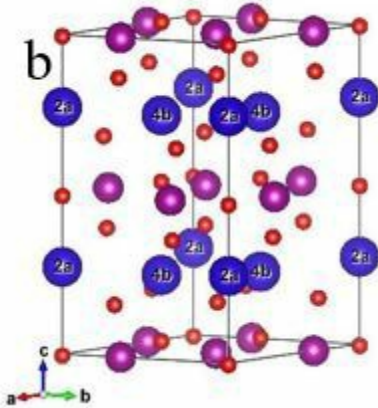


Fig. 1(a) Photograph of as-grown hexagonal DyMnO_3 single crystal. (b) Crystal structure of hexagonal DyMnO_3 . Blue, pink and red balls represent the Dy^{3+} , Mn^{3+} and O^{2-} ions. Dy^{3+} occupy the 2a and 4b Wyckoff positions shown in the figure.

Friday, August 2, 2019

8:00 AM - 10:00 AM

Fundamentals of Crystal Growth: Colloids and Crystal Growth in Solution

Location: Torrey Peak II-IV

Session Chair(s): Peter G. Vekilov, Mu Wang

8:00 AM - 8:30 AM

NUCLEATION, GROWTH AND PERFECTION OF COLLOIDAL CRYSTALS

F. Spaepen

School of Engineering and Applied Sciences, Harvard University,
UNITED STATES OF AMERICA

Colloidal particles in suspension form liquid, crystalline and glassy phases similar to those formed by atoms. Since the particles are “fat” ($\sim 1\mu\text{m}$) and “slow” ($\sim 10\text{Hz}$), they can be individually tracked in space and time by confocal microscopy. Dense colloidal systems therefore serve as “analog computers” to study the dynamics of condensed matter, and provide a direct look, at the particle level, of complex phenomena, such as phase transformations, atomic transport and plastic deformation.

For example, it is possible to observe the nucleation of crystals from the liquid directly: the formation or dissolution of crystalline fluctuations, the presence subcritical and supercritical nuclei and the large variations in the shape of the nuclei. Nevertheless, there remain serious discrepancies between the nucleation frequencies measured in these experiments and in computer simulations with identical potentials, such as hard-sphere.

It is possible to study the motion of a crystallization front under highly controlled conditions by confining the colloids in an "electric bottle", a device that concentrates them by dielectrophoresis when an electric field gradient is applied. It is possible to measure the individual jump frequencies whereby particles go back and forth between the liquid and the crystalline phase, and hence characterize the crystallization and melting kinetics. For simple crystals, such as f.c.c. and b.c.c., the kinetics are purely Brownian, and hence allow a direct look at an analog of collision-limited growth in atomic crystals.

It is possible to grow large single crystals by depositing the colloids on patterned templates. One of the phenomena that can be directly observed is the growth of misfit dislocations, with energetics and kinetics that correspond in detail to those observed in epitaxial growth of atomic crystals. The template technique also makes it possible to create tailor-made grain boundaries. From their positional fluctuations, we can determine the grain boundary stiffness and its dependence on the crystallography. The latter technique has also been applied to large, random high-angle boundaries in polycrystals.

[1]

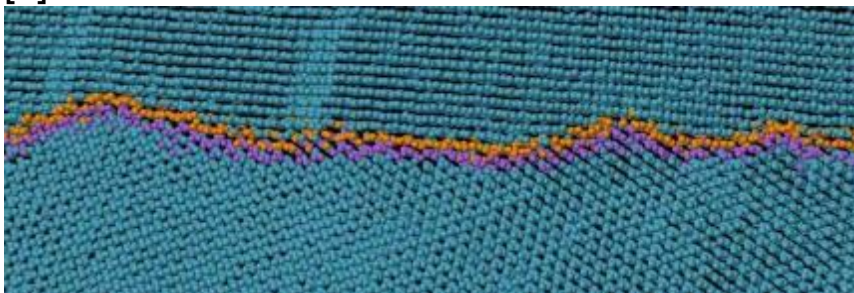


Figure 1: High-angle grain boundary between two hard-sphere colloidal crystals

8:30 AM - 8:45 AM

ANALYSIS OF DIFFUSIONLESS TRANSFORMATIONS IN

COLLOIDAL CRYSTALLITES

T. Sinno, Y.K. Lee, X. Li, C. Reina, J.C. Crocker

University of Pennsylvania, PA, UNITED STATES OF AMERICA

The existence of diffusionless, or displacive, transformations in binary colloidal crystals comprised of DNA-functionalized particles has been demonstrated experimentally in both micron- and nanoscale colloidal assemblies [1,2]. For example, in binary systems of 'A' and 'B' particles, CsCl (bcc) superlattice crystallites are homogeneously nucleated when A-B attractions become sufficiently strong. When A-A and B-B attractive interactions are then increased, CsCl crystallites are observed to spontaneously transform into a higher-coordinated CuAu (fcc) phase [2]. Different transformations have been observed as the particle size ratio and interaction combinations have been varied. The unexpected ubiquity of diffusionless transformations in these assemblies is interesting because it offers the possibility of increasing the diversity of accessible structures with spherically-symmetric, short-ranged interactions. One puzzling feature of these transformations is observation that the child configurations are generally not consistent with thermodynamic expectations: out of many energetically degenerate child configurations resulting from many equivalent transformation pathways, the experimental observation is typically that a single configuration is selected. Indeed, molecular dynamics or Brownian dynamics simulations lead to this expected outcome, generating child configurations that exhibit stacking disorder, at odds with the experiments. Jenkins et al. [3] have put forth the suggestion that hydrodynamic drag is responsible for this effect. Here, we study further this hypothesis in detail by first performing detailed simulations of the CsCl \rightarrow CuAu transformation while accounting for hydrodynamic interactions. We employ Multi-particle Collision Dynamics (MPCD) coupled with molecular dynamics (MD) to explore the role of long-range hydrodynamic interactions as a function of the solvent viscosity [4]. We also explore the role of short-ranged interactions by including a lubrication correction to the MPCD dynamics. Next, we employ Principal Component Analysis of the fluctuations of transformable crystallites to understand the nature of how hydrodynamic correlations act to bias diffusionless transformations in colloidal crystallites. We suggest that understanding

the 'softness' of certain assemblies provides another target for engineering self-assembling systems. [1] Casey, M.T., Scarlett, R.T., Rogers, W.B., Jenkins, I., Sinno, T. and Crocker, J.C., 2012. Driving diffusionless transformations in colloidal crystals using DNA handshaking. *Nature communications*, 3, p.1209. [2] Zhang, Y., Pal, S., Srinivasan, B., Vo, T., Kumar, S. and Gang, O., 2015. *Nature materials*, 14(8), p.840. [3] Jenkins, I.C., Casey, M.T., McGinley, J.T., Crocker, J.C. and Sinno, T., 2014. *Proceedings of the National Academy of Sciences*, 111(13), pp.4803-4808. [4] Malevanets, A. and Kapral, R., 1999. *The Journal of chemical physics*, 110(17), pp.8605-8613.

8:45 AM - 9:00 AM

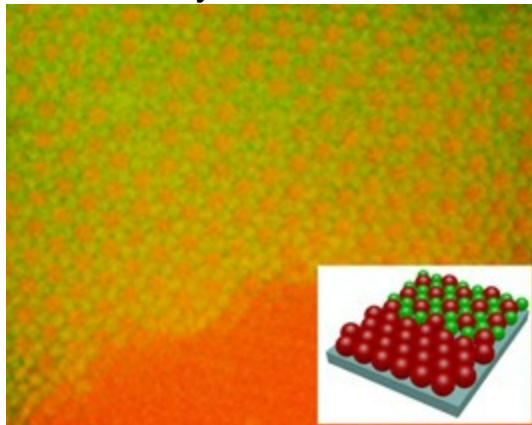
GROWTH MECHANISM OF BINARY COLLOIDAL CRYSTALS

J. Nozawa, H. Niinomi, J. Okada, S. Uda

Institute for Materials Research, Tohoku University, JAPAN

Diverse structures of colloidal crystals are now significantly demanded from various application fields of colloidal crystals, which is owing to their unique and useful optical properties. Binary colloidal crystals are promising materials to meet this requirement since it exhibits a rich structural diversity. However, to grow large size of binary colloidal crystals with high crystallinity is quite difficult, and, in contrast to single component system, the growth mechanism is poorly understood. In this study, in-situ observation is carried out on growing binary colloidal crystals and the detailed growth mechanism is discussed. Fluorescent polystyrene particles are employed in the experiment, in which various particle size (400 to 700 nm) are used. Crystallization of colloidal crystals is induced by depletion attraction by adding sodium polyacrylate. There are numbers of reports on synthesizing of binary colloidal crystals by various methods. In the binary system with attractive interaction, eutectic reaction for two components (A and B) was reported, here A and B are denoted to large and small particles, respectively. By employing certain particle ratio, strength of attractive interaction and composition (number ratio of A and B), AB_2 structure is formed with depletion attraction. We have found several features on the growth of binary colloidal crystals. First, it grows on substrate.

Figure shows 1st layer of AB₂ structure (A: red, 700 nm, B: green, 500 nm) nucleated on the edge of another crystals of an A phase. The AB₂ crystals also grow on crystals of a B phase. The specific crystallographic orientations between those crystals are recognized. Therefore, heteroepitaxial growth is found to occur for growth of AB₂ structure. Second, growth rate of binary colloidal crystals is quite small compare to that of single component system under the same particle concentration. This is attributed to complex structure of the crystals, which requires each particle to be incorporated to their own site in the crystal. Third, cluster formation at the surface of growing crystals is recognized. The ordered structure composed only of B particles is formed at surface of growing AB₂ crystals. Particles of A are incorporated into the cluster to generate AB₂ structure. This process occasionally takes place to grow AB₂ crystals. These observations well contribute to understanding of overall growth mechanism of binary colloidal crystals. In particular, we believe that heteroepitaxy is useful technique to control nucleation and growth of the binary colloidal crystals.



9:00 AM - 9:15 AM

THE ATOMIC SCALE MECHANISM OF GROWTH ADDITIVES FOR NaCl

E. Vlieg, E. Townsend, W. Van Enckevort

Radboud University, Institute for Molecules and Materials,
NETHERLANDS

The role that additives play in the growth of sodium chloride is a topic which has been widely researched but not always fully understood at

an atomic level. Lead chloride (PbCl_2) is one such additive which has been reported to have growth inhibition effects on NaCl {100} and {111}, however no definitive evidence has been reported which details the mechanism of this interaction. In this investigation, we used the technique of surface x-ray diffraction to determine the interaction between PbCl_2 and NaCl {100} and the structure at the surface. We find that Pb^{2+} replaces a surface Na^+ ion, while a Cl^- ion is located on top of the Pb^{2+} . This leads to a charge mismatch in the bulk crystal, which, as energetically unfavourable, leads to a growth blocking effect. While this is a similar mechanism as in the anticaking agent ferrocyanide, the effect of PbCl_2 is much weaker, most likely due to the fact that the Pb^{2+} ion can more easily desorb. Moreover, PbCl_2 has an even stronger effect on NaCl {111}.

9:15 AM - 9:30 AM

MONONUCLEAR AND POLYNUCLEAR GROWTH OF ELECTROLYTE CRYSTALS FROM SOLUTION

H.E.L. Madsen

Chemistry Department, University of Copenhagen, DENMARK

In crystal growth studied by recording rate of precipitation, polynuclear kinetics, also known as birth-and-spread growth, is typically observed during the initial stage, often combined with spiral growth (BCF mechanism), which takes over as saturation is approached.

Mononuclear growth, in which only one growing surface nucleus is present on any crystal face and at any time, is rather uncommon. The two mechanisms may be distinguished from the kinetic analysis, obtaining edge free energy. If the values found for this parameter is significantly higher than expected and highly variable, the explanation may be mononuclear kinetics. The main difference is a factor 3 in the denominator of the exponential in the expression for polynuclear growth, being absent in the other case. Evidently the crystal must be sufficiently large to accommodate more than one growing surface nucleus at a time on any face. This explains why reports on mononuclear growth are infrequent. In a study of crystallization of iron(III) phosphate (strengite), which forms very small crystals, both mononuclear and polynuclear kinetics was observed. In 3 cases

transition from the former to the latter occurred at intermediate supersaturation. Average edge free energies from a number of experiments were found a few percent higher in the mononuclear case. It is shown that the electrostatic energy for attachment of an ion to a small crystal is higher, i.e. less negative, than that for a large crystal, thus leading to a higher edge free energy for nuclei on small crystals., .

9:30 AM - 9:45 AM

OBSERVATION OF SOLUTION STRUCTURES AND SUPERCOOLING SUPPRESSION IN SEMICLATHRATE HYDRATE RECRYSTALLIZATION

T. Sugahara¹, H. Machida², I. Hirasawa³

¹Osaka University, JAPAN, ²Panasonic Corporation, JAPAN,

³Waseda University, JAPAN

The semiclathrate hydrates composed of quaternary onium salts and water have attracted much attention as phase change materials. A large degree of supercooling, however, is necessary to form semiclathrate hydrates. For the practical applications, to suppress supercooling is indispensable. One of the effective methods is the utilization of "memory effect", which is a kind of temperature hysteresis in the recrystallization. Different theories have been proposed about the mechanism of the memory effect: one is the residual hydrogen-bonded structures in the aqueous solution resulting from hydrate dissociation. The other is the existence of anomalous dissolved gas or ultra-fine bulk bubbles. In the present study, we observed the existence of solution structures in the aqueous solution formed by the semiclathrate hydrate with (SEM + "freeze-fracture replica method") and other analytical methods. The relation between the observed solution structures and supercooling suppression was investigated. The memory effect in the semiclathrate hydrate recrystallization is derived from the residual clusters of 10-20 nm, which exist in the aqueous solution after complete hydrate dissociation.

9:45 AM - 10:00 AM

DETACHED GROWTH PHENOMENON AND THE FUNDAMENTAL

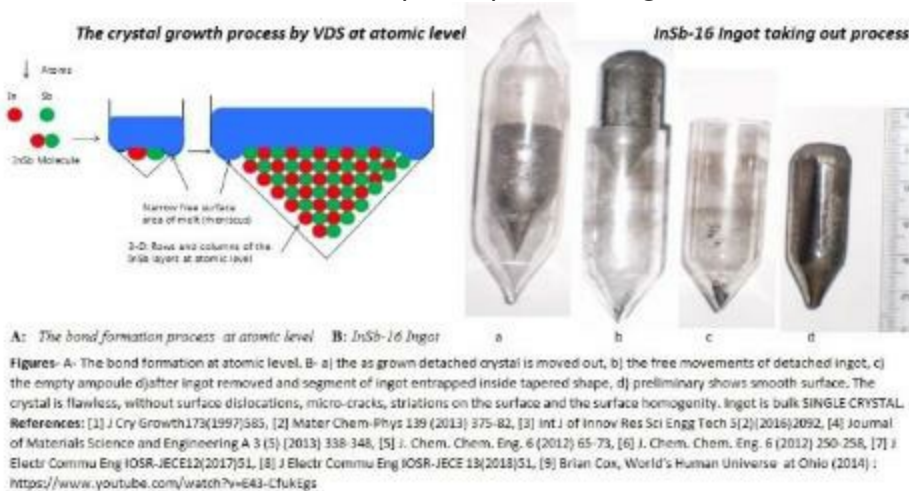
SCIENCE BEHIND: NOVEL CRYSTAL GROWTH PROCESS IN VERTICAL DIRECTIONAL SOLIDIFICATION BY SLOW FREEZING

D. Gadkari

Freelance Research and Consultant, Crystal Growth and Technology,,
INDIA

Since 1993, the research was focused on high-quality crystal growth by vertical directional solidification (VDS) [1]. The VDS process for solidification has been reliably implemented on earth for the Sb-based materials sealed in vacuum 10^{-5} torr (0.1MPa) inside an ampoule. The deleterious interactions between growing crystal and the ampoule wall was eradicated. The crystals with unprecedented elevation of structural perfection achieved by reduced buoyant thermo-gravitational convection (10^{-2} - 10^{-3} order), and concentration difference into melt [2]. In spite of the conditions in space, the entire detached solidification of Sb-based crystals were practical on Earth by VDS. The physical properties showed highest than the crystal grown ever [5,6], and p-n junction, Schottky diode and MOS structures fabrication on Sb-based VDS-substrates showed lower leakage (dark) current <0.1 nA at 300K [7,8]. The universal detached phenomenon: A solid crystal detaches serendipitously by apparition of a gap by the conjuring entire crystal [4]. In a vacuum, all objects fall with same rate, if gravity and acceleration is constant [9] as the concept of no gravitational force in vacuum as the bodies have weightlessness. This concept, we would study the influence of growth parameters in a vacuum by VDS in terrestrial lab. In view of this, the crystal growth in sealed ampoule acts as a vacuum chamber in terrestrial lab. A crystal grown away from the ampoule wall due to the influence of thermo-capillary influence and cohesive energy, as effect of a narrow free surface area (meniscus) forms. Moreover, the three phase lines as triple-point (TPL), Solid-Liquid-Gas phases on crystal periphery form. A fundamental growth process, these concepts assist Indium (In) and Antimony (Sb) molecules attract to form InSb bonds near solidifying front under cohesive energy Fig-A, and for the detached ingot taken out of ampoule Fig-B. In VDS, the seven furnace temperature steps growth profile, five self controlled process, five growth parameters, three type of growth, three type of conversion, three gap variations, which promoted entire detached solidification by slow freezing [3].

Investigations in VDS, i) the ultra-high crystal quality, micro and macroscopic homogeneity of bulk single crystal correspond to the diffusion mass transfer (DMT) and the heat mass transfer (HMT), and ii) the uniformity and homogeneously composition reveals the crystal growth rate correspond to the diffusion transfer condition (DTC) and heat transfer condition (HTC), investigations are confirmed.



Friday, August 2, 2019

8:00 AM - 10:00 AM

Modeling of Crystal Growth Processes V

Location: Crestone I, II

Session Chair(s): Daniel Vizman, Jochen Friedrich

8:00 AM - 8:30 AM

MODELING THE OPTICAL FLOATING ZONE CRYSTAL GROWTH SYSTEM FOR MATERIALS DISCOVERY

S.S. Dossa¹, J.F. Mitchell², J.J. Derby¹

¹University of Minnesota, MN, UNITED STATES OF AMERICA,

²Argonne National Laboratory, IL, UNITED STATES OF AMERICA

Optical floating zone (OFZ) crystal growth furnaces are powerful tools to grow single-crystal samples of materials that have never before been synthesized, a necessary step in the discovery of new materials with novel properties. However, full utilization of these novel crystal growth systems is hindered by operational challenges brought on by nonlinear, strongly coupled phenomena and a lack of understanding of

their underlying physical interactions. Indeed, a skilled operator is often an essential element for the successful growth of a new material in a reasonable time frame. We discuss model development and finite-element simulations for the OFZ crystal growth system. Model validation results are presented, comparing predictions to experimental results for the growth. We are particularly motivated to understand system behavior under very high pressures (up to 300 bar). Growth under such conditions offers numerous advantages over traditional systems by allowing for increased compositional control via mass exchange between the melt zone and surrounding gas and by providing access to new regions of phase space for growth. However, these new experimental parameters can further complicate system behavior, which we desire to better understand via model simulations. Finally, we discuss plans to deploy of our model as a user-friendly software package for experimental practitioners to aid in growth of novel materials.

8:30 AM - 8:45 AM

NUMERICAL STUDIES ON ASYMMETRIC THREE-PHASE LINE IN THE FLOATING ZONE SILICON

X. Han, S. Nakano, X. Liu, H. Harada, Y. Miyamura, K. Kakimoto
Research Institute for Applied Mechanics, Kyushu University, JAPAN
A numerical calculation has been carried out to study the asymmetric heat transfer, fluid flow and three-phase line in the floating zone (FZ) silicon crystal growth. In the FZ method, a needle-eye inductor is used to grow the large-diameter (>100 mm) single crystal silicon. The needle-eye inductor has one main slit and three side slits. This asymmetric configuration induces the asymmetric heating on the free surface of the silicon melt and three-phase line. In the previous study [1], spillage down of melt and deflection of three-phase line have been observed during the crystal growth because of inhomogeneous heating. To investigate the effect of asymmetric heating on the deflection of three-phase line, 3D global model considering electromagnetic (EM) and heat transfer has been developed [2]. Fig. 1 shows that the current density distribution along the three-phase line is not homogeneous as a result of existence of slits. The asymmetric current density caused asymmetric heating and deflection of three-

phase line. In Fig.2, the deflection of three-phase line is calculated to compare with the experimentally observed results [1]. Calculation results provide a similar trend with experimental results that along the rotation direction, the three-phase line descends quickly and ascends slowly below the current supplies. The inhomogeneous local growth rate at the three-phase line causes the asymmetric deflection of the three-phase line below the current supplies. When the local growth rate is lower than the pulling rate, the re-melting phenomenon occurs.

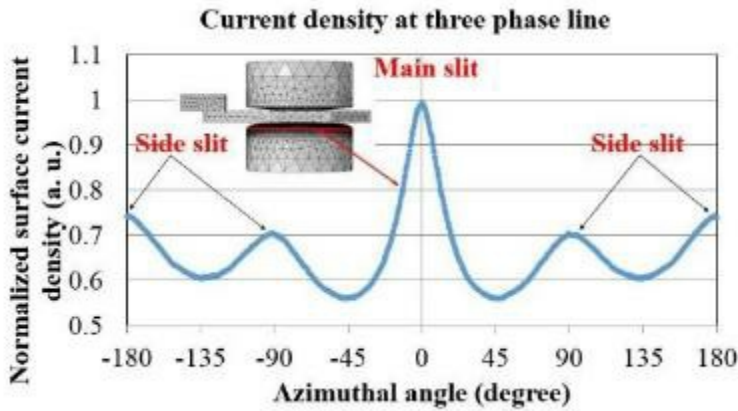


Fig. 1. Normalized surface current density distribution along the three-phase line.

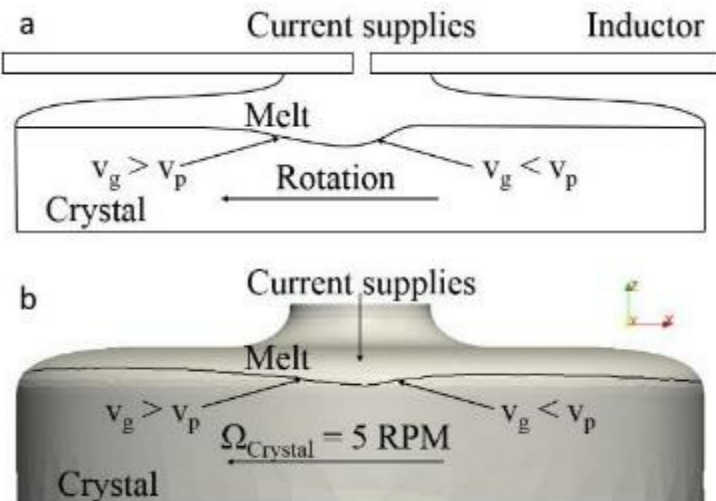


Fig. 2. Comparison of the shape of the three-phase line between experimental observation results [1] and calculation results.

Reference [1] R. Menzel, Growth Conditions for Large Diameter FZ Si Single Crystals, PhD thesis, (2013). [2] X.F. Han, X. Liu, S. Nakano, H. Harada, Y. Miyamura, K. Kakimoto, Crystal Research and Technology, (2018) 1700246. **Acknowledgement** This work was partly supported by the New Energy and Industrial Technology

Development Organization (NEDO) under the Ministry of Economy, Trade and Industry (METI)

8:45 AM - 9:00 AM

THE FLUCTUATION OF CRYSTAL/MELT INTERFACE INDUCED BY MELT FLOW INSTABILITY IN LARGE SIZE CZ-SI CRYSTAL GROWTH

J. Ding, L. Liu

Xi'an Jiaotong University, CHINA

The Czochralski (CZ) growth method is the current mainstream technology for growing high quality silicon crystals for electronic applications and solar cells. Nowadays, the melt volume and crucible diameter increase to grow large-size crystals in order to reduce costs. Many studies have found that the crystal/melt interface is the main factor affecting the crystal quality during crystal growth, which is directly influenced by the melt flow in the crucible. With the crucible size increase, the melt flow is always turbulence-characterized with velocity and temperature fluctuations. It is necessary to study the characteristics of unstable melt flow in the crucible, and investigate the influence mechanism of flow instability on the interface. In this work, the relationship between the undercooling and the growth rate is considered to develop a numerical model that can calculate the unstable melt flow and the fluctuant crystal/melt interface simultaneously. Based on this model, the fluctuations and spectral characteristics of temperature and velocity in the unstable melt flow are investigated. The influence mechanism of melt flow instability on the crystal/melt interface is clarified. The effects of some process parameters on the melt unstable flow and the fluctuation of the interface are discussed. Fig. 1 shows the effects of the crystal and crucible rotations on the fluctuation of the crystal/melt interface deflection, which is defined as the axial position difference between the center and the edge of the growing crystal. It shows that when the crystal co-rotates with crucible (Case C), the deflection of the interface is larger compared with the case of counter-rotation (Case B). However, the effect of the crystal rotation rate on the amplitude of interface shape fluctuation (the height of the box) is quite small.

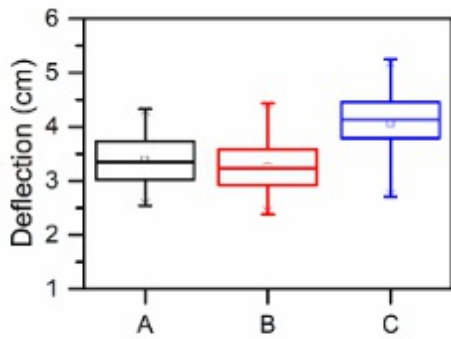


Fig. 1 The fluctuation of the crystal/melt interface deflection for different crystal and crucible rotations. (A: $\omega_{cry} = -8$ rpm, $\omega_{cru} = 6$ rpm. B: $\omega_{cry} = -12$ rpm, $\omega_{cru} = 6$ rpm. C: $\omega_{cry} = -12$ rpm, $\omega_{cru} = -6$ rpm.)

9:00 AM - 9:15 AM

EFFECT OF NUMERICAL PARAMETERS ON UNSTEADY MELT FLOW FEATURES AND IMPURITY TRANSPORT WITHIN A SIMPLIFIED CZ SI CRYSTAL GROWTH PROCESS GEOMETRY WITH EFFECT OF TRANSVERSE MAGNETIC FIELDS

S. Demina¹, A. Smirnov¹, **V. Kalaev**¹, G. Ratrieks², L. Kadinski², A. Sattler²

¹STR Group, Inc. – Soft-Impact, Ltd., RUSSIAN FEDERATION,

²Siltronic AG, GERMANY

Czochralski growth of 300 mm silicon crystals with transverse magnetic field is a main technology used worldwide for manufacturing of silicon wafers for microelectronics. Growing demand for quantity and quality of 300 mm silicon wafers requires silicon wafer and crystal manufacturers to use computer modeling to accelerate development and optimization of crystal growth processes. In this situation accuracy of computer models used for technology optimization becomes very critical. A model geometry of Cz Si growth process with high approximation orders for diffusive terms was presented in [1]. Such model geometry provides a good opportunity for benchmarking of different modeling tools and approaches. It was demonstrated that fourth approximation orders enable transition from symmetric to asymmetric melt flow structure with fully axisymmetric geometry and boundary conditions for the process with the effect of crystal rotation.

These results qualitatively agree with other works [2]. Previously presented results [1] have been obtained using steady approach. However, it is well known that the melt flow in processes with transverse magnetic fields is transient [3]. Melt flow determines transport of impurities in silicon melt due to low diffusion coefficient and high molecular Schmidt number. Thus, unsteady melt flow features might contribute to heat and mass transport. In the present work, the effect of unsteady melt flow features obtained with high approximation orders available in CGSim software package [4] is presented for the model geometry and its effect on impurity transport and melt/crystal interface shape in real cases is discussed. [1] S. Demina et al., abstract for IWMCG-9. [2] R. Yokoyama et al., J. Crystal Growth 468 (2017) 905-908. [3] R. Yokoyama et al., abstract for IWMCG-9. [4] <http://www.str-soft.com/products/CGSim/>

9:15 AM - 9:30 AM

LATTICE BOLTZMANN SIMULATION OF THREE-DIMENSIONAL INSTABILITIES IN CZOCHRALSKI CRYSTAL GROWTH

X. Xu¹, J. Zhu², B. Dai¹, J. Han¹

¹Center for Composite Materials and Structures, Harbin Institute of Technology, CHINA, ²Key Laboratory of Micro-systems and Micro-structures Manufacturing, Ministry of Education, Harbin Institute of Technology, CHINA

This study presents model extensions for a lattice Boltzmann (LB) approach to steady axisymmetric flow in a Czochralski crucible with three-dimensional perturbations. Based on the linear stability theory, the three-dimensional instability problem can be treated as a sequence of 2D-like problems by separating for different azimuthal modes. Axisymmetric lattice Boltzmann D2Q9 models are applied to simulate temperature fields and flow patterns for the base flow. Besides, the perturbation equations are solved through modifying the equilibrium distribution functions and inserting source terms into the two-dimensional LB equations. The numerical approach developed has been validated via a series of benchmark problems and then applied to a model corresponding to the melt flow in Czochralski crystal growth. The results of a numerical investigation of the effect of Prandtl number and the aspect ratio of the cylinder on the critical

Grashof number are presented.

9:30 AM - 9:45 AM

ADVANCES IN TURBULENCE MODELING OF HEAT AND MASS TRANSPORT DURING CZ SILICON CRYSTAL GROWTH

V. Artemyev¹, V. Kalaev¹, A. Smirnov¹, D. Borisov¹, A. Kuliev¹, P. Dold², R. Kunert², R. Turan³, O. Aydin³, I. Kabacelik³

¹STR Group, Inc. – Soft-Impact, Ltd., RUSSIAN FEDERATION,

²Fraunhofer CSP, GERMANY, ³iTechSolar, TURKEY

In present work we discuss modeling of turbulent heat and mass transfer during Czochralski (Cz) silicon crystal growth [1] for solar cells. The major problems of the solar cells quality are low minority carrier lifetime and light induced degradation (LID) [2]. LID is characterized by decreasing of the minority carrier lifetime, which could be related to oxygen and carbon content [3] in silicon melt and crystal. Complicated turbulent convective mass transport governs the distributions of impurities and dopants in the melt and in the crystal [4]. We have focused on the development of modified 2D Reynolds-averaged Navier-Stokes (RANS) approach for simulation of turbulent heat and mass transfer in the melt, using advanced 3D unsteady direct numerical simulation (DNS) data and available experimental measurements for validation and critical analysis. Conventional turbulence models usually fail to predict oxygen concentration in the melt mainly because turbulence anisotropy is not considered under the melt free surface and turbulent oxygen mass flux through the surface is dramatically overestimated. We suggest novel approaches for turbulence modeling: the new tensor of anisotropic turbulent viscosity M_t in the melt instead scalar m_t and a new boundary condition for the kinetic turbulent energy on the melt free surface to take into account turbulence generation by thermocapillary convection. The advanced chemical model built in CGSim software was used for prediction of oxygen and carbon transport in the melt. Several 9-inch silicon crystals were grown in EKZ 3500 facility of Fraunhofer CSP. Crystal wafers has been analyzed using the Fourier-transform infrared spectroscopy (FTIR) and the secondary ion mass spectrometry (SIMS) techniques. The carbon and oxygen content

were measured using the equipment of iTechSolar. The comparison between experimental and calculated results is discussed in detail. This work was supported by the Foundation for Assistance to Small Innovative Enterprises (FASIE, Russia) within ERA.Net RUS Plus Project, grant number ERA-RUS-41114 0042017. [1] V. Kalaev, A. Sattler, L. Kadinski, J. of Crystal Growth, V. 413, 12–16, 2015 [2] G. Hahn and A. Schonecker. New crystalline silicon ribbon materials for photovoltaics. J. Phys.: Condens. Matter, 16: R1615–R1648, 2004 [3] X. Liu, et al., J. of Crystal Growth, V. 499, 8-12, 2018 [4] A.N. Vorob'ev, A.P. Sidko, V.V. Kalaev, J. of Crystal Growth, V. 386, 226–234, 2014

9:45 AM - 10:00 AM

NEW COLD CRUCIBLE FOR SINGLE CRYSTAL GROWTH

K. Zaidat¹, H. Abouchi¹, S. Alradi¹, F. Baltaretu², M. Alradi¹, C. Garnier¹, G. Hasan¹, P. Petitpas¹, R. Ernst¹

¹SIMaP-EPM laboratory, INP Grenoble Alpes University, FRANCE,

²Technical University of Civil Engineering Bucharest, ROMANIA

Currently in the semiconductor industry more than 80% of silicon crystals are grown by the Czochralski (Cz) method. In this method, fused silica (SiO₂) crucibles and graphite heaters are used inside furnaces. The surface of the crucibles, which are in contact with the molten silicon, is gradually dissolved into the melt [1]. This reaction occurs during all the crystal growth process contributes to the presence of oxygen in silicon crystals and has a lot of consequence in the crystal quality (OSF, dislocation, precipitation of impurities...). In the eighties, Wenkus & Menashi[2] and Ciszek [3] used a cold crucible in order to decrease the oxygen contamination level. They have shown that it was possible to get a small single crystal (2.5 cm in diameter) with a very low oxygen contamination. They concluded also that one of the major problems, as yet unresolved in the use of the cold_[SEP]crucible for the growth of single crystals, is related to the stabilization and precise control of the melt flow. In this study, we have designed and modelled a new generation of cold crucible in order to stabilize the fluid flow induced by the Lorentz force inside the bulk. The model is implemented in COMSOL software where all the

physical aspect is taken into account.

Friday, August 2, 2019

8:00 AM - 10:00 AM

Nonlinear Optical and Laser Host Materials IV

Location: Red Cloud Peak

Session Chair(s): Kevin T. Zawilski, Peter G. Schunemann

8:00 AM - 8:15 AM

THEORETICAL INVESTIGATION ON THE MICROSCOPIC MECHANISM OF LATTICE THERMAL CONDUCTIVITY OF ZNXP₂ (X=SI, GE AND SN)

L. Wei

Shandong Academy of Science, CHINA

Thermal conductivity is an important physical parameter for the application of nonlinear optical single crystal materials. The underlying science of thermal transport behavior is not well established both experimentally and theoretically. In present work, we have studied the microscopic picture of lattice thermal conductivity of ZnXP₂ (X=Si, Ge, Sn), chalcopyrite ABC₂ type infrared optical crystals, by performing harmonic and anharmonic lattice dynamic method and phonon Boltzmann transport equation based on first-principle calculation. With the mass of atom X increased, the phonon frequencies and phonon group velocities of ZnXP₂ (X=Si, Ge, Sn) are shown not surprisingly decreased. Nevertheless, phonon lifetime of ZnXP₂ are unexpectedly increased, which is the governing mechanism for the increased thermal conductivity as 12.5 W/(m·k), 31.6 W/(m·k) and 35.4 W/(m·k), for ZnSiP₂, ZnGeP₂ and ZnSnP₂, respectively, at 300 K. The contributions of optical phonons (with the frequency below 150 cm⁻¹) to the total thermal conductivity are remarkable, reaching to 18%, 31%, and 34% for three compounds, due to the significantly increased phonon lifetime in the frequency range 50-150 cm⁻¹. To explore the physical insights of phonon lifetime and phonon anharmonicity, three-phonon scattering phase space and ELF analysis of X-P bond are provided. The results show that the covalent nature of X-P bonds is

enhanced with the increased mass of atom $X=Si, Ge, Sn$, which induce the reduction of three-phonon scattering phase space in the frequency range $50-150\text{ cm}^{-1}$, leading to the enhancement of phonon lifetime and thermal conductivity of $ZnXP_2$.

[1] L. Wei, X. P. Wang, B. Liu, Y. Y. Zhang, X. S. Lv, Y. G. Yang, H. J. Zhang, and X. Zhao, *AIP Advances* **5**, 127236 (2015).

[2] L. Wei *et al.*, *Phys Chem Chem Phys* **20**, 1568 (2018).

[3] L. Wei *et al.*, *Inorg Chem*, DOI: 10.1021/acs.inorgchem.8b03421 (2019).

8:15 AM - 8:30 AM

THE DESIGN AND SYNTHESSES OF HIGH PERFORMANCE IR NON D. Mei

Shanghai University of Engineering Science, CHINA

In recent years, IR nonlinear optical (NLO) materials have been widely used in laser frequency conversion, signal communication, optical parametric oscillator building, and other applications.¹ In our work, in order to solve the defects of traditional IR NLO materials, such as small second harmonic generation (SHG) and low laser damage threshold (LDT), we have made up for these defects through rational design based on the structures of the compounds. (1) Inspiring by the structure feature of oxide SrB_4O_7 that has large band gap and high LDT, we synthesized $BaAl_4S_7$ ² with the similar crystal structure. $BaAl_4S_7$ exhibits very large band gap and high LDT among the chalcogenide nonlinear optical materials. (2) Under the guidance of partly substituting Ge atoms for Ga atoms in the nonlinear optical material $LiGaS_2$ with high melting point, we designed and synthesized a new nonlinear optical crystal material $LiGaGe_2S_6$ ³ with low melting point and excellent NLO property. (3) We designed and synthesized a new quaternary Sn-containing sulfide $Sr_3MnSn_2S_8$,¹ it has a wide band gap and a strong SHG response. (4) Starting from the traditional compound $AgGaSe_2$, by introducing tetrahedron $SiSe_4$ into the structure to increase its optical band gap, and finally we obtained a IR NLO material $Ag_3Ga_3SiSe_8$ ⁴ with good property. **Reference** 1. C. Liu, D.-J. Mei, W.-Z. Cao, Y. Yang, Y.-D. Wu, G.-B. Li and Z.-S. Lin, *J.*

Mater. Chem. C, 2019, 7, 1146-1150. 2. D.-J. Mei, J.-Q. Jiang, F. Liang, S.-Y. Zhang, Y.-D. Wu, C.-T. Sun, D.-F. Xue and Z.-S. Lin, *J. Mater. Chem. C*, 2018, 6, 2684-2689. 3. D.-J. Mei, S.-Y. Zhang, F. Liang, S.-G. Zhao, J.-Q. Jiang, J.-B. Zhong, Z.-S. Lin and Y.-D. Wu, *Inorg. Chem.*, 2017, 56, 13267-13273. 4. D.-J. Mei, P.-F. Gong, Z.-S. Lin, K. Feng, J.-Y. Yao, F.-Q. Huang and Y.-C. Wu, *CrystEngComm*, 2014, 16, 6836-6840.

8:30 AM - 8:45 AM

ELABORATION OF LARGE LBO AND RTP CRYSTALS FOR NONLINEAR AND ELECTRO OPTIC APPLICATIONS

D. Balitsky¹, P. Villeval¹, D. Lupinski²

¹Cristal Laser S.A., FRANCE, ²CRISTAL LASER SA, FRANCE

In last years, many attempts were undertaken on development of high efficient and high damage resistant lithium triborate (LiB_3O_5 - LBO) and rubidium titanyl phosphate (RbTiOPO_4 - RTP). The way to damage resistant, homogeneous and low absorption crystals is adjustment of crystal growth conditions, using of high purity chemicals and successful crystallization of very large size boules. A large number of applications are based on such kind of nonlinear optics and Q-switching electro-optics [1,2,3]. Our attempts on crystal growth and processing of optical elements have allowed increasing of weight of LBO boules to 3 kg and even more, as well to get RTP Pockels cells of 9 mm² of aperture in serial production. The crystals are characterized by high optic homogeneity, high transmission and high damage resistance. Some main features of crystal growth and characterization of LBO and RTP will be discussed: - Relation of chemicals purity and absorption of crystals from NIR to UV and deep UV - Original test on thermal stability of RTP cells regarding the extinction ration in a wide range of temperatures: -50/+70°C - Use of the photo-thermal common path interferometry (PCI) [4] for characterization of RTP and LBO by absorption measurements at different wave lengths - Development of absorption measurement at 257 nm especially for characterization of deep UV grad β -BBO (BaB_2O_4) These tests allow selecting of crystals with the more suitable properties and help in adjusting of crystal growth conditions.



Left figure: RTP boule of 1200 g, for elaboration of 15x15x10 mm³ electro-optic elements. Right figure: LBO boule of 3200 g, up to 100 mm diameter of SHG wafers. [1] D.V. Balitsky, Ph. Villeval, D. Lupinski. Growth of large scale nonlinear LBO and electro-optic RTP crystals: state of the art and applications. Invited talk. Advanced Solid State Lasers Conference and Exhibition (ASSL), Berlin, GERMANY, 04-09 October 2015 [2] G Mennerat, J Rault, O Bonville, P Canal, P Villeval, B Rainaud. 115 J, 85% efficiency second harmonic generation in LBO.. Conference on Lasers and Electro-Optics, CPDA1, 2008 [3] Kokh, N. Kononova, G. Mennerat, Ph. Villeval, S. Durst, D. Lupinski, V. Vlezko, K. Kokh "Growth of high quality large size of LBO crystals for high energy second harmonic generation" Journal of Crystal growth, 312, 1774-1778, 2010 [4] A.L. Alexandrovski, M.M. Fejer, R.P. Route, and R.L. Byer. Photothermal absorption measurements in optical materials. Conference on Lasers and Electro-Optics 2000, San Francisco, CA,US, ISBN: 1-55752-634-6, 2000

8:45 AM - 9:00 AM

GROWTH OF HIGH-QUALITY SRB_4O_7 SINGLE CRYSTAL AND ITS OPTICAL PROPERTIES

Y. Tanaka¹, R. Murai², Y. Takahashi², T. Sugita³, M. Imanishi¹, Y. Mori⁴, S. Aikawa⁵, Y. Umeda⁵, Y. Funamoto⁵, T. Kamimura⁵, M. Yoshimura⁴

¹Grad. Sch. of Eng., Osaka Univ., JAPAN, ²ILE, Osaka Univ., JAPAN,

³Nikon Corp., JAPAN, ⁴SOSHO CHOKO Inc., JAPAN, ⁵Dept. of Electronics, Info. and Comm. Eng., Osaka Inst. Tech., JAPAN

In the laser processing field, short-wavelength and high-power laser sources have been developed for processing complex materials such

as glass composite substrates and carbon fiber reinforced plastics (CFRPs). However, conventional optical components used for such laser systems are very highly prone to optical damage. Thus, there is a high demand to develop new optical materials with high laser-induced damage resistance. Strontium tetraborate SrB_4O_7 (SBO) was reported to be a nonlinear optical crystal with wide transparency down to 130 nm. In this research, we grew a high-quality SBO single crystal and measured the surface DUV laser-induced damage threshold (LIDT). The SBO crystal was grown in a three-zone vertical furnace equipped with the seed cooling apparatus by the Kyropoulos method [1]. A sintered material was prepared from a mixture of SrCO_3 (99.9%) and B_2O_3 (99.9%) with the stoichiometric composition ($\text{Sr} : \text{B} = 1 : 4$). The growth temperature was about 1002°C . The seed crystal oriented along the c -axis was rotated at 5 rpm and reversed continuously every 5 min. The crucible 90 mm in diameter and 90 mm in height was rotated at 15 rpm in the opposite direction of the seed crystal. We supplied air gas at a flow rate of 3 L/min to prevent the seed from melting during the crystal growth. The average growth rate along the a -axis was controlled to be 1.1 mm/day. Figure 1 shows the as-polished SBO crystal with dimensions of $51 \times 9 \times 25 \text{ mm}^3$ ($a \times b \times c$). The crystal had no macroscopic defects, such as cracks and inclusions. We measured the surface LIDT of the crystal by 1-on-1 method at 266 nm (pulse width : 5 ns). The polarization direction was parallel to the c -axis of the (020) sample. For comparison, other samples such as synthetic silica glass and calcium fluoride (CaF_2) were also evaluated. Three samples showed a surface roughness (RMS) of 0.35 nm, 0.84 nm, and 0.84 nm, respectively. Figure 2 shows the experimental results of surface LIDT at 266 nm. The SBO crystal has higher surface LIDT (16.4 J/cm^2) than that of the synthetic silica glass (4.8 J/cm^2) and the CaF_2 (11.4 J/cm^2). This result reveals for the first time that the SBO crystal exhibit outstanding surface LIDT than conventional optical materials used for DUV laser systems.

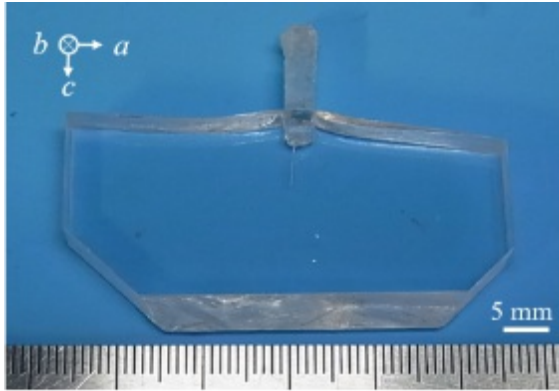


Fig.1. As-polished SBO single crystal.

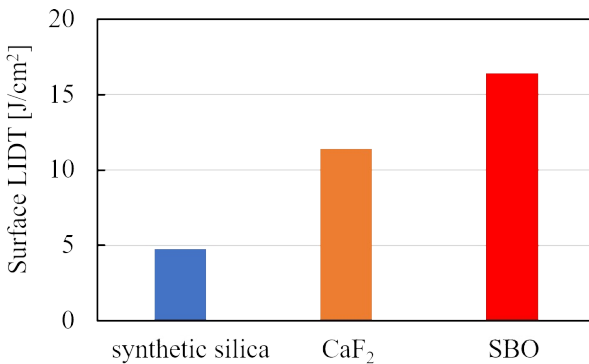


Fig.2. Surface LIDT of synthetic silica glass, CaF₂, and SBO at 266 nm.

[1] T. Kawamura *et al.*, J. Cryst. Growth **312**, 1118 (2010).

9:00 AM - 9:15 AM

STUDY OF SELF-FLUX COMPOSITION FOR GROWING CSLiB₆O₁₀ CRYSTAL WITH HIGH DUV LASER-INDUCED DEGRADATION TOLERANCE

R. Murai¹, T. Fukuhara², G. Ando¹, Y. Tanaka², Y. Takahashi¹, K. Matsumoto³, M. Maruyama², M. Imanishi², Y. Mori², **M. Yoshimura**¹
¹Institute of Laser Engineering, Osaka University, JAPAN, ²Graduate School of Engineering, Osaka University, JAPAN, ³SOSHO CHOKO Inc., JAPAN

CsLiB₆O₁₀ (CLBO) is one of the key nonlinear optical crystals for generating deep-ultraviolet (DUV) light below the wavelength of 300 nm, and has already been put to practical use in coherent DUV illumination sources for semiconductor inspection. For next-generation advanced laser processing applications, output degradation occurred

in the crystal is a critical issue associated with power scaling and long-term operation. In this research, we have investigated self-flux composition to produce high-quality CLBO crystals with high laser-induced degradation tolerance. Three types of self-flux composition were examined: conventional B-poor flux (Cs:Li:B = 1:1:5.5), B-rich flux (Cs:Li:B = 1:1:6.25), and Li-poor flux (Cs:Li:B = 1.2:0.8:6.25). The starting materials were prepared from a mixture of Cs_2CO_3 , Li_2CO_3 , and H_3BO_3 . After dissolving these materials in pure water, we charged the dried growth materials in a Pt crucible of 10 cm diameter. The crystal growth was conducted by Top Seeded Solution Growth (TSSG) method. The average crystal growth rate was controlled to about 3 mm/day by adjusting the furnace temperature. The grown crystals with weight of about 100 g are free from cracks and macro inclusions. We also confirmed that CLBO crystals grown from Li-poor and B-rich fluxes have less light scattering defects compared with crystal grown from B-poor flux. By using the accelerated degradation test [1], we evaluated 266 nm UV-induced degradation tolerance of each crystal as the lifetime. Figure 1 shows the experimental results. The CLBO crystal grown from Li-poor flux exhibits relatively longer lifetimes than crystals grown the other self-flux compositions. For obtaining larger crystal, we grew a CLBO crystal from the Li-poor flux using a Pt crucible of 15 cm diameter. The average crystal growth rate was about 3.5 mm/day and a growth period was 16.8 days. Figure 2 shows a high-quality CLBO crystal with the size of $126 \times 75 \times 55$ ($a \times c \times a'$) mm^3 and the weight of 531 g. We empirically confirmed that the viscosity of Li-poor flux solution is not so high, and therefore we consider the solution composition is suitable for growing large and high-quality CLBO crystals. Reference [1] K. Takachiho *et al.*, Opt. Mater. Express, **4**, 559-567 (2014).

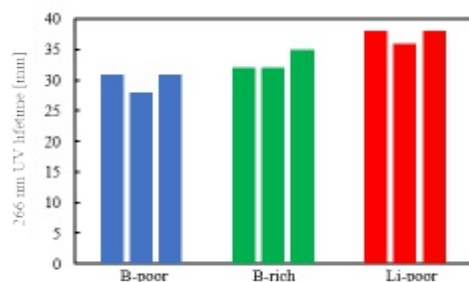


Fig. 1. 266 nm UV lifetimes of CLBO crystals grown from various self-flux compositions.



Fig. 2. A high-quality CLBO crystal with the weight of 531 g grown from Li-poor flux.

9:15 AM - 9:30 AM

BORATE MATERIALS: FROM BULK SINGLE CRYSTALS TO LOW-DIMENSIONAL STRUCTURES

N.I. Leonyuk

Lomonosov Moscow State University, Geological faculty, Department of Crystallography and Crystal Chemistry, RUSSIAN FEDERATION

Here is an overview on crystal growth and characterization of high-temperature borates, performed by the author's research group and other research centers during last several decades. This presentation is devoted to the correlation between physico-chemical characteristics of multicomponent borate melts, as well as growth mechanism and kinetics of many crystals with device potential. The author's experimental works performed within several last decades are related to the phase relationships in molybdate-based and related fluxed melts, to primary crystallization fields of huntite type borate family including their derivatives, temperature-dependent solubility diagrams, as well as growth conditions for most attractive optical and multiferroic borate crystals. Some of the key results are summarized in this report. Various aspects of their controlled crystallization in borate fluxed melts, relationships between growth conditions, composition, structure, morphology and properties of grown crystals are analyzed. Data on the synthesis and crystal chemistry of borates with mixed anions are presented as well. Particular examples state the crystallochemical prerequisites for studying the phase relationships and high-temperature crystallization of refractory borates in four- to six component systems. On particular examples, structural aspects as ways towards development of high-temperature borates' crystal growth technology from such complex fluxed melts are considered. An information is provided on liquid-phase epitaxy of one-dimensional single crystal layers of rare-earth borates doped with active ions, as well as on glass-ceramic nanocomposites. This research was supported in part by the RFBR grant ## 18-29-12091_MK and 18-05-01085a.

9:30 AM - 9:45 AM

(ISO)CYANURATES WITH NEW TYPES OF π -CONJUGATED SIX-

MEMBERED RING UNITS FOR LINEAR/NONLINEAR OPTICAL APPLICATIONS

M. Xia

Technical Institute of Physics and Chemistry, CAS, CHINA

The compounds containing π -conjugated units exhibit very large anisotropic polarizability and second harmonic generation susceptibility can be employed as birefringent and nonlinear optical (NLO) materials. For example, the β -BBO crystal has excellent NLO properties while α -BBO is a famous ultraviolet birefringent crystal. The outstanding linear and NLO properties of them are stemmed from the planar π -conjugated $(B_3O_6)^{3-}$ groups. Recently, cyanurates containing planar $(C_3N_3O_3)^{3-}$ six-membered-ring (6-MR) units that are isoelectric with $(B_3O_6)^{3-}$ groups, can be considered as new types birefringent and NLO materials. In this talk, we have grown five new (iso)cyanurates, namely $K_6Cd_3(C_3N_3O_3)_4$, $Cs_3Na(C_3N_3O_3H_2)_4 \cdot 3H_2O$, $Ba_2M(C_3N_3O_3)_2$ ($M = Ba, Sr$ and Pb). The former two compounds are noncentrosymmetric, show considerable NLO effects. The $Ba_2M(C_3N_3O_3)_2$ are uniaxial and possess optical anisotropy of $\Delta n = 0.32$ at 800 nm, two times than that of the benchmark birefringent crystal calcite. All results show that (iso)cyanurates containing π -conjugated 6-MR groups are promising birefringent and NLO materials.

9:45 AM - 10:00 AM

NASR3BE3B3O9F4 CRYSTAL GROWTH, DEFECT AND HIGH POWER OF UV LASER GENERATION

L. Liu, G. Guo, Z. Hou, X. Wang

Technical Institute of Physics and Chemistry, CHINA

Large-size of $NaSr_3Be_3B_3O_9F_4$ (NSBBF) crystal was grown by a modified top-seeded solution growth with sizes up to $45 \times 25 \times 20 \text{mm}^3$. However the crystal always has cracks inside. The mechanism for the formation of the cracks were investigated for the first time by using powder X-ray diffraction, chemical etching et.al. The ability for UV laser generation both at 355nm and 266nm were evaluated. A maximum conversion efficiency of 33.5% from 1064nm to 355nm

generation has been achieved. And a maximum output of 11mJ at 355nm was obtained with the 1064nm energy of 39mJ. Furthermore, a maximum output power exceeding 1 W at 266 nm was obtained, corresponding to a conversion efficiency of 10.3%. Stability measurement on the NSBBF crystal shows a fluctuation of 3.34% at 200 mW within 1 hour. The above results indicates that it is a promising UV nonlinear optical (NLO) material for practical applications.

Friday, August 2, 2019

8:00 AM - 10:00 AM

Silicon Carbide Materials and Devices I

Location: Crestone III, IV

Session Chair(s): Govindhan Dhanaraj, Michael Dudley

8:00 AM - 8:30 AM

ADVANCED SILICON CARBIDE SUBSTRATES AND DEFECT CHARACTERIZATION FOR POWER ELECTRONIC INDUSTRY **S. Parthasarathy**

GT Advanced Technologies, NH, UNITED STATES OF AMERICA

The growing demand for power electronic device for automotive, photovoltaic, transportation, motor drives creates an enormous demand for wide band gap semiconducting materials such as silicon carbide (SiC) and gallium nitride (GaN). While GaN based devices can be used for low voltages, SiC is the workhorse for voltages >600 volts. Progress in the availability of larger diameter SiC wafers has driven the final cost of device assembly down. Today, SiC is grown from a gas or liquid phase process that involves the following: (a) the generation of reactants (sublimation or non-congruent melt) (b) the transport of reactants to the growth surface (required temperature gradients), (c) adsorption at the growth surface (supersaturation), (d) nucleation and (e) finally crystal growth – advancement of gas solid interface or solid liquid interface. GT Advanced Technologies has been making sublimation furnace (gas phase growth) since the year 2000. The 100 mm and 150 mm 4H-N type SiC boules were grown by equipment made by GT and using the conventional PVT process with

proprietary hotzone components. OD ground material with usable heights of 7-20 mm were obtained from as-grown boules. Thermal modelling was performed to optimize the applied shear stress, which is responsible for generation of dislocations and micropipes and von Mises stress responsible for boule cracking. The axial and radial temperature gradients were optimized in order to prevent the formation of the silicon second phase (droplets) at the growth interface, which are the drivers for structural defects such as micropipes, point and planar defects. Likewise the generation of the carbon second phase has also been reduced by optimizing the hotzone geometry. A high temperature wafer annealing process was developed to reduce the BPD further. The materials produced were extensively characterized by Cross polarizer, X-Ray scan for off-axis and rocking curve measurements, light transmission microscopy with polarizer for stress and micropipe examination, optical surface analyzer for surface defects and micropipes, KOH etching studies to observe and quantify defects such as threading edge dislocation, threading screw dislocation, basal planar defects and micropipes. A detailed comparison of technology readiness of various SiC crystal growth techniques, along with defect reduction, correlation of defects to devices and cost modelling of low cost SiC wafers will be presented in the talk.

8:30 AM - 9:00 AM

GROWTH OF LARGE DIAMETER 6H SI AND 4H N+ SiC SINGLE CRYSTALS

V. Rengarajan, A. Gupta, X. Xu, K. Yang, H. Li, H. Wang, I. Zwieback, G. Ruland

II-VI INCORPORATED WORLD HEADQUARTERS, PA, UNITED STATES OF AMERICA

Silicon carbide (SiC) is a wide bandgap semiconductor with high thermal conductivity, which is ideal for high-power, high-temperature, and high-frequency electronics. High quality and larger diameter SiC substrate is required in order to improve the performance and reduce the manufacturing cost of SiC-based electronic and optoelectronic devices. In this paper, we report the growth and characteristics of large-diameter SiC substrates. Large-diameter SiC single crystals

(≥150 mm) are grown at II-VI by the Physical Vapour Transport (PVT) technique. 150 mm substrates of semi-insulating 6H/4H SiC and n-type 4H SiC are currently produced as commercial products. In 6H-SiC crystal diameter has expanded to 200 mm. Over the last few years, improvements have been made in crystal quality. In SI SiC substrates, stable semi-insulating properties are achieved by precise vanadium compensation. Electrical resistivity of SI substrates is, typically, of 10^{11} Ω·cm or above. N-type 4H-SiC substrates are produced using doping with nitrogen and substrates show uniform resistivity of 0.020 W-cm. Over the last few years the crystal quality has improved significantly. 4H n+ crystal diameter has been expanded above 200 mm. Data on crystal quality, total dislocation density, basal plane dislocation density and screw dislocation will be discussed.

9:00 AM - 9:30 AM

MODELING SOLUTIONS FOR SILICON CARBIDE CRYSTAL GROWTH AND EPITAXY

A. Galyukov

STR US, Inc., VA, UNITED STATES OF AMERICA

There are several technologies to manufacture silicon carbide crystalline materials which include sublimation and solution growth of bulk crystals and epitaxy of thin films. Computer modeling helps to get insights and advance the technology for better process control, enhanced material quality, and higher production yields while keeping the costs low. We present various application examples that illustrate the use of computer modeling in optimization of SiC production and demonstrate the range of physical phenomena involved in SiC growth and epitaxy that can be studied with the modeling tools available today. Commercial crystal growth simulator *CGSim* [1] and *Virtual Reactor* [2] by STR Group, Inc. are used.

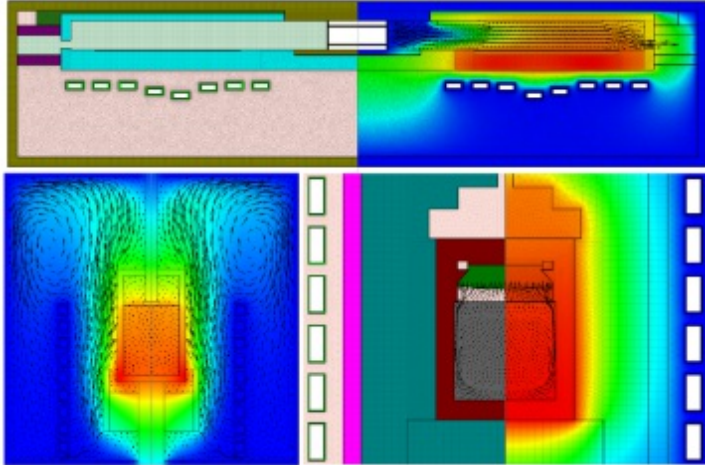


Figure 1: CVD SiC epitaxy in planetary system; SiC growth from solution; SiC sublimation growth. [1] <http://www.str-soft.com/products/CGSim> [2] http://www.str-soft.com/products/Virtual_Reactor

9:30 AM - 9:45 AM

LOW TEMPERATURE GROWTH OF SiC: EVOLUTION OF MORPHOLOGY DURING DISSOLUTION OF Al-Si EUTECTIC
N.B. Singh

University of Maryland, Baltimore County, UNITED STATES OF AMERICA

Silicon carbide crystals have been grown in 3C, 4H and 6H polytype morphology by physical vapor transport method. Recently it has been possible to use low temperature methods to produce 2H hexagonal crystals. Also, composite literatures have shown nucleation into 2H morphology in presence of some impurities. We have used Al-Si alloy to synthesize SiC and AlSiC compounds. Effect of carbon impurity on the morphology and solidification behavior of Al-12%Si alloy was studied in dynamic condition. We used carbon as alloying element and forced the mixing during crystallization of the alloy by rotation and stirring. We nucleated the material on silicon carbide substrate while alloy melt was rotated in a graphite crucible at the rotation of 30 rpm. Several experiments were performed to determine effect of soaking time, cooling rate, rotation speed and nucleation condition. We observed dendritic and cellular morphology during early stage. As the concentration increased breakdown of morphology started. Microstructure was studied by optical microscope and compositional

study was performed by SEM and EDX for the developed matrix. This study was used to explore a novel approach to develop novel low temperature process silicon carbide and also to develop understanding for grain growth to refine carbon composites.

9:45 AM - 10:00 AM

IN SITU X-RAY TOPOGRAPHY STUDIES OF 4H-SiC SUBSTRATES AND EPILAYERS

B. Raghoeamachar¹, Y. Yang¹, J. Guo¹, S. Weit², M. Dudley¹, A. Danilewsky², P.J. McNally³, B.K. Tanner⁴

¹Stony Brook University, NY, UNITED STATES OF AMERICA,

²Crystallography, Albert-Ludwigs University Freiburg, GERMANY,

³Dublin City University, IRELAND, ⁴Durham University, UNITED KINGDOM

X-ray topography is widely used for ex situ characterization of defects in single crystal materials in the form of boules, wafers and thin films. However, it is often desirable to directly observe defect behavior during growth, processing or device operation. Such studies reveal aspects of defect behavior not readily deduced from studying defect configurations after growth or processing. Synchrotron white beam X-ray topography is particularly suitable for direct imaging under in-situ conditions because of advantages such as high intensities, wide spectral range, good signal-to-noise ratio and sufficient geometrical resolutions even at large specimen-detector distances thus allowing crystals to be enclosed in desired environment conditions (heating, cooling, stress, etc.). During post-growth cooling of PVT-grown 4H-SiC boules, relaxation of thermal stresses results most frequently in deformation governed by basal plane slip involving basal plane dislocation (BPD) half-loops nucleated at the boule edges and at the sites of micropipes or inclusions and propagating into the rest of the boule. However, in situ studies on 4H-SiC crystals heated to temperatures as high as 1600°C in double ellipsoidal mirror furnace reveal the dynamical operation of multiple double-ended Frank-Read dislocation sources in the interior of the crystal. Analysis reveals that the nucleation of these sources is facilitated by a specific configuration consisting of one basal plane dislocation (BPD) segment pinned by

two threading edge dislocations (TEDs) [1]. During 4H-SiC homoepitaxy, the misfit strain induced by the nitrogen doping concentration difference between the epilayer and substrate is relaxed by an interfacial dislocation created by the glide of a mobile segment of a basal plane dislocation (BPD) in the substrate or epilayer towards the interface, leaving a trailing edge component right at the interface. This mechanism has been confirmed through direct X-ray topography observation of a n-/n+ 4H-SiC homoepitaxial sample subjected to a high-temperature heat treatment. The movement of a BPD segment in the epilayer towards the direction perpendicular to the step flow, leaving a long and straight interfacial dislocation in the path was revealed [2].

References 1. Y. Yang, J. Guo, B. Raghoeamachar, M. Dudley, Svetlana Weit, A.N. Danilewsky, P.J. McNally, B.K. Tanner, Materials Science Forum, 924, 172-175 (2018). 2. J. Guo, Y. Yang, B. Raghoeamachar, M. Dudley, Svetlana Weit, A.N. Danilewsky, P.J. McNally, B.K. Tanner, Materials Science Forum, 924, 176-179 (2018).

Friday, August 2, 2019

8:00 AM - 10:00 AM

Symposium on Epitaxy of Complex Oxides: 5d Transition Metal Oxides

Location: Grays Peak II, III

Session Chair(s): Jacobo Santamaria

8:00 AM - 8:30 AM

ENGINEERING THE ELECTRONIC STRUCTURE AND CORRELATIONS IN IRIDATES

J.K. Kawasaki

University of Wisconsin Madison, WI, UNITED STATES OF AMERICA

Dimensionality and connectivity among octahedra play important roles in determining the properties, electronic structure, and phase transitions in transition metal oxides. In this talk, I will discuss how these parameters can be tuned precisely via a feedback between molecular beam epitaxial growth and *in-situ* photoemission (core level and ARPES). I will focus on iridates as a model system, where we

have recently demonstrated that the effective mass can be tuned precisely via quantum confinement, both in ultrathin films of rutile IrO₂ [1] and in all-rutile IrO₂/TiO₂ superlattices [2]. The IrO₆ octahedral connectivity provides another important parameter, which determines the strength of electron-electron correlations. We demonstrate this via growth and ARPES measurements across a series of iridates with varying octahedral connectivity, ranging from the two dimensional Sr₂IrO₄, to the three dimensional SrIrO₃, to the hyper-connected IrO₂, in which the IrO₆ octahedra form a mixed edge and corner sharing network [3]. In all studies, the ability to probe intrinsic properties is made possible by the identification of an adsorption-controlled MBE growth window in which the stoichiometry is self-limiting. I will conclude with an outlook on how these concepts can be applied in other classes of quantum materials, e.g. Heusler compounds. This work was supported by the Kavli Institute at Cornell, ARO-YIP, and NSF-CAREER. [1] Phys. Rev. Lett. **121**, 176802 (2018); [2] Phys. Rev. Materials **2**, 054206 (2018); [3] Phys. Rev. B **94**, 121104(R) (2016)

8:30 AM - 9:00 AM

SYNTHESIS CONTROL OF QUANTUM PHASES IN 3D-5D DOUBLE PEROVSKITE OXIDE HETEROSTRUCTURES

C. Sohn, H.N. Lee

Oak Ridge National Laboratory, UNITED STATES OF AMERICA

Rich quantum phenomena are expected in 3d-5d oxide double perovskites, where both strong electron-electron correlations in 3d orbitals and the relativistic spin-orbit coupling in 5d orbitals play cooperative roles. Here, we have demonstrated synthesis control of electronic and magnetic ground states in 3d-5d double perovskite Sr₂FeReO₆ heterostructures. In the first part of presentation, we will show control of cation stoichiometry and the degree of cation ordering by using pulsed laser epitaxy. Among many growth parameters, we found a single parameter, oxygen partial pressure, can sensitively control the ratio of 3d Fe ions and 5d Re ions as well as degrees of checkerboard ordering of B-site cations. Beyond the original ferromagnetic metallic state found in stoichiometric bulk samples, we

found room-temperature ferromagnetic insulating states, which are rare in nature but required for developing spintronic devices, in Fe-rich and cation-ordered films. In the second part of presentation, we will show the evolution of electronic and magnetic ground state of $\text{Sr}_2\text{FeReO}_6$ with reducing dimensionality. While the original ferromagnetic ordering is survived even down to monolayer $\text{Sr}_2\text{FeReO}_6$, the enhancement of strong electron correlation in a quasi-two-dimensional geometry of $[\text{SrTiO}_3]_8/[\text{Sr}_2\text{FeReO}_6]_1$ superlattices induced the Mott-like metal-insulator transition. The origin of the metal-insulator transition with polarized spin states will be discussed based on optical spectroscopy and the first principle calculations. This work was supported by the U.S. Department of Energy, Office of Science, Basic Energy Sciences, Materials Sciences and Engineering Division.

9:00 AM - 9:30 AM

SPIN RECONSTRUCTIONS AT EPITAXIAL OXIDE INTERFACES

J. Santamaria

Universidad Complutense, SPAIN

The electronic reconstruction occurring at oxide interfaces may be the source of interesting device concepts for future oxide electronics. In particular, the electronic and orbital reconstructions occurring at oxide interfaces underlie deep changes in their magnetic states. While in 3d perovskite oxides with an orbital moment quenched by the octahedral crystal field, magnetism is largely determined by the spin degree of freedom, in 4d or 5d oxides the interplay between strong spin orbit interaction and correlated physics is at the bottom of exciting new electronic states. At epitaxial interfaces modified orbital filling and/or changes in orbital overlap between distorted bonds, drastically affect magnetic interactions. In this talk I will show novel forms of interfacially induced magnetism at oxide interfaces, which can be the source of novel functionalities in oxide electronic devices. I will first discuss the spin reconstruction occurring at the interfaces of a $\text{La}_{0.7}\text{Sr}_{0.3}\text{MnO}_3$ / BaTiO_3 / $\text{La}_{0.7}\text{Sr}_{0.3}\text{MnO}_3$ multiferroic tunnel junctions. It is the origin of a spin filtering functionality which enables a giant electrical modulation of the tunneling magnetoresistance between values of 10% and

1000%, that could inspire device concepts in oxides based low dissipation spintronics. As a second topic I will examine the magnetic properties of oxide interfaces involving the strong spin orbit SrIrO₃. I will show evidences of interfacially induced magnetic instability in the otherwise paramagnetic oxide and how epitaxial modification of the structure of ultrathin layers offer interesting strategies to manipulate this novel magnetic state. Work done in collaboration with J. Tornos*¹, F. Gallego *¹, S. Valencia², Y. H. Liu^{3,4}, V. Rouco⁵, V. Lauter³, R. Abrudan^{2,6}, C. Luo^{2,7}, H. Ryll², Q. Wang⁴, F. Cuellar¹, F. J. Mompean⁸, M. Garcia-Hernandez⁸, F. Radu², T. R. Charlton⁹, A. Rivera-Calzada¹, Z. Sefrioui¹, S. G. E. te Velthuis⁴, C. Leon¹ ¹GFMC, *Universidad Complutense de Madrid, 28040 Madrid, Spain.*

²*Hemholtz-Zentrum Berlin für Materialien und Energie, Albert-Einstein-Strasse 15, 12489 Berlin, Germany* ³*Neutron Scattering Division, Oak Ridge National Laboratory, Oak Ridge, Tennessee 37831, USA* ⁴*Materials Science Division, Argonne National Laboratory, Argonne, Illinois 60439, USA* ⁵*Unité Mixte de Physique, CNRS, Thales, Université Paris-Saclay, 91767 Palaiseau, France* ⁶*Institut für Experimentalphysik/Festkörperphysik, Ruhr-Universität Bochum, 44780 Bochum, Germany* ⁷*University of Regensburg, Universitätsstraße 31, 93053 Regensburg, Germany* ⁸*2D-Foundry Group, Instituto de Ciencia de Materiales de Madrid ICMN-CSIC, 28049 Madrid, Spain* ⁹*ISIS, Rutherford Appleton Laboratory, Chilton, Oxon OX11 0QX, United Kingdom*

9:30 AM - 9:45 AM

GROWTH CONTROL OF INTERFACE STRUCTURE AND SYMMETRY FOR NOVEL FUNCTIONALITIES IN 3D AND 5D OXIDE SUPERLATTICES

E. Skoropata, Z. Liao, J. Ok, H.N. Lee

Oak Ridge National Laboratory, TN, UNITED STATES OF AMERICA
Correlated oxides have been extensively studied due to the diverse physical properties arising from strong 3d electron correlations combined with lattice and orbital degrees of freedom. By comparison, 5d oxides with large spin-orbit coupling are attractive systems to host

exotic quantum states. An ability to grow high-quality epitaxial heterostructures that combine the physical properties of $3d$ and $5d$ materials in a single system is a promising route to develop novel functionalities in correlated oxide materials. We will describe our approach to this strategy of materials synthesis using pulsed laser deposition (PLD) to grow $5d$ SrIrO₃ and $3d$ transition metal oxide superlattices. A practical challenge to address is the difficulty to grow $5d$ -oxides, such as SrIrO₃, due to the tendency for target deterioration, the possible formation of volatile Ir-oxide, and competing phase formation during growth. We demonstrate well controlled growth of high-quality single phase SrIrO₃ films using PLD. Furthermore, the growth conditions were optimized to synthesize simultaneously SrIrO₃ and $3d$ perovskite oxides, opening an avenue to study the confluence of $3d$ magnetism and $5d$ spin-orbit coupling at epitaxial interfaces. The critical impact of well controlled interface growth is highlighted by our recent synthesis of SrIrO₃/LaMnO₃ superlattices with engineered interfacial A-site termination. We will show that the interfacial structure directly controls the emergence of chiral magnetism and “topological” Hall effect created by Dzyaloshinskii-Moriya interactions. We also explore the interface-driven electronic properties of all $3d$ -oxide systems using SrCuO₂/LaNiO₃ superlattices. Atomic-scale control of SrCuO₂ layer thickness allows tuning of the oxygen connectivity that can generate an unprecedentedly large orbital polarization in adjacent LaNiO₃ by transforming the local Ni-O coordination environment. These examples demonstrate a dramatic degree of control of properties emerging from oxide interfaces can be achieved from fine tuning atomic-scale synthesis of heterostructures, and open new insights to the discovery of unconventional functional properties in correlated oxide materials. *This work was supported by the U.S. Department of Energy, Office of Science, Basic Energy Sciences, Materials Sciences and Engineering Division.

9:45 AM - 10:00 AM

**SPONTANEOUS HALL EFFECT INDUCED BY LOCAL IR
MOMENTS IN THE EPITAXIAL PR2IR2O7 THIN FILMS**

L. Guo¹, N. Campbell¹, Y. Choi², J. Kim², P. Ryan², H. Huyan³, L. Li³,
T. Nan¹, J. Kang¹, C. Sundahl¹, X. Pan³, M. Rzchowski¹, C. Eom¹

¹University of Wisconsin-Madison, WI, UNITED STATES OF AMERICA, ²Argonne National Laboratory, IL, UNITED STATES OF AMERICA, ³University of California-Irvine, CA, UNITED STATES OF AMERICA

Quantum critical $\text{Pr}_2\text{Ir}_2\text{O}_7$ ¹ has attracted much attention recently. It exhibits a chiral spin liquid state suggested by a large spontaneous Hall effect without long range magnetic ordering^{2,3}. While this extraordinary phenomenon was observed below 1.5K³ in bulk, by growing the thin film on YSZ (111) under rhombohedral lattice distortion, we increased the onset temperature of the spontaneous Hall effect up to 15 K. To explore the origin of the enhancement, we employed element-resolved x-ray magnetic spectroscopy and scattering studies. Without clear indications of long-range magnetic ordering, X-ray magnetic circular dichroism (XMCD) shows that local Ir moments emerge in the film, a likely cause of the emergent high temperature magnetism, whereas the Pr magnetism is similar between the film and bulk samples. Our results highlight the effect of strain-induced trigonal distortion on the incipient Ir 5d local moments. This increase in the magnetic complexity allows for a link between the Ir electronic band structure and the observed spontaneous Hall effect at higher temperatures. Ref: 1 Y. Tokiwa, J.J. Ishikawa, S. Nakatsuji, and P. Gegenwart, Nat. Mater. 13, 356 (2014). 2 S. Nakatsuji, Y. Maehida, Y. Maeno, T. Tayama, T. Sakakibara, J. Van Duijn, L. Balicas, J.N. Millican, R.T. MacAluso, and J.Y. Chan, Phys. Rev. Lett. 96, (2006). 3 Y. Maehida, S. Nakatsuji, S. Onoda, T. Tayama, and T. Sakakibara, Nature 463, 210 (2010).

Friday, August 2, 2019

10:30 AM - 12:00 PM

Biological and Biomimetic Materials II

Location: Grays Peak I

Session Chair(s): Anna Pohl, Jinhui Tao

10:30 AM - 10:45 AM

THE OPTIMUM DESIGN OF DNA-GUIDED NANOPARTICLE SUPERLATTICES FOR DIRECT DEHYDRATION

H. Sumi¹, T. Isogai², S. Kojima¹, N. Ohta³, H. Sekiguchi³, S. Harada², T. Ujihara², M. Tagawa²

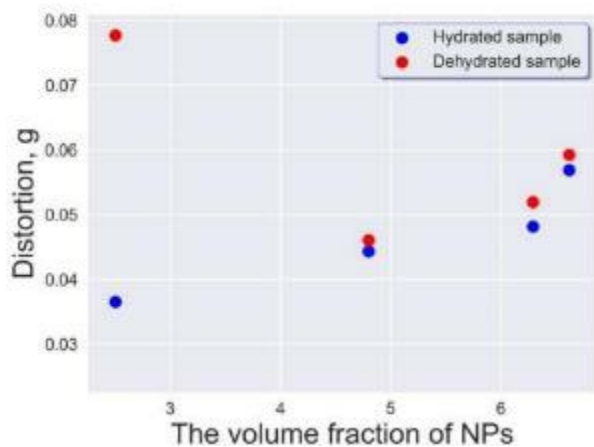
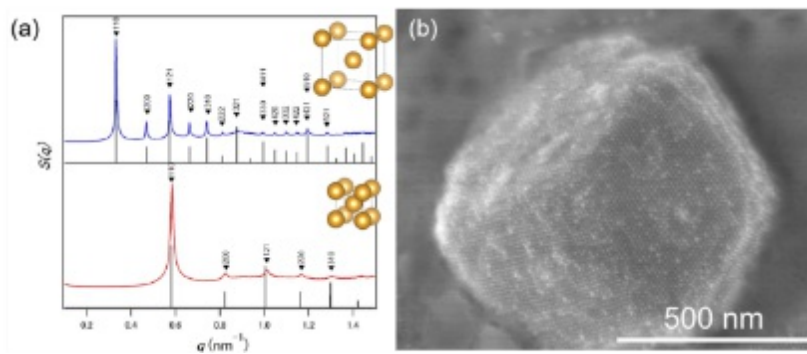
¹Graduate School of Engineering Nagoya University, JAPAN,

²Institute of Materials and Systems for Sustainability (IMaSS), JAPAN,

³Japan Synchrotron Radiation Research Institute (JASRI), JAPAN

DNA-functionalized nanoparticles (DNA-NPs) can assemble into various types of 3D nanoparticle superlattices, due to the programmability of DNA base sequences. However, DNA-NP superlattices have a problem in structure stability. Whereas DNA-NP superlattices are stable in a buffer solution, they collapse outside the solution because of the dehydration of DNA strands. We previously examined the structural stability of DNA-NP superlattices during dehydration by changing the nanoparticle volume fraction per unit cell with the different sized nanoparticles linked by the same DNA strands. Then we revealed that DNA-NP superlattices with higher nanoparticle volume fraction tended to maintain their symmetries during dehydration [1]. However, it is still challenging to realize stable dehydration of DNA-NP superlattices with nanoparticles smaller than 10 nm. Thus, it is necessary to optimize the design of DNA sequences for stable dehydration of DNA-NP superlattices. Here, we demonstrate the successful dehydration of DNA-NP superlattices with smaller sized nanoparticles by controlling volume fractions per unit cells by changing DNA base sequences. DNA-functionalized Au nanoparticles (DNA-AuNPs) assembled into superlattices by controlling the temperature sequences. The crystal structures of DNA-AuNP superlattices were analyzed by small angle X-ray scattering (SAXS) before and after dehydrations. The shapes and the surface structures of dehydrated aggregates were observed by scanning electron microscopy (SEM). Fig. 1a shows SAXS patterns of the assemblies of DNA-AuNPs with 9.6-nm nanoparticles. This result shows that DNA-AuNP aggregates are bcc structured superlattices, and they contracted while maintaining their symmetries after dehydration. Fig. 1b shows a SEM image of a dehydrated DNA-AuNP superlattice

assembled with volume fraction of 4.8 %. The dehydrated superlattice shows faceted crystal shape and ordered arrangements of Au nanoparticles on its crystal faces. Fig. 2 shows lattice distortions of DNA-AuNP superlattices calculated from diffraction peak widths and crystallite sizes. As the volume fraction increased, the distortion of hydrated superlattices increased slightly, whilst that of dehydrated superlattices decreased drastically. However, the distortions of dehydrated superlattices were always larger than that of hydrated superlattices. Thus, it is revealed that there is the optimum design which minimized the distortion of dehydrated superlattice. [1] H. Sumi *et al.*, Dehydration stability analysis of DNA-guided nanoparticle superlattices, MRS Fall Meeting & Exhibit (2018).



10:45 AM - 11:00 AM

HIERARCHICAL ASSEMBLY AND CHARACTERIZATION OF DNA NANOTUBE NETWORKS

M.S. Pacella, R. Liu, P. Singh, J. Zhang, P. Vallejo, T. Hou, J. Gunn, M. Bordui, E. Jelezniakov, R. Schulman
Johns Hopkins University, MD, UNITED STATES OF AMERICA

DNA nanotechnology offers a means to synthesize custom nanostructured materials from the ground up in a hierarchical fashion. DNA nanostructures share several interesting properties with mineral crystals; for instance, depending on the assembly conditions, they can form unique types of structures (akin to crystalline polymorphs) that can be dynamically reconfigured. The relatively large size of each component in DNA nanostructures allows us to directly observe individual assembly events and to develop models of hierarchical assembly applicable to both DNA nanostructures and, potentially, other hierarchically assembled materials such as mineral crystals. While the assembly of DNA nanostructures from small (nanometer-scale) monomeric components has been studied extensively, a general model for the hierarchical assembly of rigid or semiflexible units into multimicron-scale structures remains elusive. To study such hierarchical assembly, we have developed a system for assembling extend networks of semiflexible DNA nanotubes. These nanotubes assemble from nanometer scale tiles into materials via nucleated growth from sites on rigid, Y-shaped nanotube seeds. In this process, nanotubes first grow from these Y-shaped seeds to form 3-armed nanotube architectures. These architectures then, in turn, assemble into networks that include as many as 80 seeds and can extend over areas as large as $900 \mu\text{m}^2$. We measure the kinetics of network growth and find that the assembly of these networks can be approximated by a stochastic model of hierarchical assembly that assumes a single joining rate between DNA nanotube ends. Because the number of nucleation sites on the seeds and their spatial arrangement can be systematically varied by design, this system allows the assembly of a wide variety of networks and characterization of the assembly mechanisms that lead to different types of material architectures at length scales of tens to hundreds of microns. We have identified the ratio of inter-network vs intra-network joining events as a key parameter that controls whether networks develop into “open-branching” topologies or “closed-loop” topologies. Further, by activating/deactivating the incorporated Y-shaped DNA origami junctions via strand displacement we are also able to direct networks to change form, suggesting a model system for understanding not only the formation of filament networks at this length-scale but also their

reconfiguration.

11:00 AM - 11:15 AM

AN ORDERED 2D POLYMER TEMPLATE FOR PROTEIN CRYSTALLIZATION

E. Vlieg, W. De Poel, W. Van Enckevort, H. Elemans, A. Rowan
Radboud University, Institute for Molecules and Materials,
NETHERLANDS

2-Dimensional Polymers (2DP) are a novel class of material that consist of a monolayer of ordered molecular building blocks, that have been covalently linked. One of these monomers was self-assembled on a flat muscovite mica scaffold and subsequently the organic layer was polymerized. The resulting flat and stable 2DP layer was used as a template for protein crystallization. Crystals of insulin were epitaxially grown on the template, while insulin crystals grown on clean muscovite mica had a random orientation. The template was selective, since no epitaxially ordered crystals were formed of hen egg white lysozyme, bovine serum albumin, or talin.

11:15 AM - 11:30 AM

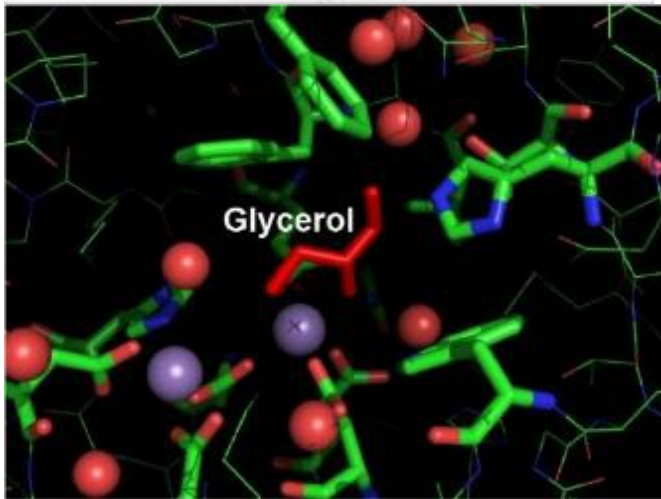
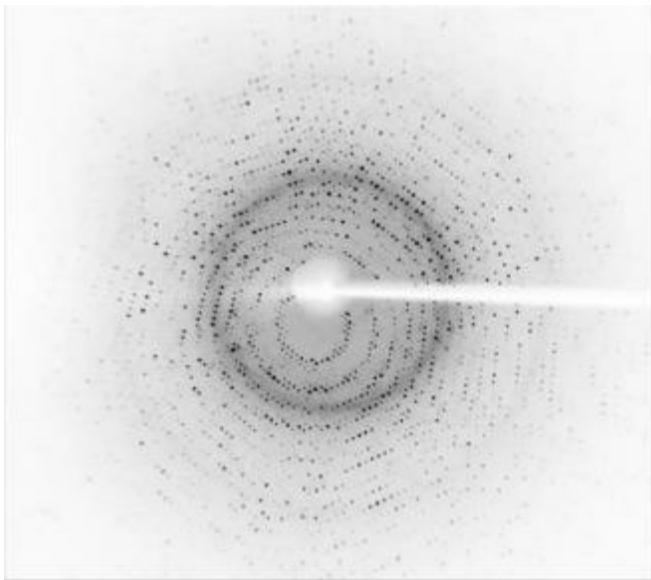
PRECIPITANT-FREE CRYSTALLIZATION OF GLUCOSE ISOMERASE SIMPLY BY CONCENTRATION IN A CRYOPROTECTANT SOLUTION

Y. Suzuki¹, N. Maita²

¹Graduate School of Technology, Industrial and Social Sciences, Tokushima University, JAPAN, ²The Institute for Advanced Enzyme Research, Tokushima University, JAPAN

Protein crystallization is usually conducted by using precipitants, whereas so-called "salting-out" phenomenon is still unclear and complex. The addition of precipitants probably results in the change in local structure of the protein molecules and sometimes irreversible precipitation of protein molecules. Although almost all structures in protein data bank (PDB) are obtained using crystals which are grown with a large amount of precipitants, such conditions are quite different from that in general living organisms; the three-dimensional structures of protein molecules would be sometimes different from native

structures. To solve the problems, we have developed a precipitant-free protein crystallization method using a centrifugal concentration apparatus [1]. Although we successfully crystallized orthorhombic hen egg-white lysozyme with the above method and revealed significant change in the 3D structure of lysozyme molecule at the atomic level [1], lysozyme is known to be easily crystallized and very stable. Thus, we need to indicate universal applicability of our method to the other proteins. An industrial-level grade GI (Nagase ChemteX, Spezyme Glpf) was used as a model protein. We repeated desalination and concentration of GI mother liquor in 30 % aqueous glycerol solution using a centrifugal filter unit (Millipore, Ultracel–3K) five times. This process was also useful for removing sorbitol which had been added in the mother liquor to inhibit enzymatic activities. During the repetition processing, nucleation of GI crystals started inside at the bottom and side walls of the filter unit. The temperature of the sample was controlled at 25 °C. After several days, an adequate-sized crystal was trapped using a nylon loop, and flash-cooled for data collection. An oscillation photograph (oscillation angle was 0.75°, and exposure time is 60 s) which was taken using in-house X-ray source (Rigaku, R-AXIS VII, output 2.025 W) is shown in Fig. 1. Clear diffraction spots were confirmed. Although no drastic changes in the overall 3D molecular structure were observed, the structure in the precipitant-free crystal seemed to shrink a bit as a whole, and several residues at water accessible surfaces seem to move significantly. In particular, a glycerol molecule was found at the activation site of the GI molecule (Fig. 2). [1] Y. Suzuki et al., *Cryst. Growth Des.* **18**, 4226 (2018).



11:30 AM - 11:45 AM

BIO-INSPIRED SYNTHESIS AND PHASE TRANSFORMATIONS OF TiO / TiO₂ FOR WATER PURIFYING MEMBRANES

L. Cruz¹, D. Kisailus²

¹Materials Science and Engineering Program, University of California at Riverside, CA, UNITED STATES OF AMERICA, ²Department of Chemical and Environmental Engineering, University of California at Riverside, CA, UNITED STATES OF AMERICA

Titanium dioxide is known to be one the of the most widely used photocatalytic materials due to its strong oxidation potential. However, many TiO₂ photocatalytic systems are particulate in nature, which necessitates a recollection process that hinders their efficiency,

increases cost, and limits their widespread application. Anchoring these nanoparticles on surfaces or within three-dimensional matrices would be beneficial. Drawing inspiration from nature, which uses organic scaffolds to guide mineralization of inorganic structures that provide structural support, we investigate the effects of annealing on the diffusion, crystal growth and phase transformation of TiO_x species within a synthetic polymer matrix. The role of temperature, atmosphere, and polymer structure on the growth and phase transformation of the TiO_x nanoparticles within carbonaceous matrices are discussed.

11:45 AM - 12:00 PM

BIOMIMETIC TEMPLATE-FREE SYNTHESIS OF Ta_3N_5 SPHERICAL NANOSHELLS FOR PHOTOCATALYTIC APPLICATIONS

T. Wang¹, D. Kisailus²

¹University of California at Riverside, UNITED STATES OF AMERICA,

²Department of Chemical and Environmental Engineering, University of California at Riverside, CA, UNITED STATES OF AMERICA

Nanoshells with nanometer pores are frequently used in nature due to the many unique physical, chemical and biological properties of the simple geometrical structure. Biomolecular nanoshells are typically formed by the self-assembly of thousands of organic structural units, like phospholipids that form a membrane in transport vesicles.

Inorganic nanoshells are also being actively studied for their unique optical, mechanical and catalytic properties. However, templates are often required for inorganic hollow structures, which increases the complexity and cost effect of the synthesis. Here, we describe the synthesis of a visible-light driven photocatalyst, tantalum nitride (Ta_3N_5).

By tuning our synthetic parameters, Ta_3N_5 spherical nanoshells have been synthesized. Using a combination of microscopic and spectroscopic methods, we describe the potential micelle-formation growth mechanism of the hollow nanospheres. Finally, we found the tantalum nitride nanoshells exhibit superior photocatalytic activity for dye degradation, which can attributed to their biomimetic structure as well as the oxygen and nitrogen content.

Friday, August 2, 2019

10:30 AM - 12:00 PM

HVPE Growth and Devices

Location: Torrey Peak II-IV

Session Chair(s): Aaron Ptak, Masakazu Sugiyama

10:30 AM - 11:00 AM

HIGH SPEED GROWTH OF III-V MATERIALS USING MOVPE AND HVPE FOR LOW COST PHOTOVOLTAICS

T. Sugaya

National Institute of Advanced Industrial Science and Technology,
JAPAN

Cost reduction and improved conversion efficiency are the most important issues in the wide-scale deployment of solar photovoltaic systems. Multijunction solar cells provide ultra-high efficiencies by the effectively utilizing the solar spectrum through the interconnection of different kinds of solar cells. Even though multijunction solar cells have the highest reported efficiencies and have been commercialized for space and concentrator applications, they are not used widely because of their high cost. Therefore, it is necessary to lower the manufacturing cost for implementing large-scale terrestrial III-V modules. High speed growth would be a possible pathway to lower the cost of III-V devices. We have developed metal organic vapor phase epitaxy (MOVPE) as well as hydride vapor-phase epitaxy (HVPE) to obtain ultrafast growth of III-V materials. We achieved high growth rates of over 100 $\mu\text{m}/\text{h}$ for GaAs using both growth techniques. 140 $\mu\text{m}/\text{h}$ and 30 $\mu\text{m}/\text{h}$ were obtained for InGaP growth in HVPE and MOVPE, respectively. The solar cell characteristics of these materials will be discussed in the presentation.

11:00 AM - 11:15 AM

UNIFORMITY OF GAAS SOLAR CELLS GROWN IN A KINETICALLY-LIMITED REGIME BY DYNAMIC HYDRIDE VAPOR PHASE EPITAXY

K.L. Schulte, W. Metaferia, J. Simon, A. Ptak

National Renewable Energy Laboratory, CO, UNITED STATES OF AMERICA

III-V solar cell devices are currently limited to high value applications, such as space power, which value the high efficiency and low weight that only III-V devices provide. Cell manufacturing costs, of which epitaxial growth comprises a significant fraction, must be reduced dramatically to enable proliferation of these high-performance devices in terrestrial applications. Dynamic hydride vapor phase epitaxy (D-HVPE) has emerged as a potential route to high-efficiency solar cell devices with reduced manufacturing cost. D-HVPE combines low-cost elemental precursors with significantly higher throughput and potentially higher reactant utilization efficiency compared with metalorganic vapor phase epitaxy, the incumbent III-V growth technique. Previously, the complexity and performance of HVPE-grown heterojunction devices were limited by an inability to form abrupt heterointerfaces. D-HVPE overcomes this difficulty, enabling the formation of abrupt arsenide/phosphide heterointerfaces at high growth rates without growth pauses, and represents a step towards in-line growth. For D-HVPE to take the next step towards industrial adoption, the performance of D-HVPE devices must be validated over larger areas. In this presentation, we demonstrate III-V growth on 2" diameter GaAs substrates by D-HVPE. We combine 3D computational fluid dynamics modeling of our reactor with a kinetic GaAs growth model, and use it to predict spatial GaAs growth rate over a 2" wafer area. We compare these predictions with experimental data from our D-HVPE reactor and find excellent agreement. We use the modeling to gain insight into the specific mechanisms that control the GaAs spatial uniformity in this growth regime. We use this understanding to produce GaAs solar cells on 2" GaAs substrates. In contrast to our prior D-HVPE devices, grown at 650°C in a transport-limited regime, these were grown at 700°C in a kinetically-limited growth regime in which the growth rate uniformity is controlled by thermally activated surface reactions. These devices exhibit an open circuit voltage up to 1.07 V, nearly identical performance to the devices grown at lower temperature. We analyze the device performance and find only a 1% variation in absolute device efficiency across the majority of the wafer. We analyze the GaAs and GaInP growth rate uniformity and GaInP

compositional uniformity, and find that any non-uniformity in device efficiency is not related to variations in these structural characteristics. These results suggest a large parameter window for the growth of high-performance optoelectronic devices by D-HVPE, possibly with large area uniformity.

11:15 AM - 11:30 AM

HETEROEPITAXY OF GAASP AND GAP ON GAAS BY LOW PRESSURE HYDRIDE VAPOR PHASE EPITAXY

A. Strömberg, G. Omanakuttan, S. Lourudoss, **Y. Sun**

Department of Applied Physics, KTH-Royal Institute of Technology, SWEDEN

Heteroepitaxy of $\text{GaAs}_x\text{P}_{(1-x)}$ and GaP on GaAs has broad applications in the fields of optoelectronics and renewable energy. $\text{GaAs}_x\text{P}_{(1-x)}$ is a promising top cell material for III-V/Si tandem solar cells aiming for conversion efficiency beyond 30%. Orientation-patterned GaP (OP-GaP) grown on GaAs has been investigated as a nonlinear optical crystal for infrared laser application enabled by frequency conversion. High growth rate and low defect density in the heteroepitaxial $\text{GaAs}_x\text{P}_{(1-x)}$ and GaP layers on GaAs are desired for various photonic device applications. In this work, low pressure hydride vapor phase epitaxy (LP-HVPE) technology is utilized to grow $\text{GaAs}_x\text{P}_{(1-x)}$ and GaP on semi-insulating (SI) (001) GaAs aiming for high growth rate and high crystalline quality. The growth was conducted at a pressure of 20 mbar. PH_3 , AsH_3 and GaCl formed by flowing HCl over molten gallium were used for $\text{GaAs}_x\text{P}_{(1-x)}$ and GaP growths. Different combinations of gas flows and growth temperatures were investigated to achieve high growth rate and high crystalline quality. The grown $\text{GaAs}_x\text{P}_{(1-x)}$ and GaP layers on GaAs were characterized by high resolution X-ray diffraction (HRXRD) for composition and crystalline quality, Hall effect for impurity concentration and carrier mobility and atomic force microscopy (AFM) for morphology. The dependence of $\text{GaAs}_x\text{P}_{(1-x)}$ composition on PH_3/AsH_3 ratio was studied. $\text{GaAs}_{0.72}\text{P}_{0.28}$ was obtained with FWHM of 230 arcsec in XRD rocking curve, which is suitable for top cell

material in high efficiency GaAsP/Si tandem solar cell application. The growth rate of 52 $\mu\text{m}/\text{hour}$ for GaAsP and more than 70 $\mu\text{m}/\text{hour}$ for GaP were achieved. GaP with FWHM of 221 arcsec in XRD rocking curve was obtained on GaAs substrate despite the large lattice mismatch about 4%. In this work we have demonstrated high growth rate of GaP and $\text{GaAs}_x\text{P}_{(1-x)}$ with tunable composition and bandgap on GaAs substrates with high crystalline quality grown by LPHVPE, which will facilitate the realization of high efficiency GaAsP/Si tandem solar cell and OP-GaP nonlinear optical crystal for frequency conversion in IR and THz regions.

11:30 AM - 11:45 AM

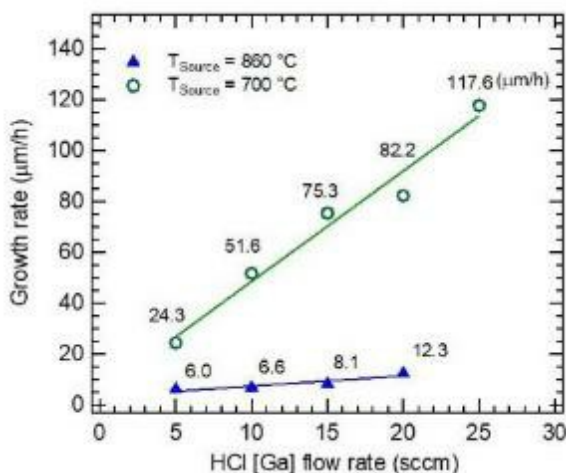
EVALUATION OF GAAS SOLAR CELLS GROWN WITH DIFFERENT GROWTH REGIMES BY HYDRIDE VAPOR PHASE EPITAXY

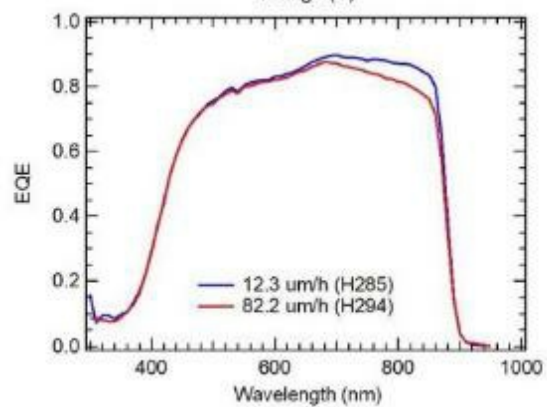
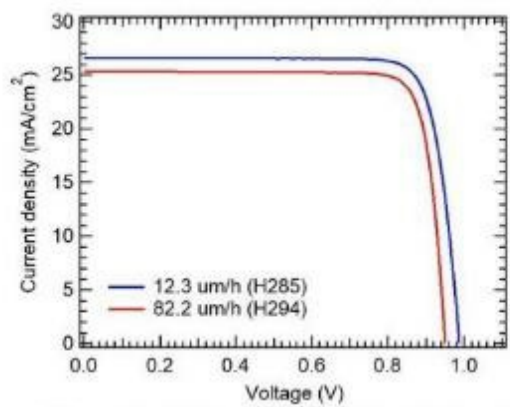
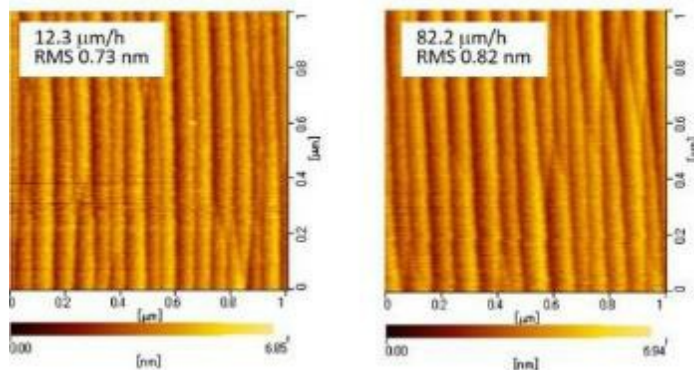
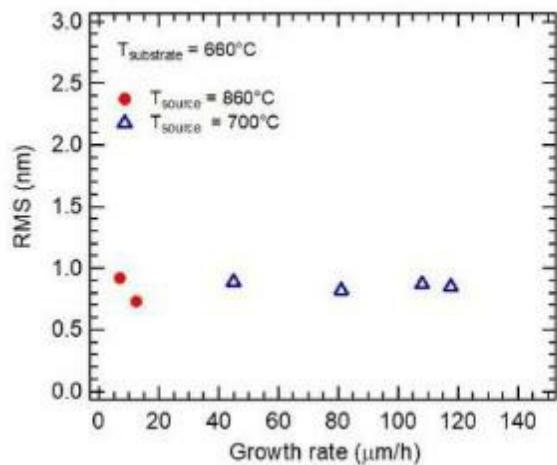
R. Oshima¹, Y. Shoji¹, K. Makita¹, A. Ubukata², T. Sugaya¹

¹National Institute of Advanced Industrial Science and Technology, JAPAN, ²Taiyo Nippon Sanso Corporation, JAPAN

At present, the use of highly efficient III-V solar cells is limited to space and high-concentration systems, owing to their high manufacturing cost. It is necessary to lower the manufacturing cost for implementing large-scale terrestrial modules. As hydride vapor-phase epitaxy (HVPE) is a high speed growth technique using less expensive group III elemental metals, it would be a possible pathway to lower the cost of III-V devices. We previously developed a vertical flow-type, atmospheric pressure HVPE with triple growth chambers and demonstrated GaAs cells with 22.1% efficiency. However, a relatively growth rate of 8 $\mu\text{m}/\text{h}$ for GaAs was a drawback to improve throughput performance. A low growth temperature of 660°C, which is required to grow high-quality InGaP/GaAs heterostructures at a single temperature, limits the growth rate due to a large kinetic barrier of GaAs formation. Despite this limitation, the kinetic barrier has been reduced in non-standard growth condition, when the group V elements reach the surface in hydrides. In this study, we examined a control of decomposition ratio of AsH_3 to achieve high growth rate for GaAs for solar cell application. The temperature of the substrate region was set

to 660°C. The flow rate of gaseous HCl over Ga metal and V/III ratio were 20 sccm and 4. When the temperature of source region (T_s) was decreased from 860 to 700°C, and at the same time, H_2 carrier flow rate that pushed AsH_3 was increased from 1 to 5 SLM, the growth rate was significantly increased from 12.3 to 82.2 $\mu\text{m/h}$. This suggests that high AsH_3 velocities at lower T_s left a significant fraction of uncracked AsH_3 until it reached the surface, leading to a change in the growth mode from kinetically limit to mass transport limit growth. In AFM measurement, small surface roughness of smaller than 0.9 nm was successfully observed for both growths. However, in solar cell measurements, the GaAs cell grown at 82.2 $\mu\text{m/h}$ yielded an efficiency (η) of 20.4% with short-circuit current density (J_{SC}) = 25.3 mA/cm^2 , open-circuit voltage (V_{OC}) = 0.95 V, and fill factor (FF) = 0.85, which was slightly lower than that of 21.8% for the cell grown at 12.3 $\mu\text{m/h}$ with J_{SC} = 26.6 mA/cm^2 , V_{OC} = 0.99 V, and FF = 0.83. In addition, quantum efficiency for the cell grown at 82.2 $\mu\text{m/h}$ was gradually decreased in longer wavelength region possibly due to a short minority carrier diffusion length.





11:45 AM - 12:00 PM

GAAS SOLAR CELLS GROWN AT GROWTH RATES EXCEEDING 300 $\mu\text{M}/\text{H}$ BY DYNAMIC-HYDRIDE VAPOR PHASE EPITAXY

W. Metaferia, K.L. Schulte, J. Simon, S. Johnston, A. Ptak

National Renewable Energy Laboratory, CO, UNITED STATES OF AMERICA

Light weight, flexibility and high conversion efficiencies are among the attributes of III-V materials that make III-V photovoltaics advantageous over commercial Si. However, high manufacturing costs have generally limited III-V PV to niche markets. Hydride vapor phase epitaxy (HVPE) has re-emerged as a potentially lower-cost alternative to today's industry standard III-V production technique, metalorganic vapor phase epitaxy (MOVPE). One way that HVPE projects to be lower cost is through the extremely high growth rates that are possible using this technique. Here, we present recent efforts to increase the growth rates for GaAs and GaInP in our custom, dynamic-HVPE (D-HVPE) reactor. We show that through optimization of the *in-situ* conversion reaction between elemental Ga and anhydrous HCl to form GaCl for the growth reaction, plus increased mass transport of reactants to the growth front and a decrease in the kinetic barrier to growth, we can achieve GaAs growth rates $> 300 \mu\text{m}/\text{h}$ by atmospheric-pressure D-HVPE at $650 \text{ }^\circ\text{C}$. We also demonstrate GaInP layers with growth rates in excess of $100 \mu\text{m}/\text{h}$, with no evidence of growth rate saturation in the range we were able to test. Although GaAs films have previously been grown using rates $\sim 300 \mu\text{m}/\text{h}$ by low pressure HVPE, no devices were demonstrated to test the material quality. We grew single junction GaAs solar cells with GaInP passivation layers at GaAs growth rates $\sim 35 - 309 \mu\text{m}/\text{h}$ and assessed the effect of growth rate on device performance. The open circuit voltage of our GaAs solar cells grown at these rates was in the range of $1.04 - 1.07 \text{ V}$ with minimal degradation as the growth rate increased, indicating that the material quality was maintained at these high growth rates. This was further confirmed by deep level transient spectroscopy measurements that identified EL2 traps with concentration $< 3 \times 10^{14} \text{ cm}^{-3}$, with no significant increase in concentration as the growth rate increased from $\sim 35 - 309 \mu\text{m}/\text{h}$.

These results have strong implications toward increasing the throughput and lowering the cost of III-V photovoltaics, enabling the deposition of high efficiency cells in mere seconds instead of hours.

Friday, August 2, 2019

10:30 AM - 12:00 PM

In Situ Observation and Characterization IV

Location: Shavano Peak

Session Chair(s):

10:30 AM - 10:45 AM

HOW MICROGRAVITY EXPERIMENTS LEAD TO A BETTER UNDERSTANDING OF PARTICLE INCORPORATION DURING CRYSTAL GROWTH

T. Jauss¹, N. Pfändler¹, C. Reimann², J. Friedrich², T. Sorgenfrei¹

¹University of Freiburg, GERMANY, ²Fraunhofer IISB, GERMANY

The incorporation of foreign phase particles during solidification might be favorable in some cases, but in most crystal growth processes it needs to be avoided. A prominent example for the second scenario is the directional solidification of multi crystalline (mc) silicon for photovoltaic applications. During this process, the silicon melt is in contact with the silicon nitride coated crucible walls and the furnace atmosphere which contains carbon monoxide. The dissolution of the crucible coating, the carbon bearing gas, and the carbon already present in the feedstock lead to the formation of silicon carbide and silicon nitride particles in the melt and subsequently in the crystal during the growth process. Besides electrical and mechanical impairments of the mc-material, the growth of the silicon grains can be influenced negatively by the presence of particles, which act as nucleation sources and lead to a grit structure of small grains and are sources for dislocations. On board of the TEXUS 51, 53, and 55 sounding rocket missions we studied the incorporation behavior of SiC, Si₃N₄ particles separately as well as both species together under microgravity, and therefore under nearly diffusive conditions. Under microgravity conditions both species of particles were incorporated at lower growth rates and in earlier stages during the growth compared

to the terrestrial experiments. From these findings during the sounding rocket missions it can be concluded that forced melt convection is an appropriate tool to prevent foreign phase particles from incorporation into the growing crystal. A remaining question that could not be answered satisfyingly in the Si-C-N system by these experiments is the response of the moving solid liquid interface to the presence of these particles shortly before and during incorporation. For this reason, we are developing a model system with a transparent melt to observe the particle-phase boundary interactions in-situ. This model system will provide further insights on these interactions during the upcoming TEXUS 56 sounding rocket mission.

10:45 AM - 11:00 AM

IN SITU OBSERVATION OF DENDRITE GROWTH IN GALLIUM ANTIMONIDE

K. Shiga, M. Kawano, K. Maeda, K. Fujiwara
Institute for Materials Research, JAPAN

Single-crystal substrates of gallium antimonide (GaSb) are used in a variety of electronic devices such as mid-infrared-emitting diodes and thermophotovoltaic cells. It is well known that electrical properties of the devices are dependent on the grain boundary structure in the substrate. In pure semiconductors Si and Ge, twin boundaries provide nucleation sites for the dendrite growth. Compared to pure semiconductors, the dendrite growth in the group III–V compound semiconductors remains less well studied. In this study, we directly observed crystal–melt interfaces of GaSb during the directional growth and elucidated the process by which faceted dendrites are formed. We used an in-situ observation system consisting of a furnace and a digital microscope with a zoom lens having a long-working-distance. The furnace was equipped with two carbon heaters that could be independently controlled to produce a thermal gradient (G) inside the furnace. GaSb was melted under an argon atmosphere, after which the temperature was decreased to promote directional growth. The crystal–melt interfaces during the directional growth were directly observed with the digital microscope. The crystallographic orientations of the GaSb dendrites in the areas observed were determined by electron backscatter diffraction (EBSD; JSM-6610A, JEOL). When the

moving velocity of the crystal–melt interface was low, the planar interface was maintained. With increasing moving velocity, the shape of the interface became instable and the faceted interface was formed. The dendrite growth was initiated at the faceted interface. Dendrite grew in either the $\langle 112 \rangle$ or $\langle 110 \rangle$ direction, and each type of dendrite exhibited a unique shape and propagation mechanism. The dendrite grown along $\langle 112 \rangle$ exhibited the continuous formation of two triangular crystals with a tip angle of 60° , and the growth direction of the triangular crystal alternately changed. Conversely, the dendrite grown along $\langle 110 \rangle$ showed that the tip angle was 120° and the growth direction of the tip did not change. It was clarified that dendrites in GaSb grow via two-dimensional nucleation at reentrant corners located at twin boundaries.

11:00 AM - 11:15 AM

INFLUENCE ON DEFECT TYPES AND DENSITIES OF 4H-SiC WITH VARYING GROWTH CONDITIONS

M.A. Roder¹, P. Wellmann², J. Steiner², M. Arzig², M. Kabukcuoglu³, S. Haaga³, A. Danilewsky¹

¹Crystallography, Albert-Ludwigs University Freiburg, GERMANY,

²Crystal Growth Lab, Material Department 6 (i-meet), GERMANY,

³Karlsruhe Institute of Technology (KIT), Institute for Photon Science and Synchrotron Radiation (IPS), GERMANY

Silicon carbide (SiC) is a semiconductor with a high application variety but a high diversity of defects like Micropipes (MP), Threading Screw Dislocation (TSD), Threading Edge Dislocation (TED), Basal Plane Dislocations (BPD), which negatively influences the device's performance [1 2]. Several SiC wafers, grown by Physical Vapor Transport [3] at various growth conditions were characterized with different X-ray methods. Synchrotron White Beam X-ray Topography (SWXRT) in back-reflection geometry was used to determine defect types. SWXRT were performed at the TopoTomo Beamline, IPS Karlsruhe institute for technology (KIT). The dominating defect types include TSDs, TEDs, MPs in different densities and small-angle grain boundaries between screw dislocations. Additionally, full wafer mappings in transmission geometry show a different defect density,

depending on the growth conditions. The wafers grown at lower temperatures, with a longer growth duration, a lower growth rate and a higher crystal diameter show a lower defect density but also an inhomogeneous defect distribution, which is highest at the wafer's edge. Furthermore, the mappings show a clear lineation of small-angle grain boundaries in direction of the crystal's misorientation. Therefore appearance and development of small-angle grain boundaries are in direct relation with angle and direction of the crystal's misorientation, which was determined with Laue precision measurements. High resolution X-ray diffractometry (HRXRD) measurements were performed at the corresponding positions to investigate the crystal quality in terms of crystal lattice strain and tilt. Rocking curves in 0004 reflection show a difference in their curve shape and full-width at half maximum (FWHM) depending on the crystal quality, which is in good agreement with the SWXRT results. Reciprocal Space maps were recorded at the same positions in the same reflection. Depending on the dominant defect type in the measured area the relation of crystal lattice strain to crystal lattice tilt changes. A higher density of TSDs and small-angle grain boundaries induces more crystal lattice tilt. The results of all measurements showed a high defect density in the wafer but inhomogeneous distribution, pointing to an inhomogeneous temperature distribution and a high temperature gradient vertically and horizontally during growth. [1] Neudeck, PH. G. et. al. *Solid State Electron*, 42(12):2157–2164, 1998. [2] Dhanaraj, Govindhan, et al., eds. *Springer handbook of crystal growth*. Springer Science & Business Media, 2010 [3] Wellmann, P. et. al. *Crys. Res. & Technol.*, 50(1):2-9, 2015

11:15 AM - 11:30 AM

***IN-SITU* SYNCHROTRON X-RAY TOPOGRAPHY STUDIES OF STACKING FAULTS EXPANSION PROCESS IN N-TYPE 4H-SiC CRYSTALS**

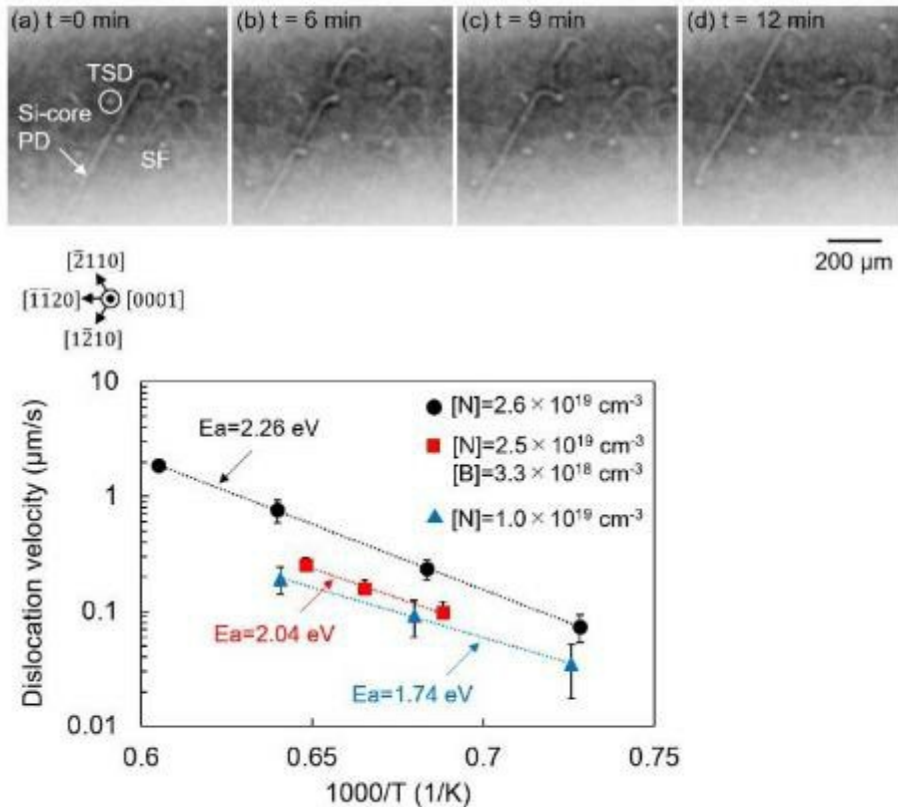
F. Fujie¹, S. Harada², H. Suo³, T. Kato⁴, T. Ujihara²

¹Department of Materials Process Engineering, Nagoya University, JAPAN, ²Institute of Materials and Systems for Sustainability (IMaSS), JAPAN, ³Showa Denko K.K., JAPAN, ⁴National Institute of Advanced

Industrial Science and Technology (AIST), JAPAN

Silicon carbide (SiC) is one of the most promising materials for power devices because of its excellent physical properties. To obtain a low resistivity n-type SiC substrate, nitrogen is doped as donor impurity. However, in heavily-nitrogen-doped 4H-SiC, the formation and expansion of double Shockley stacking faults (DSFs) has been observed to occur at typical device processing temperatures. It has been suggested that the driving force is attributed to the local energy levels associated with the SFs. The electronic energy gain induced by the electron trapping by the SF-induced energy levels leads to the negative SF energy in nitrogen-doped 4H-SiC at high temperatures. It is also reported that the nitrogen enhances the SFs expansion, whereas the boron suppresses the expansion. Recently, we developed an *in-situ* X-ray topography system using synchrotron radiation for the observation of the SFs in 4H-SiC during a high-temperature annealing process. In this study, we studied about the influence of impurities on the dynamic behavior of SFs expansion. *In-situ* X-ray topography experiments were performed using 00016 reflection. The nitrogen-doped and nitrogen-boron co-doped 4H-SiC crystal was subject to high-temperature heat treatment while sequential X-ray topography images were recorded simultaneously. Fig. 1 shows sequential X-ray topography images of 4H-SiC crystals with a nitrogen concentration of $1.0 \times 10^{19} \text{ cm}^{-3}$ taken at 1610 K. In this geometry, Si-core partial dislocation (PD) exhibits white line contrasts. The SF surrounded by straight PD was observed. During annealing, the Si-core PD glided at constant rate while accompanying the SF expansion even though it interacted with TSDs. Fig. 2 shows the Arrhenius plots for the glide velocity of the Si-core PDs. The velocity increased with nitrogen concentration, but it decreased by boron doping. As for the dislocation mobility, however, the activation energy of the dislocation increased with nitrogen concentration, but it decreased by boron doping. This means that nitrogen makes the dislocations less mobile, whereas boron facilitates the glide of the dislocations. From the above results, one can state that the varieties of the SFs expansion velocity when nitrogen and/or boron are doped would mainly come from the change of the driving force of the dislocation glide (SF energy) rather than the dislocation mobility

depending on the nitrogen and boron concentrations. This work was supported by Council for Science, Technology and Innovation (CSTI), Cross-ministerial Strategic Innovation Promotion Program (SIP), “Next-generation power electronics/ Consistent R&D of next-generation SiC power electronics” (funding agency: NEDO).

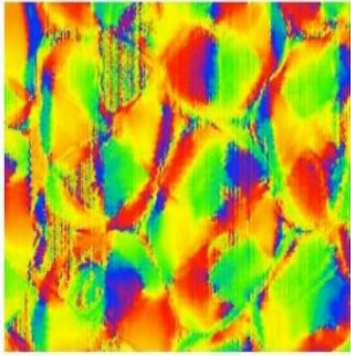


11:30 AM - 11:45 AM

OPTICAL ANOMALY OF GAN AND SIC CRYSYALS AS OBSERVED BY NEW OPTICAL MAIN AXIS MAPPING

K. Tsukamoto¹, M. Imanishi², H. Koizumi³, T. Onuma⁴, T. Ujihara⁵, Y. Mori²

¹Graduate School of Science, Tohoku University, JAPAN, ²Graduate School of Engineering, Osaka University, JAPAN, ³Institute of Materials and Systems for Sustainability (IMaSS), JAPAN, ⁴Photron Limited, JAPAN, ⁵Graduate School of Engineering and School of Engineering, Nagoya University, JAPAN



Optical anomaly that is attributed to the fine deviation of crystal symmetry from the ideal ones has been observed in various minerals and crystals with larger photo-elasticity like garnet and SiC crystals. This reduction of the symmetry was not easy to be detected by structural analysis using X-ray and has been observed by optical birefringence microscopy for the last decades. We have developed a new optical microscopy to map both phase-shift and reduction of symmetry from pixel to pixel and thus the faint shift of optical axis caused by distortion of the crystal structure in much more sensitive way and in a quicker way than birefringence microscopy or x-ray analysis. Thanks to the development of fast birefringence CCD cameras, $>10^4$ frames/s. The new method was applied to GaN and SiC crystals. Initial stage of an epitaxially grown GaN crystal, fig, clearly shows that the crystal symmetry deviates from ideal hexagonal symmetry depending the growth directions. If the crystal is real hexagonal symmetry, the colors that show the main optical axis is uniform. This method was applied also to other GaN and SiC crystals and found to be useful to characterize how and by which technique the crystals were grown. Compared to, for instance, X-ray topography, this method is more sensitive to the local anomaly of the crystal symmetry from ideal ones. Among others, this optical method has an advantage in the good time-resolution and thus is suitable to study fast phase change or grain growth like ice crystals that are already started to be investigated.

Friday, August 2, 2019

10:30 AM - 12:00 PM

Nonlinear Optical and Laser Host Materials V

Location: Red Cloud Peak

Session Chair(s): Yushi Kaneda

10:30 AM - 10:45 AM

OPTIMIZATION OF THE GROWTH OF ERBIUM DOPED YAG AND ER-TM CO-DOPED YAG FIBERS BY THE MICRO-PULLING DOWN TECHNIQUE

A. Laidoune, D. Bahloul

Faculté des Sciences de la Matière; département de physique
université Batna 1, ALGERIA

In this study we work on the optimization of the growth of erbium doped YAG and Er-Tm co-doped YAG fibers crystals grown by the micro pulling down (μ -PD) technique. The growth of these fibers is performed using a relatively recent growing technique that is the (μ -PD). This method presents several advantages over other growing method and allows a stable growth of shaped crystal fibers with very good optical quality. The obtained fibers have good transparency and stable diameter, they are homogeneous and free from defects. The absorption and emission spectra of Er:YAG and Er-Tm : YAG fibers are realized and compared using the pump excitation at 800 nm. A broad seamless emission extending from 1.37 μ m to 1.55 μ m for the Er³⁺-Tm³⁺ codoped YAG fibers were observed. The possibility of amplifying signals beyond 1600 nm is also discussed. The visible upconversion emission spectra were also recorded in order to understand the luminescence. This work confirms the importance of crystalline fibers as good candidates in the design of new photonic devices for laser application especially in medical application. The experimental results of the lifetimes are confirmed the possibility to laser production.

10:45 AM - 11:00 AM

CRYSTAL GROWTH, SPECTROSCOPY AND FEMTOSECOND LASER PERFORMANCE OF TM,HO:CNGG DISORDERED

GARNET CRYSTAL

Z. Pan¹, Y. Zhao², Y. Wang², W. Chen², L. Wang², H. Cai¹, P. Loiko³, S. Suomalainen⁴, A. Härkönen⁴, M. Guina⁴, X. Mateos⁵, U. Griebner², V. Petrov²

¹Institute of Chemical Materials, China Academy of Engineering Physics, CHINA, ²Max-Born-Institute for Nonlinear Optics and Ultrafast Spectroscopy, GERMANY, ³ITMO University, RUSSIAN FEDERATION, ⁴Optoelectronics Research Centre, Tampere University of Technology, FINLAND, ⁵Universitat Rovira i Virgili (URV), SPAIN

We report on the crystal growth, spectroscopy characterization, tunable and mode-locked laser operation of a disordered multicomponent garnet crystal, Tm,Ho:CNGG. A tunability of 204 nm has been achieved, covering the wavelength range beyond 1940 nm (from 1940 to 2144 nm), which is located outside the region of strong water vapor absorption. Mode-locked femtosecond laser based on the disordered garnet were demonstrated. Employing InGaAsSb quantum-well semiconductor saturable absorber and chirped mirrors for dispersion compensation, pulses as short as 100 fs are generated at 89.30 MHz repetition rate with an average output power of 105 mW. Using a 0.5% output coupling, pulses as short as 73 fs are produced with an average output power of 36 mW without extracavity compression.

11:00 AM - 11:15 AM

RECENT PROGRESS IN $\text{KBe}_2(\text{BO}_3)\text{F}_2$ CRYSTAL GROWTH AND APPLICATIONS

X. Wang, L. Liu, R. Li

Technical Institute of Physics and Chemistry, CAS, CHINA

In recent years, many types of potential deep-ultraviolet (UV) nonlinear optical (NLO) crystals have been discovered. However, their capability to generate deep-UV harmonic generation is based on theoretical calculations and untested. So far, $\text{KBe}_2(\text{BO}_3)\text{F}_2$ (KBBF) is still the only practical deep-UV NLO crystal that can generate coherent radiation below 200 nm by direct second harmonic. It can be deemed that the development of all-solid-state deep-UV lasers is solely based

on KBBF crystals and their prism coupled devices (PCD). KBBF crystals are also suitable for generating laser lines near 200 nm through cascaded harmonics that other NLO crystals are difficult to achieve. In this paper, we report the recent progress in KBBF crystal growth and applications, including the output of laser lines at 213nm by the fifth harmonic generation from an Nd: YAG laser, and other laser outputs at short wavelengths. Finally, we also evaluate the commercialization viability of KBBF crystals.

11:15 AM - 11:30 AM

GROWTH, ELECTRICAL, OPTICAL STUDIES AND TERAHERTZ WAVE GENERATION OF ORGANIC NLO CRYSTALS: DSTMS

B. Teng

College of Physics, Qingdao University, CHINA

The raw materials of 4-N,N-dimethylamino-4'-N'-methyl-stilbazolium 2,4,6-trimethylbenzenesulfonate (DSTMS) is synthesized by condensation method under the catalysis of piperidine. DSTMS crystals are grown by spontaneous nucleation method with methanol as solvent. The UV-Vis-NIR spectrum was recorded for the grown crystal, and critical optical properties such as the cut-off wavelength, band gap energy, absorption coefficient and refractive index were calculated. Photoluminescence (PL) spectrum of DSTMS crystal were recorded. The electric properties of the crystal were tested. The surface characteristics of the crystal were studied by chemical etching. The relative second harmonic generation efficiency (SHG) was tested to explore the nonlinear optical (NLO) property. The continuous terahertz waves in the range of 0-10 THz have been measured by optical rectification (OR).

11:30 AM - 11:45 AM

CRYSTAL GROWTH, COMPOSITION, MORPHOLOGY AND THERMAL PROPERTIES OF $REAL_{2.07}(B_4O_{10})O_{0.60}$ DIMETABORATES SOLID SOLUTIONS ($RE = LA, CE, PR$).

E. Koporulina¹, V.V. Maltsev¹, N.I. Leonyuk²

¹Lomonosov Moscow State University, Geological faculty, RUSSIAN FEDERATION, ²Lomonosov Moscow State University, Geological

faculty, Department of Crystallography and Crystal Chemistry,
RUSSIAN FEDERATION

To date, two large families of anhydrous rare earth aluminium borates are known: orthoborates $REAl_3(BO_3)_4$ ($RE = Y, Pr-Lu$), with huntite $R32$ type of structure, and their $C2$ and $C2/c$ polytypic monoclinic derivatives, and hexagonal dimetaborates $REEAl_{2.07}(B_4O_{10})O_{0.60}$ ($RE = La-Nd$) with $P-6m2$ sp.gr. which are isostructural with mineral peprossiite-(Ce) [1]. A common feature of these materials is the high concentration of RE optically active ions in their crystal structure. While the compounds of the first group have been widely investigated, information about representatives of dimetaborate family is rather fragmentary. In this work, a correlation between growth conditions, composition and morphology of $REEAl_{2.07}(B_4O_{10})O_{0.60}$ ($REE = La, Ce, Pr$) crystals and their solid solutions is discussed. The crystals of title compounds were grown by spontaneous nucleation using $K_2Mo_3O_{10}$ based fluxed melts in the temperature range of $1000-800^\circ C$ using 50 wt% of dimetaborate in the initial mixture. As a result, hexagonal plate-like crystals up to 5 mm were obtained. Their colour varies from colourless to light green depending on the type and content of the rare-earth cation. The composition, homogeneity and morphology of single crystals were studied using analytical scanning electron microscopy. Considering the plate-like habit of dimetaborate crystals, as grown surfaces without additional preparation were used for the analysis. The micromorphology of the crystal faces were investigated by atomic-force microscope (AFM) in semi-contact mode in air at room temperature. Most of the crystals grown are characterized by well-developed polygonal spirals on the $\{0001\}$ faces. Shape of these spirals corresponds to the hexagonal symmetry of the faces. According to the AFM measurements, the height of the spiral layers varies in the range of 10–30 nm; the largest steps reach 50 nm. These values do not depend on the crystal composition and, apparently, are determined by similar experimental conditions, in particular, by the cooling rates of the fluxed melts. The compositions of the grown dimetaborate crystals and their solid solutions are close to those in the initial fluxed melt. The concentration profiles showed a uniform distribution of rare-earth elements along the crystal faces. It

was determined that La-dimetaborate incongruently melts at 1165°C and LaBO_3 and $\text{Al}_{18}\text{B}_4\text{O}_{33}$ were found among decomposition products. This research was supported in part by the RFBR grants Nos. 18-05-01085 and 18-29-12091.

References: D. Yu. Pushcharovsky et al. Sov. Phys. Dokl., 1978, V.23(7), pp.450-452. N. I. Leonyuk and L. I. Leonyuk. Prog. Cryst. Growth Charact., 1995, V.31(3-4), pp.179-278.

11:45 AM - 12:00 PM

PROGRESS ON SELF-FREQUENCY-DOUBLED YB:CA₄YO(BO₃)₃ CRYSTAL

J. Wang¹, H. Yu¹, H. Zhang²

¹Shandong University, CHINA, ², CHINA

Self-frequency-doubled Yb:Ca₄YO(BO₃)₃ (Yb:YCOB) crystal with different doping concentration has been grown by the Czochralski method. A watt-level self-frequency-doubled yellow laser at the 570 nm wavelength was realized by taking advantage of the vibronic emission of Yb:YCOB crystal cut along the optimized direction with the maximum effective nonlinear coefficient. Meanwhile, a maximum green light output power of 710 mW at 523 nm with Yb:YCOB crystal was obtained by cavity design, as presented in Fig. 1.

According to the previous reports, Yb:Ca₄YO(BO₃)₃ (Yb:YCOB) crystal of good quality and large size can be grown easily by the Czochralski method. The crystal has good potential to be used for self-frequency-doubling due to its excellent combination of nonlinear and laser properties. By analysing the measured fluorescence spectra and absorption spectra, the effective gain cross sections $\sigma_g(\lambda)$ were calculated, which showed that the crystal had a small vibronic emission peak at about 1130 nm with the emission cross section of about $5 \times 10^{-22} \text{ cm}^2$. By suppressing the electronic emission, the polarized vibronic Yb:YCOB radiation was realized with the fundamental wavelength shifting from 1130 nm to 1140 nm. The self-frequency-doubled yellow laser was achieved with a maximum output power of 1.08 W at 570 nm. This work provides a way for the realization of yellow lasers and promising, attractive source with a compact structure. In the meantime, a maximum green light output

power of 710 mW at 523 nm with Yb:YCOB crystal was obtained, and this result is the best performance ever reported about the SFD green light with Yb:YCOB crystal.

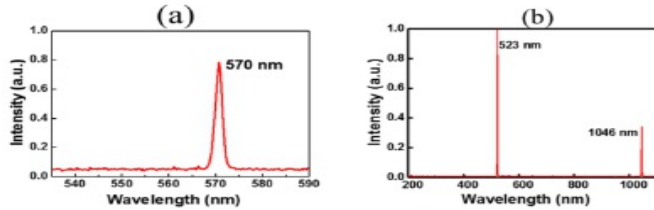


Fig. 1 Output wavelengths of the SFD yellow and green light.
[1] R. Acevedo, P. A. Tanner, T. Meruane, and V. Poblete, *Physical Review B* **54**, 3976 (1996).

Friday, August 2, 2019

10:30 AM - 12:00 PM

Silicon Carbide Materials and Devices II

Location: Crestone III, IV

Session Chair(s): Narsingh B. Singh, S. Parathasarathy

10:30 AM - 11:00 AM

EVALUATION OF DEFECTS IN BULK SiC

M. Dudley

, UNITED STATES OF AMERICA

An overview is presented of defects in PVT Grown bulk SiC crystals. Detailed Synchrotron X-ray Topography analysis shows that the observed defects can be divided into two categories: (a) those produced by phenomena occurring at the moving growth interface and (b) those produced by phenomena occurring behind the growth interface while the crystal is still in the growth chamber. Considering (a), most dislocations piercing the growth interface are simply replicated and extend as the crystal grows. In addition, opposite sign pairs of threading dislocations can be nucleated through the incorporation of inclusions at the interface. Near the crystal periphery, the interface shape can sometimes become convex leading to step

bunching and the formation of macrosteps. These macrosteps can deflect threading dislocations onto the basal plane and can also lead to the formation of stacking faults. Considering (b), dislocations behind the growth interface can experience both climb and glide. For example, threading dislocations with a c-component of Burgers vector produced by replication or nucleation processes at the interface can interact with non-equilibrium concentration of vacancies and climb into spiral type configurations. This can sometimes lead to annihilation of segments of these dislocations. In addition, dislocations with Burgers vector $1/3 \langle 11-20 \rangle$ can experience stresses due to thermal gradients leading to glide and, in some cases, multiplication processes. Both basal and prismatic slip can occur depending on the nature of the shear stresses experienced by the cooling crystal. Detailed examples of these processes will be presented. The presentation will be summarized by presenting trends in the densities of defects of all types over the past several years as well as future expectations.

11:00 AM - 11:30 AM

GROWING LARGE DIAMETER 4H SiC BOULES

G. Dhanaraj, D. Dukes, V. Torres, L. Young, G. Sandgren
Pallidus Inc., NY, UNITED STATES OF AMERICA

Silicon carbide (SiC) is a semiconductor material which is replacing and outperforming the conventionally used silicon crystal in power applications. The wide bandgap of SiC results in a low leakage current even at high temperatures. Among the 200 polytypes of silicon carbide, 4H SiC has become the matured wide band gap semiconductor. High resistive SiC material is used in military radar applications. Colorless SiC has become a popular material for gemstones applications competing with diamond because of their excellent brilliance and other properties. At present, the production of large size and high quality 4H SiC single crystals is limited to a few industrial entities worldwide. The seeded physical vapor transport (PVT), commonly known as the modified Lely method, which exploits the sublimation at above 1800°C is the only proven method for the industrial production of SiC boules. However, fabrication of the PVT system for the growth of SiC is highly instrumentation oriented, and also due to its commercial importance, the know-how, and technical

details are scarcely available in the literature. The complexity is due to the fact that the operating temperature is extreme (above 2000°C) and monitoring and controls are difficult. The growth process occurs in a nearly air-tight graphite crucible and it is not feasible to observe the growing boule or determine experimentally the exact thermal conditions in the growth zone due to high operating temperatures and the opacity of the graphite crucible. It is difficult to control the radial gradients when the diameter reaches close to 6 inches or beyond. With full modeling knowledge as well as outstanding expertise in equipment and the process technology and thermal modeling, Pallidus has developed 6 inch diameter SiC growth process technology. The technical details on the design and fabrication of the SiC PVT system, hot zone, modeling, crystal growth and characterization results will be presented.

11:30 AM - 11:45 AM

EFFECT OF NITROGEN DOPING CONCENTRATION ON LATTICE STRAIN VARIATION IN 4H-SiC SUBSTRATES

T. Ailihumaer, H. Peng, B. Raghothamachar, M. Dudley
Department of Materials Science and Chemical Engineering, Stony Brook University, NY, UNITED STATES OF AMERICA

Nitrogen-doped 4H-SiC wafers are the most promising substrate materials for applications in power electronic devices based on its superior performance under extreme conditions such as high temperature and high voltage. However, the incorporation of the nitrogen as a dopant in 4H-SiC crystals can produce significant lattice parameter variations, which can strongly affect the crystal quality and to a large extent degrade the performance of SiC-based power devices. The formation of double Shockley stacking faults in heavily doped 4H-SiC substrates can also cause inhomogeneous resistivity and a relatively large (0001) surface roughness of 4H-SiC substrates. The non-destructive synchrotron X-ray contour mapping method [1] that we reported recently is a very powerful technique to characterize the lattice strain in 4H-SiC substrates with different nitrogen concentrations. An anisotropic elasticity model [2] has been postulated based on this technique to relate the nitrogen concentration with lattice strain values. In our study, we have applied this technique to

further study the inhomogeneity of lattice strain in different nitrogen doping conditions. Lattice strain maps were derived from 11-20, 1-100 and 0008 reflections by deconvoluting the lattice strain component from lattice tilt. Lattice strain variation inside the 4H-SiC facet and non-facetted regions were studied. In order to further investigate the relationship between the nitrogen concentration and lattice strain variation, Hall measurements associated with van der Pauw method were carried out in different 4H-SiC samples. Result shows that the resistivity and Hall mobility decreases as the nitrogen concentration increases. Nitrogen concentration in facet regions was found to be over 45% higher than the non-facetted regions. Analysis of the lattice strain maps indicated that lattice strain is isotropic inside the basal plane, while along the growth direction, lattice strain variation is one magnitude lower. Besides, the distribution of lattice strain is found to be more uniform inside the facet region compared to the outside facet regions. Triple-axis rocking curve measurement was also applied for these samples. Result showed a remarkably broadening of FWHM at the facet region, which further confirmed our result. [1] J. Guo, Y. Yang, B. Raghothamachar, M. Dudley, and S. Stoupin, J. Electron. Mater. 47(2), 903-909 (2018). [2] Y. Yang, J. Guo, B. Raghothamachar, X. Chan, T. Kim, M. Dudley, J. Electron. Mater. 47(2), 938-943 (2018).

11:45 AM - 12:00 PM

DESIGN OF SiC SOLUTION GROWTH CONDITION UTILIZING PREDICTION MODEL CONSTRUCTED BY MACHINE LEARNING AND MATHEMATICAL OPTIMIZATION

S. Harada¹, H. Lin², C. Zhu¹, T. Narumi³, Y. Tsunooka⁴, T. Endo⁵, K. Ando², K. Kutsukake⁶, M. Tagawa², T. Ujihara¹

¹Institute of Materials and Systems for Sustainability (IMaSS), JAPAN,

²Department of Materials Process Engineering, Nagoya University,

JAPAN, ³Venture Business Laboratory (VBL), Nagoya University,

JAPAN, ⁴GaN Advanced Device Open Innovation Laboratory (Gan-

OIL), Nagoya University, JAPAN, ⁵Nagoya University, JAPAN,

⁶RIKEN Center for Advanced Intelligence Project (AIP), JAPAN

Solution growth of silicon carbide (SiC) is expected to produce high-

quality SiC wafers. We have revealed the mechanism of dislocation reduction process during the SiC solution growth and demonstrated the high-quality SiC crystal growth. To enlarge the size of the crystal for the high-quality SiC wafer, it is necessary to optimize the spatial distribution of carbon supersaturation, flow and temperature in the solution. Recently, we have demonstrated the rapid prediction of the computational fluid dynamics (CFD) simulation by machine learning. Furthermore, we have constructed the optimization system of the growth condition by mathematical optimization using the prediction model. In the present study, we performed the SiC solution growth under the condition which was suggested by the optimization and improved the growth condition. Figure 1 shows optimization process of the present study. Firstly, we constructed prediction model which quickly predicts the distributions of carbon supersaturation and flow in the solution from the growth condition by machine learning with a neural network. The parameters for the growth condition were the rotation speed of the seed crystal and the crucible, the inner diameter and the position of the crucible and the meniscus height. Then, multiple purpose optimization was conducted with genetic algorithm by using the constructed prediction models. In the multiple purpose optimization, we defined several objective functions about the distributions of carbon supersaturation, flow and temperature. The objective functions were modified based on the previous experimental results. Among the optimal solutions, we selected the crystal growth conditions and performed the SiC solution growth with the diameter of 85 mm. From the actual crystal growth, it is necessary to control the supersaturation near the growth surface because of the suppression of polycrystalline precipitation on the growth surface. Therefore, we defined the objective function so that the value of supersaturation ranges from 0.01 to 0.02. Furthermore, for the stabilization of surface morphology, we defined the objective functions of inward and outward flows for applying switching flow technique. Under the suggested condition by the optimization, we have obtained the grown crystal with relatively smooth morphology at whole growth surface as shown in figure 2. This result indicates that the process of the optimization of crystal growth condition, which usually spends a long time by step-by-step process, can be drastically shorten by our proposed method.

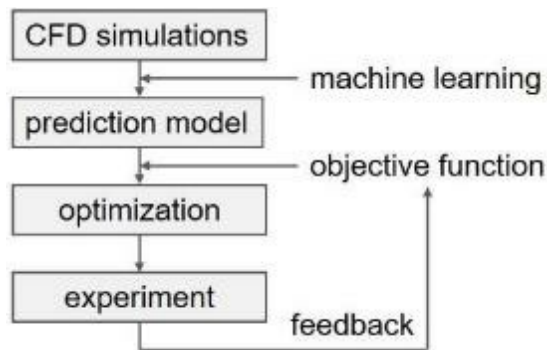


Figure 1. Optimization process of crystal growth.

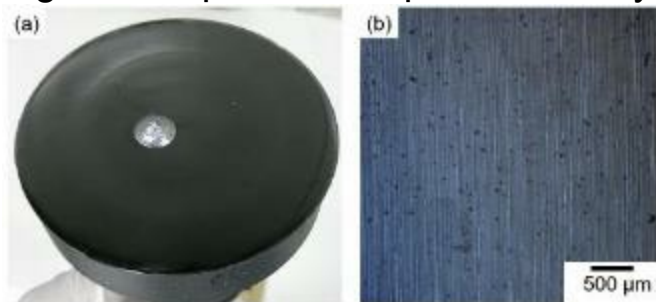


Figure 2. (a) Appearance and (b) surface morphology of the grown crystal.

Friday, August 2, 2019

10:30 AM - 12:00 PM

**Symposium on Epitaxy of Complex Oxides:
Understanding Film Growth and Solid-Phase Epitaxy**

Location: Grays Peak II, III

Session Chair(s): Lane W. Martin

10:30 AM - 11:00 AM

A NEXUS IN OXIDES: MOLECULAR BEAM EPITAXY

Y. Krockenberger, A. Ikeda, H. Yamamoto

NTT Basic Research Labs, JAPAN

Understanding of the multifariousness of electronic compartments in materials is borne out of the desire to ameliorate and hone them. While this task implies that materials with ever lower defect concentrations are required, molecular beam epitaxy (MBE) technique is regarded to cater for this need. Although other materials synthesis methods, e.g., single crystal growth, attracted high attention in the research of high temperature superconducting cuprates, the enigma

surrounding them is nowhere close to be resolved. Instead, MBE can provide by far superior research-grade materials and considerable advancements in measurement techniques and equipment have enabled state-of-the-art characterization methods to thin film materials [1,2]. The superiority in sample quality is not only due to the omnipresent crystallographically layered structures found in cuprate superconductors but also accounts for the fact that their electronic response is primarily steered by oxygen stoichiometry and cationic disorder. As oxide MBE operates significantly off thermodynamic equilibrium conditions, the thermodynamic gradient that may drive a system towards an undesired phase formation can be significantly flattened. In combination with extrinsic synthesis parameters, e.g., the epitaxial strain, superconducting Pr_2CuO_4 have been grown [3] in contrast to the common antiferromagnetic and insulating phase. Moreover, superconducting infinite-layer cuprates, a cuprate system where single crystal cannot be grown, are accessible as single crystals using MBE [4]. Superconducting cuprate thin films are conversant for their intransigently demand of the highest technological and operational level ever achieved and meeting those demands allows for the growth of other multi-cation, complex transition metal oxides, e.g., superconducting Sr_2RuO_4 thin films, ferromagnetic osmates [5], and layered palladates [6]. [1] M. Kang *et al.* Nat. Phys. <https://doi.org/10.1038/s41567-018-0401-8> (2019), in press [2] M. Horio *et al.* Phys. Rev. Lett. **120**, 257001 (2018); Phys. Rev. B **98**, 020505(R) (2018) [3] Y. Krockenberger *et al.* Appl. Phys. Ex. **8**, 053101 (2015); Sci. Rep. **3**, 2235 (2014) [4] Y. Krockenberger *et al.* Appl. Phys. Ex. **5**, 043101 (2012); J. Appl. Phys. **124**, 073905 (2018) [5] Y. Wakabayashi *et al.* Nat. Comm. **10**, 535 (2019) [6] Y. Nanao *et al.* Phys. Rev. Mat. **2**, 085003 (2018)

11:00 AM - 11:15 AM

INSIGHTS INTO THE DYNAMIC INTERFACE REARRANGEMENT IN $\text{LaFeO}_3/\text{N-SrTiO}_3(001)$ HETEROJUNCTIONS

Y. Du¹, S. Spurgeon¹, L. Wang¹, R. Comes², P. Sushko¹, S.A. Chambers¹

¹Pacific Northwest National Laboratory, WA, UNITED STATES OF

AMERICA, ²Auburn University, AL, UNITED STATES OF AMERICA
Many emergent properties and functionalities have been realized at the carefully designed complex oxide interfaces. However, complexity of the growth pathways and kinetics and their sensitivity to external conditions limit control and reproducibility of synthesis efforts. Here we demonstrate that the dynamic rearrangements of atomic planes at the polar/nonpolar junction of LaFeO₃(LFO)/n-SrTiO₃(STO) with an SrO termination can be tuned by controlling the sequence of species arriving on the substrate during the MBE growth process. Specifically, shuttering growth with alternating FeO₂ and LaO monolayers leads to the disappearance of the top-most SrO layer, and yields a TiO₂-LaO interface. Our modeling of potential kinetic pathways suggest that this dynamic rearrangement allows the incorporate oxygen of vacancies to form Fe³⁺, as SrO/Fe⁴⁺O₂ is not stable. On the other hand, co-evaporation approach can stabilize the expected TiO₂/SrO-FeO₂/LaO interface, as the La³⁺ ions are provided simultaneously to stabilize the interface Fe³⁺. The theoretical predictions are confirmed by our X-ray photoelectron, scanning transmission electron microscopy, and electron energy loss spectroscopy results. Our work highlights that subtle change in the synthesis and processing conditions can drastically affect the designed heterostructures. In addition, our modeling and experimental study into the growth kinetics and pathways may open new ways to deterministically control the structure and properties of oxide interfaces.

11:15 AM - 11:30 AM

CONTROL OF PHASES AND FUNCTIONALITIES IN EPITAXIAL PEROVSKITE OXIDE THIN FILMS THROUGH FORMATION OF OXYGEN DIODES

Q. Lu, E. Skoropata, G. Eres, H.N. Lee

Oak Ridge National Laboratory, TN, UNITED STATES OF AMERICA
Oxygen defects are essential building blocks for designing functional oxides with remarkable properties, ranging from electrical and ionic conductivity to magnetism and ferroelectricity. Oxygen stoichiometry, which can be achieved by design in synthesis of epitaxial oxide thin films, can profoundly alter crystal and electronic structures and

enables emergent phenomena unattainable with other tuning parameters. In this work, we achieved control of phases and functionalities of epitaxial perovskite thin films through triggering oxygen vacancy ordering induced by depositing SrTiO₃ (STO) capping layers in vacuum using pulsed laser epitaxy (PLE). Due to the much higher oxygen vacancy formation energy of STO compared with the perovskite layer underneath, “oxygen diode” effect can be induced which drives oxygen vacancy formation and ordering in the underlying perovskite thin film. We successfully applied this method to both La_{1-x}Sr_xMnO₃ (x = 0.3 and 0.5, denoted as LSMO) and LaCoO₃ (LCO). In LSMO, we found that depositing STO capping layer can trigger the formation of brownmillerite (BM) phase with a large expansion along the c-axis of the lattice. While in LCO, we observed an unprecedented new phase with diffraction peaks at (0 0 1/3) and (0 0 2/3) relative lattice unit, which suggests oxygen vacancy ordering every three perovskite unit cells. Further increasing the thickness of STO capping layer eventually resulted the phase transformation to BM phase in LCO. The formed BM phase LSMO and LCO still possess epitaxy and good crystal quality comparable to the pristine perovskite thin films. We quantified the chemical state changes in LSMO and LCO thin films capped with STO by using X-ray absorption spectroscopy, which clearly showed much lowered oxidation state of Mn or Co. In both LSMO and LCO, the oxygen vacancy ordered phases showed suppressed ferromagnetism and large change in optical property compared with the parent perovskite phase. Our findings provide a new pathway of tuning physical properties by designing the structure oxygen vacancies during epitaxial oxide thin film synthesis. This work was supported by the U.S. Department of Energy, Office of Science, Basic Energy Sciences, Materials Sciences and Engineering Division and as part of the Computational Materials Sciences Program.

11:30 AM - 11:45 AM

**SOLID PHASE EPITAXY OF PRALO₃ ON SRTIO₃: A
NEW GROWTH APPROACH FOR COMPLEX OXIDE THIN FILMS AI**

P. Zuo¹, Y. Chen¹, W.L..I. Waduge², N. Jayakodiarachchi², D.S. Gyan¹, T.F. Kuech³, C.H. Winter², S.E. Babcock¹, P.G. Evans¹

¹Department of Materials Science and Engineering, University of Wisconsin-Madison, WI, UNITED STATES OF AMERICA,

²Department of Chemistry, Wayne State University, MI, UNITED STATES OF AMERICA, ³Department of Chemical and Biological Engineering, University of Wisconsin, WI, UNITED STATES OF AMERICA

Solid phase epitaxy (SPE) is a promising approach for expanding the applications of epitaxial complex oxides by providing access to a broader range of compositions and enabling their formation in complex geometries. In the SPE process, oxide layers are crystallized in the solid state from amorphous layers of the same composition through solid state diffusion involving only local rearrangements of the atoms.[1] Extensive insight into SPE phenomena in semiconductors [2,3] provides a foundation on which to understand its utility for oxide epitaxy. The SPE of PrAlO_3 on SrTiO_3 serves as a model system. The interfaces between lanthanide aluminates and SrTiO_3 are also of practical interest because these interfaces can host a two-dimensional electron gas.[4] Amorphous PrAlO_3 layers were deposited on the SrTiO_3 (001) by atomic layer deposition using tris(isopropylcyclopentadienyl)praseodymium ($\text{Pr}(\text{C}_5\text{H}_4\text{iPr})_3$), trimethylaluminum (AlMe_3) and water.[5] Transmission electron microscopy (TEM) and scanning TEM (STEM) microanalysis indicated the presence of an Al_2O_3 -rich layer a few nm thick at the STO-PAO interface. The amorphous layers were crystallized by annealing in oxygen. X-ray diffraction shows the development of highly-textured, crystalline PrAlO_3 aligned predominantly with the substrate in films that were annealed at 750 °C to 800 °C for 1 to 11 hours. TEM and STEM showed the epitaxial relationship between the PrAlO_3 film and the SrTiO_3 substrate and retention of the abrupt change composition in the crystalline film that was observed in the amorphous deposit. The detailed characteristics of the Al_2O_3 -rich layer at the STO interface are under further investigation with the aim of understanding SPE mechanisms in complex oxides more fully.

References: [1] P. G. Evans, Y. Chen, J. A. Tilka, S. E. Babcock, T. F. Kuech, Crystallization of Amorphous Complex Oxides: New

Geometries and New Compositions via Solid Phase Epitaxy, Curr. Opin. Solid St. M., 2018, 22, 229-242. [2] M. G. Grimaldi, B. M. Paine, M. A. Nicolet, D. K. Sadana, Ion Implantation and Low-Temperature Epitaxial Regrowth of GaAs, J. Appl. Phys., 1981, 52 (6), 4038-4046. [3] M. G. Grimaldi, B. M. Paine, M. Maenpaa, M. Am Nicolet, D. K. Sadana, Epitaxial Regrowth of Thin Amorphous GaAs Layers, Appl. Phys. Lett., 1981, 39 (1), 70-72. [4] A. Ohtomo, H. Y. Hwang, A High-Mobility Electron Gas at the LaAlO₃/SrTiO₃ Heterointerface, Nature, 2004, 427, 423. [5] W. L. I. Waduge, Y. Chen, N. Jayakodiarachchi, T. F. Kuech, S. E. Babcock, P. G. Evans and C. H. Winter, 2019, in preparation.

11:45 AM - 12:00 PM

SOLID-STATE CRYSTALLIZATION OF AMORPHOUS AL₂O₃ ON C-PLANE SAPPHIRE

O. Elleuch¹, K. Lekhal¹, A.D. Alfieri², D.E. Savage², S.E. Babcock², P.G. Evans², T.F. Kuech¹

¹Department of Chemical and Biological Engineering, University of Wisconsin, WI, UNITED STATES OF AMERICA, ²Department of Materials Science and Engineering, University of Wisconsin-Madison, WI, UNITED STATES OF AMERICA

In solid phase epitaxy (SPE) an amorphous film is crystallized while in contact with a crystalline seed or substrate whose presence influences the phase formed, its orientation, and the kinetics of the transformation. Despite its potential impact on broad range of applications, SPE has been explored in relatively few materials. Emerging oxide materials have promise in applications in thermal transport engineering, quantum electronics, and as substrates for heteroepitaxy [1]. The synthesis of these materials from the amorphous form has significant potential benefits in expanding the range of compositions and nanoscale architectures that can be practically employed, but also requires a deep understanding of the mechanism of SPE. In the particular case of Al₂O₃, it has been reported that the α phase can be directly obtained via SPE on c-plane sapphire substrates or through seeding by small crystalline α -Al₂O₃ seed particles [2]. The sequence of phases and the kinetics depend,

however, on the sample preparation including, for example, the observation that ion-implanted amorphous layer recrystallized via two distinct phases: γ then α [3]. We have investigated the crystallization of amorphous Al_2O_3 to the stable α -phase and identified a series of epitaxial intermediate metastable microstructures. An amorphous Al_2O_3 layer with a thickness of 100 nm was deposited by atomic layer deposition (ALD) using trimethylaluminum and water precursors with deposition rate of $\sim 1 \text{ \AA/cycle}$. The amorphous/crystalline interface was prepared before the deposition by heating to 1400°C for 10 h in air to obtain a uniform step-terrace morphology. Crystallization was investigated by annealing at 900 and 1200°C for 10 h under an O_2 atmosphere to crystallize the amorphous alumina. An analysis of the crystallized samples revealed a sequence of metastable crystalline phases of Al_2O_3 . After heating to 900°C for 10 h a significant part of the layer is in the monoclinic ϑ -phase and has a preferred textural alignment with the substrate. After heating at 1200°C for 10 h the x-ray diffraction measurements show that the dominant phase has become α , the bulk sapphire phase, with no measurable ϑ -phase and is similarly in registry with the substrate with a mosaicity around $\pm 5^\circ$. This research was primarily supported by NSF Division of Materials Research through the University of Wisconsin Materials Research Science and Engineering Center (DMR-1720415).

Friday, August 2, 2019

12:15 PM - 1:45 PM

Modeling of Crystal Growth Processes VI

Location: Castle Peak III & IV

Session Chair(s): Natasha Dropka, Liverios Lymperakis

12:15 PM - 12:15 PM

PREDICTION MODEL OF COMPUTATIONAL FLUID DYNAMICS BASED ON NEURAL NETWORK CONSTRUCTED BY MACHINE LEARNING AND PROCESS OPTIMIZATION OF SIC SOLUTION GROWTH

T. Ujihara¹, **Y. Tsunooka**², **H. Lin**², **C. Zhu**¹, **T. Narumi**³, **K.**

Kutsukake⁴, S. Harada², M. Tagawa²

¹Institute of Materials and Systems for Sustainability (IMaSS), JAPAN,

²Department of Materials Process Engineering, Nagoya University,

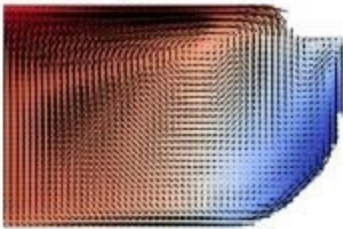
JAPAN, ³Venture Business Laboratory (VBL), Nagoya University,

JAPAN, ⁴RIKEN, JAPAN

Our final target is to realize “Cyber-Physical-System (CPS)” in crystal growth technology. In this system, crystal growth process is designed using high-speed and exact emulation of crystal growth constructed in the cyber space, and we perform crystal growth under the designed process in the physical-space. In this study, we made the high-speed and exact emulation of computation fluid dynamics (CFD) and demonstrated SiC solution growth under the optimized conditions. Silicon carbide is a semiconductor for next-generation power devices. We have developed a SiC solution growth technology, and we actually demonstrated the growth of ultra-high quality SiC crystals. However, the size of crystal was still small, e.g. 10-15 mm. It is required to enlarge it to 6 or 8 inch. The development of large diameter crystal is very tough. In the case of silicon, following the development of necking method, they spent 35-40 years to increase the diameter to 300 mm. One of difficulties is to optimize many growth parameters including design parameters of equipment. We often use the CFD simulation. Since the time of CFD simulation is also long, it is impossible to find optimized parameters comprehensively. In this study, we constructed a high-speed and exact regression model of CFD results based on neural network using machine learning. In addition, we tried to optimize the growth parameters using this regression model and we performed growth experiment of 3.5 inch, actually. The CFD simulation of about 100-300 cases are performed and the regression model is constructed on neural network by machine learning. Figure 1 shows one example of the prediction result compared to the simulation results due to same condition. They are almost same as each other. It is surprising the prediction time is 5-7 order higher than the simulation time. Moreover, we can construct a regression model as a function of design parameters, e.g. crucible size and shape. In other words, we can design a crucible, a thermal insulator and so on. Growth parameters can be decided by multi-

objective optimization with a prediction model. Firstly we defined objective functions of temperature, super cooling, solution flow and others based on our experiences. Optimization with a genomic algorithm suggested many candidates of growth parameters for high quality crystal. In actual, we performed the growth of over 3 inch SiC using the suggested growth conditions just after a few experiments (Fig. 2). Using this system, we could decrease the development period, dramatically.

(a) Prediction model



(b) Simulation



12:15 PM - 12:15 PM

ESTIMATION OF HIGH-TEMPERATURE PHYSICAL PROPERTIES

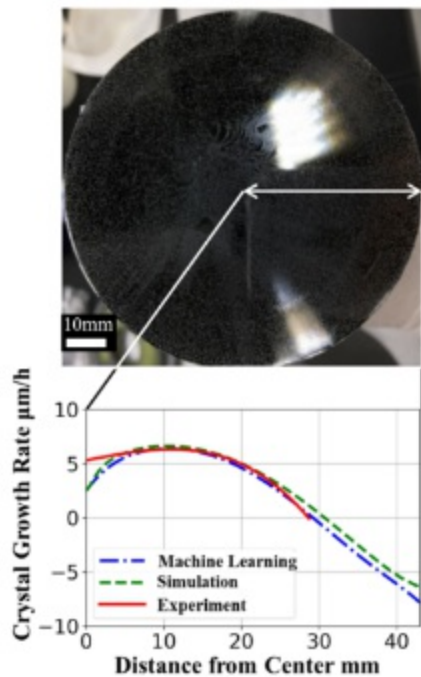
BY MACHINE LEARNING TOWARD ACCURATE NUMERICAL MODELING OF CRYSTAL GROWTH

K. Ando¹, H. Lin¹, Y. Tsunooka², T. Narumi³, C. Zhu⁴, K. Kutsukake⁵, S. Harada¹, K. Matsui⁵, I. Takeuchi⁶, Y. Koyama⁷, Y. Kawajiri¹, M. Tagawa¹, T. Ujihara⁴

¹Department of Materials Process Engineering, Nagoya University, JAPAN, ²GaN Advanced Device Open Innovation Laboratory (Gan-OIL), Nagoya University, JAPAN, ³Venture Business Laboratory (VBL), Nagoya University, JAPAN, ⁴Institute of Materials and Systems for Sustainability (IMaSS), JAPAN, ⁵RIKEN Center for Advanced Intelligence Project (AIP), JAPAN, ⁶Department of Computer Science, Nagoya Institute of Technology, JAPAN, ⁷Research and Services Division of Materials Data and Integrated System (MaDIS), National Institute for Materials Science (NIMS), JAPAN

Numerical modeling is widely employed to precisely design the transport phenomena during crystal growth and various high-temperature materials processing. However, the numerical modeling often contradicts the actual condition because many high-temperature physical properties are not assessed well. Recently, we develop the framework to find the optimal parameters for materials processing by machine learning and mathematical optimization [1-3]. In this study, this framework was applied to estimate the physical properties to improve the computational fluid dynamics (CFD) simulation of high-temperature solution growth method of silicon carbide (SiC). Firstly, a solution growth of SiC was conducted by an induction furnace using Si-Al solvent for 20 hours. The experimental growth rate was obtained from the radius distribution of grown SiC layer thickness. Next, 454 CFD simulations were conducted using randomly chosen physical properties shown in Table 1. Other conditions such as the geometry were the same as the experiment. Then, the regression model was constructed by a neural network to predict the growth rate from the physical properties. Finally, the optimal physical properties were investigated by the mathematical optimization. Fig. 1 shows the one of the radius distributions of the growth rate by the mathematical optimization together with the experimental result. It was confirmed that the regression model predicted the experimental result by using

the optimal physical properties. Since the large number of combinations of optimal physical properties was suggested, the mode values of distributions of optimal physical properties were used for comparing with the conventional values. The mode values and the conventional values were summarized in Table 1. The optimal physical properties including the interfacial reaction rate constants, which requires huge effort to obtain by experiments, were achieved in this study. To find the more specific optimal physical properties, both the experimental and the mathematical approaches are now under investigation. [1] Y. Tsunooka *et al.*, *CrystEngComm*, **20**(2018)6546. [2] Y. Tsunooka *et al.*, abstract book of ECSCRM 2018, Birmingham, MO.P.SG9. [3] Y. Jiang *et al.*, abstract book of the 66th JSAP Spring Meeting, 2019, 11p-70A-5.



Physical Property	Unit	This study	Conventional
Heat Capacity	J/kg/K	869	791
Thermal Conductivity	W/m/K	114.1	59.3
Emissivity	1	0.496	0.3
Density	kg/m ³	$-0.2708 \times T + 2992$	$-0.273 \times T + 2959$
Viscosity	Pa*s	$\exp\left(\frac{1850.5}{T} - 8.581\right)$	$\exp\left(\frac{1885}{T} - 8.58\right)$
Carbon Solubility	1	$\exp\left(-\frac{2.943 \times 10^4}{T} + 6.767\right)$	$\exp\left(-\frac{2.98 \times 10^4}{T} + 6.88\right)$
Seed Crystal / Solution Interface Reaction Rate Constant	m/s	6.92×10^{-5}	-
Graphite Crucible/ Solution Interface Reaction Rate Constant	m/s	1.38×10^{-10}	-

12:15 PM - 12:15 PM

INVESTIGATION OF PROCESS CONDITIONS ON SURFACE HEIGHT VARIATION OF KDP CRYSTALS BY RAPID GROWTH TECHNIQUE

L. Zheng, K. Hu, H. Zhang
Tsinghua University, CHINA

A rapid growth technique is often used for the growth of large sized KDP crystals. Inclusion formation during growth remains the key issue as it affects optical quality of crystals. Much studies have confirmed morphological instability as the primary factor for inclusion formation, which is directly related to the local growth rate along the crystal interface. And the local growth rate is determined not only by the interfacial kinetics at microscale but also species transport at macroscale. Thus, control of inclusion formation for high optical quality crystal requires better understanding of the underlying physics causing surface morphological instability during growth and critical process control parameters. This work presents numerical studies of morphological instability of crystal front during growth, specifically, variation of KDP crystal surface height by rapid growth technique. Computational models couple the macroscopic transport of solute and impurities with the microscopic interfacial kinetics processes. Numerical simulations are performed to study growth rate fluctuation at representative growth interfaces subjected to variations in crystal size, bulk super-saturation, rotation rate of the stirring paddle and impurities. It is found that the predicted interface moving speeds, equivalent to growth rate, are uniformly distributed normal to each pyramidal and prismatic faces at the macro-scale when considering interfacial kinetics process, however, they fluctuate wavyly at the micro-scale. The amplitude of growth rate fluctuation is at the order of micrometer. The fluctuation in growth rate will cause KDP crystal surface height variation and lead to the formation of micron-sized and nano-sized inclusions in crystals. Increasing crystal size and bulk super-saturation can intensify growth rate fluctuation, potentially reduce the quality of crystal. Increasing rotational speed can reduce growth rate fluctuation. The impurities influence growth rate of the KDP prismatic face obviously. When impurities exist in solution,

growth rate of prismatic face decreases greatly and growth rate fluctuation can be intensified by one order of magnitude.

12:15 PM - 12:15 PM

ANALYSIS OF HEAT AND MASS TRANSFER USING ROTATING BAFFLE IN VERTICAL BRIDGMAN CONFIGURATION

A.G. Ostrogorsky¹, N. Dropka², V. Riabov¹

¹Illinois Institute of Technology, IL, UNITED STATES OF AMERICA,
²IKZ, GERMANY

Analysis of Heat and Mass Transfer using Rotating Baffle in Vertical Bridgman Configuration Flow visualization and crystal growth experiments were performed using NaNO_3 to study the effect of melt flow driven by the rotating baffle on heat and mass transfer in in Vertical Bridgman configuration. 3D simulations of the process were performed for a set of material having a wide range from $0.01 < Pr < 33$, including Ge, InP, CdTe, Ga_2O_3 NaNOs and Al_2O_3 . The rotation rate of the baffle was varied in the range $0 < w < 100$ rpm. Positive slightly convex crystal-melt interface was obtained for all studied materials. The higher the Pr number of melts, the stronger is the influence of the baffle rotation. *Corresponding author, AOstrogo@IIT.edu

12:15 PM - 12:15 PM

NUMERICAL INVESTIGATION OF THERMAL AND IMPURITIES DISTRIBUTION IN THE DIRECTIONAL SOLIDIFICATION FURNACE FOR PHOTOVOLTAIC APPLICATIONS

K. V. S. M., P. Ramasamy

SSN College of Engineering, INDIA

The thermal and impurities distribution in multi-crystalline silicon were investigated in Directional Solidification (DS) system. The different heater designs were investigated for the DS system. The Oxygen impurities originate from the quartz crucible at high temperature. Oxygen impurities is affecting solar cell efficiency. Oxygen impurities are inducing light-induced degradation and more oxygen atom forms SiO_2 precipitates during the solidification time. Oxygen-related defect affects the electrical parameters in the crystal. The optimized heater

design gives the lower oxygen impurities in the melt and crystal. Because the optimized heater design reduces the melt flow velocity, lower and uniform temperature distribution in melt. The optimized heater design has produced lower temperature in the crucible wall side. So, it is reducing the dissolving rate of oxygen impurities in the crucible with lower stream function and it is improving the melt-crystal (m-c) interface shape. The melt-crystal interface shape is mainly affected by the temperature distribution. The numerical results are useful for understanding of thermal distribution, the effect of the heater design, the effect of the ratio temperature between the top and side heater systems in the Directional solidification system for reduction of oxygen impurities in the mc-Si ingots.

** Current as of 6-20-2019. Changes to the schedule will be posted on-site **